TUMOR MICROENVIRONMENT (TME) AND TUMOR IMMUNE MICROENVIRONMENT (TIME): NEW PERSPECTIVES FOR PROGNOSIS AND THERAPY

EDITED BY: Ana Karina de Oliveira, Jay William Fox, Mariane Tami Amano, Adriana Franco Paes Leme and Rodrigo Nalio Ramos

PUBLISHED IN: Frontiers in Cell and Developmental Biology

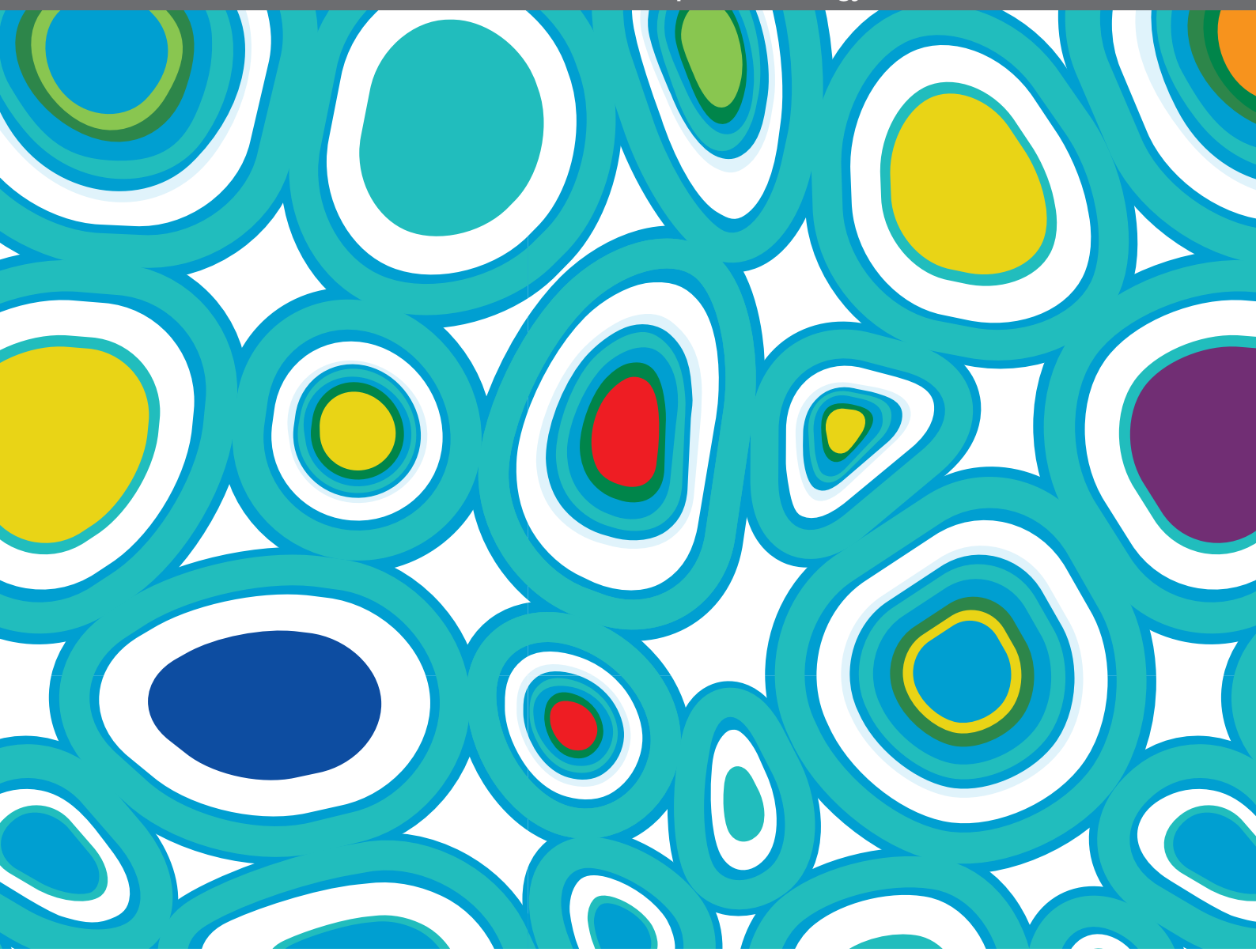

frontiers Research Topics

ISSN 1664-8714
ISBN 978-2-83250-132-0
DOI 10.3389/978-2-83250-132-0

About Frontiers

Frontiers is more than just an open-access publisher of scholarly articles: it is a pioneering approach to the world of academia, radically improving the way scholarly research is managed. The grand vision of Frontiers is a world where all people have an equal opportunity to seek, share and generate knowledge. Frontiers provides immediate and permanent online open access to all its publications, but this alone is not enough to realize our grand goals.

Frontiers Journal Series

The Frontiers Journal Series is a multi-tier and interdisciplinary set of open-access, online journals, promising a paradigm shift from the current review, selection and dissemination processes in academic publishing. All Frontiers journals are driven by researchers for researchers; therefore, they constitute a service to the scholarly community. At the same time, the Frontiers Journal Series operates on a revolutionary invention, the tiered publishing system, initially addressing specific communities of scholars, and gradually climbing up to broader public understanding, thus serving the interests of the lay society, too.

Dedication to Quality

Each Frontiers article is a landmark of the highest quality, thanks to genuinely collaborative interactions between authors and review editors, who include some of the world's best academicians. Research must be certified by peers before entering a stream of knowledge that may eventually reach the public - and shape society; therefore, Frontiers only applies the most rigorous and unbiased reviews.
Frontiers revolutionizes research publishing by freely delivering the most outstanding research, evaluated with no bias from both the academic and social point of view. By applying the most advanced information technologies, Frontiers is catapulting scholarly publishing into a new generation.

What are Frontiers Research Topics?

Frontiers Research Topics are very popular trademarks of the Frontiers Journals Series: they are collections of at least ten articles, all centered on a particular subject. With their unique mix of varied contributions from Original Research to Review Articles, Frontiers Research Topics unify the most influential researchers, the latest key findings and historical advances in a hot research area! Find out more on how to host your own Frontiers Research Topic or contribute to one as an author by contacting the Frontiers Editorial Office: frontiersin.org/about/contact

TUMOR MICROENVIRONMENT (TME) AND TUMOR IMMUNE MICROENVIRONMENT (TIME): NEW PERSPECTIVES FOR PROGNOSIS AND THERAPY

Topic Editors:
Ana Karina de Oliveira, University of Virginia, United States
Jay William Fox, University of Virginia, United States
Mariane Tami Amano, Hospital Sirio Libanes, Brazil
Adriana Franco Paes Leme, Brazilian Biosciences National Laboratory (LNBio), Brazil
Rodrigo Nalio Ramos, D'Or Institute for Research and Education (IDOR), Brazil

Citation: de Oliveira, A. K., Fox, J. W., Amano, M. T., Leme, A. F. P., Ramos, R. N., eds. (2022). Tumor Microenvironment (TME) and Tumor Immune Microenvironment (TIME): New Perspectives for Prognosis and Therapy. Lausanne: Frontiers Media SA. doi: 10.3389/978-2-83250-132-0

Table of Contents

frontiers | Frontiers in Cell and Developmental Biology

TYPE Editorial
PUBLISHED 22 August 2022
DOI 10.3389/fcell.2022.971275

OPEN ACCESS

EDITED AND REVIEWED BY
Ramani Ramchandran,
Medical College of Wisconsin,
United States

*CORRESPONDENCE
Ana Karina de Oliveira,
ak4yj@virginia.edu

SPECIALTY SECTION
This article was submitted to Cell Growth and Division, a section of the journal Frontiers in Cell and Developmental Biology

RECEIVED 16 June 2022
ACCEPTED 04 July 2022
PUBLISHED 22 August 2022

CITATION
Ramos RN, Amano MT, Paes Leme AF, Fox JW and de Oliveira AK (2022), Editorial: Tumor microenvironment (TME) and tumor immune microenvironment (TIME): New perspectives for prognosis and therapy. *Front. Cell Dev. Biol.* 10:971275. doi: 10.3389/fcell.2022.971275

Editorial: Tumor microenvironment (TME) and tumor immune microenvironment (TIME): New perspectives for prognosis and therapy

Rodrigo Nalio Ramos[1], Mariane Tami Amano[2], Adriana Franco Paes Leme[3], Jay Willian Fox[4] and Ana Karina de Oliveira[5]*

[1]Departament of Hematology and Cell Therapy, Laboratory of Medical Investigation in Pathogenesis and Directed Therapy in Onco-Immuno-Hematology (LIM-31), D'Or Institute for Research and Education (IDOR), Hospital Das Clínicas da Faculdade de Medicina da Universidade de São Paulo, São Paulo, Brazil, [2]Hospital Sirio Libanes, São Paulo, Brazil, [3]Brazilian Biosciences National Laboratory (LNBio), Brazilian Center for Research in Energy and Materials (CNPEM), Campinas, Brazil, [4]Department of Microbiology, Immunology and Cancer Biology, Office of Research Core Administration (ORCA), University of Virginia School of Medicine, Charlottesville, VA, United States, [5]Department of Pathology, University of Virginia School of Medicine, Spatial Biology Core (SBC) Facility, Charlottesville, VA, United States

KEYWORDS

tumormicroenvironment, tumor immune microenvironment, immune checkpoint blockade, immune therapeutics, tumor stroma cross-talk, prognosis

Editorial on the Research Topic
Tumor Microenvironment and Tumor Immune Microenvironment: New Perspectives for Prognosis and Therapy

The success of tumor treatment is defined by a combination of factors that include the cells that make up the tumor microenvironment (TME). TME studies have contributed to illuminating the heterogeneity of tumors and has led to the discovery of potential targets for cancer immunotherapeutics. New strategies are continually being based on these studies are being approved for clinical use at a greater rate than compared in the past decade. In the 2000s, the first studies of the effects of PD-1, PDL-1, and CTLA-4 inhibitors started, and currently, there are dozens of promising immunotherapy targets in clinical trials studies or already available in the clinical practice, including genetically modified T cells expressing chimeric antigen receptors (CAR-T cells), anti-CD20 (Rituximab) for treatment of non-Hodgkin's B cell lymphoma, anti-CD52 (Alemtuzumab) for multiple myeloma, anti-IL-6 (Siltuximab) and the anti-IL-6R (Tocilizumab) for multiple myeloma and solid tumors, anti-LAG3 (Relatlimab) immune activating checkpoints in melanoma.

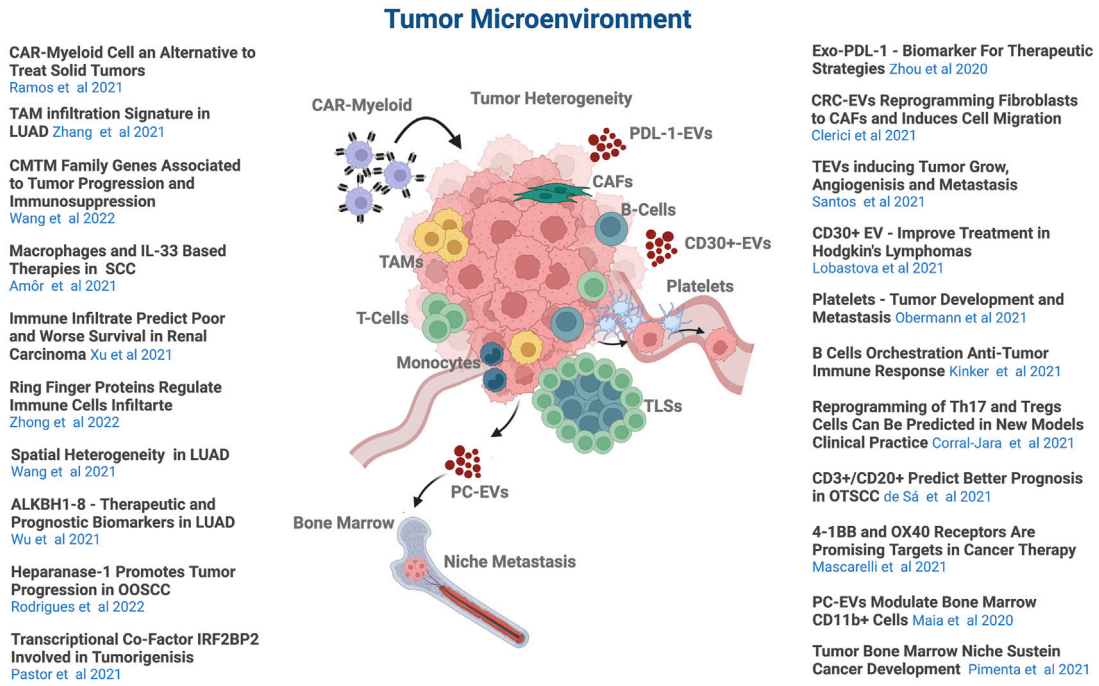

FIGURE 1
The tumor microenvironment. A schematic view of the tumor microenvironment components and all scientific contributions in this Topic Research. The picture was created with BioRender.com.

Although great advances have been made in the immunotherapeutic field, only about 30% of patients respond to these treatments. In some cases, tumors acquire resistance to immune checkpoint blockade (ICB) by losing neoantigen expression or even presenting a low frequency of T cell infiltration, or other unknown reason. Investigators still have a long way to go to improve strategies against cancer that including the discovery of new targets and strategies to activate the immune system, the modulation of phenotype and function of cells present in the TME, the re-education of immune cell function, and the induction of immune cell migration to the tumor site.

This Research Topic presents a remarkable collection of articles comprised of 9 Original Research, 2 Brief Research Reports, 8 Reviews, and 2 Mini Reviews covering novel, promising recent trends in the immune microenvironment landscape and immunotherapy field (Figure 1).

The TME is a complex ecosystem where continuous interactions sustain tumor development and growth. Recent molecular biology and immunology findings have shown that tumor-stroma communication promotes intense suppressive signals in the microenvironment, contributing to therapy failure. Tumor-stroma communication is not a unidirectional process, driven only by cancer cells. Other resident cells, like cancer-associated fibroblasts (CAFs), macrophages, lymphocytes, endothelial cells, and cancer stem cells, have intense crosstalk with each other, with secreted factors and components of the extracellular matrix (ECM). New technologies have been emerging to map these ecosystems. Machine learning (ML) is one of these promising technologies that has revolutionized this area of research. Big data combined with ML have changed many aspects of the experimental domain and may ultimately support the clinical decision process in cancer therapy.

In this context, Zhang et al. used bioinformatics approaches to build a tumor-associated macrophage (TAM) prognostic risk model. They generated a relevant gene model correlated with clinical features and predictive risk scores and thereby determined a central regulatory axis: LINC00324/miR-9-5p (miR-33b-5p)/GAB3 (IKZF1), which may play a pivotal role in regulating the risk and prognosis of TAM in patients with lung adenocarcinoma (LUAD). Using a training and validation cohort model with more than 900 patients from different databases, Wang et al. constructed a score based on the cluster model. This model was able to stratify lower-grade glioma (LGG) patients into two groups concerning the chemokine-like factor (CKLF)-like Marvel transmembrane domain-containing (CMTM) gene family: low-risk score groups associated with high tumor purity and reduced immune cell infiltration; and the high-risk score group which exhibited a poor prognosis with higher grade wild-

type isocitrate dehydrogenase (WT-IDH), high expression of CMTM genes, and increased expression levels of PD-1, PD-L1, and PD-L2.

Considering the remarkable role of extracellular vesicles (EVs) in cell-to-cell communication in the TME and the emergent number of novel studies in literature, it is no surprise that five articles in this thematic field were published on this topic. EVs can originate from either endosomal (exosome) or plasma membrane budding (microvesicles). Some have been demonstrated to have a pro-tumoral activity in the TME, impacting cancer cell proliferation, immune escape, angiogenesis, invasion, pre-metastatic niche formation, and metastasis. Based on these characteristics they may become important therapeutic targets and prognostic biomarkers as was discussed by Santos et al. in their review. Clerici et al. demonstrated another aspect of colorectal cancer-derived EVs, which reprogram fibroblasts, induce migration, and contribute to the drug resistance phenotype.

Interestingly, Maia et al. show communication between bone marrow CD11b+ and pancreatic tumor cells mediated by EVs. This communication induces genetic alterations in the TME, such as macrophage activation and expression of inflammatory molecules. Zhou et al. show the predictive potential of tumor cell-derived exosomal PD-L1+ as a marker of immunotherapeutic efficacy, while Lobastova et al. show that $CD30^+$ EVs can increase the treatment efficacy of Hodgkin's lymphomas.

Kinker et al. in their comprehensive review of tertiary lymphoid structures (TLS), highlighted the TLS structure in the TME. The TLS provides an area of intense B cell antigen presentation that induces T cell activation and effector B cell generation, which induces the antibody-secreting plasma cells and memory B cells differentiation. The TLS is a well-organized non-encapsulated structure composed of immune and stromal cells, which are associated with improved response to immune checkpoint therapies. Evaluating patients with Oral Tongue Squamous Cell Carcinoma, Sales de Sá et al. show that high expression of $CD3^+$ T cells and B cells in TLS regions are predictive of better overall survival and inflammatory response.

A number of articles discussed the participation of specific molecules in tumorigenesis and cancer metastasis. Obermann et al. reviewed the role of platelets in the formation of micrometastases and the formation of the metastatic niche. Indeed, metastatic niches seem to contribute exponentially to tumor progression. Different niches present in the bone marrow (BM) are altered during acute myeloid leukemia (AML) development. These niches that support the development of AML are also important targets for the development of future therapies since these targets are involved in critical functions of leukemia (Pimenta et al.). Pastor et al. described the involvement of Interferon regulatory factor 2-binding protein 2 (IRF2BP2) in tumor development. The role of heparinase-1 in oral squamous cell carcinoma tumor progression was investigated by Rodrigues et al.

In the domain of the emerging therapies, Ramos et al. provided a magnificent review of the new approaches of Chimeric antigen receptor (CAR) engineering in solid tumor treatment using CAR-myeloid cells. CAR therapy is an already established technology used for T cells (CAR-T) and natural killer cells (CAR-NK). In CAR T-cell therapies, whereby the patient's T-cells are genetically reprogramed to express a chimeric antigen receptor thereby driving T cells to eliminate tumors. CAR-T is used in hematologic tumors but has yet to demonstrate overall efficacy in solid tumors. Thus, the use of genetically modified macrophages and dendritic cells expressing CAR (CAR-myeloid cells) may open new perspectives in treating solid tumors.

We are confident that our Tumor Microenvironment (TME) and Tumor Immune Microenvironment (TIME): New Perspectives for Prognosis and Therapy Research Topic has highlighted important aspects of tumor microenvironment heterogeneity, new therapeutic and prognostic targets, interactions in TEM, new technologies for the study of cancer, and more importantly, and also indicated that there is yet a long path forward to provide robust cancer prognoses and therapies in cancer.

Author contributions

All authors listed have made a substantial, direct, and intellectual contribution to the work and approved it for publication.

Conflict of interest

The authors declare that the research was conducted in the absence of any commercial or financial relationships that could be construed as a potential conflict of interest.

Publisher's note

frontiers in Cell and Developmental Biology

REVIEW
published: 15 October 2020
doi: 10.3389/fcell.2020.569219

Exosomal PD-L1: New Insights Into Tumor Immune Escape Mechanisms and Therapeutic Strategies

Kaijian Zhou[1], Shu Guo[1], Fei Li[2], Qiang Sun[1] and Guoxin Liang[3]*

[1] Department of Plastic Surgery, The First Affiliated Hospital of China Medical University, Shenyang, China, [2] Department of Pharmaceutical Science, The First Affiliated Hospital of China Medical University, Shenyang, China, [3] Cancer Therapy Research Institute, The First Affiliated Hospital of China Medical University, Shenyang, China

OPEN ACCESS

Edited by:
Adriana Franco Paes Leme, Brazilian Biosciences National Laboratory (LNBio), Brazil

Reviewed by:
Hinrich Peter Hansen, University of Cologne, Germany
Mariateresa Giuliano, University of Campania Luigi Vanvitelli, Italy
Diana Noronha Nunes, A C Camargo Cancer Center, Brazil

***Correspondence:**
Shu Guo
sguo@cmu.edu.cn

Specialty section:
This article was submitted to Molecular Medicine, a section of the journal Frontiers in Cell and Developmental Biology

Received: *03 June 2020*
Accepted: *27 August 2020*
Published: *15 October 2020*

Citation:
Zhou K, Guo S, Li F, Sun Q and Liang G (2020) Exosomal PD-L1: New Insights Into Tumor Immune Escape Mechanisms and Therapeutic Strategies. Front. Cell Dev. Biol. 8:569219. doi: 10.3389/fcell.2020.569219

As a classical immune checkpoint molecule, PD-L1 on the surface of tumor cells plays a pivotal role in tumor immunosuppression, primarily by inhibiting the antitumor activities of T cells by binding to its receptor PD-1. PD-1/PD-L1 inhibitors have demonstrated unprecedented promise in treating various human cancers with impressive efficacy. However, a significant portion of cancer patients remains less responsive. Therefore, a better understanding of PD-L1-mediated immune escape is imperative. PD-L1 can be expressed on the surface of tumor cells, but it is also found to exist in extracellular forms, such as on exosomes. Recent studies have revealed the importance of exosomal PD-L1 (ExoPD-L1). As an alternative to membrane-bound PD-L1, ExoPD-L1 produced by tumor cells also plays an important regulatory role in the antitumor immune response. We review the recent remarkable findings on the biological functions of ExoPD-L1, including the inhibition of lymphocyte activities, migration to PD-L1-negative tumor cells and immune cells, induction of both local and systemic immunosuppression, and promotion of tumor growth. We also discuss the potential implications of ExoPD-L1 as a predictor for disease progression and treatment response, sensitive methods for detection of circulating ExoPD-L1, and the novel therapeutic strategies combining the inhibition of exosome biogenesis with PD-L1 blockade in the clinic.

Keywords: exosomal PD-L1, tumor microenvironment, immune escape, antitumor immune memory, abscopal effect, biomarker, detection method, immunotherapy

INTRODUCTION

Programmed cell death protein-ligand 1 (PD-L1) is an immune checkpoint molecule that interacts with programmed cell death protein-1 (PD-1) to mediate immunosuppression (Ribas and Hu-Lieskovan, 2016; Alsaab et al., 2017; Sun et al., 2018; Han et al., 2020). Binding of PD-L1 to PD-1 conveys a regulatory signal to T cells and an antiapoptotic signal to tumor cells, resulting in T cells exhaustion and tumor cell survival (Dong et al., 2002; Jiang X. et al., 2019; Jiang Y. et al., 2019). It is known that, as a membrane-bound molecule, PD-L1 is expressed on the cell surface of many tumor

types and the PD-1/PD-L1 pathway is considered to be a critical mechanism for immune escape and tumor progression (Quail and Joyce, 2013; Yu et al., 2016; Kakavand et al., 2017; Kythreotou et al., 2018; Cha et al., 2019). Therefore, anti-PD-1/PD-L1 inhibitors are able to induce durable tumor regression and represent a unique therapeutic strategy for patients with advanced cancers (Couzin-Frankel, 2013; Mahoney et al., 2015; Ribas et al., 2016; Yaghoubi et al., 2019). However, the effective rate of anti-PD-1/PD-L1 immunotherapy remains low (Xu-Monette et al., 2017; Chamoto et al., 2020; Hatae et al., 2020). Furthermore, patients exhibiting negative PD-L1 expression can also benefit from anti-PD-1/PD-L1 blockade (Patel and Kurzrock, 2015; Shukuya and Carbone, 2016; Shen and Zhao, 2018). Thus, neither the expression pattern of PD-L1 on the tumor cell surface alone is sufficient to account for the mechanism of tumor immune escape nor accurate for predicting the response to anti-PD-1/PD-L1 treatment, although tumor tissue PD-L1 is the only indicator authorized by the FDA (Festino et al., 2016; Wang Q. et al., 2017; Li et al., 2019c; Martinez-Morilla et al., 2020). Therefore, as an alternative to membrane-bound PD-L1, exosomal PD-L1 (ExoPD-L1) that is associated with exosomes secreted by tumor cells has been investigated recently.

Extracellular vesicles (EVs) are membrane-enveloped particles produced by almost all cell types and are classified into three subgroups: microvesicles, apoptotic bodies, and exosomes, according to their biogenesis, cellular source and biological properties (Gould and Raposo, 2013; Colombo et al., 2014; Yanez-Mo et al., 2015; Xu et al., 2016; Hessvik and Llorente, 2018; van Niel et al., 2018; Margolis and Sadovsky, 2019). Microvesicles and apoptotic bodies are large EVs (normally 100−1000 μm) and are shed directly from the plasma membrane (Gould and Raposo, 2013; van Niel et al., 2018; Margolis and Sadovsky, 2019). Exosomes are small EVs (typically 30−100 μm) generated by the endocytic pathway (Thery et al., 2006; Kowal et al., 2014; Lobb et al., 2015; Kalluri, 2016; Tkach and Thery, 2016; Tkach et al., 2018). After the fusion of endosomal multivesicular bodies (MVBs) with the plasma membrane, exosomes are secreted extracellularly (Carlton, 2010; Stoorvogel, 2015; Ha et al., 2016). Neutral sphingomyelinase type 2 (nSMase2) and Rab27a are two key enzymes in the biogenesis of exosomes (Hessvik and Llorente, 2018). They are involved in the inward budding of MVBs to form intraluminal vesicles (ILVs), the intracellular precursors of exosomes, and the transportation and fusion of the MVBs to the plasma membrane, respectively (Trajkovic et al., 2008; Ostrowski et al., 2010; Lallemand et al., 2018). Genetic and pharmacological manipulation of these enzymes offers an approach to determine the various roles of exosomes *in vitro* and *in vivo*. Increasing evidence indicates that exosomes derived from tumor cells can regulate the tumor microenvironment and promote cancer progression via their cargos, which include proteins, lipids, and nucleic acids (Anastasiadou and Slack, 2014; Lazaro-Ibanez et al., 2019; Zhang and Yu, 2019; Raimondo et al., 2020; Sahebi et al., 2020). Recent studies have demonstrated that PD-L1 also exists on the surface of exosomes generated by their parental tumor cells (Chen G. et al., 2018; Lubin et al., 2018; Ricklefs et al., 2018; Theodoraki et al., 2018b; Yang et al., 2018; Fan et al., 2019; Kim et al., 2019; Poggio et al., 2019; Cordonnier et al., 2020; Huang et al., 2020). Moreover, ExoPD-L1 can function as efficiently as PD-L1 on the tumor cell surface through direct ligation to PD-1 on the surface of lymphocytes in tumor foci (Chen G. et al., 2018; Lubin et al., 2018; Ricklefs et al., 2018; Theodoraki et al., 2018b; Yang et al., 2018; Fan et al., 2019; Kim et al., 2019; Poggio et al., 2019; Cordonnier et al., 2020; Huang et al., 2020). Surprisingly, although the cell-surface PD-L1 is low or absent, the ExoPD-L1 may be highly secreted by its parental tumor cells that are resistant to anti-PD-L1 therapy (Poggio et al., 2019). Overall, ExoPD-L1 plays a pivotal role in immunosuppression and tumor progression.

In this review, we summarize the various functions of ExoPD-L1 secreted by tumor cells, focusing on the recent findings regarding their expression heterogeneity, the impact on local and systemic immune response, and tumor growth. Moreover, we also discuss the clinical implications of circulating ExoPD-L1 as a non-invasive biomarker to predict tumor progression and immunotherapeutic response, and as a novel target to develop more effective antitumor strategies.

THE EXPRESSION PATTERN OF TUMOR ExoPD-L1

It is well known that the PD-L1 protein is abundantly expressed on the cell surface of various cancers (Cimino-Mathews et al., 2016; Nduom et al., 2016; Brody et al., 2017; Sunshine et al., 2017). Recent studies have shown that tumor cells can secrete PD-L1 in EVs, particularly in exosomes, which are generally present in the pellet obtained by ultracentrifugation (Chen G. et al., 2018; Yang et al., 2018; Kim et al., 2019; Poggio et al., 2019). Colocalization of PD-L1 and exosomal marker CD63 in MVBs is observed in human breast cancer tissues by immunohistochemical staining (Pols and Klumperman, 2009; Khushman et al., 2017; Farooqi et al., 2018; Yang et al., 2018). Furthermore, human ExoPD-L1 was found in the circulation of nude mice bearing human melanoma xenografts (Chen G. et al., 2018). Thereby, both human and murine tumor cells can secrete ExoPD-L1 both *in vitro* and *in vivo*.

The expression of ExoPD-L1 is highly heterogeneous in tumor cells. The variability in the levels of ExoPD-L1 is quite significant between different tumor types and even between different cell lines of the same type (**Table 1**). In addition, it appears that ExoPD-L1 levels are consistent with the levels of PD-L1 expressed in their parental tumor cells (Chen G. et al., 2018; Ricklefs et al., 2018; Fan et al., 2019; Kim et al., 2019). However, an exception is observed in prostate cancer. These tumor cells produce high levels of PD-L1-containing exosomes, but are devoid of PD-L1 on the tumor cell surface, despite expressing constitutively high levels of PD-L1 mRNA (Poggio et al., 2019). Considering the discordance between exosomal and cell-surface PD-L1 expression, the expression pattern of ExoPD-L1 from tumor cells, especially that of low or undetectable cell-surface PD-L1, should not be neglected. In addition, interferon-γ, a typical inflammatory cytokine, upregulates ExoPD-L1 production by melanoma, breast cancer, prostate cancer, glioblastoma, and non-small cell lung

TABLE 1 | Expression of ExoPD-L1 secreted by human and mouse tumor cell lines.

Tumor	High	Low	Negative	References
Breast cancer	MDA-MB-231#			Chen G. et al., 2018; Yang et al., 2018
	BT549, 4T1*	MCF-7		Yang et al., 2018
			HCC1954#, 67NR*#, SKBR&	Monypenny et al., 2018
Colon cancer	RKO			Yang et al., 2018
	MC38*			Poggio et al., 2019
Gastric cancer	MKN74	SGC7901, BGC823, NCI-N87, NUGC4, MKN45	KATOIII, AGS, MGC803	Fan et al., 2019
Glioblastoma	G34, G35, CT2A*	G44#, G157#		Ricklefs et al., 2018
Melanoma	WM9#, WM164#, UACC-903	WM1552C, WM35, WM793, WM902B	MEL624	Chen G. et al., 2018
		SK-MEL-28		Poggio et al., 2019
	B16-F10*			Chen G. et al., 2018; Cordonnier et al., 2020
	SK-MEL-2			Cordonnier et al., 2020
	A375			Chen G. et al., 2018; Huang et al., 2020
			A375	Yang et al., 2018
NSCLC	H1299#, H358#, H1264#			Chen G. et al., 2018
	H460, H1975	A549	LLC-1*	Kim et al., 2019
	HCC827			Yang et al., 2018
	A549			Cordonnier et al., 2020
Prostate cancer	PC3#, TRAMP-C2*#		LNCaP	Poggio et al., 2019

**, murine; #, IFN-γ inducible PD-L1 expression; &, IFN-γ non-inducible PD-L1 expression.*

carcinoma (NSCLC) (Chen G. et al., 2018; Monypenny et al., 2018; Ricklefs et al., 2018; Poggio et al., 2019). However, the mechanism regulating ExoPD-1 release is not fully understood. Thus, endeavors to further explore the molecular mechanisms regulating ExoPD-L1 expression are warranted.

THE IMMUNOSUPPRESSIVE EFFECTS OF ExoPD-L1

The modulatory effect of tumor cell PD-L1 occurs through binding to PD-1. PD-L1 is a typical transmembrane protein (Dong et al., 1999, 2002). Recent studies reveal that ExoPD-L1 displays the same extracellular domain topology as its cell-surface counterpart (Chen G. et al., 2018). Therefore, ExoPD-L1 may exert a similar function as tumor cell-surface PD-L1 by engaging with PD-1.

The Interaction Between ExoPD-L1 and PD-1 on T Cells

ExoPD-L1 Directly Binds to PD-1 on T Cells

In vitro binding assays showed that PD-L1 on melanoma-derived exosomes is able to ligate to soluble PD-1 molecules in a concentration-dependent manner (Chen G. et al., 2018; Ricklefs et al., 2018; Yang et al., 2018). Consistently, both PD-L1 and PD-1 blocking antibodies can disrupt the ligation in a dose-dependent manner (Chen G. et al., 2018; Ricklefs et al., 2018). The physical combination of melanoma exosomes and T cells was confirmed by using confocal microscopy, flow cytometry and enzyme linked immunosorbent assay (ELISA) (Chen G. et al., 2018; Ricklefs et al., 2018). The binding of melanoma-derived exosomes to $CD8^+$ T cells is increased when the levels of either PD-1 on $CD8^+$ T cells or ExoPD-L1 are upregulated (Chen G. et al., 2018). Studies on glioblastoma-derived exosomes also show that ExoPD-L1 binds to $CD4^+$ and $CD8^+$ T cells (Ricklefs et al., 2018). Furthermore, the *in vivo* colocalization of ExoPD-L1 to tumor-infiltrating lymphocytes (TILs) in mouse glioblastoma tissues was visualized (Ricklefs et al., 2018). Thus, ExoPD-L1 can ligate to PD-1 on T cells, which is an alternative pathway to membrane-bound PD-L1 interacting with its receptor PD-1.

ExoPD-L1 Interacts With PD-1 on T Cells After Migration to PD-L1-Negative Tumor Cells

It has been demonstrated that exosomes can transfer specific proteins, nucleic acids, and lipids from donor cells to recipient cells, thereby influencing the phenotype of the recipient cells (Milane et al., 2015; Ruivo et al., 2017; Wan et al., 2018; Lazaro-Ibanez et al., 2019). Recent studies found that tumor-derived exosomes can transport PD-L1 from PD-L1-positive tumor cells to PD-L1-negative tumor cells (Yang et al., 2018). After a 24 h incubation with ExoPD-L1 derived from breast cancer cells with constitutive PD-L1 expression, high levels of PD-L1 were detected in breast cancer cells with PD-L1 knockdown or low PD-L1 expression (Yang et al., 2018). Notably, the ExoPD-L1 migration to PD-L1-negative tumor cells was detectable in tumor masses of mice 5 days after coinjection of ExoPD-L1 (Yang et al., 2018). Furthermore, ExoPD-L1 can be transported to immune cells, including human macrophages and dendritic cells *in vitro* and murine tumor-infiltrated macrophages *in vivo* (Yang et al., 2018). More importantly, results obtained from flow cytometric analysis demonstrated that the ExoPD-L1, which settled on the surface of the PD-L1-negative tumor cells, is capable of binding to the PD-1 Fc fragment (Yang et al., 2018). Thus, the ExoPD-L1 that migrates to the surface of recipient cells from PD-L1-positive

tumor cells still maintains its ability to bind to PD-1 on T cells (Yang et al., 2018).

Notably, CD80 is also a binding partner of PD-L1 and competes with PD-1 for engaging PD-L1 (Butte et al., 2008; Park et al., 2010; Chen and Flies, 2013). The interaction of PD-L1 on tumor cells and CD80 on T cells suppresses T cell activation and survival, suggesting that dual blocking PD-1 and CD80 interaction with PD-L1 might be more favorable for improving the immunotherapy efficacy compared with single PD-1 blockade (Butte et al., 2007; Rollins and Gibbons Johnson, 2017). In addition, PD-L1 can interact in *cis* with CD80 on the same cell (Chaudhri et al., 2018). The *cis*-heterodimer of PD-L1 and CD80 on antigen presenting cells is able to restrict PD-1 function and is the requirement for triggering T cell responses (Sugiura et al., 2019; Zhao Y. et al., 2019; Mayoux et al., 2020). Therefore, it is necessary to dissect the functions contributed by the crosstalk between PD-L1/PD-1 and PD-L1/CD80 pathways in tumor microenvironment to explore new opportunities for tumor treatment.

The PD-1/PD-L1 signaling pathway in activated T cells has been reviewed in recent literatures (Ai et al., 2020; Bastaki et al., 2020; Wu et al., 2020). After PD-1 binds to PD-L1, the cytoplasmic tail of PD-1 is phosphorylated and recruits Src homology phosphatase 1 (SHP-1) and SHP-2 (Chemnitz et al., 2004; Yokosuka et al., 2012; Chinai et al., 2015). SHP-2 dephosphorylates and inhibits T cell receptor (TCR) and downstream signaling, such as zeta-chain-associated protein kinase 70 (ZAP70), phosphoinositide 3-kinase (PI3K), protein kinase B (PKB/AKT), mammalian target of rapamycin (mTOR), rat sarcoma (RAS), mitogen-activated protein kinase (MAPK/MEK), and extracellular regulated protein kinase (ERK) (Sheppard et al., 2004; Parry et al., 2005; Riley, 2009; Patsoukis et al., 2012; Hui et al., 2017). Additionally, recent studies reported that CD28, rather than the TCR, is the primary target of SHP-2 (Hui et al., 2017; Kamphorst et al., 2017), suggesting that PD-1 may target both TCR and CD28 to exert regulatory function. It has been shown that ExoPD-L1 released by breast cancer cells significantly suppresses ERK phosphorylation and nuclear factor kappa-B activation in CD3/CD28-activated T cells (Yang et al., 2018). However, whether other molecules participate in the ExoPD-L1 signaling, especially in the context of tumorigenesis, remains unclear and needs to be further investigated.

The *in vitro* Immunosuppressive Effects of ExoPD-L1

It has been reported that tumor-derived exosomes contribute to $CD8^+$ T cell dysfunction, although the mechanism is not fully understood (Ludwig et al., 2017; Maybruck et al., 2017; Huang et al., 2018; Wang T. et al., 2019). Recent studies found that ExoPD-L1 secreted by tumor cells can efficiently induce T cell dysfunction via interacting with its surface PD-1 (**Table 2**).

Protein-1 is mainly expressed on activated T cells and it is a central inhibitory receptor that regulates $CD8^+$ T cell dysfunction in tumors (Ahn et al., 2018; Miller et al., 2019). Recent studies found that the activation-signaling pathway in T cells is inhibited in a dose-dependent manner from exposure to ExoPD-L1 derived from breast cancer cells (Yang et al., 2018).

TABLE 2 | The inhibitory effects of tumor cell-derived ExoPD-L1 on T cells *in vitro*.

Cell source of ExoPD-L1	Target cell	Effect	Indicator	References
Human MDA-MB-231 breast cancer cells	PBMCs	Suppression of T cell activation	IL-2 ↓	Yang et al., 2018
Human RKO colon cancer cells	PBMCs		IL-2 ↓	Yang et al., 2018
Human HCC827 NSCLC cells	PBMCs		IL-2 ↓	Yang et al., 2018
Human PC3 prostate cancer cells	Jurkat T cells		IL-2 ↓	Poggio et al., 2019
Human NSCLC primary cells	$CD8^+$ and Jurkat T cells		IL-2 ↓, IFN-γ ↓	Kim et al., 2019
Human WM9 melanoma cells	$CD8^+$ T cells		IL-2 ↓, IFN-γ ↓, TNF-α ↓	Chen G. et al., 2018
Human SK-MEL-2 melanoma cells	PBMCs		IFN-γ ↓, PD-1 ↓	Cordonnier et al., 2020
Human MKN74 gastric cancer cells	PBMCs		CD69 ↓, PD-1 ↓	Fan et al., 2019
Human glioblastoma primary cells and murine CT2A cells	$CD8^+$ and $CD4^+$ T cells		CD69 ↓, CD25 ↓, PD-1 ↓	Ricklefs et al., 2018
Human glioblastoma primary cells and murine CT2A cells	$CD8^+$ and $CD4^+$ T cells	Inhibition of T cell proliferation	CFSE ↓	Ricklefs et al., 2018
Human WM9 melanoma and murine B16-F10 cells	$CD8^+$ T cells		CFSE ↓, Ki67 ↓	Chen G. et al., 2018
Human NSCLC primary cells and H1264 cells	$CD8^+$ T cells		CFSE ↓, Ki67 ↓	Chen G. et al., 2018
Human SK-MEL-2 melanoma cells	PBMCs		Ki67 ↓	Cordonnier et al., 2020
Human H1264 NSCLC cells	$CD8^+$ T cells	Suppression of T cell Cytotoxicity	GzmB ↓	Chen G. et al., 2018
Human MDA-MB-231 breast cancer cells	PBMCs		Tumor-cell killing ability ↓	Yang et al., 2018
Human WM9 melanoma and murine B16-F10 cells	$CD8^+$ T cells		Tumor-cell killing ability ↓, GzmB↓	Chen G. et al., 2018
Human NSCLC cells	$CD8^+$ T cells	Inhibition of T cell survival	Apoptosis ↑	Kim et al., 2019
Human HNSCC primary cells	$CD8^+$ T cells		Apoptosis ↑	Theodoraki et al., 2018a

↑, *increase;* ↓, *decrease.*

Furthermore, the production of IFN-γ, IL-2, and TNF-α by $CD8^+$ T cells was decreased in the presence of ExoPD-L1 derived from melanoma, breast cancer, NSCLC, and prostate cancer (Chen G. et al., 2018; Yang et al., 2018; Kim et al., 2019; Poggio et al., 2019; Cordonnier et al., 2020). In addition, ExoPD-L1 shuts down the expression of activation markers on $CD4^+$ and $CD8^+$ T cells, including CD69, CD25, and PD-1 (Ricklefs et al., 2018; Fan et al., 2019; Cordonnier et al., 2020). Pretreatment with anti-PD-1 antibodies or PD-L1 knockdown constructs significantly diminished the suppression of T cell activation mediated by ExoPD-L1 (Chen G. et al., 2018; Ricklefs et al., 2018; Theodoraki et al., 2018b; Yang et al., 2018; Fan et al., 2019; Kim et al., 2019). Importantly, exosomes from plasma of patients with NSCLC and headneck squamous cell carcinoma (HNSCC) display modulatory effects on T cells (Theodoraki et al., 2018a; Kim et al., 2019). Remarkably, ExoPD-L1 from tumors is not only as efficient as cellular PD-L1, but also stronger than soluble PD-L1 in suppressing T cell activation because of the high stability of ExoPD-L1 and MHC-I expression (Fan et al., 2019; Cordonnier et al., 2020).

Recent studies showed that exosomes derived from human melanoma and NSCLC significantly reduced the Ki-67 expression of T cells and $CD8^+$ T cells, which is restored in the presence anti-PD-1 blocking antibodies (Chen G. et al., 2018; Cordonnier et al., 2020). Additionally, exosomes from human glioblastoma culture block both $CD8^+$ and $CD4^+$ T cell proliferation (Ricklefs et al., 2018). Notably, ExoPD-L1 from NSCLC and HNSCC cells induced apoptosis in $CD8^+$ T cells and the amount of $CD8^+$ T cells decreased in a dose-dependent manner (Theodoraki et al., 2018a; Kim et al., 2019). Overall, tumor-derived ExoPD-L1 is able to suppress the proliferation and survival of T cells, which contributes to T cell dysfunction (Li et al., 2019b; Xia et al., 2019).

The cytotoxicity of functional effector T cells is responsible for killing cancer cells and eradicating tumors. Exosomes secreted from melanoma and NSCLC cells that express endogenous PD-L1 inhibit the expression of granzyme B (GzmB) from human peripheral and mouse splenic $CD8^+$ T cells activated by TCR stimulation (Chen G. et al., 2018). Pretreatment with exosomes from tumors, such as melanoma and breast cancer, significantly inhibited the cytotoxic T cell-mediated tumor killing, which could be counteracted by anti-PD-L1 antibodies (Chen G. et al., 2018; Yang et al., 2018; Kim et al., 2019). Thus, tumor-derived ExoPD-L1 is capable of inhibiting T cell function by modulating the proliferative capacity and effector function of T cells (**Table 2**).

Together, ExoPD-L1 secreted from tumor cells is able to mediate immunosuppression *in vitro*. The expression of inhibitory receptors is also a characteristic of T cell dysfunction, except for low proliferation and loss of effector function (Xia et al., 2019). Therefore, in addition to PD-1, the impact of ExoPD-L1 on other T cell inhibitory receptors should be investigated, including T cell immunoglobulin domain and mucin domain-3 (TIM-3), cytotoxic T lymphocyte antigen 4 (CTLA-4), lymphocyte activation gene 3 (LAG-3), T cell immunoreceptor with Ig and ITIM domains (TIGIT) (Anderson et al., 2016; Andrews et al., 2019; Wolf et al., 2019).

The Immunoinhibitory Effects of ExoPD-L1 in Mouse Tumor Models

Insight into the immunosuppressive effects of ExoPD-L1 *in vivo* is beneficial to understanding the mechanisms of tumor immune escape. Recent studies have shown that ExoPD-L1 released by tumor cells induces immunosuppressive activities at tumor sites in a paracrine-dependent manner (Chen G. et al., 2018; Yang et al., 2018; Kim et al., 2019). Additionally, exosomes can enter blood and circulate systemically, which may help ExoPD-L1 to function at distant sites in a manner similar to endocrine molecules (**Figure 1**; Seo et al., 2018; Wortzel et al., 2019).

Decreased Frequencies and Activities of TILs

A significant reduction in the number of $CD8^+$ TILs was observed in melanoma tumors of C57BL/6 mice after 24 days of an injection with PD-L1-containing exosomes (Chen G. et al., 2018). Moreover, the frequency of $Ki67^+PD\text{-}1^+CD8^+$ T cells in the tumor microenvironment decreased significantly, which was reversed by anti-PD-L1 antibodies (Chen G. et al., 2018). There was also a significant loss of $CD8^+$ TILs in the tumor area of NSCLC after an intravenous injection of PD-L1-containing exosomes in mice after 14 days (Kim et al., 2019). Furthermore, PD-L1-containing exosomes reduce cytotoxic T cell activity, as assessed by GzmB expression, in the tumor microenvironment (Yang et al., 2018). Collectively, these results suggest that ExoPD-L1 plays a key role in induction of immune escape in tumor microenvironment (**Figure 1**).

Suppression of T Cell Function in the Draining Lymph Node

It is clear that exosomes are important communicators between tumors and immune cells and they exert modulatory effects on the systemic immune response (Hood et al., 2011; Groot Kormelink et al., 2018; Czystowska-Kuzmicz et al., 2019; Sheehan and D'Souza-Schorey, 2019). Recent studies reported that PD-L1-deletion significantly increases the number, proliferation (Ki67), and effector function (GzmB) of $CD8^+$ T cells, while decreasing the exhaustion (TIM-3) of $CD8^+$ T cells in the draining lymph node of mice injected with TRAMP-C2 prostate cancer cells (Poggio et al., 2019). Meanwhile, similar to PD-L1-deletion, Rab27a-deletion, which inhibits the biogenesis of exosomes, has a promotional effect on the frequency and activity of $CD8^+$ T cells (Poggio et al., 2019). More importantly, the administration of exogenous exosomes derived from wild-type (Newton et al., 2016) prostate cancer cells leads to immunosuppression in the draining lymph node, as evidenced by a reduced number and effector function, and increased exhaustion of $CD8^+$ T cells of mice injected with Rab27a-deleted prostate cancer cells (Poggio et al., 2019). Moreover, the administration of WT melanoma cell-derived exosomes significantly reduced the proportion of $Ki67^+PD\text{-}1^+CD8^+$ T cells in the draining lymph node of mice injected with the PD-L1-deleted melanoma cells, which was counteracted by anti-PD-L1 antibodies (Chen G. et al., 2018). Thus, these findings indicate that tumor-derived ExoPD-L1 is capable of patrolling the draining lymph node and regulating T cell activation (**Figure 1**).

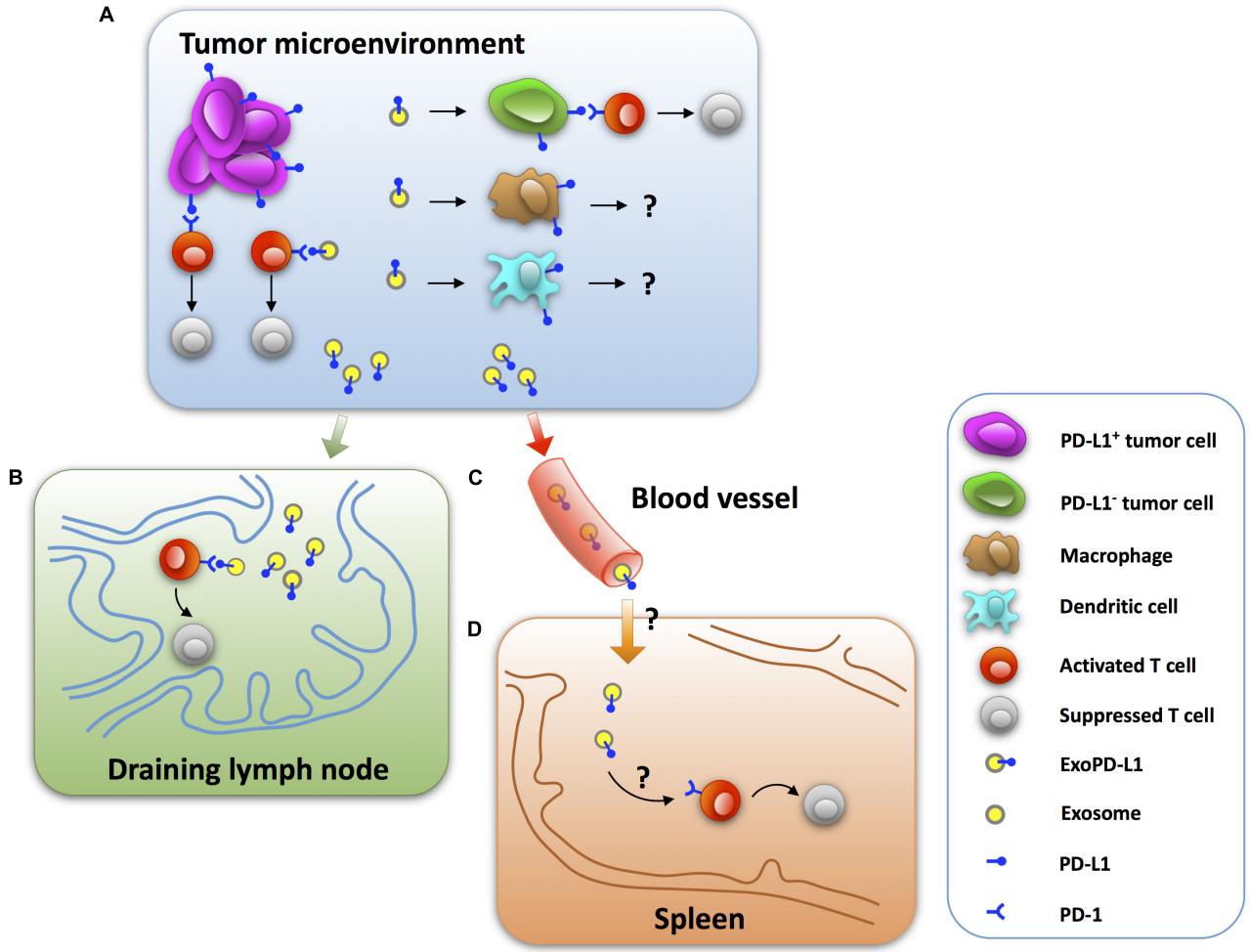

FIGURE 1 | The mechanisms by which tumor ExoPD-L1 induce immunosuppression. **(A)** ExoPD-L1 originating from tumor cells induces T cell dysfunction in the tumor microenvironment by directly ligating to PD-1 on T cells as well as stationing on PD-L1-negative tumor cells, while its immunoregulatory effect remains intact. ExoPD-L1 also migrates to macrophages and dendritic cells, but the potential effects remain unknown. **(B)** ExoPD-L1 is able to leave tumor foci and enter the draining lymph node to mediate T cell suppression. **(C)** ExoPD-L1 can enter and circulate in the blood. **(D)** ExoPD-L1 inhibits the immune response in spleen and decreases spleen size.

Reduction of Spleen Size and T Cell Proliferation in Spleen

In addition to inducing immune suppression in the draining lymph node, ExoPD-L1 can inhibit the immune response in the spleen. Recent studies reported that PD-L1-deletion significantly increases the spleen size of mice injected with TRAMP-C2 prostate cancer cells (Poggio et al., 2019). Meanwhile, Rab27a-deletion also increases the spleen size of mice injected with prostate cancer cells. Notably, intravenous injection of exogenous exosomes derived from WT prostate cancer cells resulted in decreased spleen size of mice injected with Rab27a-deleted prostate cancer cells to nearly 50% (Poggio et al., 2019). In addition, administration of WT melanoma B16-F10 cell-derived exosomes significantly reduced the proportion of $Ki67^{+}PD\text{-}1^{+}CD8^{+}$ T cells in murine spleen injected with the PD-L1-deleted melanoma cells. This effect could be counteracted by anti-PD-L1 antibody treatment (Chen G. et al., 2018). Thus, ExoPD-L1 secreted by tumor cells can enter into the circulation to inhibit the antitumor immunity systemically (**Figure 1**).

Promotion of Tumor Growth Across Different Tumor Types in an Immune-Dependent Manner

It has been shown that ExoPD-L1 derived from tumor cells promotes tumor growth *in vivo*, including cancers of the breast and prostate, colorectal cancer, melanoma, and NSCLC (Chen G. et al., 2018; Yang et al., 2018; Kim et al., 2019; Poggio et al., 2019). PD-L1 knockout leads to substantial tumor regression or even failure to grow, however, this was reversed by local or intravenous injection of exosomes derived from WT tumor cells (Chen G. et al., 2018; Yang et al., 2018; Poggio et al., 2019). Different from PD-L1 deletion, which downregulates the transcripts of PD-L1 mRNA, genetic deletion of Rab27a or nSMase2 reduces the production of ExoPD-L1 via inhibition of exosome biogenesis. *In vitro* studies showed that blockade of Rab27a or nSMase2

does not change cell proliferation in prostate cancer, colorectal cancer, or breast cancer, indicating that blockade of exosome biogenesis itself does not cause the suppression of tumor growth (Yang et al., 2018; Poggio et al., 2019). However, deletion of either Rab27a or nSMase2 significantly inhibits tumor growth in mice, including that of breast, prostate, and colorectal cancers (Yang et al., 2018; Poggio et al., 2019). These findings reveal that the inhibition of exosome biogenesis or PD-L1 deletion results in a similar suppressive effect on tumor growth. In addition, prostate and breast cancer cells experiencing a blockade of Rab27a, nSMase2 or PD-L1 failed to grow in WT mice, but grow rapidly in immunodeficient mice (Yang et al., 2018; Poggio et al., 2019). Collectively, ExoPD-L1 promotes tumor growth that is dependent on the inhibition of the antitumor immune response.

ExoPD-L1 Contributes to the Immune Suppression in Tumor Patients

It has been observed that circulating ExoPD-L1 level is positively associated with its ability to suppress the activation of $CD8^+$ T cells in HNSCC patients (Theodoraki et al., 2018b). Additionally, in metastatic gastric tumor patients, the levels of plasma ExoPD-L1 are negatively associated with $CD4^+$ and $CD8^+$ T cell counts as well as the cytotoxicity of T cells (Fan et al., 2019). These findings indicate that ExoPD-L1 contributes to immunosuppression by inducing T-cell dysfunction, suggesting that ExoPD-L1 might promote the disease progression of tumor patients (Theodoraki et al., 2018b; Fan et al., 2019).

Collectively, tumor ExoPD-L1 plays a pivotal part in mediating local and systemic immunosuppression in mouse models and tumor patients.

POTENTIAL CLINICAL IMPLICATION OF CIRCULATING ExoPD-L1 AS A BIOMARKER FOR TUMOR DIAGNOSIS, DISEASE PROGRESSION, AND IMMUNOTHERAPY RESPONSE

Tumor immunotherapy requires biomarkers for predicting disease progression, prognosis, clinical response, and the selection of suitable patients (Buder-Bakhaya and Hassel, 2018; Zhang et al., 2019). Tumor cell PD-L1 has been considered a predictor for response to immunotherapy in the clinic (Patel and Kurzrock, 2015; Aguiar et al., 2017; Lin et al., 2018; Li et al., 2019c). However, there are pitfalls of using cellular PD-L1 such as traumatic biopsy, missing small tumors, heterogeneity of PD-L1 expression within tumors, unavailability of dynamic observation, and limited sensitivity (Kaunitz et al., 2017; Bassanelli et al., 2018; Teixido et al., 2018; Davis and Patel, 2019; Stovgaard et al., 2019; Xu G. et al., 2019). Recent studies indicate that circulating ExoPD-L1 is emerging as a non-invasive and readily available biomarker, and is more easily detectable and reliable than both tissue and soluble PD-L1 in plasma (Liu et al., 2018b; Cordonnier et al., 2020; Huang et al., 2020; Pang et al., 2020).

ExoPD-L1 as a Biomarker for Diagnosis and Disease Progression

Tumor-derived exosomes can be enriched from small volumes of patient plasma and are considered to be a potential biomarker based on liquid biopsy (Crow et al., 2019; Johnsen et al., 2019; Xie C. et al., 2019; Yekula et al., 2019, 2020; Brennan et al., 2020). The number and the protein content of exosomes in the blood of breast cancer patients are higher compared with those of healthy subjects and the increased exosome numbers positively correlates with tumor growth (Hesari et al., 2018). However, in melanoma, the level of ExoPD-L1 in the blood, rather than the number and total protein content of exosomes, is elevated in metastatic melanoma patients compared with healthy subjects (Chen G. et al., 2018). Furthermore, patients with NSCLC and adenocarcinoma also exhibit higher levels of circulating ExoPD-L1 compared with healthy controls (Liu et al., 2018b; Li et al., 2019a; Huang et al., 2020; Pang et al., 2020). Therefore, circulating ExoPD-L1 may be a potential diagnostic marker. In addition, high levels of circulating ExoPD-L1 were associated with metastatic melanoma, advanced HNSCC, and poor prognosis in pancreatic cancer, further indicating that circulating ExoPD-L1 may be a useful biomarker for tumor progression (Theodoraki et al., 2018a; Lux et al., 2019; Huang et al., 2020).

Soluble PD-L1 in plasma is also considered as a potential diagnostic and predictive biomarker for tumor recurrence and prognosis (Chatterjee et al., 2017; Okuma et al., 2017; Zhou et al., 2017; Chang et al., 2019; Shigemori et al., 2019; Liu S. et al., 2020). However, the levels of soluble PD-L1 were not different between NSCLC patients and healthy donors (Li et al., 2019a). Moreover, soluble PD-L1 did not correlate with disease progression in patients with metastatic gastric cancer, HNSCC, or NSCLC (Liu et al., 2018b; Fan et al., 2019; Li et al., 2019a; Pang et al., 2020). On the contrary, circulating ExoPD-L1 in plasma is an independent biomarker to predict poor prognosis in patients with metastatic gastric cancer (Fan et al., 2019). Furthermore, the levels of ExoPD-L1 correlated with the disease progression of patients with HNSCC and NSCLC, including tumor size, lymph node status, metastasis, and clinical stage (Theodoraki et al., 2018a,b; Li et al., 2019a).

Exosomal PD-L1 DNA is present in exosomes isolated from the plasma of glioblastoma patients (Ricklefs et al., 2018). The amount of ExoPD-L1 DNA from glioblastoma patients is associated with tumor volume, although the function of PD-L1 DNA remains unknown (Ricklefs et al., 2018; Lazaro-Ibanez et al., 2019). Together, liquid biopsy analysis of ExoPD-L1 protein and DNA in blood may provide biomarkers for tumor diagnosis and disease progression.

ExoPD-L1 as a Biomarker for Efficacy of Anti-PD-1/PD-L1 Therapy

It is important to provide individualized precise treatment and to predict tumor response to immunotherapy (Madore et al., 2015; Kaunitz et al., 2017; Sui et al., 2018; Liu and Wu, 2019). To fulfill the need for real-time monitoring, the analysis of liquid biopsy-based circulating biomarkers is preferred (Nishino et al., 2013;

Ando et al., 2019; Gregg et al., 2019; Kloten et al., 2019; Tang et al., 2020). Recent studies demonstrated that melanoma patients who were less responsive to anti-PD-1 blockade had a significantly higher level of circulating ExoPD-L1 prior to treatment as compared with responders (Chen G. et al., 2018). In addition, the increasing magnitude of circulating ExoPD-L1 in melanoma patients during early treatment periods can distinguish clinical responders from non-responders (Chen G. et al., 2018). Moreover, a prospective study on melanoma indicated that monitoring the levels of circulating ExoPD-L1 may be helpful to predict therapeutic efficacy and clinical outcome (Cordonnier et al., 2020). Additionally, compared with patients exhibiting recurrence, patients who did not relapse had higher levels of tumor-enriched CD3- ExoPD-L1 prior to therapy, which significantly decreased after five weeks of therapy (Theodoraki et al., 2018a, 2019). In contrast, tumor-enriched ExoPD-L1 levels increased at week five of therapy, whereas the $CD3^+$ ExoPD-L1 levels decreased in patients with recurrence (Theodoraki et al., 2019). Thus, studying on the role of ExoPD-L1 derived from immune cells and tumor cells as biomarkers for tumor patients will be necessary. Interestingly, ExoPD-L1 mRNA can also be sequestered in exosomes of patient plasma in melanoma and NSCLC, and associated with response to anti-PD-1 inhibitors (Del Re et al., 2018; Zhao Z. et al., 2019).

Collectively, ExoPD-L1, including PD-L1 protein, DNA and mRNA, has the potential to become reliable biomarkers for immunotherapy. This is an effective complement to tumor PD-L1 and soluble PD-L1 to identify patients who may benefit from immunotherapy and to dynamically monitor therapeutic response (Chen G. et al., 2018; Theodoraki et al., 2019; Cordonnier et al., 2020; Daassi et al., 2020).

The regulation of PD-L1 expression is highly intricate and has been extensively addressed at transcriptional, posttranscriptional, translational, and posttranslational levels (Sun et al., 2018; Zerdes et al., 2018; Cha et al., 2019; Xu Y. et al., 2019; Fu et al., 2020; Han et al., 2020; Ju et al., 2020). Notably, soluble PD-L1 may be generated from ectodomain shedding mediated by either matrix metalloproteinases (MMPs) or a disintegrin and metalloproteases (ADAMs). Additionally, soluble PD-L1 may be produced by alternative splice variants omitting transmembrane domain (Dezutter-Dambuyant et al., 2016; Hira-Miyazawa et al., 2018; Aguirre et al., 2020; Orme et al., 2020; Romero et al., 2020). Although soluble PD-L1 is found in human serum and is regarded as a liquid biopsy predictor, whether soluble PD-L1 can deliver a regulatory signal through PD-1 remains elusive (Gu et al., 2018; Takeuchi et al., 2018; Abu Hejleh et al., 2019; Asanuma et al., 2020). Some studies reported that soluble PD-L1 inhibits T cell activation, while others suggested that soluble PD-L1 is likely to increase immune response by proteolytic reducing the amount of membrane-bound PD-L1 on both cell surface and exosome or by competing with membrane-bound PD-L1 for PD-1 binding (Dezutter-Dambuyant et al., 2016; Hira-Miyazawa et al., 2018; Aguirre et al., 2020; Romero et al., 2020). Furthermore, it is demonstrated that soluble PD-L1 produced by *CD274-L2A* splice variant lacks suppressive activity and functions as a PD-1 antagonist, suggesting the possibility that soluble PD-L1 might limit the immunoinhibitory effects of ExoPD-L1 (Wan et al., 2006; Steidl et al., 2011; Ng et al., 2019).

Additionally, PD-L2 is also expressed on tumor cells and involved in antitumor immune suppression (Latchman et al., 2001; Taube et al., 2014; Yearley et al., 2017; Larsen et al., 2019; Liao et al., 2019; Tanegashima et al., 2019; Nakayama et al., 2020). Moreover, PD-L2 not only possesses higher affinity for PD-1 than PD-L1 does but also may be highly coexpressed with PD-L1 in tumor cells and tissues (Youngnak et al., 2003; Cheng et al., 2013; Morales-Betanzos et al., 2017; Tang and Kim, 2019; Furuse et al., 2020; Wolkow et al., 2020). It is worth mentioning that proteolytic degradation or alternative splice variants also produce soluble PD-L2, which may be a complementary biomarker (He et al., 2004; Dai et al., 2014; Fukasawa et al., 2017; Costantini et al., 2018; Buderath et al., 2019; Wang Q. et al., 2019). Recently, a pilot study found PD-L2-expressing EVs in a murine sepsis model (Kawamoto et al., 2019). Moreover, sepsis patients displayed higher PD-L2 expression on EVs compared with healthy subjects (Kawamoto et al., 2019). Additionally, reduced exosomal PD-L2 was observed in IL-10-treated murine dendritic cells (Ruffner et al., 2009). However, it is unclear whether tumor cells are able to release exosomal PD-L2, and the function and regulation of exosomal PD-L2 in antitumor immunity are unexplored and worthy of further investigations (Solinas et al., 2020).

POTENTIAL METHODS FOR THE DETECTION OF CIRCULATING ExoPD-L1 IN CLINICAL SAMPLES

A quick, simple, and sensitive assay is a prerequisite for a point-of-care test for ExoPD-L1 as a clinical biomarker. However, due to the small size and high heterogeneity of exosomes, the methods used most widely to detect ExoPD-L1 from tumor patients required ultracentrifugation and ELISA (**Table 3**). Therefore, low efficiency and sensitivity are two bottlenecks to the classic detection of ExoPD-L1 in the clinic (Liu et al., 2017; Yang et al., 2017). Efforts have been made to improve the sensitivity of the ELISA-based methods for detecting low levels of ExoPD-L1 (Liu et al., 2018a,b; Huang et al., 2020).

Ultracentrifugation-Based Methods

Recently, a homogeneous, low-volume, efficient, and sensitive ExoPD-L1 (HOLMES-ExoPD-L1) quantitation method has been developed (Huang et al., 2020). The HOLMES-ExoPD-L1 method combining PD-L1 aptamer with separation-free thermophoresis exhibits higher sensitivity and is more rapid than the classic ELISA-based methods (Lee et al., 2019; Huang et al., 2020). To completely surmount the disadvantages of ELISA, a nanoplasmonic exosome (nPLEX) assay has been established, which involves modified surface plasmon resonance (Enderle et al., 2015) with a compact SPR biosensor (Liu et al., 2018b). Notably, the nPLEX assay is able to detect ExoPD-L1 in 50 μl serum samples in real-time, which is undetectable by ELISA (**Table 3**; Liu et al., 2018b).

TABLE 3 | Comparison of methods for detecting ExoPD-L1 in clinical samples.

Method	Instrument	Sample volume (μl)	Exosome isolation	Heterogeneous reaction system	Detection limitation	References
ELISA	Microplate reader	1000	Ultracentrifugation	Yes	200 pg/ml	Chen G. et al., 2018; Liu et al., 2018b; Theodoraki et al., 2018a,b, 2019; Fan et al., 2019; Li et al., 2019a; Lux et al., 2019; Cordonnier et al., 2020; Huang et al., 2020
HOLMES-Exo-PD-L1	Flow cytometer	1000	Ultracentrifugation	No	17.6 pg/ml	Huang et al., 2020
nPLEX assay	Compact SPR biosensor	50	Ultracentrifugation	No	Not given	Liu et al., 2018b
SERS immunoassay	Raman spectrometer	4	Fe_3O_4@TiO_2 magnetic nanobeads	No	1 PD-L1$^+$ exosome/μl	Pang et al., 2020

ELISA, enzyme linked immunosorbent assay; HOLMES-ExoPD-L1, homogeneous, low-volume, efficient, and sensitive ExoPD-L1; nPLEX, nanoplasmonic exosome; SPR, surface plasmon resonance; SERS, surface-enhanced Raman scattering.

Ultracentrifugation-Free Method

The methods described above are ultracentrifugation-based, time-consuming and yield low recovery (Momen-Heravi et al., 2013; Lobb et al., 2015). More recently, a quick and precise method for detecting ExoPD-L1 directly from clinical samples has been set up by coupling Fe_3O_4@TiO_2 isolation with a surface-enhanced Raman scattering (SERS) immunoassay (Pang et al., 2020). Although it takes less than 40 min to complete the entire procedure, the separation efficiency for exosomes is 96.5% and the detection limit is one PD-L1$^+$ exosome per microliter (Pang et al., 2020). Moreover, the number of ExoPD-L1 molecules in four μl of a patient's serum is precisely quantified using this method (Pang et al., 2020). Overall, along with the advancement of novel technologies, there should have more methods in development. It should be noted that it is necessary to validate these methods in large cohorts before routinely using ExoPD-L1 as a clinical biomarker (**Table 3**).

POTENTIAL STRATEGIES TARGETING ExoPD-L1 FOR ANTITUMOR THERAPY

Antibody blockade of PD-L1 is able to trigger an antitumor immune response, bringing about a persistent remission in a fraction of tumor patients. Recent studies have shown that the removal of ExoPD-L1 blocks tumor growth, even in mouse models which are resistant to anti-PD-L1 antibody (Chen G. et al., 2018; Yang et al., 2018; Kim et al., 2019; Poggio et al., 2019; Xie F. et al., 2019). This indicates that targeting exosome biogenesis inhibition and PD-L1 deletion represents an unexplored strategy for antitumor therapy.

Blockade of Exosome Biogenesis Provides an Efficient Way to Overcome Resistance to Anti-PD-L1 Antibody

Immune checkpoint inhibitors are effective against various cancers, including melanoma, NSCLC, and renal cancer. However, the overall response rate in patients treated with anti-PD-1/PD-L1 antibodies is low (Page et al., 2014). In some tumor types, such as prostate cancer, the number of responders is very limited (Goswami et al., 2016; Sharma et al., 2017). However, genetic deletion of PD-L1 in TRAMP-C2 prostate cancer cells, which causes a reduction of both cell-surface PD-L1 and ExoPD-L1, strikingly prevents anti-PD-L1 antibody resistant tumor to grow in mice (Foster et al., 1997; Poggio et al., 2019). More importantly, the prostate cancer cells were also unable to grow in mice when Rab27a or aSNase2 was deleted by the CRISPR/Cas9 technique, leading to a blockade of exosome biogenesis (Poggio et al., 2019). Thus, targeting the process of exosome biogenesis may yield new approaches to overcoming tumor resistance to anti-PD-L1 antibodies.

The biogenesis of ExoPD-L1 is a complicated process involving multiple molecules that impact the production of ExoPD-L1 in different ways (Chen G. et al., 2018; Monypenny et al., 2018; Yang et al., 2018; Poggio et al., 2019). The endosomal sorting complex required for transport complex (ESCRT) is a key mediator of MVB biogenesis (Henne et al., 2011; Matusek et al., 2014; Olmos and Carlton, 2016; Schoneberg et al., 2017; Furthauer, 2018). Hepatocyte growth factor-regulated tyrosine kinase substrate (HRS) is a subunit of ESCRT that mediates the recognition and sorting of exosomal cargos (Schmidt and Teis, 2012). Genetic deletion of HRS leads to a decrease in ExoPD-L1 levels but an increase in cellular PD-L1 levels. The effect of HRS blockade on tumor growth remains unknown (Chen G. et al., 2018). Apoptosis-linked gene 2-interacting protein X (ALIX), an ESCRT accessory protein, is a critical regulator potentially involved in the redistribution of PD-L1 between exosomes and cell-surface membranes (Baietti et al., 2012; Hurley and Odorizzi, 2012; Bissig and Gruenberg, 2014; Christ et al., 2017; Monypenny et al., 2018; Skowyra et al., 2018; Szymanska et al., 2018). Similar to nSMase2 or Rab27a deletion, ALIX knockdown also leads to a significant decrease in ExoPD-L1 production in breast cancer (Monypenny et al., 2018). However, in contrast to Rab27a or nSMase2 deletion, ALIX knockdown promotes, but does not suppress the tumor growth (Monypenny et al., 2018). The differential effects of these genetic deletions on cell-surface PD-L1 expression contribute to their different effects on tumor growth. Deletion of nSMase2 leads to a reduction in the levels of both cellular PD-L1 and ExoPD-L1 protein by downregulating the transcription of the PD-L1 gene (Poggio et al., 2019). Meanwhile, Rab27a deletion does not change cell-surface PD-L1 levels but causes a greater inhibition in exosome production compared with nSMase2 deletion (Poggio et al., 2019). Therefore,

deletion of either nSMase2 or Rab27a completely inhibits tumor growth (Yang et al., 2018; Poggio et al., 2019). In contrast, ALIX knockdown leads to a significant increase in cell-surface PD-L1 on breast cancer cells, and thereby increases the aggressiveness of tumors (Monypenny et al., 2018). Collectively, the distribution of PD-L1 between exosomes and cell surfaces is pivotal for the efficacy of immunotherapy. Both ExoPD-L1 and cell-surface PD-L1 should be the focus of future therapeutic strategies (**Figure 2**).

Combination of Exosome Biogenesis Inhibition With Anti-PD-L1 Antibody Enhances Immunotherapy Efficacy

It is a concern that the antitumor effect of removing ExoPD-L1 is not limited to the anti-PD-L1 resistant model of prostate cancer. Both Rab27a depletion and an nSMase2 inhibitor (GW4869) significantly inhibit the growth of breast cancer derived from 4T1 cells in mice, which is a drug-resistant model for breast cancer (Pulaski and Ostrand-Rosenberg, 2001; Lasso et al., 2019). These findings indicate that the blockade of exosome secretion is an effective tool to disrupt the growth of various tumors (Grasselly et al., 2018; Yang et al., 2018). Importantly, Rab27a knockdown and nSMase2 inhibition are more potent suppressors of breast cancer growth compared with anti-PD-L1 antibody treatment (Yang et al., 2018). More importantly, blocking either Rab27a or sMSase2 markedly enhances the therapeutic effectiveness of anti-PD-L1 antibody for the inhibition of breast cancer growth (Yang et al., 2018). Thus, combining exosome biogenesis inhibition with anti-PD-L1 antibody may be more potent for tumor suppression.

Rab27a knockout suppressed colorectal cancer growth and extended survival in MC38 mice, which is a colorectal cancer model exhibiting a partial response to anti-PD-L1 therapy (Deng et al., 2014; Poggio et al., 2019). In contrast to the resistant TRAMP-C2 prostate cancer model, either Rab27a knockout or anti-PD-L1 antibody blockade exhibited less of an effect

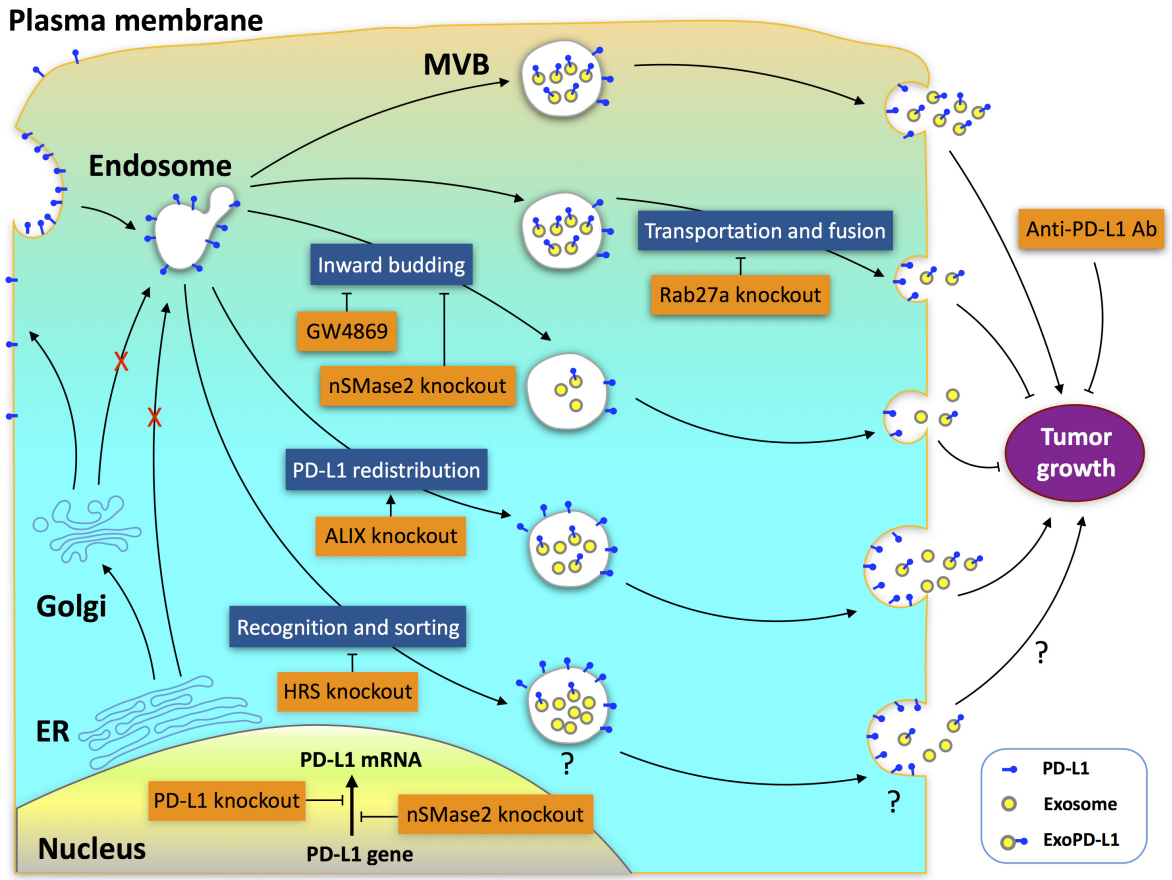

FIGURE 2 | Potential targets for antitumor therapy in ExoPD-L1 biogenesis pathways. Multiple molecules, including Rab27a, nSMase2, ALIX, and HRS, participate in the complex processes of ExoPD-L1 biogenesis, which originates from the cell surface rather than from the ER or Golgi apparatus. Deletion of Rab27a decreases ExoPD-L1, but does not alter cell-surface PD-L1 levels. Deletion of nSMase2 reduces the levels of both cellular PD-L1 and ExoPD-L1 protein. Rab27a deletion causes a greater inhibition in exosome production compared with nSMase2 deletion, while nSMase2 deletion leads to a greater inhibition of ExoPD-L1 production compared with Rab27a deletion. GW4869, an inhibitor of nSMase2, inhibits ExoPD-L1 generation, but does not increase cellular PD-L1 levels. Knockdown of ALIX, which redistributes PD-L1 between the cell-surface and exosomes, results in a reduction of ExoPD-L1 production but an increase in cell-surface PD-L1. Blockade of Rab27a or nSMase2 results in suppression, whereas ALIX knockdown promotes tumor growth. Knockdown of HRS, an ESCRT-0 subunit, confers a decrease in ExoPD-L1 levels but an increase in cellular PD-L1 levels. The effects of HRS knockdown on the cell-surface PD-L1 levels and tumor growth remain unknown.

on the MC38 colorectal cancer growth compared with PD-L1 genetic deletion (Poggio et al., 2019). However, the combination of exosome deletion with anti-PD-L1 antibody lengthened the lifespan of mice burdened with colorectal cancer to an extent similar to that of PD-L1 deletion (Poggio et al., 2019). Hence, ExoPD-L1 appears to impose an additional, but not redundant impact compared with anti-PD-L1 antibody on the suppression of tumor growth (Chen G. et al., 2018; Poggio et al., 2019). In addition, combined genetic deletion of Rab27a and PD-L1 showed a similar inhibition of tumor growth as compared with PD-L1 deletion, demonstrating that the inhibitory effect of exosomes on colorectal cancer growth occurs mainly through the deletion of ExoPD-L1 (Poggio et al., 2019). Thus, the combination of inhibitors targeting exosome secretion with anti-PD-L1 blockade targeting cell-surface PD-L1 may be a promising strategy to effectively suppress tumor growth in the clinic (Yang et al., 2018; Poggio et al., 2019).

ExoPD-L1-Deficient Tumor Cells Induce Abscopal Effect and Antitumor Immune Memory

The abscopal effect refers to that treatment of a local tumor leads to the regression of distant tumors (Postow et al., 2012; Demaria and Formenti, 2020; Fionda et al., 2020; Mondini et al., 2020). This represents a promising therapeutic strategy for tumors and has drawn increased attention (Liu et al., 2018; Ngwa et al., 2018; Rodriguez-Ruiz et al., 2018; Choi et al., 2020). Interestingly, blocking ExoPD-L1 suppresses the growth of not only the local tumor, but also tumors at a distant site (Poggio et al., 2019). In the TRAMP-C2 mouse prostate cancer model, mutant cancer cells devoid of Rab27a, nSMase2, or PD-L1 expression completely failed to grow (Chen G. et al., 2018; Yang et al., 2018; Poggio et al., 2019). Surprisingly, the growth of WT tumor cells was reduced dramatically when the above mutant cells were injected simultaneously in the opposite sides of mice (Poggio et al., 2019). This indicates that ExoPD-L1-deficient tumor cells induce an abscopal effect on tumor growth (Poggio et al., 2019). On the contrary, WT cells had little or no effect on the growth of the mutant cells (Poggio et al., 2019). Furthermore, the numbers and activities of TILs in WT tumors in mice coinjected with ExoPD-L1-deleted mutant cells were significantly increased in comparison with the mice injected with WT cells alone (Poggio et al., 2019). Thereby, local anti-ExoPD-L1 treatment is able to induce a durable immune response to suppress the growth of tumors at distant sites (**Figure 3**).

Additionally, in the prostate cancer model, the mice injected with mutant cells deleted of PD-L1, Rab27a, or nSMase2 survived more than 90 days, whereas the mice injected with WT cells died soon or had to be euthanized because of tumors greater than

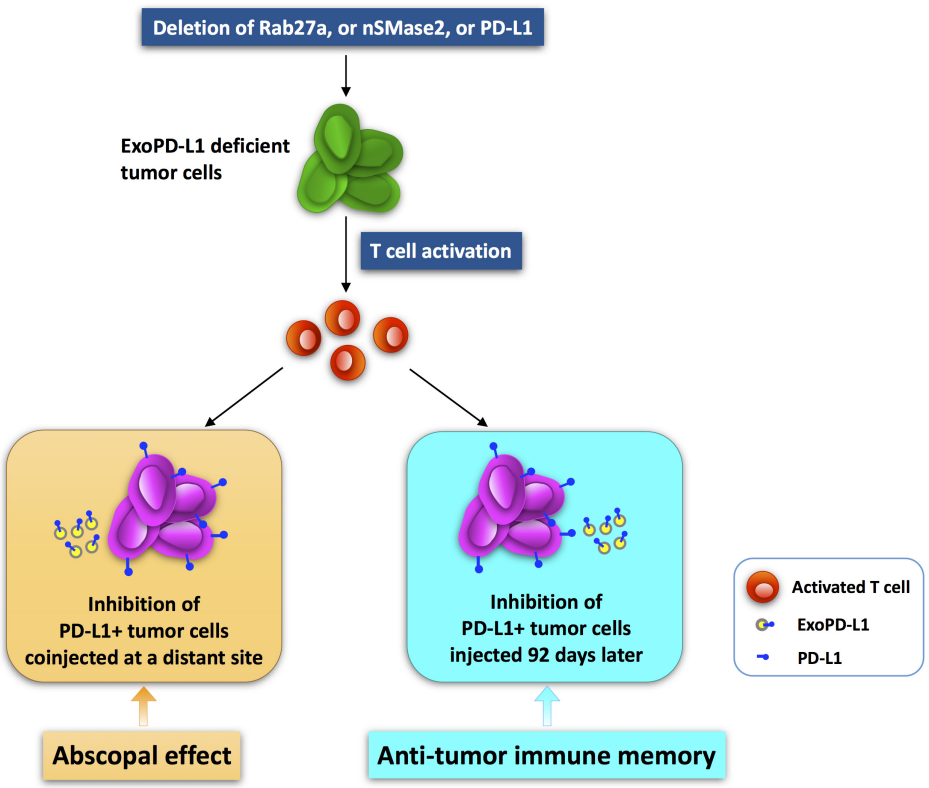

FIGURE 3 | The abscopal effect and antitumor immune memory induced by ExoPD-L1-deficient tumor cells. Tumor cells with ExoPD-L1 deletion are generated by genetic mutation of Rab27a, nSMase2, or PD-L1. The growth of PD-L1-positive tumors at a distant site is inhibited when ExoPD-L1-deleted tumor cells are coinjected simultaneously. In addition, the growth of PD-L1-positive tumors injected secondarily 92 days later is also suppressed.

2 cm in diameter (Poggio et al., 2019). At 92 days after primary injection with mutant cells, surviving mice were reinjected with WT cells on the opposite flank. Interestingly, the WT prostate cancer cells were unable to grow in the mice that were preinjected with mutant cells (Poggio et al., 2019). In contrast, they grew normally in mice that were not preinjected with mutant cells (Poggio et al., 2019). Therefore, local import of tumor cells lacking of ExoPD-L1 induced a strong antitumor memory response against secondarily challenged tumor cells that secrete ExoPD-L1 (Poggio et al., 2019). In summary, the anti-ExoPD-L1 therapy that targets the tumor at one site may be of clinical significance due to the triggering of a systemic and durable immune response against tumors at multiple sites or challenged secondarily (**Figure 3**).

Currently, a dozen of small molecules have been recognized as exosome inhibitors (Luberto et al., 2002; Johnson et al., 2016; Catalano and O'Driscoll, 2020). GW4869 and Nexinhib-20 are inhibitors of nSMase2 and Rab27a, respectively (Luberto et al., 2002; Johnson et al., 2016). Moreover, Yang et al. reported that GW4869 inhibited exosome secretion of MDA-MB-231 human breast tumor cells *in vitro* and 4T1 mouse mammary tumor cells *in vitro* and *in vivo* (Yang et al., 2018). However, neither GW4869 nor Nexinhib-20 are able to inhibit exosome release in other tumor cell lines (Phuyal et al., 2014), although genetic deletion of either nSMase2 or Rab27a leads to tremendous loss of exosome secretion (Poggio et al., 2019). It has been established that exosomes participate in a variety of physiological processes and can be released from a variety of cell types (Colombo et al., 2014; Lo Cicero et al., 2015; van Niel et al., 2018; Catalano and O'Driscoll, 2020). It is likely that exosome inhibitors might interfere with normal cell functions by affecting the exosome release from healthy cells (Kalluri, 2016; Hessvik and Llorente, 2018; van Niel et al., 2018; Catalano and O'Driscoll, 2020; Hassanpour et al., 2020). Thus, it should be noted that exploitation of exosome inhibitors for tumor immunotherapy should be conducted with caution due to the potential adverse effects on healthy tissues (Dinkins et al., 2014). In addition, similar to immune checkpoint inhibitors, the restoration of T cell activation mediated by ExoPD-L1 blockade is non-specific and may result in immune-related adverse events (Cuzzubbo et al., 2017; Wanchoo et al., 2017; Barroso-Sousa et al., 2018; Myers, 2018; Sandigursky and Mor, 2018; Sibaud, 2018; Varricchi et al., 2018; Fan et al., 2020; Gauci et al., 2020; Liu T. et al., 2020; Ueki et al., 2020; Williams et al., 2020). Collectively, exosome inhibitors that selectively target cancer cells need to be developed to maximize the antitumor immune responses and minimize the possible side effects of blocking ExoPD-L1 release (Nagai and Muto, 2018; Weinmann and Pisetsky, 2019).

CONCLUDING REMARKS

Exosomal PD-L1 derived from tumors is able to suppress antitumor immunity locally and systemically through ligation of PD-1 on T cells, which facilitates immune escape and tumor progression. Additionally, circulating ExoPD-L1 is emerging as a liquid biopsy biomarker for diagnosis, prognosis, stratifying eligible patients, and real-time monitoring of clinical response. Furthermore, the therapeutic strategies targeting ExoPD-L1 are potentially promising by inhibiting the biogenesis of PD-L1-expressing exosomes, and inducing the abscopal effect and antitumor memory response.

However, many issues remain to be resolved. First, understanding the mechanism by which cytokines regulate the biogenesis of ExoPD-L1 is needed. It has been reported that IFN-γ enhances ExoPD-L1 secretion by multiple tumors (Chen G. et al., 2018; Mimura et al., 2018; Monypenny et al., 2018; Poggio et al., 2019). Moreover, there is crosstalk between IFN-γ and epidermal growth factor in the regulation of the distribution of ExoPD-L1 and cellular PD-L1 in breast cancer cells (Monypenny et al., 2018). Recent studies have revealed that both cell-surface PD-L1 and ExoPD-L1 play crucial roles in immunosuppression, tumor progression, and response to cancer immunotherapy (Zou et al., 2016; Chen G. et al., 2018; Theodoraki et al., 2018b; Fan et al., 2019; Kim et al., 2019; Xie F. et al., 2019; Cordonnier et al., 2020; Huang et al., 2020; Tang et al., 2020). Nevertheless, the manner in which inflammatory cytokines affect PD-L1 expression on tumor cells and exosomes is still elusive (Akbay et al., 2013; Chen et al., 2015, 2019; Wang X. et al., 2017; Li et al., 2018; Lin et al., 2020). Second, studies regarding the origin of the PD-L1 nucleic acids in exosomes and their function in antitumor immunity are required. PD-L1 mRNA and DNA are found in exosomes derived from tumor cells in addition to PD-L1 protein (Del Re et al., 2018; Lubin et al., 2018; Ricklefs et al., 2018). It has been reported that RNA in cancer-derived exosomes is also relevant to the local and systemic interaction of exosomes with target cells (Skog et al., 2008; Matei et al., 2017; Yang et al., 2020). However, little is known about the role that ExoPD-L1 nucleic acids play, which should be addressed in the future. Third, immune cells and other cells in the tumor microenvironment or outside of the tumor also express PD-L1 and release exosomes. Moreover, the PD-L1 expression on immune cells is differently regulated and has an important impact on anticancer immunity (Kowanetz et al., 2018). However, the dynamics of host cell-derived ExoPD-L1 production and its potential function in immunosuppression remain unclear (Chen S. et al., 2018; Choo et al., 2018; Zhou et al., 2018; Carreras-Planella et al., 2019; Hong et al., 2019; Lan et al., 2019; Wang X. et al., 2019). Recent studies of murine tumor models indicate that PD-L1 expressed on host cells rather than on tumor cells is the primary target for immunotherapy, and determines the efficacy of the PD-1/PD-L1 blockade (Lin et al., 2018; Tang et al., 2018). Thereby, the immunoregulatory impact of ExoPD-L1 produced by host cells, such as T and B cells, macrophages, dendritic cells, epithelial cells, and mesenchymal stem cells, should be addressed. Finally, determining the regulatory role of ExoPD-L1 on various PD-1-expressing immune cells is of significant interest. In addition to T cells, PD-1 is also expressed on natural killer cells, macrophages, and dendritic cells, which are enriched in the tumor microenvironment (Karyampudi et al., 2016; Gordon et al., 2017; Hsu et al., 2018; Mariotti et al., 2019). Hence, the effect mediated by ExoPD-L1 on a group of PD-1-positive immune cells is a highly relevant issue in tumor immunology.

We believe that a better understanding of the regulatory roles of ExoPD-L1 in host resistance to immunotherapies will offer novel therapeutic strategies for cancer patients in the future (Shergold et al., 2019).

AUTHOR CONTRIBUTIONS

KZ and FL were major contributors in searching the literature and writing the manuscript. SG and GL reviewed the manuscript and provided significant revisions. QS gave guidance for figures. All authors read and approved the final manuscript.

FUNDING

This work was supported by grants from the National Natural Science Foundation of China (No. 51872332) and the National Natural Science Foundation of Liaoning Province (No. 20170541040).

REFERENCES

Abu Hejleh, T., Furqan, M., Ballas, Z., and Clamon, G. (2019). The clinical significance of soluble PD-1 and PD-L1 in lung cancer. *Crit. Rev. Oncol. Hematol.* 143, 148–152. doi: 10.1016/j.critrevonc.2019.08.009

Aguiar, P. N. Jr., De Mello, R. A., Hall, P., Tadokoro, H., and Lima Lopes, G. (2017). PD-L1 expression as a predictive biomarker in advanced non-small-cell lung cancer: updated survival data. *Immunotherapy* 9, 499–506. doi: 10.2217/imt-2016-0150

Aguirre, J. E., Beswick, E. J., Grim, C., Uribe, G., Tafoya, M., Chacon Palma, G., et al. (2020). Matrix metalloproteinases cleave membrane-bound PD-L1 on CD90+ (myo-)fibroblasts in Crohn's disease and regulate Th1/Th17 cell responses. *Int. Immunol.* 32, 57–68. doi: 10.1093/intimm/dxz060

Ahn, E., Araki, K., Hashimoto, M., Li, W., Riley, J. L., Cheung, J., et al. (2018). Role of PD-1 during effector CD8 T cell differentiation. *Proc. Natl. Acad. Sci. U.S.A.* 115, 4749–4754. doi: 10.1073/pnas.1718217115

Ai, L., Xu, A., and Xu, J. (2020). Roles of PD-1/PD-L1 Pathway: signaling. Cancer, and Beyond. *Adv. Exp. Med. Biol.* 1248, 33–59. doi: 10.1007/978-981-15-3266-5_3

Akbay, E. A., Koyama, S., Carretero, J., Altabef, A., Tchaicha, J. H., Christensen, C. L., et al. (2013). Activation of the PD-1 pathway contributes to immune escape in EGFR-driven lung tumors. *Cancer Discov.* 3, 1355–1363. doi: 10.1158/2159-8290.CD-13-0310

Alsaab, H. O., Sau, S., Alzhrani, R., Tatiparti, K., Bhise, K., Kashaw, S. K., et al. (2017). PD-1 and PD-L1 checkpoint signaling inhibition for cancer immunotherapy: mechanism, combinations, and clinical outcome. *Front. Pharmacol.* 8:561. doi: 10.3389/fphar.2017.00561

Anastasiadou, E., and Slack, F. J. (2014). Cancer. Malicious exosomes. *Science* 346, 1459–1460. doi: 10.1126/science.aaa4024

Anderson, A. C., Joller, N., and Kuchroo, V. K. (2016). Lag-3, Tim-3, and TIGIT: co-inhibitory receptors with specialized functions in immune regulation. *Immunity* 44, 989–1004. doi: 10.1016/j.immuni.2016.05.001

Ando, K., Hamada, K., Watanabe, M., Ohkuma, R., Shida, M., Onoue, R., et al. (2019). Plasma Levels of Soluble PD-L1 correlate with tumor regression in patients with lung and gastric cancer treated with immune checkpoint inhibitors. *Anticancer Res.* 39, 5195–5201. doi: 10.21873/anticanres.13716

Andrews, L. P., Yano, H., and Vignali, D. A. A. (2019). Inhibitory receptors and ligands beyond PD-1, PD-L1 and CTLA-4: breakthroughs or backups. *Nat. Immunol.* 20, 1425–1434. doi: 10.1038/s41590-019-0512-0

Asanuma, K., Nakamura, T., Hayashi, A., Okamoto, T., Iino, T., Asanuma, Y., et al. (2020). Soluble programmed death-ligand 1 rather than PD-L1 on tumor cells effectively predicts metastasis and prognosis in soft tissue sarcomas. *Sci. Rep.* 10:9077. doi: 10.1038/s41598-020-65895-0

Baietti, M. F., Zhang, Z., Mortier, E., Melchior, A., Degeest, G., Geeraerts, A., et al. (2012). Syndecan-syntenin-ALIX regulates the biogenesis of exosomes. *Nat. Cell Biol.* 14, 677–685. doi: 10.1038/ncb2502

Barroso-Sousa, R., Barry, W. T., Garrido-Castro, A. C., Hodi, F. S., Min, L., Krop, I. E., et al. (2018). Incidence of endocrine dysfunction following the use of different immune checkpoint inhibitor regimens: a systematic review and meta-analysis. *JAMA Oncol.* 4, 173–182. doi: 10.1001/jamaoncol.2017.3064

Bassanelli, M., Sioletic, S., Martini, M., Giacinti, S., Viterbo, A., Staddon, A., et al. (2018). Heterogeneity of PD-L1 Expression and Relationship with Biology of NSCLC. *Anticancer Res.* 38, 3789–3796. doi: 10.21873/anticanres.12662

Bastaki, S., Irandoust, M., Ahmadi, A., Hojjat-Farsangi, M., Ambrose, P., Hallaj, S., et al. (2020). PD-L1/PD-1 axis as a potent therapeutic target in breast cancer. *Life Sci.* 247:117437. doi: 10.1016/j.lfs.2020.117437

Bissig, C., and Gruenberg, J. (2014). ALIX and the multivesicular endosome: ALIX in Wonderland. *Trends Cell Biol.* 24, 19–25. doi: 10.1016/j.tcb.2013.10.009

Brennan, K., Martin, K., FitzGerald, S. P., O'Sullivan, J., Wu, Y., Blanco, A., et al. (2020). A comparison of methods for the isolation and separation of extracellular vesicles from protein and lipid particles in human serum. *Sci. Rep.* 10:1039. doi: 10.1038/s41598-020-57497-7

Brody, R., Zhang, Y., Ballas, M., Siddiqui, M. K., Gupta, P., Barker, C., et al. (2017). PD-L1 expression in advanced NSCLC: Insights into risk stratification and treatment selection from a systematic literature review. *Lung Cancer* 112, 200–215. doi: 10.1016/j.lungcan.2017.08.005

Buderath, P., Schwich, E., Jensen, C., Horn, P. A., Kimmig, R., Kasimir-Bauer, S., et al. (2019). Soluble programmed death receptor ligands sPD-L1 and sPD-L2 as liquid biopsy markers for prognosis and platinum response in epithelial ovarian cancer. *Front. Oncol.* 9:1015. doi: 10.3389/fonc.2019.01015

Buder-Bakhaya, K., and Hassel, J. C. (2018). Biomarkers for clinical benefit of immune checkpoint inhibitor treatment-A review from the melanoma perspective and beyond. *Front. Immunol.* 9:1474. doi: 10.3389/fimmu.2018.01474

Butte, M. J., Keir, M. E., Phamduy, T. B., Sharpe, A. H., and Freeman, G. J. (2007). Programmed death-1 ligand 1 interacts specifically with the B7-1 costimulatory molecule to inhibit T cell responses. *Immunity* 27, 111–122. doi: 10.1016/j.immuni.2007.05.016

Butte, M. J., Pena-Cruz, V., Kim, M. J., Freeman, G. J., and Sharpe, A. H. (2008). Interaction of human PD-L1 and B7-1. *Mol. Immunol.* 45, 3567–3572. doi: 10.1016/j.molimm.2008.05.014

Carlton, J. (2010). The ESCRT machinery: a cellular apparatus for sorting and scission. *Biochem. Soc. Trans.* 38, 1397–1412. doi: 10.1042/BST0381397

Carreras-Planella, L., Monguio-Tortajada, M., Borras, F. E., and Franquesa, M. (2019). Immunomodulatory effect of MSC on B cells is independent of secreted extracellular vesicles. *Front. Immunol.* 10:1288. doi: 10.3389/fimmu.2019.01288

Catalano, M., and O'Driscoll, L. (2020). Inhibiting extracellular vesicles formation and release: a review of EV inhibitors. *J. Extracell. Vesicles* 9:1703244. doi: 10.1080/20013078.2019.1703244

Cha, J. H., Chan, L. C., Li, C. W., Hsu, J. L., and Hung, M. C. (2019). Mechanisms Controlling PD-L1 expression in cancer. *Mol. Cell* 76, 359–370. doi: 10.1016/j.molcel.2019.09.030

Chamoto, K., Hatae, R., and Honjo, T. (2020). Current issues and perspectives in PD-1 blockade cancer immunotherapy. *Int. J. Clin. Oncol.* 25, 790–800. doi: 10.1007/s10147-019-01588-7

Chang, B., Huang, T., Wei, H., Shen, L., Zhu, D., He, W., et al. (2019). The correlation and prognostic value of serum levels of soluble programmed death protein 1 (sPD-1) and soluble programmed death-ligand 1 (sPD-L1) in patients with hepatocellular carcinoma. *Cancer Immunol. Immunother.* 68, 353–363. doi: 10.1007/s00262-018-2271-4

Chatterjee, J., Dai, W., Aziz, N. H. A., Teo, P. Y., Wahba, J., Phelps, D. L., et al. (2017). Clinical use of programmed cell death-1 and its ligand expression as discriminatory and predictive markers in ovarian cancer. *Clin. Cancer Res.* 23, 3453–3460. doi: 10.1158/1078-0432.CCR-16-2366

Chaudhri, A., Xiao, Y., Klee, A. N., Wang, X., Zhu, B., and Freeman, G. J. (2018). PD-L1 Binds to B7-1 only *in Cis* on the same cell surface. *Cancer Immunol. Res.* 6, 921–929. doi: 10.1158/2326-6066.CIR-17-0316

Chemnitz, J. M., Parry, R. V., Nichols, K. E., June, C. H., and Riley, J. L. (2004). SHP-1 and SHP-2 associate with immunoreceptor tyrosine-based switch motif of programmed death 1 upon primary human T cell stimulation, but only receptor ligation prevents T cell activation. *J. Immunol.* 173, 945–954. doi: 10.4049/jimmunol.173.2.945

Chen, G., Huang, A. C., Zhang, W., Zhang, G., Wu, M., Xu, W., et al. (2018). Exosomal PD-L1 contributes to immunosuppression and is associated with anti-PD-1 response. *Nature* 560, 382–386. doi: 10.1038/s41586-018-0392-8

Chen, L., and Flies, D. B. (2013). Molecular mechanisms of T cell co-stimulation and co-inhibition. *Nat. Rev. Immunol.* 13, 227–242. doi: 10.1038/nri3405

Chen, M., Sharma, A., Lin, Y., Wu, Y., He, Q., Gu, Y., et al. (2019). Insluin and epithelial growth factor (EGF) promote programmed death ligand 1(PD-L1) production and transport in colon cancer stem cells. *BMC Cancer* 19:153. doi: 10.1186/s12885-019-5364-3

Chen, N., Fang, W., Zhan, J., Hong, S., Tang, Y., Kang, S., et al. (2015). Upregulation of PD-L1 by EGFR activation mediates the immune escape in EGFR-Driven NSCLC: implication for optional immune targeted therapy for NSCLC patients with EGFR mutation. *J. Thorac. Oncol.* 10, 910–923. doi: 10.1097/JTO.0000000000000500

Chen, S., Lv, M., Fang, S., Ye, W., Gao, Y., and Xu, Y. (2018). Poly(I:C) enhanced anti-cervical cancer immunities induced by dendritic cells-derived exosomes. *Int. J. Biol. Macromol.* 113, 1182–1187. doi: 10.1016/j.ijbiomac.2018.02.034

Cheng, X., Veverka, V., Radhakrishnan, A., Waters, L. C., Muskett, F. W., Morgan, S. H., et al. (2013). Structure and interactions of the human programmed cell death 1 receptor. *J. Biol. Chem.* 288, 11771–11785. doi: 10.1074/jbc.M112.448126

Chinai, J. M., Janakiram, M., Chen, F., Chen, W., Kaplan, M., and Zang, X. (2015). New immunotherapies targeting the PD-1 pathway. *Trends Pharmacol. Sci.* 36, 587–595. doi: 10.1016/j.tips.2015.06.005

Choi, J. S., Sansoni, E. R., Lovin, B. D., Lindquist, N. R., Phan, J., Mayo, L. L., et al. (2020). Abscopal effect following immunotherapy and combined stereotactic body radiation therapy in recurrent metastatic head and neck squamous cell carcinoma: a report of two cases and literature review. *Ann. Otol. Rhinol. Laryngol.* 129, 517–522. doi: 10.1177/0003489419896602

Choo, Y. W., Kang, M., Kim, H. Y., Han, J., Kang, S., Lee, J. R., et al. (2018). M1 macrophage-derived nanovesicles potentiate the anticancer efficacy of immune checkpoint inhibitors. *ACS Nano* 12, 8977–8993. doi: 10.1021/acsnano.8b02446

Christ, L., Raiborg, C., Wenzel, E. M., Campsteijn, C., and Stenmark, H. (2017). Cellular functions and molecular mechanisms of the ESCRT membrane-scission machinery. *Trends Biochem. Sci.* 42, 42–56. doi: 10.1016/j.tibs.2016.08.016

Cimino-Mathews, A., Thompson, E., Taube, J. M., Ye, X., Lu, Y., Meeker, A., et al. (2016). PD-L1 (B7-H1) expression and the immune tumor microenvironment in primary and metastatic breast carcinomas. *Hum. Pathol.* 47, 52–63. doi: 10.1016/j.humpath.2015.09.003

Colombo, M., Raposo, G., and Thery, C. (2014). Biogenesis, secretion, and intercellular interactions of exosomes and other extracellular vesicles. *Annu. Rev. Cell Dev. Biol.* 30, 255–289. doi: 10.1146/annurev-cellbio-101512-122326

Cordonnier, M., Nardin, C., Chanteloup, G., Derangere, V., Algros, M. P., Arnould, L., et al. (2020). Tracking the evolution of circulating exosomal-PD-L1 to monitor melanoma patients. *J. Extracell. Vesicles* 9:1710899. doi: 10.1080/20013078.2019.1710899

Costantini, A., Julie, C., Dumenil, C., Helias-Rodzewicz, Z., Tisserand, J., Dumoulin, J., et al. (2018). Predictive role of plasmatic biomarkers in advanced non-small cell lung cancer treated by nivolumab. *Oncoimmunology* 7:e1452581. doi: 10.1080/2162402X.2018.1452581

Couzin-Frankel, J. (2013). Breakthrough of the year 2013. Cancer immunotherapy. *Science* 342, 1432–1433. doi: 10.1126/science.342.6165.1432

Crow, J., Samuel, G., and Godwin, A. K. (2019). Beyond tumor mutational burden: potential and limitations in using exosomes to predict response to immunotherapy. *Expert Rev. Mol. Diagn.* 19, 1079–1088. doi: 10.1080/14737159.2020.1688144

Cuzzubbo, S., Javeri, F., Tissier, M., Roumi, A., Barlog, C., Doridam, J., et al. (2017). Neurological adverse events associated with immune checkpoint inhibitors: review of the literature. *Eur. J. Cancer* 73, 1–8. doi: 10.1016/j.ejca.2016.12.001

Czystowska-Kuzmicz, M., Sosnowska, A., Nowis, D., Ramji, K., Szajnik, M., Chlebowska-Tuz, J., et al. (2019). Small extracellular vesicles containing arginase-1 suppress T-cell responses and promote tumor growth in ovarian carcinoma. *Nat. Commun.* 10:3000. doi: 10.1038/s41467-019-10979-3

Daassi, D., Mahoney, K. M., and Freeman, G. J. (2020). The importance of exosomal PDL1 in tumour immune evasion. *Nat. Rev. Immunol.* 20, 209–215. doi: 10.1038/s41577-019-0264-y

Dai, S., Jia, R., Zhang, X., Fang, Q., and Huang, L. (2014). The PD-1/PD-Ls pathway and autoimmune diseases. *Cell. Immunol.* 290, 72–79. doi: 10.1016/j.cellimm.2014.05.006

Davis, A. A., and Patel, V. G. (2019). The role of PD-L1 expression as a predictive biomarker: an analysis of all US Food and Drug Administration (FDA) approvals of immune checkpoint inhibitors. *J. Immunother. Cancer* 7:278. doi: 10.1186/s40425-019-0768-9

Del Re, M., Marconcini, R., Pasquini, G., Rofi, E., Vivaldi, C., Bloise, F., et al. (2018). PD-L1 mRNA expression in plasma-derived exosomes is associated with response to anti-PD-1 antibodies in melanoma and NSCLC. *Br. J. Cancer* 118, 820–824. doi: 10.1038/bjc.2018.9

Demaria, S., and Formenti, S. C. (2020). The abscopal effect 67 years later: from a side story to center stage. *Br. J. Radiol.* 93:20200042. doi: 10.1259/bjr.20200042

Deng, L., Liang, H., Burnette, B., Beckett, M., Darga, T., Weichselbaum, R. R., et al. (2014). Irradiation and anti-PD-L1 treatment synergistically promote antitumor immunity in mice. *J. Clin. Invest.* 124, 687–695. doi: 10.1172/JCI67313

Dezutter-Dambuyant, C., Durand, I., Alberti, L., Bendriss-Vermare, N., Valladeau-Guilemond, J., Duc, A., et al. (2016). A novel regulation of PD-1 ligands on mesenchymal stromal cells through MMP-mediated proteolytic cleavage. *Oncoimmunology* 5:e1091146. doi: 10.1080/2162402X.2015.1091146

Dinkins, M. B., Dasgupta, S., Wang, G., Zhu, G., and Bieberich, E. (2014). Exosome reduction *in vivo* is associated with lower amyloid plaque load in the 5XFAD mouse model of Alzheimer's disease. *Neurobiol. Aging* 35, 1792–1800. doi: 10.1016/j.neurobiolaging.2014.02.012

Dong, H., Strome, S. E., Salomao, D. R., Tamura, H., Hirano, F., Flies, D. B., et al. (2002). Tumor-associated B7-H1 promotes T-cell apoptosis: a potential mechanism of immune evasion. *Nat. Med.* 8, 793–800. doi: 10.1038/nm730

Dong, H., Zhu, G., Tamada, K., and Chen, L. (1999). B7-H1, a third member of the B7 family, co-stimulates T-cell proliferation and interleukin-10 secretion. *Nat. Med.* 5, 1365–1369. doi: 10.1038/70932

Enderle, D., Spiel, A., Coticchia, C. M., Berghoff, E., Mueller, R., Schlumpberger, M., et al. (2015). Characterization of RNA from exosomes and other extracellular vesicles isolated by a novel spin column-based method. *PLoS One* 10:e0136133. doi: 10.1371/journal.pone.0136133

Fan, Y., Che, X., Qu, J., Hou, K., Wen, T., Li, Z., et al. (2019). Exosomal PD-L1 retains immunosuppressive activity and is associated with gastric cancer prognosis. *Ann. Surg. Oncol.* 26, 3745–3755. doi: 10.1245/s10434-019-07431-7

Fan, Y., Geng, Y., Shen, L., and Zhang, Z. (2020). Advances on immune-related adverse events associated with immune checkpoint inhibitors. *Front. Med.* doi: 10.1007/s11684-019-0735-3 [Epub ahead of print].

Farooqi, A. A., Desai, N. N., Qureshi, M. Z., Librelotto, D. R. N., Gasparri, M. L., Bishayee, A., et al. (2018). Exosome biogenesis, bioactivities and functions as new delivery systems of natural compounds. *Biotechnol. Adv.* 36, 328–334. doi: 10.1016/j.biotechadv.2017.12.010

Festino, L., Botti, G., Lorigan, P., Masucci, G. V., Hipp, J. D., Horak, C. E., et al. (2016). Cancer treatment with Anti-PD-1/PD-L1 agents: Is PD-L1 expression a biomarker for patient selection? *Drugs* 76, 925–945. doi: 10.1007/s40265-016-0588-x

Fionda, B., Massaccesi, M., Tagliaferri, L., Dinapoli, N., Iezzi, R., and Boldrini, L. (2020). Abscopal effect and interventional oncology: state of art and future perspectives. *Eur. Rev. Med. Pharmacol. Sci.* 24, 773–776. doi: 10.26355/eurrev_202001_20058

Foster, B. A., Gingrich, J. R., Kwon, E. D., Madias, C., and Greenberg, N. M. (1997). Characterization of prostatic epithelial cell lines derived from transgenic adenocarcinoma of the mouse prostate (TRAMP) model. *Cancer Res.* 57, 3325–3330.

Fu, Y., Liu, C. J., Kobayashi, D. K., Johanns, T. M., Bowman-Kirigin, J. A., Schaettler, M. O., et al. (2020). GATA2 Regulates Constitutive PD-L1 and PD-L2 Expression in Brain Tumors. *Sci. Rep.* 10:9027. doi: 10.1038/s41598-020-65915-z

Fukasawa, T., Yoshizaki, A., Ebata, S., Nakamura, K., Saigusa, R., Miura, S., et al. (2017). Contribution of soluble forms of programmed death 1 and programmed death ligand 2 to disease severity and progression in systemic sclerosis. *Arthritis Rheumatol.* 69, 1879–1890. doi: 10.1002/art.40164

Furthauer, M. (2018). The ESCRT machinery: When function follows form. *Semin. Cell Dev. Biol.* 74, 1–3. doi: 10.1016/j.semcdb.2017.11.003

Furuse, M., Kuwabara, H., Ikeda, N., Hattori, Y., Ichikawa, T., Kagawa, N., et al. (2020). PD-L1 and PD-L2 expression in the tumor microenvironment including peritumoral tissue in primary central nervous system lymphoma. *BMC Cancer* 20:277. doi: 10.1186/s12885-020-06755-y

Gauci, M. L., Baroudjian, B., Bederede, U., Zeboulon, C., Delyon, J., Allayous, C., et al. (2020). Severe immune-related hepatitis induced by immune checkpoint inhibitors: clinical features and management proposal. *Clin. Res. Hepatol. Gastroenterol.* doi: 10.1016/j.clinre.2020.06.016 [Epub ahead of print].

Gordon, S. R., Maute, R. L., Dulken, B. W., Hutter, G., George, B. M., McCracken, M. N., et al. (2017). PD-1 expression by tumour-associated macrophages inhibits phagocytosis and tumour immunity. *Nature* 545, 495–499. doi: 10.1038/nature22396

Goswami, S., Aparicio, A., and Subudhi, S. K. (2016). Immune checkpoint therapies in prostate cancer. *Cancer J.* 22, 117–120. doi: 10.1097/PPO.0000000000000176

Gould, S. J., and Raposo, G. (2013). As we wait: coping with an imperfect nomenclature for extracellular vesicles. *J. Extracell. Vesicles* 2:20389. doi: 10.3402/jev.v2i0.20389

Grasselly, C., Denis, M., Bourguignon, A., Talhi, N., Mathe, D., Tourette, A., et al. (2018). The antitumor activity of combinations of cytotoxic chemotherapy and immune checkpoint inhibitors is model-dependent. *Front. Immunol.* 9:2100. doi: 10.3389/fimmu.2018.02100

Gregg, J. P., Li, T., and Yoneda, K. Y. (2019). Molecular testing strategies in non-small cell lung cancer: optimizing the diagnostic journey. *Transl. Lung Cancer Res.* 8, 286–301. doi: 10.21037/tlcr.2019.04.14

Groot Kormelink, T., Mol, S., de Jong, E. C., and Wauben, M. H. M. (2018). The role of extracellular vesicles when innate meets adaptive. *Semin. Immunopathol.* 40, 439–452. doi: 10.1007/s00281-018-0681-1

Gu, D., Ao, X., Yang, Y., Chen, Z., and Xu, X. (2018). Soluble immune checkpoints in cancer: production, function and biological significance. *J. Immunother. Cancer* 6:132. doi: 10.1186/s40425-018-0449-0

Ha, D., Yang, N., and Nadithe, V. (2016). Exosomes as therapeutic drug carriers and delivery vehicles across biological membranes: current perspectives and future challenges. *Acta Pharm. Sin. B* 6, 287–296. doi: 10.1016/j.apsb.2016.02.001

Han, Y., Liu, D., and Li, L. (2020). PD-1/PD-L1 pathway: current researches in cancer. *Am. J. Cancer Res.* 10, 727–742.

Hassanpour, M., Rezabakhsh, A., Rezaie, J., Nouri, M., and Rahbarghazi, R. (2020). Exosomal cargos modulate autophagy in recipient cells via different signaling pathways. *Cell Biosci.* 10:92. doi: 10.1186/s13578-020-00455-7

Hatae, R., Chamoto, K., Kim, Y. H., Sonomura, K., Taneishi, K., Kawaguchi, S., et al. (2020). Combination of host immune metabolic biomarkers for the PD-1 blockade cancer immunotherapy. *JCI Insight* 5:e133501. doi: 10.1172/jci.insight.133501

He, X. H., Liu, Y., Xu, L. H., and Zeng, Y. Y. (2004). Cloning and identification of two novel splice variants of human PD-L2. *Acta Biochim. Biophys. Sin.* 36, 284–289. doi: 10.1093/abbs/36.4.284

Henne, W. M., Buchkovich, N. J., and Emr, S. D. (2011). The ESCRT pathway. *Dev. Cell* 21, 77–91. doi: 10.1016/j.devcel.2011.05.015

Hesari, A., Golrokh Moghadam, S. A., Siasi, A., Rahmani, M., Behboodi, N., Rastgar-Moghadam, A., et al. (2018). Tumor-derived exosomes: potential biomarker or therapeutic target in breast cancer? *J. Cell. Biochem.* 119, 4236–4240. doi: 10.1002/jcb.26364

Hessvik, N. P., and Llorente, A. (2018). Current knowledge on exosome biogenesis and release. *Cell. Mol. Life Sci.* 75, 193–208. doi: 10.1007/s00018-017-2595-9

Hira-Miyazawa, M., Nakamura, H., Hirai, M., Kobayashi, Y., Kitahara, H., Bou-Gharios, G., et al. (2018). Regulation of programmed-death ligand in the human head and neck squamous cell carcinoma microenvironment is mediated through matrix metalloproteinase-mediated proteolytic cleavage. *Int. J. Oncol.* 52, 379–388. doi: 10.3892/ijo.2017.4221

Hong, P., Yang, H., Wu, Y., Li, K., and Tang, Z. (2019). The functions and clinical application potential of exosomes derived from adipose mesenchymal stem cells: a comprehensive review. *Stem Cell Res. Ther.* 10:242. doi: 10.1186/s13287-019-1358-y

Hood, J. L., San, R. S., and Wickline, S. A. (2011). Exosomes released by melanoma cells prepare sentinel lymph nodes for tumor metastasis. *Cancer Res.* 71, 3792–3801. doi: 10.1158/0008-5472.CAN-10-4455

Hsu, J., Hodgins, J. J., Marathe, M., Nicolai, C. J., Bourgeois-Daigneault, M. C., Trevino, T. N., et al. (2018). Contribution of NK cells to immunotherapy mediated by PD-1/PD-L1 blockade. *J. Clin. Invest.* 128, 4654–4668. doi: 10.1172/JCI99317

Huang, M., Yang, J., Wang, T., Song, J., Xia, J., Wu, L., et al. (2020). Homogeneous, low-volume, efficient, and sensitive quantitation of circulating exosomal PD-L1 for cancer diagnosis and immunotherapy response prediction. *Angew. Chem. Int. Ed. Engl.* 59, 4800–4805. doi: 10.1002/anie.201916039

Huang, Y., Liu, K., Li, Q., Yao, Y., and Wang, Y. (2018). Exosomes function in tumor immune microenvironment. *Adv. Exp. Med. Biol.* 1056, 109–122. doi: 10.1007/978-3-319-74470-4_7

Hui, E., Cheung, J., Zhu, J., Su, X., Taylor, M. J., Wallweber, H. A., et al. (2017). T cell costimulatory receptor CD28 is a primary target for PD-1-mediated inhibition. *Science* 355, 1428–1433. doi: 10.1126/science.aaf1292

Hurley, J. H., and Odorizzi, G. (2012). Get on the exosome bus with ALIX. *Nat. Cell Biol.* 14, 654–655. doi: 10.1038/ncb2530

Jiang, X., Wang, J., Deng, X., Xiong, F., Ge, J., Xiang, B., et al. (2019). Role of the tumor microenvironment in PD-L1/PD-1-mediated tumor immune escape. *Mol. Cancer* 18:10. doi: 10.1186/s12943-018-0928-4

Jiang, Y., Chen, M., Nie, H., and Yuan, Y. (2019). PD-1 and PD-L1 in cancer immunotherapy: clinical implications and future considerations. *Hum. Vaccin Immunother.* 15, 1111–1122. doi: 10.1080/21645515.2019.1571892

Johnsen, K. B., Gudbergsson, J. M., Andresen, T. L., and Simonsen, J. B. (2019). What is the blood concentration of extracellular vesicles? Implications for the use of extracellular vesicles as blood-borne biomarkers of cancer. *Biochim. Biophys. Acta Rev. Cancer* 1871, 109–116. doi: 10.1016/j.bbcan.2018.11.006

Johnson, J. L., Ramadass, M., He, J., Brown, S. J., Zhang, J., Abgaryan, L., et al. (2016). Identification of Neutrophil Exocytosis Inhibitors (Nexinhibs), Small Molecule Inhibitors of Neutrophil Exocytosis and Inflammation: druggability of the small GTPase Rab27a. *J. Biol. Chem.* 291, 25965–25982. doi: 10.1074/jbc.M116.741884

Ju, X., Zhang, H., Zhou, Z., and Wang, Q. (2020). Regulation of PD-L1 expression in cancer and clinical implications in immunotherapy. *Am. J. Cancer Res.* 10, 1–11.

Kakavand, H., Rawson, R. V., Pupo, G. M., Yang, J. Y. H., Menzies, A. M., Carlino, M. S., et al. (2017). PD-L1 expression and immune escape in melanoma resistance to MAPK inhibitors. *Clin. Cancer Res.* 23, 6054–6061. doi: 10.1158/1078-0432.CCR-16-1688

Kalluri, R. (2016). The biology and function of exosomes in cancer. *J. Clin. Invest.* 126, 1208–1215. doi: 10.1172/JCI81135

Kamphorst, A. O., Pillai, R. N., Yang, S., Nasti, T. H., Akondy, R. S., Wieland, A., et al. (2017). Proliferation of PD-1+ CD8 T cells in peripheral blood after PD-1-targeted therapy in lung cancer patients. *Proc. Natl. Acad. Sci. U.S.A.* 114, 4993–4998. doi: 10.1073/pnas.1705327114

Karyampudi, L., Lamichhane, P., Krempski, J., Kalli, K. R., Behrens, M. D., Vargas, D. M., et al. (2016). PD-1 blunts the function of ovarian tumor-infiltrating dendritic cells by inactivating NF-kappaB. *Cancer Res.* 76, 239–250. doi: 10.1158/0008-5472.CAN-15-0748

Kaunitz, G. J., Cottrell, T. R., Lilo, M., Muthappan, V., Esandrio, J., Berry, S., et al. (2017). Melanoma subtypes demonstrate distinct PD-L1 expression profiles. *Lab. Invest.* 97, 1063–1071. doi: 10.1038/labinvest.2017.64

Kawamoto, E., Masui-Ito, A., Eguchi, A., Soe, Z. Y., Prajuabjinda, O., Darkwah, S., et al. (2019). Integrin and PD-1 ligand expression on circulating extracellular vesicles in systemic inflammatory response syndrome and sepsis. *Shock* 52, 13–22. doi: 10.1097/SHK.0000000000001228

Khushman, M., Bhardwaj, A., Patel, G. K., Laurini, J. A., Roveda, K., Tan, M. C., et al. (2017). Exosomal Markers (CD63 and CD9) expression pattern using immunohistochemistry in resected malignant and nonmalignant pancreatic specimens. *Pancreas* 46, 782–788. doi: 10.1097/MPA.0000000000000847

Kim, D. H., Kim, H., Choi, Y. J., Kim, S. Y., Lee, J. E., Sung, K. J., et al. (2019). Exosomal PD-L1 promotes tumor growth through immune escape in non-small cell lung cancer. *Exp. Mol. Med.* 51, 1–13. doi: 10.1038/s12276-019-0295-2

Kloten, V., Lampignano, R., Krahn, T., and Schlange, T. (2019). Circulating Tumor Cell PD-L1 Expression as Biomarker for Therapeutic Efficacy of Immune Checkpoint Inhibition in NSCLC. *Cells* 8:809. doi: 10.3390/cells8080809

Kowal, J., Tkach, M., and Thery, C. (2014). Biogenesis and secretion of exosomes. *Curr. Opin. Cell Biol.* 29, 116–125. doi: 10.1016/j.ceb.2014.05.004

Kowanetz, M., Zou, W., Gettinger, S. N., Koeppen, H., Kockx, M., Schmid, P., et al. (2018). Differential regulation of PD-L1 expression by immune and tumor cells in NSCLC and the response to treatment with atezolizumab (anti-PD-L1). *Proc. Natl. Acad. Sci. U.S.A.* 115, E10119–E10126. doi: 10.1073/pnas.1802166115

Kythreotou, A., Siddique, A., Mauri, F. A., Bower, M., and Pinato, D. J. (2018). Pd-L1. *J. Clin. Pathol.* 71, 189–194. doi: 10.1136/jclinpath-2017-204853

Lallemand, T., Rouahi, M., Swiader, A., Grazide, M. H., Geoffre, N., Alayrac, P., et al. (2018). nSMase2 (Type 2-Neutral Sphingomyelinase) Deficiency or Inhibition by GW4869 Reduces Inflammation and Atherosclerosis in Apoe(-/-) Mice. *Arterioscler. Thromb. Vasc. Biol.* 38, 1479–1492. doi: 10.1161/ATVBAHA.118.311208

Lan, J., Sun, L., Xu, F., Liu, L., Hu, F., Song, D., et al. (2019). M2 macrophage-derived exosomes promote cell migration and invasion in colon cancer. *Cancer Res.* 79, 146–158. doi: 10.1158/0008-5472.CAN-18-0014

Larsen, T. V., Hussmann, D., and Nielsen, A. L. (2019). PD-L1 and PD-L2 expression correlated genes in non-small-cell lung cancer. *Cancer Commun.* 39:30. doi: 10.1186/s40880-019-0376-6

Lasso, P., Llano Murcia, M., Sandoval, T. A., Uruena, C., Barreto, A., and Fiorentino, S. (2019). Breast tumor cells highly resistant to drugs are controlled only by the immune response induced in an immunocompetent mouse model. *Integr. Cancer Ther.* 18:1534735419848047. doi: 10.1177/1534735419848047

Latchman, Y., Wood, C. R., Chernova, T., Chaudhary, D., Borde, M., Chernova, I., et al. (2001). PD-L2 is a second ligand for PD-1 and inhibits T cell activation. *Nat. Immunol.* 2, 261–268. doi: 10.1038/85330

Lazaro-Ibanez, E., Lasser, C., Shelke, G. V., Crescitelli, R., Jang, S. C., Cvjetkovic, A., et al. (2019). DNA analysis of low- and high-density fractions defines heterogeneous subpopulations of small extracellular vesicles based on their DNA cargo and topology. *J. Extracell. Vesicles* 8:1656993. doi: 10.1080/20013078.2019.1656993

Lee, H. H., Wang, Y. N., Xia, W., Chen, C. H., Rau, K. M., Ye, L., et al. (2019). Removal of N-Linked Glycosylation Enhances PD-L1 Detection and Predicts Anti-PD-1/PD-L1 Therapeutic Efficacy. *Cancer Cell* 36, 168–178.e4. doi: 10.1016/j.ccell.2019.06.008

Li, C., Li, C., Zhi, C., Liang, W., Wang, X., Chen, X., et al. (2019a). Clinical significance of PD-L1 expression in serum-derived exosomes in NSCLC patients. *J. Transl. Med.* 17:355. doi: 10.1186/s12967-019-2101-2

Li, H., van der Leun, A. M., Yofe, I., Lubling, Y., Gelbard-Solodkin, D., van Akkooi, A. C. J., et al. (2019b). Dysfunctional CD8 T cells form a proliferative, dynamically regulated compartment within human melanoma. *Cell* 176, 775–789.e18. doi: 10.1016/j.cell.2018.11.043

Li, H., Xu, Y., Wan, B., Song, Y., Zhan, P., Hu, Y., et al. (2019c). The clinicopathological and prognostic significance of PD-L1 expression assessed by immunohistochemistry in lung cancer: a meta-analysis of 50 studies with 11,383 patients. *Transl. Lung Cancer Res.* 8, 429–449. doi: 10.21037/tlcr.2019.08.04

Li, N., Wang, J., Zhang, N., Zhuang, M., Zong, Z., Zou, J., et al. (2018). Cross-talk between TNF-alpha and IFN-gamma signaling in induction of B7-H1 expression in hepatocellular carcinoma cells. *Cancer Immunol. Immunother.* 67, 271–283. doi: 10.1007/s00262-017-2086-8

Liao, H., Chen, W., Dai, Y., Richardson, J. J., Guo, J., Yuan, K., et al. (2019). Expression of programmed cell death-ligands in hepatocellular carcinoma: correlation with immune microenvironment and survival outcomes. *Front. Oncol.* 9:883. doi: 10.3389/fonc.2019.00883

Lin, H., Wei, S., Hurt, E. M., Green, M. D., Zhao, L., Vatan, L., et al. (2018). Host expression of PD-L1 determines efficacy of PD-L1 pathway blockade-mediated tumor regression. *J. Clin. Invest.* 128:1708. doi: 10.1172/JCI120803

Lin, X., Zeng, T., Lin, J., Zhang, Q., Cheng, H., Fang, S., et al. (2020). Establishment of humanized tumor microenvironment mouse models based on the injection of peripheral blood mononuclear cells and IFN-gamma to evaluate the efficacy of PD-L1/PD-1-targeted immunotherapy. *Cancer Biol. Ther.* 21, 130–138. doi: 10.1080/15384047.2019.1670520

Liu, C., Xu, X., Li, B., Situ, B., Pan, W., Hu, Y., et al. (2018a). Single-exosome-counting immunoassays for cancer diagnostics. *Nano Lett.* 18, 4226–4232. doi: 10.1021/acs.nanolett.8b01184

Liu, C., Zeng, X., An, Z., Yang, Y., Eisenbaum, M., Gu, X., et al. (2018b). Sensitive detection of exosomal proteins via a compact surface plasmon resonance biosensor for cancer diagnosis. *ACS Sens.* 3, 1471–1479. doi: 10.1021/acssensors.8b00230

Liu, F., Vermesh, O., Mani, V., Ge, T. J., Madsen, S. J., Sabour, A., et al. (2017). The exosome total isolation chip. *ACS Nano* 11, 10712–10723. doi: 10.1021/acsnano.7b04878

Liu, S., Zhu, Y., Zhang, C., Meng, X., Sun, B., Zhang, G., et al. (2020). The clinical significance of soluble programmed cell Death-Ligand 1 (sPD-L1) in patients with gliomas. *Front. Oncol.* 10:9. doi: 10.3389/fonc.2020.00009

Liu, S. Y., and Wu, Y. L. (2019). Biomarker for personalized immunotherapy. *Transl. Lung Cancer Res.* 8, S308–S317. doi: 10.21037/tlcr.2019.08.02

Liu, T., Jin, B., Chen, J., Wang, H., Lin, S., Dang, J., et al. (2020). Comparative risk of serious and fatal treatment-related adverse events caused by 19 immune checkpoint inhibitors used in cancer treatment: a network meta-analysis. *Ther. Adv. Med. Oncol.* 12:1758835920940927. doi: 10.1177/1758835920940927

Liu, Y., Dong, Y., Kong, L., Shi, F., Zhu, H., and Yu, J. (2018). Abscopal effect of radiotherapy combined with immune checkpoint inhibitors. *J. Hematol. Oncol.* 11:104. doi: 10.1186/s13045-018-0647-8

Lo Cicero, A., Stahl, P. D., and Raposo, G. (2015). Extracellular vesicles shuffling intercellular messages: for good or for bad. *Curr. Opin. Cell Biol.* 35, 69–77. doi: 10.1016/j.ceb.2015.04.013

Lobb, R. J., Becker, M., Wen, S. W., Wong, C. S., Wiegmans, A. P., Leimgruber, A., et al. (2015). Optimized exosome isolation protocol for cell culture supernatant and human plasma. *J. Extracell. Vesicles* 4:27031. doi: 10.3402/jev.v4.27031

Luberto, C., Hassler, D. F., Signorelli, P., Okamoto, Y., Sawai, H., Boros, E., et al. (2002). Inhibition of tumor necrosis factor-induced cell death in MCF7 by a novel inhibitor of neutral sphingomyelinase. *J. Biol. Chem.* 277, 41128–41139. doi: 10.1074/jbc.M206747200

Lubin, J. A., Zhang, R. R., and Kuo, J. S. (2018). Extracellular vesicles containing PD-L1 contribute to immune evasion in glioblastoma. *Neurosurgery* 83, E98–E100. doi: 10.1093/neuros/nyy295

Ludwig, S., Floros, T., Theodoraki, M. N., Hong, C. S., Jackson, E. K., Lang, S., et al. (2017). Suppression of lymphocyte functions by plasma exosomes correlates with disease activity in patients with head and neck cancer. *Clin. Cancer Res.* 23, 4843–4854. doi: 10.1158/1078-0432.CCR-16-2819

Lux, A., Kahlert, C., Grutzmann, R., and Pilarsky, C. (2019). c-Met and PD-L1 on circulating exosomes as diagnostic and prognostic markers for pancreatic cancer. *Int. J. Mol. Sci.* 20:567. doi: 10.3390/ijms20133305

Madore, J., Vilain, R. E., Menzies, A. M., Kakavand, H., Wilmott, J. S., Hyman, J., et al. (2015). PD-L1 expression in melanoma shows marked heterogeneity within and between patients: implications for anti-PD-1/PD-L1 clinical trials. *Pigment Cell Melanoma Res.* 28, 245–253. doi: 10.1111/pcmr.12340

Mahoney, K. M., Freeman, G. J., and McDermott, D. F. (2015). The next immune-checkpoint inhibitors: PD-1/PD-L1 blockade in melanoma. *Clin. Ther.* 37, 764–782. doi: 10.1016/j.clinthera.2015.02.018

Margolis, L., and Sadovsky, Y. (2019). The biology of extracellular vesicles: the known unknowns. *PLoS Biol.* 17:e3000363. doi: 10.1371/journal.pbio.3000363

Mariotti, F. R., Petrini, S., Ingegnere, T., Tumino, N., Besi, F., Scordamaglia, F., et al. (2019). PD-1 in human NK cells: evidence of cytoplasmic mRNA and protein expression. *Oncoimmunology* 8:1557030. doi: 10.1080/2162402X.2018.1557030

Martinez-Morilla, S., McGuire, J., Gaule, P., Moore, L., Acs, B., Cougot, D., et al. (2020). Quantitative assessment of PD-L1 as an analyte in immunohistochemistry diagnostic assays using a standardized cell line tissue microarray. *Lab. Invest.* 100, 4–15. doi: 10.1038/s41374-019-0295-9

Matei, I., Kim, H. S., and Lyden, D. (2017). Unshielding exosomal RNA unleashes tumor growth and metastasis. *Cell* 170, 223–225. doi: 10.1016/j.cell.2017.06.047

Matusek, T., Wendler, F., Poles, S., Pizette, S., D'Angelo, G., Furthauer, M., et al. (2014). The ESCRT machinery regulates the secretion and long-range activity of Hedgehog. *Nature* 516, 99–103. doi: 10.1038/nature13847

Maybruck, B. T., Pfannenstiel, L. W., Diaz-Montero, M., and Gastman, B. R. (2017). Tumor-derived exosomes induce CD8(+) T cell suppressors. *J. Immunother. Cancer* 5:65. doi: 10.1186/s40425-017-0269-7

Mayoux, M., Roller, A., Pulko, V., Sammicheli, S., Chen, S., Sum, E., et al. (2020). Dendritic cells dictate responses to PD-L1 blockade cancer immunotherapy. *Sci. Transl. Med.* 12:eaav7431. doi: 10.1126/scitranslmed.aav7431

Milane, L., Singh, A., Mattheolabakis, G., Suresh, M., and Amiji, M. M. (2015). Exosome mediated communication within the tumor microenvironment. *J. Control. Release* 219, 278–294. doi: 10.1016/j.jconrel.2015.06.029

Miller, B. C., Sen, D. R., Al Abosy, R., Bi, K., Virkud, Y. V., LaFleur, M. W., et al. (2019). Subsets of exhausted CD8(+) T cells differentially mediate tumor control and respond to checkpoint blockade. *Nat. Immunol.* 20, 326–336. doi: 10.1038/s41590-019-0312-6

Mimura, K., Teh, J. L., Okayama, H., Shiraishi, K., Kua, L. F., Koh, V., et al. (2018). PD-L1 expression is mainly regulated by interferon gamma associated with JAK-STAT pathway in gastric cancer. *Cancer Sci.* 109, 43–53. doi: 10.1111/cas.13424

Momen-Heravi, F., Balaj, L., Alian, S., Mantel, P. Y., Halleck, A. E., Trachtenberg, A. J., et al. (2013). Current methods for the isolation of extracellular vesicles. *Biol. Chem.* 394, 1253–1262. doi: 10.1515/hsz-2013-0141

Mondini, M., Levy, A., Meziani, L., Milliat, F., and Deutsch, E. (2020). Radiotherapy-immunotherapy combinations - perspectives and challenges. *Mol. Oncol.* 14, 1529–1537. doi: 10.1002/1878-0261.12658

Monypenny, J., Milewicz, H., Flores-Borja, F., Weitsman, G., Cheung, A., Chowdhury, R., et al. (2018). ALIX regulates tumor-mediated immunosuppression by controlling EGFR activity and PD-L1 presentation. *Cell Rep.* 24, 630–641. doi: 10.1016/j.celrep.2018.06.066

Morales-Betanzos, C. A., Lee, H., Gonzalez Ericsson, P. I., Balko, J. M., Johnson, D. B., Zimmerman, L. J., et al. (2017). Quantitative Mass Spectrometry Analysis of PD-L1 Protein Expression, N-glycosylation and Expression Stoichiometry with PD-1 and PD-L2 in Human Melanoma. *Mol. Cell Proteomics* 16, 1705–1717. doi: 10.1074/mcp.RA117.000037

Myers, G. (2018). Immune-related adverse events of immune checkpoint inhibitors: a brief review. *Curr. Oncol.* 25, 342–347. doi: 10.3747/co.25.4235

Nagai, H., and Muto, M. (2018). Optimal management of immune-related adverse events resulting from treatment with immune checkpoint inhibitors: a review and update. *Int. J. Clin. Oncol.* 23, 410–420. doi: 10.1007/s10147-018-1259-6

Nakayama, Y., Mimura, K., Kua, L. F., Okayama, H., Min, A. K. T., Saito, K., et al. (2020). Immune suppression caused by PD-L2 expression on tumor cells in gastric cancer. *Gastric Cancer*. doi: 10.1007/s10120-020-01079-z [Epub ahed of print].

Nduom, E. K., Wei, J., Yaghi, N. K., Huang, N., Kong, L. Y., Gabrusiewicz, K., et al. (2016). PD-L1 expression and prognostic impact in glioblastoma. *Neuro Oncol.* 18, 195–205. doi: 10.1093/neuonc/nov172

Newton, R., Priyadharshini, B., and Turka, L. A. (2016). Immunometabolism of regulatory T cells. *Nat. Immunol.* 17, 618–625. doi: 10.1038/ni.3466

Ng, K. W., Attig, J., Young, G. R., Ottina, E., Papamichos, S. I., Kotsianidis, I., et al. (2019). Soluble PD-L1 generated by endogenous retroelement exaptation is a receptor antagonist. *eLife* 8:e50256. doi: 10.7554/eLife.50256

Ngwa, W., Irabor, O. C., Schoenfeld, J. D., Hesser, J., Demaria, S., and Formenti, S. C. (2018). Using immunotherapy to boost the abscopal effect. *Nat. Rev. Cancer* 18, 313–322. doi: 10.1038/nrc.2018.6

Nishino, M., Giobbie-Hurder, A., Gargano, M., Suda, M., Ramaiya, N. H., and Hodi, F. S. (2013). Developing a common language for tumor response to immunotherapy: immune-related response criteria using unidimensional measurements. *Clin. Cancer Res.* 19, 3936–3943. doi: 10.1158/1078-0432.CCR-13-0895

Okuma, Y., Hosomi, Y., Nakahara, Y., Watanabe, K., Sagawa, Y., and Homma, S. (2017). High plasma levels of soluble programmed cell death ligand 1 are prognostic for reduced survival in advanced lung cancer. *Lung Cancer* 104, 1–6. doi: 10.1016/j.lungcan.2016.11.023

Olmos, Y., and Carlton, J. G. (2016). The ESCRT machinery: new roles at new holes. *Curr. Opin. Cell Biol.* 38, 1–11. doi: 10.1016/j.ceb.2015.12.001

Orme, J. J., Jazieh, K. A., Xie, T., Harrington, S., Liu, X., Ball, M., et al. (2020). ADAM10 and ADAM17 cleave PD-L1 to mediate PD-(L)1 inhibitor resistance. *Oncoimmunology* 9:1744980. doi: 10.1080/2162402X.2020.1744980

Ostrowski, M., Carmo, N. B., Krumeich, S., Fanget, I., Raposo, G., Savina, A., et al. (2010). Rab27a and Rab27b control different steps of the exosome secretion pathway. *Nat. Cell Biol.* 12, 19–30. doi: 10.1038/ncb2000

Page, D. B., Postow, M. A., Callahan, M. K., Allison, J. P., and Wolchok, J. D. (2014). Immune modulation in cancer with antibodies. *Annu. Rev. Med.* 65, 185–202. doi: 10.1146/annurev-med-092012-112807

Pang, Y., Shi, J., Yang, X., Wang, C., Sun, Z., and Xiao, R. (2020). Personalized detection of circling exosomal PD-L1 based on Fe3O4@TiO2 isolation and SERS immunoassay. *Biosens. Bioelectron.* 148:111800. doi: 10.1016/j.bios.2019.111800

Park, J. J., Omiya, R., Matsumura, Y., Sakoda, Y., Kuramasu, A., Augustine, M. M., et al. (2010). B7-H1/CD80 interaction is required for the induction and maintenance of peripheral T-cell tolerance. *Blood* 116, 1291–1298. doi: 10.1182/blood-2010-01-265975

Parry, R. V., Chemnitz, J. M., Frauwirth, K. A., Lanfranco, A. R., Braunstein, I., Kobayashi, S. V., et al. (2005). CTLA-4 and PD-1 receptors inhibit T-cell activation by distinct mechanisms. *Mol. Cell. Biol.* 25, 9543–9553. doi: 10.1128/MCB.25.21.9543-9553.2005

Patel, S. P., and Kurzrock, R. (2015). PD-L1 expression as a predictive biomarker in cancer immunotherapy. *Mol. Cancer Ther.* 14, 847–856. doi: 10.1158/1535-7163.MCT-14-0983

Patsoukis, N., Brown, J., Petkova, V., Liu, F., Li, L., and Boussiotis, V. A. (2012). Selective effects of PD-1 on Akt and Ras pathways regulate molecular components of the cell cycle and inhibit T cell proliferation. *Sci. Signal.* 5:ra46. doi: 10.1126/scisignal.2002796

Phuyal, S., Hessvik, N. P., Skotland, T., Sandvig, K., and Llorente, A. (2014). Regulation of exosome release by glycosphingolipids and flotillins. *FEBS J.* 281, 2214–2227. doi: 10.1111/febs.12775

Poggio, M., Hu, T., Pai, C. C., Chu, B., Belair, C. D., Chang, A., et al. (2019). Suppression of exosomal PD-L1 induces systemic anti-tumor immunity and memory. *Cell* 177, 414–427.e13. doi: 10.1016/j.cell.2019.02.016

Pols, M. S., and Klumperman, J. (2009). Trafficking and function of the tetraspanin CD63. *Exp. Cell Res.* 315, 1584–1592. doi: 10.1016/j.yexcr.2008.09.020

Postow, M. A., Callahan, M. K., Barker, C. A., Yamada, Y., Yuan, J., Kitano, S., et al. (2012). Immunologic correlates of the abscopal effect in a patient with melanoma. *N. Engl. J. Med.* 366, 925–931. doi: 10.1056/NEJMoa1112824

Pulaski, B. A., and Ostrand-Rosenberg, S. (2001). Mouse 4T1 breast tumor model. *Curr. Protoc. Immunol.* Chapter 20:Unit 20.2. doi: 10.1002/0471142735.im2002s39

Quail, D. F., and Joyce, J. A. (2013). Microenvironmental regulation of tumor progression and metastasis. *Nat. Med.* 19, 1423–1437. doi: 10.1038/nm.3394

Raimondo, S., Pucci, M., Alessandro, R., and Fontana, S. (2020). Extracellular vesicles and tumor-immune escape: biological functions and clinical perspectives. *Int. J. Mol. Sci.* 21:2286. doi: 10.3390/ijms21072286

Ribas, A., Hamid, O., Daud, A., Hodi, F. S., Wolchok, J. D., Kefford, R., et al. (2016). Association of pembrolizumab with tumor response and survival among patients with advanced melanoma. *JAMA* 315, 1600–1609. doi: 10.1001/jama.2016.4059

Ribas, A., and Hu-Lieskovan, S. (2016). What does PD-L1 positive or negative mean? *J. Exp. Med.* 213, 2835–2840. doi: 10.1084/jem.20161462

Ricklefs, F. L., Alayo, Q., Krenzlin, H., Mahmoud, A. B., Speranza, M. C., Nakashima, H., et al. (2018). Immune evasion mediated by PD-L1 on glioblastoma-derived extracellular vesicles. *Sci. Adv.* 4:eaar2766. doi: 10.1126/sciadv.aar2766

Riley, J. L. (2009). PD-1 signaling in primary T cells. *Immunol. Rev.* 229, 114–125. doi: 10.1111/j.1600-065X.2009.00767.x

Rodriguez-Ruiz, M. E., Vanpouille-Box, C., Melero, I., Formenti, S. C., and Demaria, S. (2018). Immunological mechanisms responsible for radiation-induced abscopal effect. *Trends Immunol.* 39, 644–655. doi: 10.1016/j.it.2018.06.001

Rollins, M. R., and Gibbons Johnson, R. M. (2017). CD80 Expressed by CD8(+) T Cells Contributes to PD-L1-Induced Apoptosis of Activated CD8(+) T Cells. *J. Immunol. Res.* 2017:7659462. doi: 10.1155/2017/7659462

Romero, Y., Wise, R., and Zolkiewska, A. (2020). Proteolytic processing of PD-L1 by ADAM proteases in breast cancer cells. *Cancer Immunol. Immunother.* 69, 43–55. doi: 10.1007/s00262-019-02437-2

Ruffner, M. A., Kim, S. H., Bianco, N. R., Francisco, L. M., Sharpe, A. H., and Robbins, P. D. (2009). B7-1/2, but not PD-L1/2 molecules, are required on IL-10-treated tolerogenic DC and DC-derived exosomes for *in vivo* function. *Eur. J. Immunol.* 39, 3084–3090. doi: 10.1002/eji.200939407

Ruivo, C. F., Adem, B., Silva, M., and Melo, S. A. (2017). The biology of cancer exosomes: insights and new perspectives. *Cancer Res.* 77, 6480–6488. doi: 10.1158/0008-5472.CAN-17-0994

Sahebi, R., Langari, H., Fathinezhad, Z., Bahari Sani, Z., Avan, A., Ghayour Mobarhan, M., et al. (2020). Exosomes: new insights into cancer mechanisms. *J. Cell. Biochem.* 121, 7–16. doi: 10.1002/jcb.29120

Sandigursky, S., and Mor, A. (2018). Immune-related adverse events in cancer patients treated with immune checkpoint inhibitors. *Curr. Rheumatol. Rep.* 20:65. doi: 10.1007/s11926-018-0770-0

Schmidt, O., and Teis, D. (2012). The ESCRT machinery. *Curr. Biol.* 22, R116–R120. doi: 10.1016/j.cub.2012.01.028

Schoneberg, J., Lee, I. H., Iwasa, J. H., and Hurley, J. H. (2017). Reverse-topology membrane scission by the ESCRT proteins. *Nat. Rev. Mol. Cell Biol.* 18, 5–17. doi: 10.1038/nrm.2016.121

Seo, N., Akiyoshi, K., and Shiku, H. (2018). Exosome-mediated regulation of tumor immunology. *Cancer Sci.* 109, 2998–3004. doi: 10.1111/cas.13735

Sharma, P., Hu-Lieskovan, S., Wargo, J. A., and Ribas, A. (2017). Primary, adaptive, and acquired resistance to cancer immunotherapy. *Cell* 168, 707–723. doi: 10.1016/j.cell.2017.01.017

Sheehan, C., and D'Souza-Schorey, C. (2019). Tumor-derived extracellular vesicles: molecular parcels that enable regulation of the immune response in cancer. *J. Cell Sci.* 132:jcs235085. doi: 10.1242/jcs.235085

Shen, X., and Zhao, B. (2018). Efficacy of PD-1 or PD-L1 inhibitors and PD-L1 expression status in cancer: meta-analysis. *BMJ* 362:k3529. doi: 10.1136/bmj.k3529

Sheppard, K. A., Fitz, L. J., Lee, J. M., Benander, C., George, J. A., Wooters, J., et al. (2004). PD-1 inhibits T-cell receptor induced phosphorylation of the ZAP70/CD3zeta signalosome and downstream signaling to PKCtheta. *FEBS Lett.* 574, 37–41. doi: 10.1016/j.febslet.2004.07.083

Shergold, A. L., Millar, R., and Nibbs, R. J. B. (2019). Understanding and overcoming the resistance of cancer to PD-1/PD-L1 blockade. *Pharmacol. Res.* 145:104258. doi: 10.1016/j.phrs.2019.104258

Shigemori, T., Toiyama, Y., Okugawa, Y., Yamamoto, A., Yin, C., Narumi, A., et al. (2019). Soluble PD-L1 Expression in Circulation as a Predictive Marker for Recurrence and Prognosis in Gastric Cancer: direct Comparison of the Clinical Burden Between Tissue and Serum PD-L1 Expression. *Ann. Surg. Oncol.* 26, 876–883. doi: 10.1245/s10434-018-07112-x

Shukuya, T., and Carbone, D. P. (2016). Predictive markers for the efficacy of Anti-PD-1/PD-L1 antibodies in lung cancer. *J. Thorac. Oncol.* 11, 976–988. doi: 10.1016/j.jtho.2016.02.015

Sibaud, V. (2018). Dermatologic reactions to immune checkpoint inhibitors : skin toxicities and immunotherapy. *Am. J. Clin. Dermatol.* 19, 345–361. doi: 10.1007/s40257-017-0336-3

Skog, J., Wurdinger, T., van Rijn, S., Meijer, D. H., Gainche, L., Sena-Esteves, M., et al. (2008). Glioblastoma microvesicles transport RNA and proteins that promote tumour growth and provide diagnostic biomarkers. *Nat. Cell Biol.* 10, 1470–1476. doi: 10.1038/ncb1800

Skowyra, M. L., Schlesinger, P. H., Naismith, T. V., and Hanson, P. I. (2018). Triggered recruitment of ESCRT machinery promotes endolysosomal repair. *Science* 360:eaar5078. doi: 10.1126/science.aar5078

Solinas, C., Aiello, M., Rozali, E., Lambertini, M., Willard-Gallo, K., and Migliori, E. (2020). Programmed Cell Death-Ligand 2: a neglected but important target in the immune response to cancer? *Transl. Oncol.* 13:100811. doi: 10.1016/j.tranon.2020.100811

Steidl, C., Shah, S. P., Woolcock, B. W., Rui, L., Kawahara, M., Farinha, P., et al. (2011). MHC class II transactivator CIITA is a recurrent gene fusion partner in lymphoid cancers. *Nature* 471, 377–381. doi: 10.1038/nature09754

Stoorvogel, W. (2015). Resolving sorting mechanisms into exosomes. *Cell Res.* 25, 531–532. doi: 10.1038/cr.2015.39

Stovgaard, E. S., Dyhl-Polk, A., Roslind, A., Balslev, E., and Nielsen, D. (2019). PD-L1 expression in breast cancer: expression in subtypes and prognostic significance: a systematic review. *Breast Cancer Res. Treat.* 174, 571–584. doi: 10.1007/s10549-019-05130-1

Sugiura, D., Maruhashi, T., Okazaki, I. M., Shimizu, K., Maeda, T. K., Takemoto, T., et al. (2019). Restriction of PD-1 function by cis-PD-L1/CD80 interactions is required for optimal T cell responses. *Science* 364, 558–566. doi: 10.1126/science.aav7062

Sui, H., Ma, N., Wang, Y., Li, H., Liu, X., Su, Y., et al. (2018). Anti-PD-1/PD-L1 Therapy for Non-Small-Cell Lung Cancer: toward Personalized Medicine and Combination Strategies. *J. Immunol. Res.* 2018, 6984948. doi: 10.1155/2018/6984948

Sun, C., Mezzadra, R., and Schumacher, T. N. (2018). Regulation and Function of the PD-L1 Checkpoint. *Immunity* 48, 434–452. doi: 10.1016/j.immuni.2018.03.014

Sunshine, J. C., Nguyen, P. L., Kaunitz, G. J., Cottrell, T. R., Berry, S., Esandrio, J., et al. (2017). PD-L1 expression in melanoma: a quantitative immunohistochemical antibody comparison. *Clin. Cancer Res.* 23, 4938–4944. doi: 10.1158/1078-0432.CCR-16-1821

Szymanska, E., Budick-Harmelin, N., and Miaczynska, M. (2018). Endosomal "sort" of signaling control: the role of ESCRT machinery in regulation of receptor-mediated signaling pathways. *Semin. Cell Dev. Biol.* 74, 11–20. doi: 10.1016/j.semcdb.2017.08.012

Takeuchi, M., Doi, T., Obayashi, K., Hirai, A., Yoneda, K., Tanaka, F., et al. (2018). Soluble PD-L1 with PD-1-binding capacity exists in the plasma of patients with non-small cell lung cancer. *Immunol. Lett.* 196, 155–160. doi: 10.1016/j.imlet.2018.01.007

Tanegashima, T., Togashi, Y., Azuma, K., Kawahara, A., Ideguchi, K., Sugiyama, D., et al. (2019). Immune suppression by PD-L2 against spontaneous and treatment-related antitumor immunity. *Clin. Cancer Res.* 25, 4808–4819. doi: 10.1158/1078-0432.CCR-18-3991

Tang, H., Liang, Y., Anders, R. A., Taube, J. M., Qiu, X., Mulgaonkar, A., et al. (2018). PD-L1 on host cells is essential for PD-L1 blockade-mediated tumor regression. *J. Clin. Invest.* 128, 580–588. doi: 10.1172/JCI96061

Tang, S., and Kim, P. S. (2019). A high-affinity human PD-1/PD-L2 complex informs avenues for small-molecule immune checkpoint drug discovery. *Proc. Natl. Acad. Sci. U.S.A.* 116, 24500–24506. doi: 10.1073/pnas.1916916116

Tang, Y., Zhang, P., Wang, Y., Wang, J., Su, M., Wang, Y., et al. (2020). The biogenesis, biology, and clinical significance of exosomal PD-L1 in cancer. *Front. Immunol.* 11:604. doi: 10.3389/fimmu.2020.00604

Taube, J. M., Klein, A., Brahmer, J. R., Xu, H., Pan, X., Kim, J. H., et al. (2014). Association of PD-1, PD-1 ligands, and other features of the tumor immune microenvironment with response to anti-PD-1 therapy. *Clin. Cancer Res.* 20, 5064–5074. doi: 10.1158/1078-0432.CCR-13-3271

Teixido, C., Vilarino, N., Reyes, R., and Reguart, N. (2018). PD-L1 expression testing in non-small cell lung cancer. *Ther. Adv. Med. Oncol.* 10:1758835918763493. doi: 10.1177/1758835918763493

Theodoraki, M. N., Hoffmann, T. K., and Whiteside, T. L. (2018a). Separation of plasma-derived exosomes into CD3((+) and CD3((-) fractions allows for association of immune cell and tumour cell markers with disease activity in HNSCC patients. *Clin. Exp. Immunol.* 192, 271–283. doi: 10.1111/cei.13113

Theodoraki, M. N., Yerneni, S., Gooding, W. E., Ohr, J., Clump, D. A., Bauman, J. E., et al. (2019). Circulating exosomes measure responses to therapy in head and neck cancer patients treated with cetuximab, ipilimumab, and IMRT. *Oncoimmunology* 8:1593805. doi: 10.1080/2162402X.2019.1593805

Theodoraki, M. N., Yerneni, S. S., Hoffmann, T. K., Gooding, W. E., and Whiteside, T. L. (2018b). Clinical significance of PD-L1(+) exosomes in plasma of head and neck cancer patients. *Clin. Cancer Res.* 24, 896–905. doi: 10.1158/1078-0432.CCR-17-2664

Thery, C., Amigorena, S., Raposo, G., and Clayton, A. (2006). Isolation and characterization of exosomes from cell culture supernatants and biological fluids. *Curr. Protoc. Cell Biol.* Chapter 3:Unit 3.22. doi: 10.1002/0471143030.cb0322s30

Tkach, M., Kowal, J., and Thery, C. (2018). Why the need and how to approach the functional diversity of extracellular vesicles. *Philos. Trans. R. Soc. Lond. B Biol. Sci.* 373:20160479. doi: 10.1098/rstb.2016.0479

Tkach, M., and Thery, C. (2016). Communication by extracellular vesicles: Where we are and where we need to go. *Cell* 164, 1226–1232. doi: 10.1016/j.cell.2016.01.043

Trajkovic, K., Hsu, C., Chiantia, S., Rajendran, L., Wenzel, D., Wieland, F., et al. (2008). Ceramide triggers budding of exosome vesicles into multivesicular endosomes. *Science* 319, 1244–1247. doi: 10.1126/science.1153124

Ueki, Y., Suzuki, M., Horikawa, Y., Watanabe, H., Yamaguchi, Y., Morita, C., et al. (2020). Pembrolizumab-induced pancytopenia in a patient with squamous cell lung cancer. *Thorac. Cancer*. doi: 10.1111/1759-7714.13582 [Epub ahead of print].

van Niel, G., D'Angelo, G., and Raposo, G. (2018). Shedding light on the cell biology of extracellular vesicles. *Nat. Rev. Mol. Cell Biol.* 19, 213–228. doi: 10.1038/nrm.2017.125

Varricchi, G., Marone, G., Mercurio, V., Galdiero, M. R., Bonaduce, D., and Tocchetti, C. G. (2018). Immune checkpoint inhibitors and cardiac toxicity: an emerging issue. *Curr. Med. Chem.* 25, 1327–1339. doi: 10.2174/0929867324666170407125017

Wan, B., Nie, H., Liu, A., Feng, G., He, D., Xu, R., et al. (2006). Aberrant regulation of synovial T cell activation by soluble costimulatory molecules in rheumatoid arthritis. *J. Immunol.* 177, 8844–8850. doi: 10.4049/jimmunol.177.12.8844

Wan, Z., Gao, X., Dong, Y., Zhao, Y., Chen, X., Yang, G., et al. (2018). Exosome-mediated cell-cell communication in tumor progression. *Am. J. Cancer Res.* 8, 1661–1673.

Wanchoo, R., Karam, S., Uppal, N. N., Barta, V. S., Deray, G., Devoe, C., et al. (2017). Adverse renal effects of immune checkpoint inhibitors: a narrative review. *Am. J. Nephrol.* 45, 160–169. doi: 10.1159/000455014

Wang, Q., Liu, F., and Liu, L. (2017). Prognostic significance of PD-L1 in solid tumor: an updated meta-analysis. *Medicine* 96:e6369. doi: 10.1097/MD.0000000000006369

Wang, Q., Zhang, J., Tu, H., Liang, D., Chang, D. W., Ye, Y., et al. (2019). Soluble immune checkpoint-related proteins as predictors of tumor recurrence, survival, and T cell phenotypes in clear cell renal cell carcinoma patients. *J. Immunother. Cancer* 7:334. doi: 10.1186/s40425-019-0810-y

Wang, T., Nasser, M. I., Shen, J., Qu, S., He, Q., and Zhao, M. (2019). Functions of exosomes in the triangular relationship between the tumor, inflammation, and immunity in the tumor microenvironment. *J. Immunol. Res.* 2019:4197829. doi: 10.1155/2019/4197829

Wang, X., Wang, G., Wang, Z., Liu, B., Han, N., Li, J., et al. (2019). PD-1-expressing B cells suppress CD4(+) and CD8(+) T cells via PD-1/PD-L1-dependent pathway. *Mol. Immunol.* 109, 20–26. doi: 10.1016/j.molimm.2019.02.009

Wang, X., Yang, L., Huang, F., Zhang, Q., Liu, S., Ma, L., et al. (2017). Inflammatory cytokines IL-17 and TNF-alpha up-regulate PD-L1 expression in human prostate and colon cancer cells. *Immunol. Lett.* 184, 7–14. doi: 10.1016/j.imlet.2017.02.006

Weinmann, S. C., and Pisetsky, D. S. (2019). Mechanisms of immune-related adverse events during the treatment of cancer with immune checkpoint inhibitors. *Rheumatology* 58, vii59–vii67. doi: 10.1093/rheumatology/kez308

Williams, S. G., Mollaeian, A., Katz, J. D., and Gupta, S. (2020). Immune checkpoint inhibitor-induced inflammatory arthritis: identification and management. *Expert Rev. Clin. Immunol.* doi: 10.1080/1744666X.2020.1804362 [Epub ahead of print].

Wolf, Y., Anderson, A. C., and Kuchroo, V. K. (2019). TIM3 comes of age as an inhibitory receptor. *Nat. Rev. Immunol.* 20, 173–185. doi: 10.1038/s41577-019-0224-6

Wolkow, N., Jakobiec, F. A., Afrogheh, A. H., Pai, S. I., and Faquin, W. C. (2020). High expression of PD-L1 and PD-L2 in ophthalmic sebaceous carcinoma: the case for a clinical trial of checkpoint inhibitors. *Am. J. Ophthalmol.* (in press). doi: 10.1016/j.ajo.2020.07.031

Wortzel, I., Dror, S., Kenific, C. M., and Lyden, D. (2019). Exosome-mediated metastasis: communication from a distance. *Dev. Cell* 49, 347–360. doi: 10.1016/j.devcel.2019.04.011

Wu, Q., Jiang, L., Li, S. C., He, Q. J., Yang, B., and Cao, J. (2020). Small molecule inhibitors targeting the PD-1/PD-L1 signaling pathway. *Acta Pharmacol. Sin.* doi: 10.1038/s41401-020-0366-x [Epub ahead of print].

Xia, A., Zhang, Y., Xu, J., Yin, T., and Lu, X. J. (2019). T cell dysfunction in cancer immunity and immunotherapy. *Front. Immunol.* 10:1719. doi: 10.3389/fimmu.2019.01719

Xie, C., Ji, N., Tang, Z., Li, J., and Chen, Q. (2019). The role of extracellular vesicles from different origin in the microenvironment of head and neck cancers. *Mol. Cancer* 18:83. doi: 10.1186/s12943-019-0985-3

Xie, F., Xu, M., Lu, J., Mao, L., and Wang, S. (2019). The role of exosomal PD-L1 in tumor progression and immunotherapy. *Mol. Cancer* 18:146. doi: 10.1186/s12943-019-1074-3

Xu, G., Sun, L., Li, Y., Xie, F., Zhou, X., Yang, H., et al. (2019). The clinicopathological and prognostic value of PD-L1 expression in cholangiocarcinoma: a meta-analysis. *Front. Oncol.* 9:897. doi: 10.3389/fonc.2019.00897

Xu, R., Greening, D. W., Zhu, H. J., Takahashi, N., and Simpson, R. J. (2016). Extracellular vesicle isolation and characterization: toward clinical application. *J. Clin. Invest.* 126, 1152–1162. doi: 10.1172/JCI81129

Xu, Y., Wu, Y., Zhang, S., Ma, P., Jin, X., Wang, Z., et al. (2019). A tumor-specific super-enhancer drives immune evasion by guiding synchronous expression of PD-L1 and PD-L2. *Cell Rep.* 29:3435. doi: 10.1016/j.celrep.2019.10.093

Xu-Monette, Z. Y., Zhang, M., Li, J., and Young, K. H. (2017). PD-1/PD-L1 blockade: Have we found the key to unleash the antitumor immune response? *Front. Immunol.* 8:1597. doi: 10.3389/fimmu.2017.01597

Yaghoubi, N., Soltani, A., Ghazvini, K., Hassanian, S. M., and Hashemy, S. I. (2019). PD-1/ PD-L1 blockade as a novel treatment for colorectal cancer. *Biomed. Pharmacother.* 110, 312–318. doi: 10.1016/j.biopha.2018.11.105

Yanez-Mo, M., Siljander, P. R., Andreu, Z., Zavec, A. B., Borras, F. E., Buzas, E. I., et al. (2015). Biological properties of extracellular vesicles and their physiological functions. *J. Extracell. Vesicles* 4:27066. doi: 10.3402/jev.v4.27066

Yang, F., Liao, X., Tian, Y., and Li, G. (2017). Exosome separation using microfluidic systems: size-based, immunoaffinity-based and dynamic methodologies. *Biotechnol. J.* 12:1600699. doi: 10.1002/biot.201600699

Yang, Y., Li, C. W., Chan, L. C., Wei, Y., Hsu, J. M., Xia, W., et al. (2018). Exosomal PD-L1 harbors active defense function to suppress T cell killing of breast cancer cells and promote tumor growth. *Cell Res.* 28, 862–864. doi: 10.1038/s41422-018-0060-4

Yang, Z., Shi, J., Xie, J., Wang, Y., Sun, J., Liu, T., et al. (2020). Large-scale generation of functional mRNA-encapsulating exosomes via cellular nanoporation. *Nat. Biomed. Eng.* 4, 69–83. doi: 10.1038/s41551-019-0485-1

Yearley, J. H., Gibson, C., Yu, N., Moon, C., Murphy, E., Juco, J., et al. (2017). PD-L2 expression in human tumors: relevance to anti-PD-1 therapy in cancer. *Clin. Cancer Res.* 23, 3158–3167. doi: 10.1158/1078-0432.CCR-16-1761

Yekula, A., Minciacchi, V. R., Morello, M., Shao, H., Park, Y., Zhang, X., et al. (2020). Large and small extracellular vesicles released by glioma cells *in vitro* and *in vivo*. *J. Extracell. Vesicles* 9:1689784. doi: 10.1080/20013078.2019.1689784

Yekula, A., Yekula, A., Muralidharan, K., Kang, K., Carter, B. S., and Balaj, L. (2019). Extracellular vesicles in glioblastoma tumor microenvironment. *Front. Immunol.* 10:3137. doi: 10.3389/fimmu.2019.03137

Yokosuka, T., Takamatsu, M., Kobayashi-Imanishi, W., Hashimoto-Tane, A., Azuma, M., and Saito, T. (2012). Programmed cell death 1 forms negative costimulatory microclusters that directly inhibit T cell receptor signaling by recruiting phosphatase SHP2. *J. Exp. Med.* 209, 1201–1217. doi: 10.1084/jem.20112741

Youngnak, P., Kozono, Y., Kozono, H., Iwai, H., Otsuki, N., Jin, H., et al. (2003). Differential binding properties of B7-H1 and B7-DC to programmed death-1. *Biochem. Biophys. Res. Commun.* 307, 672–677. doi: 10.1016/s0006-291x(03)01257-9

Yu, H., Boyle, T. A., Zhou, C., Rimm, D. L., and Hirsch, F. R. (2016). PD-L1 expression in lung cancer. *J. Thorac. Oncol.* 11, 964–975. doi: 10.1016/j.jtho.2016.04.014

Zerdes, I., Matikas, A., Bergh, J., Rassidakis, G. Z., and Foukakis, T. (2018). Genetic, transcriptional and post-translational regulation of the programmed death protein ligand 1 in cancer: biology and clinical correlations. *Oncogene* 37, 4639–4661. doi: 10.1038/s41388-018-0303-3

Zhang, L., and Yu, D. (2019). Exosomes in cancer development, metastasis, and immunity. *Biochim. Biophys. Acta Rev. Cancer* 1871, 455–468. doi: 10.1016/j.bbcan.2019.04.004

Zhang, Y., Liu, Y., Liu, H., and Tang, W. H. (2019). Exosomes: biogenesis, biologic function and clinical potential. *Cell Biosci.* 9:19. doi: 10.1186/s13578-019-0282-2

Zhao, Y., Lee, C. K., Lin, C. H., Gassen, R. B., Xu, X., Huang, Z., et al. (2019). PD-L1:CD80 Cis-Heterodimer Triggers the Co-stimulatory Receptor CD28 While Repressing the Inhibitory PD-1 and CTLA-4 Pathways. *Immunity* 51, 1059–1073.e9. doi: 10.1016/j.immuni.2019.11.003

Zhao, Z., Fan, J., Hsu, Y. S., Lyon, C. J., Ning, B., and Hu, T. Y. (2019). Extracellular vesicles as cancer liquid biopsies: from discovery, validation, to clinical application. *Lab Chip* 19, 1114–1140. doi: 10.1039/c8lc01123k

Zhou, J., Mahoney, K. M., Giobbie-Hurder, A., Zhao, F., Lee, S., Liao, X., et al. (2017). Soluble PD-L1 as a biomarker in malignant melanoma treated with checkpoint blockade. *Cancer Immunol. Res.* 5, 480–492. doi: 10.1158/2326-6066.CIR-16-0329

Zhou, K., Guo, S., Tong, S., Sun, Q., Li, F., Zhang, X., et al. (2018). Immunosuppression of human adipose-derived stem cells on t cell subsets via the reduction of NF-kappaB activation mediated by PD-L1/PD-1 and Gal-9/TIM-3 Pathways. *Stem Cells Dev.* 27, 1191–1202. doi: 10.1089/scd.2018.0033

Zou, W., Wolchok, J. D., and Chen, L. (2016). PD-L1 (B7-H1) and PD-1 pathway blockade for cancer therapy: mechanisms, response biomarkers, and combinations. *Sci. Transl. Med.* 8:328rv4. doi: 10.1126/scitranslmed.aad7118

Conflict of Interest: The authors declare that the research was conducted in the absence of any commercial or financial relationships that could be construed as a potential conflict of interest.

frontiers in Cell and Developmental Biology

BRIEF RESEARCH REPORT
published: 27 November 2020
doi: 10.3389/fcell.2020.592518

Transcriptome Reprogramming of CD11b$^+$ Bone Marrow Cells by Pancreatic Cancer Extracellular Vesicles

*Joana Maia[1,2], Andreia Hanada Otake[1,3], Juliana Poças[4,5,6], Ana Sofia Carvalho[7], Hans Christian Beck[8], Ana Magalhães[4,5], Rune Matthiesen[7], Maria Carolina Strano Moraes[1] and Bruno Costa-Silva[1]**

[1] Champalimaud Centre for the Unknown, Champalimaud Foundation, Lisbon, Portugal, [2] Graduate Program in Areas of Basic and Applied Biology, University of Porto, Porto, Portugal, [3] Center for Translational Research in Oncology, Instituto do Câncer do Estado de São Paulo, Hospital das Clínicas, Faculdade de Medicina da Universidade de São Paulo, São Paulo, Brazil, [4] i3S – Instituto de Investigação e Inovação em Saúde, Universidade do Porto, Porto, Portugal, [5] IPATIMUP – Instituto de Patologia e Imunologia Molecular da Universidade do Porto, Porto, Portugal, [6] Instituto de Ciências Biomédicas Abel Salazar, University of Porto, Porto, Portugal, [7] Computational and Experimental Biology Group, CEDOC, Chronic Diseases Research Centre, NOVA Medical School, Faculdade de Ciencias Medicas, Universidade NOVA de Lisboa, Lisbon, Portugal, [8] Centre for Clinical Proteomics, Department of Clinical Biochemistry and Pharmacology, Odense University Hospital, Odense, Denmark

OPEN ACCESS

Edited by:
Rodrigo Nalio Ramos, Institut Curie, France

Reviewed by:
Michele Bernasconi, University Children's Hospital Bern, Switzerland
Tarcio Teodoro Braga, Federal University of Paraná, Brazil

***Correspondence:**
Bruno Costa-Silva
bruno.costa-silva@research.fchampalimaud.org

Specialty section:
This article was submitted to Molecular Medicine, a section of the journal Frontiers in Cell and Developmental Biology

Received: 07 August 2020
Accepted: 27 October 2020
Published: 27 November 2020

Citation:
Maia J, Otake AH, Poças J, Carvalho AS, Beck HC, Magalhães A, Matthiesen R, Strano Moraes MC and Costa-Silva B (2020) Transcriptome Reprogramming of CD11b$^+$ Bone Marrow Cells by Pancreatic Cancer Extracellular Vesicles. Front. Cell Dev. Biol. 8:592518. doi: 10.3389/fcell.2020.592518

Pancreatic cancers (PC) are highly metastatic with poor prognosis, mainly due to delayed detection. We previously showed that PC-derived extracellular vesicles (EVs) act on macrophages residing in the liver, eliciting extracellular matrix remodeling in this organ and marked hepatic accumulation of CD11b$^+$ bone marrow (BM) cells, which support PC liver metastasis. We here show that PC-EVs also bind to CD11b$^+$ BM cells and induce the expansion of this cell population. Transcriptomic characterization of these cells shows that PC-EVs upregulate IgG and IgA genes, which have been linked to the presence of monocytes/macrophages in tumor microenvironments. We also report here the transcriptional downregulation of genes linked to monocyte/macrophage activation, trafficking, and expression of inflammatory molecules. Together, these results show for the first time the existence of a PC–BM communication axis mediated by EVs with a potential role in PC tumor microenvironments.

Keywords: tumor microenvironment, extracellular vesicles, macrophages, monocytes, metastasis, pancreatic cancer, exosomes, cancer

INTRODUCTION

Pancreatic cancer is the fourth leading cause of cancer-related deaths in the world, displaying a 5-year survival rate of about 6% and a median survival rate of about 6 months. Among pancreatic cancers, pancreatic ductal adenocarcinoma (PC) is the most common type and accounts for more than 90% of cases (Saif, 2011). A combination of factors leads to the poor prognosis of PC, including difficulties in detecting early stage disease, its high metastatic potential, and its resistance to conventional therapies. Current predictions report a worldwide escalation in the incidence of this disease and an over twofold increase in the number of new PC cases, as well as related deaths, by 2030 (Ying et al., 2016; Foucher et al., 2018).

Tumors do not exist as isolated entities, but as complex systemic networks involving cell–cell communication between transformed and non-transformed cells. The milieu created by tumor-associated cells can be composed by both local cells and cells recruited from distant sites, such as the bone marrow (BM) (Bergfeld and DeClerck, 2010), creating a tumor microenvironment thought to be a key modulator of tumor progression by providing either inhibitory or stimulatory growth signals (Bissell and Hines, 2011). In sites distant from the primary tumor, non-tumor cells can also be hijacked in order to prepare the future metastatic sites that support engraftment and survival of metastatic cells (Bergfeld and DeClerck, 2010; Lee and Margolin, 2011). Besides direct cell-to-cell communication, secreted factors play a key role in the interaction among cells. Of these, extracellular vesicles (EVs) have emerged as novel cell–cell communication players in setting up and modifying tumor microenvironments (Record et al., 2014; Maia et al., 2018).

Extracellular vesicles are vesicles released by both prokaryotic and eukaryotic cells, being involved in various physiological and pathological processes (Kalluri and LeBleu, 2020). Microvesicles and exosomes are prevalent types of EVs in biofluids. Microvesicles are generated by the direct outward budding of the plasma membrane, and they range in size from ∼100 to 1,000 nm (Stahl and Raposo, 2019). In contrast, exosomes have an endosomal origin and fall within a size range of ∼30 to 150 nm in diameter (Maia et al., 2018; Stahl and Raposo, 2019). Regardless of their type, EVs can harbor biomolecules such as proteins, DNAs, messenger RNAs, microRNAs, and other RNAs (Nolte-'t Hoen et al., 2012). Due to their cargo and capacity to transfer information both locally and to distant sites, consensus has lately emerged on their role as "signal-transducing agents" (Stahl and Raposo, 2019).

The role of EVs in oncology is currently an active area of research. We have recently described a previously unknown prometastatic circuit in which pancreatic cancer-derived EVs can induce the formation of liver premetastatic niches (LPMN) that foster metastatic development (Costa-Silva et al., 2015; Hoshino et al., 2015). We demonstrated that EVs derived from malignant pancreatic lesions play a key role in LPMN initiation by being specifically taken up by Kupffer cells (KC) in the liver, where they activate fibrotic pathways and promote a pro-inflammatory milieu that ultimately supports metastasis. In particular, we showed that exosomal macrophage migration inhibitory factor (MIF) induces the release of transforming growth factor β (TGF-β) by KCs, which, in turn, promotes activation and fibronectin production by hepatic stellate cells. Fibronectin deposits subsequently promote the arrest of CD11b$^+$ BM-derived cells in the liver, completing the formation of the LPMN (Costa-Silva et al., 2015). Although we showed that BM cells are a key component of the LPMN, it is still unknown whether PC-EVs have a potential direct effect in BM cells and in their phenotypes.

Considering that virtually any cell in the body is a potential target for these tumor-derived messages, the identification of novel cellular circuits induced by tumor-derived EVs will help to further elucidate the cellular mechanisms involved in oncologic diseases. In this work, we show that PC-EVs preferentially bind to CD11b$^+$ BM cells and induce the expansion of this cell population. Additionally, PC-EVs induce phenotypic changes in CD11b$^+$ BM cells with potential relevance to the dynamics of the tumor microenvironments. Together, these results demonstrate the existence of a PC–BM communication axis mediated by EVs with a potential role in PC tumor microenvironments.

MATERIALS AND METHODS

Cells

The C57Bl/6 murine pancreatic adenocarcinoma PAN02 (also identified as Panc02) was purchased from the DTP, DCTD Tumor Repository, NIH. Cells were cultured in RPMI supplemented with 10% fetal bovine serum (FBS, Biowest S181BH-500, Nuaillé, France) and 1% penicillin–streptomycin (Gibco 15-140-122, United States), and maintained at 37°C with 5% CO_2 levels. For conditioning, cells were cultured in RPMI supplemented with 1% penicillin–streptomycin and 10% EV-depleted FBS. FBS was depleted of bovine EVs by ultracentrifugation at 100,000 *g* for 140 min. For the preparation of the conditioned medium, 1×10^6 PAN02 cells were seeded in 150 mm culture dishes containing 20 ml of medium, and the conditioned medium was collected after 72 h of culture.

EV Isolation

The EV isolation/purification procedure was performed as previously described (Ferreira et al., 2019). Specifically, the conditioned medium was submitted to two initial centrifugations (10 min, 500 *g* and 20 min, 3,000 *g*) to remove any suspended or dead cells in the medium. To remove large EVs, media was centrifuged (20 min, 12,000 *g*) and the pellet was discarded. The supernatant enriched in small EVs was again centrifuged (2 h 20 min, 100,000 *g*), and the EV-enriched pellet was collected. For sucrose cushion purification, this pellet was resuspended in 14 ml filtered phosphate buffered saline (PBS, Corning 15313581, NY, United States) and added to the top of 4 ml sucrose solution (D2O containing 1.2 g of protease-free sucrose and 96 mg of *Tris* base adjusted to pH 7.4). A new ultracentrifugation was performed (1 h 10 min, 100,000 *g*), after which 4 ml of the sucrose fraction was collected using a 18G needle placed at the bottom of the ultracentrifugation tube (away from the pellet). Finally, 16 ml of PBS was added to the collected sucrose/EV solution and an overnight (16 h, 100,000 *g*) ultracentrifugation was performed. The pellet containing the isolated EVs was resuspended in filtered PBS.

All solutions used (PBS and sucrose cushion) were sterile (0.22 μm membrane-filtered). All centrifugation steps were performed in refrigerated conditions (10°C), and ultracentrifugation was performed with rotors 50.4Ti or 70Ti (Beckman-Coulter, CA, United States).

EV Labeling

For EV-tracking experiments, purified EVs were fluorescently labeled using PKH67 membrane dye (PKH67GL-1KT, Sigma-Aldrich, Germany). The staining was performed during the

isolation protocol according to the manufacturer's instructions. Briefly, labeling was done before the sucrose cushion step. After the fraction with labeled EVs (4 ml) was collected, the isolation protocol was performed as previously stated.

EV Characterization

All EV samples were analyzed for particle concentration and size distribution by the NS300 Nanoparticle Tracking Analysis (NTA) system with red laser (638 nm) (NanoSight – Malvern Panalytical, United Kingdom). Samples were prediluted in filtered PBS to achieve a concentration within the range for optimal NTA analysis. Video acquisitions were performed using a camera level of 16 and a threshold between 5 and 7. Five to nine videos of 30 s each were captured per sample. Analysis of particle concentration per milliliter and size distribution were performed with the NTA software v3.4.

Additionally, protein quantification of the EV preparations was assessed by BCA assay (Pierce^{TM} BCA Protein Assay kit, Thermo Fisher Scientific).

EV Treatment

All mouse work was performed in accordance with national animal experimentation guidelines (DGAV), animal protocol 0421/000/000/2018. Adult C57Bl/6 female mice (5 to 8 weeks old) were used for all experimental procedures. Mice were anesthetized using isoflurane 1.5–3%. Five micrograms of EVs were injected into the retro-orbital venous sinus in a total volume of 100 μl filtered PBS. For education experiments, mice received 5 μg of EVs every other day, three times per week for 3 weeks. In the experiments involving evaluation of EV incorporation, labeled EVs were injected 24 h prior to tissue collection, and analysis of EV$^+$ cells was performed by flow cytometry or immunofluorescence. Unlabeled EVs were used as controls for signal specificity. For education experiments, retro-orbital injection of PBS was used in the control groups.

Flow Cytometry Analysis

For tracking of labeled EVs and phenotypical analysis of murine organs, femurs were flushed and single-cell suspensions were filtered through a 40-μm strainer. Cells were washed in PBS with 1% BSA and incubated with anti-CD11b-PerCP-Cyanine5.5 (clone M1/70, 1:100, BD Biosciences – 561114) at predetermined saturating concentrations. PKH67-labeled EV-positive cells were detected using blue laser excitation and 488 nm emission. Data for 1,000,000 cells was acquired on a BD FACS Canto^{TM} cytometer with Diva software (BD) and was analyzed using FlowJo^{TM} software (TreeStar).

Collection of BM-Derived Cells and CD11b$^+$ Magnetic Sorting

C57Bl/6 female mice were euthanized and femurs and tibiae were harvested and cleaned. The bones were flushed with cold working buffer (PBS supplemented with 0.5% BSA and 2 mM EDTA), using a 26G needle. The preparation was resuspended using a 18G needle and filtered through a 40-μm strainer. The single-cell preparation was then centrifuged (500 *g*, 10 min, 4°C) and the resulting pellet resuspended in ACK buffer. After 2 min at room temperature, the lysis was stopped by adding more working buffer and the sample was centrifuged (500 *g*, 10 min, 4°C). The pellet was resuspended in working buffer and the cells were counted.

Subsequently, cells underwent MACS bead isolation using CD11b microbeads (Miltenyi Biotec, 130-049-601, Germany), which enabled the isolation of CD11b$^+$ cells from the preparation. The CD11b$^+$ cells were counted and centrifuged (500 *g*, 10 min, 4°C) and the pellet proceeded for RNA isolation.

RNA Extraction and cDNA Preparation

Prior to RNA extraction, CD11b$^+$ BM cells were run through the QIAshredder kit (79654, Qiagen, Germany). Total RNA was isolated using the RNeasy Mini kit (74104, Qiagen), following the manufacturer's instructions, and resuspended in nuclease-free water. RNA concentration and purity were estimated by spectrophotometric absorbance (260 and 280 nm) using a Nanodrop 2000 unit (Thermo Scientific). One microgram of RNA was used to prepare cDNA using the QuantiTect Reverse Transcription Kit (205311, Qiagen), according to the manufacturer's instructions.

Illumina Strand-Specific RNA Sequencing

To analyze the genes whose expression was altered in mouse CD11b$^+$ BM cells as a result of education with PAN02 EVs, animals were grouped between the ones educated with PAN02 EVs and the control animals educated with PBS. Total RNA was then isolated as described above, and the RNA quality was assessed using Bioanalyzer. The cDNA library was generated using Kappa Stranded Total RNA with Ribo-Zero Library Preparation Kit. The resultant DNA fragments (DNA library) were sequenced in the Illumina HiSeq 4000 platform, using 150 bp paired-end sequencing reads.

For the analysis of differentially expressed genes, we used the Differential Expression for RNA-Seq tool, which is a multifactorial statistical analysis tool based on a negative binomial model. It uses a generalized linear model approach influenced by the multifactorial EdgeR method (Robinson et al., 2009). The differentially expressed genes were filtered using standard conditions (van Iterson et al., 2010; Raza and Mishra, 2012), and the genes that fulfilled both conditions were listed in the results (**Supplementary Table 1**). The conditions were as follows: fold change (≥ 2 or ≤ -2) and false discovery rate (FDR) P-value ≤ 0.05.

Primer Design

The primers used in this study were designed using Integrated DNA Technologies online software PrimerQuest Tool (Integrated DNA Technologies, Inc., United States). Primer sequences and characteristics are shown in **Supplementary Table 2**.

The amplification efficiencies of each selected gene performing quantitative RT-PCR (RT-qPCR) were evaluated using cDNA dilutions (1, 1:10, 1:100, 1:1,000, 1:10,000). The amplification efficiency *E* of all primers used was measured and all displayed high *E*-values ranging from 1.8 to 2.2 (**Supplementary Table 2**).

RT-qPCR Assay and Analysis

The qRT-PCR reactions were performed in a CFX96 Touch Real-Time PCR Detection System thermocycler (Bio-Rad, United States). The reaction mix was performed using 10 μl SsoFast EvaGreen Supermix (1725200, Bio-Rad), primers at a final concentration of 500 nM, 1 μl of cDNA, and nuclease-free water to complete a final volume of 20 μl. After PCR, a melting curve program from 65 to 95°C with 0.5°C changes was applied, and the presence of a single reaction product in each well was confirmed. All reactions were performed in duplicate and technical replicates were run on the same plate. For the analysis, the threshold value used for each plate was the one defined by the software.

The relative expression was calculated using the model proposed by M.W. Pfaffl (2001) and normalized to both *Gapdh* and *Hmbs* levels, the two reference genes used.

Mass Spectrometry

Peptide Sample Preparation

The protein solution containing SDS and dithiothreitol (DTT) was loaded onto filtering columns and washed exhaustively with 8 M urea in HEPES buffer (Wisniewski et al., 2009). Proteins were reduced with DTT and alkylated with IAA. Protein digestion was performed by overnight digestion with trypsin sequencing grade (Promega).

Nano-LC-MSMS Analysis

Peptide samples were analyzed by nano-LC-MSMS (Dionex RSLCnano 3000) coupled to a Q-Exactive Orbitrap mass spectrometer (Thermo Scientific). Briefly, the samples (5 μl) were loaded onto a custom-made fused capillary precolumn (2 cm length, 360 μm OD, 75 μm ID) with a flow of 5 μl per min for 7 min. Trapped peptides were separated on a custom-made fused capillary column (20 cm length, 360 μm outer diameter, 75 μm inner diameter) packed with ReproSil-Pur C18 3-μm resin (Dr. Maish, Ammerbuch-Entringen, Germany) with a flow of 300 nl per minute using a linear gradient from 92% A (0.1% formic acid) to 28% B (0.1% formic acid in 100 acetonitrile) over 93 min followed by a linear gradient from 28 to 35% B over 20 min at a flow rate of 300 nl per minute. Mass spectra were acquired in positive ion mode applying automatic data-dependent switch between one Orbitrap survey MS scan in the mass range of 400 to 1,200 *m*/*z* followed by higher-energy collisional dissociation (HCD) fragmentation and Orbitrap detection of the 15 most intense ions observed in the MS scan. Target value in the Orbitrap for MS scan was 1,000,000 ions at a resolution of 70,000 at *m*/*z* 200. Fragmentation in the HCD cell was performed at normalized collision energy of 31 eV. Ion selection threshold was set to 25,000 counts and maximum injection time was 100 ms for MS scans and 300 and 500 ms for MSMS scans. Selected sequenced ions were dynamically excluded for 45 s.

Database Search

The obtained data from the X LC-MS runs were searched using VEMS (Matthiesen et al., 2012; Carvalho et al., 2014) and MaxQuant (Cox and Mann, 2008). A standard proteome database from UniProt (3AUP000005640), in which common contaminants were included, was also searched. Trypsin cleavage allowing a maximum of four missed cleavages was used. Carbamidomethyl cysteine was included as fixed modification. Methionine oxidation, N-terminal protein acetylation, and S, T, and Y phosphorylation were included as variable modifications; 5 ppm mass accuracy was specified for precursor ions and 0.01 *m*/*z* for fragment ions. The FDR for protein identification was set to 1% for peptide and protein identifications. No restriction was applied for minimal peptide length for VEMS search. Identified proteins were divided into evidence groups as defined (Matthiesen et al., 2012).

Negative-Staining Transmission Electron Microscopy

Extracellular vesicles were visualized by transmission electron microscopy (TEM) using negative staining. For this, 10 μl of the sample solution was mounted on formvar/carbon film-coated mesh nickel grids (Electron Microscopy Sciences, Hatfield, PA, United States). The excess liquid was removed with filter paper, and 10 μl of 1% uranyl acetate was added onto the grids. Visualization was carried out on a JEOL JEM 1400 TEM at 120 kV (Tokyo, Japan). Images were digitally recorded using a CCD digital camera (Orious 1100W Tokyo, Japan).

Statistical and Pathway Analysis

Error bars in graphical data represent means ± SEM. Statistical significance was determined using a two-tailed Student's *t*-test or by ANOVA. $P < 0.05$ was considered statistically significant. Statistical analyses were performed using the GraphPad Prism software (GraphPad software). No statistical method was used to predetermine sample size. The experiments were not randomized, and the investigators were not blinded to allocation during the experiments and outcome assessment.

Accession Codes

The raw sequencing data (**Supplementary Table 1**) have been deposited in the GEO database under accession number GSE156071.

RESULTS

Isolated EVs were characterized for morphology and size by transmission electron microscopy (**Figure 1A**) and for size distribution by Nanoparticle Tracking Analysis (**Figure 1B**) and the expression of proteins commonly identified in EVs (**Figure 1C**). Currently, there are no available methods to isolate EVs expressing endosomal features and consensus on markers

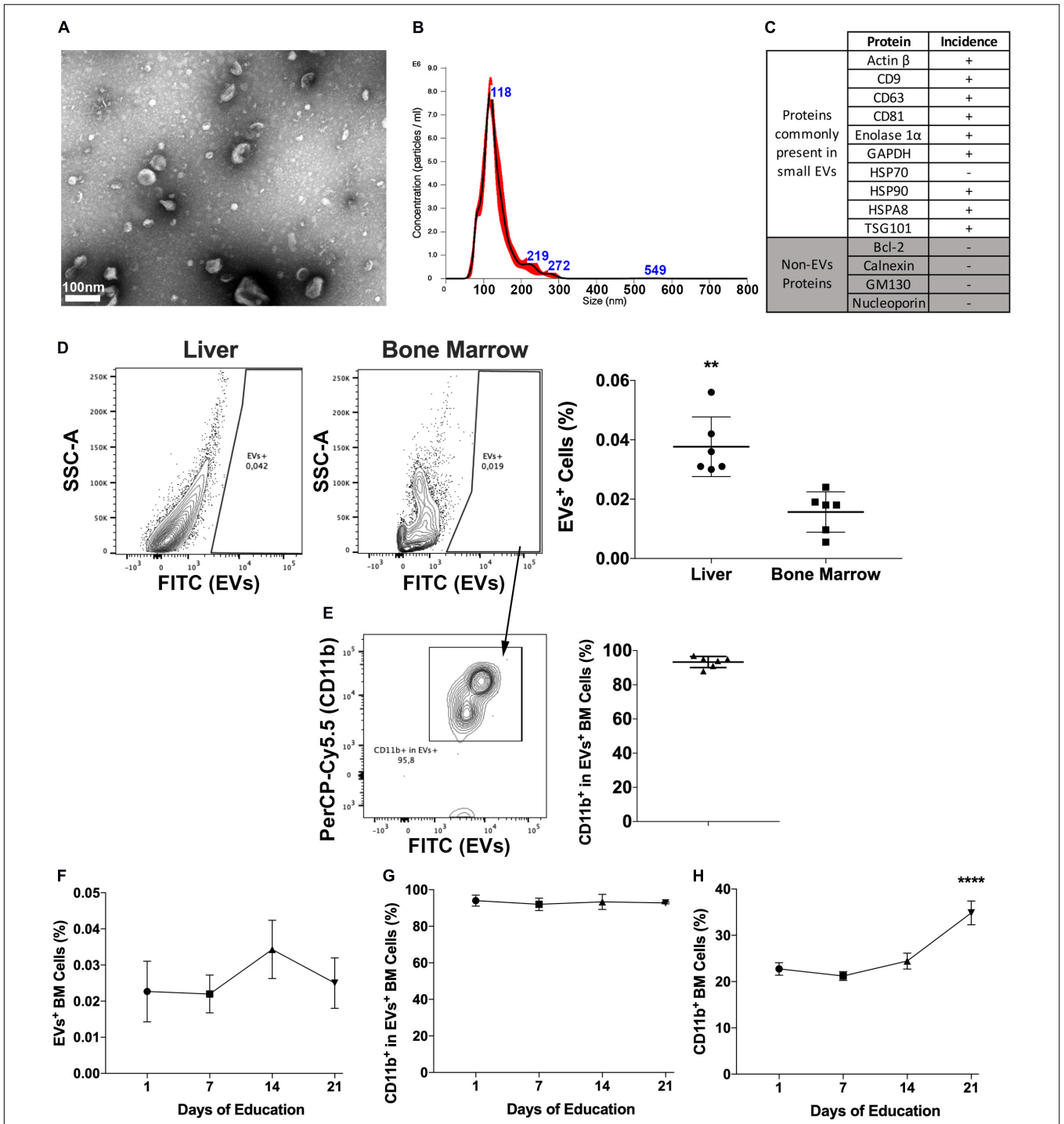

FIGURE 1 | Pancreatic cancers-derived EVs binding to BM cells. **(A)** Representative transmission electron microscopy of PAN02 EVs. **(B)** Representative Nanoparticle Tracking Analysis of PAN02 EVs. **(C)** Proteins frequently present and absent in small EVs, studied in PAN02 EVs by Protein Mass Spectrometry. **(D)** PC-EVs are taken up by liver and BM cells, 24 h post-injection. **(E)** Most of the cells that take up PC-EVs are CD11b$^+$ BM cells. **(F)** Three-week education with PC-EVs does not modify the incidence of EV$^+$ BM cells or CD11b$^+$ cells within cells that take up PC-EVs **(G)**. **(H)** Three-week education with PC-EVs induces the increase of BM CD11b$^+$ cells. $^{**}P < 0.01$, $^{****}P < 0.0001$ by ANOVA.

that could be used to differentiate endosomal (i.e., exosomes) from membrane shedding-derived vesicles (i.e., microvesicles). In fact, even molecules considered as markers of small endosomal EVs, such as HSP70, CD63, and CD9, have been reported to be present both in small and large EVs (Kowal et al., 2016). Therefore, although the majority of our vesicles display

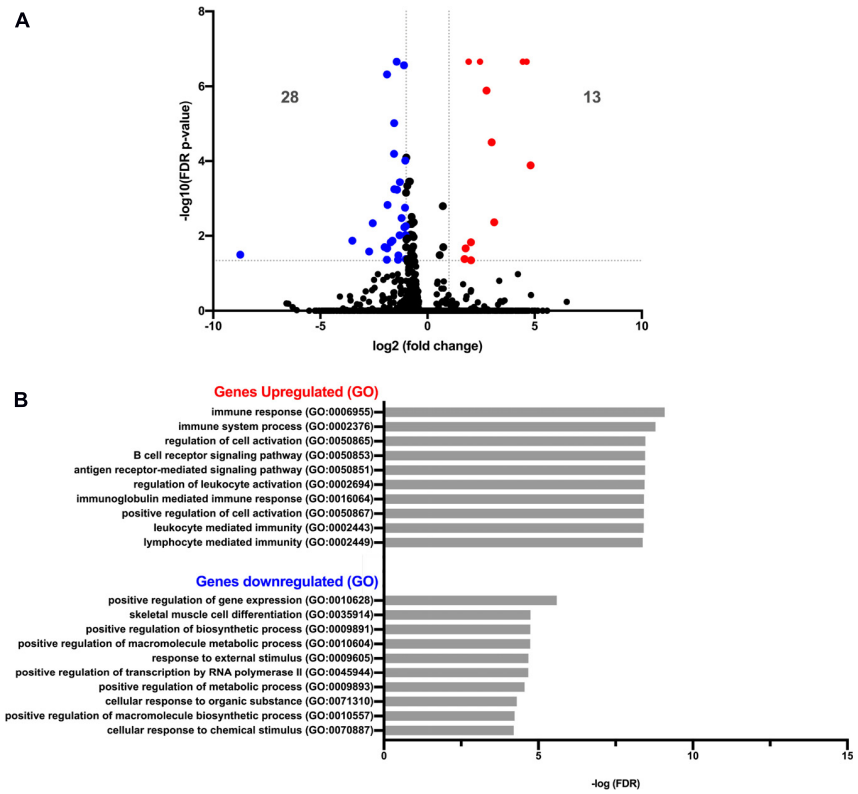

FIGURE 2 | Gene expression analysis of pancreatic cancer EV-treated bone marrow cells. **(A)** Volcano plot of RNA-Seq of PBS versus EV-treated CD11b$^+$ BM cells showing 13 and 28 genes significantly up- and downregulated (red dots and blue dots, respectively), with FDR *P*-value ≤ 0.05 and fold change > 2 or < -2. **(B)** Graph plot of the most significant processes of Gene Ontology (GO) enrichment analysis in the "Biological Process" section of up- and downregulated genes, using the Gene Ontology PANTHER Database.

exosome features, including size (**Figures 1A,B**) and molecular composition (**Figure 1C** and **Supplementary Table 3**), we decided to identify them as EVs throughout the manuscript to avoid potential sample misidentification, following the latest MISEV's recommendations (Thery et al., 2018).

To first determine the occurrence of PC–BM interaction, labeled PC-EVs were injected intravenously in mice. Besides the liver, 24-h post-injection EVs were also located in the BM, albeit the percentage of EVs$^+$ cells in the BM was lower (∼0.02%) than the one found in the liver (∼0.04%) (**Figure 1D**). In the BM, more than 80% of the cells that took up PC-EVs were CD11b$^+$ (**Figure 1E**). To our knowledge, this is the first report of a direct PC–BM communication axis mediated by EVs.

To evaluate if this proportion increased over time and upon continuous treatment, animals were also educated (3 weeks, every other day) with PC-EVs. No differences in the percentage of EVs$^+$ BM cells were found throughout the experiment (**Figure 1F**). The percentage of CD11b$^+$ cells among EVs$^+$ BM cells also did not oscillate throughout the experiment (**Figure 1G**). However, education with PC-EVs increased the percentage of CD11b$^+$ BM cells at the experiment endpoint (**Figure 1H**).

We next asked whether PC-EVs can modify the gene expression profile of CD11b$^+$ BM cells. For that, we sequenced RNA samples extracted from CD11b$^+$ BM cells of both naive and PC-EV-educated mice. The expression levels of all samples were assessed through the mapping of the high-quality reads of each sample, where 88.9 to 94.38% of the total fragments were mapped against the *Mus musculus* (GRCm38) genome. The differentially expressed genes were selected using standard conditions (FDR *P*-value ≤ 0.05 and fold change > 2 or < -2), which yielded a total of 41 genes (**Figure 2A**). Of these, 13 genes were significantly upregulated (**Table 1**) and 28 significantly downregulated (**Table 2**). These results were validated by qPCR analysis of two of the top differentially expressed genes (**Supplementary Figure 1**).

Gene Ontology (GO) analysis revealed that the upregulated genes (**Table 1**) were associated with immune response processes and immunoglobulin production (**Figure 2A**). Among those genes, we found the Immunoglobulin heavy constant gamma 3 (fragment) (*Ighg3*) gene, which is associated with the IgG3 isotype, and the genes Immunoglobulin heavy constant alpha (fragment) (*Igha*) and Immunoglobulin J chain (*Jchain*), both associated with IgA molecules. Within the downregulated genes, we found that the most significant GO processes were associated with transcriptional activation, response to stimulus, and regulation of gene

TABLE 1 | Upregulated genes.

Name	FDR *p*-value	Log2 fold change	ENSEMBL
Immunoglobulin heavy variable 1-26 (Fragment)	0	4,623730851	ENSMUSG00000094546
Immunoglobulin kappa variable 4-59 (Fragment)	0	4,447764161	ENSMUSG00000094006
Immunoglobulin J chain	0	2,449246148	ENSMUSG00000067149
Immunoglobulin heavy constant alpha (Fragment)	0	1,927167042	ENSMUSG00000095079
Immunoglobulin kappa constant (Fragment)	0	1,914161392	ENSMUSG00000076609
Ig gamma-1 chain C region secreted form (Fragment)	1,30134E-06	2,752343692	ENSMUSG00000076614
Predicted gene, 49345 (Fragment)	3,1653E-05	2,99697945	ENSMUSG00000114923
Immunoglobulin heavy variable V3-8 (Fragment)	0,000129751	4,808095452	ENSMUSG00000076674
Immunoglobulin kappa variable 1-110 (Fragment)	0,004373421	3,110850502	ENSMUSG00000093861
U3A small nuclear RNA	0,014852817	2,027515231	ENSMUSG00000106147
Immunoglobulin lambda constant 1 (Fragment)	0,021654529	1,776317776	ENSMUSG00000105906
Immunoglobulin lambda variable 1 (Fragment)	0,041671894	1,728395758	ENSMUSG00000076934
Immunoglobulin heavy constant gamma 3 (Fragment)	0,044897113	2,031085382	ENSMUSG00000076615

TABLE 2 | Downregulated genes.

Name	FDR *p*-value	Log2 fold change	ENSEMBL
Nuclear receptor subfamily 4 group A member 1	2,19745E-07	−1,435869584	ENSM USG 00000023034
Lipoprotein lipase	2,74851E-07	−1,09850161	ENSMUSG00000015568
Cyclic AMP-dependent transcription factor ATF-3	4,81325E-07	−1,887929851	ENSM USG 00000026628
ATP synthase protein 8	9,71391E-06	−1,554520723	ENSM USG 00000064356
Early growth response protein 3	6,39601E-05	−1,565012389	ENSM USG 00000033730
Krueppel-like factor 4	9,72554E-05	−1,036425344	ENSM USG 00000003032
Early growth response protein 1	0,000369143	−1,293024511	ENSMUSG00000038418
Prostaglandin G/H synthase 2	0,000573753	−1,548440352	ENSM USG 00000032487
Probable leucine–tRNA ligase, mitochondrial	0,000590408	−1,422122013	ENSM USG 00000035202
Regulator of G-protein signaling 1	0,001504139	−1,862241816	ENSM USG 00000026358
Monocyte differentiation antigen CD14	0,001783497	−1,048560286	ENSMUSG00000051439
C-C motif chemokine 3	0,003368206	−1,210768022	ENSM USG 00000000982
Predicted gene, 47075	0,0046162	−2,554952242	ENSMUSG00000114169
Cyclin-dependent kinase inhibitor 1	0,005512827	−1,012425917	ENSM USG 00000023067
Proto-oncogene c-Fos	0,005961159	−1,078598039	ENSMUSG00000021250
Transcription factor Spi-C	0,009588443	−1,02746831	ENSM USG 00000004359
Fos-related antigen 1	0,009676491	−1,304846194	ENSMUSG00000024912
Nuclear receptor subfamily 4 group A member 2	0,013476224	−1,63691541	ENSM USG 00000026826
Predicted gene, 23262	0,013476224	−3,507668615	ENSM USG 00000088948
Predicted gene 6377	0,014852817	−1,716519183	ENSM USG 00000048621
X-linked lymphocyte-regulated protein PM1	0,020080701	−1,997616005	ENSM USG 00000054626
C-C motif chemokine 2	0,021654529	−1,882312446	ENSM USG 00000035385
Predicted gene, 47088	0,026317916	−2,725652374	ENSMUSG00000113076
Predicted gene, 48275	0,031964977	−8,738521219	ENSMUSG00000111202
E3 SUMO-protein ligase EGR2	0,033340755	−1,358834793	ENSM USG 00000037868
Hematopoietic prostaglandin D synthase	0,041671894	−1,012816032	ENSMUSG00000029919
Predicted gene 45053	0,043671552	−1,376757203	ENSMUSG00000108368
Mitochondrially encoded 16S rRNA	0,043671552	−1,896767497	ENSM USG 00000064339

expression (**Figure 2B**). Specifically, most downregulated genes were transcription factors associated with monocyte and macrophage differentiation, macrophage polarization, production of pro- or anti-inflammatory cytokines, and immune cell trafficking (**Table 2**). Interestingly, the majority of downregulated genes are relevant in the tumor microenvironment context.

DISCUSSION

In the present study, we aimed to identify a novel systemic cell–cell communication axis with potential relevance to tumor microenvironment dynamics. Previously, we have demonstrated that PC-derived EVs can induce a liver microenvironment supportive of tumor development and metastasis, LPMN, by

acting in non-tumor cells in the liver. The LPMN cascade of events involves the accumulation of CD11b$^+$ BM cells in the liver, which is associated with the formation of hepatic PC metastatic lesions (Costa-Silva et al., 2015). For this reason, we asked if EVs could also mediate a direct communication between PC and CD11b$^+$ BM cells *in vivo*. We found that PC-EVs bind preferentially to CD11b$^+$ BM cells and induce the expansion of this cell population upon 3 weeks of treatment, every other day with PC-EVs. These results agree with previous reports of EVs mediating the communication of other cancer types and BM (Yu et al., 2007; Peinado et al., 2012).

We next showed that PC-EVs can reprogram the gene expression of recipient CD11b$^+$ BM cells. Indeed, various studies describe tumor EVs as capable of impacting myeloid cell function (Valenti et al., 2006; Yu et al., 2007; Shen et al., 2017) whereas PC-EVs were shown to regulate the expression of TLR4 in dendritic cells *in vitro* (Zhou et al., 2014). EVs carry all main biomolecules, including lipids, metabolites, proteins, and/or nucleic acids, which can impact the recipient cells and mediate several biological processes such as tumor growth and invasion, inflammation, and immunologic remodeling. Various studies describe the role of EV lipids, namely PGE2, in tumor growth and resistance (Record et al., 2018). The role of metabolites transported by EVs cannot be dismissed since EVs derived from MSCs are packaged with numerous metabolites that have been directly associated with immunomodulation, including M2 macrophage polarization and regulatory T lymphocyte induction (Showalter et al., 2019). Worth mentioning is also the role of microRNA within EVs, since mir-145 can regulate the polarization of tumor-associated macrophages (Shinohara et al., 2017). In the past, we also described the relevance of the protein content in tumor EV bioactivity, when we described that once taken up by hepatic resident macrophages, in a mechanism mediated by EV Integrin αVβ5 (Hoshino et al., 2015), pancreatic cancer-derived EVs containing high levels of MIF (Costa-Silva et al., 2015) induced upregulation of secreted factors associated with liver fibrosis, such as TGF-β (Costa-Silva et al., 2015), and pro-inflammatory genes involved with metastasis, such as S100A8 and S100P (Lukanidin and Sleeman, 2012; Hoshino et al., 2015). Considering the literature on this topic, we expect that the response of CD11b BM cells to PC-EVs described in this manuscript most likely involves numerous molecules and different pathways, suggesting that it could be simultaneously mediated by multiple EV biomolecules. Our work did not evaluate *in vivo* the potential role of the genes differentially expressed in BM CD11b$^+$ cells upon PC-EV education in the setup of prometastasis hepatic niches. Therefore, follow-up *in vivo* studies will be necessary to test the potential role of each of the identified genes in PC liver metastasis. Future investigation will enable the identification of which EV biomolecules mediate the transcription reprogramming here described. In addition, based on previous works that utilized plasma EVs as biomarkers for diagnosis, prognosis, and follow-up of cancer patients (Peinado et al., 2012; Costa-Silva et al., 2015; Hoshino et al., 2015, 2020; Melo et al., 2015), it is possible that EV biomolecules linked with PC-CD11b$^+$ BM cell communication may enable early detection of this process through the study of circulating plasma EVs. We will here discuss on genes regulated by PC-EVs with potential relevance to tumor microenvironments and the biology of monocytes/macrophages.

Immunoglobulin Genes

The production of immunoglobulins has been classically linked to lymphoid B cells. However, recent evidence challenged the existing dogma by showing expression of immunoglobulins outside the lymphoid lineage (e.g., monocytes and macrophages) in oncologic settings (Haziot et al., 2018; Busch et al., 2019). These works describe immunoglobulin expression as a defining feature of monocytes and also macrophages in the tumor microenvironment.

Increased levels of immunoglobulin expression in tumor microenvironments are described to result in the accumulation of immune complexes that favor tumor-promoting inflammatory responses, including recruitment and activation of several myeloid cell types (Barbera-Guillem et al., 1999). Both IgG and IgA are relevant in the tumor microenvironment, having anti- and protumoral effects. IgG is described to promote cell growth and metastasis, inhibit apoptosis, and play a role in cancer immune evasion (Wan et al., 2015; Xu et al., 2016). Synergistically, IgG and tumor cell-derived debris are able to promote metastasis of pancreatic cancer by inducing inflammation *via* M2-polarized tumor-associated macrophages (TAMs) (Chen et al., 2019). Moreover, IgGs have been shown to promote cancer development by activating Fc-γ receptors on resident and recruited leukocytes that in turn regulate recruitment, composition, and effector functions of tumor-infiltrating lymphocytes in a mouse model of squamous carcinogenesis (Andreu et al., 2010). On the other hand, some studies show IgG1 supporting immunity against tumors, inducing antibody-dependent cell-mediated cytotoxicity (ADCC) and antibody-dependent cellular phagocytosis (ADCP) (Kellner et al., 2017).

It has also been shown that IgA can block cytotoxic T-cell reactions against melanoma (O'Neill and Romsdahl, 2009). More recently, IgA$^+$ plasmocytes were shown to suppress antitumor immunity in a mouse prostate cancer model. However, in this study, it is unclear if the suppression can be attributed to IgA$^+$ plasmocytes or IgA alone (Shalapour et al., 2015). By contrast, IgA shows a therapeutic potential against cancer cells, since it activates neutrophil-mediated antibody-dependent cellular cytotoxicity better than IgG (Frontera et al., 2018; Steffen et al., 2020). It should be highlighted though that confirmation that immunoglobulins produced by non-lymphoid cells are functional is still pending, since studies on whether affinity-matured antibodies from these cells are capable of binding to antigens are not yet available. Additionally, we cannot exclude the potential presence of B1 cells, a small immunoglobulin-expressing phagocytic population that is believed to originate from B cells, within our CD11b$^+$ BM cells (Griffin and Rothstein, 2011).

In light of these findings, and taking into consideration the previously described direct association between CD11b$^+$ BM cell accumulation in the liver and the formation of hepatic PC metastatic lesions, our results suggest that PC-EV-induced immunoglobulin expression on CD11b$^+$ BM cells may play a

role in PC liver metastasis. Nevertheless, it is still unclear which specific epitopes are recognized by these antibodies and whether they contribute to tumor microenvironments (Haziot et al., 2018; Busch et al., 2019).

Genes Linked With Monocyte/Macrophage Differentiation

Among the downregulated genes identified, lipoprotein lipase (*Lpl*) (Chang et al., 2018), transcription factor Spi-c (*Spic*) (Kohyama et al., 2008; Haldar et al., 2014; Alam et al., 2017; Kurotaki et al., 2017), and Nuclear receptor subfamily 4 group A member1 (*Nr4a1*) (Hanna et al., 2011) have all been previously found to induce differentiation of monocytes. Another gene potentially linked with monocyte/macrophage differentiation is CDK inhibitor 1, which when downregulated leads to higher expression of CD11b, thus modifying cellular differentiation (Radomska et al., 2012; McClure et al., 2016). Other downregulated genes, early growth response protein 1 (*Egr1*) and 3 (*Egr3*), were believed to have an essential role in regulating monocyte/macrophage differentiation, but were later suggested to have no impact in the macrophage differentiation process (Carter and Tourtellotte, 2007). Hence, our results suggest a mixed effect of PC-EVs in CD11b$^+$ BM cell differentiation, with some of the downregulated genes found having a positive impact on the differentiation process and others having a negative impact in the same process. A more detailed functional characterization will thus be necessary to understand the final balance of the downregulation of these genes by PC-EVs in CD11b$^+$ BM cell differentiation, as well as their role in PC.

Genes Linked With Tumor Immunity

In the establishment of tumor-supportive microenvironments, macrophage polarization is pivotal. Reduced expression of Cyclic AMP-dependent transcription factor ATF-3 (*Atf3*) (Labzin et al., 2015; Sha et al., 2017), Fos-related antigen 1 (*Fosl1*) (de Marcken et al., 2019), and *Nr4a1* (Hamers et al., 2016) can impact pro-inflammatory M1 polarization and antitumor immunity (Kratochvill et al., 2015; Chiba et al., 2018), as they negatively regulate these processes. C-C chemokine ligand 3 (*Ccl3*) (Cassol et al., 2009) was also reported to be involved in the M1 macrophage polarization and CD14 was shown not only to contribute to a M1 phenotype but also to drive strong Th1/Th17 signaling in macrophages and circulating dendritic cells (Prakash et al., 2016). Reduced expression of the Proto-oncogene c-Fos (*c-fos*) and *Egr1* is expected to reduce the expression of pro-inflammatory and antitumoral cytokines, which are also involved in the M1 polarization (Krämer et al., 1994; Ray et al., 2006; Maruyama et al., 2007; Cullen et al., 2010; Hop et al., 2018; Yu et al., 2018). Conversely, reduced expression of *Atf3* (Sha et al., 2017), *Klf4* (Ahmad et al., 2018; Wen et al., 2019), and Prostaglandin G/H synthase 2 (*Pghs-2*) (Wang X. et al., 2017) in macrophages can favor a pro-inflammatory M1 polarization, hence potentially favoring antitumoral responses.

On the other hand, some of the genes downregulated by PC-EVs were also found to support tumor development, as C-C chemokine ligand 2 (*Ccl2*) (Roca et al., 2009; Li et al., 2017), *Atf3* (Sha et al., 2017), Hematopoietic prostaglandin D synthase (Abbas and Janeway, 2000), Krüppel-like factor 4 (*Klf4*) (Kapoor et al., 2015; Wang K. et al., 2017), Nuclear receptor subfamily 4 group A member 2 (*Nr4a2*) (Mahajan et al., 2015), and *Pghs-2* (Li et al., 2015) were linked to M2 polarization of macrophages. The *Egr2* gene has been described as a M2 macrophage marker and it has been implicated in fate determination in the myeloid lineage (Gabet et al., 2010; Jablonski et al., 2015). Specifically, an *Egr2* knockdown model failed to show upregulation of either M1 or M2 markers upon stimulation, and low levels of *Egr2* expression were associated with non-responsiveness of macrophages to activation signals (Veremeyko et al., 2018).

Besides the discussed effects on M1/M2 macrophage polarization, several of the downregulated genes were associated with other antitumoral effects, which may lead to a broader range of protumorigenic outcomes. That is the case of *Nr4a1*, *Ccl2*, and *Ccl3*, which antagonize tumor growth by attracting tumor-suppressive immune cells. Indeed, infiltration of inflammatory cells in the tumors of *Nr4a1*$^{-/-}$ mice was diminished when compared with *Nr4a1*$^{+/+}$ mice (Ahmad et al., 2017), and the inhibition of *Ccl2* promoted neocarcinogenesis and metastasis (Huang et al., 1994; Li et al., 2014; Lavender et al., 2017). *Ccl2* (Granot et al., 2011; Mitchem and DeNardo, 2012) has also been reported to increase the cytotoxicity of neutrophils against tumor cells. Thus, reduction of *Ccl2* expression can decrease neutrophil-mediated killing of tumor cells and promote a protumorigenic microenvironment.

We here suggest that the downregulation of these genes by PC-EVs could induce a combined anti-/protumorigenic response by BM CD11b$^+$ cells. Additional *in vivo* studies will be necessary to evaluate whether these inflammatory profiles will be reversed and/or reinforced after the influx of these cells in the liver, where Kupffer cell-derived TGF-β (Costa-Silva et al., 2015) can play a potential role in inducing protumorigenic genes (Gratchev, 2017) by BM-derived CD11b$^+$ cells.

Genes Linked With Monocyte/Macrophage Trafficking

Genes associated with monocyte and macrophage recruitment, such as *Ccl2* (Qian et al., 2011; Carson et al., 2017; Gschwandtner et al., 2019), *Ccl3* (Ntanasis-Stathopoulos et al., 2020), and *Fosl1* (Jiang et al., 2019), were found to be downregulated. The decrease in the levels of *Fosl1*, *Ccl2*, and *Ccl3* is expected to reduce the recruitment of cells that allow tumor cells to evade the immune surveillance, e.g., TAMs, regulatory T cells (Tregs), and myeloid-derived suppressor cells (MDSCs) (Jiang et al., 2019; Wculek et al., 2019; Ntanasis-Stathopoulos et al., 2020). Furthermore, downregulated *Ccl3* could reduce the recruitment of cytotoxic neutrophils, dendritic cells, and NK cells; reduce CD8$^+$ antitumor response; and lead to impaired antigen presentation, reduced levels of IFN-γ by antigen-specific T cells, and consequently, reduced cytotoxic activity (Song et al., 2007; Ntanasis-Stathopoulos et al., 2020). Overall, a decrease in the recruitment of monocytes and macrophages could shape the tumor microenvironment toward a less supportive setting for cancer progression.

Another downregulated gene, *Atf3*, has been linked with increased intrahepatic macrophage/neutrophil trafficking

(Zhu et al., 2018). Regulator of G-protein signaling 1 (*Rgs1*), also downregulated by PC-EVs, has been involved in the chemoattraction of monocytes. Specifically, *Rgs1* deactivates the chemotactic response (Denecke et al., 1999), and its deficiency leads to enhanced recruitment of macrophages (Patel et al., 2015). We speculate that the *Rgs1* downregulation in CD11b$^+$ BM cells can lead to less myeloid accumulation and more monocyte/macrophage trafficking.

In most of these studies, genes were downregulated in the whole animal, instead of only in BM cells. Therefore, more detailed *in vivo* experiments would be needed to test whether reduced expression of these genes in CD11b$^+$ BM cells could impact their trafficking to PC microenvironments.

Genes Linked With Monocyte/Macrophage Apoptosis

The downregulation of *Ccl2* (Salcedo et al., 2000; Lavender et al., 2017), *Fosl1* (Lewçn et al., 2007; Luo et al., 2009), and *Rgs1* (Hu et al., 2019) has been described to increase apoptosis and to decrease angiogenesis and tumor invasion by affecting molecules associated with these processes (e.g., VEGF, MMP-2, MMP-9). On the other hand, the downregulated genes *Egr1* (Chen et al., 2010) and *Atf3* (Wong, 2011) have been described as proapoptotic, and thus, the decrease in their expression alone might provide a higher degree of protection against apoptosis in CD11b$^+$ BM cells.

CONCLUSION

We here found a novel PC–BM communication axis mediated by PC-EVs. Our gene expression analysis showed reprogramming of genes linked to both anti- and protumorigenic activities by CD11b$^+$ cells. Their potential relevance in PC tumor microenvironments was discussed, although how the individual effects of the reprogrammed genes balance each other to a final anti- or protumorigenic effect is currently unclear. Future *in vivo* studies involving single-cell transcriptome and detailed analysis of the role of each gene in the phenotype of CD11b$^+$ BM cells will be necessary to clarify whether and how PC-EVs uptake by these cells contributes to the setup of PC microenvironments. Stepping further into the future, the study of PC-educated BM-derived cells linked with PC metastasis in the peripheral blood could be used as a minimally invasive method to detect and monitor these protumorigenic niches in clinical settings, thus having a potential impact in improving early diagnosis, treatment, and follow-up of patients with PC and other oncologic diseases. Additionally, it has the potential to contribute to the development of therapeutic targeting of BM-derived cells that promote liver metastatic disease.

DATA AVAILABILITY STATEMENT

The datasets presented in this study can be found in online repositories. The names of the repository/repositories and accession number(s) can be found in the article/**Supplementary Material**.

ETHICS STATEMENT

All mouse work was performed in accordance with national animal experimentation guidelines (DGAV), animal protocol 0421/000/000/2018.

AUTHOR CONTRIBUTIONS

JM designed and performed the experiments. AM and JP performed the transmission electron microscopy studies. AO, AC, RM, and HB performed the mass spectrometry studies. MS built the experimental setup. BC-S conceived the project. All authors wrote and reviewed the manuscript.

FUNDING

JM was supported by "Fundação para a Ciência e a Tecnologia" (PD/BD/105866/2014). This work was supported by the Champalimaud Foundation; grant 751547 from H2020-MSCA-IF-2016; EMBO Installation Grant 3921; grant 2017NovPCC1058 from Breast Cancer Now's Catalyst Programme, which is supported by funding from Pfizer; grant 765492 from H2020-MSCA-ITN-2017; and grant LCF/PR/HR19/52160014 from "La Caixa" Foundation. This work was also funded by FEDER funds through the Operational Programme for Competitiveness Factors-COMPETE and National Funds through the Foundation for Science and Technology (FCT), under the project: PTDC/MED-ONC/28489/2017 (to AM). JP acknowledges the FCT grant SFRH/BD/137319/2018.

ACKNOWLEDGMENTS

The authors would like to thank Inês Coelho, Silvia Batista, Ana Gregório, Julia Elzanowska, and Cristian Bodo for their support in the final preparation of the manuscript and Rui Fernandes (HEMS, i3S Scientific platform) for TEM image acquisition.

SUPPLEMENTARY MATERIAL

The Supplementary Material for this article can be found online at: https://www.frontiersin.org/articles/10.3389/fcell.2020.592518/full#supplementary-material

Supplementary Figure 1 | Validation of differentially expressed genes by quantitative PCR (qPCR). Depicted in the graph is the fold change of CD11b$^+$ BM cells from animals treated PC EVs or PBS (control). Ighv1-26 and Ighv4-59 relative gene expression was evaluated by qPCR. Error bars represent ± SEM for $n = 4$, each point represents a pool of at least 5 animals. qPCR samples were normalized to both reference genes (*Gapdh* and *Hmbs*).

REFERENCES

Abbas, A. K., and Janeway, C. A. Jr. (2000). Immunology: improving on nature in the twenty-first century. *Cell* 100, 129–138. doi: 10.1016/S0092-8674(00)81689-X

Ahmad, A., Barakat, D. J., Suresh, R., Barberi, T., Pienta, K. J., Simons, B. W., et al. (2018). Absence of myeloid Klf4 reduces prostate cancer growth with pro-atherosclerotic activation of tumor myeloid cells and infiltration of CD8 T cells. *PLoS One* 13:e0191188. doi: 10.1371/journal.pone.0191188

Ahmad, A., Li, X.-M., Wang, J.-R., Shen, T., Gao, S.-S., He, X.-S., et al. (2017). Nur77 deficiency in mice accelerates tumor invasion and metastasis by facilitating TNFα secretion and lowering CSF-1R expression. *PLoS One* 12:e0171347. doi: 10.1371/journal.pone.0171347

Alam, M. Z., Devalaraja, S., and Haldar, M. (2017). The heme connection: linking erythrocytes and macrophage biology. *Front. Immunol.* 8:33. doi: 10.3389/fimmu.2017.00033

Andreu, P., Johansson, M., Affara, N. I., Pucci, F., Tan, T., Junankar, S., et al. (2010). FcRγ activation regulates inflammation-associated squamous carcinogenesis. *Cancer Cell* 17, 121–134. doi: 10.1016/j.ccr.2009.12.019

Barbera-Guillem, E., May, K. F., Nyhus, J. K., and Nelson, M. B. (1999). Promotion of tumor invasion by cooperation of granulocytes and macrophages activated by anti-tumor antibodies. *Neoplasia* 1, 453–460. doi: 10.1038/sj.neo.7900054

Bergfeld, S. A., and DeClerck, Y. A. (2010). Bone marrow-derived mesenchymal stem cells and the tumor microenvironment. *Cancer Metastasis Rev.* 29, 249–261. doi: 10.1007/s10555-010-9222-7

Bissell, M. J., and Hines, W. C. (2011). Why don't we get more cancer? A proposed role of the microenvironment in restraining cancer progression. *Nat. Med.* 17, 320–329. doi: 10.1038/nm.2328

Busch, S., Talamini, M., Brenner, S., Abdulazim, A., Hänggi, D., Neumaier, M., et al. (2019). Circulating monocytes and tumor−associated macrophages express recombined immunoglobulins in glioblastoma patients. *Clin. Transl. Med.* 8:18. doi: 10.1186/s40169-019-0235-8

Carson, W. F., Salter-Green, S. E., Scola, M. M., Joshi, A., Gallagher, K. A., and Kunkel, S. L. (2017). Enhancement of macrophage inflammatory responses by CCL2 is correlated with increased miR-9 expression and downregulation of the ERK1/2 phosphatase Dusp6. *Cell. Immunol.* 314, 63–72. doi: 10.1016/j.cellimm.2017.02.005

Carter, J. H., and Tourtellotte, W. G. (2007). Early growth response transcriptional regulators are dispensable for macrophage differentiation. *J. Immunol.* 178, 3038–3047. doi: 10.4049/jimmunol.178.5.3038

Carvalho, A. S., Ribeiro, H., Voabil, P., Penque, D., Jensen, O. N., Molina, H., et al. (2014). Global mass spectrometry and transcriptomics array based drug profiling provides novel insight into glucosamine induced endoplasmic reticulum stress. *Mol. Cell Proteomics* 13, 3294–3307. doi: 10.1074/mcp.M113.034363

Cassol, E., Cassetta, L., Rizzi, C., Alfano, M., and Poli, G. (2009). M1 and M2a polarization of human monocyte-derived macrophages inhibits HIV-1 replication by distinct mechanisms. *J. Immunol.* 182, 6237–6246. doi: 10.4049/jimmunol.0803447

Chang, C. L., Garcia-Arcos, I., Nyren, R., Olivecrona, G., Kim, J. Y., Hu, Y., et al. (2018). Lipoprotein lipase deficiency impairs bone marrow myelopoiesis and reduces circulating monocyte levels. *Arterioscler. Thromb. Vasc. Biol.* 38, 509–519. doi: 10.1161/ATVBAHA.117.310607

Chen, L., Wang, S., Zhou, Y., Wu, X., Entin, I., Epstein, J., et al. (2010). Identification of early growth response protein 1 (EGR-1) as a novel target for JUN-induced apoptosis in multiple myeloma. *Blood* 115, 61–70. doi: 10.1182/blood-2009-03-210526

Chen, Q., Wang, J., Zhang, Q., Zhang, J., Lou, Y., Yang, J., et al. (2019). Tumour cell-derived debris and IgG synergistically promote metastasis of pancreatic cancer by inducing inflammation via tumour-associated macrophages. *Br. J. Cancer* 121, 786–795. doi: 10.1038/s41416-019-0595-2

Chiba, Y., Mizoguchi, I., Furusawa, J., Hasegawa, H., Ohashi, M., Xu, M., et al. (2018). Interleukin-27 exerts its antitumor effects by promoting differentiation of hematopoietic stem cells to M1 macrophages. *Cancer Res.* 78, 182–194. doi: 10.1158/0008-5472.CAN-17-0960

Costa-Silva, B., Aiello, N. M., Ocean, A. J., Singh, S., Zhang, H., Basant, K., et al. (2015). Pancreatic cancer exosomes initiate pre-metastatic niche formation in the liver. *Nat. Cell Biol.* 17, 816–826. doi: 10.1038/ncb3169

Cox, J., and Mann, M. (2008). MaxQuant enables high peptide identification rates, individualized p.p.b.-range mass accuracies and proteome-wide protein quantification. *Nat. Biotechnol.* 26, 1367–1372. doi: 10.1038/nbt.1511

Cullen, E. M., Brazil, J. C., and O'Connor, C. M. (2010). Mature human neutrophils constitutively express the transcription factor EGR-1. *Mol. Immunol.* 47, 1701–1709. doi: 10.1016/j.molimm.2010.03.003

de Marcken, M., Dhaliwal, K., Danielsen, A. C., Gautron, A. S., and Dominguez-Villar, M. (2019). TLR7 and TLR8 activate distinct pathways in monocytes during RNA virus infection. *Sci. Signal.* 12:eaaw1347. doi: 10.1126/scisignal.aaw1347

Denecke, B., Meyerdierks, A., and Böttger, E. C. (1999). RGS1 is expressed in monocytes and acts as a GTPase-activating protein for G-protein-coupled chemoattractant receptors. *J. Biol. Chem.* 274, 26860–26868. doi: 10.1074/jbc.274.38.26860

Ferreira, N., Marques, A., Aguas, H., Bandarenka, H., Martins, R., Bodo, C., et al. (2019). Label-free nanosensing platform for breast cancer exosome profiling. *ACS Sens.* 4, 2073–2083. doi: 10.1021/acssensors.9b00760

Foucher, E. D., Ghigo, C., Chouaib, S., Galon, J., Iovanna, J., and Olive, D. (2018). Pancreatic ductal adenocarcinoma: a strong imbalance of good and bad immunological cops in the tumor microenvironment. *Front. Immunol.* 9:1044. doi: 10.3389/fimmu.2018.01044

Frontera, E. D., Khansa, R. M., Schalk, D. L., Leakan, L. E., Guerin-Edbauer, T. J., Ratnam, M., et al. (2018). IgA Fc-folate conjugate activates and recruits neutrophils to directly target triple-negative breast cancer cells. *Breast Cancer Res. Treat.* 172, 551–560. doi: 10.1007/s10549-018-4941-5

Gabet, Y., Baniwal, S. K., Leclerc, N., Shi, Y., Kohn-Gabet, A. E., Cogan, J., et al. (2010). Krox20/EGR2 deficiency accelerates cell growth and differentiation in the monocytic lineage and decreases bone mass. *Blood* 116, 3964–3971. doi: 10.1182/blood-2010-01-263830

Granot, Z., Henke, E., Comen, E. A., King, T. A., Norton, L., and Benezra, R. (2011). Tumor entrained neutrophils inhibit seeding in the premetastatic lung. *Cancer Cell* 20, 300–314. doi: 10.1016/j.ccr.2011.08.012

Gratchev, A. (2017). TGF-beta signalling in tumour associated macrophages. *Immunobiology* 222, 75–81. doi: 10.1016/j.imbio.2015.11.016

Griffin, D. O., and Rothstein, T. L. (2011). A small CD11b+ human B1 cell subpopulation stimulates T cells and is expanded in lupus. *J. Exp. Med.* 208, 2591–2598. doi: 10.1084/jem.20110978

Gschwandtner, M., Derler, R., and Midwood, K. S. (2019). More than just attractive: how CCL2 influences myeloid cell behavior beyond chemotaxis. *Front. Immunol.* 10:2759. doi: 10.3389/fimmu.2019.02759

Haldar, M., Kohyama, M., So, A. Y., Kc, W., Wu, X., Briseno, C. G., et al. (2014). Heme-mediated SPI-C induction promotes monocyte differentiation into iron-recycling macrophages. *Cell* 156, 1223–1234. doi: 10.1016/j.cell.2014.01.069

Hamers, A. A., Argmann, C., Moerland, P. D., Koenis, D. S., Marinkovic, G., Sokolovic, M., et al. (2016). Nur77-deficiency in bone marrow-derived macrophages modulates inflammatory responses, extracellular matrix homeostasis, phagocytosis and tolerance. *BMC Genomics* 17:162. doi: 10.1186/s12864-016-2469-9

Hanna, R. N., Carlin, L. M., Hubbeling, H. G., Nackiewicz, D., Green, A. M., Punt, J. A., et al. (2011). The transcription factor NR4A1 (Nur77) controls bone marrow differentiation and the survival of Ly6C- monocytes. *Nat. Immunol.* 12, 778–785. doi: 10.1038/ni.2063

Haziot, A., Fuchs, T., Hahn, M., Ries, L., Giesler, S., Busch, S., et al. (2018). Expression of combinatorial immunoglobulins in macrophages in the tumor microenvironment. *PLoS One* 13:e0204108. doi: 10.1371/journal.pone.0204108

Hop, H. T., Arayan, L. T., Huy, T. X. N., Reyes, A. W. B., Vu, S. H., Min, W., et al. (2018). The key role of c-Fos for immune regulation and bacterial dissemination in brucella infected macrophage. *Front. Cell Infect. Microbiol.* 8:287. doi: 10.3389/fcimb.2018.00287

Hoshino, A., Costa-Silva, B., Shen, T.-L., Rodrigues, G., Hashimoto, A., Tesic Mark, M., et al. (2015). Tumour exosome integrins determine organotropic metastasis. *Nature* 527, 329–335. doi: 10.1038/nature15756

Hoshino, A., Kim, H. S., Bojmar, L., Gyan, K. E., Cioffi, M., Hernandez, J., et al. (2020). Extracellular vesicle and particle biomarkers define multiple human cancers. *Cell* 182, 1044–1061.e18. doi: 10.1016/j.cell.2020.07.009

Hu, X., Tang, J., Zeng, G., Hu, X., Bao, P., Wu, J., et al. (2019). RGS1 silencing inhibits the inflammatory response and angiogenesis in rheumatoid arthritis

rats through the inactivation of Toll−like receptor signaling pathway. *J. Cell. Physiol.* 234, 20432–20442. doi: 10.1002/jcp.28645

Huang, S., Singh, R. K., Xie, K., Gutman, M., Berry, K. K., Bucana, C. D., et al. (1994). Expression of theJE/MCP-1 gene suppresses metastatic potential in murine colon carcinoma cells. *Cancer Immunol. Immunother.* 39, 231–238. doi: 10.1007/BF01525986

Jablonski, K. A., Amici, S. A., Webb, L. M., Ruiz-Rosado Jde, D., Popovich, P. G., Partida-Sanchez, S., et al. (2015). Novel markers to delineate murine M1 and M2 macrophages. *PLoS One* 10:e0145342. doi: 10.1371/journal.pone.0145342

Jiang, P., Gao, W., Ma, T., Wang, R., Piao, Y., Dong, X., et al. (2019). CD137 promotes bone metastasis of breast cancer by enhancing the migration and osteoclast differentiation of monocytes/macrophages. *Theranostics* 9, 2950–2966. doi: 10.7150/thno.29617

Kalluri, R., and LeBleu, V. S. (2020). The biology, function, and biomedical applications of exosomes. *Science* 367:eaau6977. doi: 10.1126/science.aau6977

Kapoor, N., Niu, J., Saad, Y., Kumar, S., Sirakova, T., Becerra, E., et al. (2015). Transcription factors STAT6 and KLF4 implement macrophage polarization via the dual catalytic powers of MCPIP. *J. Immunol.* 194, 6011–6023. doi: 10.4049/jimmunol.1402797

Kellner, C., Otte, A., Cappuzzello, E., Klausz, K., and Peipp, M. (2017). Modulating cytotoxic effector functions by Fc engineering to improve cancer therapy. *Transfusion Med. Hemother.* 44, 327–336. doi: 10.1159/000479980

Kohyama, M., Ise, W., Edelson, B. T., Wilker, P. R., Hildner, K., Mejia, C., et al. (2008). Role for Spi-C in the development of red pulp macrophages and splenic iron homeostasis. *Nature* 457, 318–321. doi: 10.1038/nature07472

Kowal, J., Arras, G., Colombo, M., Jouve, M., Morath, J. P., Primdal-Bengtson, B., et al. (2016). Proteomic comparison defines novel markers to characterize heterogeneous populations of extracellular vesicle subtypes. *Proc. Natl. Acad. Sci. U.S.A.* 113, E968–E977. doi: 10.1073/pnas.1521230113

Krämer, B., Meichle, A., Hensel, G., Charnay, P., and Krönke, M. (1994). Characterization of an Krox-24/Egr-1-responsive element in the human tumor necrosis factor promoter. *Biochim. Biophys. Acta* 1219, 413–421. doi: 10.1016/0167-4781(94)90066-3

Kratochvill, F., Neale, G., Haverkamp, J. M., Van de Velde, L. A., Smith, A. M., Kawauchi, D., et al. (2015). TNF counterbalances the emergence of M2 tumor macrophages. *Cell Rep.* 12, 1902–1914. doi: 10.1016/j.celrep.2015.08.033

Kurotaki, D., Sasaki, H., and Tamura, T. (2017). Transcriptional control of monocyte and macrophage development. *Int. Immunol.* 29, 97–107. doi: 10.1093/intimm/dxx016

Labzin, L. I., Schmidt, S. V., Masters, S. L., Beyer, M., Krebs, W., Klee, K., et al. (2015). ATF3 is a key regulator of macrophage IFN responses. *J. Immunol.* 195, 4446–4455. doi: 10.4049/jimmunol.1500204

Lavender, N., Yang, J., Chen, S.-C., Sai, J., Johnson, C. A., Owens, P., et al. (2017). The Yin/Yan of CCL2: a minor role in neutrophil anti-tumor activity in vitro but a major role on the outgrowth of metastatic breast cancer lesions in the lung in vivo. *BMC Cancer* 17:88. doi: 10.1186/s12885-017-3074-2

Lee, S., and Margolin, K. (2011). Cytokines in cancer immunotherapy. *Cancers* 3, 3856–3893. doi: 10.3390/cancers3043856

Lewçn, S., Zhou, H., Hu, H.-D., Cheng, T., Markowitz, D., Reisfeld, R. A., et al. (2007). A Legumain-based minigene vaccine targets the tumor stroma and suppresses breast cancer growth and angiogenesis. *Cancer Immunol. Immunother.* 57, 507–515. doi: 10.1007/s00262-007-0389-x

Li, H., Yang, B., Huang, J., Lin, Y., Xiang, T., Wan, J., et al. (2015). Cyclooxygenase-2 in tumor-associated macrophages promotes breast cancer cell survival by triggering a positive-feedback loop between macrophages and cancer cells. *Oncotarget* 6, 29637–29650. doi: 10.18632/oncotarget.4936

Li, M., Knight, D. A., Snyder, L. A., Smyth, M. J., and Stewart, T. J. (2014). A role for CCL2 in both tumor progression and immunosurveillance. *Oncoimmunology* 2:e25474. doi: 10.4161/onci.25474

Li, X., Yao, W., Yuan, Y., Chen, P., Li, B., Li, J., et al. (2017). Targeting of tumour-infiltrating macrophages via CCL2/CCR2 signalling as a therapeutic strategy against hepatocellular carcinoma. *Gut* 66, 157–167. doi: 10.1136/gutjnl-2015-310514

Lukanidin, E., and Sleeman, J. P. (2012). Building the niche: the role of the S100 proteins in metastatic growth. *Semin. Cancer Biol.* 22, 216–225. doi: 10.1016/j.semcancer.2012.02.006

Luo, Y. P., Zhou, H., Krueger, J., Kaplan, C., Liao, D., Markowitz, D., et al. (2009). The role of proto-oncogene Fra-1 in remodeling the tumor microenvironment in support of breast tumor cell invasion and progression. *Oncogene* 29, 662–673. doi: 10.1038/onc.2009.308

Mahajan, S., Saini, A., Chandra, V., Nanduri, R., Kalra, R., Bhagyaraj, E., et al. (2015). Nuclear receptor Nr4a2 promotes alternative polarization of macrophages and confers protection in sepsis. *J. Biol. Chem.* 290, 18304–18314. doi: 10.1074/jbc.M115.638064

Maia, J., Caja, S., Strano Moraes, M. C., Couto, N., and Costa-Silva, B. (2018). Exosome-based cell-cell communication in the tumor microenvironment. *Front. Cell Dev. Biol.* 6:18. doi: 10.3389/fcell.2018.00018

Maruyama, K., Sano, G., Ray, N., Takada, Y., and Matsuo, K. (2007). c-Fos-deficient mice are susceptible to *Salmonella enterica* serovar Typhimurium infection. *Infect. Immun.* 75, 1520–1523. doi: 10.1128/IAI.01316-06

Matthiesen, R., Prieto, G., Amorim, A., Aloria, K., Fullaondo, A., Carvalho, A. S., et al. (2012). SIR: deterministic protein inference from peptides assigned to MS data. *J. Proteomics* 75, 4176–4183. doi: 10.1016/j.jprot.2012.05.010

McClure, C., Ali, E., Youssef, D., Yao, Z. Q., McCall, C. E., El Gazzar, M., et al. (2016). NFI-A disrupts myeloid cell differentiation and maturation in septic mice. *J. Leukoc. Biol.* 99, 201–211. doi: 10.1189/jlb.4A0415-171RR

Melo, S. A., Luecke, L. B., Kahlert, C., Fernandez, A. F., Gammon, S. T., Kaye, J., et al. (2015). Glypican-1 identifies cancer exosomes and detects early pancreatic cancer. *Nature* 523, 177–182. doi: 10.1038/nature14581

Mitchem, J. B., and DeNardo, D. G. (2012). Battle over CCL2 for control of the metastatic niche: neutrophils versus monocytes. *Breast Cancer Res.* 14:315. doi: 10.1186/bcr3149

Nolte-'t Hoen, E. N. M., Buermans, H. P. J., Waasdorp, M., Stoorvogel, W., Wauben, M. H. M., and 't Hoen, P. A. C. (2012). Deep sequencing of RNA from immune cell-derived vesicles uncovers the selective incorporation of small non-coding RNA biotypes with potential regulatory functions. *Nucleic Acids Res.* 40, 9272–9285. doi: 10.1093/nar/gks658

Ntanasis-Stathopoulos, I., Fotiou, D., and Terpos, E. (2020). CCL3 signaling in the tumor microenvironment. *Adv. Exp. Med. Biol.* 1231, 13–21. doi: 10.1007/978-3-030-36667-4_2

O'Neill, P. A., and Romsdahl, M. M. (2009). IgA as a blocking factor in human malignant melanoma. *Immunol. Commun.* 3, 427–438. doi: 10.3109/08820137409061123

Patel, J., McNeill, E., Douglas, G., Hale, A. B., de Bono, J., Lee, R., et al. (2015). RGS1 regulates myeloid cell accumulation in atherosclerosis and aortic aneurysm rupture through altered chemokine signalling. *Nat. Commun.* 6:6614. doi: 10.1038/ncomms7614

Peinado, H., Aleèkoviæ, M., Lavotshkin, S., Matei, I., Costa-Silva, B., Moreno-Bueno, G., et al. (2012). Melanoma exosomes educate bone marrow progenitor cells toward a pro-metastatic phenotype through MET. *Nat. Med.* 18, 883–891. doi: 10.1038/nm.2753

Pfaffl, M. W. (2001). A new mathematical model for relative quantification in real-time RT-PCR. *Nucleic Acids Res.* 29:e45. doi: 10.1093/nar/29.9.e45

Prakash, H., Nadella, V., Singh, S., and Schmitz-Winnenthal, H. (2016). CD14/TLR4 priming potentially recalibrates and exerts anti-tumor efficacy in tumor associated macrophages in a mouse model of pancreatic carcinoma. *Sci. Rep.* 6:31490. doi: 10.1038/srep31490

Qian, B.-Z., Li, J., Zhang, H., Kitamura, T., Zhang, J., Campion, L. R., et al. (2011). CCL2 recruits inflammatory monocytes to facilitate breast-tumour metastasis. *Nature* 475, 222–225. doi: 10.1038/nature10138

Radomska, H. S., Alberich-Jorda, M., Will, B., Gonzalez, D., Delwel, R., and Tenen, D. G. (2012). Targeting CDK1 promotes FLT3-activated acute myeloid leukemia differentiation through C/EBPalpha. *J. Clin. Invest.* 122, 2955–2966. doi: 10.1172/JCI43354

Ray, N., Kuwahara, M., Takada, Y., Maruyama, K., Kawaguchi, T., Tsubone, H., et al. (2006). c-Fos suppresses systemic inflammatory response to endotoxin. *Int. Immunol.* 18, 671–677. doi: 10.1093/intimm/dxl004

Raza, K., and Mishra, A. (2012). A novel anticlustering filtering algorithm for the prediction of genes as a drug target. *Am. J. Biomed. Eng.* 2, 206–211. doi: 10.5923/j.ajbe.20120205.03

Record, M., Carayon, K., Poirot, M., and Silvente-Poirot, S. (2014). Exosomes as new vesicular lipid transporters involved in cell–cell communication and various pathophysiologies. *Biochim. Biophys. Acta* 1841, 108–120. doi: 10.1016/j.bbalip.2013.10.004

Record, M., Silvente-Poirot, S., Poirot, M., and Wakelam, M. J. O. (2018). Extracellular vesicles: lipids as key components of their biogenesis and functions. *J. Lipid Res.* 59, 1316–1324. doi: 10.1194/jlr.E086173

Robinson, M. D., McCarthy, D. J., and Smyth, G. K. (2009). edgeR: a Bioconductor package for differential expression analysis of digital gene expression data. *Bioinformatics* 26, 139–140. doi: 10.1093/bioinformatics/btp616

Roca, H., Varsos, Z. S., Sud, S., Craig, M. J., Ying, C., and Pienta, K. J. (2009). CCL2 and interleukin-6 promote survival of human CD11b+ peripheral blood mononuclear cells and induce M2-type macrophage polarization. *J. Biol. Chem.* 284, 34342–34354. doi: 10.1074/jbc.M109.042671

Saif, M. W. (2011). Pancreatic neoplasm in 2011: an update. *JOP* 12, 316–321.

Salcedo, R., Ponce, M. L., Young, H. A., Wasserman, K., Ward, J. M., Kleinman, H. K., et al. (2000). Human endothelial cells express CCR2 and respond to MCP-1: direct role of MCP-1 in angiogenesis and tumor progression. *Blood* 96, 34–40. doi: 10.1182/blood.V96.1.34

Sha, H., Zhang, D., Zhang, Y., Wen, Y., and Wang, Y. (2017). ATF3 promotes migration and M1/M2 polarization of macrophages by activating tenascin-C via Wnt/β-catenin pathway. *Mol. Med. Rep.* 16, 3641–3647. doi: 10.3892/mmr.2017.6992

Shalapour, S., Font-Burgada, J., Di Caro, G., Zhong, Z., Sanchez-Lopez, E., Dhar, D., et al. (2015). Immunosuppressive plasma cells impede T-cell-dependent immunogenic chemotherapy. *Nature* 521, 94–98. doi: 10.1038/nature14395

Shen, Y., Guo, D., Weng, L., Wang, S., Ma, Z., Yang, Y., et al. (2017). Tumor-derived exosomes educate dendritic cells to promote tumor metastasis via HSP72/HSP105-TLR2/TLR4 pathway. *Oncoimmunology* 6:e1362527. doi: 10.1080/2162402X.2017.1362527

Shinohara, H., Kuranaga, Y., Kumazaki, M., Sugito, N., Yoshikawa, Y., Takai, T., et al. (2017). Regulated polarization of tumor-associated macrophages by miR-145 via colorectal cancer-derived extracellular vesicles. *J. Immunol.* 199, 1505–1515. doi: 10.4049/jimmunol.1700167

Showalter, M. R., Wancewicz, B., Fiehn, O., Archard, J. A., Clayton, S., Wagner, J., et al. (2019). Primed mesenchymal stem cells package exosomes with metabolites associated with immunomodulation. *Biochem. Biophys. Res. Commun.* 512, 729–735. doi: 10.1016/j.bbrc.2019.03.119

Song, R., Liu, S., and Leong, K. W. (2007). Effects of MIP-1α, MIP-3α, and MIP-3β on the induction of HIV Gag-specific immune response with DNA vaccines. *Mol. Ther.* 15, 1007–1015. doi: 10.1038/mt.sj.6300129

Stahl, P. D., and Raposo, G. (2019). Extracellular vesicles: exosomes and microvesicles, integrators of homeostasis. *Physiology* 34, 169–177. doi: 10.1152/physiol.00045.2018

Steffen, U., Koeleman, C. A., Sokolova, M. V., Bang, H., Kleyer, A., Rech, J., et al. (2020). IgA subclasses have different effector functions associated with distinct glycosylation profiles. *Nat. Commun.* 11:120. doi: 10.1038/s41467-019-13992-8

Thery, C., Witwer, K. W., Aikawa, E., Alcaraz, M. J., Anderson, J. D., Andriantsitohaina, R., et al. (2018). Minimal information for studies of extracellular vesicles 2018 (MISEV2018): a position statement of the international society for extracellular vesicles and update of the MISEV2014 guidelines. *J. Extracell. Vesicles* 7:1535750. doi: 10.1080/20013078.2018.1535750

Valenti, R., Huber, V., Filipazzi, P., Pilla, L., Sovena, G., Villa, A., et al. (2006). Human tumor-released microvesicles promote the differentiation of myeloid cells with transforming growth factor-β–mediated suppressive activity on T lymphocytes. *Cancer Res.* 66, 9290–9298. doi: 10.1158/0008-5472.CAN-06-1819

van Iterson, M., Boer, J. M., and Menezes, R. X. (2010). Filtering, FDR and power. *BMC Bioinformatics* 11:450. doi: 10.1186/1471-2105-11-450

Veremeyko, T., Yung, A. W. Y., Anthony, D. C., Strekalova, T., and Ponomarev, E. D. (2018). Early growth response gene-2 is essential for M1 and M2 macrophage activation and plasticity by modulation of the transcription factor CEBPbeta. *Front. Immunol.* 9:2515. doi: 10.3389/fimmu.2018.02923

Wan, X., Lei, Y., Li, Z., Wang, J., Chen, Z., McNutt, M., et al. (2015). Pancreatic expression of immunoglobulin g in human pancreatic cancer and associated diabetes. *Pancreas* 44, 1304–1313. doi: 10.1097/MPA.0000000000000544

Wang, K., Zhou, W., Cai, Q., Cheng, J., Cai, R., and Xing, R. (2017). SUMOylation of KLF4 promotes IL-4 induced macrophage M2 polarization. *Cell Cycle* 16, 374–381. doi: 10.1080/15384101.2016.1269045

Wang, X., Yao, B., Wang, Y., Fan, X., Wang, S., Niu, A., et al. (2017). Macrophage cyclooxygenase-2 protects against development of diabetic nephropathy. *Diabetes* 66, 494–504. doi: 10.2337/db16-0773

Wculek, S. K., Cueto, F. J., Mujal, A. M., Melero, I., Krummel, M. F., and Sancho, D. (2019). Dendritic cells in cancer immunology and immunotherapy. *Nature Rev. Immunol.* 20, 7–24. doi: 10.1038/s41577-019-0210-z

Wen, Y., Lu, X., Ren, J., Privratsky, J. R., Yang, B., Rudemiller, N. P., et al. (2019). KLF4 in macrophages attenuates TNFalpha-mediated kidney injury and fibrosis. *J. Am. Soc. Nephrol.* 30, 1925–1938. doi: 10.1681/ASN.2019020111

Wisniewski, J. R., Zougman, A., Nagaraj, N., and Mann, M. (2009). Universal sample preparation method for proteome analysis. *Nat. Methods* 6, 359–362. doi: 10.1038/nmeth.1322

Wong, R. S. Y. (2011). Apoptosis in cancer: from pathogenesis to treatment. *J. Exp. Clin. Cancer Res.* 30:87. doi: 10.1186/1756-9966-30-87

Xu, Y., Chen, B., Zheng, S., Wen, Y., Xu, A., Xu, K., et al. (2016). IgG silencing induces apoptosis and suppresses proliferation, migration and invasion in LNCaP prostate cancer cells. *Cell. Mol. Biol. Lett.* 21:27. doi: 10.1186/s11658-016-0029-6

Ying, H., Dey, P., Yao, W., Kimmelman, A. C., Draetta, G. F., Maitra, A., et al. (2016). Genetics and biology of pancreatic ductal adenocarcinoma. *Genes Dev.* 30, 355–385. doi: 10.1101/gad.275776.115

Yu, Q., Huang, Q., Du, X., Xu, S., Li, M., and Ma, S. (2018). Early activation of Egr-1 promotes neuroinflammation and dopaminergic neurodegeneration in an experimental model of Parkinson's disease. *Exp. Neurol.* 302, 145–154. doi: 10.1016/j.expneurol.2018.01.009

Yu, S., Liu, C., Su, K., Wang, J., Liu, Y., Zhang, L., et al. (2007). Tumor exosomes inhibit differentiation of bone marrow dendritic cells. *J. Immunol.* 178, 6867–6875. doi: 10.4049/jimmunol.178.11.6867

Zhou, M., Chen, J., Zhou, L., Chen, W., Ding, G., and Cao, L. (2014). Pancreatic cancer derived exosomes regulate the expression of TLR4 in dendritic cells via miR-203. *Cell. Immunol.* 292, 65–69. doi: 10.1016/j.cellimm.2014.09.004

Zhu, Q., Wang, H., Jiang, B., Ni, X., Jiang, L., Li, C., et al. (2018). Loss of ATF3 exacerbates liver damage through the activation of mTOR/p70S6K/ HIF-1alpha signaling pathway in liver inflammatory injury. *Cell Death Dis.* 9:910. doi: 10.1038/s41419-018-0894-1

Conflict of Interest: The authors declare that the research was conducted in the absence of any commercial or financial relationships that could be construed as a potential conflict of interest.

frontiers in Cell and Developmental Biology

REVIEW
published: 09 February 2021
doi: 10.3389/fcell.2021.636544

The Tumor Microenvironment in SCC: Mechanisms and Therapeutic Opportunities

*Nádia Ghinelli Amôr[1], Paulo Sérgio da Silva Santos[2] and Ana Paula Campanelli[1]**

[1] Department of Biological Sciences, Bauru School of Dentistry, University of São Paulo, Bauru, Brazil, [2] Department of Surgery, Stomatology, Pathology, and Radiology, Bauru School of Dentistry, University of São Paulo, Bauru, Brazil

Squamous cell carcinoma (SCC) is the second most common skin cancer worldwide and, despite the relatively easy visualization of the tumor in the clinic, a sizeable number of SCC patients are diagnosed at advanced stages with local invasion and distant metastatic lesions. In the last decade, immunotherapy has emerged as the fourth pillar in cancer therapy *via* the targeting of immune checkpoint molecules such as programmed cell-death protein-1 (PD-1), programmed cell death ligand-1 (PD-L1), and cytotoxic T-lymphocyte-associated protein 4 (CTLA-4). FDA-approved monoclonal antibodies directed against these immune targets have provide survival benefit in a growing list of cancer types. Currently, there are two immunotherapy drugs available for cutaneous SCC: cemiplimab and pembrolizumab; both monoclonal antibodies (mAb) that block PD-1 thereby promoting T-cell activation and/or function. However, the success rate of these checkpoint inhibitors currently remains around 50%, which means that half of the patients with advanced SCC experience no benefit from this treatment. This review will highlight the mechanisms by which the immune checkpoint molecules regulate the tumor microenvironment (TME), as well as the ongoing clinical trials that are employing single or combinatory therapeutic approaches for SCC immunotherapy. We also discuss the regulation of additional pathways that might promote superior therapeutic efficacy, and consequently provide increased survival for those patients that do not benefit from the current checkpoint inhibitor therapies.

Keywords: cutaneous squamous cell carcinoma, immunotherapy, tumor microenvironment, checkpoint inhibitors, regulatory T cell, macrophage, IL-33

OPEN ACCESS

Edited by:
Ana Karina Oliveira, National Center for Research in Energy and Materials (Brazil), Brazil

Reviewed by:
Eliana Blini Marengo, Hospital Israelita Albert Einstein, Brazil
Jamile Sá, Brazilian Biosciences National Laboratory (LNBio), Brazil

****Correspondence:***
Ana Paula Campanelli
apcampan@usp.br

Specialty section:
This article was submitted to Molecular Medicine, a section of the journal Frontiers in Cell and Developmental Biology

Received: *01 December 2020*
Accepted: *18 January 2021*
Published: *09 February 2021*

Citation:
Amôr NG, Santos PSS and Campanelli AP (2021) The Tumor Microenvironment in SCC: Mechanisms and Therapeutic Opportunities. Front. Cell Dev. Biol. 9:636544. doi: 10.3389/fcell.2021.636544

INTRODUCTION

Squamous cell carcinoma (SCC) is the second most common skin cancer worldwide and, despite the relatively easy visualization of the tumor in the clinic, a sizeable number of SCC patients are diagnosed at advanced stages with local invasion and distant metastatic lesions (Tromp et al., 2005). Worldwide, 300,000 new cases are seen each year (Thomson, 2018; Stang et al., 2019). The most significant risk factor for SCC includes sun exposure and age and is most common in white male individuals (Que et al., 2018a). Microscopically, SCC can be subcategorized according to the differentiation status of the epithelium and the presence of metastatic lesions (Que et al., 2018a). Tumor diameter and perineural involvement are highly associated with mortality risk

(Que et al., 2018a). The majority of cutaneous SCC can be surgically removed, however, high risk and advanced SCC management remained to be standardized (Que et al., 2018b).

The high risk of SCC development observed in immunocompromised individuals highlights the critical role of the immune system during skin carcinogenesis (Euvrard et al., 2003; Asgari et al., 2017; Omland et al., 2018). Conversely, increased infiltration of specific inflammatory cells, such as neutrophils, macrophages, and T lymphocytes are associated with aggressive SCC and metastasis (Duan et al., 2000; Seddon et al., 2016; Jiang et al., 2019). Such discordant observations are explained by the great capacity of tumor cells to modulate the tumor microenvironment (TME) to become a supportive niche thereby inhibiting anti-tumoral responses (Weber et al., 2005; Moussai et al., 2011; Maalouf et al., 2012). The CD28-related inhibitory receptors crucial for T cell regulation, namely cytotoxic T-lymphocyte-associated protein 4 (CTLA-4) and programmed cell-death protein-1 (PD-1), are highly expressed in human SCC samples and associated with cancer progression (Welsh et al., 2009; Gambichler et al., 2017). Blocking specific immunosuppressive pathways seems to be the most promising approach to fight cancer cells. Indeed, PD-1 blockade using monoclonal antibody has been shown to increase the infiltration of $CD4^+$ and $CD8^+$ T cells and delays SCC development in mice (Belai et al., 2014), and the immunotherapy that blocks the signaling pathway mediated by PD-1 has been approved for cutaneous SCC. However, a significant proportion of SCC patients receive no benefit from this therapy (Migden et al., 2018). Such observations highlight the need for developing alternative or combinatory targets, that take into account the complexity of the immune system and the heterogeneity of tumor-infiltrating leukocytes in SCC (Ji et al., 2020). For example, regulatory T cells (Tregs) are observed in advanced cancers and also associated with poor outcomes (Azzimonti et al., 2015). Pre-clinical model of SCC development is also accompanied by infiltration of Tregs in the skin and draining lymph nodes (LN), and depletion of these cells using anti-CD25 significantly impaired SCC progression by increasing the infiltration of activated $CD4^+$ and $CD8^+$ T cells in the TME and the production of anti-tumor cytokines such as IL-12 and IFN-γ (Ramos et al., 2012). Herein, we provide a comprehensive overview of the interactions between tumor and immune cells and highlight strategies to identify potential new targets and biomarkers for immunotherapy in SCC.

CELLULAR COMPOSITION OF THE TUMOR MICROENVIRONMENT

The SCC microenvironment is comprised of cancerous and normal epithelial cells, fibroblasts, endothelial cells (ECs), melanocytes, plasmacytoid, and dendritic cells (DCs), Langerhans cells, macrophages, myeloid-derived suppressor cells (MDSCs), natural killer (NK) cells, $CD4^+$ and $CD8^+$ T cells, and Tregs (Ji et al., 2020). Importantly, the frequency of each cell type varies considerably between patients, suggesting that the TME is not static and might be influenced by genetic and other patient-derived intrinsic factors (Ji et al., 2020). The role of the TME during SCC tumorigenesis and the mechanisms of immune escape are summarized in **Figure 1**.

The stroma adjacent to SCC is composed mainly of ECs and fibroblasts that create a fibrovascular niche (Ji et al., 2020). The association between ECs and cancer is frequently studied since angiogenesis is fundamental for SCC development (Tonini et al., 2003; Florence et al., 2011; **Figure 1A**). In addition, it has been demonstrated that tumor cell increased the expression of CD200 in ECs, which in combination with its ligand, CD200R (present in macrophages and DCs), might be a mechanism leading to immunosuppression in the TME (Belkin et al., 2013; **Figure 1A**). Fibroblasts are highly heterogeneous and multifunctional mesenchymal-derived cells embedded within the interstitial extracellular matrix that becomes activated during wound healing, tissue inflammation, and organ fibrosis (Chen and Song, 2019). Activated fibroblasts in the TME are named cancer-associated fibroblasts (CAFs) and are identified by the expression of α-smooth muscle actin (α–SMA), fibroblast-activation protein α (FAPα), and ferroptosis suppressor protein 1 (FSP-1) (Öhlund et al., 2014). CAFs directly impact the behavior of tumor cells by increasing the expression of laminin-332 γ2 chain in tumor cells through activation of the TGF-β signaling subsequently leading to enhanced cell invasion (Siljamäki et al., 2020; **Figure 1B**). CAFs also have a role in immunosurveillance and tumor escape *via* CD276 (B7-H3), which augments Tregs and inhibit cytotoxic $CD8^+$ T cell responses (Ji et al., 2020) and promote tumor development by enhancing monocyte chemoattractant protein-1 (MCP-1)–dependent macrophage infiltration and chronic inflammation (Zhang et al., 2011; **Figure 1B**). However, Zhang et al. (2013a) demonstrated that CAFs can prevent carcinogen-derived tumor formation by protecting epithelial cells from DNA damage, suggesting an ambiguous role of CAFs in cutaneous SCC.

During inflammation, neutrophils are among the first phagocytes to infiltrate the tissue, mostly through CXC chemokine-mediated chemotaxis, and these cells predominate in the SCC invasive front (Kruger et al., 2015; Simonneau et al., 2018; Khou et al., 2020). Progressive infiltration of tumor-associated neutrophils (TANs) was observed during the evolution of benign papillomas to established SCC lesions in a chemical carcinogenesis model, and tumor escape mostly involved the impairment of anti-tumor $CD8^+$ T cell responses mediated by high arginase activity, production of reactive oxygen species (ROS), nitrite (NO), and the induction of PD-1 expression on $CD8^+$ T cells (Khou et al., 2020; **Figure 1C**). Similar to CAFs, TANs can also play an anti-tumoral effect in SCC. Challacombe et al. (2006) showed that neutrophil depletion increases SCC development, suggesting their role in mediating anti-tumor responses. In addition, neutrophils were necessary for the anti-tumoral effects of the Ingenol 3-angelate in experimental SCC (Challacombe et al., 2006). Such contradictory roles of these cells might be explained by the fact that, in the TME, tumor-derived factors can modulate their phenotype and function. TANs may acquire either an anti-tumor activity (N1 neutrophils), and/or a pro-tumoral activity (N2 neutrophils) mediated by TGF-b signaling (Fridlender et al., 2009; **Figure 1C**). In a mouse uterine cancer model, TANs exhibit N2 phenotype and promoted

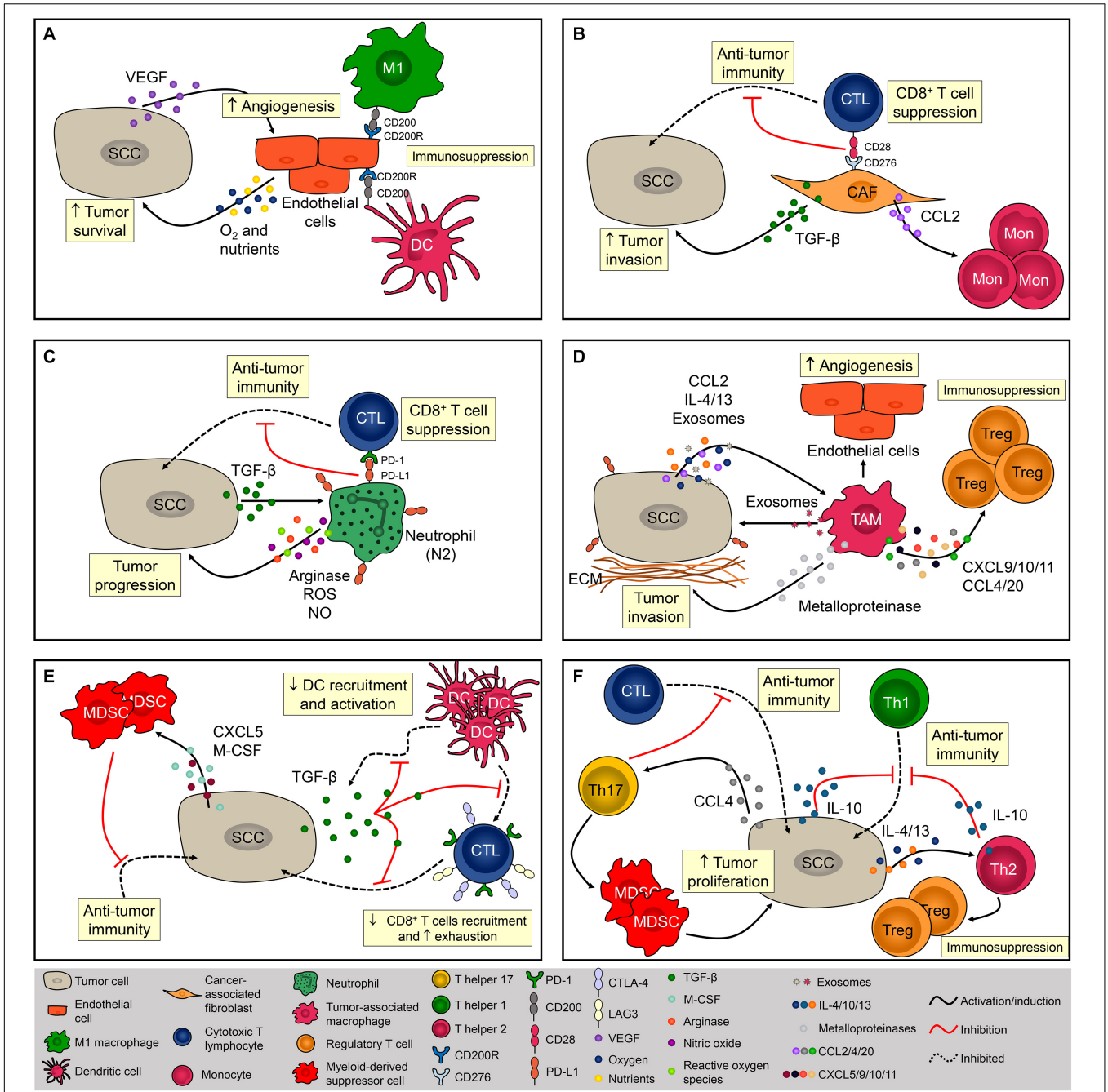

FIGURE 1 | Cellular composition of the SCC microenvironment. The SCC microenvironment is comprised of cancerous and normal epithelial cells, fibroblasts, endothelial cells, and immune cells. Each one of them can exert pro- and/or anti-tumoral effects. **(A)** Tumor cells produce VEGF that promotes angiogenesis. Endothelial cells (EC) provide oxygen and nutrients that are essential for tumor cells metabolism and promote immunosuppression *via* CD200R expression. **(B)** Cancer-associated fibroblasts (CAF) impact immunosurveillance and tumor escape *via* CD276 (B7-H3), contributing to the activation of Tregs and inhibition cytotoxic $CD8^+$ T cells. CAFS also promote tumor development by increasing the influx of monocytes *via* MCP-1 release and TGF-β production. **(C)** Neutrophils are recruited *via* CXCL8 chemotaxis. Neutrophils are polarized to N2 phenotype *via* TGF-β and promote SCC progression mostly by suppressing the activity of cytotoxic T lymphocytes (CTL) *via* PD-1/PD-L1 signaling. **(D)** Tumor-associated macrophages (TAM) are recruited *via* CCL2 chemotaxis and contribute to the progression of tumor by producing metalloproteinases (MMP) and recruiting regulatory T cells (Tregs). TAMs are polarized to a pro-tumor phenotype by IL-4, IL-13, and tumor-derived exosomes. **(E)** By secreting TGF-β1, SCC inhibits dendritic cells (DC) migration and the ability of DC to mature into a potent T cell activator. Tumor cells also promote immunosuppression by recruiting myeloid-derived suppressor cells *via* CXCL5 and M-CSF. **(F)** $CD4^+$ T cells from a chemically-induced mouse model of SCC preferentially produce IL-4 and IL-10, promoting immunosuppression by inhibiting Th1 responses and recruiting Tregs. Th17 cells are recruited to the TME *via* CCL4 chemotaxis and promote the infiltration of myeloid cells and decrease the infiltration of IFN-γ-producing $CD8^+$ T lymphocytes contributing to the immunosuppressive niche during SCC.

tumor growth through elastase release (Mahiddine et al., 2020). The authors also demonstrated that hypoxia is crucial for N2 phenotype maintenance and tumor oxygenation can revert TANs phenotype toward N1 (Mahiddine et al., 2020). Tumor-associated macrophages (TAMs) also represent a significant percentage of infiltrating phagocyte population in SCC (Kambayashi et al., 2013; Amôr et al., 2018; Simonneau et al., 2018; Jiang et al., 2019), and specific depletion of these cells inhibited tumor growth (Takahashi et al., 2009). The recruitment of monocytes into the SCC is mediated by CC chemokines such as CCL2 and, once in the TME, monocyte-derived macrophages are polarized toward a M1 or M2 phenotype (Pettersen et al., 2011; Caley et al., 2020). Due to the abundance of Th2-related cytokines such as IL-13, IL-4, and IL-10, the TME around SCC is often predominated by M2 macrophages (Linde et al., 2012b; Caley et al., 2020; **Figure 1D**). In addition to the TME cytokine profile, macrophages can also be M2-polarized through the secretion of tumor-derived exosomes. Exosomes derived from SCC promoted M2-like macrophage polarization through ERK1/2 signaling activation (Pang et al., 2020) besides promoting cell survival after ionizing radiation *in vitro* (Mutschelknaus et al., 2016; **Figure 1D**). Data from breast cancer also suggest that exosomes are capable of inducing IL-6 secretion, and a pro-survival phenotype in M2 macrophages, partially *via* gp130/STAT3 signaling (Ham et al., 2018). Interestingly, exosome-mediated communication in the TME works in both ways. Macrophage-derived exosomes increase cell migration and PD-L1 expression contributing to the establishment of an immunosuppressive TME (Bellmunt et al., 2019; **Figure 1D**). The contribution of TAMs directly to tumor growth occurs in early stages of carcinogenesis *via* malignant transformation and proliferation of epidermal cells. These cells also contribute to the progression of tumor by producing metalloproteinases (MMP) and increasing angiogenesis, thus facilitating the dissemination of tumor cells (Kerkelä et al., 2002; Linde et al., 2012a,b; Kambayashi et al., 2013; **Figure 1D**). TAMs can facilitate tumor escape by recruiting Tregs through the secretion of CXCL9/10/11 (ligands for CXCR3), CCL4 (ligands for CCR4/8), and CCL20 (ligands for CXCR3 and CCR6), which will further suppress local anti-tumoral immune responses (Ji et al., 2020; **Figure 1D**). Depletion of CCR2-expressing monocytes or macrophages with anti-CSF1R prevents the spontaneous development of SCC in transgenic mice (Antsiferova et al., 2017). Similarly, VEGFR-3 ligand blockade reduced SCC development by decreasing macrophage infiltration (Alitalo et al., 2013). Together, these findings strongly indicate the significant role of TAMs during SCC pathogenesis.

Given the importance of DCs in the skin, these cells are often thought to be the first immune cells to encounter tumor antigens from SCC (Valladeau and Saeland, 2005). SCC-derived DCs strongly induce $CD4^+$ and $CD8^+$ T-cell proliferation and IFN-γ production, thereby promoting the anti-tumoral response (Fujita et al., 2012). A significant decrease in DC infiltration has been reported in SCC and this is likely an important mechanism for tumor escape. By secreting TGF-β1, SCC inhibits DC migration and the ability of DC to mature into a potent T cell activator (**Figure 1E**; Halliday and Le, 2001; Weber et al., 2005). Further, *in vitro* stimulation of SCC-derived DCs showed an impaired ability of these cells to express costimulatory molecules when compared with DCs derived from normal skin, suggesting that SCC microenvironment display mechanisms that contribute to negative regulation in anti-tumor immune responses (Bluth et al., 2009). In SCC patients, this might be explained by the high expression of PD-L1 and PD-L2 in DCs (Jiao et al., 2017) or by the proximity of DCs to Tregs (Jang, 2008). Another myeloid cell that exerts a significant role in TME is the MDSCs, which promotes tumor progression by suppressing the effector function of anti-tumor immune cells from early to advanced stages of SCC (**Figure 1E**). Elevated circulating numbers of MDSCs were associated with high-grade SCC (Seddon et al., 2016). During early stages of tumor initiation in mice, Maalouf et al. (2012) reported an increased influx of MDSCs driven by the secretion of epidermal-derived CXCL5 and macrophage colony-stimulating factor (M-CSF) (**Figure 1E**). MDSCs were also found in advanced stages of SCC; these cells express high levels of $CD200R^+$ that may interact with $CD200^+$ tumor cells conferring immune privilege and favoring metastasis development (Stumpfova et al., 2010).

$CD8^+$ T lymphocytes can directly eliminate tumor cells through the secretion of cytolytic enzymes, which are essential mediators of the anti-tumoral response (Nasti et al., 2015). However, SCC lesions display low frequencies of $CD8^+$ T cells (Freeman et al., 2014) due, in part, to the presence of TGF-β, which inhibits $CD8^+$ T cells infiltration and induces the expression of T cell exhaustion markers such as Tim-3, CTLA-4, and PD-1 (Weber et al., 2005; Linedale et al., 2017; **Figure 1E**). Blockade of PD-1 with monoclonal antibody was shown to increase tumor-infiltrating cytotoxic T lymphocytes (CTLs) resulting in anti-tumor activity against SCC growth (Belai et al., 2014), however, the depletion of $CD8^+$ abrogated the efficacy of the anti-PD1 mAb treatment (Dodagatta-Marri et al., 2019), suggesting an association between the efficacy of PD-1 blockade therapies and the frequency of $PD\text{-}1^+$ $CD8^+$ T cells in the TME (Gros et al., 2014; Kansy et al., 2017; Kumagai et al., 2020).

Mice lacking $CD4^+$ T cells and submitted to UVB-induced carcinogenesis displayed higher tumor growth associated with increased inflammation and increased number of $p53^+$ tumor cells, demonstrating that this subset of T cells has an important role in controlling inflammation-associated carcinogenesis (Hatton et al., 2007). During skin carcinogenesis, $CD4^+$ T cells are recruited *via* CXCL9- and CXCL10-mediated chemotaxis (Winkler et al., 2011). However, tumor cells can escape from T helper-mediated immune responses by polarizing $CD4^+$ cells toward to a pro-tumor phenotype, characterized by Th2, Th17, and Treg cytokine profiles (Girardi et al., 2004; Zhang et al., 2013b; **Figure 1F**). IL-10-depleted mice are protected from UV-induced skin cancer due to their increased amounts of IFN-γ and enhanced numbers of $CD4^+$ T cells, indicating a strong Th1-driven immune response (Loser et al., 2007). $CD4^+$ T cells from a chemically-induced mouse model of SCC preferentially produced IL-4 and IL-10 (typical of Th2-type immunity) and these cells promote immunosuppression by inhibiting Th1 responses and recruiting Tregs (Yusuf et al., 2008; Nasti et al., 2011; **Figure 1F**). Th17 cells are recruited

to the TME *via* CCL4 chemotaxis (Ortiz et al., 2015) and Wang et al. (2010) demonstrated that IL-17 contributes to skin tumorigenesis directly by increasing hyperproliferation of epithelial cells. Finally, IL-17 promoted the infiltration of myeloid cells, and decreased the infiltration of IFN-γ-producing $CD8^+$ T lymphocytes contributing to the immunosuppressive niche during SCC (Wang et al., 2010; **Figure 1F**).

EVASION OF THE IMMUNE RESPONSE: POTENTIAL TARGETS FOR IMMUNOTHERAPIES

As discussed above, an effective immune response is critical to control SCC development and progression (Burton et al., 2016). To efficiently eliminate SCC, leukocytes must infiltrate the TME, initiate cell-to-cell interactions so as to exert effective anti-tumoral functions (Halliday and Le, 2001; Weber et al., 2005; Ortner et al., 2017). T cell activation involves the engagement of receptors and co-receptors (Dustin and Shaw, 1999), but this activation is countered by a series of molecules called immune checkpoints that are responsible for controlling T cell function and induce self-tolerance (Yao et al., 2013; Waldman et al., 2020).

CTLA-4 and PD-1 are the most well-studied examples of T cell immune checkpoint molecules and tumor cells exploit these molecules to evade host immunity (Miao et al., 2019). Ipilimumab, an anti-CTLA-4 blocking monoclonal antibody, was the first immune checkpoint inhibitor to be tested and approved for the treatment of cancer (Phan et al., 2003). CTLA-4 is a transmembrane molecule that competes with the co-receptors B7-1 and B7-2 for CD28 binding and negatively regulates T cell activation (Brunet et al., 1987; Linsley et al., 1992; **Figure 2A**). During photocarcinogenesis, mice treated with anti-CTLA-4 developed significantly fewer tumors (Loser et al., 2005). Moreover, mice treated with anti-CTLA-4 developed long-lasting protective immunity, and *in vitro* CTLA-4 blockade inhibited the suppressor activity of UV-induced Tregs, suggesting that anti-CTLA-4-treated mice were protected from tumor growth due to the inhibition of Treg function in the TME (Loser et al., 2005; **Figure 2A**). Despite the beneficial effects of this therapy been observed in pre-clinical models of carcinogenesis, and in patients with melanoma (Hodi et al., 2010), there is presently only one ongoing (recruiting) clinical trial assessing the efficacy of ipilimumab in cutaneous SCC (NCT04620200).

T cell activation is also regulated by PD-1 and is mediated by the interaction with its ligands, PD-L1 and PD-L2 (Freeman et al., 2000; Latchman et al., 2001), both of which are highly expressed in SCC (Belai et al., 2014; Varki et al., 2018). Blocking PD-1 resulted in a potent anti-tumoral response in a chemically induced SCC model characterized by the infiltration of activated $CD4^+$ and $CD8^+$ T cells, IFN-γ levels, and reduced levels of the immunosuppressor cytokine TGF-β (Belai et al., 2014; **Figure 2B**). Currently, two FDA-approved immunotherapies for SCC (i.e., pembrolizumab and cemiplimab) target the interaction between PD-1/PD-L1 molecules. Despite reports of adverse events in this trial, approximately half the patients with advanced SCC responded to cemiplimab therapy (Migden et al., 2018). Immune checkpoints-based therapies are of great relevance especially for patients with advanced and metastatic disease that are not ideal candidates for surgical excision. A retrospective analysis showed that PD-1 inhibition produces durable responses among patients with advanced or metastatic SCC (In et al., 2020). In a multicenter study, the overall response rate obtained among patients with advanced SCC was even higher (Salzmann et al., 2020). In both studies, the dose used was well tolerated and the response rate satisfactory, therefore adding evidence and encouraging the implementation of immune checkpoint therapies for patients with advanced and unresectable SCC lesions.

Besides T cell exhaustion, SCC development is also associated with the generation of effector Tregs (Clark et al., 2008). Tregs are characterized by CD4, CD25, and transcription factor forkhead box P3 (FOXP3) expression and, once activated, these cells suppress exacerbated immune responses and maintain self-tolerance (Sakaguchi et al., 2010; **Figure 2C**). The depletion of $CD25^+$ Tregs significantly reduced SCC development in mice (Ramos et al., 2012). Further, the presence of Tregs within the TME and the levels of PD-1 expression by Tregs directly correlate with immune evasion (Kumagai et al., 2020) and worse outcome (Azzimonti et al., 2015). Increased percentage of tumor-infiltrating Tregs was associated with loss of inflammasome activation, and SCC development in mice (Gasparoto et al., 2014). Tregs can be either locally differentiated by TGF-β (Chen et al., 2003) or recruited *via* the CCL4/CCL5-CCR5 axis (de Oliveira et al., 2017; **Figure 2C**). Tregs inhibitory function is mediated by IL-10 (Loser et al., 2007), and by the inhibition of $CD4^+$ and $CD8^+$ T cells proliferation and IFN-γ secretion (Lai et al., 2016; **Figure 2C**). Importantly, in mice, anti-TGF-β monotherapy was more efficient (approximately 20% of complete regression) than anti-PD-1 monotherapy (<3% of complete regression) and promoted long-term immunity against SCC (Dodagatta-Marri et al., 2019), therefore inhibition of Tregs recruitment or differentiation using antagonistic antibodies against CCR5 or neutralizing antibodies against TGF-β are relevant strategies for immunotherapy (**Figure 2D**). Moreover, although anti-PD-1 monotherapy elevates immunosuppressive Tregs in chemically induced SCC, 60% of complete regression in established tumors was achieved when combined with anti-TGF-β therapy, highlighting the benefits of combinatory immunotherapies for SCC (Dodagatta-Marri et al., 2019). It has recently been demonstrated that PD-1 blockade induces both recovery of dysfunctional $PD\text{-}1^+$ $CD8^+$ T cells and enhanced $PD\text{-}1^+$ Treg cell-mediated immunosuppression (Kumagai et al., 2020). This study suggests that the balance of PD-1 expression between $CD8^+$ effector T cells and Tregs in the TME should be considered as a clinically meaningful biomarker to predict the efficacy of PD-1-blocking immunotherapy in various cancers including SCC (Aksoylar and Boussiotis, 2020; Kumagai et al., 2020).

Another recently emerging area in cancer immunotherapy has focused on macrophages since these cells frequently infiltrate solid tumors, including SCC, and have a significant impact on prognosis (Takahara et al., 2009; Li, 2016; **Figure 2E**). Indeed, colony-stimulating factor 1 (CSF-1) is a key regulator of monocyte/macrophage recruitment and differentiation in the

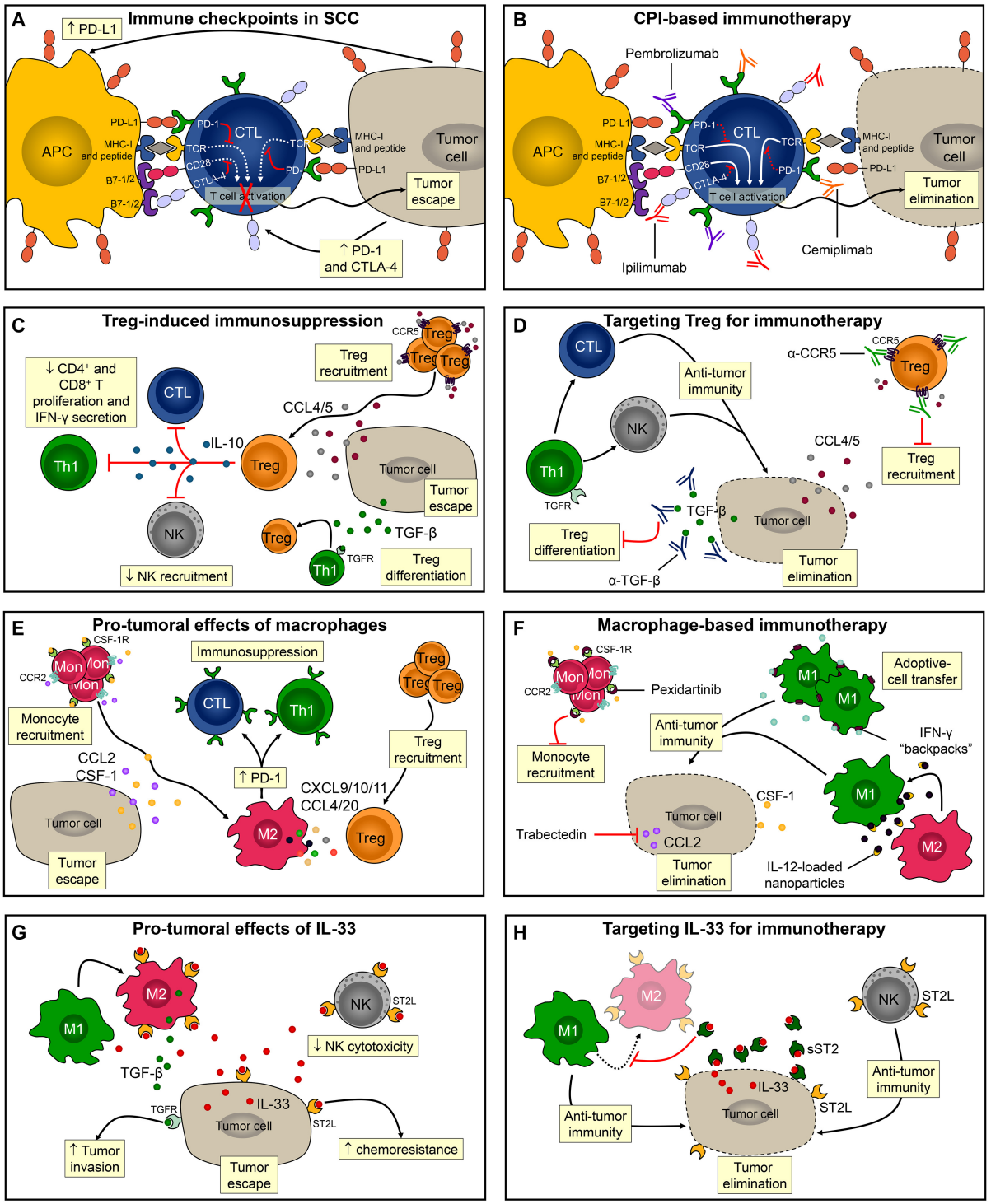

FIGURE 2 | Continued

FIGURE 2 | Evasion of the immune response and potential targets for immunotherapies. **(A)** *Via* the interaction between PD-1/PD-L1 and CTLA-4/B7, SCC cells inhibit $CD8^+$ T cell activation and escape from immunosurveillance. **(B)** Monoclonal antibodies block PD-1 (pembrolizumab and cemiplimab) and CTLA-4 (ipilimumab) thereby promoting T-cell activation and/or function. **(C)** Tregs are recruited to TME *via* CCL4 and CCL5 or locally differentiated by TGF-β. The presence of Tregs within the TME and their levels of PD-1 expression directly correlate with immune evasion. **(D)** To overcome Treg-induced immunosuppression it is necessary to block its recruitment and/or local differentiation by inhibiting CCL4-5/CCR5 signaling or by neutralizing TGF-β. **(E)** Monocytes are recruited into the TME *via* CCL2 and CSF-1 chemotaxis. Macrophages promote SCC progression by creating an immunosuppressor microenvironment. **(F)** Pexidartinib and trabectedin are two molecules known for inhibiting macrophage recruitment into the TME. Another macrophage-based therapy involves the induction and sustained polarization of macrophages toward anti-tumoral phenotype M1. **(G)** In mice, IL-33 promotes SCC development by increasing M2 macrophage infiltration and inhibiting NK cell cytotoxicity. **(H)** Using the soluble form of the IL-33 receptor, sST2, it is possible to disrupt the IL-33/ST2 signaling and promote anti-tumor immune response mediated by M1 macrophages and NK cells.

TME and promotes malignancy (Lin et al., 2001; **Figure 2E**). In a syngeneic mouse model of melanoma, pexidartinib, a potent inhibitor of the CSF-1 receptor (CSF-1R), conferred anti-tumoral response associated with TAMs reduction (Mok et al., 2014; **Figure 2F**). Pexidartinib is approved for the treatment of tenosynovial giant cell tumor (Lamb, 2019) and is currently being tested in several clinical trials, none of them for SCC but with great potential (Benner et al., 2020). CCL2, also known as MCP-1, is another monocyte chemoattractant that promotes carcinogenesis by recruiting TAMs and inducing immune evasion through PD-1 signaling (Yang et al., 2020; **Figure 2E**). A phase II trial of trabectedin, a small molecule that specifically inhibits CCL2 synthesis, showed effectiveness as a single agent in platinum-sensitive patients with advanced recurrent ovarian cancer (Krasner et al., 2007; **Figure 2F**). Although trabectedin has been used to treat ovarian and breast cancer as well as soft tissue sarcomas (D'Incalci and Zambelli, 2016), its effect against SCC has yet to be investigated. While inhibition of macrophage recruitment might seem promising, M1-polarized macrophages exert potent anti-tumoral immune responses. Accordingly, M1-polarization of TAMs reversed the immunosuppressive state of TAMs and promoted tumor regression in models of ovarian cancer, melanoma, and glioblastoma (Zhang et al., 2019; **Figure 2F**). However, macrophage-based therapies remain highly challenging due to the plasticity of these cells (i.e., M1 macrophages can easily switch for M2 phenotype upon stimulus) (Linde et al., 2012a). To overcome this, sustained M1 differentiation is required and nanoparticles containing IL-12 promote macrophage conversion from the M2 to the M1 phenotype in the TME. Notably, this strategy has protected mice from melanoma development (Wang et al., 2017; **Figure 2F**). Shields et al. (2020) also successfully demonstrated that sustaining the M1 phenotype in the TME effectively controlled melanoma progression. Interestingly, this research team developed discoidal particles called "backpacks" that attach to macrophages and constantly deliver IFN-γ to sustain the M1 phenotype (Shields et al., 2020; **Figure 2F**).

Lastly, but still of considerable importance, soluble components of the TME, such as cytokines, chemokines, and growth factors exert a critical role during tumorigenesis (Dranoff, 2004). For example, IL-33 is abundantly expressed in epithelial cells and several other cell types (Hammad and Lambrecht, 2015), and as such it appears to be a great target for cutaneous SCC therapy. Due to its central role in mediating type 2 innate and adaptive immunity *via* the ST2 receptor, IL-33 has been extensively studied in cancer and inflammatory diseases (Liew et al., 2016). In mice, IL-33 promotes SCC development by increasing M2 macrophage infiltration and decreasing NK cell cytotoxicity (Amôr et al., 2018; **Figure 2G**). IL-33 promotes differentiation of macrophages that in turn, send paracrine TGF-β signals to tumor cells consequently inducing invasive behavior (Taniguchi et al., 2020; **Figure 2G**). In addition, IL-33 can acts directly on tumor cells to enhance chemoresistance (Fang et al., 2017), highlighting that IL-33/ST2 targeting should be considered further for SCC therapies (**Figure 2G**). One possible way to disrupt the IL-33/ST2 signaling is *via* the soluble form of the IL-33 receptor, sST2, which acts as a decoy receptor and prevents the binding of IL-33 to ST2L on the cell surface (Hayakawa et al., 2007; Griesenauer and Paczesny, 2017; **Figure 2H**). Although the effects of sST2 administration have not been tested in SCC, its potential therapeutic benefits were demonstrated in colorectal carcinoma (Akimoto et al., 2016). The reduced tumor growth observed in sST2-treated mice was associated with decreased angiogenesis, and inhibition of macrophage infiltration and M2 polarization (Akimoto et al., 2016; **Figure 2H**).

CONCLUDING REMARKS AND PERSPECTIVES

Growing evidence highlights the crucial contribution of immune and non-immune cells during SCC pathogenesis, most notably in the TME, and the targeting of this supportive tumor niche is an important part of emerging therapies in this cancer. As the understanding of the mechanistic events that permit tumor evasion from immunosurveillance emerges, comprehensive treatment methods that enhance anti-tumor immunity and the sensitivity of tumor cells to chemotherapies will revolutionize the therapy landscape in SCC. Although emerged as the advent for cancer treatment, one of the major limitations of immunotherapy is the development of acquired resistance to treatment due to triggering of compensatory mechanisms resulting in tumor relapse/progression. For example, in SCC, the anti-PD-1 treatment that is supposed to reduce T cell suppression also promotes the infiltration of Tregs, which are known to directly assist tumor escape in experimental SCC (Dodagatta-Marri et al., 2019). Similarly, in head and neck SCC (HNSCC), PD-1 blockade culminated in Tim-3 upregulation, supporting a circuit of compensatory suppressor signaling allowing tumor escape (Shayan et al., 2017). Therefore, combinatory therapies are the more promising future strategies in SCC therapy. Clinical data have shown that melanoma patients treated with anti-PD-1 and anti-CTLA-4 monoclonal antibodies (mAb) presented tumor

reduction (Wolchok et al., 2013; Postow et al., 2015). Similarly, simultaneous blockade of GITR and PD-L1 demonstrated safety and efficacy against advanced solid tumors (Heinhuis et al., 2019). Results from over 50% of patients with recurrent or metastatic HNSCC have shown disease stabilization after treatment with motolimod, an agonist of TLR8 which stimulates NK, DC, and monocytes, in combination with cetuximab in a phase Ib clinical trial (Chow et al., 2017). Altogether, these studies represent an exciting new horizon that could be also tested for cutaneous SCC treatment.

Additionally, the next-generation sequencing (NGS) technology has emerged as one of the most powerful tools for cancer research since enables efficient and accurate detection of somatic mutations frequently associated with treatment resistance (Łuksza et al., 2017). Using the NGS approach, Lobl et al. (2020) identified the co-occurrence of ERBB4 and STK11 mutations in localized cutaneous SCC, which prompted the researchers to suggest a new therapeutic approach by inhibiting CDH1 and the Wnt pathway. Besides identification of tumor mutational burden, NGS also allows the prediction of response and development of a personalized treatment that might significantly improve outcomes for cancer patients (Holbrook et al., 2011; Roychowdhury et al., 2011; Chen et al., 2019). Based on that, NGS could and should be incorporated to assess mutations not only in tumor cells but also in immune cells of SCC patients that will help to overcome the differences of response rate observed among patients with similar malignancy and treatment, leading to the development of personalized therapies improving clinical outcomes.

Herein, we provide a range of alternative targets focused on the regulation of immune cells beyond T cells to promote anti-tumoral responses. However, a reasonable amount of the work regarding immunological therapeutic strategies remains to be evaluated against SCC, highlighting opportunities for therapeutic intervention. Since the composition of the TME is heterogeneous and result in different TME subclasses not only among patients or tumor types but also within a patient's tumor, it is important to consider the differences in the spatial localization, density, and functional orientation of immune cells in the TME, in order to predict and improve the clinical benefits [reviewed extensively by Pérez-Ruiz et al. (2020)]. Most exciting to us are experimental strategies around macrophage- and/or IL-33-based therapies in SCC. We concede that most of the data regarding these strategies are derived from experimental models with little clinical insight, but animal models do provide key early insights into the role of immune cells and soluble factors in SCC tumorigenesis. We contend that these limitations will be lessened as further translational investigations using human subjects and clinical trials are implemented to better assess the efficacy of alternative strategies for SCC immunotherapy.

AUTHOR CONTRIBUTIONS

NA contributed to graphic drawing and drafting of the manuscript. PS contributed to drafting of the manuscript. AC contributed to concept generation and drafting of the manuscript. All authors contributed to the article and approved the submitted version.

FUNDING

The work was supported by grants #2014/06215-1, #2018/10529-2, and #2021/00217-6 São Paulo Research Foundation (FAPESP) and by CNPq (#302578/2019-6). This study was also financed in part by the Coordenação de Aperfeiçoamento de Pessoal de Nível Superior – Brazil (CAPES) – Finance Code 001.

ACKNOWLEDGMENTS

The authors would like to thank Blooming LLC, scientific consulting and editing, for the proofreading and revision of the manuscript.

REFERENCES

Akimoto, M., Maruyama, R., Takamaru, H., Ochiya, T., and Takenaga, K. (2016). Soluble IL-33 receptor sST2 inhibits colorectal cancer malignant growth by modifying the tumour microenvironment. *Nat. Commun.* 7:13589. doi: 10.1038/ncomms13589

Aksoylar, H. I., and Boussiotis, V. A. (2020). PD-1(+) T(reg) cells: a foe in cancer immunotherapy? *Nat. Immunol.* 21, 1311–1312. doi: 10.1038/s41590-020-0801-7

Alitalo, A. K., Proulx, S. T., Karaman, S., Aebischer, D., Martino, S., Jost, M., et al. (2013). VEGF-C and VEGF-D blockade inhibits inflammatory skin carcinogenesis. *Cancer Res.* 73, 4212–4221. doi: 10.1158/0008-5472.can-12-4539

Amôr, N. G., de Oliveira, C. E., Gasparoto, T. H., Boas, V. G. V., Perri, G., Kaneno, R., et al. (2018). ST2/IL-33 signaling promotes malignant development of experimental squamous cell carcinoma by decreasing NK cells cytotoxicity and modulating the intratumoral cell infiltrate. *Oncotarget* 9:25768. doi: 10.18632/oncotarget.25768

Antsiferova, M., Piwko-Czuchra, A., Cangkrama, M., Wietecha, M., Sahin, D., Birkner, K., et al. (2017). Activin promotes skin carcinogenesis by attraction and reprogramming of macrophages. *EMBO Mol. Med.* 9, 27–45. doi: 10.15252/emmm.201606493

Asgari, M. M., Ray, G. T., Quesenberry, C. P. Jr., Katz, K. A., and Silverberg, M. J. (2017). Association of Multiple Primary Skin Cancers With Human Immunodeficiency Virus Infection. *CD4 Count. Viral Load. JAMA Dermatol.* 153, 892–896. doi: 10.1001/jamadermatol.2017.1716

Azzimonti, B., Zavattaro, E., Provasi, M., Vidali, M., Conca, A., Catalano, E., et al. (2015). Intense Foxp3+ CD25+ regulatory T-cell infiltration is associated with high-grade cutaneous squamous cell carcinoma and counterbalanced by CD8+/Foxp3+ CD25+ ratio. *Br. J. Dermatol.* 172, 64–73. doi: 10.1111/bjd.13172

Belai, E. B., de Oliveira, C. E., Gasparoto, T. H., Ramos, R. N., Torres, S. A., Garlet, G. P., et al. (2014). PD-1 blockage delays murine squamous cell carcinoma development. *Carcinogenesis* 35, 424–431. doi: 10.1093/carcin/bgt305

Belkin, D. A., Mitsui, H., Wang, C. Q., Gonzalez, J., Zhang, S., Shah, K. R., et al. (2013). CD200 upregulation in vascular endothelium surrounding cutaneous squamous cell carcinoma. *JAMA Dermatol.* 149, 178–186. doi: 10.1001/jamadermatol.2013.1609

Bellmunt, ÀM., López-Puerto, L., Lorente, J., and Closa, D. (2019). Involvement of extracellular vesicles in the macrophage-tumor cell communication in head and

neck squamous cell carcinoma. *PLoS One* 14:e0224710. doi: 10.1371/journal.pone.0224710

Benner, B., Good, L., Quiroga, D., Schultz, T. E., Kassem, M., Carson, W. E., et al. (2020). Pexidartinib, a Novel Small Molecule CSF-1R Inhibitor in Use for Tenosynovial Giant Cell Tumor: A Systematic Review of Pre-Clinical and Clinical Development. *Drug Des. Devel. Ther.* 14, 1693–1704. doi: 10.2147/dddt.s253232

Bluth, M. J., Zaba, L. C., Moussai, D., Suárez-Fariñas, M., Kaporis, H., Fan, L., et al. (2009). Myeloid dendritic cells from human cutaneous squamous cell carcinoma are poor stimulators of T-cell proliferation. *J. Invest. Dermatol.* 129, 2451–2462. doi: 10.1038/jid.2009.96

Brunet, J. F., Denizot, F., Luciani, M. F., Roux-Dosseto, M., Suzan, M., Mattei, M. G., et al. (1987). A new member of the immunoglobulin superfamily–CTLA-4. *Nature* 328, 267–270. doi: 10.1038/328267a0

Burton, K. A., Ashack, K. A., and Khachemoune, A. (2016). Cutaneous Squamous Cell Carcinoma: A Review of High-Risk and Metastatic Disease. *Am. J. Clin. Dermatol.* 17, 491–508. doi: 10.1007/s40257-016-0207-3

Caley, M. P., Martins, V. L., Moore, K., Lashari, M., Nissinen, L., Kähäri, V. M., et al. (2020). Loss of Laminin α3 induces cell invasion and macrophage infiltration in cutaneous squamous cell carcinoma. *Br. J. Dermatol.* 2020:19571. doi: 10.1111/bjd.19471

Challacombe, J. M., Suhrbier, A., Parsons, P. G., Jones, B., Hampson, P., Kavanagh, D., et al. (2006). Neutrophils are a key component of the antitumor efficacy of topical chemotherapy with ingenol-3-angelate. *J. Immunol.* 177, 8123–8132. doi: 10.4049/jimmunol.177.11.8123

Chen, W., Jin, W., Hardegen, N., Lei, K. J., Li, L., Marinos, N., et al. (2003). Conversion of peripheral CD4+CD25- naive T cells to CD4+CD25+ regulatory T cells by TGF-beta induction of transcription factor Foxp3. *J. Exp. Med.* 198, 1875–1886. doi: 10.1084/jem.20030152

Chen, X., and Song, E. (2019). Turning foes to friends: targeting cancer-associated fibroblasts. *Nat. Rev. Drug Dis.* 18, 99–115. doi: 10.1038/s41573-018-0004-1

Chen, Y., Liu, Q., Chen, Z., Wang, Y., Yang, W., Hu, Y., et al. (2019). PD-L1 expression and tumor mutational burden status for prediction of response to chemotherapy and targeted therapy in non-small cell lung cancer. *J. Exp. Clin. Cancer Res. CR* 38:193. doi: 10.1186/s13046-019-1192-1

Chow, L. Q. M., Morishima, C., Eaton, K. D., Baik, C. S., Goulart, B. H., Anderson, L. N., et al. (2017). Phase Ib Trial of the Toll-like Receptor 8 Agonist, Motolimod (VTX-2337), Combined with Cetuximab in Patients with Recurrent or Metastatic SCCHN. *Clin. Cancer Res.* 23, 2442–2450. doi: 10.1158/1078-0432.CCR-16-1934

Clark, R. A., Huang, S. J., Murphy, G. F., Mollet, I. G., Hijnen, D., Muthukuru, M., et al. (2008). Human squamous cell carcinomas evade the immune response by down-regulation of vascular E-selectin and recruitment of regulatory T cells. *J. Exp. Med.* 205, 2221–2234. doi: 10.1084/jem.20071190

de Oliveira, C. E., Gasparoto, T. H., Pinheiro, C. R., Amôr, N. G., Nogueira, M. R. S., Kaneno, R., et al. (2017). CCR5-dependent homing of T regulatory cells to the tumor microenvironment contributes to skin squamous cell carcinoma development. *Mole. Cancer Ther.* 16, 17–0341. doi: 10.1158/1535-7163.MCT-17-0341

D'Incalci, M., and Zambelli, A. (2016). Trabectedin for the treatment of breast cancer. *Exp. Opin. Investig. Drugs* 25, 105–115. doi: 10.1517/13543784.2016.1124086

Dodagatta-Marri, E., Meyer, D. S., Reeves, M. Q., Paniagua, R., To, M. D., Binnewies, M., et al. (2019). α-PD-1 therapy elevates Treg/Th balance and increases tumor cell pSmad3 that are both targeted by α-TGFβ antibody to promote durable rejection and immunity in squamous cell carcinomas. *J. Immunother. Cancer* 7:62. doi: 10.1186/s40425-018-0493-9

Dranoff, G. (2004). Cytokines in cancer pathogenesis and cancer therapy. *Nat. Rev. Cancer* 4, 11–22. doi: 10.1038/nrc1252

Duan, H., Koga, T., Masuda, T., Mashino, T., Imafuku, S., Terao, H., et al. (2000). CD1a+, CD3+, CD4+, CD8+, CD68+ and cutaneous lymphocyte-associated antigen-positive cells in Bowen's disease. *Br. J. Dermatol.* 143, 1211–1216. doi: 10.1046/j.1365-2133.2000.03890.x

Dustin, M. L., and Shaw, A. S. (1999). Costimulation: building an immunological synapse. *Science* 283, 649–650. doi: 10.1126/science.283.5402.649

Euvrard, S., Kanitakis, J., and Claudy, A. (2003). Skin cancers after organ transplantation. *N Engl J Med* 348, 1681–1691. doi: 10.1056/NEJMra022137

Fang, M., Li, Y., Huang, K., Qi, S., Zhang, J., Zgodzinski, W., et al. (2017). IL33 Promotes Colon Cancer Cell Stemness via JNK Activation and Macrophage Recruitment. *Cancer Res.* 77, 2735–2745. doi: 10.1158/0008-5472.CAN-16-1602

Florence, M. E., Massuda, J. Y., Bröcker, E. B., Metze, K., Cintra, M. L., and Souza, E. M. (2011). Angiogenesis in the progression of cutaneous squamous cell carcinoma: an immunohistochemical study of endothelial markers. *Clinics* 66, 465–468. doi: 10.1590/s1807-59322011000300018

Freeman, A., Bridge, J. A., Maruthayanar, P., Overgaard, N. H., Jung, J. W., Simpson, F., et al. (2014). Comparative immune phenotypic analysis of cutaneous Squamous Cell Carcinoma and Intraepidermal Carcinoma in immune-competent individuals: proportional representation of CD8+ T-cells but not FoxP3+ Regulatory T-cells is associated with disease stage. *PLoS One* 9:e110928. doi: 10.1371/journal.pone.0110928

Freeman, G. J., Long, A. J., Iwai, Y., Bourque, K., Chernova, T., Nishimura, H., et al. (2000). Engagement of the PD-1 immunoinhibitory receptor by a novel B7 family member leads to negative regulation of lymphocyte activation. *J. Exp. Med.* 192, 1027–1034. doi: 10.1084/jem.192.7.1027

Fridlender, Z. G., Sun, J., Kim, S., Kapoor, V., Cheng, G., Ling, L., et al. (2009). Polarization of tumor-associated neutrophil phenotype by TGF-beta: "N1" versus "N2" TAN. *Cancer Cell* 16, 183–194. doi: 10.1016/j.ccr.2009.06.017

Fujita, H., Suárez-Fariñas, M., Mitsui, H., Gonzalez, J., Bluth, M. J., Zhang, S., et al. (2012). Langerhans cells from human cutaneous squamous cell carcinoma induce strong type 1 immunity. *J. Invest. Dermatol.* 132, 1645–1655. doi: 10.1038/jid.2012.34

Gambichler, T., Gnielka, M., Rüddel, I., Stockfleth, E., Stücker, M., and Schmitz, L. (2017). Expression of PD-L1 in keratoacanthoma and different stages of progression in cutaneous squamous cell carcinoma. *Cancer Immunol. Immunother.* 66, 1199–1204. doi: 10.1007/s00262-017-2015-x

Gasparoto, T. H., de Oliveira, C. E., de Freitas, L. T., Pinheiro, C. R., Hori, J. I., Garlet, G. P., et al. (2014). Inflammasome activation is critical to the protective immune response during chemically induced squamous cell carcinoma. *PLoS One* 9:e107170. doi: 10.1371/journal.pone.0107170

Girardi, M., Oppenheim, D., Glusac, E. J., Filler, R., Balmain, A., Tigelaar, R. E., et al. (2004). Characterizing the protective component of the alphabeta T cell response to transplantable squamous cell carcinoma. *J. Invest. Dermatol.* 122, 699–706. doi: 10.1111/j.0022-202X.2004.22342.x

Griesenauer, B., and Paczesny, S. (2017). The ST2/IL-33 Axis in Immune Cells during Inflammatory Diseases. *Front. Immunol.* 8:475. doi: 10.3389/fimmu.2017.00475

Gros, A., Robbins, P. F., Yao, X., Li, Y. F., Turcotte, S., Tran, E., et al. (2014). PD-1 identifies the patient-specific $CD8^+$ tumor-reactive repertoire infiltrating human tumors. *J. Clin. Investig.* 124, 2246–2259. doi: 10.1172/JCI73639

Halliday, G. M., and Le, S. (2001). Transforming growth factor-beta produced by progressor tumors inhibits, while IL-10 produced by regressor tumors enhances. *Langerhans Cell Migrat. Skin. Int. Immunol.* 13, 1147–1154. doi: 10.1093/intimm/13.9.1147

Ham, S., Lima, L. G., Chai, E. P. Z., Muller, A., Lobb, R. J., Krumeich, S., et al. (2018). Breast Cancer-Derived Exosomes Alter Macrophage Polarization via gp130/STAT3 Signaling. *Front. Immunol.* 9:871. doi: 10.3389/fimmu.2018.00871

Hammad, H., and Lambrecht, B. N. (2015). Barrier Epithelial Cells and the Control of Type 2 Immunity. *Immunity* 43, 29–40. doi: 10.1016/j.immuni.2015.07.007

Hatton, J. L., Parent, A., Tober, K. L., Hoppes, T., Wulff, B. C., Duncan, F. J., et al. (2007). Depletion of CD4+ cells exacerbates the cutaneous response to acute and chronic UVB exposure. *J. Invest. Dermatol.* 127, 1507–1515. doi: 10.1038/sj.jid.5700746

Hayakawa, H., Hayakawa, M., Kume, A., and Tominaga, S. (2007). Soluble ST2 blocks interleukin-33 signaling in allergic airway inflammation. *J. Biol. Chem.* 282, 26369–26380. doi: 10.1074/jbc.M704916200

Heinhuis, K. M., Carlino, M., Joerger, M., di Nicola, M., Meniawy, T., Rottey, S., et al. (2019). Safety, Tolerability, and Potential Clinical Activity of a Glucocorticoid-Induced TNF Receptor-Related Protein Agonist Alone or in Combination With Nivolumab for Patients With Advanced Solid Tumors: A Phase 1/2a Dose-Escalation and Cohort-Expansion Clini. *JAMA Oncology* 6, 1–8. doi: 10.1001/jamaoncol.2019.3848

Hodi, F. S., O'Day, S. J., McDermott, D. F., Weber, R. W., Sosman, J. A., Haanen, J. B., et al. (2010). Improved survival with ipilimumab in patients with metastatic melanoma. *N. Engl. J. Med.* 363, 711–723. doi: 10.1056/NEJMoa1003466

Holbrook, J. D., Parker, J. S., Gallagher, K. T., Halsey, W. S., Hughes, A. M., Weigman, V. J., et al. (2011). Deep sequencing of gastric carcinoma reveals somatic mutations relevant to personalized medicine. *J. Translat. Med.* 9:119. doi: 10.1186/1479-5876-9-119

In, G. K., Vaidya, P., Filkins, A., Hermel, D. J., King, K. G., Ragab, O., et al. (2020). PD-1 inhibition therapy for advanced cutaneous squamous cell carcinoma: a retrospective analysis from the University of Southern California. *J. Cancer Res. Clin. Oncol.* 2020, 3458–3456. doi: 10.1007/s00432-020-03458-6

Jang, T. J. (2008). Prevalence of Foxp3 positive T regulatory cells is increased during progression of cutaneous squamous tumors. *Yonsei Med. J.* 49, 942–948. doi: 10.3349/ymj.2008.49.6.942

Ji, A. L., Rubin, A. J., Thrane, K., Jiang, S., Reynolds, D. L., Meyers, R. M., et al. (2020). Multimodal Analysis of Composition and Spatial Architecture in Human Squamous Cell Carcinoma. *Cell* 182, 497.e–514.e. doi: 10.1016/j.cell.2020.05.039

Jiang, X., Wang, M., Cyrus, N., Yanez, D. A., Lacher, R. K., Rhebergen, A. M., et al. (2019). Human keratinocyte carcinomas have distinct differences in their tumor-associated macrophages. *Heliyon* 5:e02273. doi: 10.1016/j.heliyon.2019.e02273

Jiao, Q., Liu, C., Li, W., Fang, F., Qian, Q., and Zhang, X. (2017). Programmed death-1 ligands 1 and 2 expression in cutaneous squamous cell carcinoma and their relationship with tumour- infiltrating dendritic cells. *Clin. Exp. Immunol.* 188, 420–429. doi: 10.1111/cei.12921

Kambayashi, Y., Fujimura, T., and Aiba, S. (2013). Comparison of immunosuppressive and immunomodulatory cells in keratoacanthoma and cutaneous squamous cell carcinoma. *Acta Derm Venereol.* 93, 663–668. doi: 10.2340/00015555-1597

Kansy, B. A., Concha-Benavente, F., Srivastava, R. M., Jie, H.-B., Shayan, G., Lei, Y., et al. (2017). PD-1 Status in CD8(+) T Cells Associates with Survival and Anti-PD-1 Therapeutic Outcomes in Head and Neck Cancer. *Cancer Res.* 77, 6353–6364. doi: 10.1158/0008-5472.CAN-16-3167

Kerkelä, E., Ala-aho, R., Klemi, P., Grénman, S., Shapiro, S. D., Kähäri, V. M., et al. (2002). Metalloelastase (MMP-12) expression by tumour cells in squamous cell carcinoma of the vulva correlates with invasiveness, while that by macrophages predicts better outcome. *J. Pathol.* 198, 258–269. doi: 10.1002/path.1198

Khou, S., Popa, A., Luci, C., Bihl, F., Meghraoui-Kheddar, A., Bourdely, P., et al. (2020). Tumor-Associated Neutrophils Dampen Adaptive Immunity and Promote Cutaneous Squamous Cell Carcinoma Development. *Cancers* 12:12071860. doi: 10.3390/cancers12071860

Krasner, C. N., McMeekin, D. S., Chan, S., Braly, P. S., Renshaw, F. G., Kaye, S., et al. (2007). A Phase II study of trabectedin single agent in patients with recurrent ovarian cancer previously treated with platinum-based regimens. *Br. J. Cancer* 97, 1618–1624. doi: 10.1038/sj.bjc.6604088

Kruger, P., Saffarzadeh, M., Weber, A. N., Rieber, N., Radsak, M., von Bernuth, H., et al. (2015). Neutrophils: Between host defence, immune modulation, and tissue injury. *PLoS Pathog.* 11:e1004651. doi: 10.1371/journal.ppat.1004651

Kumagai, S., Togashi, Y., Kamada, T., Sugiyama, E., Nishinakamura, H., Takeuchi, Y., et al. (2020). The PD-1 expression balance between effector and regulatory T cells predicts the clinical efficacy of PD-1 blockade therapies. *Nat. Immunol.* 21, 1346–1358. doi: 10.1038/s41590-020-0769-3

Lai, C., August, S., Albibas, A., Behar, R., Cho, S. Y., Polak, M. E., et al. (2016). OX40+ Regulatory T Cells in Cutaneous Squamous Cell Carcinoma Suppress Effector T-Cell Responses and Associate with Metastatic Potential. *Clin. Cancer Res.* 22, 4236–4248. doi: 10.1158/1078-0432.ccr-15-2614

Lamb, Y. N. (2019). Pexidartinib: First Approval. *Drugs* 79, 1805–1812. doi: 10.1007/s40265-019-01210-0

Latchman, Y., Wood, C. R., Chernova, T., Chaudhary, D., Borde, M., Chernova, I., et al. (2001). PD-L2 is a second ligand for PD-1 and inhibits T cell activation. *Nat Immunol.* 2, 261–268. doi: 10.1038/85330

Li, X. (2016). TIPE2 regulates tumor-associated macrophages in skin squamous cell carcinoma. *Tumour Biol.* 37, 5585–5590. doi: 10.1007/s13277-015-4388-9

Liew, F. Y., Girard, J.-P., and Turnquist, H. R. (2016). Interleukin-33 in health and disease. *Nat. Rev. Immunol.* 16, 676–689. doi: 10.1038/nri.2016.95

Lin, E. Y., Nguyen, A. V., Russell, R. G., and Pollard, J. W. (2001). Colony-stimulating factor 1 promotes progression of mammary tumors to malignancy. *J. Exp. Med.* 193, 727–740. doi: 10.1084/jem.193.6.727

Linde, N., Gutschalk, C. M., Hoffmann, C., Yilmaz, D., and Mueller, M. M. (2012a). Integrating macrophages into organotypic co-cultures: a 3D in vitro model to study tumor-associated macrophages. *PLoS One* 7:e40058. doi: 10.1371/journal.pone.0040058

Linde, N., Lederle, W., Depner, S., van Rooijen, N., Gutschalk, C. M., and Mueller, M. M. (2012b). Vascular endothelial growth factor-induced skin carcinogenesis depends on recruitment and alternative activation of macrophages. *J. Pathol.* 227, 17–28. doi: 10.1002/path.3989

Linedale, R., Schmidt, C., King, B. T., Ganko, A. G., Simpson, F., Panizza, B. J., et al. (2017). Elevated frequencies of CD8 T cells expressing PD-1, CTLA-4 and Tim-3 within tumour from perineural squamous cell carcinoma patients. *PLoS One* 12:e0175755. doi: 10.1371/journal.pone.0175755

Linsley, P. S., Greene, J. L., Tan, P., Bradshaw, J., Ledbetter, J. A., Anasetti, C., et al. (1992). Coexpression and functional cooperation of CTLA-4 and CD28 on activated T lymphocytes. *J. Exp. Med.* 176, 1595–1604. doi: 10.1084/jem.176.6.1595

Lobl, M. B., Clarey, D., Higgins, S., Sutton, A., Hansen, L., and Wysong, A. (2020). Targeted next-generation sequencing of matched localized and metastatic primary high-risk SCCs identifies driver and co-occurring mutations and novel therapeutic targets. *J. Dermatol. Sci.* 99, 30–43. doi: 10.1016/j.jdermsci.2020.05.007

Loser, K., Apelt, J., Voskort, M., Mohaupt, M., Balkow, S., Schwarz, T., et al. (2007). IL-10 controls ultraviolet-induced carcinogenesis in mice. *J. Immunol.* 179, 365–371. doi: 10.4049/jimmunol.179.1.365

Loser, K., Scherer, A., Krummen, M. B., Varga, G., Higuchi, T., Schwarz, T., et al. (2005). An important role of CD80/CD86-CTLA-4 signaling during photocarcinogenesis in mice. *J. Immunol.* 174, 5298–5305. doi: 10.4049/jimmunol.174.9.5298

Łuksza, M., Riaz, N., Makarov, V., Balachandran, V. P., Hellmann, M. D., Solovyov, A., et al. (2017). A neoantigen fitness model predicts tumour response to checkpoint blockade immunotherapy. *Nature* 551, 517–520. doi: 10.1038/nature24473

Maalouf, S. W., Theivakumar, S., and Owens, D. M. (2012). Epidermal α6β4 integrin stimulates the influx of immunosuppressive cells during skin tumor promotion. *J. Dermatol. Sci.* 66, 108–118. doi: 10.1016/j.jdermsci.2012.02.009

Mahiddine, K., Blaisdell, A., Ma, S., Créquer-Grandhomme, A., Lowell, C. A., and Erlebacher, A. (2020). Relief of tumor hypoxia unleashes the tumoricidal potential of neutrophils. *J. Clin. Investig.* 130, 389–403. doi: 10.1172/JCI130952

Miao, Y., Yang, H., Levorse, J., Yuan, S., Polak, L., Sribour, M., et al. (2019). Adaptive Immune Resistance Emerges from Tumor-Initiating Stem Cells. *Cell* 177, 1172.e–1186.e. doi: 10.1016/j.cell.2019.03.025

Migden, M. R., Rischin, D., Schmults, C. D., Guminski, A., Hauschild, A., Lewis, K. D., et al. (2018). PD-1 Blockade with Cemiplimab in Advanced Cutaneous Squamous-Cell Carcinoma. *N. Engl. J. Med.* 379, 341–351. doi: 10.1056/NEJMoa1805131

Mok, S., Koya, R. C., Tsui, C., Xu, J., Robert, L., Wu, L., et al. (2014). Inhibition of CSF-1 receptor improves the antitumor efficacy of adoptive cell transfer immunotherapy. *Cancer Res.* 74, 153–161. doi: 10.1158/0008-5472.can-13-1816

Moussai, D., Mitsui, H., Pettersen, J. S., Pierson, K. C., Shah, K. R., Suárez-Fariñas, M., et al. (2011). The human cutaneous squamous cell carcinoma microenvironment is characterized by increased lymphatic density and enhanced expression of macrophage-derived VEGF-C. *J. Invest. Dermatol.* 131, 229–236. doi: 10.1038/jid.2010.266

Mutschelknaus, L., Peters, C., Winkler, K., Yentrapalli, R., Heider, T., Atkinson, M. J., et al. (2016). Exosomes Derived from Squamous Head and Neck Cancer Promote Cell Survival after Ionizing Radiation. *PLoS One* 11:e0152213. doi: 10.1371/journal.pone.0152213

Nasti, T. H., Iqbal, O., Tamimi, I. A., Geise, J. T., Katiyar, S. K., and Yusuf, N. (2011). Differential roles of T-cell subsets in regulation of ultraviolet radiation induced cutaneous photocarcinogenesis. *Photochem. Photobiol.* 87, 387–398. doi: 10.1111/j.1751-1097.2010.00859.x

Nasti, T. H., Rudemiller, K. J., Cochran, J. B., Kim, H. K., Tsuruta, Y., Fineberg, N. S., et al. (2015). Immunoprevention of chemical carcinogenesis through

early recognition of oncogene mutations. *J. Immunol.* 194, 2683–2695. doi: 10.4049/jimmunol.1402125

Öhlund, D., Elyada, E., and Tuveson, D. (2014). Fibroblast heterogeneity in the cancer wound. *J. Exp. Med.* 211, 1503–1523. doi: 10.1084/jem.20140692

Omland, S. H., Ahlström, M. G., Gerstoft, J., Pedersen, G., Mohey, R., Pedersen, C., et al. (2018). Risk of skin cancer in patients with HIV: A Danish nationwide cohort study. *J. Am. Acad. Dermatol.* 79, 689–695. doi: 10.1016/j.jaad.2018.03.024

Ortiz, M. L., Kumar, V., Martner, A., Mony, S., Donthireddy, L., Condamine, T., et al. (2015). Immature myeloid cells directly contribute to skin tumor development by recruiting IL-17-producing CD4+ T cells. *J. Exp. Med.* 212, 351–367. doi: 10.1084/jem.20140835

Ortner, D., Tripp, C. H., Komenda, K., Dubrac, S., Zelger, B., Hermann, M., et al. (2017). Langerhans cells and NK cells cooperate in the inhibition of chemical skin carcinogenesis. *Oncoimmunology* 6:e1260215. doi: 10.1080/2162402x.2016.1260215

Pang, X., Wang, S.-S., Zhang, M., Jiang, J., Fan, H.-Y., Wu, J.-S., et al. (2020). OSCC cell-secreted exosomal CMTM6 induced M2-like macrophages polarization via ERK1/2 signaling pathway. *Cancer Immunol. Immunother.* 2020, 2741–2742. doi: 10.1007/s00262-020-02741-2

Pérez-Ruiz, E., Melero, I., Kopecka, J., Sarmento-Ribeiro, A. B., García-Aranda, M., and de Las Rivas, J. (2020). Cancer immunotherapy resistance based on immune checkpoints inhibitors: Targets, biomarkers, and remedies. *Drug Resist. Updates* 53:100718. doi: 10.1016/j.drup.2020.100718

Pettersen, J. S., Fuentes-Duculan, J., Suárez-Fariñas, M., Pierson, K. C., Pitts-Kiefer, A., Fan, L., et al. (2011). Tumor-associated macrophages in the cutaneous SCC microenvironment are heterogeneously activated. *J. Invest. Dermatol.* 131, 1322–1330. doi: 10.103/jid.2011.9

Phan, G. Q., Yang, J. C., Sherry, R. M., Hwu, P., Topalian, S. L., Schwartzentruber, D. J., et al. (2003). Cancer regression and autoimmunity induced by cytotoxic T lymphocyte-associated antigen 4 blockade in patients with metastatic melanoma. *Proc. Natl. Acad. Sci. U S A* 100, 8372–8377. doi: 10.1073/pnas.1533209100

Postow, M. A., Chesney, J., Pavlick, A. C., Robert, C., Grossmann, K., McDermott, D., et al. (2015). Nivolumab and ipilimumab versus ipilimumab in untreated melanoma. *N. England J. Med.* 372, 2006–2017. doi: 10.1056/NEJMoa1414428

Que, S. K. T., Zwald, F. O., and Schmults, C. D. (2018a). Cutaneous squamous cell carcinoma: Incidence, risk factors, diagnosis, and staging. *J. Am. Acad. Dermatol.* 78, 237–247. doi: 10.1016/j.jaad.2017.08.059

Que, S. K. T., Zwald, F. O., and Schmults, C. D. (2018b). Cutaneous squamous cell carcinoma: Management of advanced and high-stage tumors. *J. Am. Acad. Dermatol.* 78, 249–261. doi: 10.1016/j.jaad.2017.08.058

Ramos, R. N., Oliveira, C. E., Gasparoto, T. H., Malaspina, T. S. S., Belai, E. B., Cavassani, K. A., et al. (2012). Cd25+ T cell depletion impairs murine squamous cell carcinoma development via modulation of antitumor immune responses. *Carcinogenesis* 33:103. doi: 10.1093/carcin/bgs103

Roychowdhury, S., Iyer, M. K., Robinson, D. R., Lonigro, R. J., Wu, Y.-M., Cao, X., et al. (2011). Personalized oncology through integrative high-throughput sequencing: a pilot study. *Sci. Translat. Med.* 3:111ra121. doi: 10.1126/scitranslmed.3003161

Sakaguchi, S., Miyara, M., Costantino, C. M., and Hafler, D. A. (2010). FOXP3+ regulatory T cells in the human immune system. *Nat. Rev. Immunol.* 10, 490–500. doi: 10.1038/nri2785

Salzmann, M., Leiter, U., Loquai, C., Zimmer, L., Ugurel, S., Gutzmer, R., et al. (2020). Programmed cell death protein 1 inhibitors in advanced cutaneous squamous cell carcinoma: real-world data of a retrospective, multicenter study. *Eur. J. Cancer* 138, 125–132. doi: 10.1016/j.ejca.2020.07.029

Seddon, A., Hock, B., Miller, A., Frei, L., Pearson, J., McKenzie, J., et al. (2016). Cutaneous squamous cell carcinomas with markers of increased metastatic risk are associated with elevated numbers of neutrophils and/or granulocytic myeloid derived suppressor cells. *J. Dermatol. Sci.* 83, 124–130. doi: 10.1016/j.jdermsci.2016.04.013

Shayan, G., Srivastava, R., Li, J., Schmitt, N., Kane, L. P., and Ferris, R. L. (2017). Adaptive resistance to anti-PD1 therapy by Tim-3 upregulation is mediated by the PI3K-Akt pathway in head and neck cancer. *Oncoimmunology* 6:e1261779. doi: 10.1080/2162402X.2016.1261779

Shields, C. W., Evans, M. A., Wang, L. L., Baugh, N., Iyer, S., Wu, D., et al. (2020). Cellular backpacks for macrophage immunotherapy. *Sci. Adv.* 6:eaaz6579. doi: 10.1126/sciadv.aaz6579

Siljamäki, E., Rappu, P., Riihilä, P., Nissinen, L., Kähäri, V. M., and Heino, J. (2020). H-Ras activation and fibroblast-induced TGF-β signaling promote laminin-332 accumulation and invasion in cutaneous squamous cell carcinoma. *Matrix Biol.* 87, 26–47. doi: 10.1016/j.matbio.2019.09.001

Simonneau, M., Frouin, E., Huguier, V., Jermidi, C., Jégou, J. F., Godet, J., et al. (2018). Oncostatin M is overexpressed in skin squamous-cell carcinoma and promotes tumor progression. *Oncotarget* 9, 36457–36473. doi: 10.18632/oncotarget.26355

Stang, A., Khil, L., Kajüter, H., Pandeya, N., Schmults, C. D., Ruiz, E. S., et al. (2019). Incidence and mortality for cutaneous squamous cell carcinoma: comparison across three continents. *J. Eur. Acad. Dermatol. Venereol. JEADV* 33(Suppl. 8), 6–10. doi: 10.1111/jdv.15967

Stumpfova, M., Ratner, D., Desciak, E. B., Eliezri, Y. D., and Owens, D. M. (2010). The immunosuppressive surface ligand CD200 augments the metastatic capacity of squamous cell carcinoma. *Cancer Res.* 70, 2962–2972. doi: 10.1158/0008-5472.can-09-4380

Takahara, M., Chen, S., Kido, M., Takeuchi, S., Uchi, H., Tu, Y., et al. (2009). Stromal CD10 expression, as well as increased dermal macrophages and decreased Langerhans cells, are associated with malignant transformation of keratinocytes. *J. Cutan Pathol.* 36, 668–674. doi: 10.1111/j.1600-0560.2008.01139.x

Takahashi, T., Ibata, M., Yu, Z., Shikama, Y., Endo, Y., Miyauchi, Y., et al. (2009). Rejection of intradermally injected syngeneic tumor cells from mice by specific elimination of tumor-associated macrophages with liposome-encapsulated dichloromethylene diphosphonate, followed by induction of CD11b(+)/CCR3(-)/Gr-1(-) cells cytotoxic again. *Cancer Immunol. Immunother.* 58, 2011–2023. doi: 10.1007/s00262-009-0708-5

Taniguchi, S., Elhance, A., van Duzer, A., Kumar, S., Leitenberger, J. J., and Oshimori, N. (2020). Tumor-initiating cells establish an IL-33-TGF-β niche signaling loop to promote cancer progression. *Science* 369, aay1813. doi: 10.1126/science.aay1813

Thomson, P. J. (2018). Perspectives on oral squamous cell carcinoma prevention-proliferation, position, progression and prediction. *J. Oral Pathol. Med.* 47, 803–807. doi: 10.1111/jop.12733

Tonini, T., Rossi, F., and Claudio, P. P. (2003). Molecular basis of angiogenesis and cancer. *Oncogene* 22, 6549–6556. doi: 10.1038/sj.onc.1206816

Tromp, D. M., Brouha, X. D. R., Hordijk, G.-J., Winnubst, J. A. M., and de Leeuw, J. R. J. (2005). Patient factors associated with delay in primary care among patients with head and neck carcinoma: a case-series analysis. *Family Pract.* 22, 554–559. doi: 10.1093/fampra/cmi058

Valladeau, J., and Saeland, S. (2005). Cutaneous dendritic cells. *Semin Immunol.* 17, 273–283. doi: 10.1016/j.smim.2005.05.009

Varki, V., Ioffe, O. B., Bentzen, S. M., Heath, J., Cellini, A., Feliciano, J., et al. (2018). PD-L1, B7-H3, and PD-1 expression in immunocompetent vs. immunosuppressed patients with cutaneous squamous cell carcinoma. *Cancer Immunol. Immunother.* 67, 805–814. doi: 10.1007/s00262-018-2138-8

Waldman, A. D., Fritz, J. M., and Lenardo, M. J. (2020). A guide to cancer immunotherapy: from T cell basic science to clinical practice. *Nat. Rev. Immunol.* 2020, 1–18. doi: 10.1038/s41577-020-0306-5

Wang, L., Yi, T., Zhang, W., Pardoll, D. M., and Yu, H. (2010). IL-17 enhances tumor development in carcinogen-induced skin cancer. *Cancer Res.* 70, 10112–10120. doi: 10.1158/0008-5472.can-10-0775

Wang, Y., Lin, Y. X., Qiao, S. L., An, H. W., Ma, Y., Qiao, Z. Y., et al. (2017). Polymeric nanoparticles promote macrophage reversal from M2 to M1 phenotypes in the tumor microenvironment. *Biomaterials* 112, 153–163. doi: 10.1016/j.biomaterials.2016.09.034

Weber, F., Byrne, S. N., Le, S., Brown, D. A., Breit, S. N., Scolyer, R. A., et al. (2005). Transforming growth factor-beta1 immobilises dendritic cells within skin tumours and facilitates tumour escape from the immune system. *Cancer Immunol. Immunother.* 54, 898–906. doi: 10.1007/s00262-004-0652-3

Welsh, M. M., Applebaum, K. M., Spencer, S. K., Perry, A. E., Karagas, M. R., and Nelson, H. H. (2009). CTLA4 variants, UV-induced tolerance, and risk of non-melanoma skin cancer. *Cancer Res.* 69, 6158–6163. doi: 10.1158/0008-5472.can-09-0415

Winkler, A. E., Brotman, J. J., Pittman, M. E., Judd, N. P., Lewis, J. S. Jr., Schreiber, R. D., et al. (2011). CXCR3 enhances a T-cell-dependent epidermal proliferative response and promotes skin tumorigenesis. *Cancer Res.* 71, 5707–5716. doi: 10.1158/0008-5472.can-11-0907

Wolchok, J. D., Kluger, H., Callahan, M. K., Postow, M. A., Rizvi, N. A., Lesokhin, A. M., et al. (2013). Nivolumab plus ipilimumab in advanced melanoma. *N. England J. Med.* 369, 122–133. doi: 10.1056/NEJMoa1302369

Yang, H., Zhang, Q., Xu, M., Wang, L., Chen, X., Feng, Y., et al. (2020). CCL2-CCR2 axis recruits tumor associated macrophages to induce immune evasion through PD-1 signaling in esophageal carcinogenesis. *Mol. Cancer* 19:41. doi: 10.1186/s12943-020-01165-x

Yao, S., Zhu, Y., and Chen, L. (2013). Advances in targeting cell surface signalling molecules for immune modulation. *Nat. Rev. Drug Discov.* 12, 130–146. doi: 10.1038/nrd3877

Yusuf, N., Nasti, T. H., Katiyar, S. K., Jacobs, M. K., Seibert, M. D., Ginsburg, A. C., et al. (2008). Antagonistic roles of CD4+ and CD8+ T-cells in 7,12-dimethylbenz(a)anthracene cutaneous carcinogenesis. *Cancer Res.* 68, 3924–3930. doi: 10.1158/0008-5472.can-07-3059

Zhang, F., Parayath, N. N., Ene, C. I., Stephan, S. B., Koehne, A. L., Coon, M. E., et al. (2019). Genetic programming of macrophages to perform anti-tumor functions using targeted mRNA nanocarriers. *Nat. Commun.* 10:3974. doi: 10.1038/s41467-019-11911-5

Zhang, J., Chen, L., Liu, X., Kammertoens, T., Blankenstein, T., and Qin, Z. (2013a). Fibroblast-specific protein 1/S100A4-positive cells prevent carcinoma through collagen production and encapsulation of carcinogens. *Cancer Res.* 73, 2770–2781. doi: 10.1158/0008-5472.CAN-12-3022

Zhang, J., Chen, L., Xiao, M., Wang, C., and Qin, Z. (2011). FSP1+ fibroblasts promote skin carcinogenesis by maintaining MCP-1-mediated macrophage infiltration and chronic inflammation. *Am. J. Pathol.* 178, 382–390. doi: 10.1016/j.ajpath.2010.11.017

Zhang, S., Fujita, H., Mitsui, H., Yanofsky, V. R., Fuentes-Duculan, J., Pettersen, J. S., et al. (2013b). Increased Tc22 and Treg/CD8 ratio contribute to aggressive growth of transplant associated squamous cell carcinoma. *PLoS One* 8:e62154. doi: 10.1371/journal.pone.0062154

Conflict of Interest: The authors declare that the research was conducted in the absence of any commercial or financial relationships that could be construed as a potential conflict of interest.

frontiers in Cell and Developmental Biology

ORIGINAL RESEARCH
published: 18 February 2021
doi: 10.3389/fcell.2020.622161

Increased Tumor Immune Microenvironment CD3+ and CD20+ Lymphocytes Predict a Better Prognosis in Oral Tongue Squamous Cell Carcinoma

*Raísa Sales de Sá[1], Marisol Miranda Galvis[1,2], Bruno Augusto Linhares Almeida Mariz[1], Amanda Almeida Leite[1], Luciana Schultz[3], Oslei Paes Almeida[1], Alan Roger Santos-Silva[1], Clovis Antonio Lopes Pinto[4], Pablo Agustin Vargas[1], Kenneth John Gollob[5,6] and Luiz Paulo Kowalski[7,8]**

[1] Department of Oral Diagnosis, Piracicaba Dental School, University of Campinas, Piracicaba, Brazil, [2] Department of Oral Biology and Diagnostic Sciences, Dental College of Georgia, Augusta University, Augusta, GA, United States, [3] Department of Anatomic Pathology, Instituto de Anatomia Patologica–IAP, Santa Barbara d'Oeste, Brazil, [4] Department of Anatomic Pathology, A. C. Camargo Cancer Center, São Paulo, Brazil, [5] International Research Center, A. C. Camargo Cancer Center, São Paulo, Brazil, [6] National Institute for Science and Technology in Oncogenomics and Therapeutic Innovation, A.C. Camargo Cancer Center, São Paulo, Brazil, [7] Department of Head and Neck Surgery and Otorhinolaryngology, A. C. Camargo Cancer Center, São Paulo, Brazil, [8] Head and Neck Surgery Department, Medical School, University of São Paulo, São Paulo, Brazil

OPEN ACCESS

Edited by:
Rodrigo Nalio Ramos,
Institut Curie, France

Reviewed by:
Eleonora Timperi,
Institut Curie, France
Ana Paula Campanelli,
University of São Paulo, Brazil

***Correspondence:**
Luiz Paulo Kowalski
lp_kowalski@uol.com.br

Specialty section:
This article was submitted to Molecular Medicine, a section of the journal Frontiers in Cell and Developmental Biology

Received: 27 October 2020
Accepted: 18 December 2020
Published: 18 February 2021

Citation:
Sales de Sá R, Miranda Galvis M, Mariz BALA, Leite AA, Schultz L, Almeida OP, Santos-Silva AR, Pinto CAL, Vargas PA, Gollob KJ and Kowalski LP (2021) Increased Tumor Immune Microenvironment CD3+ and CD20+ Lymphocytes Predict a Better Prognosis in Oral Tongue Squamous Cell Carcinoma. Front. Cell Dev. Biol. 8:622161. doi: 10.3389/fcell.2020.622161

Background: Oral tongue squamous cell carcinoma (OTSCC) causes over 350,000 cases annually and particularly impacts populations in developing countries. Smoking and alcohol consumption are major risk factors. Determining the role of the tumor immune microenvironment (TIME) in OTSCC outcomes can elucidate immune mechanisms behind disease progression, and can potentially identify prognostic biomarkers.

Methods: We performed a retrospective study of 48 OTSCC surgical specimens from patients with tobacco and alcohol exposures. A panel of immunoregulatory cell subpopulations including T (CD3, CD4, CD8) and B (CD20) lymphocytes, dendritic cells (CD1a, CD83), macrophages (CD68), and immune checkpoint molecules programmed cell death protein 1 (PD-1) and ligand 1 (PD-L1) were analyzed using immunohistochemistry. The levels of immune effector cell subpopulations and markers were analyzed in relation to overall survival.

Results: Pathological characteristics of the tumor microenvironment included inflammatory infiltrates (83.3%), desmoplasia (41.6%), and perineural invasion (50.0%). The TIME contained high levels of T cells (CD3+, CD4+, and CD8+) and B cells (CD20+), as well as immature (CD1a) and mature (CD83) dendritic cells, PD-1, and PD-L1. Higher numbers of TIME infiltrating CD3+ T cells and CD20+ B cells were predictive of better survival, while higher levels of CD83+ mature dendritic cells predicted better survival. CD3+ T cells were identified as an independent prognostic marker for OTSCC. Lastly, CD3+ T cells were strongly correlated with the number of CD8+ cells and PD-L1 expression.

Conclusion: Our findings provide evidence that the TIME profile of OTSSC impacted prognosis. The high expression of CD3+ T cells and B cells are predictive of better overall survival and indicative of an immunologically active, inflammatory TIME in patients with better survival. The number of CD3+ T cells was an independent prognostic marker.

Keywords: tumor-infiltrating lymphocytes, immune microenvironment, tongue squamous cell carcinoma (TSCC), CD20 B cells+, CD3

INTRODUCTION

Oral cancer is among the 10 most frequent cancers worldwide, with an incidence of over 350,000 new cases annually (Bray et al., 2018). Oral squamous cell carcinoma (OSCC) of mucosal origin accounts for more than 90% of cases (Curado et al., 2016; Bray et al., 2018). Patients affected by oral tongue squamous cell carcinoma (OTSCC) are often elderly males over the sixth decade of life, with prolonged exposures to tobacco and alcohol (Scully and Bagan, 2009; Ng et al., 2017). Over half of cases are diagnosed and treated at locally advanced stages, consequently presenting a high risk of recurrences and locoregional metastasis (Ng et al., 2017).

Extensive research has elucidated underlying mechanisms of tumor cell survival, proliferation, and dissemination (Hanahan and Weinberg, 2000). A dynamic signaling network between tumor cells and the tumor microenvironment (TME) significantly influences cancer progression and response to conventional therapies (Hanahan and Weinberg, 2011; Salo et al., 2014). The TME contains varied components including immune cells (e.g., tumor-infiltrating lymphocytes [TILs], macrophages, and dendritic cells); cancer-associated fibroblasts, and endothelial cells; and in addition, an extracellular matrix (fibronectin and collagen fibers) and soluble factors (e.g., enzymes, growth factors, and chemokines) (Kim, 2007; Lim et al., 2018).

The tumor immune microenvironment (TIME) plays a critical role in the recognition and clearance of tumor cells, as well as the generation of detrimental immunosuppressive microenvironments (Munn and Bronte, 2016; Hadler-Olsen and Wirsing, 2019). Immune surveillance is an important process that counters carcinogenesis and maintains homeostasis (Kim, 2007; Ferris, 2015). Growing evidence suggests that the composition of immune cell infiltrates may be a potential prognostic marker in OSCC (Almangush et al., 2020; Perri et al., 2020; Zhou et al., 2020). The immune checkpoint molecule programmed cell death receptor 1 (PD-1) and its ligand, programmed cell death ligand - 1 (PD-L1), can induce immune suppression, thereby promoting the progression of disease, and protecting tumors from immune aggression (Ferris, 2015; Lim et al., 2018). Recognizing the importance of immunological components of tumors, an immunescore was developed that can provide a prognostic factor for global survival, as well as for a means for cancer classification (Galon et al., 2012; Fridman et al., 2013). In addition, tumor immune components provide a target for new therapeutic approaches, including immunotherapy via blocking anti-PD-1/PD-L1 (Moskovitz and Ferris, 2018). Importantly, environmental factors such as tobacco and alcohol consumption can modify the tumor immune profile, especially by suppressing T cell chemotaxis (de la Iglesia et al., 2020). Therefore, we aimed to characterize the TIME from a homogeneous cohort of OTSCC patients with tobacco and alcohol exposures, and to further evaluate its impact on survival outcomes.

PATIENTS AND METHODS

Study Design and Ethical Approval

Surgical specimens of OTSCC from 48 patients treated from 2010 to 2017 were retrieved from the archives of the A.C. Camargo Cancer Center (São Paulo, Brazil) and the Institute of Pathological Anatomy (Santa Bárbara d'Oeste, São Paulo State, Brazil). Eligibility criteria included previously untreated OTSCC and tobacco and alcohol consumption. Patients with previous or other concomitant primary carcinomas were not eligible. Patients' medical records were reviewed to retrieve sociodemographic characteristics (e.g., gender, age, risk habits), clinical data (e.g., clinical stage, tumor local, lymph node metastasis, and distant merastasis), therapeutic modality (surgery, radiotherapy, and/or chemotherapy), and follow-up status (Edge and Compton, 2010). Tumor stage and clinical stage were categorized as initial (I and II) or advanced (III and IV) (**Table 1**).

Two experienced pathologists reviewed and classified histologic grades according to WHO criteria (El.Naggar et al., 2017). Histological differentiation was assigned as well-differentiated (grade I), moderately differentiated (grade II), and poorly differentiated (grade III) tumors. Microscopic examination of resected surgical margins was categorized according to the distance between the tumor and the surgical resection into negative ($\geq$5 mm) and positive ($<$5 mm). Survival outcomes were evaluated as overall survival (OS), and the presence of desmoplasia, inflammatory infiltrate, vascular invasion, perineural invasion, and lymphatic invasion (**Table 1**) (El.Naggar et al., 2017). The study was approved by the Human Research Ethics Committee of A.C. Camargo Cancer Center (Number 2.481.465).

Immunohistochemistry

Immunohistochemical assays were performed on 3-μm-thick sections of paraffin-embedded tissues as specified in **Supplementary Table 1**. Antigen retrieval was performed using an electric pressure cooker for 15 min. Endogenous peroxidase activity was suppressed using 6% H_2O_2 for 15 min before the sections were incubated with primary antibodies for 2 h.

TABLE 1 | Clinicopathological features of oral squamous cell carcinoma patients.

Parameters		
Age		
Range	43–86	
Mean	61.2	
Median	61.5	
	n	**%**
Gender		
M	35	73.0
F	13	27.0
Tumor size		
T1	15	31.2
T2	13	27.1
T3	09	18.8
T4	11	22.9
Lymph node metastasis		
N0	30	62.5
N1	10	20.8
N2	8	16.7
Distant metastasis		
M	0	0
Clinical stage		
I	13	27.1
II	10	20.8
III	08	16.7
IV	17	35.4
Histological grade		
Well differentiated	16	33.3
Moderately differentiated	25	52.1
Poorly differentiated	7	14.6
Status		
Alive	31	64.6
Dead	10	20.8
Lost to follow-up	7	14.6
Recurrence		
Yes	17	35.4
No	31	64.6
Desmoplasia		
Presente	20	41.6
Absent	2	4.2
NA	26	54.2
Desmoplasia intensity		
Weak	9	45
Moderate	7	35
Strong	4	20
Inflammatory infiltrate		
Present	40	83.3
Absent	0	0
NA	8	16.7
Vascular invasion		
Present	4	8.3
Absent	43	89.6
NA	1	2.1
Perineural invasion		
Present	24	50.0
Absent	23	47.9
NA	1	2.1
Lymphatic invasion		
Present	5	10.4
Absent	42	87.5
NA	1	2.1

M: Male; F: Female; NA: Not available.

Immunohistochemical staining was performed with either the Advance (Dako, Hamburg, Germany) or Vectastain Elite ABC (Vector Laboratories, Burlingame, USA) kit, according to manufacturer's instructions. Slides were then exposed to diaminobenzidine tetrahydrochloride (Dako, Hamburg, Germany), and counterstained with Carazzi's hematoxylin.

Immunohistochemical Analysis

The expression of CD3 +, CD4 +, CD8 +, CD20+, CD68+, CD83+, CD1a+, and PD-1+ cells were analyzed in the invasive margin (IM) and tumor center (TC). The methods for counting were adapted from published methods used to analyze TILs, dendritic cell, and PD-1 (Pellicioli et al., 2017; Zhou et al., 2018; Naruse et al., 2019; Ngamphaiboon et al., 2019). PD-L1+ cells were evaluated in the TC, where only membranous positivity was considered for scoring purposes. Complete circumferential or partial membranous staining of TC at any intensity was considered PD-L1-positive (+) and using reported parameters for the specific antibody clones (Tsao et al., 2017). OTSCC slides were screened at low power (100x), and then representative fields were selected at 200× magnification, as showed in **Supplementary Figure 1**. Images of each field were captured using an optical light microscope (Leica DFC450, Germany). Quantification of positive dendritic cells (CD83 and CD1a) and PD-1+ the individual value was the average of the total of 10 positive cell fields using ImageJ software (version 2.0). The density of CD3, CD4, CD8, CD20, and CD68 expression was scored using semiquantitative score based on the percentage of positive immune cells was scored as (1) negative (<5%), (2) weak (5–30%), (3) moderate (30–80%), and (4) strong (>80%) for each field (Ngamphaiboon et al., 2019), the individual scores are the mean values of the 10 fields. The results were shown as the mean number per slide. PD-L1 was considered positive in cases >1% and negative in cases <1% (**Supplementary Table 2**).

Construction of Prognostic Score Based on Immune Characteristics

The determination of 2 groups of observations was accomplished by estimating a simple cut-point by using the maximum of the standardized log-rank statistic proposed by Lausen and Schumacher (Society, 2010). The optimal cut-points for cell surface markers were selected to enable sorting into low and high expression groups. The estimated cut-point was calculated

for each marker, such as CD3+ 1.9 (low: 12; high: 26 patients); CD4+ 1.0 (low: 06; high: 42 patients); CD8+ 1.7 (low: 19; high: 29 patients); CD20+ 1.2 (low: 11; high: 37 patients); CD68+ 1.9 (low: 29; high: 19 patients); CD83+ 1.1 (low: 02; high: 46 patients); CD1a+ 5 (low: 09; high: 39 patients) and PD-1+ 6.6 (low: 16; high: 48 patients), (**Supplementary Figure 2**).

Statistical Analysis

Analysis of the association between immune expression and patient demographic and clinicopathological characteristics was performed using Student's *t*-, Mann–Whitney *U*, Kruskal–Wallis, and Pearson's chi-square tests, as appropriate. The determination of two groups of observations for a simple cut-point was estimated by the use of the maximum of the standardized log-rank statistic proposed by Lausen and Schumacher (Society, 2010). Univariate overall survival (OS) probabilities were calculated using the Kaplan–Meier method. Comparisons among survival functions were performed with the log-rank test. The Cox semiparametric proportional hazards model was used to identify independent prognostic factors. Statistical analyses were performed using SPSS (version 23) and R (version 3.2.1) and the significance level was set at 5% for all statistical tests.

RESULTS

Clinicopathological Features and Its Correlation With Survival

Forty-eight cases of OTSSC were retrieved. The clinicopathological features are presented in **Table 1**. Briefly, the mean age was 61.2 years (range 43–86 years), and males were represented (35 cases, 73%) more than females (13 cases, 27%). Twenty-eight (58.3%) patients had initial tumor stages (T1 and T2) and 20 (41.7%) had advanced-stage tumors (T3 and T4). Lymph node metastasis was observed in 18 patients (37.5%), and no patients presented distant metastasis. Initial clinical stages (Stages I and II) accounted for 23 cases (47.9%), while 25 (52.1%) presented with advanced clinical stage tumors (Stages III and IV). Seventeen patients (35.4%) developed recurrences, with a mean time to recurrence of 37.5 months (range: 0.1–97.2 months). The assessment of histological risk factors associated with prognosis is shown in **Table 1**. Interestingly, 16 patients (33.3%) had well-differentiated, 25 (52.1%) had moderately differentiated, and 7 (14.6%) had poorly differentiated tumors. Twenty tumors (41.6%) featured a desmoplastic stroma, and 40 displayed inflammatory infiltrates (83.3%). Desmoplasia was reported as weak in 9 cases (45%) and moderate in 7 patients (35%). Perineural invasion was reported in half of the surgical specimens (24 cases [50.0%]), while lymphovascular invasion was less frequent, observed only in 5 cases (10.4%) of patients, (**Table 1**).

The OS analysis showed an average estimate of 78.5 months (HR = 5.2, 95% CI 0.4–5.7). Univariate analysis showing the associations between clinicopathological features and OS are presented in **Table 2**. T3 stage (HR 29.6, 95% CI 3.0–295.3 ($p = 0.04$), N2 stage (HR 5.9, 95% CI 1.4–24.6 ($p = 0.01$), and poor histological grade (HR 12.7, 95% [CI] 1.4–117.1 ($p = 0.02$), were correlated with OS rates. Multivariate analysis revealed T stage (HR 9.172, 95% CI, 1.6–52.8) ($p = 0.01$) as a predictor of OS.

TABLE 2 | Univariate and multivariate analysis for overall survival of oral squamous cell carcinoma patients.

	HR	95.0% CI		*P*-value
Overall survival				
Univariate model				
T stage				
T1	1.0 (Ref.)			0.009
T2	3.867	0.348	42.972	0.271
T3	29.593	2.965	295.346	**0.004**
T4	3.872	0.228	65.766	0.349
N stage				
N0	1.0 (Ref.)			0.025
N1	0.608	0.070	5.266	0.652
N2	5.906	1.417	24.614	**0.015**
Histological grade				
Well	1.0 (Ref.)			0.027
Moderately	2.887	0.337	24.730	0.333
Poorly	12.770	1.393	117.061	**0.024**
Overall survival				
Multivariate model				
T stage	9.172	1.593	52.798	**0.013**
CD3	0.229	0.060	0.868	**0.030**

Bold value is P < 0.05.

Characterization of the TIME Profile of OTSSC

To delineate the OTSCC TIME profile, stratification was based on individualized cutoff values for the optimized prognostic power of each marker (**Figures 1A**, **2AE**, **3AE**, **4AE**, **5AD**). All patients were classified into low or high expression groups for each marker, and the percentages of individuals in each group were compared.

Upon analysis of the percentage of tumors demonstrating high vs. low lymphocyte subpopulation infiltration, we observed a major increase in the high expression groups for $CD3^+$ (75.0%) (**Figure 1B**), $CD20^+$ (77.1%) (**Figure 2B**), $CD8^+$ (60.4%) (**Figure 2F**), and $CD4^+$ (87.5%) cells (**Figure 3B**). In contrast, the majority of tumors expressed low frequencies of CD68+ macrophages (**Figure 3F**). Remarkably, almost all OTSCC presented high expression profiles of mature dendritic cells, evaluated by CD83 expression (95.8%) (**Figure 4B**), as well as, immature dendritic cells assessed through CD1a expression (81.3%) (**Figure 4F**). In addition to the infiltrating cell populations, we also evaluated the expression of the immune checkpoint molecules PD-1 and PD-L1 due to their immunosuppressive activity. Both proteins were highly expressed in most of the samples with PD-1 in 66.7% (**Figure 5B**) and PD-L1 in 75.0% (**Figure 5E**).

To better understand the OTSCC immunoregulatory networks established in the TIME, we analyzed the correlation between the expression of the evaluated markers. Using the original data of the quantification of TILs and PD-L1 markers,

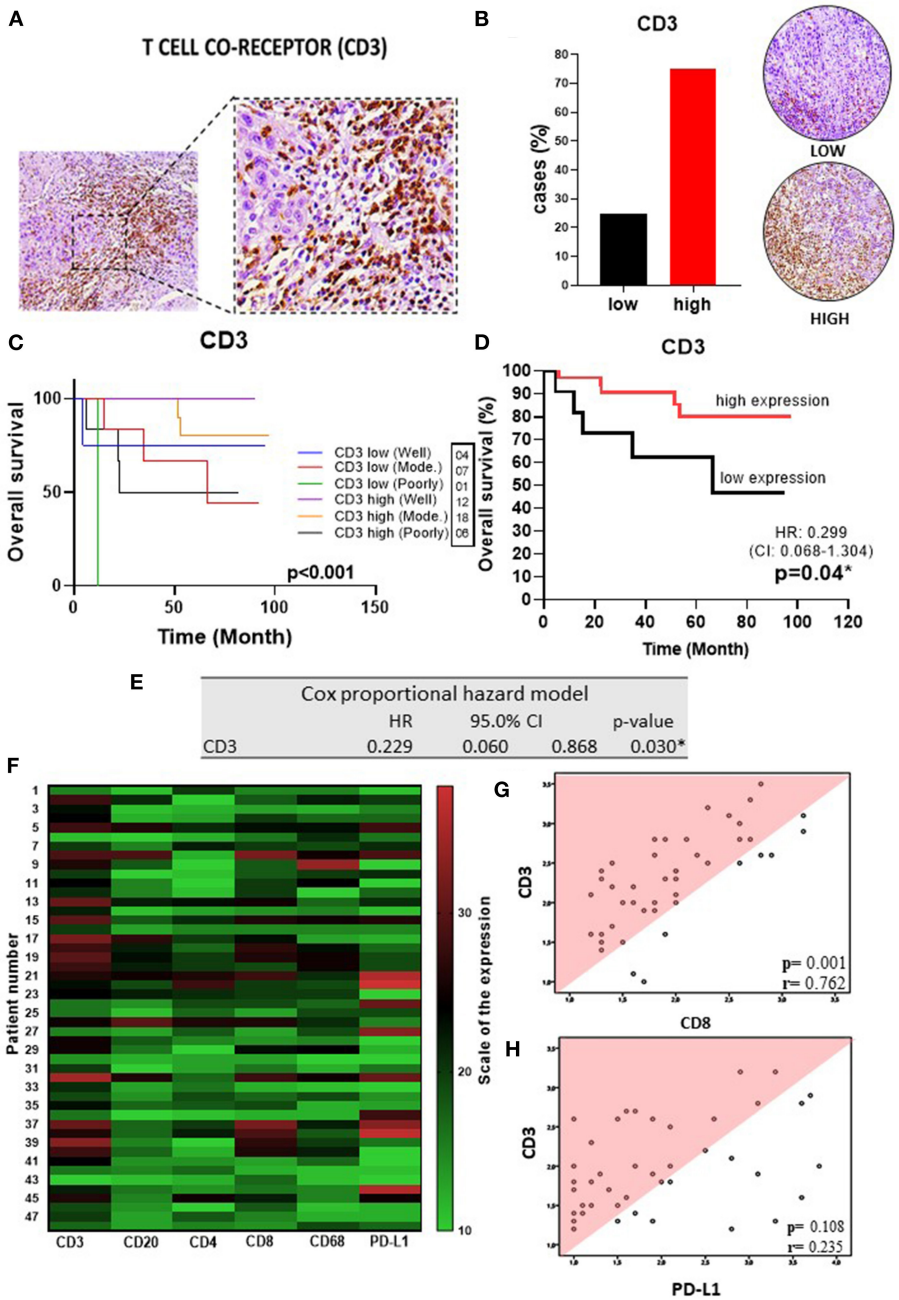

FIGURE 1 | T cell co-receptor in OSSC **(A)** CD3 (left: 200X magnification; right panel: 400X magnification). **(B)** Representative images of OSCC tissues showing low and high CD3 expression, graph showing 36 cases (75.00%) with high CD3 tissues. **(C)** Well histological grade in CD3 high was associated with improved OS ($p <$ 0.001). **(D)** High CD3 expression was associated with improved OS ($P = 0.04$). **(E)** Table showing multivariate analysis for CD3 ($p = 0.03$). **(F)** Heat map showing TILs, slim and PD-L1 expressions in OSSC. **(G)** Correlation of the CD3 rate with expression patterns of CD8 ($r = 0.76$; $p =$ <0.001) and **(H)** PD-L1 ($r = 0.411$; $p = 0.004$) by Spearman rank correlation coefficient. CI, confidence interval; HR, hazard ratio; OS, overall survival; OSCC, oral squamous cell carcinoma; CD3, T cell co-receptor; Mod, Moderately.

a heatmap was constructed showing the relative expression levels for each marker across all patient samples (**Figure 1F**). Performing a Spearman correlation analysis, we observed a clear correlation between CD3+ cells and CD8+ cells ($p < 0.05$, $R = 0.76$) (**Figure 1G**), as well as with PD-L1+ cells ($p < 0.05$, $R = 0.41$) (**Figure 1H**). In addition, the densities of CD8+ cells significantly correlated with the levels of CD3+, CD20+, CD68+ subsets with R values 0.76; 0.71; and 0.59 (Spearman correlation analysis, p-values < 0.05) (**Supplementary Table 3**); and PD-L1+ cells (**Figure 5G**).

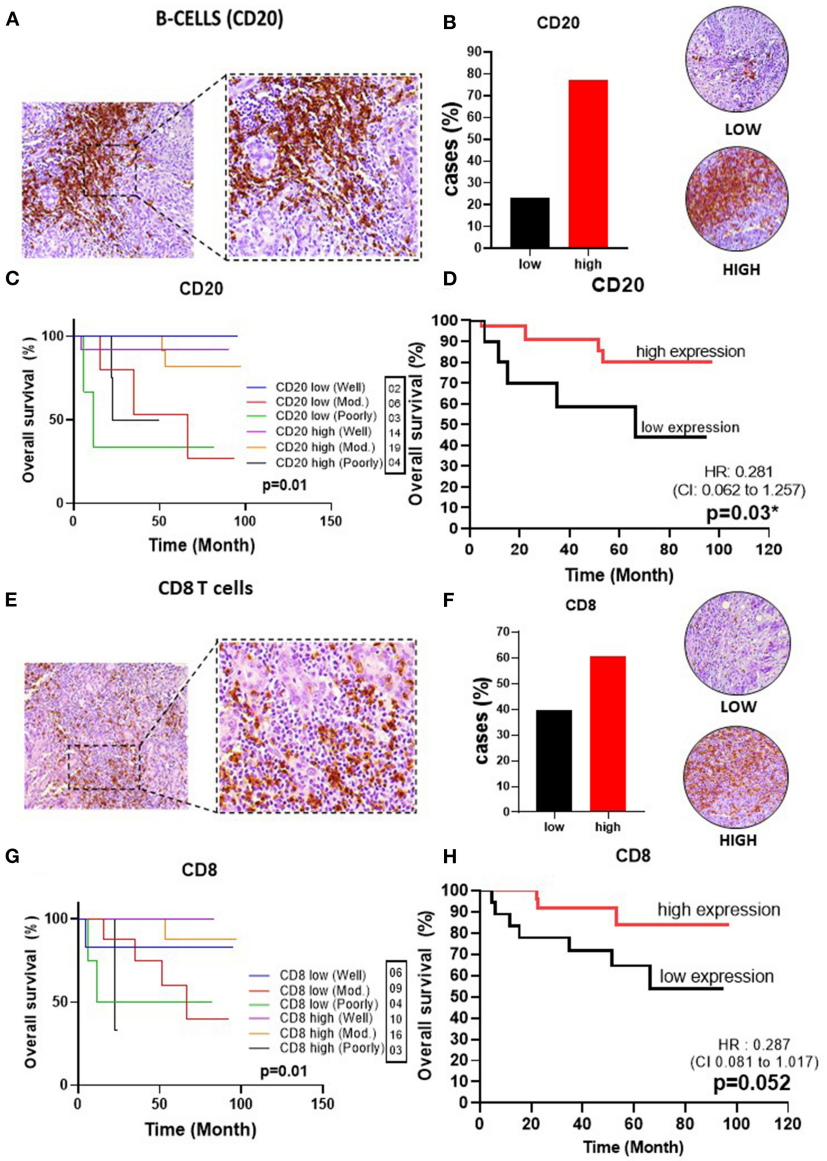

FIGURE 2 | Infiltrating lymphocytes in OSSC. **(A)** CD20 (left: 200X magnification; right panel: 400X magnification). **(B)** Representative images of OSCC tissues showing low and high expressions of CD20, graph showing 37 cases (77.08%) with high CD4 tissues. **(C)** Well histological grade in CD20 high was associated with improved OS ($p = 0.01$). **(D)** High CD20 expression was associated with improved OS ($p = 0.03$). **(E)** CD8 in OSCC (left: magnification 200X; right panel: magnification 400X). **(F)** Representative images of OSCC tissues showing low and high CD8 expressions, graph showing 29 cases (60.41%) with low CD68 **(G)** Well histological grade in CD8 high was associated with improved OS ($p = 0.01$); **(H)** High CD8 expression was associated with improved OS ($P = 0.052$). CI, confidence interval; HR, hazard ratio; OS, overall survival; OSCC, oral squamous cell carcinoma; CD20, B cell; CD8, cytotoxic T cell; Mod, Moderately.

Increased Expression of Infiltrating T and B Lymphocytes Are Correlated With Improved Survival in OTSCC

We next explored whether the expression of the immune markers influenced OS. These analyses showed that infiltrating CD3+ T cells were correlated with an improved OS ($p = 0.04$) (HR 0.3, 95%CI, 0.1–1.3) (**Figure 1D**). Also, statistically significant variables identified by univariate analysis were evaluated by using the multivariate Cox proportional regression analysis hazard model. Not surprisingly, $CD3^+$ T cells were identified as an independent prognostic factor ($p = 0.03$) (HR 0.1, 95%CI, 0.1–0.9), supporting the prognostic value of CD3 markers in OTSCC (**Figure 1E**).

Analysis of CD8+ T cells revealed that higher levels were also associated with better OS (HR 0.3, 95%CI, 0.1–1.1), with a p-value of 0.052 (**Figure 2H**). CD4+ T cells, which play an important role in immunoregulation, were not correlated with OS ($p = 0.21$) (**Figure 3D**). Lastly, we found that high CD20+ B cells were correlated with an improved OS ($p = 0.03$) (HR 0.3, 95% CI, 0.1–1.3) (**Figure 2D**).

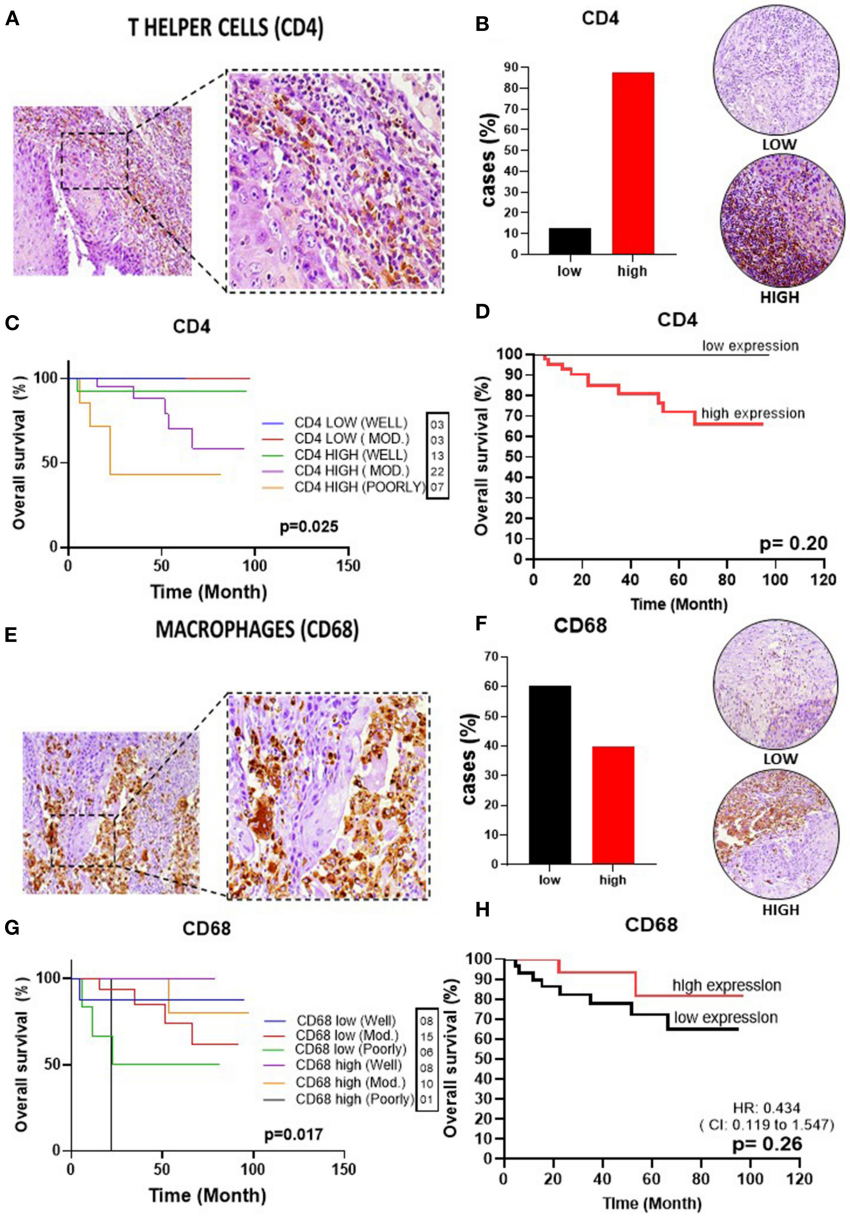

FIGURE 3 | Infiltrating T helper cells and macrophages in OSSC. **(A)** CD4 (left: 200X magnification; right panel: 400X magnification). **(B)** Representative images of OSCC tissues showing low and high CD4 expression, graph showing 42 cases (87.5%) of high CD4 tissues. **(C)**Well histological grade in CD4 low was associated with improved OS ($p = 0.02$). **(D)** High expression was unrelated to OS ($P = 0.21$). **(E)** CD68 in OSCC (left: magnification 200X; right panel: magnification 400X). **(F)** Representative images of OSCC tissues showing low and high expression, graph showing 29 cases (60.42%) with low CD68 low 60.42%; **(G)** Well histological grade in CD68 high was associated with improved OS ($p = 0.017$). **(H)** High CD68 expression was unrelated to OS ($P = 0.18$). CI, confidence interval; HR, hazard ratio; OS, overall survival; OSCC, oral squamous cell carcinoma; CD4, T helper cell; CD68, pan-macrophage; Mod, Moderately.

High Expression of Mature Dendritic Cells in the TME Are Correlated With Higher Survival

Given the importance of myeloid-derived immune effector cell subpopulations in the regulation of the TIME, we evaluated the pan-macrophage immunomarker CD68 to assess the presence of macrophages (both M1 and M2). We did not observe a correlation between expression of $CD68^{+}$ cells and OS (HR 0.4, 95%CI, 0.1–1.6) ($p = 0.27$) (**Figure 3H**). In addition, we also evaluated the presence of dendritic cells, due to their important role in T cell activation and immunoregulation. Our results demonstrated high prevalence of mature dendritic cells ($CD83^{+}$) in the TME was correlated with an improved OS (HR 0.2, 95%CI 0.0–3.4) ($p = 0.01$) (**Figure 4D**). In contrast, immature dendritic cells did not impact survival ($p = 0.18$) (**Figure 4H**).

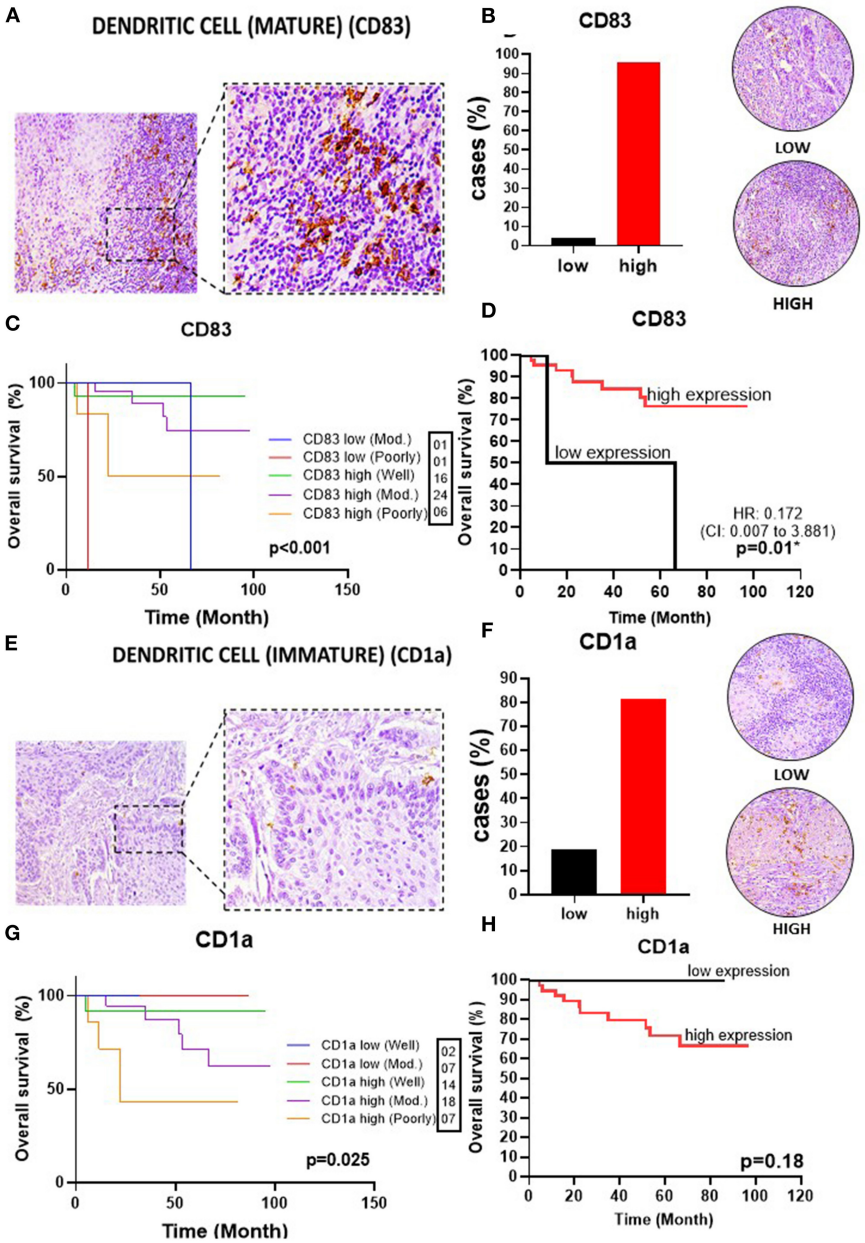

FIGURE 4 | Infiltrating dendritic cells in OSSC. **(A)** CD83 (left: 200X magnification; right panel: 400X magnification). **(B)** Representative images of OSCC tissues showing low and high CD83 expression, graph showing 46 cases (95.83%) with high CD83 tissues. **(C)** Well histological grade in CD83 high was associated with improved OS ($p < 0.001$). **(D)** High CD83 expression was associated with better OS ($P = 0.01$). **(E)** CD1a in OSCC (left: magnification 200X; right panel: magnification 400X). **(F)** Representative images of OSCC tissues showing low and high CD1a expression, graph showing 39 (81.25%) cases with high CD1a. **(G)** Well histological grade in CD1a low was associated with improved OS ($p = 0.025$). **(H)** High CD1a expression did not impact OS ($P = 0.18$). CI, confidence interval; HR, hazard ratio; OS, overall survival OSCC, oral squamous cell carcinoma; CD83, mature dendritic cell; CD1a, immature dendritic cell; Mod, Moderately.

TIME Correlates With Histological Grade and Survival in OTSCC

We stratified patients by histological grade (well, moderaty, and poorly differentiated) with the expression of the markers CD3, CD4, CD8, CD20, CD68, CD83, CD1a, and correlating with OS.

This analysis demonstrated a strong association of CD3+ and CD8+ T cells with a histological grade of well-differentiated and high expression of T lymphocytes with an improved OS ($p < 0.001$ and $p = 0.001$, respectively) (**Figures 1C**, **2G**). CD4+ T lymphocytes showed the opposite where patients with low expression show improvement in OS, but in this group no patient was found with poorly differentiated histological grade ($p = 0.025$) (**Figure 3C**). CD20+ B cells were correlated with OS improvement when

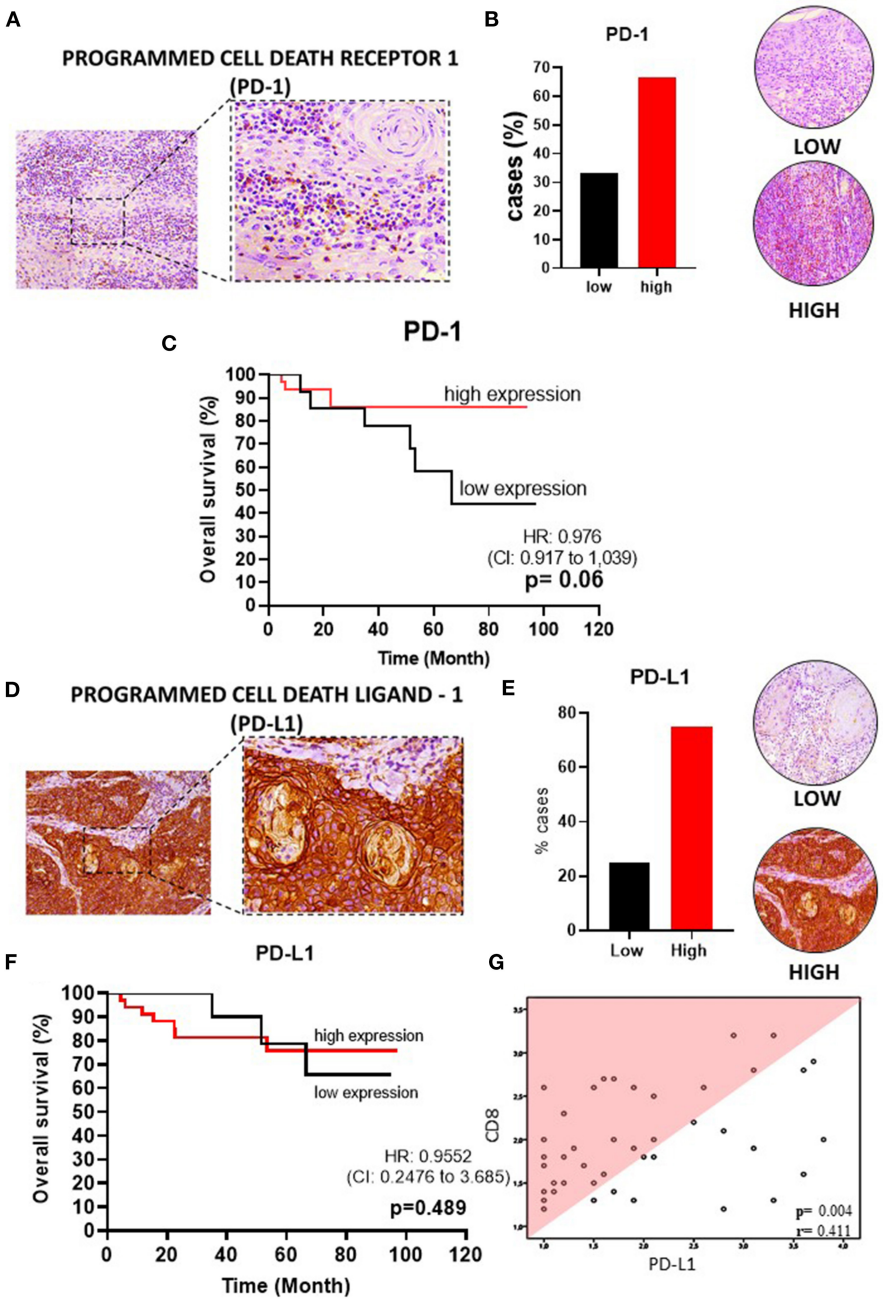

FIGURE 5 | PD-1 and PD-L1 in OSSC. **(A)** PD-1 in OSCC (left: 200X magnification; right panel: 400X magnification). **(B)** Representative images of OSCC tissues showing low and high PD-1 expression, graph showing 32 cases (66.67%) of high PD-1. **(C)** High PD-1 expression was not associated with OS ($P = 0.06$). **(D)** PD-LD-1 in OSCC (left: 200X magnification; right panel: 400X magnification). **(E)** Representative images of OSCC tissues showing low and high PDL-1 expression, graph showing 36 cases (75%) with high PD-L1. **(F)** High PD-L1 expression was not associated with OS. **(G)** Correlation of CD8+ rate with expression patterns of PD-L1 by Spearman rank correlation coefficient ($r = 0.480$; $p = 0.001$). CI, confidence interval; HR, hazard ratio; OS, overall survival; OSCC, oral squamous cell carcinoma, PD-1, programmed cell death receptor-1; PD-L1, programmed cell death ligand-1; Mod, Moderately.

they have a well-differentiated histological grade ($p = 0.01$) (**Figure 2C**).

CD68+ pan-macrophage cells showed the pattern of well histological differentiation and correlated with OS improvement ($p = 0.017$) (**Figure 3G**). CD83+ mature dendritic cells showed the pattern of high expression with improved survival when compared to low expression, independent of the degree of differentiation between these two groups ($p < 0.001$)

(**Figure 4C**). Non-low expression of the immature CD1a dendritic cell marker correlated with improved OS ($p = 0.025$) (**Figure 4G**).

TME Expression of PD-1 and PD-L1 Were not Associated With Survival Outcomes

The immune checkpoint molecules PD-1 and PD-L1 can suppress immunity, thereby preventing autoimmunity and protecting tissues from immune-mediated injury. However, in the context of cancer, they can inhibit beneficial anti-tumor immune responses. Although most of the tumors displayed high expression of both PD-1 (HR 1.0, 95% CI, 0.9–1.0, $p = 0.06$) and PD-L1 (HR 1.0, 95% CI, 0.3–3.7, $p = 0.48$), the expressions of these proteins in the TME and tumor center were not correlated with OS (**Figures 5C,F**).

To gain further insights into immunoregulatory networks in the TME, we performed a correlation matrix between all immune cell subpopulations and checkpoint inhibitor molecules. We observed a significant positive correlation ($p < 0.05$) between the densities of PD-1+ cells and cell subpopulations expressing CD3+, CD4+, CD8+, CD20+, and CD83+. In addition, a strong positive correlation was seen between CD20+ B cells and T cell subpopulations (CD3+, CD4+ and CD8+), which could be indicative of tertiary lymphoid structures (**Supplementary Table 2**).

DISCUSSION

Cancer biology research focused on the TIME has grown exponentially in recent years. Accumulating evidence suggests that OSCC is an immunosuppressive disease, and consequently immunotherapy has emerged as a novel approach to restore anti-tumor responses and to overcome escape mechanisms utilized by tumor cells (Ferris, 2015; Moskovitz and Ferris, 2018; Galvis et al., 2020). Nevertheless, it is important to recognize that the immune system is extremely complex, and that environmental factors such as tobacco and alcohol use can modify the antitumor immune response (de la Iglesia et al., 2020). Therefore, there is an acute need to recognize TIME profiles and assess their impacts on OSCC survival.

Herein we demonstrate that OTSCC in patients with tobacco and alcohol exposures is characterized by high levels of total T cells (CD3+), CD8+ T cells, and CD4+ T cells, as well as B lymphocytes (CD20+), and immature (CD1a) and mature (CD83) dendritic cells. Moreover, tumor cells showed a high expression of the immune checkpoint molecule PD-L1, while surrounding immune cells exhibited high PD-1 expression. In contrast, the TME presented low levels of macrophages (CD68). The influence of tumor immune infiltrate on survival curves showed particular promise for the CD3+ T cell co-receptor, CD20+ B cells and CD8+ T cells as predictors of survival, and identified CD3 as an independent prognostic marker.

The immune microenvironment is composed primarily of TILs (T and B lymphocytes and NK cells), macrophages, and dendritic cells (Munn and Bronte, 2016; Hadler-Olsen and Wirsing, 2019). All components play critical roles in the detection and elimination of tumor cells, thereby contributing to arresting tumor progression and proliferation (Kim, 2007; Ferris, 2015). The activation of T cells requires the T-cell receptor complex, which includes the co-receptor CD3 (Perri et al., 2020). Our findings showed that OTSCC featured a high expression of CD3+ T cells that was significantly correlated with improved survival and acts as an independent prognostic indicator. Past studies have shown that the presence of CD3+ T cells in the TME is related to improved prognosis in a wide range of tumors (Zhou et al., 2018, 2020). Supporting our findings, recent studies have reported the abundance of CD3+ T cells in the TME as an independent prognostic factor for OSCC, improving OS and recurrence-free survival (Zhou et al., 2018, 2020). Thus, the high expression of TME CD3+ cells is likely reflecting immunocompetent T lymphocytes with anti-tumor activity, and also highlights its potential roles as an accurate prognostic marker and for the selection of patient candidates for therapies targeting T lymphocytes (Almangush et al., 2020).

B lymphocytes play an important role in antigen presentation and antibody production in the early stages of tumor development (Quan et al., 2016; Taghavi et al., 2018; Hadler-Olsen and Wirsing, 2019). Our data correlated a high expression of CD20 with improved OS. Despite the importance of B cells in antitumor activity, there remains a paucity of evidence regarding their prognostic role. Our finding that TME CD20+ B cells are strongly correlated with T cells could be reflecting the formation of tertiary lymphoid structures, which have been associated with improved survival in OSCC (Wirsing et al., 2014). Notably, our results reinforce the importance of understanding the role of B cells in the TIME and their role as a prognostic factor.

Immune activation is driven through interactions between immune cells and tumor-associated antigens (Perri et al., 2020). CD8+ cytotoxic T cell activation follows interaction with antigen-presenting cells. Our data revealed that a high prevalence of T cells (likely including cytotoxic CD8+ T cells) in the invasive margin tends to be associated with higher OS. The presence of cytotoxic T cells in the TME has been highlighted as a key-point in the interactions between tumor and immune cells (Ferris, 2015; Hadler-Olsen and Wirsing, 2019; Perri et al., 2020). Our findings are consistent with previous studies showing that the high expression of CD8+ cytotoxic T cells is correlated with improved survival in OTSSC (Nguyen et al., 2016; Zhou et al., 2018; Shimizu et al., 2019). Due to all evidence and the biological role of CD8+ T cells in the TME, CD8 may prove to be a fundamental molecule to assess as a prognostic marker for OTSSC patients.

CD4+ T helper cells act as regulators of the immune response, thus avoiding exacerbated immune responses, particularly those mediated by cytotoxic T cells (Perri et al., 2020). Treg cells represent a minor heterogenic subsite of CD4+ T cells with the potential to induce suppression of CD8+ T cells and may contribute to carcinogenesis and cancer progression by two mechanisms; first, by limiting immune function upon tumor recognition; and second, by suppressing the cellular activity of cytotoxic T cells (Dayan et al., 2012; Hadler-Olsen and Wirsing, 2019; Perri et al., 2020). Our results demonstrated that patients with increased CD4+ expression tended to have a worse

prognosis, although statistical significance was not established. Previous studies evaluating the impact of CD4+ T cells also did not reach statistical significance with respect to their influence on OS. These data indicate the antagonistic effect of some T cell subpopulations in the TME, and demonstrate the importance of characterization of specific cell subpopulations in the TIME, mainly Treg cells, which often express Foxp3, a marker not included in our study (Perri et al., 2020).

Tumor-associated macrophages present two different phenotypes: M1, which exerts an antitumor role; and M2, which exerts a protumor immunosuppressive role (Alves et al., 2018). CD68 is a pan-macrophage marker, which has been related to tumor-suppressor activity (Alves et al., 2018; Hadler-Olsen and Wirsing, 2019). We did not observe statistical differences between CD68+ cells and survival outcomes. A recent meta-analysis found no significant association between the CD68 pan-macrophage marker and OS (Hadler-Olsen and Wirsing, 2019). Moreover, a recent literature review noted the difficulty in evaluating this marker due to data variability and study methodologies (Alves et al., 2018).

Dendritic cells (DC) are responsible for recognizing and presenting antigens to immune cells, especially T cells (Hansen and Andersen, 2017; Perri et al., 2020). Currently, there are a large number of markers for characterizing DC subpopulations (Pellicioli et al., 2017; Jardim et al., 2018). In our study, we selected CD83 (mature DCs) and CD1a (immature DCs) because of their well-established biological properties and previous investigations (Gomes et al., 2016; Pellicioli et al., 2017; Jardim et al., 2018). Our findings showed that OTSCC patients presented high expression of CD83+ DCs, and that they were significantly correlated with improved survival. Pellicioli *et al.* showed that the presence of mature DCs is associated with the early stages of OTSSC development (Pellicioli et al., 2017). In contrast, Jardim et al., did not find a correlation between CD83 and OS (Jardim et al., 2018).

We used CD1a expression as an indicator of immature DCs. CD1a is involved in antigen presentation by dendritic Langerhans cells to T lymphocytes (Gondak et al., 2012; Jardim et al., 2018). Our data demonstrated that increased levels of CD1a+ cells tended to result in a worse prognosis, although statistical significance was not established. However, Jardim et al. showed that lower levels of immature peritumoral DCs predict higher recurrence rates and shorter survival (Jardim et al., 2018). The presence of immature DCs often demonstrates that the immune system is in the stage of maturation and recruitment, and thus predicts worse survival. The opposite effect is suggested by the presence of mature DCs, which reflects the presence of active T lymphocytes, and predicts an active immune response and improved prognosis (Hansen and Andersen, 2017; Jardim et al., 2018).

T cells express the immunological checkpoint protein PD-1, which interacts with its receptor on neoplastic and immune cells, PD-L1, leading to the inhibition of cytolytic antitumor responses, thereby promoting immunologic escape of tumor cells (Ferris, 2015; Gato-Cañas et al., 2017; Gong et al., 2018; Moskovitz and Ferris, 2018). In our study, levels of PD-1 did not correlate with prognosis in OTSSC. Thus, our study demonstrates the presence of an active microenvironment that drives the expression of immune checkpoint inhibitors; however, this microenvironment manages to remain active through the recruitment of CD8+ T cells, reinforcing the potential use of immune checkpoint inhibitor therapies (Ferris, 2015; Gato-Cañas et al., 2017; Kansy et al., 2017; Gong et al., 2018).

The presence of PD-L1 in tumor cells indicates an active mechanism of immune escape (Ferris, 2015; Moskovitz and Ferris, 2018; Perri et al., 2020). In our study, there was no clear effect of PD-L1 expression on OS. The expression of PD-L1 by tumor cells can facilitate immunologic escape by inhibiting cytotoxic T cell function; therefore, increased PD-L1 can correlate with a worse prognosis. On the other hand, the expression of PD-L1 by tumor cells may be secondary to the production of IFN-gamma by infiltrating T cells, which is often associated with better outcomes (Moskovitz and Ferris, 2018; Perri et al., 2020). Previous studies have associated PD-L1 overexpression with reduced survival (Lin et al., 2015; De Vicente et al., 2019; Lenouvel et al., 2020) others show the opposite, where prognostic significance is not established (Huang et al., 2020). These conflicting results show the importance of the need for standardization of marking for this protein. A recent study has demonstrated several PD-L1 marker patterns in OTSCC, which associated four patterns with distinct biological processes (genetic modifications and adaptive immune resistance, immune ignorance, intrinsic induction, and immune tolerance), and demonstrated a change in survival when evaluating the different patterns (Miranda-Galvis et al., 2020). Thus, the study shows the potential prognostic value of PD-L1, however studies evaluating these patterns in different cohorts and tumors will clarify their potential as broadly used markers.

Another finding observed in our study was the stratification of the patients regarding the histological grade. The histological grade is a known prognostic factor in OTSSC, and it has been described that higher grades of TILs or increasing CD3+ or CD8 + cell densities are associated with histological grades (Giraldo et al., 2019; Almangush et al., 2020; Zhou et al., 2020). Our study observed that the presence of TIME influences survival of the patients even when stratifying the patients by the histological grade. Importantly, CD3+ T cells remained an independent marker.

Our studies limitations are; First, the strict inclusion criteria that aimed to study a more homogeneous population, defined by tobacco and alcohol consumption, led to a smaller sample size, Second, the cell population of macrophages was evaluated by using the pan-macrophage antibody, which did not allow the identification of M1 and M2 subtypes, Third, the assessment of immune cell profiles through immunohistochemistry only allows the identification of the presence of the cells, but does not address their specific immune functional activity, and Fourth, due to the sample size stratification by histological grade led to small sub-group sizes, limiting the ability to generalize these particular findings.

In summary, we provide evidence that OTSCC patients who smoke tobacco and drink alcohol have an active TIME, which is associated with better OS. We identified specific TIL subpopulations, including CD3+ T cells, CD20+ B cells, and

CD83+ mature dendritic cells, that are associated with better survival rates. Moreover, increased expression of CD3+ T cells was identified as an independent prognostic marker, suggesting a potential biomarker for therapeutic targets in OTSCC.

DATA AVAILABILITY STATEMENT

The raw data supporting the conclusions of this article will be made available by the authors, without undue reservation.

ETHICS STATEMENT

The studies involving human participants were reviewed and approved by Human Research Ethics Committee of A.C. Camargo Cancer Center. The patients/participants provided their written informed consent to participate in this study.

AUTHOR CONTRIBUTIONS

RS: study concepts, study design, data acquisition, data analysis and interpretation, statistical analysis, manuscript preparation, and manuscript editing. MM: data acquisition, data analysis and interpretation, statistical analysis, and manuscript preparation. BM: data analysis and interpretation, and manuscript preparation. AL: data interpretation and manuscript review. LS: data acquisition and quality control. OA: data acquisition and quality control, and manuscript review. AS-S: data analysis and interpretation, and manuscript review. CP: data acquisition and quality control. PV: study concepts, study design, data analysis and interpretation, and manuscript review. KG: study concepts, study design, data analysis and interpretation, and manuscript review. LK: study concepts, study design, data quality control and algorithm, data analysis and interpretation, and manuscript review. All authors contributed to the article and approved the submitted version.

FUNDING

This work was supported by the Coordination of Superior Level Staff Improvement– Brazil (CAPES) (RS, finance code 001), and by the São Paulo Research Foundation (FAPESP) – (BM grant #2018/24715-2). KG is a CNPq Research Fellow.

SUPPLEMENTARY MATERIAL

The Supplementary Material for this article can be found online at: https://www.frontiersin.org/articles/10.3389/fcell.2020.622161/full#supplementary-material

REFERENCES

Almangush, A., Mäkitie, A. A., Triantafyllou, A., de Bree, R., Strojan, P., Rinaldo, A., et al. (2020). Staging and grading of oral squamous cell carcinoma: an update. *Oral Oncol.* 107:104799. doi: 10.1016/j.oraloncology.2020.104799

Alves, A. M., Diel, L. F., and Lamers, M. L. (2018). Macrophages and prognosis of oral squamous cell carcinoma: a systematic review. *J. Oral Pathol. Med.* 47, 460–467. doi: 10.1111/jop.12643

Bray, F., Ferlay, J., Soerjomataram, I., Siegel, R. L., Torre, L. A., and Jemal, A. (2018). Global cancer statistics 2018: GLOBOCAN estimates of incidence and mortality worldwide for 36 cancers in 185 countries. *CA Cancer J. Clin.* 68, 394–424. doi: 10.3322/caac.21492

Curado, M. P., Johnson, N. W., Kerr, A. R., Silva, D. R. M., Lanfranchi, H., Pereira, D. L., et al. (2016). Oral and oropharynx cancer in South America. *Transl. Res. Oral Oncol.* 1:2057178X1665376. doi: 10.1177/2057178X16653761

Dayan, D., Salo, T., Salo, S., Nyberg, P., Nurmenniemi, S., Costea, D. E., et al. (2012). Molecular crosstalk between cancer cells and tumor microenvironment components suggests potential targets for new therapeutic approaches in mobile tongue cancer. *Cancer Med.* 1, 128–140. doi: 10.1002/cam4.24

de la Iglesia, J. V., Slebos, R. J. C., Martin-Gomez, L., Wang, X., Teer, J. K., Tan, A. C., et al. (2020). Effects of tobacco smoking on the tumor immune microenvironment in head and neck squamous cell carcinoma. *Clin. Cancer Res.* 26, 1474–1485. doi: 10.1158/1078-0432.CCR-19-1769

De Vicente, J. C., Rodríguez-Santamarta, T., Rodrigo, J. P., Blanco-Lorenzo, V., Allonca, E., and García-Pedrero, J. M. (2019). PD-L1 expression in tumor cells is an independent unfavorable prognostic factor in oral squamous cell carcinoma. *Cancer Epidemiol. Biomarkers Prev.* 28, 546–554. doi: 10.1158/1055-9965.EPI-18-0779

Edge, S. B., and Compton, C. C. (2010). The american joint committee on cancer: the 7th edition of the AJCC cancer staging manual and the future of TNM. *Ann. Surg. Oncol.* 17, 1471–1474. doi: 10.1245/s10434-010-0985-4

El.Naggar, A. K. C. J., Grandis, J. R., and Takata, T., S. P. (2017). WHO Classification of Head and Neck Tumours. (Lyon: IARC).

Ferris, R. L. (2015). Immunology and immunotherapy of head and neck cancer. *J. Clin. Oncol.* 33, 3293–3304. doi: 10.1200/JCO.2015.61.1509

Fridman, W. H., Dieu-Nosjean, M. C., Pagès, F., Cremer, I., Damotte, D., Sautès-Fridman, C., et al. (2013). The immune microenvironment of human tumors: general significance and clinical impact. *Cancer Microenviron.* 6, 117–122. doi: 10.1007/s12307-012-0124-9

Galon, J., Pagès, F., Marincola, F. M., Angell, H. K., Thurin, M., Lugli, A., et al. (2012). Cancer classification using the Immunoscore: a worldwide task force. *J. Transl. Med.* 10:205. doi: 10.1186/1479-5876-10-205

Galvis, M. M., Borges, G. A., Oliveira, T. B., de Toledo, I. P., de Castilho, R. M., Guerra, E. N. S., et al. (2020). Immunotherapy improves efficacy and safety of patients with HPV positive and negative head and neck cancer: a systematic review and meta-analysis. *Crit. Rev. Oncol. Hematol.* 150:102966. doi: 10.1016/j.critrevonc.2020.102966

Gato-Cañas, M., Ibañez-Vea, M., Escors, D., Kochan, G., Breckpot, K., Arasanz, H., et al. (2017). PD1 signal transduction pathways in T cells. *Oncotarget* 8, 51936–51945. doi: 10.18632/oncotarget.17232

Giraldo, N. A., Peske, J. D., Sautès-Fridman, C., and Fridman, W. H. (2019). Integrating histopathology, immune biomarkers, and molecular subgroups in solid cancer: the next step in precision oncology. *Virchows Arch.* 474, 463–474. doi: 10.1007/s00428-018-02517-1

Gomes, J. O., de Vasconcelos Carvalho, M., Fonseca, F. P., Gondak, R. O., Lopes, M. A., and Vargas, P. A. (2016). CD1a+ and CD83+ langerhans cells are reduced in lower lip squamous cell carcinoma. *J. Oral Pathol. Med.* 45, 433–439. doi: 10.1111/jop.12389

Gondak, R. O., Alves, D. B., Silva, L. F. F., Mauad, T., and Vargas, P. A. (2012). Depletion of Langerhans cells in the tongue from patients with advanced-stage acquired immune deficiency syndrome: relation to opportunistic infections. *Histopathology* 60, 497–503. doi: 10.1111/j.1365-2559.2011.04068.x

Gong, J., Chehrazi-Raffle, A., Reddi, S., and Salgia, R. (2018). Development of PD-1 and PD-L1 inhibitors as a form of cancer immunotherapy: a comprehensive review of registration trials and future considerations. *J. Immunother. Cancer* 6, 1–18. doi: 10.1186/s40425-018-0316-z

Hadler-Olsen, E., and Wirsing, A. M. (2019). Tissue-infiltrating immune cells as prognostic markers in oral squamous cell carcinoma: a systematic review and meta-analysis. *Br. J. Cancer* 120, 714–727. doi: 10.1038/s41416-019-0409-6

Hanahan, D., and Weinberg, R. A. (2000). The hallmarks of cancer. *Cell* 100, 57–70. doi: 10.1016/S0092-8674(00)81683-9

Hanahan, D., and Weinberg, R. A. (2011). Hallmarks of cancer: the next generation. *Cell* 144, 646–674. doi: 10.1016/j.cell.2011.02.013

Hansen, M., and Andersen, M. H. (2017). The role of dendritic cells in cancer. *Semin. Immunopathol.* 39, 307–316. doi: 10.1007/s00281-016-0592-y

Huang, W., Zhou, X., Liao, Q., Tang, Y., Zuo, L., Wang, H., et al. (2020). Clinicopathological and prognostic significance of PD-1/PD-L1 axis expression in patients with tongue squamous cell carcinoma. *J. Cell. Physiol.* 235, 6942–6953. doi: 10.1002/jcp.29590

Jardim, J. F., Gondak, R., Galvis, M. M., Pinto, C. A. L., and Kowalski, L. P. (2018). A decreased peritumoral CD1a+ cell number predicts a worse prognosis in oral squamous cell carcinoma. *Histopathology* 72, 905–913. doi: 10.1111/his.13415

Kansy, B. A., Concha-Benavente, F., Srivastava, R. M., Jie, H. B., Shayan, G., Lei, Y., et al. (2017). PD-1 status in CD8+ T cells associates with survival and anti-PD-1 therapeutic outcomes in head and neck cancer. *Cancer Res.* 77, 6353–6364. doi: 10.1158/0008-5472.CAN-16-3167

Kim, R. (2007). Cancer immunoediting: from immune surveillance to immune escape. *Cancer Immunother.* 2007, 9–27. doi: 10.1016/B978-012372551-6/50066-3

Lenouvel, D., González-Moles, M. Á., Ruiz-Ávila, I., Gonzalez-Ruiz, L., Gonzalez-Ruiz, I., and Ramos-García, P. (2020). Prognostic and clinicopathological significance of PD-L1 overexpression in oral squamous cell carcinoma: a systematic review and comprehensive meta-analysis. *Oral Oncol.* 106:104722. doi: 10.1016/j.oraloncology.2020.104722

Lim, B., Woodward, W. A., Wang, X., Reuben, J. M., and Ueno, N. T. (2018). Inflammatory breast cancer biology: the tumour microenvironment is key. *Nat. Rev. Cancer* 18, 485–499. doi: 10.1038/s41568-018-0010-y

Lin, Y. M., Sung, W. W., Hsieh, M. J., Tsai, S. C., Lai, H. W., Yang, S. M., et al. (2015). High PD-L1 expression correlates with metastasis and poor prognosis in oral squamous cell carcinoma. *PLoS ONE* 10:e0142656. doi: 10.1371/journal.pone.0142656

Miranda-Galvis, M., Piña, A. R., Sales de Sá, R., Leite, A. A., Vargas, P. A., Calsavara, V. F., et al. (2020). PD-L1 expression patterns in oral cancer as an integrated approach for further prognostic classification running title. *Oral Dis.* 1–12. doi: 10.1111/odi.13714. [Epub ahead of print].

Moskovitz, J. M., and Ferris, R. L. (2018). Tumor immunology and immunotherapy for head and neck squamous cell carcinoma. *J. Dent. Res.* 97, 622–626. doi: 10.1177/0022034518759464

Munn, D. H., and Bronte, V. (2016). Immune suppressive mechanisms in the tumor microenvironment. *Curr. Opin. Immunol.* 39, 1–6. doi: 10.1016/j.coi.2015.10.009

Naruse, T., Yanamoto, S., Okuyama, K., Ohmori, K., Tsuchihashi, H., Furukawa, K., et al. (2019). Immunohistochemical study of PD-1/PD-L1 axis expression in oral tongue squamous cell carcinomas: effect of neoadjuvant chemotherapy on local recurrence. *Pathol. Oncol. Res.* 26, 735–742. doi: 10.1007/s12253-019-00606-3

Ng, J. H., Iyer, N. G., Tan, M.-H., and Edgren, G. (2017). Changing epidemiology of oral squamous cell carcinoma of the tongue: a global study. *Head Neck* 39, 297–304. doi: 10.1002/hed.24589

Ngamphaiboon, N., Chureemas, T., Siripoon, T., Arsa, L., Trachu, N., Jiarpinitnun, C., et al. (2019). Characteristics and impact of programmed death-ligand 1 expression, CD8+ tumor-infiltrating lymphocytes, and p16 status in head and neck squamous cell carcinoma. *Med. Oncol.* 36, 1–10. doi: 10.1007/s12032-018-1241-1

Nguyen, N., Bellile, E., Thomas, D., McHugh, J., Rozek, L., Virani, S., et al. (2016). Tumor infiltrating lymphocytes and survival in patients with head and neck squamous cell carcinoma. *Head Neck* 38, 1074–1084. doi: 10.1002/hed.24406

Pellicioli, A. C. A., Bingle, L., Farthing, P., Lopes, M. A., Martins, M. D., and Vargas, P. A. (2017). Immunosurveillance profile of oral squamous cell carcinoma and oral epithelial dysplasia through dendritic and T-cell analysis. *J. Oral Pathol. Med.* 46, 928–933. doi: 10.1111/jop.12597

Perri, F., Ionna, F., Longo, F., Della Vittoria Scarpati, G., De Angelis, C., Ottaiano, A., et al. (2020). Immune response against head and neck cancer: biological mechanisms and implication on therapy. *Transl. Oncol.* 13, 262–274. doi: 10.1016/j.tranon.2019.11.008

Quan, H., Fang, L., Pan, H., Deng, Z., Gao, S., Liu, O., et al. (2016). An adaptive immune response driven by mature, antigen-experienced T and B cells within the microenvironment of oral squamous cell carcinoma. *Int. J. Cancer* 138, 2952–2962. doi: 10.1002/ijc.30019

Salo, T., Vered, M., Bello, I. O., Nyberg, P., Bitu, C. C., Zlotogorski Hurvitz, A., et al. (2014). Insights into the role of components of the tumor microenvironment in oral carcinoma call for new therapeutic approaches. *Exp. Cell Res.* 325, 58–64. doi: 10.1016/j.yexcr.2013.12.029

Scully, C., and Bagan, J. (2009). Oral squamous cell carcinoma overview. *Oral Oncol.* 45, 301–308. doi: 10.1016/j.oraloncology.2009.01.004

Shimizu, S., Hiratsuka, H., Koike, K., Tsuchihashi, K., Sonoda, T., Ogi, K., et al. (2019). Tumor-infiltrating CD8 + T-cell density is an independent prognostic marker for oral squamous cell carcinoma. *Cancer Med.* 8, 80–93. doi: 10.1002/cam4.1889

Society, I. B. (2010). Maximally Selected Rank Statistics Author (s): Berthold Lausen and Martin Schumacher Published by : International Biometric Society Stable. *Society* 48, 73–85. doi: 10.2307/2532740

Taghavi, N., Mohsenifar, Z., Baghban, A. A., and Arjomandkhah, A. (2018). CD20+ tumor infiltrating B lymphocyte in oral squamous cell carcinoma: correlation with clinicopathologic characteristics and heat shock protein 70 expression. *Patholog. Res. Int.* 2018, 1–7. doi: 10.1155/2018/4810751

Tsao, M. S., Kerr, K. M., Dacic, S., Yatabe, Y., and Hirsch, F. R. (2017). IASLC *A*tlas of PD-L1 *I*mmunohistochemistry *T*esting in *L*ung *Cancer*. Editorial Rx Press.

Wirsing, A. M., Rikardsen, O. G., Steigen, S. E., Uhlin-Hansen, L., and Hadler-Olsen, E. (2014). Characterisation and prognostic value of tertiary lymphoid structures in oral squamous cell carcinoma. *BMC Clin. Pathol.* 14, 1–10. doi: 10.1186/1472-6890-14-38

Zhou, C., Diao, P., Wu, Y., Wei, Z., Jiang, L., Zhang, W., et al. (2020). Development and validation of a seven-immune-feature-based prognostic score for oral squamous cell carcinoma after curative resection. *Int. J. Cancer* 146, 1152–1163. doi: 10.1002/ijc.32571

Zhou, C., Wu, Y., Jiang, L., Li, Z., Diao, P., Wang, D., et al. (2018). Density and location of CD3 + and CD8 + tumor-infiltrating lymphocytes correlate with prognosis of oral squamous cell carcinoma. *J. Oral Pathol. Med.* 47, 359–367. doi: 10.1111/jop.12698

Conflict of Interest: The authors declare that the research was conducted in the absence of any commercial or financial relationships that could be construed as a potential conflict of interest.

frontiers in Cell and Developmental Biology

ORIGINAL RESEARCH
published: 02 March 2021
doi: 10.3389/fcell.2021.629941

Identification of a ceRNA Network in Lung Adenocarcinoma Based on Integration Analysis of Tumor-Associated Macrophage Signature Genes

Lei Zhang[1,2†], Kai Zhang[2†], Shasha Liu[2†], Ruizhe Zhang[3], Yang Yang[1], Qi Wang[1], Song Zhao[1], Li Yang[2], Yi Zhang[2*] and Jiaxiang Wang[1*]*

[1] Department of Surgery, The First Affiliated Hospital of Zhengzhou University, Zhengzhou, China, [2] Biotherapy Center, The First Affiliated Hospital of Zhengzhou University, Zhengzhou, China, [3] Reproductive Medicine Center, The First Affiliated Hospital of Zhengzhou University, Zhengzhou, China

As research into tumor-immune interactions progresses, immunotherapy is becoming the most promising treatment against cancers. The tumor microenvironment (TME) plays the key role influencing the efficacy of anti-tumor immunotherapy, in which tumor-associated macrophages (TAMs) are the most important component. Although evidences have emerged revealing that competing endogenous RNAs (ceRNAs) were involved in infiltration, differentiation and function of immune cells by regulating interactions among different varieties of RNAs, limited comprehensive investigation focused on the regulatory mechanism between ceRNA networks and TAMs. In this study, we aimed to utilize bioinformatic approaches to explore how TAMs potentially influence the prognosis and immunotherapy of lung adenocarcinoma (LUAD) patients. Firstly, according to TAM signature genes, we constructed a TAM prognostic risk model by the least absolute shrinkage and selection operator (LASSO) cox regression in LUAD patients. Then, differential gene expression was analyzed between high- and low-risk patients. Weighted gene correlation network analysis (WGCNA) was utilized to identify relevant gene modules correlated with clinical characteristics and prognostic risk score. Moreover, ceRNA networks were built up based on predicting regulatory pairs in differentially expressed genes. Ultimately, by synthesizing information of protein-protein interactions (PPI) analysis and survival analysis, we have successfully identified a core regulatory axis: LINC00324/miR-9-5p (miR-33b-5p)/GAB3 (IKZF1) which may play a pivotal role in regulating TAM risk and prognosis in LUAD patients. The present study contributes to a better understanding of TAMs associated immunosuppression in the TME and provides novel targets and regulatory pathway for anti-tumor immunotherapy.

Keywords: tumor-associated macrophages, lung adenocarcinoma, LASSO cox regression, WGCNA, competing endogenous RNA

OPEN ACCESS

Edited by:
Mariane Tami Amano, Hospital Sirio Libanes, Brazil

Reviewed by:
Danilo Candido De Almeida, Federal University of São Paulo, Brazil
Vinícius Jardim Carvalho, University of São Paulo, Brazil

****Correspondence:***
Li Yang
fccyangl1@zzu.edu.cn
Yi Zhang
yizhang@zzu.edu.cn
Jiaxiang Wang
wangjx101@126.com

† These authors have contributed equally to this work and share first authorship

Specialty section:
This article was submitted to Molecular Medicine, a section of the journal Frontiers in Cell and Developmental Biology

Received: *16 November 2020*
Accepted: *11 February 2021*
Published: *02 March 2021*

Citation:
Zhang L, Zhang K, Liu S, Zhang R, Yang Y, Wang Q, Zhao S, Yang L, Zhang Y and Wang J (2021) Identification of a ceRNA Network in Lung Adenocarcinoma Based on Integration Analysis of Tumor-Associated Macrophage Signature Genes. Front. Cell Dev. Biol. 9:629941. doi: 10.3389/fcell.2021.629941

INTRODUCTION

As reported in World Cancer Report 2020, lung cancer continues to be the most common cancer type and the leading cause of cancer death worldwide, accounting for about 18% of all cancer deaths. Non-small-cell lung cancer represents 80–85% of lung cancers, and can be subdivided into adenocarcinoma, squamous-cell carcinoma, and large-cell carcinoma, etc (Reck and Rabe, 2017; Siegel et al., 2020). Among them, lung adenocarcinoma (LUAD) is more aggressive and possesses more morphological heterogeneity than other types of lung cancer (Zhang et al., 2018).

In spite of advances in chemotherapy, radiotherapy, and targeted therapy in the last decade, prognosis of patients with advanced lung cancer is still very poor, with a 5-year survival rate of 10–20% (Allemani et al., 2015). As research progresses, immunotherapy is becoming the most promising treatment against cancers, and has gradually revolutionized cancer treatment (Herbst et al., 2018). Although several tumor types including LUAD reveal effective response to immunotherapy especially immune checkpoint blockade, it remains a large portion of patients failed to benefit from the treatment (Chen and Mellman, 2017; Hirsch et al., 2017).

Recent studies have demonstrated that the tumor microenvironment (TME) plays the key role influencing the efficacy of anti-tumor immunotherapy, in which tumor-associated macrophages (TAMs) are the most important component (Bohn et al., 2018; Xia et al., 2020). TAMs are abundant in multiple cancers compared to adjacent tissues, supporting oncogenesis, vascularization in spite of immunosurveillance (Yang and Zhang, 2017). This raises the intriguing possibility that targeting TAMs may be an effective therapeutic strategy for intractable LUAD (Cassetta and Pollard, 2018). Actually, considering the extremely complicated microenvironment, TAMs appear to be highly heterogeneous in solid tumors. Meanwhile, TAM-associated molecular markers appear to show controversial prognostic value in pan-cancer patients (Pollard, 2004; Lu-Emerson et al., 2013; Ojalvo et al., 2018; Wang et al., 2018; Cao et al., 2019; Li et al., 2019; Liu et al., 2019; Dai et al., 2020). Collective evidence had previously demonstrated that TAMs were characterized mostly by M2-like markers and were correlated with poor prognosis in numerous malignancies, including lung cancer. Therefore, we assumed that identification of M2-like TAMs risk was more meaningful because they are primarily responsible for the prognosis of patients.

Accumulating evidences have emerged revealing competing endogenous RNAs (ceRNAs) play an essential role in regulating interactions among different varieties of RNAs and were involved in progression and immune infiltration in multiple kinds of tumors (Zhang K. et al., 2020). However, there is limited comprehensive investigation focusing on the regulatory mechanism between ceRNA networks and TAM associated signature genes, and the deep prognostic value is not yet fully explored. In this study, we aimed to utilize bioinformatic approaches analyzing public datasets to explore how TAMs potentially influence the prognosis of LUAD patients and tried to provide novel targets and directions for anti-tumor immunotherapy, especially for targeting the TAMs.

MATERIALS AND METHODS

Study Design

The workflow of the manuscript is shown in **Figure 1**. Public datasets TCGA-LUAD and an external GEO validation cohort, containing sequencing data of LUAD tumor tissues, were analyzed in this study. As for TCGA-training cohort, utilizing TAMs associated genes, we firstly constructed a TAMs prognostic risk model by LASSO cox regression. Samples were divided into high- and low-risk groups according to their calculated risk scores. Then differentially expressed genes between two groups were identified for following comprehensive analysis. WGCNA was utilized to identify relevant gene modules correlated with clinical characters and prognostic risk score and ceRNA networks were then built up in concerned WGCNA modules. At last, by synthesizing information of PPI analysis and survival analysis, we tried to identify a core regulatory axis in ceRNA networks which may play a key role in TAMs associated immunosuppression and prognostic value in LUAD patients.

Public Data Used in This Study

The TCGA-LUAD data, containing expression value of lncRNAs, miRNAs, and mRNA as well as clinical information were retrieved from the TCGA data portal[1]. Besides, another external validation set GSE72094, defined as GEO-validation cohort was obtained from the GEO website[2]. After removing patients who have ever been affected by other malignant tumors or with incomplete lncRNAs, miRNAs, and mRNAs data, 804 LUAD patients were screened for inclusion in this study. Expression value of genes was then standardized for subsequent analysis.

Construction of TAMs Related Prognostic Risk Model

According to comprehensively reported TAMs related gene signature: CD68, CD11b, CD163, CD206, IL10, CD39, MMP14, CXCL8, CCL17, CD274, TGFB1, ARG1, and IDO1, a TAMs related prognostic risk model was built up by the least absolute shrinkage and selection operator (LASSO) cox regression (Duan et al., 2016). Package "glmnet" in R software (version 3.3.2) was utilized to achieve this result. Optimized lambda was determined when the cross-validation error reach to the smallest and non-zero coefficients were selected. Subsequently, a risk score was built according to the expression value and module coefficient of each gene (Lossos et al., 2004; Chen et al., 2007; Hu et al., 2019):

$$\text{Risk score} = \sum_{i=1}^{k} \beta i Si$$

where k, βi, and Si represent the number of signature genes, the coefficient index, and the gene expression level, respectively.

[1]https://tcga-data.nci.nih.gov/tcga/

[2]https://www.ncbi.nlm.nih.gov/geo/

Subsequently, a risk score was built according to the expression value and module coefficient of each gene and therefore patients were assigned into high-risk group and low-risk group based on the risk score. At last, Kaplan-Meier survival analysis were performed to validate prognostic value of the risk model.

Survival Analysis

The univariate Cox regression model was applied to analyze the relationship between the overall survival (OS) of LUAD patients and gene expression. p-value < 0.05 was considered to be significant. Then, the selected genes were visualized with the Kaplan-Meier survival curve. Time-dependent ROC analyses were conducted by "timeROC" R package to estimate the accuracy of the predicted survival probability.

Identification of Differentially Expressed Genes

Random variance model (RVM) t-test was applied to filter the differentially expressed genes among groups. After the significant analysis and FDR analysis, we selected the differentially expressed genes according to the criterion: FDR < 0.05 and absolute FC > 1.2. Then, the relative abundances of differentially expressed lncRNAs (DElncRNAs), differentially expressed miRNAs (DEmiRNAs) and differentially expressed mRNAs (DEmRNAs) were illustrated in heatmaps by R package "gplots."

Weighted Gene Correlation Network Analysis

In order to analyze potential interconnections between DEGs, Weighted gene correlation network analysis (WGCNA) analysis was employed to identify modules containing genes with similar expression patterns via the package "WGCNA" in R software (Langfelder and Horvath, 2008). Firstly, cluster analysis was performed to remove outliers based on differential gene expression of samples. Next, to balance the relationship between scale independence and mean connectivity, a suitable soft-threshold power β was determined. Then Topological Overlap Matrix (TOM) was constructed based on β value, deriving the intergenic divergence coefficients. Cluster Dendrogram and Eigengene Adjacency Heatmap were drew to show gene clustering and module relationship. To determine the most important module for further analysis, eigengene for each module was calculated. Then eigengenes were employed to compute module-trait associations with risk score, TNM stage, age, gender, race, and RFS, etc. Finally, concerned modules were identified by considering genes numbers and association between modules and clinical features.

Gene Ontology and KEGG Pathway Enrichment Analysis

Gene ontology (GO) analysis was applied to analyze the main function of genes according to the Gene Ontology database[3], which can organize genes into hierarchical categories and uncover the gene regulatory network on the basis of biological process and molecular function. The Kyoto Encyclopedia of Genes and Genomes (KEGG)[4] (Kanehisa et al., 2010) was used to analyze the potential regulatory pathways of DEG and genes involved in concerned WGCNA modules. The functional annotations were performed by "clusterProfiler" package in R software.

Construction of ceRNA Networks

To predict the possible target mRNAs and lncRNAs of DEmiRNAs, several target gene prediction websites were utilized. Firstly, by searching miRanda[5], Targetscan[6] (Lewis et al., 2005), and miRWalk[7] databases, we got intersection of predicted miRNA-mRNA pairs with possible binding relation. Similarly, miRNA-lncRNA pairs were predicted by employing PITA[8] and miRanda databases. Then, miRNA-mRNA/miRNA-lncRNA pairs with negatively correlation were finally determined in concerned WGCNA modules separately. Ultimately, the ceRNA networks were constructed by integrating the miRNA–lncRNA-mRNA interactions by Cytoscape 3.4.0 software (Lotia et al., 2013).

Protein-Protein Interactions (PPI) Networks Analysis

The protein-protein interactions (PPI) between mRNAs in ceRNA networks were constructed by Search Tool for the Retrieval of Interacting Genes (STRING) database[9] (Szklarczyk et al., 2011). Interactions with confidence score ≥ 0.4 were demonstrated in the networks.

Quantification of Genes by Quantitative Real-Time PCR

A total of 20 surgical resection of tumor tissues from LUAD patients were obtained from the Thoracic Surgery department of the First Affiliated Hospital of Zhengzhou University. Informed consents were signed by patients before surgeries, and this research was approved by the Institutional Ethical Committee of the First Affiliated Hospital of Zhengzhou University. Total RNA was extracted from tumor tissues with TRIzol reagent (Invitrogen, United States). The purity and concentration of RNA were quantified by NanoDrop 2000 spectrophotometer (Thermo Fisher Scientific, United States). For mRNA and lncRNA detection, 1 mg total RNA was used to synthesize the first strand cDNA using PrimeScript RT reagent Kit With gDNA Eraser (TaKaRa, Japan). For miRNA detection, cDNA was synthesized with miRNA First Strand cDNA Synthesis (Tailing Reaction) (Sangon, China). qRT-PCR were carried out using SYBR Premix Ex Taq II (TaKaRa, Japan) in CXF96 System (BioRad, United States). GAPDH and U6 were used as

[3]http://www.geneontology.org

[4]http://www.kegg.jp/

[5]http://www.microrna.org/

[6]http://www.targetscan.org/

[7]http://129.206.7.150/

[8]https://genie.weizmann.ac.il/pubs/mir07/mir07_exe.html

[9]http://string-db.org/

endogenous control. The primers used in this study were listed in **Supplementary Table 5**.

RESULTS

Information of Samples and TAMs Biomarkers Enrolled in This Study

The flowchart in **Figure 1** demonstrates the overall design and process about this study. To begin with, we have screened suitable samples for analysis by removing patients who have ever been affected by other malignant tumors and only samples with expression data of lncRNA, miRNA and mRNA could be enrolled. Firstly, we randomly assigned 406 samples from TCGA-LUAD into two groups, 203 in TCGA-training cohort, and 203 in TCGA-validation cohort. Besides, another external validation set GSE72094, containing 398 LUAD samples, was defined as GEO-validation cohort. In total, 804 LUAD patients were screened for inclusion in this study. As for TAM biomarkers, 13 candidate genes which have been comprehensively reported associated with phenotype or function of TAMs were enrolled in analysis, including CD68, CD11b, CD163, CD206, IL10, CD39, MMP14, CXCL8, CCL17, CD274, TGFB1, ARG1, and IDO1, and the details about these TAM-related genes were showed in **Supplementary Table 1**.

Construction of a Prognostic Risk Model Based on TAM Signature Genes

In order to comprehensively assess the relationship between TAM-related genes and the prognosis of LUAD patients, a LASSO cox regression model was used in TCGA-Training cohort to calculate the most valuable prognostic genes. The optimized lambda determined in **Figure 2A** was utilized to select features with non-zero coefficients, and the LASSO coefficient profiles of TAM-associated genes are shown in **Figure 2B**. Based on the LASSO regression model and the prognosis of patients, 8 potential predictors were screened in the TCGA-Training cohort: CD68, ITGAM, MRC1, IL10,

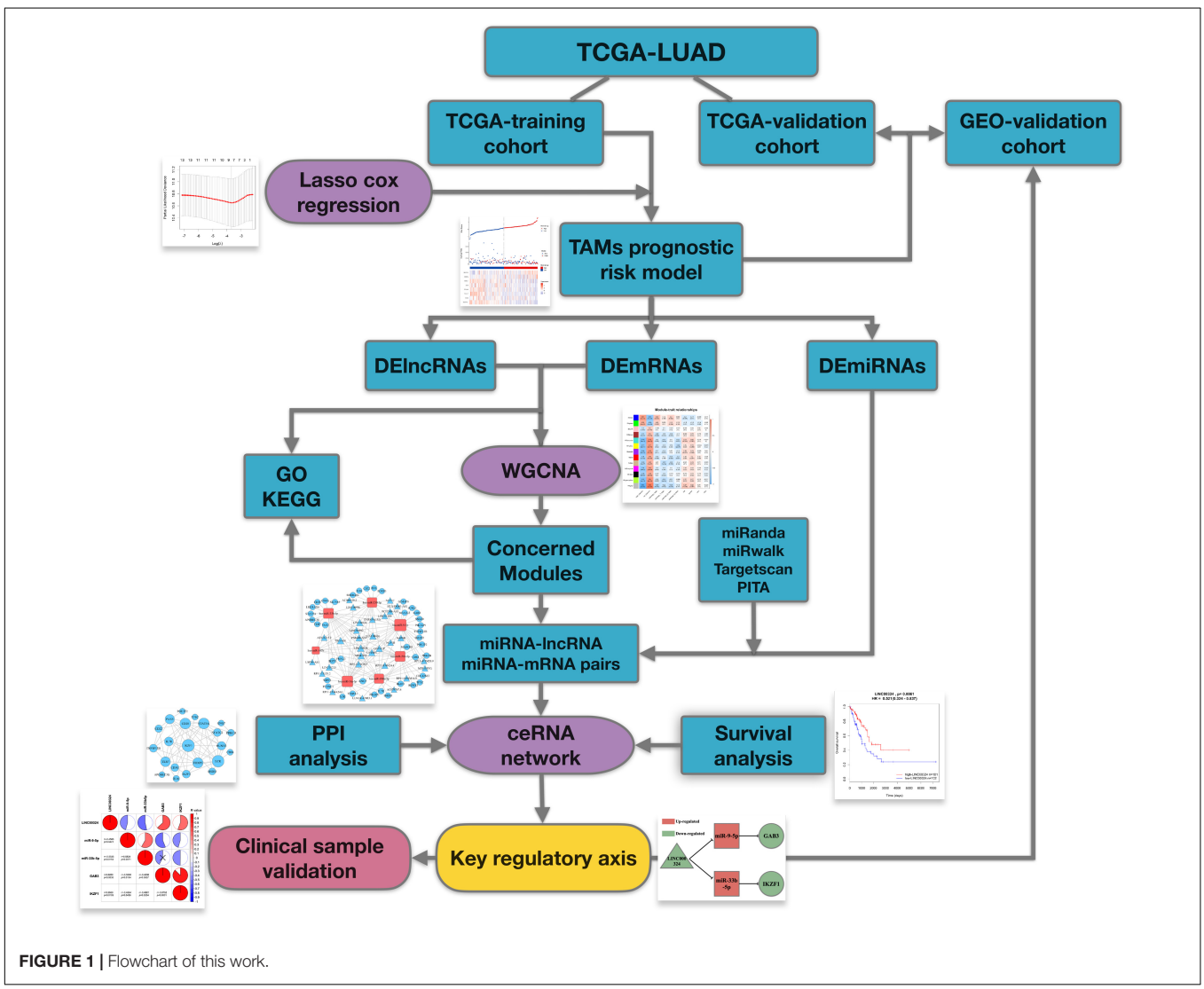

FIGURE 1 | Flowchart of this work.

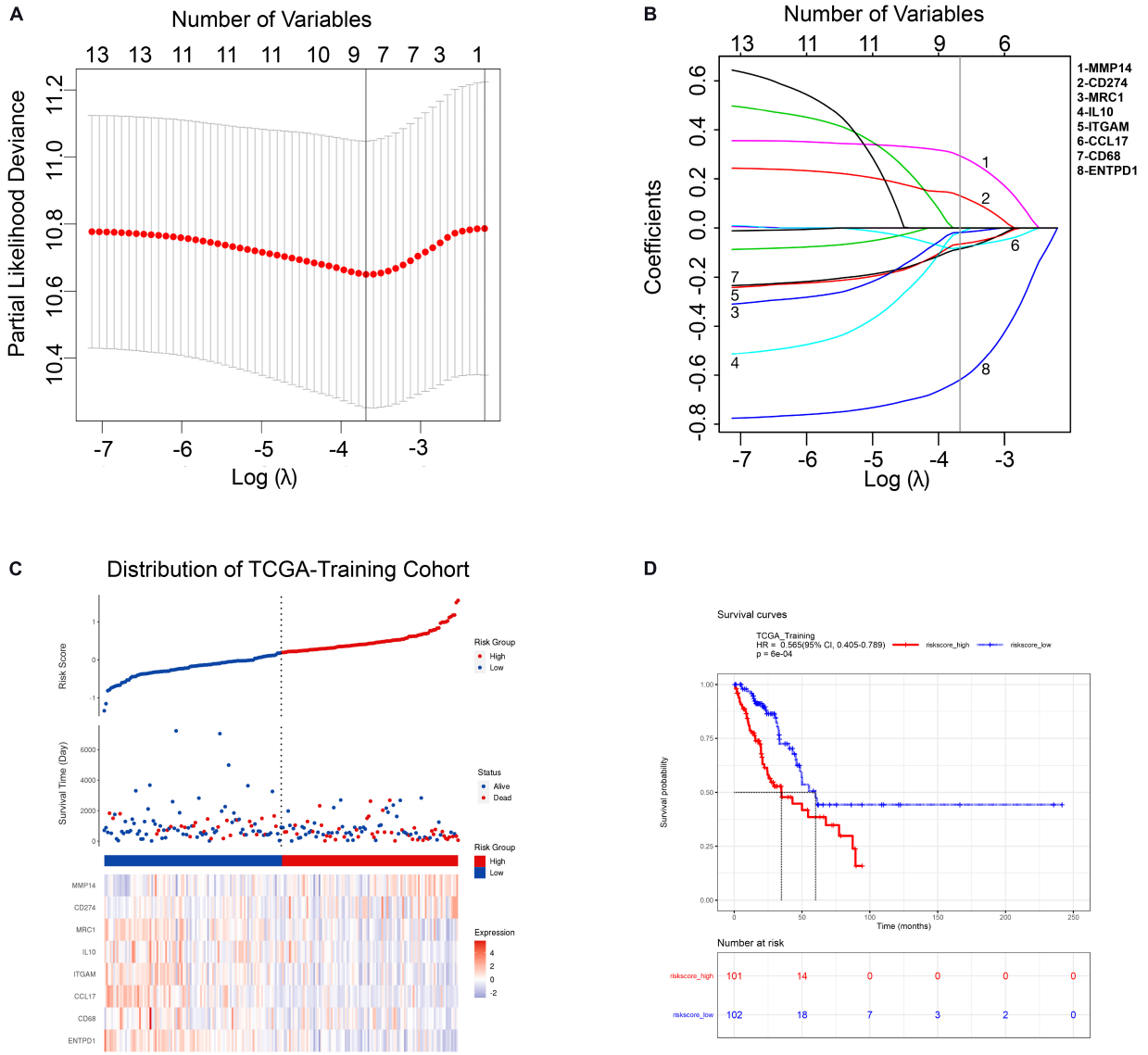

FIGURE 2 | Construction of TAM risk model in TCGA-training cohort. **(A)** Optimized lambda determined in the LASSO regression model. A vertical line is drawn at the value chosen by 10-fold cross-validation. **(B)** The LASSO coefficient spectrum of the 13 TAM-related genes. **(C)** Expression heatmap of identified 8 genes and corresponding risk score as well as survival status of patients in TCGA-training cohort. **(D)** KM survival curve for high- and low-risk group patients in TCGA-training cohort.

CD274, ENTPD1, CCL17, and MMP14. Subsequently, a risk score was built according to the expression value and module coefficient of each gene: Risk Score = (−0.085962 × CD68 expression) + (−0.065982 × ITGAM expression) + (−0.018361 × MRC1 expression) + (−0.019623 × IL10 expression) + (0.132375 × CD274 expression) + (−0.620876 × ENTPD1 expression) + (−0.080381 × CCL17 expression) + (0.295009 × MMP14 expression). Then, risk score for each patient in TCGA-Training cohort was calculated using this formula, and therefore patients were assigned into high-risk group and low-risk group according to the median of the risk score (**Figure 2C**). Univariate and multivariate analyses suggested that TAMs risk score in this study was an independent prognostic factor of LUAD patients (**Supplementary Table 6**). Kaplan-Meier survival analyses showed that the prognosis of patients in the high-risk group was significantly poor than that in the low-risk group (**Figure 2D**), indicating that the risk model we constructed had a predictive role in the prognosis of LUAD patients.

TAM Risk Model Displays a Consistent Predictive Capacity in Validation Cohort

To further evaluate the prognostic value of the risk model constructed above, similarly, the risk score formula was employed to calculate risk score for patients in TCGA-validation and

GEO-validation cohort. As a result, the distribution of patients with risk score as well as prognostic status was presented in **Figures 3A,B**, respectively. In addition, Kaplan-Meier survival analyses in **Figures 3C,D** demonstrated that patients with higher risk score in these two validation sets tend to possess a worse prognosis which was consistent with the results in TCGA-training set. Moreover, time-dependent receiver operating characteristic curve (ROC) was plotted for predictive capacity of the risk model in **Figure 3E**. From the figure we can see that the area under curve (AUC) for TCGA-training, TCGA-validation and GEO-validation was 70.7, 65.2, and 71.6% respectively. The results suggest that the risk model we constructed based on TAM signature genes reveals a good prognostic value.

Analysis of Differentially Expressed Genes Based on Risk Score

So far, we have successfully constructed a prognostic risk model in LUAD patients based on the expression of TAM-related genes. Afterward, in order to get a deeper insight into the specific molecular mechanisms that induce differences in survival prognosis between high- and low-risk samples, comprehensive analysis about differentially expressed genes between these two groups will be conducted in the following sections.

Firstly, differential gene expression analysis was performed between high- and low-risk groups in TCGA-training cohort. Genes with FDR < 0.05 and absolute FC > 1.2 were considered to be significantly changed in expression. Based on this criterion, as a result, we have identified 381 DElncRNAs, 29 DEmiRNAs, and 1976 DEmRNAs between the two groups. Compared to the low-risk group, 81 lncRNAs, 8 miRNAs and 620 mRNAs were upregulated, whereas 300 lncRNAs, 21 miRNAs and 1356 mRNAs were downregulated in the high-risk group. The relative abundances of these genes were illustrated in heatmaps by clustering analysis (**Figures 4A–C**). As mRNA encoded proteins usually perform major biological functions, biological process and pathway enrichment analysis of DEmRNAs were conducted according to Gene Ontology and KEGG databases. As depicted in **Figure 4D**, enrichment results showed that upregulated DEmRNAs in high-risk group were primarily involved in GO biological processes (GO-BP), such as "cell division," "cell proliferation," "DNA replication" and "DNA repair." Meanwhile, KEGG pathways analysis also showed that upregulated DEmRNAs were primarily involved in "cell cycle,"

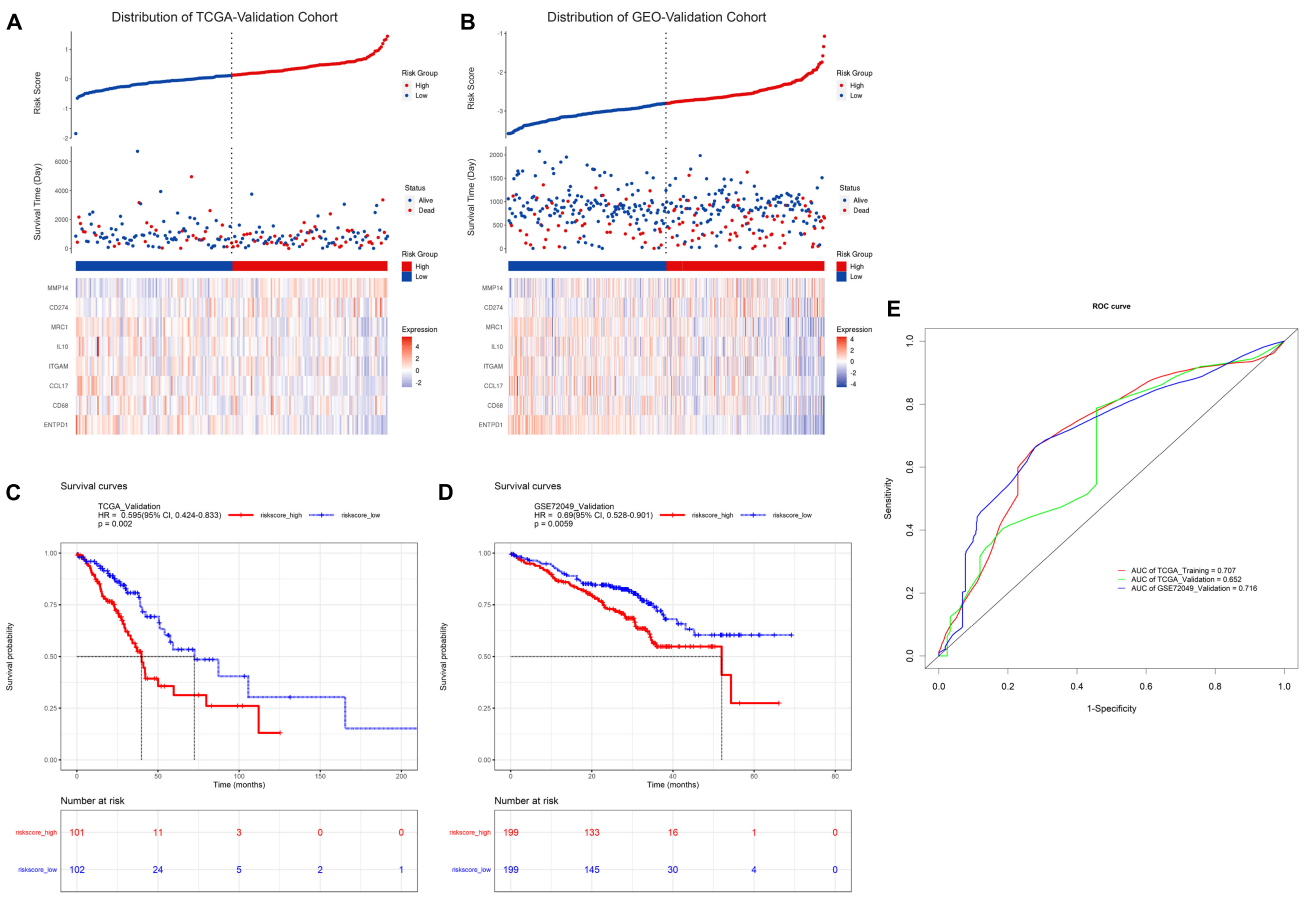

FIGURE 3 | Validation of TAM risk model in validation cohorts. Expression heatmap as well as survival status of patients in TCGA- or GEO-validation cohort are showed in **(A,B)**. KM survival curve for high- and low-risk group patients in TCGA- or GEO-validation cohort are showed in **(C,D)**. **(E)** Time-dependent ROC curve of risk score in three cohorts.

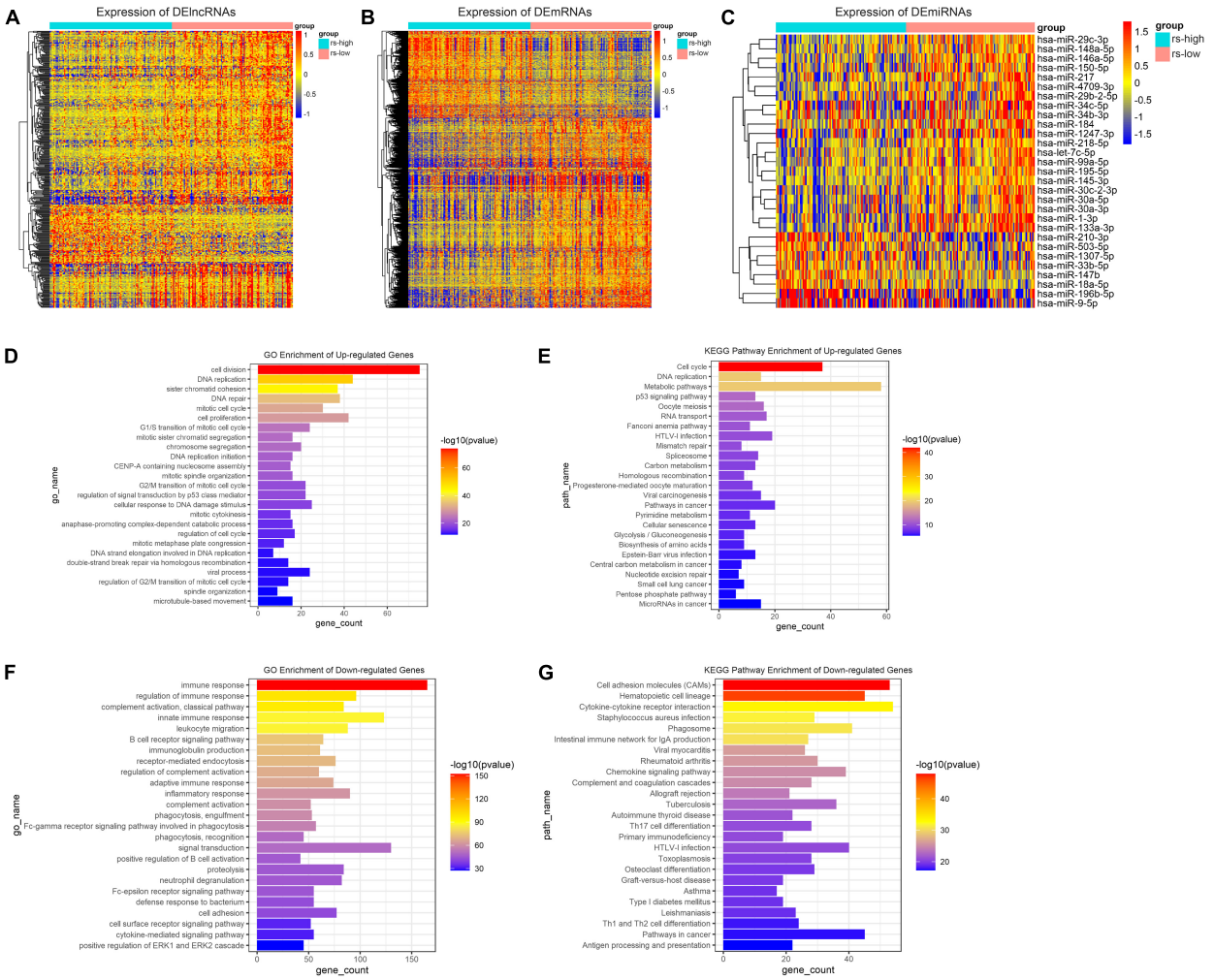

FIGURE 4 | Differential gene expression analysis and function annotation. Heatmaps demonstrate expression of DElncRNAs **(A)**, DEmRNAs **(B),** and DEmiRNAs **(C)**. The top 25 enriched GO biological processes **(D)** and KEGG pathways **(E)** of the significantly upregulated genes. The top 25 enriched GO biological processes **(F)** and KEGG pathways **(G)** of the significantly downregulated genes.

"DNA replication" and "metabolic pathways" which were related to tumor development and progression (**Figure 4E**). On the contrary, regarding to downregulated DEmRNAs in the high-risk group, it is noteworthy that downregulated genes were mainly enriched in "immune response," "phagocytosis," and "cytokine-cytokine receptor interaction" (**Figures 4F,G**). These results collectively demonstrate that DEmRNAs between high- and low-risk groups play a key role in tumor development and immunosuppression which is exactly consistent with the immunosuppression of TAMs in the TME.

Weighted Gene Correlation Network Analysis Reveals Potential Interconnections Between Differentially Expressed Genes

In the following part, in order to analyze the potential interconnections between DEGs, WGCNA analysis was employed to identify modules containing genes with similar expression patterns. Firstly, cluster analysis was performed to remove outliers based on differential gene expression of samples (**Supplementary Figure 1**). Next, the expression profiles of 381 DElncRNAs and 1976 DEmRNAs were obtained for constructing the co-expression network via the package "WGCNA" in R software. To balance the relationship between scale independence and mean connectivity, a suitable soft-threshold power β should be determined for following construction of WGCNA network. We analyzed the network topology with soft-threshold power from 1 to 20 and finally confirmed β values of 9 in lncRNAs/mRNAs co-expression network analysis (**Figure 5A**). Then we constructed Topological Overlap Matrix (TOM) based on β value, deriving the intergenic divergence coefficients. From the Cluster Dendrogram in **Figure 5B**, we could find that genes with similar expression patterns were grouped into modules with specific color. Correlation between modules were showed in Eigengene Adjacency Heatmap (**Figure 5C**), and

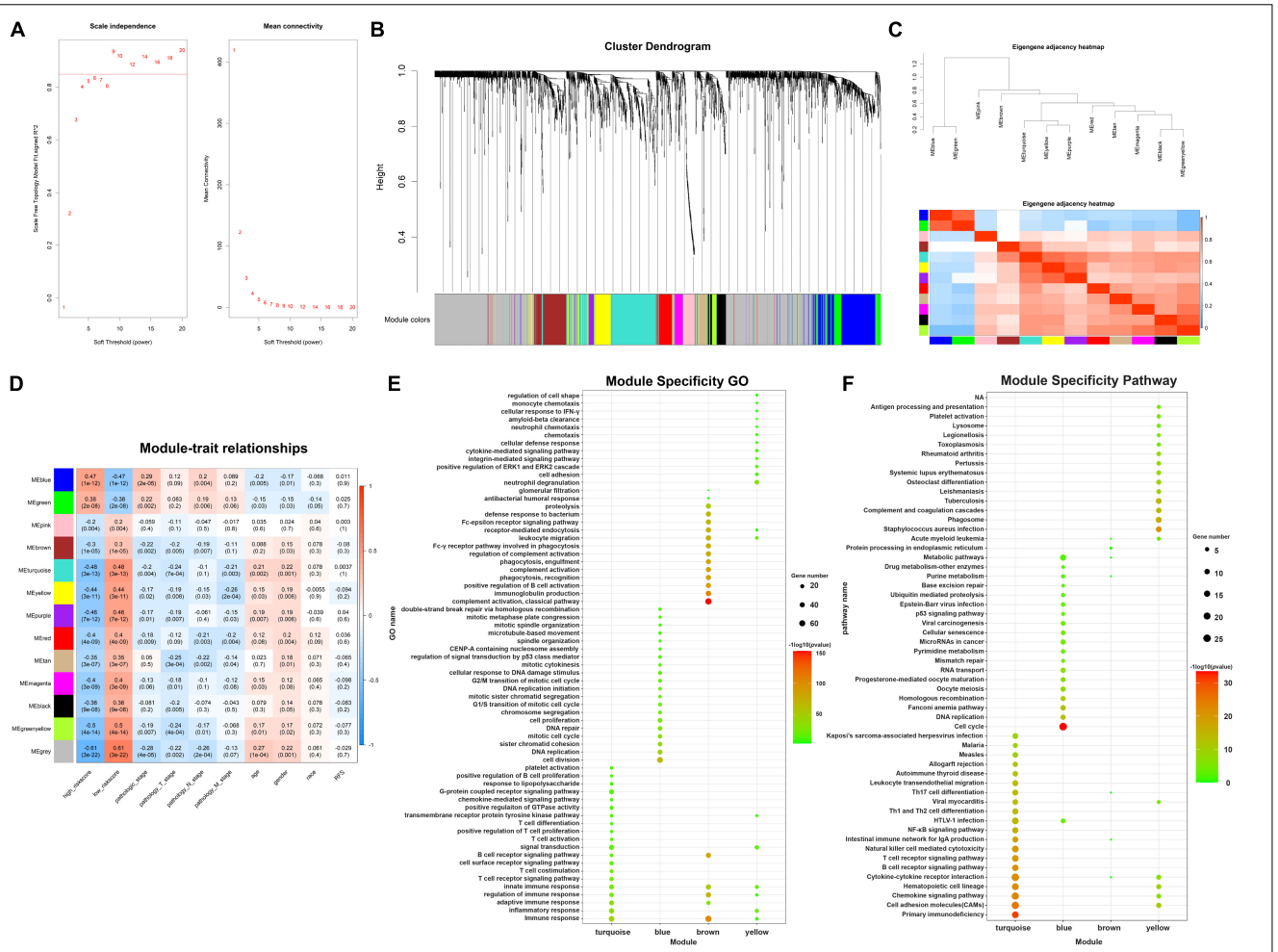

FIGURE 5 | WGCNA analysis identifying concerned modules. **(A)** Determination of soft-threshold power in the lncRNAs/mRNAs WGCNA. Left: Analysis of scale independence for various soft-thresholding powers. Right: Analysis of the mean connectivity for various soft-thresholding powers. **(B)** Cluster dendrogram was generated by hierarchical clustering based on dissimilarity measure of genes. The branches correspond to modules of highly interconnected groups of genes. **(C)** Heatmap plot of the adjacencies in the hub gene network, red represents positive correlation with high adjacency, while blue color represents negative correlation with low adjacency. **(D)** Matrix of module-trait relationships and *p*-values for selected traits. Each row corresponds to a module eigengene, and each column corresponds to a clinical character, each module contains a corresponding correlation value R and *p*-value. **(E)** Module specificity GO enrichment analysis of 4 concerned modules. **(F)** Module specificity KEGG pathway enrichment analysis of 4 concerned modules.

there were no modules with too much similarity needed to be merged. Ultimately, a total of 12 modules were generated in the lncRNAs/mRNAs co-expression network, clustering in size from 36 to 341 genes (**Supplementary Table 2**). The gray module represented a gene set containing genes not suitable for assigning to any other modules. Having assigned DEGs into different color modules, we then want to explore the correlation between modules and clinical characteristics and phenotypes of samples. As shown in **Figure 5D**, several modules correlated with clinical characteristics, such as age, gender, race, and TNM stage as well as TAM-related risk score. Modules that are positively related to TAM risk score, such as blue module and green modules, tend to be positively related to tumor pathology stage as well. On the contrary, modules negatively associated with TAM risk score, such as turquoise and yellow modules, are more likely related to an earlier pathology stage. These results are accordant with previously reported influence of TAMs on tumor progression. In order to choose suitable modules for following construction of ceRNA networks, we preferred to choose WGCNA modules which contained more lncRNAs/mRNAs co-expression pairs and correlated with clinical features. According to this criterion, the four interested modules that contained the highest number of genes were turquoise, blue, brown, and yellow module (containing 341, 264, 161, and 126 genes respectively). Meanwhile, these concerned modules revealed correlations with clinical stage and TAM risk score. Details about these four modules were enclosed in **Supplementary Table 3**. Moreover, module specificity GO enrichment analysis and module specificity KEGG pathway enrichment analysis were performed in **Figures 5E,F**. Of note, turquoise module had a significant correlation with immunosuppression while blue module tended to be associated

with tumor development. Overall, employing weighted gene correlation network analysis, we have identified four concerned modules containing co-expressed genes which may play an important role in immunosuppression and tumor development.

Construction of ceRNA Networks for Concerned WGCNA Modules

Accumulating evidences have emerged revealing that ceRNA theory plays an essential role in explaining interactions among different varieties of RNAs. Briefly, lncRNAs can share miRNA response elements to affect miRNA affinity with target mRNAs, thus regulating gene expression at the transcriptional level. Considering the concerned modules in WGCNA mainly contained lncRNAs and mRNAs with positively correlation, according to the ceRNA theory, there should present miRNAs negatively correlated with lncRNAs and mRNAs, and then collectively forms a ceRNA network. Firstly, by searching DEmiRNAs in miRanda, Targetscan and miRWalk databases, we got predicted miRNA-mRNA pairs with possible binding relation. Similarly, miRNA-lncRNA pairs were predicted by employing miRanda and PITA databases. Then, according to the predicted miRNA-mRNA/miRNA-lncRNA pairs and expression pattern of genes in clinical samples, miRNA-mRNA/miRNA-lncRNA pairs with negatively correlation were finally determined in concerned WGCNA modules separately. Ultimately, ceRNA networks for concerned modules were constructed by integrating the miRNA-lncRNA-mRNA interactions by Cytoscape software (**Figure 6**). The ceRNA network for turquoise module and blue module involved the most abundant regulatory relationships. There were 30/11 lncRNAs, 7/16 miRNAs, and 39/77 mRNAs in ceRNA network for turquoise module and blue module, respectively. As mentioned before, turquoise module contained genes appear to be associated with immune response and all of these lncRNAs and mRNAs were downregulated in high TAM risk group. Meanwhile, blue module contained

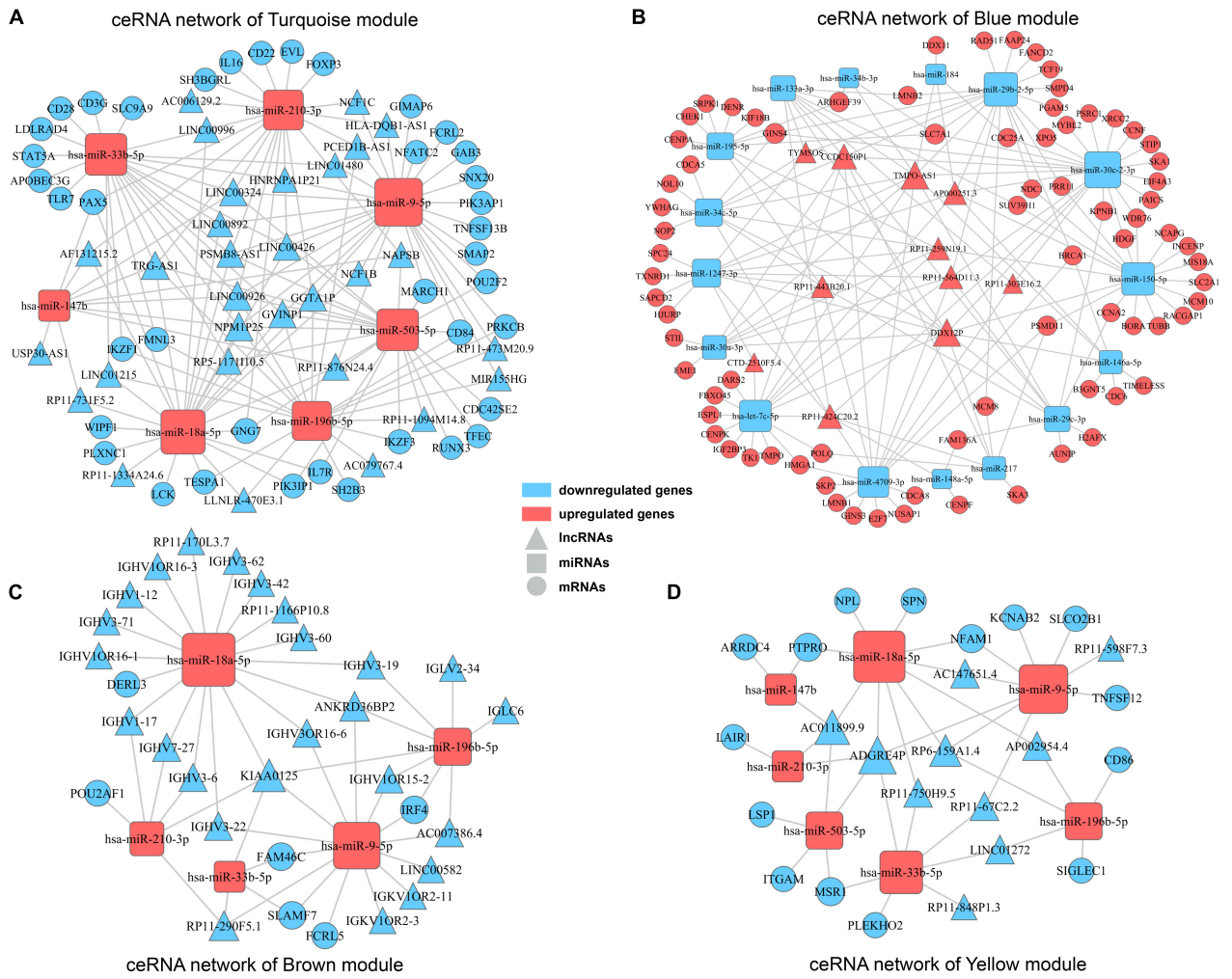

FIGURE 6 | ceRNA networks for concerned WGCNA modules. ceRNA networks were built up for turquoise module **(A)**, blue module **(B)**, brown module **(C),** and yellow module **(D),** respectively. Triangle represents lncRNAs, square represents miRNAs and round represents mRNAs. Blue color indicates downregulated genes, while red color indicates upregulated genes.

genes, upregulated in the high-risk group, were related to tumor development. Therefore, ceRNA networks in these two concerned modules may play a key role in TAMs risk and LUAD prognosis which deserves further analysis.

Identifying Core Regulatory Axis in ceRNA Network by Synthesizing Information of PPI Analysis and Survival Analysis

In order to explore intrinsic relationships between proteins encoded by mRNAs in ceRNA networks, PPI networks were constructed by employing STRING database. We identified hub genes among these DEmRNAs involved in ceRNA networks (**Figures 7A,B**). Hub genes with top node degree in turquoise module were IKZF1, LCK, CD28, STAT5A, FOXP3, TLR7, PAX5, IL7R, RUNX3, and IKZF3. As for blue module, CCNA2, CHEK1, CDC6, CDCA8, NCAPG, CENPF, NUSAP1, CENPA, MCM10, and HJURP may act as hub genes in the ceRNA network. In the meanwhile, Kaplan-Meier survival analysis was performed for all of the genes involved in ceRNA networks to identify key prognostic genes. As a result, we finally identified 127 genes with prognostic value from the ceRNA networks, including 34 lncRNAs, 7 miRNAs, and 86 mRNAs. Survival analysis results as well as ceRNA regulatory relationships in Turquoise and Blue modules could be find in **Supplementary Table 4**. According to the intersection of survival analysis results and ceRNA regulatory relationship, we tried to identify ceRNA regulatory axis containing genes with the best prognostic value. Ultimately, by synthesizing information of PPI analysis and survival analysis, we have successfully identified a core regulatory axis: LINC00324/miR-9-5p (miR-33b-5p)/GAB3 (IKZF1) (**Figure 7C**)

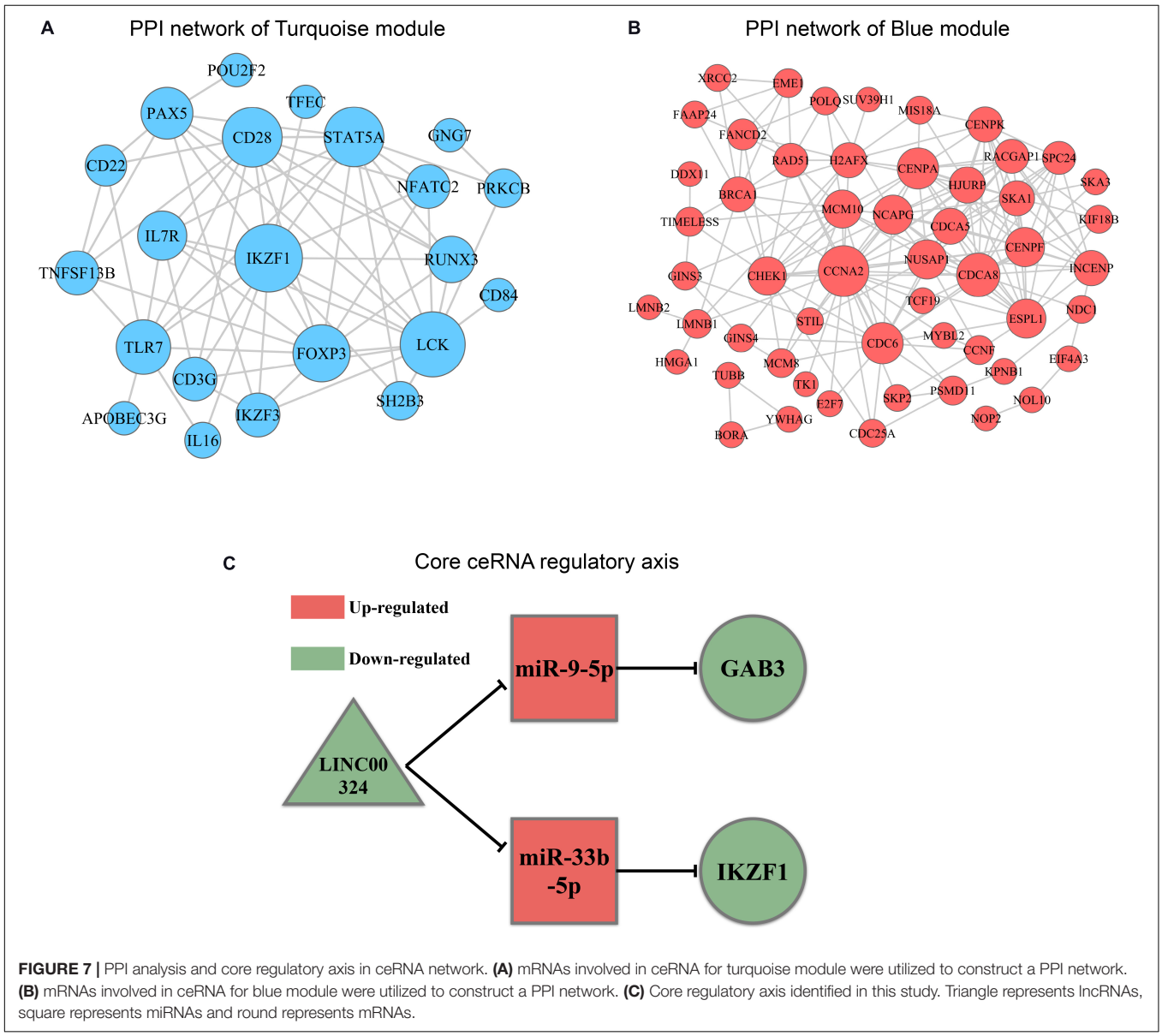

FIGURE 7 | PPI analysis and core regulatory axis in ceRNA network. **(A)** mRNAs involved in ceRNA for turquoise module were utilized to construct a PPI network. **(B)** mRNAs involved in ceRNA for blue module were utilized to construct a PPI network. **(C)** Core regulatory axis identified in this study. Triangle represents lncRNAs, square represents miRNAs and round represents mRNAs.

which may play a pivotal role in regulating TAM risk and the prognosis in LUAD patients.

External Validation of the Core Regulatory Axis in GEO Dataset and Clinical Samples

In order to validate the prognostic value and expression significance of key genes involved in the regulatory axis we identified above, survival analysis and expression analysis were also performed in an external GEO database (Samples were divided into two groups according to the median of expression of genes). As shown in **Figures 8A,B**, all of LINC00324 (HR = 0.418, $p < 0.01$), GAB3 (HR = 0.518, $p < 0.01$), and IKZF1 (HR = 0.605, $p < 0.01$) could predict a good prognosis in GEO LUAD patients, which were coincident with the result in TCGA database (HR = 0.521, $p < 0.05$ for LINC00324; HR = 0.487, $p < 0.05$ for GAB3; HR = 0.594, $p < 0.05$ for IKZF1). Due to the lack of miRNAs data in GEO database, miR-9-5p only showed prognostic significance in TCGA dataset (HR = 1.584, $p < 0.05$). Then expression difference analysis was carried out in GEO dataset. According to TAM risk model employed before, patients were divided into high- and low-risk group, as expected, all of these three genes were more highly expressed in low-risk group ($p < 0.01$), which indicating their potential role in anti-tumor immunity as mentioned before (**Figure 8C**).

In addition, small size validation with clinical samples was also employed to verify these results. According to gene relative expression results achieved by qRT-PCR and OS of LUAD patients, we analyzed expression correlations between genes and prognostic value of the core regulatory ceRNA axis. As **Figure 9A** presented, there existed a clear regulatory correlation between genes involved in the ceRNA axis. There were positive correlations between LINC00324 and GAB3/IKZF1 ($r = 0.6289$, $p = 0.003$/$r = 0.5559$, $p = 0.0109$). As for LINC00324 and miR-9-5p/miR-33b-5p, they possessed negative expression correlations ($r = -0.4583$, $p = 0.0421$/$r = -0.5333$, $p = 0.0154$). Similarly, miR-9-5p and GAB3 ($r = -0.559$, $p = 0.0104$) or miR-33b-5p and IKZF1 ($r = -0.4981$, $p = 0.0254$) also possessed negative expressions which suggested their potential regulatory relationships. Moreover, from survival analysis in **Figures 9B–F**, results suggested that high expression of LINC00324, GAB3, and IKZF1 predicted a good prognosis ($p = 0.0147$, 0.0048, and 0.0117, respectively) while miR-9-5p and miR-33b-5p

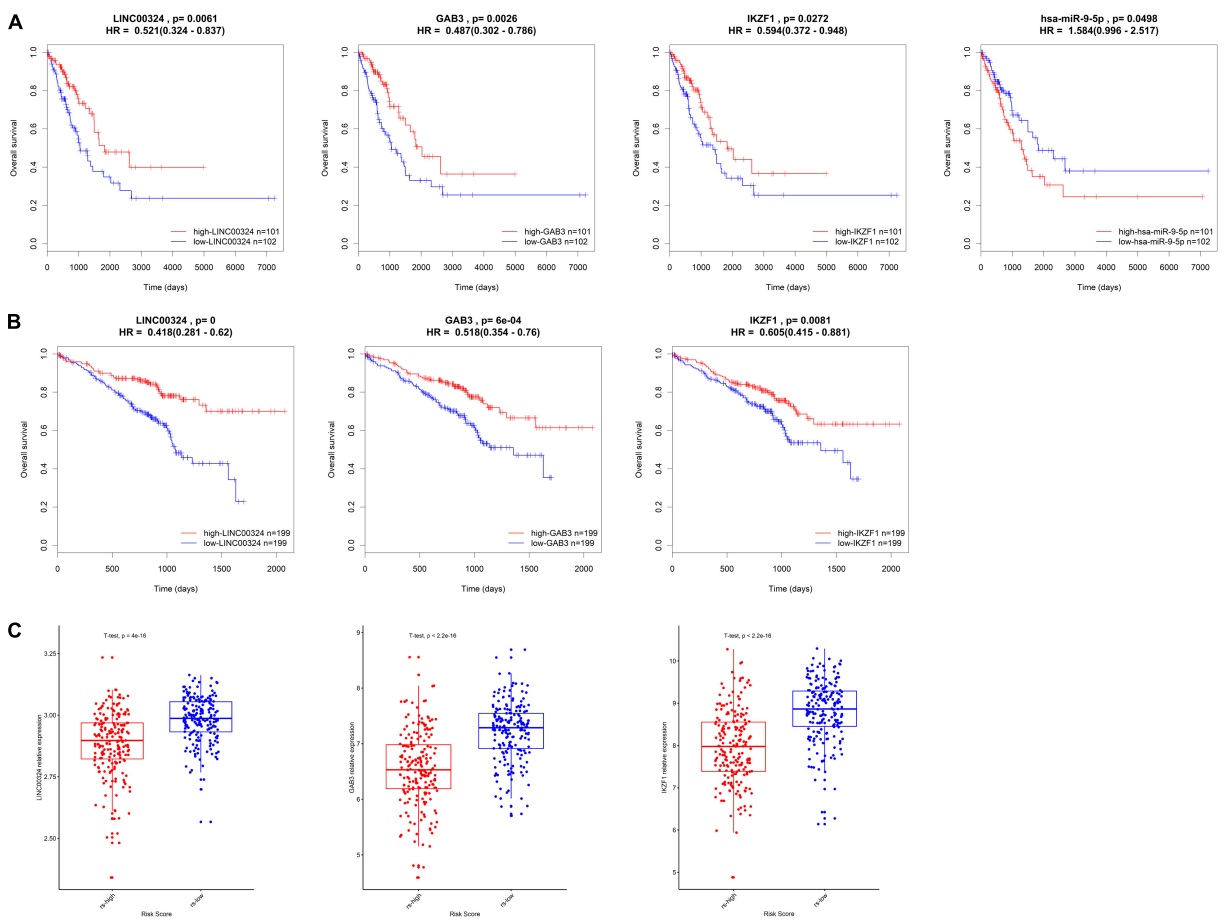

FIGURE 8 | Validation of the core regulatory axis. Survival analysis of LINC00324, GAB3, IKZF1 and miR-9-5p in TCGA database **(A)** or GEO database **(B)**. **(C)** Expression validation of LINC00324, GAB3, and IKZF1 between high- and low-risk groups in GEO cohort.

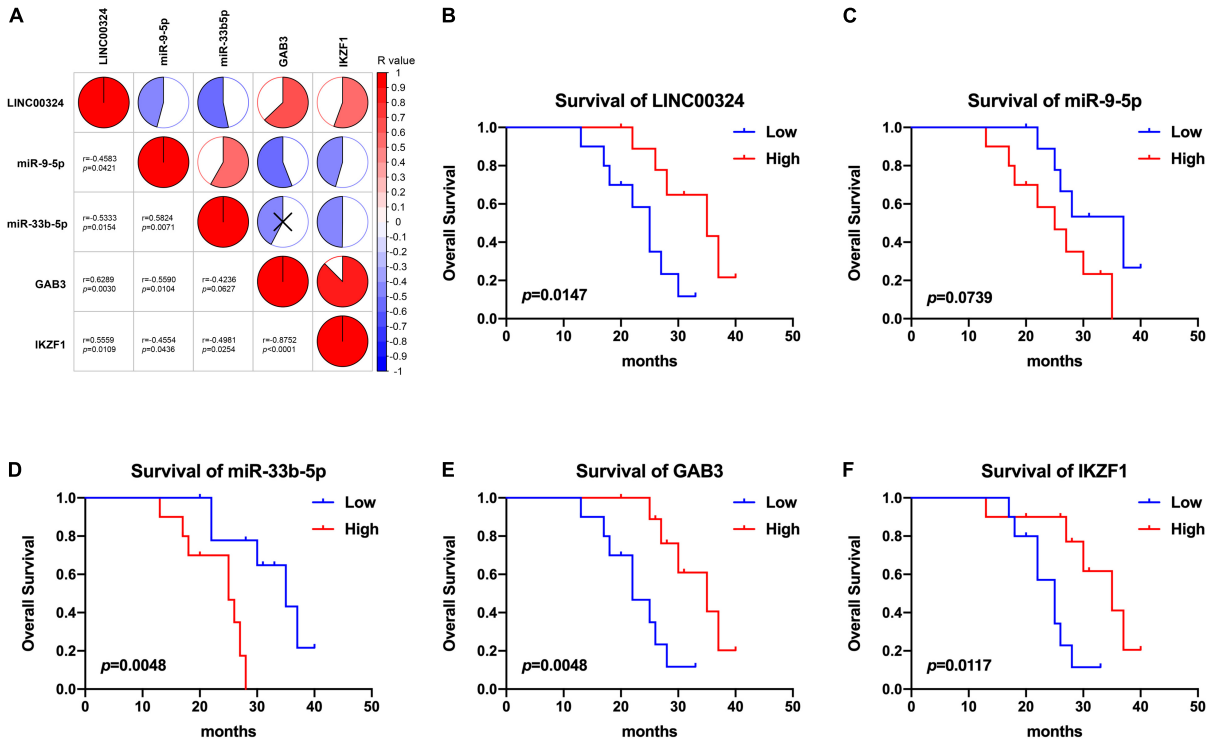

FIGURE 9 | Correlation and survival analysis of the core regulatory axis in clinical samples. **(A)** Correlations between LINC00324, miR-9-5p, miR-33b-5p, GAB3, and IKZF1. Results were analyzed according to gene relative expression achieved by qRT-PCR and correlations were tested using Pearson correlation coefficient. Kaplan-Meier analyses of overall survival in LUAD patients with low (n = 10) and high (n = 10) LINC00324 **(B)**, miR-9-5p **(C)**, miR-33b-5p **(D)**, GAB3 **(E),** and IKZF1 **(F)** expression.

appeared to predict a poor prognosis (p = 0.0739 and 0.0048, respectively), which were consistent with results analyzed from public datasets above.

Taken together, these findings demonstrated that the prognostic value and expression significance of key genes in core regulatory axis could be validated in external datasets.

DISCUSSION

Lung cancer is the most common type of cancer and remains the predominant cause of cancer deaths worldwide. LUAD is the most common histological subtype of lung cancer, with an average 5-year survival rate of 15% (Allemani et al., 2015). LUAD usually exhibits more morphological heterogeneity and relatively poor prognosis warranting the need for better treatment strategies (Zhang et al., 2018). In recent years, as research progresses, emerging evidences show that immunotherapy is becoming a promising treatment against LUAD. Although tumor immunotherapy, especially immune checkpoint blockade, has gradually revolutionized cancer treatment, there still remains a large portion of patients failed to benefit from the treatment (Horvath et al., 2020; Huang M.Y. et al., 2020). One of the key reasons for that was the obstruction of the TME which consisted of complicated cellular and molecular components (Chae et al., 2018; Seidel et al., 2018; Yang et al., 2019b; Lei et al., 2020). Recent evidences reveal that TAMs are the most abundant infiltrating immunosuppressive cells in the TME, playing a key role influencing efficacy of anti-tumor immunotherapy (Pérez-Ruiz et al., 2020). Therefore, understanding specific molecular mechanisms by which TAMs affect tumor immunotherapy is of great value for developing ideal treatment strategies for LUAD patients.

However, TAMs are highly plastic and heterogeneous in solid tumor (Ngiow and Young, 2020). Generally, Th1 cytokines such as lipopolysaccharide (LPS), interferon-γ (IFN-γ), and tumor necrosis factor-α induce macrophages into a M1-like phenotype, playing a role in antitumor inflammation. On the contrary, TAMs (M2-like) polarized by IL-4 and IL-13 play the opposite immunosuppression and pro-tumor function in the TME (Bohn et al., 2018). To our knowledge, there exists massive biomarkers of TAMs which represent function or phenotype of macrophage infiltrated in the tumors. Meanwhile, TAM-associated molecular markers appear to be showed a controversial prognostic value in pan-cancer patients for the expression of some markers are not absolutely specific (Zhao et al., 2019). Therefore, considering the heterogeneous phenotypes of TAMs, there are certain limitations making a distinction between M1-like and M2-like macrophages or predicting prognosis of patients by single molecular marker.

To this end, we aimed to comprehensively investigate broadly reported TAM signature genes to construct a precise prognostic

risk model and further explore the underlying mechanism by which TAMs influence immunotherapy and tumor progression.

TAM-associated genes enrolled in this study were broadly reported as follows: The pan-macrophage marker CD68 is now generally utilized to identify TAMs in pathological specimen and has been reported associated with controversial prognostic value in patients with cancers including breast and ovarian cancer (Wang et al., 2018); CD163 as well as CD206 tend to be associated with worse clinical outcome and have been defined as M2-related markers combined with myeloid marker CD11b in most researches (Lu-Emerson et al., 2013; Xu et al., 2020); Cytokines and chemokines, including IL-10, TGFB1, CXCL8, and CCL17, play the immunosuppressive roles in the TME via recruiting regulatory T cells and myeloid-derived suppressor cells, serving as functional biomarker of TAMs (Cassetta and Pollard, 2018; Yang et al., 2019a); Metabolic enzymes, such as ARG1, IDO1, and ENTPD1, play key roles in regulating immune balance via various metabolic signaling pathways (Takenaka et al., 2019; Vitale et al., 2019); MMP14, a matrix metalloproteinase, has also been reported to induce TAM immunosuppression and could predict the prognosis of cancers (Alonso-Herranz et al., 2020); CD274, also known as PD-L1, contributing to the well-known PD-1/PD-L1 immune checkpoint theory, was involved in TAM immunosuppression (Noguchi et al., 2017).

The LASSO regression model is a frequently used statistical method for multicollinearity problems and has been demonstrated to be suitable for high dimensional data regression analysis. In this study, according to 13 TAM-related biomarkers described above, we constructed a TAM prognostic risk model containing 8 genes with the most prognostic valuable by LASSO cox regression in LUAD patients. Therefore, every patient would be assigned a risk score based on expression of 8 TAM-related genes according to the formula obtained from the risk model. As validated in TCGA- and GEO-validation cohort, the TAM prognostic risk model revealed an ideal prognostic value and it would be possible for us to distinguish between high and low prognostic risk for patients based on risk scores.

Afterward, in order to get a deeper insight into the specific molecular mechanisms inducing different survival prognosis between high and low-risk samples, comprehensive analysis about differentially expressed genes between these two groups was crucially needed. As a result, there revealed 381 DElncRNAs, 29 DEmiRNAs, and 1976 DEmRNAs between high- and low-risk groups. GO and KEGG pathway enrichment analysis were generally used to annotate gene sets and provide hints about functions and pathways participated by concerned genes.

Enrichment results showed that upregulated DEmRNAs in high-risk group were primarily involved in GO biological processes, such as "cell division," "cell proliferation," "DNA replication," "DNA repair," and KEGG pathways, such as "cell cycle," "DNA replication" and "metabolic pathways." It suggests that there exist more genes related to tumor development and progression in TAMs high-risk patients. In the meantime, it was noteworthy that downregulated genes in high-risk group were mainly enriched in "immune response," "phagocytosis," and "cytokine-cytokine receptor interaction." These results suggest that differentially expressed genes between high-risk and low-risk groups played an imperative role in tumor development and immunosuppression which is exactly consistent with the immunosuppression of TAMs in the TME and this also illustrates the validity of our risk model.

Next, in order to further narrow the focus on specific genes, we employed WGCNA, ceRNA and PPI network analysis with these dysregulated genes. WGCNA is commonly used to enrich genes with similar expression patterns into modules associated with clinical characters. In this study, we identified two interested modules containing a large number of DEGs associated with risk score and TNM stage. Of note, GO and KEGG analysis showed that turquoise module had a significant correlation with immunosuppression while blue module tended to be associated with tumor development, which was consistent with their upregulated or downregulated patterns. As reported before, ceRNAs played an essential role in regulating interactions among different varieties of RNAs and were involved in progression and immune infiltration in multiple kinds of tumors (Zhang K. et al., 2020). We constructed ceRNA networks in concerned WGCNA modules through predictive algorithm. Prediction of complexes in PPI networks is significant for understanding the principles of cellular organization and function. In this study, we performed PPI analysis in order to explore intrinsic relationships between mRNAs and identify hub genes which may play important role in prognosis in ceRNA networks. By synthesizing information of PPI analysis and survival analysis, we have eventually identified a core regulatory axis: LINC00324/miR-9-5p (miR-33b-5p)/GAB3 (IKZF1) which may play a pivotal role in regulating TAM risk and the prognosis in LUAD patients.

In reviewing the literature, genes in the core regulatory axis function through different approaches influencing tumor progression and the immune microenvironment.

Gab3 is a kind of adaptor proteins expressed mainly in hematopoietic cells, such as lymphocytes and bone marrow-derived macrophages, functioning as scaffolding and docking molecules. The role of Gab3 in immune cells is incompletely understood. Relationship between Gab3 and macrophages was firstly reported in 2002. Rohrschneider et al., reported that Gab3 was tyrosine phosphorylated after macrophage colony stimulating factor receptor stimulation and then accelerated macrophage morphological differentiation (Liu and Rohrschneider, 2002; Wolf et al., 2002). However, further analysis demonstrated that hematopoiesis in mice lacking Gab3 was not impaired and macrophages developed in normal numbers exhibited normal function (Seiffert et al., 2003). Colucci recently indicated that Gab3 may promote expansion and function of NK cells through MAPK-ERK pathway (Colucci, 2019). Sliz et al. (2019) also found that knockout of Gab3 induced defective uNK cell expansion, suggesting that Gab3 was a key component required for cytokine-mediated NK cells priming and expansion that is essential for antitumor responses. Gab3 plays a controversial role in immune system. Cheng et al. (2018) indicated that Gab3 expression was upregulated by IFN and Gab3 demonstrated antiviral effects through enhancing IFN response and innate immune activation. However, Wang et al. (2019) illustrated the importance of Gab2/3 in controlling macrophages and $CD8^+$ T cells activation and suppressing chronic colitis.

Besides, several researches recently suggested that Gabs acted as tumor-promoting molecule in colorectal, glioma, and ovarian cancer (Jia et al., 2017; Xiang et al., 2017; Berkel and Cacan, 2020). IKZF1, same as Gab3, plays a controversial role in immune system. Ikaros is a member of the kruppel family of zinc finger DNA-binding proteins encoded by IKZF1, functioning as a master regulator of hematopoiesis and the immune system. As reported, Ikaros was widely expressed in tumors but performed anti-tumor or pro-tumor function in different researches (Dhanyamraju et al., 2020). As for immune cells, Dumortier et al. (2003) reported that Ikaros positively regulates early neutrophil differentiation. While, Singhal et al. (2016) demonstrated that Ikaros affected anti-tumor response through inhibiting APC-like neutrophils. As for macrophage, Cho et al. (2008) demonstrated that Ikaros acted as a negative regulator on LPS/IFN-γ-induced iNOS expression in macrophages. Moreover, Oh et al. (2018) described unexpected dual repressor and activator functions for Ikaros in the LPS response of murine macrophages. Of note, Chen et al. (2018) reported that IKZF1 overexpression promoted immune infiltration in several tumor types, and enhanced the efficacy of anti-PD1 and anti-CTLA4 treatment. Besides, non-coding RNAs in our study, including LINC00324 (Ni et al., 2019; Zhang M. et al., 2020), miR-9-5p (Ma et al., 2020; Wang et al., 2020), and miR-33b-5p (Huang G. et al., 2020; Ni et al., 2020), were also reported in literatures to be associated with the prognosis of various cancer types.

In our study, upregulation of LINC00324, GAB3 as well as IKZF1 in TAM low-risk group could predict a better prognosis, suggesting the potential anti-tumor immunology role in the TME. However, miR-9-5p and miR-33b-5p present as pro-tumor molecules whose immunosuppression may be achieved through regulating expression of mRNAs they targeted. To our knowledge, although there have been lots of valuable researches about these genes, how do they influence the prognosis of LUAD patients through TAMs has not been reported to date. In our study, core regulatory axis obtained from TAM risk model showed an ideal prognostic value, suggesting that these genes could influence the prognosis of LUAD through regulating polarization or infiltration of TAMs.

Several limitations need to be acknowledged regarding the present study. Firstly, findings and results in this study were indirect because we explored how TAMs potentially influenced the prognosis of LUAD patients mainly through utilizing bioinformatic approaches analyzing public datasets with TAMs biomarkers. In addition, in the validation part, the small size of clinical samples limited our validation power of the prognostic value and correlation between genes involved in the core regulatory axis. Therefore, these preliminary findings and specific deep mechanism of this axis deserve further direct experimental studies.

CONCLUSION

In conclusion, we utilized bioinformatic approaches analyzing public datasets to explore how TAMs potentially influence the prognosis of LUAD patients. Eventually, we have identified a core regulatory axis: LINC00324/miR-9-5p (miR-33b-5p)/GAB3 (IKZF1) which may play a pivotal role in regulating TAM risk and prognosis in LUAD patients. Although the current study is mainly based on public data analysis through bioinformatic approaches, findings in this work contribute to a better understanding of TAM-associated immunosuppression in the TME and provide novel targets and regulatory pathways for anti-tumor immunotherapy. In the future, we will employ more convincing experimental researches to confirm this core regulatory ceRNA axis in further studies.

DATA AVAILABILITY STATEMENT

Publicly available datasets were analyzed in this study. This data can be found here: https://tcga-data.nci.nih.gov/tcga/, https://www.ncbi.nlm.nih.gov/geo/, accession: GSE72094.

AUTHOR CONTRIBUTIONS

LZ, KZ, SL, LY, YZ, and JW designed, edited, and led out this study. LZ, KZ, and SL collected materials and conducted data analysis. RZ, YY, QW, and SZ raised critical discussions of the results and provided technical support. All authors contributed to the writing and editing of the manuscript and approved the final draft of the manuscript.

FUNDING

This work was supported by grants from the National Natural Science Foundation of China (No. 81902471) and Henan Province Medical Science and Technology Key Project Co-construction Project (SB201901033).

SUPPLEMENTARY MATERIAL

The Supplementary Material for this article can be found online at: https://www.frontiersin.org/articles/10.3389/fcell.2021.629941/full#supplementary-material

REFERENCES

Allemani, C., Weir, H. K., Carreira, H., Harewood, R., Spika, D., Wang, X. S., et al. (2015). Global surveillance of cancer survival 1995-2009: analysis of individual data for 25,676,887 patients from 279 population-based registries in 67 countries (CONCORD-2). *Lancet* 385, 977–1010. doi: 10.1016/s0140-6736(14)62038-9

Alonso-Herranz, L., Sahún-Español, Á, Paredes, A., Gonzalo, P., Gkontra, P., Núñez, V., et al. (2020). Macrophages promote endothelial-to-mesenchymal

transition via MT1-MMP/TGFβ1 after myocardial infarction. *Elife* 9:e57920. doi: 10.7554/eLife.57920

Berkel, C., and Cacan, E. (2020). GAB2 and GAB3 are expressed in a tumor stage-, grade- and histotype-dependent manner and are associated with shorter progression-free survival in ovarian cancer. *J. Cell Commun. Signal*. doi: 10.1007/s12079-020-00582-3 [Epub ahead of print].

Bohn, T., Rapp, S., Luther, N., Klein, M., Bruehl, T. J., Kojima, N., et al. (2018). Tumor immunoevasion via acidosis-dependent induction of regulatory tumor-associated macrophages. *Nat. Immunol.* 19, 1319–1329. doi: 10.1038/s41590-018-0226-8

Cao, L., Che, X., Qiu, X., Li, Z., Yang, B., Wang, S., et al. (2019). M2 macrophage infiltration into tumor islets leads to poor prognosis in non-small-cell lung cancer. *Cancer Manag. Res.* 11, 6125–6138. doi: 10.2147/cmar.S199832

Cassetta, L., and Pollard, J. W. (2018). Targeting macrophages: therapeutic approaches in cancer. *Nat. Rev. Drug Discov.* 17, 887–904. doi: 10.1038/nrd.2018.169

Chae, Y. K., Arya, A., Iams, W., Cruz, M. R., Chandra, S., Choi, J., et al. (2018). Current landscape and future of dual anti-CTLA4 and PD-1/PD-L1 blockade immunotherapy in cancer; lessons learned from clinical trials with melanoma and non-small cell lung cancer (NSCLC). *J. Immunother. Cancer* 6:39. doi: 10.1186/s40425-018-0349-3

Chen, D. S., and Mellman, I. (2017). Elements of cancer immunity and the cancer-immune set point. *Nature* 541, 321–330. doi: 10.1038/nature21349

Chen, H. Y., Yu, S. L., Chen, C. H., Chang, G. C., Chen, C. Y., Yuan, A., et al. (2007). A five-gene signature and clinical outcome in non-small-cell lung cancer. *N. Engl. J. Med.* 356, 11–20. doi: 10.1056/NEJMoa060096

Chen, J. C., Perez-Lorenzo, R., Saenger, Y. M., Drake, C. G., and Christiano, A. M. (2018). IKZF1 enhances immune infiltrate recruitment in solid tumors and susceptibility to immunotherapy. *Cell Syst.* 7, 92–103.e104. doi: 10.1016/j.cels.2018.05.020

Cheng, M., Niu, Y., Fan, J., Chi, X., Liu, X., and Yang, W. (2018). Interferon down-regulation of miR-1225-3p as an antiviral mechanism through modulating Grb2-associated binding protein 3 expression. *J. Biol. Chem.* 293, 5975–5986. doi: 10.1074/jbc.RA117.000738

Cho, S. J., Huh, J. E., Song, J., Rhee, D. K., and Pyo, S. (2008). Ikaros negatively regulates inducible nitric oxide synthase expression in macrophages: involvement of Ikaros phosphorylation by casein kinase 2. *Cell. Mol. Life Sci.* 65, 3290–3303. doi: 10.1007/s00018-008-8332-7

Colucci, F. (2019). Placentation and antitumor immunity regulated by a scaffolding protein in NK cells. *Sci. Immunol.* 4:eaax9589. doi: 10.1126/sciimmunol.aax9589

Dai, X., Lu, L., Deng, S., Meng, J., Wan, C., Huang, J., et al. (2020). USP7 targeting modulates anti-tumor immune response by reprogramming tumor-associated macrophages in lung cancer. *Theranostics* 10, 9332–9347. doi: 10.7150/thno.47137

Dhanyamraju, P. K., Iyer, S., Smink, G., Bamme, Y., Bhadauria, P., Payne, J. L., et al. (2020). Transcriptional regulation of genes by ikaros tumor suppressor in acute lymphoblastic leukemia. *Int. J. Mol. Sci.* 21:1377. doi: 10.3390/ijms21041377

Duan, J., Soussen, C., Brie, D., Idier, J., Wan, M., and Wang, Y. P. (2016). Generalized LASSO with under-determined regularization matrices. *Signal Processing* 127, 239–246. doi: 10.1016/j.sigpro.2016.03.001

Dumortier, A., Kirstetter, P., Kastner, P., and Chan, S. (2003). Ikaros regulates neutrophil differentiation. *Blood* 101, 2219–2226. doi: 10.1182/blood-2002-05-1336

Herbst, R. S., Morgensztern, D., and Boshoff, C. (2018). The biology and management of non-small cell lung cancer. *Nature* 553, 446–454. doi: 10.1038/nature25183

Hirsch, F. R., Scagliotti, G. V., Mulshine, J. L., Kwon, R., Curran, W. J. Jr., Wu, Y. L., et al. (2017). Lung cancer: current therapies and new targeted treatments. *Lancet* 389, 299–311. doi: 10.1016/s0140-6736(16)30958-8

Horvath, L., Thienpont, B., Zhao, L., Wolf, D., and Pircher, A. (2020). Overcoming immunotherapy resistance in non-small cell lung cancer (NSCLC) – novel approaches and future outlook. *Mol. Cancer* 19:141. doi: 10.1186/s12943-020-01260-z

Hu, F., Zeng, W., and Liu, X. (2019). A gene signature of survival prediction for kidney renal cell carcinoma by multi-omic data analysis. *Int. J. Mol. Sci.* 20:5720. doi: 10.3390/ijms20225720

Huang, G., Lai, Y., Pan, X., Zhou, L., Quan, J., Zhao, L., et al. (2020). Tumor suppressor miR-33b-5p regulates cellular function and acts a prognostic biomarker in RCC. *Am. J. Transl. Res.* 12, 3346–3360.

Huang, M. Y., Jiang, X. M., Wang, B. L., Sun, Y., and Lu, J. J. (2020). Combination therapy with PD-1/PD-L1 blockade in non-small cell lung cancer: strategies and mechanisms. *Pharmacol. Ther.* 219, 107694. doi: 10.1016/j.pharmthera.2020.107694

Jia, P., Li, F., Gu, W., Zhang, W., and Cai, Y. (2017). Gab3 overexpression in human glioma mediates Akt activation and tumor cell proliferation. *PLoS One* 12:e0173473. doi: 10.1371/journal.pone.0173473

Kanehisa, M., Goto, S., Furumichi, M., Tanabe, M., and Hirakawa, M. (2010). KEGG for representation and analysis of molecular networks involving diseases and drugs. *Nucleic Acids Res.* 38, D355–D360. doi: 10.1093/nar/gkp896

Langfelder, P., and Horvath, S. (2008). WGCNA: an R package for weighted correlation network analysis. *BMC Bioinformatics* 9:559. doi: 10.1186/1471-2105-9-559

Lei, Q., Wang, D., Sun, K., Wang, L., and Zhang, Y. (2020). Resistance mechanisms of Anti-PD1/PDL1 therapy in solid tumors. *Front. Cell Dev. Biol.* 8:672. doi: 10.3389/fcell.2020.00672

Lewis, B. P., Burge, C. B., and Bartel, D. P. (2005). Conserved seed pairing, often flanked by adenosines, indicates that thousands of human genes are microRNA targets. *Cell* 120, 15–20. doi: 10.1016/j.cell.2004.12.035

Li, J., Xie, Y., Wang, X., Li, F., Li, S., Li, M., et al. (2019). Prognostic impact of tumor-associated macrophage infiltration in esophageal cancer: a meta-analysis. *Future Oncol.* 15, 2303–2317. doi: 10.2217/fon-2018-0669

Liu, S., Zhang, C., Maimela, N. R., Yang, L., Zhang, Z., Ping, Y., et al. (2019). Molecular and clinical characterization of CD163 expression via large-scale analysis in glioma. *Oncoimmunology* 8:1601478. doi: 10.1080/2162402x.2019.1601478

Liu, Y., and Rohrschneider, L. R. (2002). The gift of Gab. *FEBS Lett.* 515, 1–7. doi: 10.1016/s0014-5793(02)02425-0

Lossos, I. S., Czerwinski, D. K., Alizadeh, A. A., Wechser, M. A., Tibshirani, R., Botstein, D., et al. (2004). Prediction of survival in diffuse large-B-cell lymphoma based on the expression of six genes. *N. Engl. J. Med.* 350, 1828–1837. doi: 10.1056/NEJMoa032520

Lotia, S., Montojo, J., Dong, Y., Bader, G. D., and Pico, A. R. (2013). Cytoscape app store. *Bioinformatics* 29, 1350–1351. doi: 10.1093/bioinformatics/btt138

Lu-Emerson, C., Snuderl, M., Kirkpatrick, N. D., Goveia, J., Davidson, C., Huang, Y., et al. (2013). Increase in tumor-associated macrophages after antiangiogenic therapy is associated with poor survival among patients with recurrent glioblastoma. *Neuro Oncol.* 15, 1079–1087. doi: 10.1093/neuonc/not082

Ma, N., Li, X., Wei, H., Zhang, H., and Zhang, S. (2020). Circular RNA circNFATC3 acts as a miR-9-5p sponge to promote cervical cancer development by upregulating SDC2. *Cell. Oncol. (Dordr)* doi: 10.1007/s13402-020-00555-z [Epub ahead of print].

Ngiow, S. F., and Young, A. (2020). Re-education of the tumor microenvironment with targeted therapies and immunotherapies. *Front Immunol* 11:1633. doi: 10.3389/fimmu.2020.01633

Ni, X., Xie, J. K., Wang, H., and Song, H. R. (2019). Knockdown of long non-coding RNA LINC00324 inhibits proliferation, migration and invasion of colorectal cancer cell via targeting miR-214-3p. *Eur. Rev. Med. Pharmacol. Sci.* 23, 10740–10750. doi: 10.26355/eurrev_201912_19775

Ni, Y., Li, C., Bo, C., Zhang, B., Liu, Y., Bai, X., et al. (2020). LncRNA EGOT regulates the proliferation and apoptosis of colorectal cancer by miR-33b-5p/CROT axis. *Biosci. Rep*. doi: 10.1042/bsr20193893 [Epub ahead of print].

Noguchi, T., Ward, J. P., Gubin, M. M., Arthur, C. D., Lee, S. H., Hundal, J., et al. (2017). Temporally distinct PD-L1 expression by tumor and host cells contributes to immune escape. *Cancer Immunol. Res.* 5, 106–117. doi: 10.1158/2326-6066.Cir-16-0391

Oh, K. S., Gottschalk, R. A., Lounsbury, N. W., Sun, J., Dorrington, M. G., Baek, S., et al. (2018). Dual roles for ikaros in regulation of macrophage chromatin state and inflammatory gene expression. *J. Immunol.* 201, 757–771. doi: 10.4049/jimmunol.1800158

Ojalvo, L. S., Thompson, E. D., Wang, T. L., Meeker, A. K., Shih, I. M., Fader, A. N., et al. (2018). Tumor-associated macrophages and the tumor immune microenvironment of primary and recurrent epithelial ovarian cancer. *Hum. Pathol.* 74, 135–147. doi: 10.1016/j.humpath.2017.12.010

Pérez-Ruiz, E., Melero, I., Kopecka, J., Sarmento-Ribeiro, A. B., García-Aranda, M., and De Las Rivas, J. (2020). Cancer immunotherapy resistance based on immune checkpoints inhibitors: targets, biomarkers, and remedies. *Drug Resist. Updat.* 53:100718. doi: 10.1016/j.drup.2020.100718

Pollard, J. W. (2004). Tumour-educated macrophages promote tumour progression and metastasis. *Nat. Rev. Cancer* 4, 71–78. doi: 10.1038/nrc1256

Reck, M., and Rabe, K. F. (2017). Precision diagnosis and treatment for advanced non-small-cell lung cancer. *N. Engl. J. Med.* 377, 849–861. doi: 10.1056/NEJMra1703413

Seidel, J. A., Otsuka, A., and Kabashima, K. (2018). Anti-PD-1 and Anti-CTLA-4 therapies in cancer: mechanisms of action, efficacy, and limitations. *Front. Oncol.* 8:86. doi: 10.3389/fonc.2018.00086

Seiffert, M., Custodio, J. M., Wolf, I., Harkey, M., Liu, Y., Blattman, J. N., et al. (2003). Gab3-deficient mice exhibit normal development and hematopoiesis and are immunocompetent. *Mol. Cell. Biol.* 23, 2415–2424. doi: 10.1128/mcb.23.7.2415-2424.2003

Siegel, R. L., Miller, K. D., and Jemal, A. (2020). Cancer statistics, 2020. *CA Cancer J. Clin.* 70, 7–30. doi: 10.3322/caac.21590

Singhal, S., Bhojnagarwala, P. S., O'Brien, S., Moon, E. K., Garfall, A. L., Rao, A. S., et al. (2016). Origin and role of a subset of tumor-associated neutrophils with antigen-presenting cell features in early-stage human lung cancer. *Cancer Cell* 30, 120–135. doi: 10.1016/j.ccell.2016.06.001

Sliz, A., Locker, K. C. S., Lampe, K., Godarova, A., Plas, D. R., Janssen, E. M., et al. (2019). Gab3 is required for IL-2- and IL-15-induced NK cell expansion and limits trophoblast invasion during pregnancy. *Sci. Immunol.* 4:eaav3866. doi: 10.1126/sciimmunol.aav3866

Szklarczyk, D., Franceschini, A., Kuhn, M., Simonovic, M., Roth, A., Minguez, P., et al. (2011). The STRING database in 2011: functional interaction networks of proteins, globally integrated and scored. *Nucleic Acids Res.* 39, D561–D568. doi: 10.1093/nar/gkq973

Takenaka, M. C., Gabriely, G., Rothhammer, V., Mascanfroni, I. D., Wheeler, M. A., Chao, C. C., et al. (2019). Control of tumor-associated macrophages and T cells in glioblastoma via AHR and CD39. *Nat. Neurosci.* 22, 729–740. doi: 10.1038/s41593-019-0370-y

Vitale, I., Manic, G., Coussens, L. M., Kroemer, G., and Galluzzi, L. (2019). Macrophages and metabolism in the tumor microenvironment. *Cell Metab.* 30, 36–50. doi: 10.1016/j.cmet.2019.06.001

Wang, L., Cui, M., Cheng, D., Qu, F., Yu, J., Wei, Y., et al. (2020). miR-9-5p facilitates hepatocellular carcinoma cell proliferation, migration and invasion by targeting ESR1. *Mol. Cell. Biochem.* 476, 575–583. doi: 10.1007/s11010-020-03927-z

Wang, L., Zhang, C., Zhang, Z., Han, B., Shen, Z., Li, L., et al. (2018). Specific clinical and immune features of CD68 in glioma via 1,024 samples. *Cancer Manag. Res.* 10, 6409–6419. doi: 10.2147/cmar.S183293

Wang, Z., Vaughan, T. Y., Zhu, W., Chen, Y., Fu, G., Medrzycki, M., et al. (2019). Gab2 and Gab3 redundantly suppress colitis by modulating macrophage and CD8(+) T-Cell activation. *Front. Immunol.* 10:486. doi: 10.3389/fimmu.2019.00486

Wolf, I., Jenkins, B. J., Liu, Y., Seiffert, M., Custodio, J. M., Young, P., et al. (2002). Gab3, a new DOS/Gab family member, facilitates macrophage differentiation. *Mol. Cell. Biol.* 22, 231–244. doi: 10.1128/mcb.22.1.231-244.2002

Xia, Y., Rao, L., Yao, H., Wang, Z., Ning, P., and Chen, X. (2020). Engineering macrophages for cancer immunotherapy and drug delivery. *Adv. Mater.* 32:e2002054. doi: 10.1002/adma.202002054

Xiang, S., Wang, N., Hui, P., and Ma, J. (2017). Gab3 is required for human colorectal cancer cell proliferation. *Biochem. Biophys. Res. Commun.* 484, 719–725. doi: 10.1016/j.bbrc.2017.01.095

Xu, Z. J., Gu, Y., Wang, C. Z., Jin, Y., Wen, X. M., Ma, J. C., et al. (2020). The M2 macrophage marker CD206: a novel prognostic indicator for acute myeloid leukemia. *Oncoimmunology* 9:1683347. doi: 10.1080/2162402x.2019.1683347

Yang, L., Dong, Y., Li, Y., Wang, D., Liu, S., Wang, D., et al. (2019a). IL-10 derived from M2 macrophage promotes cancer stemness via JAK1/STAT1/NF-κB/Notch1 pathway in non-small cell lung cancer. *Int. J. Cancer* 145, 1099–1110. doi: 10.1002/ijc.32151

Yang, L., Li, A., Lei, Q., and Zhang, Y. (2019b). Tumor-intrinsic signaling pathways: key roles in the regulation of the immunosuppressive tumor microenvironment. *J. Hematol. Oncol.* 12:125. doi: 10.1186/s13045-019-0804-8

Yang, L., and Zhang, Y. (2017). Tumor-associated macrophages: from basic research to clinical application. *J Hematol Oncol* 10, 58. doi: 10.1186/s13045-017-0430-2

Zhang, K., Zhang, L., Mi, Y., Tang, Y., Ren, F., Liu, B., et al. (2020). A ceRNA network and a potential regulatory axis in gastric cancer with different degrees of immune cell infiltration. *Cancer Sci.* 111, 4041–4050. doi: 10.1111/cas.14634

Zhang, M., Lin, B., Liu, Y., Huang, T., Chen, M., Lian, D., et al. (2020). LINC00324 affects non-small cell lung cancer cell proliferation and invasion through regulation of the miR-139-5p/IGF1R axis. *Mol. Cell. Biochem.* 473, 193–202. doi: 10.1007/s11010-020-03819-2

Zhang, Y., Lin, Q., Xu, T., Deng, W., Yu, J., Liao, Z., et al. (2018). Out of the darkness and into the light: new strategies for improving treatments for locally advanced non-small cell lung cancer. *Cancer Lett.* 421, 59–62. doi: 10.1016/j.canlet.2018.02.003

Zhao, Y., Ge, X., Xu, X., Yu, S., Wang, J., and Sun, L. (2019). Prognostic value and clinicopathological roles of phenotypes of tumour-associated macrophages in colorectal cancer. *J. Cancer Res. Clin. Oncol.* 145, 3005–3019. doi: 10.1007/s00432-019-03041-8

Conflict of Interest: The authors declare that the research was conducted in the absence of any commercial or financial relationships that could be construed as a potential conflict of interest.

frontiers in Cell and Developmental Biology

REVIEW
published: 16 April 2021
doi: 10.3389/fcell.2021.674553

Platelets, Constant and Cooperative Companions of Sessile and Disseminating Tumor Cells, Crucially Contribute to the Tumor Microenvironment

*Wolfgang M. J. Obermann, Katrin Brockhaus and Johannes A. Eble**

Institute of Physiological Chemistry and Pathobiochemistry, University of Münster, Münster, Germany

OPEN ACCESS

Edited by:
Ana Karina Oliveira, National Center for Research in Energy and Materials, Brazil

Reviewed by:
Yi Yang, University of North Carolina at Chapel Hill, United States
Ana Paula Campanelli, University of São Paulo, Brazil

***Correspondence:**
Johannes A. Eble
johannes.eble@uni-muenster.de

Specialty section:
This article was submitted to Molecular Medicine, a section of the journal Frontiers in Cell and Developmental Biology

Received: *01 March 2021*
Accepted: *29 March 2021*
Published: *16 April 2021*

Citation:
Obermann WMJ, Brockhaus K and Eble JA (2021) Platelets, Constant and Cooperative Companions of Sessile and Disseminating Tumor Cells, Crucially Contribute to the Tumor Microenvironment. Front. Cell Dev. Biol. 9:674553. doi: 10.3389/fcell.2021.674553

Although platelets and the coagulation factors are components of the blood system, they become part of and contribute to the tumor microenvironment (TME) not only within a solid tumor mass, but also within a hematogenous micrometastasis on its way through the blood stream to the metastatic niche. The latter basically consists of blood-borne cancer cells which are in close association with platelets. At the site of the primary tumor, the blood components reach the TME via leaky blood vessels, whose permeability is increased by tumor-secreted growth factors, by incomplete angiogenic sprouts or by vasculogenic mimicry (VM) vessels. As a consequence, platelets reach the primary tumor via several cell adhesion molecules (CAMs). Moreover, clotting factor VII from the blood associates with tissue factor (TF) that is abundantly expressed on cancer cells. This extrinsic tenase complex turns on the coagulation cascade, which encompasses the activation of thrombin and conversion of soluble fibrinogen into insoluble fibrin. The presence of platelets and their release of growth factors, as well as fibrin deposition changes the TME of a solid tumor mass substantially, thereby promoting tumor progression. Disseminating cancer cells that circulate in the blood stream also recruit platelets, primarily by direct cell-cell interactions via different receptor-counterreceptor pairs and indirectly by fibrin, which bridges the two cell types via different integrin receptors. These tumor cell-platelet aggregates are hematogenous micrometastases, in which platelets and fibrin constitute a particular TME in favor of the cancer cells. Even at the distant site of settlement, the accompanying platelets help the tumor cell to attach and to grow into metastases. Understanding the close liaison of cancer cells with platelets and coagulation factors that change the TME during tumor progression and spreading will help to curb different steps of the metastatic cascade and may help to reduce tumor-induced thrombosis.

Keywords: platelets, tumor microenvironment, coagulation, thrombus formation, fibrin, tissue factor, CLEC-2, integrins

INTRODUCTION

It may not be obvious to consider platelets and coagulation factors as components of the tumor microenvironment (TME), as they are blood components while the TME of a solid tumor mass consists of cancer cells, resident and infiltrating cells, and the dense network of extracellular matrix (ECM) (Iozzo and Sanderson, 2011; Theocharis et al., 2016; Henke et al., 2019; Martins Cavaco et al., 2020). Resident stroma cells may undergo a cancer cell-induced differentiation into cancer-associated fibroblasts (CAFs) (Pietras and Ostman, 2010; Kalluri, 2016; Wang et al., 2017), which remodel the ECM in a tumor-supportive manner (Eble and Niland, 2019). Also, infiltrating immune cells are influenced by tumor cells and thus attenuate their tumor-suppressive properties (Huber et al., 2020; Sadeghalvad et al., 2020; Yang et al., 2020). The non-cellular ECM, mostly synthesized, secreted, and arranged by CAFs, consists of collagen-containing fibrils, water-resorbing proteoglycans and glycosaminoglycans and a plethora of other ECM-proteins (Eble and Niland, 2019; Niland and Eble, 2020). Together, they form the scaffold, which keeps the tissue in shape and provides a stiff collagenous capsule of desmoplastic tumors (Leight et al., 2017; Mohammadi and Sahai, 2018; Martins Cavaco et al., 2020). Moreover, the ECM scaffold tethers growth factors, forming the morphogenic stage for cell differentiation (Lodyga and Hinz, 2020; Wei et al., 2020). Also the presence of metabolic components, such as protons, lactate, reactive oxygen species (ROS), contribute to the typical environment of cancer cells in a solid tumor mass (Oudin and Weaver, 2016).

Primarily, the site of neoplasia within epithelia or stroma tissue is not connected directly to the blood. The tumor mass seems far away from the blood, the usual environment of platelets and coagulation factors. However, in at least two scenarios, cancer cells and the blood components come close to each other: either, when the hypoxic TME induces angiogenic ingrowth of sprouting capillaries into the tumor mass (De Palma et al., 2017; Klein, 2018; Zanotelli and Reinhart-King, 2018), or when cancer cells hematogenously disseminate from their prime tumor site to colonize distant organs (Erpenbeck and Schon, 2010; Schlesinger, 2018). In both cases, cancer cells come in close contact with the blood components. Consequentially, platelets and coagulation factors play a crucial role in tumor progression and metastasis (Menter et al., 2017; Burbury and MacManus, 2018; Mege et al., 2019).

The liaison between tumor cells and platelets is clinically relevant, as tumor-induced thromboembolism is the second leading cause of death in cancer patients (Gay and Felding-Habermann, 2011a; Connolly and Francis, 2013; Mege et al., 2019; Palacios-Acedo et al., 2019). This frequent complication of enhanced and inappropriate platelet activation and blood coagulation in cancer patients has been known for one and a half century, since the physician Armand Trousseau described this type of thrombophlebitis in 1865 (Trousseau, 1865), later generally named Trousseau syndrome (Han et al., 2014).

This review highlights the molecular interactions of platelets and the coagulation system with tumor cells, thereby showing that these blood components are constituents of the TME, even only temporarily, but with an important impact on tumor progression and hematogenous metastasis.

PLATELETS, THE CELLULAR PLAYERS IN HEMOSTASIS

Platelets are anuclear cells with a diameter of 2–5 μm and a thickness of about 0.5 μm, which float in the blood stream at a density of 150,000–400,000 per μl. After they pinch off from the large megakaryocytes in the bone marrow, these small cells spend their lifetime of around 5–7 days in the blood circulation, unless they detect a damage within the endothelium-lined blood vessel wall (Andrews and Berndt, 2004). They are also recruited to more severe tissue damages, where both the endothelial lining and the underlaying basement membrane are breached, and the adventitial stroma tissue around the blood vessel is injured. There, platelets attach and close the wound. Thus, they stop the blood leakage into the tissue and fulfill their hemostatic functions, for which they are predominantly known (Andrews and Berndt, 2004, 2008; Gale, 2011; Broos et al., 2012; Menter et al., 2017).

Attachment is mediated by several cell adhesion molecules (CAMs), which not only anchor the platelets to the wound area, but also trigger signals within the platelets, that activate them (Broos et al., 2012). Activation of platelets is accompanied by a remarkable shape change (Yeung et al., 2018). Quiescent platelets have a discoid shape, which upon activation changes into a stellate-like appearance with pronounced platelet spreading and formation of lamellipodia and numerous filipodia. These protrusions enable platelets to entangle with each other, to spread on an adhesive substrate, generally at the injury site of a wounded blood vessel, and to form the primary thrombus (Gale, 2011; Broos et al., 2012; Berndt et al., 2014). Another step of platelet activation is degranulation. Platelets contain different types of granules, among them α-granules and dense granules, which upon platelet activation undergo exocytosis and release their contents (Gay and Felding-Habermann, 2011a). The former contain (i) ECM-proteins, such as von-Willebrand factor (vWF), fibrinogen, thrombospondin, (ii) coagulation factor V and VIII, the latter associated with vWF, (iii) growth factors, such as platelet-derived growth factor (PDGF), and (iv) membrane-anchored CAMs, such as P-selectin, which thus becomes exposed on the platelet surface exclusively after platelet activation. Dense granules are rich in adenosine diphosphate (ADP), adenosine triphosphate (ATP), serotonin, and histamine. Whereas the release of the ECM proteins, especially vWF, increases the adhesion of platelets (Grassle et al., 2014; Lancellotti et al., 2019), the purine nucleotides attract and activate additional platelets thereby increasing the size of the primary thrombus (Jamasbi et al., 2017; Yeung et al., 2018).

Platelet adhesion is crucial for thrombus formation (Andrews and Berndt, 2008; Broos et al., 2012; Jamasbi et al., 2017; Huang et al., 2019). Several CAMs enable platelets to attach firmly to an injured blood vessel wall, which is necessary to withstand the shear forces of the blood stream (Kunicki, 2001; Andrews and Berndt, 2008; Hansen et al., 2018). In addition to their mechanical functions, most of the CAMs also fulfill signaling

functions, via which platelets perceive the environmental cues of adhesion (Yeung et al., 2018). Thus, adhesion triggers platelet activation, which in turn reinforces the binding activity of platelet CAMs to their ECM ligands. Amongst the plethora of platelet CAMs, we will focus on the vWF-binding GPIb-complex, on the collagen-binding receptors, glycoprotein (GP) VI and integrin α2β1, and on the fibrin receptor, integrin αIIbβ3 (Kunicki, 2001; Gay and Felding-Habermann, 2011a; Jamasbi et al., 2017; Martins Lima et al., 2019).

The vWF-receptor consists of four transmembrane protein chains, GPIbα, GPIbβ, GPIX, GPV, which assemble into the GPIb-complex in a 2:2:2:1 stochiometry within the platelet membrane (Kunicki, 2001; Andrews et al., 2003; Quach and Li, 2020). The GPIbα chain harbors the binding site for vWF (Lof et al., 2018; Lancellotti et al., 2019). vWF is a large ECM molecule consisting of several modules, which are assigned to four different types of domains; A, B, C, and D (Lancellotti et al., 2019). It is stored in the Weibel-Palade bodies of endothelial cells and after exocytosis multimerizes into a scaffold within the subendothelial basement membrane. In solution, it takes on a globular structure, in which also domain A1 with its GPIb-binding site is in a cryptic state (Huck et al., 2014; Lof et al., 2018). Upon association with other immobilized ECM proteins, e.g., with collagens via its A3 domain, and under hydrodynamic shear forces, vWF unwinds into an extended shape, which makes its A1 domain accessible to the platelet GPIb complex (Huck et al., 2014; Hansen et al., 2018). Thus, vWF bridges platelet attachment to collagen even under high blood flow rates, such as observed within the arterial branch of the circulatory system (Kulkarni et al., 2000; Hansen et al., 2018). Moreover, the GPIb-complex-mediated attachment of platelets to vWF and collagen under high shear forces results in stretching of the GPIb-chain and thus triggers an activating signal which is further transduced via the phosphoprotein-binding adaptor protein 14-3-3 within the platelet (Chen et al., 2018; Scharf, 2018b; Quach and Li, 2020).

The direct interaction of platelets with collagens is mediated via two distinct receptors, GPVI and α2β1 integrin (Nuyttens et al., 2011). Apparently, GPVI is physically associated in the platelet membrane with the GPIb complex (Arthur et al., 2005). GPVI is a type I transmembrane protein consisting of an extracellular tandem domain of two immunoglobulin C2 (Ig C2)-like modules, a glycosylated mucin-like stalk domain, a transmembrane and short cytoplasmic domains (Nieswandt and Watson, 2003). The Ig C2-like domains recognize bundles of collagen molecules, which contain the posttranslationally modified hydroxyproline residues that are essential for binding (Knight et al., 1999). Binding to collagen depends on the N-linked glycoconjugates of GPVI (Kunicki et al., 2005). High affinity binding of collagen also requires dimerization of GPVI receptors, which then signals via the associated Fc-receptor γ-chain (FcRγ) (Miura et al., 2002; Nieswandt and Watson, 2003). Deficiency of GPVI (Kato et al., 2003) or its inhibition by antibodies or pharmaceuticals (Nieswandt et al., 2001; Martins Lima et al., 2019) affect thrombus formation, although hemostasis, measured as bleeding time, is affected only mildly. In contrast to GPVI, the other collagen receptor on platelets, α2β1 integrin, belongs to the large family of integrins, consisting of two non-covalently associated subunits, α and β (Madamanchi et al., 2014; Zheng and Leftheris, 2020). The two integrin chains jointly form a globular head domain, which harbors the ligand binding site (Arnaout et al., 2005). All collagen-binding integrins contain an additional A-domain, which sits on top of the α-subunit propeller domain and is responsible for collagen binding (Emsley et al., 2000; Eble, 2005). The collagen ligands do not necessarily need to bear hydroxyproline residues (Perret et al., 2003; Niland et al., 2011), but the triple helical array of a specific collagenous integrin binding motif is indispensably required (Kühn and Eble, 1994; Hamaia and Farndale, 2014). Integrins undergo substantial changes in their conformation, which is influenced by ligand occupancy and, in turn, influences ligand binding (Arnaout et al., 2005; Luo et al., 2007; Hanein and Volkmann, 2018). Moreover, upon collagen binding, α2β1 integrins cluster on the platelet surface, likely mirroring the supramolecular array of integrin binding sites on collagen fibrils (Lima et al., 2018). This is similar to the ligand-induced clustering of GPVI and other CAMs on platelets (Ozaki et al., 2013; Poulter et al., 2017), which triggers a signaling cascade and thus induces platelet activation and aggregation (Humphries et al., 2019). The redundancy of the collagen receptors, GPVI and α2β1 integrin, on platelets has prompted several discourses and models, as the individual deletion of either of them did not entirely abolish collagen-induced platelet activation (He et al., 2003; Marjoram et al., 2014). Their interplay in collagen-induced platelet activation is still not entirely clear. Apparently, the two receptors influence each other in their signaling potential, as activation of GPVI seems to be regulated by α2β1 integrin (Atkinson et al., 2003), and *vice versa* (Inoue et al., 2003). The signals of both receptors convene into an integrating network (Lima et al., 2018; Izquierdo et al., 2020). Yet, another model postulates that GPVI is more involved in signal transduction, whereas α2β1 integrin firmly attaches the platelet mechanically to the collagen thereby allowing the forming thrombus to withstand the shear forces of the blood (Kunicki, 2001; Jarvis et al., 2004; Pugh et al., 2010).

The most numerous adhesion receptor with 50,000–100,000 molecules on the surface of a quiescent platelet and with many more molecules exposed upon platelet activation is the fibrin receptor, integrin αIIbβ3 (Coller, 2015; Huang et al., 2019). Not only the numbers of surface-exposed integrin αIIbβ3 molecules, but also the activation state of these fibrin receptors is essential for effective platelet adhesion to fibrin. On quiescent platelets, integrin αIIbβ3 is in its inactive conformation, in which the globular integrin head domain bent back toward the platelet cell membrane. Only upon platelet activation, such as by the precedent binding of vWF and collagen to their respective receptors, cytoplasmic adaptor molecules, particularly talin and kindlin, bind to the αIIbβ3 integrin (Moser et al., 2008; Kasirer-Friede et al., 2014). Via this so-called in-side out signaling, the unclasping of the cytoplasmic domains and membrane-proximal stalk domains of both integrin subunits as well as a conformational extension of the integrin ectodomains is induced. This goes along with an enhancement of binding affinity to the fibrin ligand (Arnaout et al., 2005; Luo et al., 2007; Huang et al., 2019; Humphries et al., 2019) and integrin clustering (Li et al., 2017), which eventually enables platelets to firmly attach to fibrin

scaffolds and to exert contractile forces onto it (White, 2000; Haling et al., 2011).

THE PROTHROMBOTIC MICROENVIRONMENT OF SOLID TUMORS

Under healthy conditions, hemostasis aims to seal any damage of the otherwise leakproof circulatory system, to stop bleeding and to initiate tissue regeneration by providing a provisional ECM network of fibrin. These tasks are accomplished by the interdependent network of platelets, blood coagulation factors, and the blood vessel wall (Gale, 2011; Broos et al., 2012; Berndt et al., 2014).

The final product of the coagulation pathway is fibrin (Jennewein et al., 2011; Swieringa et al., 2018; Kwaan and Lindholm, 2019). Coagulation comprises a complex network of serine proteinases, which float in the blood plasma in an inactive zymogenic form (Dahlbäck, 2000; Gale, 2011). Intrinsic hemostasis is triggered intravascularly by negatively charged surfaces and kallikrein, at injured sites of the vessel wall, where endothelial cells detach and leave a desnuded basement membrane (**Figure 1**). This triggers a cascade of partial proteolysis steps, by which clotting factors XII, XI, and IX activate each other sequentially (Gale, 2011). Platelets also attach to the denuded vessel wall, are activated and thus take on a dendritic cell shape. Activated factor IX associates with activated factor VIII in a Ca^{2+} ion-dependent manner on the surface of these activated platelets, a process which is supported by the enrichment of phosphatidylserine residues in the outer membrane leaflet (de Witt et al., 2014; Swieringa et al., 2018). This intrinsic tenase complex is named according to its substrate, clotting factor X (X being the Roman numeral for 10). It proteolytically cleaves factor X, which together with activated factor V forms yet another coagulant complex on the platelet surface, the prothrombinase complex, resulting in active thrombin (factor II) (Wojtukiewicz et al., 2016; Reddel et al., 2019). In addition to fibrinogen conversion, thrombin is able to activate several upstream clotting factors, thereby perpetuating and amplifying coagulation. Moreover, thrombin elicits intracellular signals by activating protease-activated receptors (PARs), thereby reinforcing platelet activation (Wojtukiewicz et al., 2015). In the context of hemostasis, it converts soluble fibrinogen monomers into insoluble fibrin molecules. They aggregate into highly ordered supramolecular bundles that form rope-like structures and networks, that stabilize the platelet aggregates and allow the platelets to contract the resulting thrombus (Gale, 2011). Factor XIII, a transglutaminase, secreted from the platelets, covalently crosslinks the fibrin molecules, thereby strengthening thrombus stability. Several control mechanisms are implemented into this network of coagulation to avoid spatially or temporarily inappropriate or overshooting hemostasis, which would cause vascular occlusion, thrombosis and consequentially ischemia (Connolly and Francis, 2013). Among them, thrombin triggers also the anticoagulant circuit of protein C activation to confine the coagulation cascade locally and temporally (Dahlbäck, 2000; Gale, 2011).

The tight lining of endothelial cells prevents platelets and fibrinogen from getting in contact with extravascular protagonists that trigger activation of platelets and of coagulation factors (Nagy et al., 2012; Benazzi et al., 2014; Fitzgerald et al., 2018; Klein, 2018). During vessel damage and tissue injury, platelets and fibrinogen from the blood meet these prothrombotic and coagulant agents, thereby physiologically leading to hemostasis and to the generation of fibrin-scaffolded granulation tissue, which in normal tissue would be the first step in wound healing and tissue regeneration (Menter et al., 2017). However, where do platelets meet cancer cells that grow in a solid mass within epithelial or stromal tissue? How do platelets become part of the TME? The answers lay in the high permeability of blood vessels in the vicinity of a tumor mass (Nagy et al., 2012). This leakiness allows the intravascular platelets and fibrinogen to access the extravascular space, where platelets become activated and fibrinogen is converted to fibrin by coagulation (**Figure 2**). Depending on the type of tumor vessel, there are different ways, how tumor vessels lose their gatekeeper functions and allow extravasation of platelets and coagulation factors (**Figure 2**; Chouaib et al., 2010; Klein, 2018). First, the tumor mass approaches preexisting vessels due to its volume-demanding growth or by vessel co-option (Kuczynski et al., 2019; Niland and Eble, 2019). Vascular endothelial growth factor (VEGF), especially its isoform VEGF-A, and likely other chemokines from the TME increase the permeability of normal blood vessels and activate endothelial cells (Apte et al., 2019). This may result in increased leukocyte extravasion. Moreover, activation of endothelial cells is accompanied by the loss of antithrombotic surface molecules, such as thrombomodulin and heparin sulfate, from the endothelial cell surface (Klein, 2018). This increases the propensity of intravascular coagulation and thrombosis. Second, VEGF, produced by the cells of the tumor mass in response to the hypoxic TME, also stimulates angiogenesis. However, the ingrowing blood vessels are tortuous, variably calibered, and chaotically organized with a patchy and discontinuous lining of endothelial cells, while the underlying basement membrane is not fully established and defective, and the stabilizing mural cells, such as pericytes, are missing (Benazzi et al., 2014; Zanotelli and Reinhart-King, 2018). Thus, the irregular angiogenic vessels become another route for blood components to leak into the tumor mass (**Figure 2**). The blood flow in these vessels is irregular and likely turbulent, which also increases endothelium activation and leakiness. Vasculogenic mimicry (VM) vessels are a third option for extravasation of blood components into tumor tissue. Although their existence has been controversially discussed for the last two decades, VM vessels occur in a variety of solid tumors with a bad prognosis for the patient (Andonegui-Elguera et al., 2020; Wechman et al., 2020; Wei et al., 2021). These vessels are hardly or not at all lined by endothelial cells, but possess a sleeve of ECM glycoproteins. The latter are responsible for their detection with periodic acid fuchsin staining (PAS) reagent in histological sections. Moreover, in an attempt to confine the lumen of VM vessels, tumor cells align to shape a tube-like conduit. There, tumor cells are in contact with the

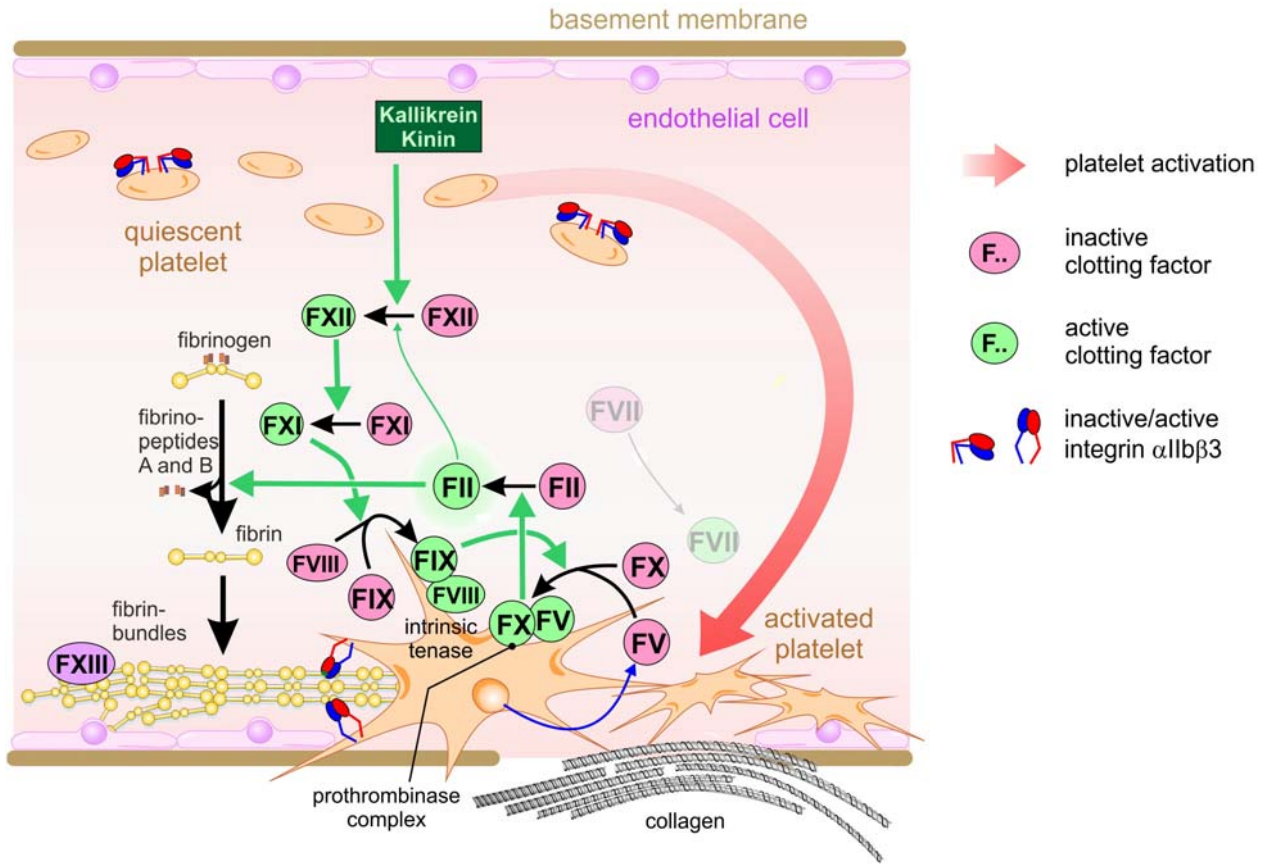

FIGURE 1 | The intrinsic coagulation pathway resulting in the hemostatic sealing of a leaky blood vessel wall. Triggered by damaged vessel walls and by exposed negatively charged surfaces, kallikrein partially cleaves and thus activates coagulation factor XII, which subsequentially activates factor XI. As the next step in this activation cascade, factor XI activates factor IX, which together with activated factor VIII associates into the intrinsic tenase complex on the surface of activated platelets which have attached to the subendothelial basement membrane or collagen fibrils at the vessel injury site. The tenase complex activates factor X, which then forms another platelet-tethered complex together with platelet-secreted factor V, the protrombinase complex. This complex turns on thrombin (factor II), resulting in fibrinogen conversion and deposition of insoluble fibrin fibrils, which are further stabilized via covalent cross-linkage by factor XIII.

blood flow and, due to their discontinuous cell-cell contacts, give another route of extravasation of blood components. Along these three routes, blood components reach the tumor mass and contribute with their high colloid-osmotic pressure to the characteristically elevated interstitial pressure within the TME. The rigidity and tension of the ECM adds to this high interstitial pressure typical of the TME (Mohammadi and Sahai, 2018; Eble and Niland, 2019).

The subendothelial basement membrane and the underlying three-dimensional ECM scaffold significantly contributes to the TME (Eble and Niland, 2019; Mongiat et al., 2019). In leaky blood vessels, it gives way for platelets and coagulation factors to reach the interstitial ECM scaffold of the tumor mass and the cancer cells (Acerbi et al., 2015; Naba et al., 2016, 2017). Within the TME, the coagulation cascade preferentially runs along the extrinsic pathway. In contrast to intrinsic hemostasis, it is alternatively triggered by tissue factor (TF) (factor III, thromboplastin, CD142), which is expressed on adventitial stroma cells and is abundant on tumor cells. It recruits factor VII, which leaks into the TME and, upon proteolytic activation, predominantly cleaves factor X, but also factor XI. Therefore, this complex on tumor cells is called the extrinsic tenase complex (Repetto and De Re, 2017; Chowdary, 2020). Activated factor X and platelet-released factor V form the prothrombinase complex on the platelet surface in a Ca^{2+} ion-dependent manner. This eventually activates thrombin (factor II), the central serine protease of coagulation (**Figure 2**).

Through the leaky tumor vessel, also platelets reach the tumor site in three subsequent steps: tethering, adhesion, and activation of platelets (Kunicki, 2001; Wong, 2013; Hansen et al., 2018; Scharf, 2018a). Platelets tether to subendothelial vWF, which is synthesized and secreted by endothelial cells. The shear forces of the turbulent blood flow in the tortuous and leaky tumor vessels change the conformation of vWF and enable its recognition by the GPIb-complex (Huck et al., 2014). This prepares the adhesion and activation steps of platelets, as tethering provides a sufficiently long period for other adhesion receptors to bind to additional ECM proteins. Then, due to their cytoskeleton rearrangement, platelets also actively migrate along the ECM into the TME (Wong, 2013).

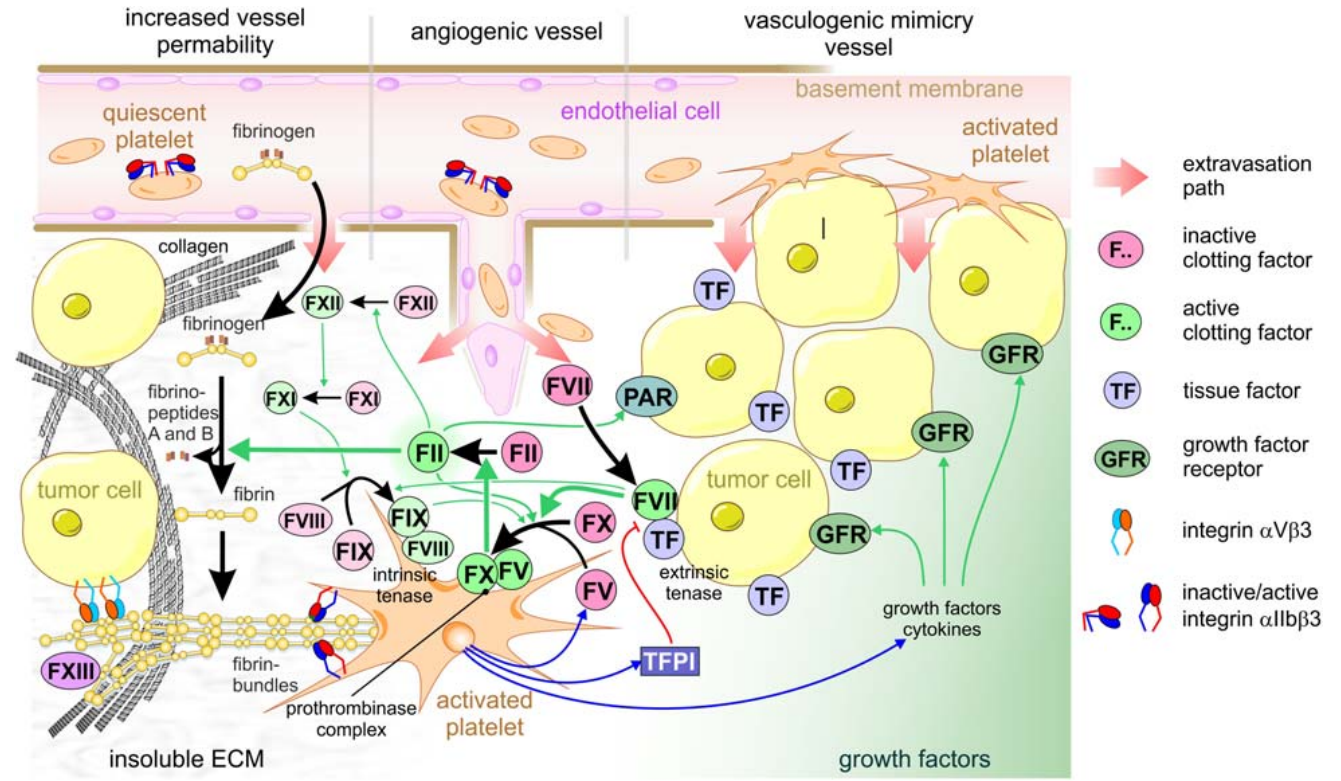

FIGURE 2 | Platelets are crucial for tumor cell-induced coagulation and contribute to the TME of solid tumors. Increased vessel permeability in the vicinity of a tumor, tumor-induced angiogenic sprouting or vasculogenic mimicry vessels are three ways that allow extravasation of platelets and clotting factors from the blood stream into the interstitial stroma of tumor tissue. After the platelets recognize vWF of the subendothelial basement membrane, or collagen of the desmoplastic TME, platelets become activated, thereby take a dendritic shape, expose phosphatidylserine on the outer leaflet of cell membrane, degranulate, and activate the adhesion receptors, especially αIIbβ3 integrin. After leaking from the blood vessel, clotting factor VII immediately is activated and associates with tissue factor, which is abundant on most tumor cells, thereby forming the extrinsic tenase complex. This activates factor X and XI, the former of which forms the prothrombinase complex, together with platelet-secreted factor V, on the surface of activated platelets exposing phosphatidylserine. This activates thrombin (factor II). In addition to this main activation path, thrombin activation is perpetuated by integrating the intrinsic coagulation pathway: thrombin > factor XII > factor XI > intrinsic tenase complex (factor IX:FVIII) > factor X > thrombin. Also, PARs are activated by thrombin on tumor cells, additionally promoting tumor progression. Activated thrombin converts soluble fibrinogen from the blood plasma to insoluble fibrin molecules that aggregate into highly ordered fibrin bundles. They change the composition of the TME substantially and allow further platelets to adhere. Activated platelets secrete not only factor V and factor VIII, but also tissue factor pathway inhibitor (TFPI), thereby feeding back on the extrinsic tenase complex, as well as growth factors. Relevant growth factor receptors, e.g., for PDGF and TGFβ, provide proliferative signals to tumor cells.

Cancer cells and their neighboring stroma cells change the composition and physical properties of the ECM in the tumor mass remarkably (Eble and Niland, 2019; Henke et al., 2019). Distinct ECM proteins are abundantly deposited in the TME, such as collagen fibrils, fibronectin variants EDA and EDB, and tenascin-W (Acerbi et al., 2015; Naba et al., 2016, 2017; Eble and Niland, 2019; Niland and Eble, 2020). They are deposited in gradients within the TME, with high concentrations of collagens and fibronectin in the periphery of the tumor mass, especially of desmoplastic tumors (Oudin and Weaver, 2016; Wang et al., 2016; Eble and Niland, 2019). Therefore, approaching the tumor from the leaky vasculature, platelets first experience and attach to collagen, either via vWF, which via its A3-domain decorates collagen, or directly via collagen receptors. Collagen belongs to the strongest activators of platelets. Activated platelets further migrate into the tumor mass, a process which is likely reinforced by the distribution of ECM proteins and by other gradients within the TME, such as mechanical stiffness and tension, or of metabolites, acidic pH and oxygen tension (Oudin and Weaver, 2016). Thus, platelets enter the TME and become a part of it.

Shortly after their discovery in 2004, neutrophil extracellular traps (NETs) were pinpointed as another way of platelet extravasation and infiltration into the TME (Cedervall et al., 2018; Masucci et al., 2020). Upon activation and arrest at a leaky tumor vessel, neutrophil granulocytes may undergo NETosis, a suicidal process, which results in the production of ROS and release of decondensed nuclear and mitochondrial DNA into the extracellular space. Histones are modified and released from the denuded chromosomal DNA leaving behind a network of nucleic acid, originally meant to entrap pathogens (Masucci et al., 2020). However, these highly negatively charged nucleic acids form the surface, on which clotting factor XII is activitated, and vWF-bound factor VIII is enriched. Activated factor XII initiates the intrinsic pathway of coagulation, also at the sites of leaky tumor vessels (Campello et al., 2018). Moreover, this nucleic acid

network also entraps platelets and allows them to extravasate at these TME-near vessel sites (Erpenbeck and Schon, 2017; Cedervall et al., 2018). Although not entirely clear today, NET-mediated platelet entrapment is an alternative route of platelet recruitment to the TME.

COOPERATION OF TUMOR CELLS AND PLATELETS WITHIN THE TME OF A SOLID TUMOR MASS

Once in the physical vicinity of the tumor cells, platelets contribute to the TME in several ways (Gay and Felding-Habermann, 2011a; Menter et al., 2017). Activated platelets release clotting factors, V and VIII, which reinforce the coagulation cascade (Swieringa et al., 2018). In particular, by secreting factor V, platelets complement the activity of the extrinsic tenase complex on the cancer cells, as both activated factors V and X form the prothrombinase complex on platelets (Camire, 2016). By flipping phosphatidylserine to their outer leaflet of the cell membrane, platelets form the platform for thrombin generation. Thrombin takes multiple roles within the TME by activating other tumor secreted proteases, by activating PARs on both platelets and cancer cells (Wojtukiewicz et al., 2015), and by remodeling the ECM scaffold and turning it to a fibrin-rich matrix (Repetto and De Re, 2017; Kwaan and Lindholm, 2019). Moreover, platelets store multiple growth factors, such as PDFG, VEGF, and transforming growth factor-β (TGFβ), as well as several cytokines (Gay and Felding-Habermann, 2011a; Swieringa et al., 2018; Bikfalvi and Billottet, 2020). This cocktail of signaling molecules is secreted from activated platelets into the TME. VEGF supports angiogenesis of endothelial cells (Sabrkhany et al., 2011; De Palma et al., 2017; Apte et al., 2019). Certain platelet-derived cytokines suppress immune cells (Palacios-Acedo et al., 2019; Bikfalvi and Billottet, 2020). PDGF and TGFβ are strong stimulators for fibroblasts to differentiate into cancer-associated fibroblasts (CAFs) (Ostman, 2017; Lodyga and Hinz, 2020). CAFs convert the TME into a cancer cell-supportive environment by remodeling the ECM, by exerting mechanical forces and interstitial tension, and supporting tumor cell invasion (Kalluri, 2016; Eble and Niland, 2019; Pakshir et al., 2020). Another way of platelet-tumor cell-communications are microvesicles, which are secreted by platelets and are taken up by tumor cells in the TME (Goubran et al., 2015; Vajen et al., 2015).

A special cooperativity between platelets and tumor cells becomes evident in the formation of the extrinsic tenase complex on tumor cells. It contains tissue factor (TF), which is abundantly expressed on several tumor cells (Han et al., 2014; Versteeg, 2015; Grover and Mackman, 2018; Unruh and Horbinski, 2020). Moreover, its expression is upregulated in many tumor entities (Han et al., 2014 and references therein) and correlates with the malignancy grade of the tumors (Callander et al., 1992; Shoji et al., 1998; Liu et al., 2011; Zhang et al., 2020). Also, CAFs are a rich source of tissue factor and also form the extrinsic tenase complex, together with the factor VII that diffuses into the TME from the leaky blood vessels (Liu et al., 2011; Zhang et al., 2020). Although it is unclear whether this prometastatic effect of TF-FVII complex on tumor cells is caused by its proteolytic activity or its signaling function, practically, TF-inhibitory antibodies or FVII-deficiency reduce metastasis in murine breast cancer models (Versteeg, 2015; Rondon et al., 2019). Conspicuously, but not entirely understood is the regulatory interplay of tissue factor pathway inhibitor (TFPI), a Kunitz type domains-containing inhibitor of the tissue factor:factor VII-complex, which is secreted by activated platelets (Dahlback, 2017; Chowdary, 2020).

Two isoforms of tissue factor are generated by alternative splicing, a full length variant (flTF) and an alternatively spliced variant (asTF) (Unruh and Horbinski, 2020). They share the same N-terminal ectodomain, which encompasses two fibronectin type III-domains, each with an intradomain disulfide bridge. Whereas flTF is anchored in the cell membrane via a single span transmembrane domain, the asTF only peripherally tethers to the cell membrane via five positively charged amino acid residues at the shortened C-terminus. Three N-glycoconjugates may influence the association affinity for activated factor VII (Stone et al., 1995). The cytoplasmic domain of flTF may be phosphorylated and palmitoylated (Unruh and Horbinski, 2020). In addition to its coagulant function, the extrinsic tenase complex on cancer cells may also cleave ephrin receptors, ephB2 and ephA2 (Kania and Klein, 2016), or PAR2 (Wojtukiewicz et al., 2015). For instance, the latter initiates a signaling process of increased protein kinase C (PKC) activity and enhanced intracellular Ca^{2+} levels within the cancer cells (Unruh and Horbinski, 2020). Both flTF and asTF can also associate with distinct β1 integrins, thereby inducing a conformational change and consequential increase of ligand binding activity and cell migration (Versteeg, 2015).

Of remarkable impact on ECM remodeling within the TME is the ability of the extrinsic tenase complex to trigger the coagulative conversion of fibrinogen into fibrin. This is not restricted to the immediate surroundings of the cancer cells, as cancer cells intensely secrete microparticles which contain flTF and phosphatidylserine. These microparticles are abundantly found in the blood of cancer patients. Due to their strong procoagulant potential, their abundance correlates with the risk of venous thromboembolism (Tesselaar et al., 2009; OwensIII, and Mackman, 2011) and may be a determinant in preparing premetastatic niches (Gkolfinopoulos et al., 2020).

At the primary tumor site, fibrin can be considered as a joint product of platelets and tumor cells, which changes the biochemical and biophysical composition of the TME (Eble and Niland, 2019). The fibrin network resembles the fibrin-rich ECM of granulation tissue during wound repair. Via cell adhesion receptors, it feeds back on both platelets and cancer cells (Kwaan and Lindholm, 2019). Whereas platelets attach to fibrin via their most numerous receptor, integrin αIIbβ3, tumor cells recognize fibrin via αVβ3 integrin (Katagiri et al., 1995). The binding sites for both integrin receptors are different from each other and located at different sites within the 50 nm long fibrin molecule, allowing both receptors to bind to the same molecule without steric competition (Springer et al., 2008). Especially for platelets, the interaction with fibrinogen and fibrin is a complex and regulated process, as both platelet and fibrinogen

are blood plasma components without interacting with each other under normal conditions. Quiescent platelets usually bear αIIbβ3 integrin in an inactive, bent conformation (Xiao et al., 2004). It does not bind to fibrinogen nor to cleaved fibrin molecules in solution (Vickers, 1998). Instead, fibrin must form highly ordered fibrils and networks or must be immobilized to surfaces to allow effective binding of αIIbβ3 integrin and platelet adhesion (Podolnikova et al., 2010). This requirement is fulfilled only after coagulation within the TME. Therefore, network formation and deposition of fibrin changes the adhesive properties of the TME for both platelets and cells. It enables αIIbβ3 integrin to be conformationally activated (Xiao et al., 2004; Podolnikova et al., 2009; Durrant et al., 2017). Like other ECM receptors, fibrin-bound αIIbβ3 integrin molecules likely cluster, in line with the pattern of integrin binding sites within the fibrin network (Ozaki et al., 2013; Martins Lima et al., 2019). Via outside-in signaling, they convey the adhesive signal into the platelet by recruiting cytoskeletal, adaptor, and kinase proteins, such as Src and focal adhesion kinase (FAK), to the cellular attachment site (Coller, 2015; Durrant et al., 2017; Huang et al., 2019). Platelets, especially those that leak out of the blood stream after the first thrombotic events are activated and reinforce the thrombotic and coagulant TME. Such adhesive clues of the fibrin-enriched and remodeled ECM, together with the platelet-secreted growth factors, cytokines, and microvesicles decisively contribute to the TME and influence the TME-embedded cells, such as cancer cells, CAFs, immune cells and endothelial cells (Kalluri, 2016; Eble and Niland, 2019).

BLOOD-BORNE TUMOR CELLS ARE SHELTERED AND SUPPORTED BY ASSOCIATING PLATELETS

The physical interaction of platelets with tumor cells is not only relevant in the TME of solid tumors, but also crucial in the formation of blood-borne tumor cell-platelet aggregates (TCPAs) and hematogenous metastasis. Immediately after entering the bloodstream, tumor cells are coated with platelets on their surface. This cloak protects them from the shear stress, that they experience from the blood flow (Egan et al., 2014), and prevents them from being eliminated by the immune system (Palumbo et al., 2007; Gay and Felding-Habermann, 2011b). The formation of TCPAs is mediated by receptors on platelets that bind to their counterreceptors on tumor cells and by the establishment of fibrin bridges between the two cell types (Erpenbeck and Schon, 2010; Schlesinger, 2018). In this process, several interactions are responsible for the firm cohesion of platelets to tumor cells, such as the binding between (i) C-type lectin-like receptor 2 (Clec-2) on platelets with podoplanin on tumor cells, (ii) P-selectin on activated platelets, and Sialyl-Lewis^x-conjugates on tumor cells, and (iii) the integrins αIIbβ3 on platelets and αVβ3 on tumor cells, which both bind to a fibrin bridge. TCPA formation is a multistep cascade initiated by Clec-2 based platelet activation followed by fibrinogen conversion and fibrin bridging (**Figure 3**).

Clec-2 is an N-glycosylated type II membrane protein with a short cytoplasmic tail containing a hemi-immunoreceptor tyrosine-based activation motif (hemITAM) and a C-type lectin-like ectodomain (Nagae et al., 2014). It is exclusively expressed on the platelet membrane. Its counter piece is podoplanin, also known as aggrus, which appears in several tissues and is overexpressed on certain types of cancer cells (Suzuki-Inoue, 2019). Podoplanin is a type I membrane protein containing a short cytoplasmic tail which anchors the receptor to the actin cytoskeleton (Quintanilla et al., 2019) and an extracellular part harboring in tandem three copies of a platelet aggregation (PLAG) stimulating motif (Nagae et al., 2014). The third PLAG motif has an O-linked disialyl sugar moiety attached (Kaneko et al., 2007). Sialyation together with the acidic amino acids glutamate and aspartate in podoplanin's PLAG3 motif is essential for electrostatic contact with three arginine residues in Clec-2 and for stimulation of platelet aggregation, as revealed by structural analysis of the Clec-2-podoplanin protein complex (Nagae et al., 2014). Interaction with its agonist podoplanin results in translocation of Clec-2 into lipid rafts (Pollitt et al., 2010), mixtures of sphingolipids, cholesterol, and proteins that form membrane microdomains (Simons and Gerl, 2010). The dense packing in rafts mediates clustering of Clec-2 receptors (Ozaki et al., 2013). The multimerization of Clec-2 increases the affinity for podoplanin and in turn causes podoplanin clustering, resulting in a strong interaction between platelets and tumor cells (Pollitt et al., 2014).

Upon podoplanin-dependent Clec-2 clustering in lipid rafts, platelet activation is initiated by Clec-2 signaling through its hemITAM sequence (Suzuki-Inoue, 2019). The hemITAM segment consists of the tyrosine phosphorylation motif YXXL adjacent to an upstream triple of acidic amino acids (Hughes et al., 2013). Phosphorylation of the hemITAM YXXL is catalyzed by a collaboration between Syk tyrosine kinase and a Src family tyrosine kinase (Spalton et al., 2009; Severin et al., 2011; Pollitt et al., 2014). This enables Syk to avidly bind with its pair of Src homology (SH2) domains to the phosphorylated hemITAM sequences of two Clec-2 molecules that form a dimer (Watson et al., 2009). Thereby, the catalytic activity of the tyrosine kinase Syk is further boosted (Suzuki-Inoue, 2019). Eventually, Syk starts a downstream signaling cascade by phosphorylation of the adaptor proteins, LAT (linker for activation of T cells) and SLP-76 (Src homology 2 domain-containing leukocyte protein of 76 kDa), leading to activation of Btk (Bruton tyrosine kinase) and PLCγ2 (phospholipase C γ2). Finally, cleavage of phosphatidylinositol-4,5-biphosphate (PIP2) by PLCγ2 generates the second messenger molecules IP3 (inositol 1,4,5-triphosphate) and DAG (diacylglycerol), that increase intracellular Ca^{2+} levels and activation of PKC (protein kinase C), resulting in platelet activation (Pollitt et al., 2010; Suzuki-Inoue, 2019). Subsequently, additional intercellular interactions are established and further tighten the cohesion between platelets and tumor cells within TCPAs (Erpenbeck and Schon, 2010).

After initial Clec-2-podoplanin mediated activation, platelets degranulate and expose P-selectin on their cell membranes (Jenne et al., 2013; van Golen et al., 2015). P-selectin on the platelet surface binds to the Sialyl-Lewis^x-tetrasaccharide conjugate of PSGL-1 (P-selectin glycoprotein ligand-1) expressed on tumor cells, thus constituting a secondary level of platelet-tumor

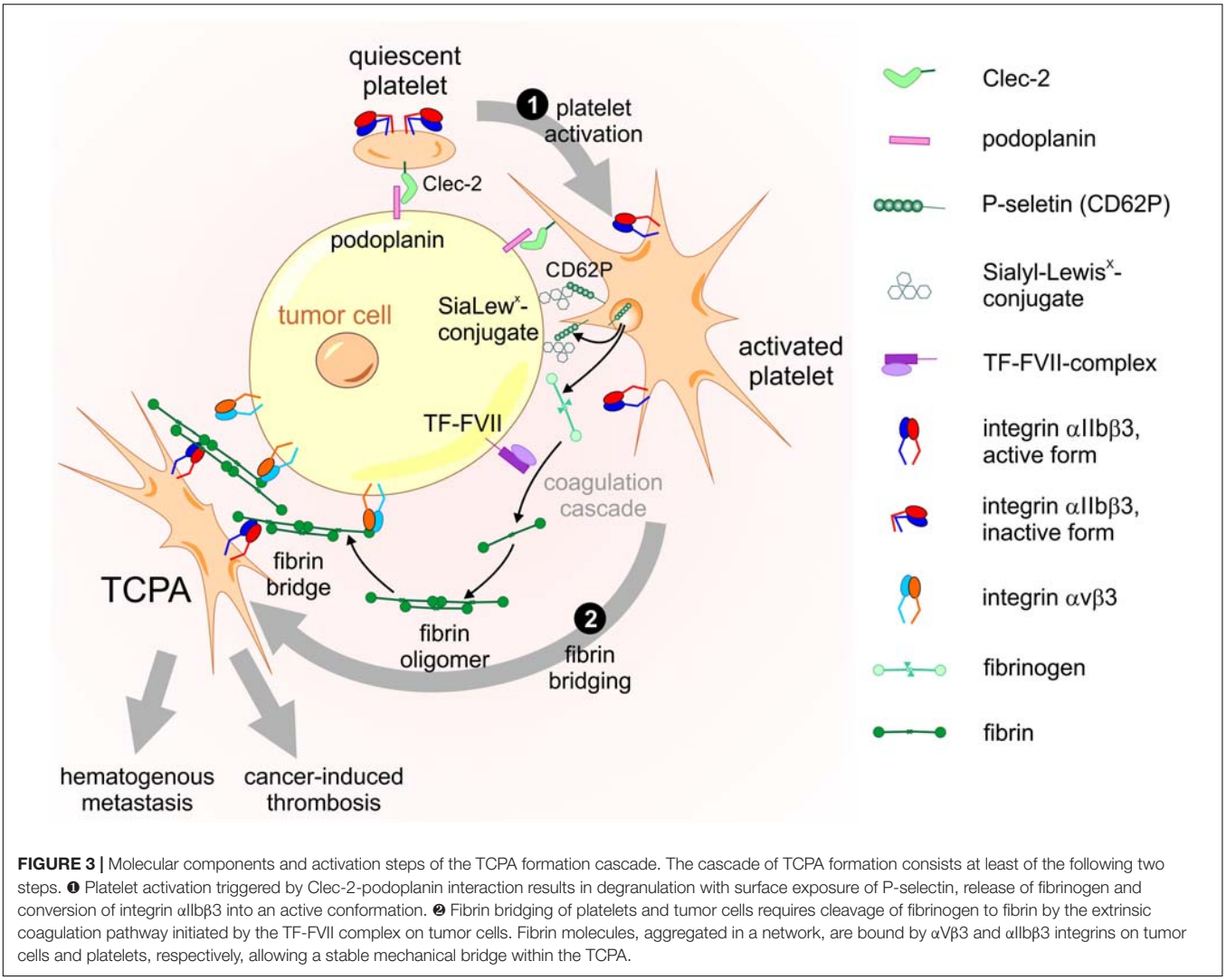

FIGURE 3 | Molecular components and activation steps of the TCPA formation cascade. The cascade of TCPA formation consists at least of the following two steps. ❶ Platelet activation triggered by Clec-2-podoplanin interaction results in degranulation with surface exposure of P-selectin, release of fibrinogen and conversion of integrin αIIbβ3 into an active conformation. ❷ Fibrin bridging of platelets and tumor cells requires cleavage of fibrinogen to fibrin by the extrinsic coagulation pathway initiated by the TF-FVII complex on tumor cells. Fibrin molecules, aggregated in a network, are bound by αVβ3 and αIIbβ3 integrins on tumor cells and platelets, respectively, allowing a stable mechanical bridge within the TCPA.

cell cohesion downstream of the Clec-2-podoplanin interaction (Coupland and Parish, 2014).

Fibrin which is generated from fibrinogen by thrombin serves as another bracket between tumor cells and platelets as it is bound by integrin αIIbβ3 on the platelet surface and by integrin αVβ3 on the tumor cell, building a firm bridge between the two cell types (Katagiri et al., 1995). While integrin αVβ3 binds to an RGD motif in the fibrinogen α subunit, integrin αIIbβ3 interacts with another peptide sequence in the γ subunit (Springer et al., 2008). As a result, platelets and tumor cells firmly cohere to form stable TCPAs connected by three different receptor pairs: Clec-2 and podoplanin, P-selectin and PSGL-1, and integrin αIIbβ3 via fibrin to integrin αVβ3 (**Figure 3**). Moreover, clotting factor FXIII, a transglutaminase, crosslinks plasma fibronectin to insoluble fibrin oligomers, thereby forming a fibrin-fibronectin network (Corbett et al., 1997) and imbedding the metastasizing tumor cell. In addition, the fibrin-fibronectin complex binds to and further activates integrin αVβ3 on tumor cells, inducing invadopodia formation and metastasis (Malik et al., 2010). Yet another way of tumor cell-platelet crosstalk has been reported recently. CD97, an adhesion dependent G protein coupled receptor on tumor cells, activates platelets by a so far unknown counterreceptor to release lysophosphatidic acid (LPA) from dense granules (Ward et al., 2018). In turn, LPA binds to its receptor on tumor cells and starts the Rho kinase signaling pathway, which is associated with tumor cell invasiveness (Ward et al., 2018).

A major threat to blood-borne cancer cells during hematogenous metastasis are natural killer cells that clear tumor cells by cytolytic attack (Nieswandt et al., 1999). In the microenvironment of TCPAs, tumor cells exploit platelets to escape their elimination by the immune system (Labelle and Hynes, 2012; Schlesinger, 2018). The presence of MHC (major histocompatibility complex) class I molecules on the surface of a cell indicates "self" to avoid activation of the immune response. Since many tumor cells traveling alone in the blood circulation show no or low expression of MHC class I molecules on their surface, they are easy prey to natural killer cells (Placke et al., 2012b). In contrast, platelets express plenty of MHC class I molecules on their membrane, which shelters them and the close-by tumor cells within the

TCPAs (Placke et al., 2012b). These platelet derived MHC class I molecules confer "self" to tumor cells and thereby circumvent destruction by natural killer cells (Placke et al., 2012a). Furthermore, activated platelets release growth factors such as PDGF and TGFβ from their α-granules. PDGF binds to PDGF receptors on the surface of natural killer cells and lowers their cytolytic activity (Gersuk et al., 1991). TGFβ impedes expression of NKG2D, a C-type lectin-like receptor on natural killer cells that normally detects transformed tumor cells (Kopp et al., 2009). Accordingly, this constricts cytotoxicity of natural killer cells and lowers disposal of interferon-γ, an anti-tumorigenic cytokine and stimulator of the immune response (Kopp et al., 2009).

THE ROLE OF PLATELETS IN PREPARING METASTATIC NICHES

Having escaped the mechanical challenges in the blood circulation and the threat of the immune system, tumor cells in TCPAs receive further support by platelets as they move to their destination site. After floating for some minutes in the bloodstream, TCPAs come to rest at the vasculature of blood vessels, where tumor cells prepare for extravasation (Labelle and Hynes, 2012). To support attachment of their accompanying tumor cells to the vessel wall, activated platelets bind with P-selectins to Sialyl-Lewis^x-conjugates on the surface of endothelial cells (Gay and Felding-Habermann, 2011a). Hence, platelets create a custom-made microenvironment to safeguard the tumor cells, help them in tethering to endothelial cells and expedite metastasis in their target tissue (Schlesinger, 2018; Palacios-Acedo et al., 2019; Gkolfinopoulos et al., 2020). Fostering the formation of metastatic niches, activated platelets release a multitude of growth factors, cytokines, ECM proteins and clotting factors, and attract different host derived cells of the myeloid lineage such as neutrophils, monocytes and macrophages to assist the piggy-backed tumor cells (Labelle and Hynes, 2012).

Platelets release cytokines CXCL5 and CXCL7 that bind to the CXCR2 receptor on neutrophils to attract them to the metastatic niche (Labelle et al., 2014; Wu et al., 2019; Jaillon et al., 2020). There, neutrophils bind to tumor cells and enforce their attachment to endothelial cells (Huh et al., 2010). Furthermore, upon stimulation by platelet delivered TGFβ, neutrophils produce reactive oxygen species (ROS), nitric oxide and arginase that prevent stimulation of immune reactive T cells (Jaillon et al., 2020). In addition, neutrophils release leukotrienes that confer a high tumorigenic and metastatic potential to tumor cells (Wculek and Malanchi, 2015). Moreover, tumor cells in TCPAs induce the secretion of acid sphingomyelinase from platelets, in turn leading to hydrolysis of sphingomyelin to ceramide (Carpinteiro et al., 2015). In the tumor cell, ceramide molecules form membrane domains in which receptor proteins, such as integrin α5β1, accumulate. Integrin α5β1 clustering further strengthens attachment of tumor cells to the endothelial wall and thereby promotes their metastatic potential (Carpinteiro et al., 2015).

TGFβ released from platelets and direct contact between platelets and tumor cells activate TGFβ-Smad and NF-κB pathways, respectively, in tumor cells (Labelle et al., 2011; Labelle and Hynes, 2012). This results in transcription of target genes, which promote transformation of tumor cells from an epithelial to a mesenchymal phenotype (Labelle et al., 2011; Mittal, 2018). Accordingly, synergistic activation of TGFβ-Smad and NF-κB pathways downregulate epithelial markers such as claudin1 and E-cadherin, but lead to upregulation of mesenchymal transcription factors such as snail and twist, and marker proteins including vimentin and fibronectin in tumor cells (Labelle et al., 2011; Mittal, 2018). Moreover, target genes of the NF-κB and TGFβ-Smad signaling pathways, such as Serpin family H member 1 (SERPINH1), Matrix metalloproteinase 9 (MMP9), Vascular endothelial growth factor C (VEGF-C), Tenascin C (TNC) and C-C motif chemokine 2 (CCL2) enhance hematogenous tumor metastasis by different mechanisms (Labelle et al., 2011; Kim et al., 2019; Xiong F. et al., 2020). For example, during epithelial-mesenchymal transition, snail dependent downregulation of E-cadherin results in loss of intercellular contacts between cancer cells, and loss of their original polarized cellular shape and tissue specific properties (Mittal, 2018). Therefore, tumor cells become mobile, allowing migration and extravasation through the endothelial barrier. Tumor cell overexpressed SERPINH1 encodes the endoplasmic reticulum resident heat shock protein 47 (Hsp47), a molecular chaperone that fosters collagen type I production and export through the secretory pathway during epithelial-mesenchymal transition (Xiong G. et al., 2020). This results in the collagen-rich desmoplastic TME also at the metastatic site. Accordingly, collagen enforces recruitment of platelets to tumor cells, thereby facilitating migration through the endothelium and induces interaction of tumor cells and cluster formation, a necessity for metastasis (Xiong F. et al., 2020). MMP9 is required for ECM remodeling, while VEGF-C and TNC are involved in endothelial cell growth and angiogenesis (Carmeliet, 2005; Rupp et al., 2016). CCL2 released from tumor cells after platelet stimulation is the ligand for chemokine receptor 2 (CCR2) expressed on monocytes and endothelial cells (Wolf et al., 2012). CCL2 binding attracts monocytes to tumor cells and confers suppression of the immune response (Mantovani and Sica, 2010). Stimulation of endothelial cells by CCL2 increases cell permeability of the endothelial wall and tumor cell extravasation by signaling via Janus kinase 2 (JAK2), which triggers downstream signal transducer and activator of transcription 5 (Stat5) and p38 mitogen-activated protein kinase (p38MAPK) activation (Wolf et al., 2012). Eventually, tumor cells that have acquired a mesenchymal, mobile phenotype break the endothelial barrier and make their way to form metastases at distant organs.

PERSPECTIVES FOR TRANSLATION INTO CLINICAL TREATMENT STRATEGIES

Platelets and coagulation play a crucial role in tumor progression and hematogenous metastasis and are therefore considered as

valid pharmaceutical targets in anti-cancer therapy (Zhang et al., 2020). The important surveillance of platelet counts during chemotherapy, their role in chemoresitance, and the potential use of platelets as drug delivery systems in chemotherapy have recently been reviewed (Swier and Versteeg, 2017; Dovizio et al., 2020; Zhang et al., 2020). Therefore, we will not focus on this platelet-dependent aspect of chemotherapy, but will here focus on targeting platelets as relevant constituents of the TME. With respect to the TME of solid tumor mass, different strategies have been chosen to target platelets and tumor cell-induced coagulation. Interestingly, a monoclonal antibody inhibiting TF-signaling via PAR2 reduces tumor growth, while another TF-directed antibody that inhibits its proteolytic function only impedes hematogenous metastasis (Versteeg et al., 2008). Another monoclonal antibody, CNTO 859, inhibits both progression and hematogenous metastasis of tumor cells (Ngo et al., 2007). Two recombinant anticoagulant proteins, the nematode anticoagulant protein c2 (NAPc2) and ixolaris from a tick species, both targeting the TF:FVII complex reduce also tumor progression and metastasis (Hembrough et al., 2003; Carneiro-Lobo et al., 2009). However, it is not entirely clear yet, which isoform of TF influences which steps of tumor progression and metastasis and via which mechanism (van den Berg et al., 2012). Also, TF-positive microvesicles are intensely studied as potential targets to reduce tumor-induced thrombosis and metastasis (Rondon et al., 2019).

Instead of inhibiting TF, another therapeutic approach utilizes TF to pharmaceutically induce tumor infarction. To this end, recombinant TF is directed to tumor vessels either in a soluble form or bound to nanoparticles (Schwöppe et al., 2010; Ding et al., 2013; Schliemann et al., 2020). By enriching TF in the tumor vessels, an excessive fibrin deposition and thrombus formation occlude the tumor vasculature (Jahanban-Esfahlan et al., 2017). The resulting hemostatic plug abolishes the blood flow and the nutrient support for the tumor, resulting in tumor infarction and regression of tumor tissue (Schliemann et al., 2020).

Targeting adhesion and infiltration of platelets within the TME of solid tumors is also tested as potential strategy to curb tumor progression. To this end, adhesive platelet receptors are molecular targets, especially as they have already been clinically addressed to treat thrombosis. RGD-mimicking compounds that interfere with ligand binding of both platelet integrin αIIbβ3 and αVβ3 on tumor cells are relevant lead structures for anti-tumor applications (Jamasbi et al., 2017; Miller et al., 2017). Their inhibitory mechanism and efficacy on RGD-dependent integrins have been derived from snake venom disintegrins (Huang et al., 2016; Estevao-Costa et al., 2018). Another toxin class from snake venoms, the C-type lectin-related proteins, are very efficient inhibitors specifically directed to the receptors for collagen and vWF (Eble, 2019).

The contact of quiescent platelets with blood-borne tumor cells initiates the formation of TCPAs, giving rise to hematogenous metastasis and cancer-induced thrombosis. Therefore, it is of upmost importance to interfere with this initial step of platelet activation right at the beginning (**Figure 3**). Since the primary contact between tumor cells and platelets likely is mediated by the Clec-2-podoplanin interaction, targeting this early step should substantially impede the entire TCPA formation cascade. Accordingly, several approaches are being followed to identify inhibitors of Clec-2 and podoplanin (Harbi et al., 2021). Among the Clec-2 targeting toxins, the snake venom rhodocytin, also named aggretin, was the first to be discovered (Suzuki-Inoue et al., 2006). It is a heterodimeric C-type lectin from the Malayan pit viper *Calloselasma rhodostoma* consisting of α and β chains covalently linked by a disulfide bridge. Crystal structure analysis identified rhodocytin as a $(\alpha\beta)_2$ heterotetramer that binds to Clec-2, induces receptor clustering on the cell surface and thereby triggers platelet activation and aggregation (Watson et al., 2008). Mutations introduced into recombinant rhodocytin expressed in E. coli preserved heterodimer formation but disturbed the oligomeric suprastructure of rhodocytin (Sasaki et al., 2018). Remarkably, such rhodocytin mutant still binds to Clec-2 but fails to induce receptor clustering, thereby blocking the Clec-2-podoplanin axis and platelet activation (Sasaki et al., 2018). Furthermore, when tested in a mouse model of podoplanin-induced lung cancer, mutant rhodocytin prevented formation of metastases, demonstrating that change of its suprastructure can turn rhodocytin from an agonist to an antagonist of tumor cell-induced platelet aggregation and TCPA formation (Sasaki et al., 2018). Since protein medications are rather circumstantial to administer, small drug-like compounds are another approach that was followed to disrupt the Clec-2-podoplanin axis. Cobalt hematoporphyrin was identified by screening a chemical compound library for inhibitors of the interaction between recombinant expressed Clec-2 and podoplanin (Tsukiji et al., 2018). When cobalt hematoporphyrin was used in a mouse model, podoplanin-induced pulmonary metastasis was blocked efficiently (Tsukiji et al., 2018), however, at a potency yet too low for clinical application (Harbi et al., 2021). In a similar approach the 5-nitrobenzoate compound 2CP was discovered as another inhibitor of the Clec-2-podoplanin interaction (Chang et al., 2015). 2CP suppressed pulmonary tumor metastasis in a xenograft mouse model, although at concentrations yet too high for clinical use (Chang et al., 2015).

Another strategy to interfere with Clec-2-podoplanin mediated TCPA formation may be function-blocking antibodies. The mouse monoclonal antibody AYP1 specifically recognizes human Clec-2 and perturbs activation and aggregation of platelets upon stimulation with podoplanin or snake venom rhodocytin (Gitz et al., 2014). However, no *in vivo* study to test this antibody in cancer metastasis has been reported so far. Likewise, monoclonal antibodies 8.1.1 and SZ168 were raised against podoplanin that block the interaction with Clec-2 and platelet activation (Rayes et al., 2017; Wang et al., 2021). When used in a mouse model, podoplanin antibody SZ168 repressed podoplanin dependent, cancer associated thrombosis (Wang et al., 2021).

These preliminary data indicate that the TME provided by the recruitment of platelets to a solid tumor mass or to blood-borne cancer cells is a valid target to curb tumor progression and metastasis. Newly developed tools targeting the multiple platelet-tumor cell interactions may open new strategies not only to reduce the fatal consequence of the Trousseau syndrome but also to impede tumor growth and dissemination.

AUTHOR CONTRIBUTIONS

WO and JE drafted and wrote the manuscript. KB helped in search for references and edited the manuscript. All authors contributed to the article and approved the submitted version.

FUNDING

This work was financially supported by the University of Münster through the Interdisciplinary Center of Clinical Research (IZKF) (IZKF-grant: Ebl/009/21 to JE) and by the Deutsche Forschungsgemeinschaft (DFG) through the SFB1009 project A09 and DFG-grant Eb177/17-1 to JE.

ACKNOWLEDGMENTS

We apologize to all researchers whose scientific contributions are not cited due to the length restrictions.

REFERENCES

Acerbi, I., Cassereau, L., Dean, I., Shi, Q., Au, A., Park, C., et al. (2015). Human breast cancer invasion and aggression correlates with ECM stiffening and immune cell infiltration. *Integr. Biol. (Camb)* 7, 1120–1134. doi: 10.1039/c5ib00040h

Andonegui-Elguera, M. A., Alfaro-Mora, Y., Caceres-Gutierrez, R., Caro-Sanchez, C. H. S., Herrera, L. A., and Diaz-Chavez, J. (2020). An overview of vasculogenic mimicry in Breast Cancer. *Front. Oncol.* 10:220. doi: 10.3389/fonc.2020.00220

Andrews, R. K., and Berndt, M. C. (2004). Platelet physiology and thrombosis. *Thromb. Res.* 114, 447–453. doi: 10.1016/j.thromres.2004.07.020

Andrews, R. K., and Berndt, M. C. (2008). Platelet adhesion: a game of catch and release. *J. Clin. Invest.* 118, 3009–3011.

Andrews, R. K., Gardiner, E. E., Shen, Y., Whisstock, J. C., and Berndt, M. C. (2003). Glycoprotein Ib-IX-V. *Int. J. Biochem. Cell Biol.* 35, 1170–1174.

Apte, R. S., Chen, D. S., and Ferrara, N. (2019). VEGF in signaling and disease: beyond discovery and development. *Cell* 176, 1248–1264. doi: 10.1016/j.cell.2019.01.021

Arnaout, M. A., Mahalingam, B., and Xiong, J. P. (2005). Integrin structure, allostery, and bidirectional signaling. *Annu. Rev. Cell Dev. Biol.* 21, 381–410. doi: 10.1146/annurev.cellbio.21.090704.151217

Arthur, J. F., Gardiner, E. E., Matzaris, M., Taylor, S. G., Wijeyewickrema, L., Ozaki, Y., et al. (2005). Glycoprotein VI is associated with GPIb-IX-V on the membrane of resting and activated platelets. *Thromb. Haemost.* 93, 716–723. doi: 10.1160/th04-09-0584

Atkinson, B. T., Jarvis, G. E., and Watson, S. P. (2003). Activation of GPVI by collagen is regulated by alpha2beta1 and secondary mediators. *J. Thromb. Haemost.* 1, 1278–1287. doi: 10.1046/j.1538-7836.2003.00245.x

Benazzi, C., Al-Dissi, A., Chau, C. H., Figg, W. D., Sarli, G., De Oliveira, J. T., et al. (2014). Angiogenesis in spontaneous tumors and implications for comparative tumor biology. *ScientificWorldJournal* 2014:919570.

Berndt, M. C., Metharom, P., and Andrews, R. K. (2014). Primary haemostasis: newer insights. *Haemophilia* 20(Suppl. 4), 15–22. doi: 10.1111/hae.12427

Bikfalvi, A., and Billottet, C. (2020). The CC and CXC chemokines: major regulators of tumor progression and the tumor microenvironment. *Am. J. Physiol. Cell Physiol.* 318, C542–C554.

Broos, K., De Meyer, S. F., Feys, H. B., Vanhoorelbeke, K., and Deckmyn, H. (2012). Blood platelet biochemistry. *Thromb. Res.* 129, 245–249. doi: 10.1016/j.thromres.2011.11.002

Burbury, K., and MacManus, M. P. (2018). The coagulome and the oncomir: impact of cancer-associated haemostatic dysregulation on the risk of metastasis. *Clin. Exp. Metastasis* 35, 237–246. doi: 10.1007/s10585-018-9875-0

Callander, N. S., Varki, N., and Rao, L. V. (1992). Immunohistochemical identification of tissue factor in solid tumors. *Cancer* 70, 1194–1201. doi: 10.1002/1097-0142(19920901)70:5<1194::aid-cncr2820700528>3.0.co;2-e

Camire, R. M. (2016). Rethinking events in the haemostatic process: role of factor V and TFPI. *Haemophilia* 22(Suppl. 5), 3–8. doi: 10.1111/hae.13004

Campello, E., Henderson, M. W., Noubouossie, D. F., Simioni, P., and Key, N. S. (2018). Contact system activation and cancer: new insights in the pathophysiology of Cancer-Associated thrombosis. *Thromb. Haemost.* 118, 251–265. doi: 10.1160/th17-08-0596

Carmeliet, P. (2005). VEGF as a key mediator of angiogenesis in cancer. *Oncology* 69(Suppl. 3), 4–10. doi: 10.1159/000088478

Carneiro-Lobo, T. C., Konig, S., Machado, D. E., Nasciutti, L. E., Forni, M. F., Francischetti, I. M., et al. (2009). Ixolaris, a tissue factor inhibitor, blocks primary tumor growth and angiogenesis in a glioblastoma model. *J. Thromb. Haemost.* 7, 1855–1864. doi: 10.1111/j.1538-7836.2009.03553.x

Carpinteiro, A., Becker, K. A., Japtok, L., Hessler, G., Keitsch, S., Pozgajova, M., et al. (2015). Regulation of hematogenous tumor metastasis by acid sphingomyelinase. *EMBO Mol. Med.* 7, 714–734. doi: 10.15252/emmm.201404571

Cedervall, J., Hamidi, A., and Olsson, A. K. (2018). Platelets. NETs and cancer. *Thromb. Res.* 164(Suppl. 1), S148–S152.

Chang, Y. W., Hsieh, P. W., Chang, Y. T., Lu, M. H., Huang, T. F., Chong, K. Y., et al. (2015). Identification of a novel platelet antagonist that binds to CLEC-2 and suppresses podoplanin-induced platelet aggregation and cancer metastasis. *Oncotarget* 6, 42733–42748. doi: 10.18632/oncotarget.5811

Chen, Y., Ruggeri, Z. M., and Du, X. (2018). 14-3-3 proteins in platelet biology and glycoprotein Ib-IX signaling. *Blood* 131, 2436–2448. doi: 10.1182/blood-2017-09-742650

Chouaib, S., Kieda, C., Benlalam, H., Noman, M. Z., Mami-Chouaib, F., and Ruegg, C. (2010). Endothelial cells as key determinants of the tumor microenvironment: interaction with tumor cells, extracellular matrix and immune killer cells. *Crit. Rev. Immunol.* 30, 529–545. doi: 10.1615/critrevimmunol.v30.i6.30

Chowdary, P. (2020). Anti-tissue factor pathway inhibitor (TFPI) therapy: a novel approach to the treatment of haemophilia. *Int. J. Hematol.* 111, 42–50. doi: 10.1007/s12185-018-2548-6

Coller, B. S. (2015). alphaIIbbeta3: structure and function. *J. Thromb. Haemost.* 13(Suppl. 1), S17–S25.

Connolly, G. C., and Francis, C. W. (2013). Cancer-associated thrombosis. *Hematol. Am. Soc. Hematol. Educ. Program* 2013, 684–691.

Corbett, S. A., Lee, L., Wilson, C. L., and Schwarzbauer, J. E. (1997). Covalent cross-linking of fibronectin to fibrin is required for maximal cell adhesion to a fibronectin-fibrin matrix. *J. Biol. Chem.* 272, 24999–25005. doi: 10.1074/jbc.272.40.24999

Coupland, L. A., and Parish, C. R. (2014). Platelets, selectins, and the control of tumor metastasis. *Semin. Oncol.* 41, 422–434. doi: 10.1053/j.seminoncol.2014.04.003

Dahlbäck, B. (2000). Blood coagulation. *Lancet* 355, 1627–1632.

Dahlback, B. (2017). Novel insights into the regulation of coagulation by factor V isoforms, tissue factor pathway inhibitoralpha, and protein S. *J. Thromb. Haemost.* 15, 1241–1250. doi: 10.1111/jth.13665

De Palma, M., Biziato, D., and Petrova, T. V. (2017). Microenvironmental regulation of tumour angiogenesis. *Nat. Rev. Cancer* 17, 457–474. doi: 10.1038/nrc.2017.51

de Witt, S. M., Verdoold, R., Cosemans, J. M., and Heemskerk, J. W. (2014). Insights into platelet-based control of coagulation. *Thromb. Res.* 133(Suppl. 2), S139–S148.

Ding, Y., Li, S., and Nie, G. (2013). Nanotechnological strategies for therapeutic targeting of tumor vasculature. *Nanomedicine (Lond)* 8, 1209–1222. doi: 10.2217/nnm.13.106

Dovizio, M., Ballerini, P., Fullone, R., Tacconelli, S., Contursi, A., and Patrignani, P. (2020). Multifaceted functions of platelets in Cancer: from tumorigenesis to liquid biopsy tool and drug delivery system. *Int. J. Mol. Sci.* 21, 9585. doi: 10.3390/ijms21249585

Durrant, T. N., Van Den Bosch, M. T., and Hers, I. (2017). Integrin alphaIIbbeta3 outside-in signaling. *Blood* 130, 1607–1619.

Eble, J. A. (2005). Collagen-binding integrins as pharmaceutical targets. *Curr. Pharm. Des* 11, 867–880. doi: 10.2174/1381612053381738

Eble, J. A. (2019). structurally robust and functionally highly Versatile-C-Type Lectin (-Related) proteins in snake venoms. *Toxins (Basel)* 11:136. doi: 10.3390/toxins11030136

Eble, J. A., and Niland, S. (2019). The extracellular matrix in tumor progression and metastasis. *Clin. Exp. Metastasis* 36, 171–198. doi: 10.1007/s10585-019-09966-1

Egan, K., Cooke, N., and Kenny, D. (2014). Living in shear: platelets protect cancer cells from shear induced damage. *Clin. Exp. Metastasis* 31, 697–704. doi: 10.1007/s10585-014-9660-7

Emsley, J., Knight, C. G., Farndale, R. W., Barnes, M. J., and Liddington, R. C. (2000). Structural basis of collagen recognition by integrin alpha2beta1. *Cell* 101, 47–56. doi: 10.1016/s0092-8674(00)80622-4

Erpenbeck, L., and Schon, M. P. (2010). Deadly allies: the fatal interplay between platelets and metastasizing cancer cells. *Blood* 115, 3427–3436. doi: 10.1182/blood-2009-10-247296

Erpenbeck, L., and Schon, M. P. (2017). Neutrophil extracellular traps: protagonists of cancer progression? *Oncogene* 36, 2483–2490. doi: 10.1038/onc.2016.406

Estevao-Costa, M. I., Sanz-Soler, R., Johanningmeier, B., and Eble, J. A. (2018). Snake venom components in medicine: from the symbolic rod of Asclepius to tangible medical research and application. *Int. J. Biochem. Cell Biol.* 104, 94–113. doi: 10.1016/j.biocel.2018.09.011

Fitzgerald, G., Soro-Arnaiz, I., and De Bock, K. (2018). The warburg effect in endothelial cells and its potential as an anti-angiogenic target in Cancer. *Front. Cell Dev. Biol.* 6:100. doi: 10.3389/fcell.2018.00100

Gale, A. J. (2011). Continuing education course #2: current understanding of hemostasis. *Toxicol. Pathol.* 39, 273–280.

Gay, L. J., and Felding-Habermann, B. (2011a). Contribution of platelets to tumour metastasis. *Nat. Rev. Cancer* 11, 123–134. doi: 10.1038/nrc3004

Gay, L. J., and Felding-Habermann, B. (2011b). Platelets alter tumor cell attributes to propel metastasis: programming in transit. *Cancer Cell* 20, 553–554. doi: 10.1016/j.ccr.2011.11.001

Gersuk, G. M., Westermark, B., Mohabeer, A. J., Challita, P. M., Pattamakom, S., and Pattengale, P. K. (1991). Inhibition of human natural killer cell activity by platelet-derived growth factor (PDGF). III. Membrane binding studies and differential biological effect of recombinant PDGF isoforms. *Scand. J. Immunol.* 33, 521–532. doi: 10.1111/j.1365-3083.1991.tb02522.x

Gitz, E., Pollitt, A. Y., Gitz-Francois, J. J., Alshehri, O., Mori, J., Montague, S., et al. (2014). CLEC-2 expression is maintained on activated platelets and on platelet microparticles. *Blood* 124, 2262–2270. doi: 10.1182/blood-2014-05-572818

Gkolfinopoulos, S., Jones, R. L., and Constantinidou, A. (2020). The emerging role of platelets in the formation of the micrometastatic niche: current evidence and future perspectives. *Front. Oncol.* 10:374. doi: 10.3389/fonc.2020.00374

Goubran, H., Sabry, W., Kotb, R., Seghatchian, J., and Burnouf, T. (2015). Platelet microparticles and cancer: an intimate cross-talk. *Transfus Apher Sci.* 53, 168–172. doi: 10.1016/j.transci.2015.10.014

Grassle, S., Huck, V., Pappelbaum, K. I., Gorzelanny, C., Aponte-Santamaria, C., Baldauf, C., et al. (2014). von Willebrand factor directly interacts with DNA from neutrophil extracellular traps. *Arterioscler. Thromb. Vasc. Biol.* 34, 1382–1389. doi: 10.1161/atvbaha.113.303016

Grover, S. P., and Mackman, N. (2018). Tissue factor: an essential mediator of hemostasis and trigger of thrombosis. *Arterioscler. Thromb. Vasc. Biol.* 38, 709–725. doi: 10.1161/atvbaha.117.309846

Haling, J. R., Monkley, S. J., Critchley, D. R., and Petrich, B. G. (2011). Talin-dependent integrin activation is required for fibrin clot retraction by platelets. *Blood* 117, 1719–1722. doi: 10.1182/blood-2010-09-305433

Hamaia, S., and Farndale, R. W. (2014). Integrin recognition motifs in the human collagens. *Adv. Exp. Med. Biol.* 819, 127–142. doi: 10.1007/978-94-017-9153-3_9

Han, X., Guo, B., Li, Y., and Zhu, B. (2014). Tissue factor in tumor microenvironment: a systematic review. *J. Hematol. Oncol.* 7:54.

Hanein, D., and Volkmann, N. (2018). Conformational equilibrium of human platelet integrin investigated by three-dimensional electron cryo-microscopy. *Subcell Biochem.* 87, 353–363. doi: 10.1007/978-981-10-7757-9_12

Hansen, C. E., Qiu, Y., Mccarty, O. J. T., and Lam, W. A. (2018). Platelet mechanotransduction. *Annu. Rev. Biomed. Eng.* 20, 253–275. doi: 10.1146/annurev-bioeng-062117-121215

Harbi, M. H., Smith, C. W., Nicolson, P. L. R., Watson, S. P., and Thomas, M. R. (2021). Novel antiplatelet strategies targeting GPVI. CLEC-2 and tyrosine kinases. *Platelets* 32, 29–41. doi: 10.1080/09537104.2020.1849600

He, L., Pappan, L. K., Grenache, D. G., Li, Z., Tollefsen, D. M., Santoro, S. A., et al. (2003). The contributions of the alpha 2 beta 1 integrin to vascular thrombosis in vivo. *Blood* 102, 3652–3657.

Hembrough, T. A., Swartz, G. M., Papathanassiu, A., Vlasuk, G. P., Rote, W. E., Green, S. J., et al. (2003). Tissue factor/factor VIIa inhibitors block angiogenesis and tumor growth through a nonhemostatic mechanism. *Cancer Res.* 63, 2997–3000.

Henke, E., Nandigama, R., and Ergun, S. (2019). Extracellular matrix in the tumor microenvironment and its impact on Cancer therapy. *Front. Mol. Biosci.* 6:160. doi: 10.3389/fmolb.2019.00160

Huang, J., Li, X., Shi, X., Zhu, M., Wang, J., Huang, S., et al. (2019). Platelet integrin alphaIIbbeta3: signal transduction, regulation, and its therapeutic targeting. *J. Hematol. Oncol.* 12:26.

Huang, T. F., Hsu, C. C., and Kuo, Y. J. (2016). Anti-thrombotic agents derived from snake venom proteins. *Thromb. J.* 14:18.

Huber, M., Brehm, C. U., Gress, T. M., Buchholz, M., Alashkar Alhamwe, B., Von Strandmann, E. P., et al. (2020). The immune microenvironment in pancreatic Cancer. *Int. J. Mol. Sci.* 21:7307.

Huck, V., Schneider, M. F., Gorzelanny, C., and Schneider, S. W. (2014). The various states of von willebrand factor and their function in physiology and pathophysiology. *Thromb. Haemost.* 111, 598–609. doi: 10.1160/th13-09-0800

Hughes, C. E., Sinha, U., Pandey, A., Eble, J. A., O'callaghan, C. A., and Watson, S. P. (2013). Critical Role for an acidic amino acid region in platelet signaling by the HemITAM (hemi-immunoreceptor tyrosine-based activation motif) containing receptor CLEC-2 (C-type lectin receptor-2). *J. Biol. Chem.* 288, 5127–5135. doi: 10.1074/jbc.m112.411462

Huh, S. J., Liang, S., Sharma, A., Dong, C., and Robertson, G. P. (2010). Transiently entrapped circulating tumor cells interact with neutrophils to facilitate lung metastasis development. *Cancer Res.* 70, 6071–6082. doi: 10.1158/0008-5472.can-09-4442

Humphries, J. D., Chastney, M. R., Askari, J. A., and Humphries, M. J. (2019). Signal transduction via integrin adhesion complexes. *Curr. Opin. Cell Biol.* 56, 14–21. doi: 10.1016/j.ceb.2018.08.004

Inoue, O., Suzuki-Inoue, K., Dean, W. L., Frampton, J., and Watson, S. P. (2003). Integrin alpha2beta1 mediates outside-in regulation of platelet spreading on collagen through activation of Src kinases and PLCgamma2. *J. Cell Biol.* 160, 769–780. doi: 10.1083/jcb.200208043

Iozzo, R. V., and Sanderson, R. D. (2011). Proteoglycans in cancer biology, tumour microenvironment and angiogenesis. *J. Cell Mol. Med.* 15, 1013–1031. doi: 10.1111/j.1582-4934.2010.01236.x

Izquierdo, I., Barrachina, M. N., Hermida-Nogueira, L., Casas, V., Moran, L. A., Lacerenza, S., et al. (2020). A comprehensive tyrosine phosphoproteomic analysis reveals novel components of the platelet CLEC-2 signaling cascade. *Thromb. Haemost.* 120, 262–276. doi: 10.1055/s-0039-3400295

Jahanban-Esfahlan, R., Seidi, K., and Zarghami, N. (2017). Tumor vascular infarction: prospects and challenges. *Int. J. Hematol.* 105, 244–256. doi: 10.1007/s12185-016-2171-3

Jaillon, S., Ponzetta, A., Di Mitri, D., Santoni, A., Bonecchi, R., and Mantovani, A. (2020). Neutrophil diversity and plasticity in tumour progression and therapy. *Nat. Rev. Cancer* 20, 485–503. doi: 10.1038/s41568-020-0281-y

Jamasbi, J., Ayabe, K., Goto, S., Nieswandt, B., Peter, K., and Siess, W. (2017). Platelet receptors as therapeutic targets: past, present and future. *Thromb. Haemost.* 117, 1249–1257. doi: 10.1160/th16-12-0911

Jarvis, G. E., Best, D., and Watson, S. P. (2004). Differential roles of integrins alpha2beta1 and alphaIIbbeta3 in collagen and CRP-induced platelet activation. *Platelets* 15, 303–313. doi: 10.1080/09537100410001710254

Jenne, C. N., Urrutia, R., and Kubes, P. (2013). Platelets: bridging hemostasis, inflammation, and immunity. *Int. J. Lab. Hematol.* 35, 254–261. doi: 10.1111/ijlh.12084

Jennewein, C., Tran, N., Paulus, P., Ellinghaus, P., Eble, J. A., and Zacharowski, K. (2011). Novel aspects of fibrin(ogen) fragments during inflammation. *Mol. Med.* 17, 568–573. doi: 10.2119/molmed.2010.00146

Kalluri, R. (2016). The biology and function of fibroblasts in cancer. *Nat. Rev. Cancer* 16, 582–598. doi: 10.1038/nrc.2016.73

Kaneko, M. K., Kato, Y., Kameyama, A., Ito, H., Kuno, A., Hirabayashi, J., et al. (2007). Functional glycosylation of human podoplanin: glycan structure of platelet aggregation-inducing factor. *FEBS Lett.* 581, 331–336. doi: 10.1016/j.febslet.2006.12.044

Kania, A., and Klein, R. (2016). Mechanisms of ephrin-Eph signalling in development, physiology and disease. *Nat. Rev. Mol. Cell Biol.* 17, 240–256. doi: 10.1038/nrm.2015.16

Kasirer-Friede, A., Kang, J., Kahner, B., Ye, F., Ginsberg, M. H., and Shattil, S. J. (2014). ADAP interactions with talin and kindlin promote platelet integrin alphaIIbbeta3 activation and stable fibrinogen binding. *Blood* 123, 3156–3165. doi: 10.1182/blood-2013-08-520627

Katagiri, Y., Hiroyama, T., Akamatsu, N., Suzuki, H., Yamazaki, H., and Tanoue, K. (1995). Involvement of alpha v beta 3 integrin in mediating fibrin gel retraction. *J. Biol. Chem.* 270, 1785–1790. doi: 10.1074/jbc.270.4.1785

Kato, K., Kanaji, T., Russell, S., Kunicki, T. J., Furihata, K., Kanaji, S., et al. (2003). The contribution of glycoprotein VI to stable platelet adhesion and thrombus formation illustrated by targeted gene deletion. *Blood* 102, 1701–1707. doi: 10.1182/blood-2003-03-0717

Kim, H. J., Park, J. H., Shin, J. M., Yang, H. W., Lee, H. M., and Park, I. H. (2019). TGF-beta1-induced HSP47 regulates extracellular matrix accumulation via Smad2/3 signaling pathways in nasal fibroblasts. *Sci. Rep.* 9:15563.

Klein, D. (2018). The tumor vascular endothelium as decision maker in Cancer therapy. *Front. Oncol.* 8:367. doi: 10.3389/fonc.2018.00367

Knight, C. G., Morton, L. F., Onley, D. J., Peachey, A. R., Ichinohe, T., Okuma, M., et al. (1999). Collagen-platelet interaction: Gly-Pro-Hyp is uniquely specific for platelet Gp VI and mediates platelet activation by collagen. *Cardiovasc. Res.* 41, 450–457. doi: 10.1016/s0008-6363(98)00306-x

Kopp, H. G., Placke, T., and Salih, H. R. (2009). Platelet-derived transforming growth factor-beta down-regulates NKG2D thereby inhibiting natural killer cell antitumor reactivity. *Cancer Res.* 69, 7775–7783. doi: 10.1158/0008-5472.can-09-2123

Kuczynski, E. A., Vermeulen, P. B., Pezzella, F., Kerbel, R. S., and Reynolds, A. R. (2019). Vessel co-option in cancer. *Nat. Rev. Clin. Oncol.* 16, 469–493. doi: 10.1038/s41571-019-0181-9

Kühn, K., and Eble, J. (1994). The structural bases of integrin-ligand interactions. *Trends Cell Biol.* 4, 256–261. doi: 10.1016/0962-8924(94)90124-4

Kulkarni, S., Dopheide, S. M., Yap, C. L., Ravanat, C., Freund, M., Mangin, P., et al. (2000). A revised model of platelet aggregation. *J. Clin. Invest.* 105, 783–791.

Kunicki, T. J. (2001). The role of platelet collagen receptor (glycoprotein Ia/IIa; integrin alpha2 beta1) polymorphisms in thrombotic disease. *Curr. Opin. Hematol.* 8, 277–285. doi: 10.1097/00062752-200109000-00003

Kunicki, T. J., Cheli, Y., Moroi, M., and Furihata, K. (2005). The influence of N-linked glycosylation on the function of platelet glycoprotein VI. *Blood* 106, 2744–2749. doi: 10.1182/blood-2005-04-1454

Kwaan, H. C., and Lindholm, P. F. (2019). Fibrin and fibrinolysis in Cancer. *Semin. Thromb. Hemost.* 45, 413–422.

Labelle, M., Begum, S., and Hynes, R. O. (2011). Direct signaling between platelets and cancer cells induces an epithelial-mesenchymal-like transition and promotes metastasis. *Cancer Cell* 20, 576–590. doi: 10.1016/j.ccr.2011.09.009

Labelle, M., Begum, S., and Hynes, R. O. (2014). Platelets guide the formation of early metastatic niches. *Proc. Natl. Acad. Sci. U S A.* 111, E3053–E3061.

Labelle, M., and Hynes, R. O. (2012). The initial hours of metastasis: the importance of cooperative host-tumor cell interactions during hematogenous dissemination. *Cancer Discov.* 2, 1091–1099. doi: 10.1158/2159-8290.cd-12-0329

Lancellotti, S., Sacco, M., Basso, M., and De Cristofaro, R. (2019). Mechanochemistry of von Willebrand factor. *Biomol Concepts* 10, 194–208. doi: 10.1515/bmc-2019-0022

Leight, J. L., Drain, A. P., and Weaver, V. M. (2017). Extracellular matrix remodeling and stiffening modulate tumor phenotype and treatment response. *Ann. Rev. Cancer Biol.* 1, 313–334. doi: 10.1146/annurev-cancerbio-050216-034431

Li, H., Deng, Y., Sun, K., Yang, H., Liu, J., Wang, M., et al. (2017). Structural basis of kindlin-mediated integrin recognition and activation. *Proc. Natl. Acad. Sci. U S A.* 114, 9349–9354. doi: 10.1073/pnas.1703064114

Lima, A. M., Wegner, S. V., Martins Cavaco, A. C., Estevao-Costa, M. I., Sanz-Soler, R., Niland, S., et al. (2018). The spatial molecular pattern of integrin recognition sites and their immobilization to colloidal nanobeads determine alpha2beta1 integrin-dependent platelet activation. *Biomaterials* 167, 107–120. doi: 10.1016/j.biomaterials.2018.03.028

Liu, Y., Jiang, P., Capkova, K., Xue, D., Ye, L., Sinha, S. C., et al. (2011). Tissue factor-activated coagulation cascade in the tumor microenvironment is critical for tumor progression and an effective target for therapy. *Cancer Res.* 71, 6492–6502. doi: 10.1158/0008-5472.can-11-1145

Lodyga, M., and Hinz, B. (2020). TGF-beta1 - a truly transforming growth factor in fibrosis and immunity. *Semin. Cell Dev. Biol.* 101, 123–139. doi: 10.1016/j.semcdb.2019.12.010

Lof, A., Muller, J. P., and Brehm, M. A. (2018). A biophysical view on von Willebrand factor activation. *J. Cell. Physiol.* 233, 799–810. doi: 10.1002/jcp.25887

Luo, B. H., Carman, C. V., and Springer, T. A. (2007). Structural basis of integrin regulation and signaling. *Annu. Rev. Immunol.* 25, 619–647. doi: 10.1146/annurev.immunol.25.022106.141618

Madamanchi, A., Santoro, S. A., and Zutter, M. M. (2014). alpha2beta1 Integrin. *Adv. Exp. Med. Biol.* 819, 41–60.

Malik, G., Knowles, L. M., Dhir, R., Xu, S., Yang, S., Ruoslahti, E., et al. (2010). Plasma fibronectin promotes lung metastasis by contributions to fibrin clots and tumor cell invasion. *Cancer Res.* 70, 4327–4334. doi: 10.1158/0008-5472.can-09-3312

Mantovani, A., and Sica, A. (2010). Macrophages, innate immunity and cancer: balance, tolerance, and diversity. *Curr. Opin. Immunol.* 22, 231–237. doi: 10.1016/j.coi.2010.01.009

Marjoram, R. J., Li, Z., He, L., Tollefsen, D. M., Kunicki, T. J., Dickeson, S. K., et al. (2014). alpha2beta1 integrin, GPVI receptor, and common FcRgamma chain on mouse platelets mediate distinct responses to collagen in models of thrombosis. *PLoS One* 9:e114035. doi: 10.1371/journal.pone.0114035

Martins Cavaco, A. C., Damaso, S., Casimiro, S., and Costa, L. (2020). Collagen biology making inroads into prognosis and treatment of cancer progression and metastasis. *Cancer Metastasis Rev.* 39, 603–623. doi: 10.1007/s10555-020-09888-5

Martins Lima, A., Martins Cavaco, A. C., Fraga-Silva, R. A., Eble, J. A., and Stergiopulos, N. (2019). From patients to platelets and back again: pharmacological approaches to glycoprotein VI, a thrilling antithrombotic target with minor bleeding risks. *Thromb. Haemost.* 119, 1720–1739. doi: 10.1055/s-0039-1695770

Masucci, M. T., Minopoli, M., Del Vecchio, S., and Carriero, M. V. (2020). The emerging role of Neutrophil Extracellular Traps (NETs) in tumor progression and metastasis. *Front. Immunol.* 11:1749. doi: 10.3389/fimmu.2020.01749

Mege, D., Aubert, M., Lacroix, R., Dignat-George, F., Panicot-Dubois, L., and Dubois, C. (2019). Involvement of platelets in Cancers. *Semin. Thromb. Hemost.* 45, 569–575. doi: 10.1055/s-0039-1693475

Menter, D. G., Kopetz, S., Hawk, E., Sood, A. K., Loree, J. M., Gresele, P., et al. (2017). Platelet "first responders" in wound response, cancer, and metastasis. *Cancer Metastasis Rev.* 36, 199–213. doi: 10.1007/s10555-017-9682-0

Miller, L. M., Pritchard, J. M., Macdonald, S. J. F., Jamieson, C., and Watson, A. J. B. (2017). Emergence of small-molecule Non-RGD-Mimetic inhibitors for RGD integrins. *J. Med. Chem.* 60, 3241–3251. doi: 10.1021/acs.jmedchem.6b01711

Mittal, V. (2018). Epithelial mesenchymal transition in tumor metastasis. *Annu. Rev. Pathol.* 13, 395–412.

Miura, Y., Takahashi, T., Jung, S. M., and Moroi, M. (2002). Analysis of the interaction of platelet collagen receptor glycoprotein VI (GPVI) with collagen. a dimeric form of GPVI, but not the monomeric form, shows affinity to fibrous collagen. *J. Biol. Chem.* 277, 46197–46204. doi: 10.1074/jbc.m204029200

Mohammadi, H., and Sahai, E. (2018). Mechanisms and impact of altered tumour mechanics. *Nat. Cell Biol.* 20, 766–774. doi: 10.1038/s41556-018-0131-2

Mongiat, M., Buraschi, S., Andreuzzi, E., Neill, T., and Iozzo, R. V. (2019). Extracellular matrix: the gatekeeper of tumor angiogenesis. *Biochem. Soc. Trans.* 47, 1543–1555. doi: 10.1042/bst20190653

Moser, M., Nieswandt, B., Ussar, S., Pozgajova, M., and Fassler, R. (2008). Kindlin-3 is essential for integrin activation and platelet aggregation. *Nat. Med.* 14, 325–330. doi: 10.1038/nm1722

Naba, A., Clauser, K. R., Ding, H., Whittaker, C. A., Carr, S. A., and Hynes, R. O. (2016). The extracellular matrix: tools and insights for the "omics" era. *Matrix Biol.* 49, 10–24. doi: 10.1016/j.matbio.2015.06.003

Naba, A., Pearce, O. M. T., Del Rosario, A., Ma, D., Ding, H., Rajeeve, V., et al. (2017). Characterization of the extracellular matrix of normal and diseased tissues using proteomics. *J. Proteome Res.* 16, 3083–3091. doi: 10.1021/acs.jproteome.7b00191

Nagae, M., Morita-Matsumoto, K., Kato, M., Kaneko, M. K., Kato, Y., and Yamaguchi, Y. (2014). A platform of C-type lectin-like receptor CLEC-2 for binding O-glycosylated podoplanin and nonglycosylated rhodocytin. *Structure* 22, 1711–1721. doi: 10.1016/j.str.2014.09.009

Nagy, J. A., Dvorak, A. M., and Dvorak, H. F. (2012). Vascular hyperpermeability, angiogenesis, and stroma generation. *Cold Spring Harb. Perspect. Med.* 2:a006544. doi: 10.1101/cshperspect.a006544

Ngo, C. V., Picha, K., Mccabe, F., Millar, H., Tawadros, R., Tam, S. H., et al. (2007). CNTO 859, a humanized anti-tissue factor monoclonal antibody, is a potent inhibitor of breast cancer metastasis and tumor growth in xenograft models. *Int. J. Cancer* 120, 1261–1267. doi: 10.1002/ijc.22426

Nieswandt, B., Hafner, M., Echtenacher, B., and Mannel, D. N. (1999). Lysis of tumor cells by natural killer cells in mice is impeded by platelets. *Cancer Res.* 59, 1295–1300.

Nieswandt, B., Schulte, V., Bergmeier, W., Mokhtari-Nejad, R., Rackebrandt, K., Cazenave, J. P., et al. (2001). Long-term antithrombotic protection by in vivo depletion of platelet glycoprotein VI in mice. *J. Exp. Med.* 193, 459–469. doi: 10.1084/jem.193.4.459

Nieswandt, B., and Watson, S. P. (2003). Platelet-collagen interaction: is GPVI the central receptor? *Blood* 102, 449–461. doi: 10.1182/blood-2002-12-3882

Niland, S., and Eble, J. A. (2019). Neuropilins in the context of tumor vasculature. *Int. J. Mol. Sci.* 20:639. doi: 10.3390/ijms20030639

Niland, S., and Eble, J. A. (2020). Hold on or cut? integrin- and MMP-Mediated cell-matrix interactions in the tumor microenvironment. *Int. J. Mol. Sci.* 22:238. doi: 10.3390/ijms22010238

Niland, S., Westerhausen, C., Schneider, S. W., Eckes, B., Schneider, M. F., and Eble, J. A. (2011). Biofunctionalization of a generic collagenous triple helix with the alpha2beta1 integrin binding site allows molecular force measurements. *Int. J. Biochem. Cell Biol.* 43, 721–731. doi: 10.1016/j.biocel.2011.01.013

Nuyttens, B. P., Thijs, T., Deckmyn, H., and Broos, K. (2011). Platelet adhesion to collagen. *Thromb. Res.* 127(Suppl. 2), S26–S29.

Ostman, A. (2017). PDGF receptors in tumor stroma: biological effects and associations with prognosis and response to treatment. *Adv. Drug Deliv. Rev.* 121, 117–123. doi: 10.1016/j.addr.2017.09.022

Oudin, M. J., and Weaver, V. M. (2016). Physical and chemical gradients in the tumor microenvironment regulate tumor cell invasion, migration, and metastasis. *Cold. Spring Harb. Symp. Quant. Biol.* 81, 189–205. doi: 10.1101/sqb.2016.81.030817

Owens, A. P. III, and Mackman, N. (2011). Microparticles in hemostasis and thrombosis. *Circ. Res.* 108, 1284–1297. doi: 10.1161/circresaha.110.233056

Ozaki, Y., Suzuki-Inoue, K., and Inoue, O. (2013). Platelet receptors activated via mulitmerization: glycoprotein VI. GPIb-IX-V, and CLEC-2. *J. Thromb. Haemost.* 11(Suppl. 1), 330–339. doi: 10.1111/jth.12235

Pakshir, P., Noskovicova, N., Lodyga, M., Son, D. O., Schuster, R., Goodwin, A., et al. (2020). The myofibroblast at a glance. *J. Cell Sci.* 133:jcs227900. doi: 10.1242/jcs.227900

Palacios-Acedo, A. L., Mege, D., Crescence, L., Dignat-George, F., Dubois, C., and Panicot-Dubois, L. (2019). Platelets, thrombo-inflammation, and Cancer: collaborating with the enemy. *Front. Immunol.* 10:1805. doi: 10.3389/fimmu.2019.01805

Palumbo, J. S., Talmage, K. E., Massari, J. V., La Jeunesse, C. M., Flick, M. J., Kombrinck, K. W., et al. (2007). Tumor cell-associated tissue factor and circulating hemostatic factors cooperate to increase metastatic potential through natural killer cell-dependent and-independent mechanisms. *Blood* 110, 133–141. doi: 10.1182/blood-2007-01-065995

Perret, S., Eble, J. A., Siljander, P. R., Merle, C., Farndale, R. W., Theisen, M., et al. (2003). Prolyl hydroxylation of collagen type I is required for efficient binding to integrin alpha 1 beta 1 and platelet glycoprotein VI but not to alpha 2 beta 1. *J. Biol. Chem.* 278, 29873–29879. doi: 10.1074/jbc.m304073200

Pietras, K., and Ostman, A. (2010). Hallmarks of cancer: interactions with the tumor stroma. *Exp. Cell Res.* 316, 1324–1331. doi: 10.1016/j.yexcr.2010.02.045

Placke, T., Orgel, M., Schaller, M., Jung, G., Rammensee, H. G., Kopp, H. G., et al. (2012a). Platelet-derived MHC class I confers a pseudonormal phenotype to cancer cells that subverts the antitumor reactivity of natural killer immune cells. *Cancer Res.* 72, 440–448. doi: 10.1158/0008-5472.can-11-1872

Placke, T., Salih, H. R., and Kopp, H. G. (2012b). GITR ligand provided by thrombopoietic cells inhibits NK cell antitumor activity. *J. Immunol.* 189, 154–160. doi: 10.4049/jimmunol.1103194

Podolnikova, N. P., O'toole, T. E., Haas, T. A., Lam, S. C., Fox, J. E., and Ugarova, T. P. (2009). Adhesion-induced unclasping of cytoplasmic tails of integrin alpha(IIb)beta3. *Biochemistry* 48, 617–629. doi: 10.1021/bi801751s

Podolnikova, N. P., Yermolenko, I. S., Fuhrmann, A., Lishko, V. K., Magonov, S., Bowen, B., et al. (2010). Control of integrin alphaIIb beta3 outside-in signaling and platelet adhesion by sensing the physical properties of fibrin(ogen) substrates. *Biochemistry* 49, 68–77. doi: 10.1021/bi9016022

Pollitt, A. Y., Grygielska, B., Leblond, B., Desire, L., Eble, J. A., and Watson, S. P. (2010). Phosphorylation of CLEC-2 is dependent on lipid rafts, actin polymerization, secondary mediators, and Rac. *Blood* 115, 2938–2946. doi: 10.1182/blood-2009-12-257212

Pollitt, A. Y., Poulter, N. S., Gitz, E., Navarro-Nunez, L., Wang, Y. J., Hughes, C. E., et al. (2014). Syk and Src family kinases regulate C-type lectin receptor 2 (CLEC-2)-mediated clustering of podoplanin and platelet adhesion to lymphatic endothelial cells. *J. Biol. Chem.* 289, 35695–35710. doi: 10.1074/jbc.m114.584284

Poulter, N. S., Pollitt, A. Y., Owen, D. M., Gardiner, E. E., Andrews, R. K., Shimizu, H., et al. (2017). Clustering of glycoprotein VI (GPVI) dimers upon adhesion to collagen as a mechanism to regulate GPVI signaling in platelets. *J. Thromb. Haemost.* 15, 549–564. doi: 10.1111/jth.13613

Pugh, N., Simpson, A. M., Smethurst, P. A., De Groot, P. G., Raynal, N., and Farndale, R. W. (2010). Synergism between platelet collagen receptors defined using receptor-specific collagen-mimetic peptide substrata in flowing blood. *Blood* 115, 5069–5079. doi: 10.1182/blood-2010-01-260778

Quach, M. E., and Li, R. (2020). Structure-function of platelet glycoprotein Ib-IX. *J. Thromb. Haemost.* 18, 3131–3141. doi: 10.1111/jth.15035

Quintanilla, M., Montero-Montero, L., Renart, J., and Martin-Villar, E. (2019). Podoplanin in inflammation and Cancer. *Int. J. Mol. Sci.* 20:707. doi: 10.3390/ijms20030707

Rayes, J., Lax, S., Wichaiyo, S., Watson, S. K., Di, Y., Lombard, S., et al. (2017). The podoplanin-CLEC-2 axis inhibits inflammation in sepsis. *Nat. Commun.* 8:2239.

Reddel, C. J., Tan, C. W., and Chen, V. M. (2019). Thrombin generation and cancer: contributors and consequences. *Cancers (Basel)* 11:100. doi: 10.3390/cancers11010100

Repetto, O., and De Re, V. (2017). Coagulation and fibrinolysis in gastric cancer. *Ann. N. Y. Acad. Sci.* 1404, 27–48. doi: 10.1111/nyas.13454

Rondon, A. M. R., Kroone, C., Kapteijn, M. Y., Versteeg, H. H., and Buijs, J. T. (2019). Role of tissue factor in tumor progression and Cancer-Associated Thrombosis. *Semin. Thromb. Hemost.* 45, 396–412. doi: 10.1055/s-0039-1687895

Rupp, T., Langlois, B., Koczorowska, M. M., Radwanska, A., Sun, Z., Hussenet, T., et al. (2016). Tenascin-C orchestrates glioblastoma angiogenesis by modulation of pro- and anti-angiogenic signaling. *Cell Rep.* 17, 2607–2619. doi: 10.1016/j.celrep.2016.11.012

Sabrkhany, S., Griffioen, A. W., and Oude Egbrink, M. G. (2011). The role of blood platelets in tumor angiogenesis. *Biochim. Biophys. Acta* 1815, 189–196.

Sadeghalvad, M., Mohammadi-Motlagh, H. R., and Rezaei, N. (2020). Immune microenvironment in different molecular subtypes of ductal breast carcinoma. *Breast Cancer Res Treat.* 185, 261–279. doi: 10.1007/s10549-020-05954-2

Sasaki, T., Shirai, T., Tsukiji, N., Otake, S., Tamura, S., Ichikawa, J., et al. (2018). Functional characterization of recombinant snake venom rhodocytin:

rhodocytin mutant blocks CLEC-2/podoplanin-dependent platelet aggregation and lung metastasis. *J. Thromb. Haemost.* 16, 960–972. doi: 10.1111/jth.13987

Scharf, R. E. (2018a). Platelet signaling in primary haemostasis and arterial thrombus formation: Part 1. *Hamostaseologie* 38, 203–210. doi: 10.1055/s-0038-1675144

Scharf, R. E. (2018b). Platelet signaling in primary haemostasis and arterial thrombus formation: Part 2. *Hamostaseologie* 38, 211–222. doi: 10.1055/s-0038-1675149

Schlesinger, M. (2018). Role of platelets and platelet receptors in cancer metastasis. *J. Hematol. Oncol.* 11:125.

Schliemann, C., Gerwing, M., Heinzow, H., Harrach, S., Schwöppe, C., Wildgruber, M., et al. (2020). First-In-Class CD13-Targeted tissue factor tTF-NGR in patients with recurrent or refractory malignant tumors: results of a phase I dose-escalation study. *Cancers (Basel)* 12, 1488. doi: 10.3390/cancers12061488

Schwöppe, C., Kessler, T., Persigehl, T., Liersch, R., Hintelmann, H., Dreischaluck, J., et al. (2010). Tissue-factor fusion proteins induce occlusion of tumor vessels. *Thromb. Res.* 125(Suppl. 2), S143–S150.

Severin, S., Pollitt, A. Y., Navarro-Nunez, L., Nash, C. A., Mourao-Sa, D., Eble, J. A., et al. (2011). Syk-dependent phosphorylation of CLEC-2: a novel mechanism of hem-immunoreceptor tyrosine-based activation motif signaling. *J. Biol. Chem.* 286, 4107–4116.

Shoji, M., Hancock, W. W., Abe, K., Micko, C., Casper, K. A., Baine, R. M., et al. (1998). Activation of coagulation and angiogenesis in cancer: immunohistochemical localization in situ of clotting proteins and vascular endothelial growth factor in human cancer. *Am. J. Pathol.* 152, 399–411.

Simons, K., and Gerl, M. J. (2010). Revitalizing membrane rafts: new tools and insights. *Nat. Rev. Mol. Cell Biol.* 11, 688–699.

Spalton, J. C., Mori, J., Pollitt, A. Y., Hughes, C. E., Eble, J. A., and Watson, S. P. (2009). The novel Syk inhibitor R406 reveals mechanistic differences in the initiation of GPVI and CLEC-2 signaling in platelets. *J. Thromb. Haemost.* 7, 1192–1199.

Springer, T. A., Zhu, J., and Xiao, T. (2008). Structural basis for distinctive recognition of fibrinogen gammaC peptide by the platelet integrin alphaIIbbeta3. *J. Cell Biol.* 182, 791–800.

Stone, M. J., Ruf, W., Miles, D. J., Edgington, T. S., and Wright, P. E. (1995). Recombinant soluble human tissue factor secreted by *Saccharomyces cerevisiae* and refolded from *Escherichia coli* inclusion bodies: glycosylation of mutants, activity and physical characterization. *Biochem. J.* 310(Pt 2), 605–614.

Suzuki-Inoue, K. (2019). Platelets and cancer-associated thrombosis: focusing on the platelet activation receptor CLEC-2 and podoplanin. *Blood* 134, 1912–1918.

Suzuki-Inoue, K., Fuller, G. L., Garcia, A., Eble, J. A., Pohlmann, S., Inoue, O., et al. (2006). A novel Syk-dependent mechanism of platelet activation by the C-type lectin receptor CLEC-2. *Blood* 107, 542–549.

Swier, N., and Versteeg, H. H. (2017). Reciprocal links between venous thromboembolism, coagulation factors and ovarian cancer progression. *Thromb. Res.* 150, 8–18.

Swieringa, F., Spronk, H. M. H., Heemskerk, J. W. M., and Van Der Meijden, P. E. J. (2018). Integrating platelet and coagulation activation in fibrin clot formation. *Res. Pract. Thromb. Haemost.* 2, 450–460.

Tesselaar, M. E., Romijn, F. P., Van Der Linden, I. K., Bertina, R. M., and Osanto, S. (2009). Microparticle-associated tissue factor activity in cancer patients with and without thrombosis. *J. Thromb. Haemost.* 7, 1421–1423.

Theocharis, A. D., Skandalis, S. S., Gialeli, C., and Karamanos, N. K. (2016). Extracellular matrix structure. *Adv. Drug Deliv. Rev.* 97, 4–27.

Trousseau, A. (1865). Plegmasia alba dolens. *Lectures Clin. Med.* 5, 281–332.

Tsukiji, N., Osada, M., Sasaki, T., Shirai, T., Satoh, K., Inoue, O., et al. (2018). Cobalt hematoporphyrin inhibits CLEC-2-podoplanin interaction, tumor metastasis, and arterial/venous thrombosis in mice. *Blood Adv.* 2, 2214–2225.

Unruh, D., and Horbinski, C. (2020). Beyond thrombosis: the impact of tissue factor signaling in cancer. *J. Hematol. Oncol.* 13:93.

Vajen, T., Mause, S. F., and Koenen, R. R. (2015). Microvesicles from platelets: novel drivers of vascular inflammation. *Thromb. Haemost.* 114, 228–236.

van den Berg, Y. W., Osanto, S., Reitsma, P. H., and Versteeg, H. H. (2012). The relationship between tissue factor and cancer progression: insights from bench and bedside. *Blood* 119, 924–932.

van Golen, R. F., Stevens, K. M., Colarusso, P., Jaeschke, H., and Heger, M. (2015). Platelet aggregation but not activation and degranulation during the acute post-ischemic reperfusion phase in livers with no underlying disease. *J. Clin. Transl. Res.* 1, 107–115.

Versteeg, H. H. (2015). Tissue factor: old and new links with Cancer biology. *Semin. Thromb. Hemost.* 41, 747–755.

Versteeg, H. H., Schaffner, F., Kerver, M., Petersen, H. H., Ahamed, J., Felding-Habermann, B., et al. (2008). Inhibition of tissue factor signaling suppresses tumor growth. *Blood* 111, 190–199.

Vickers, J. D. (1998). In contrast to fibrinogen or fibrin, peptide and peptide mimetic binding to alphaIIbbeta3 (GPIIb-IIIa) does not cause outside-in signalling as judged by measurements of phosphatidylinositol 4,5-bisphosphate. *Platelets* 9, 390–394.

Wang, M., Zhao, J., Zhang, L., Wei, F., Lian, Y., Wu, Y., et al. (2017). Role of tumor microenvironment in tumorigenesis. *J. Cancer* 8, 761–773.

Wang, X., Liu, B., Xu, M., Jiang, Y., Zhou, J., Yang, J., et al. (2021). Blocking podoplanin inhibits platelet activation and decreases cancer-associated venous thrombosis. *Thromb. Res.* 200, 72–80.

Wang, Y., Gallant, R. C., and Ni, H. (2016). Extracellular matrix proteins in the regulation of thrombus formation. *Curr. Opin. Hematol.* 23, 280–287.

Ward, Y., Lake, R., Faraji, F., Sperger, J., Martin, P., Gilliard, C., et al. (2018). Platelets promote metastasis via binding tumor CD97 leading to bidirectional signaling that coordinates transendothelial migration. *Cell Rep.* 23, 808–822.

Watson, A. A., Christou, C. M., James, J. R., Fenton-May, A. E., Moncayo, G. E., Mistry, A. R., et al. (2009). The platelet receptor CLEC-2 is active as a dimer. *Biochemistry* 48, 10988–10996.

Watson, A. A., Eble, J. A., and O'callaghan, C. A. (2008). Crystal structure of rhodocytin, a ligand for the platelet-activating receptor CLEC-2. *Protein Sci.* 17, 1611–1616.

Wculek, S. K., and Malanchi, I. (2015). Neutrophils support lung colonization of metastasis-initiating breast cancer cells. *Nature* 528, 413–417.

Wechman, S. L., Emdad, L., Sarkar, D., Das, S. K., and Fisher, P. B. (2020). Vascular mimicry: triggers, molecular interactions and in vivo models. *Adv. Cancer Res.* 148, 27–67.

Wei, J., Hu, M., Huang, K., Lin, S., and Du, H. (2020). Roles of proteoglycans and glycosaminoglycans in Cancer development and progression. *Int. J. Mol. Sci.* 21:5983.

Wei, X., Chen, Y., Jiang, X., Peng, M., Liu, Y., Mo, Y., et al. (2021). Mechanisms of vasculogenic mimicry in hypoxic tumor microenvironments. *Mol. Cancer* 20:7.

White, J. G. (2000). EDTA-induced changes in platelet structure and function: clot retraction. *Platelets* 11, 49–55.

Wojtukiewicz, M. Z., Hempel, D., Sierko, E., Tucker, S. C., and Honn, K. V. (2015). Protease-activated receptors (PARs)–biology and role in cancer invasion and metastasis. *Cancer Metastasis Rev.* 34, 775–796.

Wojtukiewicz, M. Z., Hempel, D., Sierko, E., Tucker, S. C., and Honn, K. V. (2016). Thrombin-unique coagulation system protein with multifaceted impacts on cancer and metastasis. *Cancer Metastasis Rev.* 35, 213–233.

Wolf, M. J., Hoos, A., Bauer, J., Boettcher, S., Knust, M., Weber, A., et al. (2012). Endothelial CCR2 signaling induced by colon carcinoma cells enables extravasation via the JAK2-Stat5 and p38MAPK pathway. *Cancer Cell* 22, 91–105.

Wong, A. K. (2013). Platelet biology: the role of shear. *Expert Rev. Hematol.* 6, 205–212.

Wu, L., Saxena, S., Awaji, M., and Singh, R. K. (2019). Tumor-Associated neutrophils in Cancer: going pro. *Cancers (Basel)* 11:564.

Xiao, T., Takagi, J., Coller, B. S., Wang, J. H., and Springer, T. A. (2004). Structural basis for allostery in integrins and binding to fibrinogen-mimetic therapeutics. *Nature* 432, 59–67.

Xiong, F., Hausdorf, J., Niethammer, T. R., Jansson, V. A., and Klar, R. M. (2020). Temporal TGF-beta supergene family signalling cues modulating tissue morphogenesis: chondrogenesis within a muscle tissue model? *Int. J. Mol. Sci.* 21:4863.

Xiong, G., Chen, J., Zhang, G., Wang, S., Kawasaki, K., Zhu, J., et al. (2020). Hsp47 promotes cancer metastasis by enhancing collagen-dependent cancer cell-platelet interaction. *Proc. Natl. Acad. Sci. U S A.* 117, 3748–3758.

Yang, Y., Yang, Y., Yang, J., Zhao, X., and Wei, X. (2020). Tumor microenvironment in ovarian cancer: function and therapeutic strategy. *Front. Cell Dev. Biol.* 8:758. doi: 10.3389/fcell.2020.00758

Yeung, J., Li, W., and Holinstat, M. (2018). Platelet signaling and disease: targeted therapy for thrombosis and other related diseases. *Pharmacol. Rev.* 70, 526–548.

Zanotelli, M. R., and Reinhart-King, C. A. (2018). Mechanical forces in tumor angiogenesis. *Adv. Exp. Med. Biol.* 1092, 91–112.

Zhang, B., Pang, Z., and Hu, Y. (2020). Targeting hemostasis-related moieties for tumor treatment. *Thromb. Res.* 187, 186–196.

Zheng, Y., and Leftheris, K. (2020). Insights into protein-ligand interactions in integrin complexes: advances in structure determinations. *J. Med. Chem.* 63, 5675–5696.

Conflict of Interest: The authors declare that the research was conducted in the absence of any commercial or financial relationships that could be construed as a potential conflict of interest.

frontiers in Cell and Developmental Biology

REVIEW
published: 29 April 2021
doi: 10.3389/fcell.2021.655307

The Transcriptional Co-factor IRF2BP2: A New Player in Tumor Development and Microenvironment

*Tatiane P. Pastor, Barbara C. Peixoto and João P. B. Viola**

Program of Immunology and Tumor Biology, Brazilian National Cancer Institute (INCA), Rio de Janeiro, Brazil

Interferon regulatory factor 2-binding protein 2 (IRF2BP2) encodes a member of the IRF2BP family of transcriptional regulators, which includes IRF2BP1, IRF2BP2, and IRF2BPL (EAP1). IRF2BP2 was initially identified as a transcriptional corepressor that was dependent on Interferon regulatory factor-2 (IRF-2). The IRF2BP2 protein is found in different organisms and has been described as ubiquitously expressed in normal and tumor cells and tissues, indicating a possible role for this transcriptional cofactor in different cell signaling pathways. Recent data suggest the involvement of IRF2BP2 in the regulation of several cellular functions, such as the cell cycle, cell death, angiogenesis, inflammation and immune response, thereby contributing to physiological cell homeostasis. However, an imbalance in IRF2BP2 function may be related to the pathophysiology of cancer. Some studies have shown the association of IRF2BP2 expression in hematopoietic and solid tumors through mechanisms based on gene fusion and point mutations in gene coding sequences, and although the biological functions of these types of hybrid and mutant proteins are not yet known, they are thought to be involved in an increase in the likelihood of tumor development. In this review, we address the possible involvement of IRF2BP2 in tumorigenesis through its regulation of important pathways involved in tumor development.

Keywords: IRF2BP2, tumor suppressor, transcriptional regulation, tumor development, tumor microenvironment

OPEN ACCESS

Edited by:
Mariane Tami Amano, Hospital Sirio Libanes, Brazil

Reviewed by:
Guillaume Darrasse-Jeze, Université de Paris, France
Kenneth J. Gollob, AC Camargo Cancer Center, Brazil
Felipe Valenca Pereira, University of Colorado Denver, United States

****Correspondence:***
João P. B. Viola
jpviola@inca.gov.br

Specialty section:
This article was submitted to Molecular Medicine, a section of the journal Frontiers in Cell and Developmental Biology

Received: *18 January 2021*
Accepted: *06 April 2021*
Published: *29 April 2021*

Citation:
Pastor TP, Peixoto BC and Viola JPB (2021) The Transcriptional Co-factor IRF2BP2: A New Player in Tumor Development and Microenvironment. Front. Cell Dev. Biol. 9:655307. doi: 10.3389/fcell.2021.655307

INTRODUCTION

The interferon regulatory factor 2-binding protein (IRF2BP) family of transcription regulators includes IRF2BP1, IRF2BP2, and IRF2BPL (also known as EAPI – enhanced at puberty 1), all three of which are nuclear proteins. IRF2BP2 proteins were first identified *via* a yeast two-hybrid assay as nuclear transcription corepressors of interferon regulatory factor-2 (IRF-2) that inhibit both enhancer-activated and basal transcription. More recently, IRF2BP2 was identified as a transcriptional repressor in several other biological contexts that do not require IRF-2 participation, suggesting that IRF2BP2 has IRF-2-independent functions (Childs and Goodbourn, 2003).

Interferon regulatory factor 2-binding protein 2 is encoded by a gene located on chromosome 1q42.3 in humans and has two exons producing three alternatively spliced proteins, IRF2BP2A with 587 amino acids, IRF2BP2B with 571 amino acids and IRF2BP2C with 163 amino acids. IRF2BP2 isoforms A and B share high identity and display two conserved regions: a zinc finger domain at the N-terminus, which is missing in IRF2BP2 isoform C, and a CH3C4 real

interesting new gene (RING) domain at the C-terminus. The function of these domains in the IRF2BP2 isoforms is not fully understood, but both domains have been described as being important for their ability to mediate interactions between different proteins. Between these domains, there is a region formed by arginine and lysine residues (RKRK), with the nuclear localization signal (NLS), which is conserved among family members (Carneiro et al., 2011; Teng et al., 2011). Teng et al. (2011) showed that phosphorylation of Ser360 near the NLS, as identified in IRF2BP2 isoform A, favors IRF2BP2 nuclear localization (Teng et al., 2011).

The IRF2BP2 protein is observed in different organisms and is ubiquitously expressed in different normal and tumor cells and tissues, as determined through analyses of the transcriptome and proteome, as related by Fagerberg et al. (2014), that this transcriptional cofactor plays possible roles in different cell signaling pathways.

BIOLOGICAL FUNCTIONS OF IRF2BP2

Despite being identified as a transcriptional partner of IRF-2, the IRF2BP2 protein is also observed in organisms lacking this transcription factor, showing that this protein has IRF-2-independent functions through interactions with other partners involved in transcriptional regulation (Childs and Goodbourn, 2003). Although the majority of reports available in the literature propose a role for IRF2BP2 as a repressor in the regulation of diverse genes, some studies have shown that IRF2BP2 may also act as a positive regulator of gene expression (Teng et al., 2010; Chen et al., 2015; Cruz et al., 2017). Although IRF2BP2 is an important regulator of gene expression, the mechanisms by which IRF2BP2 mediates its repression or induction have not been established and may involve interactions with different proteins that vary according to the context.

Interferon regulatory factor 2-binding protein 2 is extensively involved in regulating gene expression and other biological processes, including metabolic syndrome, nervous diseases, immunodeficiency disorders, and cancer. Recent data suggest the participation of IRF2BP2 in controlling various cellular functions, such as cell proliferation (Koeppel et al., 2009; Secca et al., 2016; Manjur et al., 2019; Yao et al., 2019; Feng et al., 2020), apoptosis (Koeppel et al., 2009; Tinnikov et al., 2009; Yeung et al., 2011; Feng et al., 2020; Li et al., 2020), angiogenesis (Teng et al., 2010), cell migration (Manjur et al., 2019; Feng et al., 2020), cell differentiation (Stadhouders et al., 2015; Kim et al., 2019; Wang et al., 2020a), inflammation (Chen et al., 2015; Cruz et al., 2017; Hari et al., 2017; Feng et al., 2020; Li et al., 2020), and immune response (Blotta et al., 2009; Carneiro et al., 2011; Soliman et al., 2014; Dorand et al., 2016; Secca et al., 2016; Wu et al., 2019), contributing to physiological homeostasis and the hallmarks of oncogenesis (**Figure 1**). Different studies have shown the association of IRF2BP2 expression in hematopoietic malignancies and solid tumors, such as breast cancer, leukemia and chondrosarcoma, through mechanisms of gene fusion and point mutations in gene coding sequences, but its exact role and the regulatory mechanism in cancers have not been explored. This review focuses on the involvement of IRF2BP2 in tumorigenesis through the regulation of important pathways in tumor development.

IRF2BP2 IN CELL PROLIFERATION

Tissue homeostasis is characterized by a delicate balance between cell proliferation and death, and several signaling mechanisms determine whether a particular cell remains quiescent, proliferates or dies. Therefore, proliferation is an important part of cancer development and progression and manifests with altered expression and/or activity of cell cycle-related proteins (Malumbres and Barbacid, 2001; Caglar and Avci, 2020).

Several studies have demonstrated the important function of IRF2BP2 in controlling the cell cycle and cell proliferation. Koeppel et al. (2009) identified *IRF2BP2* as a novel gene directly targeted by the p53 protein, influencing cell fate. In this study, it was shown that in response to genotoxic stress, p53 binds to an upstream site in the *IRF2BP2* promoter and activates its expression. Consequently, IRF2BP2 overexpression represses the p53-mediated transactivation of the p21 gene and can induce changes in the cell cycle of living cells, mainly changing the number of cells in the S-phase population, which decreases after actinomycin D (Act. D) treatment, favoring cell cycle arrest and survival of U2OS osteosarcoma cells (Koeppel et al., 2009).

Viola's study demonstrated that the ectopic overexpression of IRF2BP2 in primary CD4 T cells leads to a decrease in cell proliferation upon activation and reduces the expression of the activation markers CD69 and CD25 *in vitro*. In addition, CD4 T cells overexpressing IRF2BP2 were transferred to sublethally irradiated C57/BL6 recipient mice to observe their expansion *in vivo*. The lymphocytes transduced with *IRF2BP2* showed reduced cell expansion, indicating that this protein had a negative effect on the survival of these cells (Secca et al., 2016).

Manjur et al. (2019) analyzed the role of IRF2BP2 in the regulation of glucocorticoid (GC) signaling. For this study, IRF2BP2 was silenced by siRNA in HEK293-GR cells, and gene expression was analyzed using RNA-seq. IRF2BP2 modulated the transcription of approximately one half of the GC-responsive genes, leading to a reduction in the proliferation of HEK293-GR cells. To investigate the predicted effect of IRF2BP2 silencing on HEK293-GR proliferation, a live-cell imaging assay was performed, and the results confirmed those obtained *via* RNA-seq, suggesting that IRF2BP2 acts as a positive regulator of cell proliferation and is part of the GR transcription regulatory complex and functions as a novel coregulator of a subset of target genes associated with glucocorticoid functions (Manjur et al., 2019).

Another study found that IRF2BP2 is a direct target of components in the Hippo pathway, an evolutionarily conserved regulator of cell growth. Interestingly, IRF2BP2 overexpression in two hepatocellular carcinoma (HCC) cell lines (HepG2 and Huh7 cells) negatively regulated YAP activity and decreased the expression levels of YAP target genes. An MTT analysis of cell proliferation and a colony formation assay showed that cells stably overexpressing IRF2BP2 exhibited suppressed growth and reduced colony formation ability, respectively. In addition,

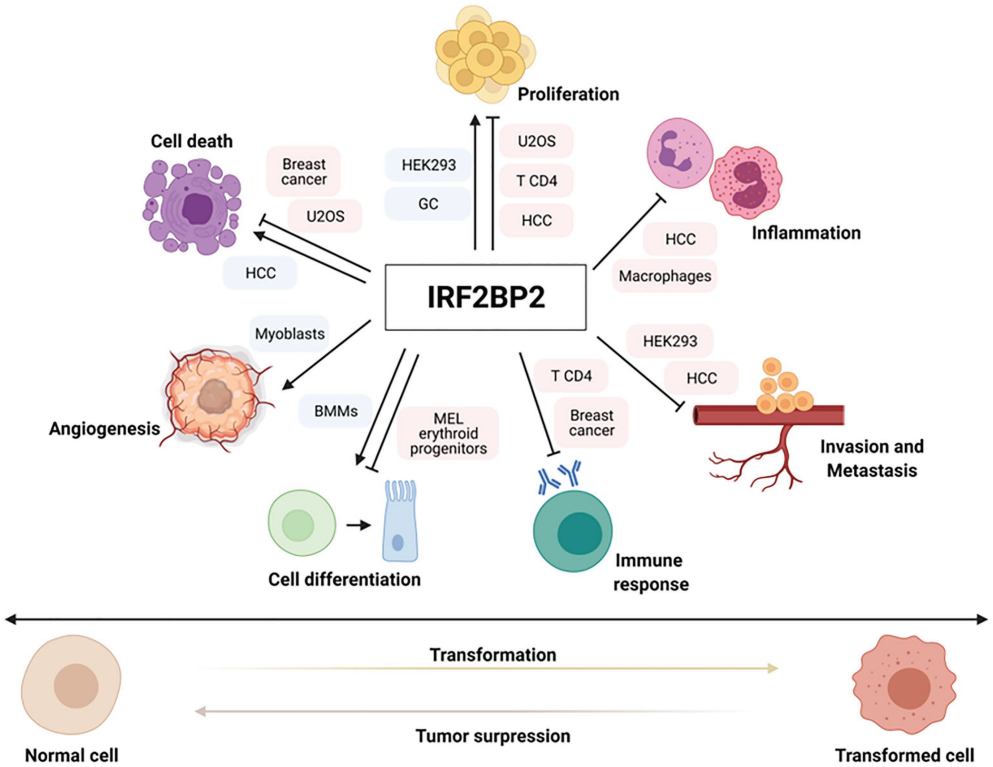

FIGURE 1 | Important pathways for tumor development are regulated by interferon regulatory factor 2-binding protein 2 (IRF2BP2). IRF2BP2 proteins are involved in regulating positive or negative expression of genes related to various hallmarks of oncogenesis, such as cell proliferation, apoptosis, cell differentiation, angiogenesis, immune response, inflammation and invasion/metastasis in normal and cancer setting. Boxes indicate normal and tumor cells where IRF2BP2 protein acts as a positive (blue) or negative (red) regulator of different cell functions.

HCC cells overexpressing IRF2BP2 were inoculated in the flanks of nude mice, and interestingly, IRF2BP2 overexpression failed to lead to tumors formation, compared to their formation in control groups. To confirm these results, the authors examined the loss-of-function phenotypes of IRF2BP2 in HepG2 cells. IRF2BP2-deficient (IRF2BP2−/−) cells were established by the CRISPR-CAS9 technique. IRF2BP2 depletion led to enhanced cell growth and colony formation and promoted HepG2 xenograft tumor growth. Taken together, these results showed that IRF2BP2 exhibits tumor-suppressor activity in the liver, inhibiting liver cancer cell growth and tumor formation (Feng et al., 2020).

On the other hand, recent study showed an opposite effect of IRF2BP2 on cell proliferation. MTT and colony formation assay results suggested that knocking down IRF2BP2 by siRNAs significantly decreased the proliferation and colony formation rates of human gastric (GC) cell lines. Additionally, GC cells expressing IRF2BP2 shRNA were inoculated subcutaneously in mice to construct xenograft models, and the results showed that knocking down IRF2BP2 significantly inhibited tumor growth. This study demonstrated that IRF2BP2 knockdown decreased cell proliferation by inhibiting the binding of TEAD4 to YAP1, which then could no longer promote the transcription of genes downstream of YAP1, such as CTCF, an important oncogene related to the promotion of GC cell proliferation (Yao et al., 2019). It important to note that, the differences in cellular proliferation phenotypes observed in previous studies may be associated with the different interaction partners and/or target genes of the IRF2BP2, which may be involved with the type of cell and tumor involved.

Furthermore, Barysch et al. (2021) investigated the functional consequences of endothelial growth factor (EGF)-dependent deSUMOylation of IRF2BP2 protein. They demonstrated that IRF2BP2 protein lost SUMO upon EGF treatment in HeLa cells and this deSUMOylation is very transient. Two SUMO motifs that were conserved within the family IRF2BP have been identified, one of which is located in the C-terminal region. IRF2BP2 knockdown in HeLa cells led to an upregulation of EGFR which may contribute to enhanced proliferation in response to EGF, a potent regulator of cellular growth as well as in cancer progression (Barysch et al., 2021).

IRF2BP2 IN THE REGULATION OF APOPTOSIS

To prevent cell proliferation, programmed cell death processes follow ordered sequences of events that lead to cell death. The process of programmed cell death, or apoptosis, is generally characterized by distinct morphological characteristics and is considered a vital component of various processes, including

normal cell turnover. However, inappropriate apoptosis is a factor in many human conditions, including different types of cancer (Elmore, 2007).

Koeppel et al. (2009) showed that IRF2BP2, in addition to inhibiting the expression of the p21 gene, also acts as a repressor of p53-mediated transactivation of the BAX gene, a potent proapoptotic gene. U2OS cells were transfected with IRF2BP2 and treated with doxorubicin to induce apoptosis. In the *IRF2BP2*-transfected cells, treatment with doxorubicin failed to induce an increase in the population of apoptotic cells (as indicated by the sub-G1 population). To investigate the function of IRF2BP2 in apoptosis under physiological conditions, endogenous levels of IRF2BP2 were downregulated by siRNAs in U2OS cells. Upon the treatment with Act. D and doxorubicin, the IRF2BP2-knockdown cells showed high levels of activated Caspase 3. According to the authors, these results suggest that IRF2BP2 is an important factor in the determination between cell survival and cell death (Koeppel et al., 2009).

Interferon regulatory factor 2-binding protein 2 isoform A was identified in a yeast double-hybrid assay, revealing its interaction with NRIF3, which is a proapoptotic factor in breast cancer cells. In this study, different breast cancer cell lines were transfected with a siRNA that targets IRF2BP2A mRNA, and all of the cell lines exhibited an increased apoptosis rate, suggesting that IRF2BP2A acted to selectively repress proapoptotic genes and thus functioned as an anti-apoptotic factor (Tinnikov et al., 2009). In 2011, the same group showed that IRF2BP2A performs this function by suppressing the proapoptotic gene FASTKD2. Through chromatin immunoprecipitation and mass spectrometry analyses, the IRF2BP2A protein was identified as one of the members of a large protein complex that also includes IRF2BP1 and EAP1 proteins. These proteins interact through their C4 zinc finger domains and bind to DNA near the transcription region of the FASTKD2 gene, repressing its transactivation and thus selectively modulating the cell survival and apoptosis of breast cancer cells (Yeung et al., 2011).

Feng et al. (2020) showed that IRF2BP2 overexpression not only inhibited cell growth and tumor formation but also induced apoptosis, as indicated by the elevated expression of cleaved PARP in HCC cell lines, suggesting that this protein plays the role of tumor suppressor in these cells (Feng et al., 2020). A recent study reported that IRF2BP2 overexpression significantly suppressed cell death in lipopolysaccharide (LPS)-challenged mice, which was indicated by the reduced expression of proapoptotic Bax and cleaved caspase 3 and increased the expression of antiapoptotic Bcl2 (Li et al., 2020).

IRF2BP2 IN ANGIOGENESIS

Angiogenesis is an important factor in the progression of cancer, and in the absence of vascular support, tumor may become necrotic or and tumor cells may even become apoptotic. Angiogenesis is stimulated when tumor tissues require nutrients and oxygen and is necessary for the metastatic spread of cancerous tissue (Nishida et al., 2006). Angiogenesis is regulated by both activator and inhibitor molecules, including vascular EGF (VEGF), a powerful angiogenic agent in neoplastic tissues, as well as in normal tissues (Liekens et al., 2001).

A study developed by Stewart's group identified IRF2BP2 as a novel coactivator of VEGFA expression in muscle cells. It was demonstrated that IRF2BP2 participates in a transcriptional complex that includes TEAD4/VGLL4 proteins and coactivates VEGFA promoter expression. Interestingly, the co-expression of IRF2BP2 and TEAD1 was sufficient to coactivate the VEGFA promoter in myoblasts. Moreover, it was observed that IRF2BP2 protein levels are increased in both ischemic skeletal and cardiac muscle, showing that IRF2BP2 plays an important role in the regulation of tissue angiogenesis (Teng et al., 2010).

IRF2BP2 IN THE REGULATION OF INFLAMMATION

The inflammatory process is a cofactor in carcinogenesis. The inflammatory microenvironment of tumors is characterized by the presence of host leucocytes both in the supporting stroma and in tumor areas. Tumor-infiltrating lymphocytes may contribute to cancer growth and metastasis and to the immunosuppression associated with malignant disease (Coussens and Werb, 2002).

Several studies have demonstrated the importance of IRF2BP2 in regulating the inflammatory process. Feng et al. (2020) demonstrated that hepatocyte-specific IRF2BP2-deficient mouse lines (IRF2BP2-HKO cells) showed hepatic steatosis, insulin resistance, and inflammation. Real-time PCR analysis of liver tissues in high-fat diet groups revealed that the mRNA levels of inflammatory cytokines, such as TNF, were higher in the IRF2BP2-HKO mice. In contrast to these results, IRF2BP2 overexpression significantly alleviated hepatic and systemic inflammation. Moreover, complete depletion of IRF2BP2 in human hepatocytes (IRF2BP2-KO cells) led to an increase in the mRNA levels of inflammatory cytokines. This study provided evidence that IRF2BP2 regulates hepatocyte inflammation by repressing activating transcription factor 3 (ATF3) gene transcription through physical DNA binding; however, the mechanisms by which IRF2BP2 represses ATF3 gene expression are not yet clear (Feng et al., 2020).

A study developed by Chen et al. (2015) demonstrated the important function of IRF2BP2 in macrophage-mediated inflammation. They generated animals with IRF2BP2-deficient macrophages and observed the participation of IRF2BP2 in the polarization of macrophages. IRF2BP2 overexpression is involved in the differentiation of M2 type macrophages through the regulation of the expression of the anti-inflammatory transcription factor Krüppel-like factor 2 (KLF2). In addition, mice with IRF2BP2-deficient macrophages developed severe atherosclerosis (Chen et al., 2015). In a more recent study from the same group, it was observed that the loss of IRF2BP2 in microglia was associated with the reduced activation of many M2 anti-inflammatory markers and increased expression of inflammatory cytokines. IRF2BP2 is necessary to mediate the anti-inflammatory and protective effects of IFN-β cytokines on stroke injury (Cruz et al., 2017), and IRF2BP2-deficient

microglia block the anxiolytic effect of enhanced postnatal care (EPC) by reducing inflammatory cytokine expression in the hypothalamus (Hari et al., 2017).

It is important to highlight the study performed by Li et al. (2020) that reported IRF2BP2 as a negative regulator of septic cardiomyopathy. Overexpression of IRF2BP2 in the heart inhibited NF-κB signaling and blocked the production of proinflammatory cytokines. Additionally, IRF2BP2 reduced inflammatory cell infiltration by suppressing the accumulation of CD11b-positive cells in the heart after lipopolysaccharide (LPS) treatment (Li et al., 2020).

IRF2BP2 IN CELL MIGRATION AND INVASION

Cell migration is required for many biological processes, such as tissue repair and regeneration. Aberrant regulation of cell migration drives the progression of many diseases, including cancer invasion and metastasis. Malignant cancer cells utilize their intrinsic migratory ability to invade adjacent tissues and the vasculature and ultimately to metastasize (Yamaguchi and Condeelis, 2007).

Manjur et al. (2019) used RNA-seq data and wound healing assays to demonstrate that the silencing of IRF2BP2 increased the migration of HEK293 cells upon dexamethasone treatment (Manjur et al., 2019). On the basis of transwell and wound healing assays, another study showed that IRF2BP2 overexpression inhibited the migration of HCC cells. On the other hand, knocking out IRF2BP2 promoted cell migration and invasion. Together, these studies showed that IRF2BP2 may play an important role in controlling cell mobility (Feng et al., 2020).

IRF2BP2 IN THE REGULATION OF CELL DIFFERENTIATION

Cell differentiation constitutes a complex biological process that regulates the expression of a large number of genes linked to the control of cell proliferation. Carcinogenesis, in turn, is characterized by the production of cell clones with genetic and epigenetic changes, which mainly result in loss of control over cell differentiation and proliferation (Chen and Dent, 2014).

Stadhouders et al. (2015) demonstrated that IRF2BP2 appears to be important for erythropoiesis and erythroid gene regulation *in vitro* and *in vivo*. IRF2BP2 interacts with the transcription factor ETO2 and favors its repressive activity in erythroid progenitor cells. The ETO2-IRF2BP2 axis recruits the NCOR1/SMRT corepressor complex and suppresses the expression of the vast majority of erythroid genes and pathways involved in terminal differentiation. The functional relevance of IRF2BP2 repressive activity was confirmed *in vivo*. It was observed that homozygous IRF2BP2-deficient mice have a lethal phenotype, dying during pregnancy or in the first weeks of life due to severe growth retardation (Stadhouders et al., 2015).

Interferon regulatory factor 2-binding protein 2 was identified as a novel determinant in the fate of neutrophil-macrophage progenitor cells, favoring macrophage development during definitive myelopoiesis in zebrafish. IRF2BP2-deficient embryos showed a significant decrease in neutrophil markers and an increase in monocyte and macrophage markers. IRF2BP2 acts as a direct target of C/ebpa and represses pu.1 gene transcription by binding directly to its promoter, and the repressive activity of IRF2BP2 is dependent on SUMOylation (Wang et al., 2020a).

A study developed by Kim et al. (2019) revealed that IRF2BP2 controls osteoclast and osteoblast differentiation *via* KLF2. IRF2BP2 overexpression increased KLF2 expression, significantly inhibited osteoclast differentiation and promoted osteoblast differentiation in bone marrow-derived macrophage cells (BMMs). Taken together, these results suggest that the IRF2BP2/KLF2 axis regulates bone homeostasis and may be a potential therapeutic target for various bone diseases (Kim et al., 2019).

IRF2BP2 IN CANCER IMMUNOMODULATION

Immune checkpoints are known to be essential regulators of immune responses. These factors are related to tumor cell escape mechanisms, for example, through the skewed regulation of the programmed death-ligand 1/programmed cell death 1 (PD-L1/PD-1) axis (Garcia-Diaz et al., 2017); this immune checkpoint promotes a break in T lymphocyte activation, leading to immune response suppression and culminating in the impairment of cytokine production and lymphocyte cytolytic activity (Garcia-Diaz et al., 2017). PD-L1 overexpression is a relevant tumor feature in several tumor types. PD-L1 is a transmembrane protein that is regulated transcriptionally by IRF-1 in response to high IFN-γ levels. IRF-1 is an IRF-2 antagonist, and these transcription factors are described as PD-L1 positive and negative regulators, respectively (Dorand et al., 2016). The tumor microenvironment is an inflammatory milieu that contains cytokines, such as the TNF and IFN family members IL-6 and IL-17. This inflammatory microenvironment contributes to tumor initiation and establishment (Zhang et al., 2018). In addition, IFN-γ in the microenvironment induces IRF-1-mediated PD-L1 transcription, establishing a critical tumor immune escape mechanism through the PD-L1/PD-1 axis (Dorand et al., 2016).

Dorand et al. (2016) observed an IRF-2 and IRF2BP2 increase in CD4 T cells deficient in Cdk5, a serine–threonine kinase that is highly active in many cancers and important in immune evasion of tumor cells. An IRF2BP2 increase is followed by hyperphosphorylation, which is essential for its nuclear localization and function (Dorand et al., 2016). Furthermore, the same study identified IRF2BP2 as an indirect PD-L1 repressor *via* IRF-2 increases and posttranslational IRF2BP2 modification, even in the presence of persistent IFN-γ stimuli (Dorand et al., 2016). Moreover, the relationship between PD-L1 and IRF2BP2 in cancer cells was also investigated by Soliman et al. (2014), who associated low IRF2BP2 levels with high PD-L1 expression in breast cancer cells (Soliman et al., 2014). Although many studies have demonstrated that IRF2BP2 participates in PD-L1 regulation, the mechanism involved in this pathway

remains unclear. It must be further investigated due to its potential relevance and putative applicability in cancer immunotherapy; for example, the induction of PD-L1 downregulation may control tumor development.

Additionally, VGLL4 was recently associated with IRF2BP2 in PD-L1 expression modulation. VGLL4 is a transcriptional suppressor that competes with YAP to bind TEADs, thereby restraining YAP-induced overgrowth and tumorigenesis. Furthermore, VGLL4 promotes IRF2BP2 stability, and *Vgll4* deficiency is followed by decreased PD-L1 expression (Wu et al., 2019). IRF2BP2 absence prevents the *Cd274* transcription induced by IFN-γ, and consequently, its protein levels are reduced. Thus, VGLL4 appears to be a PD-L1 expression regulator and plays a key role in the VGLL4 and YAP association in tumor immunity modulation. Therefore, the authors suggest that IFN-γ stimulation promotes IRF-2 release from the PD-L1 promoter to favor IRF2BP2-IRF-2 binding, allowing PD-L1 expression (Wu et al., 2019). However, the mechanisms of this regulation need to be further investigated to improve cancer therapy. For instance, VGLL4 is used as an inhibition target to promote indirect *Cd274* transcription repression through IRF2BP2 stabilization.

Furthermore, another protein associated with several tumors is the transcription factor NFAT. The NFAT family is characterized as inducers of several cellular processes, including lymphocyte development, activation, and differentiation (Rao et al., 1997). NFAT1-5 expression was identified at the mRNA and protein levels in several cell types in different tumors (Mancini and Toker, 2009). The NFAT family is expressed in several cancer cell types and plays roles in survival, invasive migration, angiogenesis, and inflammatory microenvironment maintenance (Ryeom et al., 2008). In breast cancer cells, a member of the NFAT family, NFAT1, is ubiquitinated by the E3 ubiquitin ligase murine double minute 2 (MDM2) downstream of Akt and GSK-3 signaling (Wang et al., 2020b). Activated NFAT1 promotes the migration and invasion of breast cancer cells *in vitro* (Jauliac et al., 2002). Therefore, our group has identified IRF2BP2 as an NFAT1 protein interaction partner. Ectopic IRF2BP2 expression in CD4 T cells represses IL-2 and IL-4-induced NFAT1-mediated transcription; however, although these data suggest IRF2BP2 is an important immune modulator, the mechanisms involved in these processes are unclear (Carneiro et al., 2011).

Based on the importance of NFAT1 in the immune response and tumor cells, it is crucial to elucidate the repressor mechanisms mediated by IRF2BP2. Our group also demonstrated that IRF2BP2 overexpression in CD4 T lymphocytes repressed STAT5 phosphorylation and the expression of the IL-2 high-affinity receptor α-chain (CD25). Moreover, IRF2BP2 downregulates CD69 expression. Taken together, these data demonstrated that IRF2BP2 regulating CD4 T cell activation by repressing IL-2 signaling, and restraining CD4 T cells clonal expansion (Secca et al., 2016).

To investigate new antigens capable of inducing a proper and efficient immune response and cell transformation control, Blotta et al. (2009) performed a screening of a recombinant cDNA expression library from the serum of patients with monoclonal gammopathy of undetermined significance (MGUS). IRF2BP2 was identified among these newly tracked antigens. Nonetheless, the mechanisms involved in lining IRF2BP2 expression to the malignancy of plasma cells during the evolution from MGUS to multiple myeloma (MM) were not explored (Blotta et al., 2009).

These data are driving substantial demand for investigations of IRF2BP2 in cancer and immunological contexts. We know that IRF2BP2 represses NFAT1 transcriptional activity, inhibits STAT5 phosphorylation, downregulates CD69, and indirectly re-primes PD-L1 transcription in Cdk5-deficient T CD4 cells, and plays other roles (**Figure 2**). Together, these findings indicate roles for IRF2BP2 in the cancer immune response and cancer

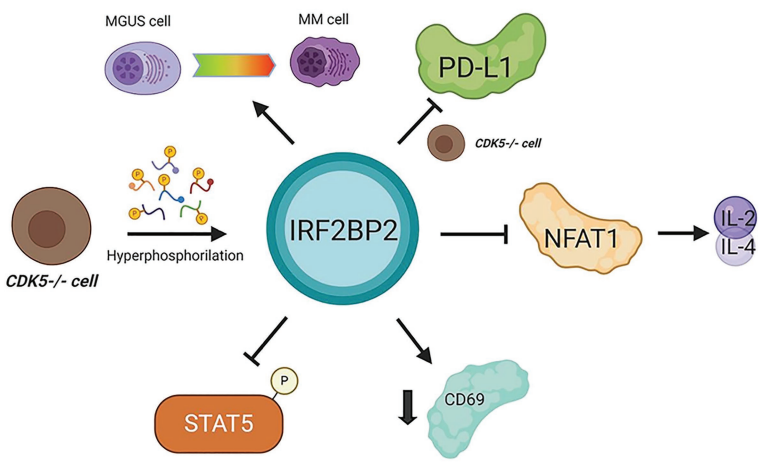

FIGURE 2 | Interferon regulatory factor 2-binding protein 2 in cancer immunomodulation. IRF2BP2 was described as being involved in monoclonal gammopathy of undetermined significance (MGUS) transformation to multiple myeloma (MM) cells. When CDK5 is depleted programmed death-ligand 1 (PD-L1) is inhibited. In CD4 T lymphocytes, IRF2BP2 is associated with restraining the IL-2 and IL-4 transcription mediated by NFAT1, decreasing the CD69 marker levels and inhibiting STAT5 phosphorylation. CDK5 depletion leads to IRF2BP2 hyperphosphorylation. MGUS, monoclonal gammopathy of undetermined significance; MM, multiple myeloma.

response, and this association must be elucidated. Here, we instigate a provocative and needed challenge to investigate this relationship more deeply.

ROLE OF IRF2BP2 AND ITS GENETIC VARIATIONS IN THE DEVELOPMENT OF TUMOR

The identification of molecular mechanisms and gene expression profiles necessary for tumor development and maintenance are fundamental and contribute to the diagnosis, prognosis and possible therapeutic interventions of cancer.

Some studies have reported the participation of IRF2BP2 in the development of different kinds of cancer (**Figure 3**) through gene fusion, copy number variations and mutations. To date, some reports have published studies on a novel fusion gene important for acute promyelocytic leukemia (APL) development. APL is characterized by the fusion of RARA with PML; however, a rare variant of this fusion gene, IRF2BP2-RARA, was identified in APL patients. This fusion gene caused some unusual clinical features and influenced the response to conventional treatment with all-trans-retinoic acid (ATRA; Yin et al., 2015; Shimomura et al., 2016; Jovanovic et al., 2017; Mazharuddin et al., 2018; Liu et al., 2019).

Furthermore, a newly discovered fusion of genes encoding IRF2BP2 and the transcription factor CDX1 was reported in mesenchymal chondrosarcomas. This in-frame t(1;5)(q42;q32) fusion results in an IRF2BP2-CDX1 translocation between exon 1 of the IRF2BP2 gene on chromosome 1 and intron 1 of the CDX1 gene on chromosome 5; however, the biological implications of this predicted fusion gene remain unknown (Nyquist et al., 2012).

Fusion involving the IRF2BP2 gene has also been identified in lung adenocarcinoma. Through next-generation sequencing, tumor samples were subjected to mutational profiling, and an in-frame gene rearrangement involving IRF2BP2 exon 1 and NTRK1 exons 8–16 was identified. No other oncogenic alterations were identified, supporting the idea that the IRF2BP2-NTRK1 fusion gene acts as a potent oncogenic driver (Wang et al., 2019). In thyroid carcinoma, a kinase involving IRF2BP2-NTRK1 fusion was found in one patient (Chu et al., 2020).

A study by He et al. (2020) identified IRF2BP2 as a novel triple-negative breast cancer (TNBC) candidate driver gene by integrating DNA copy number changes and mRNA expression omics data. The biological function of IRF2BP2 in controlling TNBC cell proliferation was assessed by siRNA-mediated loss-of-function screening of two TNBC cell lines (BT549 and SUM149T cells), and the results showed that IRF2BP2 is important in promoting proliferation in TNBC cells. In addition, copy number gain (CNG) recurrence of IRF2BP2 was found in 10/20 TNBC cell lines, indicating that this gene exhibited CNG/amplification and high expression in breast tumors (He et al., 2020).

Mutations in the IRF2BP2 gene have also been identified in primary central nervous system lymphoma (PCNSL). IRF2BP2 was sequenced to determine the coding exons by pyrosequencing, and somatic variations (nonsense mutations) were found in 14% of the PCNSL cases (Bruno et al., 2014). Alterations in the IRF2BP2 gene were predicted to be a potential prognostic markers and therapeutic targets in the treatment and management of multiple myeloma (Ni et al., 2012). A chromosomal gain was identified at region 1q42.3, which encodes IRF2BP2, in six of eight MM patients with the BCL1/JH t(11;14) translocation gene, with high penetrance (75%). Although the expression of IRF2BP2 at the mRNA level was not investigated, chromosome

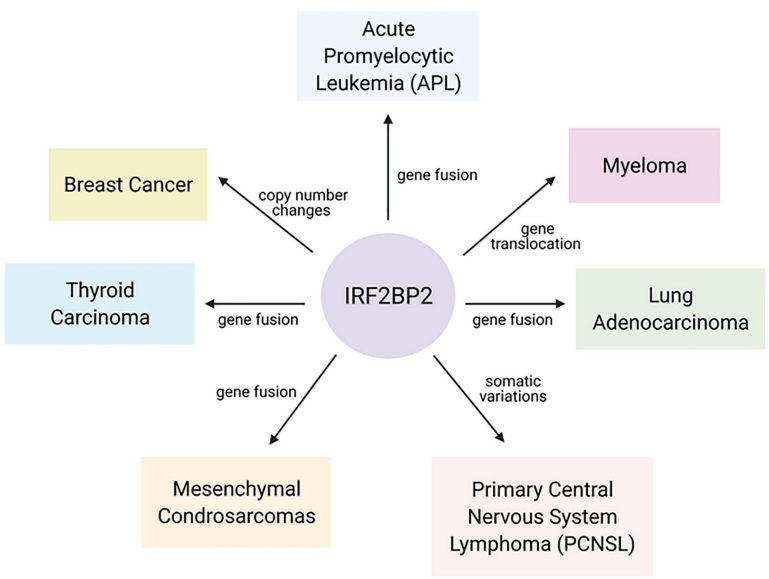

FIGURE 3 | Interferon regulatory factor 2-binding protein 2 in the malignancy of hematopoietic and solid tumors. Gene fusion, copy number changes and mutations in IRF2BP2 coding sequences were found in different kinds of cancer and are linked to an increased probability of cancer development.

1q gain is frequently associated with poor prognosis for myeloma patients (Ni et al., 2012).

CONCLUSION AND PERSPECTIVES

Initially, IRF2BP2 was described as a nuclear protein that interacts with IRF-2, although it has IRF-2-independent functions. Recently, IRF2BP2 has emerged as an important novel transcriptional cofactor in different biological systems, acting as a positive and negative regulator of gene expression. Although the IRF2BP2 protein is an important regulator of gene expression, little is known about how it exerts control. The details of IRF2BP2 regulation and the mechanism by which this protein regulates gene expression will be essential to understand its role in different biological processes. Recent data suggest the participation of IRF2BP2 in controlling various hallmarks of oncogenesis, acting as a tumor suppressor or oncogene depending on the cellular context and show the association of the expression of IRF2BP2 in hematopoietic and solid tumors. The details of IRF2BP2 regulation and the mechanisms involved in the relationship between the expression of IRF2BP2 and cell malignancy are not yet fully understood, and it is of great interest to understand how it influences the transcription of important genes for tumor development.

AUTHOR CONTRIBUTIONS

TP and BP reviewed the literature and wrote the manuscript. JV wrote and reviewed the manuscript. All authors contributed to the article and approved the submitted version.

FUNDING

This work was supported by grants from CNPq to JV (408127/2016-3 and 307042/2017-0) and FAPERJ (203.007/2016 and 202.640/2019).

ACKNOWLEDGMENTS

Work in the JV laboratory was supported by grants from Fundação de Amparo à Pesquisa do Estado do Rio de Janeiro (FAPERJ), Conselho Nacional de Desenvolvimento Tecnológico e Científico (CNPq), and Coordenação de Aperfeiçoamento de Pessoal de Nível Superior (CAPES). TP and BP were supported by fellowships from Instituto Nacional de Câncer (INCA).

REFERENCES

Barysch, S. V., Stankovic-Valentin, N., Miedema, T., Karaca, S., Doppel, J., Achour, T. N., et al. (2021). Transient deSUMOylation of IRF2BP proteins controls early transcription in EGFR signaling. *EMBO Rep.* 22:e49651. doi: 10.15252/embr.201949651

Blotta, S., Tassone, P., Prabhala, R. H., Tagliaferri, P., Cervi, D., Amin, S., et al. (2009). Identification of novel antigens with induced immune response in monoclonal gammopathy of undetermined significance. *Blood* 114, 3276–3284. doi: 10.1182/blood-2009-04-219436

Bruno, A., Boisselier, B., Labreche, K., Marie, Y., Polivka, M., Jouvet, A., et al. (2014). Mutational analysis of primary central nervous system lymphoma. *Oncotarget* 5, 5065–5075. doi: 10.18632/oncotarget.2080

Caglar, H., and Avci, C. (2020). Alterations of cell cycle genes in cancer: unmasking the role of cancer stem cells. *Mol. Biol. Rep.* 47, 3065–3076. doi: 10.1007/s11033-020-05341-6

Carneiro, F. R., Ramalho-Oliveira, R., Mognol, G. P., and Viola, J. P. (2011). Interferon regulatory factor 2 binding protein 2 is a new NFAT1 partner and represses its transcriptional activity. *Mol. Cell. Biol.* 31, 2889–2901. doi: 10.1128/MCB.00974-10

Chen, T., and Dent, S. (2014). Chromatin modifiers: regulators of cellular differentiation. *Nat. Rev. Genet.* 15, 93–106. doi: 10.1038/nrg3607

Chen, H. H., Keyhanian, K., Zhou, X., Vilmundarson, R. O., Almontashiri, N. A. M., Cruz, S. A., et al. (2015). IRF2BP2 reduces macrophage inflammation and susceptibility to atherosclerosis. *Circ. Res.* 117, 671–683. doi: 10.1161/CIRCRESAHA.114.305777

Childs, K. S., and Goodbourn, S. (2003). Identification of novel co-repressor molecules for interferon regulatory factor-2. *Nucleic Acids Res.* 31, 3016–3026. doi: 10.1093/nar/gkg431

Chu, Y. H., Wirth, L. J., Farahani, A. A., Nosé, V., Faquin, W. C., Dias-Santagata, D., et al. (2020). Clinicopathologic features of kinase fusion-related thyroid carcinomas: an integrative analysis with molecular characterization. *Mod. Pathol.* 33, 2458–2472. doi: 10.1038/s41379-020-0638-5

Coussens, L., and Werb, Z. (2002). Inflammation and cancer. *Nature* 420, 860–867. doi: 10.1038/nature01322

Cruz, S. A., Hari, A., Qin, Z., Couture, P., Huang, H., Lagace, D. C., et al. (2017). Loss of IRF2BP2 in microglia increases inflammation and functional deficits after focal ischemic brain injury. *Front. Cell. Neurosci.* 11:201. doi: 10.3389/fncel.2017.00201

Dorand, R. D., Nthale, J., Myers, J. T., Barkauskas, D. S., Avril, S., Chirieleison, S. M., et al. (2016). Cdk5 disruption attenuates tumor PD-L1 expression and promotes antitumor immunity. *Science* 353, 399–403. doi: 10.1126/science.aae0477

Elmore, S. (2007). Apoptosis: a review of programmed cell death. *Toxicol. Pathology* 35, 495–516. doi: 10.1080/01926230701320337

Fagerberg, L., Hallström, B. M., Oksvold, P., Kampf, C., Djureinovic, D., Odeberg, J., et al. (2014). Analysis of the human tissue-specific expression by genome-wide integration of transcriptomics and antibody-based proteomics. *Mol. Cell. Proteomics* 13, 397–406. doi: 10.1074/mcp.M113.035600

Feng, X., Lu, T., Li, J., Yang, R., Hu, L., Ye, Y., et al. (2020). The tumor suppressor interferon regulatory factor 2 binding protein 2 regulates hippo pathway in liver cancer by a feedback loop in mice. *Hepatology* 71, 1988–2004. doi: 10.1002/hep.30961

Garcia-Diaz, A., Shin, D. S., Moreno, B. H., Saco, J., Escuin-Ordinas, H., Rodriguez, G. A., et al. (2017). Interferon receptor signaling pathways regulating PD-L1 and PD-L2 expression. *Cell Rep.* 19, 1189–1201. doi: 10.1016/j.celrep.2017.04.031

Hari, A., Cruz, S. A., Qin, Z., Couture, P., Vilmundarson, R. O., Huang, H., et al. (2017). IRF2BP2-deficient microglia block the anxiolytic effect of enhanced postnatal care. *Sci. Rep.* 7:9836. doi: 10.1038/s41598-017-10349-3

He, J., McLaughlin, R., van der Beek, L., Canisius, S., Wessels, L., Smid, M., et al. (2020). Integrative analysis of genomic amplification-dependent expression and loss-of-function screen identifies ASAP1 as a driver gene in triple-negative breast cancer progression. *Oncogene* 39, 4118–4131. doi: 10.1038/s41388-020-1279-3

Jauliac, S., López-Rodriguez, C., Shaw, L. M., Brown, L. F., Rao, A., and Toker, A. (2002). The role of NFAT transcription factors in integrin-mediated carcinoma invasion. *Nat. Cell Biol.* 4, 540–544. doi: 10.1038/ncb816

Jovanovic, J. V., Chillón, M. C., Vincent-Fabert, C., Dillon, R., Voisset, E., Gutiérrez, N. C., et al. (2017). The cryptic IRF2BP2-RARA fusion transforms hematopoietic stem/progenitor cells and induces retinoid-sensitive acute promyelocytic leukemia. *Leukemia* 31, 747–751. doi: 10.1038/leu.2016.338

Kim, I., Kim, J. H., Kim, K., Seong, S., and Kim, N. (2019). The IRF2BP2-KLF2 axis regulates osteoclast and osteoblast differentiation. *BMB Rep.* 52, 469–474. doi: 10.5483/BMBRep.2019.52.7.104

Koeppel, M., van Heeringen, S. J., Smeenk, L., Navis, A. C., Jansen-Megens, E. M., and Lohrum, M. (2009). The novel p53 target gene IRF2BP2 participates in cell survival during the p53 stress response. *Nucleic Acids Res.* 37, 322–335. doi: 10.1093/nar/gkn940

Li, T., Luo, Q., He, L., Li, D., Li, Q., Wang, C., et al. (2020). Interferon regulatory factor-2 binding protein 2 ameliorates sepsis-induced cardiomyopathy via AMPK-mediated anti-inflammation and anti-apoptosis. *Inflammation* 43, 1464–1475. doi: 10.1007/s10753-020-01224-x

Liekens, S., de Clercq, E., and Neyts, J. (2001). Angiogenesis: regulators and clinical applications. *Biochem. Pharmacol.* 61, 253–270. doi: 10.1016/S0006-2952(00)00529-3

Liu, Y., Xu, F., Hu, H., Wen, J., Su, J., Zhou, Q., et al. (2019). A rare case of acute promyelocytic leukemia with IRF2BP2-RARA fusion; and literature review. *Onco. Targets. Ther.* 12, 6157–6163. doi: 10.2147/OTT.S217622

Malumbres, M., and Barbacid, M. (2001). To cycle or not to cycle: a critical decision in cancer. *Nat. Rev. Cancer* 1, 222–231. doi: 10.1038/35106065

Mancini, M., and Toker, A. (2009). NFAT proteins: emerging roles in cancer progression. *Nat. Rev. Cancer* 9, 810–820. doi: 10.1038/nrc2735

Manjur, K., Lempiäinen, J. K., Malinen, M., Palvimo, J. J., and Niskanena, E. A. (2019). IRF2BP2 modulates the crosstalk between glucocorticoid and TNF signaling. *J. Steroid Biochem. Mol. Biol.* 192:105382. doi: 10.1016/j.jsbmb.2019.105382

Mazharuddin, S., Chattopadhyay, A., Levy, M. Y., and Redner, R. L. (2018). IRF2BP2-RARA t(1;17)(q42.3;q21.2) APL blasts differentiate in response to all-trans retinoic acid. *Leuk. Lymphoma* 59, 2246–2249. doi: 10.1080/10428194.2017.1421761

Ni, I., Ching, N. G., Meng, C. K., and Zakaria, Z. (2012). Translocation t(11;14)(q13;q32) and genomic imbalances in multi-ethnic multiple myeloma patients: a Malaysian study. *Hematol. Rep.* 4:e19. doi: 10.4081/hr.2012.e19

Nishida, N., Yano, H., Nishida, T., Kamura, T., and Kojiro, M. (2006). Angiogenesis in cancer. *Vasc. Health Risk Manag.* 2, 213–219. doi: 10.2147/vhrm.2006.2.3.213

Nyquist, K. B., Panagopoulos, I., Thorsen, J., Haugom, L., Gorunova, L., Bjerkehagen, B., et al. (2012). Whole-transcriptome sequencing identifies novel IRF2BP2-CDX1 fusion gene brought about by translocation t(1;5)(q42;q32) in mesenchymal chondrosarcoma. *PLoS One* 7:e49705. doi: 10.1371/journal.pone.0049705

Rao, A., Luo, C., and Hogan, P. G. (1997). Transcription factors of the NFAT family: regulation and function. *Annu. Rev. Immunol.* 15, 707–747. doi: 10.1146/annurev.immunol.15.1.707

Ryeom, S., Baek, K.-H., and Rioth, M. J. (2008). Targeted deletion of the calcineurin inhibitor DSCR1 suppresses tumor growth. *Cancer Cell* 13, 420–431. doi: 10.1016/j.ccr.2008.02.018

Secca, C., Faget, D. V., Hanschke, S. C., Carneiro, M. S., Bonamino, M. H., De Araujo-Souza, P. S., et al. (2016). IRF2BP2 transcriptional repressor restrains naive CD4 T cell activation and clonal expansion induced by TCR triggering. *J. Leukoc. Biol.* 100, 1081–1091. doi: 10.1189/jlb.2A0815-368R

Shimomura, Y., Mitsui, H., Yamashita, Y., Kamae, T., Kanai, A., Matsui, H., et al. (2016). New variant of acute promyelocytic leukemia with IRF2BP2-RARA fusion. *Cancer Sci.* 107, 1165–1168. doi: 10.1111/cas.12970

Soliman, H., Khalil, F., and Antonia, S. (2014). PD-L1 expression is increased in a subset of basal type breast cancer cells. *PLoS One* 9:e88557. doi: 10.1371/journal.pone.0088557

Stadhouders, R., Cico, A., Stephen, T., Thongjuea, S., Kolovos, P., Baymaz, I., et al. (2015). Control of developmentally primed erythroid genes by combinatorial co-repressor actions. *Nat. Commun.* 6:8893. doi: 10.1038/ncomms9893

Teng, A. C., Al-Montashiri, N. A., Cheng, B. L., Lou, P., Ozmizrak, P., Chen, H. H., et al. (2011). Identification of a phosphorylation-dependent nuclear localization motif in interferon refulatory factor 2 binding protein 2. *PLoS One* 6:e24100. doi: 10.1371/journal.pone.0024100

Teng, A. C., Kuratis, D., Deeke, S. A., Ahmadi, A., Dugan, S. G., Cheng, B. L. M., et al. (2010). IRF2BP2 is a skeletal and cardiac muscle-enriched ischemia-inducible activator of VEGFA. *FASEB J.* 24, 4825–4834. doi: 10.1096/fj.10-167049

Tinnikov, A. A., Yeung, K. T., Das, S., and Samuels, H. H. (2009). Identification of a novel pathway that selectively modulates apoptosis of breast cancer cells. *Cancer Res.* 69, 1375–1382. doi: 10.1158/0008-5472.CAN-08-2896

Wang, B., Gao, Y., Huang, Y., Ou, Q., Fang, T., Tang, C., et al. (2019). Durable clinical response to crizotinib in IRF2BP2-NTRK1 non-small-cell lung cancer. *Clin. Lung Cancer* 20, e233–e237. doi: 10.1016/j.cllc.2018.12.017

Wang, L., Gao, S., Wang, H., Xue, C., Liu, X., Yuan, H., et al. (2020a). Interferon regulatory factor 2 binding protein 2b regulates neutrophil versus macrophage fate during zebrafish definitive myelopoiesis. *Haematologica* 105, 325–337. doi: 10.3324/haematol.2019.217596

Wang, W., Zafar, A., Rajaei, M., and Zhang, R. (2020b). Two birds with one stone: NFAT1-MDM2 dual inhibitors for cancer therapy. *Cell* 9:1176. doi: 10.3390/cells9051176

Wu, A., Wu, Q., Deng, Y., Liu, Y., Lu, J., Liu, L., et al. (2019). Loss of VGLL4 suppresses tumor PD-L1 expression and immune evasion. *EMBO J.* 38:e99506. doi: 10.15252/embj.201899506

Yamaguchi, H., and Condeelis, J. (2007). Regulation of the actin cytoskeleton in cancer cell migration and invasion. *Biochim. Biophys. Acta* 1773, 642–652. doi: 10.1016/j.bbamcr.2006.07.001

Yao, Y., Wang, Y., Li, L., Xiang, X., Li, J., Chen, J., et al. (2019). Down-regulation of interferon regulatory factor 2 binding protein 2 suppresses gastric cancer progression by negatively regulating connective tissue growth factor. *J. Cell. Mol. Med.* 23, 8076–8089. doi: 10.1111/jcmm.14677

Yeung, K. T., Das, S., Zhang, J., Lomniczi, A., Ojeda, S. R., Xu, C. F., et al. (2011). A novel transcription complex that selectively modulates apoptosis of breast cancer cells through regulation of FASTKD2. *Mol. Cell. Biol.* 31, 2287–2298. doi: 10.1128/MCB.01381-10

Yin, C., Jain, N., Mehrotra, M., Zhagn, J., Protopopov, A., Zuo, Z., et al. (2015). Identification of a novel fusion gene, IRF2BP2-RARA, in acute promyelocytic leukemia. *J. Natl. Compr. Cancer Netw.* 13, 19–22. doi: 10.6004/jnccn.2015.0005

Zhang, S., Yang, X., Wang, L., and Zhang, C. (2018). Interplay between inflammatory tumor microenvironment and cancer stem cells. *Oncol. Lett.* 16, 679–686. doi: 10.3892/ol.2018.8716

Conflict of Interest: The authors declare that the research was conducted in the absence of any commercial or financial relationships that could be construed as a potential conflict of interest.

frontiers in Cell and Developmental Biology

REVIEW
published: 07 May 2021
doi: 10.3389/fcell.2021.675099

Modeling the Th17 and Tregs Paradigm: Implications for Cancer Immunotherapy

*Karla F. Corral-Jara[1], Gonçalo Rosas da Silva[2], Nora A. Fierro[3] and Vassili Soumelis[4]**

[1] Computational Systems Biology Team, Institut de Biologie de l'Ecole Normale Supérieure, CNRS UMR 8197, INSERM U1024, Ecole Normale Supérieure, PSL Research University, Paris, France, [2] School of Biological Sciences, Queen's University Belfast, Belfast, United Kingdom, [3] Department of Immunology, Biomedical Research Institute, National Autonomous University of Mexico, Mexico City, Mexico, [4] Université de Paris, INSERM U976, France and AP-HP, Hôpital Saint-Louis, Immunology-Histocompatibility Department, Paris, France

CD4 + T cell differentiation is governed by gene regulatory and metabolic networks, with both networks being highly interconnected and able to adapt to external stimuli. Th17 and Tregs differentiation networks play a critical role in cancer, and their balance is affected by the tumor microenvironment (TME). Factors from the TME mediate recruitment and expansion of Th17 cells, but these cells can act with pro or anti-tumor immunity. Tregs cells are also involved in tumor development and progression by inhibiting antitumor immunity and promoting immunoevasion. Due to the complexity of the underlying molecular pathways, the modeling of biological systems has emerged as a promising solution for better understanding both CD4 + T cell differentiation and cancer cell behavior. In this review, we present a context-dependent vision of CD4 + T cell transcriptomic and metabolic network adaptability. We then discuss CD4 + T cell knowledge-based models to extract the regulatory elements of Th17 and Tregs differentiation in multiple CD4 + T cell levels. We highlight the importance of complementing these models with data from omics technologies such as transcriptomics and metabolomics, in order to better delineate existing Th17 and Tregs bifurcation mechanisms. We were able to recompilate promising regulatory components and mechanisms of Th17 and Tregs differentiation under normal conditions, which we then connected with biological evidence in the context of the TME to better understand CD4 + T cell behavior in cancer. From the integration of mechanistic models with omics data, the transcriptomic and metabolomic reprograming of Th17 and Tregs cells can be predicted in new models with potential clinical applications, with special relevance to cancer immunotherapy.

Keywords: Th17, Tregs, mathematical models, omics data, tumor microenvironment

OPEN ACCESS

Edited by:
Rodrigo Nalio Ramos, Institut National de la Santé et de la Recherche Médicale (INSERM) U1138 Centre de Recherche des Cordeliers (CRC), France

Reviewed by:
Rafael Ribeiro Almeida, University of São Paulo, Brazil
Youliang Wang, Beijing Institute of Technology, China

***Correspondence:**
Vassili Soumelis
vassili.soumelis@aphp.fr

Specialty section:
This article was submitted to Molecular Medicine, a section of the journal Frontiers in Cell and Developmental Biology

Received: *02 March 2021*
Accepted: *12 April 2021*
Published: *07 May 2021*

Citation:
Corral-Jara KF, Rosas da Silva G, Fierro NA and Soumelis V (2021) Modeling the Th17 and Tregs Paradigm: Implications for Cancer Immunotherapy. Front. Cell Dev. Biol. 9:675099. doi: 10.3389/fcell.2021.675099

INTRODUCTION

CD4 + T cell differentiation requires a combination of external signals to induce changes at the membrane, cytoplasmic and nuclear levels. This requires the activation of complex gene regulatory networks, involving transcriptional and non-coding RNA, cell signaling and epigenetic regulation (Christie and Zhu, 2014; Schmidl et al., 2018). This process of differentiation is also supported by distinct metabolic reaction networks (Buck et al., 2015).

This can be shown by how Th17 and Tregs CD4 + T cell phenotypes play a central role in cancer, and how to the conditions within the tumor microenvironment (TME) can lead to a deregulation and hijacking of these T cell networks for tumor proliferation (Guéry and Hugues, 2015). Flexibility between Th17 and Tregs cells is well-documented in the TME (Diller et al., 2016). For instance, Th17 cells have been shown to progressively transdifferentiate into IL-17A^{+}FOXP3^{+} and IL-17A^{-}FOXP3^{+} T cells during tumor development (Downs-Canner et al., 2017).

With the recent increase of immunotherapy as a promising therapeutic option against cancer, the regulation and differentiation of Th17 and Tregs cells has gained recognition as essential part of this equation (Zanetti, 2015; Sadozai et al., 2017). Elucidating the factors underlying changes in Th17 and Tregs networks will potentiate the development of innovative therapeutic strategies by manipulating metabolic and transcriptional intracellular pathways (Kim et al., 2018; Rivadeneira and Delgoffe, 2018).

The evolution of the field of systems biology has led to several advances in the mechanistic comprehension of the immune system (Smolke and Silver, 2011; Calder et al., 2018). Systems biology heavily relies on expansive, well-curated databases and prior literature, so the field has benefited from the integration of expanding omics technologies for several years (Karahalil, 2016). Metabolomics in particular, often via incorporation into existing models, are being increasingly integrated into both model development and new therapeutic/analytical approaches (Misra et al., 2017; Chong et al., 2018).

In this review, we address the mechanisms behind the decisions governing Th17 and Tregs cell fate, as explained by a systems biology point of view, through *in silico* simulations/predictions and their relation with the TME. We then offer an explanation of the biological adaptability of CD4 + T cells as the basis for understanding Th17 and Tregs plasticity. Subsequently, we present a recompilation of the molecular mechanisms behind Th17 and Tregs function, highlighted on theory-data-driven models, and connect this information with biological evidence in the context of the TME. Finally, we describe how cancer immunotherapeutic applications have been developed based on mathematical modeling strategies and omics data integration.

GENE REGULATORY MEDIATING CD4 + T CELL DIFFERENTIATION

Th17 cells belong to the effector CD4 + T cell lineage (Teffs), while periphery-induced regulatory T (iTregs) and thymic regulatory T cells (tTregs) belong to the regulatory lineage. CD4 + T cells are regulated across three main regulatory layers; the cell membrane, cytoplasm, and nucleus (DuPage and Bluestone, 2016), with molecular and other signaling pathways occurring within and between these layers, and giving rise to gene regulatory networks (GRN) (**Figure 1A**), that contribute to the expression of genes involved in metabolic networks (Klosik et al., 2017; Hiemer et al., 2019) (**Figure 1A**).

The differentiation processes of these cells are also known, though not fully-established; CD4 + T cell signal differentiation is initiated in the T cell receptor (TCR) pathway, with cytokines and co-stimulatory molecules binding their receptors to the cell membrane. This then activates signaling pathways in the cytoplasm, which act as an intermediary between the membrane and the nucleus, in which the endpoints of these pathways will induce an overexpression of specific transcription factors (TFs). These TFs will then induce a particular CD4 + T cell subtype cytokines signature (Christie and Zhu, 2014) (**Figure 2**).

Previously, it was thought that the process of differentiating toward each individual CD4 + T cell subtype was modulated by a single lineage-specific TF and mutually inhibited by the others (Zheng and Flavell, 1997; Szabo et al., 2000). However, it has since been discovered that a CD4 + T cell lineage-specific TF could be expressed among multiple CD4 + T cell subtypes, introducing the concept of transcription factor co-expression (Evans and Jenner, 2013). Similarly, gene regulatory network variability at the single-cell level has been observed (Padovan-Merhar and Raj, 2013). A single CD4 + T cell may acquire different molecular phenotypes associated with transcriptomic and proteomic fluctuations (Vieira Braga et al., 2016). This adds significant complexity to our understanding of differentiation in these cells.

CD4 + T CELL DIFFERENTIATION AND METABOLIC FLUX NETWORK ADAPTATIONS

Similarly, CD4 + T cells react differently to different nutritional stimuli, activating different metabolic routes in the cytoplasm, such as glucose and its promotion of glycolysis. In most cases, in contrast to GRN, metabolic networks terminate in the mitochondria with the generation of adenosine triphosphate (ATP), the main energy source for the cell (Shyer et al., 2020).

There have been continuous efforts to define the metabolic hallmarks for each CD4 + T cell subtype. In general, CD4 + effector T cells prioritize glycolysis and lactate production under aerobic conditions. Conversely, Tregs immediately undergo fatty acid oxidation (FAO) leading the generation of ATP (Wang and Solt, 2016). Specifically, murine tTregs engage in glycolysis and glutaminolysis at levels comparable to effector T cells, despite expressing forkhead box 3 (FOXP3) (Priyadharshini et al., 2018), while murine iTregs have been shown to preferentially use FAO, despite the fact that human iTregs heavily rely on glycolysis (Pacella et al., 2018). Fatty acid synthesis (FAS) is an anabolic hallmark of CD4 + effector T cells, but not of Tregs, which require fatty acid uptake (FAU) (Buck et al., 2015; Howie et al., 2018).

These metabolic networks do not remain static during CD4 + T cell differentiation, and adapt in response to diverse stimuli. Instances of CD4 + effector T cells activating/relying on FAO and Tregs differentiating through glycolysis have both been documented. For example, CD4 + effector T cells rely on FAS and glutaminolysis as principal sources of energy in response to low glucose levels, but their normal functions

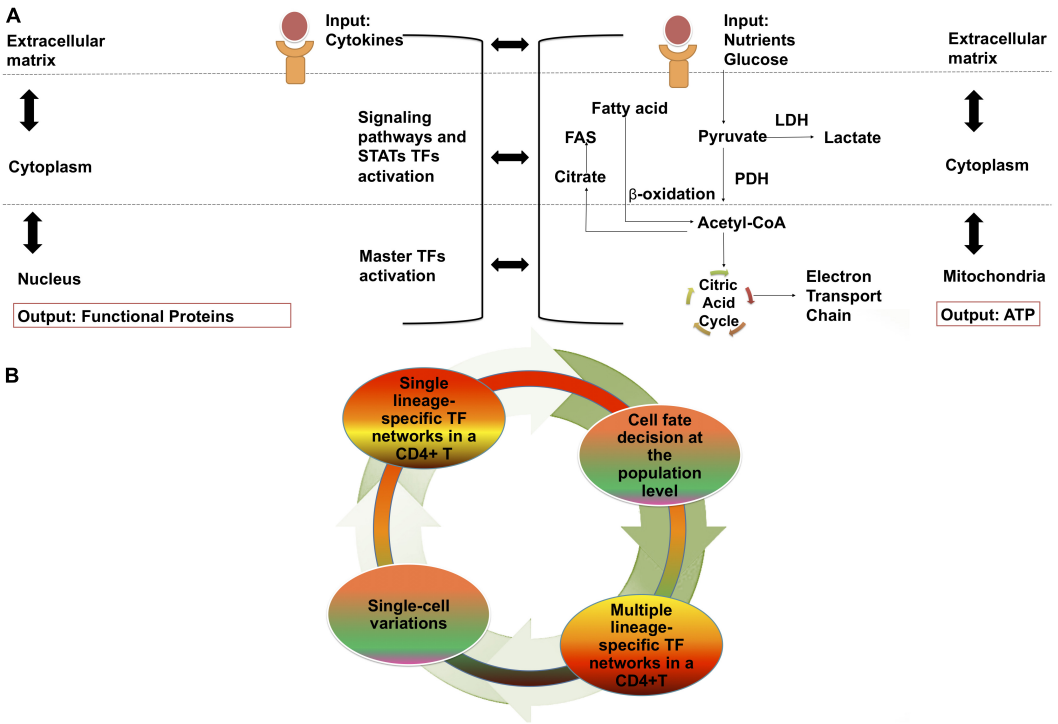

FIGURE 1 | CD4 + T cell differentiation: Cellular regulation layouts and dynamism of transcriptional and metabolic networks. **(A)** Levels of cellular regulation in gene regulatory networks. Membrane: TCR, cytokines and binding of co-stimulatory molecules. Cytoplasm: signaling pathways and activation of STATs. Nuclear: activation of master TFs and transcription of functional proteins. And levels of cellular regulation in metabolic networks. Membrane: nutrients binding to receptors. Cytoplasm: activation of metabolic fluxes. Mitochondria: activation of the electron transport chain for the generation of ATP. **(B)** CD4 + T cell differentiation and network components dynamic. Under different external stimuli changes occurring on a intracellular level are observed. Among a set of cells that receives the same signal, individual cell variability is also presented. STATs, signal transducer and activator of transcription; FAS, fatty acid synthesis; LDH, lactate dehydrogenase; PDH, pyruvate dehydrogenase; ATP, adenosine triphosphate; TF, Transcription factor.

and their capacity to synthesize IFN-γ are both compromised (Ecker et al., 2018). Simultaneously, Tregs take advantage of glucose scarcity and lactate abundance to undergo differentiation (Angelin et al., 2017). However, under certain conditions, Tregs rely on glycolysis to maintain their expression of FOXP3 and potentiate their suppressive functions (Fan and Turka, 2018). This evidence strongly suggests that, similar to GRN, metabolic networks are flexible and widely stimulus-dependent.

MUTUAL EFFECTS OF GENE REGULATORY NETWORKS AND METABOLIC NETWORKS IN CD4 + T CELL DIFFERENTIATION

The activation of the TCR signaling pathway in the cytoplasm acts as an intermediate domain between the GRN and metabolic networks (Klosik et al., 2017). This pathway is responsible for the activation of the phosphatidylinositol 3-kinase/mammalian target of rapamycin/protein kinase B (PI3K/mTOR/AKT) pathway, which is a key component of CD4 + T cell metabolism. This pathway involves the phosphorylation of phosphatidylinositol 4,5-bisphosphate (PIP2) by PI3K, converting it to phosphatidylinositol (3,4,5)-trisphosphate (PIP3), in a reaction negatively regulated by phosphatase and tensin homolog (PTEN) phosphatase. PIP3 promotes mTOR complex 2 (mTORC2) activation to phosphorylate AKT (Carlson et al., 2009; Liu et al., 2015).

Following TCR engagement, two mutually inhibited molecules, mTOR and AMP-activated protein kinase (AMPK) are expressed. mTOR is promoted in CD4 + effector T cells, while AMPK is expressed in Tregs. mTOR, a key signaling protein, is also related to the activation of metabolic processes such as glycolysis via Hypoxia Inducible Factor subunit alpha (HIF-1α) and FAS via sterol regulatory element-binding protein 2 (SREBP2), while AMPK can sense the cellular AMP/ATP ratio and respond to low energy conditions, inhibiting FAS and promoting FAO (Salmond, 2018).

Gene regulatory networks intermediates can also induce metabolism-related gene activation and vice-versa; metabolism-related genes regulate the transcriptional fingerprints on CD4 + T cells, since some metabolic pathway-related enzymes are transported to the nucleus and interact with mRNAs, thus impacting their stability and translation. For example, the glycolytic enzyme Gapdh in murine T cells can suppress

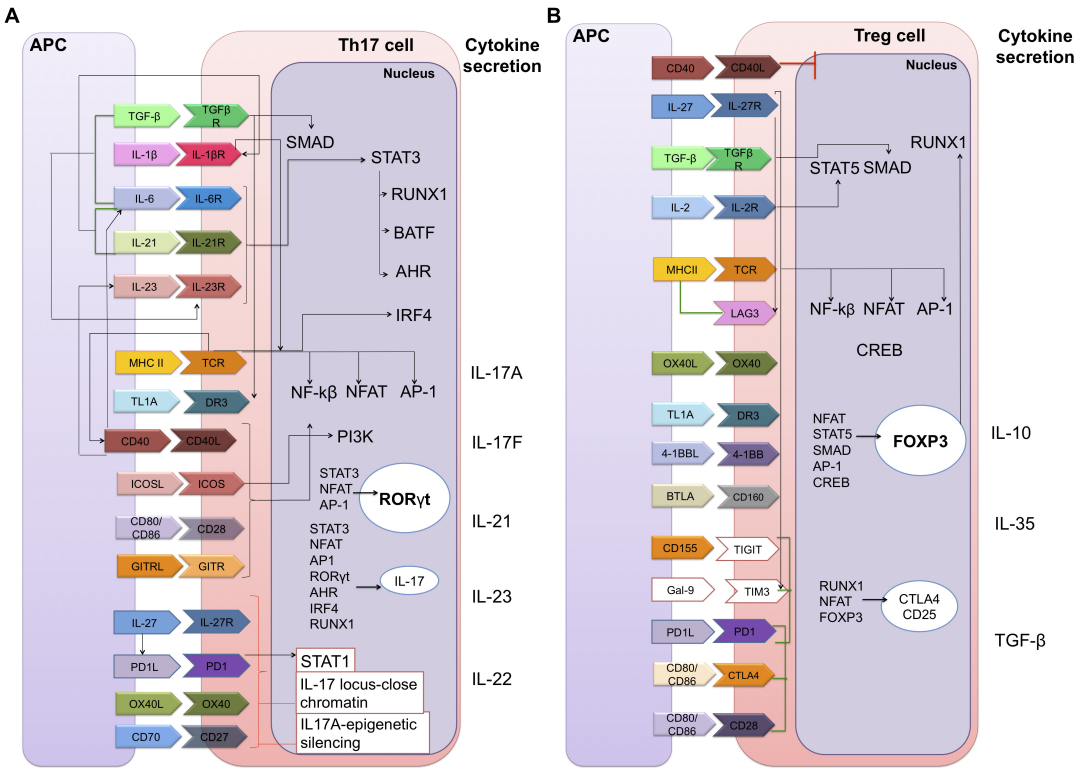

FIGURE 2 | Static gene regulatory networks of CD4 + T cell differentiation: Th17 and Tregs. Each CD4 + T cell subset can be defined by their distinct abilities to sense, program and function in the control of specific pathogen or immune pathologies. The inductive cytokines, polarizing transcription factors and cytokines or chemokine receptors that are characteristic of each subset are shown. **(A)** Th17 cell differentiation. The Th17 subset is a key mediator of the inflammatory response; its functional attributes are the recruitment of neutrophils that are necessary for the clearance of extracellular bacterial and fungal infections. **(B)** Regulatory T cell differentiation. Tregs are vital to maintaining balance in the system since they allow tolerance and prevent autoimmune diseases by suppressing the function of Effector T cells. Membrane components: TGF-β, transforming growth factor beta; TGFβR, TGF-beta receptor; IL-1β, interleukin 1-beta; IL-1βR, interleukin 1-beta receptor; MHC II, major histocompatibility complex class II; TCR, T-cell receptor; TL1A, TNF-like ligand A1; DR3, death receptor 3; CD40, cluster of differentiation 40; CD40L, CD40 ligand; ICOS, inducible T-cell co-stimulator; GITR, glucocorticoid-induced TNFR family related gene; PD1, programed cell death protein 1; OX40, tumor necrosis factor receptor superfamily, member 4; LAG3, lymphocyte-activation gene 3; 4-1BB (or CD137). BTLA, B- and T-lymphocyte attenuator; TIGIT, T cell immunoreceptor with Ig and ITIM domains; Gal-9, galectin 9; TIM3, T-cell immunoglobulin and mucin-domain containing-3; CTLA4, cytotoxic T-lymphocyte-associated protein 4. Nuclear components: SMAD, smad family members; STAT3, signal transducer and activator of transcription 3; RUNX1, runt-related transcription factor 1; BATF, basic leucine zipper ATF-like transcription factor; AHR, aryl hydrocarbon receptor; IRF4, interferon regulatory factor 4; NF-kβ, nuclear factor-kappa B; NFAT, nuclear factor of activated T-cells; AP-1, activator protein 1; PI3K, phosphoinositide 3-kinases; RORγt, RAR-related orphan receptor gamma; CREB, C-AMP response element-binding protein; FOXP3, forkhead box P3. Extracellular secretion: IL-17A, IL-17F, IL-21, IL-23, IL-22, IL-10, IL-35, and TGF-β. Black lines means a positive direct interaction. Red lines are negative direct interactions and green lines indicate a bibliographic support on the synergistic function of the components in the differentiation of cellular subtypes.

the translation of IFN-γ by binding to the 3-UTR in mRNA (Chang et al., 2013).

Small variations in these gene and metabolic networks will result in a different immune response (**Figure 1B**). These significant differences in the mechanisms on which separate immune cell lines rely for energy production and the ways in which they react to external stimuli (especially from glucose and lactate) are also of special interest for cancer immunotherapy. Many cancers are known to be metabolically aberrant, causing significant alterations to their own biochemical composition and that of their TMEs (Ganapathy-Kanniappan, 2017). Competition for glucose (glycolysis) and mitochondrial metabolism between T cells and tumor cells have been identified as key events in determining the success of anti-tumor T cell activation (Yin et al., 2019), and the harting and "taming" of these metabolic traits have long been points of interest for cancer immunotherapy.

TH17 AND TREGS BALANCE APPROACHED THROUGH SYSTEMS BIOLOGY: MULTIPLE CELL REGULATORY LAYERS

The non-linear, cooperative and stochastic nature of the interactions in the immune system can make it difficult to delineate a mechanistic understanding of T cell differentiation, and also makes it more difficult to implement this knowledge into improving cancer immunotherapy outcomes. Computational

modeling is increasingly involved in confronting these challenges, bridging the gaps left by unclear immunological processes (Chakraborty, 2017). An inspection of the published literature indicates that, within the field of systems biology applied specifically to understanding CD4 + T cells, a significant portion of studies looked at differentiation or immunotherapy implications.

Systems biology methodologies aim to predict how changes in the concentration of a particular component, or in the efficiency levels of a function relating to that component, will influence the overall activity of the system (Germain et al., 2011). Combining the organization-based approach of theory-driven models (to identify novel interactions) with the amount of data and the novelty of the network component obtained from data-driven models, highly predictive, hybrid models are ultimately expected to be constructed, with which we could achieve a better understanding of CD4 + T cells in TME context (Carbo et al., 2014; Morel et al., 2017). The goal is to find the appropriate balance between the oversimplification of system descriptions and inclusion of overly complex details (Klosik et al., 2017).

CD4 + T cell knowledge-based models are presented in the following sections, as means to identify Th17 and Tregs regulatory elements, including feedback loops and feed-forward loops in multiple cell layers, with the goal of finding their connections in a tumoral context.

MODELING OF TH17 CELLS AND TREGS AT THE MEMBRANE LEVEL FOR UNDERSTANDING A TME

On the basis of model simulations, it has been concluded that both Tregs and Th17 cells are highly plastic and labile across different environmental conditions (Mendoza and Xenarios, 2006; Naldi et al., 2010; Mendoza, 2013). In addition, the behavior of master TFs has been modeled, leading to new discoveries such as FOXP3 expression being lost or transient in the absence of IL-2, while the expression of RORγt is more robust (Naldi et al., 2010; Hong et al., 2011). During differentiation, the Tregs phenotype passes through an additional intermediate state where they produce IL-2 before "activating" PTEN, enabling permanent activation of FOXP3 (Miskov-Zivanov et al., 2013).

However, Tregs are prevalent in nearly all cancers and act as immunosuppressive regulators of the body's immune response making them a unique obstacle in cancer immunotherapy. The precise molecular mechanisms that guide Tregs cell stability in tumors remain elusive, but a cell-intrinsic role of the alarmin interleukin (IL)-33-ST2 axis in the functional stability of Tregs cells in the TME has been identified (Hatzioannou et al., 2020); more specifically, a feedback loop in which conventional mouse CD11c(+) dendritic cells (DC) stimulated by IL-33 secrete IL-2 to selectively expand IL-33R [ST2(+)]-suppressive CD4(+)Foxp3(+) Tregs was found (Matta et al., 2014). This suggests an important role for external cytokines in the mediation of CD4 + T cells in the TME.

Models of regulatory networks aimed at determining how external stimuli are processed to determine CD4 + T cell responses have also been developed (Naldi et al., 2010; Abou-Jaoudé et al., 2015). According to these simulations, several differentiated Th subtypes can be reprogramed from an initial state into various other subtypes by sequentially using proper environmental input conditions. Similarly, in response to varied cytokine mixtures, cells co-express lineage-specific proteins at diverse levels, such that the cell population spans a continuum of intermediate states between canonical cell phenotypes (Eizenberg-Magar et al., 2017).

In Th17 models, pitchfork bifurcations with TGF-β concentrations have been analysed by several teams. Increasing the TGF-β concentration caused the transformation of FOXP3 single-positive Tregs into RORγt-expressing Th17 cells and doubly positive cells expressing FOXP3high RORγthigh (Hong et al., 2011; Martinez-Sanchez et al., 2018). TGF-β can have a determining impact on T cells within the TME since it could promote Tregs or Th17 expansion and present a pleiotropic function (Dahmani and Delisle, 2018).

In the TME, Th17-Tregs differentiation is typically directed by multiple external signals driving opposing regulatory pathways. Studies on the effects of combining lineage-specifying cytokines on polarization and the acquired non-canon cell phenotypes are becoming more common. A data-driven computational model predicted a new function for IL-12 as an inducer of IL-17F, but not of IL-17A in an IL-1β signaling context (Grandclaudon et al., 2019). Subsequently, a hierarchical additive regression model was constructed, providing a framework for the prediction of cellular responses to new cytokine combinations and doses. In this case, the input conditions of TGF-β + IL-6 + IL-12 + IL-4 + IL-2 supported the *in silico* expression of IL-17A (Eizenberg-Magar et al., 2017).

IL-12 in particular has emerged as one of the most potent cytokines in mediating antitumor activity in a variety of preclinical models. IL-12 establishes a link between innate and adaptive immunity that involves different immune effector cells and cytokines depending on the type of tumor or the affected tissue (Tugues et al., 2015). Therefore, these mechanistic models could provide the first clues about the anti-tumoral response of IL-12, possibly through the induction of effector cytokines, such as IL-17A (Corral-Jara et al., 2021).

The Th17-Tregs balance has strong implications in autoimmunity and cancer immunotherapy (Knochelmann et al., 2018), and it may exhibit a range of sensitivities to altered concentrations of cytokines as they switch from one phenotype to another (**Figure 3**).

MODELING OF TH17 CELLS AND TREGS AT THE TRANSCRIPTIONAL LEVEL FOR UNDERSTANDING A TME

A model aimed at understanding the mechanisms mediated by TFs in Th17 cells and Tregs has corroborated that increasing the concentrations of PPARγ in Th17 cells would lead to the downregulation of RORγt and IL-17 and the upregulation of

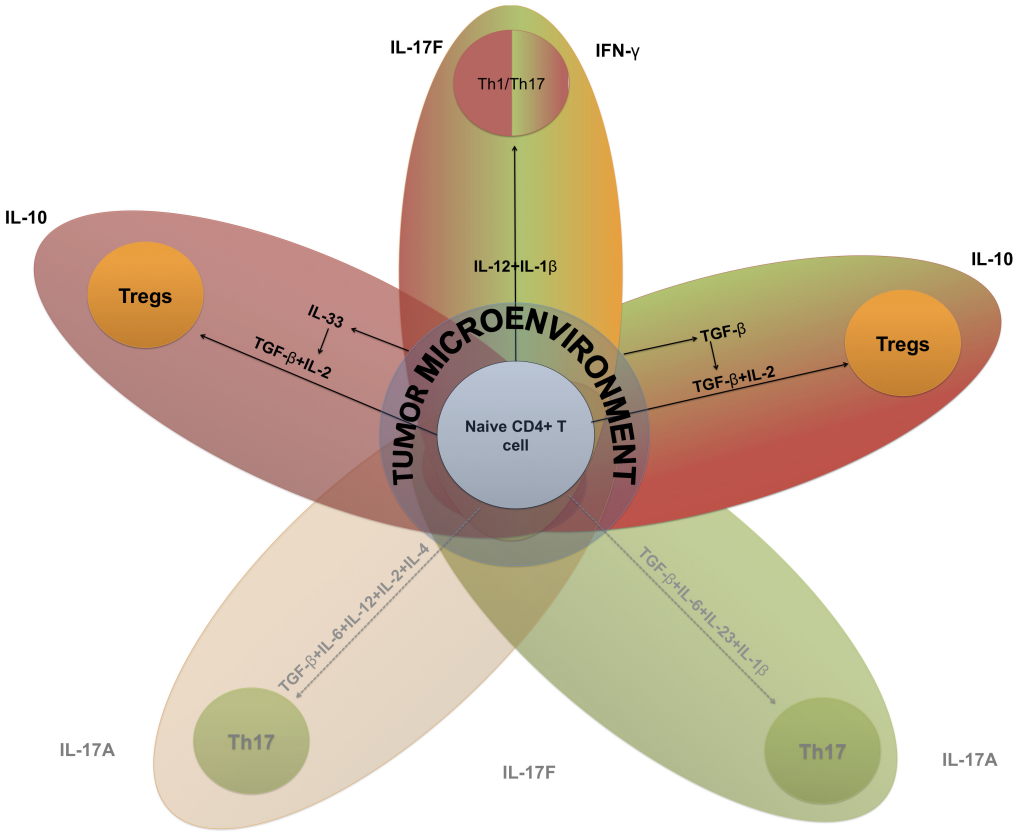

FIGURE 3 | Key elements of Th17-Tregs differentiation based on systems biology-extracted information. Cytokine-driven T cell plasticity in a tumor microenvironment. The key inductive cytokines IL-12, IL-6, IL-4, IL-1β, I-L23, TGF-β, and IL-2, alone or in concert, can polarize naive CD4 + T cells toward different functions. This figure is intended to reveal the interconnectedness of these different programs based on the capacity of these inductive cytokines to promote polarization between subsets. These subsets include Th1–Th17, hybrid cells that produce IFN-γ and IL17 cytokines from a mixture of inductive cytokines characteristic of Th1 and Th17. TME, tumor microenvironment. Black lines represent positive interactions and dotted lines represent inhibited processes.

FOXP3 upon the addition of external TGF-β and external IL-6 *in silico* (Carbo et al., 2013).

PPARγ induces the expression of genes associated with FAU, a feature of Tregs, and controls glucose oxidation by inhibiting pyruvate dehydrogenase (PDH) (Howie et al., 2018). The inhibition of PDH by pyruvate dehydrogenase kinase 1 (PDHK1) is required for Th17 cell development (Gerriets et al., 2015). In contrast, Th1 and Th2 cells are inhibited by TOFA, an inhibitor of ACC1 (a master enzyme of FAS, a feature of CD4 + effector T cells); however, there are discrepancies regarding the Th17-TOFA effect (Berod et al., 2014; Angela et al., 2016), indicating that PPARγ and FAU may also support a Th17 cytokine signature (Nicholas et al., 2017) and be a potential mechanism to consider in immunotherapeutic approaches.

Lipids are a key part of the TME (Luo et al., 2018), and fatty acid binding proteins (FABPs) play important roles in fatty acid uptake from the microenvironment. FABP5 is one of the most highly expressed FABPs in T cells (Rolph et al., 2006), and its inhibition has been shown to minimize IL-17 cytokine production and skew T cells toward a Tregs phenotype *in vitro* (Field et al., 2020). FABP5 has also been associated with the development of diverse types of cancer (Carbonetti et al., 2019), indicating the importance of considering metabolic aspects of CD4 + T cells in the TME.

MODELING OF TH17 CELLS AND TREGS AT THE SIGNALING LEVEL FOR UNDERSTANDING A TME

Signaling and metabolic modulations of Th17-Tregs differentiation are directly related to the intensity of TCR signaling. Computational modeling assays have been performed to determine how the TCR signal strength engages alternate signaling networks to control cell fate decisions. Weak TCR signals generated elevated PIP2 and reduced PIP3 levels, and high PIP3 levels activate mTOR/AKT signaling completely toward glycolisis (Hawse and Cattley, 2019). Using a model of multiple interleukin 2 tyrosine kinase (ITK) signaling circuits, a tyrosine kinase required for full TCR-induced activation of mTOR, it was predicted that inositol (1,3,4,5) tetrakisphosphate (IP4) might promote ITK binding to PIP3 through cooperative allosteric selection (Mukherjee et al., 2013).

Analyzing Th17 and Tregs differentiation, it has been demonstrated that CD4 + T cells deficient in ITK exhibit decreased IL-17A expression, decreased IL-2-induced phosphorylation of mTOR and increased FOXP3 induction due to PTEN activation (Gomez-Rodriguez et al., 2009, 2014). In the TME, data from a murine colon adenocarcinoma model demonstrated a decline in functionality of Tregs cells from $Itk^{-/-}$ mice, which further supports the connection between decreased ITK expression and decreased Tregs cell functionality (Lutsiak et al., 2008).

Revu et al. (2018), stated that CD28 co-stimulation suppresses the induction of the Th17 cell transcriptional program, activating the mTOR/AKT pathway to high levels, indicating that some mTOR/AKT activation is required despite high mTOR/AKT activity suppressing Th17 cell development (Revu et al., 2018). This supposition suggests that the plasticity of Th17 and Tregs can be modulated by dedicated doses of external factors that have an effect on cell signaling pathways.

Thymic regulatory T cells require a strong TCR signal since their metabolism is based on glycolysis, and iTregs require a low TCR signal due to their relying primarily on fatty acid metabolism. In the case of Th17 cells, there are discrepancies about the strength of the TCR signaling required to drive their differentiation (DuPage and Bluestone, 2016), as has been previously discussed. It is possible that, at the beginning of Th17 cell differentiation *in vivo*, a low TCR signal is required, leading to increases in STAT5 and PIP2, and a decrease in PIP3-ITK interactions. This will lead to a decrease in the activity of the mTOR pathway. At an intermediate time, a strong signal from the TCR is required, reversing the aforementioned processes. Upon the conclusion of this process, the TCR signal may decrease again (**Figure 4A**).

The TME has an intricate and profound effect on CD4 + T cell signaling pathways. For instance, lactate released by tumor and stromal cells generates extracellular acidity, and inhibits the PI3K/Akt/mTOR pathway, thus also inhibiting T cell glycolysis. Additionally, acidification of the TME impairs Teffs to a much greater extent compared to Tregs, mostly because Teffs acquire energy mainly through glycolysis, while Tregs can rely on FAO (Yin et al., 2019) (**Figure 4B**).

TH17-TREGS BALANCE AND OMICS DATA: A COMPLEMENT TO THE THEORETICAL MODEL APPROACH

The intricately-linked networks by which CD4 + T cells differentiate have been broadly approached to date (Koch and Radtke, 2011), with a body of research being steadily built over several years and benefiting/accelerating largely based on factors such as the increased accessibility of DNA and RNA sequencing technologies (Frio, 2015).

Most of the current systems biology-based approaches derived from real biological/medical data are based on the genome, transcriptome or proteome of an organism, a situation partially attributable to these datasets being measured by established and tested methods, and the continued capacity of these methods to iterate and integrate new protocols, such as single-cell transcriptomics (Stubbington et al., 2017). Analyses of these datasets are slowly becoming more accurate and manageable due to the frequent release and update of new dedicated tools (Chong et al., 2018; Marco-Ramell et al., 2018) and, in addition to the increased resolution, throughput capacity and accuracy that might be expected over time, developments that enable the exploration of new paradigms, such as single-cell metabolomics (Zenobi, 2013).

TH17 AND TREGS DIFFERENTIATION-TRANSCRIPTOMICS-BASED APPROACH AND TME IMPLICATIONS

Some teams have experimented with high-throughput data to construct a Th17 cell differentiation network, and reported that there are three transcriptional phases that control mouse Th17 cell differentiation: early, intermediate and late (Ciofani et al., 2012; Yosef et al., 2013). As proposed, there are also three possible metabolic phases of Th17 cell differentiation in which TCR-AKT-mTOR pathway activity is modulated. Determining the mechanisms of GRN-metabolic network integration is a promising concept in TME comprehension.

The early transcription phase is characterized by *cis* regions bound by BATF/IRF4 complex under TCR stimulation conditions (Th0 cells), and with promoted chromatin accessibility, binding strongly with STAT3, RORγt, c-Maf, and p300 in cells (Ciofani et al., 2012).

The transition to the intermediate phase is marked by the induction of RORγt and another TFs, known (*e.g.*, Ahr) and novel (*e.g.*, Trps1) (Yosef et al., 2013). RORγt is sensitive to changing environmental signals and is essential for licensing the expression of a select few loci; it functions as a rheostat to tune mRNA levels to those of a Th17-specific program. RORγt can also limit target expression, including that of the regulators of metabolism and quiescence, e.g., IL-10, HIF-1α, Egln3, Foxo1, and IL-7R (Ciofani et al., 2012).

HIF-1α is induced by mTOR and mediates glycolytic activity, thereby contributing to the Th17 cell or Tregs lineage switch (Shi et al., 2011). We suggest that, in the late stages of Th17 cell differentiation, the inhibition of the mTOR pathway and HIF-1α, may subsequently be required in order to ensure the transition toward the final stage of the process. During the conclusion of the differentiation step, Th17 cells induce IL-23R, which plays an important role in the late phase (Yosef et al., 2013).

It has been suggested that, during the late stage of Th17 differentiation, HIF-1α must be decreased. HIF-1α is highly expressed in Th17 cells, priming at physiological oxygen tension in the presence of inflammatory cytokines. HIF-1α plays a prominent role in Th17 cell differentiation and it helps recruit CBP/p300 to the RORγt transcription complex, but does not directly bind to the IL-17 promoter. Additionally, HIF-1α increases glycolysis by inducing the expression of glycolytic enzymes, which further contributes to Th17 development. However, HIF-1α also promotes carcinogenesis and is a prominent cancer target, and various HIF-1α inhibitors have

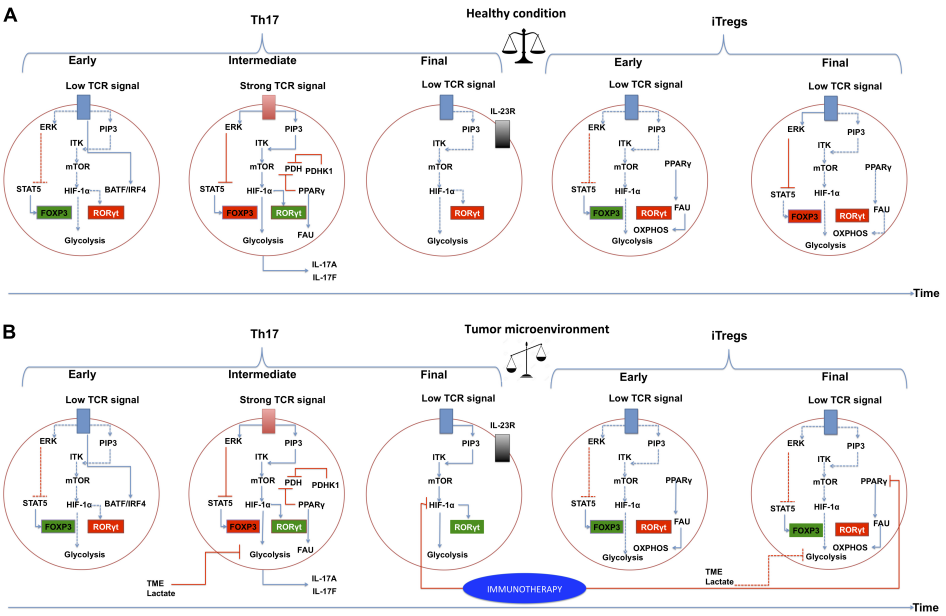

FIGURE 4 | The PI3K–AKT–mTOR pathway and metabolic programs converge to regulate the differentiation of inflammatory versus regulatory T cells in a tumor microenvironment. Links between extracellular cues, T-cell receptor (TCR) strength, the phosphatidylinositol 3-kinase (PI3K)–AKT–mammalian target of rapamycin (mTOR) pathway, metabolic programs and gene regulation are depicted. **(A)** Normal conditions. Three stages of differentiation over time are shown for Th17, at the end of the timeline, Tregs differentiation is presented to indicate that these require more time to differentiate. IL-2-inducible T-cell kinase (ITK) and TCR signaling play a critical role in regulating the expression of transcription factor hypoxia-inducible factor (HIF-1α) by functioning as a rheostat that determines the extent of activation of PI3K and mTOR-activated pathways. HIF-1α is activated in intermediate and deactivated in final steps of Th17 differentiation. A balance between Th17 cells and Tregs is achieved and they can co-exist in the time. PPARγ in Tregs should be deactivated in a specific time. **(B)** Tumor microenvironment conditions. We suggest a deregulation of the signaling pathways in Th17 cells and Tregs. It is likely that HIF-1α is not inactivated in a tumor microenvironment, leading to a higher expression of RORγt, and generating an exhausted Th17. Likewise, PPARγ may not be deactivated in Tregs, leading to functional Tregs. Immunotherapy proposals could be directed at targets such as HIF-1α and PPARγ. Activated interactions between components are indicated by solid lines, whereas inactivated links between proteins are denoted with dashed lines. The blue lines indicate positive direct interactions between the components. Red lines indicate direct negative interactions. The green squares indicate that the component is active, the red square indicates that the component is inactive. ERK, extracellular-signal-regulated kinase pathway; PIP3, phosphatidylinositol (3,4,5)-trisphosphate; STAT5, signal transducer and activator of transcription 5; FOXP3, forkhead box P3; RORγt, RAR-related orphan receptor gamma; PDH, pyruvate dehydrogenase; PDHK1, pyruvate dehydrogenase kinase 1; PPARγ, peroxisome proliferator-activated receptor gamma; FAU, fatty acid uptake; TME, tumor microenvironment.

been identified and are currently being studied for their efficacy in cancer therapy (Chou et al., 2016). Although Th17 cells are prevalent within the TME, their functional role in tumor immunity is controversial (Ye et al., 2013), and the three suggested steps of Th17 differentiation and HIF-1α participation could provide partial explanations.

TH17 AND TREGS DIFFERENTIATION-METABOLOMICS-BASED APPROACH AND TME IMPLICATIONS

CD4 + T cell differentiation networks have been classified at the genomic and proteomic level (Zhu and Paul, 2010; Liston and Schlenner, 2015), but incorporating metabolism has proven difficult, since gene expression is not directly correlated to the activity of the encoded metabolic enzyme (Wang et al., 2017).

Metabolomics concerns the study of metabolites, the downstream results of the many processes in tissues and fluids that comprise the functions of life, and it is a relatively recent branch of the omics family of technologies. Despite the high cost and difficulty of metabolomic data interpretation, its possible integration into systems biology methodologies and its capacity to define CD4 + T cell phenotypic traits, as opposed to purely genotypic traits, make it an interesting tool (Misra et al., 2017; Trivedi et al., 2017).

CD4 + T cell differentiation is also known to be heavily influenced by external factors, such as the modulation induced by obesity, specific nutritional choices (Maruyama et al., 2011; Endo et al., 2015) and the presence and effects of the gut microbiota under physiological conditions (Frankel et al., 2017), giving increased importance to metabolomics as a valuable cellular phenotype-centered method for screening pathways and networks of exposotypes. Ideally, this will result in a more comprehensive systems biology approach (Rattray et al., 2018).

Metabolomics has been used to characterize the actions of Tregs. Specifically, short-chain fatty acids (SCFAs) produced by commensal microorganisms during starch fermentation have an immunomodulatory effect on the balance of pro- and anti-inflammatory cells. For instance, butyrate, a known histone deacetylase inhibitor, facilitates extrathymic generation of Tregs due to increased Foxp3 protein acetylation (Arpaia et al.,

2013). Another SCFA, pentanoate, also shows potent histone deacetylase-inhibitory activity in CD4 + T cells and reduces IL-17A production and Th17 cell differentiation; however, it does not have an impact on Tregs development, despite being able to induce the production of IL-10 (a Tregs-promoting cytokine) in lymphocytes by reprograming their metabolic activity toward elevated glucose oxidation, supplying additional pentanoate-originated acetyl-CoA for histone acetyltransferases, and allowing IL-10 transcription after pentanoate-triggered enhancement of mTOR activity (Luu et al., 2019). High blood butyrate and propionate levels are also associated with resistance to CTLA-4 blockade and higher proportion of Tregs cells in TME (Coutzac et al., 2020).

Using metabolomics data, a key bifurcation point between T cell glycolytic and oxidative metabolism was discovered, specifically, the TCR-signaling-dependent activation of PDHK1, an inhibitor of PDH, was found to be involved (Menk et al., 2018). PDHK1 plays a role in CD4 + T cell fate through mechanisms depending on the CD4 + effector T cell subtype, as indicated by the enzyme being expressed in Th17 cells but not in Th1 cells and being required for Th17 cell but not Tregs function *in vitro* (Gerriets et al., 2015). In addition, a differential coupling of serine metabolism based on lineage choices and the production of cytokines IL-17 or IFN-γ were demonstrated by a data-driven metabolic network in an untargeted metabolomics analysis, while targeting the serine pathway promoted Tregs lineage development (Andrejeva, 2018).

Differential T cell metabolism can be used as a target to produce a specific CD4 + T cell phenotype, due to its strong relation with GRN components. In addition to these metabolomics and systems biology studies focusing on physiology and function, these technologies have also been employed in the search for diagnostics and markers of disease status and outcome, giving them another layer of potential use within the field of cancer immunotherapy (Li H. et al., 2019).

IMMUNOTHERAPY APPLICATIONS: OMICS DATA AND MATHEMATICAL MODELS AND LIMITATIONS

We have emphasized strong functional indicators of the differentiation and roles that Tregs and Th17 cells have in the progression and in the treatment of cancer, as well as in how they react to external stimuli. The Th plasticity between these also plays an important role in the TME. This plasticity/reprograming can occur simultaneously or sequentially in response to specific microenvironmental cues to ultimately fuel complex immune interactions that participate in tumor progression (Jäger et al., 2009). This complex interplay adds new dimensions to the immunometabolism of T cells, and can present a hurdle for data interpretation.

The differentiated Tregs cells can be converted into Th17 cells under the influence of strong inflammatory conditions (Xu et al., 2007). For instance, hypoxia induced the expression of IL-17 in $FOXP3^+$ Tregs in colorectal cáncer (CRC), $FOXP3^+IL\text{-}17^+$ T cells were then capable of inducing CRC-associated cell markers in bone marrow-derived mononuclear cells and drove the cells to be cancer-initiating cells (Yang et al., 2011).

It is also important to note that, while much of the literature on effector T cells in the TME focuses at least in part on Th17 and Tregs, due to how their balance is known to influence prognosis, the TME is populated by other T cell subsets with important roles. Th9 and IL-9 are similarly considered complementary to Th17 cells, and have similarly been found to promote cancer metastasis, potentially in combination with Th17. Accordingly, inhibition of IL-9 or IL-17 cytokines by neutralizing antibodies decreased epithelial-mesenchymal transition (EMT) and slowed lung cancer progression and metastasis (Salazar et al., 2020).

An anti-tumor property of Th1/Th17 hybrid cells have also been reported. The heightened effector function and prolonged persistence of Th1 and Th17 cells, respectively, are the key features of these hybrid cells. The enhanced anti-tumor cells were dependent on the increased NAD(+)-dependent activity of the histone deacetylase Sirt1 (Chatterjee et al., 2018). Th1, in similarly to Th17, depends on glutaminase activity and glutamine metabolism (Johnson et al., 2018). Glutamine metabolism affected histone modifications in human breast cancer cell lines, and the treatment of non-invasive epitelial and invasive mesenchymal breast cancer cell lines with a glutaminase inhibitor induce a downregulation of epigenetic regulatory genes, such as Sirt1. The interplay of metabolism and epigenetic regulatory mechanisms has become a focal point for a better understanding of cancer development and progression (Simpson et al., 2012; Renaude et al., 2020).

Similarly, Tregs have attracted attention due to their well-defined metabolic hallmarks, such as their reliance on FAO and oxidative phosphorylation for energy production and the centrality of mTORC1 for their maintenance. These features, have led to them also being targeted for metabolic modulation within the TME for therapeutic purposes, through targets such as TLR8. TLR8 signaling-mediated reprograming of glucose metabolism and function in human Tregs cells can enhance anti-tumor immunity *in vivo* in a melanoma adoptive transfer T cell therapy model (Li L. et al., 2019).

Singling out immunotherapy, for which one of the major modern challenges has been the balancing of patient benefit with a low toxicity profile, the fact that metabolites are the products and byproducts of cellular biochemical activities places them downstream of all other "omics" technologies; this makes them excellent biomarkers for disease and toxic stimuli/conditions within the body (Metallo and Vander Heiden, 2013; Zhang et al., 2015).

Factors such as the inherent variability of cancer and the complexity of the TME make it very difficult to detect a viable and reproducible metabolic fingerprint, especially when considering how certain components of the TME, such as Th17 cells and other subsets with IL-17 and IL-23, can help both fight (Muranski et al., 2008) and promote cancer growth (Numasaki et al., 2005; Dawod et al., 2020), but it is also notable that positive results have been achieved recently during attempts to find biomarkers of chemotherapeutic responses (Cardoso et al., 2018; Amin et al., 2019; Ghini et al., 2020). Biomarkers for response to immune checkpoint inhibitor therapy (ICI), such as the ratio of

serum kynurenine/tryptophan, have shown promise in detecting negative outcomes for treatment in advanced melanoma and renal cell carcinoma patients treated with nivolumab, an antibody against programed cell death protein 1 (PD1) (Li H. et al., 2019). Metabolites are also routinely integrated (together with proteomics and transcriptomics) in proposed diagnostic tools for multiple types of cancer (Argelaguet et al., 2018; MacMullan et al., 2019).

The ubiquity of metabolomics data when studying immunotherapy is especially notable due to the presence of this technology in many of the most recent trends in the field, such as the acknowledgment of the importance of the microbiome (Gopalakrishnan et al., 2018), and how selectively-enriched fauna can influence treatment outcomes (Botticelli et al., 2020). Keen et al. (2018) also proposed the inclusion of high-throughput proteomics and metabolomics (in addition to genomic sequencing) in future large-scale studies that aim to show that ICI success is dependent on the microbiome to better characterize the mechanisms at play. The use of immunometabolomics is slowly uncovering new therapies and helping to better understand the behavior of these cells.

However, it is equally important to acknowledge that these options do not exist in isolation and serve best when incorporated with existing modalities. As an example of this, a recent single cells *in silico* based on single-cell RNA-Seq and flux balance analysis by Wagner et al. (2020) showed that, Th17 cell metabolic diversity reflects a balance between glycolysis and FAO, which is associated with pathogenicity. Pathogenic Th17 cells maintain higher aerobic glycolysis and TCA activity, whereas non-pathogenic Th17 cells oxidize fatty acids to produce ATP (Wagner et al., 2020). It agrees with our hypotheses proposed in previous sections, indicating that the processes of differentiation of Th17 and Tregs is changing over time and can go through various processes of activation or inhibition of signaling pathways (**Figure 4**).

This also reinforce the notion that, as useful as a metabolomics approach can be, it benefits from being incorporated into a larger toolkit that helps to make these results more context-sensitive. Mathematical modeling of cancer metabolism has been undertaken for decades (Markert and Vazquez, 2015) and has recently been an active part of drug discovery and therapeutic design (Sun et al., 2016; Roy and Finley, 2017), but the extreme complexity of the TME and the associated signaling and cross talk between lymphocytes and other cells has made precise modeling and interpretation very difficult, however, this situation is slowly improving due to systems biology integration (Pinu et al., 2019). For instance, a set of mathematical equations has been used to describe the pharmacodynamics of radiotherapy in combination with two immunotherapies, the blockers PD1-PDL1 axis and of the CTLA-4 pathway. This model explained several experimental results reported in preclinical and clinical settings, and paves the way for the efficient *in silico* design and optimization of combined anticancer therapies (Serre et al., 2016).

Despite some limitations in System Biology and omics approaches, including difficulties in collecting and processing data, lack of a suitably optimized immunometabolism-dedicated metabolite database, and potential technological limitations, there have been several promising advances in the disparate omics fields and continuous efforts are being taken to achieve their seamless integration on fundamental levels (Mitchell et al., 2015). This could potentially be beneficial for the study and treatment to other immune-mediated diseases, ranging from rheumatoid arthritis to multiple sclerosis and Alzheimer's disease (Ferretti et al., 2016; Ciccocioppo et al., 2019), assuming the datasets generated are of high enough quality.

For example, simultaneous single-cell multiomics data collection will likely result in higher quality and more reproducible or directly comparable data sets. When coupled with efforts for further methodological and instrumental standardization, these data collection methods present unique opportunities to gain understanding on the fundamentals of CD4 + T cell differentiation and CD4 + T cell-focused applications in future immunotherapies.

DISCUSSION

The effect of Th lymphocytes on carcinogenesis may largely depend on the context of the tumor type and cancer stage, cytokine availability, receptor distribution, and crosstalk among different stimuli, cell types, and signaling pathways.

The complexity of CD4 + T cell function in TME has contributed to some of the limitations found in system biology interpretation, therefore, the complementarity of these methods with omics data will be necessary to obtain more precise hypotheses.

Intracellular network modeling has been used because of the importance of understanding that a range of dynamic cell population behaviors, including cellular synchronization, delays, and bimodal responses, can emerge from simple networks (Eizenberg-Magar et al., 2017; Thurley et al., 2018). The function of Th17 and Tregs modeling will allow for the prediction of the effect of these subpopulations on tumor development.

Omics integration is reaching its maximum point in the definition toward a better response and understanding of the TME. The integration of metabolomics has presented useful future applications to understand CD4 + T cell behavior in TME. In particular, it has recently produced promising results in the subcellular imaging of specific metabolite distributions (Pareek et al., 2020), revealing novel potential techniques for monitoring immune cell metabolic signals. However, few current examples of a full system biology integration with other omics data are known, despite promising clinical applications and toward a better CD4 + T cell function delineation in the TME (Lazarus et al., 2019; Kirshtein et al., 2020; Paterson et al., 2020).

AUTHOR CONTRIBUTIONS

KC-J and GR contributed equally to the writing of the manuscript. NF and VS contributed to its revision. All authors contributed to the article and approved the submitted version.

REFERENCES

Abou-Jaoudé, W., Monteiro, P. T., Naldi, A., Grandclaudon, M., Soumelis, V., Chaouiya, C., et al. (2015). Model checking to assess T-helper cell plasticity. *Front. Bioeng. Biotechnol.* 2:86. doi: 10.3389/fbioe.2014.00086

Amin, S., Rattner, J., Keramati, M. R., Farshidfar, F., McNamara, M. G., Knox, J. J., et al. (2019). A strategy for early detection of response to chemotherapy drugs based on treatment-related changes in the metabolome. *PLoS One* 14:e0213942. doi: 10.1371/journal.pone.0213942

Andrejeva, G. (2018). Metabolomics analysis reveals differential t-cell serine metabolism as a target in autoimmunity. *J. Immunol.* 200:167.7.

Angela, M., Endo, Y., Asou, H. K., Yamamoto, T., Tumes, D. J., Tokuyama, H., et al. (2016). Fatty acid metabolic reprogramming via MTOR-mediated inductions of PPARγ directs early activation of T cells. *Nat. Commun.* 7:13683. doi: 10.1038/ncomms13683

Angelin, A., Gil-de-Gómez, L., Dahiya, S., Jiao, J., Guo, L., Levine, M. H., et al. (2017). Foxp3 reprograms T cell metabolism to function in low-glucose, high-lactate environments. *Cell. Metabol.* 25, 1282–1293. doi: 10.1016/j.cmet.2016.12.018

Argelaguet, R., Velten, B., Arnol, D., Dietrich, S., Zenz, T., Marioni, J. C., et al. (2018). Multi-omics factor analysis—a framework for unsupervised integration of multi-omics data sets. *Mol. Syst. Biol.* 14:e8124. doi: 10.15252/msb.20178124

Arpaia, N., Campbell, C., Fan, X., Dikiy, S., van der Veeken, J., deRoos, P., et al. (2013). Metabolites produced by commensal bacteria promote peripheral regulatory T-cell generation. *Nature* 504, 451–455. doi: 10.1038/nature12726

Berod, L., Friedrich, C., Nandan, A., Freitag, J., Hagemann, S., Harmrolfs, K., et al. (2014). De novo fatty acid synthesis controls the fate between regulatory T and T helper 17 cells. *Nat. Med.* 20, 1327–1333. doi: 10.1038/nm.3704

Botticelli, A., Vernocchi, P., Marini, F., Quagliariello, A., Cerbelli, B., Reddel, S., et al. (2020). Gut metabolomics profiling of non-small cell lung cancer (NSCLC) patients under immunotherapy treatment. *J. Transl. Med.* 18:49. doi: 10.1186/s12967-020-02231-0

Buck, M. D., O'Sullivan, D., and Pearce, E. L. T. (2015). Cell metabolism drives immunity. *J. Exper. Med.* 212, 1345–1360. doi: 10.1084/jem.20151159

Calder, M., Craig, C., Culley, D., de Cani, R., Donnelly, C. A., Douglas, R., et al. (2018). Computational modelling for decision-making: where, why, what, who and how. *R. Soc. open sci.* 5:172096. doi: 10.1098/rsos.172096

Carbo, A., Hontecillas, R., Andrew, T., Eden, K., Mei, Y., Hoops, S., et al. (2014). Computational modeling of heterogeneity and function of CD4+ T cells. *Front. Cell Dev. Biol.* 2:31. doi: 10.3389/fcell.2014.00031

Carbo, A., Hontecillas, R., Kronsteiner, B., Viladomiu, M., Pedragosa, M., Lu, P., et al. (2013). Systems modeling of molecular mechanisms controlling cytokine-driven CD4+ T cell differentiation and phenotype plasticity. *PLoS Comput. Biol.* 9:e1003027. doi: 10.1371/journal.pcbi.1003027

Carbonetti, G., Wilpshaar, T., Kroonen, J., Studholme, K., Converso, C., d'Oelsnitz, S., et al. (2019). FABP5 coordinates lipid signaling that promotes prostate cancer metastasis. *Sci. Rep.* 9:18944. doi: 10.1038/s41598-019-55418-x

Cardoso, M., Santos, J., Ribeiro, M., Talarico, M., Viana, L., and Derchain, S. (2018). A metabolomic approach to predict breast cancer behavior and chemotherapy response. *Int. J. Mol. Sci.* 19:617. doi: 10.3390/ijms19020617

Carlson, C. B., Robers, M. B., Vogel, K. W., and Machleidt, T. (2009). Development of lanthascreen^{TM} cellular assays for key components within the PI3K/AKT/MTOR pathway. *J. Biomol. Screen* 14, 121–132. doi: 10.1177/1087057108328132

Chakraborty, A. K. A. (2017). Perspective on the role of computational models in immunology. *Annu. Rev. Immunol.* 35, 403–439. doi: 10.1146/annurev-immunol-041015-055325

Chang, C.-H., Curtis, J. D., Maggi, L. B., Faubert, B., Villarino, A. V., O'Sullivan, D., et al. (2013). Posttranscriptional control of T cell effector function by aerobic glycolysis. *Cell* 153, 1239–1251. doi: 10.1016/j.cell.2013.05.016

Chatterjee, S., Daenthanasanmak, A., Chakraborty, P., Wyatt, M. W., Dhar, P., Selvam, S. P., et al. (2018). CD38-NAD+Axis regulates immunotherapeutic anti-tumor T cell response. *Cell. Metabol.* 27, 85–100. doi: 10.1016/j.cmet.2017.10.006

Chong, J., Soufan, O., Li, C., Caraus, I., Li, S., Bourque, G., et al. (2018). MetaboAnalyst 4.0: towards more transparent and integrative metabolomics analysis. *Nucleic Acids Res.* 46, W486–W494. doi: 10.1093/nar/gky310

Chou, T.-F., Chuang, Y.-T., Hsieh, W.-C., Chang, P.-Y., Liu, H.-Y., Mo, S.-T., et al. (2016). Tumour suppressor death-associated protein kinase targets cytoplasmic HIF-1α for Th17 suppression. *Nat. Commun.* 7:11904. doi: 10.1038/ncomms11904

Christie, D., and Zhu, J. (2014). Transcriptional regulatory networks for CD4 T cell differentiation. *Curr. Top. Microbiol. Immunol.* 381, 125–172. doi: 10.1007/82_2014_372

Ciccocioppo, F., Lanuti, P., Pierdomenico, L., Simeone, P., Bologna, G., Ercolino, E., et al. (2019). The characterization of regulatory T-cell profiles in Alzheimer's disease and multiple sclerosis. *Sci. Rep.* 9:8788. doi: 10.1038/s41598-019-45433-3

Ciofani, M., Madar, A., Galan, C., Sellars, M., Mace, K., Pauli, F., et al. (2012). Validated regulatory network for Th17 cell specification. *Cell* 151, 289–303. doi: 10.1016/j.cell.2012.09.016

Corral-Jara, K. F., Chauvin, C., Abou-Jaoudé, W., Grandclaudon, M., Naldi, A., Soumelis, V., et al. (2021). Interplay between SMAD2 and STAT5A is a critical determinant of IL-17A/IL-17F differential expression. *Mol. Biomed.* 2021, 2–16.

Coutzac, C., Jouniaux, J.-M., Paci, A., Schmidt, J., Mallardo, D., Seck, A., et al. (2020). Systemic short chain fatty acids limit antitumor effect of CTLA-4 blockade in hosts with cancer. *Nat. Commun.* 11:2168. doi: 10.1038/s41467-020-16079-x

Dahmani, A., and Delisle, J.-S. (2018). TGF-β in T cell biology: implications for cancer immunotherapy. *Cancers* 10:194. doi: 10.3390/cancers10060194

Dawod, B., Liu, J., Gebremeskel, S., Yan, C., Sappong, A., Johnston, B., et al. (2020). Myeloid-derived suppressor cell depletion therapy targets IL-17A-expressing mammary carcinomas. *Sci. Rep.* 10:13343. doi: 10.1038/s41598-020-70231-7

Diller, M. L., Kudchadkar, R. R., Delman, K. A., Lawson, D. H., and Ford, M. L. (2016). Balancing inflammation: the link between Th17 and regulatory T cells. *Mediators Inflamm.* 2016, 1–8. doi: 10.1155/2016/6309219

Downs-Canner, S., Berkey, S., Delgoffe, G. M., Edwards, R. P., Curiel, T., Odunsi, K., et al. (2017). Suppressive IL-17A+Foxp3+ and Ex-Th17 IL-17AnegFoxp3+ Treg cells are a source of tumour-associated treg cells. *Nat. Commun.* 8:14649. doi: 10.1038/ncomms14649

DuPage, M., and Bluestone, J. A. (2016). Harnessing the plasticity of CD4+ T cells to treat immune-mediated disease. *Nat. Rev. Immunol.* 16, 149–163. doi: 10.1038/nri.2015.18

Ecker, C., Guo, L., Voicu, S., Gil-de-Gómez, L., Medvec, A., Cortina, L., et al. (2018). Differential reliance on lipid metabolism as a salvage pathway underlies functional differences of T cell subsets in poor nutrient environments. *Cell. Rep.* 23, 741–755. doi: 10.1016/j.celrep.2018.03.084

Eizenberg-Magar, I., Rimer, J., Zaretsky, I., Lara-Astiaso, D., Reich-Zeliger, S., and Friedman, N. (2017). Diverse continuum of CD4 $^{+}$ T-cell states is determined by hierarchical additive integration of cytokine signals. *Proc. Natl. Acad. Sci. USA* 114, E6447–E6456. doi: 10.1073/pnas.1615590114

Endo, Y., Asou, H. K., Matsugae, N., Hirahara, K., Shinoda, K., Tumes, D. J., et al. (2015). Obesity drives Th17 cell differentiation by inducing the lipid metabolic kinase, ACC1. *Cell. Rep.* 12, 1042–1055. doi: 10.1016/j.celrep.2015.07.014

Evans, C. M., and Jenner, R. G. (2013). Transcription factor interplay in t helper cell differentiation. *Briefings Funct. Genom.* 12, 499–511. doi: 10.1093/bfgp/elt025

Fan, M. Y., and Turka, L. A. (2018). Immunometabolism and PI(3)K signaling as a link between IL-2, Foxp3 expression, and suppressor function in regulatory T cells. *Front. Immunol.* 9:69. doi: 10.3389/fimmu.2018.00069

Ferretti, M. T., Merlini, M., Späni, C., Gericke, C., Schweizer, N., Enzmann, G., et al. (2016). T-cell brain infiltration and immature antigen-presenting cells in transgenic models of Alzheimer's disease-like cerebral amyloidosis. *Brain Behav. Immun.* 54, 211–225. doi: 10.1016/j.bbi.2016.02.009

Field, C. S., Baixauli, F., Kyle, R. L., Puleston, D. J., Cameron, A. M., Sanin, D. E., et al. (2020). Mitochondrial integrity regulated by lipid metabolism is a cell-intrinsic checkpoint for treg suppressive function. *Cell Metabol.* 31, 422–437. doi: 10.1016/j.cmet.2019.11.021

Frankel, A. E., Coughlin, L. A., Kim, J., Froehlich, T. W., Xie, Y., Frenkel, E. P., et al. (2017). Metagenomic shotgun sequencing and unbiased metabolomic profiling identify specific human gut microbiota and metabolites associated with immune checkpoint therapy efficacy in melanoma patients. *Neoplasia* 19, 848–855. doi: 10.1016/j.neo.2017.08.004

Frio, T. R. (2015). "High-Throughput Technologies: DNA and RNA Sequencing Strategies and Potential," in *Pan-cancer Integrative Molecular Portrait Towards*

a New Paradigm in Precision Medicine, eds C. Le Tourneau and M. Kamal (New York city, NY: Springer International Publishing).

Ganapathy-Kanniappan, S. (2017). Taming tumor glycolysis and potential implications for immunotherapy. *Front. Oncol.* 7:36. doi: 10.3389/fonc.2017.00036

Germain, R. N., Meier-Schellersheim, M., Nita-Lazar, A., and Fraser, I. D. C. (2011). Systems biology in immunology: a computational modeling perspective. *Annu. Rev. Immunol.* 29, 527–585. doi: 10.1146/annurev-immunol-030409-101317

Gerriets, V. A., Kishton, R. J., Nichols, A. G., Macintyre, A. N., Inoue, M., Ilkayeva, O., et al. (2015). Metabolic programming and PDHK1 control CD4+ T cell subsets and inflammation. *J. Clin. Invest.* 125, 194–207. doi: 10.1172/JCI76012

Ghini, V., Laera, L., and Fantechi, B. (2020). Metabolomics to assess response to immune checkpoint inhibitors in patients with non-small-cell lung cancer. *Cancers* 12:3574.

Gomez-Rodriguez, J., Sahu, N., Handon, R., Davidson, T. S., Anderson, S. M., Kirby, M. R., et al. (2009). Differential expression of interleukin-17A and -17F Is coupled to T cell receptor signaling via inducible T cell kinase. *Immunity* 31, 587–597. doi: 10.1016/j.immuni.2009.07.009

Gomez-Rodriguez, J., Wohlfert, E. A., Handon, R., Meylan, F., Wu, J. Z., Anderson, S. M., et al. (2014). Itk-mediated integration of T cell receptor and cytokine signaling regulates the balance between Th17 and regulatory T cells. *J. Exper. Med.* 211, 529–543. doi: 10.1084/jem.20131459

Gopalakrishnan, V., Helmink, B. A., Spencer, C. N., Reuben, A., and Wargo, J. A. (2018). The influence of the gut microbiome on cancer, immunity, and cancer immunotherapy. *Cancer Cell.* 33, 570–580. doi: 10.1016/j.ccell.2018.03.015

Grandclaudon, M., Perrot-Dockès, M., Trichot, C., Karpf, L., Abouzid, O., Chauvin, C., et al. (2019). Quantitative multivariate model of human dendritic cell-T helper cell communication. *Cell* 179, 432–447. doi: 10.1016/j.cell.2019.09.012

Guéry, L., and Hugues, S. (2015). Th17 cell plasticity and functions in cancer immunity. *BioMed. Res. Int.* 2015, 1–11. doi: 10.1155/2015/314620

Hatzioannou, A., Banos, A., Sakelaropoulos, T., Fedonidis, C., Vidali, M.-S., Köhne, M., et al. (2020). An intrinsic role of IL-33 in treg cell–mediated tumor immunoevasion. *Nat. Immunol.* 21, 75–85. doi: 10.1038/s41590-019-0555-2

Hawse, W. F., and Cattley, R. T. (2019). T cells transduce T-cell receptor signal strength by generating different phosphatidylinositols. *J. Biol. Chem.* 294, 4793–4805. doi: 10.1074/jbc.RA118.006524

Hiemer, S., Jatav, S., Jussif, J., Alley, J., Lathwal, S., Piotrowski, M., et al. (2019). Integrated metabolomic and transcriptomic profiling reveals novel activation-induced metabolic networks in human T cells. *bioRxiv* 46.

Hong, T., Xing, J., Li, L., and Tyson, J. J. A. (2011). Mathematical model for the reciprocal differentiation of T helper 17 cells and induced regulatory T cells. *PLoS Comput. Biol.* 7:e1002122. doi: 10.1371/journal.pcbi.1002122

Howie, D., Ten Bokum, A., Necula, A. S., Cobbold, S. P., and Waldmann, H. (2018). The role of lipid metabolism in T lymphocyte differentiation and survival. *Front. Immunol.* 8:1949. doi: 10.3389/fimmu.2017.01949

Jäger, A., Dardalhon, V., Sobel, R. A., Bettelli, E., and Kuchroo, V. K. (2009). Th1, Th17, and Th9 effector cells induce experimental autoimmune encephalomyelitis with different pathological phenotypes. *J. Immunol.* 183, 7169–7177. doi: 10.4049/jimmunol.0901906

Johnson, M. O., Wolf, M. M., Madden, M. Z., Andrejeva, G., Sugiura, A., Contreras, D. C., et al. (2018). Distinct regulation of Th17 and Th1 cell differentiation by glutaminase-dependent metabolism. *Cell* 175, 1780–1795. doi: 10.1016/j.cell.2018.10.001

Karahalil, B. (2016). Overview of systems biology and omics technologies. *Curr. Med. Chem.* 23, 4221–4230. doi: 10.2174/0929867323666160926150617

Keen, E. C., Crofts, T. S., and Dantas, G. (2018). Checkpoint checkmate: microbiota modulation of cancer immunotherapy. *Clin. Chem.* 64, 1280–1283. doi: 10.1373/clinchem.2017.286229

Kim, S.-H., Roszik, J., Grimm, E. A., and Ekmekcioglu, S. (2018). Impact of L-arginine metabolism on immune response and anticancer immunotherapy. *Front. Oncol.* 8:67. doi: 10.3389/fonc.2018.00067

Kirshtein, A., Akbarinejad, S., Hao, W., Le, T., Su, S., Aronow, R. A., et al. (2020). Data driven mathematical model of colon cancer progression. *J. Clin. Med.* 9:3947. doi: 10.3390/jcm9123947

Klosik, D. F., Grimbs, A., Bornholdt, S., and Hütt, M.-T. (2017). The interdependent network of gene regulation and metabolism is robust where it needs to be. *Nat. Commun.* 8:534. doi: 10.1038/s41467-017-00587-4

Knochelmann, H. M., Dwyer, C. J., Bailey, S. R., Amaya, S. M., Elston, D. M., Mazza-McCrann, J. M., et al. (2018). When worlds collide: Th17 and treg cells in cancer and autoimmunity. *Cell. Mol. Immunol.* 15, 458–469. doi: 10.1038/s41423-018-0004-4

Koch, U., and Radtke, F. (2011). Mechanisms of T cell development and transformation. *Annu. Rev. Cell Dev. Biol.* 27, 539–562. doi: 10.1146/annurev-cellbio-092910-154008

Lazarus, J., Oneka, M. D., Barua, S., Maj, T., Lanfranca, M. P., Delrosario, L., et al. (2019). Mathematical modeling of the metastatic colorectal cancer microenvironment defines the importance of cytotoxic lymphocyte infiltration and presence of PD-L1 on antigen presenting cells. *Ann. Surg. Oncol.* 26, 2821–2830. doi: 10.1245/s10434-019-07508-3

Li, H., Bullock, K., Gurjao, C., Braun, D., Shukla, S. A., Bossé, D., et al. (2019). Metabolomic adaptations and correlates of survival to immune checkpoint blockade. *Nat. Commun.* 10:4346. doi: 10.1038/s41467-019-12361-9

Li, L., Liu, X., Sanders, K. L., Edwards, J. L., Ye, J., Si, F., et al. (2019). TLR8-mediated metabolic control of human treg function: a mechanistic target for cancer immunotherapy. *Cell. Metabol.* 29, 103–123. doi: 10.1016/j.cmet.2018.09.020

Liston, A., and Schlenner, S. M. (2015). Regulatory T cell differentiation: cooperation saves the day. *EMBO J.* 34, 1145–1146. doi: 10.15252/embj.201591169

Liu, P., Gan, W., Chin, Y. R., Ogura, K., Guo, J., Zhang, J., et al. (2015). PtdIns(3,4,5)P_3-dependent activation of the MTORC2 kinase complex. *Cancer Discov.* 5, 1194–1209. doi: 10.1158/2159-8290.CD-15-0460

Luo, X., Zhao, X., Cheng, C., Li, N., Liu, Y., and Cao, Y. (2018). The implications of signaling lipids in cancer metastasis. *Exp. Mol. Med.* 50:127. doi: 10.1038/s12276-018-0150-x

Lutsiak, M. E. C., Tagaya, Y., Adams, A. J., Schlom, J., and Sabzevari, H. (2008). Tumor-induced impairment of TCR signaling results in compromised functionality of tumor-infiltrating regulatory T cells. *J. Immunol.* 180, 5871–5881. doi: 10.4049/jimmunol.180.9.5871

Luu, M., Pautz, S., Kohl, V., Singh, R., Romero, R., Lucas, S., et al. (2019). The short-chain fatty acid pentanoate suppresses autoimmunity by modulating the metabolic-epigenetic crosstalk in lymphocytes. *Nat. Commun.* 10:760. doi: 10.1038/s41467-019-08711-2

MacMullan, M. A., Dunn, Z. S., Graham, N., Yang, L., and Wang, P. (2019). Quantitative proteomics and metabolomics reveal biomarkers of disease as potential immunotherapy targets and indicators of therapeutic efficacy. *Theranostics* 9, 7872–7888. doi: 10.7150/thno.37373

Marco-Ramell, A., Palau-Rodriguez, M., Alay, A., Tulipani, S., Urpi-Sarda, M., Sanchez-Pla, A., et al. (2018). Evaluation and comparison of bioinformatic tools for the enrichment analysis of metabolomics data. *BMC Bioinform.* 19:1. doi: 10.1186/s12859-017-2006-0

Markert, E. K., and Vazquez, A. (2015). Mathematical models of cancer metabolism. *Cancer Metab.* 3:14. doi: 10.1186/s40170-015-0140-6

Martinez-Sanchez, M. E., Huerta, L., Alvarez-Buylla, E. R., and Villarreal Luján, C. (2018). Role of cytokine combinations on CD4+ T cell differentiation, partial polarization, and plasticity: continuous network modeling approach. *Front. Physiol.* 9:877. doi: 10.3389/fphys.2018.00877

Maruyama, T., Mimura, K., Izawa, S., Shiba, S., Watanabe, M., Kawaguchi, Y., et al. (2011). Immunonutritional diet modulates natural killer cell activation and Th17 cell distribution in patients with gastric and esophageal cancer. *Nutrition* 27, 146–152. doi: 10.1016/j.nut.2010.07.007

Matta, B. M., Lott, J. M., Mathews, L. R., Liu, Q., Rosborough, B. R., Blazar, B. R., et al. (2014). IL-33 Is an unconventional alarmin that stimulates IL-2 secretion by dendritic cells to selectively expand IL-33R/ST2$^+$ regulatory T cells. *J. Immunol.* 193, 4010–4020. doi: 10.4049/jimmunol.1400481

Mendoza, L., and Xenarios, I. A. (2006). Method for the generation of standardized qualitative dynamical systems of regulatory networks. *Theor. Biol. Med. Model.* 3:13. doi: 10.1186/1742-4682-3-13

Mendoza, L. A. (2013). Virtual culture of CD4+ T lymphocytes. *Bull. Math. Biol.* 75, 1012–1029. doi: 10.1007/s11538-013-9814-9

Menk, A. V., Scharping, N. E., Moreci, R. S., Zeng, X., Guy, C., Salvatore, S., et al. (2018). Early TCR signaling induces rapid aerobic glycolysis enabling distinct acute T cell effector functions. *Cell. Rep.* 22, 1509–1521. doi: 10.1016/j.celrep.2018.01.040

Metallo, C. M., and Vander Heiden, M. G. (2013). Understanding metabolic regulation and its influence on cell physiology. *Mol. Cell.* 49, 388–398. doi: 10.1016/j.molcel.2013.01.018

Miskov-Zivanov, N., Turner, M. S., Kane, L. P., Morel, P. A., and Faeder, J. R. (2013). The duration of T cell stimulation is a critical determinant of cell fate and plasticity. *Sci. Signal.* 6:ra97. doi: 10.1126/scisignal.2004217

Misra, B. B., Fahrmann, J. F., and Grapov, D. (2017). Review of emerging metabolomic tools and resources: 2015-2016: general. *ELECTROPHORESIS* 38, 2257–2274. doi: 10.1002/elps.201700110

Mitchell, C. J., Getnet, D., Kim, M.-S., Manda, S. S., Kumar, P., Huang, T.-C., et al. (2015). Multi-omic analysis of human naïve CD4+ T cells. *BMC Syst. Biol.* 9:75. doi: 10.1186/s12918-015-0225-4

Morel, P. A., Lee, R. E. C., and Faeder, J. R. (2017). Demystifying the cytokine network: mathematical models point the way. *Cytokine* 98, 115–123. doi: 10.1016/j.cyto.2016.11.013

Mukherjee, S., Rigaud, S., Seok, S.-C., Fu, G., Prochenka, A., Dworkin, M., et al. (2013). In silico modeling of Itk activation kinetics in thymocytes suggests competing positive and negative IP4 mediated feedbacks increase robustness. *PLoS One* 8:e73937. doi: 10.1371/journal.pone.0073937

Muranski, P., Boni, A., Antony, P. A., Cassard, L., Irvine, K. R., Kaiser, A., et al. (2008). Tumor-specific Th17-polarized cells eradicate large established melanoma. *Blood* 112, 362–373. doi: 10.1182/blood-2007-11-120998

Naldi, A., Carneiro, J., Chaouiya, C., and Thieffry, D. (2010). Diversity and plasticity of Th cell types predicted from regulatory network modelling. *PLoS Comput. Biol.* 6:e1000912. doi: 10.1371/journal.pcbi.1000912

Nicholas, D., Proctor, E. A., Jones, A., Raval, F., Habib, C., Corkey, B., et al. (2017). Fatty acid uptake unexpectedly supports a Th17 cytokine signature in type 2 diabetes (T2D) inflammation. *J. Immunol.* 198:197.21.

Numasaki, M., Watanabe, M., Suzuki, T., Takahashi, H., Nakamura, A., McAllister, F., et al. (2005). IL-17 enhances the net angiogenic activity and in vivo growth of human non-small cell lung cancer in SCID mice through promoting CXCR-2-dependent angiogenesis. *J. Immunol.* 175, 6177–6189. doi: 10.4049/jimmunol.175.9.6177

Pacella, I., Procaccini, C., Focaccetti, C., Miacci, S., Timperi, E., Faicchia, D., et al. (2018). Fatty acid metabolism complements glycolysis in the selective regulatory T cell expansion during tumor growth. *Proc. Natl. Acad. Sci. U S A.* 115, E6546–E6555. doi: 10.1073/pnas.1720113115

Padovan-Merhar, O., and Raj, A. (2013). Using variability in gene expression as a tool for studying gene regulation: characterizing gene regulation using expression variability. *WIREs Syst. Biol. Med.* 5, 751–759. doi: 10.1002/wsbm.1243

Pareek, V., Tian, H., Winograd, N., and Benkovic, S. J. (2020). Metabolomics and mass spectrometry imaging reveal channeled de novo purine synthesis in cells. *Science* 368, 283–290. doi: 10.1126/science.aaz6465

Paterson, C., Clevers, H., and Bozic, I. (2020). Mathematical model of colorectal cancer initiation. *Proc. Natl. Acad. Sci. USA* 117, 20681–20688. doi: 10.1073/pnas.2003771117

Pinu, F. R., Beale, D. J., Paten, A. M., Kouremenos, K., Swarup, S., Schirra, H. J., et al. (2019). Systems biology and multi-omics integration: viewpoints from the metabolomics research community. *Metabolites* 9:76. doi: 10.3390/metabo9040076

Priyadharshini, B., Loschi, M., Newton, R. H., Zhang, J.-W., Finn, K. K., Gerriets, V. A., et al. (2018). Cutting edge: TGF-β and phosphatidylinositol 3-kinase signals modulate distinct metabolism of regulatory T cell subsets. *J. Immunol.* 201, 2215–2219. doi: 10.4049/jimmunol.1800311

Rattray, N. J. W., Deziel, N. C., Wallach, J. D., Khan, S. A., Vasiliou, V., Ioannidis, J. P. A., et al. (2018). Beyond genomics: understanding exposotypes through metabolomics. *Hum. Genom.* 12:4. doi: 10.1186/s40246-018-0134-x

Renaude, E., Kroemer, M., Loyon, R., Binda, D., Borg, C., Guittaut, M., et al. (2020). The fate of Th17 cells is shaped by epigenetic modifications and remodeled by the tumor microenvironment. *Int. J. Mol. Sci.* 21:1673. doi: 10.3390/ijms21051673

Revu, S., Wu, J., Henkel, M., Rittenhouse, N., Menk, A., Delgoffe, G. M., et al. (2018). IL-23 and IL-1β drive human Th17 cell differentiation and metabolic reprogramming in absence of CD28 costimulation. *Cell. Rep.* 22, 2642–2653. doi: 10.1016/j.celrep.2018.02.044

Rivadeneira, D. B., and Delgoffe, G. M. (2018). Antitumor T-cell reconditioning: improving metabolic fitness for optimal cancer immunotherapy. *Clin. Cancer Res.* 24, 2473–2481. doi: 10.1158/1078-0432.CCR-17-0894

Rolph, M. S., Young, T. R., Shum, B. O. V., Gorgun, C. Z., Schmitz-Peiffer, C., Ramshaw, I. A., et al. (2006). Regulation of dendritic cell function and T cell priming by the fatty acid-binding protein AP2. *J. Immunol.* 177, 7794–7801. doi: 10.4049/jimmunol.177.11.7794

Roy, M., and Finley, S. D. (2017). Computational model predicts the effects of targeting cellular metabolism in pancreatic cancer. *Front. Physiol.* 8:217. doi: 10.3389/fphys.2017.00217

Sadozai, H., Gruber, T., Hunger, R. E., and Schenk, M. (2017). Recent successes and future directions in immunotherapy of cutaneous melanoma. *Front. Immunol.* 8:1617. doi: 10.3389/fimmu.2017.01617

Salazar, Y., Zheng, X., Brunn, D., Raifer, H., Picard, F., Zhang, Y., et al. (2020). Microenvironmental Th9 and Th17 lymphocytes induce metastatic spreading in lung cancer. *J. Clin. Invest.* 130, 3560–3575. doi: 10.1172/JCI124037

Salmond, R. J. (2018). MTOR regulation of glycolytic metabolism in T Cells. *Front. Cell Dev. Biol.* 6:122. doi: 10.3389/fcell.2018.00122

Schmidl, C., Delacher, M., Huehn, J., and Feuerer, M. (2018). Epigenetic mechanisms regulating T-cell responses. *J. Allergy Clin. Immunol.* 142, 728–743. doi: 10.1016/j.jaci.2018.07.014

Serre, R., Benzekry, S., Padovani, L., Meille, C., André, N., Ciccolini, J., et al. (2016). Mathematical modeling of cancer immunotherapy and its synergy with radiotherapy. *Cancer Res.* 76, 4931–4940. doi: 10.1158/0008-5472.CAN-15-3567

Shi, L. Z., Wang, R., Huang, G., Vogel, P., Neale, G., Green, D. R., et al. (2011). HIF1α–dependent glycolytic pathway orchestrates a metabolic checkpoint for the differentiation of TH17 and treg cells. *J. Exper. Med.* 208, 1367–1376. doi: 10.1084/jem.20110278

Shyer, J. A., Flavell, R. A., and Bailis, W. (2020). Metabolic signaling in T cells. *Cell. Res.* 30, 649–659. doi: 10.1038/s41422-020-0379-5

Simpson, N. E., Tryndyak, V. P., Pogribna, M., Beland, F. A., and Pogribny, I. P. (2012). Modifying metabolically sensitive histone marks by inhibiting glutamine metabolism affects gene expression and alters cancer cell phenotype. *Epigenetics* 7, 1413–1420.

Smolke, C. D., and Silver, P. A. (2011). Informing biological design by integration of systems and synthetic biology. *Cell* 144, 855–859. doi: 10.1016/j.cell.2011.02.020

Stubbington, M. J. T., Rozenblatt-Rosen, O., Regev, A., and Teichmann, S. A. (2017). Single-cell transcriptomics to explore the immune system in health and disease. *Science* 358, 58–63. doi: 10.1126/science.aan6828

Sun, X., Bao, J., and Shao, Y. (2016). Mathematical modeling of therapy-induced cancer drug resistance: connecting cancer mechanisms to population survival rates. *Sci. Rep.* 6:22498. doi: 10.1038/srep22498

Szabo, S. J., Kim, S. T., Costa, G. L., Zhang, X., Fathman, C. G., and Glimcher, L. H. A. (2000). Novel transcription factor, T-bet, directs Th1 lineage commitment. *Cell* 100, 655–669. doi: 10.1016/S0092-8674(00)80702-3

Thurley, K., Wu, L. F., and Altschuler, S. J. (2018). Modeling cell-to-cell communication networks using response-time distributions. *Cell. Syst.* 6, 355–367. doi: 10.1016/j.cels.2018.01.016

Trivedi, D. K., Hollywood, K. A., and Goodacre, R. (2017). Metabolomics for the masses: the future of metabolomics in a personalized world. *Eur. J. Mol. Clin. Med.* 3:294. doi: 10.1016/j.nhtm.2017.06.001

Tugues, S., Burkhard, S. H., Ohs, I., Vrohlings, M., Nussbaum, K., vom Berg, J., et al. (2015). New insights into IL-12-mediated tumor suppression. *Cell. Death Differ.* 22, 237–246. doi: 10.1038/cdd.2014.134

Vieira Braga, F. A., Teichmann, S. A., and Chen, X. (2016). Genetics and immunity in the era of single-cell genomics. *Hum. Mol. Genet.* 25, R141–R148. doi: 10.1093/hmg/ddw192

Wagner, A., Wang, C., DeTomaso, D., Avila-Pacheco, J., Zaghouani, S., Fessler, J., et al. (2020). In silico modeling of metabolic state in single Th17 cells reveals novel regulators of inflammation and autoimmunity. *J. Immunol.* 204:150.22.

Wang, R., and Solt, L. A. (2016). Metabolism of murine T $_H$ 17 cells: impact on cell fate and function. *Eur. J. Immunol.* 46, 807–816. doi: 10.1002/eji.201545788

Wang, Z., Danziger, S. A., Heavner, B. D., Ma, S., Smith, J. J., Li, S., et al. (2017). Combining inferred regulatory and reconstructed metabolic networks enhances phenotype prediction in yeast. *PLoS Comput. Biol.* 13:e1005489. doi: 10.1371/journal.pcbi.1005489

Xu, L., Kitani, A., Fuss, I., and Strober, W. (2007). Cutting edge: regulatory T cells induce CD4 $^{+}$ CD25 $^{-}$ Foxp3 $^{-}$ T cells or are self-induced to become Th17 cells in the absence of exogenous TGF-β. *J. Immunol.* 178, 6725–6729. doi: 10.4049/jimmunol.178.11.6725

Yang, S., Wang, B., Guan, C., Wu, B., Cai, C., Wang, M., et al. (2011). Foxp3 $^{+}$ IL-17 $^{+}$ T cells promote development of cancer-initiating cells in colorectal cancer. *J. Leukocyte Biol.* 89, 85–91. doi: 10.1189/jlb.0910506

Ye, J., Livergood, R. S., and Peng, G. (2013). The role and regulation of human Th17 cells in tumor immunity. *Am. J. Pathol.* 182, 10–20. doi: 10.1016/j.ajpath.2012.08.041

Yin, Z., Bai, L., Li, W., Zeng, T., Tian, H., and Cui, J. (2019). Targeting T cell metabolism in the tumor microenvironment: an anti-cancer therapeutic strategy. *J. Exp. Clin. Cancer Res.* 38:403. doi: 10.1186/s13046-019-1409-3

Yosef, N., Shalek, A. K., Gaublomme, J. T., Jin, H., Lee, Y., Awasthi, A., et al. (2013). Dynamic regulatory network controlling TH17 cell differentiation. *Nature* 496, 461–468. doi: 10.1038/nature11981

Zanetti, M. (2015). Tapping CD4 T cells for cancer immunotherapy: the choice of personalized genomics. *J. Immunol.* 194, 2049–2056. doi: 10.4049/jimmunol.1402669

Zenobi, R. (2013). Single-cell metabolomics: analytical and biological perspectives. *Science* 342:1243259. doi: 10.1126/science.1243259

Zhang, A., Sun, H., Yan, G., Wang, P., and Wang, X. (2015). Metabolomics for biomarker discovery: moving to the clinic. *BioMed. Res. Int.* 2015, 1–6. doi: 10.1155/2015/354671

Zheng, W., and Flavell, R. A. (1997). The transcription factor GATA-3 is necessary and sufficient for Th2 cytokine gene expression in CD4 T cells. *Cell* 89, 587–596. doi: 10.1016/S0092-8674(00)80240-8

Zhu, J., and Paul, W. E. (2010). Peripheral CD4+ T-cell differentiation regulated by networks of cytokines and transcription factors: transcription factor network in Th cells. *Immunol. Rev.* 238, 247–262. doi: 10.1111/j.1600-065X.2010.00951.x

Conflict of Interest: The authors declare that the research was conducted in the absence of any commercial or financial relationships that could be construed as a potential conflict of interest.

frontiers in Cell and Developmental Biology

ORIGINAL RESEARCH
published: 03 June 2021
doi: 10.3389/fcell.2021.633927

ALKBH1-8 and FTO: Potential Therapeutic Targets and Prognostic Biomarkers in Lung Adenocarcinoma Pathogenesis

Geting Wu[1†], Yuanliang Yan[2†], Yuan Cai[1], Bi Peng[1], Juanni Li[1], Jinzhou Huang[3], Zhijie Xu[1,4] and Jianhua Zhou[1*]*

[1] Department of Pathology, Xiangya Hospital, Central South University, Changsha, China, [2] Department of Pharmacy, Xiangya Hospital, Central South University, Changsha, China, [3] Department of Oncology, Mayo Clinic, Rochester, MN, United States, [4] National Clinical Research Center for Geriatric Disorders, Xiangya Hospital, Central South University, Changsha, China

OPEN ACCESS

Edited by:
Rodrigo Nalio Ramos, INSERM U1138 Centre de Recherche des Cordeliers (CRC), France

Reviewed by:
Jimena Tosello, Institut Curie, France
Kewa Gao, University of California, Davis, United States

***Correspondence:**
Zhijie Xu
xzj1322007@csu.edu.cn
Jianhua Zhou
zhoujh15@163.com

[†] *These authors have contributed equally to this work*

Specialty section:
This article was submitted to Molecular Medicine, a section of the journal Frontiers in Cell and Developmental Biology

Received: *26 November 2020*
Accepted: *03 May 2021*
Published: *03 June 2021*

Citation:
Wu G, Yan Y, Cai Y, Peng B, Li J, Huang J, Xu Z and Zhou J (2021) ALKBH1-8 and FTO: Potential Therapeutic Targets and Prognostic Biomarkers in Lung Adenocarcinoma Pathogenesis. Front. Cell Dev. Biol. 9:633927. doi: 10.3389/fcell.2021.633927

The AlkB family consists of Fe(II)- and α-ketoglutarate-dependent dioxygenases that can catalyze demethylation on a variety of substrates, such as RNA and DNA, subsequently affecting tumor progression and prognosis. However, their detailed functional roles in lung adenocarcinoma (LUAD) have not been clarified in a comprehensive manner. In this study, several bioinformatics databases, such as ONCOMINE, TIMER, and DiseaseMeth, were used to evaluate the expression profiles and prognostic significance of the AlkB family (ALKBH1-8 and FTO) in LUAD. The expression levels of ALKBH1/2/4/5/7/8 were significantly increased in LUAD tissues, while the expression levels of ALKBH3/6 and FTO were decreased. The main functions of differentially expressed AlkB homologs are related to the hematopoietic system and cell adhesion molecules. We also found that the expression profiles of the AlkB family are highly correlated with infiltrating immune cells (i.e., B cells, CD8 + T cells, CD4 + T cells, macrophages, neutrophils and dendritic cells). In addition, DNA methylation analysis indicated that the global methylation levels of ALKBH1/2/4/5/6/8 and FTO were decreased, while the global methylation levels of ALKBH3/7 were increased. In addition, the patients with upregulated ALKBH2 have significantly poor overall survival (OS) and post-progressive survival (PPS). Taken together, our work could provide insightful information about aberrant AlkB family members as potential biomarkers for the diagnostic and prognostic evaluation of LUAD. Especially, ALKBH2 could be served as a therapeutic candidate for treating LUAD.

Keywords: AlkB family, lung adenocarcinoma, expression profiles, prognosis, methylation, immune cell infiltration

INTRODUCTION

Lung cancer is one of the most common malignant tumors in the world (Yan et al., 2019). Thousands of patients die from this malignant disease every year. In addition, the incidence of lung cancer continues to increase (Lin et al., 2019; Subedi et al., 2019; Arbyn et al., 2020). Lung adenocarcinoma (LUAD) is the most common histological subtype of lung cancer (Wei et al., 2019). At present, great progress has been made in the diagnosis and treatment of LUAD (Lim and Ma, 2019; Zhang et al., 2019b), but there is still a lack

of advanced diagnosis and treatment programs (Oberndorfer and Mullauer, 2018). Therefore, it is urgent to identify more therapeutic targets and prognostic biomarkers.

The AlkB family of Fe(II) and α-ketoglutarate-dependent dioxygenases is a universal class of direct reversal DNA repair enzymes (Pilzys et al., 2019; Xu et al., 2020). This family of enzymes can remove alkyl adducts from nucleobases by oxidative dealkylation, protecting the bacterial genome from alkylation damage (Trewick et al., 2002; Liu et al., 2018). Research has found that there are currently 9 homologs of the AlkB protein, including ALKBH1-8 and FTO (Du et al., 2019; Xiao et al., 2020). They have multiple biological functions, such as regulation of RNA metabolism, involvement in the DNA damage response or participation in fatty acid metabolism (Wu et al., 2016; Bian et al., 2019; Rajecka et al., 2019).

Many studies have found that the AlkB family plays a key role in the occurrence and development of tumors either directly or indirectly, including breast cancer, ovarian cancer, and bladder cancer (Fujii et al., 2013; Tao et al., 2016; Zhu et al., 2019). However, the detailed role of the AlkB family in LUAD remains to be further elucidated. With the rapid development of second-generation gene sequencing technology and the establishment of various databases, a comprehensive analysis of the AlkB family is beneficial to the clarification of the AlkB family in LUAD pathogenesis and treatment. In this study, we conducted a thorough and comprehensive bioinformatics analysis of the AlkB family (including ALKBH1-8 and FTO) in LUAD. Moreover, we evaluated their potential as therapeutic targets and prognostic biomarkers based on multiple public bioinformatics databases. The purpose of this study is to help clinicians choose appropriate therapeutic drugs and more accurately predict the long-term prognosis of patients with LUAD.

MATERIALS AND METHODS

Oncomine3.0

Oncomine3.0[1] is a cancer microarray database and web-based data mining platform with 40 microarray data sets and approximately 100 differential expression analyses. It provides users with powerful, comprehensive genome-wide expression analysis (Rhodes et al., 2004, 2007). In this research, $p < 0.05$ and genes ranked in the top 10% were taken as the significance thresholds. Student's t test was used to analyze the difference in AlkB family expression in LUAD. Specific information is summarized in **Supplementary Table 1**.

GEPIA2

GEPIA2[2], Gene Expression Profiling Interactive Analysis, is a web-based that provides key interactive and customizable features, including differential expression analysis, correlation analysis, and patient survival analysis (Tang et al., 2017, 2019). In this study, we used the "single gene analysis" module of GEPIA to analyze mRNA expression differences between tumors and normal tissues. At the same time, multiple gene comparison analysis of the AlkB family was performed using the "Multiple Gene Comparison" module and the "KIRC" GEPIA dataset. Student's t test was used to generate p values for expression, and $p < 0.05$ was considered statistically significant.

UALCAN

UALCAN[3] is an interactive network resource based on TCGA datasets that can compare the primary tumor and normal tissue samples based on pathological stage, tumor grade and other clinicopathological characteristics (Chandrashekar et al., 2017). In our research, the expression data of the AlkB family were obtained through the "stage analysis" module and the "KIRC" data set of UALCAN. Differences in transcriptional expression were compared by Student's t test, and $p < 0.05$ was considered statistically significant.

The Human Protein Atlas

The Human Protein Atlas is a database of tools that can be used to identify clinically useful biomarkers using produced antibody and protein expression data (Asplund et al., 2012). Researchers can study the expression patterns of different proteins expressed in specific tumors. In this study, we directly compared the protein expression of Alkb family members in normal and LUAD tissues by immunohistochemistry.

Kaplan-Meier Plotter

Kaplan-Meier plotter[4] was used to analyze the prognostic value of the AlkB family in LUAD (Sun et al., 2019; Wang et al., 2019). To analyze OS and PPS in patients with LUAD, the patient samples were divided into two groups by median expression (high and low expression) and were evaluated by the K-M survival chart. Information on the number of high-risk cases, median mRNA expression levels, HR, 95% CI, and p values can be found on the K-M plotter website. A $p < 0.05$ was considered statistically significant.

cBioPortal

c-BioPortal[5], a comprehensive network of resources, can be used to explore, visualize and analyze multidimensional cancer genomics and clinical data. It contains more than 200 cancer genomics studies, including all the data on TCGA (Cerami et al., 2012; Wu et al., 2019). In this study, we analyzed the genome map of the AlkB family, which includes mutation and mRNA expression data. The mRNA expression z scores (RNA Seq V2 RSEM) were obtained using a z score threshold of ± 0.75.

GeneMANIA

Given a list of genes to query, GeneMANIA[6] can use vast amounts of genomics and proteomics data to find genes with similar functions. In addition, GeneMANIA can predict gene function.

[1]http://www.oncomine.org

[2]http://gepia.cancer-pku.cn/index.html

[3]http://ualcan.path.uab.edu/index.html

[4]http://kmplot.com/analysis/

[5]http://cbioportal.org

[6]http://genemania.org

Given a query gene, GeneMANIA finds genes that might share the target gene's function based on their interactions (Zuberi et al., 2013; Franz et al., 2018).

Cytoscape

Cytoscape can integrate biomolecular interaction networks with high-throughput expression data and other molecular states into a unified conceptual framework (Shannon et al., 2003). In this study, we performed functional integration on 284 co-expressed molecules of AlkB family members screened from cBioPortal (the molecular names are provided in **Supplementary Table 2**). According to the degree values between the interacting proteins decided the nodes size. The higher the degree, the larger the circles.

WebGestalt

WebGestalt[7] is a comprehensive, powerful, flexible, and interactive web-based analysis toolkit (Wang et al., 2017). Gene ontology (GO) enrichment analysis and Kyoto Encyclopedia of Genes and Genomes (KEGG) pathway analysis were performed in this study using WebGestalt.

TIMER2.0

TIMER2.0[8] can assess immune cell infiltration and the clinical impact of 10,897 tumors from 32 cancer types (Li et al., 2017). In our study, the "Gene Module" was used to assess the association between the AlkB family and immune cell infiltration. The "survival module" was used to assess the correlation of clinical outcomes with immune cell infiltration and the AlkB family. The multivariable cox proportional hazard model is used as the statistical method.

DiseaseMeth2.0

DiseaseMeth2.0[9] aims to provide information on abnormal DNA methylation in human diseases, especially all sorts of cancer, in the most complete collection and comments (Lv et al., 2012; Xiong et al., 2017). We used Wanderer to screen the possible methylation value of the AlkB family. A $p < 0.05$ was considered as statically significant.

RESULTS

Abnormal Expression of the AlkB Family in Patients With LUAD

We first searched the expression levels of the AlkB family (ALKBH1-ALKBH8, FTO) in LUAD and normal lung tissue using the Oncomine database. The results are shown in **Table 1**. The results demonstrated that the expression levels of ALKBH1/2/4/5/7/8 were significantly elevated in LUAD. Five datasets showed that ALKBH1 expression in LUAD was higher than that in normal lung tissue (Garber et al., 2001; Su et al., 2007; Landi et al., 2008; Hou et al., 2010; Okayama et al., 2012). In the Selamat and Hou datasets, the expression level of ALKBH2 in LUAD was significantly upregulated (Hou et al., 2010; Selamat et al., 2012). The results of Selamat (Selamat et al., 2012), Okayama (Okayama et al., 2012), Hou (Hou et al., 2010), and Su (Su et al., 2007) all suggest that ALKBH4 expression was significantly higher in LUAD compared with normal samples. The expression levels of ALKBH5 and ALKBH7 in LUAD were markedly higher than those in normal lung tissues in the Okayama (Okayama et al., 2012) and Hou (Hou et al., 2010) datasets. However, Selamat et al. (2012) found a decreased level of ALKBH8 in LUAD. Next, mRNA expression levels of the AlkB family in LUAD and normal lung tissue were verified in the GEPIA database. As shown in **Figure 1A**, the results showed clear support that the expression levels of ALKBH1/2/4/5/7/8 in LUAD were significantly elevated, while the expression levels of ALKBH3/6 and FTO were reduced compared with normal lung tissues. GEPIA was also used to compare the relative expression levels of the AlkB family in LUAD, and this analysis revealed that ALKBH5/7 had the highest relative expression levels among all AlkB family molecules (**Figure 1B**). After a comprehensive analysis of the mRNA expression levels of Alkb family in LUAD, we used the Human Protein Atlas to explore the protein expression levels of Alkb family in LUAD. The results showed that, ALKB1/2/4/5/7/8 was medium or high expression in LUAD. However, ALKB3/6 and FTO had low or no detect expression in LUAD. The results are shown in **Figure 1C**. This result is consistent with our previous findings on mRNA levels of expression. Moreover, UALCAN was used to analyze the relationship between the mRNA expression of AlkB family members and the clinicopathological staging of LUAD. From the results, it is clear that the mRNA expression level of ALKBH1/2/4/6 was positively correlated with tumor stage. In contrast, the mRNA expression levels of ALKBH7 and FTO were negatively correlated with tumor stage (**Figure 2A**).

TABLE 1 | The expression profiles of the AlkB family in patients with LUAD using the Oncomine database.

Name	Dataset	Fold change	*p* values	References
ALKBH1	Garber Lung	4.353	1.61E-4	Garber et al. (2001)
	Okayama Lung	1.368	5.58E-8	Okayama et al. (2012)
	Su Lung	1.100	0.035	Su et al. (2007)
	Landi Lung	1.069	0.016	Landi et al. (2008)
	Hou Lung	1.108	0.009	Hou et al. (2010)
ALKBH2	Selamat Lung	1.204	6.56E-5	Selamat et al. (2012)
	Hou Lung	1.211	9.00E-4	Hou et al. (2010)
ALKBH4	Su Lung	1.684	8.00E-4	Su et al. (2007)
	Hou Lung	1.181	8.88E-7	Hou et al. (2010)
	Selamat Lung	1.113	7.63E-4	Selamat et al. (2012)
	Okayama Lung	1.226	0.002	Okayama et al. (2012)
ALKBH5	Okayama Lung	1.227	0.004	Okayama et al. (2012)
	Hou Lung	1.093	0.006	Hou et al. (2010)
ALKBH7	Okayama Lung	1.117	0.015	Okayama et al. (2012)
	Hou Lung	1.052	0.047	Hou et al. (2010)
ALKBH8	Selamat Lung	1.219	1.19E-5	Selamat et al. (2012)

[7]http://www.webgestalt.org

[8]https://cistrome.shinyapps.io/timer/

[9]http://bioinfo.hrbmu.edu.cn/diseasemeth/

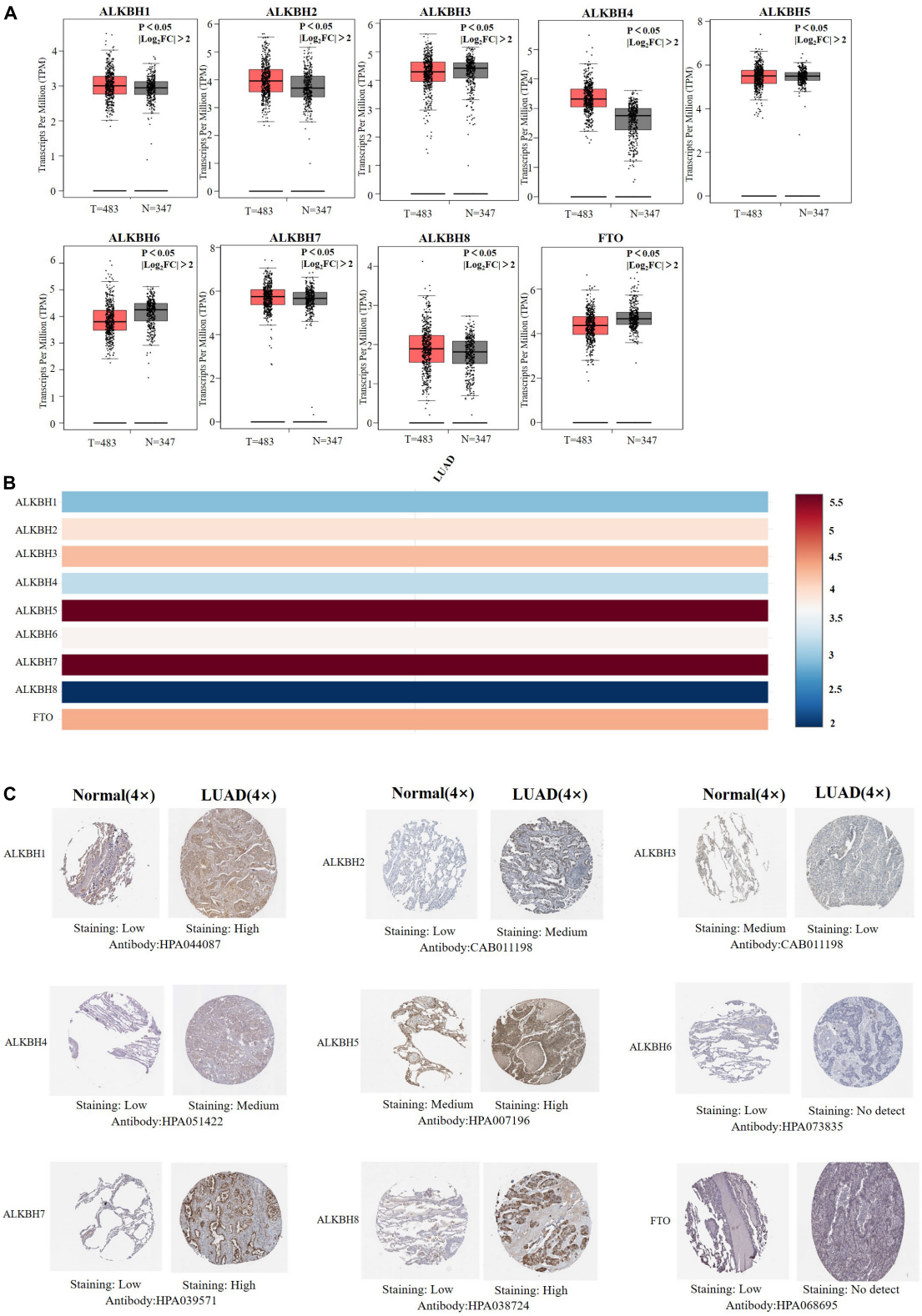

FIGURE 1 | (A) mRNA expression levels of different AlkB family members in LUAD and normal lung samples (GEPIA). T and N indicated the LUAD tissues and normal tissues, respectively. **(B)** The relative expression of the AlkB family in LUAD. **(C)** Immunohistochemical expression of ALKB family in LUAD tissue and normal lung tissue (the Human Protein Atlas).

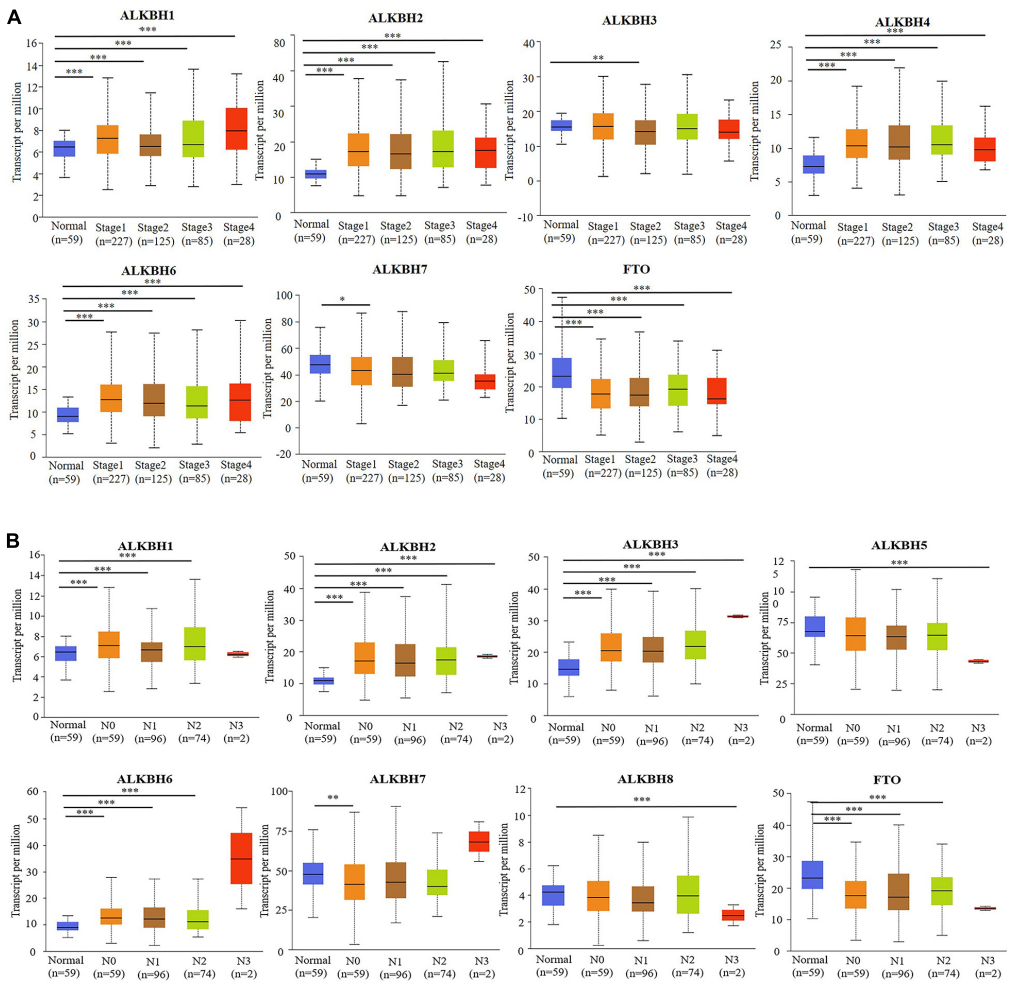

FIGURE 2 | (A) The relationship between mRNA expression and pathological stage of LUAD patients with different members of the AlkB family (UALCAN). **(B)** The relationship between mRNA expression of distinct AlkB family members with lymph node metastasis of LUAD patients (UALCAN). $^{*}p < 0.05$, $^{**}p < 0.01$, $^{***}p < 0.001$.

Similarly, the mRNA expression level of AlkB family members was also significantly correlated with lymph node metastasis. The highest mRNA expression levels of ALKBH2 and ALKBH3 were found in tumor N3 and were significantly correlated. At the same time, the mRNA expression levels of ALKBH2, ALKBH3, and ALKBH6 had a trend to upper expression in tumors with lymph node metastasis, although this was not significant. That may be caused by insufficient sample size and other reasons. Conversely, the expression levels of ALKBH5, ALKBH8 and FTO were lower than those in normal tissues at any stage of lymph node metastasis (**Figure 2B**).

Prognostic Value of mRNA Expression of the AlkB Family in LUAD Patients

Next, we used Kaplan-Meier plotter to analyze the prognostic values of the mRNA expression of AlkB family members in LUAD patients, including overall survival (OS) and post-progressive survival (PPS). The curves of OS are presented in **Figure 3A**. It is interesting to note that patients with higher transcription levels of ALKBH2, ALKBH4, and ALKBH7 displayed shorter OS times. The downregulations of ALKBH1, ALKBH3, ALKBH8, and FTO were significantly correlated with longer OS. However, ALKBH5 and ALKBH6 mRNA transcription showed no obvious correlation with the OS of LUAD patients. Moreover, the higher the transcription level of ALKBH2, the shorter the PPS in patients, while the higher the transcription levels of ALKBH3, ALKBH8 and FTO, the longer the PPS in patients. These results are summarized in **Figure 3B**.

Genetic Alteration and Functional Analysis of the AlkB Family in LUAD Patients

We conducted a comprehensive biological function analysis to further grasp the molecular characteristics of the differentially expressed AlkB family. The genetic alterations of the differentially expressed AlkB family were evaluated in the temporary TCGA

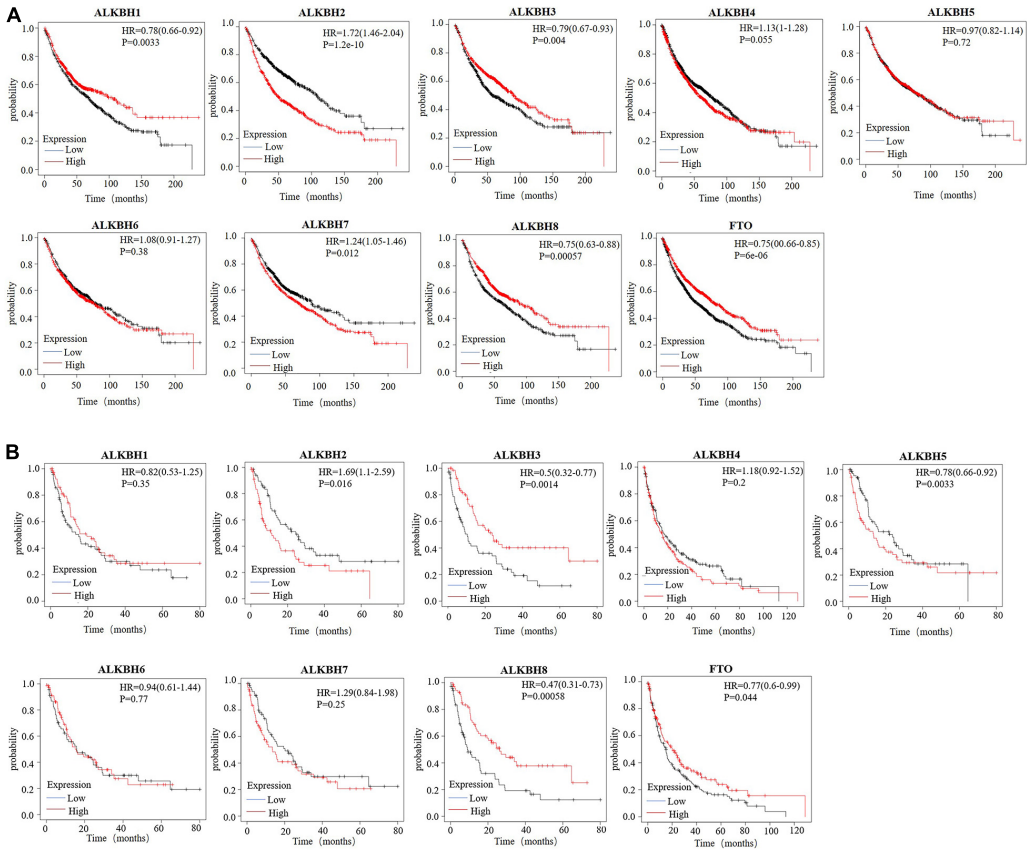

FIGURE 3 | (A) The overall survival curve of AlkB molecules in LUAD patients (Kaplan-Meier plotter). **(B)** The post-progressive survival curve of the AlkB molecules in LUAD patients (Kaplan-Meier plotter).

dataset. The results are shown in **Figure 4A**. ALKBH1, ALKBH2, ALKBH3, ALKBH4, ALKBH5, ALKBH6, ALKBH7, ALKBH8, and FTO were all altered, with 12, 6, 2, 2.8, 2.2, 3, 1, 2, and 1.8% alterations in the LUAD samples, respectively. We calculated the correlation by mRNA expression in the GEPIA online database, and Pearson's correction was included. There was a strongly negative correlation between ALKBH2 and FTO, ALKBH7 and ALKBH8. ALKBH5 was positively correlated with FTO, and ALKBH1 was positively correlated with ALKBH8 (**Figure 4B**).

In fact, multiple of cellular proteins can work in a synergistic manner by forming multi-protein complexes. Moreover, protein-protein interactions (PPIs) play important roles among the different functions of a cell. Therefore, exploring PPI patterns is essential for understanding the structure and function of protein complexes (Planas-Iglesias et al., 2013; Furmanova et al., 2018). Afterward, to discover the PPI patterns between the differentially expressed AlkB family, we downloaded 248 co-expressed molecules with the highest correlation with AlkB family members using the cBioPortal database and modified them with Cytoscape (**Figure 5A**). These data suggest that TNF, ITGAM, ITGB2, ITGAX, DOCK2, IRF4, IRF8, CXCR5, CSF2RB, ZAP70, and TBX21 were primarily associated with the modulation and function of AlkB family in LUAD. In addition, GO analysis could be used to annotate the biological meaning of candidate biomarkers and their functions in various organisms. It is composed of molecular functions, biological processes and cellular components (Gene Ontology Consortium, 2019). And KEGG, a genome encyclopedia, can be used to perform biological interpretation of fully sequenced genomes and infer the systematic behaviors of targeted gene sets (Kanehisa et al., 2017). To probe the biological functions of these co-expressed molecules, WebGestalt was used to conduct GO annotation and KEGG pathway analysis for this study. GO annotation recognized that the AlkB family is mainly located on the cell membrane and is involved in biological regulation processes. In terms of molecular function, the family mainly participates in protein binding (**Figure 5B**). The corresponding pathways, as shown **Figure 5C**, were hematopoietic cell lineage, viral myocarditis and cell adhesion molecules (CAMs).

Immune Cell Infiltration of the AlkB Family in LUAD Patients

Members of the AlkB family are involved in the inflammatory response and the infiltration of immune cells in the tumor (Zhang et al., 2019a), thereby affecting the clinical outcomes of LUAD patients. The TIMER database was used to discuss the correlation between the differential expression of the AlkB

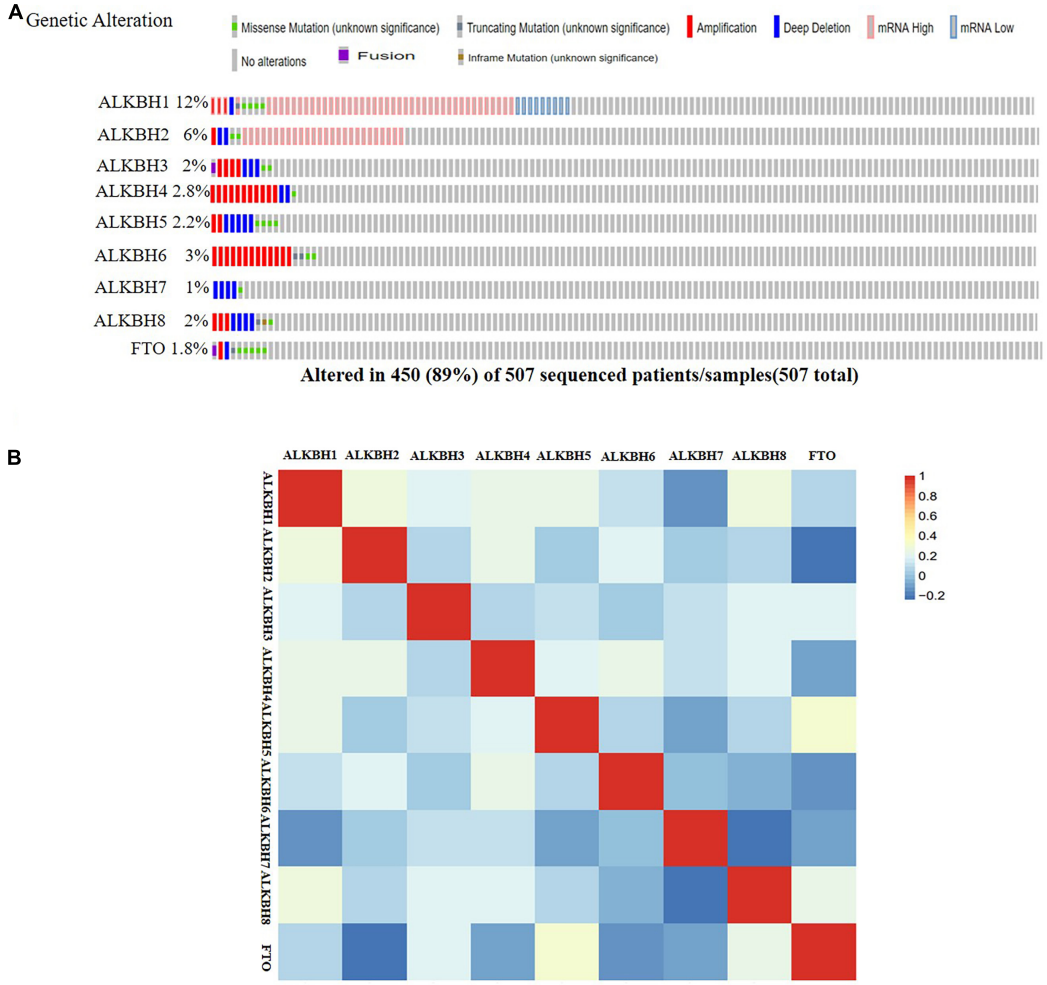

FIGURE 4 | Genetic alternatives and correlation analysis of the AlkB family in LUAD. **(A)** Summary of the mutation rates in each AlkB family member in LUAD. **(B)** Correlation between different AlkB family in LUAD (GEPIA).

family and immune cell infiltration. ALKBH1 and FTO were positively correlated with B cells, CD8 + T cells, CD4 + T cells, macrophages, neutrophils and dendritic cells (**Figures 6A,I**), but ALKBH2 was negatively correlated with these immune cells (**Figure 6B**). There were positive correlations between ALKBH3 expression and the infiltration of B cells, CD4 + cells, neutrophils and dendritic cells (**Figure 6C**) and negative correlations between ALKBH4 expression and the infiltration of CD8 + T cells and macrophages (**Figure 6D**). Similarly, ALKBH5 was positively correlated with CD4 + T cells (**Figure 6E**). In contrast, ALKBH6 and ALKBH7 were negatively correlated with CD8 + T cells and macrophages (**Figures 6F,G**). We also found that ALKBH8 was positively correlated with CD4 + T cells, CD8 + T cells, macrophages, neutrophils and dendritic cells (**Figure 6H**). We also evaluated the correlation between the expression levels of the AlkB family and immune cell infiltration. After adjusting for some confounding factors, including B cells, CD8 + T cells, CD4 + T cells, macrophages, neutrophils and dendritic cells, we used the Cox proportional hazard model to find that B cells were significantly associated with the clinical outcome of LUAD patients (**Table 2**).

Methylation Expression Levels of the AlkB Family in LUAD Patients

DNA methylation is negatively correlated with gene expression (Gensous et al., 2020; Kronfol et al., 2020). And we want to evaluate the effect of methylation on the expression levels of Alkb family members. We downloaded the methylation expression data of AlkB family members from the DiseaseMeth database. The results reflect that the methylation expression levels of ALKBH1, ALKBH2, and ALKBH6 are lower in LUAD samples than in normal samples. Furthermore, the methylation expression levels of ALKBH3 were higher in LUAD samples (**Supplementary Figure 1**). Previous findings indicated the upregulated ALKBH1/2 and downregulated ALKBH3 in LUAD samples (**Figure 1**). Thus, the abnormal expression of ALKBH1/2/3 might be due to the changes in their methylation values.

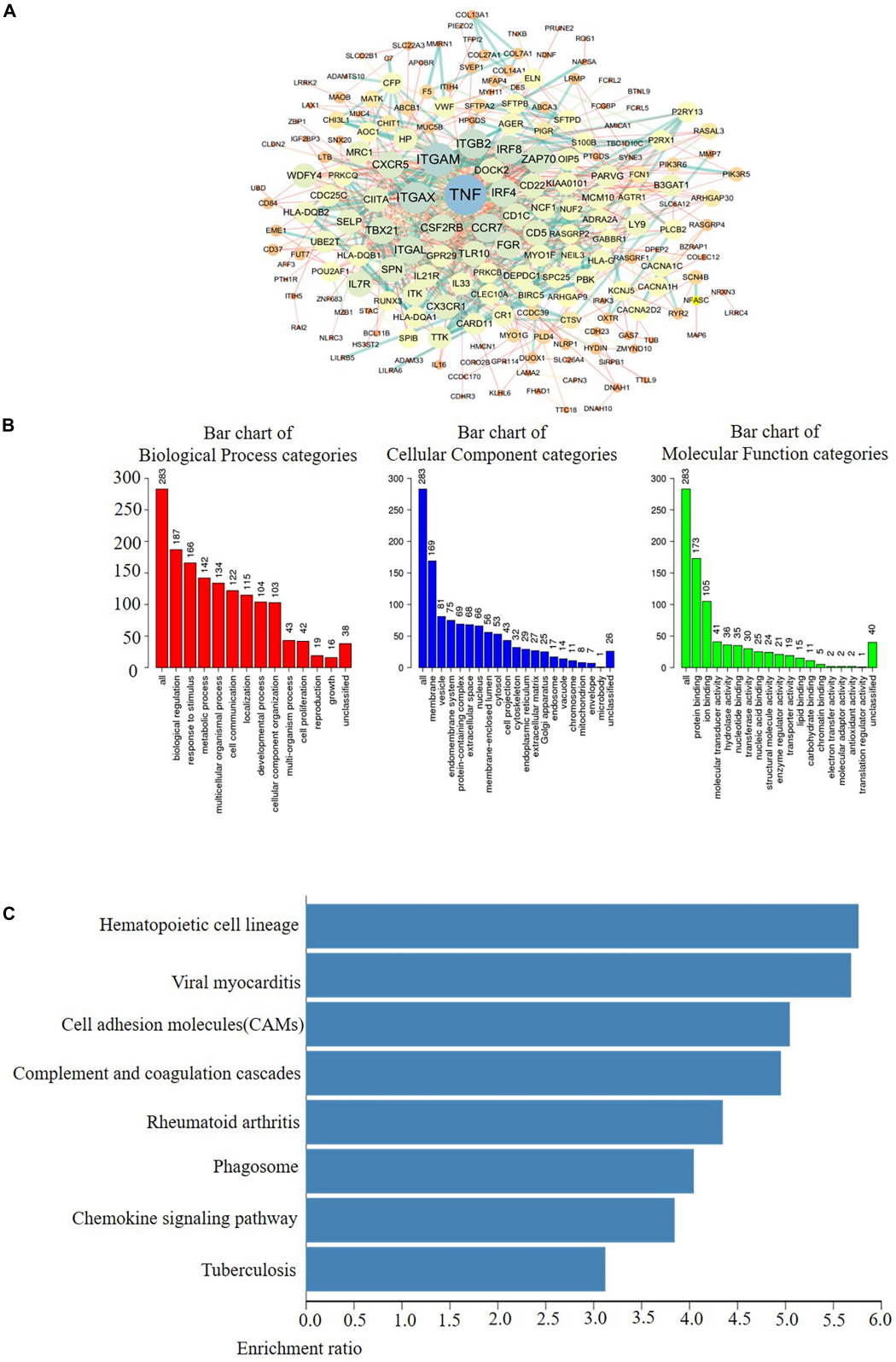

FIGURE 5 | Coexpression network analysis of the AlkB family in LUAD. **(A)** The PPI network of AlkB family interaction partners generated by the frequently used c-BioPortal and Cytoscape. **(B)** Primary molecular functions, biological processes and cell components related to the biology of the AlkB family were identified using WebGestalt. **(C)** Bar plot of KEGG enriched terms analyzed by WebGestalt.

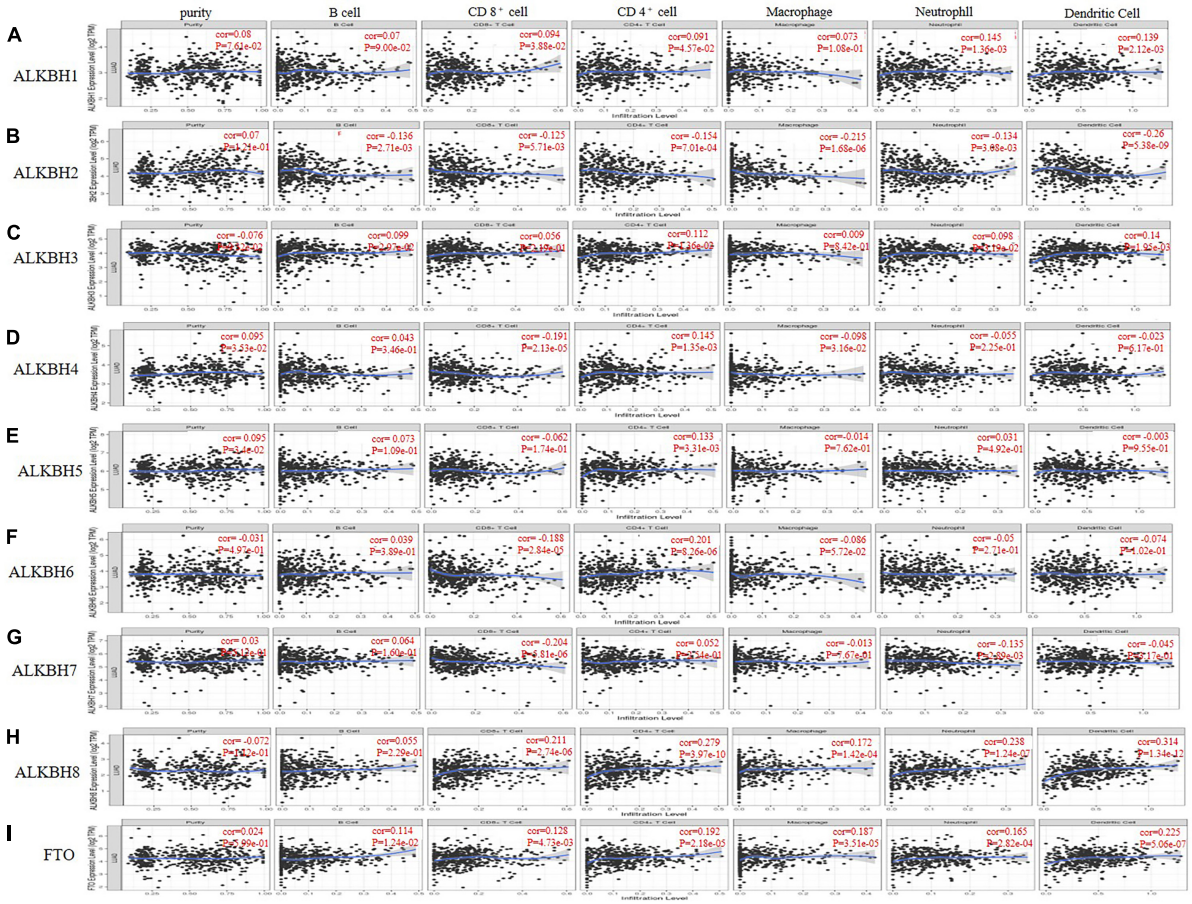

FIGURE 6 | The correlations between differentially expressed AlkB family and immune cell infiltration. **(A–I)** The effect of ALKBH1-8 and FTO on the immune cell infiltration analyzed by TIMER2.0.

DISCUSSION

Emerging reports have revealed that DNA damage induces autophagy, apoptosis and senescence of cells, thus playing pivotal roles in the development of malignant tumors (Lord and Ashworth, 2012; Roos et al., 2016). As a classic reversal DNA repair enzyme, the AlkB family cannot be ignored in the development of multiple cancers (Xie et al., 2018; Zhu et al., 2019). At present, some scholars have discovered that ALKBH5 regulates epithelial-mesenchymal transition and angiogenesis to promote cancer progression (Panneerdoss et al., 2018). Chen et al. found that ALKBH3 can promote the proliferation, migration and invasion of cancer cells (Panneerdoss et al., 2018). Although a few members of the AlkB family have been discovered to play critical roles in lung cancer (Tasaki et al., 2011; Wu et al., 2011), the specific roles of other members of the AlkB family in LUAD have not yet been elucidated.

In this research, the AlkB family was studied comprehensively in terms of its expression and clinical prognostic value in LUAD. For the first time, we summarized the mRNA expression levels of nine members of the ALKBH family in LUAD compared with normal tissues. Next, a further novel finding is that the AlkB family is closely related to individual clinicopathological stages and lymph node metastasis. In addition, higher expression levels of ALKBH2/4/7 were significantly associated with shorter OS times. Lower expression levels of ALKBH1/3/8 and FTO were significantly associated with longer OS times. The patients with elevated ALKBH3/8 and FTO levels had long PPS, while patients with decreased ALKBH2 levels had shortened PPS. The process of tumor occurrence is intricate and multifaceted, and genetic alterations play a significant role in this process (Martincorena et al., 2017; Sondka et al., 2018; Coelho et al., 2019). The AlkB family shows evidence of frequent gene alterations in LUAD. The expression alteration of mRNA is one of the most typical mutations. These results comprehensively demonstrated that differential expression of the AlkB family probably plays a critical role in LUAD.

After discovering that the AlkB family is differentially expressed in LUAD and normal tissues, we next explored their molecular biological functions. We focused on the functional analysis of the AlkB family and their 247 frequently altered neighboring genes in LUAD. DNA repair- and protein methyltransferase activity-related genes, including

TABLE 2 | The Cox proportional hazard model of the ALKB family and six tumor-infiltrating immune cells in LUAD.

	coef	HR	95%CI_l	95%CI_u	*p* value	sig
B cell	−5.066	0.006	0.000	0.088	0.000	***
CD8_Tcell	0.223	1.249	0.191	8.170	0.816	
CD4_Tcell	2.450	11.588	0.674	199.263	0.091	
Macrophage	−0.438	0.645	0.047	8.932	0.744	
Neutrophil	−0.368	0.692	0.014	33.222	0.852	
Dendritic	−0.038	0.962	0.249	3.714	0.955	
ALKBH1	−0.042	0.959	0.624	1.474	0.848	
ALKBH2	0.000	1.000	0.762	1.311	0.999	
ALKBH3	−0.088	0.915	0.720	1.164	0.471	
ALKBH4	−0.361	0.697	0.472	1.030	0.070	
ALKBH5	0.234	1.263	0.877	1.819	0.209	
ALKBH6	0.048	1.049	0.806	1.366	0.721	
ALKBH7	0.109	1.115	0.839	1.482	0.452	
ALKBH8	0.269	1.308	0.956	1.791	0.094	
FTO	−0.201	0.818	0.584	1.147	0.244	

****p < 0.001.*

ASCC3 and TRMT112, were highly linked to AlkB family alterations. Protein network interactions showed that TNF, ITGAM, ITGB2, ITGAX, DOCK2, IRF4, and IRF8 were primarily associated with the modulation and function of the differentially expressed AlkB family in LUAD. KEGG pathway analysis showed that AlkB family members were closely related to the CAMs. Multiple of CAM molecules have been proved to involve in the synaptic connection formation, maturation, function, and plasticity among cells. In a variety of human malignancies, including LUAD, tumor progression has been observed to be associated with altered CAM signaling pathways (Johnson, 1991). Similarly, Fujii and colleague reported the stimulative roles of ALKBH2 on the MUC1, an anti-adhesion molecule, on tumor cell growth (Fujii et al., 2013).

Increasing evidence shows that tumor progression and recurrence will be affected by immune cell infiltration and become an important determinant of immunotherapy response and clinical outcome (Lopes et al., 2019; Rotte, 2019). In our study, we found a significant correlation between the expression of the AlkB family and the infiltration of six immune cells, including B cells, CD8 + T cells, CD4 + T cells, macrophages, neutrophils and dendritic cells. Previous studies have shown that the relationship between tumor cells and immune microenvironment plays a key role in the occurrence and development of tumors (Varn et al., 2017). Many researchers have found that the infiltration of immune cells is closely related to the OS or disease-specific survival rate (DSS) of many cancers, including LUAD (Kadara et al., 2017; Hofman, 2020; Luo et al., 2020). As a kind of immune cells, B cells can fight against tumors through the production of antibodies, antigen royalty or the secretion of immune regulatory factors (Stoycheva et al., 2021). Han et al. (2020) found that B cells can be used as an independent indicator of OS prediction in LUAD. It is well known that methylation plays an important role in the development of cancer. In this study, we have found that Alkb family has abnormal expression of DNA methylation in LUAD. In fact, many researchers have also made some breakthroughs in the modification of RNA methylation in Alkb family. N6-methyladenosine is the most common RNA modification. ALKBH5, A member of the Alkb family, is the most widespread m^6A demethylase. It has been shown that ALKBH5 can inhibit tumor growth and metastasis (Ji et al., 2020; Jin et al., 2020). Zhu et al. (2020) found that m^6A-related gene ALKBH5 had a good predictive value in pathological staging and prognosis of LUAD. The results of our study reflect that the AlkB family not only can be used as prognostic indicators but also reflect immune status.

In this study, we comprehensively analyzed the expression and prognosis of the AlkB family in LUAD from the perspective of bioinformatics. Through a comprehensive analysis, we found that high ALKBH2 expression was significantly related to poor OS and PPS in LUAD patients. In addition, abnormally expressed ALKBH2 could also alter the immune cell infiltration in LUAD. These results provide novel biomarkers for the diagnosis of LUAD in the future and will help clinicians design potential therapeutic strategies for LUAD patients to improve the survival rate.

DATA AVAILABILITY STATEMENT

The original contributions presented in the study are included in the article/**Supplementary Material**, further inquiries can be directed to the corresponding authors.

AUTHOR CONTRIBUTIONS

GW, JL, and ZX: acquisition of the data. YY: analysis and interpretation of the data. JZ: conception and design. YC and BP: data curation. JH: development of the methodology. GW and ZX: writing the manuscript. All authors contributed to the article and approved the submitted version.

FUNDING

This work was supported by grants from the National Natural Science Foundation of China (No. 81803035), the Natural Science Foundation of Hunan Province (2020JJ5934 and 2019JJ50932), and the China Postdoctoral Science Foundation (2020M672521).

SUPPLEMENTARY MATERIAL

The Supplementary Material for this article can be found online at: https://www.frontiersin.org/articles/10.3389/fcell.2021.633927/full#supplementary-material

Supplementary Figure 1 | The methylation expression of AlkB family members in LUAD patients (DiseaseMeth).

REFERENCES

Arbyn, M., Weiderpass, E., Bruni, L., de Sanjose, S., Saraiya, M., Ferlay, J., et al. (2020). Estimates of incidence and mortality of cervical cancer in 2018: a worldwide analysis. *Lancet Glob. Health* 8, e191–e203. doi: 10.1016/S2214-109X(19)30482-6

Asplund, A., Edqvist, P. H., Schwenk, J. M., and Ponten, F. (2012). Antibodies for profiling the human proteome-The Human Protein Atlas as a resource for cancer research. *Proteomics* 12, 2067–2077. doi: 10.1002/pmic.201100504

Bian, K., Lenz, S. A. P., Tang, Q., Chen, F., Qi, R., Jost, M., et al. (2019). DNA repair enzymes ALKBH2, ALKBH3, and AlkB oxidize 5-methylcytosine to 5-hydroxymethylcytosine, 5-formylcytosine and 5-carboxylcytosine in vitro. *Nucleic Acids Res.* 47, 5522–5529. doi: 10.1093/nar/gkz395

Cerami, E., Gao, J., Dogrusoz, U., Gross, B. E., Sumer, S. O., Aksoy, B. A., et al. (2012). The cBio cancer genomics portal: an open platform for exploring multidimensional cancer genomics data. *Cancer Discov.* 2, 401–404. doi: 10.1158/2159-8290.CD-12-0095

Chandrashekar, D. S., Bashel, B., Balasubramanya, S. A. H., Creighton, C. J., Ponce-Rodriguez, I., Chakravarthi, B., et al. (2017). UALCAN: a portal for facilitating tumor subgroup gene expression and survival analyses. *Neoplasia* 19, 649–658. doi: 10.1016/j.neo.2017.05.002

Coelho, M. C., Pinto, R. M., and Murray, A. W. (2019). Heterozygous mutations cause genetic instability in a yeast model of cancer evolution. *Nature* 566, 275–278. doi: 10.1038/s41586-019-0887-y

Du, K., Zhang, L., Lee, T., and Sun, T. (2019). m(6)A RNA methylation controls neural development and is involved in human diseases. *Mol. Neurobiol.* 56, 1596–1606. doi: 10.1007/s12035-018-1138-1

Franz, M., Rodriguez, H., Lopes, C., Zuberi, K., Montojo, J., Bader, G. D., et al. (2018). GeneMANIA update 2018. *Nucleic Acids Res.* 46, W60–W64. doi: 10.1093/nar/gky311

Fujii, T., Shimada, K., Anai, S., Fujimoto, K., and Konishi, N. (2013). ALKBH2, a novel AlkB homologue, contributes to human bladder cancer progression by regulating MUC1 expression. *Cancer Sci.* 104, 321–327. doi: 10.1111/cas.12089

Furmanova, K., Byska, J., Groller, E. M., Viola, I., Palecek, J. J., and Kozlikova, B. (2018). COZOID: contact zone identifier for visual analysis of protein-protein interactions. *BMC Bioinformatics* 19:125. doi: 10.1186/s12859-018-2113-6

Garber, M. E., Troyanskaya, O. G., Schluens, K., Petersen, S., Thaesler, Z., Pacyna-Gengelbach, M., et al. (2001). Diversity of gene expression in adenocarcinoma of the lung. *Proc. Natl. Acad. Sci. U.S.A.* 98, 13784–13789. doi: 10.1073/pnas.241500798

Gene Ontology Consortium (2019). The gene ontology resource: 20 years and still GOing strong. *Nucleic Acids Res.* 47, D330–D338. doi: 10.1093/nar/gky1055

Gensous, N., Garagnani, P., Santoro, A., Giuliani, C., Ostan, R., Fabbri, C., et al. (2020). One-year Mediterranean diet promotes epigenetic rejuvenation with country- and sex-specific effects: a pilot study from the NU-AGE project. *Geroscience* 42, 687–701. doi: 10.1007/s11357-019-00149-0

Han, L., Shi, H., Luo, Y., Sun, W., Li, S., Zhang, N., et al. (2020). Gene signature based on B cell predicts clinical outcome of radiotherapy and immunotherapy for patients with lung adenocarcinoma. *Cancer Med.* 9, 9581–9594. doi: 10.1002/cam4.3561

Hofman, P. (2020). New insights into the interaction of the immune system with non-small cell lung carcinomas. *Transl. Lung Cancer Res.* 9, 2199–2213. doi: 10.21037/tlcr-20-178

Hou, J., Aerts, J., den Hamer, B., van Ijcken, W., den Bakker, M., Riegman, P., et al. (2010). Gene expression-based classification of non-small cell lung carcinomas and survival prediction. *PLoS One* 5:e10312. doi: 10.1371/journal.pone.0010312

Ji, G., Huang, C., He, S., Gong, Y., Song, G., Li, X., et al. (2020). Comprehensive analysis of m6A regulators prognostic value in prostate cancer. *Aging* 12, 14863–14884. doi: 10.18632/aging.103549

Jin, D., Guo, J., Wu, Y., Yang, L., Wang, X., Du, J., et al. (2020). m(6)A demethylase ALKBH5 inhibits tumor growth and metastasis by reducing YTHDFs-mediated YAP expression and inhibiting miR-107/LATS2-mediated YAP activity in NSCLC. *Mol. Cancer* 19:40. doi: 10.1186/s12943-020-01161-1

Johnson, J. P. (1991). Cell adhesion molecules of the immunoglobulin supergene family and their role in malignant transformation and progression to metastatic disease. *Cancer Metastasis Rev.* 10, 11–22. doi: 10.1007/BF00046840

Kadara, H., Choi, M., Zhang, J., Parra, E. R., Rodriguez-Canales, J., Gaffney, S. G., et al. (2017). Whole-exome sequencing and immune profiling of early-stage lung adenocarcinoma with fully annotated clinical follow-up. *Ann. Oncol.* 28, 75–82. doi: 10.1093/annonc/mdw436

Kanehisa, M., Furumichi, M., Tanabe, M., Sato, Y., and Morishima, K. (2017). KEGG: new perspectives on genomes, pathways, diseases and drugs. *Nucleic Acids Res.* 45, D353–D361. doi: 10.1093/nar/gkw1092

Kronfol, M. M., Jahr, F. M., Dozmorov, M. G., Phansalkar, P. S., Xie, L. Y., Aberg, K. A., et al. (2020). DNA methylation and histone acetylation changes to cytochrome P450 2E1 regulation in normal aging and impact on rates of drug metabolism in the liver. *Geroscience* 42, 819–832. doi: 10.1007/s11357-020-00181-5

Landi, M. T., Dracheva, T., Rotunno, M., Figueroa, J. D., Liu, H., Dasgupta, A., et al. (2008). Gene expression signature of cigarette smoking and its role in lung adenocarcinoma development and survival. *PLoS One* 3:e1651. doi: 10.1371/journal.pone.0001651

Li, T., Fan, J., Wang, B., Traugh, N., Chen, Q., Liu, J. S., et al. (2017). TIMER: a web server for comprehensive analysis of tumor-infiltrating immune cells. *Cancer Res.* 77, e108–e110. doi: 10.1158/0008-5472.CAN-17-0307

Lim, Z. F., and Ma, P. C. (2019). Emerging insights of tumor heterogeneity and drug resistance mechanisms in lung cancer targeted therapy. *J. Hematol. Oncol.* 12:134. doi: 10.1186/s13045-019-0818-2

Lin, L., Yan, L., Liu, Y., Yuan, F., Li, H., and Ni, J. (2019). Incidence and death in 29 cancer groups in 2017 and trend analysis from 1990 to 2017 from the Global Burden of Disease Study. *J. Hematol. Oncol.* 12:96. doi: 10.1186/s13045-019-0783-9

Liu, Y., Yuan, Q., and Xie, L. (2018). The AlkB family of Fe (II)/alpha-ketoglutarate-dependent dioxygenases modulates embryogenesis through epigenetic regulation. *Curr. Stem Cell Res. Ther.* 13, 136–143. doi: 10.2174/1574888X12666171027105532

Lopes, A., Vandermeulen, G., and Preat, V. (2019). Cancer DNA vaccines: current preclinical and clinical developments and future perspectives. *J. Exp. Clin. Cancer Res.* 38:146. doi: 10.1186/s13046-019-1154-7

Lord, C. J., and Ashworth, A. (2012). The DNA damage response and cancer therapy. *Nature* 481, 287–294. doi: 10.1038/nature10760

Luo, C., Lei, M., Zhang, Y., Zhang, Q., Li, L., Lian, J., et al. (2020). Systematic construction and validation of an immune prognostic model for lung adenocarcinoma. *J. Cell. Mol. Med.* 24, 1233–1244. doi: 10.1111/jcmm.14719

Lv, J., Liu, H., Su, J., Wu, X., Liu, H., Li, B., et al. (2012). DiseaseMeth: a human disease methylation database. *Nucleic Acids Res.* 40, D1030–D1035. doi: 10.1093/nar/gkr1169

Martincorena, I., Raine, K. M., Gerstung, M., Dawson, K. J., Haase, K., Van Loo, P., et al. (2017). Universal patterns of selection in cancer and somatic tissues. *Cell* 171, 1029–1041.e21. doi: 10.1016/j.cell.2017.09.042

Oberndorfer, F., and Mullauer, L. (2018). Molecular pathology of lung cancer: current status and perspectives. *Curr. Opin. Oncol.* 30, 69–76. doi: 10.1097/CCO.0000000000000429

Okayama, H., Kohno, T., Ishii, Y., Shimada, Y., Shiraishi, K., Iwakawa, R., et al. (2012). Identification of genes upregulated in ALK-positive and EGFR/KRAS/ALK-negative lung adenocarcinomas. *Cancer Res.* 72, 100–111. doi: 10.1158/0008-5472.CAN-11-1403

Panneerdoss, S., Eedunuri, V. K., Yadav, P., Timilsina, S., Rajamanickam, S., Viswanadhapalli, S., et al. (2018). Cross-talk among writers, readers, and erasers of m(6)A regulates cancer growth and progression. *Sci. Adv.* 4:eaar8263. doi: 10.1126/sciadv.aar8263

Pilzys, T., Marcinkowski, M., Kukwa, W., Garbicz, D., Dylewska, M., Ferenc, K., et al. (2019). ALKBH overexpression in head and neck cancer: potential target for novel anticancer therapy. *Sci. Rep.* 9:13249. doi: 10.1038/s41598-019-49550-x

Planas-Iglesias, J., Bonet, J., Garcia-Garcia, J., Marin-Lopez, M. A., Feliu, E., and Oliva, B. (2013). Understanding protein-protein interactions using local structural features. *J. Mol. Biol.* 425, 1210–1224. doi: 10.1016/j.jmb.2013.01.014

Rajecka, V., Skalicky, T., and Vanacova, S. (2019). The role of RNA adenosine demethylases in the control of gene expression. *Biochim. Biophys. Acta Gene Regul. Mech.* 1862, 343–355. doi: 10.1016/j.bbagrm.2018.12.001

Rhodes, D. R., Kalyana-Sundaram, S., Mahavisno, V., Varambally, R., Yu, J., Briggs, B. B., et al. (2007). Oncomine 3.0: genes, pathways, and networks in a collection of 18,000 cancer gene expression profiles. *Neoplasia* 9, 166–180. doi: 10.1593/neo.07112

Rhodes, D. R., Yu, J., Shanker, K., Deshpande, N., Varambally, R., Ghosh, D., et al. (2004). ONCOMINE: a cancer microarray database and integrated data-mining platform. *Neoplasia* 6, 1–6. doi: 10.1016/s1476-5586(04)80047-2

Roos, W. P., Thomas, A. D., and Kaina, B. (2016). DNA damage and the balance between survival and death in cancer biology. *Nat. Rev. Cancer* 16, 20–33. doi: 10.1038/nrc.2015.2

Rotte, A. (2019). Combination of CTLA-4 and PD-1 blockers for treatment of cancer. *J. Exp. Clin. Cancer Res.* 38:255. doi: 10.1186/s13046-019-1259-z

Selamat, S. A., Chung, B. S., Girard, L., Zhang, W., Zhang, Y., Campan, M., et al. (2012). Genome-scale analysis of DNA methylation in lung adenocarcinoma and integration with mRNA expression. *Genome Res.* 22, 1197–1211. doi: 10.1101/gr.132662.111

Shannon, P., Markiel, A., Ozier, O., Baliga, N. S., Wang, J. T., Ramage, D., et al. (2003). Cytoscape: a software environment for integrated models of biomolecular interaction networks. *Genome Res.* 13, 2498–2504. doi: 10.1101/gr.1239303

Sondka, Z., Bamford, S., Cole, C. G., Ward, S. A., Dunham, I., and Forbes, S. A. (2018). The COSMIC cancer gene census: describing genetic dysfunction across all human cancers. *Nat. Rev. Cancer* 18, 696–705. doi: 10.1038/s41568-018-0060-1

Stoycheva, D., Simsek, H., Weber, W., Hauser, A. E., and Klotzsch, E. (2021). External cues to drive B cell function towards immunotherapy. *Acta Biomater.* 2021:S1742-7061(21)00121-5. doi: 10.1016/j.actbio.2021.02.026

Su, L. J., Chang, C. W., Wu, Y. C., Chen, K. C., Lin, C. J., Liang, S. C., et al. (2007). Selection of DDX5 as a novel internal control for Q-RT-PCR from microarray data using a block bootstrap re-sampling scheme. *BMC Genomics* 8:140. doi: 10.1186/1471-2164-8-140

Subedi, P., Nembrini, S., An, Q., Zhu, Y., Peng, H., Yeh, F., et al. (2019). Telomere length and cancer mortality in American Indians: the Strong Heart Study. *Geroscience* 41, 351–361. doi: 10.1007/s11357-019-00080-4

Sun, C. C., Li, S. J., Hu, W., Zhang, J., Zhou, Q., Liu, C., et al. (2019). Comprehensive analysis of the expression and prognosis for E2Fs in human breast cancer. *Mol. Ther.* 27, 1153–1165. doi: 10.1016/j.ymthe.2019.03.019

Tang, Z., Kang, B., Li, C., Chen, T., and Zhang, Z. (2019). GEPIA2: an enhanced web server for large-scale expression profiling and interactive analysis. *Nucleic Acids Res.* 47, W556–W560. doi: 10.1093/nar/gkz430

Tang, Z., Li, C., Kang, B., Gao, G., Li, C., and Zhang, Z. (2017). GEPIA: a web server for cancer and normal gene expression profiling and interactive analyses. *Nucleic Acids Res.* 45, W98–W102. doi: 10.1093/nar/gkx247

Tao, Y., Hu, K., Tan, F., Zhang, S., Zhou, M., Luo, J., et al. (2016). SH3-domain binding protein 1 in the tumor microenvironment promotes hepatocellular carcinoma metastasis through WAVE2 pathway. *Oncotarget* 7, 18356–18370. doi: 10.18632/oncotarget.7786

Tasaki, M., Shimada, K., Kimura, H., Tsujikawa, K., and Konishi, N. (2011). ALKBH3, a human AlkB homologue, contributes to cell survival in human non-small-cell lung cancer. *Br. J. Cancer* 104, 700–706. doi: 10.1038/sj.bjc.6606012

Trewick, S. C., Henshaw, T. F., Hausinger, R. P., Lindahl, T., and Sedgwick, B. (2002). Oxidative demethylation by *Escherichia coli* AlkB directly reverts DNA base damage. *Nature* 419, 174–178. doi: 10.1038/nature00908

Varn, F. S., Wang, Y., Mullins, D. W., Fiering, S., and Cheng, C. (2017). Systematic pan-cancer analysis reveals immune cell interactions in the tumor microenvironment. *Cancer Res.* 77, 1271–1282. doi: 10.1158/0008-5472.CAN-16-2490

Wang, B., Ran, Z., Liu, M., and Ou, Y. (2019). Prognostic significance of potential immune checkpoint member HHLA2 in human tumors: a comprehensive analysis. *Front. Immunol.* 10:1573. doi: 10.3389/fimmu.2019.01573

Wang, J., Vasaikar, S., Shi, Z., Greer, M., and Zhang, B. (2017). WebGestalt 2017: a more comprehensive, powerful, flexible and interactive gene set enrichment analysis toolkit. *Nucleic Acids Res.* 45, W130–W137. doi: 10.1093/nar/gkx356

Wei, C., Dong, X., Lu, H., Tong, F., Chen, L., Zhang, R., et al. (2019). LPCAT1 promotes brain metastasis of lung adenocarcinoma by up-regulating PI3K/AKT/MYC pathway. *J. Exp. Clin. Cancer Res.* 38:95. doi: 10.1186/s13046-019-1092-4

Wu, P., Heins, Z. J., Muller, J. T., Katsnelson, L., de Bruijn, I., Abeshouse, A. A., et al. (2019). Integration and analysis of CPTAC proteomics data in the context of cancer genomics in the cBioPortal. *Mol. Cell. Proteomics* 18, 1893–1898. doi: 10.1074/mcp.TIR119.001673

Wu, S. S., Xu, W., Liu, S., Chen, B., Wang, X. L., Wang, Y., et al. (2011). Down-regulation of ALKBH2 increases cisplatin sensitivity in H1299 lung cancer cells. *Acta Pharmacol. Sin.* 32, 393–398. doi: 10.1038/aps.2010.216

Wu, T. P., Wang, T., Seetin, M. G., Lai, Y., Zhu, S., Lin, K., et al. (2016). DNA methylation on N(6)-adenine in mammalian embryonic stem cells. *Nature* 532, 329–333. doi: 10.1038/nature17640

Xiao, M. Z., Liu, J. M., Xian, C. L., Chen, K. Y., Liu, Z. Q., and Cheng, Y. Y. (2020). Therapeutic potential of ALKB homologs for cardiovascular disease. *Biomed. Pharmacother.* 131:110645. doi: 10.1016/j.biopha.2020.110645

Xie, Q., Wu, T. P., Gimple, R. C., Li, Z., Prager, B. C., Wu, Q., et al. (2018). N(6)-methyladenine DNA modification in glioblastoma. *Cell* 175, 1228–1243.e20. doi: 10.1016/j.cell.2018.10.006

Xiong, Y., Wei, Y., Gu, Y., Zhang, S., Lyu, J., Zhang, B., et al. (2017). DiseaseMeth version 2.0: a major expansion and update of the human disease methylation database. *Nucleic Acids Res.* 45, D888–D895. doi: 10.1093/nar/gkw1123

Xu, Z., Peng, B., Cai, Y., Wu, G., Huang, J., Gao, M., et al. (2020). N6-methyladenosine RNA modification in cancer therapeutic resistance: current status and perspectives. *Biochem. Pharmacol.* 182:114258. doi: 10.1016/j.bcp.2020.114258

Yan, Y., Chen, X., Wang, X., Zhao, Z., Hu, W., Zeng, S., et al. (2019). The effects and the mechanisms of autophagy on the cancer-associated fibroblasts in cancer. *J. Exp. Clin. Cancer Res.* 38:171. doi: 10.1186/s13046-019-1172-5

Zhang, C., Fu, J., and Zhou, Y. A. (2019a). Review in research progress concerning m6A methylation and immunoregulation. *Front. Immunol.* 10:922. doi: 10.3389/fimmu.2019.00922

Zhang, C., Leighl, N. B., Wu, Y. L., and Zhong, W. Z. (2019b). Emerging therapies for non-small cell lung cancer. *J. Hematol. Oncol.* 12:45. doi: 10.1186/s13045-019-0731-8

Zhu, H., Gan, X., Jiang, X., Diao, S., Wu, H., and Hu, J. (2019). ALKBH5 inhibited autophagy of epithelial ovarian cancer through miR-7 and BCL-2. *J. Exp. Clin. Cancer Res.* 38:163. doi: 10.1186/s13046-019-1159-2

Zhu, J., Wang, M., and Hu, D. (2020). Deciphering N(6)-methyladenosine-related genes signature to predict survival in lung adenocarcinoma. *Biomed Res. Int.* 2020:2514230. doi: 10.1155/2020/2514230

Zuberi, K., Franz, M., Rodriguez, H., Montojo, J., Lopes, C. T., Bader, G. D., et al. (2013). GeneMANIA prediction server 2013 update. *Nucleic Acids Res.* 41, W115–W122. doi: 10.1093/nar/gkt533

Conflict of Interest: The authors declare that the research was conducted in the absence of any commercial or financial relationships that could be construed as a potential conflict of interest.

frontiers in Cell and Developmental Biology

REVIEW
published: 07 June 2021
doi: 10.3389/fcell.2021.678127

B Cell Orchestration of Anti-tumor Immune Responses: A Matter of Cell Localization and Communication

Gabriela Sarti Kinker[1†], Glauco Akelinghton Freire Vitiello[1,2†], Wallax Augusto Silva Ferreira[1,3†], Alexandre Silva Chaves[1†], Vladmir Cláudio Cordeiro de Lima[4,5] and Tiago da Silva Medina[1,6]*

[1] Translational Immuno-oncology Group, International Research Center, A.C. Camargo Cancer Center, São Paulo, Brazil, [2] Department of Pathological Sciences, Londrina State University, Londrina, Brazil, [3] Laboratory of Tissue Culture and Cytogenetics, Environment Section (SAMAM), Evandro Chagas Institute, Ananindeua, Brazil, [4] Instituto do Câncer do Estado de São Paulo (ICESP), São Paulo, Brazil, [5] Oncologia D'Or São Paulo, Rede D'or, São Paulo, Brazil, [6] National Institute of Science and Technology in Oncogenomics and Therapeutic Innovation, São Paulo, Brazil

The immune system plays a crucial role in cancer development either by fostering tumor growth or destroying tumor cells, which has open new avenues for cancer immunotherapy. It was only over the last decade that the role of B cells in controlling anti-tumor immune responses in the tumor milieu has begun to be appreciated. B and plasma cells can exert anti-tumor effects through antibody-dependent cell cytotoxicity (ADCC) and activation of the complement cascade, even though their effector functions extend beyond the classical humoral immunity. In tumor tissues, B cells can be found in lymphoid aggregates, known as tertiary lymphoid structures (TLSs), well-organized non-encapsulated structures composed of immune and stromal cells. These structures reflect a process of lymphoid neogenesis occurring in peripheral tissues upon long-lasting exposure to inflammatory signals. The TLS provides an area of intense B cell antigen presentation that can lead to optimal T cell activation and effector functions, as well as the generation of effector B cells, which can be further differentiated in either antibody-secreting plasma cells or memory B cells. Of clinical interest, the crosstalk between B cells and antigen-experienced and exhausted $CD8^+$ T cells within mature TLS was recently associated with improved response to immune checkpoint blockade (ICB) in melanoma, sarcoma and lung cancer. Otherwise, B cells sparsely distributed in the tumor microenvironment or organized in immature TLSs were found to exert immune-regulatory functions, inhibiting anti-tumor immunity through the secretion of anti-inflammatory cytokines. Such phenotype might arise when B cells interact with malignant cells rather than T and dendritic cells. Differences in the spatial distribution likely underlie discrepancies between the role of B cells inferred from human samples or mouse models. Many fast-growing orthotopic tumors develop a malignant cell-rich bulk with reduced stroma and are devoid of TLSs, which highlights the importance of carefully selecting pre-clinical models. In summary, strategies that promote TLS formation in close proximity to tumor cells are likely to favor immunotherapy responses. Here, the cellular and molecular programs coordinating B cell development, activation and organization within TLSs will be reviewed, focusing on their translational relevance to cancer immunotherapy.

Keywords: B lymphocytes, tertiary lymphoid structures, germinal center, T lymphocytes, tumor, anti-tumor responses, pro-tumor responses

OPEN ACCESS

Edited by:
Adriana Franco Paes Leme, Brazilian Biosciences National Laboratory (LNBio), Brazil

Reviewed by:
Gaofeng Xiong, University of Kentucky, United States
Dong-Joo (Ellen) Cheon, Albany Medical College, United States

***Correspondence:**
Tiago da Silva Medina
tiago.medina@accamargo.org.br

† These authors have contributed equally to this work

Specialty section:
This article was submitted to Molecular Medicine, a section of the journal Frontiers in Cell and Developmental Biology

Received: *08 March 2021*
Accepted: *27 April 2021*
Published: *07 June 2021*

Citation:
Kinker GS, Vitiello GAF, Ferreira WAS, Chaves AS, Cordeiro de Lima VC and Medina TS (2021) B Cell Orchestration of Anti-tumor Immune Responses: A Matter of Cell Localization and Communication. Front. Cell Dev. Biol. 9:678127. doi: 10.3389/fcell.2021.678127

INTRODUCTION

Cancer arises from the accumulation of genetic mutations that ultimately lead to global epigenetic changes within transformed cells. These genetic and epigenetic alterations can potentially give rise to neoantigens whose recognition by the immune system is fundamental for tumor control. In particular, $CD8^+$ T cells exert potent anti-tumor activities through the recognition of tumor neoantigens presented on class I major histocompatibility complex (MHC-I) molecules. However, when governed by an immunosuppressive microenvironment, immune cells may seed a fertile niche for tumor growth (Jones et al., 2019). Among the established hallmarks of cancer, tumor-promoting inflammation and tumor evasion from the immune response have emerged as important processes for cancer development and progression (Hanahan and Weinberg, 2011). The recognition that the immune system can counterintuitively be involved in either cancer development or control, depending on the milieu, represented a milestone in cancer research and has led to significant breakthroughs in clinical care for a growing list of malignancies (Farkona et al., 2016).

The field of immuno-oncology, however, is not as new as one might think: evidence demonstrating that the immune system is capable of eliminating tumors dates back to the early civilizations, when historical reports have documented spontaneous regression of tumors associated with concomitant infections and fever. In the nineteenth century, Rudolf Virchow was the first pathologist to observe the presence of inflammatory cells in solid tumors. Later, William Coley's pioneering empirical work reported tumor shrinkage in cancer patients who had severe postoperative infections. This groundbreaking observation led him to inoculate *Streptococcus pyogenes* into tumors to promote inflammation and tumor regression. Reaching the 1950s and 1960s, transplantation of chemically induced tumors between syngeneic animals pointed to the existence of anti-tumor-specific immunity endowed with memory (Dobosz and Dzieciatkowski, 2019).

Since then, leveraged by the outstanding technical and scientific progress made in molecular biology and immunology, the mechanisms behind tumor recognition by the immune system have been dissected (Dobosz and Dzieciatkowski, 2019). Over the past years, cytotoxic $CD8^+$ T lymphocytes have been in the center of this debate, as their anti-tumor response can optimally eliminate tumor cells by specifically recognizing tumor antigens that originate from mutated or aberrantly expressed proteins linked to MHC-I on the surface of tumor cells (Schumacher and Schreiber, 2015).

Further advances in immunology have helped to elucidate why $CD8^+$ T cells often fail to efficiently control the development of cancer, revealing that immune regulatory mechanisms operate in the cancer milieu. The inflammatory counterbalance promoted by immune regulatory mechanisms is essential to prevent undesirable local tissue damage. Accordingly, multiple immune regulatory processes can be induced in the tumor microenvironment and include, but are not limited to, suboptimal priming of lymphocytes by immature dendritic cells maintained in the absence of inflammatory signals, tolerance mechanisms triggered by autoantigens expressed in tumor cells, as well as T cell exhaustion due to chronic antigenic stimulation (van der Leun et al., 2020). This accumulated knowledge paved the way for the development of several therapies aimed to overcome these barriers, including cytokine therapies, cellular vaccines employing *ex-vivo* activated dendritic cells, and immune checkpoint blockade (ICB) therapies, which are currently approved for several types of cancers (Zhang and Zhang, 2020).

Despite the major impact that immunotherapies, specially ICB, have had on cancer treatment, several challenges still persist for their widespread application, as evidenced by the significant number of patients that do not derive clinical benefits and the cancer types wherein their efficacy is still to be proved. Thus, further clarification of the immune mechanisms operating in the tumor microenvironment is needed in order to identify novel therapeutic targets and biomarkers of response (Gibney et al., 2016; Bai et al., 2020).

As previously highlighted, cytotoxic T lymphocytes, thought to be the major effector cells in anti-tumor immune responses, have received the greatest attention throughout the history of the immuno-oncology field. However, more recently it has become apparent that these cells are not capable of acting independently, relying on a complex network of interactions with other immune and stromal cells for their coordinated activation, maintenance and function (Garner and de Visser, 2020). In this context, the pivotal role of B lymphocytes on anti-tumor immune responses has only begun to be appreciated. These cells can mediate both pro-and anti-tumor effects and perform a plethora of roles in the tumor milieu, such as secretion of antibodies and cytokines, antigen presentation for both cytotoxic ($CD8^+$) and helper ($CD4^+$) T lymphocytes, and coordination and maintenance of lymphoid aggregates known as tertiary lymphoid structures (TLS), which are privileged sites for antigen presentation and T cell (re-)activation (Sautes-Fridman et al., 2019; Sharonov et al., 2020).

In this review, we outline the multiple functions of B lymphocytes in anti-tumor immune responses. In particular, we briefly describe B cell biology from genesis to effector functions. We also discuss the spatial organization of B cells in the tumor microenvironment, highlighting the molecular mechanisms that promote B and T cell compartmentalization within TLSs in chronic inflammatory processes, focusing mainly on cancer. We then present evidence for both pro-and anti-tumor responses of B cells depending on what cellular niche these cells occupy. We also describe how the spatial organization within TLS can shape anti-tumor effector B and T cell responses and we provide evidence that mature TLSs are an ideal environment capable of triggering optimal T cell activation, which ultimately leads to the expression of clinically relevant immune checkpoints.

B LYMPHOCYTE BIOLOGY: FROM B CELL ONTOGENY TO ACTIVATION AND ITS ROLE IN ANTIGEN PRESENTATION

B lymphocytes are the main cellular components of the humoral compartment of adaptive immunity (Sebina and Pepper, 2018). Their development occurs mainly in the liver during fetal life and

in the bone marrow (BM) after birth through several sequential steps of differentiation, wherein hematopoietic stem cells (HSCs) reach the common lymphoid progenitor (CLP) stage, which gives rise to either B, T or Natural Killer (NK) cells (Rieger and Schroeder, 2012). B lymphocytes derived from the fetal liver belong to the B-1a lineage and comprise a population of long-lived and self-renewing B lymphocytes that occupy body cavities and mucosae and constitutively secret IgM antibodies ("natural antibodies") of restricted specificity (Baumgarth, 2017). The vast majority of B lymphocytes in adults is derived from the BM and can be divided into the B-1b lineage, which are functionally similar to B-1a cells, and the B-2 lineage, which migrate from the BM to the spleen to further differentiate into marginal-zone or follicular B lymphocytes (Pieper et al., 2013).

The ontogeny of lymphocytes initiates with the differentiation of HSCs into a lymphoid-primed multipotent progenitor (LMPP), which expresses the lymphoid-specific recombinases RAG1 and RAG2 that promote LMPP differentiation into the earliest lymphoid progenitor (ELP) and then into CLPs. In mice, the commitment of the B cell lineage is critically dependent on the expression of the cytokine receptors FLT3 and IL-7R (Medina and Singh, 2005), while IL-7 signaling does not seem to be essential in humans (Pieper et al., 2013).

The early transcription factors (TFs) involved in B lymphocyte commitment, E2A and EBF, act coordinately to repress key molecular programs from other cell lineages and promote the expression of PAX5, which further stabilizes lineage commitment, thus defining the pro-B stage (Sigvardsson, 2018). Next, developing B cells begin to mount their antigen specific B-cell receptors (BCR) that are constituted by accessory signaling proteins coupled to transmembrane isoforms of IgM antibodies. These are composed of two heavy chains generated through recombination between variable regions (V_H, D_H, and J_H) from the Ig heavy (H) locus, each combined with a light chain, generated through recombination between variable regions VL and JL from Ig κ or λ light (L) chain *loci* (Jung and Alt, 2004). This process generates approximately 5×10^{13} B lymphocyte clones, each expressing a unique BCR that recognizes a different epitope (Pieper et al., 2013).

Initially, E2A and EBF1 direct RAG1 and RAG2 recombinases to the IgH locus in pro-B cells, promoting D_H-J_H recombination (Romanow et al., 2000). Then, V_H-DJ_H recombination is facilitated by PAX5-promoted "contraction" of IgH *locus* (Fuxa et al., 2004; Jung et al., 2006). The terminal deoxynucleotidyl transferase (TdT) is specifically expressed during this phase and further increases the junctional diversity by adding random nucleotides in recombination sites (Bertocci et al., 2006). After recombination, IgH forms a complex with the polypeptide chains V Pre-B and λ5, which substitute the Ig light chain. IgH also interacts with Igα (CD79a), and Igβ (CD79b), giving rise to the pre-BCR, whose expression is regulated by the key TFs that characterize the pre-B stage (Sigvardsson, 2018).

The correct assembly of pre-BCR represents an important checkpoint for B cell development. This receptor signals through the Burton's tyrosine kinase (BTK) and the adapter protein BLNK to promote cell survival, proliferation and activation of the TFs NF-κB and interferon response factor 4 (IRF4), which have been shown to be essential for the rearrangement of IgL chains. The recombination events are initiated in Ig κ locus and followed by λ locus if κ rearrangements for both alleles result in a non-functional or self-reactive BCR (Pieper et al., 2013; Sigvardsson, 2018). Complex molecular mechanisms ensure that Ig rearrangements for IgH and IgL occur at one allele at a time, promoting the usage of the other allele only if the first recombination is unproductive. The mechanisms behind this process, named allelic exclusion, are not yet fully understood (Vettermann and Schlissel, 2010).

Developing B cells that successfully produce non-self-reactive BCRs undergo molecular changes including a decrease in the chemokine receptor CXCR4 signaling (Beck et al., 2014) and an increase in the expression of sphingosine-1-phosphate receptor 1 (S1P1) (Cinamon et al., 2004), which mediate the migration of B cells to the spleen, where they complete their maturation to marginal zone or follicular B cells, depending on the strength of BCR signaling to self-antigens and NF-κB, BAFF, and Notch2 signaling pathways (Pillai and Cariappa, 2009). Marginal-zone B cells remain on the spleen mediating mainly T-independent responses to blood-borne antigens from diverse chemical natures (proteins, lipids, carbohydrates); whereas follicular B cells migrate through B-cell zones (or follicles) in lymph nodes throughout the body, guided by the interaction between CXCR5, expressed on their cell surface, and CXCL13, a chemokine produced by follicular dendritic cells (FDCs). Then, the encounter between naïve B lymphocytes and their cognate antigens, either captured from peripheral tissues by FDCs or freely borne through lymph, is favored in follicular B-cell zones (Cyster and Allen, 2019).

As part of the innate immune response, complement system-derived peptides can bind to the surface of pathogens/antigens. FDCs capture complement-covered pathogens and antigens in peripheral tissues through complement-specific receptors present on their cell membranes and transport them to lymph nodes. In follicles, BCR interacts with surface antigens, and high-affinity interactions promote both BCR signaling and internalization of the bound antigen through a clathrin-dependent mechanism. Activation of co-receptors on B cell surface, such as complement receptors and pathogen-associated molecular pattern recognition receptors, such as Toll-like receptors (TLRs), amplifies BCR signaling and diminishes the B cell activation threshold, while inhibitory receptors that recognize self-molecules, such as CD22, or antibodies, such as FcγRIIb, may increase the threshold for B cell activation, acting as a negative feedback to prevent auto-reactivity and exacerbated immune responses (Cyster and Allen, 2019).

As a consequence of early B cell activation, these cells downregulate the expression of S1P1 and begin to express CCR7 and EBI2, which direct them to the interface between B cell follicles and adjacent T cell zones, following CCL21 and CCL19 gradients. In parallel, these cells process the internalized antigen to present antigen-derived peptides bound to MHC-II on their cell surface along with co-stimulatory ligands, such as CD80/CD86 and ICOSL. Altogether, these phenotypic

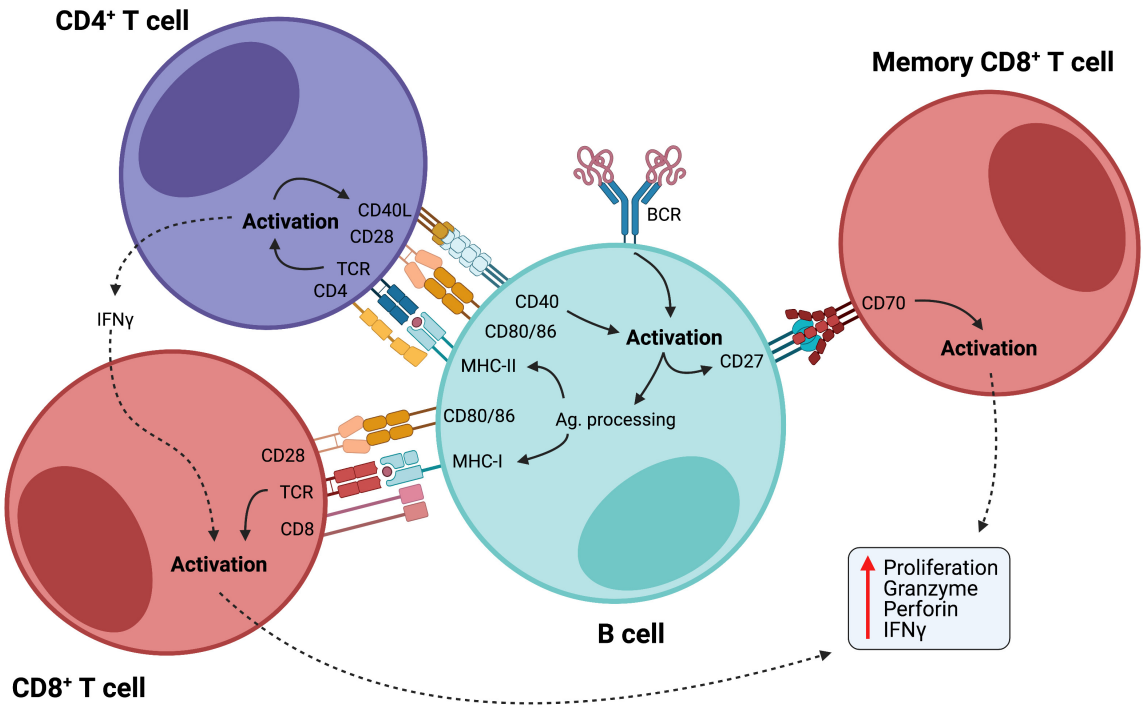

FIGURE 1 | B cells as activators of cellular immunity. B cells are initially activated by antigen recognition through BCR. Internalized antigens are then presented through class II MHC to $CD4^+$ helper T cells, which provide co-stimulatory signals for B cell activation. Activated B cells acquire enhanced potential for antigen presentation with upregulation of MHC-I and II and co-stimulatory molecules, such as CD80/86, further activating both $CD4^+$ and $CD8^+$ T cells. Also, CD27 is upregulated in activated B cells, and interaction between this molecule and CD70 on the membrane of memory $CD8^+$ T cells promotes their maintenance and facilitates their activation in an antigen-independent manner. $CD8^+$ T cell activation leads to efficient cell proliferation and production of potent inflammatory mediators, such as granzymes, perforin, and IFN-γ.

changes favor B cell interaction with activated $CD4^+$ helper T cells migrating in the opposite direction. The recognition of MHC-II-bound peptides by $CD4^+$ T cells along with co-stimulatory signals promote their activation and differentiation into follicular-helper T cells (T_{FH}), which express CD40L, that interact with CD40 on B cells. This intimate B-T cell interaction in the presence of cytokines, such as IL-4 and IL-21, promotes B cell survival, proliferation and activation (Cyster and Allen, 2019).

Activated B cells also undergo class-switch recombination (CSR), in which the conserved region of expressed antibodies is changed from those derived from Cμ and Cσ loci to those coded by Cγ, Cα, or Cε loci. This allows the replacement of IgM and IgD by IgG, IgA, or IgE, depending on the inflammatory stimulus. Each conserved region holds different effector functions and is induced by different cytokines secreted by T_{FH} cells. For instance, IFN-γ promotes IgG2a and IgG3 production, while IL-4 facilitates switching to IgE, and TGF-β favors IgA (Zhang, 2003). CSR is depends on the activated induced deaminase (AID) expressed in B cells, which also promotes hypermutation of the Ig variable region, further increasing antibody diversification and affinity maturation in a clonal fashion (Cyster and Allen, 2019).

In summary, B cells capture, process and present antigens to $CD4^+$ T cells, what may lead to mutual activation. Once activated, B cells undergo proliferation while changing their antibody repertoire by inducing class-switching and affinity maturation. This drives the development of a germinal center (GC), composed of a "dark zone" (DZ), where B cells interact with T_{FH} cells and undergo activation and clonal expansion, and a "light zone" (LZ), characterized by cells derived from the DZ undergoing CSR and affinity maturation. In the LZ, cells that effectively produce high-affinity antibodies differentiate either into antibody-secreting plasma cells or memory B cells (Gatto and Brink, 2010).

The ability of B cells to efficiently present antigens and activate T cells through the expression of co-stimulatory molecules is of particular interest, as a large body of evidence has shown that B cells can present antigens as efficiently as professional APCs, such as dendritic cells, and promote T cell mediated immune responses in various contexts (Rivera et al., 2001; Chen and Jensen, 2008; de Wit et al., 2010; Adler et al., 2017; Hong et al., 2018), including cancer (Nielsen et al., 2012; Rossetti et al., 2018), where B cells demonstrated high capacity of cross-presenting internalized antigens via MHC-I to activate cytotoxic T cells (Gnjatic et al., 2003). Additionally, the interaction between CD27-expressing B cells and CD70-expressing $CD8^+$ T lymphocytes induces cytotoxic T cell responses in an antigen-independent manner (Deola et al., 2008), demonstrating another way by which B cells stimulate T cell responses (**Figure 1**).

SECONDARY LYMPHOID ORGANS AND TERTIARY LYMPHOID STRUCTURES: FUNCTIONALLY SIMILAR, BUT SLIGHTLY DIFFERENT IN COMPOSITION

The formation of TLSs is a phenomenon associated with chronic inflammatory conditions, such as autoimmune diseases and cancer, reflecting a process of lymphatic neogenesis that creates a local hub for antigen presentation and immune responses (Pitzalis et al., 2014). Though the main cellular components of TLSs are lymphocytes and dendritic cells, the adequate organization of this complex environment is sustained by a network of non-hematopoietic stromal cells. Populations of lymphatic and blood endothelial cells and immunofibroblasts are at the core of this framework (Buckley et al., 2015).

Key steps involved in the formation of secondary lymphoid organs (SLOs) during organogenesis are also commonly observed in the formation of TLSs. However, while SLO development occurs in predefined areas during embryogenesis, TLSs are ectopically formed at sites of chronic inflammation. A crucial step for the fetal development of the secondary lymphoid tissue is the migration of integrin $\alpha4\beta7^+$ lymphoid tissue inducer cells (LTis) that interact with MadCAM-1^+ high endothelial venules (HEVs) in the lymph node anlagen (Mebius et al., 1996). LTis originate from common lymphoid progenitors in the fetal liver and undergo maturation through a process involving the Notch signaling pathway and the transcriptional repressor Id2. This generates terminally differentiated LTis expressing RORγT and α4β7 integrin (Cherrier et al., 2012). Retinoic acid produced by nerve endings allows mesenchymal cells to express the chemokine CXCL13, whose gradient attracts LTis via interaction with the receptor CXCR5. Although both CXCL13 and CCL21 chemokines have the capacity of attracting LTis during the early embryonic phases, only CXCL13 is expressed in all lymph node anlagen at that time (van de Pavert et al., 2009).

Once properly recruited to the anlagen, LTis activate stromal lymphoid tissue organizer cells (LTos) through the interaction between the lymphotoxin (LT) α1β2 and its receptor, LTβR. This favors the expression of several adhesion molecules by LTos, such as VCAM-1, ICAM-1, and MadCAM-1, which, together with the homeostatic chemokines CCL19, CCL21, and CXCL13, promotes the recruitment of lymphocytes and the retention of LTis (Peduto et al., 2009; Vondenhoff et al., 2009). Another interesting point is that while chemokines promote the recruitment of DCs, NK, T and B cells, LTβR signaling aids the development of lymph nodes, as well as cell clustering and spatial organization. LTos develop further into follicular (FC) and fibroblastic reticular cells (FRC) that provide the conduit framework on which T and B cells migrate and interact with each other, allowing the proper development of adaptive immunity (Veiga-Fernandes et al., 2007; van de Pavert et al., 2009).

Much of the current knowledge about TLS formation and function comes from murine models of autoimmunity (Pipi et al., 2018). In human Sjogren's Syndrome (SS) and murine models of SS, TLS assembly is strictly dependent on a network of $gp38^+$ immunofibroblasts that are phenotypically and functionally similar to FRC networks in SLO. In both cases, the coordinated action of IL-22, LTα1β2, and Th2 cytokines seems to be associated with such network formation. Although lymphocytes are not needed for the priming of immunofibroblast progenitors, they contribute for the network expansion and activation. While $ROR\gamma T^+$ LTis play a critical role in the development of fibroblast reticular cells in SLOs, they are not required for priming and expansion of TLS immunofibroblasts in SS (Nayar et al., 2019). Of note, IL-21-producing Th17 cells might work as LTi cells that initiate TLS organogenesis and GC formation (Deteix et al., 2010). A murine model of experimental autoimmune encephalomyelitis (EAE) demonstrated that $gp38^+$ Th17 cells stably producing Th17 cytokines induce the expression of CXCL13 in the central nervous system and the development of follicle-like structures (Peters et al., 2011). These structures were composed of B cell clusters, surrounded by a mantle of T cells and collagen fibers; the latter could extend into the center of B cell clusters. Moreover, the expression of GC markers GL7 and PNA revealed the existence B cell aggregates with different levels of maturation.

Germinal Center Maturation in Chronically Inflamed Scenarios

So far, we have presented a sketch of the TLS structure, briefly pointing out what makes them different from SLOs. However, we have not delved into a particular aspect, common to both structures, that may draw special attention: the GC maturation (**Figure 2**). Classical markers of GC B cells include lack of surface IgD, upregulation of CD38, high expression levels of Fas and n-glycolylneuraminic acid, along with the selective expression of BCL-6 and AID. When mature, GCs constitute well-structured regions with two dynamic compartments: the DZ and LZ. The gradient of CXCL12 and CXCL13, along with the expression of their respective receptors CXCR4 and CXCR5, dictates the spatial distribution of B cells. During the events taking place into GCs, activated B cells acquire new features and functions. The CXCR4-expressing centroblasts are mostly located in the DZ, due to the CXCL12 abundance, whereas the CXCR5-expressing centrocytes move to the LZ, in favor of the CXCL13 gradient (Gatto and Brink, 2010). Besides moving through the GC zones in response to a chemokine gradient, B cells can also be engaged in short, dynamic interactions with both T cells and antigens.

This whole process can be observed in well-structured TLS, as they are analogous in structure and function to SLOs (Germain et al., 2014). In immature TLSs, on the other hand, B cells cannot interact and expand properly, hampering the formation of active GCs. Indeed, in early steps of hepatocellular carcinoma progression, immature TLSs are associated with inefficient immune responses and tumor evasion (Meylan et al., 2020). Maturation of murine TLSs can be induced by LT-producing B cells, as it has been shown that the reconstitution of $LT\alpha^{-/-}$ recipients with bone marrows containing LT-producing B cells was critical for skewing immature TLSs into mature TLSs (Lorenz et al., 2003; McDonald et al., 2005).

In colorectal cancer, multi-parameter immunofluorescence detection of CD21, CD23 and CXCL13 revealed three different

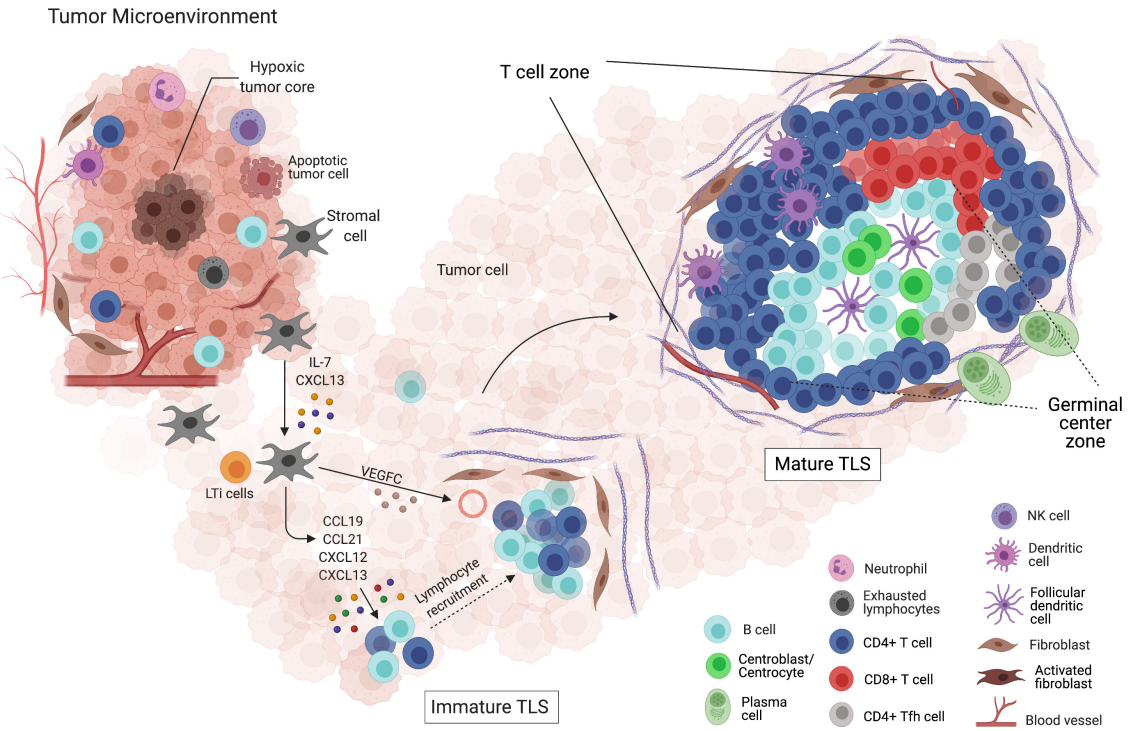

FIGURE 2 | Formation and maturation of tertiary lymphoid structures (TLSs) within the tumor microenvironment. (I) Depiction of the tumor microenvironment and its interactions with both innate and adaptive immune cells, and the non-immune components. (II) LTis attracted by the CXCL13 gradient, produced by activated stromal cells, migrate to the site of TLS initiation. Chemokines, such as CCL19, CCL21, CXCL12, and CXCL13, allow the migration and retention of additional LTis along with lymphocytes. The gathering of leukocytes surrounded by an extracellular matrix net produced by fibroblasts and newly formed blood vessels supports immature TLS formation, which fails to mount effective anti-tumor responses. (III) The presence of clearly delimited T cell and B cell zones, as well as a GC-like structure, defines mature TLSs. In this structure, the induction of plasma cells and memory B cells takes place, reflecting the interaction with other specific cell types, such as FDCs, T_{FH}, and $CD8^+$ T cells. Surrounded by pericytes and expressing adhesion molecules, the normal high endothelial venules (HEVs) located at the TLS vicinity favor the formation of mature TLSs, which are thought to be a rich niche of anti-tumor B and T cell responses.

states of TLS maturation: (i) early TLS as dense lymphocytic aggregates; (ii) primary follicle-like TLS, composed of B cell clusters with FDC networks, but devoid of GCs; and (iii) the secondary follicle-like TLS, including active GCs with $CD23^+$ B cells (Posch et al., 2018). In melanoma samples, mature GCs composed of highly proliferative $KI67^+$ B cells were associated with higher frequencies of antigen-experienced $CD4^+$ T cells expressing the anti-apoptotic molecule BCL2 (Cabrita et al., 2020). Such structures also included $TCF7^+IL7R^+$ naive and/or memory $CD4^+$ and $CD8^+$ T cells. In a cohort of esophago-gastric primary adenocarcinomas, approximately 48% of patients presented TLSs along the tumor invasive margin, as well as tumor-specific antibodies in the serum, underscoring the presence of B cell-dependent anti-tumor responses (Schlosser et al., 2019). In line with these observations, $CD3^+CD4^+CCR7^-CD45RA^-CXCR5^+$ T_{FH} cells and $CD20^-CD27^+CD38^+$ plasmablasts were found to be enriched in tumor samples compared to peripheral blood. Interestingly, the number of B cells was reduced in the microenvironment of tumors that expressed PD-L1 or lacked the expression of HLA-I (Schlosser et al., 2019).

In autoimmune diseases, spontaneous GC development often contributes to the disease severity due to self-reactive B cells (Domeier et al., 2017). In this case, IFN-γ plays a major role through its signaling pathway, as IFNγR signaling phosphorylates STAT1 and upregulates T-bet in B cells, which is required for spontaneous GC formation and class switching to IgG2b and IgG2c antibodies (Domeier et al., 2016). A different perspective can be seen in the context of chronic infectious diseases. In a C57BL/6 mouse model of *Mycobacterium tuberculosis* infection with H37Rv or HN878 strains (Hertz et al., 2020), sex affected the appropriate formation of B cell follicles upon infection, as chronically H37Rv-infected male mice expressed diminished levels of CXCL13 and CCL19 in the lungs, in comparison with female mice. Besides, when HN878 strain infection developed, there was a significantly higher amount of IL-17A, IL-23, and IL-1β in female lungs (Hertz et al., 2020). Perhaps in this scenario, sex differences between hosts and their genetic background may impact the assembly of mature TLSs (Hertz and Schneider, 2019). In a *Helicobacter pylori* infection model, $CXCR5^{-/-}$ mice failed to induce the formation of TLSs and Peyer's patches, which generated less antigen-loaded DCs, diminished T cell priming and impaired T cell-dependent B cell response against the pathogen (Winter et al., 2010).

But what should be expected when cancer-related scenarios are considered? We will next explore in detail the biological and

clinical relevance of the spatial organization of B cells in different types of tumors. We will also speculate how this system may be exploited clinically to improve patient prognosis and responses to immunotherapy.

PRO-TUMOR FUNCTIONS OF B LYMPHOCYTES

Our understanding of the multifaceted functions of B lymphocytes in tumor immunity has improved substantially in recent years. Current evidence suggests that the tumor microenvironment may have distinct B cell subpopulations that can exert both pro– or anti–tumor activities (Germain et al., 2014; Shimabukuro-Vornhagen et al., 2014; Shalapour et al., 2015; Wouters and Nelson, 2018; **Figure 3**), hence affecting patient outcomes (Mauri and Menon, 2017; Hu et al., 2019). The balance between the dual role of B cells is influenced by several factors, such as hypoxia (Caro-Maldonado et al., 2014; Shin et al., 2014; Meng et al., 2018), cytokines and metabolites produced by tumor cells (Wejksza et al., 2013; Pimenta et al., 2015; Ricciardi et al., 2015; Somasundaram et al., 2017; Ye et al., 2018), other immune cells [e.g., regulatory T cells (Tregs) and myeloid-derived suppressor cells (MDSC); Zhao et al., 2006; Shen et al., 2018; Wang Y. et al., 2018], inhibitory factors produced by B cells (Kessel et al., 2012; Khan et al., 2015; Shalapour et al., 2015) and immune checkpoints (Nishimura et al., 1998; Okazaki et al., 2001; Haas, 2011; Escors et al., 2018).

When outside the TLS, B cells can acquire a plethora of suppressive functions, meaning that B cell spatial distribution across the tumor microenvironment influences their activities. Thus, it is tempting to speculate that B cells acquire pro-inflammatory features that fully activate T cell responses when compartmentalized within TLS, while B cells outside the TLS are likely to acquire anti-inflammatory features that contribute to tumor growth (Cabrita et al., 2020). Within TLSs, it is possible that the mantle of T cells physically protects B cells from immunosuppressive stimuli found in the tumor tissue. The recent advent of technical approaches capable of interrogating the spatial architecture of tumor tissues (e.g., spatial transcriptomics) will allow the detailed exploitation of the TLS composition and function (Vickovic et al., 2019). Therefore, identifying strategies that reconfigure the spatial architecture of immune cells in the tumor microenvironment might have a great impact on the outcome of cancer patients.

Several studies have provided solid evidence that the tumor-promoting effects are mainly led by a diverse population of B cells known as regulatory B cells (Breg) (Schwartz et al., 2016; Sarvaria et al., 2017; Matsushita, 2019; Sharonov et al., 2020; Wang et al., 2020). Multiple Breg phenotypes that fulfill an immunosuppressive role have been described in different human solid tumors (Lee-Chang et al., 2013; Shao et al., 2014; Zhou et al., 2014; Wang et al., 2015; Wei et al., 2016; Roya et al., 2020; Wu et al., 2020a), as well as in peritumoral tissues (Garaud et al., 2019), peripheral blood (Qian et al., 2015; Wang K. et al., 2018; Karim and Wang, 2019; Murakami et al., 2019) and tumor-draining lymph nodes (Ganti et al., 2015), suggesting their broad clinical relevance and potential therapeutic application. Nevertheless, due to intricate origins and activation pathways, there is still no clear consensus on Breg-cell-specific phenotypic or lineage commitment markers, and the transcription factors that specifically drive the development of these cells remain elusive (Oleinika et al., 2019; Wang et al., 2020).

In both human and mice, most studies of Bregs are concentrated in memory $CD27^+$ and transitional $CD38^+$ B cells, sharing markers such as IgA^+CD138^+ and IgM^+CD147^+ with plasma cells (Fremd et al., 2013; Schwartz et al., 2016). Recently, a solution to this problem was proposed employing Toll-like receptor ligands, together with high dimensional data-analysis (Chaye et al., 2021). The available data suggest that Breg cells can arise at various stages during B cell development and differentiation in response to various cues, including cytokines (e.g., IL-35, IL-21, IL-1β, and IL-6) (Yoshizaki et al., 2012; Rosser et al., 2014; Wang et al., 2014; Dambuza et al., 2017), large amounts of calcium influx (Matsumoto et al., 2011; Matsumoto and Baba, 2013) and activation of surface molecules such as TLRs, CD40 and BCRs (Fillatreau et al., 2002; Yoshizaki et al., 2012; Rosser et al., 2014; Menon et al., 2016; Ran et al., 2020).

Breg cells support carcinogenesis, tumor progression and metastasis predominantly, although not exclusively, through the production of IL-10, TGF-β, and IL-35 or by intercellular contact (Ammirante et al., 2010; Shao et al., 2014; Tao et al., 2015; Wang et al., 2015; Schwartz et al., 2016; Xiao et al., 2016; Sarvaria et al., 2017). IL-10-producing Bregs can induce dendritic cells to produce IL-4 and downregulate IL-12, thereby affecting the Th1/Th2 balance (Moulin et al., 2000); they can suppress $CD4^+$ T cell differentiation into Th1 (suppressing IFN-γ and TNF-α production) and Th17 (suppressing IL-17 production); they also suppress TNF-α-producing monocytes (Iwata et al., 2011). Bregs can also induce the polarization of naïve $CD4^+$T cells into both $FOXP3^+$ Treg cells and IL-10-producing Tr1 cells, modulating cancer progression and increasing tumor metastasis (Olkhanud et al., 2011). Additionally, Bregs can promote apoptosis of effector $CD4^+$ T cells through the expression of FasL (Fillatreau et al., 2002; Iwata et al., 2011; Matsumoto et al., 2014; Wang et al., 2015; Zhou et al., 2016). Furthermore, IL-10-producing Breg cells have been shown to contribute to tumor progression by positively regulating the differentiation of tumor-associated macrophages (TAMs), skewed toward a M2 macrophage phenotype, that ultimately inhibit effector T and NK cells (Rosser et al., 2014; Wu et al., 2020b). It is currently unclear whether Bregs actively promote tumor growth, or an increase in the Breg population merely reflects the immune response against the tumor (Sarvaria et al., 2017).

Breg cells have also been reported to have other immunosuppressive mechanisms, such as (i) B cell expression of programmed cell death-1 (PD-1) via TLR4 activation, which induces T cell dysfunction and foster cancer progression; (ii) expression of other inhibitory molecules such as programmed death-ligand 1 (PD-L1) and FasL, which regulate humoral immunity mediated by $CD4^+CXCR5^+PD\text{-}1^+$ T_{FH} cells via PD-1; (iii) combined secretion of IgG4 and IL-10; (iv) IL-21–mediated induction of GZMB, which efficiently suppresses T cell proliferation by GrB-dependent TCR-ζ degradation;

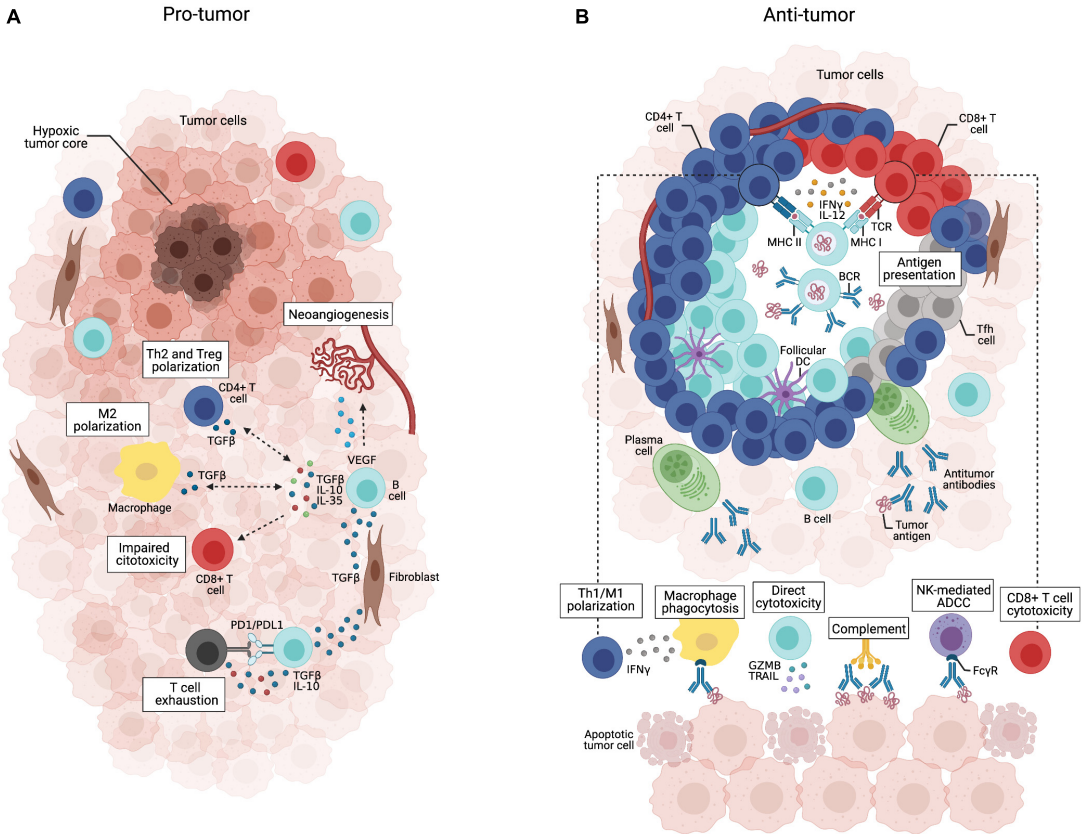

FIGURE 3 | Dual role of tumor-infiltrating B cells. **(A)** B cells scatteredly distributed throughout the tumor bulk may acquire immunosuppressive phenotypes in response to stimulation with TGF-β secreted by fibroblasts, Tregs or M2 macrophages. They can release IL-10, IL-35, and TGF-β that support Treg expansion and Th2/M2 polarization, while suppressing effector T cell activity, which is potentialized by B cell PD-L1 expression. VEGF-producing B cells may also promote tumor progression through neoangiogenesis.**(B)** Tumor-infiltrating B cells organized in well-structured TLSs coordinate anti-tumor immune responses through multiple mechanisms. They can present tumor-derived antigens to T cells and secrete cytokines such as IFN-γ and IL-12 that support Th1/M1 polarization and $CD8^+$ T cell cytotoxicity. Tumor-specific antibodies secreted by plasma cells can trigger the complement cascade, mediate phagocytosis of tumor cells, and antibody-dependent cell cytotoxicity by NK cells. Activated B cells may also directly kill tumor cells by secreting TRAIL and granzyme B.

(v) production of adenosine 5'-monophosphate (AMP) and adenosine (ADO), which suppresses activated T cells; (vi) activation of geranylgeranyl pyrophosphate (GGPP) (an intermediate of cholesterol metabolism), permitting transduction of signaling cascades necessary for IL-10 expression; (vii) production of indoleamine 2,3-dioxygenase (IDO), which inhibits T cell responses; (viii) expression of Aryl hydrocarbon receptor (AhR), which modulates the differentiation and function of Bregs, specially by suppressing their pro-inflammatory transcriptional program; and (ix) TLR4-mediated BCL6 upregulation that induces T cell dysfunction through PD-1 expression and IL-10 secretion (Gotot et al., 2012; Lindner et al., 2013; Saze et al., 2013; van de Veen et al., 2013; Khan et al., 2015; Nouel et al., 2015; Ren et al., 2016; Xiao et al., 2016; Piper et al., 2019; Bibby et al., 2020). Furthermore, glioma cell-derived placental growth factors (PIGFs) have been shown to promote proliferation of intratumoral B cells by inducing their differentiation into TGF-β-producing Bregs that suppress CD8 T cell anti-tumor activities (Han et al., 2014).

Akin to murine studies, other human B cells are key mediators of tumor growth. In melanoma, gastric, lung, liver and prostate cancers, tumor-infiltrating B cells can persistently express VEGF (vascular endothelial growth factor) and other pro-angiogenic genes via STAT3 signaling, fostering tumor progression by increasing angiogenesis (Yang et al., 2013). Another subset of STAT3-activated B cells found in human prostate, non-small cell lung, and ovarian cancers, $CD5^+$ B cells promote tumor progression upon IL-6 activation (Zhang et al., 2016). Furthermore, IL35-producing B cells ($CD1d^{high}CD5^+$) are required to support growth of early pancreatic neoplasia, more specifically $KRAS^{G12D}$-harboring neoplastic lesions (Pylayeva-Gupta et al., 2016). In addition, a hypoxic tumor microenvironment restrains the TLS formation and limits tumor elimination. Indeed, pancreas-specific hypoxia-inducible factor 1α (HIF1α) deletion increased CXCL13 secretion and B-cell infiltration and was associated with accelerated tumor growth (Lee K.E. et al., 2016). This supports the idea that a compromised tumor microenvironment is likely to disrupt

the spatial architecture of immune cells, largely perturbing the migration of immune cell populations and their organization in privileged sites, particularly TLSs, that elicit optimal activation and maintenance of anti-tumor immune responses. There is now great interest in understanding whether intratumoral perturbations, including aberrant neoangiogenesis, hypoxia, acidification, intense cell death by necrosis or apoptosis and fibrosis, could negatively impact TLS formation. Furthermore, $CD19^+$ B cells in metastatic ovarian carcinoma and $CD20^+$ and $CD138^+$ B cells infiltration in epithelial ovarian cancer were associated with poor outcome (Dong et al., 2006; Lundgren et al., 2016). Taken together, a better understanding of immunosuppressive B cell subpopulations and their underlying roles may open new avenues for cancer immunotherapy.

ANTI-TUMOR ROLE OF TLS B CELLS

Accumulating evidence indicates that TLSs play a major role in controlling tumor progression (Teillaud and Dieu-Nosjean, 2017; **Figure 3**). Overall, despite the heterogeneity of methods used for quantifying TLSs, studies have consistently found that high densities of intra and peritumoral TLSs are associated with prolonged overall survival and disease-free survival in more than 10 types of malignancies (**Table 1**), including sarcoma (Petitprez et al., 2020), melanoma (Cabrita et al., 2020), lung (Dieu-Nosjean et al., 2008; Germain et al., 2014; Tang et al., 2020; Rakaee et al., 2021), breast (Lee H.J. et al., 2016; Liu X. et al., 2017), colorectal (Coppola et al., 2011; Vayrynen et al., 2014) and pancreatic cancers (Hiraoka et al., 2015; Castino et al., 2016). The cellular composition and spatial organization of tumor-associated TLSs indicate that the development of B cell-dependent anti-tumor immunity lay the basis for the contribution of such structures to a favorable prognosis.

The presence of active GCs with AID^+ and $BCL\text{-}6^+$ B cells, as well as differentiated memory B cells and plasma cells, has been detected within TLSs from diverse cancer types (Cipponi et al., 2012; Germain et al., 2014; Kroeger et al., 2016; Montfort et al., 2017; Garaud et al., 2019). Analysis of the repertoire of immunoglobulins in melanoma (Cipponi et al., 2012; Helmink et al., 2020), ovarian cancer (Kroeger et al., 2016) and invasive breast ductal carcinoma (Nzula et al., 2003) samples demonstrated B cell clonal amplification, somatic hypermutation (SHM) and CSR, revealing a local antigen-driven response and antibody affinity maturation. Similarly, a comprehensive characterization of immune cells from triple-negative breast cancer patients using paired single-cell RNA and TCR/BCR sequencing revealed that tumor-infiltrating B cells were mostly $CD27^+$ memory B cells and had higher clonality, CSR and SHM than those in the blood (Hu et al., 2021). Unsupervised clustering further identified a group of $AICDA^+$ and $MKI67^+$ proliferative B cells and $CD38^+$ plasma cells in tumor samples, underscoring the existence of functionally active GCs. Widespread B cell clonal expansions and immunoglobulin subclass switch events were also evidenced in multiple human cancers by a large-scale report, analyzing more than 30 million IgH complementarity-determining region 3 sequences assembled from ∼9,000 tumor RNA-seq samples (32 cancer types) in The Cancer Genome Atlas (TCGA, Hu et al., 2019).

Activated TLS B cells may modulate T cell phenotypes within the tumor microenvironment through their ability to present tumor-derived peptides. Multiple studies have shown that tumor-infiltrating B cells with an activated/memory phenotype express markers of antigen presentation, including MHC class I and II and costimulatory molecules such as CD40, CD80, and CD86 (Nielsen et al., 2012; Shi et al., 2013; Bruno et al., 2017; Rossetti et al., 2018). Although dendritic cells are the major APCs that provide initial T cell activation in the lymph nodes, antigen-presenting B cells can contribute to additional $CD4^+$ T cell expansion intratumorally, as demonstrated by *ex vivo* co-culture assays (Bruno et al., 2017; Rossetti et al., 2018). Accordingly, in lung tumors, a high density of TLS B cells was associated with increased $CD4^+$ T cell receptor repertoire clonality (Zhu et al., 2015) and with a reduced percentage of Tregs (Germain et al., 2021). The capacity of B cells to cross-present antigens to $CD8^+$ T cells is also well established (Heit et al., 2004; Hon et al., 2005; Marino et al., 2012) and has been demonstrated in the context of the cancer testis antigen NY-ESO-1 (Gnjatic et al., 2003). Moreover, in ovarian cancer, antigen-experienced $CD20^+$ B cells colocalized with activated $CD8^+$ T cells, and the presence of both populations correlated with increased patient survival compared with the presence of $CD8^+$ T cells alone (Nielsen et al., 2012). Memory B cells may also possess tumor-killing potential by producing IFN-γ, interleukin 12*p*40 (IL-12*p*40), granzyme B, and TRAIL (Shi et al., 2013).

Plasma cells generated within tumor-associated TLSs may reside locally and produce significant amounts of tumor-specific antibodies, as shown for breast cancer (Coronella et al., 2002; Pavoni et al., 2007), melanoma (Erdag et al., 2012), non-small cell lung cancer (Lohr et al., 2013; Germain et al., 2014), and high-grade serous ovarian cancer (Montfort et al., 2017). Importantly, the isotype and specificity of such antibodies can drive distinct immune responses (Sharonov et al., 2020). The IgG1 antibody class is of primary importance for anti-tumor cytotoxic responses, as these antibodies can bind to Fcγ receptors and trigger antibody-dependent cellular cytotoxicity and phagocytosis, complement activation, and enhance antigen presentation by dendritic cells (Gilbert et al., 2011; Boyerinas et al., 2015; Carmi et al., 2015). Accordingly, high intratumoral IgG1 has been associated with longer patient survival, while IgA may drive an opposite pattern (Welinder et al., 2016; Bolotin et al., 2017; Isaeva et al., 2019). Additionally, analysis of more than 5,000 TCGA RNA-seq samples revealed that high levels of IgG3–1 switch are associated with prolonged survival in patients with high SHM rates, whereas IgG3–1 levels are not prognostic in low SHM samples, underscoring the role of SHM in generating BCR sequences with high binding affinity to the exposed tumor antigens (Hu et al., 2019).

In prostate cancer and hepatocellular carcinoma, IgA-producing plasma cells have been shown to function as potent immunosuppressive cell populations through the expression of IL-10 and PD-L1 (Shalapour et al., 2015, 2017). On the other hand, in ovarian cancer, a recent report demonstrated that protective humoral responses are dominated by the production

TABLE 1 | B cell and TLS presence and abundance as prognostic factors in different tumors.

Author, year	Tumor type	N	Sample type	Method of assessment	Finding
B lymphocytes					
Ladanyi et al. (2011)	Cutaneous melanoma	106	FFPE	Immunohistochemistry	High number of $CD20^+$ B cells (intratumoral and peritumoral) associated with improved OS
Mahmoud et al. (2012)	Breast cancer	1,470	FFPE	Immunohistochemistry	Higher total $CD20^+$ B cell counts associated with better DFI and BCSS
Woo et al. (2014)	Prostate carcinoma	53	FFPE	Immunohistochemistry	Intratumoral $CD20^+$ B cells associated with cancer recurrence and progression
Germain et al. (2014)	Lung cancer	74 early stage 122 advanced stage	FFPE	Immunohistochemistry	High density of follicular $CD20^+$ B cells within TLSs associated with better OS
Castino et al. (2016)	Pancreatic cancer	104	FFPE	Immunohistochemistry	High density of B cells within TLSs associated with improved DSS.
Miligy et al. (2017)	Breast DCIS	36	FFPE	Immunohistochemistry	High number of $CD20^+$ B cells associated with shorter RFI
Sakimura et al. (2017)	Gastric cancer	226	FFPE	Immunohistochemistry	High number of $CD20^+$ B cells associated with longer OS
Arias-Pulido et al. (2018)	Inflammatory breast cancer	221	FFPE	Immunohistochemistry	$CD20^+PD\text{-}L1^+$ lymphocytes were an independent favorable prognostic factor for DFS and BCSS
Edin et al. (2019)	Colorectal	316	FFPE	Multiplexed immunohistochemistry and multispectral imaging	High number of $CD20^+$ B cells associated with improved DSS
Murakami et al. (2019)	Gastric cancer	59	FFPE	Double staining immunohistochemistry (CD19 and IL-10)	Regulatory B cells ($CD19^+IL10^+$) associated with worse 5-year OS rate
Chen et al. (2020)	NK/T-cell lymphoma	56	FFPE	Immunohistochemistry	High density of $CD20^+$ B cells associated with improved OS
Petitprez et al. (2020)	Sarcoma	496	STS public datasets (TCGA SARC, GSE21050, GSE21122 and GSE30929)	Gene expression (TME deconvolution)	B cell signature associated with improved OS
TLS					
Coppola et al. (2011)	Colorectal cancer	21	Fresh tumor	Microarray	Higher expression of a 12-chemokine TLS signature in long-term survivors
Vayrynen et al. (2014)	Colorectal cancer	418 (cohort 1)	FFPE	H&E	Higher TLS density (the number of follicles/the length of the invasive front) associated with improved 5-year survival
Hiraoka et al. (2015)	Pancreatic cancer	308	FFPE	Immunohistochemistry	Higher relative area of intratumoral TLSs associated with improved OS and DFS
Schweiger et al. (2016)	Colorectal cancer (lung metastases)	57	FFPE	Immunohistochemistry	The presence of TLSs was not associated with improved RFS or OS
Lee H.J. et al. (2016)	Resected triple negative breast cancer	769	FFPE	H&E	Moderate or abundant TLSs associated with better DFS
Liu X. et al., 2017	Invasive breast cancer	248	FFPE	Immunohistochemistry	Presence of TLS associated with improved DFS in $HER2^+$ tumors
Silina et al. (2018)	Resected squamous cell lung carcinoma	138	FFPE	H&E	Number of TLSs per mm^2 was the strongest prognostic factor
Calderaro et al. (2019)	Resected hepatocellular carcinoma	273	FFPE	H&E	Presence of intratumoral TLSs associated with lower risk of early tumor relapse following surgery
Sofopoulos et al. (2019)	Ductal breast carcinoma	112	FFPE	H&E	Patients with peritumoral TLSs had worse DFS and OS
Cabrita et al. (2020)	Cutaneous melanoma	117	FFPE	Immunohistochemistry	Presence of TLSs and tumor associated $CD8^+$ cells associated with improved OS
Li et al. (2020)	Resected oral cancer	65	FFPE	H&E	Patients whose tumors were enriched for intratumoral TLSs had better DFS and OS

(Continued)

TABLE 1 | Continued

Author, year	Tumor type	N	Sample type	Method of assessment	Finding
Tang et al. (2020)	Lung cancer	133	FFPE	Immunohistochemistry	High TLS number per mm^2 and relative area associated with improved 10-year survival
Rakaee et al. (2021)	Lung cancer	553	FFPE	Immunohistochemistry	TLS score was an independent positive prognostic factor of DFS and OS, regardless of the quantification strategy used (four-scale semi-quantitative; absolute count of total TLSs; absolute count of total TLSs with germinal center)

TLS, tertiary lymphoid structures; FFPE, formalin-fixed paraffin-embedded samples; DFI, disease-free interval; BCSS, breast cancer specific survival; RFI, relapse-free interval; DCIS, ductal carcinoma in situ; DSS, disease-specific survival; OS, overall survival; STS, soft tissue sarcoma; RFS, recurrence-free survival; H&E, hematoxylin and eosin staining.

of polyclonal IgA, which binds to polymeric IgA receptors universally expressed on the tumor cells (Biswas et al., 2021). Interestingly, IgA responses were shown to impair ovarian cancer growth through complementary mechanisms: antigen-specific IgA redirected myeloid cells against cell-surface antigen-positive tumor cells, while transcytosis of non-antigen-specific IgA by tumor cells induced broad transcriptional changes, including the upregulation of IFN-γ receptors and several DUSP phosphatases, which antagonize the RAS pathway.

Accumulating evidence shows that the functional state of tumor-infiltrating B cells is shaped by whether they are organized or not in well-structured mature TLSs (**Figure 3**). Careful examination of tissue slides from adenocarcinoma of the pancreas (Castino et al., 2016) and the esophagogastric junction (Knief et al., 2016) revealed that a high density of $CD20^+$ B cells was associated with increased patient survival, but only if B cells were organized within TLSs. Similarly, the abundance of $CD20^+$ B cells in ovarian cancer was only associated with improved prognosis in the presence of the TLS marker CXCL13. $CD20^{hi}CXCL13^{hi}$ tumors had significantly longer overall survival and progression-free survival than the $CD20^{lo}$ or $CXCL13^{lo}$ counterparts (Yang et al., 2021). Regulatory phenotypes may arise when B cells are scattered throughout the stroma and have substantial interaction with malignant (Zhao et al., 2018) and TGFβ-producing cells, as suggested by the low T cell activity in immature TLSs (Cabrita et al., 2020). It is, thus, crucial to consider the spatial distribution of B cells to properly understand their dual role in controlling tumor progression. Importantly, experiments with pre-clinical murine models should be interpreted with caution, as fast-growing orthotopic tumors might develop a malignant cell-rich bulk with reduced stroma and devoid of TLSs (Spear et al., 2019).

It is noteworthy that TLS-rich tumors are typically more infiltrated by $CD8^+$ T cells, which may express inhibitory immune checkpoints following persistent antigen exposure and/or inflammatory signals. In mature TLSs of sarcoma patients, the intimate contact between B and T cells was sufficient to induce high expression of the immune checkpoint PD-1 on T cells (Petitprez et al., 2020). Similarly, expression levels of the inhibitory receptors TIGIT and CTLA-4 were elevated in TLS^{hi} non-small cell lung cancer samples compared to the TLS^{lo} ones (Rakaee et al., 2021). Thus, TLSs may represent a rich site of expression of clinically relevant immune checkpoints.

CLINICAL APPLICATIONS AND FUTURE PERSPECTIVES

Recent studies have demonstrated a prominent association between B cell-dependent anti-tumor immunity and responsiveness to immunotherapy in different types of cancer. Analysis of post-treatment resection specimens of non-small-cell lung carcinoma patients in the first trial of neoadjuvant anti-PD-1 (nivolumab) showed that immune-mediated tumor clearance was characterized by local formation of TLSs and the presence of plasma cells (Cottrell et al., 2018). Notably, a TLS gene expression signature predicted clinical outcomes to ICB with anti-CTLA-4 and/or anti-PD-1 in multiple cohorts of melanoma samples (Cabrita et al., 2020). At baseline, melanoma-infiltrating B cells from responders were shown to have increased BCR clonality and diversity, as well as a higher proportion of $CD27^+$ memory B cells (Helmink et al., 2020). A similar predictive role for B cells organized in TLSs was observed for ICB responses in patients with renal cell carcinoma (Helmink et al., 2020) and soft tissue sarcoma (Petitprez et al., 2020). Interestingly, higher expression of the TLS marker CXCL13 was independently associated with prolonged survival and objective response in muscle-invasive bladder cancer patients treated with ICB, while no significant results were observed for non–ICB-treated patients (Groeneveld et al., 2021).

Although mounting evidence highlights the central role of B lymphocytes and TLS in priming effective anti-tumor immune responses (Sautes-Fridman et al., 2019), they have largely been overlooked in clinical trials that have mostly focused on reversing T cell exhaustion. Except for drugs developed to treat B cell lymphomas and leukemias, clinical strategies that directly modulate B lymphocytes or harness the formation of TLSs have not yet been developed for solid tumors.

Barbera-Guillem et al. (2000) used rituximab to deplete B cells in a mouse model of liver metastasis of colorectal carcinoma (CRC) and demonstrated a reduction in the number of metastases following treatment. In the same study, fourteen metastatic CRC patients received rituximab, and among the 8 patients who completed treatment, half had tumor regression

and 1 achieved stable disease as evaluated by positron emission tomography (Barbera-Guillem et al., 2000).

LIGHT (TNFSF14) is a cytokine important to the development and maintenance of SLOs and TLSs. In a preclinical murine model of pancreatic cancer, the administration of LIGHT linked to a vascular targeting peptide (LIGHT-VTP) promoted the formation of TLSs, stimulated intratumoral T cell infiltration, enhanced response to anti-PD1 and anti-CTLA4 therapies and strongly synergized with anti-tumor vaccination (Johansson-Percival et al., 2017).

In a phase I/II study (J0810) involving potentially resectable pancreatic cancer, 59 patients were randomized, with a 1:1:1 ratio, to receive GVAX, a GM-CSF-secreting irradiated pancreatic tumor vaccine, administered intradermally alone (arm A) or in combination with low dose intravenous (arm B) or oral cyclophosphamide (arm C) before and after surgery. Fifty-four patients underwent surgery, five of them did not have pancreatic adenocarcinoma, 1 had an ampullary cancer and 11 had cancer recurrence immediately following surgery, all these patients were excluded from further analysis. Among the remaining 39 patients, 33 (85%) developed intratumoral TLS, whereas none of 54 unvaccinated patients from a previous study had lymphoid aggregates in their tumors. Besides, vaccinated patients had improved antigen specific (anti-mesothelin) T cell response and enhanced T effector/T regulatory ratio. The authors did not include a control group treated with cyclophosphamide only, and despite they suggested that TLS formation was associated with longer survival; this result was underpowered and biased due to patient selection (Lutz et al., 2014). Recently, Zheng et al. (2021) updated the results of this trial after the inclusion of 38 additional patients (87 in total). Combining low dose cyclophosphamide with GVAX promoted worse disease-free survival (arm A × B × C: 18.92 × 8.54 × 5.56 months) and overall survival (34.2 × 15.4 × 16.5) compared to GVAX alone. Increased density of intratumoral TLS was associated with longer overall survival (Zheng et al., 2021).

In another study, metastatic pancreatic adenocarcinoma (PDAC) patients were treated in a random fashion (2:1 ratio) with two doses of GVAX followed by 4 doses of live-attenuated *Listeria monocytogenes* expressing mesothelin (CRS-207) (arm A) or 6 doses of GVAX plus cyclophosphamide (arm B). The combination of GVAX and CRS-207 improved median overall survival (primary endpoint) from 3.9 months in arm B to 6.1 months in arm A (HR 0.59; $p = 0.02$). Mesothelin-specific T cell number was higher in arm A as well. However, no objective responses were observed, and progression-free survival was similar in both arms, which makes it challenging to rule out an imbalance due to the effect of subsequent treatments in overall survival (Le et al., 2015).

On the other hand, Tsujikawa et al. (2020) randomized 93 metastatic PDAC patients to receive the same treatment mentioned above (GVAX+ low dose cyclophosphamide+ CRS−207) with or without nivolumab (an anti-PD1 monoclonal antibody). They did not observe any difference in overall survival. The authors also analyzed 22 paired tumor samples before and after treatment and found an increase lymphoid cell density, an increased frequency of PD1-EOMES-$CD8^+$ T cells and a decrease in $CD68^+$ myeloid cells within the tumor microenvironment after cycle 3 in patients treated with GVAX and nivolumab (Tsujikawa et al., 2020).

Similarly, Wu A. A. et al. (2020) randomized 82 metastatic PDAC patients who obtained at least stable disease following 8–12 cycles of FOLFIRINOX (5-fluorouracil, leucovorin, irinotecan and oxaliplatin) to continue FOLFIRINOX or receive 4 doses of ipilimumab (an anti-CTLA4 monoclonal antibody) plus GVAX every 3 weeks. The study was stopped due to futility after an interim analysis; OS was shorter in the GVAX arm (9.38 × 14.7 months). Nevertheless, the authors observed an increase in effector and memory T cells in peripheral blood following treatment with GVAX+ ipilimumab. Similarly, they observed an increase in total $CD4^+$ and $CD8^+$ T cells, late effector memory $CD8^+$ T cells and M1 macrophages and a decrease in $CD4^+FOXP3^+$ Tregs, early effector, exhausted $CD8^+$ T cells and M2 macrophages in the tumor microenvironment comparing tumor samples obtained before and after treatment. However, it is difficult to tease out which intervention (GVAX alone, ipilimumab or the combination) promoted the aforementioned modifications.

On the other hand, corticosteroids, diet, rituximab and chemotherapy can impair the formation of TLS and reduce the development of GCs, potentially blunting anti-tumor immune response (Liu L. et al., 2017; Silina et al., 2018; Ryan et al., 2020).

Overall, these data indicate that strategies modulating TLS development in tumor milieu may hold promise in cancer treatment and extend the use of TLS and B cells beyond prognostic and therapeutic biomarkers to therapeutic targets. Studies in the basic research field aiming to further elucidate the mechanisms governing TLS evolution in cancer may pave the way for the development of new therapeutic approaches in this sense.

CONCLUDING REMARKS

There is a growing appreciation that prominent anti-tumor immune responses are elicited when immune cells are spatially organized in privileged sites, namely TLSs, that facilitate cell-to-cell interaction and optimal antigen presentation. The detailed characterization of such complex intratumoral cellular networks is gaining momentum due to their clinical relevance, since TLSs can be used as a biomarker to classify cancer patients that are likely to benefit from immunotherapy approaches. More importantly, due to their capacity of mounting coordinated anti-tumor T and B cell responses, TLSs can be used to identify clinically relevant cancer-related immune checkpoints, and further research may reveal strategies capable of modulating TLS formation in the tumor microenvironment. Previously neglected, B cells are now considered key cellular components that initiate and sustain anti-tumor responses, as they appear to be indispensable T lymphocyte allies in the fight against cancer cells.

AUTHOR CONTRIBUTIONS

GK, GV, WF, and AC designed the figures. All authors wrote and approved the manuscript before submission.

FUNDING

This work was supported by funds from the São Paulo Research Foundation (FAPESP) to GK (fellowship 2019/25129-2) and TM (grant 2018/14034-8), by the Coordination for the Improvement of Higher Education Personnel (CAPES) fellowship to AC, by grants from the National Institute of Science and Technology in Oncogenomics and Therapeutic Innovation (INCITO) funded by FAPESP (grant 2014/50943-1), and the National Council for Scientific and Technological Development (CNPq, grant 465682/2014-6).

REFERENCES

Adler, L. N., Jiang, W., Bhamidipati, K., Millican, M., Macaubas, C., Hung, S. C., et al. (2017). The Other Function: Class II-Restricted Antigen Presentation by B Cells. *Front. Immunol.* 8:319. doi: 10.3389/fimmu.2017.00319

Ammirante, M., Luo, J. L., Grivennikov, S., Nedospasov, S., and Karin, M. (2010). B-cell-derived lymphotoxin promotes castration-resistant prostate cancer. *Nature* 464, 302–305. doi: 10.1038/nature08782

Arias-Pulido, H., Cimino-Mathews, A., Chaher, N., Qualls, C., Joste, N., Colpaert, C., et al. (2018). The combined presence of CD20 + B cells and PD-L1 + tumor-infiltrating lymphocytes in inflammatory breast cancer is prognostic of improved patient outcome. *Breast Cancer Res. Treat.* 171, 273–282. doi: 10.1007/s10549-018-4834-7

Bai, R., Lv, Z., Xu, D., and Cui, J. (2020). Predictive biomarkers for cancer immunotherapy with immune checkpoint inhibitors. *Biomark Res.* 8:34.

Barbera-Guillem, E., Nelson, M. B., Barr, B., Nyhus, J. K., May, K. F. Jr., Feng, L., et al. (2000). B lymphocyte pathology in human colorectal cancer. Experimental and clinical therapeutic effects of partial B cell depletion. *Cancer Immunol. Immunother.* 48, 541–549. doi: 10.1007/pl00006672

Baumgarth, N. (2017). A Hard(y) Look at B-1 Cell Development and Function. *J. Immunol.* 199, 3387–3394. doi: 10.4049/jimmunol.1700943

Beck, T. C., Gomes, A. C., Cyster, J. G., and Pereira, J. P. (2014). CXCR4 and a cell-extrinsic mechanism control immature B lymphocyte egress from bone marrow. *J. Exp. Med.* 211, 2567–2581. doi: 10.1084/jem.20140457

Bertocci, B., De Smet, A., Weill, J. C., and Reynaud, C. A. (2006). Nonoverlapping functions of DNA polymerases mu, lambda, and terminal deoxynucleotidyltransferase during immunoglobulin V(D)J recombination in vivo. *Immunity* 25, 31–41. doi: 10.1016/j.immuni.2006.04.013

Bibby, J. A., Purvis, H. A., Hayday, T., Chandra, A., Okkenhaug, K., Rosenzweig, S., et al. (2020). Cholesterol metabolism drives regulatory B cell IL-10 through provision of geranylgeranyl pyrophosphate. *Nat. Commun.* 11:3412.

Biswas, S., Mandal, G., Payne, K. K., Anadon, C. M., Gatenbee, C. D., Chaurio, R. A., et al. (2021). IgA transcytosis and antigen recognition govern ovarian cancer immunity. *Nature* 591, 464–470. doi: 10.1038/s41586-020-03144-0

Bolotin, D. A., Poslavsky, S., Davydov, A. N., Frenkel, F. E., Fanchi, L., Zolotareva, O. I., et al. (2017). Antigen receptor repertoire profiling from RNA-seq data. *Nat. Biotechnol.* 35, 908–911. doi: 10.1038/nbt.3979

Boyerinas, B., Jochems, C., Fantini, M., Heery, C. R., Gulley, J. L., Tsang, K. Y., et al. (2015). Antibody-Dependent Cellular Cytotoxicity Activity of a Novel Anti-PD-L1 Antibody Avelumab (MSB0010718C) on Human Tumor Cells. *Cancer Immunol. Res.* 3, 1148–1157. doi: 10.1158/2326-6066.cir-15-0059

Bruno, T. C., Ebner, P. J., Moore, B. L., Squalls, O. G., Waugh, K. A., Eruslanov, E. B., et al. (2017). Antigen-Presenting Intratumoral B Cells Affect CD4(+) TIL Phenotypes in Non-Small Cell Lung Cancer Patients. *Cancer Immunol. Res.* 5, 898–907. doi: 10.1158/2326-6066.cir-17-0075

Buckley, C. D., Barone, F., Nayar, S., Benezech, C., and Caamano, J. (2015). Stromal cells in chronic inflammation and tertiary lymphoid organ formation. *Annu. Rev. Immunol.* 33, 715–745. doi: 10.1146/annurev-immunol-032713-120252

Cabrita, R., Lauss, M., Sanna, A., Donia, M., Skaarup Larsen, M., Mitra, S., et al. (2020). Tertiary lymphoid structures improve immunotherapy and survival in melanoma. *Nature* 577, 561–565. doi: 10.1038/s41586-019-1914-8

Calderaro, J., Petitprez, F., Becht, E., Laurent, A., Hirsch, T. Z., Rousseau, B., et al. (2019). Intra-tumoral tertiary lymphoid structures are associated with a low risk of early recurrence of hepatocellular carcinoma. *J. Hepatol.* 70, 58–65. doi: 10.1016/j.jhep.2018.09.003

Carmi, Y., Spitzer, M. H., Linde, I. L., Burt, B. M., Prestwood, T. R., Perlman, N., et al. (2015). Allogeneic IgG combined with dendritic cell stimuli induce antitumour T-cell immunity. *Nature* 521, 99–104. doi: 10.1038/nature14424

Caro-Maldonado, A., Wang, R., Nichols, A. G., Kuraoka, M., Milasta, S., Sun, L. D., et al. (2014). Metabolic reprogramming is required for antibody production that is suppressed in anergic but exaggerated in chronically BAFF-exposed B cells. *J. Immunol.* 192, 3626–3636. doi: 10.4049/jimmunol.1302062

Castino, G. F., Cortese, N., Capretti, G., Serio, S., Di Caro, G., Mineri, R., et al. (2016). Spatial distribution of B cells predicts prognosis in human pancreatic adenocarcinoma. *Oncoimmunology* 5:e1085147. doi: 10.1080/2162402x.2015.1085147

Chaye, M. A. M., Tontini, C., Ozir-Fazalalikhan, A., Voskamp, A. L., and Smits, H. H. (2021). Use of Toll-Like Receptor (TLR) Ligation to Characterize Human Regulatory B-Cells Subsets. *Methods Mol. Biol.* 2270, 235–261. doi: 10.1007/978-1-0716-1237-8_13

Chen, M. M., Zeng, G. P., Li, J., Fu, J. H., Long, Y. Y., Pan, J. Y., et al. (2020). High infiltration of CD20(+) B lymphocytes in extranodal natural killer/T-cell lymphoma is associated with better prognosis. *Br. J. Haematol.* 191, e116–e120.

Chen, X., and Jensen, P. E. (2008). The role of B lymphocytes as antigen-presenting cells. *Arch. Immunol. Ther. Exp.* 56, 77–83.

Cherrier, M., Sawa, S., and Eberl, G. (2012). Notch, Id2, and RORgammat sequentially orchestrate the fetal development of lymphoid tissue inducer cells. *J. Exp. Med.* 209, 729–740. doi: 10.1084/jem.20111594

Cinamon, G., Matloubian, M., Lesneski, M. J., Xu, Y., Low, C., Lu, T., et al. (2004). Sphingosine 1-phosphate receptor 1 promotes B cell localization in the splenic marginal zone. *Nat. Immunol.* 5, 713–720. doi: 10.1038/ni1083

Cipponi, A., Mercier, M., Seremet, T., Baurain, J. F., Theate, I., Van Den Oord, J., et al. (2012). Neogenesis of lymphoid structures and antibody responses occur in human melanoma metastases. *Cancer Res.* 72, 3997–4007. doi: 10.1158/0008-5472.can-12-1377

Coppola, D., Nebozhyn, M., Khalil, F., Dai, H., Yeatman, T., Loboda, A., et al. (2011). Unique ectopic lymph node-like structures present in human primary colorectal carcinoma are identified by immune gene array profiling. *Am. J. Pathol.* 179, 37–45. doi: 10.1016/j.ajpath.2011.03.007

Coronella, J. A., Spier, C., Welch, M., Trevor, K. T., Stopeck, A. T., Villar, H., et al. (2002). Antigen-driven oligoclonal expansion of tumor-infiltrating B cells in infiltrating ductal carcinoma of the breast. *J. Immunol.* 169, 1829–1836. doi: 10.4049/jimmunol.169.4.1829

Cottrell, T. R., Thompson, E. D., Forde, P. M., Stein, J. E., Duffield, A. S., Anagnostou, V., et al. (2018). Pathologic features of response to neoadjuvant anti-PD-1 in resected non-small-cell lung carcinoma: a proposal for quantitative immune-related pathologic response criteria (irPRC). *Ann. Oncol.* 29, 1853–1860. doi: 10.1093/annonc/mdy218

Cyster, J. G., and Allen, C. D. C. (2019). B Cell Responses: Cell Interaction Dynamics and Decisions. *Cell* 177, 524–540. doi: 10.1016/j.cell.2019.03.016

Dambuza, I. M., He, C., Choi, J. K., Yu, C. R., Wang, R., Mattapallil, M. J., et al. (2017). IL-12p35 induces expansion of IL-10 and IL-35-expressing regulatory B cells and ameliorates autoimmune disease. *Nat. Commun.* 8:719.

de Wit, J., Souwer, Y., Jorritsma, T., Klaasse Bos, H., Ten Brinke, A., Neefjes, J., et al. (2010). Antigen-specific B cells reactivate an effective cytotoxic T cell response against phagocytosed *Salmonella* through cross-presentation. *PLoS One* 5:e13016. doi: 10.1371/journal.pone.0013016

Deola, S., Panelli, M. C., Maric, D., Selleri, S., Dmitrieva, N. I., Voss, C. Y., et al. (2008). Helper B cells promote cytotoxic T cell survival and proliferation independently of antigen presentation through CD27/CD70 interactions. *J. Immunol.* 180, 1362–1372. doi: 10.4049/jimmunol.180.3.1362

Deteix, C., Attuil-Audenis, V., Duthey, A., Patey, N., Mcgregor, B., Dubois, V., et al. (2010). Intragraft Th17 infiltrate promotes lymphoid neogenesis and hastens clinical chronic rejection. *J. Immunol.* 184, 5344–5351. doi: 10.4049/jimmunol.0902999

Dieu-Nosjean, M. C., Antoine, M., Danel, C., Heudes, D., Wislez, M., Poulot, V., et al. (2008). Long-term survival for patients with non-small-cell lung cancer

with intratumoral lymphoid structures. *J. Clin. Oncol.* 26, 4410–4417. doi: 10.1200/jco.2007.15.0284

Dobosz, P., and Dzieciatkowski, T. (2019). The Intriguing History of Cancer Immunotherapy. *Front. Immunol.* 10:2965. doi: 10.3389/fimmu.2019.02965

Domeier, P. P., Chodisetti, S. B., Soni, C., Schell, S. L., Elias, M. J., Wong, E. B., et al. (2016). IFN-gamma receptor and STAT1 signaling in B cells are central to spontaneous germinal center formation and autoimmunity. *J. Exp. Med.* 213, 715–732. doi: 10.1084/jem.20151722

Domeier, P. P., Schell, S. L., and Rahman, Z. S. (2017). Spontaneous germinal centers and autoimmunity. *Autoimmunity* 50, 4–18. doi: 10.1080/08916934.2017.1280671

Dong, H. P., Elstrand, M. B., Holth, A., Silins, I., Berner, A., Trope, C. G., et al. (2006). NK- and B-cell infiltration correlates with worse outcome in metastatic ovarian carcinoma. *Am. J. Clin. Pathol.* 125, 451–458. doi: 10.1309/15b66dqmfyym78cj

Edin, S., Kaprio, T., Hagstrom, J., Larsson, P., Mustonen, H., Bockelman, C., et al. (2019). The Prognostic Importance of CD20(+) B lymphocytes in Colorectal Cancer and the Relation to Other Immune Cell subsets. *Sci. Rep.* 9:19997.

Erdag, G., Schaefer, J. T., Smolkin, M. E., Deacon, D. H., Shea, S. M., Dengel, L. T., et al. (2012). Immunotype and immunohistologic characteristics of tumor-infiltrating immune cells are associated with clinical outcome in metastatic melanoma. *Cancer Res.* 72, 1070–1080. doi: 10.1158/0008-5472.can-11-3218

Escors, D., Gato-Canas, M., Zuazo, M., Arasanz, H., Garcia-Granda, M. J., Vera, R., et al. (2018). The intracellular signalosome of PD-L1 in cancer cells. *Signal. Transduct. Target Ther.* 3:26.

Farkona, S., Diamandis, E. P., and Blasutig, I. M. (2016). Cancer immunotherapy: the beginning of the end of cancer? *BMC Med.* 14:73. doi: 10.1186/s12916-016-0623-5

Fillatreau, S., Sweenie, C. H., Mcgeachy, M. J., Gray, D., and Anderton, S. M. (2002). B cells regulate autoimmunity by provision of IL-10. *Nat. Immunol.* 3, 944–950. doi: 10.1038/ni833

Fremd, C., Schuetz, F., Sohn, C., Beckhove, P., and Domschke, C. (2013). B cell-regulated immune responses in tumor models and cancer patients. *Oncoimmunology* 2:e25443. doi: 10.4161/onci.25443

Fuxa, M., Skok, J., Souabni, A., Salvagiotto, G., Roldan, E., and Busslinger, M. (2004). Pax5 induces V-to-DJ rearrangements and locus contraction of the immunoglobulin heavy-chain gene. *Genes Dev.* 18, 411–422. doi: 10.1101/gad.291504

Ganti, S. N., Albershardt, T. C., Iritani, B. M., and Ruddell, A. (2015). Regulatory B cells preferentially accumulate in tumor-draining lymph nodes and promote tumor growth. *Sci. Rep.* 5:12255.

Garaud, S., Buisseret, L., Solinas, C., Gu-Trantien, C., De Wind, A., Van Den Eynden, G., et al. (2019). Tumor infiltrating B-cells signal functional humoral immune responses in breast cancer. *JCI Insight* 5:e129641.

Garner, H., and de Visser, K. E. (2020). Immune crosstalk in cancer progression and metastatic spread: a complex conversation. *Nat. Rev. Immunol.* 20, 483–497. doi: 10.1038/s41577-019-0271-z

Gatto, D., and Brink, R. (2010). The germinal center reaction. *J. Allerg. Clin. Immunol.* 126, 898–907.

Germain, C., Devi-Marulkar, P., Knockaert, S., Biton, J., Kaplon, H., Letaief, L., et al. (2021). Tertiary Lymphoid Structure-B Cells Narrow Regulatory T Cells Impact in Lung Cancer Patients. *Front. Immunol.* 12:626776. doi: 10.3389/fimmu.2021.626776

Germain, C., Gnjatic, S., Tamzalit, F., Knockaert, S., Remark, R., Goc, J., et al. (2014). Presence of B cells in tertiary lymphoid structures is associated with a protective immunity in patients with lung cancer. *Am. J. Respir. Crit. Care Med.* 189, 832–844. doi: 10.1164/rccm.201309-1611oc

Gibney, G. T., Weiner, L. M., and Atkins, M. B. (2016). Predictive biomarkers for checkpoint inhibitor-based immunotherapy. *Lancet Oncol.* 17, e542–e551.

Gilbert, A. E., Karagiannis, P., Dodev, T., Koers, A., Lacy, K., Josephs, D. H., et al. (2011). Monitoring the systemic human memory B cell compartment of melanoma patients for anti-tumor IgG antibodies. *PLoS One* 6:e19330. doi: 10.1371/journal.pone.0019330

Gnjatic, S., Atanackovic, D., Matsuo, M., Jager, E., Lee, S. Y., Valmori, D., et al. (2003). Cross-presentation of HLA class I epitopes from exogenous NY-ESO-1 polypeptides by nonprofessional APCs. *J. Immunol.* 170, 1191–1196. doi: 10.4049/jimmunol.170.3.1191

Gotot, J., Gottschalk, C., Leopold, S., Knolle, P. A., Yagita, H., Kurts, C., et al. (2012). Regulatory T cells use programmed death 1 ligands to directly suppress autoreactive B cells in vivo. *Proc. Natl. Acad. Sci. U. S. A.* 109, 10468–10473. doi: 10.1073/pnas.1201131109

Groeneveld, C. S., Fontugne, J., Cabel, L., Bernard-Pierrot, I., Radvanyi, F., Allory, Y., et al. (2021). Tertiary lymphoid structures marker CXCL13 is associated with better survival for patients with advanced-stage bladder cancer treated with immunotherapy. *Eur. J. Cancer* 148, 181–189. doi: 10.1016/j.ejca.2021.01.036

Haas, K. M. (2011). Programmed cell death 1 suppresses B-1b cell expansion and long-lived IgG production in response to T cell-independent type 2 antigens. *J. Immunol.* 187, 5183–5195. doi: 10.4049/jimmunol.1101990

Han, S., Feng, S., Ren, M., Ma, E., Wang, X., Xu, L., et al. (2014). Glioma cell-derived placental growth factor induces regulatory B cells. *Int. J. Biochem. Cell Biol.* 57, 63–68. doi: 10.1016/j.biocel.2014.10.005

Hanahan, D., and Weinberg, R. A. (2011). Hallmarks of cancer: the next generation. *Cell* 144, 646–674. doi: 10.1016/j.cell.2011.02.013

Heit, A., Huster, K. M., Schmitz, F., Schiemann, M., Busch, D. H., and Wagner, H. (2004). CpG-DNA aided cross-priming by cross-presenting B cells. *J. Immunol.* 172, 1501–1507. doi: 10.4049/jimmunol.172.3.1501

Helmink, B. A., Reddy, S. M., Gao, J., Zhang, S., Basar, R., Thakur, R., et al. (2020). B cells and tertiary lymphoid structures promote immunotherapy response. *Nature* 577, 549–555.

Hertz, D., Dibbern, J., Eggers, L., Von Borstel, L., and Schneider, B. E. (2020). Increased male susceptibility to Mycobacterium tuberculosis infection is associated with smaller B cell follicles in the lungs. *Sci. Rep.* 10:5142.

Hertz, D., and Schneider, B. (2019). Sex differences in tuberculosis. *Semin. Immunopathol.* 41, 225–237.

Hiraoka, N., Ino, Y., Yamazaki-Itoh, R., Kanai, Y., Kosuge, T., and Shimada, K. (2015). Intratumoral tertiary lymphoid organ is a favourable prognosticator in patients with pancreatic cancer. *Br. J. Cancer* 112, 1782–1790. doi: 10.1038/bjc.2015.145

Hon, H., Oran, A., Brocker, T., and Jacob, J. (2005). B lymphocytes participate in cross-presentation of antigen following gene gun vaccination. *J. Immunol.* 174, 5233–5242. doi: 10.4049/jimmunol.174.9.5233

Hong, S., Zhang, Z., Liu, H., Tian, M., Zhu, X., Zhang, Z., et al. (2018). B Cells Are the Dominant Antigen-Presenting Cells that Activate Naive CD4(+) T Cells upon Immunization with a Virus-Derived Nanoparticle Antigen. *Immunity* 49:e694.

Hu, Q., Hong, Y., Qi, P., Lu, G., Mai, X., Xu, S., et al. (2021). Atlas of breast cancer infiltrated B-lymphocytes revealed by paired single-cell RNA-sequencing and antigen receptor profiling. *Nat. Commun.* 12:2186.

Hu, X., Zhang, J., Wang, J., Fu, J., Li, T., Zheng, X., et al. (2019). Landscape of B cell immunity and related immune evasion in human cancers. *Nat. Genet.* 51, 560–567. doi: 10.1038/s41588-018-0339-x

Isaeva, O. I., Sharonov, G. V., Serebrovskaya, E. O., Turchaninova, M. A., Zaretsky, A. R., Shugay, M., et al. (2019). Intratumoral immunoglobulin isotypes predict survival in lung adenocarcinoma subtypes. *J. Immunother. Cancer* 7:279.

Iwata, Y., Matsushita, T., Horikawa, M., Dilillo, D. J., Yanaba, K., Venturi, G. M., et al. (2011). Characterization of a rare IL-10-competent B-cell subset in humans that parallels mouse regulatory B10 cells. *Blood* 117, 530–541. doi: 10.1182/blood-2010-07-294249

Johansson-Percival, A., He, B., Li, Z. J., Kjellen, A., Russell, K., Li, J., et al. (2017). De novo induction of intratumoral lymphoid structures and vessel normalization enhances immunotherapy in resistant tumors. *Nat. Immunol.* 18, 1207–1217. doi: 10.1038/ni.3836

Jones, P. A., Ohtani, H., Chakravarthy, A., and De Carvalho, D. D. (2019). Epigenetic therapy in immune-oncology. *Nat. Rev. Cancer* 19, 151–161. doi: 10.1038/s41568-019-0109-9

Jung, D., and Alt, F. W. (2004). Unraveling V(D)J recombination; insights into gene regulation. *Cell* 116, 299–311. doi: 10.1016/s0092-8674(04)00039-x

Jung, D., Giallourakis, C., Mostoslavsky, R., and Alt, F. W. (2006). Mechanism and control of V(D)J recombination at the immunoglobulin heavy chain locus. *Annu. Rev. Immunol.* 24, 541–570. doi: 10.1146/annurev.immunol.23.021704.115830

Karim, M. R., and Wang, Y. F. (2019). Phenotypic identification of CD19(+)CD5(+)CD1d(+) regulatory B cells that produce interleukin 10 and transforming growth factor beta1 in human peripheral blood. *Arch. Med. Sci.* 15, 1176–1183. doi: 10.5114/aoms.2018.77772

Kessel, A., Haj, T., Peri, R., Snir, A., Melamed, D., Sabo, E., et al. (2012). Human CD19(+)CD25(high) B regulatory cells suppress proliferation of CD4(+) T cells and enhance Foxp3 and CTLA-4 expression in T-regulatory cells. *Autoimmun. Rev.* 11, 670–677. doi: 10.1016/j.autrev.2011.11.018

Khan, A. R., Hams, E., Floudas, A., Sparwasser, T., Weaver, C. T., and Fallon, P. G. (2015). PD-L1hi B cells are critical regulators of humoral immunity. *Nat. Commun.* 6:5997.

Knief, J., Reddemann, K., Petrova, E., Herhahn, T., Wellner, U., and Thorns, C. (2016). High Density of Tumor-infiltrating B-Lymphocytes and Plasma Cells Signifies Prolonged Overall Survival in Adenocarcinoma of the Esophagogastric Junction. *Anticancer Res.* 36, 5339–5345. doi: 10.21873/anticanres.11107

Kroeger, D. R., Milne, K., and Nelson, B. H. (2016). Tumor-Infiltrating Plasma Cells Are Associated with Tertiary Lymphoid Structures. *Cytol. T Cell Resp.* 22, 3005–3015. doi: 10.1158/1078-0432.ccr-15-2762

Ladanyi, A., Kiss, J., Mohos, A., Somlai, B., Liszkay, G., Gilde, K., et al. (2011). Prognostic impact of B-cell density in cutaneous melanoma. *Cancer Immunol. Immunother.* 60, 1729–1738.

Le, D. T., Wang-Gillam, A., Picozzi, V., Greten, T. F., Crocenzi, T., Springett, G., et al. (2015). Safety and survival with GVAX pancreas prime and Listeria Monocytogenes-expressing mesothelin (CRS-207) boost vaccines for metastatic pancreatic cancer. *J. Clin. Oncol.* 33, 1325–1333. doi: 10.1200/jco.2014.57.4244

Lee-Chang, C., Bodogai, M., Martin-Montalvo, A., Wejksza, K., Sanghvi, M., Moaddel, R., et al. (2013). Inhibition of breast cancer metastasis by resveratrol-mediated inactivation of tumor-evoked regulatory B cells. *J. Immunol.* 191, 4141–4151. doi: 10.4049/jimmunol.1300606

Lee, H. J., Park, I. A., Song, I. H., Shin, S. J., Kim, J. Y., Yu, J. H., et al. (2016). Tertiary lymphoid structures: prognostic significance and relationship with tumour-infiltrating lymphocytes in triple-negative breast cancer. *J. Clin. Pathol.* 69, 422–430. doi: 10.1136/jclinpath-2015-203089

Lee, K. E., Spata, M., Bayne, L. J., Buza, E. L., Durham, A. C., Allman, D., et al. (2016). Hif1a Deletion Reveals Pro-Neoplastic Function of B Cells in Pancreatic Neoplasia. *Cancer Discov.* 6, 256–269. doi: 10.1158/2159-8290.cd-15-0822

Li, K., Guo, Q., Zhang, X., Dong, X., Liu, W., Zhang, A., et al. (2020). Oral cancer-associated tertiary lymphoid structures: gene expression profile and prognostic value. *Clin. Exp. Immunol.* 199, 172–181. doi: 10.1111/cei.13389

Lindner, S., Dahlke, K., Sontheimer, K., Hagn, M., Kaltenmeier, C., Barth, T. F., et al. (2013). Interleukin 21-induced granzyme B-expressing B cells infiltrate tumors and regulate T cells. *Cancer Res.* 73, 2468–2479. doi: 10.1158/0008-5472.can-12-3450

Liu, L., Nishihara, R., Qian, Z. R., Tabung, F. K., Nevo, D., Zhang, X., et al. (2017). Association Between Inflammatory Diet Pattern and Risk of Colorectal Carcinoma Subtypes Classified by Immune Responses to Tumor. *Gastroenterology* 153:e1514.

Liu, X., Tsang, J. Y. S., Hlaing, T., Hu, J., Ni, Y. B., Chan, S. K., et al. (2017). Distinct Tertiary Lymphoid Structure Associations and Their Prognostic Relevance in HER2 Positive and Negative Breast Cancers. *Oncologist* 22, 1316–1324. doi: 10.1634/theoncologist.2017-0029

Lohr, M., Edlund, K., Botling, J., Hammad, S., Hellwig, B., Othman, A., et al. (2013). The prognostic relevance of tumour-infiltrating plasma cells and immunoglobulin kappa C indicates an important role of the humoral immune response in non-small cell lung cancer. *Cancer Lett.* 333, 222–228. doi: 10.1016/j.canlet.2013.01.036

Lorenz, R. G., Chaplin, D. D., Mcdonald, K. G., Mcdonough, J. S., and Newberry, R. D. (2003). Isolated lymphoid follicle formation is inducible and dependent upon lymphotoxin-sufficient B lymphocytes, lymphotoxin beta receptor, and TNF receptor I function. *J. Immunol.* 170, 5475–5482. doi: 10.4049/jimmunol.170.11.5475

Lundgren, S., Berntsson, J., Nodin, B., Micke, P., and Jirstrom, K. (2016). Prognostic impact of tumour-associated B cells and plasma cells in epithelial ovarian cancer. *J. Ovarian Res.* 9:21.

Lutz, E. R., Wu, A. A., Bigelow, E., Sharma, R., Mo, G., Soares, K., et al. (2014). Immunotherapy converts nonimmunogenic pancreatic tumors into immunogenic foci of immune regulation. *Cancer Immunol. Res.* 2, 616–631. doi: 10.1158/2326-6066.cir-14-0027

Mahmoud, S. M., Lee, A. H., Paish, E. C., Macmillan, R. D., Ellis, I. O., and Green, A. R. (2012). The prognostic significance of B lymphocytes in invasive carcinoma of the breast. *Breast Cancer Res. Treat.* 132, 545–553. doi: 10.1007/s10549-011-1620-1

Marino, E., Tan, B., Binge, L., Mackay, C. R., and Grey, S. T. (2012). B-cell cross-presentation of autologous antigen precipitates diabetes. *Diabetes* 61, 2893–2905. doi: 10.2337/db12-0006

Matsumoto, M., Baba, A., Yokota, T., Nishikawa, H., Ohkawa, Y., Kayama, H., et al. (2014). Interleukin-10-producing plasmablasts exert regulatory function in autoimmune inflammation. *Immunity* 41, 1040–1051. doi: 10.1016/j.immuni.2014.10.016

Matsumoto, M., and Baba, Y. (2013). [Role of STIM-dependent Ca(2+) influx in regulatory B cells]. *Yakugaku Zasshi* 133, 419–425. doi: 10.1248/yakushi.12-00227-2

Matsumoto, M., Fujii, Y., Baba, A., Hikida, M., Kurosaki, T., and Baba, Y. (2011). The calcium sensors STIM1 and STIM2 control B cell regulatory function through interleukin-10 production. *Immunity* 34, 703–714. doi: 10.1016/j.immuni.2011.03.016

Matsushita, T. (2019). Regulatory and effector B cells: Friends or foes? *J. Dermatol. Sci.* 93, 2–7. doi: 10.1016/j.jdermsci.2018.11.008

Mauri, C., and Menon, M. (2017). Human regulatory B cells in health and disease: therapeutic potential. *J. Clin. Invest.* 127, 772–779. doi: 10.1172/jci85113

McDonald, K. G., Mcdonough, J. S., and Newberry, R. D. (2005). Adaptive immune responses are dispensable for isolated lymphoid follicle formation: antigen-naive, lymphotoxin-sufficient B lymphocytes drive the formation of mature isolated lymphoid follicles. *J. Immunol.* 174, 5720–5728. doi: 10.4049/jimmunol.174.9.5720

Mebius, R. E., Streeter, P. R., Michie, S., Butcher, E. C., and Weissman, I. L. (1996). A developmental switch in lymphocyte homing receptor and endothelial vascular addressin expression regulates lymphocyte homing and permits CD4+ CD3- cells to colonize lymph nodes. *Proc. Natl. Acad. Sci. U. S. A.* 93, 11019–11024. doi: 10.1073/pnas.93.20.11019

Medina, K. L., and Singh, H. (2005). Gene regulatory networks orchestrating B cell fate specification, commitment, and differentiation. *Curr. Top Microbiol. Immunol.* 290, 1–14. doi: 10.1007/3-540-26363-2_1

Meng, X., Grotsch, B., Luo, Y., Knaup, K. X., Wiesener, M. S., Chen, X. X., et al. (2018). Hypoxia-inducible factor-1alpha is a critical transcription factor for IL-10-producing B cells in autoimmune disease. *Nat. Commun.* 9:251.

Menon, M., Blair, P. A., Isenberg, D. A., and Mauri, C. (2016). A Regulatory Feedback between Plasmacytoid Dendritic Cells and Regulatory B Cells Is Aberrant in Systemic Lupus Erythematosus. *Immunity* 44, 683–697. doi: 10.1016/j.immuni.2016.02.012

Meylan, M., Petitprez, F., Lacroix, L., Di Tommaso, L., Roncalli, M., Bougouin, A., et al. (2020). Early Hepatic Lesions Display Immature Tertiary Lymphoid Structures and Show Elevated Expression of Immune Inhibitory and Immunosuppressive Molecules. *Clin. Cancer Res.* 26, 4381–4389.

Miligy, I., Mohan, P., Gaber, A., Aleskandarany, M. A., Nolan, C. C., Diez-Rodriguez, M., et al. (2017). Prognostic significance of tumour infiltrating B lymphocytes in breast ductal carcinoma in situ. *Histopathology* 71, 258–268. doi: 10.1111/his.13217

Montfort, A., Pearce, O., Maniati, E., Vincent, B. G., Bixby, L., Bohm, S., et al. (2017). A Strong B-cell Response Is Part of the Immune Landscape in Human High-Grade Serous Ovarian Metastases. *Clin. Cancer Res.* 23, 250–262. doi: 10.1158/1078-0432.ccr-16-0081

Moulin, V., Andris, F., Thielemans, K., Maliszewski, C., Urbain, J., and Moser, M. (2000). B lymphocytes regulate dendritic cell (DC) function in vivo: increased interleukin 12 production by DCs from B cell-deficient mice results in T helper cell type 1 deviation. *J. Exp. Med.* 192, 475–482. doi: 10.1084/jem.192.4.475

Murakami, Y., Saito, H., Shimizu, S., Kono, Y., Shishido, Y., Miyatani, K., et al. (2019). Increased regulatory B cells are involved in immune evasion in patients with gastric cancer. *Sci. Rep.* 9:13083.

Nayar, S., Campos, J., Smith, C. G., Iannizzotto, V., Gardner, D. H., Mourcin, F., et al. (2019). Immunofibroblasts are pivotal drivers of tertiary lymphoid structure formation and local pathology. *Proc. Natl. Acad. Sci. U. S. A.* 116, 13490–13497. doi: 10.1073/pnas.1905301116

Nielsen, J. S., Sahota, R. A., Milne, K., Kost, S. E., Nesslinger, N. J., Watson, P. H., et al. (2012). CD20+ tumor-infiltrating lymphocytes have an atypical CD27- memory phenotype and together with CD8+ T cells promote favorable prognosis in ovarian cancer. *Clin. Cancer Res.* 18, 3281–3292. doi: 10.1158/1078-0432.ccr-12-0234

Nishimura, H., Minato, N., Nakano, T., and Honjo, T. (1998). Immunological studies on PD-1 deficient mice: implication of PD-1 as a negative regulator for B cell responses. *Int. Immunol.* 10, 1563–1572. doi: 10.1093/intimm/10.10.1563

Nouel, A., Pochard, P., Simon, Q., Segalen, I., Le Meur, Y., Pers, J. O., et al. (2015). B-Cells induce regulatory T cells through TGF-beta/IDO production in A CTLA-4 dependent manner. *J. Autoimmun.* 59, 53–60. doi: 10.1016/j.jaut.2015.02.004

Nzula, S., Going, J. J., and Stott, D. I. (2003). Antigen-driven clonal proliferation, somatic hypermutation, and selection of B lymphocytes infiltrating human ductal breast carcinomas. *Cancer Res.* 63, 3275–3280.

Okazaki, T., Maeda, A., Nishimura, H., Kurosaki, T., and Honjo, T. (2001). PD-1 immunoreceptor inhibits B cell receptor-mediated signaling by recruiting src homology 2-domain-containing tyrosine phosphatase 2 to phosphotyrosine. *Proc. Natl. Acad. Sci. U. S. A.* 98, 13866–13871. doi: 10.1073/pnas.231486598

Oleinika, K., Mauri, C., and Salama, A. D. (2019). Effector and regulatory B cells in immune-mediated kidney disease. *Nat. Rev. Nephrol.* 15, 11–26. doi: 10.1038/s41581-018-0074-7

Olkhanud, P. B., Damdinsuren, B., Bodogai, M., Gress, R. E., Sen, R., Wejksza, K., et al. (2011). Tumor-evoked regulatory B cells promote breast cancer metastasis by converting resting CD4(+) T cells to T-regulatory cells. *Cancer Res.* 71, 3505–3515. doi: 10.1158/0008-5472.can-10-4316

Pavoni, E., Monteriu, G., Santapaola, D., Petronzelli, F., Anastasi, A. M., Pelliccia, A., et al. (2007). Tumor-infiltrating B lymphocytes as an efficient source of highly specific immunoglobulins recognizing tumor cells. *BMC Biotechnol.* 7:70. doi: 10.1186/1472-6750-7-70

Peduto, L., Dulauroy, S., Lochner, M., Spath, G. F., Morales, M. A., Cumano, A., et al. (2009). Inflammation recapitulates the ontogeny of lymphoid stromal cells. *J. Immunol.* 182, 5789–5799. doi: 10.4049/jimmunol.0803974

Peters, A., Pitcher, L. A., Sullivan, J. M., Mitsdoerffer, M., Acton, S. E., Franz, B., et al. (2011). Th17 cells induce ectopic lymphoid follicles in central nervous system tissue inflammation. *Immunity* 35, 986–996. doi: 10.1016/j.immuni.2011.10.015

Petitprez, F., De Reynies, A., Keung, E. Z., Chen, T. W., Sun, C. M., Calderaro, J., et al. (2020). B cells are associated with survival and immunotherapy response in sarcoma. *Nature* 577, 556–560.

Pieper, K., Grimbacher, B., and Eibel, H. (2013). B-cell biology and development. *J. Allergy Clin. Immunol.* 131, 959–971.

Pillai, S., and Cariappa, A. (2009). The follicular versus marginal zone B lymphocyte cell fate decision. *Nat. Rev. Immunol.* 9, 767–777. doi: 10.1038/nri2656

Pimenta, E. M., De, S., Weiss, R., Feng, D., Hall, K., Kilic, S., et al. (2015). IRF5 is a novel regulator of CXCL13 expression in breast cancer that regulates CXCR5(+) B- and T-cell trafficking to tumor-conditioned media. *Immunol. Cell Biol.* 93, 486–499. doi: 10.1038/icb.2014.110

Piper, C. J. M., Rosser, E. C., Oleinika, K., Nistala, K., Krausgruber, T., Rendeiro, A. F., et al. (2019). Aryl Hydrocarbon Receptor Contributes to the Transcriptional Program of IL-10-Producing Regulatory B Cells. *Cell Rep.* 29, 1878–1892 e7.

Pipi, E., Nayar, S., Gardner, D. H., Colafrancesco, S., Smith, C., and Barone, F. (2018). Tertiary Lymphoid Structures: Autoimmunity Goes Local. *Front. Immunol.* 9:1952. doi: 10.3389/fimmu.2018.01952

Pitzalis, C., Jones, G. W., Bombardieri, M., and Jones, S. A. (2014). Ectopic lymphoid-like structures in infection, cancer and autoimmunity. *Nat. Rev. Immunol.* 14, 447–462. doi: 10.1038/nri3700

Posch, F., Silina, K., Leibl, S., Mundlein, A., Moch, H., Siebenhuner, A., et al. (2018). Maturation of tertiary lymphoid structures and recurrence of stage II and III colorectal cancer. *Oncoimmunology* 7:e1378844. doi: 10.1080/2162402x.2017.1378844

Pylayeva-Gupta, Y., Das, S., Handler, J. S., Hajdu, C. H., Coffre, M., Koralov, S. B., et al. (2016). IL35-Producing B Cells Promote the Development of Pancreatic Neoplasia. *Cancer Discov.* 6, 247–255. doi: 10.1158/2159-8290.cd-15-0843

Qian, L., Bian, G. R., Zhou, Y., Wang, Y., Hu, J., Liu, X., et al. (2015). Clinical significance of regulatory B cells in the peripheral blood of patients with oesophageal cancer. *Cent. Eur. J. Immunol.* 40, 263–265. doi: 10.5114/ceji.2015.52840

Rakaee, M., Kilvaer, T. K., Jamaly, S., Berg, T., Paulsen, E. E., Berglund, M., et al. (2021). Tertiary lymphoid structure score: a promising approach to refine the TNM staging in resected non-small cell lung cancer. *Br. J. Cancer*. doi: 10.1038/s41416-021-01307-y [Epub Online ahead of print].

Ran, Z., Yue-Bei, L., Qiu-Ming, Z., and Huan, Y. (2020). Regulatory B Cells and Its Role in Central Nervous System Inflammatory Demyelinating Diseases. *Front. Immunol.* 11:1884. doi: 10.3389/fimmu.2020.01884

Ren, Z., Peng, H., and Fu, Y. X. (2016). PD-1 Shapes B Cells as Evildoers in the Tumor Microenvironment. *Cancer Discov.* 6, 477–478. doi: 10.1158/2159-8290.cd-16-0307

Ricciardi, M., Zanotto, M., Malpeli, G., Bassi, G., Perbellini, O., Chilosi, M., et al. (2015). Epithelial-to-mesenchymal transition (EMT) induced by inflammatory priming elicits mesenchymal stromal cell-like immune-modulatory properties in cancer cells. *Br. J. Cancer* 112, 1067–1075. doi: 10.1038/bjc.2015.29

Rieger, M. A., and Schroeder, T. (2012). Hematopoiesis. *Cold Spring Harb. Perspect. Biol.* 140, 2463–2467.

Rivera, A., Chen, C. C., Ron, N., Dougherty, J. P., and Ron, Y. (2001). Role of B cells as antigen-presenting cells in vivo revisited: antigen-specific B cells are essential for T cell expansion in lymph nodes and for systemic T cell responses to low antigen concentrations. *Int. Immunol.* 13, 1583–1593. doi: 10.1093/intimm/13.12.1583

Romanow, W. J., Langerak, A. W., Goebel, P., Wolvers-Tettero, I. L., Van Dongen, J. J., Feeney, A. J., et al. (2000). E2A and EBF act in synergy with the V(D)J recombinase to generate a diverse immunoglobulin repertoire in nonlymphoid cells. *Mol. Cell* 5, 343–353. doi: 10.1016/s1097-2765(00)80429-3

Rosser, E. C., Oleinika, K., Tonon, S., Doyle, R., Bosma, A., Carter, N. A., et al. (2014). Regulatory B cells are induced by gut microbiota-driven interleukin-1beta and interleukin-6 production. *Nat. Med.* 20, 1334–1339. doi: 10.1038/nm.3680

Rossetti, R. A. M., Lorenzi, N. P. C., Yokochi, K., Rosa, M., Benevides, L., Margarido, P. F. R., et al. (2018). B lymphocytes can be activated to act as antigen presenting cells to promote anti-tumor responses. *PLoS One* 13:e0199034. doi: 10.1371/journal.pone.0199034

Roya, N., Fatemeh, T., Faramarz, M. A., Milad, S. G., Mohammad-Javad, S., Najmeh, S. V., et al. (2020). Frequency of IL-10+CD19+ B cells in patients with prostate cancer compared to patients with benign prostatic hyperplasia. *Afr. Health Sci.* 20, 1264–1272. doi: 10.4314/ahs.v20i3.31

Ryan, S. T., Zhang, J., Burner, D. N., Liss, M., Pittman, E., Muldong, M., et al. (2020). Neoadjuvant rituximab modulates the tumor immune environment in patients with high risk prostate cancer. *J. Transl. Med.* 18:214.

Sakimura, C., Tanaka, H., Okuno, T., Hiramatsu, S., Muguruma, K., Hirakawa, K., et al. (2017). B cells in tertiary lymphoid structures are associated with favorable prognosis in gastric cancer. *J. Surg. Res.* 215, 74–82. doi: 10.1016/j.jss.2017.03.033

Sarvaria, A., Madrigal, J. A., and Saudemont, A. (2017). B cell regulation in cancer and anti-tumor immunity. *Cell Mol. Immunol.* 14, 662–674. doi: 10.1038/cmi.2017.35

Sautes-Fridman, C., Petitprez, F., Calderaro, J., and Fridman, W. H. (2019). Tertiary lymphoid structures in the era of cancer immunotherapy. *Nat. Rev. Cancer* 19, 307–325. doi: 10.1038/s41568-019-0144-6

Saze, Z., Schuler, P. J., Hong, C. S., Cheng, D., Jackson, E. K., and Whiteside, T. L. (2013). Adenosine production by human B cells and B cell-mediated suppression of activated T cells. *Blood* 122, 9–18. doi: 10.1182/blood-2013-02-482406

Schlosser, H. A., Thelen, M., Lechner, A., Wennhold, K., Garcia-Marquez, M. A., Rothschild, S. I., et al. (2019). B cells in esophago-gastric adenocarcinoma are highly differentiated, organize in tertiary lymphoid structures and produce tumor-specific antibodies. *Oncoimmunology* 8:e1512458. doi: 10.1080/2162402x.2018.1512458

Schumacher, T. N., and Schreiber, R. D. (2015). Neoantigens in cancer immunotherapy. *Science* 348, 69–74.

Schwartz, M., Zhang, Y., and Rosenblatt, J. D. (2016). B cell regulation of the anti-tumor response and role in carcinogenesis. *J. Immunother. Cancer* 4:40.

Schweiger, T., Berghoff, A. S., Glogner, C., Glueck, O., Rajky, O., Traxler, D., et al. (2016). Tumor-infiltrating lymphocyte subsets and tertiary lymphoid structures in pulmonary metastases from colorectal cancer. *Clin. Exp. Metastasis* 33, 727–739. doi: 10.1007/s10585-016-9813-y

Sebina, I., and Pepper, M. (2018). Humoral immune responses to infection: common mechanisms and unique strategies to combat pathogen immune evasion tactics. *Curr. Opin. Immunol.* 51, 46–54. doi: 10.1016/j.coi.2018.02.001

Shalapour, S., Font-Burgada, J., Di Caro, G., Zhong, Z., Sanchez-Lopez, E., Dhar, D., et al. (2015). Immunosuppressive plasma cells impede T-cell-dependent immunogenic chemotherapy. *Nature* 521, 94–98. doi: 10.1038/nature14395

Shalapour, S., Lin, X. J., Bastian, I. N., Brain, J., Burt, A. D., Aksenov, A. A., et al. (2017). Inflammation-induced IgA+ cells dismantle anti-liver cancer immunity. *Nature* 551, 340–345. doi: 10.1038/nature24302

Shao, Y., Lo, C. M., Ling, C. C., Liu, X. B., Ng, K. T., Chu, A. C., et al. (2014). Regulatory B cells accelerate hepatocellular carcinoma progression via CD40/CD154 signaling pathway. *Cancer Lett.* 355, 264–272. doi: 10.1016/j.canlet.2014.09.026

Sharonov, G. V., Serebrovskaya, E. O., Yuzhakova, D. V., Britanova, O. V., and Chudakov, D. M. (2020). B cells, plasma cells and antibody repertoires in the tumour microenvironment. *Nat. Rev. Immunol.* 20, 294–307. doi: 10.1038/s41577-019-0257-x

Shen, M., Wang, J., Yu, W., Zhang, C., Liu, M., Wang, K., et al. (2018). A novel MDSC-induced PD-1(-)PD-L1(+) B-cell subset in breast tumor microenvironment possesses immuno-suppressive properties. *Oncoimmunology* 7:e1413520. doi: 10.1080/2162402x.2017.1413520

Shi, J. Y., Gao, Q., Wang, Z. C., Zhou, J., Wang, X. Y., Min, Z. H., et al. (2013). Margin-infiltrating CD20(+) B cells display an atypical memory phenotype and correlate with favorable prognosis in hepatocellular carcinoma. *Clin. Cancer Res.* 19, 5994–6005. doi: 10.1158/1078-0432.ccr-12-3497

Shimabukuro-Vornhagen, A., Schlosser, H. A., Gryschok, L., Malcher, J., Wennhold, K., Garcia-Marquez, M., et al. (2014). Characterization of tumor-associated B-cell subsets in patients with colorectal cancer. *Oncotarget* 5, 4651–4664.

Shin, D. H., Lin, H., Zheng, H., Kim, K. S., Kim, J. Y., Chun, Y. S., et al. (2014). HIF-1alpha-mediated upregulation of TASK-2 K(+) channels augments Ca(2)(+) signaling in mouse B cells under hypoxia. *J. Immunol.* 193, 4924–4933. doi: 10.4049/jimmunol.1301829

Sigvardsson, M. (2018). Molecular Regulation of Differentiation in Early B-Lymphocyte Development. *Int. J. Mol. Sci.* 19:1928. doi: 10.3390/ijms19071928

Silina, K., Soltermann, A., Attar, F. M., Casanova, R., Uckeley, Z. M., Thut, H., et al. (2018). Germinal Centers Determine the Prognostic Relevance of Tertiary Lymphoid Structures and Are Impaired by Corticosteroids in Lung Squamous Cell Carcinoma. *Cancer Res.* 78, 1308–1320. doi: 10.1158/0008-5472.can-17-1987

Sofopoulos, M., Fortis, S. P., Vaxevanis, C. K., Sotiriadou, N. N., Arnogiannaki, N., Ardavanis, A., et al. (2019). The prognostic significance of peritumoral tertiary lymphoid structures in breast cancer. *Cancer Immunol. Immunother.* 68, 1733–1745. doi: 10.1007/s00262-019-02407-8

Somasundaram, R., Zhang, G., Fukunaga-Kalabis, M., Perego, M., Krepler, C., Xu, X., et al. (2017). Tumor-associated B-cells induce tumor heterogeneity and therapy resistance. *Nat. Commun.* 8:607.

Spear, S., Candido, J. B., Mcdermott, J. R., Ghirelli, C., Maniati, E., Beers, S. A., et al. (2019). Discrepancies in the Tumor Microenvironment of Spontaneous and Orthotopic Murine Models of Pancreatic Cancer Uncover a New Immunostimulatory Phenotype for B Cells. *Front. Immunol.* 10:542. doi: 10.3389/fimmu.2019.00542

Tang, J., Ramis-Cabrer, D., Curull, V., Wang, X., Mateu-Jimenez, M., Pijuan, L., et al. (2020). B Cells and Tertiary Lymphoid Structures Influence Survival in Lung Cancer Patients with Resectable Tumors. *Cancers* 12:2644. doi: 10.3390/cancers12092644

Tao, H., Lu, L., Xia, Y., Dai, F., Wang, Y., Bao, Y., et al. (2015). Antitumor effector B cells directly kill tumor cells via the Fas/FasL pathway and are regulated by IL-10. *Eur. J. Immunol.* 45, 999–1009. doi: 10.1002/eji.201444625

Teillaud, J. L., and Dieu-Nosjean, M. C. (2017). Tertiary lymphoid structures: an anti-tumor school for adaptive immune cells and an antibody factory to fight cancer? *Front. Immunol.* 8:830. doi: 10.3389/fimmu.2017.00830

Tsujikawa, T., Crocenzi, T., Durham, J. N., Sugar, E. A., Wu, A. A., Onners, B., et al. (2020). Evaluation of Cyclophosphamide/GVAX Pancreas Followed by Listeria-Mesothelin (CRS-207) with or without Nivolumab in Patients with Pancreatic Cancer. *Clin. Cancer Res.* 26, 3578–3588. doi: 10.1158/1078-0432.ccr-19-3978

van de Pavert, S. A., Olivier, B. J., Goverse, G., Vondenhoff, M. F., Greuter, M., Beke, P., et al. (2009). Chemokine CXCL13 is essential for lymph node initiation and is induced by retinoic acid and neuronal stimulation. *Nat. Immunol.* 10, 1193–1199. doi: 10.1038/ni.1789

van de Veen, W., Stanic, B., Yaman, G., Wawrzyniak, M., Sollner, S., Akdis, D. G., et al. (2013). IgG4 production is confined to human IL-10-producing regulatory B cells that suppress antigen-specific immune responses. *J. Allergy Clin. Immunol.* 131, 1204–1212. doi: 10.1016/j.jaci.2013.01.014

van der Leun, A. M., Thommen, D. S., and Schumacher, T. N. (2020). CD8(+) T cell states in human cancer: insights from single-cell analysis. *Nat. Rev. Cancer* 20, 218–232. doi: 10.1038/s41568-019-0235-4

Vayrynen, J. P., Sajanti, S. A., Klintrup, K., Makela, J., Herzig, K. H., Karttunen, T. J., et al. (2014). Characteristics and significance of colorectal cancer associated lymphoid reaction. *Int. J. Cancer* 134, 2126–2135. doi: 10.1002/ijc.28533

Veiga-Fernandes, H., Coles, M. C., Foster, K. E., Patel, A., Williams, A., Natarajan, D., et al. (2007). Tyrosine kinase receptor RET is a key regulator of Peyer's patch organogenesis. *Nature* 446, 547–551. doi: 10.1038/nature05597

Vettermann, C., and Schlissel, M. S. (2010). Allelic exclusion of immunoglobulin genes: models and mechanisms. *Immunol. Rev.* 237, 22–42. doi: 10.1111/j.1600-065x.2010.00935.x

Vickovic, S., Eraslan, G., Salmen, F., Klughammer, J., Stenbeck, L., Schapiro, D., et al. (2019). High-definition spatial transcriptomics for in situ tissue profiling. *Nat. Methods* 16, 987–990. doi: 10.1038/s41592-019-0548-y

Vondenhoff, M. F., Greuter, M., Goverse, G., Elewaut, D., Dewint, P., Ware, C. F., et al. (2009). LTbetaR signaling induces cytokine expression and up-regulates lymphangiogenic factors in lymph node anlagen. *J. Immunol.* 182, 5439–5445. doi: 10.4049/jimmunol.0801165

Wang, K., Liu, J., and Li, J. (2018). IL-35-producing B cells in gastric cancer patients. *Medicine* 97:e0710. doi: 10.1097/md.0000000000010710

Wang, L., Fu, Y., and Chu, Y. (2020). Regulatory B Cells. *Adv. Exp. Med. Biol.* 1254, 87–103.

Wang, R. X., Yu, C. R., Dambuza, I. M., Mahdi, R. M., Dolinska, M. B., Sergeev, Y. V., et al. (2014). Interleukin-35 induces regulatory B cells that suppress autoimmune disease. *Nat. Med.* 20, 633–641. doi: 10.1038/nm.3554

Wang, W. W., Yuan, X. L., Chen, H., Xie, G. H., Ma, Y. H., Zheng, Y. X., et al. (2015). CD19+CD24hiCD38hiBregs involved in downregulate helper T cells and upregulate regulatory T cells in gastric cancer. *Oncotarget* 6, 33486–33499. doi: 10.18632/oncotarget.5588

Wang, Y., Schafer, C. C., Hough, K. P., Tousif, S., Duncan, S. R., Kearney, J. F., et al. (2018). Myeloid-Derived Suppressor Cells Impair B Cell Responses in Lung Cancer through IL-7 and STAT5. *J. Immunol.* 201, 278–295. doi: 10.4049/jimmunol.1701069

Wei, X., Jin, Y., Tian, Y., Zhang, H., Wu, J., Lu, W., et al. (2016). Regulatory B cells contribute to the impaired antitumor immunity in ovarian cancer patients. *Tumour. Biol.* 37, 6581–6588. doi: 10.1007/s13277-015-4538-0

Wejksza, K., Lee-Chang, C., Bodogai, M., Bonzo, J., Gonzalez, F. J., Lehrmann, E., et al. (2013). Cancer-produced metabolites of 5-lipoxygenase induce tumor-evoked regulatory B cells via peroxisome proliferator-activated receptor alpha. *J. Immunol.* 190, 2575–2584. doi: 10.4049/jimmunol.1201920

Welinder, C., Jirstrom, K., Lehn, S., Nodin, B., Marko-Varga, G., Blixt, O., et al. (2016). Intra-tumour IgA1 is common in cancer and is correlated with poor prognosis in bladder cancer. *Heliyon* 2:e00143. doi: 10.1016/j.heliyon.2016.e00143

Winter, S., Loddenkemper, C., Aebischer, A., Rabel, K., Hoffmann, K., Meyer, T. F., et al. (2010). The chemokine receptor CXCR5 is pivotal for ectopic mucosa-associated lymphoid tissue neogenesis in chronic *Helicobacter* pylori-induced inflammation. *J. Mol. Med.* 88, 1169–1180. doi: 10.1007/s00109-010-0658-6

Woo, J. R., Liss, M. A., Muldong, M. T., Palazzi, K., Strasner, A., Ammirante, M., et al. (2014). Tumor infiltrating B-cells are increased in prostate cancer tissue. *J. Transl. Med.* 12:30. doi: 10.1186/1479-5876-12-30

Wouters, M. C. A., and Nelson, B. H. (2018). Prognostic Significance of Tumor-Infiltrating B Cells and Plasma Cells in Human Cancer. *Clin. Cancer Res.* 24, 6125–6135. doi: 10.1158/1078-0432.ccr-18-1481

Wu, A. A., Bever, K. M., Ho, W. J., Fertig, E. J., Niu, N., Zheng, L., et al. (2020). A Phase II Study of Allogeneic GM-CSF-Transfected Pancreatic Tumor Vaccine (GVAX) with Ipilimumab as Maintenance Treatment for Metastatic Pancreatic Cancer. *Clin. Cancer Res.* 26, 5129–5139. doi: 10.1158/1078-0432.ccr-20-1025

Wu, H., Su, Z., and Barnie, P. A. (2020a). The role of B regulatory (B10) cells in inflammatory disorders and their potential as therapeutic targets. *Int. Immunopharmacol.* 78:106111. doi: 10.1016/j.intimp.2019.106111

Wu, H., Xia, L., Jia, D., Zou, H., Jin, G., Qian, W., et al. (2020b). PD-L1(+) regulatory B cells act as a T cell suppressor in a PD-L1-dependent manner in melanoma patients with bone metastasis. *Mol. Immunol.* 119, 83–91. doi: 10.1016/j.molimm.2020.01.008

Xiao, X., Lao, X. M., Chen, M. M., Liu, R. X., Wei, Y., Ouyang, F. Z., et al. (2016). PD-1hi Identifies a Novel Regulatory B-cell Population in Human Hepatoma That Promotes Disease Progression. *Cancer Discov.* 6, 546–559. doi: 10.1158/2159-8290.cd-15-1408

Yang, C., Lee, H., Pal, S., Jove, V., Deng, J., Zhang, W., et al. (2013). B cells promote tumor progression via STAT3 regulated-angiogenesis. *PLoS One* 8:e64159. doi: 10.1371/journal.pone.0064159

Yang, M., Lu, J., Zhang, G., Wang, Y., He, M., Xu, Q., et al. (2021). CXCL13 shapes immunoactive tumor microenvironment and enhances the efficacy of PD-1 checkpoint blockade in high-grade serous ovarian cancer. *J. Immunother. Cancer* 9:e001136 doi: 10.1136/jitc-2020-001136

Ye, L., Zhang, Q., Cheng, Y., Chen, X., Wang, G., Shi, M., et al. (2018). Tumor-derived exosomal HMGB1 fosters hepatocellular carcinoma immune evasion by promoting TIM-1(+) regulatory B cell expansion. *J. Immunother. Cancer* 6:145.

Yoshizaki, A., Miyagaki, T., Dilillo, D. J., Matsushita, T., Horikawa, M., Kountikov, E. I., et al. (2012). Regulatory B cells control T-cell autoimmunity through IL-21-dependent cognate interactions. *Nature* 491, 264–268. doi: 10.1038/nature11501

Zhang, C., Xin, H., Zhang, W., Yazaki, P. J., Zhang, Z., Le, K., et al. (2016). CD5 Binds to Interleukin-6 and Induces a Feed-Forward Loop with the Transcription Factor STAT3 in B Cells to Promote Cancer. *Immunity* 44, 913–923. doi: 10.1016/j.immuni.2016.04.003

Zhang, K. (2003). Accessibility control and machinery of immunoglobulin class switch recombination. *J. Leukoc Biol.* 73, 323–332. doi: 10.1189/jlb.0702339

Zhang, Y., and Zhang, Z. (2020). The history and advances in cancer immunotherapy: understanding the characteristics of tumor-infiltrating immune cells and their therapeutic implications. *Cell Mol. Immunol.* 17, 807–821. doi: 10.1038/s41423-020-0488-6

Zhao, D. M., Thornton, A. M., Dipaolo, R. J., and Shevach, E. M. (2006). Activated CD4+CD25+ T cells selectively kill B lymphocytes. *Blood* 107, 3925–3932. doi: 10.1182/blood-2005-11-4502

Zhao, Y., Shen, M., Feng, Y., He, R., Xu, X., Xie, Y., et al. (2018). Regulatory B cells induced by pancreatic cancer cell-derived interleukin-18 promote immune tolerance via the PD-1/PD-L1 pathway. *Oncotarget* 9, 14803–14814. doi: 10.18632/oncotarget.22976

Zheng, L., Ding, D., Edil, B. H., Judkins, C., Durham, J. N., Thomas, D. L. II, et al. (2021). Vaccine-Induced Intratumoral Lymphoid Aggregates Correlate with Survival Following Treatment with a Neoadjuvant and Adjuvant Vaccine in Patients with Resectable Pancreatic Adenocarcinoma. *Clin. Cancer Res.* 27, 1278–1286. doi: 10.1158/1078-0432.ccr-20-2974

Zhou, J., Min, Z., Zhang, D., Wang, W., Marincola, F., and Wang, X. (2014). Enhanced frequency and potential mechanism of B regulatory cells in patients with lung cancer. *J. Transl. Med.* 12:304.

Zhou, X., Su, Y. X., Lao, X. M., Liang, Y. J., and Liao, G. Q. (2016). CD19(+)IL-10(+) regulatory B cells affect survival of tongue squamous cell carcinoma patients and induce resting CD4(+) T cells to CD4(+)Foxp3(+) regulatory T cells. *Oral. Oncol.* 53, 27–35. doi: 10.1016/j.oraloncology.2015.11.003

Zhu, W., Germain, C., Liu, Z., Sebastian, Y., Devi, P., Knockaert, S., et al. (2015). A high density of tertiary lymphoid structure B cells in lung tumors is associated with increased CD4(+) T cell receptor repertoire clonality. *Oncoimmunology* 4:e1051922. doi: 10.1080/2162402x.2015.1051922

Conflict of Interest: The authors declare that the research was conducted in the absence of any commercial or financial relationships that could be construed as a potential conflict of interest.

frontiers in Cell and Developmental Biology

MINI REVIEW
published: 30 June 2021
doi: 10.3389/fcell.2021.692982

Boosting Antitumor Response by Costimulatory Strategies Driven to 4-1BB and OX40 T-cell Receptors

*Daniele E. Mascarelli[1,2], Rhubia S. M. Rosa[1,2], Jessica M. Toscaro[1,3], Isadora F. Semionatto[1,2], Luciana P. Ruas[1], Carolinne T. Fogagnolo[1,4], Gabriel C. Lima[1,5] and Marcio C. Bajgelman[1,2,3]**

[1] Brazilian Biosciences National Laboratory (LNBio), Brazilian Center for Research in Energy and Materials (CNPEM), Campinas, Brazil, [2] Faculty of Pharmaceutical Sciences, University of Campinas, Campinas, Brazil, [3] Medical School, University of Campinas (UNICAMP), Campinas, Brazil, [4] Medical School of Ribeirão Preto (FMRP), University of São Paulo, Ribeirão Preto, Brazil, [5] Pro Rectory of Graduation, University of São Paulo, São Paulo, Brazil

Immunotherapy explores several strategies to enhance the host immune system's ability to detect and eliminate cancer cells. The use of antibodies that block immunological checkpoints, such as anti–programed death 1/programed death 1 ligand and cytotoxic T-lymphocyte–associated protein 4, is widely recognized to generate a long-lasting antitumor immune response in several types of cancer. Evidence indicates that the elimination of tumors by T cells is the key for tumor control. It is well known that costimulatory and coinhibitory pathways are critical regulators in the activation of T cells. Besides blocking checkpoints inhibitors, the agonistic signaling on costimulatory molecules also plays an important role in T-cell activation and antitumor response. Therefore, molecules driven to costimulatory pathways constitute promising targets in cancer therapy. The costimulation of tumor necrosis factor superfamily receptors on lymphocytes surface may transduce signals that control the survival, proliferation, differentiation, and effector functions of these immune cells. Among the members of the tumor necrosis factor receptor superfamily, there are 4-1BB and OX40. Several clinical studies have been carried out targeting these molecules, with agonist monoclonal antibodies, and preclinical studies exploring their ligands and other experimental approaches. In this review, we discuss functional aspects of 4-1BB and OX40 costimulation, as well as the progress of its application in immunotherapies.

Keywords: immunotherapy, T cell costimulation, TNFR, 4-1BB, OX40, cancer therapy, aptamers, agonistic antibody

OPEN ACCESS

Edited by:
Rodrigo Nalio Ramos, INSERM U1138 Centre de Recherche des Cordeliers (CRC), France

Reviewed by:
Maximilien Grandclaudon, Dana–Farber Cancer Institute, United States
Sarantis Korniotis, INSERM U976 Immunologie, Dermatologie, Oncologie, France

***Correspondence:**
Marcio C. Bajgelman
marcio.bajgelman@lnbio.cnpem.br

Specialty section:
This article was submitted to Molecular Medicine, a section of the journal Frontiers in Cell and Developmental Biology

Received: *09 April 2021*
Accepted: *27 May 2021*
Published: *30 June 2021*

Citation:
Mascarelli DE, Rosa RSM, Toscaro JM, Semionatto IF, Ruas LP, Fogagnolo CT, Lima GC and Bajgelman MC (2021) Boosting Antitumor Response by Costimulatory Strategies Driven to 4-1BB and OX40 T-cell Receptors. Front. Cell Dev. Biol. 9:692982. doi: 10.3389/fcell.2021.692982

INTRODUCTION

Immunotherapy explores the host immune system to enhance antitumor response. The inhibition of immunological checkpoints, on T cells, such as anti–programed death 1 (PD-1)/programed death 1 ligand (PD-L1) and cytotoxic T-lymphocyte–associated protein 4 (CTLA-4), has been shown to generate long-lasting antitumor immune responses in cancer therapy. However, this approach is effective in only 30% of patients because of mechanisms of tumor resistance (Chen and Mellman, 2013; Swart et al., 2016). There are several signaling mechanisms that may drive T-cell phenotype switching the balance between immunotolerance and surveillance.

The tumor necrosis factor receptor superfamily (TNFRSF) encodes T-cell costimulatory receptors that may regulate survival, proliferation, differentiation, and effector functions of immune cells, being a potential target for immunotherapy (Calderhead et al., 1993; Godfrey et al., 1994; Wilcox et al., 2002; Zhang et al., 2010; Melero et al., 2013).

Early experiments with activated T cells have described the cell surface 4-1BB receptor (Kwon and Weissman, 1989; Schwarz et al., 1993). The 4-1BB receptor, also known as TNFRSF9 or CD137, is a 24-kDa protein located on chromosome 1 p36 (Pollok et al., 1993; Hurtado et al., 1997), which encodes 255 amino acids harboring 64% homology to the murine sequence (Alderson et al., 1994; Zhou et al., 1995; Chin et al., 2018). The 4-1BB receptor is expressed on activated T and B cells, monocytes, macrophages, dendritic cells (DCs), regulatory T cells (Tregs), and natural killer (NK) cells (Pollok et al., 1993; Langstein et al., 1998; Melero et al., 1998; Laderach et al., 2002; Kim et al., 2008; Schoenbrunn et al., 2012). The 4-1BB receptor harbors two cytoplasmic domains that can bind to the TNFR-associated factor (TRAF) in T cells. The mammal TRAF may exhibit conserved C-terminal domains (Bouwmeester et al., 2004; Xu et al., 2004), and CD137 can interact with TRAF1, TRAF2, and TRAF3 (Jang et al., 1998). The interaction between CD137, TRAF1, and TRAF2 activates different signaling cascades such as nuclear factor κB (NF-κB), MAPK (protein kinase activated by mitogen) (Shuford et al., 1997; Arch and Thompson, 1998; Kim et al., 1998), ERK (kinase regulated by extracellular signal), and JNK (Jun N-terminal kinase) (Rothe et al., 1995; Froelich et al., 1996; Arch and Thompson, 1998; Jang et al., 1998; Saoulli et al., 1998; Cannons et al., 2001; Song et al., 2004; Sabbagh et al., 2008). The activation of the NF-κB pathway upregulates survival genes such as Bcl-XL and Bfl-1, downregulates proapoptotic molecules such as BIM, and transmits signals that stimulate cell division (Hockenbery et al., 1990; Lee et al., 2002; Bukczynski et al., 2003). Moreover, the 4-1BB/4-1BB ligand (4-1BBL) signaling triggers biochemical signals that increase T_H1 cytokines, such as interleukin 6 (IL-6), IL-8, TNF, IL-12, and interferon γ (IFN-γ); suppress T_H2 cytokines; potentiate activation, survival, proliferation, and cytotoxicity of T cells; increase IL-2 production; and provoke the maturation of DCs (Shuford et al., 1997; Kim et al., 1998; Laderach et al., 2002; Lee et al., 2002; Wen et al., 2002; Lippert et al., 2008; Fröhlich et al., 2020).

The expression of 4-1BB may be experimentally induced in human and murine T cells, using different mitogenic agents such as PMA (phorbol 12-myristate 13-acetate), phytohemagglutinin, anti-CD3, lipopolysaccharide, and IL-1β (Pollok et al., 1995; Zhou et al., 1995; Tan et al., 2000). The receptor interacts with 4-1BBL, on the surface of activated antigen-presenting cells (APCs), B cells, macrophages, and other myeloid-derived cells (Goodwin et al., 1993; Pollok et al., 1994; DeBenedette et al., 1997). The expression of 4-1BBL also was observed in cancer cells (Salih et al., 2000). The 4-1BB costimulation of T cells does not require additional CD28 signaling when a strong engagement of T-cell receptors (TCRs) occurs, producing high levels of IL-2 and enhancing T_H1 response and cytotoxic T-cell activity (Shuford et al., 1997; Saoulli et al., 1998; Takahashi et al., 1999; Cannons et al., 2000; Dawicki et al., 2004).

Another T-cell costimulatory receptor that belongs to the TNFRSF family is the OX40 receptor, also known as CD134, TNFRSF4, and ACT35. The OX40 receptor and its ligand (OX40L, TNFSF4, CD252) were first described in mice and harbor 63% homology to that of human (Paterson et al., 1987; Mallett et al., 1990; Godfrey et al., 1994). The human OX40 gene is located in on chromosome 1p36, encodes 277 amino acids, a 29-kDa protein (Latza et al., 1994).

The OX40 is expressed in activated $CD4^+$ and $CD8^+$ T cells, Tregs, T follicular helper cells, NK cells, and neutrophils (Mallett et al., 1990; Godfrey et al., 1994; Melero et al., 1998; Bansal-Pakala et al., 2004; Baumann et al., 2004; Vu et al., 2007; Zaini et al., 2007; Tahiliani et al., 2017). The antigenic stimulation of the TCR by major histocompatibility complex molecules upregulates OX40 expression on the surface of T cells, which may be potentiated by a CD28–CD80 signaling (Walker et al., 1999; Rogers et al., 2001). The OX40 peak expression is seen from 24 to 72 h after the TCR activation (Rogers et al., 2001; Song et al., 2008; Sadler et al., 2014). Once expressed, OX40 can bind to OX40L, which is mainly expressed on APCs (Linton et al., 2003; Jenkins et al., 2007; Karulf et al., 2010). The OX40/OX40L interaction triggers a signaling cascade, similar to 4-1BB/4-1BBL, inducing transcriptional changes to modulate the immune response, such as T-cell proliferation and survival. The immunomodulatory functions associated with OX40, such as the PKB pathway, promote the inhibition of cellular apoptosis, as well as increase the signaling by TCR antigenic stimuli (Song et al., 2004). The OX40 stimulation activates NF-κB pathway, which indirectly increases expression of apoptosis-suppressing proteins prolonging cell survival, and the activated T-cell nuclear factor (NFAT) pathway that leads to an increase in the synthesis of cytokines such as IL-2, IL-4, IL-5, and IFN-γ (So and Croft, 2007). Although, some data suggest the importance of OX40/OX40L signaling for primary and memory T_H2 response (Salek-Ardakani et al., 2003; Jenkins et al., 2007; Pattarini et al., 2017), there are also evidences that OX40 costimulation plays an important role in the T_H1 response (Weinberg et al., 1999; De Smedt et al., 2002; Gajdasik et al., 2020). Therefore, it was observed that OX40 costimulation may enhance both a T_H1 and a T_H2 response without supporting the role for switching polarization of $CD4^+$ T cells (De Smedt et al., 2002).

In this review, functional aspects of 4-1BB and OX4 will be discussed, as well as the progress of its application in immunotherapies.

COSTIMULATION OF 4-1BB AND OX40 RECEPTORS ENHANCES T-CELL ACTIVITY AND POTENTIATES ANTITUMOR RESPONSE

Both 4-1BB and OX40 costimulatory signaling on T cells are reported to boost antitumor immune responses (**Figure 1**).

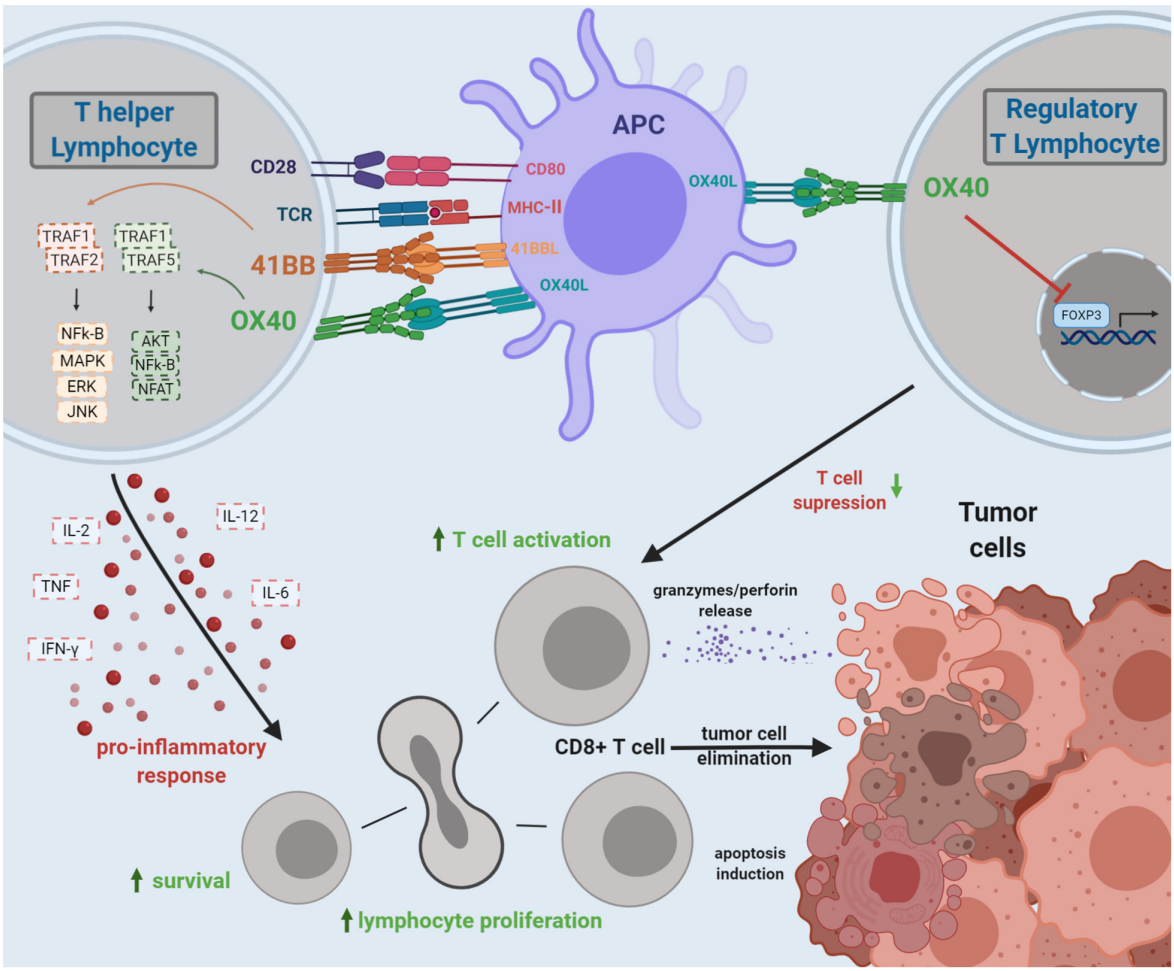

FIGURE 1 | Costimulation by 4-1BB and OX40 TCRs and the overall effects on antitumor T-cell immunity. 4-1BB and OX40 bind to their ligands, triggering a signaling cascade leading to T-cell activation and expansion of cytotoxic $CD8^+$ T lymphocytes. Costimulation of OX40 may also inhibit the FOXP3 transcription factor on $CD4^+$ T cells, impairing the Treg function, diminishing tumor immunosuppression, and boosting the antitumor immune response. The 4-1BB/4-1BBL signaling triggers biochemical signals that increase T_H1 cytokines and suppress T_H2 cytokines; potentiate activation, survival, proliferation, and cytotoxicity of T cells; and provoke the maturation of dendritic cells. The OX40/OX40L interaction triggers a signaling cascade, similar to 4-1BB/4-1BBL, inducing transcriptional changes to modulate the immune response. The OX40 costimulation may promote T-cell proliferation and survival. The agonistic signaling transduced by OX40 on Treg may impair FOXP3 expression, enhancing antitumor response.

The costimulatory 4-1BB signaling induces clonal expansion, proliferation, cytokine secretion, and long-term T-cell survival (Wen et al., 2002). The 4-1BB costimulation improves the mitochondrial function of T cells, leading to greater longevity and memory capacity of these cells (Menk et al., 2018). Although 4-1BB costimulation transduces a robust costimulatory signal, mainly acting on $CD8^+$ T cells (Habib-Agahi et al., 2007), mice that constitutively express 4-1BB on $CD4^+$ T cells exhibited heightened and sustained proliferative activity and enhancement of T-cell priming, driving T_H1 immune responses, increasing the number of tumor-infiltrating lymphocytes (TILs) in tumor masses, augmenting IFN-γ production by T-cell population, mediating tumor suppression, and prolonging mice survival (Kim et al., 2003). This persistence of T cells is crucial for the success of chimeric antigenic receptor (CAR) T-cell therapy. The CAR has an extracellular domain that recognizes a target antigen, transducing a signaling to an intracellular domain that boosts T-cell activation. This technology is being used mainly in hematological cancers, with promising results (Kalos et al., 2011; Porter et al., 2011). CAR T cells may employ a cytoplasmic domain of 4-1BB molecule to enhance the antitumor efficacy, the so-called third generation of CART cells. The 4-1BB intracellular signaling domain provides a second costimulatory signal that makes the CAR T-cells more effective and long lasting (van der Stegen et al., 2015).

Similar to 4-1BB/4-1BBL, the OX40/OX40L pathway also triggers strong costimulatory signaling on $CD4^+$ and $CD8^+$ T cells, although this effect is more prominent in $CD4^+$ T cells (Xiao et al., 2004). The OX40 costimulatory signaling promotes the activation, expansion, proliferation, differentiation,

proinflammatory cytokine production, supporting survival of T lymphocytes, and tumor regression (Rogers et al., 2001; Linch et al., 2016; Peng et al., 2019; Kuang et al., 2020). It was demonstrated that high expression of OX40 in the tumor-infiltrating immune cells in small cell lung cancer induced increased levels of IFN-γ expression and favorable prognosis in patients (Massarelli et al., 2019). The OX40 costimulatory signaling on exhausted $CD8^+$ T cells could rescue their proliferative potential and cytokine production (Buchan et al., 2015).

In addition, agonistic OX40 signaling in Tregs may impair the expression of FOXP3, which is a master key to regulate the Treg-immunosuppressive phenotype (So and Croft, 2007; Vu et al., 2007; Piconese et al., 2008). As Tregs may antagonize antitumor response inhibiting T-cell proliferation (Liu et al., 2009; Xu et al., 2010; Chang et al., 2012), the costimulation of OX40 may inhibit the immunosuppressive activity of Tregs and also the conversion of effector T (Teff) $CD4^+$ T cells into a regulatory T-cell phenotype (So and Croft, 2007; Piconese et al., 2008; Kitamura et al., 2009). The role of agonistic 4-1BB signaling on Tregs is controversial. Although most studies demonstrated 4-1BB agonistic signaling enhanced the immunosurveillance activity, there are other reports that describes immunosuppressive activity, as expanding Tregs (Irie et al., 2007; Zhang et al., 2007; Lubrano di Ricco et al., 2020).

ENHANCING ANTITUMOR IMMUNITY BY AGONISTIC ANTIBODIES DRIVEN TO 4-1BB AND OX40 T-CELL COSTIMULATION

The agonistic 4-1BB or OX40 costimulation by monoclonal antibodies (mAbs) is widely explored in cancer immunotherapy (Wilcox et al., 2002; Vinay and Kwon, 2014). There are several clinical trials exploring the therapeutic benefit of mAbs (**Table 1**). The TNFRSF-targeted costimulatory strategy may be used in combination with chemotherapy and radiotherapy, improving antitumor response (Shi and Siemann, 2006; Ju et al., 2008). 4-1BB agonist antibodies promote increased T-cell proliferation and survival. These antibodies may also activate NK cells (Klatzmann et al., 1984; Lin et al., 2008; Rajasekaran et al., 2015; Makkouk et al., 2016). The binding of an agonistic mAb induces 4-1BB cell surface receptor internalization, which may trigger signaling from endosomatic compartments, as the polyubiquitination of K63 to recruit TRAF2 and starting the T-cell activation cascade (Martinez-Forero et al., 2013). The agonistic 4-1BB antibody may act on depletion of Treg cells, and this stimulus seems to be associated with its FCγR engagement and antibody isotype. It was observed the immunoglobulin G1 (IgG1) mAb isotype induced an enhanced CD8 T-cell costimulation in an established solid tumor microenvironment. The IgG2a isotype has shown intratumoral Treg depletion and optimal antitumor activity in preclinical model (Buchan et al., 2018). The main 4-1BB agonist antibodies used in the clinic are utomilumab (PF-05082566) and urelumab (BMS-663513). Both mAbs are already being used in cancer clinical trials. Whereas the IgG2 utomilumab is safe with relatively low efficacy, the IgG4 urelumab has a great antitumor efficacy, but causes liver damage (Segal et al., 2014; Gopal et al., 2017; Tolcher et al., 2017). In addition, urelumab can induce a cluster of 4-1BBL–dependent receptors, unlike utomilumab (Chin et al., 2018). The preliminary results of urelumab trials in 2008 demonstrated efficacy against cancers in advanced stages. However, the treatment with mAb induced liver damage, interrupting the clinical trials. Toxicity is suggested as a consequence of FcγRIIB-mediated $CD8^+$ T-cell activation in the liver, once FcγRIIB is expressed on liver sinusoidal endothelial cells and Kupffer cells (Qi et al., 2019). Urelumab has been evaluated as monotherapy or in combination with other drugs, such as rituximab, cetuximab, elotuzumab, and nivolumab, at lower doses, with no damage to the liver. When associated with rituximab, in the treatment of patients with relapsing or refractory non-Hodgkin lymphomas, the urelumab has demonstrated safety, tolerability, and improvement of the host immune response. Utomilumab promoted a long-lasting

TABLE 1 | Clinical protocols in progress using costimulatory anti–4-1BB and anti-OX40 monoclonal antibodies.

mAbs	Target	Phase	Tumor	Combination	Protocol
Utomilumab	41BB	II	HER2 + Breast cancer	Avehnnab (anti-PD-Ll)	NCT03414658
Utomilumab	41BB	I	HER2 + Breast cancer	Trasluzumab (anti-HER2)	NCT03364348
Urelumab	41BB	I	Glioblastoma	Nivolumab (anti-PDl)	NCT02658981
AGEN2373	41BB	I	Advanced Solid Tumor	–	NCT04121676
MEDI0562	OX40	I	Head/Neck squamous cell carcinoma Melanoma	–	NCT03336606
MEDI6469	OX40	Ib	Head/Neck squamous cell carcinoma	Surgical resection	NCT02274155
MEDI6469	OX40	I/Ib	Metastatic colorectal cancer	Radiofrequency ablation	NCT02559024
INBRX-106	OX40	I	Locally Advanced/Metastatic tumor	Pembrolizumab	NCT04198766
PF04518600	OX40	I/II	Acute myeloid leukemia	Avelumab (anti-PD-Ll) Azacitidine	NCT03390296
PF04518600	OX40	II	Metastatic kidney cancer	Axitinib (TK inhibitor)	NCT03092856
PF04518600	OX40	II	Triple negative breast cancer	Avelumab (anti-PD-Ll)	NCT03971409
PF-04518600	OX40	I/II	Advanced malignancies	Avelumab (antiPD-Ll) Radiation	NCT03217747
INCAGN01949	OX40	I/II	Pancreatic cancer	VLP-encapsulated TLR9	NCT04387071
SL-279252	OX40	I	Advanced solid tumor/Lymphoma	Fc anti-PDl	NCT03894618

response and reduced toxicity in patients with lymphomas. This mAb is being extensively tested in combination with other immunotherapies for different tumors, such as non-small cell lung cancer, kidney, head, and neck cancer (Tolcher et al., 2017; Gopal et al., 2020).

Innovative strategies based on bispecific antibodies also may be used to overcome systemic toxicity of agonistic 4-1BB, targeting the costimulatory activity to tumor site. A bispecific 4-1BB/HER-2 antibody was engineered to bind HER-2–positive tumor cells and to costimulate T cells. This bispecific antibody was shown to inhibit tumor growth in humanized mice model (Hinner et al., 2019).

In addition to the costimulatory 4-1BB mAbs, several studies have also demonstrated the antitumor effect of OX40 agonist antibodies. Mice treated with OX40 mAbs accumulated $CD4^+$ T cells and augmented $CD4^+$ T-cell survival and developing memory T cells (Cannons et al., 2001; Tolcher et al., 2017). The OX40 agonistic antibody may inhibit immune tolerance (Gramaglia et al., 2000; Maxwell et al., 2000).

The use of OX40 agonistic antibody in preclinical models has shown tumor regression in sarcomas, melanoma, colon carcinoma, and glioma (Kjaergaard et al., 2000; Weinberg et al., 2000; Andarini et al., 2004). In several preclinical and clinical models, OX40 agonist antibodies induce tumor regression due to their ability to prevent the suppression of antitumor immune responses mediated by Tregs. The OX40 costimulation may inhibit Treg activity in three different ways: (i) inhibiting the activity of natural Treg or even the conversion of T cells to Treg phenotype, due to impairing of FOXP3 expression (So and Croft, 2007; Vu et al., 2007; Song et al., 2008); (ii) reducing the suppressive activity by increasing the production of IL-2 and other cytokines (Valzasina et al., 2005); and (iii) depleting intratumoral Treg cells in an FcγR-dependent manner (Bulliard et al., 2014).

A phase I clinical trial in patients, with incurable metastatic carcinoma, lymphoma, or sarcoma (NCT01644968), using 9B12, a murine agonistic anti-human OX40 mAb, demonstrated that OX40 mAb treatment induced proliferation of $CD4^+$ and $CD8^+$ T cells and NK cells, enhanced production of IFN-γ by $CD8^+$ T cells, boosted T- and B-cell antitumor reactivity, and increased memory T cells (Curti et al., 2013). The MOXR 0916, also known as pogalizumab, is a humanized agonistic IgG antibody specific for OX40 that has immunostimulatory and antineoplastic activities. Pogalizumab binds and selectively activates OX40. The activation of OX40 promotes the proliferation of Teff lymphocytes and inhibits the activity of Treg cells in the presence of tumor antigens (Infante et al., 2016).

The combination of agonistic OX40 mAb to the PDL1 inhibitor atezolizumab is being tested in patients who have advanced solid neoplasms (NCT02410512). Recently, Kuang et al. (2020) reported the development of a new anti-OX40 antibody, the IBI101. This mAb promotes both FcγR-dependent and independent agonistic activities. The combination of IBI101 and anti–PD-L1 has shown a better inhibition of tumor growth in mice model, when compared to the combination of pogalizumab and anti–PD-L1 (Kuang et al., 2020).

There are several clinical trials exploring the application of costimulatory anti-OX40 mAbs as adjuvants in other therapies, as anti-OX40 combined to chemotherapy and radiotherapy (NCT01303705), anti-OX40 combined to other immunotherapy and chemotherapy (NCT03390296), and anti-OX40 combined to radiotherapy (NCT01862900, NCT02559024), among others.

AGONISTIC SIGNALING STRATEGIES MEDIATED BY THE TNFSF LIGANDS 4-1BBL AND OX40L POTENTIATE T CELL–MEDIATED ANTITUMOR RESPONSE

As reported above, agonistic TNFRSF-driven antibodies may exhibit toxicity associated with the systemic use, as the expression of TNFRs is ubiquitous, and, consequently, the action of these antibodies is not specific to tumor microenvironment (Ascierto et al., 2010). Therefore, a challenge faced by researchers is to induce a tumor-specific effect, which may reduce toxicity. Back in 2009, the group of Shirwan has developed a murine recombinant 4-1BBL molecule fused to streptavidin (SA–4-1BBL) that exhibited less toxicity when compared to agonistic antibody, lacking FcγR activation (Schabowsky et al., 2009). SA–4-1BBL forms tetramers and oligomers in soluble form, inducing a powerful T-cell costimulatory activity. Further studies have shown this molecule to be safe and effective in murine model of cervical cancer (Sharma et al., 2010). SA–4-1BBL could induce an efficient $CD4^+$ T-cell activation while blocking the development of $CD4^+$ Tregs, increasing the Teff-to-Treg ratio (Curti et al., 2013). Prophylactic administration of SA–4-1BBL to tumor-challenged mice was shown to prevent tumor growth, and this was dependent on $CD4^+$ T cell, NK, and IFN-γ production (Barsoumian et al., 2016).

Murine studies with 4-1BBL have shown that NK cells are activated and may respond to the antitumor activity due to 4-1BBL administration (Houot et al., 2009). Dowell et al. have demonstrated that stimulation of human PBMC, both from healthy donors and ovarian carcinoma patients with soluble 4-1BBL and IL-2, promoted expansion of $CD56^+$ NK cells (Dowell et al., 2012). Cancer cells transduced with 4-1BBL promote expansion of cytotoxic T cells (Sharma et al., 2010; Barsoumian et al., 2016), as well as NK cells (Gong et al., 2010). It was also observed that stimulation of human NK cells with recombinant 4-1BBL (rh4-1BB) in combination to anti–HER-2 therapy (trastuzumab) enhanced antitumor cytotoxicity in gastric cancer cells (Misumi et al., 2018).

The 4-1BBL has also been used in cell-based strategies to stimulate TILs. Gene-pulsed DCs with 4-1BBL enhanced IFN-γ production and T-cell activation (Youlin et al., 2013). A lipid-based nanoparticle harboring 4-1BBL is being used for T-cell costimulation, in clinical trials for cancer therapy (NCT03323398, NCT03739931).

As seen for 4-1BBL, the OX40L-expressing cells also stimulate antitumor response. Intratumoral administration of OX40L-expressing DCs promoted the generation of

tumor-specific $CD4^+$ and NK T cells, contributing to impaired tumor growth (Zaini et al., 2007). Modification of tumor cells with an adenovirus encoding OX40L promoted an efficient T_H1 immune response associated with cytotoxic T lymphocytes (Andarini et al., 2004).

As observed for combinations of costimulatory mAbs, the OX40L and 4-1BBL dual costimulation has been shown to be effective in reducing tumor growth and enhances mainly the $CD8^+$ T-cell response (Weinberg et al., 2000; Cuadros et al., 2005; Lee et al., 2006; Gray et al., 2008; Redmond et al., 2009; Manrique-Rincón et al., 2017). We and others have shown that the synergy between OX40/OX40L and 4-1BB/4-1BBL also contributes to enhance antitumor immune response (Lee et al., 2004, 2006; Munks et al., 2004; Manrique-Rincón et al., 2017; Fu et al., 2020). Indeed, our group has previously developed tumor-derived vaccines using B16 melanoma cells line, transduced with 4-1BBL and/or OX40L. We have shown that combination of these vaccines increased antitumor T cell–mediated cytotoxicity, reduction of Tregs, and contributing to tumor rejection *in vivo*, besides generating a protective effect on rechallenged animals (Manrique-Rincón et al., 2017). Moreover, extracellular vesicles (EVs) secreted by 4-1BBL and OX40L B16 vaccines were shown to induce T-cell proliferation and inhibit the generation of inducible Treg *in vitro* (Semionatto et al., 2020). These findings highlight the exploration of tumor-derived EVs as a potential tool for immunotherapy (Zaini et al., 2007).

OLIGONUCLEOTIDE-DERIVED APTAMERS MAY BE ENGINEERED AS COSTIMULATORY MOLECULES TO ENHANCE ANTITUMOR IMMUNITY

Aptamers are small molecules of single-stranded RNA or DNA oligonucleotides that may exhibit high affinity and selectivity for targets (Ellington and Szostak, 1990; Tuerk and Gold, 1990). These molecules exhibit similar properties to antibodies and may have some advantages: (i) aptamers are chemically synthesized and (ii) exhibit high tissue permeability and cell internalization due to its reduced size; (iii) aptamers usually exhibit low toxicity and immunogenicity, and (iv) aptamers may be inactivated by an antidote (Ellington and Szostak, 1990; Bompiani et al., 2012; Cheng et al., 2013; Bouvier-Müller and Ducongé, 2018).

Several aptamer-based therapeutic application has been explored for cancer (Morita et al., 2018; Maimaitiyiming et al., 2019).

Preclinical studies have demonstrated an equivalent or even superior functionality of these oligonucleotides compared to mAb molecules, as well as a decrease of the commonly observed side effects of mAbs (Miller and Chapman, 2001; Dollins et al., 2008; McNamara et al., 2008; Pastor et al., 2011; Pratico et al., 2013; Schrand et al., 2014, 2015; Rajagopalan et al., 2017). Aptamers may be employed as antagonist, agonist, and delivery tools (Pastor et al., 2018). The first aptamer driven to tumor immunomodulation was an antagonist CTLA-4 aptamer, and then, a number of new aptamers with immunomodulatory activity have been proposed (Santulli-Marotto et al., 2003).

As T-cell surface receptors such as TNFRSF are activated because of cross-link, multivalent aptamer models have been explored to lead T-cell activation and costimulation (Dollins et al., 2008; McNamara et al., 2008; Pratico et al., 2013). The possibility of using synthetic linkers of different size and composition was shown. This multimerization strategy allowed to generate functional aptamer molecules that could costimulate 4-1BB and OX40 receptors in T cells that would address improvement of the antitumor immune response (Dollins et al., 2008; McNamara et al., 2008). These studies have shown that treatment with aptamers induces a costimulatory effect on tumor environment comparable to the treatment with the corresponding mAb (Dollins et al., 2008; McNamara et al., 2008; Pratico et al., 2013).

Considering the side effects of systemic administration of mAb 4-1BB (Niu et al., 2007) due to plasticity of engineering, aptamers have been investigated to overcome toxicity, opening a new field of research based on bispecific aptamers. The aim of these approaches is to decrease the off-target effect by driving the costimulatory effect specifically on target cells (Pastor et al., 2011; Schrand et al., 2014, 2015). A first study involving a proof of concept of these aptamers developed a bifunctional 4-1BB–prostate-specific membrane antigen (PSMA) conjugate. The PSMA is a membrane antigen highly expressed in some prostate cells. In this way, the 4-1BB portion had a T-cell costimulatory activity, whereas the PSMA portion could drive the molecule to PSMA-expressing tumor cells. The study showed that systemic administrations of bispecific aptamer were able to inhibit tumor growth with the administration of a 10-fold lower dose without occurrence of side effects (Pastor et al., 2011).

Another technological approach that has been pursued is the generation of chimeric aptamer to vehiculate siRNA to target cells. Aptamers may bind to cell surface receptors to deliver siRNA to the target cell. This approach is target specific and may reduce possible off-target effects, improving the therapeutic index of the use of siRNA as drug treatment (Berezhnoy et al., 2012). A functional study has shown that 4-1BB aptamer was conjugated to a siRNA that negatively regulate the mTOR pathway, decreasing the generation of memory cells in treated animals (Berezhnoy et al., 2014).

Despite the variety of preclinical studies involving aptamer molecules for 4-1BB and OX40 and the positive results achieved, these molecules have not been tested in clinical studies yet. The use of aptamer molecules as a therapeutic strategy is considered recent when compared to mAbs, and it has raised attention in the scientific community, proving its safety profile with the first drug approved for clinical use (Ng et al., 2006) and with other molecules being pursued for clinical study in the field of tumor immunology (Zboralski et al., 2017; Steurer et al., 2019).

CONCLUSION

The 4-1BB and OX40 TNFRSF receptors are associated with several signaling that contribute to potentiate T-cell antitumor

activity. Agonistic antibodies are widely used in clinical trials and represent the most explored TNFSF-based costimulatory strategies. The development of agonistic oligonucleotide-derived aptamers driven to TNFSFR elements is also an interesting alternative to antibodies because of the simplicity of production through chemical synthesis and engineering possibilities to generate bispecific aptamers or even vehiculated targeted cargos to enhance T-cell function. Signal transduction at TNFSFR receptors can also be mediated by approaches using 4-1BBL or OX40L ligands. These ligands may be expressed in antitumor vaccines or even used in soluble form, exhibiting therapeutic effect. The costimulatory potential of TNFSF molecules is also explored for T-cell engineering, such as chimeric receptors that encode 4-1BB intracellular domains, which are known to play an important role in the costimulation and maintenance of the activated lymphocyte phenotype. Therapeutic strategies that employ 4-1BB and OX40 costimulation work to switch the balance of the immune system toward immunosurveillance. These strategies can also be associated with immunological checkpoint inhibitors, which target the inhibition of immunosuppression mechanisms favoring the detection and elimination of tumor cells.

AUTHOR CONTRIBUTIONS

All authors listed have made a substantial, direct and intellectual contribution to the work, and approved it for publication.

FUNDING

MB – FAPESP, grant 2019/04458-8, IS – FAPESP, PhD fellowship 2018/16449-0, CF – FAPESP, fellowship 2019/13573-5, GL – FAPESP, fellowship 2019/150491, RR – CAPES PhD fellowship, DM – CAPES M.Sc fellowship.

REFERENCES

Alderson, M. R., Smith, C. A., Tough, T. W., Davis-Smith, T., Armitage, R. J., Falk, B., et al. (1994). Molecular and biological characterization of human 4-1BB and its ligand. *Eur. J. Immunol.* 24, 2219–2227.

Andarini, S., Kikuchi, T., Nukiwa, M., Pradono, P., Suzuki, T., Ohkouchi, S., et al. (2004). Adenovirus vector-mediated in vivo gene transfer of OX40 ligand to tumor cells enhances antitumor immunity of tumor-bearing hosts. *Cancer Res.* 64, 3281–3287. doi: 10.1158/0008-5472.can-03-3911

Arch, R. H., and Thompson, C. B. (1998). 4-1BB and Ox40 are members of a tumor necrosis factor (TNF)-nerve growth factor receptor subfamily that bind TNF receptor-associated factors and activate nuclear factor kappaB. *Mol. Cell. Biol.* 18, 558–565. doi: 10.1128/mcb.18.1.558

Ascierto, P. A., Simeone, E., Sznol, M., Fu, Y.-X., and Melero, I. (2010). Clinical experiences with anti-CD137 and anti-PD1 therapeutic antibodies. *Semin Oncol.* 37, 508–516. doi: 10.1053/j.seminoncol.2010.09.008

Bansal-Pakala, P., Halteman, B. S., Cheng, M. H.-Y., and Croft, M. (2004). Costimulation of CD8 T cell responses by OX40. *J. Immunol.* 172, 4821–4825. doi: 10.4049/jimmunol.172.8.4821

Barsoumian, H. B., Yolcu, E. S., and Shirwan, H. (2016). 4-1BB signaling in conventional T cells drives IL-2 production that overcomes CD4+CD25+FoxP3+ Tregulatory cell suppression. *PLoS One* 11:e0153088. doi: 10.1371/journal.pone.0153088

Baumann, R., Yousefi, S., Simon, D., Russmann, S., Mueller, C., and Simon, H.-U. (2004). Functional expression of CD134 by neutrophils. *Eur. J. Immunol.* 34, 2268–2275. doi: 10.1002/eji.200424863

Berezhnoy, A., Brenneman, R., Bajgelman, M., Seales, D., and Gilboa, E. (2012). Thermal stability of siRNA modulates aptamer- conjugated siRNA inhibition. *Mol. Ther. Nucleic Acids* 1:e51. doi: 10.1038/mtna.2012.41

Berezhnoy, A., Castro, I., Levay, A., Malek, T. R., and Gilboa, E. (2014). Aptamer-targeted inhibition of mTOR in T cells enhances antitumor immunity. *J. Clin. Invest.* 124, 188–197. doi: 10.1172/jci69856

Bompiani, K. M., Monroe, D. M., Church, F. C., and Sullenger, B. A. (2012). A high affinity, antidote-controllable prothrombin and thrombin-binding RNA aptamer inhibits thrombin generation and thrombin activity. *J. Thromb. Haemost.* 10, 870–880. doi: 10.1111/j.1538-7836.2012.04679.x

Bouvier-Müller, A., and Ducongé, F. (2018). Application of aptamers for in vivo molecular imaging and theranostics. *Adv. Drug Deliv. Rev.* 134, 94–106. doi: 10.1016/j.addr.2018.08.004

Bouwmeester, T., Bauch, A., Ruffner, H., Angrand, P.-O., Bergamini, G., Croughton, K., et al. (2004). A physical and functional map of the human TNF-alpha/NF-kappa B signal transduction pathway. *Nat. Cell Biol.* 6, 97–105.

Buchan, S., Manzo, T., Flutter, B., Rogel, A., Edwards, N., Zhang, L., et al. (2015). OX40- and CD27-mediated costimulation synergizes with anti-PD-L1 blockade by forcing exhausted CD8+ T cells to exit quiescence. *J. Immunol.* 194, 125–133. doi: 10.4049/jimmunol.1401644

Buchan, S. L., Dou, L., Remer, M., Booth, S. G., Dunn, S. N., Lai, C., et al. (2018). Antibodies to costimulatory receptor 4-1BB enhance anti-tumor immunity via T regulatory cell depletion and promotion of CD8 T cell effector function. *Immunity* 49, 958–970.e7. doi: 10.1016/j.immuni.2018.09.014

Bukczynski, J., Wen, T., and Watts, T. H. (2003). Costimulation of human CD28-T cells by 4-1BB ligand. *Eur. J. Immunol.* 33, 446–454. doi: 10.1002/immu.200310020

Bulliard, Y., Jolicoeur, R., Zhang, J., Dranoff, G., Wilson, N. S., and Brogdon, J. L. (2014). OX40 engagement depletes intratumoral Tregs via activating FcγRs, leading to antitumor efficacy. *Immunol. Cell Biol.* 92, 475–480. doi: 10.1038/icb.2014.26

Calderhead, D. M., Buhlmann, J. E., van den Eertwegh, A. J., Claassen, E., Noelle, R. J., and Fell, H. P. (1993). Cloning of mouse Ox40: a T cell activation marker that may mediate T-B cell interactions. *J. Immunol.* 151, 5261–5271.

Cannons, J. L., Choi, Y., and Watts, T. H. (2000). Role of TNF receptor-associated factor 2 and p38 mitogen-activated protein kinase activation during 4-1BB-dependent immune response. *J. Immunol.* 165, 6193–6204. doi: 10.4049/jimmunol.165.11.6193

Cannons, J. L., Lau, P., Ghumman, B., DeBenedette, M. A., Yagita, H., Okumura, K., et al. (2001). 4-1BB ligand induces cell division, sustains survival, and enhances effector function of CD4 and CD8 T cells with similar efficacy. *J. Immunol.* 167, 1313–1324. doi: 10.4049/jimmunol.167.3.1313

Chang, L.-Y., Lin, Y.-C., Mahalingam, J., Huang, C.-T., Chen, T.-W., Kang, C.-W., et al. (2012). Tumor-derived chemokine CCL5 enhances TGF-β-mediated killing of CD8(+) T cells in colon cancer by T-regulatory cells. *Cancer Res.* 72, 1092–1102. doi: 10.1158/0008-5472.can-11-2493

Chen, D. S., and Mellman, I. (2013). Oncology meets immunology: the cancer-immunity cycle. *Immunity* 39, 1–10. doi: 10.1016/j.immuni.2013.07.012

Cheng, C., Chen, Y. H., Lennox, K. A., Behlke, M. A., and Davidson, B. L. (2013). In vivo SELEX for Identification of brain-penetrating aptamers. *Mol. Ther. Nucleic Acids* 2:e67. doi: 10.1038/mtna.2012.59

Chin, S. M., Kimberlin, C. R., Roe-Zurz, Z., Zhang, P., Xu, A., Liao-Chan, S., et al. (2018). Structure of the 4-1BB/4-1BBL complex and distinct binding and functional properties of utomilumab and urelumab. *Nat. Commun.* 9:4679. doi: 10.1038/s41467-018-07136-7

Cuadros, C., Dominguez, A. L., Lollini, P.-L., Croft, M., Mittler, R. S., Borgström, P., et al. (2005). Vaccination with dendritic cells pulsed with apoptotic tumors in combination with anti-OX40 and anti-4-1BB monoclonal antibodies induces T cell-mediated protective immunity in Her-2/neu transgenic mice. *Int. J. Cancer* 116, 934–943. doi: 10.1002/ijc.21098

Curti, B. D., Kovacsovics-Bankowski, M., Morris, N., Walker, E., Chisholm, L., Floyd, K., et al. (2013). OX40 is a potent immune-stimulating target in late-stage cancer patients. *Cancer Res.* 73, 7189–7198. doi: 10.1158/0008-5472.can-12-4174

Dawicki, W., Bertram, E. M., Sharpe, A. H., and Watts, T. H. (2004). 4-1BB and OX40 act independently to facilitate robust CD8 and CD4 recall responses. *J. Immunol.* 173, 5944–5951. doi: 10.4049/jimmunol.173.10.5944

De Smedt, T., Smith, J., Baum, P., Fanslow, W., Butz, E., and Maliszewski, C. (2002). Ox40 costimulation enhances the development of T cell responses induced by dendritic cells in vivo. *J. Immunol.* 168, 661–670. doi: 10.4049/jimmunol.168.2.661

DeBenedette, M. A., Shahinian, A., Mak, T. W., and Watts, T. H. (1997). Costimulation of CD28- T lymphocytes by 4-1BB ligand. *J. Immunol.* 158, 551–559.

Dollins, C. M., Nair, S., Boczkowski, D., Lee, J., Layzer, J. M., Gilboa, E., et al. (2008). Assembling OX40 aptamers on a molecular scaffold to create a receptor-activating aptamer. *Chem. Biol.* 15, 675–682. doi: 10.1016/j.chembiol.2008.05.016

Dowell, A. C., Oldham, K. A., Bhatt, R. I., Lee, S. P., and Searle, P. F. (2012). Long-term proliferation of functional human NK cells, with conversion of CD56(dim) NK cells to a CD56 (bright) phenotype, induced by carcinoma cells co-expressing 4-1BBL and IL-12. *Cancer Immunol. Immunother.* 61, 615–628. doi: 10.1007/s00262-011-1122-3

Ellington, A. D., and Szostak, J. W. (1990). In vitro selection of RNA molecules that bind specific ligands. *Nature* 346, 818–822. doi: 10.1038/346818a0

Froelich, C. J., Orth, K., Turbov, J., Seth, P., Gottlieb, R., Babior, B., et al. (1996). New paradigm for lymphocyte granule-mediated cytotoxicity. Target cells bind and internalize granzyme B, but an endosomolytic agent is necessary for cytosolic delivery and subsequent apoptosis. *J. Biol. Chem.* 271, 29073–29079. doi: 10.1074/jbc.271.46.29073

Fröhlich, A., Loick, S., Bawden, E. G., Fietz, S., Dietrich, J., Diekmann, E., et al. (2020). Comprehensive analysis of tumor necrosis factor receptor TNFRSF9 (4-1BB) DNA methylation with regard to molecular and clinicopathological features, immune infiltrates, and response prediction to immunotherapy in melanoma. *EBioMedicine* 52, 1–14.

Fu, Y., Lin, Q., Zhang, Z., and Zhang, L. (2020). Therapeutic strategies for the costimulatory molecule OX40 in T-cell-mediated immunity. *Acta Pharm. Sin. B* 10, 414–433. doi: 10.1016/j.apsb.2019.08.010

Gajdasik, D. W., Gaspal, F., Halford, E. E., Fiancette, R., Dutton, E. E., Willis, C., et al. (2020). Th1 responses in vivo require cell-specific provision of OX40L dictated by environmental cues. *Nat. Commun.* 11:3421. doi: 10.1038/s41467-020-17293-3

Godfrey, W. R., Fagnoni, F. F., Harara, M. A., Buck, D., and Engleman, E. G. (1994). Identification of a human OX-40 ligand, a costimulator of CD4+ T cells with homology to tumor necrosis factor. *J. Exp. Med.* 180, 757–762. doi: 10.1084/jem.180.2.757

Gong, W., Xiao, W., Hu, M., Weng, X., Qian, L., Pan, X., et al. (2010). Ex vivo expansion of natural killer cells with high cytotoxicity by K562 cells modified to co-express major histocompatibility complex class I chain-related protein A, 4-1BB ligand, and interleukin-15. *Tissue Antigens* 76, 467–475. doi: 10.1111/j.1399-0039.2010.01535.x

Goodwin, R. G., Din, W. S., Davis-Smith, T., Anderson, D. M., Gimpel, S. D., Sato, T. A., et al. (1993). Molecular cloning of a ligand for the inducible T cell gene 4-1BB: a member of an emerging family of cytokines with homology to tumor necrosis factor. *Eur. J. Immunol.* 23, 2631–2641. doi: 10.1002/eji.1830231037

Gopal, A., Levy, R., Houot, R., Patel, S., Hatake, K., Popplewell, L., et al. (2017). A phase I study of utomilumab (PF-05082566), A 4-1BB/CD137 agonist, in combination with rituximab in patients with CD20+ Non-Hodgkin's Lymphoma. *Hematol. Oncol.* 35:260. doi: 10.1002/hon.2438_127

Gopal, A. K., Levy, R., Houot, R., Patel, S. P., Popplewell, L., Jacobson, C., et al. (2020). First-in-human study of utomilumab, a 4-1BB/CD137 agonist, in combination with rituximab in patients with follicular and other CD20(+) Non-Hodgkin Lymphomas. *Clin. Cancer Res.* 26, 2524–2534. doi: 10.1158/1078-0432.ccr-19-2973

Gramaglia, I., Jember, A., Pippig, S. D., Weinberg, A. D., Killeen, N., and Croft, M. (2000). The OX40 costimulatory receptor determines the development of CD4 memory by regulating primary clonal expansion. *J. Immunol.* 165, 3043–3050. doi: 10.4049/jimmunol.165.6.3043

Gray, J. C., French, R. R., James, S., Al-Shamkhani, A., Johnson, P. W., and Glennie, M. J. (2008). Optimising anti-tumour CD8 T-cell responses using combinations of immunomodulatory antibodies. *Eur. J. Immunol.* 38, 2499–2511. doi: 10.1002/eji.200838208

Habib-Agahi, M., Phan, T. T., and Searle, P. F. (2007). Co-stimulation with 4-1BB ligand allows extended T-cell proliferation, synergizes with CD80/CD86 and can reactivate anergic T cells. *Int. Immunol.* 19, 1383–1394. doi: 10.1093/intimm/dxm106

Hinner, M. J., Aiba, R. S. B., Jaquin, T. J., Berger, S., Dürr, M. C., Schlosser, C., et al. (2019). Tumor-localized costimulatory T-cell engagement by the 4-1BB/HER2 bispecific antibody-anticalin fusion PRS-343. *Clin. Cancer Res.* 25, 5878–5889. doi: 10.1158/1078-0432.ccr-18-3654

Hockenbery, D., Nuñez, G., Milliman, C., Schreiber, R. D., and Korsmeyer, S. J. (1990). Bcl-2 is an inner mitochondrial membrane protein that blocks programmed cell death. *Nature* 348, 334–336. doi: 10.1038/348334a0

Houot, R., Goldstein, M. J., Kohrt, H. E., Myklebust, J. H., Alizadeh, A. A., Lin, J. T., et al. (2009). Therapeutic effect of CD137 immunomodulation in lymphoma and its enhancement by Treg depletion. *Blood* 114, 3431–3438. doi: 10.1182/blood-2009-05-223958

Hurtado, J. C., Kim, Y. J., and Kwon, B. S. (1997). Signals through 4-1BB are costimulatory to previously activated splenic T cells and inhibit activation-induced cell death. *J. Immunol.* 158, 2600–2609.

Infante, J. R., Ahlers, C. M., Hodi, F. S., Postel-Vinay, S., Schellens, J. H. M., Heymach, J., et al. (2016). ENGAGE-1: a first in human study of the OX40 agonist GSK3174998 alone and in combination with pembrolizumab in patients with advanced solid tumors. *J. Clin. Oncol.* 34(15_Suppl.):TS3107. doi: 10.1200/JCO.2016.34.15_suppl.TPS3107

Irie, J., Wu, Y., Kachapati, K., Mittler, R. S., and Ridgway, W. M. (2007). Modulating protective and pathogenic CD4+ subsets via CD137 in type 1 diabetes. *Diabetes* 56, 186–196. doi: 10.2337/db06-0793

Jang, I. K., Lee, Z. H., Kim, Y. J., Kim, S. H., and Kwon, B. S. (1998). Human 4-1BB (CD137) signals are mediated by TRAF2 and activate nuclear factor-kappa B. *Biochem. Biophys. Res. Commun.* 242, 613–620. doi: 10.1006/bbrc.1997.8016

Jenkins, S. J., Perona-Wright, G., Worsley, A. G. F., Ishii, N., and MacDonald, A. S. (2007). Dendritic cell expression of OX40 ligand acts as a costimulatory, not polarizing, signal for optimal Th2 priming and memory induction in vivo. *J. Immunol.* 179, 3515–3523. doi: 10.4049/jimmunol.179.6.3515

Ju, S.-A., Cheon, S.-H., Park, S.-M., Tam, N. Q., Kim, Y. M., An, W. G., et al. (2008). Eradication of established renal cell carcinoma by a combination of 5-fluorouracil and anti-4-1BB monoclonal antibody in mice. *Int. J. Cancer* 122, 2784–2790. doi: 10.1002/ijc.23457

Kalos, M., Levine, B. L., Porter, D. L., Katz, S., Grupp, S. A., Bagg, A., et al. (2011). T cells with chimeric antigen receptors have potent antitumor effects and can establish memory in patients with advanced leukemia. *Sci. Transl. Med.* 3:95ra73. doi: 10.1126/scitranslmed.3002842

Karulf, M., Kelly, A., Weinberg, A. D., and Gold, J. A. (2010). OX40 ligand regulates inflammation and mortality in the innate immune response to sepsis. *J. Immunol.* 185, 4856–4862. doi: 10.4049/jimmunol.1000404

Kim, D.-H., Chang, W.-S., Lee, Y.-S., Lee, K.-A., Kim, Y.-K., Kwon, B. S., et al. (2008). 4-1BB engagement costimulates NKT cell activation and exacerbates NKT cell ligand-induced airway hyperresponsiveness and inflammation. *J. Immunol.* 180, 2062–2068. doi: 10.4049/jimmunol.180.4.2062

Kim, J., Choi, S. P., La, S., Seo, J.-S., Kim, K. K., Nam, S. H., et al. (2003). Constitutive expression of 4-1BB on T cells enhances CD4+ T cell responses. *Exp. Mol. Med.* 35, 509–517. doi: 10.1038/emm.2003.66

Kim, Y. J., Kim, S. H., Mantel, P., and Kwon, B. S. (1998). Human 4-1BB regulates CD28 co-stimulation to promote Th1 cell responses. *Eur. J. Immunol.* 28, 881–890. doi: 10.1002/(sici)1521-4141(199803)28:03<881::aid-immu881>3.0.co;2-0

Kitamura, N., Murata, S., Ueki, T., Mekata, E., Reilly, R. T., Jaffee, E. M., et al. (2009). OX40 costimulation can abrogate Foxp3+ regulatory T cell-mediated suppression of antitumor immunity. *Int. J. Cancer* 125, 630–638. doi: 10.1002/ijc.24435

Kjaergaard, J., Tanaka, J., Kim, J. A., Rothchild, K., Weinberg, A., and Shu, S. (2000). Therapeutic efficacy of OX-40 receptor antibody depends on tumor immunogenicity and anatomic site of tumor growth. *Cancer Res.* 60, 5514–5521.

Klatzmann, D., Barré-Sinoussi, F., Nugeyre, M. T., Danquet, C., Vilmer, E., Griscelli, C. et al. (1984). Selective tropism of lymphadenopathy associated virus (LAV) for helper-inducer T lymphocytes. *Science* 225, 59–63. doi: 10.1126/science.6328660

Kuang, Z., Jing, H., Wu, Z., Wang, J., Li, Y., Ni, H., et al. (2020). Development and characterization of a novel anti-OX40 antibody for potent immune activation. *Cancer Immunol. Immunother.* 69, 939–950. doi: 10.1007/s00262-020-02501-2

Kwon, B. S., and Weissman, S. M. (1989). cDNA sequences of two inducible T-cell genes. *Proc. Natl. Acad. Sci. U.S.A.* 86, 1963–1967. doi: 10.1073/pnas.86.6.1963

Laderach, D., Movassagh, M., Johnson, A., Mittler, R. S., and Galy, A. (2002). 4-1BB co-stimulation enhances human CD8(+) T cell priming by augmenting the proliferation and survival of effector CD8(+) T cells. *Int. Immunol.* 14, 1155–1167. doi: 10.1093/intimm/dxf080

Langstein, J., Michel, J., Fritsche, J., Kreutz, M., Andreesen, R., and Schwarz, H. (1998). CD137 (ILA/4-1BB), a member of the TNF receptor family, induces monocyte activation via bidirectional signaling. *J. Immunol.* 160, 2488–2494.

Latza, U., Dürkop, H., Schnittger, S., Ringeling, J., Eitelbach, F., Hummel, M., et al. (1994). The human OX40 homolog: cDNA structure, expression and chromosomal assignment of the ACT35 antigen. *Eur. J. Immunol.* 24, 677–683. doi: 10.1002/eji.1830240329

Lee, H.-W., Park, S.-J., Choi, B. K., Kim, H. H., Nam, K.-O., and Kwon, B. S. (2002). 4-1BB promotes the survival of CD8+ T lymphocytes by increasing expression of Bcl-xL and Bfl-1. *J. Immunol.* 169, 4882–4888. doi: 10.4049/jimmunol.169.9.4882

Lee, S.-J., Myers, L., Muralimohan, G., Dai, J., Qiao, Y., Li, Z., et al. (2004). 4-1BB and OX40 dual costimulation synergistically stimulate primary specific CD8 T cells for robust effector function. *J. Immunol.* 173, 3002–3012. doi: 10.4049/jimmunol.173.5.3002

Lee, S.-W., Park, Y., Song, A., Cheroutre, H., Kwon, B. S., and Croft, M. (2006). Functional dichotomy between OX40 and 4-1BB in modulating effector CD8 T cell responses. *J. Immunol.* 177, 4464–4472. doi: 10.4049/jimmunol.177.7.4464

Lin, W., Voskens, C. J., Zhang, X., Schindler, D. G., Wood, A., Burch, E., et al. (2008). Fc-dependent expression of CD137 on human NK cells: insights into "agonistic" effects of anti-CD137 monoclonal antibodies. *Blood* 112, 699–707. doi: 10.1182/blood-2007-11-122465

Linch, S. N., Kasiewicz, M. J., McNamara, M. J., Hilgart-Martiszus, I. F., Farhad, M., and Redmond, W. L. (2016). Combination OX40 agonism/CTLA-4 blockade with HER2 vaccination reverses T-cell anergy and promotes survival in tumor-bearing mice. *Proc. Natl. Acad. Sci. U.S.A.* 113, E319–E327.

Linton, P.-J., Bautista, B., Biederman, E., Bradley, E. S., Harbertson, J., Kondrack, R. M., et al. (2003). Costimulation via OX40L expressed by B cells is sufficient to determine the extent of primary CD4 cell expansion and Th2 cytokine secretion in vivo. *J. Exp. Med.* 197, 875–883. doi: 10.1084/jem.20021290

Lippert, U., Zachmann, K., Ferrari, D. M., Schwarz, H., Brunner, E., Mahbub-Ul Latif, A. H. M., et al. (2008). CD137 ligand reverse signaling has multiple functions in human dendritic cells during an adaptive immune response. *Eur. J. Immunol.* 38, 1024–1032. doi: 10.1002/eji.200737800

Liu, Z., Kim, J. H., Falo, L. D. Jr., and You, Z. (2009). Tumor regulatory T cells potently abrogate antitumor immunity. *J. Immunol.* 182, 6160–6167. doi: 10.4049/jimmunol.0802664

Lubrano di Ricco, M., Ronin, E., Collares, D., Divoux, J., Grégoire, S., Wajant, H., et al. (2020). Tumor necrosis factor receptor family costimulation increases regulatory T-cell activation and function via NF-κB. *Eur. J. Immunol.* 50, 972–985. doi: 10.1002/eji.201948393

Maimaitiyiming, Y., Hong, D., Yang, C., and Naranmandura, H. (2019). Novel insights into the role of aptamers in the fight against cancer. *J. Cancer Res. Clin. Oncol.* 145, 797–810. doi: 10.1007/s00432-019-02882-7

Makkouk, A., Chester, C., and Kohrt, H. E. (2016). Rationale for anti-CD137 cancer immunotherapy. *Eur. J. Cancer* 54, 112–119. doi: 10.1016/j.ejca.2015.09.026

Mallett, S., Fossum, S., and Barclay, A. N. (1990). Characterization of the MRC OX40 antigen of activated CD4 positive T lymphocytes–a molecule related to nerve growth factor receptor. *EMBO J.* 9, 1063–1068. doi: 10.1002/j.1460-2075.1990.tb08211.x

Manrique-Rincón, A. J., Beraldo, C. M., Toscaro, J. M., and Bajgelman, M. C. (2017). Exploring synergy in combinations of tumor-derived vaccines that harbor 4-1BBL, OX40L, and GM-CSF. *Front. Immunol.* 8:1150. doi: 10.3389/fimmu.2017.01150

Martinez-Forero, I., Azpilikueta, A., Bolaños-Mateo, E., Nistal-Villan, E., Palazon, A., Teijeira, A., et al. (2013). T cell costimulation with anti-CD137 monoclonal antibodies is mediated by K63-polyubiquitin-dependent signals from endosomes. *J. Immunol.* 190, 6694–6706. doi: 10.4049/jimmunol.1203010

Massarelli, E., Lam, V. K., Parra, E. R., Rodriguez-Canales, J., Behrens, C., Diao, L., et al. (2019). High OX-40 expression in the tumor immune infiltrate is a favorable prognostic factor of overall survival in non-small cell lung cancer. *J. Immunother. Cancer* 7:351.

Maxwell, J. R., Weinberg, A., Prell, R. A., and Vella, A. T. (2000). Danger and OX40 receptor signaling synergize to enhance memory T cell survival by inhibiting peripheral deletion. *J. Immunol.* 164, 107–112. doi: 10.4049/jimmunol.164.1.107

McNamara, J. O., Kolonias, D., Pastor, F., Mittler, R. S., Chen, L., Giangrande, P. H., et al. (2008). Multivalent 4-1BB binding aptamers costimulate CD8+ T cells and inhibit tumor growth in mice. *J. Clin. Invest.* 118, 376–386. doi: 10.1172/jci33365

Melero, I., Hirschhorn-Cymerman, D., Morales-Kastresana, A., Sanmamed, M. F., and Wolchok, J. D. (2013). Agonist antibodies to TNFR molecules that costimulate T and NK cells. *Clin. Cancer Res.* 19, 1044–1053. doi: 10.1158/1078-0432.ccr-12-2065

Melero, I., Johnston, J. V., Shufford, W. W., Mittler, R. S., and Chen, L. (1998). NK1.1 cells express 4-1BB (CDw137) costimulatory molecule and are required for tumor immunity elicited by anti-4-1BB monoclonal antibodies. *Cell. Immunol.* 190, 167–172. doi: 10.1006/cimm.1998.1396

Menk, A. V., Scharping, N. E., Rivadeneira, D. B., Calderon, M. J., Watson, M. J., Dunstane, D., et al. (2018). 4-1BB costimulation induces T cell mitochondrial function and biogenesis enabling cancer immunotherapeutic responses. *J. Exp. Med.* 215, 1091–1100. doi: 10.1084/jem.20171068

Miller, G. A., and Chapman, J. P. (2001). Misunderstanding analysis of covariance. *J. Abnorm. Psychol.* 110, 40–48. doi: 10.1037/0021-843x.110.1.40

Misumi, T., Tanabe, K., Fujikuni, N., and Ohdan, H. (2018). Stimulation of natural killer cells with rhCD137 ligand enhances tumor-targeting antibody efficacy in gastric cancer. *PLoS One* 13:e0204880. doi: 10.1371/journal.pone.0204880

Morita, Y., Leslie, M., Kameyama, H., Volk, D. E., and Tanaka, T. (2018). Aptamer therapeutics in cancer: current and future. *Cancers* 10:80. doi: 10.3390/cancers10030080

Munks, M. W., Mourich, D. V., Mittler, R. S., Weinberg, A. D., and Hill, A. B. (2004). 4-1BB and OX40 stimulation enhance CD8 and CD4 T-cell responses to a DNA prime, poxvirus boost vaccine. *Immunology* 112, 559–566. doi: 10.1111/j.1365-2567.2004.01917.x

Ng, E. W. M., Shima, D. T., Calias, P., Cunningham, E. T., Guyer, D. R., and Adamis, A. P. (2006). Pegaptanib, a targeted anti-VEGF aptamer for ocular vascular disease. *Nat. Rev. Drug Discov.* 5, 123–132. doi: 10.1038/nrd1955

Niu, L., Strahotin, S., Hewes, B., Zhang, B., Zhang, Y., Archer, D., et al. (2007). Cytokine-mediated disruption of lymphocyte trafficking, hemopoiesis, and induction of lymphopenia, anemia, and thrombocytopenia in anti-CD137-treated mice. *J. Immunol.* 178, 4194–4213. doi: 10.4049/jimmunol.178.7.4194

Pastor, F., Berraondo, P., Etxeberria, I., Frederick, J., Sahin, U., Gilboa, E., et al. (2018). An RNA toolbox for cancer immunotherapy. *Nat. Rev. Drug Discov.* 17, 751–767. doi: 10.1038/nrd.2018.132

Pastor, F., Kolonias, D., McNamara, J. O. II, and Gilboa, E. (2011). Targeting 4-1BB costimulation to disseminated tumor lesions with bi-specific oligonucleotide aptamers. *Mol. Ther.* 19, 1878–1886. doi: 10.1038/mt.2011.145

Paterson, D. J., Jefferies, W. A., Green, J. R., Brandon, M. R., Corthesy, P., Puklavec, M., et al. (1987). Antigens of activated rat T lymphocytes including a molecule of 50,000 Mr detected only on CD4 positive T blasts. *Mol. Immunol.* 24, 1281–1290. doi: 10.1016/0161-5890(87)90122-2

Pattarini, L., Trichot, C., Bogiatzi, S., Grandclaudon, M., Meller, S., Keuylian, Z., et al. (2017). TSLP-activated dendritic cells induce human T follicular helper cell differentiation through OX40-ligand. *J. Exp. Med.* 214, 1529–1546. doi: 10.1084/jem.20150402

Peng, W., Williams, L. J., Xu, C., Melendez, B., McKenzie, J. A., Chen, Y., et al. (2019). Anti-OX40 antibody directly enhances the function of tumor-reactive CD8(+) T cells and synergizes with PI3Kβ inhibition in PTEN loss melanoma. *Clin. Cancer Res.* 25, 6406–6416. doi: 10.1158/1078-0432.ccr-19-1259

Piconese, S., Valzasina, B., and Colombo, M. P. (2008). OX40 triggering blocks suppression by regulatory T cells and facilitates tumor rejection. *J. Exp. Med.* 205, 825–839. doi: 10.1084/jem.20071341

Pollok, K. E., Kim, S. H., and Kwon, B. S. (1995). Regulation of 4-1BB expression by cell-cell interactions and the cytokines, interleukin-2 and interleukin-4. *Eur. J. Immunol.* 25, 488–494. doi: 10.1002/eji.1830250227

Pollok, K. E., Kim, Y. J., Hurtado, J., Zhou, Z., Kim, K. K., and Kwon, B. S. (1994). 4-1BB T-cell antigen binds to mature B cells and macrophages, and costimulates anti-mu-primed splenic B cells. *Eur. J. Immunol.* 24, 367–374. doi: 10.1002/eji.1830240215

Pollok, K. E., Kim, Y. J., Zhou, Z., Hurtado, J., Kim, K. K., Pickard, R. T., et al. (1993). Inducible T cell antigen 4-1BB. analysis of expression and function. *J. Immunol.* 150, 771–781.

Porter, D. L., Levine, B. L., Kalos, M., Bagg, A., and June, C. H. (2011). Chimeric antigen receptor-modified T cells in chronic lymphoid leukemia. *N. Engl. J. Med.* 365, 725–733. doi: 10.1056/nejmoa1103849

Pratico, E. D., Sullenger, B. A., and Nair, S. K. (2013). Identification and characterization of an agonistic aptamer against the T cell costimulatory receptor, OX40. *Nucleic Acid Ther.* 23, 35–43. doi: 10.1089/nat.2012.0388

Qi, X., Li, F., Wu, Y., Cheng, C., Han, P., Wang, J., et al. (2019). Optimization of 4-1BB antibody for cancer immunotherapy by balancing agonistic strength with FcγR affinity. *Nat. Commun.* 10:2141.

Rajagopalan, A., Berezhnoy, A., Schrand, B., Puplampu-Dove, Y., and Gilboa, E. (2017). Aptamer-targeted attenuation of IL-2 signaling in CD8(+) T cells enhances antitumor immunity. *Mol. Ther.* 25, 54–61. doi: 10.1016/j.ymthe.2016.10.021

Rajasekaran, N., Chester, C., Yonezawa, A., Zhao, X., and Kohrt, H. E. (2015). Enhancement of antibody-dependent cell mediated cytotoxicity: a new era in cancer treatment. *Immunotargets Ther.* 4, 91–100. doi: 10.2147/itt.s61292

Redmond, W. L., Ruby, C. E., and Weinberg, A. D. (2009). The role of OX40-mediated co-stimulation in T-cell activation and survival. *Crit. Rev. Immunol.* 29, 187–201. doi: 10.1615/critrevimmunol.v29.i3.10

Rogers, P. R., Song, J., Gramaglia, I., Killeen, N., and Croft, M. (2001). OX40 promotes Bcl-xL and Bcl-2 expression and is essential for long-term survival of CD4 T cells. *Immunity* 15, 445–455. doi: 10.1016/s1074-7613(01)00191-1

Rothe, M., Sarma, V., Dixit, V. M., and Goeddel, D. V. (1995). TRAF2-mediated activation of NF-kappa B by TNF receptor 2 and CD40. *Science* 269, 1424–1427. doi: 10.1126/science.7544915

Sabbagh, L., Pulle, G., Liu, Y., Tsitsikov, E. N., and Watts, T. H. (2008). ERK-dependent Bim modulation downstream of the 4-1BB-TRAF1 signaling axis is a critical mediator of CD8 T cell survival in vivo. *J. Immunol.* 180, 8093–8101. doi: 10.4049/jimmunol.180.12.8093

Sadler, R., Bateman, E. A. L., Heath, V., Patel, S. Y., Schwingshackl, P. P., Cullinane, A. C., et al. (2014). Establishment of a healthy human range for the whole blood "OX40" assay for the detection of antigen-specific CD4+ T cells by flow cytometry. *Cytometry B Clin. Cytom.* 86, 350–361.

Salek-Ardakani, S., Song, J., Halteman, B. S., Jember, A. G.-H., Akiba, H., Yagita, H., et al. (2003). OX40 (CD134) controls memory T helper 2 cells that drive lung inflammation. *J. Exp. Med.* 198, 315–324. doi: 10.1084/jem.20021937

Salih, H. R., Kosowski, S. G., Haluska, V. F., Starling, G. C., Loo, D. T., Lee, F., et al. (2000). Constitutive expression of functional 4-1BB (CD137) ligand on carcinoma cells. *J. Immunol.* 165, 2903–2910. doi: 10.4049/jimmunol.165.5.2903

Santulli-Marotto, S., Nair, S. K., Rusconi, C., Sullenger, B., and Gilboa, E. (2003). Multivalent RNA aptamers that inhibit CTLA-4 and enhance tumor immunity. *Cancer Res.* 63, 7483–7489.

Saoulli, K., Lee, S. Y., Cannons, J. L., Yeh, W. C., Santana, A., Goldstein, M. D., et al. (1998). CD28-independent, TRAF2-dependent costimulation of resting T cells by 4-1BB ligand. *J. Exp. Med.* 187, 1849–1862. doi: 10.1084/jem.187.11.1849

Schabowsky, R.-H., Elpek, K. G., Madireddi, S., Sharma, R. K., Yolcu, E. S., Bandura-Morgan, L., et al. (2009). A novel form of 4-1BBL has better immunomodulatory activity than an agonistic anti-4-1BB Ab without Ab-associated severe toxicity. *Vaccine* 28, 512–522. doi: 10.1016/j.vaccine.2009.09.127

Schoenbrunn, A., Frentsch, M., Kohler, S., Keye, J., Dooms, H., Moewes, B., et al. (2012). A converse 4-1BB and CD40 ligand expression pattern delineates activated regulatory T cells (Treg) and conventional T cells enabling direct isolation of alloantigen-reactive natural Foxp3+ Treg. *J. Immunol.* 189, 5985–5994. doi: 10.4049/jimmunol.1201090

Schrand, B., Berezhnoy, A., Brenneman, R., Williams, A., Levay, A., and Gilboa, E. (2015). Reducing toxicity of 4-1BB costimulation: targeting 4-1BB ligands to the tumor stroma with bi-specific aptamer conjugates. *Oncoimmunology* 4:e970918. doi: 10.4161/21624011.2014.970918

Schrand, B., Berezhnoy, A., Brenneman, R., Williams, A., Levay, A., Kong, L.-Y., et al. (2014). Targeting 4-1BB costimulation to the tumor stroma with bispecific aptamer conjugates enhances the therapeutic index of tumor immunotherapy. *Cancer Immunol. Res.* 2, 867–877. doi: 10.1158/2326-6066.cir-14-0007

Schwarz, H., Tuckwell, J., and Lotz, M. (1993). A receptor induced by lymphocyte activation (ILA): a new member of the human nerve-growth-factor/tumor-necrosis-factor receptor family. *Gene* 134, 295–298. doi: 10.1016/0378-1119(93)90110-o

Segal, N. H., Gopal, A. K., Bhatia, S., Kohrt, H. E., Levy, R., Pishvaian, M. J., et al. (2014). A phase 1 study of PF-05082566 (anti-4-1BB) in patients with advanced cancer. *J. Clin. Oncol.* 32(15_Suppl.):3007. doi: 10.1200/jco.2014.32.15_suppl.3007

Semionatto, I. F., Palameta, S., Toscaro, J. M., Manrique-Rincón, A. J., Ruas, L. P., Paes Leme, A. F., et al. (2020). Extracellular vesicles produced by immunomodulatory cells harboring OX40 ligand and 4-1BB ligand enhance antitumor immunity. *Sci. Rep.* 10:15160.

Sharma, R. K., Srivastava, A. K., Yolcu, E. S., MacLeod, K. J., Schabowsky, R.-H., Madireddi, S., et al. (2010). SA-4-1BBL as the immunomodulatory component of a HPV-16 E7 protein based vaccine shows robust therapeutic efficacy in a mouse cervical cancer model. *Vaccine* 28, 5794–5802. doi: 10.1016/j.vaccine.2010.06.073

Shi, W., and Siemann, D. W. (2006). Augmented antitumor effects of radiation therapy by 4-1BB antibody (BMS-469492) treatment. *Anticancer Res.* 26, 3445–3453.

Shuford, W. W., Klussman, K., Tritchler, D. D., Loo, D. T., Chalupny, J., Siadak, A. W., et al. (1997). 4-1BB costimulatory signals preferentially induce CD8+ T cell proliferation and lead to the amplification in vivo of cytotoxic T cell responses. *J. Exp. Med.* 186, 47–55. doi: 10.1084/jem.186.1.47

So, T., and Croft, M. (2007). Cutting edge: OX40 inhibits TGF-beta- and antigen-driven conversion of naive CD4 T cells into CD25+Foxp3+ T cells. *J. Immunol.* 179, 1427–1430. doi: 10.4049/jimmunol.179.3.1427

Song, J., Salek-Ardakani, S., Rogers, P. R., Cheng, M., Van Parijs, L., and Croft, M. (2004). The costimulation-regulated duration of PKB activation controls T cell longevity. *Nat. Immunol.* 5, 150–158. doi: 10.1038/ni1030

Song, J., So, T., and Croft, M. (2008). Activation of NF-kappaB1 by OX40 contributes to antigen-driven T cell expansion and survival. *J. Immunol.* 180, 7240–7248. doi: 10.4049/jimmunol.180.11.7240

Steurer, M., Montillo, M., Scarfò, L., Mauro, F. R., Andel, J., Wildner, S., et al. (2019). Olaptesed pegol (NOX-A12) with bendamustine and rituximab: a phase IIa study in patients with relapsed/refractory chronic lymphocytic leukemia. *Haematologica* 104, 2053–2060. doi: 10.3324/haematol.2018.205930

Swart, M., Verbrugge, I., and Beltman, J. B. (2016). Combination approaches with immune-checkpoint blockade in cancer therapy. *Front. Oncol.* 6:233. doi: 10.3389/fonc.2016.00233

Tahiliani, V., Hutchinson, T. E., Abboud, G., Croft, M., and Salek-Ardakani, S. (2017). OX40 Cooperates with ICOS To amplify follicular Th cell development and germinal center reactions during infection. *J. Immunol.* 198, 218–228. doi: 10.4049/jimmunol.1601356

Takahashi, C., Mittler, R. S., and Vella, A. T. (1999). Cutting edge: 4-1BB is a bona fide CD8 T cell survival signal. *J. Immunol.* 162, 5037–5040.

Tan, J. T., Ha, J., Cho, H. R., Tucker-Burden, C., Hendrix, R. C., Mittler, R. S., et al. (2000). Analysis of expression and function of the costimulatory molecule 4-1BB in alloimmune responses. *Transplantation* 70, 175–183.

Tolcher, A. W., Sznol, M., Hu-Lieskovan, S., Papadopoulos, K. P., Patnaik, A., Rasco, D. W., et al. (2017). Phase Ib study of utomilumab (PF-05082566), a 4-1BB/CD137 agonist, in combination with pembrolizumab (MK-3475) in patients with advanced solid tumors. *Clin. Cancer Res.* 23, 5349–5357. doi: 10.1158/1078-0432.ccr-17-1243

Tuerk, C., and Gold, L. (1990). Systematic evolution of ligands by exponential enrichment: RNA ligands to bacteriophage T4 DNA polymerase. *Science* 249, 505–510. doi: 10.1126/science.2200121

Valzasina, B., Guiducci, C., Dislich, H., Killeen, N., Weinberg, A. D., and Colombo, M. P. (2005). Triggering of OX40 (CD134) on CD4+CD25+ T cells blocks their inhibitory activity: a novel regulatory role for OX40 and its comparison with GITR. *Blood* 105, 2845–2851. doi: 10.1182/blood-2004-07-2959

van der Stegen, S. J. C., Hamieh, M., and Sadelain, M. (2015). The pharmacology of second-generation chimeric antigen receptors. *Nat. Rev. Drug Discov.* 14, 499–509. doi: 10.1038/nrd4597

Vinay, D. S., and Kwon, B. S. (2014). 4-1BB (CD137), an inducible costimulatory receptor, as a specific target for cancer therapy. *BMB Rep.* 47, 122–129. doi: 10.5483/bmbrep.2014.47.3.283

Vu, M. D., Xiao, X., Gao, W., Degauque, N., Chen, M., Kroemer, A., et al. (2007). OX40 costimulation turns off Foxp3 + Tregs. *Blood* 110, 2501–2510. doi: 10.1182/blood-2007-01-070748

Walker, L. S., Gulbranson-Judge, A., Flynn, S., Brocker, T., Raykundalia, C., Goodall, M., et al. (1999). Compromised OX40 function in CD28-deficient mice is linked with failure to develop CXC chemokine receptor 5-positive CD4 cells and germinal centers. *J. Exp. Med.* 190, 1115–1122. doi: 10.1084/jem.190.8.1115

Weinberg, A. D., Rivera, M. M., Prell, R., Morris, A., Ramstad, T., Vetto, J. T., et al. (2000). Engagement of the OX-40 receptor in vivo enhances antitumor immunity. *J. Immunol.* 164, 2160–2169. doi: 10.4049/jimmunol.164.4.2160

Weinberg, A. D., Wegmann, K. W., Funatake, C., and Whitham, R. H. (1999). Blocking OX-40/OX-40 ligand interaction in vitro and in vivo leads to decreased T cell function and amelioration of experimental allergic encephalomyelitis. *J. Immunol.* 162, 1818–1826.

Wen, T., Bukczynski, J., and Watts, T. H. (2002). 4-1BB ligand-mediated costimulation of human T cells induces CD4 and CD8 T cell expansion, cytokine production, and the development of cytolytic effector function. *J. Immunol.* 168, 4897–4906. doi: 10.4049/jimmunol.168.10.4897

Wilcox, R. A., Chapoval, A. I., Gorski, K. S., Otsuji, M., Shin, T., Flies, D. B., et al. (2002). Cutting edge: expression of functional CD137 receptor by dendritic cells. *J. Immunol.* 168, 4262–4267. doi: 10.4049/jimmunol.168.9.4262

Xiao, Y., Hendriks, J., Langerak, P., Jacobs, H., and Borst, J. (2004). CD27 is acquired by primed B cells at the centroblast stage and promotes germinal center formation. *J. Immunol.* 172, 7432–7441. doi: 10.4049/jimmunol.172.12.7432

Xu, L., Xu, W., Qiu, S., and Xiong, S. (2010). Enrichment of CCR6+Foxp3+ regulatory T cells in the tumor mass correlates with impaired CD8+ T cell function and poor prognosis of breast cancer. *Clin. Immunol.* 135, 466–475. doi: 10.1016/j.clim.2010.01.014

Xu, L.-G., Li, L.-Y., and Shu, H.-B. (2004). TRAF7 potentiates MEKK3-induced AP1 and CHOP activation and induces apoptosis. *J. Biol. Chem.* 279, 17278–17282. doi: 10.1074/jbc.c400063200

Youlin, K., Li, Z., Xin, G., Mingchao, X., Xiuheng, L., and Xiaodong, W. (2013). Enhanced function of cytotoxic T lymphocytes induced by dendritic cells modified with truncated PSMA and 4-1BBL. *Hum. Vaccin. Immunother.* 9, 766–772. doi: 10.4161/hv.23116

Zaini, J., Andarini, S., Tahara, M., Saijo, Y., Ishii, N., Kawakami, K., et al. (2007). OX40 ligand expressed by DCs costimulates NKT and CD4+ Th cell antitumor immunity in mice. *J. Clin. Invest.* 117, 3330–3338. doi: 10.1172/jci32693

Zboralski, D., Hoehlig, K., Eulberg, D., Frömming, A., and Vater, A. (2017). Increasing tumor-infiltrating T cells through inhibition of CXCL12 with NOX-A12 synergizes with PD-1 blockade. *Cancer Immunol. Res.* 5, 950–956. doi: 10.1158/2326-6066.cir-16-0303

Zhang, P., Gao, F., Wang, Q., Wang, X., Zhu, F., Ma, C., et al. (2007). Agonistic anti-4-1BB antibody promotes the expansion of natural regulatory T cells while maintaining Foxp3 expression. *Scand. J. Immunol.* 66, 435–440. doi: 10.1111/j.1365-3083.2007.01994.x

Zhang, X., Voskens, C. J., Sallin, M., Maniar, A., Montes, C. L., Zhang, Y., et al. (2010). CD137 promotes proliferation and survival of human B cells. *J. Immunol.* 184, 787–795. doi: 10.4049/jimmunol.0901619

Zhou, Z., Kim, S., Hurtado, J., Lee, Z. H., Kim, K. K., Pollok, K. E., et al. (1995). Characterization of human homologue of 4-1BB and its ligand. *Immunol. Lett.* 45, 67–73. doi: 10.1016/0165-2478(94)00227-i

Conflict of Interest: The authors declare that the research was conducted in the absence of any commercial or financial relationships that could be construed as a potential conflict of interest.

frontiers in Cell and Developmental Biology

ORIGINAL RESEARCH
published: 15 July 2021
doi: 10.3389/fcell.2021.696373

Colorectal Cancer Cell-Derived Small Extracellular Vesicles Educate Human Fibroblasts to Stimulate Migratory Capacity

*Stefano Piatto Clerici[1], Maikel Peppelenbosch[2], Gwenny Fuhler[2], Sílvio Roberto Consonni[1] and Carmen Veríssima Ferreira-Halder[1]**

[1] Department of Biochemistry and Tissue Biology, Institute of Biology, University of Campinas, Campinas, Brazil,
[2] Department of Gastroenterology and Hepatology, Erasmus University Medical Center Rotterdam, Rotterdam, Netherlands

OPEN ACCESS

Edited by:
Rodrigo Nalio Ramos, INSERM U1138 Centre de Recherche des Cordeliers (CRC), France

Reviewed by:
Hocine R. Hocine, Memorial Sloan Kettering Cancer Center, United States
Lorena Martin Jaular, Institut Curie, France

***Correspondence:**
Carmen Veríssima Ferreira-Halder
carmenv@unicamp.br

Specialty section:
This article was submitted to Molecular Medicine, a section of the journal Frontiers in Cell and Developmental Biology

Received: *16 April 2021*
Accepted: *14 June 2021*
Published: *15 July 2021*

Citation:
Clerici SP, Peppelenbosch M, Fuhler G, Consonni SR and Ferreira-Halder CV (2021) Colorectal Cancer Cell-Derived Small Extracellular Vesicles Educate Human Fibroblasts to Stimulate Migratory Capacity. Front. Cell Dev. Biol. 9:696373. doi: 10.3389/fcell.2021.696373

Colorectal cancer (CRC) is in the top 10 cancers most prevalent worldwide, affecting equally men and women. Current research on tumor-derived extracellular vesicles (EVs) suggests that these small extracellular vesicles (sEVs) play an important role in mediating cell-to-cell communication and thus potentially affecting cancer progression *via* multiple pathways. In the present study, we hypothesized that sEVs derived from different CRC cell lines differ in their ability to reprogram normal human fibroblasts through a process called tumor education. The sEVs derived from CRC cell lines (HT29 and HCT116) were isolated by a combination of ultrafiltration and polymeric precipitation, followed by characterization based on morphology, size, and the presence or absence of EV and non-EV markers. It was observed that the HT29 cells displayed a higher concentration of sEVs compared with HCT116 cells. For the first time, we demonstrated that HT29-derived sEVs were positive for low-molecular-weight protein tyrosine phosphatase (Lmwptp). CRC cell-derived sEVs were uptake by human fibroblasts, stimulating migratory ability *via* Rho-Fak signaling in co-incubated human fibroblasts. Another important finding showed that HT29 cell-derived sEVs are much more efficient in activating human fibroblasts to cancer-associated fibroblasts (CAFs). Indeed, the sEVs produced by the HT29 cells that are less responsive to a cytotoxic agent display higher efficiency in educating normal human fibroblasts by providing them advantages such as activation and migratory ability. In other words, these sEVs have an influence on the CRC microenvironment, in part, due to fibroblasts reprogramming.

Keywords: colorectal cancer, small extracellular vesicles, tumor education, Lmwptp, cancer-associated fibroblast, tumor microenvironment

INTRODUCTION

Colorectal cancer (CRC) is the third most frequently diagnosed cancer type around the world, resulting in at least 800,000 related deaths occurring in 2018 (Bray et al., 2018). This makes CRC the fourth leading cause of cancer-related deaths in the world (Buccafusca et al., 2019). More than 40,000 new cases of CRC will affect the Brazilian population in 2020/22

(Instituto Nacional de Câncer José Alencar Gomes da Silva (INCA), 2019). CRC patients are expected to have a high life expectancy with an overall 5-year survival rate of 64.9%, but approximately 25% of CRC patients present metastatic events at distant organs resulting in chemoresistance, poor prognostic, and lower survival rate (Buccafusca et al., 2019).

The actual understanding of metastatic events revealed a process that involved many actors and complex cross talk between the cancer cells and their surrounding microenvironment, called tumor microenvironment (TME), which is constituted by a variety of multiple and heterogeneous populations of resident and infiltrating host cells (Hida et al., 2018; Gok Yavuz et al., 2019; Hinshaw and Shevde, 2019; Kobayashi et al., 2019), secreted factors, and extracellular matrix (Eble and Niland, 2019).

In the present study, we focused on two players that can be found in TME, cancer-associated fibroblasts (CAFs), and small extracellular vesicles (sEVs). sEVs are vesicles smaller than 200 nm, as defined according to Minimal Information for Studies of Extracellular Vesicles 2018 (Théry et al., 2019). CAFs are the major component of TME and support pro-tumoral actions related to tumor progression such as tumor growth, angiogenesis, tumor resistance, and immune suppression (Erez et al., 2010; Quail and Joyce, 2013; Borriello et al., 2017; Tao et al., 2017; Gok Yavuz et al., 2019; Kobayashi et al., 2019) and are now considered an attractive target for therapeutic approaches (Liu et al., 2019). sEVs derived from cancer cells appear as early players of microenvironment reprogramming through the transfer of oncogenic signaling pathway mediators from cancer cells to TME and distant cells *via* a process called tumor education (Kahlert and Kalluri, 2013; Milane et al., 2015; Zhao et al., 2016; Richards et al., 2017; Shephard et al., 2017; Zhang et al., 2018; Milman et al., 2019; Stefanius et al., 2021).

The present study highlights that the CRC cell line (HT29) that is less sensitive to death stimuli in comparison with HCT116 cells (Lopes-Costa et al., 2017; Attoub et al., 2018) produces higher amounts of sEVs, which have biological relevance regarding fibroblasts, as proved by an increase of migration and morphological changes. Accordingly, it was observed that Rho and FAK signaling pathways, which are key mediators of cytoskeletal reorganization, were modulated by the coculture of human fibroblasts with CRC cell-derived sEVs. Of great interest, low-molecular-weight protein tyrosine phosphatase (Lmwptp) was found to be part of cargoes of CRC cell-derived sEVs. This observation opens new avenues regarding the molecular mechanism by which this phosphatase gives an advantage to CRC cells.

MATERIALS AND METHODS

Cells and Culture Conditions

Colorectal cancer cells (HCT116 and HT29) were purchased from the Rio de Janeiro Cell Bank (Rio de Janeiro, RJ, Brazil). HCT116 and HT29 cells were cultured in McCoy's 5A medium containing 100 U/ml penicillin, 100 μg/ml streptomycin, and 10% fetal bovine serum (FBS) at 37°C in a humidified 5% carbon dioxide atmosphere. Human normal skin fibroblasts were kindly donated by Dr. Gustavo Facchini from Kosmoscience Group (Campinas, Brazil) and cultured in Dulbecco's modified Eagle medium (DMEM) with high glucose, 100 U/mL penicillin, 100 μg/ml streptomycin, and 15% FBS at 37°C in a humidified 5% carbon dioxide atmosphere. The medium was changed every 3 days for CRC cells and twice a week for fibroblasts. Cells were *Mycoplasma* spp.-free.

Small Extracellular Vesicles Isolation

HCT116 and HT29 cells were plated in T75 flasks (5×10^4 cells/cm^2) and grown in a complete medium for 48 h until they reached approximately 85–95% confluence. After, cells were washed three times with 0.22-μm filtered PBS and incubated with McCoy's 5A culture medium without FBS for the following 24 h. After that, the conditioned medium was collected. Conditioned medium was precleared by centrifugation at 4,000 × *g* for 30 min to remove cell debris. The supernatant was filtered through 0.22-μm filtered PBS and concentrated 30× using a Vivaspin Turbo 15 10,000 MWCO (Sartorius, United Kingdom) filter capsule by centrifugation at 4,000 × *g* for 15 min. After that, the concentrates were centrifuged at 15,000 × *g* for 20 min to remove microvesicles (Patel et al., 2019). Next, 0.5 v:v of Total Exosome Reagent (Thermo Fisher Scientific, MA, United States) was added to the concentrated medium and incubated overnight at 4°C under agitation. Next, samples were centrifuged at 10,000 × *g*, 4°C for 1 h. The fraction of pelleted sEVs was washed in 0.22-μm filtered PBS followed by the second step of 10,000 × *g* centrifugation at 4°C for 1 h. Pelleted sEVs were resuspended in 100 μl of 0.22-μm filtered PBS. The remaining cells (EVs donor cells) were scraped and lysed for Western blotting, as described in the following section. We have submitted all relevant data to the EV-TRACK knowledgebase (EV-TRACK ID: EV210162; Van Deun et al., 2017).

Nanoparticle Tracking Analysis

Estimated concentration and size distribution of nanoparticles in purified isolated sEV samples were determined by nanoparticle tracking analysis using a NanoSight NS300 instrument (Amesbury, United Kingdom) equipped with a 405-nm laser. Each sEV fraction was diluted 1:100 in 0.22-μm filtered PBS to obtain a concentration within the range from 10^7 to 10^{10} particles/ml. Five different videos of 30 s were recorded for each sample. The temperature was monitored and set at 25°C throughout the measurements. Videos recorded for each sample were analyzed with the NanoSight software version 2.3. For analysis, auto settings were used for blur, screen gain 4, camera level 14, and detection threshold 3.

Transmission Electron Microscopy

Transmission electron microscopy (TEM) was conducted by the Electron Microscopy Laboratory of the Institute of Biology, University of Campinas. Four microliters of aliquots of resuspended sEVs were applied on 0.5-cm^2 glow-discharged Formvar/carbon-coated electron microscopy grids and allowed to adsorb at room temperature until a thin-layer film remained.

To contrast the samples, grids were transferred to 2% uranyl acetate for 5 min. Grids were left to dry and stored in appropriate grid storage boxes, then observed under an LEO 906 transmission electron microscope (Carl Zeiss, Germany) at 60 kV.

Lipophilic Labeling of Colorectal Cancer Cell-Derived Small Extracellular Vesicles and Uptake Visualization

Colorectal cancer cell-derived sEVs were fluorescently labeled with PKH26 (Sigma-Aldrich, United States), as described by Torreggiani et al. (2014) with minor modifications. Briefly, sEVs (2 μg resuspended in 10 μl of filtered PBS) or an equal volume of filtered PBS were added to 50 μl of Diluent C. One microliter of PKH26 dye was added to 50 μl of Diluent C before being added to the sEVs and the control. Samples were mixed gently and maintained for 15 min at 37°C before 100 μl of 1% bovine serum albumin (BSA) were added to bind the excess of dye. Samples (PKH26-sEVs and PKH26-PBS control) were then filtered through Exosome Spin Columns (MW3000, Invitrogen, Thermo Fisher, United States) following the manufacturer's instructions. Human fibroblasts (1×10^4 cells) were cultured in glass coverslips in wells of a 24-well plate. Cells were serum harvested for the next 24 h, and then, PKH26-labeled CRC cell-derived sEVs (2 μg resuspended in 50 μl of DMEM serum-free) or the same volume of PKH26-PBS control were added to the cells for 6, 24, and 48 h. Cells were then washed with PBS and analyzed by fluorescent microscopy. Nuclei were stained with 4′,6-diamidino-2-phenylindole. After 48 h, cells were fixed with 4% paraformaldehyde for 10 min. Actin fibers were stained with ActinGreen 488 (Thermo Fisher, United States) following the manufacturer's instructions before imaging by Cytation5 (BioTek Instruments).

Cell Motility

In vitro cell migration was performed by classical wound healing assay and transwell migration assay. Wound healing assay was performed following a methodology described by Jana and Trivedi (2018). Human normal fibroblasts (1×10^4 cells) were seeded in a 24-well plate to form a monolayer. Cells were serum harvested for the next 24 h. A scratch was generated using a micropipette tip, and cells were washed with PBS to remove cell debris. Purified CRC cell-derived sEVs (2 μg/ml) in serum-free medium or vehicle (PBS) were added to normal human fibroblasts, and wound healing was monitored by capturing images with Lumascope 620 (Etaluma, Inc) for 24 and 48 h. *In vitro* cell migration assays were performed in a 24-well transwell plate with 8-μm polycarbonate membrane filters (Corning) separating the lower and upper culture chambers. Human fibroblasts were grown to subconfluence. After detachment with trypsin, cells were washed with PBS and resuspended in a serum-free medium, after which the cell suspension (1×10^5 cells) was added to the upper chamber. Purified CRC cell-derived sEVs (2 μg/ml) in serum-free medium or vehicle (PBS) were added to both upper and lower chambers. Cells were maintained in culture conditions for 48 h. The cells that had not migrated were removed from the upper face of the filters using cotton swabs, and the cells that had migrated to the lower face of the filters were fixed with 4% paraformaldehyde for 15 min at room temperature and then permeabilized by 100% methanol for 15 min at room temperature. Cells that had migrated were stained with 0.5% crystal violet solution for 30 min at room temperature. Images of at least five random fields were captured from each membrane using a × 10 objective (Lumascope 620, Etaluma), and the number of migratory cells was counted. All values are representative of at least two independent experiments.

Signaling Pathway Analysis

Human fibroblasts (5×10^5 cells) were seeded in 100-mm dishes and maintained in culture conditions for 24 h. Next, cells were serum harvested for the following 24 h. Then, cells were co-cultured with purified CRC cell-derived sEVs (2 μg/ml) or equal amounts of PBS for 15 min, 1, 6, 24, and 48 h. Western blotting analysis was performed as described in the next session.

Western Blotting Analysis

Standard Western blotting was performed according to a published paper (Ferreira et al., 2004) by our group with modifications in the sample preparation steps. Extracellular vesicle (EV)-specific protein markers and non-EV markers in the isolated vesicles and donor cells were examined by Western blotting as also signaling pathway mediators analysis in human fibroblasts co-cultured with CRC cell-derived sEVs. Briefly, CRC cells and human fibroblasts were washed 3× with PBS, scraped, and lysed in a radioimmunoprecipitation assay buffer containing a protease and phosphatase inhibitor for 2 h on ice. Protein extracts were cleared by centrifugation at 14,000 × *g* for 10 min (Hettich Universal 320R, Germany). Pelleted sEVs were directly lysed by radioimmunoprecipitation assay buffer. Protein concentration was determined using the microBCA kit (Thermo Fisher Scientific, MA, United States). A sample buffer (100-mM Tris-hydrochloride pH 6.8, 200-mM β-mercaptoethanol, 4% sodium dodecyl sulfate, 0.1% bromophenol blue, and 20% glycerol) was added to the samples in a 1:1 ratio, and samples were boiled for 10 min. To the sEVs' samples, a sample buffer under reducing and non-reducing conditions was added (1:1 ratio). For CRC cells, 20 μg of proteins were used; for human fibroblasts, 10 μg of proteins were required, whereas, for EVs characterization, 20 μg of lysed EVs were required. Proteins were applied to sodium dodecyl sulfate–polyacrylamide gel electrophoresis gel (10–12%) and transferred to PVDF membranes. Blocked membranes [3% BSA in Tris–buffered saline (TBS)-Tween 20 (0.05%)] were incubated overnight with specific antibodies at 1:1,000 dilution. After the washing steps in TBS-Tween 20 (0,05%), membranes were incubated with appropriate horseradish peroxidase (HRP)-conjugated secondary antibodies at 1:10,000 dilution in 1% BSA in TBS-Tween 20 (0.05%) for 3 h. Immunoblots were detected by chemiluminescence in Alliance 6.7 (UVITEC, Cambridge, United Kingdom). The following primary antibodies were used: anti-Alix mouse monoclonal (#2171, Cell Signaling); anti-Hrs rabbit monoclonal (#15087, Cell Signaling); anti-Lamp1 rabbit monoclonal (#9091, Cell Signaling); anti-Lamp2

rabbit monoclonal (#49067, Cell Signaling); anti-Lmwptp mouse monoclonal (sc390190, Santa Cruz); anti-Rab11 rabbit monoclonal (#5589, Cell Signaling); anti-Rab27A rabbit monoclonal (#95394, Cell Signaling); anti-Rab27B rabbit polyclonal (GTX64616, GeneTex); anti-Rab5 rabbit monoclonal (#3547, Cell Signaling); anti-Rab7 rabbit monoclonal (#9367, Cell Signaling); anti-Stam2 rabbit monoclonal (#53674, Cell Signaling); anti-Tsg101 rabbit polyclonal (GTX118736, GeneTex); anti-Gm130 rabbit monoclonal (#12480, Cell Signaling); anti-Cd81 mouse monoclonal (GTX43505, GeneTex); anti-α-Tubulin rabbit polyclonal (#2144, Cell Signaling); anti-β-Actin mouse monoclonal (sc47778, Santa Cruz); anti-phospho-Fak (Tyr397; #8556, Cell Signaling); anti-GAPDH (#2118, Cell Signaling); anti-Rock1 rabbit monoclonal (#4035, Cell Signaling); anti-Src rabbit monoclonal (#2123, Cell Signaling); anti-phospho-Src (Tyr527) rabbit polyclonal (#2105, Cell Signaling); anti-RhoA rabbit monoclonal (#2117, Cell Signaling); anti-RhoC rabbit monoclonal (#3430, Cell Signaling); and anti-Rac family rabbit monoclonal (#2465, Cell Signaling). Also, the following secondary antibodies were used: anti-mouse IgG/HRP conjugated (#7076, Cell Signaling) and anti-rabbit IgG/HRP conjugated (#7074, Cell Signaling).

Fibroblast Activation Assay for α-Smooth Muscle Actin

Activation of normal human fibroblasts with CRC cell-derived sEVs was performed as described by Rai et al. (2019). Briefly, fibroblasts were seeded in glass coverslips (4×10^4 cells) and maintained for 24 h in 400 μl of DMEM high glucose with 15% of EV-depleted FBS (Thermo Fisher, United States). Cells were treated with CRC cell-derived sEVs (10 μg/ml) or vehicle (PBS) for a further 48 h. Cells were then analyzed for α-smooth muscle actin (α-SMA) expression using immunofluorescence assay.

Immunofluorescence

Immunofluorescence was performed as previously described (Faria et al., 2020) with modifications. Cells were cultured on a glass coverslip on a 24-well plate. Briefly, cells were fixed in 100% methanol for 15 min at 4°C, washed in PBS, and then permeabilized using 0.1% de Triton X-100 in PBS for 15 min at room temperature. Cells were then washed in PBS and blocked with 1% BSA, glycine (22.52 mg/ml) in PBS for 1 h at room temperature. Next, cells were incubated with primary antibody (rabbit anti-α-SMA, 1:100; Cell Signaling; #19245) in 1% BSA and 0.3% Triton X-100 in PBS overnight at 4°C. Coverslips were incubated with secondary antibody (1:500) Alexa Fluor Rabbit 488 (Thermo Fisher Scientific, MA, United States) in 1% BSA and 0.3% Triton X-100 in PBS for 3 h at room temperature in the dark. Nuclei were stained with 4′,6-diamidino-2-phenylindole. Cells were imaged using Lumascope 620 (Etaluma, Inc.).

Statistical Analysis

Results were expressed as mean ± standard error of the mean. Statistical analysis was assessed using Student's *t*-test between only two groups. One-way analysis of variance was performed with multiple groups. $P < 0.05$ is considered to be statistically significant. $^{*}P < 0.05$, $^{**}P < 0.01$, and $^{***}P < 0.001$. All data were analyzed using GraphPad Prism Software, version 5.0.

RESULTS

Colorectal Cancer Cell Lines With Different Sensitivity to Cytotoxic Agents Display Different Efficiency in Small Extracellular Vesicle Production

We firstly focused on the characterization of EVs for size and purity (**Figure 1**), which was demonstrated by TEM that these vesicles displayed a compatible and expected morphology for sEVs (**Figure 1A**). Nanoparticle tracking analysis was used to characterize the size and estimated concentration (number particles/milliliter) of CRC cell-derived EVs. As shown in **Figures 1B,C**, the isolation protocol applied in this study, which is based on ultrafiltration and polymeric precipitation, purified a heterogeneous population of nanoparticles with mean diameters of 135.850 ± 31.250 and 140.200 ± 13.400, respectively, and a mean mode values of 109.650 ± 7.750 and 104.900 ± 4.200 for HCT116 and HT29, respectively. According to the Minimal Information for Studies of Extracellular Vesicles 2018 (Théry et al., 2019) and to a previous study (Patel et al., 2019) showing a mixture of different vesicle types isolated by this commercial isolation reagent, the use of the term sEVs to describe vesicles smaller than 200 nm was used. A significantly higher concentration of sEVs was released by HT29 as compared with HCT116: $2.090 \times 10^{10} \pm 1.518 \times 10^{9}$ *vs.* $1.223 \times 10^{10} \pm 1.453 \times 10^{9}$ particles/ml ($p = 0.0021$; **Figure 1D**) even if we analyzed the ratio number of particles per cells: 214 ± 38 *vs.* 81 ± 10 ($p = 0.007$; **Figure 1E**). In addition, we observed that a Western blot analysis was used to identify the presence or absence of a selection of EVs and non-EVs markers to confirm the efficiency of our isolation protocol and the purity of the isolated vesicles. sEVs are characterized by the enrichment of transmembrane proteins associated with the plasma membrane and/or endosomes such as tetraspanins (Cd9, Cd63, and Cd81) and cytosolic proteins recovered in EVs named Alix and Tsg101. Our results showed that CRC cell-derived sEVs were positive for Cd81 and Tsg101 markers and negative for non-EV marker Gm130 (Golgi marker), confirming an enrichment in sEVs in the samples (**Figure 1E**). We also observed that Lmwptp is a cargo of HT29-sEVs.

Colorectal Cancer Cell Lines Display Different Levels of Small Extracellular Vesicle Biogenesis Mediators

Based on the difference in sEV production by CRC cell lines, we then analyzed the protein profile of HCT116 and HT29 at proteins involved in EV biogenesis and transport. HT29 cells displayed a higher amount of lysosomal proteins, Lamp1, Lamp2, and Src protein (**Figures 2A,B**). It was also observed low intracellular levels of Tsg101, Alix, Hrs, and Stam2 in HT29 compared with HCT116 (**Figure 2B**). Rab5 and Rab7, components of early and late endosomes, were lower expressed

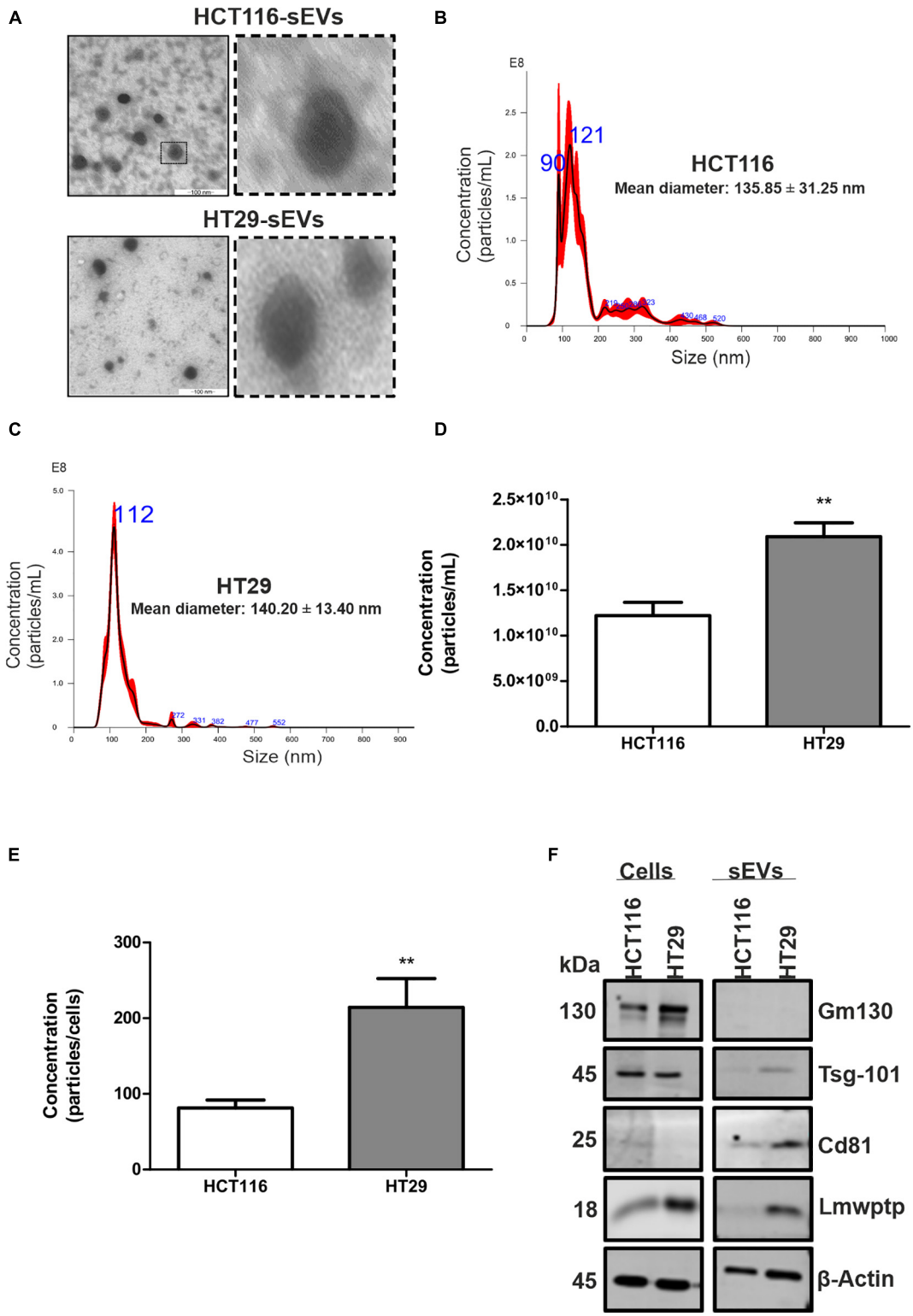

FIGURE 1 | Characterization of sEVs derived from HCT116 and HT29 cells. **(A)** Transmission electron microscopy micrographs of sEVs derived from HCT116 and HT29 cells depicting cup-shaped morphology. Scale bar: 100 nm. Representative graphs illustrating size distribution of sEVs from HCT116 **(B)** and HT29 **(C)** measured by nanoparticle tracking analysis. **(D)** Particle concentration measured by nanoparticle tracking analysis from HCT116- and HT29-derived sEVs. **(E)** Ratio of particle concentration and number of cells. **(F)** Representative images of Western blotting analysis from HCT116 and HT29 whole cell lysates and sEVs isolated from conditioned medium obtained from these cells, showing enrichment of EV markers and absence of non-EVs markers. Lmwptp is a cargo of HT29-derived sEVs ($N = 3$). All values are displayed as mean ± SEM, where $^{**}P < 0.01$, assessed with Student *t*-test.

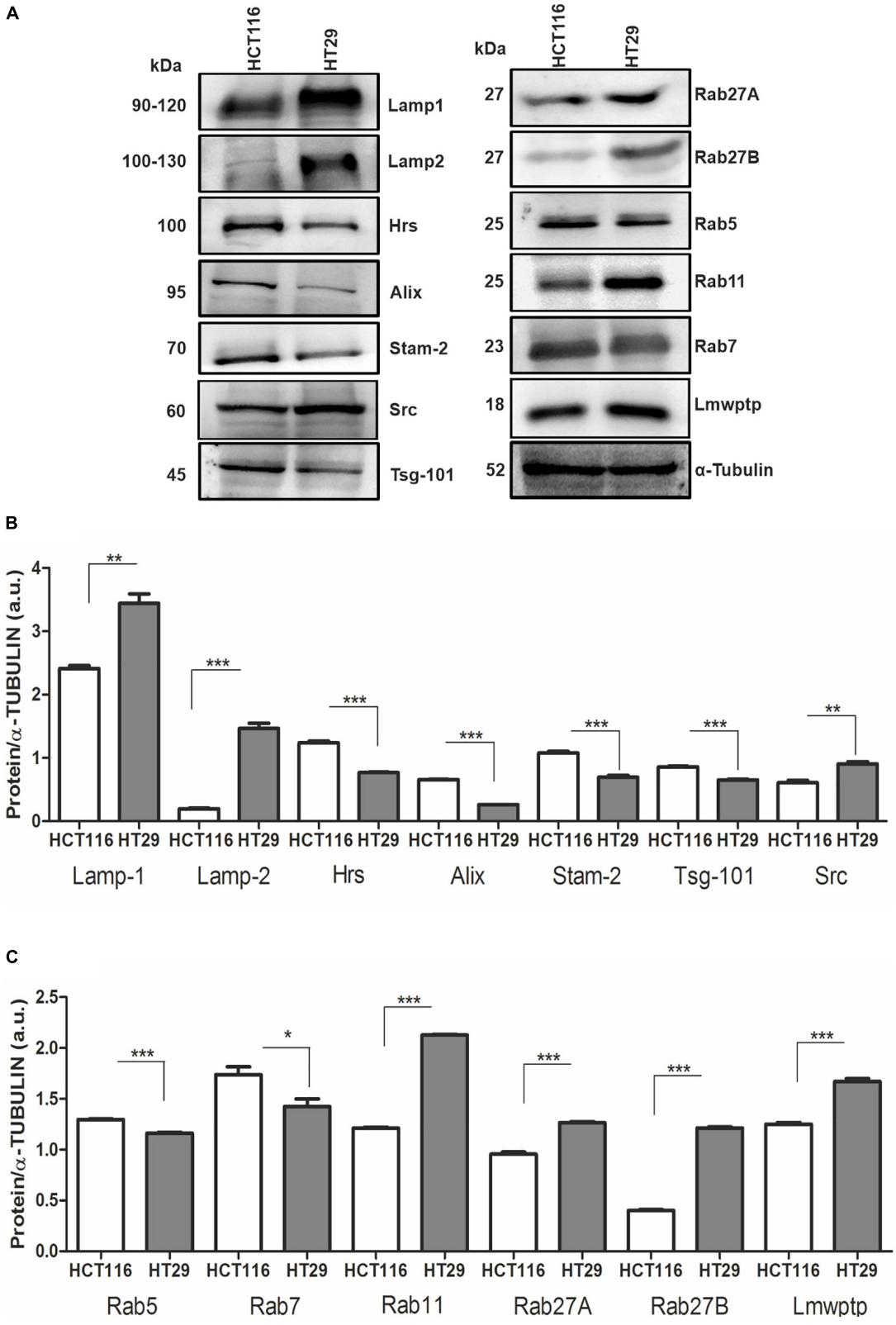

FIGURE 2 | Protein profile from HCT116 and HT29-sEV donor cells. **(A)** Representative images of Western blotting analysis performed for the indicated proteins. α-Tubulin serves as a loading control. **(B,C)** Densitometry values were corrected for loading controls. ($N = 3$ independent experiments). Values are represented as mean ± SEM. $^{*}P < 0.05$, $^{**}P < 0.01$, and $^{***}P < 0.001$, assessed with Student *t*-test.

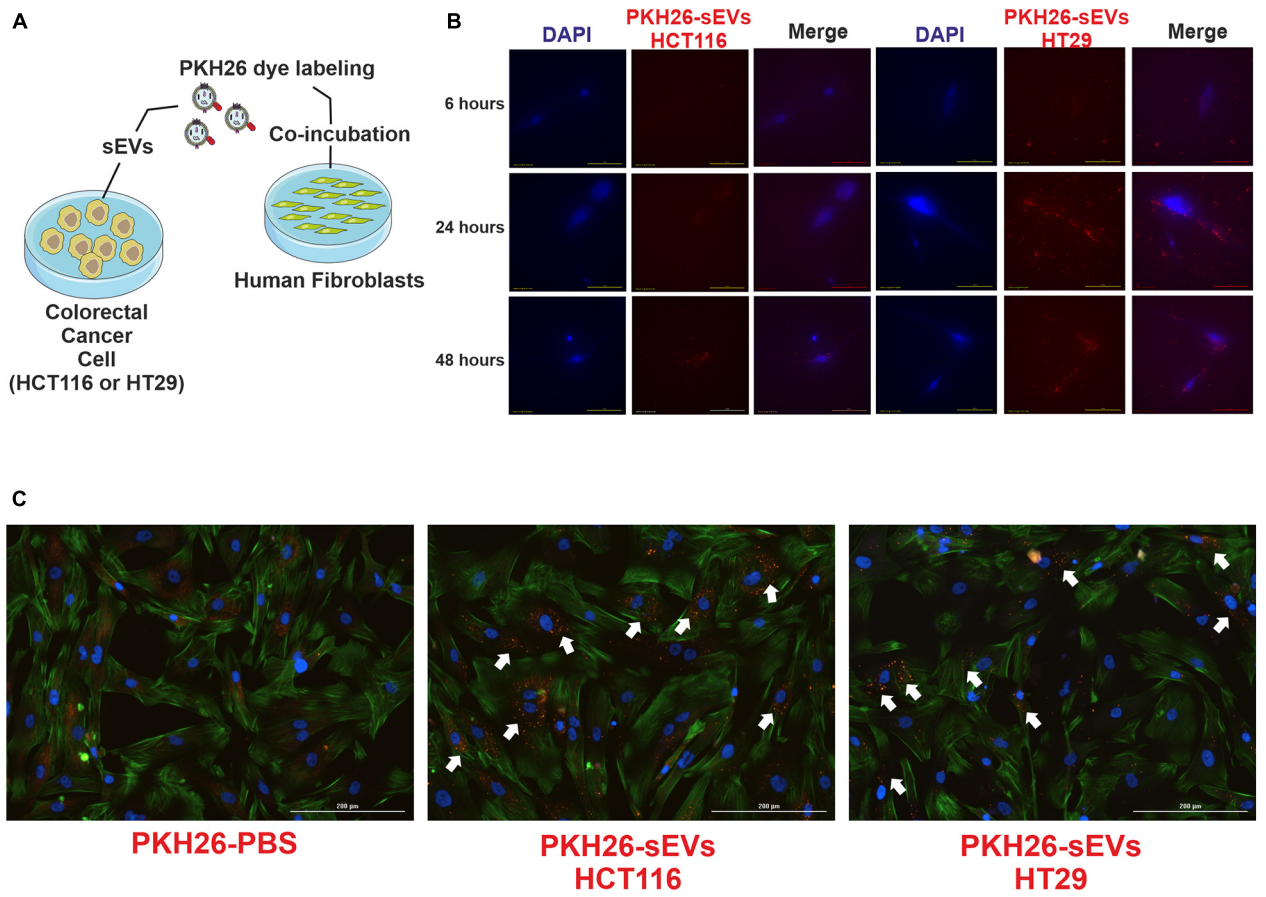

FIGURE 3 | HCT116 and HT29 cell-derived sEVs were uptake by human fibroblasts. **(A)** Schematic diagram of experimental procedures. CRC cell-derived sEVs labeled with PKH26 were added to culture media of human fibroblasts. **(B)** Fluorescent microscopic analysis of normal human fibroblasts incubated with PKH26-stained HCT116-sEVs or HT29-sEVs (2 μg, 6, 24, and 48 h; red). Nuclei were stained with 4′,6-diamidino-2-phenylindole (blue). Scale bar: 100 μm. **(C)** Representative images of human fibroblasts incubated for 48 h with PKH26-stained HCT116-sEVs or HT29-sEVs (2 μg, red); nuclei were stained in blue and actin in green (ActinGreen 488, Thermo Fisher). Scale bar: 100 μm.

in HT29 compared with HCT116 (**Figure 2C**). Rab proteins related to EV trafficking, such as Rab11, Rab27A and Rab27B, were significantly enriched in HT29 compared with HCT116 (**Figure 2C**). Taken together, these expression patterns suggest a differential secretion of EVs subtypes in HT29 cells.

Small Extracellular Vesicles Released by Colorectal Cancer Cells Are Readily Uptake by Normal Human Fibroblasts

Cancer progression is dependent on the crosstalk between tumor cells and the microenvironment, which is enriched in sEVs that are effective on cell-to-cell communication. Then, we investigated the effect of CRC cell-derived sEVs on normal human fibroblasts, expecting to identify a tumor education process mediated by CRC cell-derived sEVs. To demonstrate uptake by fibroblasts (recipient cells), HCT116- and HT29- (donor cells) derived sEVs were labeled with lipophilic tracer PKH26 and incubated with normal human fibroblasts (**Figure 3**). The tracking of the probe using fluorescence microscopy revealed that both CRC cell-derived sEVs were uptake by normal human fibroblasts within 6 h (**Figure 3B**), and this uptake remained active until at least 48 h of co-incubation (**Figure 3C**).

Colorectal Cancer Cell-Derived Small Extracellular Vesicles Educate Human Fibroblasts and Stimulate Migration

The effects of CRC cell-derived sEVs on the migration properties of normal human fibroblasts were confirmed by classical wound healing assay and Transwell system (**Figure 4**). Scratch assay results showed that both CRC cell-derived sEVs significantly promoted cell migration in 24 and 48 h, which is confirmed by counting the migrated cells to the wound area compared with the PBS group. Interestingly, HT29-derived sEVs promoted the most significant improvement in cell migration (**Figures 4B,C**). CRC cell-derived sEVs were used as a chemoattractant in a Transwell migration assay to evaluate the ability of normal human fibroblasts to migrate through a pore membrane. Transwell migration assay

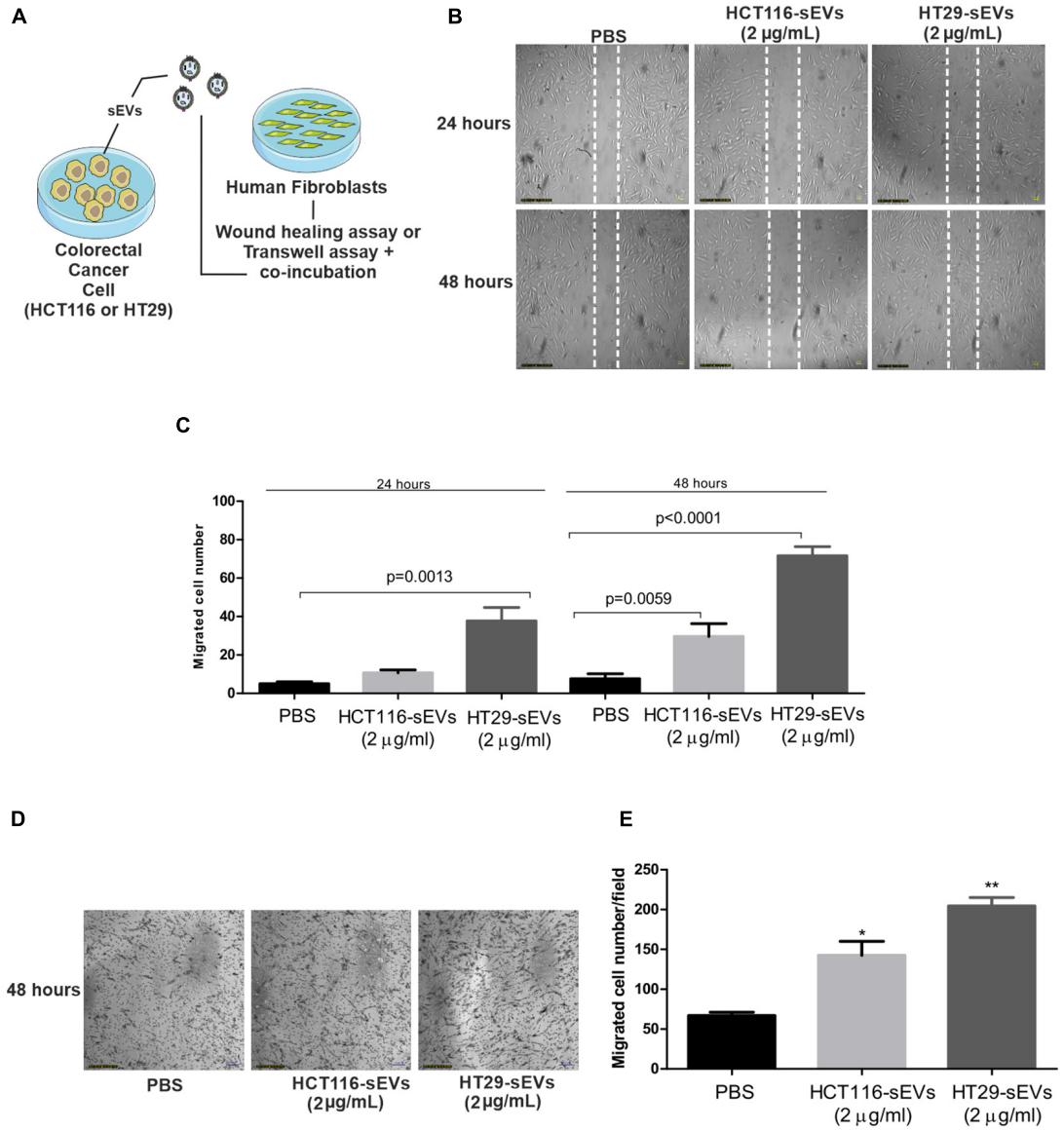

FIGURE 4 | sEVs increase human fibroblast cell migration. **(A)** Schematic diagram of experimental procedures. For wound healing assay, 1×10^4 human fibroblasts were cultured and serum-starved for 24 h. Scratch was made using a pipette tip, and cells were exposed to HCT116 and HT29 cell-derived sEVs (2 µg/ml) or vehicle (PBS) for 24 and 48 h. **(B)** Representative photographs of wound healing assay. **(C)** Quantification of migrated cells. For Transwell assay, human fibroblasts (1×10^5) were incubated for 48 h with HCT116 and HT29 cell-derived sEVs (2 µg/ml) or vehicle (PBS) in serum-free medium. Treatments were incubated both in upper and lower chambers. After 48 h of incubation, migration activity was quantified by counting migrated cells on lower surface of membrane of at least five fields per chamber of a Transwell using a ×10 objective. **(D)** Representative photographs of Transwell migration assay. **(E)** Quantification of migrated cells. All values are representative of mean of at least two independent experiments with similar results and are displayed as mean ± SEM, where $^*P < 0.05$ and $^{**}P < 0.01$, assessed with Student *t*-test.

(**Figures 4D,E**) indicated that the number of traversed fibroblasts significantly increased with both CRC cell-derived sEVs at 48 h compared with the PBS group, but importantly, it was much more intense when the chemoattractant was HT29-derived sEVs (**Figure 4E**). It is important to mention that the effect of sEVs in stimulating migration is independent of fibroblast proliferation, observed by BrdU incorporation after 48 h of sEVs co-incubation with human fibroblasts (**Supplementary Figure 1**).

Colorectal Cancer Cell-Derived Small Extracellular Vesicles Stimulate Rho-Mediated and Focal Adhesion Signaling

Since it was shown that sEVs from CRC cells were transferred to normal human fibroblasts and stimulated their migration, we examined the relevance of this transference under molecular context, up to 48 h after co-incubation (**Figure 5A**). Cellular

migration is dependent on the strict regulation of assembly and disassembly of focal adhesion sites. The process is mediated by the FAK-Src complex and downstream substrates and regulated by phosphorylation of tyrosine residues of FAK and Src, controlling activation or inhibition. Based on these data, we next examine the underlying mechanism of this enhanced migration, as we can see in **Figure 4**. It was detected that the amount of Src kinase and its phosphorylated form (Tyr527) dropped in fibroblasts co-incubated with CRC cell-derived sEVs compared with zero point, especially after 48 h of co-incubation by both CRC cell-derived sEVs (**Figures 5B,C**).

We then analyzed Rho GTPase family proteins. We observed reduced expression of Rho-associated protein kinase (Rock1) in human fibroblasts co-incubated with both CRC cell-derived sEVs (**Figures 5B,C**), especially after 48 h of co-incubation. RhoA and RhoC presented a similar profile in fibroblasts co-incubated with both CRC cell-derived sEVs. RhoA was elevated at 15 min after co-incubation with HCT116-derived sEVs. Although not reaching statistical significance, we observed a trend toward a reduced expression of RhoA after 24 and 48 h in those fibroblasts co-incubated with HCT116-derived sEVs. RhoC expression did not display significant alterations in those fibroblasts treated with HCT116-derived sEVs. On the other hand, RhoA and RhoC were significantly increased after 24 h of co-incubation with HT29-derived sEVs following a trend toward the reduced expression of RhoA and RhoC in human fibroblasts coculture with HT29-derived sEVs (**Figures 5B,C**). Rac family was reduced in fibroblasts co-incubated with HCT116-derived sEVs after 24 h, whereas no statistical significance was observed in fibroblasts co-incubated with HT29-derived sEVs.

As seen in **Figure 5D**, CRC cell-derived sEVs induce morphology changes of human fibroblasts after 24 and 48 h of co-incubation under a light microscope. Our analysis revealed a significant reduction of FAK Tyr397 phosphorylation in human fibroblasts co-incubated with both HCT116- and HT29-derived sEVs in 24 and 48 h compared with the non-treated fibroblasts (**Figures 5E,F**), thus suggesting an involvement of Rho-FAK signaling.

Normal Human Fibroblasts Acquire Cancer-Associated Fibroblasts Phenotype by Coculture With Colorectal Cancer Cell-Derived Small Extracellular Vesicles

The morphological changes of fibroblasts triggered by HCT116- and HT29-derived sEVs prompted us to investigate whether these cells were also activated by monitoring α-SMA. Although there are several markers, α-SMA that assembles into contractile filamentous stress fibers running longitudinally, is routinely used as a marker of CAFs.

To confirm CAF activation, we maintained normal human fibroblasts in culture in the presence of culture medium with EV-depleted FBS, and then, we co-incubated 10 μg/ml of CRC cell-derived sEVs for 48 h (**Figure 6A**). Fluorescent microscopy revealed that both HCT116-derived sEVs and HT29-derived sEVs induced expression of α-SMA filamentous structures in human fibroblasts (**Figure 6B**). In contrast, vehicle-treated control human fibroblasts supported only sparse α-SMA filaments. This suggests that CRC cell-derived sEVs, but more robust with HT29-derived sEVs, are capable of triggering activation of normal human fibroblasts.

DISCUSSION

In recent years, our knowledge regarding sEVs and their role in health and disease have increased drastically. As these vesicles carry a broad spectrum of bioactive molecules, they can communicate with local and distant cells (Valadi et al., 2007; Peinado et al., 2012; Colombo et al., 2014; Rai et al., 2019) and subsequently change the metabolism of these cells (Costa-Silva et al., 2015; Zhao et al., 2016; Zhang et al., 2018). sEVs have emerged as key players in different steps of cancer progression, including invasion, the acquisition of resistant phenotypes, and TME reprogramming (Kahlert and Kalluri, 2013; Chen et al., 2014; Minciacchi et al., 2015; Lugini et al., 2016; Wortzel et al., 2019; Stefanius et al., 2021). Therefore, in the present study, we questioned whether sEVs released by different CRC cell lines could have the same capacity to educate normal human fibroblasts.

Firstly, it was observed that the concentration of EVs produced by HT29 cells was higher compared with HCT116 ones, which was in accordance with molecular markers of biogenesis of these vesicles. It is well known that some tetraspanins, as Cd81 and ESCRT proteins such as Tsg101, are EV-specific markers and are commonly used for EV characterization (Théry et al., 2019). In the present study, the CRC cell-derived EVs were Cd81 and Tsg101 positive with a size smaller than 200 nm. We decided to refer to them as sEVs because the commercial isolation reagent may isolate a mixture of different EVs subtypes (Patel et al., 2019). Furthermore, the vesicle incorporation by normal human fibroblasts cells was confirmed by PKH26 staining, indicating that sEVs could potentially mediate cell-to-cell communication, transferring tumor information from CRC donor cells to normal human fibroblasts (recipient cells).

The literature has shown that tumoral exosomes are able to activate fibroblasts to CAFs. Goulet et al. (2018) studied bladder exosomes that are internalized by normal fibroblasts. The authors observed activation of these fibroblasts revealed by enhanced proliferation and migratory capacity accompanied by a high α-SMA gene expression. In concordance, Zhou et al. (2018) observed that murine fibroblasts have 3T3 internalized PKH26 dye-labeled melanoma-derived exosomes.

In the CRC context, a study conducted by Rai et al. (2019) showed that two distinct CRC cells that release exosomes with differential metastatic capacity could induce different changes in human fibroblasts reprogramming. Both SW480-exos and SW620 induce CAF activation by measuring α-SMA fluorescence. The co-incubation of quiescent fibroblasts with SW480-exos induces high proliferative ability and the secretion of pro-angiogenic factors, whereas the co-incubation of quiescent fibroblasts with SW620-exos induces invasive capacity due to

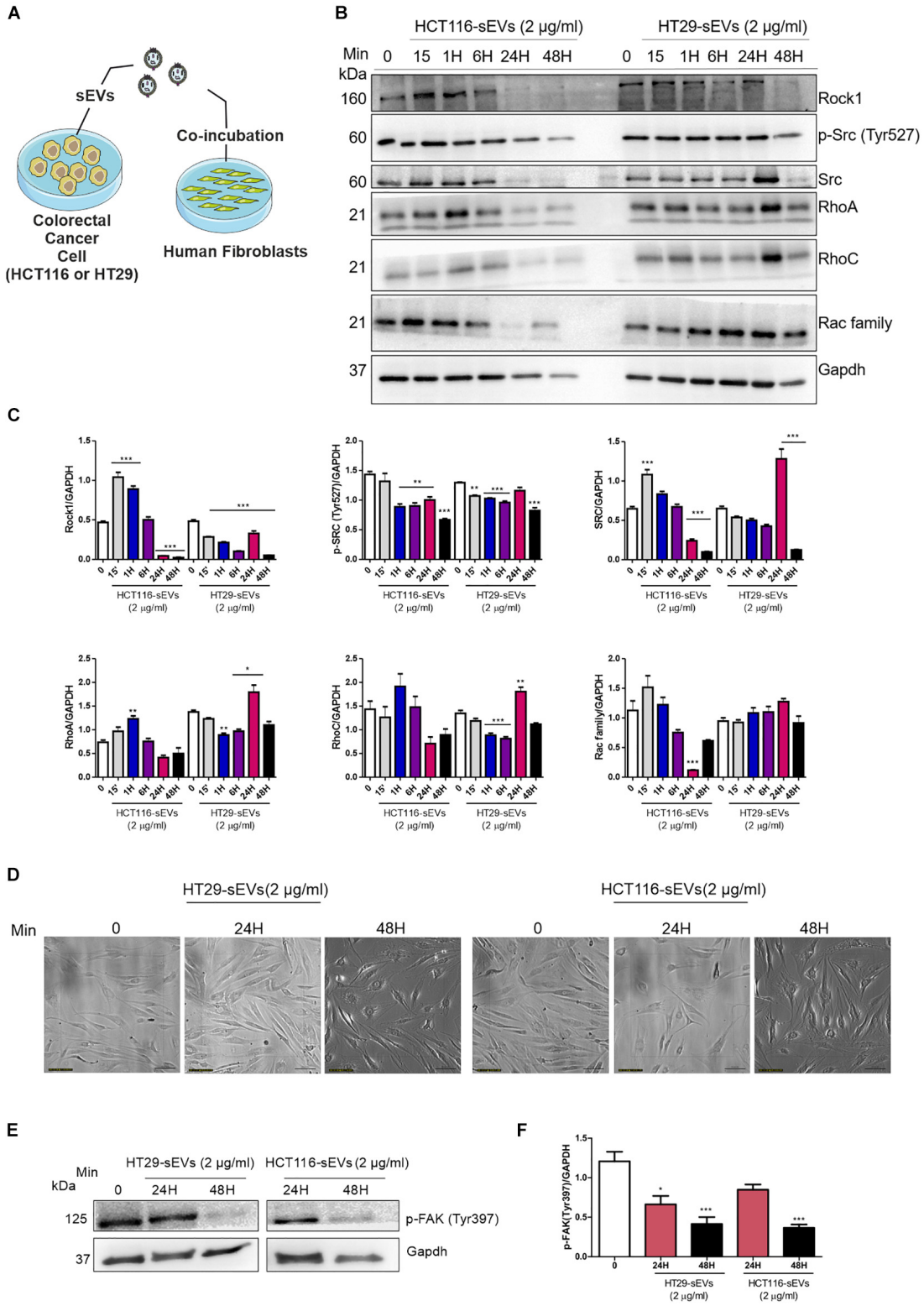

FIGURE 5 | Western Blotting analysis. **(A)** Schematic diagram of the experimental procedures. Human fibroblasts were exposed to one dose of 2 µg/ml of HCT116 and HT29 cell-derived sEVs for 15 min, 1, 6, 24, and 48 h as indicated or vehicle (PBS $t = 0$). **(B,E)** Western blot was used to analyze cell lysates with the indicated antibodies. GAPDH serves as a loading control. **(C,F)** Densitometry values were corrected for loading controls. ($N = 3$ independent experiments). Values are represented as mean ± SEM. $^{*}P < 0.05$, $^{**}P < 0.01$, and $^{***}P < 0.001$, assessed with one way-ANOVA followed by Tukey post-test. **(D)** Bright field representative images of human fibroblast exposed to HCT116 and HT29 cell-derived sEVs followed each treatment time. Scale bar: 100 µm.

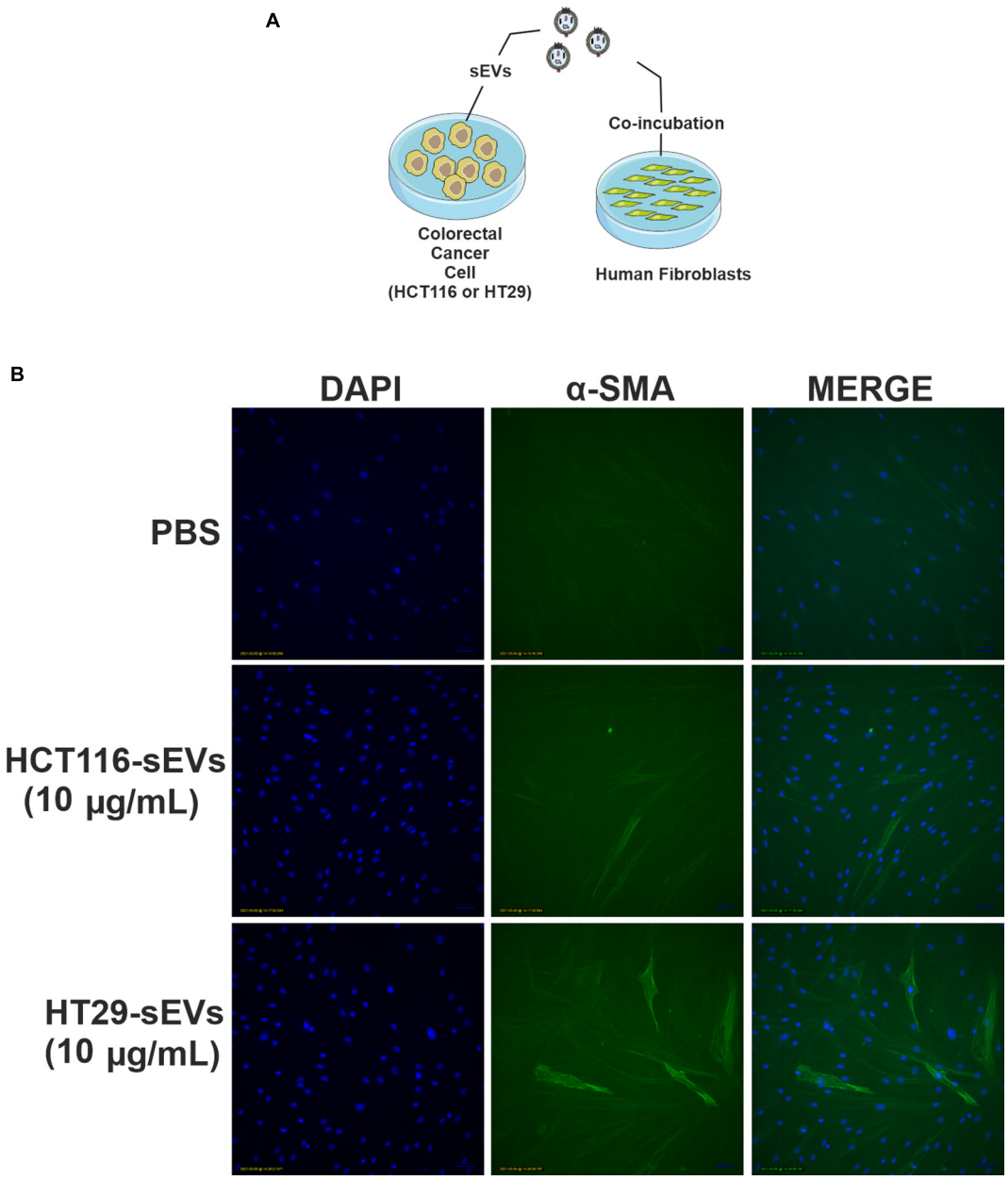

FIGURE 6 | HCT116 and HT29 cell-derived sEVs activate and transform human fibroblasts. **(A)** Schematic diagram of the experimental procedures. **(B)** Fluorescent microscopic analysis of α-SMA (green) expression in human fibroblasts exposed to HCT116 and HT29 cell-derived sEVs (10 μg/ml) or vehicle (PBS) for 48 h. Nuclei were stained with 4′,6-diamidino-2-phenylindole (blue). Scale bar: 100 μm.

the high expression of MMP11, which are able to remodel the extracellular matrix.

We observed an internalization by normal human fibroblasts of PKH26-labeled CRC (HT29 and HCT116 cells)-derived sEVs that culminated in cell migration advantage, which was higher in the case of HT29-derived sEVs. We also have identified that both CRC cell-derived sEVs can activate normal human fibroblasts through the augmented fluorescence of α-SMA in fibroblasts, especially to a greater extent in those co-incubated with HT29-derived sEVs. Our results support the premise that CRC cell-derived sEVs are important players in inducing changes in the fibroblasts' morphology and inducing migration (**Figures 7A,B**).

The findings discussed so far demonstrated that the incubation of fibroblasts with sEVs derived from CRC cells (HT29 and HCT116) stimulated three processes: vesicles uptake and fibroblast migration and activation. Increased stromal cells, especially CAFs, are important in extracellular matrix remodeling to enhance tumor growth and the spreading of tumor cells. Actomyosin contractility is a key

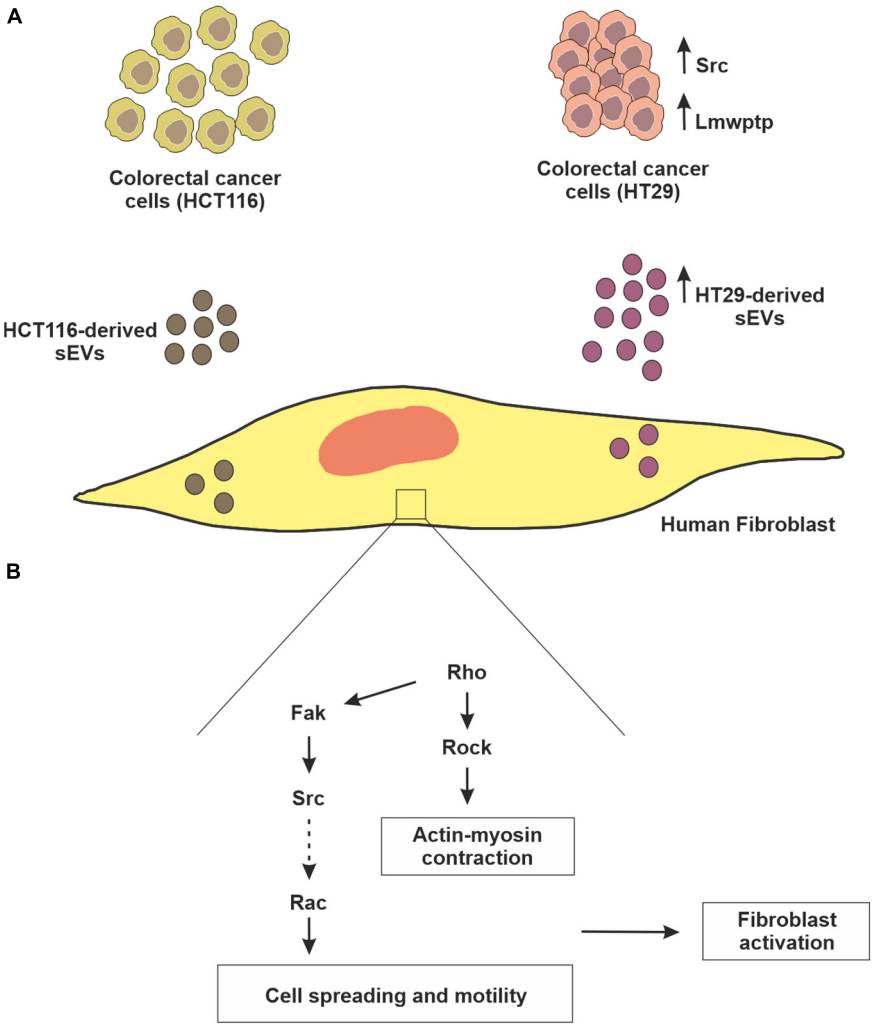

FIGURE 7 | | Schematic representation of fibroblast reprogramming (education) by CRC cell-derived sEVs. **(A)** Although both colorectal cancer cell lines (HCT116 and HT29) release sEVs, HT29 produces these vesicles in greater concentration, which can be explained, at least in part, due to higher amounts of mediators of biogenesis pathway, as well as Src kinase. Interestingly, HT29 not only has a higher amount of Lmwptp, but this protein is part of the sEVs cargo. **(B)** In relation to the biological relevance of these sEVs, in the present study, it was observed that they can educate normal fibroblasts, stimulating them to proliferate, migrate and acquire the characteristic of myoblasts.

regulator in actin cytoskeletal reorganization and cell motility (Gunst and Zhang, 2008). To confirm these processes, we analyzed the expression/phosphorylation status of signaling mediators involved in cytoskeleton remodeling. The Rho GTPase network is vital for mediating the intracellular responses that regulate cell adhesion, spreading, and endocytosis (Lawson and Ridley, 2018). Rock controls the formation of stress fibers and focal adhesions in the central part of cultured fibroblasts (Katoh et al., 2001; Katoh, 2017). FAK regulates the organization of new stress fibers and focal adhesions by Katoh (2017) examined the function of FAK at the time of focal adhesion formation in fibroblasts. They observed that Rock activation induced focal adhesion formation in FAK knockout mice. In the same way, Lee et al. (2020) observed a significant reduction of RhoA and Rock1 gene expression in CAFs co-incubated with tumor exosomes isolated from ovarian cancer cells, suggesting that these genes are important in regulating cytoskeletal alterations in CAFs. We observed reduced expression of Rho-associated protein kinase (Rock1) in both human fibroblasts co-incubated with CRC cell-derived sEVs concomitant with reduced phosphorylation of FAK Tyr397. Previous studies demonstrated that the treatment of CAFs, with Rock inhibitor (Y-27632), has smaller focal adhesions (Piltti et al., 2015), which were less stable, resulting in migration (Wang et al., 2017).

Another evidence suggests that p190RhoGEF can also bind to FAK, resulting in increases in RhoA activity contributing to the migration of fibroblasts (Lim et al., 2008). Our results showed reduced expression of RhoA and RhoC at 48 h, followed by co-incubation of CRC cell-derived sEVs with human fibroblasts, especially with HT29-derived sEVs. Chiarugi et al. (2000) used a model of Lmwptp overexpression in 3T3 fibroblasts, which results in downregulation of p190Rho-GAP, a Rho signaling

downstream protein related to cytoskeleton rearrangement. In agreement with FAK's role in fibroblasts migration, a study conducted by Rigacci et al. (2002) showed reduced focal adhesion and high motility capacity in Lmwptp overexpressed fibroblasts due to a reduced p125FAK phosphorylation.

Focal adhesions are integrin-based adhesions linking the actin cytoskeleton to the extracellular matrix, allowing the cell to sense and adapt to abrupt changes in their environment (Geiger et al., 2009). Tyrosine phosphorylation is a key signaling event at the assembly and disassembly of focal adhesions. Tyrosine phosphorylation of FAK recruits several different adhesion proteins by providing docking sites for SH2-containing proteins, such as the Src family (Xing et al., 1994). Downstream signaling can alter cell cytoskeletal dynamics to produce mechanical force for cell motility, and these pathways are under the control of tyrosine kinases and tyrosine phosphatases. As we observed that the FAK Tyr397 phosphorylation decreased after 24 and 48 h of co-incubation of human fibroblasts with CRC cell-derived sEVs and this phospho-residue creates new sites to Src interaction, we next checked Src kinase. Interestingly, a reduced Src expression, as well as its phosphorylation at Tyr527 (inhibitory site), was detected at 48 h after CRC cell-derived sEV co-incubation with human fibroblasts. This reduced phosphorylation of Src Tyr572 might culminate in Src activation, but the reduced phosphorylation of FAK Tyr397 might not create new sites for Src interaction, despite its activity. The literature mentioned that PTPN12, a kind of phosphatase, dephosphorylates FAK, thus reducing the number of focal contacts and consequently increasing tumor cell migration and invasion (Zheng et al., 2009, 2011).

Our group has shown that the Lmwptp contributes to CRC cells' aggressiveness, low response to chemotherapy, and migration. In addition, this enzyme expression follows a stepwise augment from healthy tissue to dysplastic adenoma and carcinoma, and therefore, we claimed that it could be understood as a biomarker of aggressiveness and poor prognosis for CRC patients (Hoekstra et al., 2015). In this study, we show for the first time that a CRC cell line (HT29) that is less sensitive to therapeutics (Lopes-Costa et al., 2017; Attoub et al., 2018) not only produces more sEVs (**Figure 7**) but also releases the Lmwptp as a cargo.

CONCLUSION

An emerging physiological significance of tumoral sEVs is to transfer a "prototype" message that reflects mutations, genetics, and protein profile from donor cells to recipient cells in the TME. The present study revealed that sEVs produced by CRC cells not only are able to educate normal fibroblasts *via* uptake of these vesicles but also modulate Rho and FAK, which culminate in migration and activation of fibroblasts (**Figure 7**). Of great interest, the Lmwptp was found to be part of cargoes of CRC cell-derived sEVs. This observation opens new avenues regarding the molecular mechanism by which this phosphatase gives an advantage to CRC.

DATA AVAILABILITY STATEMENT

The raw data supporting the conclusions of this article will be made available by the authors, without undue reservation.

AUTHOR CONTRIBUTIONS

SPC designed the methodology and conducted the research investigation. SRC designed and conducted the TEM methodology. The head group leader CVF-H contributed to the article conceptualization. SPC was responsible for the original writing. SPC and CVF-H were responsible for reviewing and editing. CVF-H, MP, and GF supervised the work. All authors read and approved the final manuscript.

FUNDING

This work was supported by the Sao Paulo Research Foundation (FAPESP) under grants 2018/03593-6 (SPC) and 2015/20412-7 (CVF-H).

ACKNOWLEDGMENTS

The authors are grateful for the financial support provided during the research from Sao Paulo Research Foundation (FAPESP)—(grants 2015/20412-7 and 2018/03593-6). The authors are grateful for the equipment support from Laboratório Multiusuário de Biologia Celular e Molecular and from Laboratório de Microscopia Eletrônica, Institute of Biology, University of Campinas. The authors are grateful to Gustavo Facchini from Kosmoscience Group for providing the human skin fibroblast.

SUPPLEMENTARY MATERIAL

The Supplementary Material for this article can be found online at: https://www.frontiersin.org/articles/10.3389/fcell.2021.696373/full#supplementary-material

REFERENCES

Attoub, S., Arafat, K., Khalaf, T., Sulaiman, S., and Iratni, R. (2018). Frondoside a enhances the anti-cancer effects of oxaliplatin and 5-fluorouracil on colon cancer cells. *Nutrients* 10:560. doi: 10.3390/nu10050560

Borriello, L., Nakata, R., Sheard, M. A., Fernandez, G. E., Sposto, R., Malvar, J., et al. (2017). Cancer-associated fibroblasts share characteristics and protumorigenic activity with mesenchymal stromal cells. *Cancer Res.* 77, 5142–5157. doi: 10.1158/0008-5472.CAN-16-2586

Bray, F., Ferlay, J., Soerjomataram, I., Siegel, R. L., Torre, L. A., and Jemal, A. (2018). Global cancer statistics 2018: GLOBOCAN estimates of incidence and

mortality worldwide for 36 cancers in 185 countries. *CA Cancer J. Clin.* 68, 394–424. doi: 10.3322/caac.21492

Buccafusca, G., Proserpio, I., Tralongo, A. C., Rametta Giuliano, S., and Tralongo, P. (2019). Early colorectal cancer: diagnosis, treatment and survivorship care. *Crit. Rev. Oncol. Hematol.* 136, 20–30. doi: 10.1016/j.critrevonc.2019.01.023

Chen, W. X., Liu, X. M., Lv, M. M., Chen, L., Zhao, J. H., Zhong, S. L., et al. (2014). Exosomes from drug-resistant breast cancer cells transmit chemoresistance by a horizontal transfer of MicroRNAs. *PLoS One* 9:e95240. doi: 10.1371/journal.pone.0095240

Chiarugi, P., Cirri, P., Taddei, L., Giannoni, E., Camici, G., Manao, G., et al. (2000). The low M(r) protein-tyrosine phosphatase is involved in Rho-mediated cytoskeleton rearrangement after integrin and platelet-derived growth factor stimulation. *J. Biol. Chem.* 275, 4640–4646. doi: 10.1074/jbc.275.7.4640

Colombo, M., Raposo, G., and Théry, C. (2014). Biogenesis, secretion, and intercellular interactions of exosomes and other extracellular vesicles. *Annu. Rev. Cell Dev. Biol.* 30, 255–289. doi: 10.1146/annurev-cellbio-101512-122326

Costa-Silva, B., Aiello, N. M., Ocean, A. J., Singh, S., Zhang, H., Thakur, B. K., et al. (2015). Pancreatic cancer exosomes initiate pre-metastatic niche formation in the liver. *Nat. Cell Biol.* 17, 816–826. doi: 10.1038/ncb3169

Eble, J. A., and Niland, S. (2019). The extracellular matrix in tumor progression and metastasis. *Clin. Exp. Metastasis* 36, 171–198. doi: 10.1007/s10585-019-09966-1

Erez, N., Truitt, M., Olson, P., and Hanahan, D. (2010). Cancer-associated fibroblasts are activated in incipient neoplasia to orchestrate tumor-promoting inflammation in an NF-κB-dependent manner. *Cancer Cell* 17, 135–147. doi: 10.1016/j.ccr.2009.12.041

Faria, A. V. S., Clerici, S. P., de Souza Oliveira, P. F., Queiroz, K. C. S., Peppelenbosch, M. P., and Ferreira-Halder, C. V. (2020). LMWPTP modulates the antioxidant response and autophagy process in human chronic myeloid leukemia cells. *Mol. Cell. Biochem.* 466, 83–89. doi: 10.1007/s11010-020-03690-1

Ferreira, C. V., Bos, C. L., Versteeg, H. H., Justo, G. Z., Durán, N., and Peppelenbosch, M. P. (2004). Molecular mechanism of violacein-mediated human leukemia cell death. *Blood* 104, 1459–1464. doi: 10.1182/blood-2004-02-0594

Geiger, B., Spatz, J. P., and Bershadsky, A. D. (2009). Environmental sensing through focal adhesions. *Nat. Rev. Mol. Cell Biol.* 10, 21–33. doi: 10.1038/nrm2593

Gok Yavuz, B., Gunaydin, G., Gedik, M. E., Kosemehmetoglu, K., Karakoc, D., Ozgur, F., et al. (2019). Cancer associated fibroblasts sculpt tumour microenvironment by recruiting monocytes and inducing immunosuppressive PD-1 + TAMs. *Sci. Rep.* 9:3172. doi: 10.1038/s41598-019-39553-z

Goulet, C. R., Bernard, G., Tremblay, S., Chabaud, S., Bolduc, S., and Pouliot, F. (2018). Exosomes induce fibroblast differentiation into cancer-associated fibroblasts through TGFb signaling. *Mol. Cancer Res.* 16, 1196–1204. doi: 10.1158/1541-7786.MCR-17-0784

Gunst, S. J., and Zhang, W. (2008). Actin cytoskeletal dynamics in smooth muscle : a new paradigm for the regulation of smooth muscle contraction. *Am. J. Physiol. Physiol.* 295, 576–587. doi: 10.1152/ajpcell.00253.2008

Hida, K., Maishi, N., Annan, D. A., and Hida, Y. (2018). Contribution of tumor endothelial cells in cancer progression. *Int. J. Mol. Sci.* 19:1272. doi: 10.3390/ijms19051272

Hinshaw, D. C., and Shevde, L. A. (2019). The tumor microenvironment innately modulates cancer progression. *Cancer Res.* 79, 4557–4567. doi: 10.1158/0008-5472.CAN-18-3962

Hoekstra, E., Kodach, L. L., Das, A. M., Ruela-de-Sousa, R. R., Ferreira, C. V., Hardwick, J. C., et al. (2015). Low molecular weight protein tyrosine phosphatase (LMWPTP) upregulation mediates malignant potential in colorectal cancer. *Oncotarget* 6, 8300–8312. doi: 10.18632/oncotarget.3224

Instituto Nacional de Câncer José Alencar Gomes da Silva (INCA) (2019). *Estimativa 2020 : Incidência de Câncer no Brasil / Instituto Nacional de Câncer José Alencar Gomes da Silva*. Rio de Janeiro : INCA.

Jana, S., and Trivedi, M. K. (2018). Wound healing activity of consciousness energy healing treatmenton HFF-1 Cells and DMEM using scratch assay. *Investig. Dermatol. Venereol. Res.* 4, 50–54. doi: 10.15436/2381-0858.18.2036

Kahlert, C., and Kalluri, R. (2013). Exosomes in tumor microenvironment influence cancer progression and metastasis. *J. Mol. Med.* 91, 431–437. doi: 10.1007/s00109-013-1020-6

Katoh, K. (2017). Activation of Rho-kinase and focal adhesion kinase regulates the organization of stress fibers and focal adhesions in the central part of fibroblasts. *PeerJ* 5:e4063. doi: 10.7717/peerj.4063

Katoh, K., Kano, Y., Amano, M., Kaibuchi, K., and Fujiwara, K. (2001). Stress fiber organization regulated by MLCK and Rho-kinase in cultured human fibroblasts. *Am. J. Physiol. Physiol.* 280, 1669–1679.

Kobayashi, H., Enomoto, A., Woods, S. L., Burt, A. D., Takahashi, M., and Worthley, D. L. (2019). Cancer-associated fibroblasts in gastrointestinal cancer. *Nat. Rev. Gastroenterol. Hepatol.* 16, 282–295. doi: 10.1038/s41575-019-0115-0

Lawson, C. D., and Ridley, A. J. (2018). Rho GTPase signaling complexes in cell migration and invasion. *J. Cell Biol.* 217, 447–457. doi: 10.1083/jcb.201612069

Lee, A. H., Ghosh, D., Quach, N., Schroeder, D., and Dawson, M. R. (2020). Ovarian cancer exosomes trigger differential biophysical response in tumor-derived fibroblasts. *Sci. Rep.* 10:8686. doi: 10.1038/s41598-020-65628-3

Lim, Y., Lim, S., Tomar, A., Gardel, M., Bernard-trifi, J. A., Chen, X. L., et al. (2008). PyK2 and FAK connections to p190Rho guanine nucleotide exchange factor regulate RhoA activity, focal adhesion formation, and cell motility. *J. Cell Biol.* 180, 187–203. doi: 10.1083/jcb.200708194

Liu, T., Han, C., Wang, S., Fang, P., Ma, Z., Xu, L., et al. (2019). Cancer-associated fibroblasts: an emerging target of anti-cancer immunotherapy. *J. Hematol. Oncol.* 12:86. doi: 10.1186/s13045-019-0770-1

Lopes-Costa, E., Abreu, M., Gargiulo, D., Rocha, E., Ramos, A. A., Abreu, M., et al. (2017). Anticancer effects of seaweed compounds fucoxanthin and phloroglucinol, alone and in combination with 5-fluorouracil in colon cells. *J. Toxicol. Environ. Heal. Part A* 80, 776–787. doi: 10.1080/15287394.2017.1357297

Lugini, L., Valtieri, M., Federici, C., Cecchetti, S., Meschini, S., Condello, M., et al. (2016). Exosomes from human colorectal cancer induce a tumor-like behavior in colonic mesenchymal stromal cells. *Oncotarget* 7, 50086–50098. doi: 10.18632/oncotarget.10574

Milane, L., Singh, A., Mattheolabakis, G., Suresh, M., and Amiji, M. M. (2015). Exosome mediated communication within the tumor microenvironment. *J. Control. Release* 219, 278–294. doi: 10.1016/j.jconrel.2015.06.029

Milman, N., Ginini, L., and Gil, Z. (2019). Exosomes and their role in tumorigenesis and anticancer drug resistance. *Drug Resist. Updat.* 45, 1–12. doi: 10.1016/j.drup.2019.07.003

Minciacchi, V. R., Freeman, M. R., and Di Vizio, D. (2015). Extracellular vesicles in cancer: exosomes, microvesicles and the emerging role of large oncosomes. *Semin. Cell Dev. Biol.* 40, 41–51. doi: 10.1016/j.semcdb.2015.02.010

Patel, G. K., Khan, M. A., Zubair, H., and Srivastava, S. K. (2019). Comparative analysis of exosome isolation methods using culture supernatant for optimum yield, purity and downstream applications. *Sci. Rep.* 9:5335. doi: 10.1038/s41598-019-41800-2

Peinado, H., Alečković, M., Lavotshkin, S., Matei, I., Costa-Silva, B., Moreno-Bueno, G., et al. (2012). Melanoma exosomes educate bone marrow progenitor cells toward a pro-metastatic phenotype through MET. *Nat. Med.* 18, 883–891. doi: 10.1038/nm.2753

Piltti, J., Varjosalo, M., Qu, C., Häyrinen, J., and Lammi, M. J. (2015). Rho-kinase inhibitor Y-27632 increases cellular proliferation and migration in human foreskin fibroblast cells. *Proteomics* 15, 2953–2965. doi: 10.1002/pmic.201400417

Quail, D. F., and Joyce, J. A. (2013). Microenvironmental regulation of tumor progression and metastasis. *Nat. Med.* 19, 1423–1437. doi: 10.1038/nm.3394

Rai, A., Greening, D. W., Chen, M., Xu, R., Ji, H., and Simpson, R. J. (2019). Exosomes derived from human Primary and metastatic colorectal cancer cells contribute to functional heterogeneity of activated fibroblasts by reprogramming their proteome. *Proteomics* 19:e1800148. doi: 10.1002/pmic.201800148

Richards, K. E., Zeleniak, A. E., Fishel, M. L., Wu, J., Littlepage, L. E., and Hill, R. (2017). Cancer-associated fibroblast exosomes regulate survival and proliferation of pancreatic cancer cells. *Oncogene* 36, 1770–1778. doi: 10.1038/onc.2016.353

Rigacci, S., Rovida, E., Dello Sbarba, P., and Berti, A. (2002). Low M r phosphotyrosine protein phosphatase associates and dephosphorylates p125 focal adhesion kinase, interfering with cell motility and spreading. *J. Biol. Chem.* 277, 41631–41636. doi: 10.1074/jbc.M201709200

Shephard, A. P., Yeung, V., Clayton, A., and Webber, J. P. (2017). Prostate cancer exosomes as modulators of the tumor microenvironment. *J. Cancer Metastasis Treat.* 3:288. doi: 10.20517/2394-4722.2017.32

Stefanius, K., Servage, K., and Orth, K. (2021). Exosomes in cancer development. *Curr. Opin. Genet. Dev.* 66, 83–92. doi: 10.1016/j.gde.2020.12.018

Tao, L., Huang, G., Song, H., Chen, Y., and Chen, L. (2017). Cancer associated fibroblasts : an essential role in the tumor microenvironment. *Oncol. Lett.* 14, 2611–2620. doi: 10.3892/ol.2017.6497

Théry, C., Witwer, K. W., Aikawa, E., Alcaraz, M. J., Anderson, J. D., Andriantsitohaina, R., et al. (2019). Minimal information for studies of extracellular vesicles 2018 (MISEV2018): a position statement of the International society for extracellular vesicles and update of the MISEV2014 guidelines. *J. Extracell. Vesicles* 8:1535750. doi: 10.1080/20013078.2018.1535750

Torreggiani, E., Perut, F., Roncuzzi, L., Zini, N., Baglìo, S. R., and Baldini, N. (2014). Exosomes : novel effectors of human platelet lysate activity. *Eur. Cell Mater.* 28, 137–151. doi: 10.22203/ecm.v028a11

Valadi, H., Ekström, K., Bossios, A., Sjöstrand, M., Lee, J. J., and Lötvall, J. O. (2007). Exosome-mediated transfer of mRNAs and microRNAs is a novel mechanism of genetic exchange between cells. *Nat. Cell Biol.* 9, 654–659. doi: 10.1038/ncb1596

Van Deun, J., Mestdagh, P., Agostinis, P., Akay, Ö, Anand, S., Anckaert, J., et al. (2017). EV-TRACK: transparent reporting and centralizing knowledge in extracellular vesicle research. *Nat. Methods* 14, 228–232. doi: 10.1038/nmeth.4185

Wang, T., Kang, W., Du, L., and Ge, S. (2017). Rho-kinase inhibitor Y-27632 facilitates the proliferation, migration and pluripotency of human periodontal ligament stem cells. *J. Cell. Mol. Med.* 21, 3100–3112. doi: 10.1111/jcmm.13222

Wortzel, I., Dror, S., Kenific, C. M., and Lyden, D. (2019). Exosome-mediated metastasis: communication from a distance. *Dev. Cell* 49, 347–360. doi: 10.1016/j.devcel.2019.04.011

Xing, Z., Chen, H., Nowlen, J. K., Taylor, S. J., Shalloway, D., and Guan, J. (1994). Direct interaction of v-Src with the focal adhesion kinase mediated by the Src SH2 domain. *Mol. Biol. Cell* 5, 413–421. doi: 10.1091/mbc.5.4.413

Zhang, Q., Jeppesen, D. K., Higginbotham, J. N., Demory Beckler, M., Poulin, E. J., Walsh, A. J., et al. (2018). Mutant KRAS exosomes alter the metabolic state of recipient colonic epithelial cells. *Cell. Mol. Gastroenterol. Hepatol.* 5, 627–629.e6. doi: 10.1016/j.jcmgh.2018.01.013

Zhao, H., Yang, L., Baddour, J., Achreja, A., Bernard, V., Moss, T., et al. (2016). Tumor microenvironment derived exosomes pleiotropically modulate cancer cell metabolism. *Elife* 5:e10250. doi: 10.7554/eLife.10250

Zheng, Y., Xia, Y., Hawke, D., Halle, M., Tremblay, M. L., Gao, X., et al. (2009). FAK phosphorylation by ERK primes ras-induced tyrosine dephosphorylation of FAK mediated by PIN1 and PTP-PEST. *Mol. Cell* 35, 11–25. doi: 10.1016/j.molcel.2009.06.013

Zheng, Y., Yang, W., Xia, Y., Hawke, D., Liu, D. X., and Lu, Z. (2011). Ras-induced and extracellular signal-regulated kinase 1 and 2 phosphorylation-dependent isomerization of protein tyrosine phosphatase (PTP)-PEST by PIN1 promotes FAK dephosphorylation by PTP-PEST. *Mol. Cell. Biol.* 31, 4258–4269. doi: 10.1128/mcb.05547-11

Zhou, X., Yan, T., Huang, C., Xu, Z., Wang, L., Jiang, E., et al. (2018). Melanoma cell-secreted exosomal miR-155-5p induce proangiogenic switch of cancer-associated fibroblasts via SOCS1/JAK2/STAT3 signaling pathway 11 medical and health sciences 1112 oncology and carcinogenesis 06 biological sciences 0601 biochemistry and cell biology. *J. Exp. Clin. Cancer Res.* 37:242. doi: 10.1186/s13046-018-0911-3

Conflict of Interest: The authors declare that the research was conducted in the absence of any commercial or financial relationships that could be construed as a potential conflict of interest.

frontiers in Cell and Developmental Biology

BRIEF RESEARCH REPORT
published: 30 July 2021
doi: 10.3389/fcell.2021.698503

CD30-Positive Extracellular Vesicles Enable the Targeting of CD30-Negative DLBCL Cells by the CD30 Antibody-Drug Conjugate Brentuximab Vedotin

*Liudmila Lobastova[1,2,3,4], Marcus Lettau[5,6], Felix Babatz[7], Thais Dolzany de Oliveira[1,2,3,4], Phuong-Hien Nguyen[1,2,3,4], Bianca Alves Pauletti[8], Astrid C. Schauss[7], Horst Dürkop[9], Ottmar Janssen[5], Adriana F. Paes Leme[8], Michael Hallek[1,2,3,4] and Hinrich P. Hansen[1,2,3,4]**

[1] Department I of Internal Medicine, University of Cologne, Cologne, Germany, [2] Center for Integrated Oncology Aachen Bonn Cologne Duesseldorf, Cologne, Germany, [3] Center for Molecular Medicine Cologne, University of Cologne, Cologne, Germany, [4] CECAD Center of Excellence on Cellular Stress Responses in Aging-Associated Diseases, Cologne, Germany, [5] Institute of Immunology, Christian-Albrechts-University of Kiel and University Hospital Schleswig-Holstein, Kiel, Germany, [6] Department of Hematology, University Hospital Schleswig-Holstein, Kiel, Germany, [7] CECAD Center of Excellence on Cellular Stress Responses in Aging-Associated Diseases, Imaging Facility, Cologne, Germany, [8] Laboratório de Espectrometria de Massas, Laboratório Nacional de Biociências, Centro Nacional de Pesquisa em Energia e Materiais, Campinas, Brazil, [9] Pathodiagnostik Berlin MVZ GmbH Berlin, Berlin, Germany

OPEN ACCESS

Edited by:
Jay William Fox,
University of Virginia, United States

Reviewed by:
Youliang Wang,
Beijing Institute of Technology, China
Salvatrice Mancuso,
University of Palermo, Italy

***Correspondence:**
Hinrich P. Hansen
h.hansen@uni-koeln.de

Specialty section:
This article was submitted to Molecular and Cellular Pathology, a section of the journal Frontiers in Cell and Developmental Biology

Received: *21 April 2021*
Accepted: *07 July 2021*
Published: *30 July 2021*

Citation:
Lobastova L, Lettau M, Babatz F, de Oliveira TD, Nguyen P-H, Pauletti BA, Schauss AC, Dürkop H, Janssen O, Paes Leme AF, Hallek M and Hansen HP (2021) CD30-Positive Extracellular Vesicles Enable the Targeting of CD30-Negative DLBCL Cells by the CD30 Antibody-Drug Conjugate Brentuximab Vedotin. Front. Cell Dev. Biol. 9:698503. doi: 10.3389/fcell.2021.698503

CD30, a member of the TNF receptor superfamily, is selectively expressed on a subset of activated lymphocytes and on malignant cells of certain lymphomas, such as classical Hodgkin Lymphoma (cHL), where it activates critical bystander cells in the tumor microenvironment. Therefore, it is not surprising that the CD30 antibody-drug conjugate Brentuximab Vedotin (BV) represents a powerful, FDA-approved treatment option for $CD30^+$ hematological malignancies. However, BV also exerts a strong anti-cancer efficacy in many cases of diffuse large B cell lymphoma (DLBCL) with poor CD30 expression, even when lacking detectable $CD30^+$ tumor cells. The mechanism remains enigmatic. Because CD30 is released on extracellular vesicles (EVs) from both, malignant and activated lymphocytes, we studied whether EV-associated CD30 might end up in $CD30^-$ tumor cells to provide binding sites for BV. Notably, $CD30^+$ EVs bind to various DLBCL cell lines as well as to the FITC-labeled variant of the antibody-drug conjugate BV, thus potentially conferring the BV binding also to $CD30^-$ cells. Confocal microscopy and imaging cytometry studies revealed that BV binding and uptake depend on $CD30^+$ EVs. Since BV is only toxic toward $CD30^-$ DLBCL cells when $CD30^+$ EVs support its uptake, we conclude that EVs not only communicate within the tumor microenvironment but also influence cancer treatment. Ultimately, the CD30-based BV not only targets $CD30^+$ tumor cell but also $CD30^-$ DLBCL cells in the presence of $CD30^+$ EVs. Our study thus provides a feasible explanation for the clinical impact of BV in $CD30^-$ DLBCL and warrants confirming studies in animal models.

Keywords: tumor microenvironment, cellular crosstalk, immune therapy, antibody-drug conjugate, extracellular vesicle

INTRODUCTION

CD30 is a transmembrane protein of the TNF receptor superfamily (TNFRSF8). It is restricted to a small population of activated T and B immunoblasts in lymphoid tissue of healthy individuals (Stein et al., 1985; Horie and Watanabe, 1998). In T cells, CD30 serves as a costimulatory receptor, which is upregulated by T cell receptor (TCR) and CD28 ligation in addition to the action of cytokines, such as IL-4 (Gilfillan et al., 1998). Normal $CD30^+$ B cells are mostly class-switched and express CD27 (TNFRSF7) (Weniger et al., 2018). The corresponding ligand (CD30L/TNFSF8) is also a transmembrane protein, which is weakly expressed on various immune cells including neutrophils, eosinophils, lymphocytes, myeloid cells, and mast cells. Here, the binding of membrane-associated CD30 causes reverse signaling and context-dependent pleiotropic effects, ranging from degranulation-free activation of myeloid cells to B cell inhibition (Wiley et al., 1996; Cerutti et al., 2000). In mice, constitutively active CD30 in B cells is associated with augmented B1-B and plasma cell counts, implicating NF-κB signaling and STAT 3 and STAT6 phosphorylation (Sperling et al., 2019). When aged, such mice have an enhanced risk of lymphomagenesis. Additionally, CD30 is expressed in transformed cells of certain malignant lymphomas, such as classical Hodgkin Lymphoma (cHL) and systemic Anaplastic Large Cell Lymphoma (sALCL; Horie and Watanabe, 1998). Because of its selective expression in malignant cells, CD30 became of interest for targeted immunotherapy with the monomethyl auristatin E (MMAE)-coupled humanized CD30 antibody drug conjugate (ADC) Brentuximab Vedotin (BV; Wahl et al., 2002). After internalization of the ADC, the acidic milieu of the lysosomes releases MMAE that is able to inhibit microtubule formation (Sutherland et al., 2006). In a pivotal study, BV treatment of sALCL and cHL patients, who relapsed after standard therapy, resulted in an overall response rate of 86 and 75%, respectively (Younes et al., 2012). Interestingly, BV proved also effective against other malignancies with less pronounced CD30 expression.

Recent clinical studies revealed that a minor percentage of diffuse large B cell lymphoma (DLBCL) patients had tumor cells with CD30 expression (Hu et al., 2013). Visually assessed immunohistochemistry (IHC) identified $CD30^+$ tumor cells in about 25% of DLBCL cases (Slack et al., 2014). However, unbiased computer-assisted IHC, which calculates also non-malignant $CD30^+$ cells, identified higher case numbers (36%) (Bartlett et al., 2017). Remarkably, clinical trials with BV in DLBCL patients suggested that the response to BV-treatment did not correlate with the amount of $CD30^+$ tumor cells. In one case, a complete remission was achieved with BV even when $CD30^+$ tumor cells were not detectable (Jacobsen et al., 2015). These data suggest that the CD30 transfer from non-malignant cells might contribute to the clinical efficacy of BV.

Extracellular vesicles (EVs) are released by virtually all cell types. They originate from the outward budding of multivesicular endosomes or budding from the plasma membrane. Endosome-derived EVs are referred to as small EVs (s-EVs, exosomes) and are generally smaller than plasma membrane-derived large EVs (l-EVs or microvesicles) (Thery et al., 2009; Nishimura et al., 2021). Both EV types are membrane-enclosed particles and harbor typical traits of the donor cells, including nucleic acids, lipids, and soluble and membrane-associated proteins. By binding to or fusing with cells in the proximity or at distant sites, EVs are able to communicate *in trans* in a cell contact-like manner with recipient cells and thus undoubtedly represent an important intercellular communication tool (Tkach and Thery, 2016).

In a previous study, we showed that EVs of cHL cells, carry CD30 as a cargo and bind to and are taken up by typical bystander cells (Hansen et al., 2016). In the presence of BV, the $CD30^+$ EVs are able to mediate cell damage also to $CD30^-$ cells in a $CD30^+$ EV-dependent manner. Thus, the transport of CD30 to bystander cells enables a dual targeting of $CD30^+$ tumor and $CD30^-$ supporter cells. Since DLBCL presents as a heterogeneous disease, encompassing cases with variable $CD30^+$ tumor and/or $CD30^+$ bystander cells, a functional EV-dependent transport from $CD30^+$ cells to $CD30^-$ DLBCL cells might explain the efficacy of BV in cases with $CD30^-$ tumor cells. In our study, we provide strong evidence, that $CD30^+$ EVs are able to bind and transport BV functionally to $CD30^+$ or $CD30^-$ DLBCL cells.

MATERIALS AND METHODS

Cells and Reagents

The cell lines L540, THP-1, P30/OHKUBO and DoHH-2 were purchased from the DSMZ (Braunschweig, Germany). Karpas 422 was from Sigma Aldrich (St. Louis, MO, United States). Cells were cultivated at 37°C and 5% CO_2 in RPMI 1640 containing 10% FBS, supplemented with GlutaMAX, 100 U/mL penicillin and 100 μg/mL streptomycin. The following additional reagents were used: PE Annexin V (RRID: AB_2561298), PE anti-human CD30 (RRID: AB:2207595), PE goat anti mouse IgG (RRID: AB_315010), anti-human CD81 (RRID: AB_10643417), anti-human CD9 (RRID: AB_314907), anti-human CD63 (RRID: AB_11204263), anti-human CD54 (RRID: AB_535974). The SGN30 antibody was from Seattle Genetics (Bothell, WA, United States). In fluorescence studies, the antibody was coupled with FITC (Sigma) in a 0.2 M carbonate buffer at pH 9.2 and purified by subsequent gel filtration. The CD30 antibody Ki-3 (Horn-Lohrens et al., 1995) was labeled with the deep red fluorescence dye CF 594 (Sigma) according to the manufacturer's instruction. The sheddase inhibitor Ro 32-7315 was kindly provided by Roche Diagnostics, Penzberg, Germany. The anti-CD30 hybridoma HeFi-1 was kindly provided by Dr. Ellis, Loyola Univ., Maywood, IL, United States.

Vesicle Isolation

Cells were cultivated under serum-free conditions at 5×10^6/mL for 2 h in the presence of 10 μM Ro 32-7315. Cell supernatant was collected and cleared by three consecutive centrifugation steps, i.e., 5 min at 300 × *g*, 10 min at 1,000 × *g*, 20 min at 3,500 × *g*. Cleared supernatants were sedimented in an ultracentrifuge for 2 h at 100,000 × *g*. Vesicle-containing pellets were washed twice with PBS by ultracentrifugation. Particle concentration and size

distribution of isolated EVs were determined by nanoparticle tracking analysis (NTA, Nanosight NS300, Malvern Instruments). The means of five consecutive measurements of 1 min were evaluated to adjust the EV concentration to 1×10^{10} EVs/mL.

Flow Cytometry of EVs

Extracellular vesicles were incubated at 4°C overnight with 4.5 μm Polybead carboxylate microspheres (Polysciences, Warrington, PA, United States). The beads were blocked with 1% BSA (v/w) in PBS for 1h at 800 rpm. Then, aliquots were incubated with fluorescence-labeled antibodies. Beads were evaluated by flow cytometry on a Gallios device (Beckman Coulter).

Electron Microscopy

Extracellular vesicles were fixed with 2% formaldehyde (Merck). A 100 mesh formvar coated copper grid (Science Services) was placed onto 5 μL of sample and incubated for 20 min. Grids were washed seven times for 2 min in PBS and place for 5 min on a drop of 1% glutaraldehyde (Merck). Grids were washed eight times in ddH_2O. Grids were placed for 4 min onto a drop of 1.5% aqueous uranyl acetate and blotted with a filter paper. Images were acquired using a JEM-2100 Plus Transmission Electron Microscope (JEOL) operating at 80kV equipped with a OneView 4K camera (Gatan).

EV-Labeling With DiD

Extracellular vesicles were isolated and washed with PBS by ultracentrifugation at 100,000 × *g* and subsequently labeled with 40 nM of the membrane dye DiD (1,1′-Dioctadecyl-3,3,3′,3′-tetramethylindo-dicarbo-cyanine, 4-Chlorobenzenesulfonate salt, Thermo Fisher Scientific). Then, EVs were incubated for 20 min at 37°C and washed by ultracentrifugation at 100,000 × *g* for 1 h at 4°C. Afterward DiD-labeled EVs were added to the target cell lines, incubated for 2 h at 4°C and cells were then analyzed by flow cytometry.

LC-MS/MS

The peptide mixture was analyzed in an LTQ Orbitrap Velos (Thermo Fisher Scientific) mass spectrometer coupled to nanoflow liquid chromatography on an EASY-nLC system (Proxeon Biosystems) with a Proxeon nanoelectrospray ion source. The parameters for MS analysis are described in further detail in **Supplementary Figure 1**. The mass spectrometry proteomics data have been deposited to the ProteomeXchange Consortium via the PRIDE partner repository with the dataset identifier PXD025442 (Perez-Riverol et al., 2019).

Confocal Laser-Scanning Microscopy

Eight-well μ-slides (Ibidi) were coated over night with 0.01% poly-L-lysine at 37°C and afterwards washed three times with medium. Cells were let to adhere and incubated with Ki-3-CF594-loaded EVs for 1 h. Then, the medium was carefully removed and replaced with fresh medium, containing CellMask™ Deep Red Plasma membrane stain (649/666 nm; Thermo Fisher Scientific) and Hoechst 33342 dye (NucBlue™ Live ReadyProbes™, Thermo Fisher Scientific). After 5 min incubation, the dye-containing medium was substituted by fresh medium and the samples immediately subjected to the confocal laser scanning microscope (Leica TCS SP8, 63x PlanApo oil objective N.A. 1.4) with super resolution (∼50 nm lateral, 120 nm axial).

Measurement of EV Uptake by Imaging Flow Cytometry (ImageStream)

Target cells (5×10^5) were washed twice with FACS buffer before incubation with SGN30-FITC ± EVs for 1 h at RT to allow EV binding and internalization. Then, cells were washed once with cold FACS-buffer and then fixed with 1% PFA in PBS and subsequently kept on ice until internalization could be analyzed by imaging flow cytometry.

Internalization of FITC-labeled SGN30 antibody and $CD30^+$ EVs by Karpas 422 or P30-OH/KUBO cells was quantified by imaging flow cytometry using an ImageStream X Mark II one camera system with 351, 488, 562, 658 and 732 nm lasers (Merck Millipore, Burlington, MA, United States). The system was calibrated using SpeedBeads (Merck Millipore) prior to use and at least 10,000 events with an area >12.5 μm^2 based on bright field images were acquired. Moreover, 500–1,000 events of single stained compensation control samples gated on appropriate signal size were acquired with both the bright field channel and the 732 nm laser turned off. Images (bright field in channel 1 and FITC in channel 2 (505–560 nm) were acquired at 60-fold magnification. The integrated software INSPIRE® was used for data collection as raw image files. Single color controls were used to calculate a spectral crosstalk matrix that was applied to each raw image file for spectral compensations in the detection channels. The analysis was performed on the compensated image files using the IDEAS® image analysis software. The bright field gradient root mean square (RMS) feature was used to gate on focused cells and dot plots of the bright field area versus the aspect ratio were used to gate on single cells. The internalization wizard was used to calculate the internalization score that is defined as the ratio of the intensity inside the cell to the intensity of the entire cell mapped to a logarithmic scale.

Toxicity Test

Target cells (1×10^5 cells/well) were cultivated in 500 μL medium/well in a 24-well plate ± 10^9 EVs from L540 or THP-1 along with different amounts of BV ± HeFi-1 antibody (1 μg/mL final concentration) or medium alone as control. After 24 h another 250 μL of culture medium was added to each well. The cells were further incubated for 48 h and cell viability was assessed by flow cytometry. To this end, the cells were washed once with FACS buffer, then stained with propidium iodide (PI; 0.5 μg/mL) for 30 min at 4°C, washed twice with FACS buffer and PI^+ cells were determined by flow cytometry.

Statistical Analysis

If not stated otherwise, all experiments were performed in at least three independent replicates. Results obtained from representative experiments are shown. Data ($n \geq 3$) are presented as mean ± standard errors of the mean (SEM) and were analyzed using GraphPad Prism 7 software. Statistical significance was calculated as indicated in the Figures.

RESULTS

Production of CD30$^+$ EVs

In many cases of DLBCL, cells with variable expression of CD30 are admixed in the affected tissue. They are either malignant themselves or reactive immunoblasts (**Figure 1A**). Here, we studied whether EVs from CD30$^+$ cells contribute to the efficacy of BV in DLBCL. In order to generate CD30$^+$ EVs for subsequent experiments, we cultivated the CD30$^+$ L540 cell line for 1 h under serum-free conditions and harvested the cell supernatant. The l-EVs sediment at lower gravity than the s-EVs (Nishimura et al., 2021). In order to determine, which EV type preferentially contains CD30, we compared EVs that sediment at different gravity. After two centrifugation steps at low gravity to remove cell debris, we collected vesicles that sediment at 10,000 × *g* and another portion from a subsequent ultracentrifugation step at 100,000 × *g* (**Figure 1B**). Nanoparticle tracking analysis (NTA) revealed that the 10,000 × *g* fraction contained roughly 4× less but larger vesicles than the 100,000 × *g* fraction, i.e., $6.97 \times 10^8 \pm 3.94 \times 10^7$ particles/mL with a mean diameter of 205 nm and $3.24 \times 10^9 \pm 1.03 \times 10^8$ with a mean diameter of 143 nm, respectively. Because both particle fractions are deliberately released into the environment, they are candidate vehicles, provided they contain CD30. Mass spectrometry demonstrated that both EV fractions yielded a similar amount of protein hits with largely overlapping genes, including CD30, i.e., 81% of the 10,000 × *g* and 83% of the 100,000 × *g* fraction (**Figure 1C** and **Supplementary Table 1**). Interestingly, both EV preparations contained almost exclusively hits, which are found in the EV protein database Vesiclepedia, i.e., 98.5 and 97.3% in the 10,000 × *g* and 100,000 × *g* fractions, respectively (**Supplementary Figure 1**). Also, categorization of the protein hits with the Funrich 3.1.4 software revealed that similar percentages were allocated to different cellular components, whereof the category of exosomes was the most prominent one. Because of the similar protein composition, particularly the presence of CD30, we pooled the 10,000 × *g* and the 100,000 × *g* fraction for further experiments. EVs from the CD30$^-$ cell line THP-1 were tested as a control. Transmission electron microscopy of the pooled fractions identified in both cases (OsO_4-stained) membrane-enclosed particles of variable diameter within the range of EVs. NTA measurement showed a similar EV diameter in the pooled fractions from L540 and the THP1 cell, i.e., 165.0 ± 67.5 nm (L540) and 172 ± 63.9 nm (THP-1) (**Figure 1D**). As expected, EVs from both cell types expressed typical EV markers such as phosphatidylserine and tetraspanins (CD63, CD81, and CD82) but only EVs from L540 cells contained CD30 (**Figure 1E**). Therefore, we used L540 EVs as CD30 carriers and THP-1 EVs as negative controls in subsequent experiments.

Targeting of Leukemia Cells With CD30$^+$ EVs

To study the efficacy of CD30$^+$ EVs in mediating BV toxicity in non-Hodgkin B cell leukemia, we examined three target cell lines for endogenous CD30 expression, binding of donor cell EVs and enrichment of CD30 through EV binding. Flow cytometry showed that the cell lines Karpas 422 and DoHH-2 (GC-DLBCL) had no detectable CD30, whereas P30-OH/KUBO was positive for CD30 (**Figure 2A**, left). All tested cell lines were able to bind or take up fluorescence-labeled EVs from both L540 and THP-1 cells (**Figure 2A**, middle). As expected, only the addition of EVs from L540 cells cumulated CD30 at the cell surface of the CD30$^-$ cell lines (**Figure 2A**, right). We determined the EV-dependent enrichment of CD30 in the cells by flow cytometry, comparing the CD30-depending mean fluorescence intensity between untreated and EV-treated cells. The bars indicate, that among the tested cells, Karpas 422 showed better cell surface enrichment of EV-borne CD30 than DoHH-2 after 2 h of incubation time. In P30-OH/KUBO with endogenous CD30, EVs from L540 did not contribute much to the overall cell surface expression of CD30. Our data showed that universally membrane-labeled EVs generate a stronger signal on target cells than the anti-CD30 staining. As shown in a dot-plot, only a limited percentage of target cells accumulates CD30$^+$ EVs (median 0.52–6.55%, $N = 11$; **Figure 2B**). This is not surprising because EVs from one source are generally very heterogeneous in protein composition and only a certain percentage might contain CD30 (Lee et al., 2018). In addition, the internalization rate of CD30 might be different between cell types upon ligation, and a variable amount of CD30 might have been internalized following antibody binding. Because CD30 antibody internalization is the aim in therapy, we studied the internalization of anti-CD30 antibody. To approach this question, we performed a series of imaging experiments, after coincubation of target cells with EVs and fluorescent anti-CD30 antibody. Unfortunately, the antigen binding of BV dropped after labeling with FITC, so for this set of experiments we used either SGN30, which is the humanized backbone of BV or the murine CD30 antibody Ki-3, which belongs to the same serological cluster as SGN30/35 (Horn-Lohrens et al., 1995). Confocal microscopy indicated that both CD30$^-$ Karpas 422 and DoHH-2 have a clear CD30$^+$ EV-dependent uptake of CD30 antibody (**Figure 2C**). CD30$^-$ EVs from THP1 cells did not support this effect. Microscopy suggested a stronger signal inside the cells than on the cell surface, partially explaining the low EV-dependent surface CD30 in **Figures 2A,B**. Quantification of the antibody uptake was approached by imaging flow cytometry (**Figure 2D**). We determined the internalization score of SGN30-FITC from cells incubated with L540-EVs, resulting in values of 3.1 ($N = 2156$) for Karpas 422 cells and 2.1 ($N = 1086$) for P30-OH/KUBO cells. These data indicate that both cell types display uptake of the BV antibody backbone in the presence of CD30$^+$ EVs.

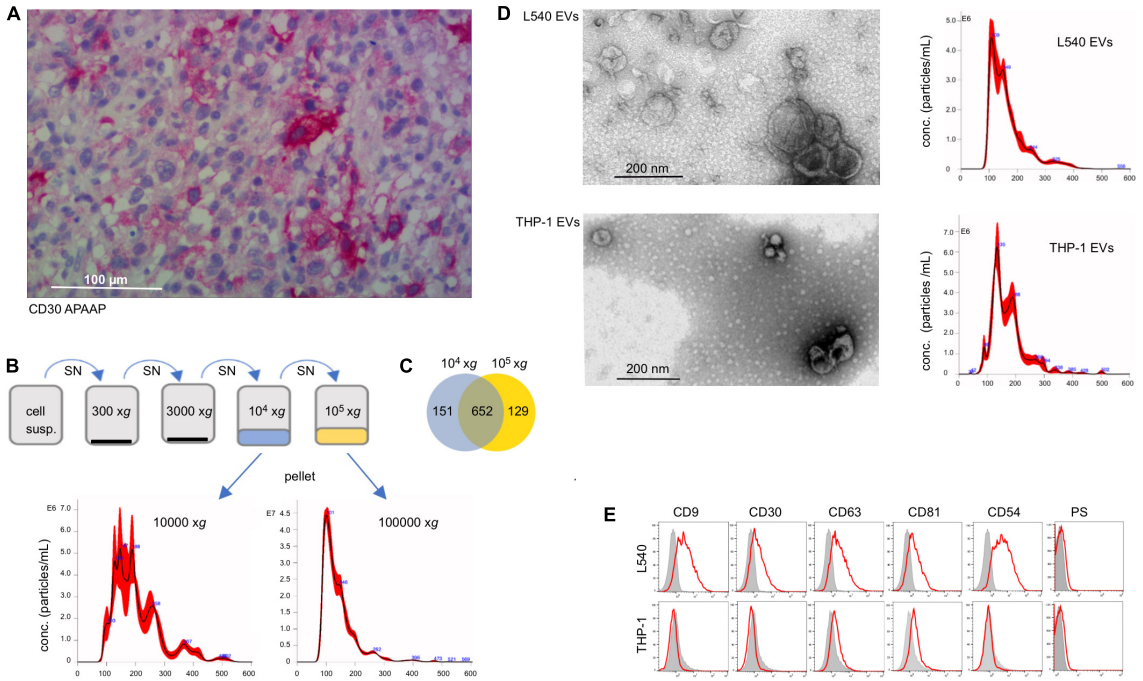

FIGURE 1 | Characterization of CD30$^+$ EVs. **(A)** Tissue section of lymph node infiltrated with DLBCL cells, which was stained with CD30 mAb (Ber-H2). The bar indicates 100 µm. **(B)** Characterization of EVs from the cell supernatant of L540 cells. They were isolated by a series of centrifugation steps. The 10,000 × *g* and the subsequent 100,000 × *g* fraction were studied by NTA and mass spectrometry. **(C)** The common and individual mass spectrum hits are shown in a Venn diagram. **(D)** The pooled 10,000 × *g* and 100,000 × *g* EV fractions of L540 and THP-1 supernatants were studied by transmission electron microscopy. The diameter (x-axis) and count (y-axis) of the EVs from the cell supernatant of L540 and THP-1 cells were analyzed by NTA. **(E)** The EVs were bound to 10 µm microspheres and analyzed by flow cytometry. The EVs were stained for CD9, CD30, CD63, CD81, CD54, and phosphatidylserine (red) and compared to the isotype controls (gray).

We also determined the functionality of CD30$^+$ EVs regarding BV-induced cytotoxicity in CD30$^-$ Karpas 422 cells (**Figure 3**). BV alone had no significant influence on the cell viability after three days of incubation, resulting in 93.6, 93.4, and 92.2% viability after treatment with 1, 3 and 10 µg/mL BV, respectively. However, after the addition of CD30$^+$ EVs (1×10^9/mL), the cell viability decreased significantly upon BV treatment, consequently resulting in cell viability of 86.5, 84.9, and 66.2% respectively. This effect was dependent on CD30 because the addition of the competitive CD30 antibody HeFi-1 could neutralize the toxicity, yielding improved cell viability of 90.3, 91.9, and 86.9%. The antibody-dependent neutralization provides a strong argument that the cytotoxicity of BV in such CD30$^-$ target cells is indeed dependent on CD30$^+$ EVs. We also tested the influence of CD30$^+$ EVs on the toxicity of BV in the CD30$^+$ cell line P30-OH/KUBO (**Supplementary Figure 2**). Although these cells constitutively express CD30 and BV is able to directly target them, this experiment provides initial evidence that CD30$^+$ EVs might contribute to or enhance the toxicity of BV even in CD30$^+$ cells (**Figure 4**).

DISCUSSION

The functional efficacy of the CD30 ADC BV is well-established in the treatment of lymphomas with high expression of CD30 in tumor cells (Younes et al., 2012). In DLBCL, the CD30 expression is variable, ranging from cases with a high percentage to cases without detectable CD30 expression. Depending on the sensitivity of the readout and whether bystander cells were included in the calculation, the CD30$^+$ cases range from 12 to 36% (Slack et al., 2014). However, DLBCL patients without CD30$^+$ tumor cells still profit from the BV therapy, in rare cases even with complete remission. This observation raises the question of the underlying mode of action in CD30$^-$ tumor cells. Here, we studied a possible function of CD30$^+$ EVs conveying the anti-tumor functionality of BV. Major findings of our study are that (i) the targeting antigen CD30 is present on l-EVs and s-EVs from L540 cells, (ii) such EVs bind to both, the immunotoxin BV and the DLBCL cells, (iii) EVs are taken up by target cells, and (iv) dependent on BV and CD30$^+$ EVs, such BV-loaded EVs also damage CD30$^-$ DLBCL cells dependent on BV and CD30$^+$ EVs (**Figure 4**).

In most cases, tumor cells do not grow independently but require the support of other malignant cells and tumor-(re)programmed non-malignant bystander cells. Therefore, in addition to addressing the malignant cells quantitatively, the targeting of the supporting tumor microenvironment has become an emerging focus of modern cancer therapy. As an example, the targeting of tumor-supporting CD25$^+$ Treg cells with ^{90}Y-daclizumab (anti-CD25) significantly improves clinical responses in cHL patients (Janik et al., 2015). This effect has also

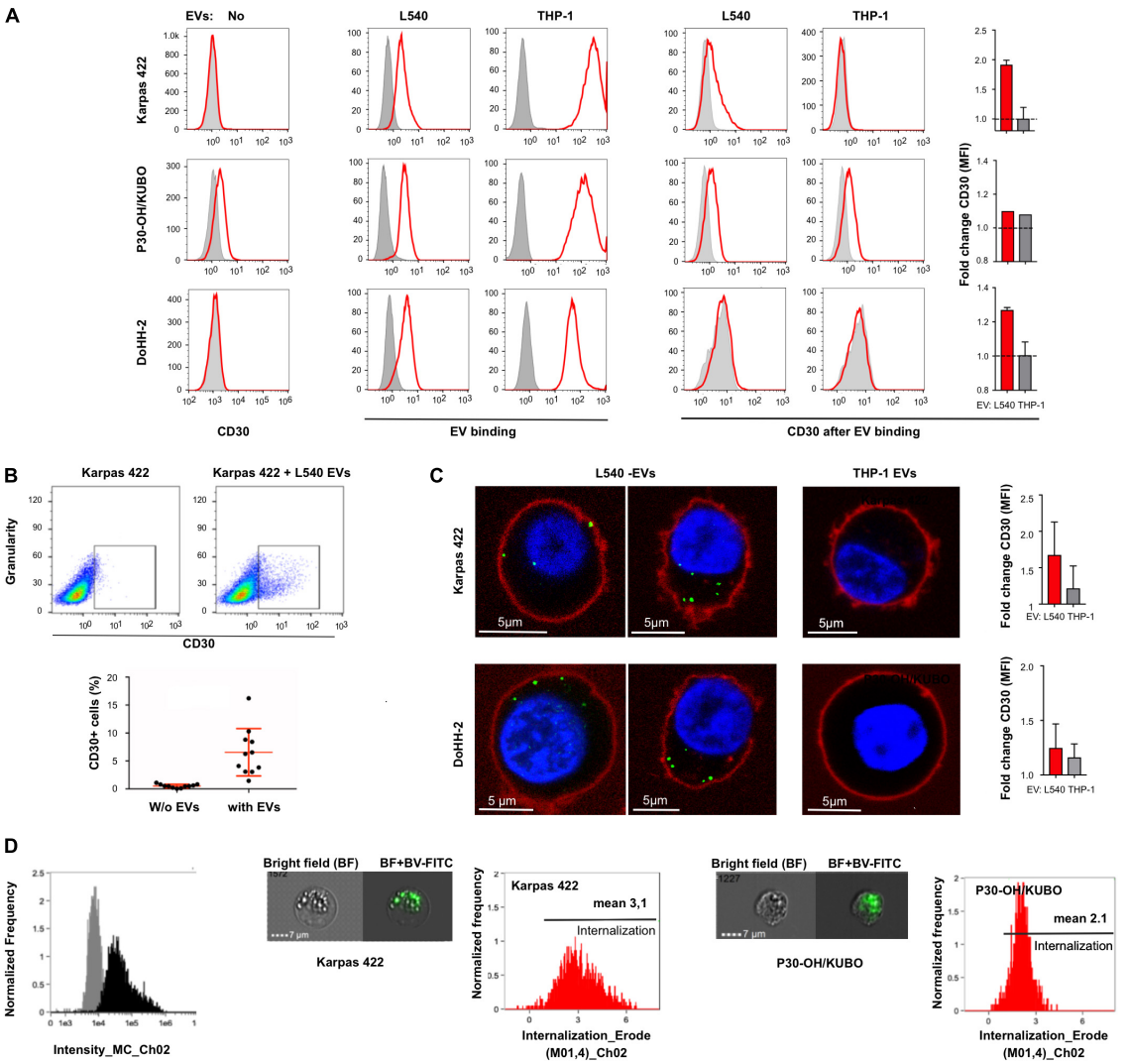

FIGURE 2 | Extracellular vesicle-dependent binding and incorporation of CD30 and BV. **(A)** The first column of graphs shows a flow cytometric analysis of the CD30 expression on the target cells Karpas 422, P30-OH/KUBO and DoHH-2 (red) compared to the isotype control (gray). The next two columns show the binding/uptake of purified EVs from the supernatant of L540 or THP-1 cells (red). For that, the cells were treated for 2 h at 4°C with DiD-labeled EVs. Untreated cells served as controls (gray). To the right, the two columns show the amount of CD30 after binding of EVs from L540 or THP-1 cells (red) as compared to the isotype control (gray). The adjacent bars indicate the relative increase of the CD30 mean fluorescence intensity (MFI) by the indicated EVs. **(B)** CD30 expression of Karpas 422 measured by flow cytometry, first gated on living cells and then the percentage of $CD30^+$ cells was calculated with and without EVs; shown as a representative image without EVs **(upper left)** and with EVs **(upper right)**, and in a diagram summarizing the results of 11 measurements. **(C)** Confocal microscopy of Karpas 422 and DoHH-2 with L540 EVs **(left panel)** or THP-1 EVs **(right)**. Cells were incubated with Ki-3-CF594-loaded EVs and the cell membrane was subsequently stained with CellMask deep red. The fold change of CD30 expression after L540 and THP-1 EVs binding was measured by flow cytometry and normalized to the samples without EVs. **(D)** The internalization process was further analyzed by one imaging flow cytometry investigation. The specific intensity of the green fluorescence is depicted [**(left)**, black]. Representative images are shown of Karpas 422 and P30-OH/KUBO cells, incubated with FITC-labeled SGN30 and EVs from L540 cells for 60 min at 37°C. Scale bars represent 7 µm. Histograms displaying the internalization score are shown.

been explained by the collateral damage of the radio isotope, targeting primarily tumor-rosetting T cells and also neighboring tumor cells. Such a crossfire effect was also suggested for the functionality of BV. After uptake of BV and cleavage of the toxic MMAE in the target cells, it was suggested that a small amount of MMAE passively penetrates the plasma membrane and diffuses back into the cell environment where it damages neighboring cells (Okeley et al., 2010).

In the last decade, the understanding of the role of EVs in the intercellular communication has significantly improved. Such EVs are also advancing cancer treatment and their influence on the PD1/PD-L1 system might be regarded as a typical example. In many malignant tumors, the immune surveillance fails because the malignant cells express programmed cell death ligands such as PD-L1, which, after cell contact, inhibit PD-1-expressing immune surveillance cells. Recently, it was shown, that malignant

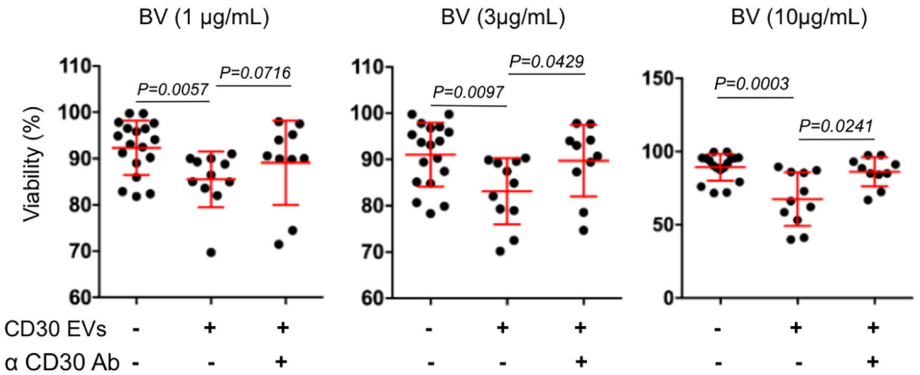

FIGURE 3 | Viability assay of Karpas 422. Viability assay of Karpas 422 ± EVs from L540 cells with the addition of BV in different concentrations 1, 3, and 10 µg/mL (from left to right); ± the inhibitory anti-CD30 antibody HeFi-1. The percentage of living cells was analyzed by flow cytometry using the propidium iodide (PI) staining. For the statistical analysis the Mann–Whitney test was used.

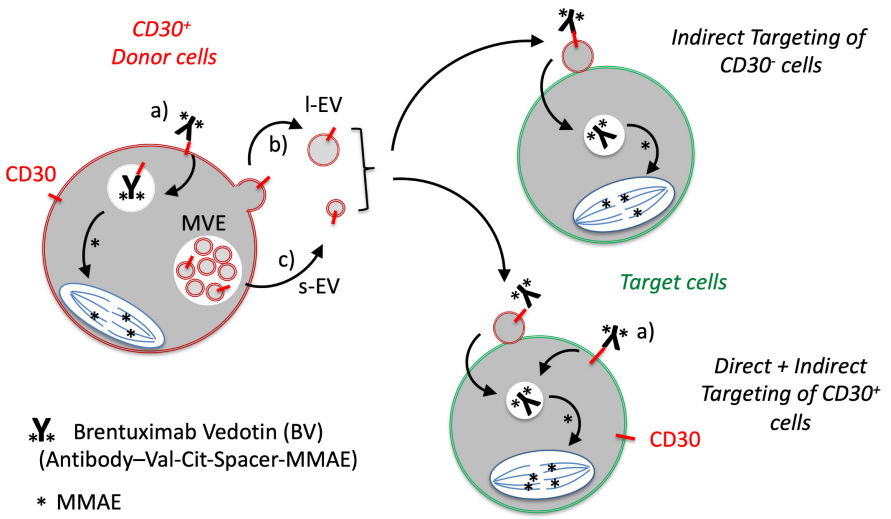

FIGURE 4 | Proposed model for the role of EVs in the targeting of CD30-negative tumor cells with the CD30 antibody drug conjugate BV. CD30 is expressed by a number of malignant DLBCL cells and activated immunoblasts. a) The CD30 ADC BV binds to $CD30^+$ tumor cells, is internalized and the cytotoxic compound monomethylauristatin E (MMAE; *) is selectively cleaved and activated at the dipeptide valine (Val)-citrulline (Cit) by the lysosomal peptidase cathepsin B. CD30 is also released in b) large EVs (l-EVs) by budding from the surface and c) in small EVs (s-EVs) by plasma membrane fusion of multivesicular endosomes. d) $CD30^+$ EVs bind BV and target different cells within the tumor microenvironment, such as $CD30^+$ or $CD30^-$ DLBCL cells. This crossfire effect might be responsible for the strong clinical efficacy of BV even in cases with $CD30^-$ tumor cells.

cells also release PD-L1 on EVs, which increases the extent of immunosuppression (Chen et al., 2018). EVs are small, mobile membrane-enclosed particles, which are released by virtually all cell types. They are regarded as fingerprints of the donor cell and thus carry and present many typical traits of the originating cell to malignant or bystander cells of the microenvironment, in a membrane-associated context. For example, chronic lymphocytic leukemia cells can activate each other during disease progression by transferring S100-A9 in EVs (Prieto et al., 2017).

CD30 is also transported by l-EVs and s-EVs along with its active releasing enzyme ADAM10. Because CD30 is expressed almost exclusively by certain tissue-associated cells and the EVs thereof, the releasing enzyme processed most CD30 before such EVs end up in the circulation (Hansen et al., 2016). This explains how blood contains predominantly the proteolytically processed soluble product sCD30. Our model argues that CD30 is only transiently expressed on EVs and the highest concentration and functionality is restricted to the vicinity of the donor cell. Because (i) CD30 antibodies are poorly internalized in many $CD30^+$ cell lines (Matthey et al., 2004), (ii) EVs together with CD30 antibody show a good uptake in confocal microscopy and imaging flow cytometry, and (iii) CD30 EVs contribute to the toxicity of BV even in the $CD30^+$ target cell P30-OH/KUBO (**Supplementary Figure 2**), we speculate that BV-loaded EVs play a major role in the therapeutic functionality of BV. However, animal models might be helpful to further substantiate our findings.

At the moment it is still not clear why CD30 does not accumulate in large quantities at the target cell surface, whereas EVs do. We know from earlier immunoelectron microscopic studies that many EVs from L540 cells do not carry CD30 (Hansen et al., 2014). In particular, very small EVs more often lack CD30 compared to larger ones. This is also a reason not to focus on small EVs alone in this study and also include larger vesicles from the 10,000 × *g* fraction. One might speculate that a certain EV type preferentially participates in EV-dependent targeting of DLBCL cells. Based on their size, EVs are arbitrarily categorized into multivesicular body-derived small (30–100 nm) or large exosomes (80–120 nm), plasma membrane-derived microvesicles (100–1,000 nm) and apoptotic bodies (>1,000 nm), the latter derived from dying cells. Except for apoptotic bodies, healthy cells constitutively and especially upon stimulation release a mixture of different vesicle types. Notably, EVs can be isolated by different methods and the selected procedure might influence the enrichment of individual types of vesicles. To avoid this risk, we pooled the EV fractions. Another interesting aspect is the fact that EVs show a strong expression of ADAM10, a major sheddase of CD30. The sheddase is not only active on cells but also cleaving CD30 on EVs (Hansen et al., 2016). A slow depletion of CD30 might be the reason that $CD30^+$ EVs are barely found in the peripheral blood of cHL patients. The limitation of $CD30^+$ EVs to the tumor microenvironment is at least partially explaining the robust clinical efficacy and the mild systemic off-target effects of BV.

CONCLUSION

The detailed mode of action of the CD30 antibody-drug conjugate BV in DLBCL is not well understood in all aspects since the clinical outcome seems to be partially independent of the CD30 expression on the tumor cells. Since $CD30^+$ bystander cells are enriched in the tumor tissue in many cases of DLBCL, CD30 might however be released with EVs. We thus propose a model that even in the absence of CD30 on the tumor cells to be targeted, EVs can transport the targeting protein from cells of the tumor microenvironment to tumor cells (**Figure 4**). This *in vitro* model explains the clinical efficacy of BV also in cases when tumor cells lack the targeting antigen. Because CD30 is not only overexpressed on certain lymphomas but also on certain activated bystander cells in other diseases, BV might be a promising therapeutic option to treat other malignancies or immune diseases.

DATA AVAILABILITY STATEMENT

The datasets presented in this study can be found in online repositories. The names of the repository/repositories and accession number(s) can be found below: The mass spectrometry proteomics data have been deposited to the ProteomeXchange Consortium via the PRIDE partner repository with the dataset identifier PXD025442.

ETHICS STATEMENT

The studies involving human participants were reviewed and approved by Geschäftsstelle Ethikkommision, Universität zu Köln, 50931 Köln. The patients/participants provided their written informed consent to participate in this study.

AUTHOR CONTRIBUTIONS

LL was the main investigator who performed most experiments. ML and OJ performed the Image Stream analysis. AS performed the microscopy. FB performed and analyzed the TEM. HD performed and analyzed the DLBCL microscopy. BP and AP performed and evaluated the mass spectrometry. P-HN and MH provided important clinical impact and critically evaluated the manuscript. HH designed and supervised the project. HH, OJ, and AS wrote the manuscript. All authors read and approved the final version of the manuscript.

FUNDING

The project was generously supported by a grant from the German Research Council (DFG) to HH (HA2432/5-2).

ACKNOWLEDGMENTS

The authors thank Christian Jüngst from the Imaging Facility of the CECAD in Cologne for valuable help with confocal microscopy.

SUPPLEMENTARY MATERIAL

The Supplementary Material for this article can be found online at: https://www.frontiersin.org/articles/10.3389/fcell.2021.698503/full#supplementary-material

Supplementary Figure 1 | Enrichment analysis of the protein hits of the 10,000 x*g* and 100,000 x*g* fraction of L540 EVs.

Supplementary Figure 2 | Viability assay of P30-OH/KUBO.

Supplementary Table 1 | Gene list of mass spectrum hits of the 10,000 x*g* and the 100,000 x*g* fraction of L540 EVs.

REFERENCES

Bartlett, N. L., Smith, M. R., Siddiqi, T., Advani, R. H., O'Connor, O. A., and Sharman, J. P. (2017). Brentuximab vedotin activity in diffuse large B-cell lymphoma with CD30 undetectable by visual assessment of conventional immunohistochemistry. *Leuk. Lymphoma* 58, 1607–1616. doi: 10.1080/10428194.2016.1256481

Cerutti, A., Schaffer, A., Goodwin, R. G., Shah, S., Zan, H., Ely, S., et al. (2000). Engagement of CD153 (CD30 ligand) by CD30+ T cells inhibits class switch DNA recombination and antibody production in human IgD+ IgM+ B cells. *J. Immunol.* 165, 786–794. doi: 10.4049/jimmunol.165.2.786

Chen, G., Huang, A. C., Zhang, W., Zhang, G., Wu, M., and Xu, W. (2018). Exosomal PD-L1 contributes to immunosuppression and is associated with anti-PD-1 response. *Nature* 560, 382–386. doi: 10.1038/s41586-018-0392-8

Gilfillan, M. C., Noel, P. J., Podack, E. R., Reiner, S. L., and Thompson, C. B. (1998). Expression of the costimulatory receptor CD30 is regulated by both CD28 and cytokines. *J. Immunol.* 160, 2180–2187.

Hansen, H. P., Engels, H. M., Dams, M., Paes Leme, A. F., Pauletti, B. A., and Simhadri, V. L. (2014). Protrusion-guided extracellular vesicles mediate CD30 trans-signalling in the microenvironment of Hodgkin's lymphoma. *J. Pathol.* 232, 405–414. doi: 10.1002/path.4306

Hansen, H. P., Trad, A., Dams, M., Zigrino, P., Moss, M., Tator, M., et al. (2016). CD30 on extracellular vesicles from malignant Hodgkin cells supports damaging of CD30 ligand-expressing bystander cells with Brentuximab-Vedotin, in vitro. *Oncotarget* 7, 30523–30535. doi: 10.18632/oncotarget.8864

Horie, R., and Watanabe, T. (1998). CD30: expression and function in health and disease. *Semin. Immunol.* 10, 457–470. doi: 10.1006/smim.1998.0156

Horn-Lohrens, O., Tiemann, M., Lange, H., Kobarg, J., Hafner, M., Hansen, H., et al. (1995). Shedding of the soluble form of CD30 from the Hodgkin-analogous cell line L540 is strongly inhibited by a new CD30-specific antibody (Ki-4). *Int. J. Cancer* 60, 539–544. doi: 10.1002/ijc.2910600419

Hu, S., Xu-Monette, Z. Y., Balasubramanyam, A., Manyam, G. C., Visco, C., Tzankov, A., et al. (2013). CD30 expression defines a novel subgroup of diffuse large B-cell lymphoma with favorable prognosis and distinct gene expression signature: a report from the International DLBCL Rituximab-CHOP Consortium Program Study. *Blood* 121, 2715–2724. doi: 10.1182/blood-2012-10-461848

Jacobsen, E. D., Sharman, J. P., Oki, Y., Advani, R. H., Winter, J. N., Bello, C. M., et al. (2015). Brentuximab vedotin demonstrates objective responses in a phase 2 study of relapsed/refractory DLBCL with variable CD30 expression. *Blood* 125, 1394–1402. doi: 10.1182/blood-2014-09-598763

Janik, J. E., Morris, J. C., O'Mahony, D., Pittaluga, S., Jaffe, E. S., and Redon, C. E. (2015). 90Y-daclizumab, an anti-CD25 monoclonal antibody, provided responses in 50% of patients with relapsed Hodgkin's lymphoma. *Proc. Natl. Acad. Sci. U. S. A.* 112, 13045–13050. doi: 10.1073/pnas.1516107112

Lee, K., Fraser, K., Ghaddar, B., Yang, K., Kim, E., Balaj, L., et al. (2018). Multiplexed Profiling of Single Extracellular Vesicles. *ACS Nano* 12, 494–503. doi: 10.1021/acsnano.7b07060

Matthey, B., Borchmann, P., Schnell, R., Tawadros, S., Lange, H., Huhn, M., et al. (2004). Metalloproteinase inhibition augments antitumor efficacy of the anti-CD30 immunotoxin Ki-3(scFv)-ETA' against human lymphomas in vivo. *Int. J. Cancer* 111, 568–574. doi: 10.1002/ijc.20278

Nishimura, T., Oyama, T., Hu, H. T., Fujioka, T., Hanawa-Suetsugu, K., Ikeda, K., et al. (2021). Filopodium-derived vesicles produced by MIM enhance the migration of recipient cells. *Dev. Cell* 56, 842–859.e8. doi: 10.1016/j.devcel.2021.02.029

Okeley, N. M., Miyamoto, J. B., Zhang, X., Sanderson, R. J., Benjamin, D. R., Sievers, E. L., et al. (2010). Intracellular activation of SGN-35, a potent anti-CD30 antibody-drug conjugate. *Clin. Cancer Res.* 16, 888–897. doi: 10.1158/1078-0432.CCR-09-2069

Perez-Riverol, Y., Csordas, A., Bai, J., Bernal-Llinares, M., Hewapathirana, S., Kundu, D. J., et al. (2019). The PRIDE database and related tools and resources in 2019: improving support for quantification data. *Nucleic Acids Res.* 47, D442–D450. doi: 10.1093/nar/gky1106

Prieto, D., Sotelo, N., Seija, N., Sernbo, S., Abreu, C., Duran, R., et al. (2017). S100-A9 protein in exosomes from chronic lymphocytic leukemia cells promotes NF-kappaB activity during disease progression. *Blood* 130, 777–788. doi: 10.1182/blood-2017-02-769851

Slack, G. W., Steidl, C., Sehn, L. H., and Gascoyne, R. D. (2014). CD30 expression in de novo diffuse large B-cell lymphoma: a population-based study from British Columbia. *Br. J. Haematol.* 167, 608–617. doi: 10.1111/bjh.13085

Sperling, S., Fiedler, P., Lechner, M., Pollithy, A., Ehrenberg, S., Schiefer, A. I., et al. (2019). Chronic CD30 signaling in B cells results in lymphomagenesis by driving the expansion of plasmablasts and B1 cells. *Blood* 133, 2597–2609. doi: 10.1182/blood.2018880138

Stein, H., Mason, D. Y., Gerdes, J., O'Connor, N., Wainscoat, J., Pallesen, G., et al. (1985). and et al.: the expression of the Hodgkin's disease associated antigen Ki-1 in reactive and neoplastic lymphoid tissue: evidence that Reed-Sternberg cells and histiocytic malignancies are derived from activated lymphoid cells. *Blood* 66, 848–858. doi: 10.1182/blood.v66.4.848.bloodjournal664848

Sutherland, M. S., Sanderson, R. J., Gordon, K. A., Andreyka, J., Cerveny, C. G., Yu, C., et al. (2006). Lysosomal trafficking and cysteine protease metabolism confer target-specific cytotoxicity by peptide-linked anti-CD30-auristatin conjugates. *J. Biol. Chem.* 281, 10540–10547. doi: 10.1074/jbc.M510026200

Thery, C., Ostrowski, M., and Segura, E. (2009). Membrane vesicles as conveyors of immune responses. *Nat. Rev. Immunol.* 9, 581–593. doi: 10.1038/nri2567

Tkach, M., and Thery, C. (2016). Communication by Extracellular Vesicles: where We Are and Where We Need to Go. *Cell* 164, 1226–1232. doi: 10.1016/j.cell.2016.01.043

Wahl, A. F., Klussman, K., Thompson, J. D., Chen, J. H., Francisco, L. V., Risdon, G., et al. (2002). The anti-CD30 monoclonal antibody SGN-30 promotes growth arrest and DNA fragmentation in vitro and affects antitumor activity in models of Hodgkin's disease. *Cancer Res.* 62, 3736–3742.

Weniger, M. A., Tiacci, E., Schneider, S., Arnolds, J., Ruschenbaum, S., Duppach, J., et al. (2018). Human CD30+ B cells represent a unique subset related to Hodgkin lymphoma cells. *J. Clin. Invest.* 128, 2996–3007. doi: 10.1172/JCI95993

Wiley, S. R., Goodwin, R. G., and Smith, C. A. (1996). Reverse signaling via CD30 ligand. *J. Immunol.* 157, 3635–3639.

Younes, A., Gopal, A. K., Smith, S. E., Ansell, S. M., Rosenblatt, J. D., Savage, K. J., et al. (2012). Results of a pivotal phase II study of brentuximab vedotin for patients with relapsed or refractory Hodgkin's lymphoma. *J. Clin. Oncol.* 30, 2183–2189. doi: 10.1200/JCO.2011.38.0410

Conflict of Interest: HD was employed by the company Pathodiagnostik Berlin MVZ GmbH.

The remaining authors declare that the research was conducted in the absence of any commercial or financial relationships that could be construed as a potential conflict of interest.

Publisher's Note: All claims expressed in this article are solely those of the authors and do not necessarily represent those of their affiliated organizations, or those of the publisher, the editors and the reviewers. Any product that may be evaluated in this article, or claim that may be made by its manufacturer, is not guaranteed or endorsed by the publisher.

frontiers in Cell and Developmental Biology

ORIGINAL RESEARCH
published: 25 August 2021
doi: 10.3389/fcell.2021.638374

Single-Cell Analysis Reveals Spatial Heterogeneity of Immune Cells in Lung Adenocarcinoma

Youyu Wang[1†], Xiaohua Li[2†], Shengkun Peng[3†], Honglin Hu[4†], Yuntao Wang[5†], Mengqi Shao[1], Gang Feng[1*], Yu Liu[4*] and Yifeng Bai[4*]*

[1] Department of Thoracic Surgery, Sichuan Provincial People's Hospital, University of Electronic Science and Technology of China, Chengdu, China, [2] Department of Respiratory and Critical Care Medicine, Sixth People's Hospital of Chengdu, Chengdu, China, [3] Department of Radiology, Sichuan Academy of Medical Sciences and Sichuan Provincial People's Hospital, University of Electronic Science and Technology of China, Chengdu, China, [4] Department of Oncology, Sichuan Provincial People's Hospital, University of Electronic Science and Technology of China, Chengdu, China, [5] Department of Oncology, The Fifth People's Hospital Affiliated to Chengdu University of Traditional Chinese Medicine the Second Clinical Medical College, Chengdu, China

OPEN ACCESS

Edited by:
Rodrigo Nalio Ramos, INSERM U1138 Centre de Recherche des Cordeliers (CRC), France

Reviewed by:
Jian Zhang, Southern Medical University, China
Christopher Auger, Beth Israel Deaconess Medical Center and Harvard Medical School, United States

***Correspondence:**
Mengqi Shao
agrimony2009@live.cn
Gang Feng
steedvan@163.com
Yu Liu
14067599@qq.com
Yifeng Bai
baiyifeng@med.uestc.edu.cn

[†]These authors have contributed equally to this work

Specialty section:
This article was submitted to Molecular and Cellular Pathology, a section of the journal Frontiers in Cell and Developmental Biology

Received: 06 December 2020
Accepted: 13 July 2021
Published: 25 August 2021

Citation:
Wang Y, Li X, Peng S, Hu H, Wang Y, Shao M, Feng G, Liu Y and Bai Y (2021) Single-Cell Analysis Reveals Spatial Heterogeneity of Immune Cells in Lung Adenocarcinoma. Front. Cell Dev. Biol. 9:638374. doi: 10.3389/fcell.2021.638374

The impacts of the tumor microenvironment (TME) on tumor evolvability remain unclear. A challenge for nearly all cancer types is spatial heterogeneity, providing substrates for the emergence and evolvability of drug resistance and leading to unfavorable prognosis. Understanding TME heterogeneity among different tumor sites would provide deeper insights into personalized therapy. We found 9,992 cell profiles of the TME in human lung adenocarcinoma (LUAD) samples at a single-cell resolution. By comparing different tumor sites, we discovered high TME heterogeneity. Single-sample gene set enrichment analysis (ssGSEA) was utilized to explore functional differences between cell subpopulations and between the core, middle and edge of tumors. We identified 8 main cell types and 27 cell subtypes of T cells, B cells, fibroblasts and myeloid cells. We revealed $CD4^+$ naive T cells in the tumor core that express high levels of immune checkpoint molecules and have a higher activity of immune-exhaustion signaling. $CD8^+$ T cell subpopulations in the tumor core correlate with the upregulated activity of transforming growth factor-β (TGF-β) and fibroblast growth factor receptor (FGFR) signaling and downregulated T cell activity. B cell subtypes in the tumor core downregulate cytokine production. In this study, we revealed that there was immunological heterogeneity in the TME of patients with LUAD that have different ratios of immune cells and stromal cells, different functions, and various degrees of activation of immune-related pathways in different tumor parts. Therefore, clarifying the spatial heterogeneity of the tumor in the immune microenvironment can help clinicians design personalized treatments.

Keywords: single-cell sequencing, spatial heterogeneity, lung adenocarcinoma, immune microenvironment, immunity

Abbreviations: TME, tumor microenvironment; LUAD, lung adenocarcinoma; ssGSEA, single-sample gene set enrichment analysis; TGF-β, transforming growth factor-β; FGFR, fibroblast growth factor receptor; LUSC, lung squamous cell carcinoma; scRNA-seq, single-cell RNA sequencing; IL, interleukin; UMI, unique molecular identifier; MsigDB, Molecular Signatures Database; COPD, chronic obstructive pulmonary disease; PCs, principle components; NK, natural killer; γδ T cells, gamma delta T cells; Tregs, regulatory T cells; MALT, mucosa-associated lymphoid tissue; TILs, tumor-infiltrating lymphocytes; Th1, T helper 1; HIF, hypoxia inducible factor; H&E, hematoxylin and eosin.

INTRODUCTION

Tumors are hierarchical, heterogeneous and evolving complex ecosystems. The continuous interaction between tumor cells and their microenvironment greatly promotes the development, metastasis and evolution of tumors (Sharma et al., 2019; Turajlic et al., 2019). Cancer cells respond to treatment under the action of other cell types in the tumor microenvironment (TME). Recently, the TME has become an important therapeutic target (Lin et al., 2019, 2020). In addition, the spatial heterogeneity of tumors has caused substantial challenges for tumor treatment (Allam et al., 2020). There are hundreds to thousands of subclones in each tumor, which makes it difficult for researchers to fully understand the TME in different areas of the tumor. Therefore, clarifying the spatial heterogeneity of the tumor within the TME would help clinicians design personalized treatments (Allam et al., 2020).

Studies of tumor heterogeneity and tumor evolution using multiregion samples and spatial transcriptome analysis have provided much help for understanding tumor pathogenesis and treatment. Sharma et al. (2019) used multiregion samples of lung squamous cell carcinoma (LUSC) after bulk sequencing from genome, transcriptome, and tumor-immune interactions and histopathology to analyze the intratumoral heterogeneity (ITH) and tumor evolution process of LUSC. Darmanis et al. (2017) performed single-cell RNA sequencing (scRNA-seq) on a total of 3,587 cells in the tumor core and surrounding areas from 4 malignant glioma patients and found that the tumor core contained a concentrated distribution of macrophages and high expression of anti-inflammatory genes and pro-angiogenic factors, such as the anti-inflammatory regulator interleukin (IL)-1 receptor antagonist (IL1RN); in contrast, the surrounding area was mainly enriched in microglia and highly expressed pro-inflammatory genes, such as the inflammation marker IL-1α/β.

ScRNA-seq reveals the functional state of cells at a single-cell resolution and is a powerful tool for studying the TME (Liu et al., 2020). Single-cell transcriptome data provide a more comprehensive understanding of the complexity of the immune system of the TME of lung cancer. The immune microenvironments of different parts of tumors, of tumors from different individuals, and in different disease states are obviously different. With an understanding of the immune microenvironment at a single-cell resolution (Lambrechts et al., 2018; Smith and Hodges, 2019; Maynard et al., 2020), we have a more comprehensive understanding of how the immune system kills tumors.

Recently, studies on immune cells in the immune microenvironment from different levels of lung adenocarcinoma (LUAD) have not been reported. In addition, there is very little research on immune cells and interstitial cells at the single-cell level to different levels of LUAD. By studying this topic, we can understand the immune infiltration of LUAD at different levels from different spatial dimensions. The situation and the activation of abnormal pathways of different immune cell subtypes could finally help achieve personalized medicine.

MATERIALS AND METHODS

Single-Cell Gene Expression Quantification and Determination of the Major Cell Types

Raw gene expression matrices that were generated in each sample using Cell Ranger (version 2.0.0) were combined in R (version 3.6.1) and converted to a Seurat object using the Seurat R package (version 3.1.4). From this, all cells that had either fewer than 201 UMIs, over 6,000 or below 101 expressed genes, or over 10% UMIs derived from the mitochondrial genome were removed. The FindIntegrationAnchors function and IntegrateData function were used to eliminate the batch effects. To reduce the dimensionality of this dataset, the first 5,000 variably expressed genes were summarized by principal component analysis, and the first 9 PCs were further summarized using tSNE dimensionality reduction using the default settings of the RunTSNE function.

scRNA-Seq Data Acquisition and Data Preprocessing

The raw sequencing data from 3 sets of LUAD specimens were downloaded from the ArrayExpress database (accessions E-MTAB-6149 and E-MTAB-6653) (Lambrechts et al., 2018). Each LUAD patient had 4 samples: samples from the core of the tumor, the middle of the tumor, the edge of the tumor and the adjacent tissues. The sampling sites, the clinical characteristics, upstream analysis and downstream analysis (including quality control (QC) and clustering) details of scRNA-seq of these three LUAD patients have been published elsewhere (**Supplementary Table 1**; Lambrechts et al., 2018). **Supplementary Figures 1A–C** shows the gene number, the unique molecular identifier (UMI), the mitochondrial content of these 12 samples, their correlation, and the origin of these samples and batches. In addition, the details of the raw data analysis and data preprocessing are shown in **Supplementary Methods** and **Figure 1A**.

Dimensionality Reduction, Clustering and Reclustering of the Main Cell Types

After QC (**Supplementary Figures 2A–F**), we used the Seurat R package to perform data normalization (LogNormalize), dimensionality reduction, and clustering analysis. The cellular components in the immune microenvironment of LUAD were identified using the FindNeighbors, FindClusters and FindAllMarkers functions to cluster cells and identify genes that were differentially expressed in the cell subsets [with cutoffs of min.pct = 0.15 and logfc.threshold = log2(2)]. Then, published literature and the CellMarker database were used to annotate the marker genes of each cluster, and we identified a total of 8 types of cells. To further identify the cell subpopulations in each cluster, we performed separate clustering and downstream analysis on each of the types of cells. To determine the cell subgroups in each cluster, we used marker genes in published literature (Lambrechts et al., 2018) and the CellMarker database to annotate each cell subgroup (Zhang et al., 2019).

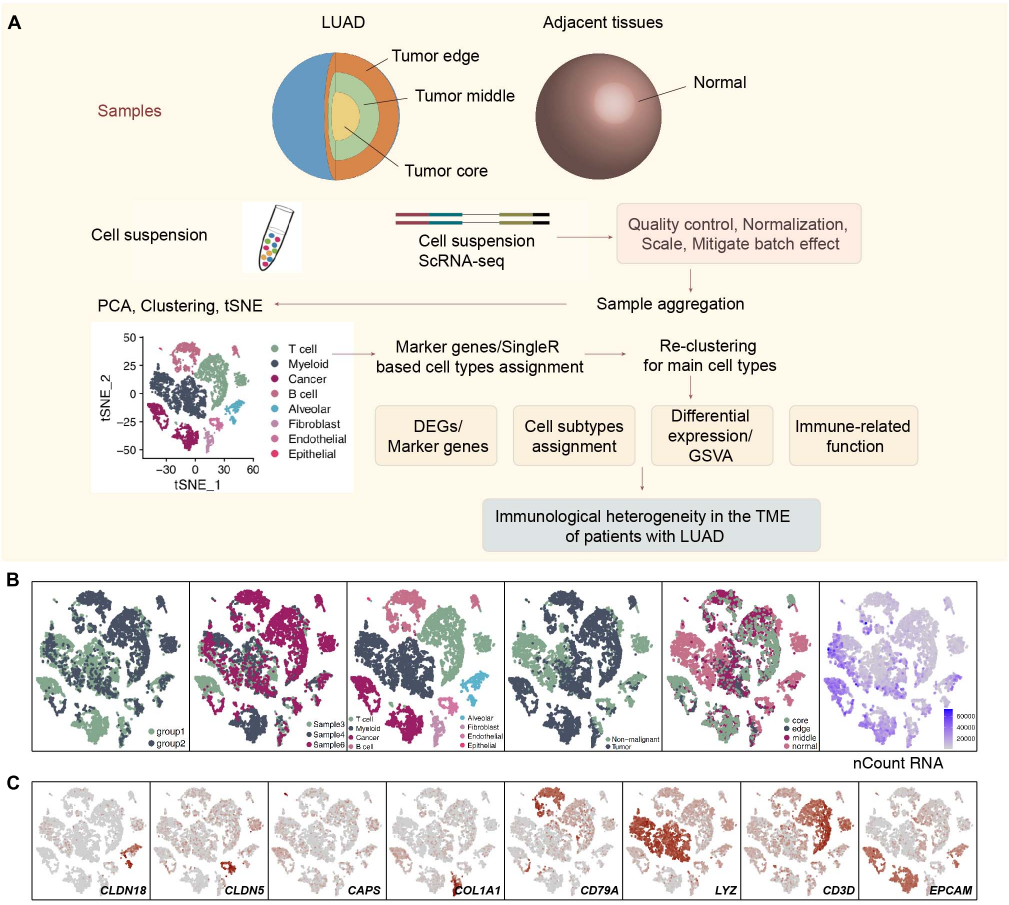

FIGURE 1 | Overview of 9,993 single cells from LUAD and adjacent non-malignant LUAD. **(A)** Overview of the scRNA-seq analysis in this study. **(B)** tSNE of the 9,993 cells profiled, with each cell color-coded for (left to right) its batch group (batch 1 and batch 2), the corresponding patient, the associated cell type and the sample origin (tumor or non-malignant tissue), and the number of transcripts (UMIs) detected in that cell (log scale is defined in the inset). **(C)** Expression of marker genes for the cell types defined above each panel.

Cell Function, Immune Function, and Trajectory Analyses

To identify the differences in cell function in different areas, the single-sample gene set enrichment analysis (ssGSEA) (Liberzon et al., 2015) algorithm in the gene set variation analysis (GSVA) (Hänzelmann et al., 2013) package was used to evaluate the activity of different pathways [from the Molecular Signatures Database (MsigDB)] (Liberzon et al., 2011) in each cell, and the ssGSEA score was used to reflect the activation and inhibition of the pathway in each cell. Lists of immune checkpoint inhibitors and cytotoxicity molecules were extracted from published literature (Rooney et al., 2015; Lambrechts et al., 2018; Li et al., 2018). The monocle package was used to reconstruct the development and differentiation trajectories of immune cells (Qiu et al., 2017).

Statistics

For gene expression, comparisons between two groups were performed using an unpaired two-tailed Mann-Whitney *U*-test. For the ssGSEA score, comparisons between the two groups were performed using the limma R package. Box plot, violin plot and histograms in the ggplot2 (Wickham, 2011) package were used for visualization. The pathways presented in the heatmaps were significantly different between the two groups (adjusted $P < 0.05$). All statistical analyses were performed using R (version 3.6.1).

RESULTS

ScRNA-Seq Transcriptomic Profiles of LUAD

All 3 LUAD patients had undergone lobectomy, and nearly 66.7% of these LUAD patients (2/3; 66.7%) had mild chronic obstructive pulmonary disease (COPD). Four samples, namely, a sample from the center, edge, and periphery of the tumor and a sample of normal tissue from each patient with LUAD were obtained from the end of the same lung tissue. These samples were all examined using single-cell sequencing with the 10X genomics protocol. We used CellRanger software to analyze the original

data (see **Supplementary Methods** for details). According to the coloring of the sample batch of each cell, we found that the samples of the two batches of data were not well integrated, and there was an obvious batch effect (**Supplementary Figure 1C**). We used the FindIntegrationAnchors and the IntegrateData functions in the Seurat package to integrate the first 5,000 variably expressed genes and remove batches of genes (**Supplementary Figure 2A**). In addition, we colored each cell according to the COPD type, sex, patient source, sampling site, and sample type (**Supplementary Figures 2B–F**). Next, we performed cluster analysis on this batch of cells. According to the differences between the first 5,000 variably expressed genes and the first 9 principle components (PCs), 9,992 cells were clustered to obtain a total of 8 cell types. A total of 3,313 cells (33.2%) belonged to non-tumor tissues, and 6,679 cells (66.8%) belonged to tumor tissues (**Figure 1B**), which were defined according to the specific high expression genes of each cell subgroup (**Supplementary Table 2**). We defined 3 lymphocyte subgroups [myeloid cells (marker gene: LYZ), T cells (marker gene: CD3D), and B cells (marker gene: CD79A)], endothelial cells (marker gene: CLDN5), alveolar cells (marker gene: CLDN18), fibroblasts (marker gene: COL1A1), epithelial cells (marker gene: CAPS), and cancer cells (marker gene: EPCAM) (**Figure 1C** and **Supplementary Table 3**).

Immunological Differences Among the T Cell Subpopulations

With 1,928 cells detected, T cells represented the most prevalent cells. T lymphocytes were regrouped into 6 cell subgroups (**Figure 2A** and **Supplementary Table 4**). Most of the cells were located in the core and middle of the tumor, which are $CD4^+$ naive T cells (SELL, CCR7, and C1orf162; clusters 0 and 2); regulatory T cells (Tregs; FOXP3, IL2RA, TNFRSF18, and TNFRSF4; cluster 4); $CD8^+$ T cells/natural killer (NK) cells (CD8A, GZMA, GZMB, and NKG7; clusters 1 and 3) and other T cells (unclassified; cluster 6; **Figure 2B**). Next, we used the ssGSEA algorithm to estimate the activity of each cell in the 6 types of T cell subgroups in the pathological pathway and compared the up- or downregulated pathological or immune-related pathways of each T cell subgroup (**Figure 2C**). $CD4^+$ naive T cells significantly upregulated the activity of gamma delta T cells (γδ T cells). The activity of $CD8^+$ T cells/NK cells in the cell cycle and DNA damage-related pathways is significantly higher than that of other T cell subgroups.

To further explore the differences between the subgroups of 932 $CD4^+$ naive T cells and the functional differences in each subgroup at different tumor sites (**Figure 3A** and **Supplementary Table 4**), we found that the $CD4^+$ naive T cells (cluster 0) located at the core of the tumor in the activities of angiogenesis and Wnt-regulating cell proliferation are significantly higher than those at the edge of the tumor; in contrast, the activity in cytokines (such as interferon) and inflammatory response as significantly lower at the core of the tumor than at the edge of the tumor (**Figure 3B**). Similarly, $CD4^+$ naive T cells (cluster 0) located at the core of the tumor have significantly higher activation levels in angiogenesis, epoxygenase cytochrome P450, NOTCH3 signaling, lipid particle organization and other pathways than those at the edge of the tumor. $CD4^+$ naive T cells (cluster 0 and cluster 2) at the core of the tumor express more immune checkpoint molecules, such as CTLA4, which has been used in clinical practice, and LAG3, HAVCR2, and TNFRSF9/CD137, which are currently undergoing clinical trials (**Figure 3C**) than those at other locations. Additionally, the functional activity of some immunostimulation-related pathways in $CD4^+$ naive T cells (clusters 0 and 2) located at the core of the tumor was significantly lower than that of $CD4^+$ naive T cells located in the middle or periphery of the tumor; these pathways included cytokine synthesis, which mediates the recruitment of lymphocytes (**Figure 3D**). In contrast, some pathway activities related to immune depletion were significantly activated in $CD4^+$ naive T cells (clusters 0 and 2) located in the core of the tumor; these pathways included FGFR signaling, lipid fatty acid synthesis, and MAPK signaling (**Figure 3D**).

$CD8^+$ T cells and NK cells play an important role in killing tumor cells. We reclustered 719 $CD8^+$ T cells and NK cells (**Figure 4A** and **Supplementary Table 4**) and identified 4 subgroups based on their marker genes (**Figure 4B** and **Supplementary Figure 4A**): exhausted $CD8^+$ T cells (marker gene: HAVCR2; cluster 0); naive $CD8^+$ T cells (marker gene: CCR7; cluster 1); proliferating $CD8^+$ T cells (marker gene: MKI67; clusters 2 and 4), and NK cells (marker gene: KLRC1, KLRB1, and SEC11C; clusters 3 and 5). We also compared the expression levels of marker genes in $CD8^+$ T cell NK cells at different tumor sites (**Supplementary Figure 3A**). $CD8^+$ T cells, $CD4^+$ naive T cells, and Tregs have different expression levels of marker genes in different tumor sites (**Supplementary Figures 3B–D**). In addition, we found that compared with that of proliferating $CD8^+$ T cells, the expression of proliferation gene markers in exhausted $CD8^+$ T cells and naive $CD8^+$ T cells was lower (**Supplementary Figure 4B**). Compared with those in the middle or periphery of the tumor, the exhausted $CD8^+$ T cells located in the core of the tumor had a lower proliferation function (**Supplementary Figure 4C**). In addition, we found that different subgroups of $CD8^+$ T cells may perform different cellular functions. For example, exhausted $CD8^+$ T cells (cluster 0) had a higher degree of activation in the FGFR, transforming growth factor-β (TGF-β) and fatty acid synthesis pathways. In contrast, proliferating $CD8^+$ T cells (cluster 2) were significantly more active in ATP, cytolysis, and MHC-IB signaling than other cell subgroups (**Figure 4C**). Similarly, immune checkpoint molecules, such as PDCD1, CTLA4, HAVCR2, and TNFRSF9/CD137, were significantly higher in exhausted $CD8^+$ T cells (cluster 0) than in other cell subsets; in contrast, cytotoxic molecules, such as GZMK, were significantly lower in exhausted $CD8^+$ T cells than in naive $CD8^+$ T cells (cluster 1) and proliferating $CD8^+$ T cells (cluster 2; **Figure 4D**). Next, we compared the functional differences between each $CD8^+$ T cell subgroup at different tumor sites (**Figures 4E,F**). Most of the pathway activities were related to immune depletion and included fatty acid lipid metabolism, stem cell proliferation, and fibroblast growth. Factor receptor signaling is significantly higher in the $CD8^+$ T cell subgroups

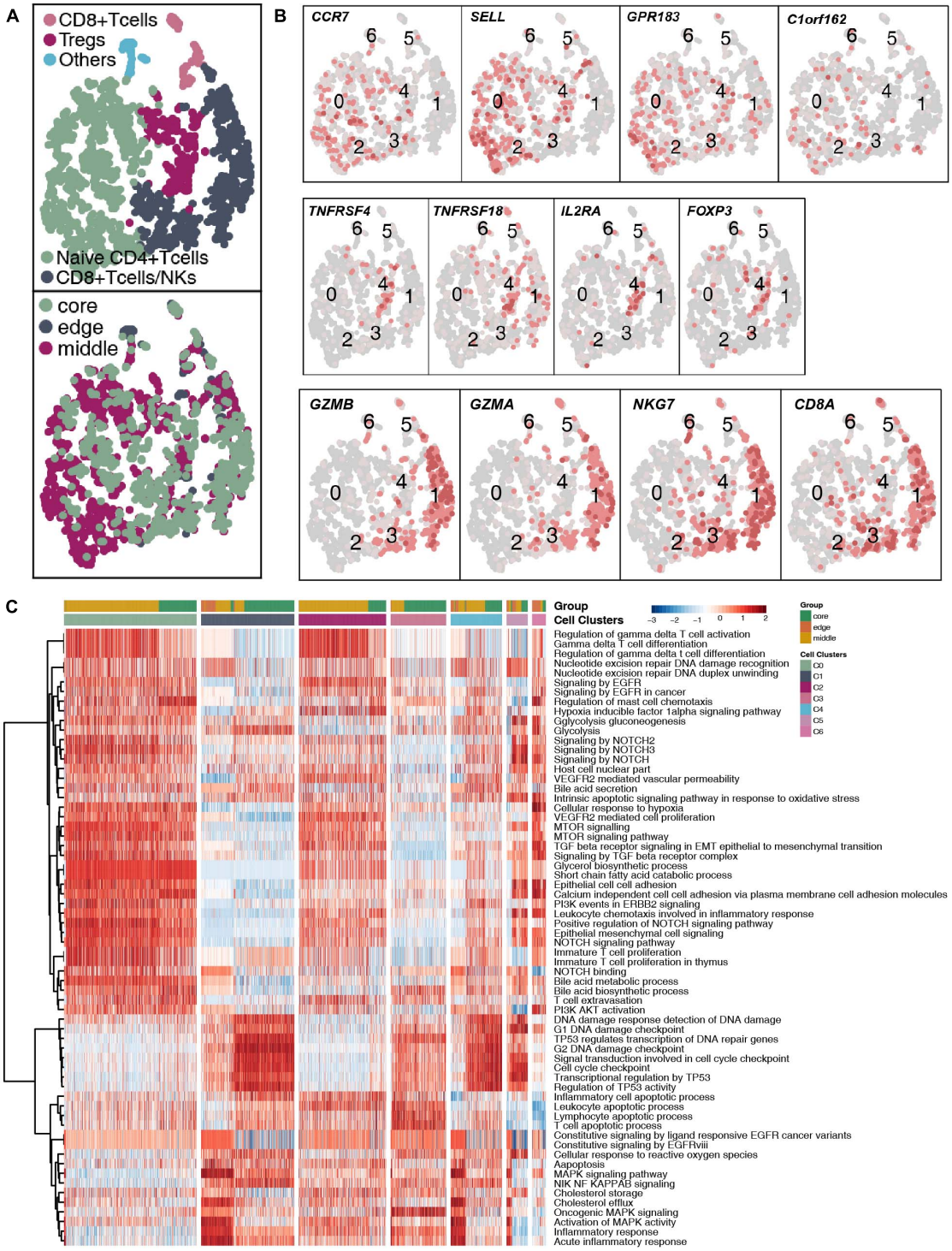

FIGURE 2 | T cell clusters in LUAD. **(A)** tSNE plot of 1,928 T cells, which are color-coded by their associated cluster or the sample location. **(B)** tSNE plot, which is color-coded for expression of marker genes for the cell types, as indicated. **(C)** Differences in pathway activities scored per cell by ssGSEA between the different T cell clusters.

located at the core of the tumor than in the $CD8^+$ T cell subgroups located at the edge of the tumor. In contrast, the activities of immune-related cytokine synthesis, chemokines, inflammatory response and other pathways at the core of the tumor were significantly lower than those of the $CD8^+$ T cell subgroups located at the edge of the tumor. Since the existence

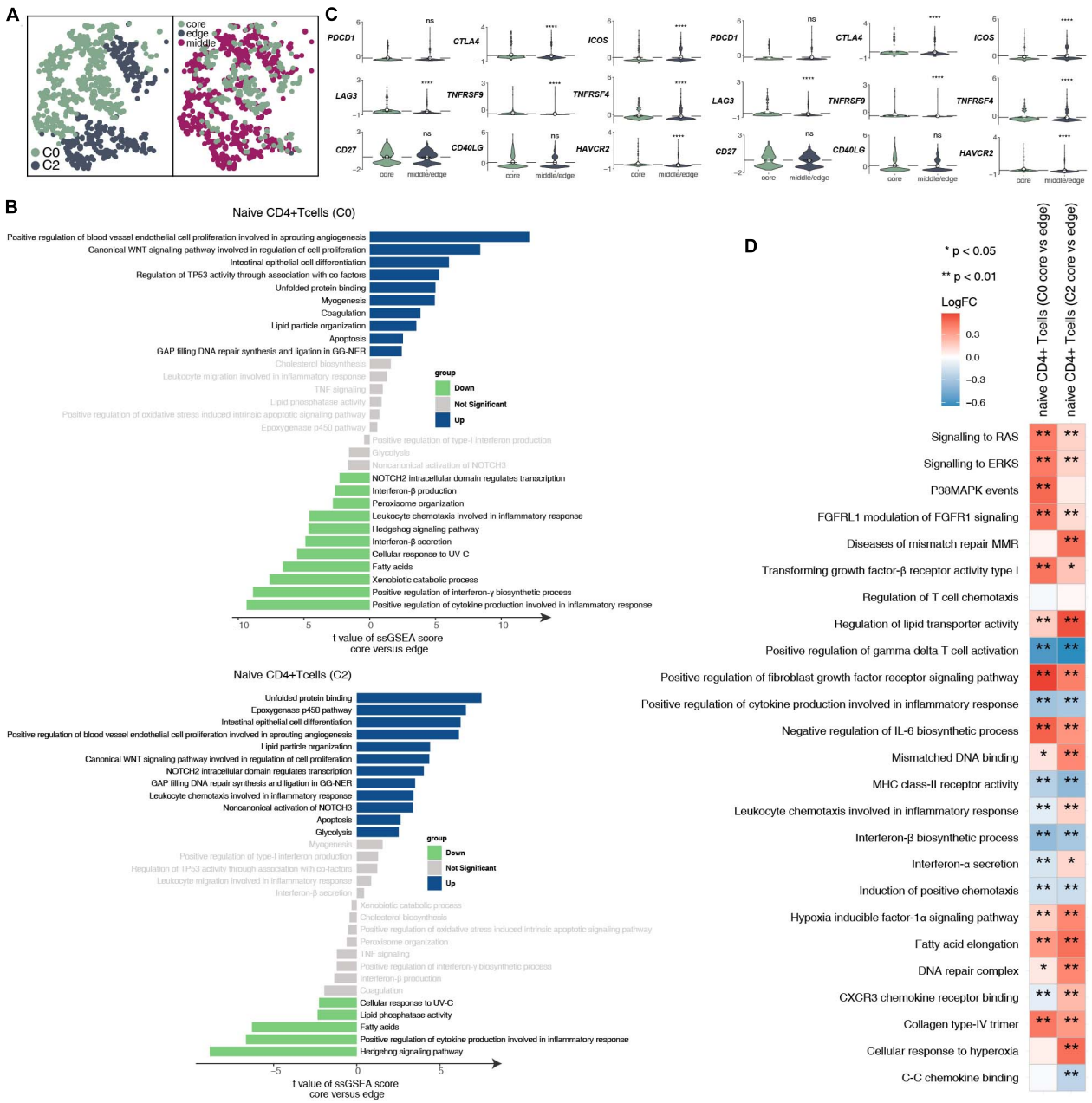

FIGURE 3 | CD4$^+$ naive T cell clusters in LUAD. **(A)** tSNE plot of 932 CD4$^+$ naive T cells, which are color-coded by their associated cluster or the sample location. **(B)** Differences in pathway activities scored per cell by GSVA between the tumor core and tumor edge in the CD4$^+$ naive T cells (cluster 0) and CD4$^+$ naive T cells (cluster 2). *T*-values are from a linear model. **(C)** Violin plots showing the smoothed expression distribution of selected genes involved in T cell activity and in immune checkpoints, stratified by CD4$^+$ naive T cell clusters (clusters 0 and 2). **(D)** Heatmap depicting the mean differences in pathway activities scored per cell by GSVA between the tumor core and tumor edge across the CD4$^+$ naive T cells (cluster 0) and CD4$^+$ naive T cells (cluster 2). The *x*-axis of the heatmap indicates different CD4$^+$ naive T cell clusters, and the *y*-axis indicates pathway activities scored per cell by GSVA. Each square represents the fold change or difference in each indicated pathway activity scored per cell by GSVA between the tumor core and tumor edge across the CD4$^+$ naive T cells (cluster 0) and CD4$^+$ naive T cells (cluster 2). Red indicates upregulation, while blue indicates downregulation. *$P < 0.05$; **$P < 0.01$; ****$P < 0.0001$.

of exhausted CD8$^+$ T cells had a great impact on the efficacy and prognosis of immunotherapy, we further compared the functional activities of exhausted CD8$^+$ T cells in different parts of the tumor. We found that the exhausted CD8$^+$ T cells located in the core of the tumor had a higher expression of immune checkpoint molecules, including PDCD1, CTLA4, LAG3, TNFRSF9/CD137, CD27, and HAVCR2. In contrast, there were significantly more cytotoxic markers, such as GZMB, in exhausted CD8$^+$ T cells at the edge of the tumor than at the core of the tumor (**Figure 4G**). Trajectory analysis based on

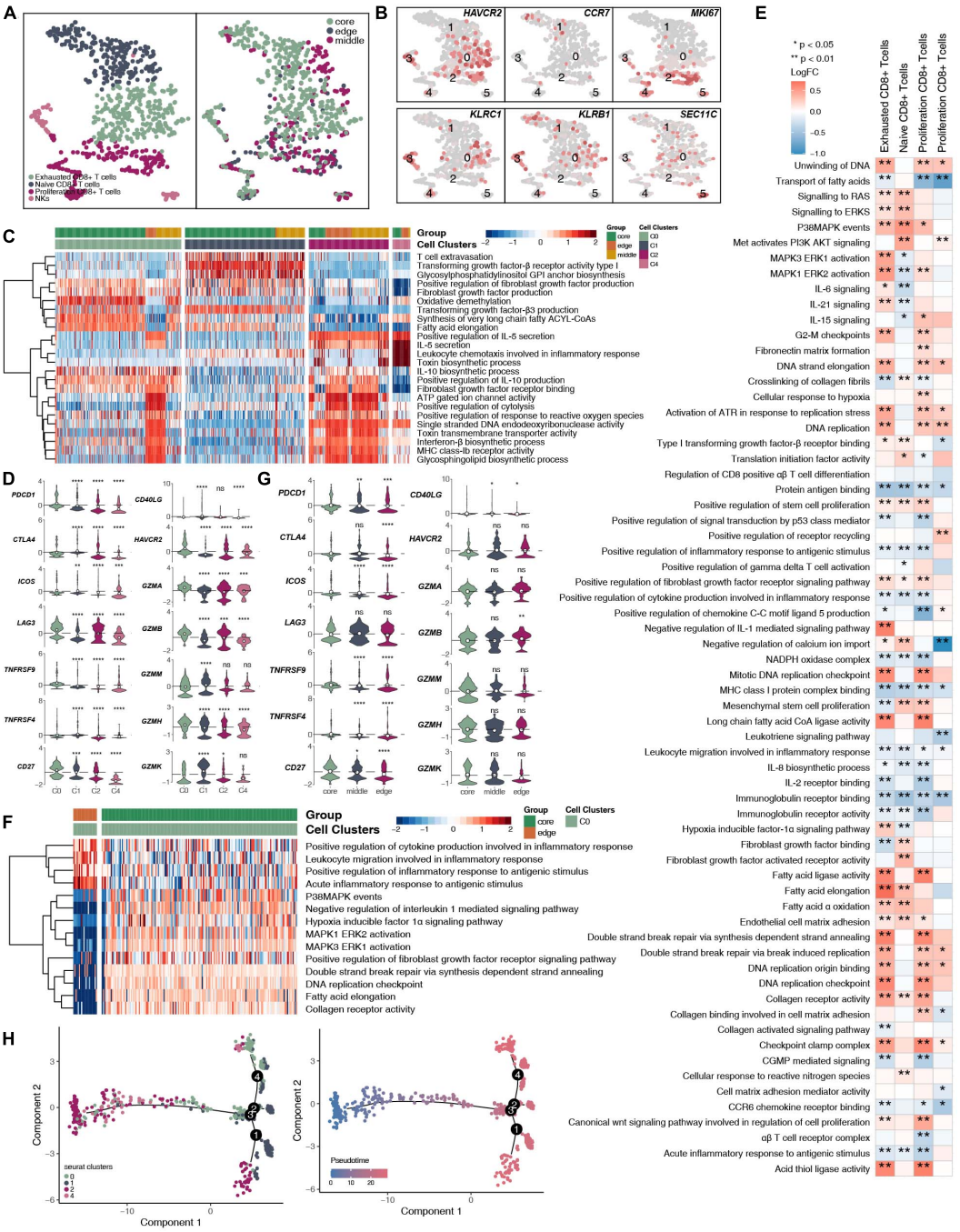

FIGURE 4 | CD8$^+$ T cells/NK cells cluster in LUAD. **(A)** tSNE plot of 719 CD8$^+$ T cells/NK cells, which are color-coded by their associated cluster or the sample location. **(B)** tSNE plot, which color-coded for the expression of marker genes for the cell types, as indicated. **(C)** Heatmap of the ssGSEA score, as estimated using gene sets from the MsigDB, for four CD8$^+$ T cell clusters: exhausted CD8$^+$ T cells (cluster 0), CD8$^+$ naive T cells (cluster 1), proliferating CD8$^+$ T cells (cluster 2), and proliferating CD8$^+$ T cells (cluster 4). **(D)** Violin plots showing the smoothed expression distribution of selected genes involved in T cell activity and in immune checkpoints, stratified by CD8$^+$ T cell clusters: exhausted CD8$^+$ T cells (cluster 0), CD8$^+$ naive T cells (cluster 1), proliferating CD8$^+$ T cells (cluster 2), and proliferating CD8$^+$ T cells (cluster 4). **(E)** Heatmap depicting the mean differences in pathway activities scored per cell by GSVA between tumor core and tumor edge across the exhausted CD8$^+$ T cells (cluster 0), CD8$^+$ naive T cells (cluster 1), proliferating CD8$^+$ T cells (cluster 2), and proliferating CD8$^+$ T cells (cluster 4). The *x*-axis of the heatmap indicates different CD8$^+$ T cell clusters, and the *y*-axis indicates pathway activities scored per cell by GSVA. Each square represents the fold change or difference in each indicated pathway activity scored per cell by GSVA between the tumor core and tumor edge across the exhausted CD8$^+$ T cells (cluster 0), CD8$^+$ naive T cells (cluster 1), proliferating CD8$^+$ T cells (cluster 2), and proliferating CD8$^+$ T cells (cluster 4). Red indicates upregulation, while blue indicates downregulation. **(F)** Heatmap of the ssGSEA score, as estimated using gene sets from MsiDB, between the tumor core and tumor edge across the exhausted CD8$^+$ T cells (cluster 0). **(G)** Violin plots showing the smoothed expression distribution of selected genes involved in T cell activity and in immune checkpoints between the tumor core and tumor edge across the exhausted CD8$^+$ T cells (cluster 0). **(H)** The cell trajectory of CD8$^+$ T cells. $^*P < 0.05$; $^{**}P < 0.01$; $^{***}P < 0.001$; $^{****}P < 0.0001$.

$CD8^+$ T cells suggests that proliferating $CD8^+$ T cells (clusters 2 and 4) may eventually gradually transition to exhausted $CD8^+$ T cells (**Figure 4H**).

Immunological Differences Among the B Cell Subpopulations

We detected 1,136 B cells, and reclustering revealed 5 B cell subgroups (**Figure 5A** and **Supplementary Table 4**). Among these B cell subgroups, we found that follicular B cells (clusters 0, 1, and 3) highly expressed CD20 (MS4A1), memory B cells (cluster 2) highly expressed CD27, plasma cells (cluster 7) highly expressed CD9, and mucosa-associated lymphoid tissue-derived (MALT) B cells highly expressed IGLL5 (clusters 5 and 8; **Figure 5B** and **Supplementary Figure 5A**). Next, we further compared the functional activity of the five types of B cell subgroups (**Figure 5C**), and follicular B cells (clusters 0 and 3) had a higher activity in the TGF-β, NOTCH and other pathways. However, follicular B cells (cluster 1) had a significantly higher activity in the cell cycle and DNA damage repair pathways than other B cell subgroups. Plasma cells (cluster 7) had a higher functional activity in MHC-I synthesis. We found that follicular B cells (clusters 0, 1, and 3) and plasma cells (cluster 7) located in the core of the tumor were significantly more active in immune depletion-related pathways than the B cell subsets located at the edge of the tumor; these pathways included epithelial cell adhesion, fibroblast growth factor binding, VEGFR2-mediated cell proliferation, oxidative stress-stimulated hypoxia, and stress-inhibited cytokine synthesis (**Figure 5D**). Similarly, the memory B cells (cluster 2) located in the core of the tumor significantly increased the activity of the angiogenesis, lipid synthesis, NOTCH signaling and other pathways but significantly downregulated the functional activity of inflammatory factor synthesis (**Figure 5E**).

Immunological Differences Among the Myeloid Cell and Fibroblast Subpopulations

A total of 1,524 myeloid cells were reclustered into 5 categories (**Figure 6A** and **Supplementary Table 4**). Two types of cells were annotated as macrophages; their marker genes are FOLR2 (cluster 0) and CRIP1 (cluster 2). The other type of cells were Langerhans cells (cluster 1; **Supplementary Figure 5B**), which highly expressed FCER1A, CD1A, CD1C, and CD1E, and cross-presenting dendritic cells (cluster 3), which highly express IDO1. The last category is granulocytes, which highly express S100A12 (**Figure 6B**). Then, to further explore the differences in cell functions among the five subgroups, we found that the two types of macrophages had similar activation levels in autophagy, macrophage chemotaxis and other pathways. Langerhans cells (cluster 1) had a significantly higher activity in pathways such as antigen presentation and IL-1 production than the other subgroups. Cross-presenting dendritic cells (cluster 3) have higher antigen presentation and cytokine production (IL-9, IL-21, IL-35, IL-6) activities (**Figure 6C**). To compare the differences in the cell functions of the myeloid cell subgroups in the different tumor sites, we analyzed the differences in the ssGSEA scores of the pathways of each subgroup according to the tumor site and displayed them in the form of heatmaps (**Figure 6D**). We found that each type was located at the core of the tumor. The vascular proliferation, FGFR, fatty acid synthesis and hypoxia activities were significantly higher in the cell subpopulations at the core of the tumor than at the cell subpopulations the edge of the tumor. In contrast, the activities of cytokines (such as interferons and interleukins), antigen presentation, inflammatory response, chemokine recruitment and other pathways were significantly higher in the various subgroups located at the edge of the tumor than in the various cell subgroups located at the core of the tumor.

After reclustering, 259 fibroblasts were divided into 3 categories, of which 2 types of cells were annotated as fibroblasts (clusters 0 and 2); the other type of cells was normal lung fibroblasts. These cells are rarely located in the core of the tumor, and most of these cells are located at the edge and in the middle of the tumor (**Figure 7A** and **Supplementary Table 4**). Fibroblasts (cluster 0) highly expressed COL10A1, SFRP4, SULF1, ASPN, and HTRA3. Normal lung fibroblasts (cluster 1) highly expressed CFD and PTGDS. Fibroblasts (cluster 2) highly expressed COL4A1 and PDGFRB (**Figure 7B**). We found that extracellular matrix collagen binding, cell adhesion, TGF-β, FGFR, IL-10 and other pathway activities were significantly higher in fibroblasts (cluster 0) than in the other cell subgroups (**Figure 7C**). In addition, fibroblasts (clusters 0 and 2) located at the edge of the tumor had a higher activity in regulating lymphocyte chemotaxis and cytokine synthesis pathways (**Figures 7D,E**).

DISCUSSION

The discovery and development of immune checkpoints has opened the door to hope to overcome tumors. However, the efficacy of tumor immunotherapy is limited to some patients, and there are obvious individual differences (Whiteside et al., 2016). How to improve the efficacy of immunotherapy and expand the population that received benefits have become the focus of tumor immunotherapy research. Growing evidence attributes the difference in treatment outcomes to the heterogeneity of the TME (Tang et al., 2016). The development of scRNA-seq technology has greatly aided the understanding of the TME (Lambrechts et al., 2018; Maynard et al., 2020). In this study, we compared the immune microenvironment of LUAD at different tumor sites from the resolution of the single-cell transcriptome and found that there is a large immunogenic heterogeneity at different tumor sites. The proportion of cells in the immune microenvironment of different parts of the tumor and the functions of immune and stromal cells are quite different. Understanding the role of the immune microenvironment in different parts of a tumor can better help researchers understand tumor evolution.

The TME is composed of tumor cells and infiltrating immune cells around the tumor, new blood vessels and their endothelial cells, cancer-associated fibroblasts (CAFs) and the extracellular matrix, which can promote tumor deterioration, increase tumor invasiveness, and increase the antitherapeutic response (Swartz et al., 2012; Lin et al., 2019; Sharma et al., 2019). In the TME,

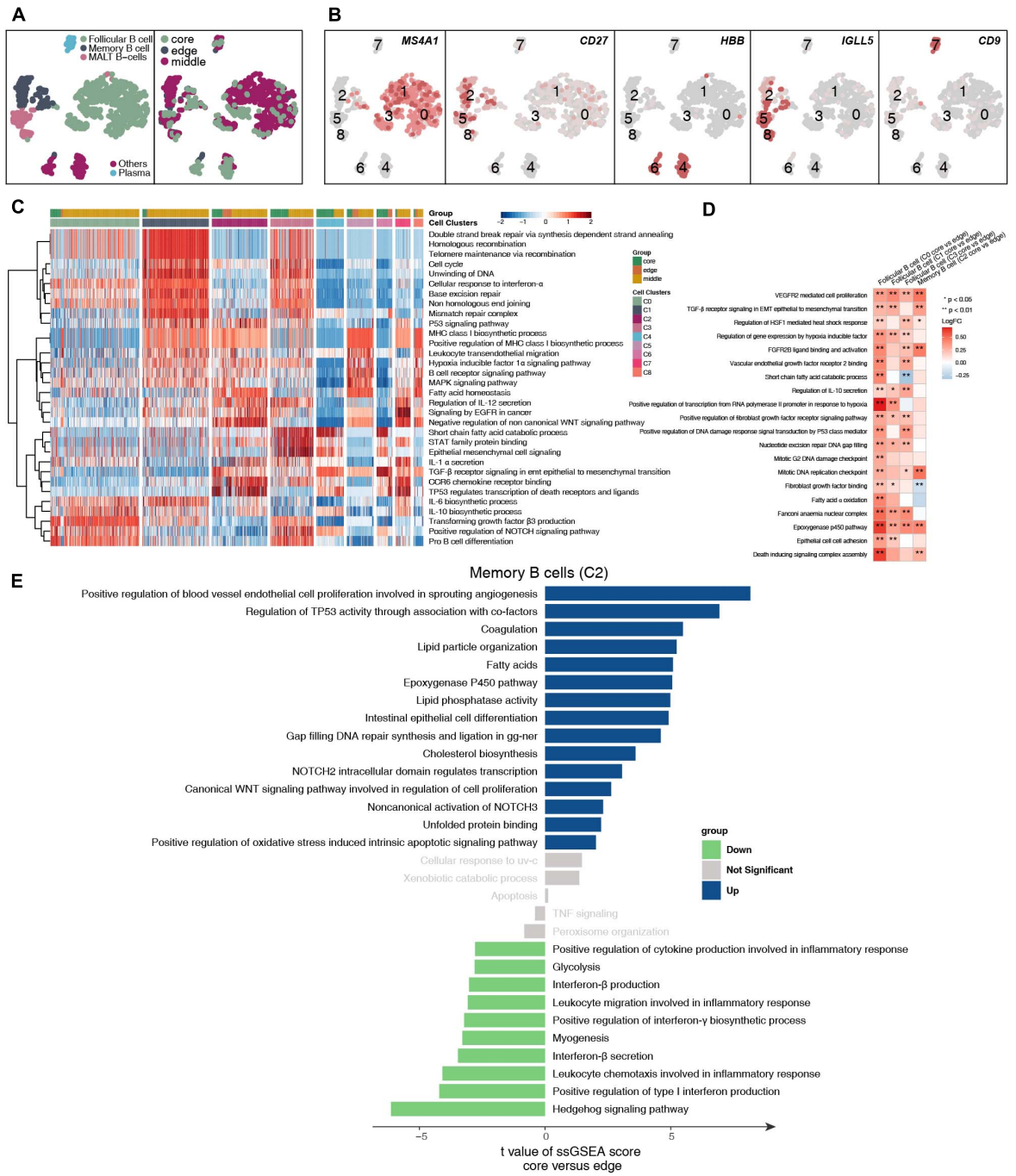

FIGURE 5 | B cell clusters in LUAD. **(A)** tSNE plot of 1,136 B cells, which are color-coded by their associated cluster or the sample location. **(B)** tSNE plot, which is color-coded for expression of marker genes for the cell types, as indicated. **(C)** Heatmap of the ssGSEA score, as estimated using gene sets from MsiDB, for eight B cell clusters: follicular B cells (cluster 0), follicular B cells (cluster 1), memory B cells (cluster 2), follicular B cells (cluster 3), other B cells (cluster 4), MALT B cells (cluster 5), other B cells (cluster 6), plasma B cells (cluster 7), and MALT B cells (cluster 8). **(D)** Heatmap depicting the mean differences in pathway activities scored per cell by GSVA between the tumor core and tumor edge across the follicular B cells (cluster 0), follicular B cells (cluster 1), memory B cells (cluster 2), follicular B cells (cluster 3), other B cells (cluster 4), MALT B cells (cluster 5), other B cells (cluster 6), plasma B cells (cluster 7), MALT B cells (cluster 8). The *x*-axis of the heatmap indicates different B cell clusters, and the *y*-axis indicates pathway activities scored per cell by GSVA. Each square represents the fold change or difference in each indicated pathway activity scored per cell by GSVA between the tumor core and tumor edge across the follicular B cells (cluster 0), follicular B cells (cluster 1), memory B cells (cluster 2), follicular B cells (cluster 3), other B cells (cluster 4), MALT B cells (cluster 5), other B cells (cluster 6), plasma B cells (cluster 7), and MALT B cells (cluster 8). Red indicates upregulation, while blue indicates downregulation. **(E)** Differences in pathway activities scored per cell by GSVA between tumor core and tumor edge in the follicular B cells (cluster 0), follicular B cells (cluster 1), memory B cells (cluster 2), follicular B cells (cluster 3), other B cells (cluster 4), MALT B cells (cluster 5), other B cells (cluster 6), plasma B cells (cluster 7), and MALT B cells (cluster 8). *T*-values are from a linear model. $^{*}P < 0.05$; $^{**}P < 0.01$.

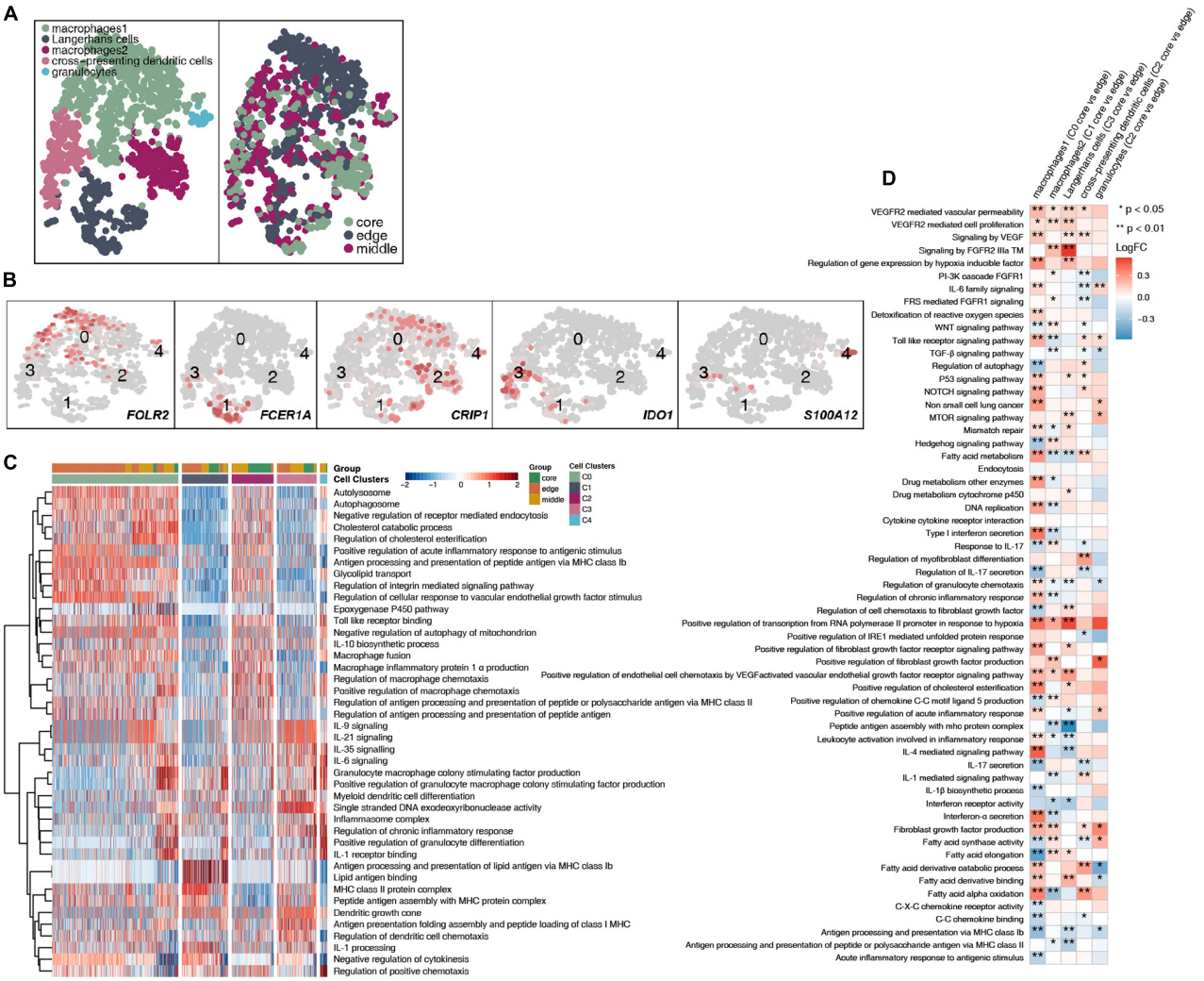

FIGURE 6 | Myeloid cell clusters in LUAD. **(A)** tSNE plot of 1,524 myeloid cells, which are color-coded by their associated cluster or the sample location. **(B)** tSNE plot, which is color-coded for expression of marker genes for the cell types, as indicated. **(C)** Heatmap of the ssGSEA score, as estimated using gene sets from MsiDB, for five myeloid cell clusters from macrophages (cluster 0), Langerhans cells (cluster 1), macrophages (cluster 2), cross-presenting dendritic cells (cluster 3) and granulocytes (cluster 4). **(D)** Heatmap depicting the mean differences in pathway activities scored per cell by GSVA between the tumor core and tumor edge across the macrophages (cluster 0), Langerhans cells (cluster 1), macrophages (cluster 2), cross-presenting dendritic cells (cluster 3) and granulocytes (cluster 4). The *x*-axis of the heatmap indicates different myeloid cell clusters, and the *y*-axis indicates pathway activities scored per cell by GSVA. Each square represents the fold change or difference in each indicated pathway activity scored per cell by GSVA between the tumor core and tumor edge across macrophages (cluster 0), Langerhans cells (cluster 1), macrophages (cluster 2), cross-presenting dendritic cells (cluster 3) and granulocytes (cluster 4). Red indicates upregulation, while blue indicates downregulation. $^{*}P < 0.05$; $^{**}P < 0.01$.

tumor-infiltrating lymphocytes (TILs) serve as the target cells of immune checkpoint inhibitors, and their infiltration degree and type significantly affect the effect of immunotherapy. Studies have pointed out that in a variety of solid tumors, the composition and degree of infiltration of TILs in patient tissue samples have value in predicting the prognosis of patients receiving immunotherapy (Lin et al., 2019, 2020). For example, high infiltration of $CD8^+$ T cells or $CD4^+$ T helper 1 (Th1) cells suggests a better prognosis (Lin et al., 2019, 2020; Zhang et al., 2020). However, infiltrating immune cells can have many different subtypes. These cell populations can have tumor-promoting or antitumor functions, and their activation status, functions, intratumoral localization and density will be different (Tosolini et al., 2011). In this study, we found that $CD4^+$ naive T cells located at the core of the tumor had higher expression levels of immune checkpoint molecules than those in other locations of the tumor. For example, $CD4^+$ naive T cells (cluster 0/cluster 2) located at the core of the tumor expressed more immune checkpoint molecules, such as CTLA4, LAG3, HAVCR2, and TNFRSF9/CD137 (Pardoll, 2012). In addition, $CD4^+$ naive T cells located at the core of the tumor had significantly higher VEGF-mediated angiogenesis and Wnt regulation of cell proliferation than those located at the edge of the tumor; in contrast, the cytokine (such as interferon) and inflammatory response activity of these cells was significantly

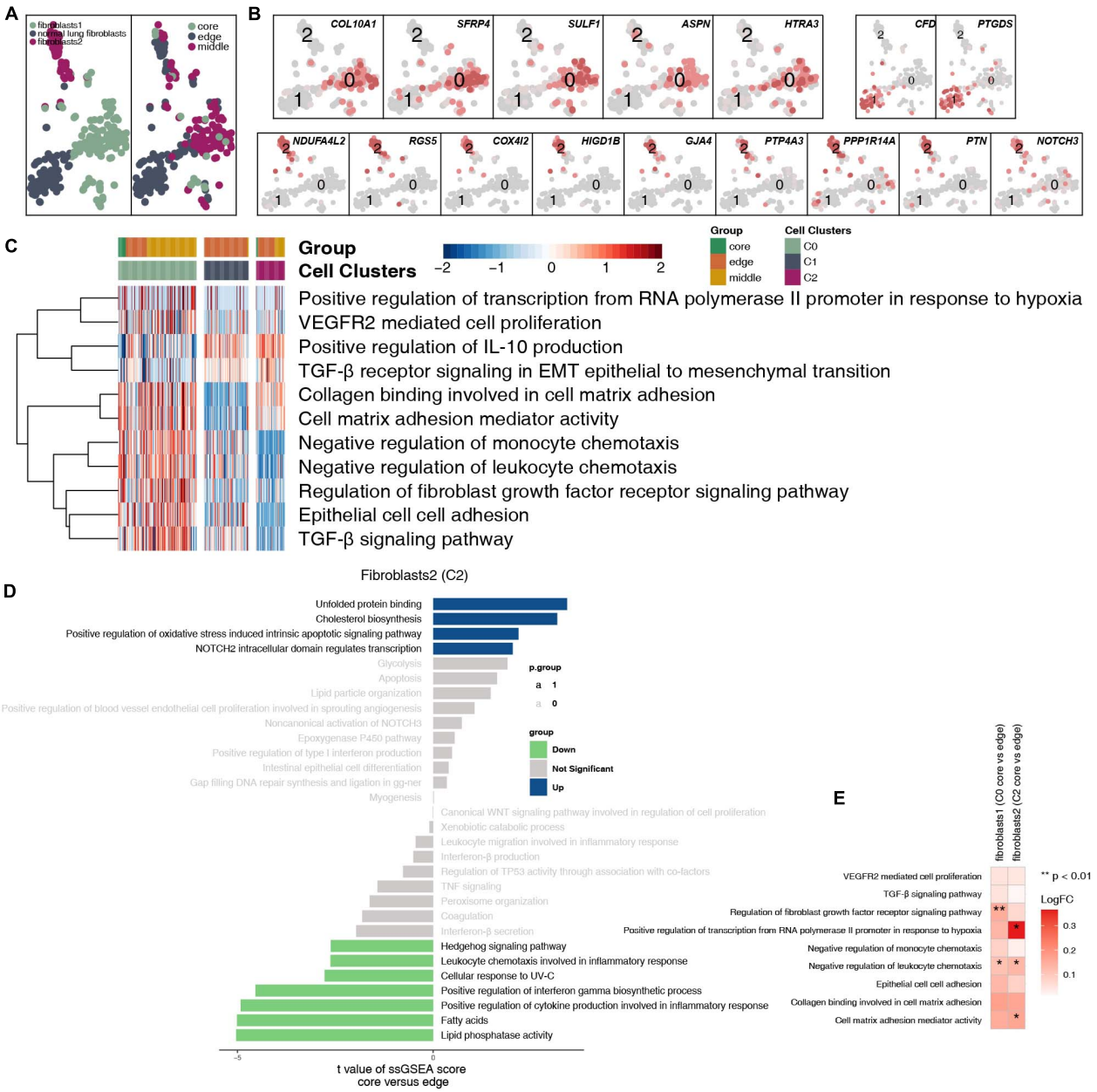

FIGURE 7 | Fibroblast clusters in LUAD. **(A)** tSNE plot of 259 fibroblasts, which are color-coded by their associated cluster or the sample location. **(B)** tSNE plot, which is color-coded for expression of marker genes for the cell types, as indicated. **(C)** Heatmap of the ssGSEA score, as estimated using gene sets from MsiDB, for three fibroblast clusters from fibroblasts (cluster 0), normal lung fibroblasts (cluster 1), and fibroblasts (cluster 2). **(D)** Differences in pathway activities scored per cell by GSVA between the tumor core and tumor edge in fibroblasts (cluster 0), normal lung fibroblasts (cluster 1), and fibroblasts (cluster 2). *T*-values are from a linear model. **(E)** Heatmap depicting the mean differences in pathway activities scored per cell by GSVA between the tumor core and tumor edge across fibroblasts (cluster 0), normal lung fibroblasts (cluster 1), and fibroblasts (cluster 2). The *x*-axis of the heatmap indicates different fibroblast clusters, and the *y*-axis indicates pathway activities scored per cell by GSVA. Each square represents the fold change or difference in each indicated pathway activity scored per cell by GSVA between the tumor core and tumor edge across fibroblasts (cluster 0), normal lung fibroblasts (cluster 1), and fibroblasts (cluster 2). Red indicates upregulation, while blue indicates downregulation. $^{*}P < 0.05$; $^{**}P < 0.01$.

lower at core of the tumor than at the edge of the tumor. Tumor cells use inhibitory signaling pathways in the immune system, such as the PD-1/PD-L1, CTLA-4, LAG-3, Tim-3, and CD160 signaling pathways, to inhibit the function of TILs in the TME, resulting in tumor immunosuppression (Wherry, 2011; Chen and Flies, 2013). Tumor cells can also secrete immunosuppressive factors, such as VEGF, into the microenvironment to increase tumor microvessel density and inhibit immune cell function, ultimately inhibiting antitumor effects (Beatty and Gladney, 2015; Span and Bussink, 2015).

In addition, we found that most of the processes related to immune depletion, including fatty acid metabolism, stem cell proliferation, FGFR signaling, and TGF-β signaling, were significantly higher in the $CD8^+$ T cell subgroups located at the core of the tumor than in those at the edge of the tumor. In contrast, the immune-related cytokine synthesis, chemokine, inflammatory response pathway and cytotoxicity marker (GZMB) activity in $CD8^+$ T cells in the core of the tumor was significantly lower than that in the same cells at the edge of the tumor. Mariathasan et al. (2018) found that TGF-β may ultimately lead to reduced antitumor immunity by limiting the infiltration of T cells, and the use of TGF-β inhibitors and PD-L1 inhibitors together in a mouse model not only inhibited the TGF-β signaling pathway in interstitial cells but also promoted $CD8^+$ T cells to enter the tumor and increases the secretion of granzyme B, which ultimately enhanced antitumor immunity and reduced the size of the tumors. In addition, functionally quiescent T cells showed high levels of oxidization and metabolism of fatty acids/lipids, and increased fatty acid transport and uptake were found to promote cancer metastasis (Kim et al., 2019; Zhao et al., 2019).

Tumor-infiltrating B cells have been identified, but their overall functional role in cancer is not fully understood (Garg et al., 2016; Tsou et al., 2016; Sarvaria et al., 2017). Preliminary evidence shows that there is a correlation between the response to immunotherapy and the presence of B cells, but the exact role of B cells in immunotherapy is still unclear (Griss et al., 2019). Helmink et al. (2020) showed that the same properties responsible for the functions of memory B cells and plasma cells in adaptive immune responses may also contribute to effective T cell responses with immunotherapy. B cells may change the activation state and function of T cells. For example, memory B cells can act as antigen-presenting cells, driving the expansion of memory B cells and naive tumor-associated T cells. B cells can also secrete a series of cytokines (including TNF, IL-2, IL-6, and IFNγ), which can activate and recruit other immune effector cells, including T cells. We found that plasma cells located at the core of the tumor had significantly increased activity in immune depletion-related processes, such as epithelial cell adhesion, FGF binding, VEGFR2-mediated cell proliferation, oxidative stress-stimulated hypoxia, and inhibitory cytokine synthesis, than the B cell subsets located at the edge of the tumor. Similarly, the memory B cells located in the core of the tumor had significantly increased angiogenesis, lipid synthesis, NOTCH signaling and other processes, but inflammatory factor synthesis was significantly lower in memory B cells in the core of the tumor than in those in the periphery of the tumor. In tumor tissues, a variety of transcription factors, such as hypoxia inducible factor (HIF), can trigger the expression of VEGF and other proangiogenic factors, leading to an increase in tumor microvessel density. Hypoxia can promote the formation of tumor blood vessels by upregulating the expression of proangiogenic factors and HIF-1α (Brahimi-Horn et al., 2007), inducing tumor cells to undergo epithelial-mesenchymal transition, increasing their malignancy and triggering tumor spread and metastasis (Wu et al., 2011). We found that the macrophages located at the core of the tumor had significantly higher blood vessel proliferation, FGFR signaling, fatty acid synthesis and hypoxia signaling than the cell subsets at the edge of the tumor. In contrast, the activities of cytokines (such as interferons and interleukins), antigen presentation, the inflammatory response, chemokine recruitment and other processes were significantly higher in the various subgroups located at the edge of the tumor than in the various cell subgroups located at the core of the tumor. MHC-II on macrophages activates T cells by presenting antigens to produce a powerful inflammatory response (Lambrechts et al., 2018). In addition, fibroblasts located at the core of the tumor had significantly higher extracellular matrix collagen binding, cell adhesion, and TGF-β, FGFR, IL-10, and other signaling than other fibroblasts at the tumor margins. The secretion of collagen promotes the reconstruction of the microenvironmental matrix and enhances the ability of tumor cells to invade along the collagen fiber (Shimoda et al., 2010; Lambrechts et al., 2018). Tumor cells can also secrete immunosuppressive factors, such as TGF-β, IL-2, IL-10, and VEGF, into the microenvironment and train infiltrating immune cells to inhibit their antitumor effects (Beatty and Gladney, 2015; Maynard et al., 2020).

However, our research has certain limitations. First, we discuss only the heterogeneity of the TME from the perspective of single-cell transcriptomes. In the future, we still need to explore the heterogeneity of the tumor immune microenvironment from the perspective of multiomics. Second, we used only bioinformatics algorithms to infer the function of each type of cell and compare the functional differences of different cell types; however, in future analyses, we still need to explore the interactions between cells.

CONCLUSION

Our research shows that there is heterogeneity in the immune microenvironment in different parts of the tumor, and this includes the different ratios of immune cells and stromal cells, different functions, and the activation degree of immune-related pathways in different tumor parts. Therefore, clarifying the spatial heterogeneity of the tumor in the immune microenvironment could help clinicians design personalized treatments.

DATA AVAILABILITY STATEMENT

All the data generated or analyzed during this study are included in the ArrayExpress database (accessions E-MTAB-6149 and E-MTAB-6653).

AUTHOR CONTRIBUTIONS

MS, GF, YL, and YB: conceptualization and supervision. YYW, XL, YTW, SP, GF, and HH: formal analysis, software, and visualization. YYW, SP, HH, and XL: writing–original draft and writing–review and editing. All authors contributed to the article and approved the submitted version.

FUNDING

This work was supported by the grants from the Key Research and Development Project of Science and Technology Department of Sichuan Province (2021YFS0128).

ACKNOWLEDGMENTS

The authors would like to thank TopScience Editing for English language polishing.

SUPPLEMENTARY MATERIAL

The Supplementary Material for this article can be found online at: https://www.frontiersin.org/articles/10.3389/fcell.2021.638374/full#supplementary-material

Supplementary Figure 1 | Before QC of single cells. **(A)** Before QC, overview of the number of mRNAs, the mRNA reads, and the percentage of mitochondrial genes in this study. **(B)** Before QC, the relationship among the percentage of mitochondrial genes, the mRNA reads and the amount of mRNA. **(C)** Before QC, the tSNE plot showing the sample position and batch effect.

Supplementary Figure 2 | After QC of single cells. **(A)** After QC, tSNE plot showing the batch group. **(B)** After QC, tSNE plot showing the COPD status. **(C)** After QC, tSNE plot showing the sex of the patient. **(D)** After QC, tSNE plot showing the corresponding patient. **(E)** After QC, tSNE plot showing the tumor site. **(F)** After QC, tSNE plot showing the sample type of origin.

Supplementary Figure 3 | (A) Violin plots showing the smoothed expression distribution of selected genes involved in marker genes of $CD8^+$ T cells/NK cells between tumor core, tumor middle and tumor edge across the $CD8^+$ T cells/NK cells. **(B)** Violin plots showing the smoothed expression distribution of selected genes involved in marker genes of $CD8^+$ T cells between the tumor core, tumor middle and tumor edge across $CD8^+$ T cells. **(C)** Violin plots showing the smoothed expression distribution of selected genes involved in marker genes of $CD4^+$ naive T cells between tumor core, tumor middle, and tumor edge across $CD4^+$ naive T cells. **(D)** Violin plots showing the smoothed expression distribution of selected genes involved in marker genes of Tregs between the tumor core, tumor middle, and tumor edge across the Tregs.

Supplementary Figure 4 | (A) tSNE plot, which is color-coded for expression of additional marker genes of $CD8^+$ T cells for the cell types, as indicated. **(B)** Violin plots showing the smoothed expression distribution of selected genes involved in proliferation between exhausted $CD8^+$ T cells (cluster 0), $CD8^+$ naive T cells (cluster 1), proliferating $CD8^+$ T cells (cluster 2), and proliferating $CD8^+$ T cells (cluster 4). **(C)** Violin plots showing the smoothed expression distribution of selected genes involved in proliferation between tumor core, tumor middle, and tumor edge tumors across the exhausted $CD8^+$ T cells (cluster 0).

Supplementary Figure 5 | (A) tSNE plot, which is color-coded for expression of additional marker genes of B cells for the cell types, as indicated. **(B)** tSNE plot, which is color-coded for expression of additional marker genes of Langerhans cells for the cell types, as indicated.

Supplementary Table 1 | Detailed information on the clinical characteristics of scRNA-seq in LUAD samples.

Supplementary Table 2 | The differentially expressed genes between the eight cell clusters.

Supplementary Table 3 | The marker genes for the eight cell clusters.

Supplementary Table 4 | Subtype characteristics for the four cell types.

REFERENCES

Allam, M., Cai, S., and Coskun, A. F. (2020). Multiplex bioimaging of single-cell spatial profiles for precision cancer diagnostics and therapeutics. *NPJ Precis. Oncol.* 4:11. doi: 10.1038/s41698-020-0114-1

Beatty, G. L., and Gladney, W. L. (2015). Immune escape mechanisms as a guide for cancer immunotherapy. *Clin. Cancer Res.* 21, 687–692. doi: 10.1158/1078-0432.CCR-14-1860

Brahimi-Horn, M. C., Chiche, J., and Pouysségur, J. (2007). Hypoxia and cancer. *J. Mol. Med. (Berl.)* 85, 1301–1307. doi: 10.1007/s00109-007-0281-3

Chen, L., and Flies, D. B. (2013). Molecular mechanisms of T cell co-stimulation and co-inhibition. *Nat. Rev. Immunol.* 13, 227–242. doi: 10.1038/nri3405

Darmanis, S., Sloan, S. A., Croote, D., Mignardi, M., Chernikova, S., Samghababi, P., et al. (2017). Single-cell RNA-Seq analysis of infiltrating neoplastic cells at the migrating front of human glioblastoma. *Cell Rep.* 21, 1399–1410. doi: 10.1016/j.celrep.2017.10.030

Garg, K., Maurer, M., Griss, J., Brüggen, M.-C., Wolf, I. H., Wagner, C., et al. (2016). Tumor-associated B cells in cutaneous primary melanoma and improved clinical outcome. *Hum. Pathol.* 54, 157–164. doi: 10.1016/j.humpath.2016.03.022

Griss, J., Bauer, W., Wagner, C., Simon, M., Chen, M., Grabmeier-Pfistershammer, K., et al. (2019). B cells sustain inflammation and predict response to immune checkpoint blockade in human melanoma. *Nat. Commun.* 10:4186. doi: 10.1038/s41467-019-12160-2

Hänzelmann, S., Castelo, R., and Guinney, J. (2013). GSVA: gene set variation analysis for microarray and RNA-Seq data. *BMC Bioinformatics* 14:7. doi: 10.1186/1471-2105-14-7

Helmink, B. A., Reddy, S. M., Gao, J., Zhang, S., Basar, R., Thakur, R., et al. (2020). B cells and tertiary lymphoid structures promote immunotherapy response. *Nature* 577, 549–555. doi: 10.1038/s41586-019-1922-8

Kim, Y.-S., Jung, J., Jeong, H., Lee, J.-H., Oh, H. E., Lee, E. S., et al. (2019). High membranous expression of fatty acid transport protein 4 is associated with tumorigenesis and tumor progression in clear cell renal cell carcinoma. *Dis. Markers* 2019, 1–7. doi: 10.1155/2019/5702026

Lambrechts, D., Wauters, E., Boeckx, B., Aibar, S., Nittner, D., Burton, O., et al. (2018). Phenotype molding of stromal cells in the lung tumor microenvironment. *Nat. Med.* 24, 1277–1289. doi: 10.1038/s41591-018-0096-5

Li, H. H., Durbin, R., Hellmann, M. D., Nathanson, T., Rizvi, H., Creelan, B. C., et al. (2018). The immune landscape of cancer. *Nature* 33:34. doi: 10.1038/ng.3677

Liberzon, A., Birger, C., Thorvaldsdóttir, H., Ghandi, M., Mesirov, J. P., and Tamayo, P. (2015). The molecular signatures database hallmark gene set collection. *Cell Syst.* 1, 417–425. doi: 10.1016/j.cels.2015.12.004

Liberzon, A., Subramanian, A., Pinchback, R., Thorvaldsdottir, H., Tamayo, P., and Mesirov, J. P. (2011). Molecular signatures database (MSigDB) 3.0. *Bioinformatics* 27, 1739–1740. doi: 10.1093/bioinformatics/btr260

Lin, A., Wei, T., Meng, H., Luo, P., and Zhang, J. (2019). Role of the dynamic tumor microenvironment in controversies regarding immune checkpoint inhibitors for the treatment of non-small cell lung cancer (NSCLC) with EGFR mutations. *Mol. Cancer* 18:139. doi: 10.1186/s12943-019-1062-7

Lin, A., Zhang, H., Hu, X., Chen, X., Wu, G., Luo, P., et al. (2020). Age, sex, and specific gene mutations affect the effects of immune checkpoint inhibitors in colorectal cancer. *Pharmacol. Res.* 159:105028. doi: 10.1016/j.phrs.2020.105028

Liu, Y., Hu, J., Liu, D., Zhou, S., Liao, J., Liao, G., et al. (2020). Single-cell analysis reveals immune landscape in kidneys of patients with chronic transplant rejection. *Theranostics* 10, 8851–8862. doi: 10.7150/thno.48201

Mariathasan, S., Turley, S. J., Nickles, D., Castiglioni, A., Yuen, K., Wang, Y., et al. (2018). TGFβ attenuates tumour response to PD-L1 blockade by contributing to exclusion of T cells. *Nature* 554, 544–548. doi: 10.1038/nature25501

Maynard, A., McCoach, C. E., Rotow, J. K., Harris, L., Haderk, F., Kerr, D. L., et al. (2020). Therapy-induced evolution of human lung cancer revealed by single-cell rna sequencing. *Cell* 182, 1232–1251.e22. doi: 10.1016/j.cell.2020.07.017

Pardoll, D. M. (2012). The blockade of immune checkpoints in cancer immunotherapy. *Nat. Rev. Cancer* 12, 252–264. doi: 10.1038/nrc3239

Qiu, X., Mao, Q., Tang, Y., Wang, L., Chawla, R., Pliner, H. A., et al. (2017). Reversed graph embedding resolves complex single-cell trajectories. *Nat. Methods* 14, 979–982. doi: 10.1038/nmeth.4402

Rooney, M. S., Shukla, S. A., Wu, C. J., Getz, G., and Hacohen, N. (2015). Molecular and genetic properties of tumors associated with local immune cytolytic activity. *Cell* 160, 48–61. doi: 10.1016/j.cell.2014.12.033

Sarvaria, A., Madrigal, J. A., and Saudemont, A. (2017). B cell regulation in cancer and anti-tumor immunity. *Cell. Mol. Immunol.* 14, 662–674. doi: 10.1038/cmi.2017.35

Sharma, A., Merritt, E., Hu, X., Cruz, A., Jiang, C., Sarkodie, H., et al. (2019). Non-genetic intra-tumor heterogeneity is a major predictor of phenotypic heterogeneity and ongoing evolutionary dynamics in lung tumors. *Cell Rep.* 29, 2164–2174.e5. doi: 10.1016/j.celrep.2019.10.045

Shimoda, M., Mellody, K. T., and Orimo, A. (2010). Carcinoma-associated fibroblasts are a rate-limiting determinant for tumour progression. *Semin. Cell Dev. Biol.* 21, 19–25. doi: 10.1016/j.semcdb.2009.10.002

Smith, E. A., and Hodges, H. C. (2019). The spatial and genomic hierarchy of tumor ecosystems revealed by single-cell technologies. *Trends Cancer* 5, 411–425. doi: 10.1016/j.trecan.2019.05.009

Span, P. N., and Bussink, J. (2015). Biology of hypoxia. *Semin. Nucl. Med.* 45, 101–109. doi: 10.1053/j.semnuclmed.2014.10.002

Swartz, M. A., Iida, N., Roberts, E. W., Sangaletti, S., Wong, M. H., Yull, F. E., et al. (2012). Tumor microenvironment complexity: emerging roles in cancer therapy. *Cancer Res.* 72, 2473–2480. doi: 10.1158/0008-5472.CAN-12-0122

Tang, H., Qiao, J., and Fu, Y.-X. (2016). Immunotherapy and tumor microenvironment. *Cancer Lett.* 370, 85–90. doi: 10.1016/j.canlet.2015.10.009

Tosolini, M., Kirilovsky, A., Mlecnik, B., Fredriksen, T., Mauger, S., Bindea, G., et al. (2011). Clinical impact of different classes of infiltrating t cytotoxic and helper cells (Th1, Th2, Treg, Th17) in patients with colorectal cancer. *Cancer Res.* 71, 1263–1271. doi: 10.1158/0008-5472.CAN-10-2907

Tsou, P., Katayama, H., Ostrin, E. J., and Hanash, S. M. (2016). The Emerging Role of B Cells in Tumor Immunity. *Cancer Res.* 76, 5597–5601. doi: 10.1158/0008-5472.CAN-16-0431

Turajlic, S., Sottoriva, A., Graham, T., and Swanton, C. (2019). Resolving genetic heterogeneity in cancer. *Nat. Rev. Genet.* 20, 404–416. doi: 10.1038/s41576-019-0114-6

Wherry, E. J. (2011). T cell exhaustion. *Nat. Immunol.* 12, 492–499. doi: 10.1038/ni.2035

Whiteside, T. L., Demaria, S., Rodriguez-Ruiz, M. E., Zarour, H. M., and Melero, I. (2016). Emerging opportunities and challenges in cancer immunotherapy. *Clin. Cancer Res.* 22, 1845–1855. doi: 10.1158/1078-0432.CCR-16-0049

Wickham, H. (2011). ggplot2. *Wires Comput. Stat.* 3, 180–185. doi: 10.1002/wics.147

Wu, M.-Z., Tsai, Y.-P., Yang, M.-H., Huang, C.-H., Chang, S.-Y., Chang, C.-C., et al. (2011). Interplay between HDAC3 and WDR5 is essential for hypoxia-induced epithelial-mesenchymal transition. *Mol. Cell* 43, 811–822. doi: 10.1016/j.molcel.2011.07.012

Zhang, J., Zhou, N., Lin, A., Luo, P., Chen, X., Deng, H., et al. (2020). ZFHX3 mutation as a protective biomarker for immune checkpoint blockade in non-small cell lung cancer. *Cancer Immunol. Immunother*. 70:137–151. doi: 10.1007/s00262-020-02668-8

Zhang, X., Lan, Y., Xu, J., Quan, F., Zhao, E., Deng, C., et al. (2019). CellMarker: a manually curated resource of cell markers in human and mouse. *Nucleic Acids Res.* 47, D721–D728. doi: 10.1093/nar/gky900

Zhao, G., Cardenas, H., and Matei, D. (2019). Ovarian cancer-why lipids matter. *Cancers* 11:1870. doi: 10.3390/cancers11121870

Conflict of Interest: The authors declare that the research was conducted in the absence of any commercial or financial relationships that could be construed as a potential conflict of interest.

Publisher's Note: All claims expressed in this article are solely those of the authors and do not necessarily represent those of their affiliated organizations, or those of the publisher, the editors and the reviewers. Any product that may be evaluated in this article, or claim that may be made by its manufacturer, is not guaranteed or endorsed by the publisher.

frontiers in Cell and Developmental Biology

MINI REVIEW
published: 31 August 2021
doi: 10.3389/fcell.2021.737449

Tumor-Derived Extracellular Vesicles: Modulation of Cellular Functional Dynamics in Tumor Microenvironment and Its Clinical Implications

Nathalia Leal Santos[1], Silvina Odete Bustos[1], Darshak Bhatt[1,2], Roger Chammas[1] and Luciana Nogueira de Sousa Andrade[1]**

[1] Center for Translational Research in Oncology, Instituto do Câncer do Estado de São Paulo, Hospital das Clínicas da Faculdade de Medicina da Universidade de São Paulo, São Paulo, Brazil, [2] Department of Medical Microbiology and Infection Prevention, University Medical Center Groningen, University of Groningen, Groningen, Netherlands

OPEN ACCESS

Edited by:
Ana Karina Oliveira, National Center for Research in Energy and Materials, Brazil

Reviewed by:
Ariane Lopes, National Center for Research in Energy and Materials, Brazil
Hinrich Peter Hansen, University of Cologne, Germany

***Correspondence:**
Roger Chammas
rchammas@usp.br
Luciana Nogueira de Sousa Andrade
luciana.nsandrade@hc.fm.usp.br

Specialty section:
This article was submitted to Molecular and Cellular Pathology, a section of the journal Frontiers in Cell and Developmental Biology

Received: *07 July 2021*
Accepted: *09 August 2021*
Published: *31 August 2021*

Citation:
Santos NL, Bustos SO, Bhatt D, Chammas R and Andrade LNS (2021) Tumor-Derived Extracellular Vesicles: Modulation of Cellular Functional Dynamics in Tumor Microenvironment and Its Clinical Implications. Front. Cell Dev. Biol. 9:737449. doi: 10.3389/fcell.2021.737449

Cancer can be described as a dynamic disease formed by malignant and stromal cells. The cellular interaction between these components in the tumor microenvironment (TME) dictates the development of the disease and can be mediated by extracellular vesicles secreted by tumor cells (TEVs). In this review, we summarize emerging findings about how TEVs modify important aspects of the disease like continuous tumor growth, induction of angiogenesis and metastasis establishment. We also discuss how these nanostructures can educate the immune infiltrating cells to generate an immunosuppressive environment that favors tumor progression. Furthermore, we offer our perspective on the path TEVs interfere in cancer treatment response and promote tumor recurrence, highlighting the need to understand the underlying mechanisms controlling TEVs secretion and cargo sorting. In addition, we discuss the clinical potential of TEVs as markers of cell state transitions including the acquisition of a treatment-resistant phenotype, and their potential as therapeutic targets for interventions such as the use of extracellular vesicle (EV) inhibitors to block their pro-tumoral activities. Some of the technical challenges for TEVs research and clinical use are also presented.

Keywords: extracellular vesicles, tumor microenvironment, cell communication, tumor progression, functional dynamics

INTRODUCTION

Malignant tumors are defined as a microenvironment composed not only by different clones of tumor cells, but also by stromal cells as well as extracellular matrix (ECM) (Quail and Joyce, 2013). All these components interact with each other dictating the natural history of the disease and the response to treatment. From an ecological point of view, these interactions can be described as cooperative or competitive and, in both cases, depend on the mechanism of cellular communication (Pelham et al., 2020). In fact, these interactions are dynamic and mediated not only by soluble factors secreted by cells or trapped in the ECM, but also by extracellular vesicles (EVs) (Tkach and Théry, 2016).

Extracellular vesicles are spherical lipid bilayer structures secreted by many cell types which play an important role in tumor progression (Schubert and Boutros, 2021). In the last decade, it has become clear that EVs shuttle messages between cells at short and large distances, changing the way cell communication has been described so far (Raposo and Stahl, 2019). Two major classes of EVs, exosomes (or small vesicles, from 30 to up 150 nm in size) and microvesicles (or large vesicles, from > 100 nm to 1 μm) are the most studied and better characterized among the other EVs types. Exosomes have endocytic origin, being formed as intraluminal vesicles (ILVs) by inward budding of the limiting membrane of late endosomes. After the fusion of multivesicular bodies with the plasma membrane, exosomes are released into the extracellular environment. By contrast, microvesicles are formed by outward budding of the plasma membrane (van Niel et al., 2018). The other classes of EVs, like large oncosomes, apoptotic bodies and platelet-derived vesicles, will not be discussed in this Review.

Amongst the diverse means of communication, EVs are the only ones that are known to carry almost all types of signaling molecules varying from DNA, different types of RNAs, protein/ligands, enzymes, metabolites, growth factors, lipids and even cytokines as recently described (Fitzgerald et al., 2018; Anand et al., 2019; Lázaro-Ibáñez et al., 2019; O'Brien et al., 2020). In general; EVs exert their effects by the transfer of their cargo to recipient cells modulating their phenotype and function (Yáñez-Mó et al., 2015). In this review, we will discuss some examples of how EVs can orchestrate cellular communication in the tumor microenvironment (TME) to promote tumor progression. In addition, we will exploit the role of these EVs in treatment response and discuss the gaps and future directions for clinics and EVs research. We apologize to all authors whose relevant and important work could not be cited due to space constraints.

TEVs AS IMPORTANT MEDIATORS OF CELL COMMUNICATION DURING MALIGNANT TRANSFORMATION AND TUMOR PROGRESSION

In the past years, several groups showed that extracellular vesicles secreted by tumor cells (Tumor–Derived Extracellular Vesicles, TEVs) can modulate the cancer hallmarks described in 2011 (Hanahan and Weinberg, 2011). For example, it is already known that TEVs are able to promote cooperation with stromal cells like endothelial cells to allow tumor development (Aslan et al., 2019), to suppress the anti-tumor immune response in cancer patients (Sharma et al., 2020), and to signal at distant sites to resident cells for the establishment of pre-metastatic niche (Costa-Silva et al., 2015).

In fact, TEVs can also participate in tumor initiation and propagation. In the study of Kalra et al. (2019), TEVs from colorectal cancer (CRC) cells harboring β-catenin mutation were shown to transfer this protein to wild-type CRC recipient cells, inducing the activation of WNT signaling pathway in these cells and, consequently, boosting tumor growth in xenograft models. Similarly, Fonseka et al. (2019) showed that TEVs secreted by N-myc-amplified neuroblastoma cells increased the proliferative and migratory potential of N-myc-non-amplified tumor cells, increasing tumor aggressiveness. Furthermore, very recently, an interesting study conducted by Kilinc et al. (2021) demonstrated that oncogene activation led to regulation of EVs release and cargo, suggesting that these nanostructures are biologically relevant even in the initial phases of the disease (**Figure 1A**).

Beyond this scenario, an important hallmark of solid tumors is the induction of angiogenesis – a *sine qua non-condition* for continuous tumor growth and progression (Folkman, 1975). More recently, several groups showed that TEVs are one of the mediators for this process (Yang et al., 2018; Bai et al., 2019; He et al., 2019; Wang et al., 2019; Shang et al., 2020; Biagioni et al., 2021). Indeed; in 2017, it was demonstrated that TEVs from glioma stem-like cells carried VEGF-A (Treps et al., 2017). One year later, Tang et al. (2018) observed that TEVs from ovarian cancer contained E-cadherin in their surface which were able to form heterodimers with VE-cadherin in endothelial cells, promoting their sprouting and angiogenesis *in vivo*. Furthermore, Sato et al. (2019) demonstrated that higher expression of EPHB2 within EVs isolated from head and neck squamous carcinoma cell lines were able to promote angiogenesis through the activation of ephrin reverse signaling in endothelial cells. Interestingly, Ko et al. (2019) observed that TEVs from ovarian cancer induced migration and tube formation by endothelial cells through a bevacizumab-insensitive VEGF presented in vesicles, showing that TEVs can also impair the efficacy of anti-angiogenic therapies. Furthermore, the pro-angiogenic role of TEVs can also be a consequence of their uptake by other stromal cells like fibroblasts, inducing a pro-tumoral phenotype in these cells (Zhou et al., 2018; Fan et al., 2020; **Figure 1B**).

Additionally, environmental stimuli like hypoxia can somehow modify TEVs release and/or TEVs cargo leading to increased angiogenesis (Chen X. et al., 2018; Guo et al., 2018; Wang et al., 2018; Park et al., 2019; Qian et al., 2020). Under hypoxia, for example, lung cancer cells produce more exosomes in comparison to normoxia. Elevated levels of miR-23a were found inside these exosomes which targeted prolyl hydroxylase 1 and 2 (PHD1 and 2), leading to an increase in HIF-1 alpha in endothelial recipient cells and sustained angiogenesis and tumor growth *in vivo*. Furthermore, enrichment of Wnt4 protein and carbonic anhydrase 9 (CA9) in TEVs in response to hypoxia were demonstrated to be responsible for increased angiogenesis in colorectal cancer (Horie et al., 2017; Huang and Feng, 2017). Beyond angiogenesis, TEVs secreted under hypoxia can also promote cancer progression through the induction of drug resistance (Dorayappan et al., 2018), stemness phenotype and increased invasive capability (Ramteke et al., 2015).

In fact, concerning metastasis, the mechanisms triggered by TEVs are quite diverse. EVs derived from the plasma of CRC patients were enriched with ITGβL1 and associated with lung and liver metastasis. This effect was caused by the activation of resident fibroblasts, which were induced to secret pro-inflammatory cytokines, promoting the establishment of the

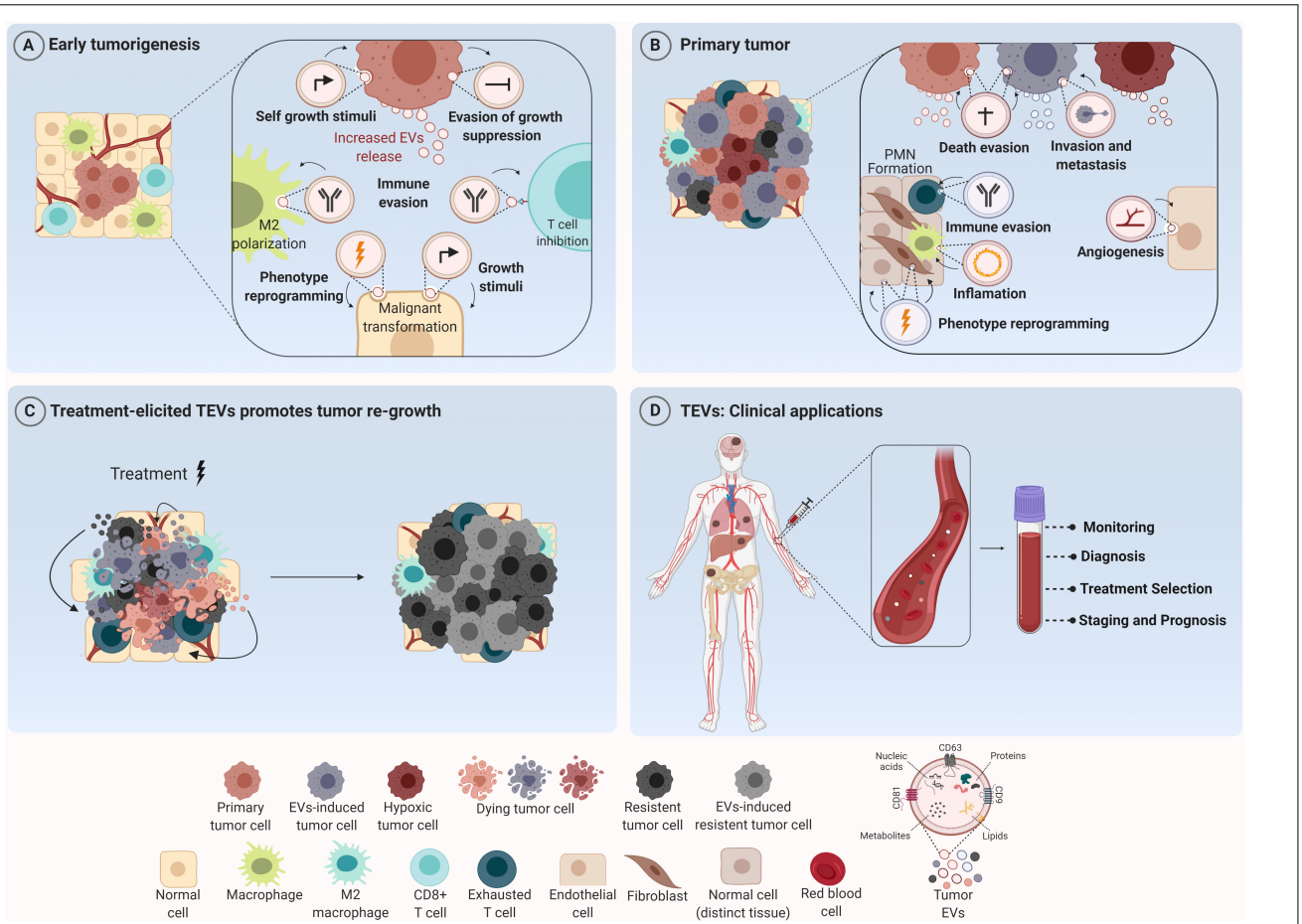

FIGURE 1 | Tumor-derived extracellular vesicles (TEVs) as mediators of tumor development and their use as potential theranostic biomarkers in oncology. **(A)** TEVs have been recognized as important modulators of many biological processes that govern tumor initiation such as sustained cell growth, evasion of antiproliferative and death stimuli, and immune evasion. Their uptake by tumor and stromal cells induces phenotype reprogramming that supports malignant transformation and tumor establishment. **(B)** Along tumor progression these nanostructures are able to create a permissive microenvironment characterized by sustained angiogenesis, inflammatory and immunosuppressive milieu at short and long distances supporting the formation of the pre-metastatic niche (PNM). **(C)** In addition, TEVs secreted in response to therapy can elicit a bystander effect in both tumor and stromal cells, inducing cell survival and outgrowth resulting in tumor recurrence. **(D)** In the clinical setting, since TEVs can reach all body fluids, they can be found in peripheral circulation and used for cancer diagnosis, prognosis and also as biomarkers for monitoring tumor response to therapies. Figure created using Biorender.

pre-metastatic niche (Ji et al., 2020). Similarly, EVs secreted by pancreatic tumor cells were shown to be selectively taken up by Kupffer cells (KC) in the liver leading to the release of TGFβ and the production of fibronectin by hepatic stellate cells, which recruited bone marrow-derived macrophages to establish a pro-inflammatory milieu to facilitate tumor metastasis (Costa-Silva et al., 2015). Few years later, Zeng et al. (2018) observed that TEVs from CRC not only increased vascular permeability, but also enhanced CRC metastasis in liver and lungs. Moreover, exosomes carrying miR-122 released by breast cancer cells reduced glucose uptake by normal recipient cells in pre-metastatic niche, increasing nutrient supply for metastatic cells Fong et al., 2015). Then, the metastatic effect by TEVs can also be mediated by their effect in stromal cells like fibroblasts (Fang et al., 2018; Xu et al., 2019); macrophages (Liang et al., 2019; Zhao et al., 2020) and in bone stroma (Dai et al., 2019) at long distances (**Figure 1B**).

THE ESTABLISHMENT OF AN IMMUNOSUPPRESSIVE ENVIRONMENT BY TEVs

Regarding the regulation of immune cells in TME, TEVs can educate infiltrating immune cells to cooperate with malignant cells, creating a permissive environment for tumor progression. In this context, EVs shed by GBM cells displaying PD-L1 were able to induce CD8 T cells exhaustion by directly binding to PD-1, thus facilitating tumor progression and impairing immunotherapy treatment efficacy (Ricklefs et al., 2018). Similar results were obtained for EVs derived from metastatic melanoma (Chen G. et al., 2018). In NSCLC patients, PD-L1 enriched exosomes from these patients inhibited IL-2 and IFN-γ production by T $CD8^+$ lymphocytes (Kim et al., 2019). In fact, exosomal PD-L1 is already pointed

out as an important biomarker in treatment management which demonstrates the translation of these findings into clinical practice. In hepatocarcinoma cells, TEVs can induce an immunosuppressive phenotype also in infiltrating B cells (Ye et al., 2018). In addition, interestingly, these immunosuppressive effects of TEVs also occur at long distances beyond the primary tumor site. Hsieh et al. (2018) showed that EVs shed by head and neck cancer cells induced M2 polarization through the transfer of miR-21 to $CD14^+$ human monocytes, favoring tumor growth (**Figure 1B**). In fact, this work shows that these cooperative relationships mediated by TEVs are not restricted to the tumor primary site and indeed can be established even at larger distances due to their presence in all body fluids, reinforcing the notion of cancer as a systemic disease under the influence of vesicles.

TREATMENT-ELICITED TEVs PROMOTES TUMOR RE-GROWTH

Tumor recurrence is considered one of the major causes of treatment failure, being directly correlated with a poor prognosis. The cellular mechanisms behind this involve intrinsic and/or acquired resistance (Zhu et al., 2021). The latter one can be mediated by vesicular cargo transfer of multidrug resistance transporters (Bebawy et al., 2009; Corcoran et al., 2012), anti-apoptotic and pro-tumorigenic molecules (Khan et al., 2012; Vella et al., 2017) from resistant to sensitive tumor cells, for example. Mrowczynski et al. (2018) showed that EVs derived from nervous system cancer cells upon Ionizing Radiation (IR) therapy could induce cell death evasion and consequent treatment resistance. Interestingly, higher radiation doses were significantly correlated with more expressive decrease in tumor suppressive molecules (STAT4, TPM1, miR-516, and miR-365) and greater increase of oncogenic cargo (CCND1, ANXA2, NPM1, and miR-889). Also, vesicles derived from dying pancreatic cancer cells after radiotherapy were shown to be enriched with miR-194-5p and could potentiate the survival of recipient cells by up-regulating DNA damage responses. In addition, the inhibition of TEVs release by aspirin significantly suppressed tumor re-growth and increased the survival of tumor-bearing mice (Jiang et al., 2020).

Moreover, EVs released upon chemotherapy have also been reported to promote tumor resistance. Survivin was found to be enriched in EVs secreted by chemotherapy-treated breast cancer cells and was able to promote the survival of tumor cells and tumor associated fibroblasts exposed to paclitaxel (Kreger et al., 2016). Furthermore, targeted therapy treatment with vemurafenib in BRAF-mutated melanoma cells resulted in altered miRNA and protein profile within EVs, inducing increased resistance in recipient cells (Lunavat et al., 2017). In accordance with these findings, Marconi et al. (2021) demonstrated that TEVs secreted by ERBB2 + breast cancer cells in response to trastuzumab carry a different protein cargo that are known to be associated with cytokinesis, lipid metabolism and organelle organization, indicating that this process might be altered in the recipient cells.

Our group recently demonstrated that EVs release by melanoma cells treated with temozolomide are taken up not only by tumor cells, which showed an increase in pluripotent and DNA repair gene expression levels, but were also able to induce a M2-phenotype in macrophages, promoting tumor repopulation in nude mice (Andrade et al., 2019). Additionally, EVs released by breast cancer cells upon paclitaxel or doxorubicin treatment were reported to contain higher amounts of ANXA6 protein, which could induce the pre-metastatic niche formation, by promoting Ccl2 expression, monocyte expansion and NF-kβ-dependent endothelial cells activation in pulmonary tissues, favoring lung metastasis at *in vivo* models (Keklikoglou et al., 2019). In myelomas, TEVs released upon chemotherapy were able to induce ECM remodeling and promote chemoresistance and relapse (Bandari et al., 2018; **Figure 1C**).

Still under this context, another process which is often sped up and induced by cytotoxic therapy is the autophagic flux. In the last few years, some studies have shown cross-regulation between autophagy and exosome release. Initially, autophagy was known as a catabolic process of intracellular degradation of proteins and organelles destined to the recycling of material and the balance of energetic cellular metabolism maintaining cellular homeostasis. However, autophagy can also interfere within the TME communication through its secretory function called secretory autophagy (SA) in a similar way as observed for TEVs (Thorburn et al., 2009; Claude-Taupin et al., 2018; Rak, 2020). Based on studies showing the similarities between EVs and autophagy concerning their biogenesis and secretory function (Murrow et al., 2015; Galluzzi et al., 2017; Pathan et al., 2019), one might speculate that this interconnection can be used by tumor cells to establish a cooperative relationship among different cells in the TME, impacting both tumor progression and treatment response in some tumors as discussed below.

Few years ago, Dutta et al. (2014) observed that exosomes released by breast cancer cells were taken up by normal epithelial cells, which was accompanied by an increase in ROS levels and autophagy in recipient cells. Consequently, these cells secreted soluble growth factors that induced the proliferation of malignant cells. More recently, cooperation among different cells in TME was shown to be dependent on the synergism between these two secretory pathways. In response to oxidative stress, pancreatic ductal adenocarcinoma cells released exosomes enriched in $KRAS^{G12D}$ during autophagy-dependent ferroptosis. These vesicles were engulfed by macrophages which, in turn, were polarized to M2 phenotype and promoted tumor growth in a mouse model (Dai E. et al., 2020).

About tumor response to therapy, it has been demonstrated that the use of chemotherapy and inhibitors of mTOR pathway led to an increased autophagic flux and, simultaneously, the exosome release (Hessvik et al., 2016; Xu J. et al., 2018; Ma et al., 2019). Exosomes harvested from irradiated brain cells carrying the miR-7 induced autophagy and transferred this signal to non-irradiated lung cells, mediating a bystander effect of autophagy in the lung after brain irradiation (Cai et al., 2017). In non-small cell lung carcinoma cells, exosomal miR-425-3p released in response to cisplatin decreased responsiveness to this drug via targeting the AKT1/mTOR signaling pathway and upregulation of autophagic

activity in recipient cells. On the other hand, enhanced miR-567 levels in HER2 + breast cancer cells were packaged into exosomes which were responsible for suppressing autophagy and reversing chemoresistance by targeting ATG5 in recipient cells (Han et al., 2020).

TEVs: FROM THE BENCH TO THE BEDSIDE

As already discussed, TEVs are multifaceted regulators of tumor progression and response to different therapeutic modalities. Although some aspects regarding their biogenesis and cargo sorting are still largely unknown, their diagnostic and therapeutic potential in oncology have been explored with enthusiasm for several groups. At some level, TEVs cargo reflects the molecular composition of malignant cells and, since these nanostructures can be found in all body fluids, they can serve as circulating biomarkers in liquid biopsy (LeBleu and Kalluri, 2020). Moreover, many studies demonstrated that the level of EVs in plasma is significant higher in cancer patients than healthy individuals as reported for esophageal squamous cell carcinoma (Matsumoto et al., 2016) and glioblastoma (Osti et al., 2019), indicating that EVs plasma quantification can be a useful surrogate indicator for cancer screening. Besides that, it has been demonstrated that plasma exosomal level increases with tumor stage progression as observed in patients with non-small cell lung cancer (Liu et al., 2018) and can be used also as an indicator of disease progression (**Figure 1D**).

Another aspect of EVs biology that has been explored in translational studies relies on the presence of macromolecules carried by these nanostructures. A very recent study by Hoshino et al. (2020) identified tissue-specific and tumor derived proteins in TEVs from cancer plasma patients in comparison to health individuals, indicating the potential use of vesicular proteins in cancer diagnosis. Moreover, in colorectal patients (CRC), it

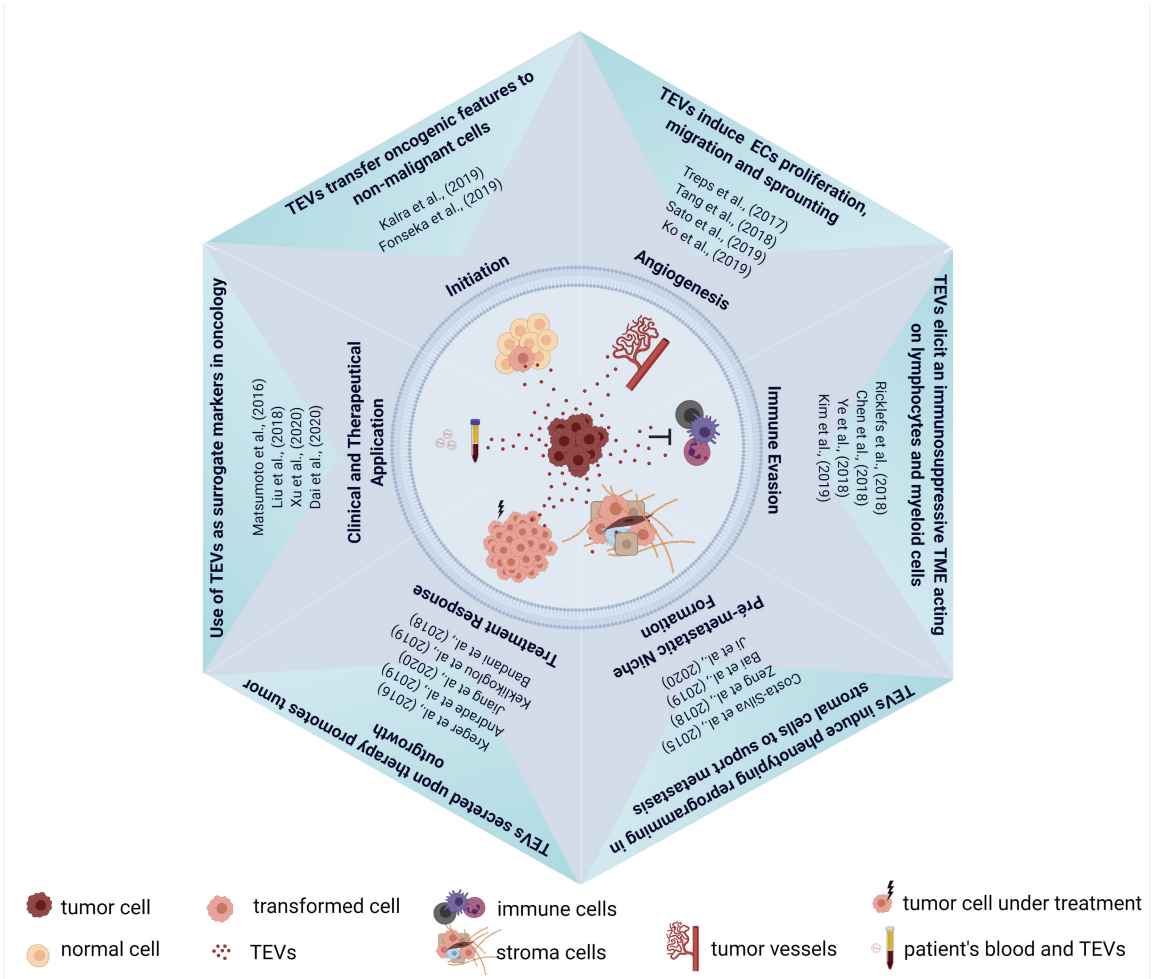

FIGURE 2 | Schematic representation of TEVs in cancer biology. Upper corner: pro-tumorigenic effect of TEVs in tumor initiation and progression. Right corner: establishment of an immunosuppressive environment by TEVs. Lower corner: effect of TEVs in pre-metastatic niche formation and in tumor repopulation after therapy. Left corner: the use of TEVs as theranostic biomarkers in oncology. Some of the published articles illustrating these mains findings of TEVs were cited in the figure. Figure created using Biorender.

was found that elevated levels of serum exosomal circ-PNN, a circular RNA, can be used for CRC diagnosis according to the validation analysis conducted by the authors (Xie et al., 2020). Interestingly, even the lipidic profile of plasma exosomes shows to be a promising biomarker in cancer (Bestard Escalas et al., 2021). To date, there are 16 clinical studies registered in Clinicaltrials.gov that aim to evaluate EVs potential in cancer diagnosis for different tumors, demonstrating that although the biology behind these nanostructures is still largely unknown, their use in clinical practice has been already explored.

Another promising use of TEVs in clinical settings is the potential of EVs as vehicles for the delivery of therapeutic agents which has also generated considerable excitement in the field. In fact, several studies evaluating the use of exosomes for the delivery of miRNAs, mRNAs, proteins, peptides, and synthetic drugs have been performed in the last years (Xu R. et al., 2018; Dai J. et al., 2020). Drugs such as doxorubicin (Srivastava et al., 2016), paclitaxel (Kim et al., 2016) and siRNA against oncogenic KRASG12D (Kamerkar et al., 2017) were successfully loaded in EVs and demonstrated potential anticancer effects *in vitro* and *in vivo*.

On the other hand, one alternative to explore the use of TEVs in cancer therapy is to reduce the exosome production or inhibit their secretion by tumor cells (Qi et al., 2016). A plenty of exosome inhibitors have been discovered and tested *in vitro* and in pre-clinical models to evaluate their effectiveness against transformed cells especially as neoadjuvant compounds. Most of them were developed to target important molecules of the exosome biogenesis machinery such as Rab27A and sphingomyelinases (Zhang et al., 2020) showing exciting results.

OUTSTANDING QUESTIONS, GAPS, AND CONCLUSION

Although remarkable progress has been made in the EVs field, as summarized in **Figure 2**, there are some gaps in our understanding of molecular mechanisms that control vesicle packaging and also how the cargo loading can be modified in response to different stimuli such as cancer therapies. This aspect is crucial for the comprehension of how EVs can promote resistance and tumor recurrence after therapy and to design new therapeutic strategies to minimize and block these pro-tumoral effects. Furthermore, EVs heterogeneity should be considered in pre-clinical and clinical studies and our understanding of functional differences among EVs classes is still limited. The answer for this question in particular will be necessary especially for the use of EVs as biomarkers in cancer diagnosis and prognosis.

Second, technical challenges are still debated in the EVs community and an effort for the standardization of methods for EV isolation, purification, quantification, and molecular characterization has been made to allow interlaboratory comparisons of pre-clinical and clinical data.

Third, even though interventions in TEVs like the ones involving drug loading and the use of EVs secretion inhibitors indicate therapeutic potential, new criteria become relevant to be investigated such as the timing of therapy, tumors to be treated and chemo-radio-immunotherapy combinations. It is also crucial to determine how the effect of different strategies to regulate exosomes in particular could influence the autophagy machinery or vice versa. Nevertheless, beyond these considerations, we believe that the study of the complex regulation between both pathways after chemo and radiotherapy, among other modalities, may open avenues for the design of novel therapies as well as improve the current ones, avoiding tumor recurrence. Then, in our opinion, the comprehension of the tumor-driven cooperation mediated by TEVs during tumor progression and upon therapy will pave the way to improve therapy outcomes in cancer patients.

AUTHOR CONTRIBUTIONS

RC and LA conceptualized the manuscript, reviewed, and edited the manuscript before submission. LA, NS, SB, DB, and RC provided intellectual input, analyzed the literature, and participated in the writing. NS prepared the figures. All authors read and approved the final version of the manuscript.

FUNDING

This research was supported by grants from FAPESP (Grant Number 2020/09176-8 and 2019/07278-0) and CNPq (Grant Number 305700/2017-0). The funder did not play any role in design, interpretation, or writing of the review.

REFERENCES

Anand, S., Samuel, M., Kumar, S., and Mathivanan, S. (2019). Ticket to a bubble ride: Cargo sorting into exosomes and extracellular vesicles. *Biochim. Biophys. Acta Proteins Proteom.* 1867:140203. doi: 10.1016/j.bbapap.2019.02.005

Andrade, L. N. S., Otake, A. H., Cardim, S. G. B., da Silva, F. I., Ikoma Sakamoto, M. M., Furuya, T. K., et al. (2019). Extracellular vesicles shedding promotes melanoma growth in response to chemotherapy. *Sci. Rep.* 9:14482. doi: 10.1038/s41598-019-50848-z

Aslan, C., Maralbashi, S., Salari, F., Kahroba, H., Sigaroodi, F., Kazemi, T., et al. (2019). Tumor-derived exosomes: implication in angiogenesis and antiangiogenesis cancer therapy. *J. Cell Physiol.* 234, 16885–16903. doi: 10.1002/jcp.28374

Bai, M., Li, J., Yang, H., Zhang, H., Zhou, Z., Deng, T., et al. (2019). miR-135b delivered by gastric tumor exosomes inhibits foxo1 expression in endothelial cells and promotes angiogenesis. *Mol. Ther.* 27, 1772–1783. doi: 10.1016/j.ymthe.2019.06.018

Bandari, S. K., Purushothaman, A., Ramani, V. C., Brinkley, G. J., Chandrashekar, D. S., Varambally, S., et al. (2018). Chemotherapy induces secretion of exosomes loaded with heparanase that degrades extracellular matrix and impacts tumor and host cell behavior. *Matrix Biol.* 65, 104–118. doi: 10.1016/j.matbio.2017.09.001

Bebawy, M., Combes, V., Lee, E., Jaiswal, R., Gong, J., Bonhoure, A., et al. (2009). Membrane microparticles mediate transfer of P-glycoprotein to drug sensitive cancer cells. *Leukemia* 23, 1643–1649. doi: 10.1038/leu.2009.76

Bestard Escalas, J., Reigada, R., Reyes, J., de la Torre, P., Liebisch, G., and Barceló-Coblijn, G. (2021). Fatty acid unsaturation degree of plasma exosomes in

colorectal cancer patients: a promising biomarker. *Int. J. Mol. Sci.* 22:60. doi: 10.3390/ijms22105060

Biagioni, A., Laurenzana, A., Menicacci, B., Peppicelli, S., Andreucci, E., Bianchini, F., et al. (2021). uPAR-expressing melanoma exosomes promote angiogenesis by VE-Cadherin, EGFR and uPAR overexpression and rise of ERK1,2 signaling in endothelial cells. *Cell Mol. Life Sci.* 78, 3057–3072. doi: 10.1007/s00018-020-03707-4

Cai, S., Shi, G. S., Cheng, H. Y., Zeng, Y. N., Li, G., Zhang, M., et al. (2017). Exosomal miR-7 mediates bystander autophagy in lung after focal brain irradiation in mice. *Int. J. Biol. Sci.* 13, 1287–1296. doi: 10.7150/ijbs.18890

Chen, G., Huang, A. C., Zhang, W., Zhang, G., Wu, M., Xu, W., et al. (2018). Exosomal PD-L1 contributes to immunosuppression and is associated with anti-PD-1 response. *Nature* 560, 382–386. doi: 10.1038/s41586-018-0392-8

Chen, X., Zhou, J., Li, X., Wang, X., and Lin, Y. (2018). Exosomes derived from hypoxic epithelial ovarian cancer cells deliver microRNAs to macrophages and elicit a tumor-promoted phenotype. *Cancer Lett.* 435, 80–91. doi: 10.1016/j.canlet.2018.08.001

Claude-Taupin, A., Bissa, B., Jia, J., Gu, Y., and Deretic, V. (2018). Role of autophagy in IL-1β export and release from cells. *Semin. Cell Dev. Biol.* 83, 36–41. doi: 10.1016/j.semcdb.2018.03.012

Corcoran, C., Rani, S., O'Brien, K., O'Neill, A., Prencipe, M., Sheikh, R., et al. (2012). Docetaxel-resistance in prostate cancer: evaluating associated phenotypic changes and potential for resistance transfer via exosomes. *PLoS One* 7:e50999. doi: 10.1371/journal.pone.0050999

Costa-Silva, B., Aiello, N. M., Ocean, A. J., Singh, S., Zhang, H., Thakur, B. K., et al. (2015). Pancreatic cancer exosomes initiate pre-metastatic niche formation in the liver. *Nat. Cell Biol.* 17, 816–826. doi: 10.1038/ncb3169

Dai, E., Han, L., Liu, J., Xie, Y., Kroemer, G., Klionsky, D. J., et al. (2020). Autophagy-dependent ferroptosis drives tumor-associated macrophage polarization via release and uptake of oncogenic KRAS protein. *Autophagy* 16, 2069–2083. doi: 10.1080/15548627.2020.1714209

Dai, J., Escara-Wilke, J., Keller, J. M., Jung, Y., Taichman, R. S., Pienta, K. J., et al. (2019). Primary prostate cancer educates bone stroma through exosomal pyruvate kinase M2 to promote bone metastasis. *J. Exp. Med.* 216, 2883–2899. doi: 10.1084/jem.20190158

Dai, J., Su, Y., Zhong, S., Cong, L., Liu, B., Yang, J., et al. (2020). Exosomes: key players in cancer and potential therapeutic strategy. *Signal Transduct. Target Ther.* 5:145. doi: 10.1038/s41392-020-00261-0

Dorayappan, K. D. P., Wanner, R., Wallbillich, J. J., Saini, U., Zingarelli, R., Suarez, A. A., et al. (2018). Hypoxia-induced exosomes contribute to a more aggressive and chemoresistant ovarian cancer phenotype: a novel mechanism linking STAT3/Rab proteins. *Oncogene* 37, 3806–3821. doi: 10.1038/s41388-018-0189-0

Dutta, S., Warshall, C., Bandyopadhyay, C., Dutta, D., and Chandran, B. (2014). Interactions between exosomes from breast cancer cells and primary mammary epithelial cells leads to generation of reactive oxygen species which induce DNA damage response, stabilization of p53 and autophagy in epithelial cells. *PLoS One* 9:e97580. doi: 10.1371/journal.pone.0097580

Fan, J., Xu, G., Chang, Z., Zhu, L., and Yao, J. (2020). miR-210 transferred by lung cancer cell-derived exosomes may act as proangiogenic factor in cancer-associated fibroblasts by modulating JAK2/STAT3 pathway. *Clin. Sci.* 134, 807–825. doi: 10.1042/CS20200039

Fang, T., Lv, H., Lv, G., Li, T., Wang, C., Han, Q., et al. (2018). Tumor-derived exosomal miR-1247-3p induces cancer-associated fibroblast activation to foster lung metastasis of liver cancer. *Nat. Commun.* 9:191. doi: 10.1038/s41467-017-02583-0

Fitzgerald, W., Freeman, M. L., Lederman, M. M., Vasilieva, E., Romero, R., and Margolis, L. (2018). A System of Cytokines Encapsulated in ExtraCellular Vesicles. *Sci. Rep.* 8:8973. doi: 10.1038/s41598-018-27190-x

Folkman, J. (1975). Tumor angiogenesis: a possible control point in tumor growth. *Ann. Intern. Med.* 82, 96–100. doi: 10.7326/0003-4819-82-1-96

Fong, M. Y., Zhou, W., Liu, L., Alontaga, A. Y., Chandra, M., Ashby, J., et al. (2015). Breast-cancer-secreted miR-122 reprograms glucose metabolism in premetastatic niche to promote metastasis. *Nat. Cell Biol.* 17, 183–194. doi: 10.1038/ncb3094

Fonseka, P., Liem, M., Ozcitti, C., Adda, C. G., Ang, C. S., and Mathivanan, S. (2019). Exosomes from N-Myc amplified neuroblastoma cells induce migration and confer chemoresistance to non-N-Myc amplified cells: implications of intra-tumour heterogeneity. *J. Extracell. Vesicles.* 8:1597614. doi: 10.1080/20013078.2019.1597614

Galluzzi, L., Baehrecke, E. H., Ballabio, A., Boya, P., Bravo-San Pedro, J. M., Cecconi, F., et al. (2017). Molecular definitions of autophagy and related processes. *EMBO J.* 36, 1811–1836. doi: 10.15252/embj.201796697

Guo, X., Qiu, W., Liu, Q., Qian, M., Wang, S., Zhang, Z., et al. (2018). Immunosuppressive effects of hypoxia-induced glioma exosomes through myeloid-derived suppressor cells via the miR-10a/Rora and miR-21/Pten Pathways. *Oncogene* 37, 4239–4259. doi: 10.1038/s41388-018-0261-9

Han, M., Hu, J., Lu, P., Cao, H., Yu, C., Li, X., et al. (2020). Exosome-transmitted miR-567 reverses trastuzumab resistance by inhibiting ATG5 in breast cancer. *Cell Death Dis.* 11:43. doi: 10.1038/s41419-020-2250-5

Hanahan, D., and Weinberg, R. A. (2011). Hallmarks of cancer: the next generation. *Cell* 144, 646–674. doi: 10.1016/j.cell.2011.02.013

He, L., Zhu, W., Chen, Q., Yuan, Y., Wang, Y., Wang, J., et al. (2019). Ovarian cancer cell-secreted exosomal miR-205 promotes metastasis by inducing angiogenesis. *Theranostics* 9, 8206–8220. doi: 10.7150/thno.37455

Hessvik, N. P., Øverbye, A., Brech, A., Torgersen, M. L., Jakobsen, I. S., Sandvig, K., et al. (2016). PIKfyve inhibition increases exosome release and induces secretory autophagy. *Cell Mol. Life Sci.* 73, 4717–4737. doi: 10.1007/s00018-016-2309-8

Horie, K., Kawakami, K., Fujita, Y., Sugaya, M., Kameyama, K., Mizutani, K., et al. (2017). Exosomes expressing carbonic anhydrase 9 promote angiogenesis. *Biochem. Biophys. Res. Commun.* 492, 356–361. doi: 10.1016/j.bbrc.2017.08.107

Hoshino, A., Kim, H. S., Bojmar, L., Gyan, K. E., Cioffi, M., Hernandez, J., et al. (2020). Extracellular Vesicle and Particle Biomarkers Define Multiple Human Cancers. *Cell* 182, 1044–1061. doi: 10.1016/j.cell.2020.07.009

Hsieh, C. H., Tai, S. K., and Yang, M. H. (2018). Snail-overexpressing Cancer Cells Promote M2-Like Polarization of Tumor-Associated Macrophages by Delivering MiR-21-Abundant Exosomes. *Neoplasia* 20, 775–788. doi: 10.1016/j.neo.2018.06.004

Huang, Z., and Feng, Y. (2017). Exosomes Derived From Hypoxic Colorectal Cancer Cells Promote Angiogenesis Through Wnt4-Induced β-Catenin Signaling in Endothelial Cells. *Oncol. Res.* 651–661. doi: 10.3727/096504016X14752792816791

Ji, Q., Zhou, L., Sui, H., Yang, L., Wu, X., Song, Q., et al. (2020). Primary tumors release ITGBL1-rich extracellular vesicles to promote distal metastatic tumor growth through fibroblast-niche formation. *Nat. Commun.* 11:1211. doi: 10.1038/s41467-020-14869-x

Jiang, M. J., Chen, Y. Y., Dai, J. J., Gu, D. N., Mei, Z., Liu, F. R., et al. (2020). Dying tumor cell-derived exosomal miR-194-5p potentiates survival and repopulation of tumor repopulating cells upon radiotherapy in pancreatic cancer. *Mol. Cancer* 19:68. doi: 10.1186/s12943-020-01178-6

Kalra, H., Gangoda, L., Fonseka, P., Chitti, S. V., Liem, M., Keerthikumar, S., et al. (2019). Extracellular vesicles containing oncogenic mutant β-catenin activate Wnt signalling pathway in the recipient cells. *J. Extracell. Vesicles* 8:1690217. doi: 10.1080/20013078.2019.1690217

Kamerkar, S., LeBleu, V. S., Sugimoto, H., Yang, S., Ruivo, C. F., Melo, S. A., et al. (2017). Exosomes facilitate therapeutic targeting of oncogenic KRAS in pancreatic cancer. *Nature* 546, 498–503. doi: 10.1038/nature22341

Keklikoglou, I., Cianciaruso, C., Güç, E., Squadrito, M. L., Spring, L. M., Tazzyman, S., et al. (2019). Chemotherapy elicits pro-metastatic extracellular vesicles in breast cancer models. *Nat. Cell Biol.* 21, 190–202. doi: 10.1038/s41556-018-0256-3

Khan, S., Jutzy, J. M., Valenzuela, M. M., Turay, D., Aspe, J. R., Ashok, A., et al. (2012). Plasma-derived exosomal survivin, a plausible biomarker for early detection of prostate cancer. *PLoS One* 7:e46737. doi: 10.1371/journal.pone.0046737

Kilinc, S., Paisner, R., Camarda, R., Gupta, S., Momcilovic, O., Kohnz, R. A., et al. (2021). Oncogene-regulated release of extracellular vesicles. *Dev. Cell* 2021:14. doi: 10.1016/j.devcel.2021.05.014

Kim, D. H., Kim, H., Choi, Y. J., Kim, S. Y., Lee, J. E., Sung, K. J., et al. (2019). Exosomal PD-L1 promotes tumor growth through immune escape in non-small cell lung cancer. *Exp. Mol. Med.* 51, 1–13. doi: 10.1038/s12276-019-0295-2

Kim, M. S., Haney, M. J., Zhao, Y., Mahajan, V., Deygen, I., Klyachko, N. L., et al. (2016). Development of exosome-encapsulated paclitaxel to overcome MDR in cancer cells. *Nanomedicine* 12, 655–664. doi: 10.1016/j.nano.2015.10.012

Ko, S. Y., Lee, W., Kenny, H. A., Dang, L. H., Ellis, L. M., Jonasch, E., et al. (2019). Cancer-derived small extracellular vesicles promote angiogenesis by

heparin-bound, bevacizumab-insensitive VEGF, independent of vesicle uptake. *Commun. Biol.* 2:386. doi: 10.1038/s42003-019-0609-x

Kreger, B. T., Johansen, E. R., Cerione, R. A., and Antonyak, M. A. (2016). The Enrichment of Survivin in Exosomes from Breast Cancer Cells Treated with Paclitaxel Promotes Cell Survival and Chemoresistance. *Cancers* 2016:8120111. doi: 10.3390/cancers8120111

Lázaro-Ibáñez, E., Lässer, C., Shelke, G. V., Crescitelli, R., Jang, S. C., Cvjetkovic, A., et al. (2019). DNA analysis of low- and high-density fractions defines heterogeneous subpopulations of small extracellular vesicles based on their DNA cargo and topology. *J. Extracell. Vesicles* 8:1656993. doi: 10.1080/20013078.2019.1656993

LeBleu, V. S., and Kalluri, R. (2020). Exosomes as a Multicomponent Biomarker Platform in Cancer. *Trends Cancer* 6, 767–774. doi: 10.1016/j.trecan.2020.03.007

Liang, Z. X., Liu, H. S., Wang, F. W., Xiong, L., Zhou, C., Hu, T., et al. (2019). LncRNA RPPH1 promotes colorectal cancer metastasis by interacting with TUBB3 and by promoting exosomes-mediated macrophage M2 polarization. *Cell Death Dis.* 10:829. doi: 10.1038/s41419-019-2077-0

Liu, Q., Xiang, Y., Yuan, S., Xie, W., Li, C., Hu, Z., et al. (2018). Plasma exosome levels in non-small-cell lung cancer: Correlation with clinicopathological features and prognostic implications. *Cancer Biomark.* 22, 267–274. doi: 10.3233/CBM-170955

Lunavat, T. R., Cheng, L., Einarsdottir, B. O., Olofsson Bagge, R., Veppil Muralidharan, S., Sharples, R. A., et al. (2017). BRAF(V600) inhibition alters the microRNA cargo in the vesicular secretome of malignant melanoma cells. *Proc. Natl. Acad. Sci. U S A.* 114, E5930–E5939. doi: 10.1073/pnas.1705206114

Ma, Y., Yuwen, D., Chen, J., Zheng, B., Gao, J., Fan, M., et al. (2019). Exosomal Transfer Of Cisplatin-Induced miR-425-3p Confers Cisplatin Resistance In NSCLC Through Activating Autophagy. *Int. J. Nanomedicine* 14, 8121–8132. doi: 10.2147/IJN.S221383

Marconi, S., Santamaria, S., Bartolucci, M., Stigliani, S., Aiello, C., Gagliani, M. C., et al. (2021). Trastuzumab Modulates the Protein Cargo of Extracellular Vesicles Released by ERBB2. *Membranes* 2021:11030199. doi: 10.3390/membranes11030199

Matsumoto, Y., Kano, M., Akutsu, Y., Hanari, N., Hoshino, I., Murakami, K., et al. (2016). Quantification of plasma exosome is a potential prognostic marker for esophageal squamous cell carcinoma. *Oncol. Rep.* 36, 2535–2543. doi: 10.3892/or.2016.5066

Mrowczynski, O. D., Madhankumar, A. B., Sundstrom, J. M., Zhao, Y., Kawasawa, Y. I., Slagle-Webb, B., et al. (2018). Exosomes impact survival to radiation exposure in cell line models of nervous system cancer. *Oncotarget* 9, 36083–36101. doi: 10.18632/oncotarget.26300

Murrow, L., Malhotra, R., and Debnath, J. (2015). ATG12-ATG3 interacts with Alix to promote basal autophagic flux and late endosome function. *Nat. Cell Biol.* 17, 300–310. doi: 10.1038/ncb3112

O'Brien, K., Breyne, K., Ughetto, S., Laurent, L. C., and Breakefield, X. O. (2020). RNA delivery by extracellular vesicles in mammalian cells and its applications. *Nat. Rev. Mol. Cell Biol.* 21, 585–606. doi: 10.1038/s41580-020-0251-y

Osti, D., Del Bene, M., Rappa, G., Santos, M., Matafora, V., Richichi, C., et al. (2019). Clinical Significance of Extracellular Vesicles in Plasma from Glioblastoma Patients. *Clin. Cancer Res.* 25, 266–276. doi: 10.1158/1078-0432.CCR-18-1941

Park, J. E., Dutta, B., Tse, S. W., Gupta, N., Tan, C. F., Low, J. K., et al. (2019). Hypoxia-induced tumor exosomes promote M2-like macrophage polarization of infiltrating myeloid cells and microRNA-mediated metabolic shift. *Oncogene* 38, 5158–5173. doi: 10.1038/s41388-019-0782-x

Pathan, M., Fonseka, P., Chitti, S. V., Kang, T., Sanwlani, R., Van Deun, J., et al. (2019). Vesiclepedia 2019: a compendium of RNA, proteins, lipids and metabolites in extracellular vesicles. *Nucleic Acids Res.* 47, D516–D519. doi: 10.1093/nar/gky1029

Pelham, C. J., Nagane, M., and Madan, E. (2020). Cell competition in tumor evolution and heterogeneity: Merging past and present. *Semin. Cancer Biol.* 63, 11–18. doi: 10.1016/j.semcancer.2019.07.008

Qi, H., Liu, C., Long, L., Ren, Y., Zhang, S., Chang, X., et al. (2016). Blood Exosomes Endowed with Magnetic and Targeting Properties for Cancer Therapy. *ACS Nano* 10, 3323–3333. doi: 10.1021/acsnano.5b06939

Qian, M., Wang, S., Guo, X., Wang, J., Zhang, Z., Qiu, W., et al. (2020). Hypoxic glioma-derived exosomes deliver microRNA-1246 to induce M2 macrophage polarization by targeting TERF2IP via the STAT3 and NF-κB pathways. *Oncogene* 39, 428–442. doi: 10.1038/s41388-019-0996-y

Quail, D. F., and Joyce, J. A. (2013). Microenvironmental regulation of tumor progression and metastasis. *Nat. Med.* 19, 1423–1437. doi: 10.1038/nm.3394

Rak, J. (2020). L(C3)icensing of exosomes for RNA export. *Nat. Cell Biol.* 22, 137–139. doi: 10.1038/s41556-020-0466-3

Ramteke, A., Ting, H., Agarwal, C., Mateen, S., Somasagara, R., Hussain, A., et al. (2015). Exosomes secreted under hypoxia enhance invasiveness and stemness of prostate cancer cells by targeting adherens junction molecules. *Mol. Carcinog.* 54, 554–565. doi: 10.1002/mc.22124

Raposo, G., and Stahl, P. D. (2019). Extracellular vesicles: a new communication paradigm? *Nat. Rev. Mol. Cell Biol.* 20, 509–510. doi: 10.1038/s41580-019-0158-7

Ricklefs, F. L., Alayo, Q., Krenzlin, H., Mahmoud, A. B., Speranza, M. C., Nakashima, H., et al. (2018). Immune evasion mediated by PD-L1 on glioblastoma-derived extracellular vesicles. *Sci. Adv.* 4:eaar2766. doi: 10.1126/sciadv.aar2766

Sato, S., Vasaikar, S., Eskaros, A., Kim, Y., Lewis, J. S., Zhang, B., et al. (2019). EPHB2 carried on small extracellular vesicles induces tumor angiogenesis via activation of ephrin reverse signaling. *JCI Insight* 4:132447. doi: 10.1172/jci.insight.132447

Schubert, A., and Boutros, M. (2021). Extracellular vesicles and oncogenic signaling. *Mol. Oncol.* 15, 3–26. doi: 10.1002/1878-0261.12855

Shang, D., Xie, C., Hu, J., Tan, J., Yuan, Y., Liu, Z., et al. (2020). Pancreatic cancer cell-derived exosomal microRNA-27a promotes angiogenesis of human microvascular endothelial cells in pancreatic cancer via BTG2. *J. Cell Mol. Med.* 24, 588–604. doi: 10.1111/jcmm.14766

Sharma, P., Diergaarde, B., Ferrone, S., Kirkwood, J. M., and Whiteside, T. L. (2020). Melanoma cell-derived exosomes in plasma of melanoma patients suppress functions of immune effector cells. *Sci. Rep.* 10:92. doi: 10.1038/s41598-019-56542-4

Srivastava, A., Amreddy, N., Babu, A., Panneerselvam, J., Mehta, M., Muralidharan, R., et al. (2016). Nanosomes carrying doxorubicin exhibit potent anticancer activity against human lung cancer cells. *Sci. Rep.* 6:38541. doi: 10.1038/srep38541

Tang, M. K. S., Yue, P. Y. K., Ip, P. P., Huang, R. L., Lai, H. C., Cheung, A. N. Y., et al. (2018). Soluble E-cadherin promotes tumor angiogenesis and localizes to exosome surface. *Nat. Commun.* 9:2270. doi: 10.1038/s41467-018-04695-7

Thorburn, J., Horita, H., Redzic, J., Hansen, K., Frankel, A. E., and Thorburn, A. (2009). Autophagy regulates selective HMGB1 release in tumor cells that are destined to die. *Cell Death Differ.* 16, 175–183. doi: 10.1038/cdd.2008.143

Tkach, M., and Théry, C. (2016). Communication by Extracellular Vesicles: Where We Are and Where We Need to Go. *Cell* 164, 1226–1232. doi: 10.1016/j.cell.2016.01.043

Treps, L., Perret, R., Edmond, S., Ricard, D., and Gavard, J. (2017). Glioblastoma stem-like cells secrete the pro-angiogenic VEGF-A factor in extracellular vesicles. *J. Extracell. Vesicles* 6:1359479. doi: 10.1080/20013078.2017.1359479

van Niel, G., D'Angelo, G., and Raposo, G. (2018). Shedding light on the cell biology of extracellular vesicles. *Nat. Rev. Mol. Cell Biol.* 19, 213–228. doi: 10.1038/nrm.2017.125

Vella, L. J., Behren, A., Coleman, B., Greening, D. W., Hill, A. F., and Cebon, J. (2017). Intercellular Resistance to BRAF Inhibition Can Be Mediated by Extracellular Vesicle-Associated PDGFRβ. *Neoplasia* 19, 932–940. doi: 10.1016/j.neo.2017.07.002

Wang, X., Luo, G., Zhang, K., Cao, J., Huang, C., Jiang, T., et al. (2018). Hypoxic Tumor-Derived Exosomal miR-301a Mediates M2 Macrophage Polarization via PTEN/PI3Kγ to Promote Pancreatic Cancer Metastasis. *Cancer Res.* 78, 4586–4598. doi: 10.1158/0008-5472.CAN-17-3841

Wang, Z. F., Liao, F., Wu, H., and Dai, J. (2019). Glioma stem cells-derived exosomal miR-26a promotes angiogenesis of microvessel endothelial cells in glioma. *J. Exp. Clin. Cancer Res.* 38:201. doi: 10.1186/s13046-019-1181-4

Xie, Y., Li, J., Li, P., Li, N., Zhang, Y., Binang, H., et al. (2020). RNA-Seq Profiling of Serum Exosomal Circular RNAs Reveals Circ-PNN as a Potential Biomarker for Human Colorectal Cancer. *Front. Oncol.* 10:982. doi: 10.3389/fonc.2020.00982

Xu, J., Camfield, R., and Gorski, S. M. (2018). The interplay between exosomes and autophagy partners in crime. *J. Cell Sci.* 131:215210. doi: 10.1242/jcs.215210

Xu, R., Rai, A., Chen, M., Suwakulsiri, W., Greening, D. W., and Simpson, R. J. (2018). Extracellular vesicles in cancer - implications for future improvements

in cancer care. *Nat. Rev. Clin. Oncol.* 15, 617–638. doi: 10.1038/s41571-018-0036-9

Xu, Z., Zheng, X., and Zheng, J. (2019). Tumor-derived exosomes educate fibroblasts to promote salivary adenoid cystic carcinoma metastasis via NGF-NTRK1 pathway. *Oncol. Lett.* 18, 4082–4091. doi: 10.3892/ol.2019.10740

Yáñez-Mó, M., Siljander, P. R., Andreu, Z., Zavec, A. B., Borràs, F. E., Buzas, E. I., et al. (2015). Biological properties of extracellular vesicles and their physiological functions. *J. Extracell Vesicles.* 4:27066. doi: 10.3402/jev.v4.27066

Yang, H., Zhang, H., Ge, S., Ning, T., Bai, M., Li, J., et al. (2018). Exosome-Derived miR-130a Activates Angiogenesis in Gastric Cancer by Targeting C-MYB in Vascular Endothelial Cells. *Mol. Ther.* 26, 2466–2475. doi: 10.1016/j.ymthe.2018.07.023

Ye, L., Zhang, Q., Cheng, Y., Chen, X., Wang, G., Shi, M., et al. (2018). Tumor-derived exosomal HMGB1 fosters hepatocellular carcinoma immune evasion by promoting TIM-1. *J. Immunother. Cancer.* 6:145. doi: 10.1186/s40425-018-0451-6

Zeng, Z., Li, Y., Pan, Y., Lan, X., Song, F., Sun, J., et al. (2018). Cancer-derived exosomal miR-25-3p promotes pre-metastatic niche formation by inducing vascular permeability and angiogenesis. *Nat. Commun.* 9:5395. doi: 10.1038/s41467-018-07810-w

Zhang, H., Lu, J., Liu, J., Zhang, G., and Lu, A. (2020). Advances in the discovery of exosome inhibitors in cancer. *J. Enzyme Inhib. Med. Chem.* 35, 1322–1330. doi: 10.1080/14756366.2020.1754814

Zhao, S., Mi, Y., Guan, B., Zheng, B., Wei, P., Gu, Y., et al. (2020). Tumor-derived exosomal miR-934 induces macrophage M2 polarization to promote liver metastasis of colorectal cancer. *J. Hematol. Oncol.* 13:156. doi: 10.1186/s13045-020-00991-2

Zhou, X., Yan, T., Huang, C., Xu, Z., Wang, L., Jiang, E., et al. (2018). Melanoma cell-secreted exosomal miR-155-5p induce proangiogenic switch of cancer-associated fibroblasts via SOCS1/JAK2/STAT3 signaling pathway. *J. Exp. Clin. Cancer Res.* 37:242. doi: 10.1186/s13046-018-0911-3

Zhu, X., Li, S., Xu, B., and Luo, H. (2021). Cancer evolution: A means by which tumors evade treatment. *Biomed. Pharmacother.* 133:111016. doi: 10.1016/j.biopha.2020.111016

Conflict of Interest: The authors declare that the research was conducted in the absence of any commercial or financial relationships that could be construed as a potential conflict of interest.

Publisher's Note: All claims expressed in this article are solely those of the authors and do not necessarily represent those of their affiliated organizations, or those of the publisher, the editors and the reviewers. Any product that may be evaluated in this article, or claim that may be made by its manufacturer, is not guaranteed or endorsed by the publisher.

frontiers in Cell and Developmental Biology

REVIEW
published: 19 November 2021
doi: 10.3389/fcell.2021.764698

The Bone Marrow Microenvironment Mechanisms in Acute Myeloid Leukemia

*Débora Bifano Pimenta†, Vanessa Araujo Varela†, Tarcila Santos Datoguia, Victória Bulcão Caraciolo, Gabriel Herculano Lopes and Welbert Oliveira Pereira**

Faculdade Israelita de Ciências da Saúde Albert Einstein, Hospital Israelita Albert Einstein, São Paulo, Brazil

Bone marrow (BM) is a highly complex tissue that provides important regulatory signals to orchestrate hematopoiesis. Resident and transient cells occupy and interact with some well characterized niches to produce molecular and cellular mechanisms that interfere with differentiation, migration, survival, and proliferation in this microenvironment. The acute myeloid leukemia (AML), the most common and severe hematological neoplasm in adults, arises and develop in the BM. The osteoblastic, vascular, and reticular niches provide surface co-receptors, soluble factors, cytokines, and chemokines that mediate important functions on hematopoietic cells and leukemic blasts. There are some evidences of how AML modify the architecture and function of these three BM niches, but it has been still unclear how essential those modifications are to maintain AML development. Basic studies and clinical trials have been suggesting that disturbing specific cells and molecules into the BM niches might be able to impair leukemia competencies. Either through niche-specific molecule inhibition alone or in combination with more traditional drugs, the bone marrow microenvironment is currently considered the potential target for new strategies to treat AML patients. This review describes the cellular and molecular constitution of the BM niches under healthy and AML conditions, presenting this anatomical compartment by a new perspective: as a prospective target for current and next generation therapies.

Keywords: acute myeloid leukemia, bone marrow, endosteal niche, vascular niche, reticular niche, molecular targets, hematopoiesis, treatment

OPEN ACCESS

Edited by:
Ana Karina Oliveira, University of Virginia, United States

Reviewed by:
Elisa Dorantes, Federico Gómez Children's Hospital, Mexico
Luciana Daniele Trino, National Center for Research in Energy and Materials (Brazil), Brazil

****Correspondence:***
Welbert Oliveira Pereira
welbertop@gmail.com

†These authors have contributed equally to this work

Specialty section:
This article was submitted to Molecular and Cellular Pathology, a section of the journal Frontiers in Cell and Developmental Biology

Received: *25 August 2021*
Accepted: *20 October 2021*
Published: *19 November 2021*

Citation:
Pimenta DB, Varela VA, Datoguia TS, Caraciolo VB, Lopes GH and Pereira WO (2021) The Bone Marrow Microenvironment Mechanisms in Acute Myeloid Leukemia. Front. Cell Dev. Biol. 9:764698. doi: 10.3389/fcell.2021.764698

INTRODUCTION

The bone marrow (BM) is a soft and viscous tissue within the bone cavities that holds a highly complex and dynamic microenvironment. The BM microenvironment is formed by heterogeneous cells populations, blood vessels and a variety of molecules allocated in niches that provide important regulatory signals to support hematopoiesis, which importantly contribute to the physiological homeostasis throughout life in several aspects, including blood regeneration and immune system maintenance (Yin and Li 2006; Medyouf 2017; Shafat, Gnaneswaran, et al., 2017; Méndez-Ferrer et al., 2020).

The hematopoietic stem cells (HSC) are self-renewing progenitors of the hematopoietic system that reside and remain in the BM until maturation. HSCs and some of their derived subpopulations are dynamically exposed to several stimuli that orchestrate survival, self-renewal, quiescence, migration, and differentiation driving to an adequate hematopoiesis. Considering the hematopoietic cells, there are two core cell lineages in the BM: the common myeloid progenitor

line dedicated to megakaryocyte/erythrocyte lineage and to granulocyte/macrophage lineage; and the common lymphoid progenitor line that ultimately originates the lymphocytes (B and T), NK and NKT cell (Passegué et al., 2003; Medyouf 2017; Shafat, Gnaneswaran, et al., 2017).

Homeostasis is affected on many levels by the correct hematopoietic system regulation. For example, immune system cells are associated with neurological functions, endocrine and cardiovascular regulation, metabolism control and cancer surveillance (Malcangio 2019; Ahmari, Hayward, and Zubcevic 2020; Vidal and Pacheco 2020; Klein 2021; Kologrivova et al., 2021). Thus, disturbances in the bone marrow microenvironment may contribute to the development and exacerbation of a range of diseases.

Genes and pathways related to normal development of HSCs may be affected by mutations and trigger hematological oncogenesis with reported changes in the BM microenvironment organization. However, the interaction of leukemia stem cells (LSC) and BM niches are still incompletely described (Passegué et al., 2003; Huntly and Gilliland 2005; Ugel et al., 2015; Méndez-Ferrer et al., 2020). What comes first? BM niches disturbance or LSC arising? How leukemic BM niches might contribute to AML? Such answers may lead researchers toward a next generation of diagnosis markers and therapeutic approaches reaching promising clinical outcomes.

ACUTE MYELOID LEUKEMIA: GENERAL ASPECTS AND CLINICAL FEATURES

Acute myeloid leukemia (AML) is a clonal malignant hematopoietic disorder originating from genetic and molecular changes in normal hematopoietic stem cells. As a result, there is a production of immature cells that proliferate and accumulate in the bone marrow (named blasts) (Deschler and Lübbert 2006). These are non-functional cells that compete with and replace normal hematopoietic precursors, which classically leads to cytopenias and leukocytosis (Estey and Döhner 2006). Recent epidemiological data revealed an incidence of 4.3 cases per 100,000 with median age at diagnosis of 68 years and 24% of 5 years survival in United States (Shallis et al., 2019).

Similarly to most of the tumors, AML emerges from accumulation of somatic drivers and secondary mutations (Ley et al., 2013), and diagnosis is currently based on cytogenetic analysis and next generation sequencing (NGS) (Patel et al., 2012). Mutated genes related to signaling pathways and protein kinase activation, such as *FLT3*, are associated to aberrant activation and proliferation of leukemic blasts (DiNardo and Cortes 2016). *FLT3* has a special role in leukemogenesis by collaborating with other mutations, especially those involving the *NPM1* gene. Patients with *NPM1* mutation are stratified as favorable prognostic. However the risk stratification is changed and the clinical course is associated with early relapses when both mutations coexist (*FLT3* and *NPM1*) (Martelli et al., 2013; Papaemmanuil et al., 2016). Other important group of founder mutation are related to genes that regulate epigenetic DNA methylation and chromatin modification. *DNMT3A* mutation, for example, impairs and blocks HSC differentiation and *TET2* mutation impairs myeloid differentiation (Papaemmanuil et al., 2016). Major cytogenetic alterations are also described as responsible for AML development (such as chromosomal translocation, gene amplification, insertion or deletion) and these marks are also important for risk classification and treatment strategy (Short, Rytting, and Cortes 2018; Eisfeld et al., 2020).

AML presents as a heterogeneous disease that typically implicates bone marrow and peripheral blood (PB), and in several cases extramedullary tissues (Narayanan and Weinberg 2020). Pancytopenia (decrease in all blood cell lineages, i.e., anemia, neutropenia, and thrombocytopenia) arises from BM failure and occupation by leukemic blasts.

The common clinical presentation comprises weakness, fatigue, recurrent infections and bleeding disorders (bruise, ecchymosis, epistaxis) (Weinberg et al., 2019). In the leukemic process, fever occurs through 2 mechanisms: neoplastic fever, arising from clonal proliferation process, or due to neutropenia and subsequent recurrent infections. Extramedullary symptoms comprise hepatosplenomegaly, lymphadenopathy, and bone lesions (Rose-Inman and Kuehl 2014).

Coagulation disorders (thrombotic or hemorrhagic) are probably the most severe presentations of AML and can lead patients to death in about 7% of cases (Franchini et al., 2013). All types of AML can present with coagulation impairment although it commonly occurs in acute promyelocytic leukemia (Naymagon and Mascarenhas 2020). Leukostasis is another clinical presentation defined as symptomatic hyperleukocytosis, which is a medical emergency observed in 10–20% of AML patients. Although leukostasis can manifest itself through pathological changes in many organs, the main clinical and potentially fatal symptoms are related to the central nervous system (CNS) and lungs (Stahl et al., 2020).

Diagnosis is set with the presence of 20% blasts in BM or PB, except in a few cases where cytogenetic by itself is sufficient to confirm AML (Arber et al., 2016). Bone marrow aspiration is assessed for several diagnostic tools: morphological analysis, flow cytometry (to define subtypes of the disease), cytogenetic (to search for chromosomal alteration), and NGS (for gene mutations) (Jongen-Lavrencic et al., 2018).

The success of AML treatment is to bring the disease to remission (undetectable blats and molecular marks). There is a well established protocol divided into two stages basically: induction and consolidation therapy (De Kouchkovsky and Abdul-Hay 2016). Intensive induction chemotherapy comprises the first-line treatment and aims at maximum reduction of the leukemic blast count (<5% in BM). For patients eligible for intensive chemotherapy, standard chemotherapy is a combination of Cytarabine for 7 days and Daunorubicin or Idarubicin for 3 days (7 + 3 protocol), and this strategy is responsible for disease remission in more than 50% of patients of all ages since 1970 (Lichtman 2013; Döhner et al., 2017). An initial evaluation is required to determine treatment modalities, for example, patients with advanced age are not candidates for intensive induction chemotherapy. Alternative

options can also reflect good results in terms of overall survival and quality of life with hypomethylation-inducers combined with Venetoclax or Cytarabine low dose as recently published (DiNardo et al., 2020; Wei et al., 2020). Consolidation therapy is the second step after induction treatment and aims to improve remission achieved with initial treatment. Depending on risk stratification (Datoguia et al., 2018), the patient can be treated with high-dose chemotherapy or undergo to bone marrow transplant with curative intent (Shimomura et al., 2021).

After a period of remission, relapse episodes are frequent with more drug-resistant leukemic clones leading patients to death due to disease complications, and only 24% of patients achieve a 5-year overall survival (Hirabayashi et al., 2021). Unfortunately, combination of re-induction protocols with target therapies (for example, tyrosine kinase inhibitors) did not produce any longer survival in the patients (Daver et al., 2020).

A specific and distinct subtype of AML classified by the World Health Organization (WHO) and currently referred as APL with *PML-RARA* (O'Donnell et al., 2017) is the Ate promyelocytic leukemia (APL), also named as AML-M3 by the French-American-British (FAB) classification system (Warrell et al., 1993; Puccetti and Ruthardt 2004). It is a separate entity comparing to the others AML by presenting histological and clinical characteristics such as the morphology of Auer's rods and the propensity to exhibit disseminated intravascular coagulation (Mistry et al., 2003). From a therapeutic point of view, there is also divergence. While AMLs as a whole are treated with 7 + 3 protocol (cytarabine with daunorubicin/or idarubicin), patients diagnosed with low-risk APL receive induction treatment with arsenic trioxide plus all-trans retinoic acid (Burnett et al., 2015), which leads to disease remission with excellent results in terms of overall survival (Wang and Chen 2008). Thus, non-APL AMLs are the main current issue for the scientists.

In recent years, there has been a significant improvement in different features of AML's physiology with a focus on BM niches, and other drugs have been addressed to interfere with niche-specific cell populations, extracellular matrix components, varied growth factors, and cell adhesion molecules produced by niche cells. Researchers intend to impair leukemia development or progression by interfering in the bone marrow microenvironment, and ultimately improving the clinical outcomes (Zhang et al., 2019; Ladikou et al., 2020).

HEALTHY AND LEUKEMIC BONE MARROW NICHES

Raymond Schofield was the first one to propose the niche concept for the human hematopoietic system. The niches were described as areas in which the hematopoietic stem cells not only reside but may establish associations with other cells to modulate their behavior (Schofield 1978). Currently, niches are commonly defined as microenvironments that combine non-hematopoietic cells and the architecture of the bone marrow to promote self-renewal and differentiation of HSCs by providing invaluable and essential factors (Morrison and Spradling 2008; Szade et al., 2018).

Collectively, the components of the niches orchestrate the phenomenon of hematopoiesis. Significant progress in bone marrow imaging technologies has provided a better understanding of the molecular and cellular complexity of the bone marrow. However, compartmentalization of this space remains a challenge due to the anatomical and functional connectivity and the numerous and simultaneous interactions between the HSCs and the surrounding cells. Nevertheless, many publications divide the bone marrow, geographically, into vascular, endosteal, and reticular niches (Behrmann, Wellbrock, and Fiedler 2018). Although there are no anatomical boundaries to physically segregate the most diverse constituents of the marrow microenvironment, the niches have specific components that define their role on the homeostasis of hematopoietic stem cells.

In summary, the endosteal niche, more hypoxic, keeps the HSCs in a quiescent state, leading to a long-term storage of the hematopoietic cells and regulating the size of the stem and progenitor cells pool in the bone. Oppositely, the vascular niche, more vascularized and rich in oxygen, supports the progenitors that are actively proliferating and differentiating to form the various hematopoietic cell lineages. The reticular niche takes part in the regulation of stem cell factors from surrounding cells secretion. Additionally, there are other cell groups whose addressing within the marrow microenvironment still causes disagreement among scientists, but whose role in the regulation of hematopoietic cells is worthy of being analyzed in this review. Considering how complex the crosstalk among niches and HSC, it is expected how a disturbance of this regulatory and integrating network can lead to, or at least be related to hematological diseases such as leukemias (Ghobrial et al., 2018). Literature provides pieces of evidence about normal and leukemic bone marrow functional architecture, and the next paragraphs will elucidate how AML modifies and takes advantage from this altered BM microenvironment.

The Physiological Endosteal Niche

The endosteal niche, also entitled osteoblastic niche, is characterized by its proximity to the trabecular or cortical bone (Nilsson, Johnston, and Coverdale 2001; Behrmann, Wellbrock, and Fiedler 2018). It is well established that this compartment is filled with mesenchymal stromal cells (MSCs), osteoprogenitor cells, pre-osteoblasts, mature osteoblasts, osteocytes, and osteoclasts (Le, Andreeff, and Battula 2018).

The mesenchymal stromal cells, also called mesenchymal stem cells or bone marrow stromal cells, are multipotent stem cells capable of renewing themselves and have the ability to differentiate and to give rise to cells such as marrow adipose tissue, bone cartilage and occasionally myofibers. In the endosteal niche, these cells are surrounding pre-osteoblasts and osteoblasts of the bone-lining cell. However, MSCs have also been described in the perivascular region, around sinusoidal endothelial cells (Yusop et al., 2018). MSCs express key hematopoietic factors such as stem cell factor (SCF) and stromal cell–derived factor 1 (SDF-1). They are also sources of trophic factors modulating the immune system and inducing intrinsic stem cells to repair damaged tissues (Prockop 1997, 1998; Bianco et al., 2013;

Shafat et al., 2017; Yusop et al., 2018; Waclawiczek et al., 2020; Rodríguez-Fuentes et al., 2021).

The osteoblastic population derived from mesenchymal precursors constitutes the main cell group resident in the endosteum, playing key roles in bone development including the synthesis and mineralization of the extracellular bone matrix (Sugiyama and Nagasawa 2012). In addition, osteoblasts are related to self-renewal and maintenance of HSCs in an undifferentiated and quiescent stage (Le, Andreeff, and Battula 2018).

The cross-talk between osteoblastic cells and HSCs is mediated by several pairs of molecules such as soluble cytokines, cytokine receptors and adhesion molecules (Goulard, Dosquet, and Bonnet 2018). The duo Notch 1/Jagged 1 constitutes an important axis in the regulation of hematopoiesis. Several studies have demonstrated that activation of Notch 1 maintains the immature profile of hematopoietic precursors, both *in vitro* and *in vivo*. The physiological activation of this signaling occurs through the interaction between the transmembrane glycoprotein receptor Notch, present on the membrane surface of hematopoietic precursor cells, and one of its possible ligands such as Jagged 1, a transmembrane protein expressed notably by osteoblasts. The cellular response to this pathway comprehends an increased self-renewal and concentration of the pool of HSCs (Stier et al., 2002).

The noncanonical Wnt signaling axis represents another central pathway associated with the long-term maintenance of quiescent HSCs. Flamingo (Fmi) and Frizzled 8 (Fz8) compose a group of molecules that mediate the activation of this signaling. Fmi is a cadherin family molecule, a mediator of homophilic adhesive interaction between pre-osteoblasts and HSCs. Fz8, in turn, is a protein of seven transmembrane domains coupled to the Fmi that regulate intracellular calcium levels. Together, Fmi and Fz8 impair the nuclear translocation of NFAT, a transcription factor, preventing the expression of IFNγ, a significant molecule in the activation of HSCs (Kimura et al., 2006). Conversely, the canonical Wnt signaling (β-catenin-mediated) is associated with maturation of progenitors under bone marrow stress conditions, meanwhile the role of the canonical route on the maintenance of HSCs is still uncertain. In homeostatic conditions, pre-osteoblasts express noncanonical Wnt ligands and inhibitors of the canonical Wnt pathway. In consequence, the interaction between pre-osteoblasts and HSCs triggers noncanonical Wnt signaling and contribute to HSC quiescence by downregulation of IFNγ production and by antagonization of the canonical Wnt route (Sugimura et al., 2012).

Arai et al. (2004) revealed Tie2/Angiopoietin-1 signaling as another important pathway implicated in the quiescence of HSCs. Tie2 is a tyrosine-kinase receptor expressed in the HSC population, more precisely the long-term repopulating HSCs (LTR-HSCs). In contrast, angiopoietin-1 is a glycoprotein secreted by osteoblasts. Apparently, Ang-1 binding is succeeded by phosphorylation of Tie2, resulting in activation of the phosphatidylinositol 3-kinase (PI3-K)/Akt signaling pathway, which promotes the maintenance of the self-renewal capacity and protection against bone marrow stresses. Furthermore, the Tie2/Ang-1 axis has been shown to be critical for positive regulation of β1-integrin, which allows the maintenance of HSCs in a primitive phenotypic state by adhering to stromal cells (Arai et al., 2004).

Osteoblasts are known to secrete various proteins for the composition of the extracellular matrix (ECM), including collagen (COL) and fibronectin (FN), the main components of ECM of BM microenvironment (Hackney et al., 2002). Ang-1 promotes FN- and COL-mediated cell adhesion of $Tie2^+$ HSCs to ECM, and increased levels of Ang-1 stimulate an elevation in the adhesion of HSCs to the bone surface *in vivo*, which may be related to cell survival (Arai et al., 2004).

Upregulation of β1-integrin is also involved in the modulation of HSCs quiescence via the THPO/MPL (thrombopoietin/thrombopoietin receptor) pathway. MPL is the product of the transcription and translation of the c-MPL gene (Vigon et al., 1992). THPO, in turn, was identified as a primary cytokine, a regulator of megakaryocyte development and platelet production (Kaushansky 1995). However, recent studies have demonstrated the role of these molecules associated with self-renewal and quiescence of HSCs in adult BM. Evidence suggests that MPL^+ HSCs adhere to THPO-producing osteoblastic cells and THPO- or MPL-knockout mice show a decrease in the number of HSCs (Kimura et al., 1998). Experiments involving a neutralizing anti-MPL provoked a reduction in the proportion of quiescent HSCs and HSCs-niche interactions. Furthermore, an increase in the number of HSCs in G0 state was observed by exogenous THPO infusion *in vivo*. Altogether, these observations suggest that THPO/MPL signaling regulates quiescent HSCs and HSC-niche interactions on the endosteal surface and contribute to the hematopoiesis process (Yoshihara et al., 2007).

A study by Susan K. Nilsson et al. provided significant evidence that osteopontin (Opn) is an essential component in the regulation of HSCs. Osteopontin is a phosphorylated glycoprotein that has multiple domains (Chen et al., 1993). The binding of this molecule to its distinct receptors explains the most diverse cellular functions that osteopontin may modulate (Denhardt and Guo 1993). In the context of hematopoiesis, this protein is expressed at high levels by endosteal osteoblasts. Similar to the Tie2/Ang-1 and THPO/MPL axes, Opn-HSCs interaction occurs via β1-integrin. Experiments involving Opn-knockout mice reported a significant increase in HSCs cycling, suggesting that, under normal conditions of osteopontin expression, this molecule acts as a negative regulator of stem cell pool size, actively maintaining the quiescence of these cells by inhibiting the entry of HSCs into the cell cycle and, consequently, blocking cell proliferation (Nilsson et al., 2005; Stier et al., 2005).

A conflicting signaling mechanism is observed on the N-cadherin pathway. N-cadherin is characterized as a cell-cell adhesion molecule dependent on the presence of calcium íons, enabling homophilic interactions between neighboring cells (Song et al., 2002). Studies are suggesting that N-cadherin acts in the regulation of HSCs quiescence. According to the observations of these groups, the HSCs N-cadherin is anchored to the N-cadherin expressed in osteoblasts, and silencing of N-cadherin results in loss of HSCs long-term engraftment (Hosokawa et al., 2010). On the other hand,

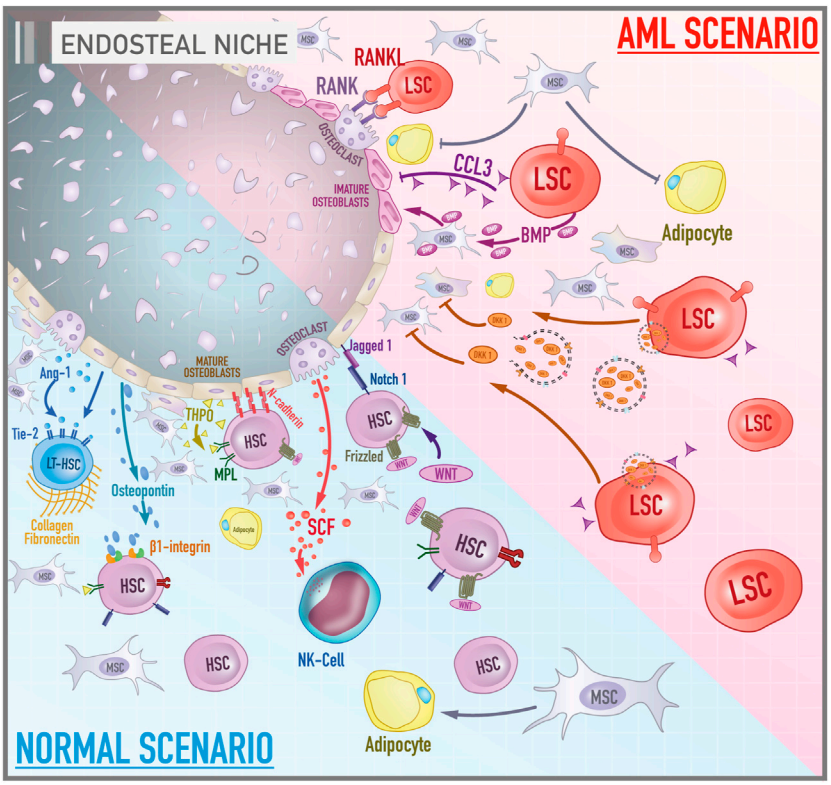

FIGURE 1 | Cellular and molecular components of bone marrow endosteal niche in both healthy and leukemic scenarios. The illustration contrasts the activities and components of the endosteal niche under physiological conditions and during the course of acute myeloid leukemia. In a normal scenario, signaling pathways such as MPL/THPO, Jagged 1/Notch 1, and Ang-1/Tie-2 promote the maintenance of hematopoietic cells in a primitive profile and their capacity for self-renewal. Osteopontin, via β1-integrin, acts as a negative regulator of stem cell pool size by blocking cell proliferation. N-cadherin constitutes a cell adhesion mechanism between HSCs and osteoblasts. In contrast, the role of the canonical Wnt signaling on the maintenance of HSCs is still debated. Collagen and fibronectin constitute the main components of the extracellular matrix of the bone marrow microenvironment. Mesenchymal stromal cells give rise to osteoblasts and adipocytes. In the AML scenario, leukemic stem cells secrete a variety of molecules such as BMP, DKK1, CCL3 that, together, lead to inhibition of adipogenic differentiation of MSCs, promotion of the osteogenic lineage, impairment of osteoblast functioning and an environment rich in immature osteoblasts. In addition, the RANK/RANKL signaling pathway leads to osteoclastogenesis and increased osteoclast survival.

another evidence indicates that N-cadherin-mediated HSCs-osteoblasts interactions are dispensable for the maintenance of hematopoietic cells in the endosteal surface (Kiel et al., 2009; Greenbaum et al., 2012). Experiments with deletion of encoding N-cadherin from HSCs revealed no change in the behavior of stem cells (Kiel, Radice, and Morrison 2007). Similar results were obtained with the deletion of N-cadherin expressed by osteolineage cells, revealing that the loss of interaction through this pathway did not have a significant effect on the status of the HSCs cycle. Consistent with these studies, it has been increasingly proposed that redundant pathways involving other cadherins such as E-cadherin, C-cadherin, and R-cadherin may compensate the loss of N-cadherin, enabling the maintenance of HSCs quiescent phenotype in the endosteum (Greenbaum et al., 2012).

Osteoclasts are also important cells on the endosteal surface. They are involved in the reabsorption of the mineralized bone matrix, but their role in the regulation of HSCs is controversial. There is evidence that osteoclasts, through secretion of proteolytic enzymes such as cathepsin K, promote the degradation of the endosteal niche components like stromal cell-derived factor 1 (SDF-1), stem cell factor (SCF), and osteopontin, leading to the mobilization of hematopoietic progenitor cells (Kollet et al., 2006). In contrast, one study elucidate the role of osteoclasts in the mobilization of hematopoietic progenitors by ablation of osteoclasts under administration of zoledronate in mice. Results revealed higher mobilization of hematopoietic cells confirming that osteoclasts are not required for the mobilization of HSC-derived progenitors (Winkler et al., 2010). But it is still clear that further studies are needed to clarify in detail the role of osteoclasts in hematopoiesis.

The Leukemic Endosteal Niche in Acute Myeloid Leukemia

The leukemic endosteal niche is marked by the loss of fine balance between bone formation and resorption, which may be associated with oncogenic events (**Figure 1**). A critical pathway in bone remodeling is RANK/RANKL. The receptor activator of nuclear factor kappa-B ligand (RANKL) is a membrane protein found on the surface of stromal and osteoblast cells, but which is also

expressed by blasts of AML patients. The receptor activator of nuclear factor kappa-B (RANK) is a transmembrane protein found on the surface of osteoclasts. Activation of this axis leads to osteoclastogenesis and increases the survival of osteoclasts (Schmiedel, Grosse-Hovest, and Salih 2013).

Battula et al. revealed that AML cells support leukemogenesis through switching from adipogenic to osteogenesis differentiation of MSCs by a bone morphogenetic protein (BMP)-dependent mechanism. Leukemic cells release BMP that activates Smad 1/5 signaling on MSCs to drive osteoblast lineage differentiation (Battula et al., 2017). Several studies have also reported that the leukemic endosteal niche is marked by osteoprogenitor cells and immature osteoblasts, delaying the maturation process of these cells and promoting deficient bone mineralization. Early-stage osteoblasts markers such as osterix, RUNX2, and Col1a1 are expressed in mesenchymal cells of AML patients. On the other hand, markers of mature osteoblasts such as osteocalcin are not found in AML-MSCs (Battula et al., 2017; Le et al., 2018). Frisch et al. brought a possible explanation for this phenomenon. The chemokine CCL3, also known as macrophage inflammatory protein 1α (MIP1α), secreted by AML cells appears to inhibit osteoblast function decreasing osteocalcin levels in the blood in murine AML model of AML patients (Frisch et al., 2012).

In fact, blocking the terminal differentiation of MSCs into mature osteoblasts seems to contribute to AML progression. Another interesting mechanism is the secretion of DKK1-containing exosomes by AML blast cells (DKK is a negative regulator of osteogenesis and normal hematopoiesis). And the pharmacological inhibition of DKK1 in AML murine model increased mice survival by impairing the progression of the disease. The inhibition of exosome release targeting Rab27a is also able to damage AML progression *in vivo* (Kumar et al., 2018). Together, these studies show how intricate and diverse the apparatus of AML is to manage the endosteal niche to create a proficuous environment for malignant cells.

In addition to the loss of fine control of endosteal physiology, various studies indicated that MSC can interfere with hematologic malignancies via inhibiting the proliferation of tumor cells. The most commonly accepted mechanism is that MSCs induce tumor cell cycle arrest (Fathi et al., 2019; Fathi et al., 2019). Li et al. (2018) showed that Umbilical Cord-MSCs (UC-MSCs) inhibited the proliferation of HL-60 and THP-1 (AML cell lines) by a mechanism dependent on cytokines release (Li et al., 2018; Fathi et al., 2019). Furthermore, *in vitro* studies have shown that bone marrow MSCs can support leukemia progenitor cell survival and provide resistance to cytotoxic therapies (Azadniv et al., 2020). It is reasonable to hypothesize that the MSC population could be associated with minimal residual disease maintenance with low rate of proliferation but high resistance to chemotherapy-induced apoptosis, and AML clone evolution would have important advantages to avoid MSC differentiation. More studies with stratification of sample patients (for instance undifferentiated AML, promyelocytic AML) are necessary to understand not only the clinical and prognostic relevance of the leukemia-endosteal niche relationship, but also to offer new perspectives of coadjuvant treatments and molecular markers.

The Physiological Vascular Niche

Whereas the osteoblastic niche offers a microenvironment for the maintenance of non-differentiated conditions of stem cells, the vascular niche, according to the literature, acts on their maturation. First of all, the architecture of the vascular niche provides a microenvironment with a higher concentration of oxygen and endocrine growth factors, which, in comparison to the endosteal, stimulates a distinct cellular behaviour. As a result, HSCs assume a proliferative and differentiating profile, which allows the proper generation and release of the hematopoietic populations to the peripheral circulation (Kopp et al., 2005).

The vascular niche (**Figure 2**), composed primarily of sinusoidal endothelial cells, pericytes, and unmyelinated Schwann cells (glial cells of the peripheral nervous system involving small axons of autonomous post-ganglion neurons), is located in a more centralized area of the bone marrow and can be characterized as an intertwined vessels with vascular arrangements subdivided into sinusoidal and arteriolar endothelium. Stromal cells and extracellular matrix work as surrounding support components (Nombela-Arrieta et al., 2013). This dense vascular network is responsible for the renewal of nutrients, oxygenation of the medullary tissue, and regulation of the entry and exit of cells, such as late plasma cells coming to BM to occupy specific locations and the newly differentiated granulocytes. Blood vessels, in general, are made up of different cell types. The inner layer of the vessel is composed of endothelial cells (ECs), which are covered by perivascular cells called pericytes. These are incorporated into the subendothelial basement membrane and connect the ECs to smooth muscle cells that cover large vessels such as arteries and veins (Sivaraj and Adams 2016). However, bone marrow vascularization, in particular, is mainly formed by a sinusoidal endothelium composed of a single layer of ECs (Tavassoli 1981). This non-stratified endothelial arrangement allows blood cells to pass through a sinusoidal wall easily, supporting transendothelial migration of hematopoietic cells from the medullary tissue into the bloodstream. Thus, the role of the vascular niche includes not only the regulation of HSCs differentiation and proliferation but also the immediate release of the progeny of these cells into the bloodstream (Wright et al., 2001; Kopp et al., 2005).

More specifically, the bone marrow vascularization is configured in a special way: the arteries align longitudinally to the perimeter of the diaphysis of long bones, branching into small arterioles to infiltrate the bone marrow and, finally, forming a network capillary, which is divided into two capillary subtypes, called H and L, which can be distinguished according to their structure, function and surface marker (Kusumbe, Ramasamy, and Adams 2014; Kusumbe et al., 2016; Sivaraj and Adams 2016). In the capillary network, blood flows through type H capillaries, located in the metaphysis, which are connected to the mentioned small arterioles and, later, it flows towards the more permeable type L sinusoidal capillaries, located in the transition between the metaphase and the diaphysis (Kusumbe, Ramasamy, and Adams

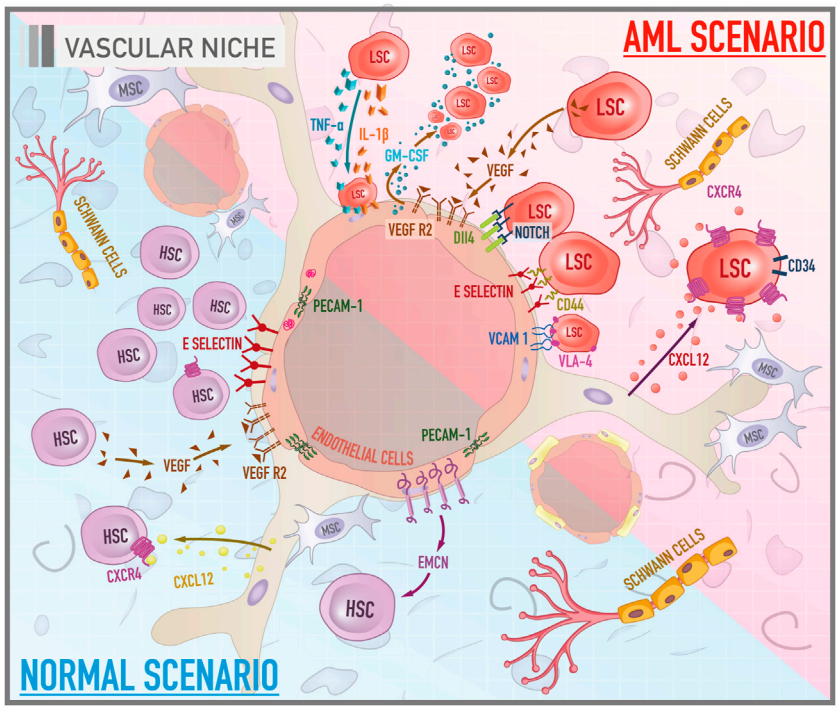

FIGURE 2 | Cellular and molecular components of bone marrow vascular niche in both healthy and leukemic scenarios. The illustration compares the functioning of the vascular niche under a normal context and during leukemogenesis. In a physiological scenario, HSCs acquire a proliferative profile and differentiated phenotype. PECAM-1 stabilizes the endothelial layer. EMCN, in turn, is a potential molecule related to angiogenesis. Another pathway associated with vessel morphogenesis is the VEGF/VEGFR. E-selectin acts as a promoter of HSCs proliferation. In the AML scenario, there are important axes that mediate the anchorage of leukemic stem cells (LSCs) to endothelial cells such as E-selectin/CD44 and VCAM-1/VLA-4. Signaling pathways such as VEGF/VEGFR and Notch/Dll4, in turn, are related to tumor angiogenesis. GM-CSF is a molecule with mitotic properties on LSCs, secreted by VEGF-stimulated endothelial cells. Cytokines, especially IL-1 beta and TNF-alpha, secreted by LSCs promote the attachment of these cells to the endothelium.

2014; Ramasamy et al., 2014). These capillaries can be differentiated by the molecules that are expressed on their surface and by the cells that surround them. Type H capillaries, surrounded by osteoprogenitors, express high levels of CD31 and endomucin. On the other hand, type L capillaries, surrounded by leptin receptor $(LEPR)^{+}$ and CXCL12-abundant reticular (CAR) cells, exhibit low levels of CD31 and endomucin on their surface. Thus, these capillaries form a dense and overly branched sinusoidal network within the medullary cavity, responsible for regulating the HSCs compartment (Sugiyama et al., 2006; Ding et al., 2012). Finally, at the exit of the bone marrow, the capillaries drain into a wide central vein that passes through a massive, calcified bone matrix towards the periphery (Kusumbe et al., 2016).

The deficiency of direct arterial supply contributes to a more hypoxic diaphysis, while the metaphysis, marked by the presence of capillaries, is configured as a better oxygenated region. In consequence, this vascular configuration contributes to the formation of metabolically distinct microenvironments, playing different roles in the regulation of hematopoietic cells. Hypoxia is known to act as an essential regulator of HSCs dormancy (Eliasson and Jönsson 2010; Takubo et al., 2010). Low oxygen levels can affect cellular energy metabolism, redirecting it from oxidative phosphorylation to cytoplasmic glycolysis (Semenza 2007). Hematopoietic cells residing in the endosteal niche have a predominance of glycolysis as energy metabolism, a less efficient process to obtain ATP molecules compared to oxidative phosphorylation prevalent in HSCs residing in the vascular niche. As a consequence, HSCs are induced to assume a dormant state for energy saving (Zhang and Sadek 2014). Another effect of this energy redirection is the lower intracellular production of reactive oxygen species (ROS). The maintenance of HSCs in a quiescent state depends on the careful management of ROS levels. Excessive levels of these substances can lead to damage to the genetic material and its products, which is associated with the development of leukemias, marked by genomic instability (Sallmyr, Fan, and Rassool 2008).

Similar to the endosteal niche, the vascular one also has molecules and signaling pathways that are essential for maintaining the architecture of the microenvironment and regulating HSCs behavior. The platelet endothelial cell adhesion molecule (PECAM-1), for example, also known as cluster of differentiation 31 (CD31) is a transmembrane glycoprotein that forms a significant part of the intercellular junctions of the endothelium and stabilizes the endothelial cell monolayer. This protein belongs to the immunoglobulin family and its properties suggest that it is involved in leukocyte transmigration, angiogenesis, and integrin activation

(Hashimoto et al., 2012; Kim et al., 2013; Lertkiatmongkol et al., 2016).

Whether in the organogenesis of bone marrow or in the homeostatic response to several stimuli, angiogenesis is a physiological process co-regulated by osteoblasts and performs an important function in the vascular niche (Schipani et al., 2013).

It is a process that consists of the formation of new vessels that grow from existing vessels through branched morphogenesis, which is a fundamental event for many physiological and pathological processes, such as embryonic development, wound healing, tumor growth, and metastasis (Carmeliet 2005). Several highly orchestrated stages are involved in angiogenesis. First, there is the degradation of the cell matrix by endothelial cells mediated by the release of metalloproteinases, followed by the migration, proliferation, and alignment of these cells. Therefore, the lumen is established and, finally, the anastomosis of the newly formed vessel with adjacent vascular structures occurs (Conway, Collen, and Carmeliet 2001). These phases are regulated by a variety of soluble growth factors as well as cellular interactions.

One of the main regulators of angiogenic responses is the vascular endothelial growth factor (VEGF), a signal protein that acts through the VEGF receptor 2 (VEGFR2) and activates endothelial cells by signaling cascades that allow subsequent branching of the vessel (Leung et al., 1989). The downstream intracellular signaling triggers p42/44 MAPK and PI3K/Akt, which promotes the migration, proliferation, survival and differentiation of ECs (Gerber et al., 1998; Kobayashi et al., 2010). Ang-1, a ligand also derived from pericytes, inhibits the apoptosis of ECs, thereby promoting the regulation of HSCs (Dimmeler and Zeiher 2000). Another molecule with a potential role in angiogenesis is endomucin-1 (EMCN). Experiments involving the modulation of the levels of this glycoprotein, present in the venous and capillary endothelium, showed that EMCN knockdown reduces the migration and proliferation of endothelial cells associated with the suppression of tube formation as well as a reduction in the levels of phospho-VEGFR2, phospho-ERK1/2, and phospho-p38-MAPK, suggesting suppression of the signaling pathway by VEGF. On the other hand, overexpression of EMCN had a positive impact on vessel morphogenesis (Park-Windhol et al., 2017).

The characterization of the vascular microenvironment as a proliferative niche for HSCs is consistent with studies that indicate E-selectin, an adhesion molecule expressed exclusively by endothelial cells, as a promoter of the proliferation of HSCs. Experiments involving administration of an E-selectin antagonist or observation of E-selectin knockout mice reported improvement in the dormant state of HSCs as well as potentiation of the self-renewal capacity, strengthening the idea that E-selectin plays a central role in the proliferation of hematopoietic cells (Winkler et al., 2012).

The Leukemic Vascular Niche in Acute Myeloid Leukemia

Studies have shown that the vascular microenvironment is consistently altered in the evolution of acute myeloid leukemia (**Figure 2**). Also, it seems that blast cells have the ability to create conditions that favor their proliferation and survival, which may have important implications for the pathophysiology of leukemia (Wang and Zhong 2018). In fact there is a cross-talk between endothelial cells and leukemic cells through autocrine and paracrine stimuli (Cogle et al., 2014). Stucki et al. demonstrated a synergy of adhesive receptors and cytokines, mainly IL-1 beta and TNF-alpha, secreted by blast cells, to produce the attachment of AML blast cells to the endothelium (Stucki et al., 2001). Important axes that mediate the anchorage of leukemic stem cells (LSCs) to endothelial cells most documented in the literature are CD44/E-selectin and VLA-4/VCAM-1 (Cavenagh et al., 1993). As previously mentioned, E-selectin is an adhesive molecule highly expressed by endothelial cells that can bind to CD44, a glycoprotein widely expressed on the membrane surface of LSCs. The vascular cell adhesion protein 1 (VCAM-1), a member of the immunoglobulin superfamily, is an endothelial ligand for very late antigen-4 (VLA-4), belonging to the β1 subfamily of integrins, expressed by leukemic cells. Together, these adhesive interactions can enable the migration of LSCs through the vascular wall and result in the establishment of disease outside the bone marrow. Some promising studies have revealed that the antagonization of E-selectin and VCAM-1 increases myeloblast mobilization and chemosensitivity, compromising their refuge in the protective niche and, consequently, their survival (Cavenagh et al., 1993; Barbier et al., 2020).

Another key component that is deregulated in this leukemic microenvironment is angiogenesis. It is well established that, although angiogenesis is considered a physiological phenomenon, it is an essential factor for the viability and development of solid tumors (Falcon et al., 2016). Because of this, the angiogenic phenomenon was initially underestimated in liquid tumors such as AML, which does not have a compact structure. Nevertheless, the formation of vessels is, in fact, crucial for, not only the progression of AML but also for its establishment in extra medullary sites. A parameter for the evaluation of vascularization in leukemic patients is the microvascular density of the bone marrow (MVD). Clinical data revealed that the bone marrow biopsy of AML patients compared to healthy donors has an increased number of sinusoidal blood vessels (Padró et al., 2000). Thus, the degree of MVD might be used as a prognostic marker, making it possible to identify the risk of recurrence and estimate the overall survival of AML patients (Kuzu et al., 2004). Important signaling pathways such as VEGF/VEGFR and Notch/Dll4 (Delta-like ligand 4) are implicated in tumor angiogenesis. Zhang et al. (2013) revealed that untreated AML patients had higher levels of VEGF, VEGFR2, Notch1, and Delta-like ligand 4 (Dll4) compared to healthy donors. Another observation was that the activation of Notch/Dll4 pathway is associated with a poor prognosis. Also, an *in vitro* experiment pointed to a rise in LSC-mediated endothelial cell proliferation that was related to activation of Notch/Dll4 signaling, which led to an increase in metalloproteinase levels, enhancing endothelial cells mobilization and formation of new blood vessels (Zhang et al., 2013). The impact of the interaction between LSCs and endothelial cells on proliferation is mutual. Fiedler et al. showed through a culture of endothelial cells in the presence of the pro-angiogenic factor VEGF led to a dose-dependent increase in granulocyte-macrophage colony-stimulating (GM-CSF),

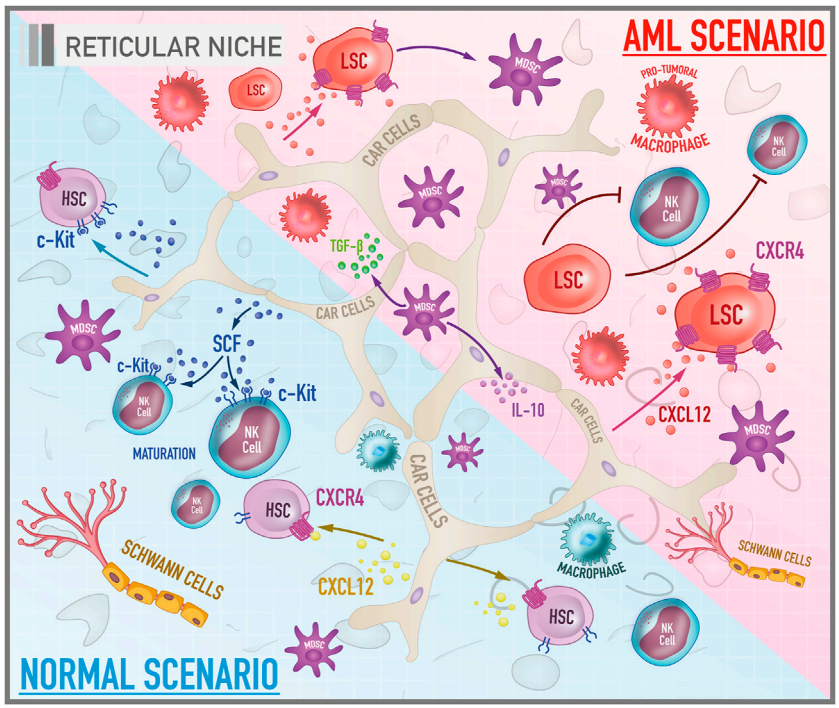

FIGURE 3 | Cellular and molecular components of bone marrow reticular niche in both healthy and leukemic scenarios. The illustration shows the reticular niche which is characterized by being a transitional niche between the endosteal and the vascular ones, responsible for the survival, homing and maintenance of HSCs and other hematopoietic progenitors in a proliferative, but undifferentiated profile. Under physiological conditions, the most important pathways are CXCL-12/CXCR-4 and SCF/c-Kit. In the AML scenario, the CXCL-12/CXCR-4 signaling plays a role in the trafficking and infiltration of leukemic cells into the protective niches of the bone marrow.

secreted by endothelial cells and known as a mitogen for AML cells (Fiedler et al., 1997).

The Physiological Reticular Niche

Although it is frequently described as containing only two niches (endosteal and vascular), the literature also elucidates the emerging role of a third microenvironment in the bone marrow: the reticular niche. However, there is little documented information about this one. This environment is associated with the maintenance of HSCs in a proliferative profile, similar to the vascular, but in an undifferentiated state, analogous to the endosteal, configuring itself as a transitional niche (**Figure 3**). Mesenchymal stromal cells, which include CXCL12-abundant reticular (CAR) cells and Nestin-expressing cells, seem to make up the predominant cell group set in this microenvironment (Nagasawa et al., 2011). These cells constitute the dominant stromal cells in the medullary cavity and are located adjacent to the sinusoidal endothelial cells (Weiss 1976; Sugiyama et al., 2006). A study that investigated the location of HSCs and potential cell niches in association with these cells revealed that most HSCs are in contact with CAR cells, responsible for the production of the most essential hematopoietic cytokines such as CXCL12 and SCF (Sugiyama et al., 2006). Not only HSCs, but precursors of B lymphocytes, plasma cells, plasmacytoid dendritic cells, and NK cells also establish interactions with the components of the reticular niche, suggesting that CAR cells may also function as a niche for immune cells (Tokoyoda et al., 2004; Kohara et al., 2007; Noda et al., 2011). Nestin-expressing cells, in turn, are associated geographically with adrenergic nerve fibers and are known to express genes related to the maintenance of HSCs. Depletion of Nestin^{+} MSCs was related to a significant reduction in HSCs pool in the bone marrow and homing of HSPCs (Méndez-Ferrer et al., 2020).

CAR cells are mesenchymal progenitors with the potential to differentiate into adipocytes and osteoblasts for their ability to express adipogenic and osteogenic genes such as PPARγ, runx2, and osterix (Osx). In addition, these cells preserve the proliferation of HSCs and lymphoid progenitors. An experiment involving selective ablation of CAR cells by the administration of diphtheria toxin in an *in vivo* model revealed that the conditioned deletion of these cells results in a decrease in the number, size, and dormancy potentiation of HSCs, as well as an increased expression of genes related to differentiation in a myeloid lineage (Omatsu et al., 2010). Another effect described was the general reduction in CXCL12 and SCF levels. Although other cell groups also produce these cytokines, the study revealed that CAR cells are primarily responsible for supplying these molecules. The potential for differentiation in adipogenic and osteogenic lines was also compromised, as well as for proliferation of erythroid and B cell progenitors, dependent on the support provided by the adipo-osteogenic progenitors (Omatsu et al., 2010). Together,

these observations reflect the impact of CAR cells in promoting bone marrow homeostasis.

Consistently with the other described niches, the reticular niche also has important molecule pairs that make possible the maintenance of HSCs in a proliferative, but undifferentiated state. The CXCL12/CXCR4 axis is an example. CXCL12, also known as a factor derived from stromal cells (SDF-1), is a chemokine with chemotactic properties, whose physiological receptor is CXC-chemokine 4 (CXCR4), also known as cluster of differentiation 184 (CD184), a protein with a structure formed by seven transmembrane domains coupled to a heterotrimeric G protein (Baggiolini et al., 1997). The signaling provided by this axis results not only in homing of HSCs, but also promotes the development of the immune system cells such as B lymphocytes (Tokoyoda et al., 2004; Nagasawa 2006). Another important axis of the reticular niche is the SCF/c-Kit axis. Stem cell factor (SCF) is a cytokine that can be soluble or transmembrane. Its c-kit receptor, also known as the cluster of differentiation 117 (CD117), is a tyrosine kinase receptor expressed on the surface of HSCs and hematopoietic progenitors. The binding of SCF to its respective receptor causes c-kit to homodimerize and autophosphorylate in tyrosine residues, triggering a signaling cascade, being able to activate pathways such as RAS/ERK, PI3-kinase, and JAK/STAT (Rönnstrand 2004). The secretion of SCF has similar effects to CXCL-12 such as increased survival, homing, and maintenance of HSCs and other hematopoietic progenitors (Kent et al., 2008).

The Leukemic Reticular Niche

Among the various soluble factors secreted by microenvironment cells that regulate AML cells, the chemokine CXCL12 is one of the most important. Mesenchymal stromal cells, in particular CAR cells, along with having a notable capacity to differentiate into other cell groups, secrete high levels of CXCL12, making them an interesting and potential therapeutic target in the AML scenario (**Figure 3**). In physiological conditions, this chemokine is involved in the induction and regulation of trafficking in leukocytes by chemotaxis. However, the interaction of CXCL12 with its CXCR4 receptor appears to be implicated as a critical mediator of the association between stromal and leukemic cells (Peled and Tavor 2013). A study by Möhle et al. showed that leukemic $CD34^+$ blasts from AML patients have considerable amounts of functionally active CXCR4 on their surface what may play a role in regulating the trafficking of malignant cells (Möhle et al., 1998). Moreover, it appears that the CXCL12/CXCR4 axis constitutes a critical signaling pathway for the infiltration of leukemic cells into the protective niches of the bone marrow which, under normal conditions, are restricted to hematopoietic cells (Wang and Zhong 2018). Therefore, it is essential to understand the factors that lead to expression of the CXCL12 receptor by leukemic blasts. It is well established that the mutation in the FTL3 gene promotes the activation of CXCR4 signaling in AML cells (Zeng et al., 2009). Another factor that induces the expression of this receptor is the stress induced by chemotherapy. A study by Spoo et al. showed that low expression of CXCR4 in cells of AML patients correlated with a longer relapse-free and longer overall survival compared to patients with intermediate and high levels. Thus, the expression of CXCR4 might be related to the migratory and adhesive behaviour of leukemic cells among the three BM niches, and could be considered as a prognostic predictor for AML patients (Spoo et al., 2007).

OTHER CELLS INVOLVED IN HEALTHY AND LEUKEMIC BONE MARROW.

There are also non-permanent resident cells on the bone marrow microenvironment that migrate and interact with the niches in healthy conditions or during pathological processes such as tumors. They are also reported in and associated with some aspects of physiopathology or immune response to AML.

Natural Killer Cells

Natural killer cells (NK) are a type of cytotoxic lymphocytes that exhibit an innate and adaptive immune response against tumor cells, including leukemic cells. The bone marrow is the main site of generation and maturation of NK cells in adulthood. NK cells are formed from NK cell progenitors (NKPs) that originate from Common Lymphoid Progenitors (CLPs) based on their interactions with stromal cells, cytokines, growth factors, and other soluble molecules that form a microenvironment characterized by presence of SCF, FLT3L, and IL-7 (Vacca et al., 2011; Di Vito, Mikulak, and Mavilio 2019).

Many strategies used by AML cells to escape the immune system response have been identified, amongst them, the increased expression of inhibitory molecules on the membrane and the secretion of immunosuppressive cytokines, thus creating an immunosuppressive microenvironment that avoids recognition mediated by NK cells, triggering tumor immune escape (Barrett and Le Blanc 2010; Baragaño Raneros et al., 2019).

This tumor immunosuppressive microenvironment results in decreased activity of NK cells by several mechanisms including the defective NK maturation, lysis inhibition by immune checkpoints (PD-1, TIM3, and TIGIT expressed on the cell surface of NK cells, recognize their ligands, which are expressed on the cell surface of AML cells, and as a consequence, activating pathways involved in NK cell regulation are inhibited, promoting NK cell anergy) and modulation of the NK receptor repertoire (NK functions are exhaustively regulated by the balance between activating and inhibitory receptors, however, during AML development the repertoire of NK cells is modified, reducing the level of expression of activating receptors and increasing that of inhibitory receptors) (Chiossone et al., 2017; Baragaño Raneros et al., 2019).

The literature does not make it clear whether NK inhabit the BM and interact with the niches, but possibly the NK migration and interactions are not restricted to one specific site. The ability to perform immune surveillance is conditioned by the expression of a repertoire of inhibitory/activator receptors, chemokine receptors and adhesion molecules that work together to drive NK migration. In a multiple myeloma study, authors demonstrated that CXCR3-and CXCR4 are important receptors to guarantee NK infiltration into bone marrow, and the absence of this signaling is sufficient to decrease NK infiltrating cells. These data are important to sustain the hypothesis of the presence of NK in endosteal, vascular and reticular niches since all of them offer such chemoattractant signals, but also

to suggest that any disturbance in the BM microenvironment promoted by AML scenario is able to difficult NK immune surveillance (Raulet, Vance, and McMahon 2001; Morris and Ley 2004; Ponzetta et al., 2015).

Myeloid-Derived Suppressor Cells

Myeloid-Derived Suppressor Cells (MDSC) are a heterogeneous population of myeloid cells in the early stages of development with an immunosuppressive profile that negatively regulates immune responses and collaborates to tumor development. The literature describes three MDSC subpopulations: the neutrophilic (PMN-MDSC), the monocytic (M-MDSC), and the immature (i-MDSC) (Talmadge and Gabrilovich 2013; Solito et al., 2014; Bronte et al., 2016; Wei et al., 2016; Ibáñez-Vea et al., 2018). These three rare populations can be present in bone marrow, peripheral blood, lymph nodes, spleen, and tumors. However, an altered hematopoietic differentiation pathway leads to an exacerbated production, expansion, and accumulation of these cells as a consequence of pathological conditions such as chronic inflammation, infections, stress, and cancer (Solito et al., 2014; Damuzzo et al., 2015; Bronte et al., 2016; Heine et al., 2017).

In general, MDSC population can suppress specific antitumor adaptive immune responses, increase the growth of already established tumors through citokines secretion (such as IL-10, TGF-β, IL-6, and IL-1β), and provide a spark for the onset of oncogenesis in the inflammatory microenvironment (Kusmartsev and Gabrilovich 2006; Wahl et al., 2006; Gabrilovich and Nagaraj 2009; Ugel et al., 2015; Yaseen et al., 2020; Weber et al., 2021).

Clinical studies have already shown that MDSC is accumulated in the peripheral blood and BM of AML patients comparing to healthy donors (Pyzer et al., 2017). Furthermore, the AML scenario promotes the expansion of the immunosuppressive population of MDSC in the BM (Taghiloo and Asgarian-Omran 2021) and there is a relevant positive correlation between increased MDSC population and poorer prognosis of patients. In fact, the detection of minimal residual disease is directly associated with the presence of MDSC population (Sun et al., 2015).

Although MDSC are not reported occupying a specific site of BM, they are potentially distributed through the three niches following and responding to the blasts presence, and offering back pro-leukemic support.

M1 and M2 Macrophages

There are resident and monocyte-derived macrophages in the BM, however there is no consensus concerning the specifically niche localization. They have been described to have the ability to adapt to the environment and play roles in maintaining homeostasis and responding to inflammation and infection. Under normal conditions, macrophages have the main function of responding to pathogens and modulating the adaptive immune response through the processing and presentation of antigens. More specifically, M1 macrophages (classically activated), are known to promote Th1 responses, secrete high levels of pro-inflammatory cytokines such as IL-1-beta, TNF-alpha, IL-12, IL-18, and IL-23, they are important in defense against bacterial infections, in addition to presenting high production of reactive oxygen and nitrogen species and causing tissue damage. On the other hand, M2 macrophages (alternatively activated) are described as immunoregulatory and promotors of tissue remodeling. They secrete large amounts of IL-10 and low levels of IL-12 and also secrete CCL17, CCL22, and CCL24 (Gentek et al., 2014; Varol et al., 2015; Wynn and Vannella 2016; Kaur et al., 2017; Kloc et al., 2019; Seyfried et al., 2020).

In cancers, monocytes are recruited by neoplastic and altered stromal cells and differentiate to tumor-associated macrophages (TAM). TAM is activated by an abnormal malignant microenvironment which contributes to tumor progression through promoting genetic instability, nurturing cancer stem cells, supporting metastasis, and regulating adaptive immunity. Depending on the factors offered by the microenvironment, TAM can acquire an M1 (anti-tumorigenic) or M2 (pro-tumorigenic) phenotype. It has been described that TAM preferentially acquires an M2 phenotype, which favors tumor growth, promotes cell survival, proliferation, dissemination, and metastasis (Mantovani et al., 1992; Mantovani et al., 2002; Solinas et al., 2009; Galdiero et al., 2013; Galdiero et al., 2013; Haas and Obenauf 2019; Li et al., 2020).

In leukemia, these cells are currently leukemia-associated macrophages (LAM) (Li et al., 2020). Although the mechanisms are not yet elucidated, Al-Matary et al. (2016) suggest that the LAM protect the AML cells from apoptosis induced by chemotherapy treatment with cytarabine (Al-Matary et al., 2016; Li et al., 2020). Moreover, Yang et al. (2018) observed that bone marrow LAM differentiated with M1 characteristics, while splenic LAM evolved mostly with M2 in AML models (Yang et al., 2018; Li et al., 2020).

Adipocytes

In the bone marrow, adipocytes constitute a cell group derived from MSC. Although many authors describe these cells close to the endosteal surface, these cells can occupy the entire interior of the medullary cavity, covering up to 70% of the bone marrow in human adults. Nevertheless, the number of these cells may vary according to nutritional conditions and cytotoxic stress. Further studies are needed to confirm the precise location of these cells in the bone marrow and their behavior under physiological and also AML context (Rosen et al., 2009; Reagan and Rosen 2016; Méndez-Ferrer et al., 2020).

In contrast to the idea of being a trivial stock of fat, adipocytes act as regulators of medullary homeostasis by the secretion of molecules such as adipokines (Horowitz et al., 2017). Although it has been described in the literature that chemotherapy can induce adipogenesis with consequences for the bioavailability of drugs in the medullary cavity, the role of adipocytes in leukemogenesis remains controversial (Sheng et al., 2016). Some studies have been done to elucidate the importance of adipocytes to AML development. The research line of Boyd's group revealed that myelo-erythropoiesis is interrupted in acute myeloid leukemia by the disruption of the adipogenesis (Boyd et al., 2017). In the same way, Battula et al. (2017) showed interruption of the differentiation of mesenchymal cells in the adipogenic lineage in the AML (Battula et al., 2017). Alternatively, Shafat's studies provide evidences in the opposite direction: adipocytes support AML blasts *in vitro* and *in vivo* by transference of fatty acids to the malignant cells, interfering with metabolism and increasing survival and proliferation. The study also showed that co-culture of adipocytes with leukemic blasts increases the fatty acid-binding protein-4 (FABP4) messenger RNA levels. Interestingly, FABP4 blockage reversed

the protection of AML cells mediated by adipocytes (Shafat et al., 2017). Accordingly, Tabe and colleagues raised evidence that the AML cells-adipocytes interactions reduces apoptosis of the monocytic cells by increasing fatty acid β-oxidation (FAO) and expression of genes such as PPARγ, FABP4, CD36, and BCL2. Consequently, the pharmacological inhibition of β-oxidation of fatty acids led to the apoptosis of AML cells. Such observation suggests that the disruption of the oxidation of these energetic molecules can act as a therapeutic strategy in controlling AML progress (Tabe et al., 2017). The association between FAO and leukemic cells was also investigated by Lee et al. (2015), who identified avocatin B, a FAO inhibitor, as a compound with cytotoxic activity in AML cells (Lee et al., 2015). An even more recent study compared adipogenic potential of MSCs derived from healthy donors or AML patients. AML-MSCs presented improved ability to support the survival of leukemia progenitor cells through a mechanism dependent on decreased expression of SOX9 (Azadniv et al., 2020). Taken together, literature give to BM resident adipocytes an important role in normal and AML scenario, what confirm them as interesting cellular targets for new therapies.

Sympathetic Neural Cells

Although sympathetic neural cells are poorly described in the literature compared to other cells in the bone marrow microenvironment, these cells act on the regulation of the HSCs compartment and, indirectly, is implicated in the AML modulation. A study by Spiegel et al. (2007) revealed that $CD34^+$ cells express beta-2 adrenergic and dopamine receptors and their mobility and proliferation can be regulated by adrenaline and noradrenaline (Spiegel et al., 2007). Additionally, unmyelinated Schwann cells seem to express molecules that activate the latent form of TGF-β, which is produced by a diversity of cells, impacting the maintenance and repopulation capacity of HSCs. Consequently, autonomic nerve denervation leads to glial cell death, inducing rapid loss of HSCs (Yamazaki et al., 2011). In myeloproliferative neoplasms, the Schwann cells and $Nestin^+$ MSCs are reduced due to neural damage of the bone marrow mediated by IL-1β, produced by malignant cells, which resulted in an expansion of deffective mesenchymal stem and progenitor cells. Pharmacological treatment with β3-adrenergic agonists reduced $Nestin^+$ MSCs loss and disrupted myeloproliferative neoplasm evolution (Arranz et al., 2014). Thus, sympathetic neural cells clearly work regulating MSCs response, but there is no robust evidence to confirm consequences for AML development.

THE EXTRAMEDULLARY ACUTE MYELOID LEUKEMIA MICROENVIRONMENT

Extramedullary acute myeloid leukemia (eAML) is defined as a tumor infiltration composed of myeloid blasts outside bone marrow, what includes both hematopoietic (spleen, liver) and non-hematopoietic tissues (skin, gums, and central nervous system) (Comings et al., 1965; Byrd et al., 1995; Shallis et al., 2019). eAML may occur simultaneously with or before bone marrow presentation, and also during relapses (with and without prior allogeneic stem cell transplant) (Solh et al., 2016). Around 0.8–2% of AML cases will develop extramedullary manifestation (Movassaghian et al., 2015; Goyal et al., 2017). Most cases are related to *de novo* AML but can also appear in acute blastic transformation of myelodysplastic syndrome, myelodysplastic/myeloproliferative neoplasms or myeloproliferative disorders (Traweek et al., 1993). Clinical presentation in the skin or gums is often concomitant to bone marrow involvement with isolated sites in lymph nodes, intestine, mediastinum and orbit (Neiman et al., 1981). The three most common sites of presentation are connective/soft tissues (31.3%), skin/breast (12.3%), and digestive system (10.3%) (Goyal et al., 2017). The prognostic impact of extramedullary disease in AML is widely discussed in literature and some authors defend that extramedullary disease brings an independent prognostic effect, others describe as inferior outcomes (Shimizu et al., 2013).

The tissue architecture of eAML lesions is simpler comparing to the bone marrow niches already described in this review. The leukemic infiltrate is histologically characterized by hyperleukocytosis with a monotone accumulation of myeloblasts/monoblasts that interact closely with stromal cells (Goyal et al., 2017; Shallis et al., 2021).

There is extent information regarding how mesenchymal stromal cells regulate AML inside bone marrow, what includes cytokine/chemokine secretion, microRNA-containing exosomes release and cell-cell contact by gap junctions, for example (Barrera-Ramirez et al., 2017; Forte et al., 2020; Kouzi et al., 2020). Because their presence in a variety of non-hematopoietic tissues in the body, they potentially would exert an additional role in extramedullary infiltration (Carter et al., 2016), but such mechanisms was not explored in the literature.

Although it has been reported an angiogenic process during eAML lesions constitution (Piccaluga et al., 2018), it remains unclear if AML blast cells establish some functional crosstalk with endothelial cells similarly to the phenomena observed in vascular niches in the bone marrow.

Chemotaxis and cellular adhesion seems to be critical for the extramedullary infiltration. Notwithstanding the equivalent expression of CD56 in leukemic cells from patients with or without eAML, some evidences support that CD56, a glycoprotein responsible for cell-cell adhesion, could promote the attachment of leukemic blasts to adipose, skeletal muscle, gastrointestinal, testicular, and brain tissue. In addition, although there was not confirmed evidence of a cause-effect relationship, it is clarified that overexpression of CD11b (β2-integrin member macrophage-1 antigen) in myelomonocytic and monocytic blasts positively correlates to eAML episodes (Ganzel et al., 2016; Shallis et al., 2021). Further contribution have been provided by studies involving skin eAML biopsies from pediatric patients that presented overexpression of CXCR4 and CXCR7, which are bone marrow specific homing chemokine receptors and whose connection with skin CXCL12 may result in the evolution of skin eAML (Faaij et al., 2010).

A fibrotic pattern with collagen deposition is also reported in the eAML sites (Cunningham et al., 2019). In other cancer models and tissues, fibrosis is associated to the frequency and activation of MDSC and M2 macrophages (Hammerich and Tacke 2015; Tang et al., 2019). A study by Hui Sun and colleagues showed that MDSC levels positively correlated with extramedullary infiltration in *de novo* AML patients (Sun et al., 2015). If eAML present similar mechanisms, the axis MDSC-M2 should

TABLE 1 | Studies registered on ClinicalTrials.gov investigating bone marrow niches-related molecular targets in AML.

ClinicalTrials.gov Identifier	Stage	Intervention	Condition or disease	Age (Years)
ENDOSTEAL NICHE				
NCT04460963	Phase 1	Adrenomedullin inhibition	AML	18 +
NCT00827138	Phase 1	New inhibitor of BCR-ABL, Flt3, Tie2 and other kinases	CML, AML	18 +
NCT01555268	Phase 1	Neutralizing peptibodie agains Angiopoietin 1/2	AML	18 +
VASCULAR NICHE				
NCT00542971	Phase 1/2	Co-treatment with VEGFR-kinase inhibitor	MDS, AML	15–60
NCT00071006	Phase 2	VEGFR-, PDGFR- and BCR-ABL-kinase inhibitor	MDS, AML	18 +
NCT00015951	Phase 2	Co-treatment with monoclonal antibody against VEGFR	Leukemias	18–120
NCT04518345	Phase 1/2	Novel specific kinase-inhibitor against ALX receptors	AML	18 +
NCT03616470	Phase 3	Specific E-selectin antagonist	AML	18–75
RETICULAR NICHE				
NCT00989261	Phase 2	FLT3 inhibitor	AML	18–85
NCT02634827	Phase 2	Pan kinase-inhibitor	AML	60 +
NCT02984995	Phase 2	FLT3-inhibitor	AML	20 +
NCT00045942	Phase 1/2	PKC-inhibitor	MDS, AML	18 +
NCT01445080	Phase 1/2	VEGFR-, PDGFR-kinase inhibitor	AML, solid tumor	2–21
NCT02954653	Phase 1	Monoclonal antibody against CXCR4	AML	18 +
NCT01546038	Phase 2	Sonic Hedgehog-inhibitor	MDS, AML	18 +

CML, Chronic Myeloid Leukemia; MDS, Myelodisplastic Syndrome.

be considered in participating on the extramedullary infiltration. Nonetheless, the role of M2 macrophages has not yet been elucidated in the context of eAML.

The current effort to investigate AML niches as targets for therapy certainly will naturally include extramedullary lesions in the focus of the researches, and relevant discoveries may give to eAML additional prognostic value.

PERSPECTIVES FOR ACUTE MYELOID LEUKEMIA THERAPIES TARGETING BONE MARROW NICHES.

The poor outcomes achieved by the current AML therapies are constantly encouraging researchers to propose new and better strategies to mitigate the leukemia development and evolution. The increased understanding about BM niches and about how these microenvironments cross-talk and regulate AML has allowed the discovery of potential novel approaches. Interestingly, part of these studies is testing well known drugs which act on common pathways and receptors shared by niches and blasts. Other groups of trials are targeting some niche-specific molecules. **Table 1** summarizes some of the main ongoing clinical trials related to BM-associated molecules described in this review.

Membrane receptors such as VEGFR, PDGFR, c-Kit, and CXCR4 are important targets in these studies not only due to their relevance in the maintenance of BM homeostasis and niches dynamics, but also because there are several inhibitors and antagonist already tested in other models and patients. Most of them presented successful results in solid or other hematological neoplasms, and the current understanding about vascular and endosteal contributed to the interesting in investigating them on AML.

Other groups of niches-related molecules have been also explored. The blockage of ligands, such as angiopoietin and CXCL12, or the inactivation of adhesion molecules, such as E-Selectin, have been tested with neutralizing peptides or antagonist small molecules. New combination protocols with traditional chemotherapy plus niche-related drugs are also common attempts observed in the ongoing trials.

The hypothesis of all these protocols is the same: disturbing the AML bone marrow organization by interfering with niche-related mechanisms and damaging proliferation, differentiation, or resistance to apoptosis. Besides additional basic studies, hematologists wait for further phase-3 clinical trials to finally confirm the efficacy of this tendency for new protocols.

AUTHOR CONTRIBUTIONS

DP, VV, and VC actively participated of the literature study and leaded the writing of the manuscript. TD reviewed the literature and leaded the writing concerning clinical aspects of AML and clinical trials. GH actively participated of the literature review and designed the figures according to the literature data. WP designed the idea of the manuscript, leaded the literature investigation, actively participated of the writing and finally reviewed the work to submit.

FUNDING

This work was supported by Amigos da Oncologia e Hematologia (AmigoH), CNPq, CAPES, and Instituto Israelita de Ensino e Pesquisa do Hospital Israelita Albert Einstein.

ACKNOWLEDGMENTS

The authors thank the Amigos da Oncologia e Hematologia (AmigoH) for the financial support for this work.

REFERENCES

Ahmari, N., Hayward, L. F., and Zubcevic, J. (2020). The Importance of Bone Marrow and the Immune System in Driving Increases in Blood Pressure and Sympathetic Nerve Activity in Hypertension. *Exp. Physiol.* 105 (11), 1815–1826. doi:10.1113/EP088247

Al-Matary, Y. S., Botezatu, L., Opalka, B., Hönes, J. M., Lams, R. F., Thivakaran, A., et al. (2016). Acute Myeloid Leukemia Cells Polarize Macrophages towards a Leukemia Supporting State in a Growth Factor independence 1 Dependent Manner. *Haematologica* 101 (10), 1216–1227. doi:10.3324/haematol.2016.143180

Arai, F., Hirao, A., Ohmura, M., Sato, H., Matsuoka, S., Takubo, K., et al. (2004). Tie2/angiopoietin-1 Signaling Regulates Hematopoietic Stem Cell Quiescence in the Bone Marrow Niche. *Cell* 118 (2), 149–161. doi:10.1016/j.cell.2004.07.004

Arber, D. A., Orazi, A., Hasserjian, R., Thiele, J., Borowitz, M. J., Le Beau, M. M., et al. (2016). The 2016 Revision to the World Health Organization Classification of Myeloid Neoplasms and Acute Leukemia. *Blood* 127 (20), 2391–2405. doi:10.1182/blood-2016-03-643544

Arranz, L., Sánchez-Aguilera, A., Martín-Pérez, D., Isern, J., Langa, X., Tzankov, A., et al. (2014). Neuropathy of Haematopoietic Stem Cell Niche Is Essential for Myeloproliferative Neoplasms. *Nature* 512 (7512), 78–81. doi:10.1038/nature13383

Azadniv, M., Myers, J. R., McMurray, H. R., Guo, N., Rock, P., Coppage, M. L., et al. (2020). Bone Marrow Mesenchymal Stromal Cells from Acute Myelogenous Leukemia Patients Demonstrate Adipogenic Differentiation Propensity with Implications for Leukemia Cell Support. *Leukemia* 34 (2), 391–403. doi:10.1038/s41375-019-0568-8

Baggiolini, M., Dewald, B., and Moser, B. (1997). Human Chemokines: an Update. *Annu. Rev. Immunol.* 15, 675–705. doi:10.1146/annurev.immunol.15.1.675

Baragaño Raneros, A., López-Larrea, C., and Suárez-Álvarez, B. (2019). Acute Myeloid Leukemia and NK Cells: Two Warriors Confront Each Other. *OncoImmunology* 8, e1539617. doi:10.1080/2162402X.2018.1539617

Barbier, V., Erbani, J., Fiveash, C., Davies, J. M., Tay, J., Tallack, M. R., et al. (2020). Endothelial E-Selectin Inhibition Improves Acute Myeloid Leukaemia Therapy by Disrupting Vascular Niche-Mediated Chemoresistance. *Nat. Commun.* 11 (1), 2042. doi:10.1038/s41467-020-15817-5

Barrera-Ramirez, J., Lavoie, J. R., Maganti, H. B., Stanford, W. L., Ito, C., Sabloff, M., et al. (2017). Micro-RNA Profiling of Exosomes from Marrow-Derived Mesenchymal Stromal Cells in Patients with Acute Myeloid Leukemia: Implications in Leukemogenesis. *Stem Cel. Rev. Rep.* 13 (6), 817–825. doi:10.1007/s12015-017-9762-0

Barrett, A. J., and Le Blanc, K. (2010). Immunotherapy Prospects for Acute Myeloid Leukaemia. *Clin. Exp. Immunol.* 161 (2), no. doi:10.1111/j.1365-2249.2010.04197.x

Battula, V. L., Le, P. M., Sun, J. C., Nguyen, K., Yuan, B., Zhou, X., et al. (2017). AML-induced Osteogenic Differentiation in Mesenchymal Stromal Cells Supports Leukemia Growth. *JCI Insight 2(13)* 2. doi:10.1172/jci.insight.90036

Behrmann, L., Wellbrock, J., and Fiedler, W. (2018). Acute Myeloid Leukemia and the Bone Marrow Niche-Take a Closer Look. *Front. Oncol.* 8, 444. doi:10.3389/fonc.2018.00444

Bianco, P., Cao, X., Frenette, P. S., Mao, J. J., Robey, P. G., Simmons, P. J., et al. (2013). The Meaning, the Sense and the Significance: Translating the Science of Mesenchymal Stem Cells into Medicine. *Nat. Med.* 19 (1), 35–42. doi:10.1038/nm.3028

Boyd, A. L., Reid, J. C., Salci, K. R., Aslostovar, L., Benoit, Y. D., Shapovalova, Z., et al. (2017). Acute Myeloid Leukaemia Disrupts Endogenous Myelo-Erythropoiesis by Compromising the Adipocyte Bone Marrow Niche. *Nat. Cel. Biol.* 19 (11), 1336–1347. doi:10.1038/ncb3625

Bronte, V., Brandau, S., Chen, S.-H., Colombo, M. P., Frey, A. B., Greten, T. F., et al. (2016). Recommendations for Myeloid-Derived Suppressor Cell Nomenclature and Characterization Standards. *Nat. Commun.* 7, 12150. doi:10.1038/ncomms12150

Burnett, A. K., Russell, N. H., Hills, R. K., Bowen, D., Kell, J., Knapper, S., et al. (2015). Research Institute Acute Myeloid Leukaemia Working GroupArsenic Trioxide and All-Trans Retinoic Acid Treatment for Acute Promyelocytic Leukaemia in All Risk Groups (AML17): Results of a Randomised, Controlled, Phase 3 Trial. *Lancet Oncol.* 16 (13), 1295–1305. doi:10.1016/S1470-2045(15)00193-X

Byrd, J. C., Edenfield, W. J., Shields, D. J., and Dawson, N. A. (1995). Extramedullary Myeloid Cell Tumors in Acute Nonlymphocytic Leukemia: a Clinical Review. *Jco* 13 (7), 1800–1816. doi:10.1200/JCO10.1200/jco.1995.13.7.1800

Carmeliet, P. (2005). Angiogenesis in Life, Disease and Medicine. *Nature* 438 (7070), 932–936. doi:10.1038/nature04478

Carter, B. Z., Mak, P. Y., Chen, Y., Mak, D. H., Mu, H., Jacamo, R., et al. (2016). Anti-apoptotic ARC Protein Confers Chemoresistance by Controlling Leukemia-Microenvironment Interactions through a NFκB/IL1β Signaling Network. *Oncotarget* 7 (15), 20054–20067. doi:10.18632/oncotarget.7911

Cavenagh, J. D., Gordon-Smith, E. C., Gibson, F. M., and Gordon, M. Y. (1993). Acute Myeloid Leukaemia Blast Cells Bind to Human Endothelium *In Vitro* Utilizing E-Selectin and Vascular Cell Adhesion Molecule-1 (VCAM-1). *Br. J. Haematol.* 85 (2), 285–291. doi:10.1111/j.1365-2141.1993.tb03168.x

Chen, J., Singh, K., Mukherjee, B. B., and Sodek, J. (1993). Developmental Expression of Osteopontin (OPN) mRNA in Rat Tissues: Evidence for a Role for OPN in Bone Formation and Resorption. *Matrix* 13 (2), 113–123. doi:10.1016/s0934-8832(11)80070-3

Chiossone, L., Vienne, M., Kerdiles, Y. M., and Vivier, E. (2017). Natural Killer Cell Immunotherapies against Cancer: Checkpoint Inhibitors and More. *Semin. Immunol.* 31, 55–63. doi:10.1016/j.smim.2017.08.003

Cogle, C. R., Goldman, D. C., Madlambayan, G. J., Leon, R. P., Al Masri, A., Clark, H. A., et al. (2014). Functional Integration of Acute Myeloid Leukemia into the Vascular Niche. *Leukemia* 28 (10), 1978–1987. doi:10.1038/leu.2014.109

Comings, D. E., Fayen, A. W., and Carter, P. (1965). Myeloblastoma Preceding Blood and Marrow Evidence of Acute Leukemia. *Cancer* 18, 253–258. doi:10.1002/1097-0142(196502)18:2<253:aid-cncr2820180218>3.0.co;2-#

Conway, E. M., Collen, D., and Carmeliet, P. (2001). Molecular Mechanisms of Blood Vessel Growth. *Cardiovasc. Res.* 49 (3), 507–521. doi:10.1016/s0008-6363(00)00281-9

Cunningham, I., Hamele-Bena, D., Guo, Y., Shiomi, T., Papp, A. C., Chakravarti, B., et al. (2019). Extramedullary Leukemia Behaving as Solid Cancer: Clinical, Histologic, and Genetic Clues to Chemoresistance in Organ Sites. *Am. J. Hematol.* 94 (11), 1200–1207. doi:10.1002/ajh.25594

Damuzzo, V., Pinton, L., Desantis, G., Solito, S., Marigo, I., Bronte, V., et al. (2015). Complexity and Challenges in Defining Myeloid-Derived Suppressor Cells. *Cytometry B Clin. Cytom.* 88 (2), 77–91. doi:10.1002/cyto.b.21206

Datoguia, T. S., R.P Velloso, E. D., Helman, R., Musacchio, J. G., Salvino, M. A., Soares, R. A., et al. (2018). Overall Survival of Brazilian Acute Myeloid Leukemia Patients According to the European LeukemiaNet Prognostic Scoring System: a Cross-Sectional Study. *Med. Oncol.* 35 (11), 141. doi:10.1007/s12032-018-1179-3

Daver, N., Wei, A. H., Pollyea, D. A., Fathi, A. T., Vyas, P., and DiNardo, C. D. (2020). New Directions for Emerging Therapies in Acute Myeloid Leukemia: the Next Chapter. *Blood Cancer J.* 10 (10), 107. doi:10.1038/s41408-020-00376-1

De Kouchkovsky, I., and Abdul-Hay, M. (2016). 'Acute Myeloid Leukemia: a Comprehensive Review and 2016 Update'. *Blood Cancer J.* 6 (7), e441. doi:10.1038/bcj.2016.50

Denhardt, D. T., and Guo, X. (1993). Osteopontin: a Protein with Diverse Functions. *FASEB J.* 7 (15), 1475–1482. doi:10.1096/fasebj.7.15.8262332

Deschler, B., and Lübbert, M. (2006). Acute Myeloid Leukemia: Epidemiology and Etiology. *Cancer* 107 (9), 2099–2107. doi:10.1002/cncr.22233

Di Vito, C., Mikulak, J., and Mavilio, D. (2019). On the Way to Become a Natural Killer Cell. *Front. Immunol.* 10, 1812. doi:10.3389/fimmu.2019.01812

Dimmeler, S., and Zeiher, A. M. (2000). Akt Takes center Stage in Angiogenesis Signaling. *Circ. Res.* 86 (1), 4–5. doi:10.1161/01.res.86.1.4

DiNardo, C. D., and Cortes, J. E. (2016). Mutations in AML: Prognostic and Therapeutic Implications. *Hematol. Am. Soc. Hematol. Educ. Program* 2016 (1), 348–355. doi:10.1182/asheducation-2016.1.348

DiNardo, C. D., Jonas, B. A., Pullarkat, V., Thirman, M. J., Garcia, J. S., Wei, A. H., et al. (2020). Azacitidine and Venetoclax in Previously Untreated Acute Myeloid Leukemia. *N. Engl. J. Med.* 383 (7), 617–629. doi:10.1056/NEJMoa2012971

Ding, L., Saunders, T. L., Enikolopov, G., and Morrison, S. J. (2012). Endothelial and Perivascular Cells Maintain Haematopoietic Stem Cells. *Nature* 481 (7382), 457–462. doi:10.1038/nature10783

Döhner, H., Estey, E., Grimwade, D., Amadori, S., Appelbaum, F. R., Büchner, T., et al. (2017). Diagnosis and Management of AML in Adults: 2017 ELN Recommendations from an International Expert Panel. *Blood* 129 (4), 424–447. doi:10.1182/blood-2016-08-733196

Eisfeld, A. K., Kohlschmidt, J., Mims, A., Nicolet, D., Walker, C. J., Blachly, J. S., et al. (2020). C. D. BloomfieldAdditional Gene Mutations May Refine the 2017 European LeukemiaNet Classification in Adult Patients with De Novo Acute Myeloid Leukemia Aged <60 Years. *Leukemia* 34 (12), 3215–3227. doi:10.1038/s41375-020-0872-3

Eliasson, P., and Jönsson, J. I. (2010). The Hematopoietic Stem Cell Niche: Low in Oxygen but a Nice Place to Be. *J. Cel. Physiol.* 222 (1), 17–22. doi:10.1002/jcp.21908

Estey, E., and Döhner, H. (2006). Acute Myeloid Leukaemia. *Lancet* 368 (9550), 1894–1907. doi:10.1016/S0140-6736(06)69780-8

Faaij, C. M., Willemze, A. J., Révész, T., Balzarolo, M., Tensen, C. P., Hoogeboom, M., et al. (2010). Chemokine/chemokine Receptor Interactions in Extramedullary Leukaemia of the Skin in Childhood AML: Differential Roles for CCR2, CCR5, CXCR4 and CXCR7. *Pediatr. Blood Cancer* 55 (2), 344–348. doi:10.1002/pbc.22500

Falcon, B. L., Chintharlapalli, S., Uhlik, M. T., and Pytowski, B. (2016). Antagonist Antibodies to Vascular Endothelial Growth Factor Receptor 2 (VEGFR-2) as Anti-angiogenic Agents. *Pharmacol. Ther.* 164, 204–225. doi:10.1016/j.pharmthera.2016.06.001

Fathi, E., Farahzadi, R., Valipour, B., and Sanaat, Z. (2019). Cytokines Secreted from Bone Marrow Derived Mesenchymal Stem Cells Promote Apoptosis and Change Cell Cycle Distribution of K562 Cell Line as Clinical Agent in Cell Transplantation. *PLoS One* 14 (4), e0215678. doi:10.1371/journal.pone.0215678

Fathi, E., Sanaat, Z., and Farahzadi, R. (2019). Mesenchymal Stem Cells in Acute Myeloid Leukemia: a Focus on Mechanisms Involved and Therapeutic Concepts. *Blood Res.* 54 (3), 165–174. doi:10.5045/br.2019.54.3.165

Fiedler, W., Graeven, U., Ergün, S., Verago, S., Kilic, N., Stockschläder, M., et al. (1997). Vascular Endothelial Growth Factor, a Possible Paracrine Growth Factor in Human Acute Myeloid Leukemia. *Blood* 89 (6), 1870–1875. doi:10.1182/blood.v89.6.1870

Forte, D., García-Fernández, M., Sánchez-Aguilera, A., Stavropoulou, V., Fielding, C., Martín-Pérez, D., et al. (2020). Bone Marrow Mesenchymal Stem Cells Support Acute Myeloid Leukemia Bioenergetics and Enhance Antioxidant Defense and Escape from Chemotherapy. *Cell Metab.* 32 (5), 829–843. doi:10.1016/j.cmet.2020.09.001

Franchini, M., Frattini, F., Crestani, S., and Bonfanti, C. (2013). Bleeding Complications in Patients with Hematologic Malignancies. *Semin. Thromb. Hemost.* 39 (1), 94–100. doi:10.1055/s-0032-1331154

Frisch, B. J., Ashton, J. M., Xing, L., Becker, M. W., Jordan, C. T., and Calvi, L. M. (2012). Functional Inhibition of Osteoblastic Cells in an *In Vivo* Mouse Model of Myeloid Leukemia. *Blood* 119 (2), 540–550. doi:10.1182/blood-2011-04-348151

Gabrilovich, D. I., and Nagaraj, S. (2009). Myeloid-derived Suppressor Cells as Regulators of the Immune System. *Nat. Rev. Immunol.* 9 (3), 162–174. doi:10.1038/nri2506

Galdiero, M. R., Bonavita, E., Barajon, I., Garlanda, C., Mantovani, A., and Jaillon, S. (2013). Tumor Associated Macrophages and Neutrophils in Cancer. *Immunobiology* 218 (11), 1402–1410. doi:10.1016/j.imbio.2013.06.003

Galdiero, M. R., Garlanda, C., Jaillon, S., Marone, G., and Mantovani, A. (2013). Tumor Associated Macrophages and Neutrophils in Tumor Progression. *J. Cel. Physiol.* 228 (7), 1404–1412. doi:10.1002/jcp.24260

Ganzel, C., Manola, J., Douer, D., Rowe, J. M., Fernandez, H. F., Paietta, E. M., et al. (2016). 2016. Extramedullary Disease in Adult Acute Myeloid Leukemia Is Common but Lacks Independent Significance: Analysis of Patients in ECOG-ACRIN Cancer Research Group Trials, 1980-2008. *J. Clin. Oncol.* 34 (29), 3544–3553. doi:10.1200/JCO10.1200/jco.2016.67.5892

Gentek, R., Molawi, K., and Sieweke, M. H. (2014). Tissue Macrophage Identity and Self-Renewal. *Immunol. Rev.* 262 (1), 56–73. doi:10.1111/imr.12224

Gerber, H. P., McMurtrey, A., Kowalski, J., Yan, M., Keyt, B. A., Dixit, V., et al. (1998). Vascular Endothelial Growth Factor Regulates Endothelial Cell Survival through the Phosphatidylinositol 3'-kinase/Akt Signal Transduction Pathway. Requirement for Flk-1/KDR Activation. *J. Biol. Chem.* 273 (46), 30336–30343. doi:10.1074/jbc.273.46.30336

Ghobrial, I. M., Detappe, A., Anderson, K. C., and Steensma, D. P. (2018). The Bone-Marrow Niche in MDS and MGUS: Implications for AML and MM. *Nat. Rev. Clin. Oncol.* 15 (4), 219–233. doi:10.1038/nrclinonc.2017.197

Goulard, M., Dosquet, C., and Bonnet, D. (2018). Role of the Microenvironment in Myeloid Malignancies. *Cell Mol. Life Sci.* 75 (8), 1377–1391. doi:10.1007/s00018-017-2725-4

Goyal, G., Bartley, A. C., Patnaik, M. M., Litzow, M. R., Al-Kali, A., and Go, R. S. (2017). Clinical Features and Outcomes of Extramedullary Myeloid Sarcoma in the United States: Analysis Using a National Data Set. *Blood Cancer J.* 7 (8), e592. doi:10.1038/bcj.2017.79

Greenbaum, A. M., Revollo, L. D., Woloszynek, J. R., Civitelli, R., and Link, D. C. (2012). N-cadherin in Osteolineage Cells Is Not Required for Maintenance of Hematopoietic Stem Cells. *Blood* 120 (2), 295–302. doi:10.1182/blood-2011-09-377457

Haas, L., and Obenauf, A. C. (2019). Allies or Enemies-The Multifaceted Role of Myeloid Cells in the Tumor Microenvironment. *Front. Immunol.* 10, 2746. doi:10.3389/fimmu.2019.02746

Hackney, J. A., Charbord, P., Brunk, B. P., Stoeckert, C. J., Lemischka, I. R., and Moore, K. A. (2002). A Molecular Profile of a Hematopoietic Stem Cell Niche. *Proc. Natl. Acad. Sci. U S A.* 99 (20), 13061–13066. doi:10.1073/pnas.192124499

Hammerich, L., and Tacke, F. (2015). Emerging Roles of Myeloid Derived Suppressor Cells in Hepatic Inflammation and Fibrosis. *World J. Gastrointest. Pathophysiol.* 6 (3), 43–50. doi:10.4291/wjgp.v6.i3.43

Hashimoto, K., Kataoka, N., Nakamura, E., Hagihara, K., Okamoto, T., Kanouchi, H., et al. (2012). Live-cell Visualization of the Trans-cellular Mode of Monocyte Transmigration across the Vascular Endothelium, and its Relationship with Endothelial PECAM-1. *J. Physiol. Sci.* 62 (1), 63–69. doi:10.1007/s12576-011-0181-8

Heine, A., Held, S. A. E., Schulte-Schrepping, J., Wolff, J. F. A., Klee, K., Ulas, T., et al. (2017). Generation and Functional Characterization of MDSC-like Cells. *Oncoimmunology* 6 (4), e1295203. doi:10.1080/2162402X.2017.1295203

Hirabayashi, S., Uozumi, R., Kondo, T., Arai, Y., Kawata, T., Uchida, N., et al. (2021). Personalized Prediction of Overall Survival in Patients with AML in Non-complete Remission Undergoing Allo-HCT. *Cancer Med.* 10 (13), 4250–4268. doi:10.1002/cam4.3920

Horowitz, M. C., Berry, R., Holtrup, B., Sebo, Z., Nelson, T., Fretz, J. A., et al. (2017). Bone Marrow Adipocytes. *Adipocyte* 6 (3), 193–204. doi:10.1080/21623945.2017.1367881

Hosokawa, K., Arai, F., Yoshihara, H., Iwasaki, H., Nakamura, Y., Gomei, Y., et al. (2010). Knockdown of N-Cadherin Suppresses the Long-Term Engraftment of Hematopoietic Stem Cells. *Blood* 116 (4), 554–563. doi:10.1182/blood-2009-05-224857

Huntly, B. J., and Gilliland, D. G. (2005). Leukaemia Stem Cells and the Evolution of Cancer-Stem-Cell Research. *Nat. Rev. Cancer* 5 (4), 311–321. doi:10.1038/nrc1592

Ibáñez-Vea, M., Zuazo, M., Gato, M., Arasanz, H., Fernández-Hinojal, G., Escors, D., et al. (2018). Myeloid-Derived Suppressor Cells in the Tumor Microenvironment: Current Knowledge and Future Perspectives. *Arch. Immunol. Ther. Exp. (Warsz)* 66 (2), 113–123. doi:10.1007/s00005-017-0492-4

Jongen-Lavrencic, M., Grob, T., Hanekamp, D., Kavelaars, F. G., Al Hinai, A., Zeilemaker, A., et al. (2018). Molecular Minimal Residual Disease in Acute Myeloid Leukemia. *N. Engl. J. Med.* 378 (13), 1189–1199. doi:10.1056/NEJMoa1716863

Kaur, S., Raggatt, L. J., Batoon, L., Hume, D. A., Levesque, J. P., and Pettit, A. R. (2017). Role of Bone Marrow Macrophages in Controlling Homeostasis and Repair in Bone and Bone Marrow Niches. *Semin. Cel. Dev. Biol.* 61, 12–21. doi:10.1016/j.semcdb.2016.08.009

Kaushansky, K. (1995). Thrombopoietin: the Primary Regulator of Megakaryocyte and Platelet Production. *Thromb. Haemost.* 74 (1), 521–525. doi:10.1055/s-0038-1642732

Kent, D., Copley, M., Benz, C., Dykstra, B., Bowie, M., and Eaves, C. (2008). Regulation of Hematopoietic Stem Cells by the Steel Factor/KIT Signaling Pathway. *Clin. Cancer Res.* 14 (7), 1926–1930. doi:10.1158/1078-0432.CCR-07-5134

Kiel, M. J., Acar, M., Radice, G. L., and Morrison, S. J. (2009). Hematopoietic Stem Cells Do Not Depend on N-Cadherin to Regulate Their Maintenance. *Cell Stem Cell* 4 (2), 170–179. doi:10.1016/j.stem.2008.10.005

Kiel, M. J., Radice, G. L., and Morrison, S. J. (2007). Lack of Evidence that Hematopoietic Stem Cells Depend on N-Cadherin-Mediated Adhesion to Osteoblasts for Their Maintenance. *Cell Stem Cell* 1 (2), 204–217. doi:10.1016/j.stem.2007.06.001

Kim, M. H., Jin, E., Zhang, H. Z., and Kim, S. W. (2013). Robust Angiogenic Properties of Cultured Human Peripheral Blood-Derived CD31$^+$ Cells. *Int. J. Cardiol.* 166 (3), 709–715. doi:10.1016/j.ijcard.2011.11.097

Kimura, H., Usui, T., Tsubouchi, A., and Uemura, T. (2006). Potential Dual Molecular Interaction of the Drosophila 7-pass Transmembrane Cadherin Flamingo in Dendritic Morphogenesis. *J. Cel. Sci.* 119 (Pt 6), 1118–1129. doi:10.1242/jcs.02832

Kimura, S., Roberts, A. W., Metcalf, D., and Alexander, W. S. (1998). Hematopoietic Stem Cell Deficiencies in Mice Lacking C-Mpl, the Receptor for Thrombopoietin. *Proc. Natl. Acad. Sci. U S A.* 95 (3), 1195–1200. doi:10.1073/pnas.95.3.1195

Klein, J. R. (2021). Dynamic Interactions between the Immune System and the Neuroendocrine System in Health and Disease. *Front. Endocrinol. (Lausanne)* 12, 655982. doi:10.3389/fendo.2021.655982

Kloc, M., Ghobrial, R. M., Wosik, J., Lewicka, A., Lewicki, S., and Kubiak, J. Z. (2019). Macrophage Functions in Wound Healing. *J. Tissue Eng. Regen. Med.* 13 (1), 99–109. doi:10.1002/term.2772

Kobayashi, H., Butler, J. M., O'Donnell, R., Kobayashi, M., Ding, B. S., Bonner, B., et al. (2010). Angiocrine Factors from Akt-Activated Endothelial Cells Balance Self-Renewal and Differentiation of Haematopoietic Stem Cells. *Nat. Cel. Biol.* 12 (11), 1046–1056. doi:10.1038/ncb2108

Kohara, H., Omatsu, Y., Sugiyama, T., Noda, M., Fujii, N., and Nagasawa, T. (2007). Development of Plasmacytoid Dendritic Cells in Bone Marrow Stromal Cell Niches Requires CXCL12-CXCR4 Chemokine Signaling. *Blood* 110 (13), 4153–4160. doi:10.1182/blood-2007-04-084210

Kollet, O., Dar, A., Shivtiel, S., Kalinkovich, A., Lapid, K., Sztainberg, Y., et al. (2006). Osteoclasts Degrade Endosteal Components and Promote Mobilization of Hematopoietic Progenitor Cells. *Nat. Med.* 12 (6), 657–664. doi:10.1038/nm1417

Kologrivova, I., Shtatolkina, M., Suslova, T., and Ryabov, V. (2021). Cells of the Immune System in Cardiac Remodeling: Main Players in Resolution of Inflammation and Repair after Myocardial Infarction. *Front. Immunol.* 12, 664457. doi:10.3389/fimmu.2021.664457

Kopp, H. G., Avecilla, S. T., Hooper, A. T., and Rafii, S. (2005). The Bone Marrow Vascular Niche: home of HSC Differentiation and Mobilization. *Physiology (Bethesda)* 20, 349–356. doi:10.1152/physiol.00025.2005

Kouzi, F., Zibara, K., Bourgeais, J., Picou, F., Gallay, N., Brossaud, J., et al. (2020). Disruption of gap Junctions Attenuates Acute Myeloid Leukemia Chemoresistance Induced by Bone Marrow Mesenchymal Stromal Cells. *Oncogene* 39 (6), 1198–1212. doi:10.1038/s41388-019-1069-y

Kumar, B., Garcia, M., Weng, L., Jung, X., Murakami, J. L., Hu, X., et al. (2018). Acute Myeloid Leukemia Transforms the Bone Marrow Niche into a Leukemia-Permissive Microenvironment through Exosome Secretion. *Leukemia* 32 (3), 575–587. doi:10.1038/leu.2017.259

Kusmartsev, S., and Gabrilovich, D. I. (2006). Role of Immature Myeloid Cells in Mechanisms of Immune Evasion in Cancer. *Cancer Immunol. Immunother.* 55 (3), 237–245. doi:10.1007/s00262-005-0048-z

Kusumbe, A. P., Ramasamy, S. K., and Adams, R. H. (2014). Coupling of Angiogenesis and Osteogenesis by a Specific Vessel Subtype in Bone. *Nature* 507 (7492), 323–328. doi:10.1038/nature13145

Kusumbe, A. P., Ramasamy, S. K., Itkin, T., Mäe, M. A., Langen, U. H., Betsholtz, C., et al. (2016). Corrigendum: Age-dependent Modulation of Vascular Niches for Haematopoietic Stem Cells. *Nature* 539 (7628), 314. doi:10.1038/nature19782

Kuzu, I., Beksac, M., Arat, M., Celebi, H., Elhan, A. H., and Erekul, S. (2004). Bone Marrow Microvessel Density (MVD) in Adult Acute Myeloid Leukemia (AML): Therapy Induced Changes and Effects on Survival. *Leuk. Lymphoma* 45 (6), 1185–1190. doi:10.1080/1042819032000159915

Ladikou, E. E., Sivaloganathan, H., Pepper, A., and Chevassut, T. (2020). Acute Myeloid Leukaemia in its Niche: the Bone Marrow Microenvironment in Acute Myeloid Leukaemia. *Curr. Oncol. Rep.* 22 (3), 27. doi:10.1007/s11912-020-0885-0

Le, P. M., Andreeff, M., and Battula, V. L. (2018). Osteogenic Niche in the Regulation of normal Hematopoiesis and Leukemogenesis. *Haematologica* 103 (12), 1945–1955. doi:10.3324/haematol.2018.197004

Lee, E. A., Angka, L., Rota, S. G., Hanlon, T., Mitchell, A., Hurren, R., et al. (2015). Targeting Mitochondria with Avocatin B Induces Selective Leukemia Cell Death. *Cancer Res.* 75 (12), 2478–2488. doi:10.1158/0008-5472.CAN-14-2676

Lertkiatmongkol, P., Liao, D., Mei, H., Hu, Y., and Newman, P. J. (2016). Endothelial Functions of Platelet/endothelial Cell Adhesion Molecule-1 (CD31). *Curr. Opin. Hematol.* 23 (3), 253–259. doi:10.1097/MOH.0000000000000239

Leung, D. W., Cachianes, G., Kuang, W. J., Goeddel, D. V., and Ferrara, N. (1989). Vascular Endothelial Growth Factor Is a Secreted Angiogenic Mitogen. *Science* 246 (4935), 1306–1309. doi:10.1126/science.2479986

Ley, T. J., Miller, C., Ding, L., Raphael, B. J., Mungall, A. J., Robertson, A., et al.Cancer Genome Atlas Research Network (2013). Genomic and Epigenomic Landscapes of Adult De Novo Acute Myeloid Leukemia. *N. Engl. J. Med.* 368 (22), 2059–2074. doi:10.1056/NEJMoa1301689

Li, Q., Pang, Y., Liu, T., Tang, Y., Xie, J., Zhang, B., et al. (2018). Effects of Human Umbilical Cord-Derived Mesenchymal Stem Cells on Hematologic Malignancies. *Oncol. Lett.* 15 (5), 6982–6990. doi:10.3892/ol.2018.8254

Li, Y., You, M. J., Yang, Y., Hu, D., and Tian, C. (2020). The Role of Tumor-Associated Macrophages in Leukemia. *Acta Haematol.* 143 (2), 112–117. doi:10.1159/000500315

Lichtman, M. A. (2013). A Historical Perspective on the Development of the Cytarabine (7days) and Daunorubicin (3days) Treatment Regimen for Acute Myelogenous Leukemia: 2013 the 40th Anniversary of 7+3. *Blood Cell Mol. Dis.* 50 (2), 119–130. doi:10.1016/j.bcmd.2012.10.005

Malcangio, M. (2019). Role of the Immune System in Neuropathic Pain. *Scand. J. Pain* 20 (1), 33–37. doi:10.1515/sjpain-2019-0138

Mantovani, A., Bottazzi, B., Colotta, F., Sozzani, S., and Ruco, L. (1992). The Origin and Function of Tumor-Associated Macrophages. *Immunol. Today* 13 (7), 265–270. doi:10.1016/0167-5699(92)90008-U

Mantovani, A., Sozzani, S., Locati, M., Allavena, P., and Sica, A. (2002). Macrophage Polarization: Tumor-Associated Macrophages as a Paradigm for Polarized M2 Mononuclear Phagocytes. *Trends Immunol.* 23 (11), 549–555. doi:10.1016/s1471-4906(02)02302-5

Martelli, M. P., Sportoletti, P., Tiacci, E., Martelli, M. F., and Falini, B. (2013). Mutational Landscape of AML with normal Cytogenetics: Biological and Clinical Implications. *Blood Rev.* 27 (1), 13–22. doi:10.1016/j.blre.2012.11.001

Medyouf, H. (2017). The Microenvironment in Human Myeloid Malignancies: Emerging Concepts and Therapeutic Implications. *Blood* 129 (12), 1617–1626. doi:10.1182/blood-2016-11-696070

Méndez-Ferrer, S., Bonnet, D., Steensma, D. P., Hasserjian, R. P., Ghobrial, I. M., Gribben, J. G., et al. (2020). Bone Marrow Niches in Haematological Malignancies. *Nat. Rev. Cancer* 20 (5), 285–298. doi:10.1038/s41568-020-0245-2

Mistry, A. R., Pedersen, E. W., Solomon, E., and Grimwade, D. (2003). The Molecular Pathogenesis of Acute Promyelocytic Leukaemia: Implications for the Clinical Management of the Disease. *Blood Rev.* 17 (2), 71–97. doi:10.1016/s0268-960x(02)00075-9

Möhle, R., Bautz, F., Rafii, S., Moore, M. A., Brugger, W., and Kanz, L. (1998). The Chemokine Receptor CXCR-4 Is Expressed on CD34+ Hematopoietic Progenitors and Leukemic Cells and Mediates Transendothelial Migration Induced by Stromal Cell-Derived Factor-1. *Blood* 91 (12), 4523–4530.

Morris, M. A., and Ley, K. (2004). Trafficking of Natural Killer Cells. *Curr. Mol. Med.* 4 (4), 431–438. doi:10.2174/1566524043360609

Morrison, S. J., and Spradling, A. C. (2008). Stem Cells and Niches: Mechanisms that Promote Stem Cell Maintenance throughout Life. *Cell* 132 (4), 598–611. doi:10.1016/j.cell.2008.01.038

Movassaghian, M., Brunner, A. M., Blonquist, T. M., Sadrzadeh, H., Bhatia, A., Perry, A. M., et al. (2015). Presentation and Outcomes Among Patients with Isolated Myeloid Sarcoma: a Surveillance, Epidemiology, and End Results Database Analysis. *Leuk. Lymphoma* 56 (6), 1698–1703. doi:10.3109/10428194.2014.963080

Nagasawa, T. (2006). Microenvironmental Niches in the Bone Marrow Required for B-Cell Development. *Nat. Rev. Immunol.* 6 (2), 107–116. doi:10.1038/nri1780

Nagasawa, T., Omatsu, Y., and Sugiyama, T. (2011). Control of Hematopoietic Stem Cells by the Bone Marrow Stromal Niche: the Role of Reticular Cells. *Trends Immunol.* 32 (7), 315–320. doi:10.1016/j.it.2011.03.009

Narayanan, D., and Weinberg, O. K. (2020). How I Investigate Acute Myeloid Leukemia. *Int. J. Lab. Hematol.* 42 (1), 3–15. doi:10.1111/ijlh.13135

Naymagon, L., and Mascarenhas, J. (2020). Hemorrhage in Acute Promyelocytic Leukemia: Can it Be Predicted and Prevented. *Leuk. Res.* 94, 106356. doi:10.1016/j.leukres.2020.106356

Neiman, R. S., Barcos, M., Berard, C., Bonner, H., Mann, R., Rydell, R. E., et al. (1981). Granulocytic Sarcoma: a Clinicopathologic Study of 61 Biopsied Cases. *Cancer* 48 (6), 1426–1437. doi:10.1002/1097-014210.1002/1097-0142(19810915)48:6<1426:aid-cncr2820480626>3.0.co;2-g

Nilsson, S. K., Johnston, H. M., and Coverdale, J. A. (2001). Spatial Localization of Transplanted Hemopoietic Stem Cells: Inferences for the Localization of Stem Cell Niches. *Blood* 97 (8), 2293–2299. doi:10.1182/blood.v97.8.2293

Nilsson, S. K., Johnston, H. M., Whitty, G. A., Williams, B., Webb, R. J., Denhardt, D. T., et al. (2005). Osteopontin, a Key Component of the Hematopoietic Stem Cell Niche and Regulator of Primitive Hematopoietic Progenitor Cells. *Blood* 106 (4), 1232–1239. doi:10.1182/blood-2004-11-4422

Noda, M., Omatsu, Y., Sugiyama, T., Oishi, S., Fujii, N., and Nagasawa, T. (2011). CXCL12-CXCR4 Chemokine Signaling Is Essential for NK-Cell Development in Adult Mice. *Blood* 117 (2), 451–458. doi:10.1182/blood-2010-04-277897

Nombela-Arrieta, C., Pivarnik, G., Winkel, B., Canty, K. J., Harley, B., Mahoney, J. E., et al. (2013). Quantitative Imaging of Haematopoietic Stem and Progenitor Cell Localization and Hypoxic Status in the Bone Marrow Microenvironment. *Nat. Cel. Biol.* 15 (5), 533–543. doi:10.1038/ncb2730

O'Donnell, M. R., Tallman, M. S., Abboud, C. N., Altman, J. K., Appelbaum, F. R., Arber, D. A., et al. (2017). Acute Myeloid Leukemia, Version 3.2017, NCCN Clinical Practice Guidelines in Oncology. *J. Natl. Compr. Canc Netw.* 15 (7), 926–957. doi:10.6004/jnccn.2017.0116

Omatsu, Y., Sugiyama, T., Kohara, H., Kondoh, G., Fujii, N., Kohno, K., et al. (2010). The Essential Functions of Adipo-Osteogenic Progenitors as the Hematopoietic Stem and Progenitor Cell Niche. *Immunity* 33 (3), 387–399. doi:10.1016/j.immuni.2010.08.017

Padró, T., Ruiz, S., Bieker, R., Bürger, H., Steins, M., Kienast, J., et al. (2000). Increased Angiogenesis in the Bone Marrow of Patients with Acute Myeloid Leukemia. *Blood* 95 (8), 2637–2644. doi:10.1182/blood.v95.8.2637.008k07_2637_2644

Papaemmanuil, E., Gerstung, M., Bullinger, L., Gaidzik, V. I., Paschka, P., Roberts, N. D., et al. (2016). Genomic Classification and Prognosis in Acute Myeloid Leukemia. *N. Engl. J. Med.* 374 (23), 2209–2221. doi:10.1056/NEJMoa1516192

Park-Windhol, C., Ng, Y. S., Yang, J., Primo, V., Saint-Geniez, M., and D'Amore, P. A. (2017). Endomucin Inhibits VEGF-Induced Endothelial Cell Migration, Growth, and Morphogenesis by Modulating VEGFR2 Signaling. *Sci. Rep.* 7 (1), 17138. doi:10.1038/s41598-017-16852-x

Passegué, E., Jamieson, C. H., Ailles, L. E., and Weissman, I. L. (2003). Normal and Leukemic Hematopoiesis: Are Leukemias a Stem Cell Disorder or a Reacquisition of Stem Cell Characteristics. *Proc. Natl. Acad. Sci. U S A.* 1: 11842–11849. doi:10.1073/pnas.2034201100

Patel, J. P., Gönen, M., Figueroa, M. E., Fernandez, H., Sun, Z., Racevskis, J., et al. (2012). Prognostic Relevance of Integrated Genetic Profiling in Acute Myeloid Leukemia. *N. Engl. J. Med.* 366 (12), 1079–1089. doi:10.1056/NEJMoa1112304

Peled, A., and Tavor, S. (2013). Role of CXCR4 in the Pathogenesis of Acute Myeloid Leukemia. *Theranostics* 3 (1), 34–39. doi:10.7150/thno.5150

Piccaluga, P. P., Paolini, S., Navari, M., Etebari, M., Visani, G., and Ascani, S. (2018). Increased Angiogenesis Seems to Correlate with Inferior Overall Survival in Myeloid Sarcoma Patients. *Pol. J. Pathol.* 69 (3), 254–265. doi:10.5114/pjp.2018.79545

Ponzetta, A., Benigni, G., Antonangeli, F., Sciumè, G., Sanseviero, E., Zingoni, A., et al. (2015). Multiple Myeloma Impairs Bone Marrow Localization of Effector Natural Killer Cells by Altering the Chemokine Microenvironment. *Cancer Res.* 75 (22), 4766–4777. doi:10.1158/0008-5472.CAN-15-1320

Prockop, D. J. (1998). Marrow Stromal Cells as Stem Cells for Continual Renewal of Nonhematopoietic Tissues and as Potential Vectors for Gene Therapy. *J. Cel. Biochem.* 72 (S30-31), 284–285. doi:10.1002/(SICI)1097-4644(1998)72:30/31+<284:AID-JCB34>3.0.CO;2-I

Prockop, D. J. (1997). Marrow Stromal Cells as Stem Cells for Nonhematopoietic Tissues. *Science* 276 (5309), 71–74. doi:10.1126/science.276.5309.71

Puccetti, E., and Ruthardt, M. (2004). Acute Promyelocytic Leukemia: PML/RARalpha and the Leukemic Stem Cell. *Leukemia* 18 (7), 1169–1175. doi:10.1038/sj.leu.2403367

Pyzer, A. R., Stroopinsky, D., Rajabi, H., Washington, A., Tagde, A., Coll, M., et al. (2017). MUC1-mediated Induction of Myeloid-Derived Suppressor Cells in Patients with Acute Myeloid Leukemia. *Blood* 129 (13), 1791–1801. doi:10.1182/blood-2016-07-730614

Ramasamy, S. K., Kusumbe, A. P., Wang, L., and Adams, R. H. (2014). Endothelial Notch Activity Promotes Angiogenesis and Osteogenesis in Bone. *Nature* 507 (7492), 376–380. doi:10.1038/nature13146

Raulet, D. H., Vance, R. E., and McMahon, C. W. (2001). Regulation of the Natural Killer Cell Receptor Repertoire. *Annu. Rev. Immunol.* 19, 291–330. doi:10.1146/annurev.immunol.19.1.291

Reagan, M. R., and Rosen, C. J. (2016). Navigating the Bone Marrow Niche: Translational Insights and Cancer-Driven Dysfunction. *Nat. Rev. Rheumatol.* 12 (3), 154–168. doi:10.1038/nrrheum.2015.160

Rodríguez-Fuentes, D. E., Fernández-Garza, L. E., Samia-Meza, J. A., Barrera-Barrera, S. A., Caplan, A. I., and Barrera-Saldaña, H. A. (2021). Mesenchymal Stem Cells Current Clinical Applications: A Systematic Review. *Arch. Med. Res.* 52 (1), 93–101. doi:10.1016/j.arcmed.2020.08.006

Rönnstrand, L. (2004). Signal Transduction via the Stem Cell Factor Receptor/c-Kit. *Cel Mol Life Sci* 61 (19-20), 2535–2548. doi:10.1007/s00018-004-4189-6

Rose-Inman, H., and Kuehl, D. (2014). Acute Leukemia. *Emerg. Med. Clin. North. Am.* 32 (3), 579–596. doi:10.1016/j.emc.2014.04.004

Rosen, C. J., Ackert-Bicknell, C., Rodriguez, J. P., and Pino, A. M. (2009). Marrow Fat and the Bone Microenvironment: Developmental, Functional, and Pathological Implications. *Crit. Rev. Eukaryot. Gene Expr.* 19 (2), 109–124. doi:10.1615/critreveukargeneexpr.v19.i2.20

Sallmyr, A., Fan, J., and Rassool, F. V. (2008). Genomic Instability in Myeloid Malignancies: Increased Reactive Oxygen Species (ROS), DNA Double Strand Breaks (DSBs) and Error-Prone Repair. *Cancer Lett.* 270 (1), 1–9. doi:10.1016/j.canlet.2008.03.036

Schipani, E., Wu, C., Rankin, E. B., and Giaccia, A. J. (2013). Regulation of Bone Marrow Angiogenesis by Osteoblasts during Bone Development and Homeostasis. *Front. Endocrinol. (Lausanne)* 4, 85. doi:10.3389/fendo.2013.00085

Schmiedel, B. J., Grosse-Hovest, L., and Salih, H. R. (2013). A Vicious Cycle of NK-Cell Immune Evasion in Acute Myeloid Leukemia Mediated by RANKL. *Oncoimmunology* 2 (5), e23850. doi:10.4161/onci.23850

Schofield, R. (1978). The Relationship between the Spleen colony-forming Cell and the Haemopoietic Stem Cell. *Blood Cells* 4 (1-2), 7–25.

Semenza, G. L. (2007). Life with Oxygen. *Science* 318 (5847), 62–64. doi:10.1126/science.1147949

Seyfried, A. N., Maloney, J. M., and MacNamara, K. C. (2020). Macrophages Orchestrate Hematopoietic Programs and Regulate HSC Function during Inflammatory Stress. *Front. Immunol.* 11, 1499. doi:10.3389/fimmu.2020.01499

Shafat, M. S., Gnaneswaran, B., Bowles, K. M., and Rushworth, S. A. (2017). The Bone Marrow Microenvironment - Home of the Leukemic Blasts. *Blood Rev.* 31 (5), 277–286. doi:10.1016/j.blre.2017.03.004

Shafat, M. S., Oellerich, T., Mohr, S., Robinson, S. D., Edwards, D. R., Marlein, C. R., et al. (2017). Leukemic Blasts Program Bone Marrow Adipocytes to Generate a Protumoral Microenvironment. *Blood* 129 (10), 1320–1332. doi:10.1182/blood-2016-08-734798

Shallis, R. M., Gale, R. P., Lazarus, H. M., Roberts, K. B., Xu, M. L., Seropian, S. E., et al. (2021). Myeloid Sarcoma, Chloroma, or Extramedullary Acute Myeloid Leukemia Tumor: A Tale of Misnomers, Controversy and the Unresolved. *Blood Rev.* 47, 100773. doi:10.1016/j.blre.2020.100773

Shallis, R. M., Wang, R., Davidoff, A., Ma, X., and Zeidan, A. M. (2019). Epidemiology of Acute Myeloid Leukemia: Recent Progress and Enduring Challenges. *Blood Rev.* 36, 70–87. doi:10.1016/j.blre.2019.04.005

Sheng, X., Tucci, J., Parmentier, J. H., Ji, L., Behan, J. W., Heisterkamp, N., et al. (2016). Adipocytes Cause Leukemia Cell Resistance to Daunorubicin via Oxidative Stress Response. *Oncotarget* 7 (45), 73147–73159. doi:10.18632/oncotarget.12246

Shimizu, H., Saitoh, T., Hatsumi, N., Takada, S., Handa, H., Jimbo, T., et al. (2013). Prevalence of Extramedullary Relapses Is Higher after Allogeneic Stem Cell Transplantation Than after Chemotherapy in Adult Patients with Acute Myeloid Leukemia. *Leuk. Res.* 37 (11), 1477–1481. doi:10.1016/j.leukres.2013.08.017

Shimomura, Y., Hara, M., Hirabayashi, S., Kondo, T., Mizuno, S., Uchida, N., et al. (2021). Comparison of Fludarabine, a Myeloablative Dose of Busulfan, and Melphalan vs Conventional Myeloablative Conditioning Regimen in Patients with Relapse and Refractory Acute Myeloid Leukemia in Non-remission Status. *Bone Marrow Transpl.* doi:10.1038/s41409-021-01380-0

Short, N. J., Rytting, M. E., and Cortes, J. E. (2018). Acute Myeloid Leukaemia. *Lancet* 392 (10147), 593–606. doi:10.1016/S0140-6736(18)31041-9

Sivaraj, K. K., and Adams, R. H. (2016). Blood Vessel Formation and Function in Bone. *Development* 143 (15), 2706–2715. doi:10.1242/dev.136861

Solh, M., Solomon, S., Morris, L., Holland, K., and Bashey, A. (2016). Extramedullary Acute Myelogenous Leukemia. *Blood Rev.* 30 (5), 333–339. doi:10.1016/j.blre.2016.04.001

Solinas, G., Germano, G., Mantovani, A., and Allavena, P. (2009). Tumor-associated Macrophages (TAM) as Major Players of the Cancer-Related Inflammation. *J. Leukoc. Biol.* 86 (5), 1065–1073. doi:10.1189/jlb.0609385

Solito, S., Marigo, I., Pinton, L., Damuzzo, V., Mandruzzato, S., and Bronte, V. (2014). Myeloid-derived Suppressor Cell Heterogeneity in Human Cancers. *Ann. N. Y Acad. Sci.* 1319, 47–65. doi:10.1111/nyas.12469

Song, X., Zhu, C. H., Doan, C., and Xie, T. (2002). Germline Stem Cells Anchored by Adherens Junctions in the Drosophila Ovary Niches. *Science* 296 (5574), 1855–1857. doi:10.1126/science.1069871

Spiegel, A., Shivtiel, S., Kalinkovich, A., Ludin, A., Netzer, N., Goichberg, P., et al. (2007). Catecholaminergic Neurotransmitters Regulate Migration and Repopulation of Immature Human CD34+ Cells through Wnt Signaling. *Nat. Immunol.* 8 (10), 1123–1131. doi:10.1038/ni1509

Spoo, A. C., Lübbert, M., Wierda, W. G., and Burger, J. A. (2007). CXCR4 Is a Prognostic Marker in Acute Myelogenous Leukemia. *Blood* 109 (2), 786–791. doi:10.1182/blood-2006-05-024844

Stahl, M., Shallis, R. M., Wei, W., Montesinos, P., Lengline, E., Neukirchen, J., et al. (2020). Management of Hyperleukocytosis and Impact of Leukapheresis Among Patients with Acute Myeloid Leukemia (AML) on Short- and Long-Term Clinical Outcomes: a Large, Retrospective, Multicenter, International Study. *Leukemia* 34 (12), 3149–3160. doi:10.1038/s41375-020-0783-3

Stier, S., Cheng, T., Dombkowski, D., Carlesso, N., and Scadden, D. T. (2002). Notch1 Activation Increases Hematopoietic Stem Cell Self-Renewal *In Vivo* and Favors Lymphoid over Myeloid Lineage Outcome. *Blood* 99 (7), 2369–2378. doi:10.1182/blood.v99.7.2369

Stier, S., Ko, Y., Forkert, R., Lutz, C., Neuhaus, T., Grünewald, E., et al. (2005). Osteopontin Is a Hematopoietic Stem Cell Niche Component that Negatively Regulates Stem Cell Pool Size. *J. Exp. Med.* 201 (11), 1781–1791. doi:10.1084/jem.20041992

Stucki, A., Rivier, A. S., Gikic, M., Monai, N., Schapira, M., and Spertini, O. (2001). Endothelial Cell Activation by Myeloblasts: Molecular Mechanisms of Leukostasis and Leukemic Cell Dissemination. *Blood* 97 (7), 2121–2129. doi:10.1182/blood.v97.7.2121

Sugimura, R., He, X. C., Venkatraman, A., Arai, F., Box, A., Semerad, C., et al. (2012). Noncanonical Wnt Signaling Maintains Hematopoietic Stem Cells in the Niche. *Cell* 150 (2), 351–365. doi:10.1016/j.cell.2012.05.041

Sugiyama, T., Kohara, H., Noda, M., and Nagasawa, T. (2006). Maintenance of the Hematopoietic Stem Cell Pool by CXCL12-CXCR4 Chemokine Signaling in Bone Marrow Stromal Cell Niches. *Immunity* 25 (6), 977–988. doi:10.1016/j.immuni.2006.10.016

Sugiyama, T., and Nagasawa, T. (2012). Bone Marrow Niches for Hematopoietic Stem Cells and Immune Cells. *Inflamm. Allergy Drug Targets* 11 (3), 201–206. doi:10.2174/187152812800392689

Sun, H., Li, Y., Zhang, Z. F., Ju, Y., Li, L., Zhang, B. C., et al. (2015). Increase in Myeloid-Derived Suppressor Cells (MDSCs) Associated with Minimal Residual Disease (MRD) Detection in Adult Acute Myeloid Leukemia. *Int. J. Hematol.* 102 (5), 579–586. doi:10.1007/s12185-015-1865-2

Szade, K., Gulati, G. S., Chan, C. K. F., Kao, K. S., Miyanishi, M., Marjon, K. D., et al. (2018). Where Hematopoietic Stem Cells Live: The Bone Marrow Niche. *Antioxid. Redox Signal.* 29 (2), 191–204. doi:10.1089/ars.2017.7419

Tabe, Y., Yamamoto, S., Saitoh, K., Sekihara, K., Monma, N., Ikeo, K., et al. (2017). Bone Marrow Adipocytes Facilitate Fatty Acid Oxidation Activating AMPK and a Transcriptional Network Supporting Survival of Acute Monocytic Leukemia Cells. *Cancer Res.* 77 (6), 1453–1464. doi:10.1158/0008-5472.CAN-16-1645

Taghiloo, S., and Asgarian-Omran, H. (2021). Immune Evasion Mechanisms in Acute Myeloid Leukemia: A Focus on Immune Checkpoint Pathways. *Crit. Rev. Oncol. Hematol.* 157, 103164. doi:10.1016/j.critrevonc.2020.103164

Takubo, K., Goda, N., Yamada, W., Iriuchishima, H., Ikeda, E., Kubota, Y., et al. (2010). Regulation of the HIF-1alpha Level Is Essential for Hematopoietic Stem Cells. *Cell Stem Cell* 7 (3), 391–402. doi:10.1016/j.stem.2010.06.020

Talmadge, J. E., and Gabrilovich, D. I. (2013). History of Myeloid-Derived Suppressor Cells. *Nat. Rev. Cancer* 13 (10), 739–752. doi:10.1038/nrc3581

Tang, P. M., Nikolic-Paterson, D. J., and Lan, H. Y. (2019). Macrophages: Versatile Players in Renal Inflammation and Fibrosis. *Nat. Rev. Nephrol.* 15 (3), 144–158. doi:10.1038/s41581-019-0110-2

Tavassoli, M. (1981). Structure and Function of Sinusoidal Endothelium of Bone Marrow. *Prog. Clin. Biol. Res.* 59B, 249–256.

Tokoyoda, K., Egawa, T., Sugiyama, T., Choi, B. I., and Nagasawa, T. (2004). Cellular Niches Controlling B Lymphocyte Behavior within Bone Marrow during Development. *Immunity* 20 (6), 707–718. doi:10.1016/j.immuni.2004.05.001

Traweek, S. T., Arber, D. A., Rappaport, H., and Brynes, R. K. (1993). Extramedullary Myeloid Cell Tumors. An Immunohistochemical and Morphologic Study of 28 Cases. *Am. J. Surg. Pathol.* 17 (10), 1011–1019. doi:10.1097/00000478-199310000-00006

Ugel, S., De Sanctis, F., Mandruzzato, S., and Bronte, V. (2015). Tumor-induced Myeloid Deviation: when Myeloid-Derived Suppressor Cells Meet Tumor-Associated Macrophages. *J. Clin. Invest.* 125 (9), 3365–3376. doi:10.1172/JCI80006

Vacca, P., Vitale, C., Montaldo, E., Conte, R., Cantoni, C., Fulcheri, E., et al. (2011). CD34+ Hematopoietic Precursors Are Present in Human Decidua and Differentiate into Natural Killer Cells upon Interaction with Stromal Cells. *Proc. Natl. Acad. Sci. U S A.* 108 (6), 2402–2407. doi:10.1073/pnas.1016257108

Varol, C., Mildner, A., and Jung, S. (2015). Macrophages: Development and Tissue Specialization. *Annu. Rev. Immunol.* 33, 643–675. doi:10.1146/annurev-immunol-032414-112220

Vidal, P. M., and Pacheco, R. (2020). The Cross-Talk between the Dopaminergic and the Immune System Involved in Schizophrenia. *Front. Pharmacol.* 11, 394. doi:10.3389/fphar.2020.00394

Vigon, I., Mornon, J. P., Cocault, L., Mitjavila, M. T., Tambourin, P., Gisselbrecht, S., et al. (1992). Molecular Cloning and Characterization of MPL, the Human Homolog of the V-Mpl Oncogene: Identification of a Member of the Hematopoietic Growth Factor Receptor Superfamily. *Proc. Natl. Acad. Sci. U S A.* 89 (12), 5640–5644. doi:10.1073/pnas.89.12.5640

Waclawiczek, A., Hamilton, A., Rouault-Pierre, K., Abarrategi, A., Albornoz, M. G., Miraki-Moud, F., et al. (2020). Mesenchymal Niche Remodeling Impairs Hematopoiesis via Stanniocalcin 1 in Acute Myeloid Leukemia. *J. Clin. Invest.* 130 (6), 3038–3050. doi:10.1172/JCI133187

Wahl, S. M., Wen, J., and Moutsopoulos, N. (2006). TGF-beta: a mobile Purveyor of Immune Privilege. *Immunol. Rev.* 213, 213–227. doi:10.1111/j.1600-065X.2006.00437.x

Wang, A., and Zhong, H. (2018). Roles of the Bone Marrow Niche in Hematopoiesis, Leukemogenesis, and Chemotherapy Resistance in Acute Myeloid Leukemia. *Hematology* 23 (10), 729–739. doi:10.1080/10245332.2018.1486064

Wang, Z. Y., and Chen, Z. (2008). Acute Promyelocytic Leukemia: from Highly Fatal to Highly Curable. *Blood* 111 (5), 2505–2515. doi:10.1182/blood-2007-07-102798

Warrell, R. P., de Thé, H., Wang, Z. Y., and Degos, L. (1993). Acute Promyelocytic Leukemia. *N. Engl. J. Med.* 329 (3), 177–189. doi:10.1056/NEJM199307153290307

Weber, R., Groth, C., Lasser, S., Arkhypov, I., Petrova, V., Altevogt, P., et al. (2021). IL-6 as a Major Regulator of MDSC Activity and Possible Target for Cancer Immunotherapy. *Cell Immunol.* 359, 104254. doi:10.1016/j.cellimm.2020.104254

Wei, A. H., Montesinos, P., Ivanov, V., DiNardo, C. D., Novak, J., Laribi, K., et al. (2020). Venetoclax Plus LDAC for Newly Diagnosed AML Ineligible for

Intensive Chemotherapy: a Phase 3 Randomized Placebo-Controlled Trial. *Blood* 135 (24), 2137–2145. doi:10.1182/blood.2020004856

Wei, W. C., Lin, S. Y., Lan, C. W., Huang, Y. C., Lin, C. Y., Hsiao, P. W., et al. (2016). Inhibiting MDSC Differentiation from Bone Marrow with Phytochemical Polyacetylenes Drastically Impairs Tumor Metastasis. *Sci. Rep.* 6, 36663. doi:10.1038/srep36663

Weinberg, O. K., Hasserjian, R. P., Baraban, E., Ok, C. Y., Geyer, J. T., S.S Philip, J. K., et al. (2019). Clinical, Immunophenotypic, and Genomic Findings of Acute Undifferentiated Leukemia and Comparison to Acute Myeloid Leukemia with Minimal Differentiation: a Study from the Bone Marrow Pathology Group. *Mod. Pathol.* 32 (9), 1373–1385. doi:10.1038/s41379-019-0263-3

Weiss, L. (1976). The Hematopoietic Microenvironment of the Bone Marrow: an Ultrastructural Study of the Stroma in Rats. *Anat. Rec.* 186 (2), 161–184. doi:10.1002/ar.1091860204

Winkler, I. G., Barbier, V., Nowlan, B., Jacobsen, R. N., Forristal, C. E., Patton, J. T., et al. (2012). Vascular Niche E-Selectin Regulates Hematopoietic Stem Cell Dormancy, Self Renewal and Chemoresistance. *Nat. Med.* 18 (11), 1651–1657. doi:10.1038/nm.2969

Winkler, I. G., Sims, N. A., Pettit, A. R., Barbier, V., Nowlan, B., Helwani, F., et al. (2010). Bone Marrow Macrophages Maintain Hematopoietic Stem Cell (HSC) Niches and Their Depletion Mobilizes HSCs. *Blood* 116 (23), 4815–4828. doi:10.1182/blood-2009-11-253534

Wright, D. E., Wagers, A. J., Gulati, A. P., Johnson, F. L., and Weissman, I. L. (2001). Physiological Migration of Hematopoietic Stem and Progenitor Cells. *Science* 294 (5548), 1933–1936. doi:10.1126/science.1064081

Wynn, T. A., and Vannella, K. M. (2016). Macrophages in Tissue Repair, Regeneration, and Fibrosis. *Immunity* 44 (3), 450–462. doi:10.1016/j.immuni.2016.02.015

Yamazaki, S., Ema, H., Karlsson, G., Yamaguchi, T., Miyoshi, H., Shioda, S., et al. (2011). Nonmyelinating Schwann Cells Maintain Hematopoietic Stem Cell Hibernation in the Bone Marrow Niche. *Cell* 147 (5), 1146–1158. doi:10.1016/j.cell.2011.09.053

Yang, X., Feng, W., Wang, R., Yang, F., Wang, L., Chen, S., et al. (2018). Repolarizing Heterogeneous Leukemia-Associated Macrophages with More M1 Characteristics Eliminates Their Pro-leukemic Effects. *Oncoimmunology* 7 (4), e1412910. doi:10.1080/2162402X.2017.1412910

Yaseen, M. M., Abuharfeil, N. M., Darmani, H., and Daoud, A. (2020). Mechanisms of Immune Suppression by Myeloid-Derived Suppressor Cells: the Role of Interleukin-10 as a Key Immunoregulatory Cytokine. *Open Biol.* 10 (9), 200111. doi:10.1098/rsob.200111

Yin, T., and Li, L. (2006). The Stem Cell Niches in Bone. *J. Clin. Invest.* 116 (5), 1195–1201. doi:10.1172/JCI28568

Yoshihara, H., Arai, F., Hosokawa, K., Hagiwara, T., Takubo, K., Nakamura, Y., et al. (2007). Thrombopoietin/MPL Signaling Regulates Hematopoietic Stem Cell Quiescence and Interaction with the Osteoblastic Niche. *Cell Stem Cell* 1 (6), 685–697. doi:10.1016/j.stem.2007.10.020

Yusop, N., Battersby, P., Alraies, A., Sloan, A. J., Moseley, R., and Waddington, R. J. (2018). Isolation and Characterisation of Mesenchymal Stem Cells from Rat Bone Marrow and the Endosteal Niche: A Comparative Study. *Stem Cell Int.* 2018, 6869128. doi:10.1155/2018/6869128

Zeng, Z., Shi, Y. X., Samudio, I. J., Wang, R. Y., Ling, X., Frolova, O., et al. (2009). Targeting the Leukemia Microenvironment by CXCR4 Inhibition Overcomes Resistance to Kinase Inhibitors and Chemotherapy in AML. *Blood* 113 (24), 6215–6224. doi:10.1182/blood-2008-05-158311

Zhang, C. C., and Sadek, H. A. (2014). Hypoxia and Metabolic Properties of Hematopoietic Stem Cells. *Antioxid. Redox Signal.* 20 (12), 1891–1901. doi:10.1089/ars.2012.5019

Zhang, J., Ye, J., Ma, D., Liu, N., Wu, H., Yu, S., et al. (2013). Cross-talk between Leukemic and Endothelial Cells Promotes Angiogenesis by VEGF Activation of the Notch/Dll4 Pathway. *Carcinogenesis* 34 (3), 667–677. doi:10.1093/carcin/bgs386

Zhang, P., Zhang, C., Li, J., Han, J., Liu, X., and Yang, H. (2019). The Physical Microenvironment of Hematopoietic Stem Cells and its Emerging Roles in Engineering Applications. *Stem Cel. Res. Ther.* 10 (1), 327. doi:10.1186/s13287-019-1422-7

Conflict of Interest: The authors declare that the research was conducted in the absence of any commercial or financial relationships that could be construed as a potential conflict of interest.

Publisher's Note: All claims expressed in this article are solely those of the authors and do not necessarily represent those of their affiliated organizations, or those of the publisher, the editors and the reviewers. Any product that may be evaluated in this article, or claim that may be made by its manufacturer, is not guaranteed or endorsed by the publisher.

frontiers in Cell and Developmental Biology

ORIGINAL RESEARCH
published: 06 December 2021
doi: 10.3389/fcell.2021.785410

Prognostic Immunophenotyping Clusters of Clear Cell Renal Cell Carcinoma Defined by the Unique Tumor Immune Microenvironment

Wenhao Xu[1†], Aihetaimujiang Anwaier[1†], Chunguang Ma[1†], Wangrui Liu[2†], Xi Tian[1], Jiaqi Su[1], Wenkai Zhu[1], Guohai Shi[1], Shiyin Wei[2], Hong Xu[2], Yuanyuan Qu[1]*, Dingwei Ye[1]* and Hailiang Zhang[1]**

[1]Department of Urology, Fudan University Shanghai Cancer Center, Shanghai Medical College, Fudan University, Shanghai, China, [2]Affiliated Hospital of Youjiang Medical University for Nationalities, Baise, China

Background: The tumor microenvironment affects the occurrence and development of cancers, including clear cell renal cell carcinoma (ccRCC). However, how the immune contexture interacts with the cancer phenotype remains unclear.

Methods: We identified and evaluated immunophenotyping clusters in ccRCC using machine-learning algorithms. Analyses for functional enrichment, DNA variation, immune cell distribution, association with independent clinicopathological features, and predictive responses for immune checkpoint therapies were performed and validated.

Results: Three immunophenotyping clusters with gradual levels of immune infiltration were identified. The intermediate and high immune infiltration clusters (Clusters B and C) were associated with a worse prognosis for ccRCC patients. Tumors in the immune-hot Clusters B and C showed pro-tumorigenic immune infiltration, and these patients showed significantly worse survival compared with patients in the immune-cold Cluster A in the training and testing cohorts (n = 422). In addition to distinct immune cell infiltrations of immunophenotyping, we detected significant differences in DNA variation among clusters, suggesting a high degree of genetic heterogeneity. Furthermore, expressions of multiple immune checkpoint molecules were significantly increased. Clusters B and C predicted favorable outcomes in 64 ccRCC patients receiving immune checkpoint therapies from the FUSCC cohort. In 360 ccRCC patients from the FUSCC validation cohort, Clusters B and C significantly predicted worse prognosis compared with Cluster A. After immunophenotyping of ccRCC was confirmed, significantly increased tertiary lymphatic structures, aggressive phenotype, elevated glycolysis and PD-L1 expression, higher abundance of $CD8^+$ T cells, and TCRn cell infiltration were found in the immune-hot Clusters B and C.

OPEN ACCESS

Edited by:
Ana Karina Oliveira,
University of Virginia, United States

Reviewed by:
Patrick Lizotte,
Dana–Farber Cancer Institute, United States
Jianfeng Yang,
Shanghai University of Traditional Chinese Medicine, China
Youyang Shi,
Shanghai University of Traditional Chinese Medicine, China

***Correspondence:**
Hong Xu
295833493@qq.com
Yuanyuan Qu
quyy1987@163.com
Dingwei Ye
dwyelie@163.com
Hailiang Zhang
zhanghl918@163.com

[†]These authors have contributed equally to this work

Specialty section:
This article was submitted to Molecular and Cellular Pathology, a section of the journal Frontiers in Cell and Developmental Biology

Received: 29 September 2021
Accepted: 29 October 2021
Published: 06 December 2021

Citation:
Xu W, Anwaier A, Ma C, Liu W, Tian X, Su J, Zhu W, Shi G, Wei S, Xu H, Qu Y, Ye D and Zhang H (2021) Prognostic Immunophenotyping Clusters of Clear Cell Renal Cell Carcinoma Defined by the Unique Tumor Immune Microenvironment. Front. Cell Dev. Biol. 9:785410. doi: 10.3389/fcell.2021.785410

Abbreviations: ccRCC, clear cell renal cell carcinoma; CI, confidence interval; CNV, copy numbers variation; DEGs, differentially expressed genes; EMT, epithelial mesenchymal transitions; FUSCC, Fudan University Shanghai Cancer Center; GSEA, gene set enrichment analysis; HE, hematoxylin-eosin; HR, hazard ratio; ICTs, immune checkpoint therapies; IHC, immunohistochemistry; MSI, microsatellite instability; RCC, renal cell carcinoma; SNP, single nucleotide polypeptides; TLS, Tertiary lymphoid structure; TME, tumor microenvironment; TKIs, tyrosine kinase inhibitors.

Conclusion: This study described immunophenotyping clusters that improved the prognostic accuracy of the immune contexture in the ccRCC microenvironment. Our discovery of the novel independent prognostic indicators in ccRCC highlights the relationship between tumor phenotype and immune microenvironment.

Keywords: clear cell renal cell carcinoma, immunophenotyping, immune checkpoint therapies, prognosis (carcinoma), tumor microenvironment, machine-learning algorithms

HIGHLIGHTS

- This study identified immunophenotyping clusters that show the prognostic accuracy of the immune contexture in the ccRCC microenvironment.
- The immune-hot Clusters B and C showed a transcriptional signature indicative of pro-tumorigenic immune infiltration and show significantly worse survival compared with the immune-cold Cluster A.
- Our discovery of the novel independent prognostic indicators in ccRCC highlights the relationship between tumor phenotype and the immune contexture.

INTRODUCTION

Renal cell carcinoma (RCC) is one of the most common malignant tumors of the genitourinary system, accounting for about 5% of all new cases in adult male patients and 3% of new cases in female patients (Siegel et al., 2020). RCC is classified into three main histological subtypes, including clear cell RCC (ccRCC), papillary RCC, and chromophobe RCC, which are considered to arise from different cell types in the nephron (Linehan, 2012; Moch et al., 2016; Hsieh et al., 2017). ccRCC is the predominant subtype of RCC, accounting for 70%–85% of all RCC patients, and is highly malignant (Gerlinger et al., 2012; Miller et al., 2019). Although classic histological heterogeneity has been widely accepted in the research and treatment of RCC, the latest advances in genomic technologies have revealed different clinically relevant molecular subtypes, which have aided in elucidating the molecular basis of RCC as well as mechanisms underlying the occurrence and development of RCC. These findings have led to improved targeted treatment measures for patients with RCC.

Although satisfactory prognosis of localized ccRCC can be achieved through radical or nephron-preserving nephrectomy, metastatic or advanced ccRCC requires systematic treatment strategies (Hofmann et al., 2020). The standard first-line systematic treatment for metastatic or advanced ccRCC includes tyrosine kinase inhibitors (TKIs) such as sunitinib or pazopanib that target the vascular endothelial growth factor receptor (VEGFR) (Motzer et al., 2007; Escudier et al., 2019; Porta et al., 2019). While anti-angiogenic drugs effectively inhibit tumor proliferation and prolong the overall survival of low-risk ccRCC patients, the objective response rate of these treatments is unsatisfactory (Heng et al., 2009; Motzer et al., 2009; Sternberg et al., 2010). Recently, new immune checkpoint therapies (ICTs) represented by PD-1/PD-L1 and CTLA-4 inhibitors have been demonstrated in clinical trials as treatments for ccRCC (Motzer et al., 2019). However, because of the high tumor heterogeneity and low somatic mutation burden of ccRCC, an accurate and effective model for the prediction of clinical treatment is required (Grimm et al., 2019; Kotecha et al., 2019).

To reveal the underlying molecular heterogeneity of ccRCC, Brannon et al. analyzed the transcriptional expression profiles of 48 ccRCC patients and identified two molecular subtypes of ccRCC (ccA and ccB) (Brannon et al., 2010). A meta-analysis of large-scale ccRCC subsequently confirmed this classification and identified a new subtype (cluster_3) associated with von Hippel-Lindau (VHL) gene mutation (Brannon et al., 2012). The Cancer Genomic Atlas (TCGA) analyzed extensive transcriptional profiles of ccRCC patients and recognized four molecular subtypes of ccRCC (m1–m4) with various somatic mutations and distinct prognosis (Cancer Genome Atlas Research Network, 2013). In the metastatic setting, four molecular subtypes (ccrcc1–4) related to the objective response rate and overall survival (OS) of angiogenesis inhibitors sunitinib and pazopanib were identified. These subtypes differ not only in mRNA expression profiles but also in somatic mutations, methylation status, and immune cell infiltration in the tumor microenvironment (TME) (Beuselinck et al., 2015).

The cells and molecules in the TME are in a process of dynamic change, reflecting the evolutionary nature of cancer, and together these factors promote the proliferation, apoptosis, metastasis, and immune escape of cancer cells (Fridman et al., 2017). A large amount of evidence has shown that not only does the efficacy of immunotherapy depend on activation of the tumor immune microenvironment, but the efficacy of traditional targeted therapy also depends on the strength of the individual antitumor immune response (Fridman et al., 2017; Kawakami et al., 2017). ICTs combined with TKIs effectively inhibit the occurrence and development of advanced ccRCC and induces the normalization of antitumor immunity, which depends on a deep understanding of the interaction between tumor cells and TME (Chen and Mellman, 2017). ccRCC patients are mainly of immune infiltrating type (73%), enriched with antitumor M1 macrophages, activated CD^{4+} memory T cells, and activated NK cells, but the immune contexture failed to accurately predict the efficacy of anti-PD-1 therapy and mTOR inhibitors (Braun et al., 2020). Our previous studies identified a relationship between immune component infiltration in TME and prognosis of ccRCC patients as well as TME regulatory cytokines and emphasized the role of TME-related markers in the prognosis of ccRCC patients; our findings also supported the use of precise immunotherapy for high-risk ccRCC patients (Xu et al., 2019). Therefore, exploring the underlying mechanism of TME-driven tumorigenesis and

development is of great significance for developing potential therapeutic prediction models, improving the effectiveness of existing treatment strategies, and discovering novel precise targets for ccRCC treatment.

The TME affects the development, occurrence, and treatment resistance of cancers including ccRCC. However, how the immune cell mixture interacts with the cancer phenotype and affects pathogenesis remains unclear. We therefore sought to identify novel immunophenotyping subtypes of ccRCC that may help improve the prognostic accuracy and of immune contexture in the ccRCC microenvironment based on large-scale data, with the aim of providing a theoretical basis for the development of individual precise treatment strategies of ICTs.

METHODS

Data download and preprocessing from the training, testing, and validation cohorts

The RNA sequencing data of 531 ccRCC patients were obtained from The Cancer Genome Atlas (TCGA, https://portal.gdc.cancer.gov) with gene IDs converted from Ensembl ID to gene symbol matrix. The FPKM gene expression profile was measured experimentally using the Illumina HiSeq 2000 RNA Sequencing platform by the University of North Carolina TCGA genome characterization center. Level 3 data were downloaded from the TCGA data coordination center, with available clinicopathological and survival data. In addition, the phenotypic and clinical data of 531 ccRCC patients were obtained from the TCGA training cohort and 91 ccRCC patients from the International Cancer Genome Consortium (ICGC, https://dcc.icgc.org/) testing cohort. A total of 770 genes were downloaded from The nCounter® PanCancer Immune Profiling panel (https://www.nanostring.com/products/ncounter-assays-panels/oncology/pancancer-immune-profiling/) and 758 immune genes were matched in the TCGA database for further analysis (Cesano, 2015).

A total of 64 ccRCC patients receiving ICTs alone or combined with TKI treatments were enrolled from the Fudan University Shanghai Cancer Center (FUSCC, Shanghai, China) cohort. A total of 360 ccRCC patients with long-term follow-up information from FUSCC cohort were enrolled as prognostic validation cohort of immunophenotyping clusters.

Construction of immune-phenotyping and subgroup analysis

To identify prognostic clusters based on tumor immune microenvironment features, we enrolled large-scale ccRCC cohorts with available RNA-seq data and constructed immune clusters based on 758 immune genes; the association between the immune clusters and tumor heterogeneity was then explored.

The correlation matrix was calculated based on the expression of 758 genes. The R "pheatmap" package was utilized to hierarchically cluster the correlation matrix of patients, where the correlation was used as the clustering distance and ward.D as a link (Galili et al., 2018). Besides, cutree function was utilized to identify subgroups of ccRCC samples. In order to determine the optimal number of clusters for each queue, "Cluster" package of R software was used to perform a contour analysis on KMeans. The subgroup myeloid infiltration score, dryness index score, immune score, and mutation were calculated, and the survival analysis of the subgroups was performed using the Kaplan–Meier method.

Construction of a classifier to predict immunophenotyping clusters

Next, the immunophenotyping clusters were established using a machine-learning algorithm and used to categorize ccRCC patients for easier clinical application. Immune subgroups were predicted by binomial logistic regression using R software "glmnet" package (Engebretsen and Bohlin, 2019), which could assign samples divided into groups without unsupervised clustering. The risks score of 28 hub immune genes used for predicting immunophenotying clusters of ccRCC are shown in the supplementary tables and mentioned in the results section.

The binomial distribution was used to develop a logistic regression predicting the classification based on the gene expression profile. Besides, operating characteristic curve (ROC) curves were plotted using the R software "pROC" package. The area under the curve (AUC) is used to evaluate the specificity and sensitivity of the clusters. Logistic regression coefficients were used to calculate the risk scores of each ccRCC sample.

Assessment of immune cell infiltration

To assess the absolute proportion of 22 infiltrating immune cells in ccRCC samples from TCGA, we performed the CIBERSORT algorithm (Chen et al., 2018). As a deconvolution algorithm, CIBERSORT utilizes a set of reference gene expression values (547 genes) to predict the proportion of immune cell types using support vector regression. In order to evaluate the reliability of the deconvolution method, the "CIBERSORT" R package provides a p value for each sample using a default feature matrix with perm = 100 times for analysis.

Single sample gene set enrichment analysis

The GSVA Bioconductor R package was used for genome functional enrichment analysis. The C2 and hallmark datasets were downloaded from the MSigDB database (https://www.gsea-msigdb.org/gsea/msigdb), collecting a variety of function annotations including epithelial–mesenchymal transitions (EMTs), stem cell proliferation, and cell cycle-related pathways.

Assessment of DNA variation

The single-nucleotide polypeptide (SNP) data and MAF profile of ccRCC patients were downloaded from FireBrowse (http://firebrowse.org/) and analyzed using the R "maftools" package. The copy number variation (CNV) data with level 3 was downloaded from Broad Institute and analyzed using the GISTIC2 module in the GenePattern cloud platform, with Reference Genome Fileselects selecting "hg19."

Assessment of immunotherapy efficacy and long-term prognostic implications

Differential immune checkpoint molecular expression, including PD-L1, PD-L2, LAG-3, IL-8, PDCD1, CTLA4, and TIGIT, and PBRM1 expression were enrolled between immunophenotyping clusters. Then, we enrolled 35 ccRCC patients receiving ICTs from the CA209-009 cohort with gene-specific enrichment in clinical benefits. Moreover, RT-qPCR was utilized to evaluate the relative expression of hub genes and immunophenotyping clusters. A total of 64 ccRCC patients receiving ICTs alone or combined with TKI treatments were enrolled from the Fudan University Shanghai Cancer Center (FUSCC, Shanghai, China) cohort. A total of 360 ccRCC patients with long-term follow-up information from the FUSCC cohort were enrolled as a prognostic validation cohort of immunophenotyping clusters.

Evaluation of tumor immune microenvironment characterizations

The tertiary lymphoid structure (TLS) was assessed using hematoxylin–eosin (HE) staining, and immunohistochemistry (IHC) was utilized to evaluate the expression level of Ki-67 (ab15580; Abcam), Glut-1 (ab115730; Abcam), and PD-L1 (ab205921; Abcam) according to procedures, as previously described (Wang et al., 2020). Then, an opal multispectral was used to identify differential immune cell infiltration. CD3 (Kit-0003, Maxim, Shenzhen, China), CD4, (RMA-0620, Maxim, China), CD8 (RMA-0514, Maxim, China), CK (Kit-0009, Maxim, China), FoxP3 (98377, CST), and PD-L1 (13684, CST) antibodies were added to the slide and incubated overnight in a humidified chamber at 4°C. An HRP-labeled goat anti-rabbit/mouse secondary antibody was added dropwise and incubated at 37°C for 30 min. Finally, the slices are imaged and quantitatively analyzed on a multispectral imaging system (Vectra® Polaris™, Shanghai, China).

Statistical analysis

In the statistical analyses, the Wilcox test was used to compare the differences between the two groups of samples. The survminer of the R package and X-tile, a single-function software developed by Yale University, were utilized to take the best cutoff value for all survival analyses. The survival curve was analyzed by Kaplan–Meier, and the log-rank test was used to determine the significance of the difference. The receiver operating characteristic (ROC) is used to evaluate prediction sensitivity and specificity of immunophenotyping clusters in the disease progression, and the AUC is used to evaluate the specificity and sensitivity of the model.

RESULTS

The TME has been implicated in various malignant biological processes, including carcinogenesis, irregular cellular metabolism, and abnormal immune regulation. This study was conducted in three phases to explore immunophenotyping clusters of ccRCC, and the study flow is shown in **Figure 1**. First, we enrolled large-scale ccRCC cohorts with available RNA-seq data and constructed immune clusters based on 758 immune genes; the association between the immune clusters and tumor heterogeneity was then explored. Second, the immunophenotyping clusters were established using a machine-learning algorithm and used to categorize ccRCC patients; the clusters showed differences in DNA variation, functional enrichment, clinical features, survival benefits, immunotherapy responses, immune cell distribution, and the tumor immune microenvironment *in silico*. Third, immunophenotyping clusters were used to estimate TME characterizations, long-term prognosis, and predictive responses to ICTs for ccRCC patients from public to real-world validation cohorts.

Screening and initial construction of subgroups based on 758 immune genes

First, we matched immune genes in the nCounter® PanCancer Immune Profiling panel with those in transcriptome data from the TCGA database and obtained the expression profile of 758 immune genes (**Supplementary Table S1A,B**). We then obtained the correlation matrix, hierarchically clustered the correlation matrix of ccRCC patients, and confirmed three subgroups (Clusters A, B, and C) as the optimal clustering (**Figures 2A,B**; **Supplementary Table S1C**). We enrolled traditional clinicopathological indicators of 531 ccRCC samples from the TCGA database and found that the expression of immune genes in Cluster C patients was markedly higher than that of the other two subgroups, and the expression of immune genes in Cluster A was at an intermediate level (**Figure 2C**).

Relation between immune clusters and tumor heterogeneity of ccRCC

We next analyzed the immune clusters and tumor heterogeneity information at genetic and epigenetic levels (**Figure 3A**). The results indicated that VHL and PBRM1 genes were the most frequently mutated genes in ccRCC, and Cluster A showed a relatively higher mutation rate than Clusters B and C. We also performed subgroup analysis of ccRCC and found significantly differential heterogeneity in methylation, miRNA, and mRNA levels among the three subgroups ($p < 0.05$). Next, we measured the myeloid infiltration score (StromalScore), immune score (ImmuneScore), tumor purity (ESTIMATEScore), and stemness index score (mRNAsi) among subgroups based on RNA expression data from the TCGA database (**Figures 3B–E**; **Supplementary Table S2A**). Overall, these results revealed significant differences in tumor heterogeneity among the three immune clusters using the Kruskal–Wallis test ($p < 0.001$).

Immune clusters predict outcomes of ccRCC in training and testing cohorts

We analyzed the prognosis of the three immune subgroups and found that patients in Clusters B and C showed similar outcomes

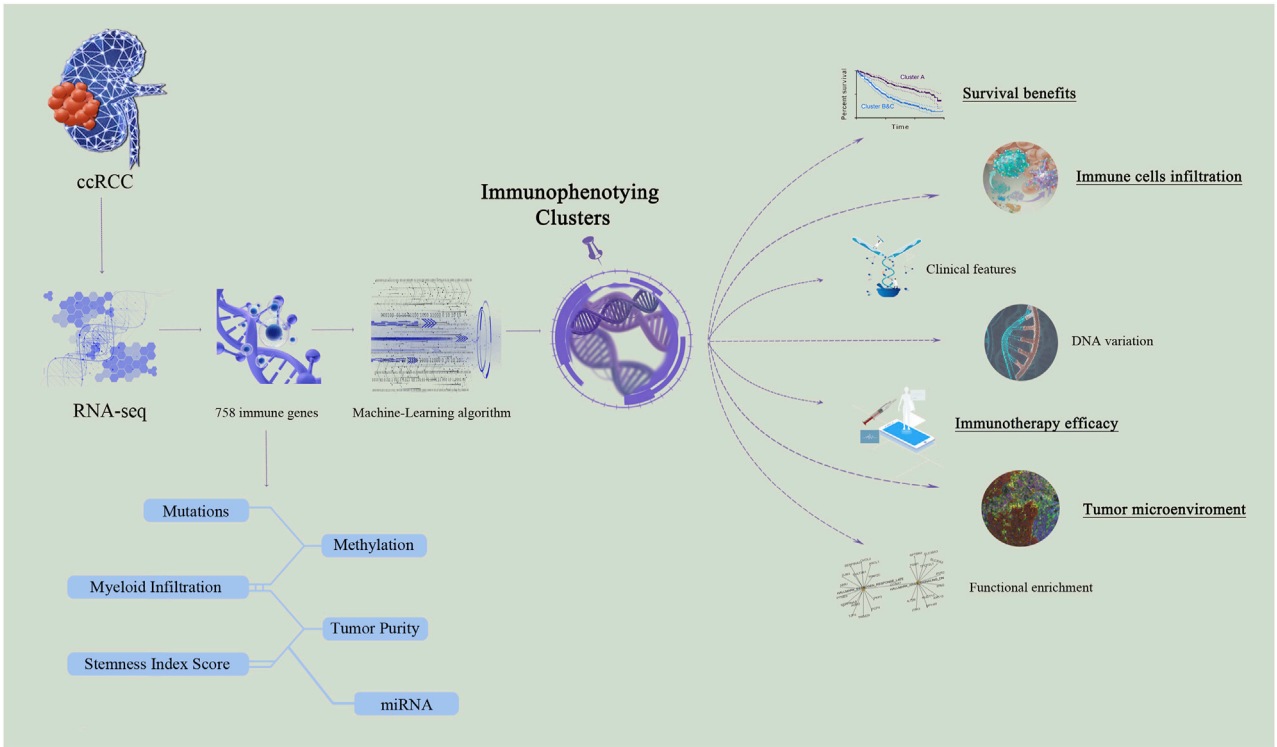

FIGURE 1 | Computational and experimental workflow for immunophenotyping clusters.

and significantly poorer survival compared with Cluster A (p < 0.0001; **Figure 3F**). We then combined Clusters B and Clusters C into the newly defined Clusters B and C (**Supplementary Table S2B**) and compared the prognosis between Cluster A and Cluster B and C. The results revealed markedly poor survival in Clusters B and C compared with Cluster A (p < 0.0001; **Figure 3G**). To validate the prognostic value of the immune clusters, we enrolled 91 ccRCC patients with available RNA-seq data from the ICGC cohort (**Figure 3H**; **Supplementary Table S3**). The clinical outcomes among three subgroups showed no significant differences (p = 0.085; **Figure 3I**). However, significantly poorer prognosis was observed in Clusters B and C compared with Cluster A (p = 0.049; **Figure 3J**).

Construction of a classifier to predict immune subgroups using machine-learning algorithms

To further explore differences between the subgroups and improve the clinical translational efficacy, we implemented a series of machine-learning algorithms to develop a simple predictor predicting immune clusters, thereby randomly assigning all samples to the group with poor or good prognosis until the best prediction efficiency is obtained. A total of 28 hub immune genes were identified for the prognostic predictor for subgroup classification, named immunophenotyping clusters (AUC = 0.914; **Figure 4A**; **Supplementary Table S4A**). As shown in **Supplementary Figure S3**, we summarized prognostic implications of significant hub immune genes in ccRCC. The K–M survival analysis emphasized the prognostic significance of SOCS1, SAA1, TLR3, PRKCE, HNRNPA2B1, PDCD1, IL1R2, FCGR1A, CD36, CASP3, CARD11, and BCL2 as cancer-promoting factors of ccRCC. For the training set samples, immunophenotyping clustering was used to analyze whether the samples belonged to Cluster A or Clusters B and C. Through model prediction, 91.9% of the samples were assigned to Cluster A, and 90.8% of samples were assigned to clusters B and C (**Figure 4B**; **Supplementary Table S4B**). We observed significant differences in survival between the immunophenotyping clusters of ccRCC patients (p < 0.0001; **Figure 4C**). The logistic regression coefficient was further used to calculate the risk score of each sample; the risk score of Clusters B and C was significantly higher than that of Cluster A (p < 2e-16; **Figure 4D**; **Supplementary Table S4C**).

Clinicopathological characteristics of immunophenotyping clusters

Next, we analyzed the differences of various clinical indicators in the different immunophenotyping clusters. Interestingly, we found a significantly decreased tumor purity in Clusters B and C, which showed with worse prognosis, compared with Cluster A (p = 2.9e-08; **Supplementary Figure S2A**). The methylation and mRNA expression levels of CDKN2A in Clusters B and C were significantly higher than in Cluster A (p < 1e-04; **Supplementary**

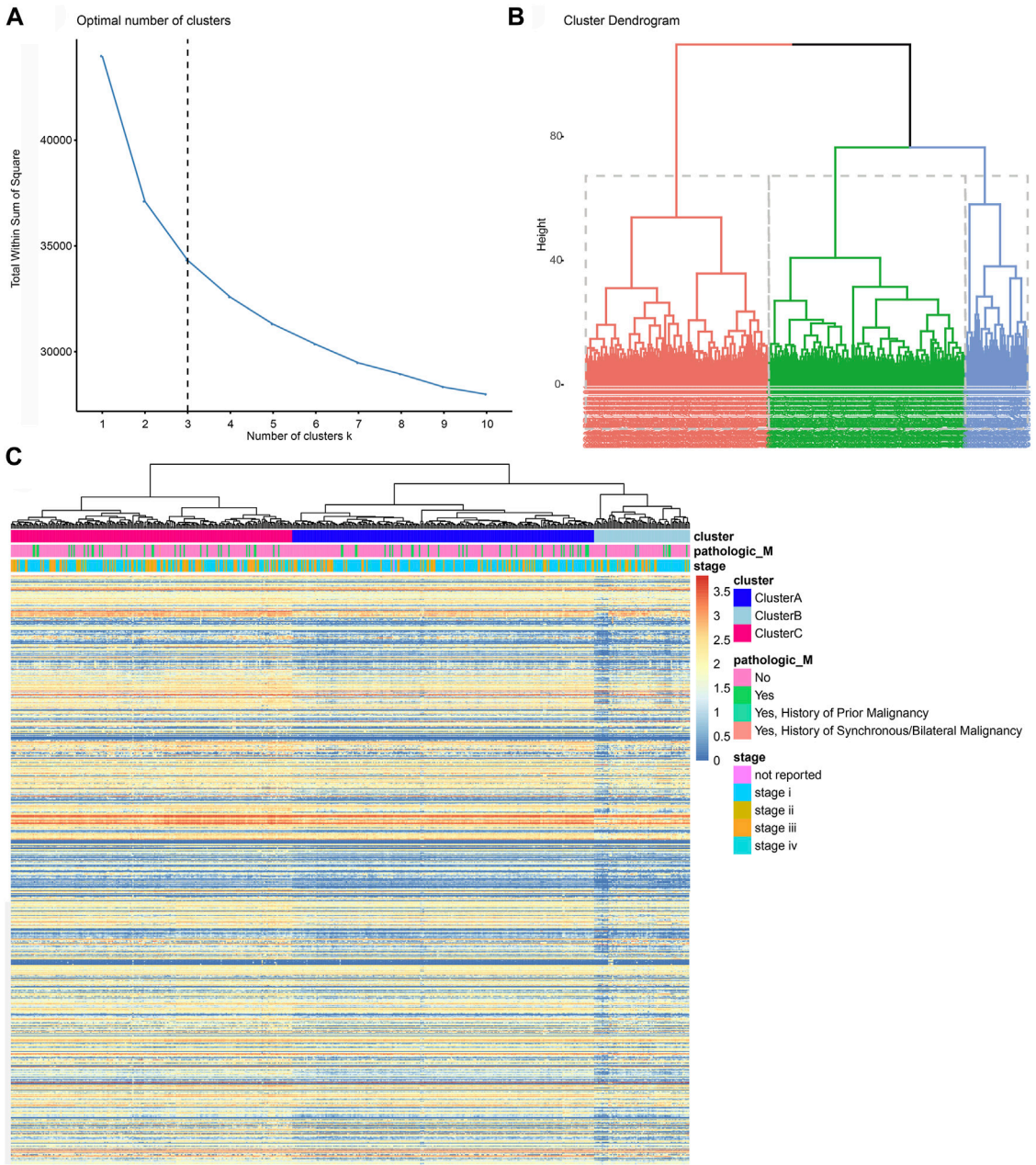

FIGURE 2 | Screening and initial construction of subgroups based on 758 immune genes. **(A, B)** Hierarchically clustering of 758 immune genes from the nCounter® PanCancer Immune Profiling panel. **(C)** Construction of subgroups based on 758 immune genes enrolled traditional clinicopathological indicators of 531 ccRCC samples from the TCGA database.

Figure S2B,C), while the total number of mutations between the two clusters did not show significant differences (p = 0.16; **Supplementary Figure S2D**).

We also analyzed other phenotypic indicators between the immunophenotyping clusters, such as sex, age, tumor stage, smoking status, microsatellite instability (MSI), resection, or biopsy site. We found significantly more ccRCC patients from Clusters B and C in the smoker group and fewer patients from Clusters B and C in the non-smoker group (p < 0.05; **Supplementary Figure S2E**). Clusters B and C also showed a significantly elevated risk score compared with Cluster A regardless of smoking status (p < 0.001; **Supplementary Figure S2F**). Significantly higher numbers of male patients were present in Clusters B and C (p < 0.05; **Supplementary Figure S2G**). MSI and age did not show differences in the two subgroups (p < 0.05; **Supplementary Figure S2H,I**). As shown in **Supplementary Figure S2J**, more patients from Clusters B and C were in advanced stages compared with patients in Cluster A.

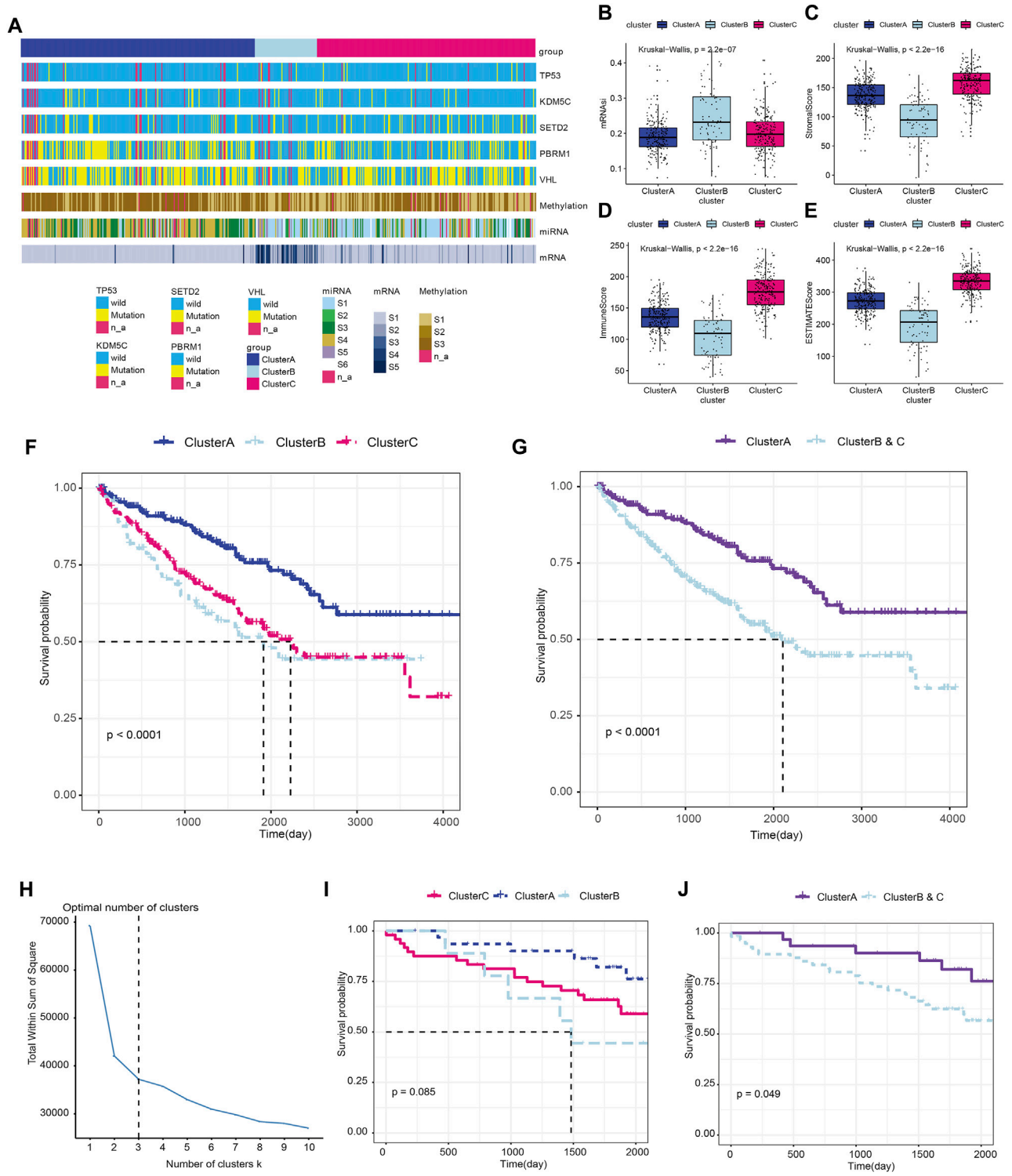

FIGURE 3 | Immune clusters predict tumor heterogeneity and outcomes of ccRCC in training and testing cohorts. **(A)** Association between the immune clusters and tumor heterogeneity in genetic and epigenetic levels. **(B–E)** The myeloid infiltration score (StromalScore), immune score (ImmuneScore), tumor purity (ESTIMATEScore), and stemness index score (mRNAsi) based on RNA expression data from the TCGA database were measured among subgroups using the Kruskal–Wallis test. **(F)** Prognosis was compared in the three immune subgroups in the TCGA-ccRCC cohort. **(G)** Prognosis was compared between Cluster A and the newly defined Clusters B and C in the training cohort. **(H–J)** Prognostic value of the immune clusters in 91 ccRCC patients from the ICGC testing cohort.

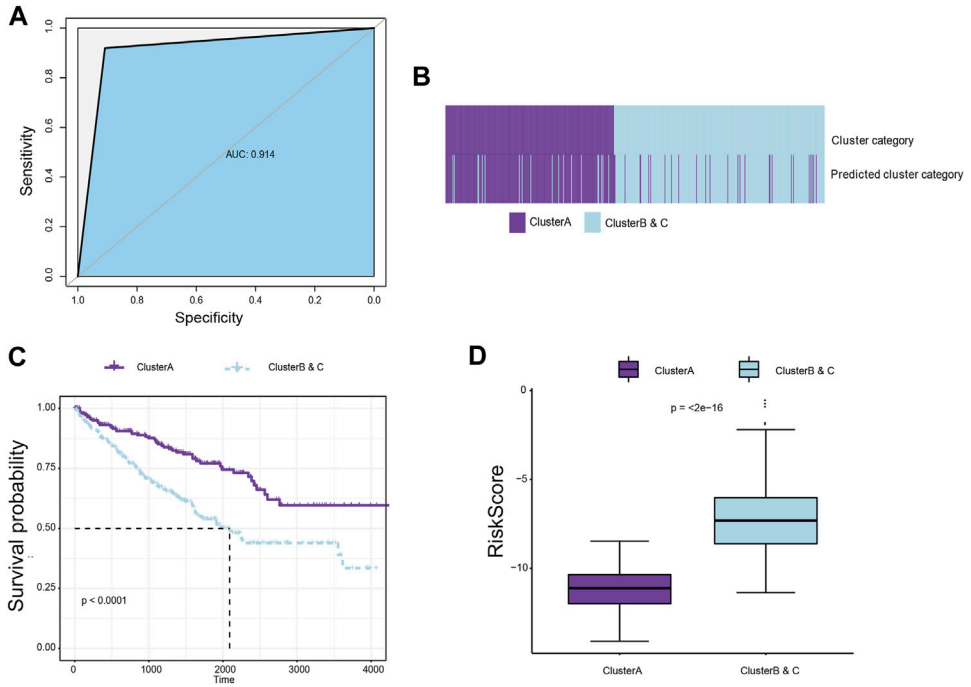

FIGURE 4 | Construction of a classifier to predict immune subgroups using machine-learning algorithms. **(A)** Machine-learning algorithms were used to develop a simple predictor to predict immune clusters, thereby randomly assigning all samples to the group with poor or good prognosis until the best prediction efficiency is obtained. A total of 26 hub immune genes were identified for the prognostic predictor for subgroup classification. **(B)** For the training set samples, immunophenotyping clustering was used to determine whether the samples belonged to Cluster A or Clusters B and C. **(C)**. Survival difference between immunophenotyping clusters of ccRCC patients in the training cohort. **(D)** The logistic regression coefficient was further used to calculate the risk score of each sample.

Immune cell infiltration analysis of immunophenotyping clusters

To explore differences in immune cell distribution, the CIBERSORT algorithm was used to analyze the absolute proportion of 22 infiltrating immune cells in ccRCC samples from the TCGA database (**Supplementary Table S5**). There were significant differences in immune cell infiltration between the immunophenotyping clusters, especially in plasma cells, CD4 memory resting T cells, follicular helper T cells, regulatory T cells (Tregs), resting dendritic cells, and resting mast cells (**Figures 5A,B**). A significant increase of $CD8^+$ T cells was found in Clusters B and C compared with Cluster A. We also assessed the distribution of risk ratios in each immune cell infiltration and identified the prognostic implications. As shown in **Supplementary Figure S3**, there were significantly differences in survival associated with CD4 memory-activated T cell, follicular helper T cell, Tregs, CD4 memory resting T cell, and resting mast cell infiltration. In addition, we examined the prognostic value of lymphocyte-derived and myeloid-derived immune cell infiltration using univariate Cox analysis, as shown in **Figure 5C**. The results suggested that elevated lymphocyte-derived $CD4^+$ memory activated T cells (HR = 1.15), Tfh cells (HR = 1.12), and Treg cells (HR = 1.10) were significantly correlated with poor outcomes for ccRCC patients, while elevated myeloid-derived resting mast cells (HR = 0.89) predicted favorable prognosis for ccRCC patients.

Function enrichment analysis of immunophenotyping clusters

To evaluate the differences in biological function between the two immunophenotyping clusters, we performed genomic function enrichment analysis using GSVA. The Wilcox test was used to identify differentially expressed genes (DEGs) in the two immunophenotyping clusters. According to the screening criteria of $|\log_2 FC|>1$ and adj.pvalue<0.01, we screened out 1,045 DEGs, with 157 genes upregulated in Cluster A and 888 genes upregulated in Cluster B and C (**Supplementary Table S6A**). GSEA was used to explore the functional annotations of the upregulated DEGs in Clusters B and C, and these DEGs were significantly enriched in C2 functions such as TP53 targets, REACTOME innate immune system, and tumorigenesis hallmarks such as estrogen response late and KRAS signaling down (**Figures 5D,E**; **Supplementary Table S6B,C**). Furthermore, the GSVA algorithm suggested that samples in Cluster A were highly enriched in immune and metabolic hallmarks such as hedgehog signaling, pancreas beta cells, and fatty acid metabolism. In Clusters B and C, samples were highly enriched in proliferation functions such as the mitotic cell cycle, hypoxia, and EMT process (**Figure 5F**, **Supplementary Table S6D**). Next, the generalized linear model Cox regression model was used to test the contribution of each function to risk of prognosis for patients with ccRCC (**Figure 5G**). These results indicated

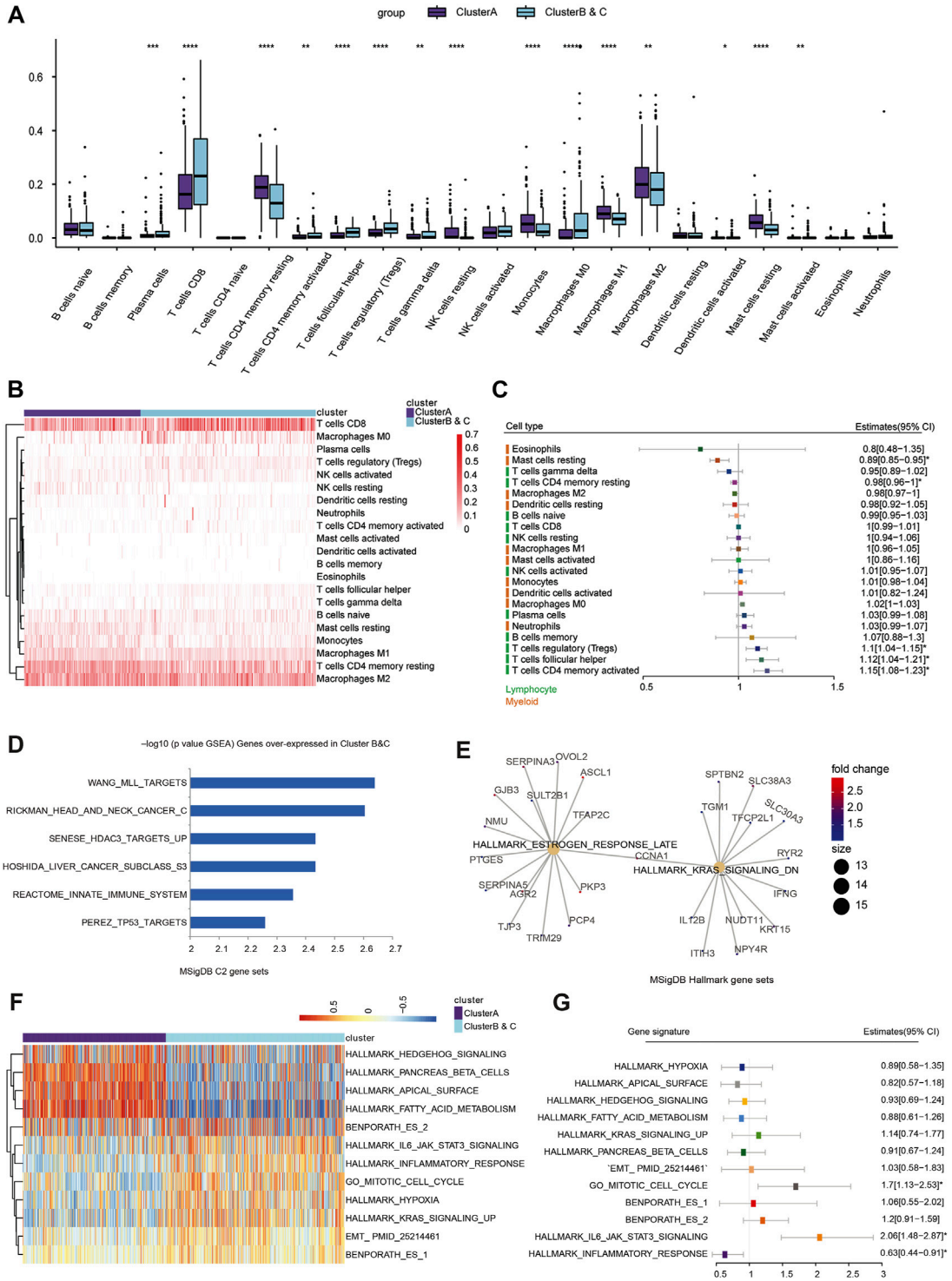

FIGURE 5 | Immune cell infiltration and function enrichment analysis of immunophenotyping clusters. **(A, B)** The CIBERSORT algorithm was performed to analyze the absolute proportion of 22 infiltrating immune cells and explore differential immune cell distribution in ccRCC samples from TCGA. **(C)** Prognostic value of lymphocyte-derived and myeloid-derived immune cell infiltration using univariate Cox regression analysis in a forest plot. **(D, E)** To evaluate the differences in biological function between the two immunophenotyping clusters, the Wilcox test was used to identify DEGs in the two immunophenotyping clusters. According to the screening criteria of $|\log_2 FC|>1$ and adj.Pvalue<0.01 (**Supplementary Materials**), GSEA was used to explore the functional annotations of upregulated DEGs in Clusters B and C. **(F)** The GSVA algorithm suggested significantly enriched hallmarks in Cluster A and Clusters B and C. **(G)** Generalized linear model Cox regression model was used to test the contribution of each function to Clusters B and C and Cluster A.

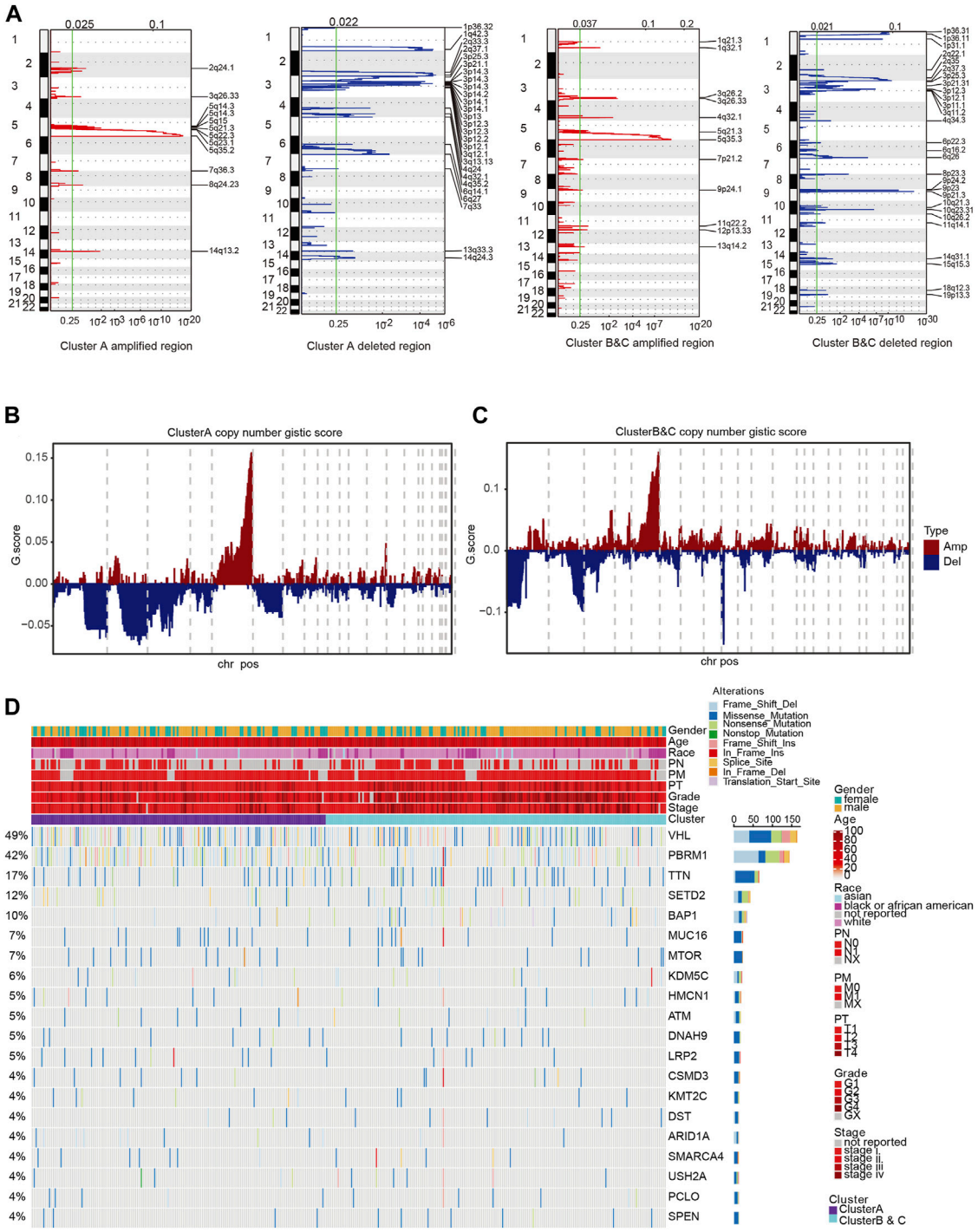

FIGURE 6 | Clinicopathological characteristics of immunophenotyping clusters. **(A)** Differences of various clinical indicators in different immunophenotyping clusters. **(B, C)** Methylation and mRNA expression level of CDKN2A in immunophenotyping clusters. **(D)** Total number of mutations in immunophenotyping clusters. **(E–I)** Phenotypic indicators, such as gender, age, tumor stage, smoking status, MSI, resection, and biopsy site, in the immunophenotyping clusters. **(J)** Patients in immunophenotyping clusters distributed according to AJCC stages.

that inflammatory response signaling has a positive effect on prognosis, while the mitotic cell cycle and IL6/JAK/STAT3 signaling are prominent risk factors for ccRCC patients. Based on these results, we hypothesized that IL6/JAK/STAT3 signaling or proliferative phenotype could be a factor leading to the poor prognosis of Clusters B and C.

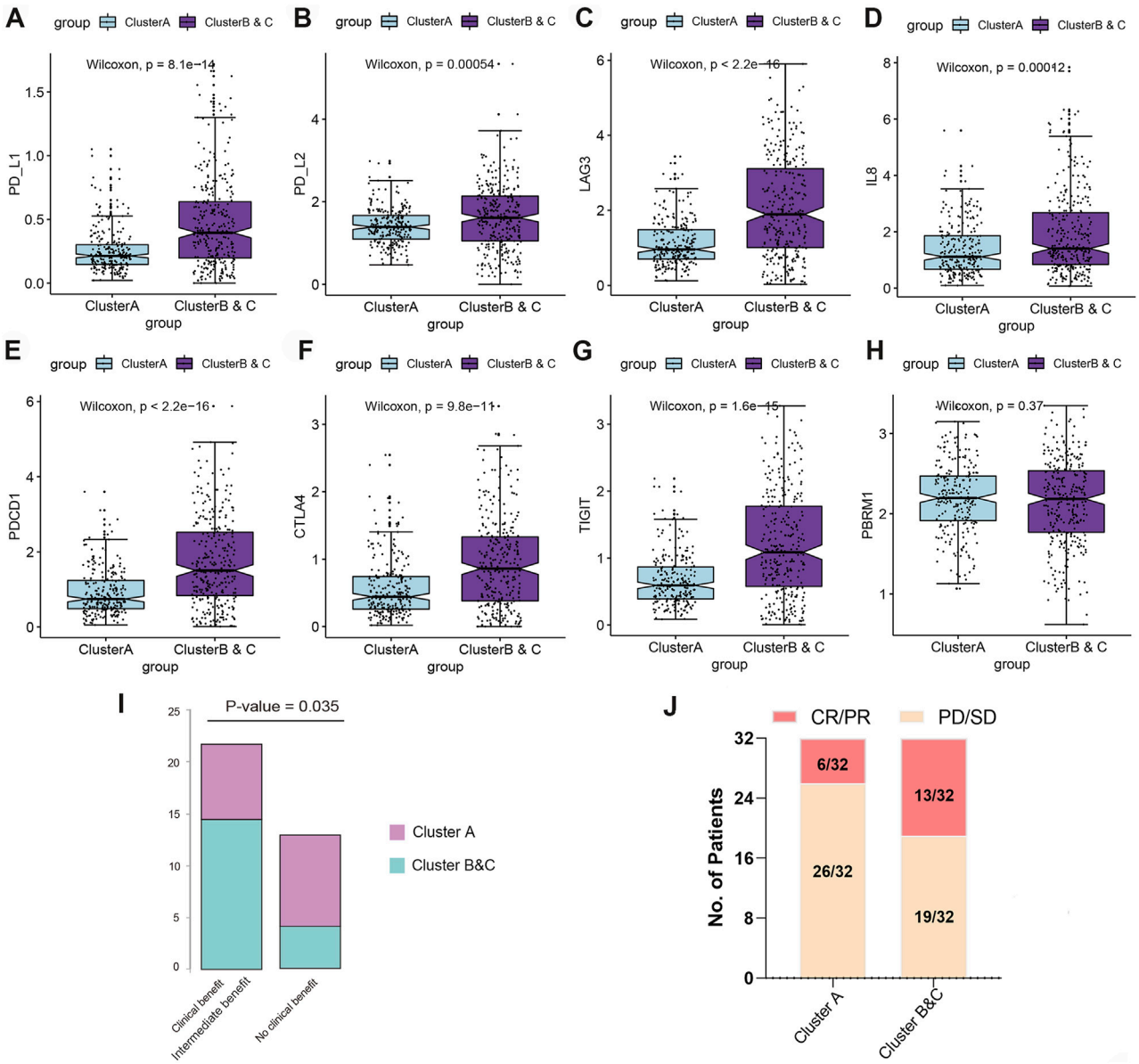

FIGURE 7 | Immunotherapy efficacy analysis of immunophenotyping clusters. **(A–H)** Expressions of immune checkpoint molecules, including PD-L1, PD-L2, LAG3, IL-8, PDCD1, CTLA-4, and TIGIT, and PBRM1, were compared using Students' *t* test. **(I)** A total of 35 ccRCC patients receiving ICTs from the CA209-009 cohort with RNA-seq data and clinical responses to treatment. **(J)** Response status in 64 ccRCC patients receiving ICTs alone or combined with TKIs from the FUSCC cohort.

DNA variation landscape of immunophenotyping clusters

To further explore DNA variation profiles of the two subgroups, we analyzed the differences in single-nucleotide polymorphisms (SNPs) and CNVs between groups. We found marked differences between copy number amplification and deletion in the two subgroups (**Figure 6A**). Amplified regions in Cluster A were largely located in 5q11.4, 5q21.3, and 5q35.2, while deleted regions were mainly located in 1q42.3, 2q37.1, 3p14.3, and 6q27. Amplified regions in Clusters B and C were largely located in 3q26.33, 5q21.3, and 5q35.3, which is similar with Cluster A, while deleted regions were mainly located in 1p36.11, 3p25.3, 3q12.3, 9q21.3, and 10q23.31, which were different compared with Cluster A. Additionally, there were significant differences in the Gistic score of the two groups (**Figures 6B,C**; **Supplementary Table S6E,F**). We next performed clustering analysis between the immunophenotyping clusters based on SNP, genes with frequent mutations or alterations, and clinical characteristics (**Figure 6D**). The

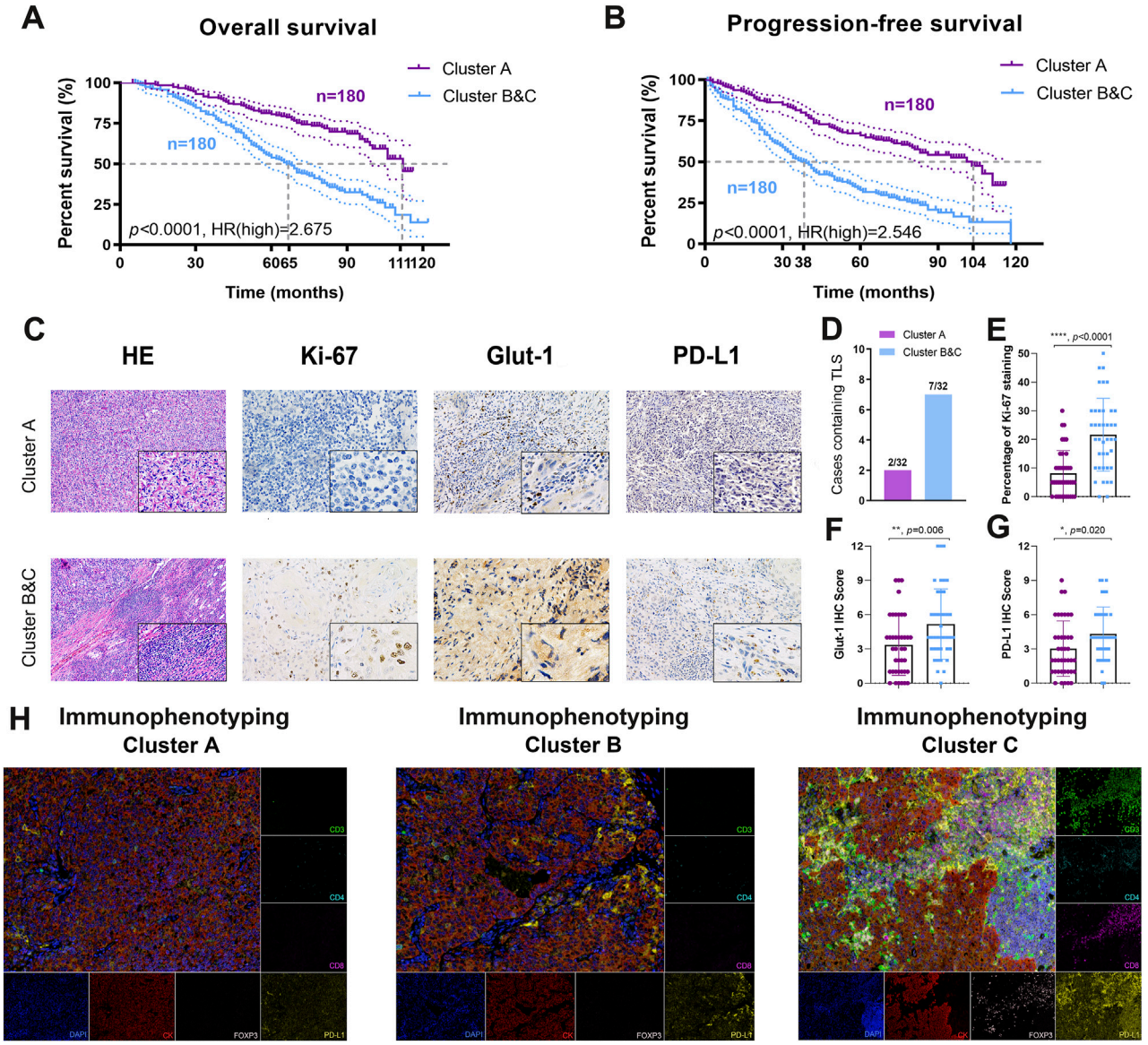

FIGURE 8 | Prognostic implications and TME characterizations of immunophenotyping clusters in a real-world validation cohort. **(A, B)** A total of 360 ccRCC patients with long-term follow-up information from the FUSCC cohort were enrolled to identify the prognostic value of immunophenotyping clusters in the validation cohort. **(C–G)** Characteristics of the tumor microenvironment between immunophenotyping clusters were explored using **(H, E)** and immunohistochemical staining analysis in different clusters. **(H)** Opal multi-label IHC staining was used to identify the abundance of CD^{8+} T cells, $CD^{4+}FOXP^{3+}$ Treg cells, and $CD^{3+}CD^{4+}CD^{8+}$ TCRn immune cell infiltration and PD-L1 expression in clusters.

results indicated that Clusters B and C were accompanied with advanced clinical indicators and frequent TTN, SETD2, and BAP1 gene mutations.

Immunotherapy efficacy analysis of immunophenotyping clusters

To further investigate the predicted responses of immunophenotyping clusters to ICTs, we compared immune checkpoint gene expressions and found that expressions of PD-L1, PD-L2, LAG-3, IL-8, PDCD1, CTLA-4, and TIGIT were significantly elevated in Clusters B and C compared with Cluster A, suggesting an immune-infiltrated TME of ccRCC (**Figures 7A–G**). No differences in PBRM1 expression were observed in the two subgroups (**Figure 7H**). We then enrolled 35 ccRCC patients receiving ICTs from the CA209-009 cohort with specific RNA-seq data and clinical response data. Patients in Clusters B and C were significantly inclined to clinical or intermediate benefit (n = 22) rather than the no clinical benefit group (n = 13) (p = 0.035; **Figure 7I**). Moreover, after grouping 64 ccRCC patients receiving ICTs alone or combined with TKI in the FUSCC cohort, we found prominently increased

ccRCC patients from Clusters B and C (13/32) with CR/PR status than patients in Cluster A (6/32) (**Figure 7J**).

Prognostic implications of immunophenotyping clusters in 360 ccRCC patients from the FUSCC validation cohort.

Although immunophenotyping clusters markedly defined the poor prognosis of ccRCC patients in the training cohort (TCGA, $n = 531$) and testing cohort (ICGA, $n = 91$), large-scale real-world validation evidence was required to confirm the clinical translational value. We thus identified immunophenotyping clusters of 360 ccRCC patients with long-term follow-up information from the FUSCC validation cohort and performed survival analysis (**Supplementary Table S7**). The results showed that Clusters B and C significantly predicted worse OS compared with Cluster A ($p < 0.0001$, HR = 2.675). The median OS time in Clusters B and C was 66 months compared with 11 months in Cluster A (**Figure 8A**). In addition, Clusters B and C significantly correlated with poor PFS compared with Cluster A ($p < 0.0001$, HR = 2.822). The median PFS in Clusters B and C was 38 months, while that in Cluster A was 104 months (**Figure 8B**).

The TME characterizations differ in immunophenotyping clusters

To provide more experimental evidence for clinical translation, we explored characteristics of the TME in the immunophenotyping clusters. After identification and classification of 64 ccRCC samples receiving ICTs in the FUSCC cohort, we performed H&E and immunohistochemical (IHC) staining analysis in the different clusters (**Figure 8C**). We found markedly more cases containing TLS in Clusters B and C (37.5%) than in Cluster A (37.5%), suggesting a relatively immune-enriched microenvironment with increased accumulation of mature tumor-infiltrated lymphocytes, such as $CD8^+$ T cells (**Figure 8D**). IHC analysis revealed a significantly more aggressive malignant phenotype, elevated activated glycolysis effect, and PD-L1 expression in Clusters B and C (**Figures 8E–G**). After opal multi-label IHC staining, we found an increased abundance of $CD4^+FoxP3^+$ Treg cells, $CD8^+$ T cells, and CD-predicted favorable response to ICTs for patients with $3^+CD4^+CD8^+$ TCRn immune cell infiltration in immune-excluded Clusters B and C compared with immune-desert Cluster A (**Figure 8H**). Besides, the expression level of PD-L1 was also significantly increased in the Cluster B and C group. Overall, the findings suggested that the pro-tumorigenic Clusters B and C may be associated with an immune-enriched TME and the ccRCC.

DISCUSSION

This study identified three immunophenotyping clusters in ccRCC with gradual levels of immune infiltration using 758 immune-related genes. As an immune-hot Cluster, Clusters B and C were associated with worse prognosis independent of known clinicopathological indicators, such as myeloid infiltration score, immune score, dryness index score, and mutation. The relatively immune-hot Clusters B and C showed a transcriptional signature indicative of pro-tumorigenic immune infiltration in tumors, and these patients showed significantly worse survival compared with the immune-cold Cluster A. To improve the clinical translational value of the model, we constructed a logistic regression algorithm and identified 26 immune genes constituting a prognostic predictor for subgroup classification. In addition to the distinct immune cell infiltrations in immunophenotyping, there were significant differences in SNVs and CNVs, suggesting a high degree of genetic heterogeneity between the subgroups. We identified two mutually exclusive aggressive tumor phenotypes in ccRCC. Through phenotypic analysis, we found that proliferation and mitotic cell cycle and IL6/JAK/STAT3 signaling were risk factors for Clusters B and C, and multiple metabolic pathways contributed to the survival benefits of Cluster A. Furthermore, the expressions of multiple immune checkpoint molecules, such as PD-1, PD-L1, PD-L2, CTLA-4, and TIGIT, were significantly increased. Importantly, Clusters B and C predicted favorable outcome in 64 ccRCC patients receiving ICTs in the FUSCC cohort. In 360 ccRCC patients in the FUSCC cohort, Clusters B and C significantly predicted worse prognosis compared with the immune-cold Cluster A. After immunophenotyping of ccRCC was confirmed, significantly abundant tertiary lymphatic structures, aggressive phenotype, elevated glycolysis and PD-L1 expression, higher abundance of $CD8^+$ T cells and $CD4^+$ $FOXP3^+$ Treg cells, and M1 macrophage cell infiltration was found in the immune-infiltrated Clusters B and C compared with immune-excluded Cluster A. Therefore, under a paradigm of targeted therapies, such as TKIs, two of the clusters that are "immune-hot" exerted poorer prognosis but might be uniquely responsive to immune checkpoint blockade, thereby improving treatment outcomes for ccRCC patients.

Previous studies have demonstrated that molecular classification of ccRCC showed a prognostic impact in patients treated with VEGFR-TKIs (Beuselinck et al., 2018). The molecular ccrcc1–4 classification of metastatic ccRCC revealed a high predictive value with a significantly higher PFS and OS in patients who received targeted therapy with sunitinib (Verbiest et al., 2018). Mutation of PBRM1 and tumor mutation burden were significantly correlated with poor and good outcome, respectively, which is clinically instructive for the application of molecular targeted therapy and ICTs (Kapur et al., 2013). A previous investigation identified 34 prognosis-related genes through analyzing RNA sequencing expression data and constructed a classifier that divides ccRCC patients into low- (ccA) and high-risk (ccB) groups (Brannon et al., 2010). When the ccrcc1–4 classifier was used to verify the ccA and ccB clusters, a high degree of similarity was found between ccrcc2 and ccA clusters, as well as ccrcc1/4 and ccB clusters (de Velasco et al., 2017). Different from other tumors, in ccRCC, non-synonymous mutations, neoantigens, insertions, or deletions caused by chromosomal structural changes and somatic CNVs were not associated with the efficacy of PD-1 inhibitors (Braun et al., 2020). In addition, the higher level of $CD8^+$ T cell infiltration in ccRCC was associated with a poorer prognosis, which was also observed in patients from the Cluster B and C group in this study (Darrow et al., 2020; Black and McGranahan, 2021). However, a large

amount of evidence has suggested that not all TMB-high solid tumors are sensitive to ICTs, and high tumor neoantigens are not necessarily accompanied by an increased abundance of $CD8^+$ T cell infiltration (McGrail, 2021). Therefore, further tumor type-specific studies are warranted in investigating biomarkers for ICTs.

This study is the first that accurately groups the immune microenvironment in the ccRCC microenvironment. We found that the immune-hot Clusters B and C have pro-tumorigenic immune infiltration and a significantly worse survival than the immune-cold Cluster A, which can be implemented as a novel independent prognostic indicator, highlighting the close relationship between tumor phenotype and the immune contexture. We also developed the construction of classifiers for different immunophenotyping clusters and identified a simple prediction classifier through machine-learning algorithms. The prediction efficiency of the original model was highly consistent, which greatly improved the clinical transformation efficiency. Further phenotypic analysis and functional annotation revealed two mutually exclusive invasive tumor phenotypes in ccRCC: one is related to mitotic cell cycle process, and the other is related to metabolism, suggesting heterogeneity between the ccRCC immunophenotyping clusters. In addition, a high-quality signature for ccRCC to predict the efficacy of immunotherapy was developed. A large amount of evidence in this study shows that the new immunophenotyping of ccRCC significantly predicts the response to ICTs. Besides, describing the correlation between TLS and the clinical benefit of cancer patients, indicating that TLS may be a prognostic and predictive factor, could arouse strong interest in studying the role of TLS in ccRCC.

This study had several limitations. First, this study has not clarified the underlying mechanism of the immunophenotyping clusters of ccRCC. Our future studies will include ccRCC specimens receiving ICTs to explore differences in the immune environment and intratumoral heterogeneity of TME between clusters. Second, although the classifier was constructed and validated using multiple public and real-world datasets, because of the limitation of retrospective analysis, further multicenter studies and prospective trials are warranted for clinical application for patients with ccRCC.

CONCLUSION

This study described immunophenotyping clusters that improve the prognostic accuracy of the immune contexture in the ccRCC microenvironment. The immune-hot Clusters B and C showed a transcriptional signature indicative of pro-tumorigenic immune infiltration and significantly worse outcome than the immune-cold Cluster A. Our discovery of novel independent prognostic indicators in ccRCC highlights the relationship between tumor phenotype and the immune contexture.

DATA AVAILABILITY STATEMENT

The datasets presented in this study can be found in online repositories. The names of the repository/repositories and accession number(s) can be found in the article/ **Supplementary Material**.

ETHICS STATEMENT

The studies involving human participants were reviewed and approved by the Fudan University Shanghai Cancer Center (Approved No. 050432-4-1805C). The patients/participants provided their written informed consent to participate in this study. Written informed consent was obtained from the individual(s) for the publication of any potentially identifiable images or data included in this article.

AUTHOR CONTRIBUTIONS

Conceptualization: WX, CM, AA, and WL. Data curation and formal analysis: WX, CM, AA, JS, WZ, and GS. Funding acquisition: WX, YQ, HZ, and DY. Investigation and methodology: WX, CM, AA, WL, HX, WZ, and GS. Resources and software: GS, SW, HX, YQ, HZ, and DY. Supervision: SW, HX, YQ, HZ, and DY. Validation and visualization: WX, CM, AA, and WL. Original draft: WX, CM, AA, and WL. Editing: HX, YQ, HZ, and DY.

FUNDING

This work is supported by Grants from Fuqing Scholar Student Scientific Research Program of Shanghai Medical College, Fudan University (No. FQXZ202112B), National Key Research and Development Project (No. 2019YFC1316000), the National Natural Science Foundation of China (Nos. 81802525, 82172817, 81872099, 82172741), the Natural Science Foundation of Shanghai (No. 20ZR1413100), and the Shanghai Municipal Health Bureau (No. 2020CXJQ03).

ACKNOWLEDGMENTS

We are grateful to all patients for their dedicated participation in the current study. We expressed our sincere gratitude to Zoo for editing Figures and the schematic diagram for this study.

SUPPLEMENTARY MATERIAL

The Supplementary Material for this article can be found online at: https://www.frontiersin.org/articles/10.3389/fcell.2021.785410/full#supplementary-material

REFERENCES

Beuselinck, B., Job, S., Becht, E., Karadimou, A., Verkarre, V., Couchy, G., et al. (2015). Molecular Subtypes of Clear Cell Renal Cell Carcinoma Are Associated With Sunitinib Response in the Metastatic Setting. *Clin. Cancer Res.* 21 (6), 1329–1339. doi:10.1158/1078-0432.ccr-14-1128

Beuselinck, B., Verbiest, A., Couchy, G., Job, S., de Reynies, A., Meiller, C., et al. (2018). Pro-Angiogenic Gene Expression Is Associated With Better Outcome on Sunitinib in Metastatic Clear-Cell Renal Cell Carcinoma. *Acta Oncologica.* 57 (4), 498–508. doi:10.1080/0284186x.2017.1388927

Black, J. R. M., and McGranahan, N. (2021). Genetic and Non-genetic Clonal Diversity in Cancer Evolution. *Nat. Rev. Cancer* 21 (6), 1–14. doi:10.1038/s41568-021-00336-2

Brannon, A. R., Haake, S. M., Hacker, K. E., Pruthi, R. S., Wallen, E. M., Nielsen, M. E., et al. (2012). Meta-Analysis of Clear Cell Renal Cell Carcinoma Gene Expression Defines a Variant Subgroup and Identifies Gender Influences on Tumor Biology. *Eur. Urol.* 61 (2), 258–268. doi:10.1016/j.eururo.2011.10.007

Brannon, A. R., Reddy, A., Seiler, M., Arreola, A., Moore, D. T., Pruthi, R. S., et al. (2010). Molecular Stratification of Clear Cell Renal Cell Carcinoma by Consensus Clustering Reveals Distinct Subtypes and Survival Patterns. *Genes & Cancer.* 1 (2), 152–163. doi:10.1177/1947601909359929

Braun, D. A., Hou, Y., Bakouny, Z., Ficial, M., Sant' Angelo, M., Forman, J., et al. (2020). Interplay of Somatic Alterations and Immune Infiltration Modulates Response to PD-1 Blockade in Advanced Clear Cell Renal Cell Carcinoma. *Nat. Med.* 26 (6), 909–918. doi:10.1038/s41591-020-0839-y

Cesano, A. (2015). nCounter PanCancer Immune Profiling Panel (NanoString Technologies, Inc., Seattle, WA). *J. Immunotherapy Cancer.* 3, 42. doi:10.1186/s40425-015-0088-7

Chen, B., Khodadoust, M. S., Liu, C. L., Newman, A. M., and Alizadeh, A. A. (2018). Profiling Tumor Infiltrating Immune Cells With CIBERSORT. *Methods Mol. Biol.* 1711, 243–259. doi:10.1007/978-1-4939-7493-1_12

Chen, D. S., and Mellman, I. (2017). Elements of Cancer Immunity and the Cancer-Immune Set point. *Nature.* 541 (7637), 321–330. doi:10.1038/nature21349

Cancer Genome Atlas Research Network (2013). Comprehensive Molecular Characterization of Clear Cell Renal Cell Carcinoma. *Nature.* 499 (7456), 43–49. doi:10.1038/nature12222

Darrow, J. J., Avorn, J., and Kesselheim, A. S. (2020). FDA Approval and Regulation of Pharmaceuticals, 1983-2018. *JAMA.* 323 (2), 164–176. doi:10.1001/jama.2019.20288

de Velasco, G., Culhane, A. C., Fay, A. P., Hakimi, A. A., Voss, M. H., Tannir, N. M., et al. (2017). Molecular Subtypes Improve Prognostic Value of International Metastatic Renal Cell Carcinoma Database Consortium Prognostic Model. *Oncol.* 22 (3), 286–292. doi:10.1634/theoncologist.2016-0078

Engebretsen, S., and Bohlin, J. (2019). Statistical Predictions With Glmnet. *Clin. Epigenet.* 11 (1), 123. doi:10.1186/s13148-019-0730-1

Escudier, B., Porta, C., Schmidinger, M., Rioux-Leclercq, N., Bex, A., Khoo, V., et al. (2019). Renal Cell Carcinoma: ESMO Clinical Practice Guidelines for Diagnosis, Treatment and Follow-Up. *Ann. Oncol.* 30 (5), 706–720. doi:10.1093/annonc/mdz056

Fridman, W. H., Zitvogel, L., Sautès–Fridman, C., and Kroemer, G. (2017). The Immune Contexture in Cancer Prognosis and Treatment. *Nat. Rev. Clin. Oncol.* 14 (12), 717–734. doi:10.1038/nrclinonc.2017.101

Galili, T., O'Callaghan, A., Sidi, J., and Sievert, C. (2018). Heatmaply: an R Package for Creating Interactive Cluster Heatmaps for Online Publishing. *Bioinformatics.* 34 (9), 1600–1602. doi:10.1093/bioinformatics/btx657

Gerlinger, M., Rowan, A. J., Horswell, S., Math, M., Larkin, J., Endesfelder, D., et al. (2012). Intratumor Heterogeneity and Branched Evolution Revealed by Multiregion Sequencing. *N. Engl. J. Med.* 366 (10), 883–892. doi:10.1056/NEJMoa1113205

Grimm, M.-O., Bex, A., De Santis, M., Ljungberg, B., Catto, J. W. F., Rouprêt, M., et al. (2019). Safe Use of Immune Checkpoint Inhibitors in the Multidisciplinary Management of Urological Cancer: The European Association of Urology Position in 2019. *Eur. Urol.* 76 (3), 368–380. doi:10.1016/j.eururo.2019.05.041

Heng, D. Y. C., Xie, W., Regan, M. M., Warren, M. A., Golshayan, A. R., Sahi, C., et al. (2009). Prognostic Factors for Overall Survival in Patients With Metastatic Renal Cell Carcinoma Treated With Vascular Endothelial Growth Factor-Targeted Agents: Results From a Large, Multicenter Study. *J. Clin. Oncol.* 27 (34), 5794–5799. doi:10.1200/jco.2008.21.4809

Hofmann, F., Hwang, E. C., Lam, T. B., Bex, A., Yuan, Y., Marconi, L. S., et al. (2020). Targeted Therapy for Metastatic Renal Cell Carcinoma. *Cochrane Database Syst. Rev.* 10, CD012796. doi:10.1002/14651858.CD012796.pub2

Hsieh, J. J., Purdue, M. P., Signoretti, S., Swanton, C., Albiges, L., Schmidinger, M., et al. (2017). Renal Cell Carcinoma. *Nat. Rev. Dis. Primers.* 3, 17009. doi:10.1038/nrdp.2017.9

Kapur, P., Peña-Llopis, S., Christie, A., Zhrebker, L., Pavía-Jiménez, A., Rathmell, W. K., et al. (2013). Effects on Survival of BAP1 and PBRM1 Mutations in Sporadic Clear-Cell Renal-Cell Carcinoma: a Retrospective Analysis With Independent Validation. *Lancet Oncol.* 14 (2), 159–167. doi:10.1016/s1470-2045(12)70584-3

Kawakami, F., Sircar, K., Rodriguez-Canales, J., Fellman, B. M., Urbauer, D. L., Tamboli, P., et al. (2017). Programmed Cell Death Ligand 1 and Tumor-infiltrating Lymphocyte Status in Patients With Renal Cell Carcinoma and Sarcomatoid Dedifferentiation. *Cancer.* 123 (24), 4823–4831. doi:10.1002/cncr.30937

Kotecha, R. R., Motzer, R. J., and Voss, M. H. (2019). Towards Individualized Therapy for Metastatic Renal Cell Carcinoma. *Nat. Rev. Clin. Oncol.* 16 (10), 621–633. doi:10.1038/s41571-019-0209-1

Linehan, W. M. (2012). Genetic Basis of Kidney Cancer: Role of Genomics for the Development of Disease-Based Therapeutics. *Genome Res.* 22 (11), 2089–2100. doi:10.1101/gr.131110.111

McGrail, D. J. (2021). High Tumor Mutation burden Fails to Predict Immune Checkpoint Blockade Response across All Cancer Types. *Ann. Oncol.* 32 (5), 661–672. doi:10.1016/j.annonc.2021.02.006

Miller, K. D., Nogueira, L., Mariotto, A. B., Rowland, J. H., Yabroff, K. R., Alfano, C. M., et al. (2019). Cancer Treatment and Survivorship Statistics, 2019. *CA A. Cancer J. Clin.* 69 (5), 363–385. doi:10.3322/caac.21565

Moch, H., Cubilla, A. L., Humphrey, P. A., Reuter, V. E., and Ulbright, T. M. (2016). The 2016 WHO Classification of Tumours of the Urinary System and Male Genital Organs-Part A: Renal, Penile, and Testicular Tumours. *Eur. Urol.* 70 (1), 93–105. doi:10.1016/j.eururo.2016.02.029

Motzer, R. J., Hutson, T. E., Tomczak, P., Michaelson, M. D., Bukowski, R. M., Oudard, S., et al. (2009). Overall Survival and Updated Results for Sunitinib Compared with Interferon Alfa in Patients With Metastatic Renal Cell Carcinoma. *J. Clin. Oncol.* 27 (22), 3584–3590. doi:10.1200/jco.2008.20.1293

Motzer, R. J., Hutson, T. E., Tomczak, P., Michaelson, M. D., Bukowski, R. M., Rixe, O., et al. (2007). Sunitinib Versus Interferon Alfa in Metastatic Renal-Cell Carcinoma. *N. Engl. J. Med.* 356 (2), 115–124. doi:10.1056/nejmoa065044

Motzer, R. J., Rini, B. I., McDermott, D. F., Arén Frontera, O., Hammers, H. J., Carducci, M. A., et al. (2019). Nivolumab Plus Ipilimumab Versus Sunitinib in First-Line Treatment for Advanced Renal Cell Carcinoma: Extended Follow-Up of Efficacy and Safety Results from a Randomised, Controlled, Phase 3 Trial. *Lancet Oncol.* 20 (10), 1370–1385. doi:10.1016/s1470-2045(19)30413-9

Porta, C., Cosmai, L., Leibovich, B. C., Powles, T., Gallieni, M., and Bex, A. (2019). The Adjuvant Treatment of Kidney Cancer: a Multidisciplinary Outlook. *Nat. Rev. Nephrol.* 15 (7), 423–433. doi:10.1038/s41581-019-0131-x

Siegel, R. L., Miller, K. D., and Jemal, A. (2020). Cancer Statistics, 2020. *CA A. Cancer J. Clin.* 70 (1), 7–30. doi:10.3322/caac.21590

Sternberg, C. N., Davis, I. D., Mardiak, J., Szczylik, C., Lee, E., Wagstaff, J., et al. (2010). Pazopanib in Locally Advanced or Metastatic Renal Cell Carcinoma: Results of a Randomized Phase III Trial. *J. Clin. Oncol.* 28 (6), 1061–1068. doi:10.1200/jco.2009.23.9764

Verbiest, A., Couchy, G., Job, S., Zucman-Rossi, J., Caruana, L., Lerut, E., et al. (2018). Molecular Subtypes of Clear Cell Renal Cell Carcinoma Are Associated With Outcome During Pazopanib Therapy in the Metastatic

Setting. *Clin. genitourinary Cancer.* 16 (3), e605–e612. doi:10.1016/j.clgc.2017.10.017

Wang, J., Xu, W., Wang, B., Lin, G., Wei, Y., Abudurexiti, M., et al. (2020). GLUT1 Is an AR Target Contributing to Tumor Growth and Glycolysis in Castration-Resistant and Enzalutamide-Resistant Prostate Cancers. *Cancer Lett.* 485, 45–55. doi:10.1016/j.canlet.2020.05.007

Xu, W.-H., Xu, Y., Wang, J., Wan, F.-N., Wang, H.-K., Cao, D.-L., et al. (2019). Prognostic Value and Immune Infiltration of Novel Signatures in clear Cell Renal Cell Carcinoma Microenvironment. *Aging.* 11 (17), 6999–7020. doi:10.18632/aging.102233

Conflict of Interest: The authors declare that the research was conducted in the absence of any commercial or financial relationships that could be construed as a potential conflict of interest.

Publisher's Note: All claims expressed in this article are solely those of the authors and do not necessarily represent those of their affiliated organizations, or those of the publisher, the editors, and the reviewers. Any product that may be evaluated in this article, or claim that may be made by its manufacturer, is not guaranteed or endorsed by the publisher.

frontiers in Cell and Developmental Biology

REVIEW
published: 10 December 2021
doi: 10.3389/fcell.2021.784421

Myeloid Immune Cells CARrying a New Weapon Against Cancer

Rodrigo Nalio Ramos[1,2]*, *Samuel Campanelli Freitas Couto*[1,3], *Theo Gremen M. Oliveira*[1,3], *Paulo Klinger*[1], *Tarcio Teodoro Braga*[4,5], *Eduardo Magalhães Rego*[1,2], *José Alexandre M. Barbuto*[1,6] *and Vanderson Rocha*[1,2,3,7]

[1]Laboratory of Medical Investigation in Pathogenesis and Directed Therapy in Onco-Immuno-Hematology (LIM-31), Departament of Hematology and Cell Therapy, Hospital das Clínicas HCFMUSP, Faculdade de Medicina, University of São Paulo, São Paulo, Brazil, [2]Instituto D'Or de Ensino e Pesquisa, São Paulo, Brazil, [3]Fundação Pró-Sangue–Hemocentro de São Paulo, São Paulo, Brazil, [4]Department of Pathology, Federal University of Parana, Curitiba, Brazil, [5]Graduate Program in Biosciences and Biotechnology, Instituto Carlos Chagas, Fiocruz-Parana, Curitiba, Brazil, [6]Departamento de Imunologia, Instituto de CienciasBiomedicas, Universidade de Sao Paulo, São Paulo, Brazil, [7]Churchill Hospital, Department of Hematology, University of Oxford, Oxford, United Kingdom

Chimeric antigen receptor (CAR) engineering for T cells and natural killer cells (NK) are now under clinical evaluation for the treatment of hematologic cancers. Although encouraging clinical results have been reported for hematologic diseases, pre-clinical studies in solid tumors have failed to prove the same effectiveness. Thus, there is a growing interest of the scientific community to find other immune cell candidate to express CAR for the treatment of solid tumors and other diseases. Mononuclear phagocytes may be the most adapted group of cells with potential to overcome the dense barrier imposed by solid tumors. In addition, intrinsic features of these cells, such as migration, phagocytic capability, release of soluble factors and adaptive immunity activation, could be further explored along with gene therapy approaches. Here, we discuss the elements that constitute the tumor microenvironment, the features and advantages of these cell subtypes and the latest studies using CAR-myeloid immune cells in solid tumor models.

Keywords: CAR (chimeric antigen receptor), monocyte, myeloid cells, solid tumor (malignancy and long term complications), macrophages, dendritic cell (DC)

OPEN ACCESS

Edited by:
Ander Izeta,
Biodonostia Health Research Institute (IIS Biodonostia), Spain

Reviewed by:
Carlos Del Fresno,
University Hospital La Paz Research Institute (IdiPAZ), Spain
Susana García-Silva,
Spanish National Cancer Research Center (CNIO), Spain

***Correspondence:**
Rodrigo Nalio Ramos
rodrigo.nalio@gmail.com

Specialty section:
This article was submitted to Molecular and Cellular Pathology, a section of the journal Frontiers in Cell and Developmental Biology

Received: *27 September 2021*
Accepted: *22 November 2021*
Published: *10 December 2021*

Citation:
Ramos RN, Couto SCF, Oliveira TGM, Klinger P, Braga TT, Rego EM, Barbuto JAM and Rocha V (2021) Myeloid Immune Cells CARrying a New Weapon Against Cancer. Front. Cell Dev. Biol. 9:784421. doi: 10.3389/fcell.2021.784421

INTRODUCTION

The myeloid immune cell compartment is composed by distinct cell subtypes that present a variety of functions once they have differentiated and maturated at the periphery. Within this compartment, besides the other cell types, the mononuclear phagocyte cells include subsets of monocytes, macrophages and dendritic cells (DC).

Monocytes are mostly found in the blood and macrophages are exclusively found in the tissues, while DC subsets can be found both in circulation and tissues.

Many phenotypic characteristics of DC associated with the induction of various T-cell response patterns have been described. It allows, for example, the association of the conventional Dendritic Cell 1 (cDC1) phenotype with the induction of CD8+ cytotoxic T lymphocytes (CTL) (Bachem et al., 2010), the conventional Dendritic Cell 2 (cDC2) phenotype with that of various Th subtypes (Segura et al., 2005; Rojas et al., 2017) but also of Treg cells (Watchmaker et al., 2014), while the plasmacytoid Dendritic Cell (pDC) phenotype has been mostly associated with the production of type I interferon (Reizis et al., 2011). However, this is

an incomplete picture which is quickly being filled outand much still needs to be determined before one can predict the *in vivo* response from any DC phenotype introduced in the system.

Most recently, distinct groups have described other DC subset such as inflammatory-DCs (Segura et al., 2013) and type 3 DC (DC3) (Dutertre et al., 2019; Bourdely et al., 2020).

Several studies have highlighted the critical role of myeloid immune cells during tumor growth and metastasis, as reviewed by Engblom and collaborators (Engblom et al., 2016). Collective findings have put evidence on the association of tumor-associated macrophages (TAMs) with poor patients' outcome for distinct tumor types (Medrek et al., 2012; Ino et al., 2013; Reinartz et al., 2014; Yang et al., 2018; Ramos et al., 2020; Guo et al., 2021). In contrast, mature DC subsets are currently associated to good prognosis, mostly due to their anti-tumoral role by stimulating T cell responses (Ladányi et al., 2007; Goc et al., 2014; Truxova et al., 2018). Also, an important role of type I IFNs has been discussed as being critical for the innate and adaptive immunity cross-talk (Demaria et al., 2019). Nucleic-acid-sensing cytosolic receptors, such as cGAS-STING pathways, found in the tumor microenvironment may trigger the production of type I IFNs that promote activation of NK cells, which subsequently stimulate DCs and T lymphocytes and anti-tumoral responses.

Numerous studies have reported the use of distinct strategies to overcome the immunosuppressive tumor microenvironment via the stimulation of myeloid immune cells (Chaib et al., 2020; Neophytou et al., 2020). These approaches include: the recruitment of a new wave of immune cells; the stimulation of cells via agonists/ligands; cytokine-based treatments; blockage of receptors by monoclonal antibodies and drug-mediated reprogramming of cells.

Very recently, some reports have described the insertion of chimeric antigen receptor (CAR) on macrophages (Klichinsky et al., 2020; Morrissey et al., 2018; W. Zhang et al., 2019; Zhang L. et al., 2020), an already known technology used for T cells (CAR-T) and natural killer cells (CAR-NK). CAR-T and CAR-NK cell therapies have achieved encouraging results in hematological tumors (Waldman et al., 2020). There has been a rapid growth of published data associated with CAR-T cells. Around 700 active clinical trials can be found at ClinicalTrials.gov database using CAR-T as a treatment modality. Most studies focus on hematologic malignancies, while 45 studies are related to solid tumor treatment. The inherent cytotoxicity of natural killer (NK) cells against tumors and their potential as an "off-the-shelf" cell therapy product have encouraged several clinical trials using CAR expressing NK cells to treat a number of malignant diseases (Xie et al., 2020). There are currently 19 active CAR-NK registered clinical trials, most of them targeting CD19+ hematological malignancies.

The myeloid lineages, especially the mononuclear phagocyte system, present an auspicious future, considering their functional capacity, which includes phagocytosis, antigen presentation, T cell co-stimulation, extracellular matrix remodeling and infiltration into the tumor microenvironment (Anderson et al., 2021; Chen et al., 2021). Despite technical issues concerning transfection, gene delivery and stable expression of CAR on myeloid immune cells (Dokka et al., 2000; Stroh et al., 2010; Keller et al., 2018), preliminary *in vitro* and pre-clinical results using CAR-Macrophages (CAR-Mac) have shown exciting data. We discuss here some important features of monocytes, DCs and macrophages for cancer therapy and the newly reported studies engineering myeloid cells to express CAR.

ONTOGENY OF MYELOID IMMUNE CELLS

The mononuclear phagocyte system was originally described as bone marrow-derived myeloid cells that circulate in the blood as monocytes and reside in tissues as macrophages in both the steady state and inflammation (Furth and Cohn 1968). It is now known that different progenitors can give rise to several cell subsets with distinct phenotypes and particular biological functions. Additionally, migration to tissues and the differentiation of lineage-committed progenitors might be influenced by the surrounding microenvironment such as the inflammatory milieu (Serbina et al., 2008). Monocytes respond to their environment by differentiating into a variety of macrophages and DC-like cells to mount specific functional programs (Taylor and Gordon 2003). The generation and development of monocytes, macrophages and DCs is driven by the association of specific cytokines and growth factors with receptors expressed in hematopoietic stem cell-derived precursors (Sasmono et al., 2003). The bone marrow-derived progenitors are responsible for the renewal of a substantial set of myeloid cells, although many tissue-resident macrophages and DCs subsets (microglia and Langerhans cells) seem to be able to self-renewal, and, thus, independent of this developmental pathway (Ajami et al., 2007; Merad and Manz 2009).

The first myeloid cells originate from hematopoietic progenitors in the human yolk sac at 2 to 3 weeks post conception (Ginhoux and Jung 2014; Epelman et al., 2014). Primitive hematopoietic stem cells (HSCs) enter the circulation and seed the fetal liver, giving rise to the first population of granulocyte-monocyte progenitors (GMPs) and blood monocytes (Hoeffel and Ginhoux 2015; Hoeffel et al., 2015). Under inflammatory conditions, monocytes exit to the blood and enter tissues, giving rise to subsets of macrophages and to inflammatory DCs (Auffray et al., 2009). It is noteworthy that monocytes do not give rise to cDCs and pDCs but are the main contributors of monocyte-derived DCs (Mo-DCs) during inflammation (Coillard and Segura 2019). Alternatively, commitment to the human cDC lineage can occur in early lympho-myeloid progenitors, from multipotent lymphoid progenitors (MLPs) that can give rise to monocytes, pDCs and cDCs (Helft et al., 2017; Doulatov et al., 2010) (**Figure 1**). Most recently, distinct groups have described a third subset of DC (also called DC3) (Dutertre et al., 2019; Bourdely et al., 2020). DC3 usually present a mixed phenotypic and functional status, between that of monocytes and cDC2, and are differentiated from a distinct pre-DC3 progenitor in a GM-CSF dependent-fashion. The DC3 subset closely resembles the monocyte-derived

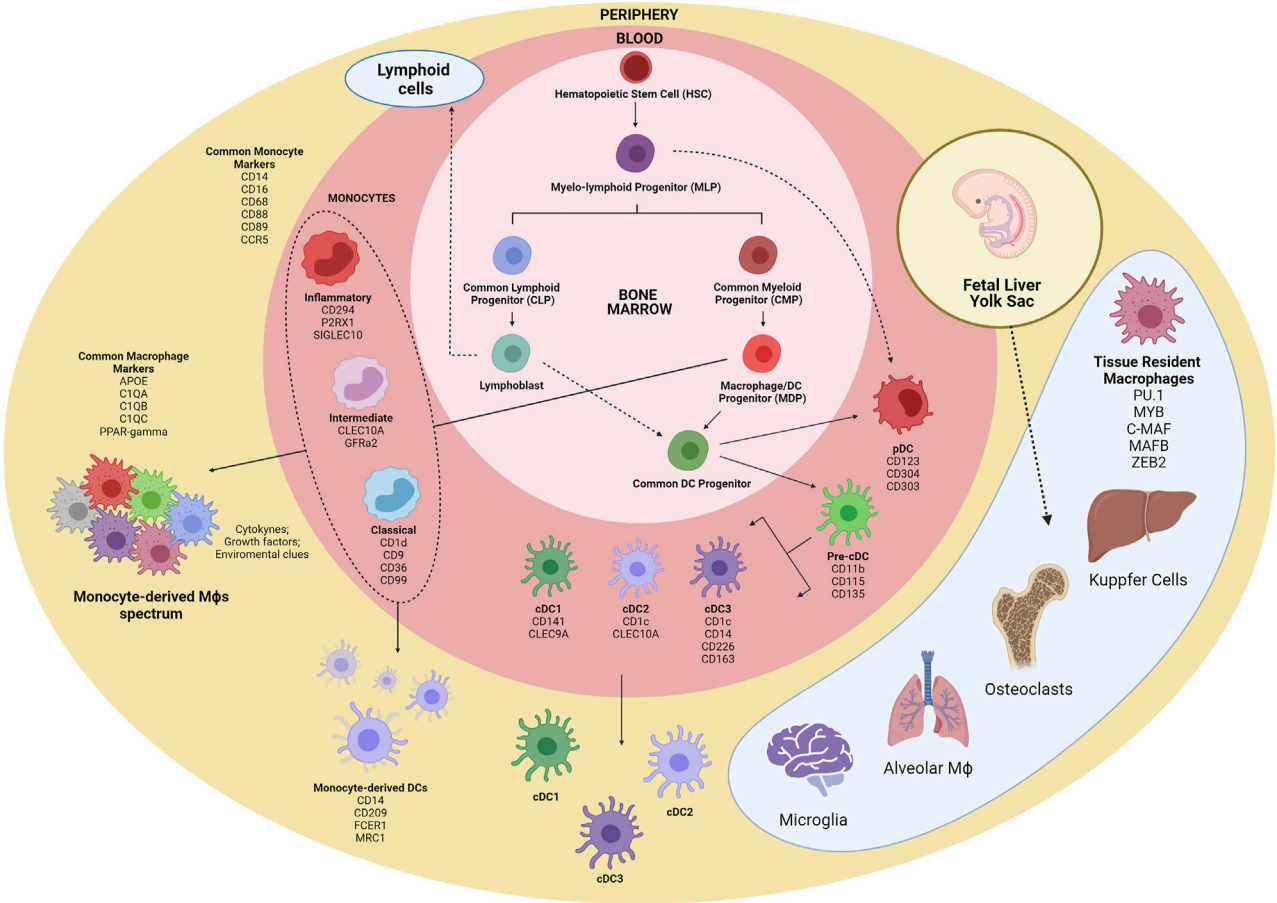

FIGURE 1 | Schematic overview of myeloid cells ontogeny. The first myeloid cells arise in the embryonic phase from yolk sac-derived primitive HSCs and expand in the fetal liver, originating GMPs and blood monocytes. Tissue-resident macrophages are established before birth and are mostly repopulated by self-renewal. Within the bone marrow, CMPs give rise to GMPs and MDPs. MDPs are responsible for the contribution of many macrophages and DC subsets. MDPs differentiate into monocytes and CDPs, which in turn differentiate into pDC and pre-cDCs. Following exit from the BM, pre-cDCs enter peripheral organs and mature into cDC1, cDC2, and cDC3. Alternatively, pDCs and cDCs may also originate from MLPs. Inflammatory cues contribute to monocyte migration to tissues, where they differentiate into macrophages and Mo-DCs. HSC, hematopoeticstem-cell; GMP, granulocyte-monocyte progenitor; CMP, common myeloid progenitor; MDP, macrophage/DC progenitor; MLP, myelo-lymphoid progenitor; CDP, common DC precursor; pre-cDC, precursor of classical DC; Mo-DC, monocyte-derived DC; cDC, classical DC; pDC, plasmacytoid DC.

dendritic cells, differentiated *in vitro* from blood monocytes, and normally accumulate under inflammatory conditions.

Several studies have been conducted to unravel the origin of the terminally differentiated cells of the mononuclear phagocyte system. The analysis of cell surface markers to separate different subpopulations of cells with myeloid origin has been shown to be very limited, since there is significant phenotypic overlap in the expression of cell surface markers among these cells (Guermonprez et al., 2019). Characteristic monocyte surface markers such as CD14, CD16, CD68, and CCR5 are shared with macrophages, and the expression of general macrophage specific surface markers (C1QC and VEGF) and tissue specific markers (VCAM1 and PPARγ) are necessary for proper discrimination between monocytes and macrophages (Ginhoux and Jung 2014; Hoeffel and Ginhoux 2015).

Macrophage subsets could be further segregated into tissue-resident and monocyte-derived cells. A great variety of tissue-resident macrophages are distributed in the human body presenting specialized functional features. Distinct studies have reported *PU.1*, *MYB*, *C-MAF*, *MAF-B*, and *ZEB2* ascore transcriptional factors (TFs) shared by tissue-resident macrophages regardless of the tissue imprinting cues (Blériot et al., 2020). Under inflammatory conditions, intrinsic local signals as cytokines, growth factors, metabolites and others contribute for shaping the macrophage programing and function, generating a much more complex range of phenotypes.

The current DC classification can be quite troublesome, and there is still little consensus on the identification and naming of DC populations (Villar and Segura 2020). Nevertheless, there is a general consensus of classification of DCs into three main groups, based on their cellular and molecular ontogeny (Guilliams et al., 2014): 1) pDC; 2) conventional DC1 and DC2; and 3) DC3. The expression of the CD123, CD304, and CD303 surface markers defines pDCs, whereas CD141 and Clec9A are cDC1 specific

markers, and expression of CD1c and CLEC10A seems to be restricted to cDC2. DC3/Mo-DCs share the expression of CD1c with cDC2, and CD14 with monocytes and macrophages, although they present specific subset markers, such as CD226 and CD163.

Studies on mice and *in vitro* culture of human cells have provided a better understanding of the developmental programs that seem to be hard-wired in hematopoietic progenitor cells to originate different myeloid cells (Epelman et al., 2014). These studies involved the selection of specific gene expression programs, including important TFs responsible for cell fate choices (Auffray et al., 2009; Merad and Manz 2009). The myeloid transcription factor PU.1 is required for the earliest steps of myeloid lineage commitment in HSCs (Sarrazin et al., 2009). This TF plays a role in myeloid lineage diversification, particularly during fate choice of monocytes into macrophage or DC (Bakri et al., 2005). The expression level of PU.1 in certain progenitor stages dictates the fate of a specific myeloid progenitor. Intermediate expression of PU.1 in GMPs favors differentiation to macrophages instead of granulocytes (Laslo et al., 2006). The ectopic expression of TFs Maf-B, c-Maf, Egr1, IRF8, IRF4, and PU.1 in early progenitors can drive monocyte/macrophage and DC fates, and the given function of any factor depends on cooperating or antagonistic TFs that are expressed at each specific progenitor stage (Laslo et al., 2006). According to the current classification of DCs based on ontogeny, a discussion is being raised whether certain DC populations might only be considered as distinct subsets if their developmental pathway is controlled by specific TFs (Villar and Segura 2020). Plasmacytoid DCs develop from progenitors that express the E2-2, ZEB2, IRF8, and IRF4 TFs. Conventional DC1 arise from expression of IRF8 and BATF3, while cCD2 progenitors express ZEB2, IRF4 and Notch2/KLF4 TFs. Monocyte-derived DCs generation depend on the expression of the MAFB and KLF4 TFs (Collin and Bigley 2018; Guermonprez et al., 2019). The DC3 subset developmental pathway is still a matter of discussion, although recent studies have shed some light on this ongoing debate. Cultures of purified monocytes or monocyte-committed precursors with $IRF8^{low}$ expression were able to differentiate into DC3, while $IRF8^{high}$ progenitors gave rise to pDC and DC2 (Bourdely et al., 2020; Cytlak et al., 2020). Besides TFs, epigenetic modification and micro-RNAs have been described to be important determinants of lineage choice (O'Connell et al., 2007; O'Connell et al., 2008).

Altogether, the possibility of generating various terminally differentiated subsets of myeloid cells *in vitro* with cytokine and growth factor cocktails can be harnessed in immunotherapy approaches to develop novel cellular therapy products with optimized biological functions (Salmon et al., 2016).

ROLE OF MONOCYTES, MACROPHAGES AND DENDRITIC CELLS IN CANCER

The Tumor Microenvironment and its Chemoattractive *millieu*

Macrophages are critical cells that participate of tissue homeostasis and regulation and may represent up to 50% of total immune cells that infiltrate solid tumors (Ramos et al., 2020). The great majority of TAMs are derived from blood monocytes due to the chemo attractive milieu from the tumor microenvironment, constituted by a large spectrum of soluble factors that includes M-CSF, CCL2, CCL3, CCL4, CCL5, CCL8, SDF1, VEGF, MIP-1, and MIF (Panni et al., 2013). The chemokine CCL2 was extensively studied and reported as one of the key factors inducing the accumulation of circulating monocytes within tumors (Kitamura et al., 2015; Cassetta and Pollard 2018). Due to the mostly suppressive activity of TAMs, a series of reports have proposed strategies to block the CCL2-CCR2 axis aiming to avoid monocyte trafficking and accumulation into the tumor tissues. These studies revealed a significant impact on tumor growth and metastasis in pre-clinical settings (Qian et al., 2011; Macanas-Pirard et al., 2017; Nywening et al., 2018), but clinical trials failed to demonstrate similar efficacy (Fetterly et al., 2013; Pienta et al., 2013). Importantly, the restoration of the CCL2-CCR2 axis after blockage promotes new waves of monocyte recruitment and accumulation, inducing an acceleration of tumor growth on mice (Bonapace et al., 2014). In addition, no effect was noted on established tissue-resident macrophages in the tumor microenvironment after CCL2-CCR2 blockage (Zhu et al., 2017). Other molecules have been identified as promoting monocyte recruitment to tumor sites. The inhibition of CCL5-CCR5 interaction has been shown to have an impact on tumor growth and metastasis (Cambien et al., 2011; Ban et al., 2017). In fact, some studies have described CCL5 as a critical chemokine present in the tumor microenvironment that is able to promote the recruitment of DC to the tumor mass (Böttcher et al., 2018; Cueto et al., 2021). Once accumulated in the tissue, intratumoral DCs will, in turn, produce important levels of CXCL9 and CXCL10, critical chemokines that attract T cells within tumors (Spranger et al., 2017). This sequence of events may generate the stimulation of anti-tumor T cell responses and tumor control.

Targeting CXCR4, a receptor for CXCL12 molecule, has also been demonstrated to have an impact on monocyte recruitment in a colorectal tumor mouse model (Jung et al., 2017). More recently, two studies highlighted new signaling pathways able to induce monocyte/macrophage attraction and accumulation on tumors. Zhang and others showed that IFN-γ affects CXCL8-CXCR2 signaling and consequently reduced TAM trafficking within the tumor microenvironment (Zhang M. et al., 2020, 8). Takahashi et al. used *in vitro* assays to reveal the role of soluble-VCAM-1 molecule produced by pancreatic cancer cells in the chemo attraction of murine macrophages (Takahashi et al., 2020). Thus, a mixture of soluble factors may drive the migration of myeloid immune cells into the tumor microenvironment. The effective manipulation of the chemo attractive signals along with proper macrophage differentiation may promote the infiltration and accumulation of subpopulations of these cells capable of controlling the tumor.

Monocytes

Human monocytes represent around 10% of mononuclear cells in peripheral blood. For decades, many authors have used flow cytometry to further describe these cells into three major subsets

with distinct proportions: classical monocytes $CD14^{high}CD16^{neg}$ (around 90% of total monocytes), intermediate monocytes $CD14^{high}$CD16+ (around 2% of total monocytes) and inflammatory monocytes $CD14^{low}CD16^{high}$ (around 8% of total monocytes) (Passlick et al., 1989; Ziegler-Heitbrock et al., 2010; Wong et al., 2012). Microarray mRNA analysis of FACS-sorted monocytes revealed unique transcriptional gene profiles for each of these subsets (Wong et al., 2011). Among newly described markers, authors revealed, both at mRNA and at protein levels, that classical monocytes express higher levels of CD1d, CD99, CD9 and CD36; intermediate monocytes showed higher levels of CLEC10A and GFRa2; and inflammatory monocytes showed elevated expression of CD294, P2RX1, and SIGLEC10. Additional studies using pseudo-time scRNAseq analysis have confirmed that both non-classical monocytes subsets may originate from classical monocytes, in mice and humans (Mildner et al., 2017; Villani et al., 2017). Of note, the CD163 scavenger receptor, which has been extensively used to describe macrophages subsets (Ruffell and Coussens 2015; Ramos et al., 2020), is also expressed by monocytes and newly described DC subsets (Villani et al., 2017) and is significantly more expressed in both classical and intermediate monocytes, in comparison to inflammatory monocytes. More recently, single-cell approaches have re-oriented the description of monocyte subsets by revealing new markers and functional features of these cells. Two new markers, CD88 and CD89, were described as specifically expressed by human classical monocytes, discriminating these cells from other immune cell subsets (Dutertre et al., 2019; Bourdely et al., 2020). These new findings are of great interest, considering that the characterization of monocytes in tissues is still challenging, since many of their surface markers are shared with macrophages (e.g., CD14, CD68, and CD163).

Hematopoietic stem cells give rise to progenitors that will progressively generate monocyte-committed progenitors and, subsequently, monocytes. Importantly, elevated counts of blood monocytes were described in cancer patients and tumor-bearing mice (Cortez-Retamozo et al., 2012; Sanford et al., 2013; Trovato et al., 2019), where increased numbers of blood monocytes were associated to worse prognoses (Lee, 2012; Shigeta et al., 2016; Hayashi et al., 2017; Feng et al., 2018). This phenomenon is further supported by the elevated serum levels of CCL2, a critical cytokine for monocyte mobilization from bone marrow (Monti et al., 2003; Dehqanzada et al., 2007; Sanford et al., 2013). Coherently, additional factors were found increased in cancer patients' serum, including the classical growth factors: G-CSF, GM-CSF, and M-CSF (Scholl et al., 1996; Wu et al., 2014; Ribechini and Hutchinson 2017). Notably, M-CSF is critical during monocyte development, promoting survival and proliferation of myeloid progenitors towards monocytic cell lineages (Rieger et al., 2009). Moreover, blood monocytes under high concentrations of M-CSF may acquire an anti-inflammatory profile, giving rise to potential suppressive mature macrophages (Menetrier-Caux et al., 1998; Jaguin et al., 2013; Ramos et al., 2020).

There are emerging data indicating that tumor-derived factors can affect monocyte differentiation remotely, altering bone marrow progenitors. A series of studies have uncovered an altered transcriptomic profile of circulating monocytes in both cancer patients (Chittezhath et al., 2014; Cassetta et al., 2019; Kiss et al., 2020; Ramos et al., 2020) and mouse tumor models (Torroella-Kouri et al., 2013; Stone et al., 2014) when compared to tumor-free individuals. One important consequence of this phenomenon is the biased differentiation programming found in patients' monocytes when compared to healthy donors, which gives rise to dysfunctional DC and macrophages (Ramos et al., 2012; Ramos et al., 2020), thus impacting adaptive anti-tumoral responses.

Due to their elevated degree of plasticity and sensitivity, monocytes can rapidly migrate and respond to inflammation in tissues. However, tumor-derived factors can also influence their process of differentiation by modulating their phenotype, differentiation and functions at tumor sites and systemically. Harnessing the great plasticity of monocytes and the precise definition of their differentiation pathways, it would be possible to recruit specifically functional cells, representing a great gain for the development of new therapies for cancer.

Macrophages

The function and phenotype of macrophages in the tumor microenvironment have been extensively described in the last decades (Ruffell and Coussens 2015). Most of the reports have associated the features of macrophages to an oversimplified bipolar model M1 (pro-inflammatory) x M2 (anti-inflammatory) (Lacey et al., 2012; Jaguin et al., 2013). Pro-inflammatory M1-macrophages have been mostly associated to anti-tumoral responses, while M2-macrophages have shown pro-angiogenic and immunosuppressive capabilities (Pollard 2004). Based on this model, many studies have used M1 or M2-like markers to describe TAMs in distinct human tumor types. Most of the markers used included CD68, CD14, CD163, and CD206 (Steidl et al., 2010; Ruffell and Coussens 2015). CD68 and CD14 molecules are expressed by monocytes, macrophages and some DC subsets, regardless of their functional status. CD163 and CD206 markers currently correspond to an M2 immunosuppressive-like macrophages status, and are associated to poor patient prognosis for several solid and hematologic tumors, such as: breast (Medrek et al., 2012; Ramos et al., 2020), ovarian (Reinartz et al., 2014), pancreatic (Ino et al., 2013) and acute myeloid leukemia (Yang et al., 2018; Guo et al., 2021). In the recent years, with new technologies using large-scale single-cell approaches, the bipolar model of macrophage differentiation–M1 versus M2-macrophages–has been gradually replaced by a multidimensional landscape (Chevrier et al., 2017; Lavin et al., 2017; Azizi et al., 2018). Three new markers have emerged from recent studies using single-cell approaches redefining macrophage features on tumors: APOE (Apolipoprotein E), TREM2 (Triggering receptor expressed on myeloid cells 2) and FOLR2 (Folate receptor 2). APOE has been associated to a new pan-macrophage marker, distinguishing these cells from blood monocytes (Lavin et al., 2017; Azizi et al., 2018). TREM2 was described as expressed on suppressive monocyte-derived macrophages that are accumulated on tumor sites

(Katzenelenbogen et al., 2020; Molgora et al., 2020; Ardighieri et al., 2021). FOLR2 molecule is expressed on tissue-resident macrophages in a variety of tissues and was also found on stromal areas from human tumors (Sharma et al., 2020; Ramos et al., 2021).

Considering that macrophages are one of the most frequent immune infiltrating cells in solid tumors, a crescent number of reports have described anti-tumor strategies that target the immunosuppressive functions of TAMs (Liu and Wang 2020). These new "omics-studies" have uncovered distinct subsets of TAM and tissue-resident macrophages presenting a complex functional programming that offer new targets for molecular targeting and new perspectives for clinical interventions.

Dendritic Cells

Dendritic cells constitute a very heterogenous group of innate cells with specialized functions that are distributed in a wide variety of tissues. DC subsets are conserved across diverse human tumors and tissues (Gerhard et al., 2021). In contrast to other APCs, such as macrophages, B cells and monocytes, DC have a unique ability to migrate, transport and present tumor-antigens to naïve T cell in the lymphoid organs (Mildner and Jung 2014; Ruhland et al., 2020), being critical for the initiation of adaptive immune responses. A great range of tumors are devoid of DC infiltration (Broz et al., 2014), and it may explain the failure of anti-tumor T cell immunity in tumor control (Spranger et al., 2017).

Studies focused on DC biology in cancer have associated the presence of these cells with good patient outcome for distinct tumor types (Malietzis et al., 2015; Truxova et al., 2018; Melaiu et al., 2020). Not only the presence of DCs but their activation status and tissue spatial localization have highlighted the functional impact of these cells in patients. Ruffel and collaborators (Ruffell et al., 2012) have shown a decrease in frequency of tumor-infiltrating DCs in tumor areas when compared to normal adjacent tissues. Besides that, tumor-infiltrating DCs were described as dysfunctional and immature (Bell et al., 1999; Gervais et al., 2005; Dieu-Nosjean et al., 2008), and may participate in the tumor angiogenesis (Fainaru et al., 2008). In fact, DCs were also described as immature in tumor bed, in contrast to activated DCs found in tumor periphery (Treilleux et al., 2004; Baleeiro et al., 2008). A study by Goc and collaborators (Goc et al., 2014) correlated a lower risk of death in lung cancer patients with the presence of mature DCs and Th1-like lymphocytes in peritumoral tertiary lymphoid structures (TLS). Many studies have explored the tumor-induced mechanisms responsible for the blockage of DC maturation and antigen presentation for T cells. Thomachot and others (Thomachot et al., 2004) showed that products derived from human breast carcinoma cell lines were able to block the *in vitro* maturation of DC derived from CD34+ progenitors. The accumulation of some metabolites such as fatty acid and lactic acid also impair the antigen processing and presentation as well as the production of pro-inflammatory cytokines by DC (Herber et al., 2010; Cao et al., 2014; Caronni et al., 2018). In addition, a variety of cytokines were reported as critical for dampening DC functionality. The vascular endothelial growth factor (VEGF) is highly expressed in the tumor microenvironment from distinct tumor types and inhibit the activity of FMS-like tyrosine kinase 3 ligand (FLT3L), a critical factor for DC development and maturation (Gabrilovich et al., 1996). IL-6 and IL-10 are known to play a critical role in the blockage of DC functions by promoting STAT3 activation, which may impede IL-12 production and promote IL-10 amplification (Diao et al., 2011; Tang et al., 2015). Farren and others (Farren et al., 2014) suggested that tumor-derived factors sustained STAT3 up-regulation on myeloid cells progenitors avoiding the activation of ERK and NF-kB signaling, which may limit the monocyte capacity to be differentiated into DCs. Furthermore, TGF-β present in the tumor microenvironment has been reported as critical to suppress DC maturation and inhibit their production of pro-inflammatory cytokines such as IL-12 and TNF-α, hampering the activation of T cells (Belladonna et al., 2008; Flavell et al., 2010). Importantly, tumor factors may also affect myeloid APCs at circulation, since defective subpopulations of DCs were described in the blood of cancer patients (Satthaporn et al., 2004).

Recent reports using transgenic mice models and single-cell approaches have further detailed the intrinsic features of the distinct DC subsets in the oncology field. Both mouse and human cDC1 were described as highly efficient for cross-presentation in the tumor context by stimulating CD8+ T cells responses (Jongbloed et al., 2010; Wculek et al., 2019). Additional studies have described that type I interferon may enhance anti-tumor properties of cDC1 cross-presentation and CD8+ T cell stimulation (Diamond et al., 2011; Fuertes et al., 2011). The cDC2 subset constitute the most heterogenous population of conventional DCs presenting a wide diversity of phenotypes (Villani et al., 2017; Dutertre et al., 2019). These cells can produce a large spectrum of cytokines and are involved in the induction of diverse CD4+ T helper subsets in both inflammatory and cancer contexts (Binnewies et al., 2019; Bosteels et al., 2020). The recently described DC3 is still under deep characterization. A study by Bourdely and others (Bourdely et al., 2020) have described the DC3 subset as effective for the priming of CD8+CD103+ tissue-resident memory T cells via the production of TGF-beta. In agreement, presence of DC3 are also associated to the accumulation of CD8+ T tissue-resident memory cells in human breast cancer tissues. Dutertre and collaborators (Dutertre et al., 2019) also reported that DC3 are capable to expand CD4+ T helper cells *in vitro*. Of note, CD14+CD163+ DC3 subset were strong inducers of CD4+IL17A+ Th17-likecells when compared to cDC2 subtype, suggesting their role in inflammatory responses.

The plasmacytoid DC subset has been extensively characterized in the tumor field. These cells were associated to a poor patients' prognosis in distinct types of cancer (Wculek et al., 2020). In fact, various reports have described a tolerogenic profile of tumor-infiltrating pDCs. Breast cancer infiltrating pDCs have shown an impaired capability to secrete IFN-α (Sisirak et al., 2012), which may be partially explained by the higher concentrations of TGF-β and TNF-α found in the tumor microenvironment (Sisirak et al., 2013). Similarly, the dysfunctional pDCs profiling was described for other tumor types including ovarian (Labidi-Galy et al., 2011)

and melanoma (Camisaschi et al., 2014). Other studies also uncovered the pDC role in the induction of suppressive CD4+ regulatory T cells in breast cancer patients, suggesting the mechanisms that explain their pro-tumorigenic profile (Faget et al., 2012; Sisirak et al., 2012).

Another critical DC subset described in many inflammatory conditions, including cancer, is the monocyte-derived DC. These cells can be found in the tissues from both mice and humans and emerge via the recruitment of CCR2+ monocytes from the blood (Schlitzer et al., 2015). *In vivo*, is still challenging to exactly define Mo-DCs phenotype and function due to their high plasticity and its profiling that overlaps with other DC subsets and macrophages (Collin and Bigley 2018). Many reports have described strategies for the manipulation of Mo-DCs due to the possibility of Mo-DC *in vitro* differentiation from blood monocytes (Sallusto and Lanzavecchia 1994) or CD34+ progenitors (Caux et al., 1996). It has allowed researchers to develop clinical protocols using Mo-DC based-vaccines to treat distinct diseases, including cancer (Barbuto et al., 2004; Neves et al., 2005). Mo-DCs plasticity can be also explored by treating monocytes with soluble factors, cytokines, TLR-L and other compounds to drive their cellular functions towards the stimulation of a variety of T helper responses and/or CD8+ T cell activation (Harris 2011; Goudot et al., 2017). *In vivo*, Mo-DC has been associated to an anti-tumor function. Kuhn and collaborators (Kuhn et al., 2015) reported that the blockage of Mo-DC recruitment and differentiation in tumor sites impede the stimulation of anti-tumor immunity in mice models. In addition, Mo-DCs isolated from cancer patients are capable to cross-present tumor antigens and activate cytotoxic CD8+ T cells *ex vivo* (Tang-Huau et al., 2018).

Altogether, DCs critically participate in the initiation and expansion of anti-tumor adaptive immune responses with specialized functions and intrinsic roles for each subset. Despite all the uncertainty, however, DC continues as a central piece in tumor immunotherapy. From one side, the effectiveness of other immunotherapeutic modalities highlights the immune system's effector mechanisms potential in cancer therapy and DCs remain the best-known cells to initiate the immune responses that would recruit such mechanisms.

Another fact that should be considered when looking at DC in the context of immunotherapy is, from one side, the heterogeneity and plasticity of the immune response and, from the other, our still incomplete knowledge of its role in each disease. Although improving the scenario is still uncertain. However, the use of a cell, itself heterogeneous and plastic, and that is hardly constrained by our manipulations, leaves the door open to "unexpected" results, which might become those that actually point to the "right" way to achieve success. The comprehensive use of these cells by exploring their skills and improving their clinical application alone or in combination with other therapies may represent a great gain for cancer patients' treatment.

CHIMERIC ANTIGEN RECEPTOR ON T CELLS AND NATURAL KILLER CELLS

The development of T cells expressing CAR date from the first studies performed in the 80's by Gross and collaborators (Gross et al., 1989). This strategy was further optimized in the subsequent years by the comprehension of the critical mechanisms for CAR-T cell activation, expansion and *in vivo* survival (Krause et al., 1998; Maher et al., 2002; Brentjens et al., 2003). The first trials using genetically engineered T cells highlighted its safety and its impact on cancer patients' survival (Morgan et al., 2006; Kochenderfer et al., 2010), paving the way for the subsequent clinical applications. Since 2017, the Food and Drug Administration department (FDA, United States) has approved five products of CAR-T for refractory non-Hodgkin B cell lymphoma, acute lymphocytic leukemia and multiple myeloma (Maude et al., 2018; Park et al., 2018; Munshi et al., 2021). Lately, clinical trials using CAR-T cells have been really encouraging with studies reporting residual disease-negative complete responses for about 70% of patients with distinct hematological malignancies (Ortíz-Maldonado et al., 2021). More recently, studies have also focused on the improvement of the manufacturing process of CAR-T cells by aiming to diminish the time for production and costs, while ameliorating the quality and the life-spam of the cells *in vivo*. The creation of the 4th generation (Chmielewski and Abken 2020) and bispecific CAR-T cells (Shah et al., 2020; Fousek et al., 2021) are examples of such improvements to be applied in the clinics.

Another recent strategy was the manufacture of NK cells expressing CAR. Many advantages were considered in the use of these cells to treat malignances, including: its intrinsic ability to eliminate cells with down regulated HLA expression, its application in allogenic scenarios and a lower potential of toxicity, which will reduce side-effects and costs with patients' conditioning (Moretta et al., 2011; Simonetta et al., 2017; Xie et al., 2020; Albinger et al., 2021). Pre-clinical reports have demonstrated that CAR-NKs generated from both peripheral blood and umbilical cord blood have effective capabilities to eliminate CD19+ target tumor cells *in vitro* (Herrera et al., 2019). In the clinical settings, trials using cord blood-derived CAR-NK for patients with B-cell malignancies showed very enthusiastic results, by reporting clinical responses in around 70% of treated individuals and CAR-NK persistence at the periphery for around 1 year (Liu et al., 2020).

Despite great success of CAR-T and CAR-NK treatment for hematological cancers, first clinical trials using CAR-T cells for solid tumors have reported disappointing results (Kershaw et al., 2006; Lamers et al., 2011; Thistlethwaite et al., 2017). Most clinical trials using CAR-NK for solid tumors are still ongoing and no conclusive results were presented so far. Many authors have extensively discussed the possible limitations for the success of CAR-T and CAR-NK in solid tumors (Hanahan and Coussens 2012; Li et al., 2018; Marofi et al., 2021). Main cited reasons include but are not limited to: the high mutational burden generating a diversity of tumor antigens, the dense extracellular matrix that may promote T cell exclusion, the absence of chemo-attractive factors for T cells, the limited *in vivo* persistence of CAR-T cells and the immunosuppressive microenvironment.

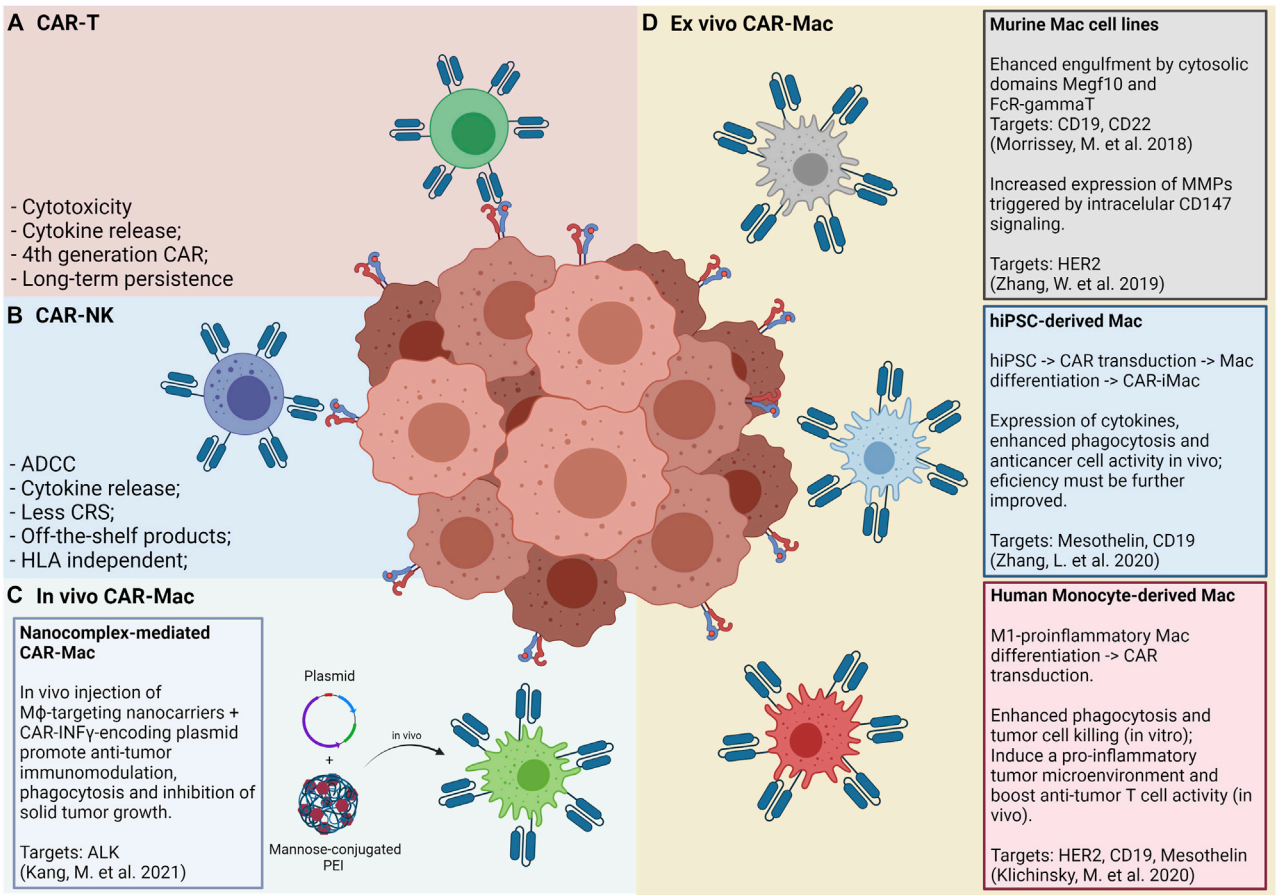

FIGURE 2 | Panels **(A)** and **(B)** show the "classic" CAR-T and CAR-NK approaches, respectively, and its main features and advantages. Panel **(C)** shows an *in vivo* approach for CAR-Mac production, in which a nanocomplex composed of mannose-conjugated PEI and DNA plasmids is intratumorally or intraperitonially administered and internalized by local macrophages. Panel **(D)** shows the approaches so far tested for generating and applying CAR-Mac cells against solid tumors (Morrissey et al., 2018; Zhang et al., 2019; Klichinsky et al., 2020; Zhang L. et al., 2020). Both murine and human macrophages were reprogrammed to target at least four tumor markers (CD19, CD22, HER2, and Mesothelin). Human macrophages were obtained from peripheral blood monocytes and from iPS cells.

CHIMERIC ANTIGEN RECEPTOR ON MYELOID IMMUNE CELLS

The low efficacy of CAR-T cell therapies for solid tumors may be, probably, explained by the inability of these cells to effectively infiltrate the tumor mass. Among the main reasons for this failure are the lack of classical T-attractive chemokines (e.g., CXCL9 and CXCL10), the dense tumor microenvironment matrix and the higher tumor-antigen heterogeneity, as compared to hematologic tumors. To overcome these difficulties, recent studies have suggested the use of CAR-engineered monocytes/macrophages for the elimination of solid tumors. Still, few reports have described CAR-Mac functionalities, but this emerging topic has called the attention of the scientific community. We summarize below the key works recently published using CAR-Mac technologies highlighting their particularities (**Figure 2**).

The study by Morrissey and collaborators (2018) (Morrissey et al., 2018) used murine CAR-Mac constructs strategies to enhance the phagocytosis of cancer cells. The authors' strategy consists in an extracellular single-chain antibody variable fragment (ScFv) specific for CD19 or CD22 with the CD8 transmembrane domain linked to a cytoplasmatic domain able to promote macrophage phagocytosis. By screening a library of intracellular domains of engulfment receptors, the authors selected the cytosolic domains from Megf10 and FcR-gamma, achieving a robust engulfment of antigen-coated synthetic particles. Macrophages expressing anti-CD19 or anti-CD22 CARs linked with the cytosolic domain Megf10 showed superior abilities of phagocytosis of synthetic beads with up to 20 μm of size when compared to CAR-GFP controls. Authors further demonstrated that the synapse of CAR-Mac cell-bead interaction induced stimulation via phosphotyrosine expression at comparative levels of CD3ζ signaling. Authors next tested the phagocytic capabilities of J774A.1 CAR-Mac expressing Megf10 and FcRγ intracellular domains in co-culture with human Raji B cell lines, cells that express CD19 endogenously. Elegant images showed that CAR-Mac with both intracellular domains presented a significant higher capability to promote trogocytosis or to engulf tumor cells when compared to control CAR-Mac GFP+. This

effect was further improved when the authors engineered CAR-Mac to increase the PI3K employment by fusing the CD19 cytoplasmatic domain, which is able to recruit the p85 subunit of PI3K. Altogether, this study provides an attractive engineered strategy to increase engulfment and elimination of tumor cells by CAR-Mac.

Another interesting study reported by Zhang and others (2019) (Zhang et al., 2019) described a murine anti-HER2 CAR-Mac Raw264.7 engineered with an intracellular signaling domain of CD147 (CAR-147-Mac), able to trigger the expression of matrix metalloproteinase (MMPs) after antigen recognition. This strategy aims to remodel the tumor microenvironment extracellular matrix, facilitating the infiltration of immune cells or drugs. Authors showed that CAR-147-Mac were able to produce significant high levels of mRNA for distinct MMPs upon HER2 antigen binding in co-cultures with 4T1 cell lines during 24 and 48 h. A more pronounced expression of *MMP3, MMP9, MMP10*, and *MMP13* was noted when compared to co-cultures between 4T1 cell lines lacking HER2 antigen expression. For *in vivo* assays, CAR-147-Mac were found in liver and tumors of mice even after 7 days of intravenous infusion. No differences were noted in total body weight of HER2+ 4T1 tumor-bearing mice injected with both CAR-147-Mac or control CAR-Mac, but significant reduction of the weight of the spleen and tumor mass was noted in animals that received CAR-147-Mac. The infusion of CAR-147-Mac significantly inhibited HER2+ 4T1 tumor growth in mice along with an up-regulation of the anti-tumor cytokines such as IL-12 and IFN-gamma, thus suggesting that this strategy involves both local modulation and systemic anti-tumor responses. In addition, CAR-147-Mac treatment promoted an increase in T-cell infiltration and a reduction of GR1+ myeloid cells into tumors. Added, no differences were found in the infiltration of DCs, NKs, and TAMs as well as in markers of activation for T cells (PD-1, CD44, CD62L, and CD107a) when comparing tumor-bearing mice that received CAR-147-Mac or control CAR-Mac. In agreement, authors used balb/c nude mice model to demonstrate that no effect in tumor control was noted after CAR-147-Mac infusion. By showing IHC images from tumor sections authors reported a significant reduction in tumor collagen deposition in mice treated by CAR-147-Mac. Using a human *in vitro* 3D spheroid system by co-culturing THP CAR-147-Mac with HER2+ MDA-MB-453 tumor cell line authors showed an increased mRNA expression of various MMPs allowing the infiltration and accumulation of T cells. In conclusion, this study provided an interesting approach using engineered macrophages able to modify the extracellular matrix, allowing T cell infiltration in the tumor mass.

More recently, two additional studies reported strategies for CAR-Mac manufacturing using human cells as primary resources. Zhang and collaborators (Zhang L. et al., 2020) focused on undifferentiated stem cells by developing a three-step procedure: I) reprogramming human PBMCs towards an induced pluripotent stem cell (iPSCs) using non-integrating episomal vectors; II) engineering CAR expression on IPSCs by lentiviral transduction; III) promoting macrophage differentiation from CAR-iPSCs using a cocktail of growth factors and cytokines including bFGF, VEGF, SCF, IGF-1, IL-3, M-CSF, and GM-CSF to obtain a final cell product of CAR induced macrophages (CAR-iMac). Authors firstly characterized and validated CAR-iMac phenotype at both transcriptional and protein levels. By flow cytometry iCAR-Mac closely resembled to primarily differentiated macrophages by showing the expression of typical proteins, such as CD11b, CD14, CD163, and CD68. At the transcriptional level CAR-iMac displayed a distinct programing from those undifferentiated IPS and clustered with primary differentiated macrophages. In addition, CAR-iMac present enrichment for genes related to GO pathways ofinnate immunity, antigen processing and presentation and positive regulation of cytokine production while expressing high levels of characteristic macrophage genes such as*AIF1*, *CSFR1*, and *SPI1*. Authors also implied scRNA-seq analysis and found that CAR-iMac cells clustered with macrophages already described in public datasets. Subsequently, authors aimed to validate functional features of iCAR-Mac against two antigens, CD19 and mesothelin. Anti-CD19 CAR-iMac co-cultured with CD19+ K562 cells expressed higher levels of *TNF*, *IL1A*, *IL1B*, and *IL-6* and displayed enrichment on pathways related to antigen process and presentation and positive regulation of cytokine production when compared to control CD19- K562 cells. Authors also showed an increased phagocytosis of anti-CD19 CAR-iMac when K562 target cells expressed CD19. Similar results were obtained for *in vitro* assays using Meso+ OVCAR3 cells lines. For *in vivo* assays, NSG mice were injected with luciferase-expressing Meso+ HO8910 cell lines intraperitoneally, prior to anti-meso CAR-iMac infusion. Data showed a significant reduction in bioluminescent tumor cells when compared to PBS-treated mice at days 4, 11, and 14 post-treatment. Considering that pluripotent stem cells have a great expansion potential it could be maintained as an unlimited source. Thus, the platform for iPSC-derived engineered CAR-Mac emerges as a very promising approach to be further explored for a variety of malignancies and tumor antigens.

An elegant study by Klichinsky and others (Klichinsky et al., 2020) reported the engineering of CAR-Mac from human monocyte-derived macrophages applying the classical M1-like *in vitro* protocol based on GM-CSF treatment. Moreover, the authors established a new protocol for primary macrophage transduction with high reproducibility (validated in more than 10 distinct monocyte donors) and efficiency (>75% of CAR-positive cells) by using the chimeric adenoviral vector Ad5f35. CAR-Mac manufactured with Ad5f35 adenovirus were able to efficiently phagocyte tumor cells from both hematological and solid tumor lines as well as control tumor growth in xenograft mouse models when administered via intravenous or intraperitoneal routes. Interestingly, CAR-Mac transfected with Ad5f35 showed superior phagocytic capacity than control M1-like macrophages and presented a stable pro-inflammatory phenotype in the tumor microenvironment. CAR-Mac were also found infiltrating distinct organs from tumor bearing-mice and persisted for up to 62 days in tumor-free animals. Surprisingly, the authors also reported efficient cross-presentation promoted by CAR-Mac transfected with Ad5f35, since in co-cultures with CAR-Mac pre-incubated with NYESO1+ tumor cell lines in an HLA-A201+ restricted

context, an increase in NYESO1+CD8+CD69+ activated T lymphocytes and an up-regulation of IFN-gamma secretion was detected. In addition, CAR-Mac were able to efficiently recruit both resting and activated T cells in chemotaxis assays and to induce activation of immature DCs via soluble factors. Importantly, this study by Klichinsky and others (Klichinsky et al., 2020) paved the way for the first phase-I clinical trial using CAR-Mac launched in 2020 for a variety of HER2-overexpressing solid tumors (NCT04660929). In this study, the authors estimate the recruitment of patients with no available curative treatment options that will be separated into two treatment groups. One group will undergo intra subject dose escalation of IV administrations of up to 500 million cells on D+0, up to 1.5 billion cells on D+3, and up to 3 billion cells on D+5. The other group will receive a single dose of up to 5 billion cells on D+0. As primary endpoints, the investigators will evaluate the safety and tolerability of the infused product by estimating the frequency and severity of adverse events (i.e., CRS) in the trial subjects during a 14 months follow-up period. The feasibility of manufacturing anti-HER2 CAR-Mac will also be assessed by describing the percentage of products that pass the release criteria. The Overall Response Rate (ORR), as well as the Progression Free Survival (PFS) of subjects that receive at least one dose of the product will be assessed as secondary endpoints within a time frame of 24 months.

More recently, Kang and collaborators (Kang et al., 2021) have described an *in vivo* approach for CAR-Mac reprograming using mannose-conjugated polyethylenimine (MPEI) nanocomplex as a gene delivery of plasmids for anti-ALK (anaplastic lymphoma kinase) CAR and IFN-gamma. Based on the fact that TAMs with anti-inflammatory properties may overexpress the mannose receptor (CD206), authors took advantage of this system to target macrophages *in situ*. They added in the plasmid construction the *IFN-γ* gene, a classical known cytokine able to stimulate a pro-inflammatory phenotype (Ramos et al., 2020). Both ALK-CAR and IFN-γ genes were cloned using the non-viral transposon system of piggyBac, for stable and persistent CAR expression. Using this systems authors proposed to target ALK tumor-antigen as well as to reprogram TAMs to acquire pro-inflammatory properties inducing adaptive immune T cell responses. Authors firstly validated the manufacturing of MPEI/pCAR-IFN-γ nanocomplexes indicating homogenous sizes and a great stability in serum for up to 7 days. Also, no cytotoxicity was noted in treated-bone marrow derived macrophages (BMDM), whereas CAR and IFN-gamma expression were validated in *in vitro* treated M2-BMDM. Of note, the efficiency of transfection was about 14% in M2-BMDM treated cells with a 20-fold increasing in IFN-gamma expression. In terms of functional *in vitro* assays, authors reported an increase of phagocytosis capability of M2-BMDM MPEI/pCAR-IFN-γ treated cells for distinct ratios of BMDM: ALK+ target Neuro-2a tumor cell. In addition, M2-BMDM presented a shift of phenotype towards a M1-like profile once treated by MPEI/IFN-γ or MPEI/pCAR-IFN-γ by showing a significantly down-regulation of CD163, CD206, IL-10, and arginase-1 concomitantly with an up-regulation of CD80, CD86, and TNF-alpha. Subsequently, authors tested the *in vivo* effects of MPEI/pCAR-IFN-γ and variations of this construction in tumor growth and tumor microenvironment modulation. Using a Neuro-2a syngeneic tumor-bearing mice model, authors reported a significant control of tumor growth in animals receiving both MPEI/pCAR or MPEI/IFN-γ, but this anti-tumoral effect was further increased under intratumoral infusion of the MPEI/pCAR-IFN-γ full construct. By analyzing the tumor microenvironment composition after MPEI/pCAR-IFN-γ treatment, authors found a significant increase in CD8+ T cell infiltration and INOS expression along with a strongly reduced expression of Arginase-1, TGF-beta, and IL10, indicating local immune modulation effects. Alternatively, by injecting MPEI/pCAR-IFN-γ intraperitoneally in tumor-bearing mice authors showed presence of CAR+ immune cells in liver, kidney and tumor mass as well as a significant effect on tumor control, even considering it less pronounced than intratumoral infusion. In conclusion, the transfection efficiency observed in this study was lower than that of lentiviral transduction and should be further improved. Importantly, *in vivo* infusion of MPEI/pCAR-IFN-γ nanocomplex allows the transfection of a variety of immune cells, including DCs and T lymphocytes, possibly amplifying the anti-tumoral effects. Thus, this nanocomplex strategy may overcome the high costs, the exhaustive process for CAR-Mac manufacturing and avoid the concerns of the use of viral vectors representing an important new avenue for future strategies.

LIMITATIONS OF CAR-MYELOID CELLS

We have summarized in **Table 1** the main differences among CAR-T, CAR-NK, and CAR-myeloid cells by highlighting the process for manufacturing of these cells and their potential applications. Two important obstacles of using myeloid cells in CAR-based therapies are the inability of primary macrophages and DCs to expand *in vitro* and the difficulty in delivering exogenous genetic material (Keller et al., 2018). Viral and non-viral delivery systems were tested in macrophages and DCs in the past decades and both presented limitations. Professional phagocytes present a powerful immune response against viral DNA making it difficult to efficiently deliver a transgene through viral vectors. On the other hand, the application of physical transfection such as nucleoporation or nucleofection did not elicit important immune responses but caused important changes in gene expression profile and functional status of macrophages and DCs (Harizaj et al., 2021). As a matter of comparison, the main steps of CAR-T cell production involve the reprogramming and expansion of T cells in order to obtain a high number of CAR+ cells before infusion. New studies have described the use of artificial APCs to stimulate T cells. The distinct approaches include cell lines modified to provide antigen-presentation and co-stimulation (Couture et al., 2019; Schmidts et al., 2020) and synthetic complexes of mesoporous silica microrods loaded with soluble mitogenic compounds and T-cell ligands (Zhang D. K. Y. et al., 2020). Recent studies have also described strategies to stimulate NK cells based on cytokine cocktails, generating a memory-like phenotype (Pahl et al., 2018). These cells present

TABLE 1 | Comparison of key manufacturing steps for CAR-based cellular products (CAR-T, CAR-NK, and CAR-Myeloid cells) and its specific advantages and disadvantages. PEI, Polyethylenimine; GM-CSF, Granulocyte-macrophage colony-stimulating factor; M-CSF, Macrophage colony-stimulating factor.

	CAR-T cells	CAR-NK cells	CAR-myeloid cells (CAR-Mac, CAR-DC)
1. Cell type and selection	Positive selection of CD3+ and/or CD4+ or CD8+ cells	Positive selection of CD56+ cells	Positive or negative selection of CD14+ cells
2. Activation/ differentiation	Beads/antibodies anti-CD3/CD28 Artificial APC cell lines	Beads/antibodies anti-CD335/CD2 Culture with IL-2, IL-15 and/or IL-21	Culture with GM-CSF, M-CSF, TNF-alpha, IFN-gamma TLR-Ligands
3. Gene delivery			
3.1 CAR viral delivery	Retroviral vector Lentiviral vector	Retroviral vector Lentiviral vector	Adenoviral vector Lentiviral vector
3.2 Non-Viral CAR delivery	Nucleoporation Liposomes Expression systems Sleeping Beauty; PiggyBac; mRNA Nanoplasmids	Nucleoporation Liposomes Expression systems Sleeping Beauty; PiggyBac; mRNA Nanoplasmids	Nanocomplex (Mannose-associated PEI + DNA plasmid) Expression systems PiggyBac
4. Expansion	Culture with IL-2, IL-7, IL-15 and/or IL-21	K562 feeder cells expressing membrane bound IL-21 Culture with IL-12 and IL-15 Memory-like phenotype: IL-12, IL-15, and IL-18	Primary human macrophages cannot be expanded *ex vivo* THP-1 cell line spontaneously expands *in vitro* and can be differentiated when cultured with PMA.
5. Final Product			
5.1 Lifespan	Long-term persistence after tumor remission	Mid-term lifespan *in vivo*	Short-term lifespan of myeloid cells *in vivo* (no available data for CAR-Myeloid)
5.2 Advantages	Efficient selection, activation and easy handling	Applicable in allogenic scenarios Low toxicity Can be obtained from multiple sources	Applicable in allogenic scenarios Low toxicity in animal models Potential application in solid tumors CAR-DCs may present a migratory potential to lymphoid organs
5.3 Disadvantages	Long-term cultures and/or high doses of IL-2 can induce terminally differentiated/exhausted T cells or biased expansion of regulatory CD4+ T cells Cytokine release syndrome (CRS) and/or Immune effector cell associated neurotoxicity syndrome (ICANS) may occur Long-term "on-target, off-tumor" effects (ex.: B cell aplasia when targeting CD19)	Few cells are obtained after selection Laborious expansion and genetic modification	Laborious transfection procedures Difficult genetic reprogramming due to the recognition of foreign genetic material No results from clinical trials so far

a long-lived profiling by expanding and producing IFN-gamma some weeks post-infusion. Considering that macrophages and DCs do not have the same potential of expansion as compared to T or NK cells, the number of CAR-Mac or CAR-DCs available for infusion would be significantly lower than in CAR-T or CAR-NK applications, which may limit their use in large tumors or in strategies using multiple doses.

Besides, the relatively short lifespan of CAR-Mac compared to CAR-T cells and CAR-NKs is a topic of concern. As discussed above, first studies are encouraging, but additional pre-clinical tests are needed to evaluate the functional status, the persistence of CAR-Mac *in vivo*, as well as the variation of cell number needed for infusion. To assure that CAR-Mac will reach the tumor mass in the shortest possible time after infusion, diverse routes of injection should be further explored in tumors of distinct origins since tissue arquiteture may vary considerably. So far, few targets have been tested in the use of pre-clinical CAR-Mac and clinical translation of CAR-myeloid cells and the future of its application relies on the overcome of technical obstacles.

CONCLUDING REMARKS

Myeloid immune cells engineered to express CAR opened a new pathway to treat cancer that, apparently, bypasses the limitations of CAR-T or CAR-NK cells. Additional advantages of myeloid cells should be further explored and combined with CAR-

engineering. In addition, the lack of response to a checkpoint inhibitor would be better explained by the absence of a response to be released from its inhibitors and, thus, DC and macrophages associated to CAR expression would be ideal candidates to add to checkpoint inhibition, a combination that is already under investigation (Wilgenhof et al., 2016). We highlighted below some key points to be considered in the use of CAR-expressing myeloid cells for solid cancers:

I) Migratory ability: monocytes and DC subtypes have great migratory skills towards a variety of inflamed and/or lymphoid tissues. The manipulation of these features needs to be further enhanced to drive these cells into specific tissues or tumor mass in a more controlled way.
II) Plasticity potential: numerous protocols of differentiation and activation may allow a better phenotypical and functional fine-tuning adjustment of monocytes, macrophages and DCs to be adapted for distinct tumor contexts and tissues. The combined use of growth factors, cytokines/chemokines, TLR-L and drugs may generate a more effective and functional manufactured CAR-myeloid cell.
III) Phagocytic skills: macrophages and DCs have unique abilities of phagocytosis and clearance for a variety of particles. The manufacturing of cells with an improved engulfment ability to eliminate tumor cells may represent a great gain in the control of malignances.
IV) Tissue remodeling: monocytes/macrophages could be reprogrammed to release a series of enzymes, cathepsins, MMPs and other modulatory factors not only to remodel the tumor microenvironment matrix but also to attract, allow the infiltration and stimulate T cells.
V) Stimulation of adaptive immunity: myeloid immune cells are capable of efficiently present tumor antigens, provide co-stimulatory signals and produce cytokines able to efficiently stimulate lymphocyte activation and expansion.

There is an emergent need to evaluate CAR-myeloid immune cells in distinct pre-clinical tumor types, considering intrinsic tissue-related factors, matrix architecture and cellular composition. Tumor growth and its intrinsic features deeply vary among models and, possibly, additional adjusts should be implemented in the manufacture of CAR-Mac. Importantly, the use of myeloid cells expressing CAR could be further combined with other clinical approaches able to disrupt the compact matrix of solid tumors and may represent a great gain for patients' outcome. These therapies include, but are not limited to, chemotherapy, radiotherapy, oncolytic virus and/or monoclonal agonistic antibodies.

AUTHOR CONTRIBUTIONS

RR and VR Conceptualization, writting and review of the article; TO, SC, PK, TB, ER, and JB writting, figure preparation and review of the article.

ACKNOWLEDGMENTS

RR, SC, TO, PK and VR are supported by CNPq #442676/2020-4. JB is supported by CNPq: # 308053/2017-6. Figures were created using Biorender.com.

REFERENCES

Ajami, B., Bennett, J. L., Krieger, C., Tetzlaff, W., and Rossi, F. M. V. (2007). Local Self-Renewal Can Sustain CNS Microglia Maintenance and Function throughout Adult Life. *Nat. Neurosci.* 10 (12), 1538–1543. doi:10.1038/nn2014

Albinger, N., Hartmann, J., and Ullrich, E. (2021). Current Status and Perspective of CAR-T and CAR-NK Cell Therapy Trials in Germany. *Gene Ther.* 28 (9), 513–527. doi:10.1038/s41434-021-00246-w

Anderson, N. R., Minutolo, N. G., Gill, S., and Klichinsky, M. (2021). Macrophage-Based Approaches for Cancer Immunotherapy. *Cancer Res.* 81 (5), 1201–1208. doi:10.1158/0008-5472.CAN-20-2990

Ardighieri, L., Missale, F., Bugatti, M., Gatta, L. B., Pezzali, I., Monti, M., et al. (2021). Infiltration by CXCL10 Secreting Macrophages Is Associated with Antitumor Immunity and Response to Therapy in Ovarian Cancer Subtypes. *Front. Immunol.* 12 (junho), 690201. doi:10.3389/fimmu.2021.690201

Auffray, C., Sieweke, M. H., and Geissmann, F. (2009). Blood Monocytes: Development, Heterogeneity, and Relationship with Dendritic Cells. *Annu. Rev. Immunol.* 27 (1), 669–692. doi:10.1146/annurev.immunol.021908.132557

Azizi, E., Carr, A. J., Plitas, G., Cornish, A. E., Konopacki, C., Prabhakaran, S., et al. (2018). Single-Cell Map of Diverse Immune Phenotypes in the Breast Tumor Microenvironment. *Cell* 174 (5), 1293–1308.e36. doi:10.1016/j.cell.2018.05.060

Bachem, A., Güttler, S., Hartung, E., Ebstein, F., Schaefer, M., Tannert, A., et al. (2010). Superior Antigen Cross-Presentation and XCR1 Expression Define Human CD11c+CD141+ Cells as Homologues of Mouse CD8+ Dendritic Cells. *J. Exp. Med.* 207 (6), 1273–1281. doi:10.1084/jem.20100348

Bakri, Y., Sarrazin, S., Mayer, U. P., Tillmanns, S., Nerlov, C., Boned, A., et al. (2005). Balance of MafB and PU.1 Specifies Alternative Macrophage or Dendritic Cell Fate. *Blood* 105 (7), 2707–2716. doi:10.1182/blood-2004-04-1448

Baleeiro, R. B., Anselmo, L. B., Soares, F. A., Pinto, C. A. L., Ramos, O., Gross, J. L., et al. (2008). High Frequency of Immature Dendritic Cells and Altered *In Situ* Production of Interleukin-4 and Tumor Necrosis Factor-α in Lung Cancer. *Cancer Immunol. Immunother.* 57 (9), 1335–1345. doi:10.1007/s00262-008-0468-7

Ban, Y., Mai, J., Li, X., Mitchell-Flack, M., Zhang, T., Zhang, L., et al. (2017). Targeting Autocrine CCL5-CCR5 Axis Reprograms Immunosuppressive Myeloid Cells and Reinvigorates Antitumor Immunity. *Cancer Res.* 77 (11), 2857–2868. doi:10.1158/0008-5472.CAN-16-2913

Barbuto, J. A. M., Ensina, L. F. C., Neves, A. R., Bergami-Santos, P., Leite, K. R. M., Marques, R., et al. (2004). Dendritic Cell?Tumor Cell Hybrid Vaccination for Metastatic Cancer. *Cancer Immunol. Immunother.* 53 (12), 1111–1118. doi:10.1007/s00262-004-0551-7

Bell, D., Chomarat, P., Broyles, D., Netto, G., Harb, G. M., Lebecque, S., et al. (1999). In Breast Carcinoma Tissue, Immature Dendritic Cells Reside within the Tumor, whereas Mature Dendritic Cells Are Located in Peritumoral Areas. *J. Exp. Med.* 190 (10), 1417–1426. doi:10.1084/jem.190.10.1417

Belladonna, M. L., Volpi, C., Bianchi, R., Vacca, C., Orabona, C., Pallotta, M. T., et al. (2008). Cutting Edge: Autocrine TGF-β Sustains Default Tolerogenesis by Ido-Competent Dendritic Cells. *J. Immunol.* 181 (8), 5194–5198. doi:10.4049/jimmunol.181.8.5194

Binnewies, M., Mujal, A. M., Pollack, J. L., Combes, A. J., Hardison, E. A., Barry, K. C., et al. (2019). Unleashing Type-2 Dendritic Cells to Drive Protective Antitumor CD4+ T Cell Immunity. *Cell* 177 (3), 556–571.e16. doi:10.1016/j.cell.2019.02.005

Blériot, C., Chakarov, S., and Ginhoux, F. (2020). Determinants of Resident Tissue Macrophage Identity and Function. *Immunity* 52 (6), 957–970. doi:10.1016/j.immuni.2020.05.014

Bonapace, L., Coissieux, M.-M., Wyckoff, J., Mertz, K. D., Varga, Z., Junt, T., et al. (2014). Cessation of CCL2 Inhibition Accelerates Breast Cancer Metastasis by Promoting Angiogenesis. *Nature* 515 (7525), 130–133. doi:10.1038/nature13862

Bosteels, C., Neyt, K., Vanheerswynghels, M., van Helden, M. J., Sichien, D., Debeuf, N., et al. (2020). Inflammatory Type 2 CDCs Acquire Features of CDC1s and Macrophages to Orchestrate Immunity to Respiratory Virus Infection. *Immunity* 52 (6), 1039–1056.e9. doi:10.1016/j.immuni.2020.04.005

Böttcher, J. P., Bonavita, E., Chakravarty, P., Blees, H., Cabeza-Cabrerizo, M., Sammicheli, S., et al. (2018). NK Cells Stimulate Recruitment of CDC1 into the Tumor Microenvironment Promoting Cancer Immune Control. *Cell* 172 (5), 1022–1037.e14. doi:10.1016/j.cell.2018.01.004

Bourdely, P., Anselmi, G., Vaivode, K., RamosRamos, R. N., Missolo-Koussou, Y., Hidalgo, S., et al. (2020). Transcriptional and Functional Analysis of CD1c+ Human Dendritic Cells Identifies a CD163+ Subset Priming CD8+CD103+ T Cells. *Immunity* 53 (2), 335–352.e8. doi:10.1016/j.immuni.2020.06.002

Brentjens, R. J., Latouche, J.-B., Santos, E., Marti, F., Gong, M. C., Lyddane, C., et al. (2003). Eradication of Systemic B-Cell Tumors by Genetically Targeted Human T Lymphocytes Co-stimulated by CD80 and Interleukin-15. *Nat. Med.* 9 (3), 279–286. doi:10.1038/nm827

Broz, M. L., Binnewies, M., Boldajipour, B., Nelson, A. E., Pollack, J. L., Erle, D. J., et al. (2014). Dissecting the Tumor Myeloid Compartment Reveals Rare Activating Antigen-Presenting Cells Critical for T Cell Immunity. *Cancer Cell* 26 (5), 638–652. doi:10.1016/j.ccell.2014.09.007

Cambien, B., Richard-Fiardo, P., Karimdjee, B. F., Martini, V., Ferrua, B., Pitard, B., et al. (2011). CCL5 Neutralization Restricts Cancer Growth and Potentiates the Targeting of PDGFRβ in Colorectal Carcinoma. *PLoS ONE* 6 (12), e28842. doi:10.1371/journal.pone.0028842

Camisaschi, C., De Filippo, A., Beretta, V., Vergani, B., Villa, A., Vergani, E., et al. (2014). Alternative Activation of Human Plasmacytoid DCs *In Vitro* and in Melanoma Lesions: Involvement of LAG-3. *J. Invest. Dermatol.* 134 (7), 1893–1902. doi:10.1038/jid.2014.29

Cao, W., Ramakrishnan, R., Tuyrin, V. A., Veglia, F., Condamine, T., Amoscato, A., et al. (2014). Oxidized Lipids Block Antigen Cross-Presentation by Dendritic Cells in Cancer. *J.I.* 192 (6), 2920–2931. doi:10.4049/jimmunol.1302801

Caronni, N., Simoncello, F., Stafetta, F., Guarnaccia, C., Ruiz-Moreno, J. S., Opitz, B., et al. (2018). Downregulation of Membrane Trafficking Proteins and Lactate Conditioning Determine Loss of Dendritic Cell Function in Lung Cancer. *Cancer Res.* 78 (7), 1685–1699. doi:10.1158/0008-5472.CAN-17-1307

Cassetta, L., Fragkogianni, S., Sims, A. H., Swierczak, A., Forrester, L. M., Zhang, H., et al. (2019). Human Tumor-Associated Macrophage and Monocyte Transcriptional Landscapes Reveal Cancer-specific Reprogramming, Biomarkers, and Therapeutic Targets. *Cancer Cell* 35 (4), 588–602.e10. doi:10.1016/j.ccell.2019.02.009

Cassetta, L., and Pollard, J. W. (2018). Targeting Macrophages: Therapeutic Approaches in Cancer. *Nat. Rev. Drug Discov.* 17 (12), 887–904. doi:10.1038/nrd.2018.169

Caux, C., Vanbervliet, B., Massacrier, C., Dezutter-Dambuyant, C., de Saint-Vis, B., JacquetYoneda, C., et al. (1996). CD34+ Hematopoietic Progenitors from Human Cord Blood Differentiate along Two Independent Dendritic Cell Pathways in Response to GM-CSF+TNF Alpha. *J. Exp. Med.* 184 (2), 695–706. doi:10.1084/jem.184.2.695

Chaib, M., Chauhan, S. C., and Makowski, L. (2020). Friend or Foe? Recent Strategies to Target Myeloid Cells in Cancer. *Front. Cel Dev. Biol.* 8 (maio), 351. doi:10.3389/fcell.2020.00351

Chen, Y., Yu, Z., Tan, X., Jiang, H., Xu, Z., Fang, Y., et al. (2021). CAR-macrophage: A New Immunotherapy Candidate against Solid Tumors. *Biomed. Pharmacother.* 139 (julho), 111605. doi:10.1016/j.biopha.2021.111605

Chevrier, S., Levine, J. H., Zanotelli, V. R. T., Silina, K., Schulz, D., Bacac, M., et al. (2017). An Immune Atlas of Clear Cell Renal Cell Carcinoma. *Cell* 169 (4), 736–749.e18. doi:10.1016/j.cell.2017.04.016

Chittezhath, M., Dhillon, M. K., Lim, J. Y., Laoui, D., Shalova, I. N., Teo, Y. L., et al. (2014). Molecular Profiling Reveals a Tumor-Promoting Phenotype of Monocytes and Macrophages in Human Cancer Progression. *Immunity* 41 (5), 815–829. doi:10.1016/j.immuni.2014.09.014

Chmielewski, M., and Abken, H. (2020). TRUCKS, the Fourth-generation CAR T Cells: Current Developments and Clinical Translation. *Adv. Cel Gene Ther* 3 (3), 84. doi:10.1002/acg2.84

Coillard, A., and Segura, E. (2019). *In Vivo* Differentiation of Human Monocytes. *Front. Immunol.* 10 (agosto), 1907. doi:10.3389/fimmu.2019.01907

Collin, M., and Bigley, V. (2018). Human Dendritic Cell Subsets: An Update. *Immunology* 154 (1), 3–20. doi:10.1111/imm.12888

Cortez-Retamozo, V., Etzrodt, M., Newton, A., Rauch, P. J., Chudnovskiy, A., Berger, C., et al. (2012). Origins of Tumor-Associated Macrophages and Neutrophils. *Proc. Natl. Acad. Sci.* 109 (7), 2491–2496. doi:10.1073/pnas.1113744109

Couture, A., Garnier, A., Docagne, F., Boyer, O., Vivien, D., Le-Mauff, B., et al. (2019). HLA-class II Artificial Antigen Presenting Cells in CD4+ T Cell-Based Immunotherapy. *Front. Immunol.* 10 (maio), 1081. doi:10.3389/fimmu.2019.01081

Cueto, F. J., del Fresno, C., Brandi, P., Combes, A. J., Hernández-García, E., Sánchez-Paulete, A. R., et al. (2021). DNGR-1 Limits Flt3L-Mediated Antitumor Immunity by Restraining Tumor-Infiltrating Type I Conventional Dendritic Cells. *J. Immunother. Cancer* 9 (5), e002054. doi:10.1136/jitc-2020-002054

Cytlak, U., Resteu, A., Pagan, S., Green, K., Milne, P., McDonald, S., et al. (2020). Differential IRF8 Transcription Factor Requirement Defines Two Pathways of Dendritic Cell Development in Humans. *Immunity* 53 (2), 353–370.e8. doi:10.1016/j.immuni.2020.07.003

Dehqanzada, Z., Storrer, C. E., Hueman, M. T., Foley, R. J., Harris, K. A., Jama, Y. H., et al. (2007). Assessing Serum Cytokine Profiles in Breast Cancer Patients Receiving a HER2/Neu Vaccine Using Luminex Technology. *Oncol. Rep.* 17 (3), 687–694. doi:10.3892/or.17.3.687

Demaria, O., Cornen, S., Daëron, M., Morel, Y., Medzhitov, R., and Vivier, E. (2019). Harnessing Innate Immunity in Cancer Therapy. *Nature* 574 (7776), 45–56. doi:10.1038/s41586-019-1593-5

Diamond, M. S., Kinder, M., Matsushita, H., Mashayekhi, M., Dunn, G. P., Archambault, J. M., et al. (20112003). Type I Interferon Is Selectively Required by Dendritic Cells for Immune Rejection of Tumors. *J. Exp. Med.* 208 (10), 1989–2003. doi:10.1084/jem.20101158

Diao, J., Zhao, J., Winter, E., and Cattral, M. S. (2011). Tumors Suppress *In Situ* Proliferation of Cytotoxic T Cells by Promoting Differentiation of Gr-1+ Conventional Dendritic Cells through IL-6. *J.I.* 186 (9), 5058–5067. doi:10.4049/jimmunol.1004125

Dieu-Nosjean, M.-C., Antoine, M., Danel, C., Heudes, D., Wislez, M., Poulot, V., et al. (2008). Long-Term Survival for Patients with Non-small-cell Lung Cancer with Intratumoral Lymphoid Structures. *J. Clin. Oncol.* 26 (27), 4410–4417. doi:10.1200/JCO.2007.15.0284

Dokka, S., Toledo, D., Shi, X., Ye, J., and Rojanasakul, Y. (2000). High-Efficiency Gene Transfection of Macrophages by Lipoplexes. *Int. J. Pharm.* 206 (1–2), 97–104. doi:10.1016/S0378-5173(00)00531-7

Doulatov, S., Notta, F., Eppert, K., Nguyen, L. T., OhashiOhashi, P. S., and Dick, J. E. (2010). Revised Map of the Human Progenitor Hierarchy Shows the Origin of Macrophages and Dendritic Cells in Early Lymphoid Development. *Nat. Immunol.* 11 (7), 585–593. doi:10.1038/ni.1889

Dutertre, C.-A., Becht, E., Irac, S. E., Khalilnezhad, A., Narang, V., Khalilnezhad, S., et al. (2019). Single-Cell Analysis of Human Mononuclear Phagocytes Reveals Subset-Defining Markers and Identifies Circulating Inflammatory Dendritic Cells. *Immunity* 51 (3), 573–589.e8. doi:10.1016/j.immuni.2019.08.008

Engblom, C., Pfirschke, C., and Pittet, M. J. (2016). The Role of Myeloid Cells in Cancer Therapies. *Nat. Rev. Cancer* 16 (7), 447–462. doi:10.1038/nrc.2016.54

Epelman, S., Lavine, K. J., and Randolph, G. J. (2014). Origin and Functions of Tissue Macrophages. *Immunity* 41 (1), 21–35. doi:10.1016/j.immuni.2014.06.013

Faget, J., Bendriss-Vermare, N., Gobert, M., Durand, I., Olive, D., Biota, C., et al. (2012). ICOS-ligand Expression on Plasmacytoid Dendritic Cells Supports Breast Cancer Progression by Promoting the Accumulation of Immunosuppressive CD4+ T Cells. *Cancer Res.* 72 (23), 6130–6141. doi:10.1158/0008-5472.CAN-12-2409

Fainaru, O., Adini, A., Benny, O., Adini, I., Short, S., Bazinet, L., et al. (2008). Dendritic Cells Support Angiogenesis and Promote Lesion Growth in a Murine Model of Endometriosis. *FASEB j.* 22 (2), 522–529. doi:10.1096/fj.07-9034com

Farren, M. R., Carlson, L. M., Netherby, C. S., Lindner, I., Abrams, L. P.-K., Gabrilovich, D. I., et al. (2014). Tumor-Induced STAT3 Signaling in Myeloid Cells Impairs Dendritic Cell Generation by Decreasing PKCβII Abundance. *Sci. Signal.* 7 (313), 4656. doi:10.1126/scisignal.2004656

Feng, F., Zheng, G., Wang, Q., Liu, S., Liu, Z., Xu, G., et al. (2018). Low Lymphocyte Count and High Monocyte Count Predicts Poor Prognosis of Gastric Cancer. *BMC Gastroenterol.* 18 (1), 148. doi:10.1186/s12876-018-0877-9

Fetterly, G. J., Aras, U., Meholick, P. D., Takimoto, C., Seetharam, S., McIntosh, T., et al. (2013). Utilizing Pharmacokinetics/pharmacodynamics Modeling to Simultaneously Examine Free CCL2, Total CCL2 and Carlumab (CNTO 888) Concentration Time Data. *J. Clin. Pharmacol.* 53 (10), 1020–1027. doi:10.1002/jcph.140

Flavell, R. A., Sanjabi, S., Wrzesinski, S. H., and Licona-Limón, P. (2010). The Polarization of Immune Cells in the Tumour Environment by TGFβ. *Nat. Rev. Immunol.* 10 (8), 554–567. doi:10.1038/nri2808

Fousek, K., Watanabe, J., Joseph, S. K., George, A., An, X., Byrd, T. T., et al. (2021). CAR T-Cells that Target Acute B-Lineage Leukemia Irrespective of CD19 Expression. *Leukemia* 35 (1), 75–89. doi:10.1038/s41375-020-0792-2

Fuertes, M. B., Kacha, A. K., KlineWoo, J., Woo, S.-R., Kranz, D. M., Murphy, K. M., et al. (2011). Host Type I IFN Signals Are Required for Antitumor CD8+ T Cell Responses through CD8α+ Dendritic Cells. *J. Exp. Med.* 208 (10), 2005–2016. doi:10.1084/jem.20101159

Gabrilovich, D. I., Chen, H. L., Girgis, K. R., Cunningham, H. T., Girgis, K. R., Cunningham, H. T., et al. (1996). Production of Vascular Endothelial Growth Factor by Human Tumors Inhibits the Functional Maturation of Dendritic Cells. *Nat. Med.* 2 (10), 1096–1103. doi:10.1038/nm1096-1096

Gerhard, G. M., Bill, R., Messemaker, M., Klein, A. M., and Pittet, M. J. (2021). Tumor-Infiltrating Dendritic Cell States Are Conserved across Solid Human Cancers. *J. Exp. Med.* 218 (1), 264. doi:10.1084/jem.20200264

Gervais, A., Levêque, J., Bouet-Toussaint, F., Burtin, F., Lesimple, T., Sulpice, L., et al. (2005). Dendritic Cells Are Defective in Breast Cancer Patients: A Potential Role for Polyamine in This Immunodeficiency. *Breast Cancer Res.* 7 (3), 1. doi:10.1186/bcr1001

Ginhoux, F., and Jung, S. (2014). Monocytes and Macrophages: Developmental Pathways and Tissue Homeostasis. *Nat. Rev. Immunol.* 14 (6), 392–404. doi:10.1038/nri3671

Goc, J., Germain, C., Vo-Bourgais, T. K. D., Lupo, A., Klein, C., Knockaert, S., et al. (2014). Dendritic Cells in Tumor-Associated Tertiary Lymphoid Structures Signal a Th1 Cytotoxic Immune Contexture and License the Positive Prognostic Value of Infiltrating CD8+ T Cells. *Cancer Res.* 74 (3), 705–715. doi:10.1158/0008-5472.CAN-13-1342

Goudot, C., Coillard, A., Villani, A.-C., Gueguen, P., Cros, A., Sarkizova, S., et al. (2017). Aryl Hydrocarbon Receptor Controls Monocyte Differentiation into Dendritic Cells versus Macrophages. *Immunity* 47 (3), 582–596.e6. doi:10.1016/j.immuni.2017.08.016

Gross, G., Waks, T., and Eshhar, Z. (1989). Expression of Immunoglobulin-T-Cell Receptor Chimeric Molecules as Functional Receptors with Antibody-type Specificity. *Proc. Natl. Acad. Sci.* 86 (24), 10024–10028. doi:10.1073/pnas.86.24.10024

Guermonprez, P., Gerber-Ferder, Y., Vaivode, K., Bourdely, P., and Helft, J. (2019). Origin and Development of Classical Dendritic Cells. *Int. Rev. Cel Mol. Biol.* 349, 1–54. doi:10.1016/bs.ircmb.2019.08.002

Guilliams, M., Ginhoux, F., Jakubzick, C., Naik, S. H., Onai, N., Schraml, B. U., et al. (2014). Dendritic Cells, Monocytes and Macrophages: A Unified Nomenclature Based on Ontogeny. *Nat. Rev. Immunol.* 14 (8), 571–578. doi:10.1038/nri3712

Guo, R., Lü, M., Cao, F., Wu, G., Gao, F., Pang, H., et al. (2021). Single-Cell Map of Diverse Immune Phenotypes in the Acute Myeloid Leukemia Microenvironment. *Biomark Res.* 9 (1), 15. doi:10.1186/s40364-021-00265-0

Hanahan, D., and Coussens, L. M. (2012). Accessories to the Crime: Functions of Cells Recruited to the Tumor Microenvironment. *Cancer Cell* 21 (3), 309–322. doi:10.1016/j.ccr.2012.02.022

Harizaj, A., De Smedt, S. C., Lentacker, I., and Braeckmans, K. (2021). Physical Transfection Technologies for Macrophages and Dendritic Cells in Immunotherapy. *Expert Opin. Drug Deliv.* 18 (2), 229–247. doi:10.1080/17425247.2021.1828340

Harris, K. M. (2011). Monocytes Differentiated with GM-CSF and IL-15 Initiate Th17 and Th1 Responses that Are Contact-dependent and Mediated by IL-15. *J. Leukoc. Biol.* 90 (4), 727–734. doi:10.1189/jlb.0311132

Hayashi, T., Fujita, K., Nojima, S., Hayashi, Y., Nakano, K., Ishizuya, Y., et al. (2017). Peripheral Blood Monocyte Count Reflecting Tumor-Infiltrating Macrophages Is a Predictive Factor of Adverse Pathology in Radical Prostatectomy Specimens. *Prostate* 77 (14), 1383–1388. doi:10.1002/pros.23398

Helft, J., Anjos-Afonso, F., van der Veen, A. G., Chakravarty, P., Bonnet, D., Reis e Sousa, C., et al. (2017). Dendritic Cell Lineage Potential in Human Early Hematopoietic Progenitors. *Cel Rep.* 20 (3), 529–537. doi:10.1016/j.celrep.2017.06.075

Herber, D. L., Cao, W., Nefedova, Y., Novitskiy, S. V., Nagaraj, S., Tyurin, V. A., et al. (2010). Lipid Accumulation and Dendritic Cell Dysfunction in Cancer. *Nat. Med.* 16 (8), 880–886. doi:10.1038/nm.2172

Herrera, L., Santos, S., Vesga, M. A., Anguita, J., Martin-Ruiz, I., Carrascosa, T., et al. (2019). Adult Peripheral Blood and Umbilical Cord Blood NK Cells Are Good Sources for Effective CAR Therapy against CD19 Positive Leukemic Cells. *Sci. Rep.* 9 (1), 18729. doi:10.1038/s41598-019-55239-y

Hoeffel, G., Chen, J., Lavin, Y., Low, D., Almeida, F. F., See, P., et al. (2015). C-Myb+ Erythro-Myeloid Progenitor-Derived Fetal Monocytes Give Rise to Adult Tissue-Resident Macrophages. *Immunity* 42 (4), 665–678. doi:10.1016/j.immuni.2015.03.011

Hoeffel, G., and Ginhoux, F. (2015). Ontogeny of Tissue-Resident Macrophages. *Front. Immunol.* 6 (setembro), 486. doi:10.3389/fimmu.2015.00486

Ino, Y., Shimada, K., Yamazaki-Itoh, R., Shimada, K., Iwasaki, M., Kosuge, T., et al. (2013). Immune Cell Infiltration as an Indicator of the Immune Microenvironment of Pancreatic Cancer. *Br. J. Cancer* 108 (4), 914–923. doi:10.1038/bjc.2013.32

Jaguin, M., Houlbert, N., Fardel, O., and Lecureur, V. (2013). Polarization Profiles of Human M-CSF-Generated Macrophages and Comparison of M1-Markers in Classically Activated Macrophages from GM-CSF and M-CSF Origin. *Cell Immunol.* 281 (1), 51–61. doi:10.1016/j.cellimm.2013.01.010

Jongbloed, S. L., Kassianos, A. J., McDonald, K. J., Angel, C. G. J., Chen, C-J. J., Ju, X., et al. (2010). Human CD141+ (BDCA-3)+ Dendritic Cells (DCs) Represent a Unique Myeloid DC Subset that Cross-Presents Necrotic Cell Antigens. *J. Exp. Med.* 207 (6), 1247–1260. doi:10.1084/jem.20092140

Jung, K., Heishi, T., Incio, J., Huang, Y., Beech, E. Y., Pinter, M., et al. (2017). Targeting CXCR4-dependent Immunosuppressive Ly6Clow Monocytes Improves Antiangiogenic Therapy in Colorectal Cancer. *Proc. Natl. Acad. Sci. USA* 114 (39), 10455–10460. doi:10.1073/pnas.1710754114

Kang, M., Lee, S. H., Kwon, M., Byun, J., Kim, D., Kim, C., et al. (2021). Nanocomplex-Mediated *In Vivo* Programming to Chimeric Antigen Receptor-M1 Macrophages for Cancer Therapy. *Adv. Mater.* 33 (43), 2103258. doi:10.1002/adma.202103258

Katzenelenbogen, Y., Sheban, F., Yalin, A., Yofe, I., Svetlichnyy, D., Jaitin, D. A., et al. (2020). Coupled ScRNA-Seq and Intracellular Protein Activity Reveal an Immunosuppressive Role of TREM2 in Cancer. *Cell* 182 (4), 872–885.e19. doi:10.1016/j.cell.2020.06.032

Keller, A.-A., Maeß, M. B., Schnoor, M., Scheiding, B., and Lorkowski, S. (2018). "Transfecting Macrophages," in *Methods in Molecular Biology* (New York, NY: Springer New York), 187–195. doi:10.1007/978-1-4939-7837-3_18

Kershaw, M. H., Westwood, J. A., Parker, L. L., Wang, G., Eshhar, Z., Mavroukakis, S. A., et al. (2006). A Phase I Study on Adoptive Immunotherapy Using Gene-Modified T Cells for Ovarian Cancer. *Clin. Cancer Res.* 12 (20), 6106–6115. doi:10.1158/1078-0432.CCR-06-1183

Kiss, M., Caro, A. A., Raes, G., and Laoui, D. (2020). Systemic Reprogramming of Monocytes in Cancer. *Front. Oncol.* 10 (setembro), 1399. doi:10.3389/fonc.2020.01399

Kitamura, T., Qian, B.-Z., Soong, D., Cassetta, L., Noy, R., Sugano, G., et al. (2015). CCL2-Induced Chemokine Cascade Promotes Breast Cancer Metastasis by Enhancing Retention of Metastasis-Associated Macrophages. *J. Exp. Med.* 212 (7), 1043–1059. doi:10.1084/jem.20141836

Klichinsky, M., Ruella, M., Shestova, O., Lu, X. M., Best, A., Zeeman, M., et al. (2020). Human Chimeric Antigen Receptor Macrophages for Cancer Immunotherapy. *Nat. Biotechnol.* 38 (8), 947–953. doi:10.1038/s41587-020-0462-y

Kochenderfer, J. N., Wilson, W. H., Janik, J. E., Dudley, M. E., Stetler-Stevenson, M., Feldman, S. A., et al. (2010). Eradication of B-Lineage Cells and Regression of Lymphoma in a Patient Treated with Autologous T Cells Genetically Engineered to Recognize CD19. *Blood* 116 (20), 4099–4102. doi:10.1182/blood-2010-04-281931

Krause, A., Guo, H.-F., Latouche, J.-B., Tan, C., Cheung, N.-K. V., and Sadelain, M. E. M. (1998). Antigen-dependent CD28 Signaling Selectively Enhances Survival and Proliferation in Genetically Modified Activated Human Primary T Lymphocytes. *J. Exp. Med.* 188 (4), 619–626. doi:10.1084/jem.188.4.619

Kuhn, S., Yang, J., and Ronchese, F. (2015). Monocyte-Derived Dendritic Cells Are Essential for CD8+ T Cell Activation and Antitumor Responses after Local Immunotherapy. *Front. Immunol.* 6 (novembro), 584. doi:10.3389/fimmu.2015.00584

Labidi-Galy, S. I., Sisirak, V., Meeus, P., Gobert, M., Treilleux, I., Bajard, A., et al. (2011). Quantitative and Functional Alterations of Plasmacytoid Dendritic Cells Contribute to Immune Tolerance in Ovarian Cancer. *Cancer Res.* 71 (16), 5423–5434. doi:10.1158/0008-5472.CAN-11-0367

Lacey, D. C., Achuthan, A., Fleetwood, A. J., Dinh, H., Roiniotis, J., Scholz, G. M., et al. (2012). Defining GM-CSF- and Macrophage-CSF-dependent Macrophage Responses by *In Vitro* Models. *J.I.* 188 (11), 5752–5765. doi:10.4049/jimmunol.1103426

Ladányi, A., Kiss, J., Somlai, B., Gilde, K., Fejős, Z., Mohos, A., et al. (2007). Density of DC-LAMP+ Mature Dendritic Cells in Combination with Activated T Lymphocytes Infiltrating Primary Cutaneous Melanoma Is a Strong Independent Prognostic Factor. *Cancer Immunol. Immunother.* 56 (9), 1459–1469. doi:10.1007/s00262-007-0286-3

Lamers, C. H. J., Willemsen, R., van Elzakker, P., van Steenbergen-Langeveld, S., Broertjes, M., Oosterwijk-Wakka, J., et al. (2011). Immune Responses to Transgene and Retroviral Vector in Patients Treated with Ex Vivo-engineered T Cells. *Blood* 117 (1), 72–82. doi:10.1182/blood-2010-07-294520

Laslo, P., Spooner, C. J., Warmflash, A., Lancki, D. W., Lee, H.-J., Sciammas, R., et al. (2006). Multilineage Transcriptional Priming and Determination of Alternate Hematopoietic Cell Fates. *Cell* 126 (4), 755–766. doi:10.1016/j.cell.2006.06.052

Lavin, Y., Kobayashi, S., Leader, A., Amir, E.-A. D., Elefant, N., Bigenwald, C., et al. (2017). Innate Immune Landscape in Early Lung Adenocarcinoma by Paired Single-Cell Analyses. *Cell* 169 (4), 750–765.e17. doi:10.1016/j.cell.2017.04.014

Leal Rojas, I. M., Mok, W.-H., Pearson, F. E., Minoda, Y., Kenna, T. J., Barnard, R. T., et al. (2017). Human Blood CD1c+ Dendritic Cells Promote Th1 and Th17 Effector Function in Memory CD4+ T Cells. *Front. Immunol.* 8 (agosto), 971. doi:10.3389/fimmu.2017.00971

Lee, Y.-Y., Choi, C. H., Sung, C. O., Do, I.-G., Huh, S., Song, T., et al. (2012). Prognostic Value of Pre-treatment Circulating Monocyte Count in Patients with Cervical Cancer: Comparison with SCC-Ag Level. *Gynecol. Oncol.* 124 (1), 92–97. doi:10.1016/j.ygyno.2011.09.034

Li, J., Li, W., Huang, K., Zhang, Y., Kupfer, G., and Zhao, Q. (2018). Chimeric Antigen Receptor T Cell (CAR-T) Immunotherapy for Solid Tumors: Lessons Learned and Strategies for Moving Forward. *J. Hematol. Oncol.* 11 (1), 22. doi:10.1186/s13045-018-0568-6

Liu, E., Marin, D., Banerjee, P., Macapinlac, H. A., Thompson, P., Basar, R., et al. (2020). Use of CAR-Transduced Natural Killer Cells in CD19-Positive Lymphoid Tumors. *N. Engl. J. Med.* 382 (6), 545–553. doi:10.1056/NEJMoa1910607

Liu, Y., and Wang, R. (2020). Immunotherapy Targeting Tumor-Associated Macrophages. *Front. Med.* 7 (novembro), 583708. doi:10.3389/fmed.2020.583708

Macanas-Pirard, P., Quezada, T., Navarrete, L., Broekhuizen, R., Leisewitz, A., Nervi, B., et al. (2017). The CCL2/CCR2 Axis Affects Transmigration and Proliferation but Not Resistance to Chemotherapy of Acute Myeloid Leukemia Cells. *PLOS ONE* 12 (1), e0168888. doi:10.1371/journal.pone.0168888

Maher, J., Brentjens, R. J., Gunset, G., Rivière, I., and Sadelain, M. (2002). Human T-Lymphocyte Cytotoxicity and Proliferation Directed by a Single Chimeric TCRζ/CD28 Receptor. *Nat. Biotechnol.* 20 (1), 70–75. doi:10.1038/nbt0102-70

Malietzis, G., Lee, G. H., Jenkins, J. T., Bernardo, D., Moorghen, M., Knight, S. C., et al. (2015). Prognostic Value of the Tumour-Infiltrating Dendritic Cells in Colorectal Cancer: A Systematic Review. *Cel Commun. Adhes.* 22 (1), 9–14. doi:10.3109/15419061.2015.1036859

Marofi, F., Motavalli, R., Safonov, V. A., Thangavelu, L., Yumashev, A. V., Alexander, M., et al. (2021). CAR T Cells in Solid Tumors: Challenges and Opportunities. *Stem Cel Res Ther* 12 (1), 81. doi:10.1186/s13287-020-02128-1

Maude, S. L., Laetsch, T. W., Buechner, J., Rives, S., Boyer, M., Bittencourt, H., et al. (2018). Tisagenlecleucel in Children and Young Adults with B-Cell Lymphoblastic Leukemia. *N. Engl. J. Med.* 378 (5), 439–448. doi:10.1056/NEJMoa1709866

Medrek, C., Pontén, F., Jirström, K., and Leandersson, K. (2012). The Presence of Tumor Associated Macrophages in Tumor Stroma as a Prognostic Marker for Breast Cancer Patients. *BMC Cancer* 12 (1), 306. doi:10.1186/1471-2407-12-306

Melaiu, O., Chierici, M., Lucarini, V., Jurman, G., Conti, L. A., De Vito, R., et al. (2020). Cellular and Gene Signatures of Tumor-Infiltrating Dendritic Cells and Natural-Killer Cells Predict Prognosis of Neuroblastoma. *Nat. Commun.* 11 (1), 5992. doi:10.1038/s41467-020-19781-y

Menetrier-Caux, C., Montmain, G., Dieu, M. C., Bain, C., Favrot, M. C., Caux, C., et al. (1998). Inhibition of the Differentiation of Dendritic Cells from CD34+ Progenitors by Tumor Cells: Role of Interleukin-6 and Macrophage Colony-Stimulating Factor. *Blood* 92 (12), 4778–4791. doi:10.1182/blood.v92.12.4778

Merad, M., and Manz, M. G. (2009). Dendritic Cell Homeostasis. *Blood* 113 (15), 3418–3427. doi:10.1182/blood-2008-12-180646

Mildner, A., and Jung, S. (2014). Development and Function of Dendritic Cell Subsets. *Immunity* 40 (5), 642–656. doi:10.1016/j.immuni.2014.04.016

Mildner, A., Schönheit, J., Giladi, A., David, E., Lara-Astiaso, D., Lorenzo-Vivas, E., et al. (2017). Genomic Characterization of Murine Monocytes Reveals C/EBPβ Transcription Factor Dependence of Ly6C – Cells. *Immunity* 46 (5), 849–862.e7. doi:10.1016/j.immuni.2017.04.018

Molgora, M., Esaulova, E., Vermi, W., Hou, J., Chen, Y., Luo, J., et al. (2020). TREM2 Modulation Remodels the Tumor Myeloid Landscape Enhancing Anti-PD-1 Immunotherapy. *Cell* 182 (4), 886–900.e17. doi:10.1016/j.cell.2020.07.013

Monti, P., Leone, B. E., Marchesi, F., Balzano, G., Zerbi, A., Scaltrini, F., et al. (2003). The CC Chemokine MCP-1/CCL2 in Pancreatic Cancer Progression: Regulation of Expression and Potential Mechanisms of Antimalignant Activity. *Cancer Res.* 63 (21), 7451–7461.

Moretta, L., Locatelli, F., Pende, D., Marcenaro, E., Mingari, M. C., and Moretta, A. (2011). Killer Ig-like Receptor-Mediated Control of Natural Killer Cell Alloreactivity in Haploidentical Hematopoietic Stem Cell Transplantation. *Blood* 117 (3), 764–771. doi:10.1182/blood-2010-08-264085

Morgan, R. A., Dudley, M. E., Hughes, M. S., Yang, J. C., Sherry, R. M., Royal, R. E., et al. (2006). Cancer Regression in Patients after Transfer of Genetically Engineered Lymphocytes. *Science* 314 (5796), 126–129. doi:10.1126/science.1129003

Morrissey, M. A., Williamson, A. P., Steinbach, A. M., Roberts, E. W., Kern, N., Headley, M. B., et al. (2018). Chimeric Antigen Receptors that Trigger Phagocytosis. *ELife* 7 (junho), e36688. doi:10.7554/eLife.36688

Munshi, N. C., Anderson, L. D., Shah, N., Madduri, D., Berdeja, J., Lonial, S., et al. (2021). Idecabtagene Vicleucel in Relapsed and Refractory Multiple Myeloma. *N. Engl. J. Med.* 384 (8), 705–716. doi:10.1056/NEJMoa2024850

Neophytou, C. M., Pierides, C., Christodoulou, M.-I., Costeas, P., Kyriakou, T.-C., and Papageorgis, P. (2020). The Role of Tumor-Associated Myeloid Cells in Modulating Cancer Therapy. *Front. Oncol.* 10 (junho), 899. doi:10.3389/fonc.2020.00899

Neves, A. R., Ensina, L. F. C., Leite, K. R. M., Buzaid, A. C., Câmara-Lopes, L. H., and Barbuto, J. A. M. (2005). Dendritic Cells Derived from Metastatic Cancer Patients Vaccinated with Allogeneic Dendritic Cell?Autologous Tumor Cell Hybrids Express More CD86 and Induce Higher Levels of Interferon-Gamma in Mixed Lymphocyte Reactions. *Cancer Immunol. Immunother.* 54 (1), 61–66. doi:10.1007/s00262-004-0550-8

Nywening, T. M., Belt, B. A., Cullinan, D. R., PanniPanni, R. Z., Han, B. J., Sanford, D. E., et al. (2018). Targeting Both Tumour-Associated CXCR2+ Neutrophils and CCR2+ Macrophages Disrupts Myeloid Recruitment and Improves Chemotherapeutic Responses in Pancreatic Ductal Adenocarcinoma. *Gut* 67 (6), 1112–1123. doi:10.1136/gutjnl-2017-313738

O'Connell, R. M., Rao, D. S., Chaudhuri, A. A., Boldin, M. P., Taganov, K. D., Nicoll, J., et al. (2008). Sustained Expression of MicroRNA-155 in Hematopoietic Stem Cells Causes a Myeloproliferative Disorder. *J. Exp. Med.* 205 (3), 585–594. doi:10.1084/jem.20072108

O'Connell, R. M., Taganov, K. D., Boldin, M. P., Cheng, G., and Baltimore, D. (2007). MicroRNA-155 Is Induced during the Macrophage Inflammatory Response. *Proc. Natl. Acad. Sci.* 104 (5), 1604–1609. doi:10.1073/pnas.0610731104

Ortíz-Maldonado, V., Rives, S., Castellà, M., Alonso-Saladrigues, A., Benítez-Ribas, D., Caballero-Baños, M., et al. (2021). CART19-BE-01: A Multicenter Trial of ARI-0001 Cell Therapy in Patients with CD19+

Relapsed/Refractory Malignancies. *Mol. Ther.* 29 (2), 636–644. doi:10.1016/j.ymthe.2020.09.027

Pahl, J. H. W., Cerwenka, A., and Ni, J. (2018). Memory-Like NK Cells: Remembering a Previous Activation by Cytokines and NK Cell Receptors. *Front. Immunol.* 9 (novembro), 2796. doi:10.3389/fimmu.2018.02796

Panni, R. Z., Linehan, D. C., and DeNardo, D. G. (2013). Targeting Tumor-Infiltrating Macrophages to Combat Cancer. *Immunotherapy* 5 (10), 1075–1087. doi:10.2217/imt.13.102

Park, J. H., Rivière, I., Gonen, M., Wang, X., Sénéchal, B., Curran, K. J., et al. (2018). Long-Term Follow-Up of CD19 CAR Therapy in Acute Lymphoblastic Leukemia. *N. Engl. J. Med.* 378 (5), 449–459. doi:10.1056/NEJMoa1709919

Passlick, B., Flieger, D., and Ziegler-Heitbrock, H. (1989). Identification and Characterization of a Novel Monocyte Subpopulation in Human Peripheral Blood. *Blood* 74 (7), 2527–2534. doi:10.1182/blood.v74.7.2527.bloodjournal7472527

Pienta, K. J., Machiels, J.-P., Schrijvers, D., Alekseev, B., Shkolnik, M., Crabb, S. J., et al. (2013). Phase 2 Study of Carlumab (CNTO 888), a Human Monoclonal Antibody against CC-Chemokine Ligand 2 (CCL2), in Metastatic Castration-Resistant Prostate Cancer. *Invest. New Drugs* 31 (3), 760–768. doi:10.1007/s10637-012-9869-8

Pollard, J. W. (2004). Tumour-Educated Macrophages Promote Tumour Progression and Metastasis. *Nat. Rev. Cancer* 4 (1), 71–78. doi:10.1038/nrc1256

Qian, B.-Z., Li, J., Zhang, H., Kitamura, T., Zhang, J., Campion, L. R., et al. (2011). CCL2 Recruits Inflammatory Monocytes to Facilitate Breast-Tumour Metastasis. *Nature* 475 (7355), 222–225. doi:10.1038/nature10138

Ramos, R. N., Chin, L. S., dos Santos, A. P. S. A., Bergami-Santos, P. C., Laginha, F., and Barbuto, J. A. M. (2012). Monocyte-Derived Dendritic Cells from Breast Cancer Patients Are Biased to Induce CD4+CD25+Foxp3+ Regulatory T Cells. *J. Leukoc. Biol.* 92 (3), 673–682. doi:10.1189/jlb.0112048

Ramos, R. N., Missolo-Koussou, Y., Gerber-Ferder, Y., Bromley, C., Bugatti, M., Núñez, N. G., et al. (2021). Tissue-resident FOLR2+ Macrophages Associate with Tumor-Infiltrating CD8+ T Cells and with Increased Survival of Breast Cancer Patients. *Preprint. Immunol.* doi:10.1101/2021.04.12.439412

Ramos, R. N., Rodriguez, C., Hubert, M., Ardin, M., Treilleux, I., Ries, C. H., et al. (2020). CD163 + Tumor-associated Macrophage Accumulation in Breast Cancer Patients Reflects Both Local Differentiation Signals and Systemic Skewing of Monocytes. *Clin. Transl Immunol.* 9 (2), 1108. doi:10.1002/cti2.1108

Reinartz, S., Schumann, T., Finkernagel, F., Wortmann, A., Jansen, J. M., Meissner, W., et al. (2014). Mixed-polarization Phenotype of Ascites-associated Macrophages in Human Ovarian Carcinoma: Correlation of CD163 Expression, Cytokine Levels and Early Relapse. *Int. J. Cancer* 134 (1), 32–42. doi:10.1002/ijc.28335

Reizis, B., Bunin, A., Ghosh, H. S., LewisLewis, K. L., and Sisirak, V. (2011). Plasmacytoid Dendritic Cells: Recent Progress and Open Questions. *Annu. Rev. Immunol.* 29 (1), 163–183. doi:10.1146/annurev-immunol-031210-101345

Ribechini, E., Hutchinson, J. A., Hergovits, S., Heuer, M., Lucas, J., Schleicher, U., et al. (2017). Novel GM-CSF Signals via IFN-Γr/irf-1 and AKT/mTOR License Monocytes for Suppressor functionNovel GM-CSF Signals via IFN-Γr/irf-1 and AKT/MTOR License Monocytes for Suppressor Function. *Blood Adv.* 1 (14), 947–960. doi:10.1182/bloodadvances.2017006858

Rieger, M. A., Hoppe, P. S., Smejkal, B. M., Eitelhuber, A. C., and Schroeder, T. (2009). Hematopoietic Cytokines Can Instruct Lineage Choice. *Science* 325 (5937), 217–218. doi:10.1126/science.1171461

Ruffell, B., Au, A., Rugo, H. S., Esserman, L. J., Hwang, E. S., and Coussens, L. M. (2012). Leukocyte Composition of Human Breast Cancer. *Proc. Natl. Acad. Sci.* 109 (8), 2796–2801. doi:10.1073/pnas.1104303108

Ruffell, B., and Coussens, L. M. (2015). Macrophages and Therapeutic Resistance in Cancer. *Cancer Cell* 27 (4), 462–472. doi:10.1016/j.ccell.2015.02.015

Ruhland, M. K., Roberts, E. W., Cai, E., Mujal, A. M., Marchuk, K., Beppler, C., et al. (2020). Visualizing Synaptic Transfer of Tumor Antigens Among Dendritic Cells. *Cancer Cell* 37 (6), 786–799.e5. doi:10.1016/j.ccell.2020.05.002

Sallusto, F., and Lanzavecchia, A. (1994). Efficient Presentation of Soluble Antigen by Cultured Human Dendritic Cells Is Maintained by Granulocyte/Macrophage Colony-Stimulating Factor Plus Interleukin 4 and Downregulated by Tumor Necrosis Factor Alpha. *J. Exp. Med.* 179 (4), 1109–1118. doi:10.1084/jem.179.4.1109

Salmon, H., Idoyaga, J., Rahman, A., Leboeuf, M., Remark, R., Jordan, S., et al. (2016). Expansion and Activation of CD103 + Dendritic Cell Progenitors at the Tumor Site Enhances Tumor Responses to Therapeutic PD-L1 and BRAF Inhibition. *Immunity* 44 (4), 924–938. doi:10.1016/j.immuni.2016.03.012

Sanford, D. E., Belt, B. A., Panni, R. Z., Mayer, A., Deshpande, A. D., Carpenter, D., et al. (2013). Inflammatory Monocyte Mobilization Decreases Patient Survival in Pancreatic Cancer: A Role for Targeting the CCL2/CCR2 Axis. *Clin. Cancer Res.* 19 (13), 3404–3415. doi:10.1158/1078-0432.CCR-13-0525

Sarrazin, S., Mossadegh-Keller, N., Fukao, T., Aziz, A., Mourcin, F., Vanhille, L., et al. (2009). MafB Restricts M-CSF-dependent Myeloid Commitment Divisions of Hematopoietic Stem Cells. *Cell* 138 (2), 300–313. doi:10.1016/j.cell.2009.04.057

Sasmono, R. T., Oceandy, D., Pollard, J. W., Tong, W., Pavli, P., Wainwright, B. J., et al. (2003). A Macrophage colony-stimulating Factor Receptor-green Fluorescent Protein Transgene Is Expressed throughout the Mononuclear Phagocyte System of the Mouse. *Blood* 101 (3), 1155–1163. doi:10.1182/blood-2002-02-0569

Satthaporn, S., Robins, A., Vassanasiri, W., El-Sheemy, M., Jibril, J. A., Clark, D., et al. (2004). Dendritic Cells Are Dysfunctional in Patients with Operable Breast Cancer. *Cancer Immunol. ImmunotherapyImmunotherapy* 53 (6), 510–518. doi:10.1007/s00262-003-0485-5

Schlitzer, A., McGovern, N., and Ginhoux, F. (2015). Dendritic Cells and Monocyte-Derived Cells: Two Complementary and Integrated Functional Systems. *Semin. Cel Develop. Biol.* 41 (maio), 9–22. doi:10.1016/j.semcdb.2015.03.011

Schmidts, A., Marsh, L. C., Srivastava, A. A., Bouffard, A. A., Boroughs, A. C., Scarfò, I., et al. (2020). Cell-Based Artificial APC Resistant to Lentiviral Transduction for Efficient Generation of CAR-T Cells from Various Cell Sources. *J. Immunother. Cancer* 8 (2), e000990. doi:10.1136/jitc-2020-000990

Scholl, S. M., Lidereau, R., de la Rochefordière, A., Cohen-Solal Le-Nir, C., Mosseri, V., Noguès, C., et al. (1996). Circulating Levels of the Macrophage Colony Stimulating Factor CSF-1 in Primary and Metastatic Breast Cancer Patients. A Pilot Study. *Breast Cancer Res. Tr* 39 (3), 275–283. doi:10.1007/BF01806155

Segura, E., Amigorena, S., and Théry, C. (2005). Mature Dendritic Cells Secrete Exosomes with Strong Ability to Induce Antigen-specific Effector Immune Responses. *Blood Cell Mol. Dis.* 35 (2), 89–93. doi:10.1016/j.bcmd.2005.05.003

Segura, E., Touzot, M., Bohineust, A., Cappuccio, A., Chiocchia, G., Hosmalin, A., et al. (2013). Human Inflammatory Dendritic Cells Induce Th17 Cell Differentiation. *Immunity* 38 (2), 336–348. doi:10.1016/j.immuni.2012.10.018

Serbina, N. V., Jia, T., Hohl, T. M., and Pamer, E. G. (2008). Monocyte-Mediated Defense against Microbial Pathogens. *Annu. Rev. Immunol.* 26 (1), 421–452. doi:10.1146/annurev.immunol.26.021607.090326

Shah, N. N., Johnson, B. D., Schneider, D., Zhu, F., Szabo, A., Keever-Taylor, C. A., et al. (2020). Bispecific Anti-CD20, Anti-CD19 CAR T Cells for Relapsed B Cell Malignancies: A Phase 1 Dose Escalation and Expansion Trial. *Nat. Med.* 26 (10), 1569–1575. doi:10.1038/s41591-020-1081-3

Sharma, A., Seow, J. J. W., Dutertre, C.-A., Pai, R., Blériot, C., Mishra, A., et al. (2020). Onco-Fetal Reprogramming of Endothelial Cells Drives Immunosuppressive Macrophages in Hepatocellular Carcinoma. *Cell* 183 (2), 377–394.e21. doi:10.1016/j.cell.2020.08.040

Shigeta, K., Kosaka, T., Kitano, S., Yasumizu, Y., Miyazaki, Y., Mizuno, R., et al. (2016). High Absolute Monocyte Count Predicts Poor Clinical Outcome in Patients with Castration-Resistant Prostate Cancer Treated with Docetaxel Chemotherapy. *Ann. Surg. Oncol.* 23 (12), 4115–4122. doi:10.1245/s10434-016-5354-5

Simonetta, F., Alvarez, M., and Negrin, R. S. (2017). Natural Killer Cells in Graft-Versus-Host-Disease after Allogeneic Hematopoietic Cell Transplantation. *Front. Immunol.* 8 (abril), 465. doi:10.3389/fimmu.2017.00465

Sisirak, V., Faget, J., Gobert, M., Goutagny, N., Vey, N., Treilleux, I., et al. (2012). Impaired IFN-α Production by Plasmacytoid Dendritic Cells Favors Regulatory T-Cell Expansion that May Contribute to Breast Cancer Progression. *Cancer Res.* 72 (20), 5188–5197. doi:10.1158/0008-5472.CAN-11-3468

Sisirak, V., Vey, N., Goutagny, N., Renaudineau, S., Malfroy, M., Thys, S., et al. (2013). Breast Cancer-Derived Transforming Growth Factor-β and Tumor Necrosis Factor-α Compromise Interferon-α Production by Tumor-Associated Plasmacytoid Dendritic Cells. *Int. J. Cancer* 133 (3), 771–778. doi:10.1002/ijc.28072

Spranger, S., Dai, D., Horton, B., and Gajewski, T. F. (2017). Tumor-Residing Batf3 Dendritic Cells Are Required for Effector T Cell Trafficking and Adoptive T Cell Therapy. *Cancer Cell* 31 (5), 711–723.e4. doi:10.1016/j.ccell.2017.04.003

Steidl, C., Lee, T., Shah, S. P., Farinha, P., Han, G., Nayar, T., et al. (2010). Tumor-Associated Macrophages and Survival in Classic Hodgkin's Lymphoma. *N. Engl. J. Med.* 362 (10), 875–885. doi:10.1056/NEJMoa0905680

Stone, S. C., Rossetti, R. A. M., Bolpetti, A., Boccardo, E., de Araujo Souza, P. S., and Lepique, A. P. (2014). HPV16-Associated Tumors Control Myeloid Cell Homeostasis in Lymphoid Organs, Generating a Suppressor Environment for T Cells. *J. Leukoc. Biol.* 96 (4), 619–631. doi:10.1189/jlb.3A0513-282R

Stroh, T., Erben, U., Kühl, A. A., Zeitz, M., and Siegmund, B. (2010). Combined Pulse Electroporation - A Novel Strategy for Highly Efficient Transfection of Human and Mouse Cells. *PLoS ONE* 5 (3), e9488. doi:10.1371/journal.pone.0009488

Takahashi, R., Ijichi, H., Sano, M., Miyabayashi, K., Mohri, D., Kim, J., et al. (2020). Soluble VCAM-1 Promotes Gemcitabine Resistance via Macrophage Infiltration and Predicts Therapeutic Response in Pancreatic Cancer. *Sci. Rep.* 10 (1), 21194. doi:10.1038/s41598-020-78320-3

Tang, M., Diao, J., Gu, H., Khatri, I., Zhao, J., and Cattral, M. S. (2015). Toll-like Receptor 2 Activation Promotes Tumor Dendritic Cell Dysfunction by Regulating IL-6 and IL-10 Receptor Signaling. *Cel Rep.* 13 (12), 2851–2864. doi:10.1016/j.celrep.2015.11.053

Tang-Huau, T.-L., Gueguen, P., Goudot, C., Durand, M., Bohec, M., Baulande, S., et al. (2018). Human In Vivo-Generated Monocyte-Derived Dendritic Cells and Macrophages Cross-Present Antigens through a Vacuolar Pathway. *Nat. Commun.* 9 (1), 2570. doi:10.1038/s41467-018-04985-0

Taylor, P. R., and Gordon, S. (2003). Monocyte Heterogeneity and Innate Immunity. *Immunity* 19 (1), 2–4. doi:10.1016/S1074-7613(03)00178-X

Thistlethwaite, F. C., Gilham, D. E., Guest, R. D., Rothwell, D. G., Pillai, M., Burt, D. J., et al. (2017). The Clinical Efficacy of First-Generation Carcinoembryonic Antigen (CEACAM5)-specific CAR T Cells Is Limited by Poor Persistence and Transient Pre-conditioning-dependent Respiratory Toxicity. *Cancer Immunol. Immunother.* 66 (11), 1425–1436. doi:10.1007/s00262-017-2034-7

Thomachot, M. C. c., Bendriss-Vermare, N., Massacrier, C., Biota, C., Treilleux, I., Goddard, S., et al. (2004). Breast Carcinoma Cells Promote the Differentiation of CD34+ Progenitors towards 2 Different Subpopulations of Dendritic Cells with CD1ahighCD86?Langerin- and CD1a+CD86+Langerin+ Phenotypes. *Int. J. Cancer* 110 (5), 710–720. doi:10.1002/ijc.20146

Torroella-Kouri, M., Rodríguez, D., and Caso, R. (2013). Alterations in Macrophages and Monocytes from Tumor-Bearing Mice: Evidence of Local and Systemic Immune Impairment. *Immunol. Res.* 57 (1–3), 86–98. doi:10.1007/s12026-013-8438-3

Treilleux, I., Blay, J.-Y., Bendriss-Vermare, N., Ray-Coquard, I., Bachelot, T., Guastalla, J.-P., et al. (2004). Dendritic Cell Infiltration and Prognosis of Early Stage Breast Cancer. *Clin. Cancer Res.* 10 (22), 7466–7474. doi:10.1158/1078-0432.CCR-04-0684

Trovato, R., Fiore, A., Sartori, S., Canè, S., Giugno, R., Cascione, L., et al. (2019). Immunosuppression by Monocytic Myeloid-Derived Suppressor Cells in Patients with Pancreatic Ductal Carcinoma Is Orchestrated by STAT3. *J. Immunother. Cancer* 7 (1), 255. doi:10.1186/s40425-019-0734-6

Truxova, I., Kasikova, L., Hensler, M., Skapa, P., Laco, J., Pecen, L., et al. (2018). Mature Dendritic Cells Correlate with Favorable Immune Infiltrate and Improved Prognosis in Ovarian Carcinoma Patients. *J. Immunother. Cancer* 6 (1), 139. doi:10.1186/s40425-018-0446-3

van Furth, R., and Cohn, Z. A. (1968). The Origin and Kinetics of Mononuclear Phagocytes. *J. Exp. Med.* 128 (3), 415–435. doi:10.1084/jem.128.3.415

Villani, A.-C., Satija, R., Reynolds, G., Sarkizova, S., Shekhar, K., Fletcher, J., et al. (2017). Single-Cell RNA-Seq Reveals New Types of Human Blood Dendritic Cells, Monocytes, and Progenitors. *Science* 356 (6335), eaah4573. doi:10.1126/science.aah4573

Villar, J., and Segura, E. (2020). Decoding the Heterogeneity of Human Dendritic Cell Subsets. *Trends Immunol.* 41 (12), 1062–1071. doi:10.1016/j.it.2020.10.002

Waldman, A. D., Fritz, J. M., and Lenardo, M. J. (2020). A Guide to Cancer Immunotherapy: From T Cell Basic Science to Clinical Practice. *Nat. Rev. Immunol.* 20 (11), 651–668. doi:10.1038/s41577-020-0306-5

Watchmaker, P. B., Lahl, K., Lee, M., Baumjohann, D., Morton, J., KimKim, S. J., et al. (2014). Comparative Transcriptional and Functional Profiling Defines Conserved Programs of Intestinal DC Differentiation in Humans and Mice. *Nat. Immunol.* 15 (1), 98–108. doi:10.1038/ni.2768

Wculek, S. K., Amores-Iniesta, J., Conde-Garrosa, R., Khouili, S. C., Melero, I., and Sancho, D. (2019). Effective Cancer Immunotherapy by Natural Mouse Conventional Type-1 Dendritic Cells Bearing Dead Tumor Antigen. *J. Immunotherapy Cancer* 7 (1), 100. doi:10.1186/s40425-019-0565-5

Wculek, S. K., Cueto, F. J., Mujal, A. M., Melero, I., Krummel, M. F., and Sancho, D. (2020). Dendritic Cells in Cancer Immunology and Immunotherapy. *Nat. Rev. Immunol.* 20 (1), 7–24. doi:10.1038/s41577-019-0210-z

Wilgenhof, S., Corthals, J., Heirman, C., van Baren, N., Lucas, S., Kvistborg, P., et al. (2016). Phase II Study of Autologous Monocyte-Derived MRNA Electroporated Dendritic Cells (TriMixDC-MEL) Plus Ipilimumab in Patients with Pretreated Advanced Melanoma. *J. Clin. Oncol.* 34 (12), 1330–1338. doi:10.1200/JCO.2015.63.4121

Wong, K. L., Tai, J. J.-Y., Wong, W.-C., Han, H., Sem, X., Yeap, W.-H., et al. (2011). Hao Han, Xiaohui Sem, Wei-Hseun Yeap, Philippe Kourilsky, and Siew-Cheng WongGene Expression Profiling Reveals the Defining Features of the Classical, Intermediate, and Nonclassical Human Monocyte Subsets. *Blood* 118 (5), e16–e31. doi:10.1182/blood-2010-12-326355

Wong, K. L., Yeap, W. H., Tai, J. J. Y., Ong, S. M., Dang, T. M., and Wong, S. C. (2012). The Three Human Monocyte Subsets: Implications for Health and Disease. *Immunol. Res.* 53 (1–3), 41–57. doi:10.1007/s12026-012-8297-3

Wu, W.-C., Sun, H.-W., Chen, H.-T., Liang, J., Yu, X.-J., Wu, C., et al. (2014). Circulating Hematopoietic Stem and Progenitor Cells Are Myeloid-Biased in Cancer Patients. *Proc. Natl. Acad. Sci.* 111 (11), 4221–4226. doi:10.1073/pnas.1320753111

Xie, G., Dong, H., Liang, Y., HamHam, J. D., Rizwan, R., and Chen, J. (2020). CAR-NK Cells: A Promising Cellular Immunotherapy for Cancer. *EBioMedicine* 59 (setembro), 102975. doi:10.1016/j.ebiom.2020.102975

Yang, X., Feng, W., Wang, R., Yang, F., Wang, L., Chen, S., et al. (2018). Repolarizing Heterogeneous Leukemia-Associated Macrophages with More M1 Characteristics Eliminates Their Pro-leukemic Effects. *OncoImmunology* 7 (4), e1412910. doi:10.1080/2162402X.2017.1412910

Zhang, D. K. Y., Cheung, A. S., and Mooney, D. J. (2020). Activation and Expansion of Human T Cells Using Artificial Antigen-Presenting Cell Scaffolds. *Nat. Protoc.* 15 (3), 773–798. doi:10.1038/s41596-019-0249-0

Zhang, L., Tian, L., Dai, X., Yu, H., Wang, J., Lei, A., et al. (2020). Pluripotent Stem Cell-Derived CAR-Macrophage Cells with Antigen-dependent Anti-cancer Cell Functions. *J. Hematol. Oncol.* 13 (1), 153. doi:10.1186/s13045-020-00983-2

Zhang, M., Huang, L., Ding, G., Huang, H., Cao, G., Sun, X., et al. (2020). Interferon Gamma Inhibits CXCL8-CXCR2 axis Mediated Tumor-Associated Macrophages Tumor Trafficking and Enhances Anti-PD1 Efficacy in Pancreatic Cancer. *J. Immunother. Cancer* 8 (1), e000308. doi:10.1136/jitc-2019-000308

Zhang, W., Liu, L., Su, H., Liu, Q., Shen, J., Dai, H., et al. (2019). Chimeric Antigen Receptor Macrophage Therapy for Breast Tumours Mediated by Targeting the Tumour Extracellular Matrix. *Br. J. Cancer* 121 (10), 837–845. doi:10.1038/s41416-019-0578-3

Zhu, Y., Herndon, J. M., Sojka, D. K., Kim, K.-W., Knolhoff, B. L., Zuo, C., et al. (2017). Tissue-Resident Macrophages in Pancreatic Ductal Adenocarcinoma Originate from Embryonic Hematopoiesis and Promote Tumor Progression. *Immunity* 47 (2), 323–338.e6. doi:10.1016/j.immuni.2017.07.014

Ziegler-Heitbrock, L., Ancuta, P., Crowe, S., Dalod, M., Grau, V., Hart, D. N., et al. (2010). Nomenclature of Monocytes and Dendritic Cells in Blood. *Blood* 116 (16), e74–e80. doi:10.1182/blood-2010-02-258558

Conflict of Interest: The authors declare that the research was conducted in the absence of any commercial or financial relationships that could be construed as a potential conflict of interest.

Publisher's Note: All claims expressed in this article are solely those of the authors and do not necessarily represent those of their affiliated organizations, or those of the publisher, the editors and the reviewers. Any product that may be evaluated in this article, or claim that may be made by its manufacturer, is not guaranteed or endorsed by the publisher.

frontiers in Cell and Developmental Biology

ORIGINAL RESEARCH
published: 09 February 2022
doi: 10.3389/fcell.2021.754873

Functions of RNF Family in the Tumor Microenvironment and Drugs Prediction in Grade II/III Gliomas

Jingwei Zhang[1,2†], Zeyu Wang[1,2†], Hao Zhang[1], Ziyu Dai[1], Xisong Liang[1], Shuwang Li[1], Xun Zhang[1], Fangkun Liu[1], Zhixiong Liu[1,2,3], Kui Yang[1,2] and Quan Cheng[1,2,3,4*]*

[1]Department of Neurosurgery, Xiangya Hospital, Central South University, Changsha, China, [2]National Clinical Research Center for Geriatric Disorders, Changsha, China, [3]Clinical Diagnosis and Therapy Center for Glioma of Xiangya Hospital, Central South University, Changsha, China, [4]Department of Clinical Pharmacology, Xiangya Hospital, Central South University, Changsha, China

OPEN ACCESS

Edited by:
Rodrigo Nalio Ramos,
INSERM U1138 Centre de Recherche des Cordeliers (CRC), France

Reviewed by:
Haitao Zhao,
Peking Union Medical College Hospital (CAMS), China
Kexin Yan,
China Medical University, China
Jianbin Bi,
China Medical University, China

***Correspondence:**
Quan Cheng
chengquan@csu.edu.cn
Kui Yang
kui.yang@csu.edu.cn

[†]These authors have contributed equally to this work

Specialty section:
This article was submitted to Molecular and Cellular Pathology, a section of the journal Frontiers in Cell and Developmental Biology

Received: 07 August 2021
Accepted: 29 November 2021
Published: 09 February 2022

Citation:
Zhang J, Wang Z, Zhang H, Dai Z, Liang X, Li S, Zhang X, Liu F, Liu Z, Yang K and Cheng Q (2022) Functions of RNF Family in the Tumor Microenvironment and Drugs Prediction in Grade II/III Gliomas. Front. Cell Dev. Biol. 9:754873. doi: 10.3389/fcell.2021.754873

Increasing evidence has demonstrated that RING finger (RNF) proteins played a vital role in cellular and physiological processes and various diseases. However, the function of RNF proteins in low-grade glioma (LGG) remains unknown. In this study, 138 RNF family members revealed their role in LGG. The TCGA database was used as the training cohort; two CGGA databases and GSE108474 were selected as external validation cohorts. Patients were grouped into cluster 1 and cluster 2, both in the training and validation cohorts, using consensus clustering analysis. The prognosis of patients in cluster 1 is significantly better than that in cluster 2. Meanwhile, biofunction prediction was further introduced to explore the potential mechanisms that led to differences in survival outcomes. Patients in Cluster 2 showed more complicated immunocytes infiltration and highly immunosuppressive features than cluster 1. Enrichment pathways such as negative regulation of mast cell activation, DNA replication, mismatch repair, Th17 cell differentiation, antigen processing and presentation, dendritic cell antigen processing and presentation, dendritic cell differentiation were also enriched in cluster 2 patients. For the last, the main contributors were distinguished by employing a machine learning algorithm. A lot of targeted and small molecule drugs that are sensitive to patients in cluster 2 were predicted. Importantly, we discovered TRIM8, DTX2, and TRAF5 as the most vital contributors from the RNF family, which were related to immune infiltration in LGG tumor immune landscape. In this study, we demonstrated the predicted role of RNF proteins in LGG. In addition, we found out three markers among RNF proteins that are closely related to the immune aspects of LGG, which might serve as novel therapeutic targets for immunotherapy in the future.

Keywords: lower-grade glioma, tumor microenvironment, immunotherapy, RING finger proteins, Chemotherapy

INTRODUCTION

Diffuse gliomas, including LGG and glioblastomas (GBM), are the most common malignant tumors among adults in the central nervous system (CNS) (Miller et al., 2019). To data, maximum safe surgical resection, radiotherapy, and chemotherapy remain the mainstay of therapeutic methods for gliomas (Zhang et al., 2019; Funakoshi et al., 2021). However, the prognosis of malignant and invasive gliomas is still far from satisfactory, even with recent improvements in diagnosis and

treatment methods (Tan et al., 2020; McKinnon et al., 2021). For example, the median overall survival (OS) of LGG patients is less than 2 years, whereas 5-year survival rate of GBM patients is only about 5% (Alexander and Cloughesy, 2017; An et al., 2020; Zhang et al., 2021a). In addition, several clinicopathological and molecular features determine the outcome of patients with gliomas, such as WHO grade, isocitrate dehydrogenase 1/2 (IDH1/2) mutations, 1p/19q co-deletion, MGMT promoter methylation, subtype (Reifenberger et al., 2017; Molinaro et al., 2019). Nowadays, increasing evidence indicates that tumor immunotherapy focusing on blocking immune checkpoints has achieved remarkable benefits, providing a promising direction for glioma patients (Hodges et al., 2017; Aslan et al., 2020).

The tumor microenvironment (TME) is a highly dynamic and complex ecosystem consisting of tumor cells, stromal cells, extracellular matrix, and various cellular molecules (Giraldo et al., 2019; Baghban et al., 2020). Tumors exhibit immunosuppression and immune evasion through immune checkpoints secreted from stromal cells or tumor cells in the TME, resulting in tumor growth and metastasis. Inhibitors and vaccines targeting classical immune checkpoint molecules in the TME, such as programmed cell death-1 (PD-1) and cytotoxic T-lymphocyte-associated antigen 4 (CTLA-4), have achieved remarkable progress in several types of cancers (Wang et al., 2019; Andrews et al., 2021). Our previous study showed that upregulated CTLA-4 expression was associated with a worse prognosis in glioma (Liu et al., 2020; Zhang et al., 2021b). Meanwhile, the infiltrated immune cells such as tumor-associated macrophages (TAMs), dendritic cells (DCS), natural killer cells (NK), and regulatory T cells (Tregs) in the TME also participate in every step of tumor immune progression (Galli et al., 2020; Li et al., 2021). The glioma tumor microenvironment has proved to play a significant role in promoting angiogenesis, immunosuppression, migration, tumor metastasis, and drug resistance (De Vleeschouwer et al., 2017; Simon et al., 2020; Liu et al., 2021).

The RNF proteins are a group of transmembrane proteins containing a unique three-dimensional domain which is consists of C3HC4 amino acid residues with eight conserved cysteine and histidine residues that combine two zinc cations (Cham et al., 2017; Cham et al., 2018; Kuhns et al., 2020). Most RNF proteins act as E3 ubiquitin ligases and regulate the ubiquitination of membrane proteins under physiological conditions (Campbell et al., 2012). In addition, studies revealed that transmembrane RNF proteins play an essential role in many organelles and cellular progress, including protein transportation, cell proliferation, differentiation, apoptosis, immunomodulatory and mitochondrial dynamics (Amal et al., 2019; Wei et al., 2019). However, in recent years, more and more studies have started to explore the function of RNF proteins in oncogenesis and tumor metastasis (Wang et al., 2016; Liu et al., 2018). For example, Rong Geng et al. (Geng et al., 2017) found that the elevated RNF183 protein in tumor samples promotes the migration and metastasis of colorectal cancer cells through activating the NF-κB-IL-8 axis. Moreover, the overexpressed RNF38 was found to inhibit the expression of neuroblast differentiation-associated protein (AHNAK) and activate the transforming growth factor-β (TGF-β) signaling pathway through ubiquitinating, which is associated with the poor outcome and high recurrence rate of hepatocellular carcinoma patients (Peng et al., 2019). However, the role of RNF proteins in LGG remains largely unclear.

Therefore, we analyzed the clinical and RNA-sequencing data of LGG patients from three different datasets to clarify the whole aspects of RNF proteins in the LGG tumor microenvironment.

MATERIALS AND METHODS

Data Collection

We collected the clinical and transcriptomic data of LGGs from the TCGA (http://cancergenome.nih.gov/), the CGGA-array (Fang et al., 2017) (mRNA microarray database), the CGGA-sequence (Zhao et al., 2017) (mRNA sequencing database) (http://www.cgga.org.cn) and Rembrandt datasets (also known as GSE108474) (Gusev et al., 2018). The Gliovis data portal predicted the (Bowman et al., 2017) subtype of LGG. RNF family members are downloaded from the HGNC database (https://www.genenames.org/).

Consensus Clustering Analysis

The intersection between RNF family members and gene lists from the TCGA and CGGA databases is performed. Then consensus cluster analysis is introduced with the R package "ConsensusClusterPlus" (Wilkerson and Hayes, 2010) based on data from the TCGA dataset. Parameters of cluster model are set as, distance = "Pearson," maxK = 10, reps = 1000, pItem = 0.8, pFeature = 1, clusterAlg = "kmdist," corUse = "complete.obs." PCA diagram shows the classification of the cluster model.

Immunogenicity Evaluation

ESTIMATE (Yoshihara et al., 2013) algorithm is applied to calculate the immune score, stromal score, and tumor purity. CIBERSORT (Newman et al., 2019) and xCell (Aran et al., 2017) algorithms are used to show the infiltration ratio of immunocytes. The expression profile of immune escape-associated genes from previous work is mapped with a boxplot. Two types of immunogram (Karasaki et al., 2017; Kobayashi et al., 2020) from previous works are reconstructed based on the "ssgsea" algorithm and shown with radar diagram, boxplot, and heatmap.

Bio Function Analysis

The Gene Ontology (GO) and Kyoto Encyclopedia of Genes and Genomes (KEGG) based on Gene Set Enrichment Analysis (GSEA) and Gene Set Variation Analysis (GSVA) were used to exploring enrichment signaling pathways between clusters or groups.

Main Contributor Identification

Main contributors of the cluster model from RNF family members are identified by employing multiple machine learning methods. First, univariate Cox regression analysis and LASSO regression analysis, as previously described, are performed to determine LGG prognosis-associated markers. Then, the xgboost algorithm is performed with the R package "xgboost." For the last, the Boruta algorithm is introduced to label family members with "Confirmed" or "Rejected" based on the cluster model, and "Confirmed" markers are filtered out. Finally,

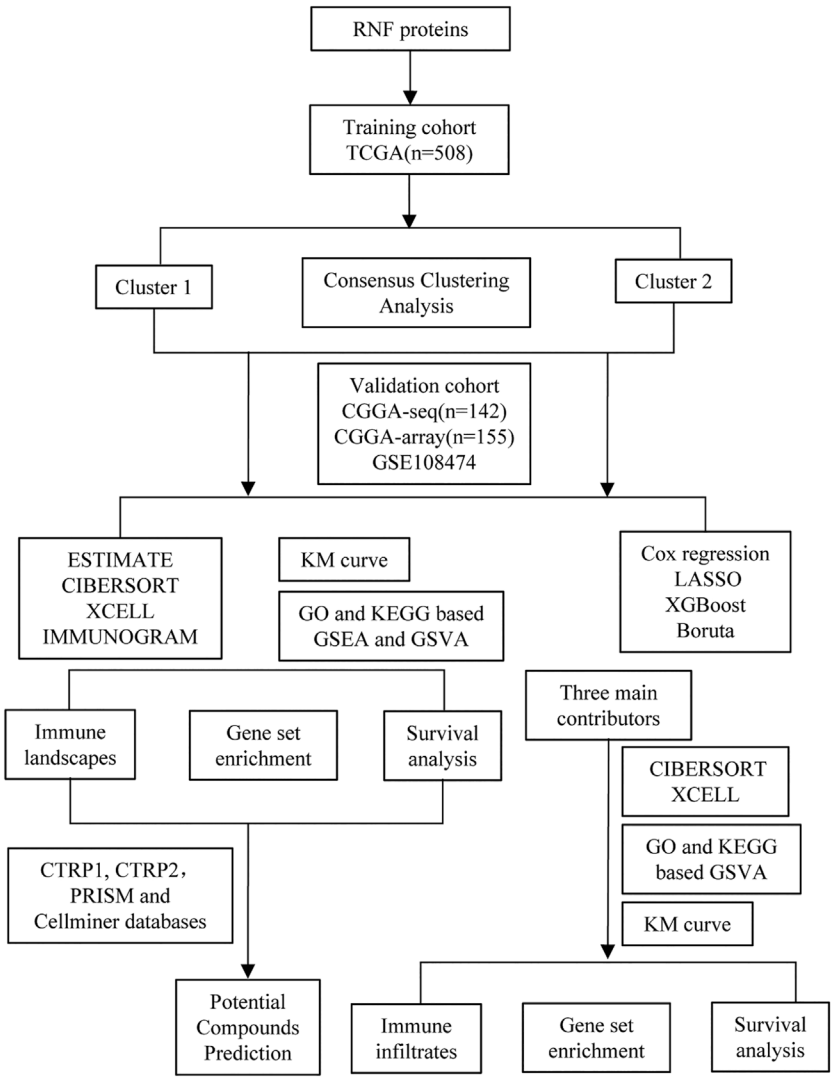

FIGURE 1 | The flow chart of the entire study.

the Venn diagram shows the intersection of results, which are also selected as leading contributors, from those three methods.

Potential Compounds Prediction

Drug sensitivity from PRISM and CTRP database and cell line expression profile from CCLE database is integrated to predict potential sensitivity compounds based on the cluster model. Preparation of drug sensitivity matrix and cell line expression matrix is performed as previous work stated. R package "pRRophetic" is used for potential compounds prediction. Similar strategies are also applied to identify compounds from the CellMiner database.

Statistical Analysis

The Wilcox test was used to compare two groups. In addition, the Kaplan-Meier analysis was applied to analyze the survival prognosis between two groups, and log-rank was used for examination. The ROC curve and corresponding AUC were generated by using the R package "timeROC." * p-value < 0.05, ** p-value < 0.01, *** p-value < 0.001, and p-value < 0.05 is significantly statistical. All analyses were performed with R (version 3.6.1).

RESULTS

Clustering Model Based on RNF Genes Identified Two Clusters with Distinct Outcomes and Clinicopathological Features

First, to clarify the prognostic role of RNF proteins in LGG, a total of 138 RNF family members were selected from the public database-GENECARDS (**Supplementary Table S1**). The flow

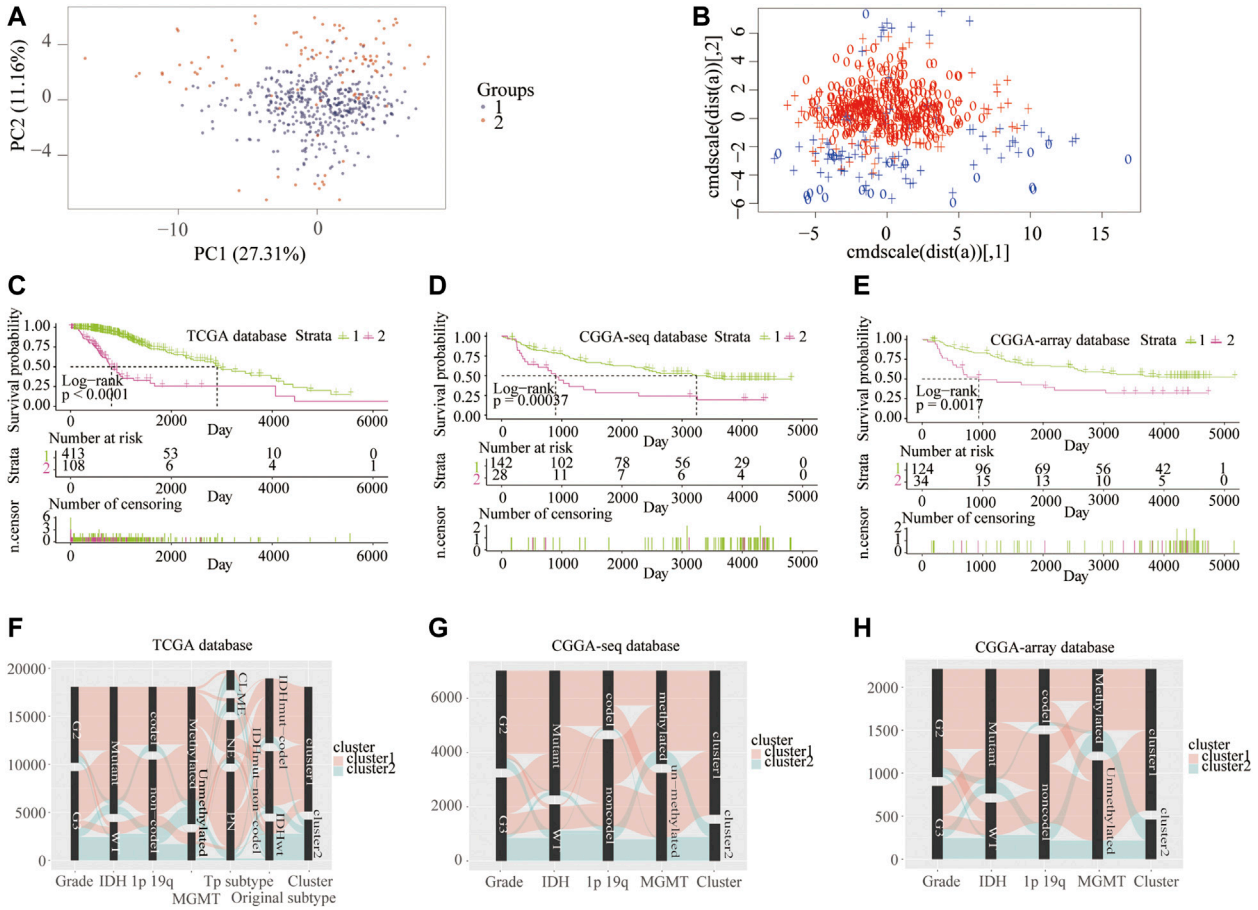

FIGURE 2 | Consensus clustering of samples into cluster 1 and cluster 2 from the training and validation cohorts. Consensus clustering patients into two clusters using principal component **(A)** and support vector machine analysis **(B)** from the TCGA database. Kaplan–Meier overall survival curve between two clusters from the TCGA **(C)**, CGGA-sequence **(D)**, and CGGA-array **(E)** databases. Sankey diagram shows LGG clinicopathologic features between two clusters from the TCGA **(F)**, CGGA-sequence **(G)**, and CGGA-array **(H)** databases.

chart of the entire study is shown in **Figure 1**, we used the TCGA as the training set, and two CGGA and the Rembrandt (GSE108474) datasets were treated as validation sets. The clinicopathological characteristics of four public databases are shown in **Supplementary Table S2**. Based on the clustering analysis, the optimal number of clusters was 2 (**Supplementary Figure S1A**). Then, patients in the TCGA database were divided into two subgroups through the consensus clustering method (**Figures 2A,B**). Kaplan-Meier analysis in the TCGA database between two clusters showed that patients in cluster 1 had a better prognosis than cluster 2 during the overall survival time ($p <$ 0.0001; **Figure 2C**). Meanwhile, in the CGGA sequence ($p < 0.001$; **Figure 2D**) and CGGA array ($p < 0.01$; **Figure 2E**) database, the patients in cluster 1 also had better results than cluster 2 during the overall survival time. Moreover, the patients in cluster 1 also had a better outcome than cluster 2 during the overall survival time in the GSE108474 dataset (**Supplementary Figure S1B**). We then calculated the AUC of the cluster model in the TCGA dataset (**Supplementary Figure S1C**), which is 0.74. However, the AUC in three validation sets is 0.61 (CGGAseq; **Supplementary Figure S1D**), 0.65 (CGGAarray; **Supplementary Figure S1E**), 0.64 (GSE108474; **Supplementary Figure S1F**). We thought that the AUC in these validation datasets was lower than 0.7 resulting from the number of samples in validation sets being less than that in the training set. In addition, the Sankey diagram in the TCGA database showed that patients in cluster 1 tend to exhibit favorable clinicopathologic features: IDH mutation and IDH mut-codel subtype (**Figure 2F**), which were also verified in CCGA-sequence (**Figure 2G**) and CCGA-array (**Figure 2H**) databases. These results indicated that the expression of RNF genes is associated with patient's prognosis in low-grade gliomas and might have a close relationship with the IDH status.

Functional Enrichment Analysis Between Two Clusters

Next, we analyzed the related enrichment signaling pathways between clusters 1 and 2 using GO and KEGG-based GSEA and GSVA. GO analysis in the TCGA database showed that several signaling pathways related to immune response were enriched in cluster 2, including positive regulation of natural killer cell-mediated immune response to the tumor cell, negative

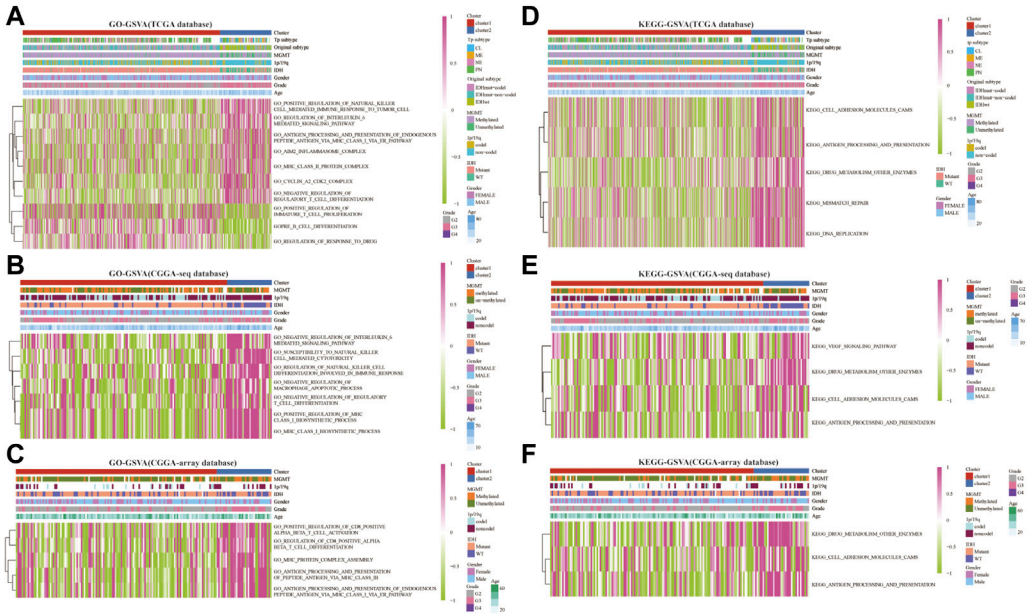

FIGURE 3 | RNF proteins-related biological functions in cluster 1 and cluster 2 from the training and validation cohorts. Gene set variation analysis in cluster 1 and cluster 2 based on GO database from the TCGA **(A)**, CGGA-sequence **(B)**, and CGGA-array **(C)** databases. Gene set variation analysis in cluster 1 and cluster 2 based on the KEGG database from the TCGA **(D)**, CGGA-sequence **(E)**, and CGGA-array **(F)** databases.

regulation of IL-6 and mast cell activation, regulation of antigen processing, and presentation, inflammasome and MHC class II protein complex, cyclin A2/CDK2 complex, negative regulation of regulatory T cell differentiation (**Figure 3A** and **Supplementary Figure S2A**). Meanwhile, the pathways of positive regulation of immature T cell proliferation, B cell differentiation, and regulation of response to the drug were enriched in cluster 1. Furthermore, GO analysis in the CGGA-sequence database showed that the pathways of susceptibility to natural killer cell-mediated cytotoxicity, negative regulation of IL-6, negative regulation of T cell differentiation and macrophage apoptotic process, positive regulation of MHC class I biosynthetic process were enriched in cluster 2 (**Figure 3B** and **Supplementary Figure S2B**). In addition, GO analysis in the CGGA-array showed that several immune-related pathways, such as positive regulation of $CD8^{+}\alpha\beta$T cell activation and differentiation, antigen processing, and presentation of peptide antigen *via* MHC classIbiosynthetic process (**Figure 3C** and **Supplementary Figure S2C**). Furthermore, KEGG analysis indicated that the pathways such as antigen processing and presentation, DNA replication, drug metabolism, other enzymes, cell adhesion molecules CAMs were enriched in cluster 2 in the training and validation databases (**Figures 3D–F** and **Supplementary Figures S2D–F**).

Immune Infiltration Analysis Between Two Clusters

Therefore, we examined the immune aspects in the LGG TME between cluster 1 and cluster 2. The results from the TCGA database demonstrated that the expression of TME immune cells in cluster 1 was significantly different from that in cluster 2, including M1 macrophages, monocytes, plasma cells, CD4 memory T cells, and Tregs ($p < 0.05$; **Figures 4A,D** and **Supplementary Figures S3A,D**). The immune cell types infiltrated in cluster 1 and cluster 2 from the CGGA sequence database were also significantly different, such as eosinophils, macrophages, and NK cells ($p < 0.05$; **Figures 4B,E** and **Supplementary Figures S3B,E**). Results from the CGGA-array database showed that large amounts of immune cells in the TME were different from cluster 1 and cluster 2, including memory B cells, dendritic cells, M1 macrophages, activated CD4 memory T cells, and follicular helper T cells ($p < 0.05$; **Figures 4C,F** and **Supplementary Figures S3C,F**). Moreover, the tumor purify was higher in cluster 1, whereas the estimated score, stromal score, and immune score were lower in cluster 1, both in the TCGA ($p < 0.001$; **Supplementary Figure S4A**), CGGA-sequence ($p < 0.05$; **Supplementary Figure S4B**) and CGGA-array ($p < 0.05$; **Supplementary Figure S4C**) databases.

Immunosuppressive Aspects Analysis Between Two Clusters

Then, we analyzed the patient-specific landscapes of the tumor microenvironment in the LGG using two types of immunogram (2017, 2010). Results showed that several immunosuppressive progresses, including the absence of checkpoint expression, trafficking, and infiltration, absence of inhibitory molecules, T cell immunity, priming, and activation, were significantly enriched in cluster 2 from the TCGA ($p < 0.001$; **Figures**

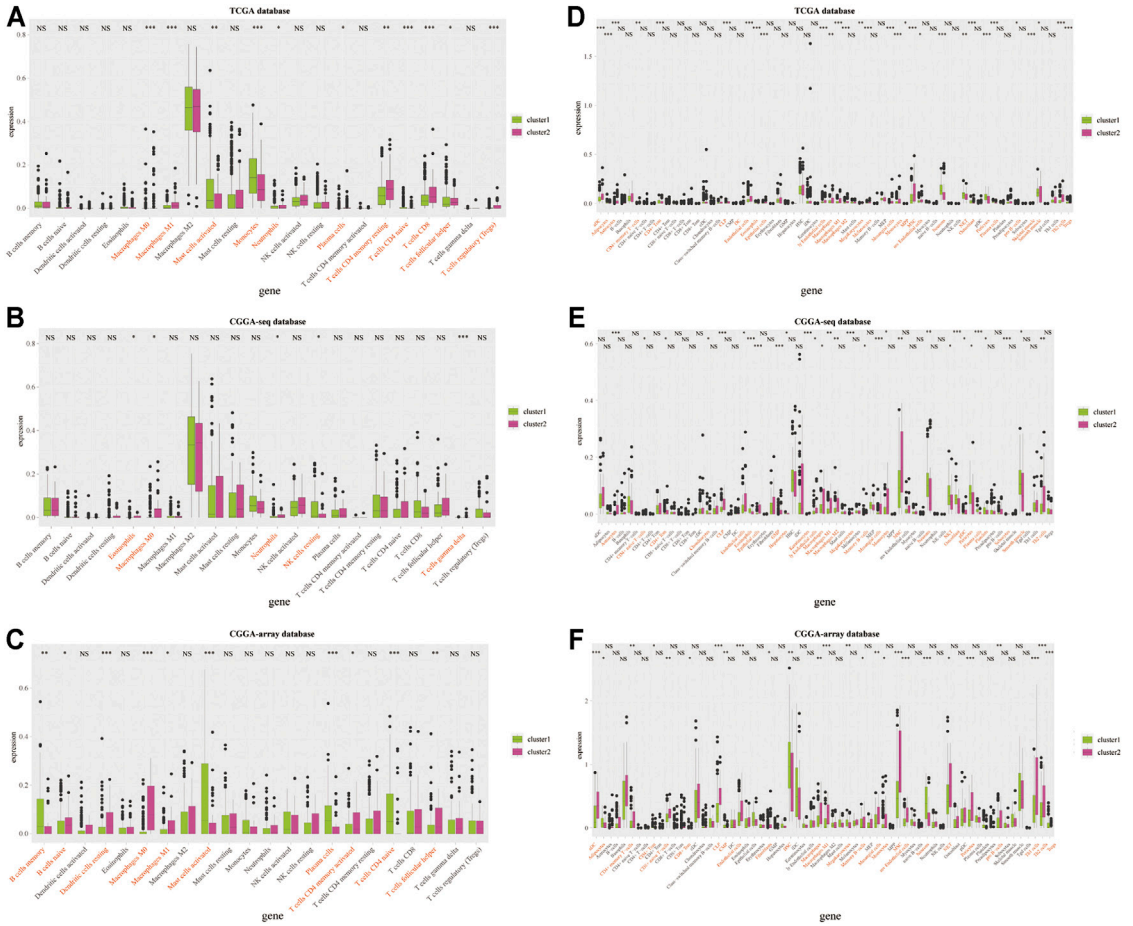

FIGURE 4 | Infiltrated immune cells in cluster 1 and cluster 2 from the training and validation cohorts. Immune infiltrates in two clusters based on the CIBERSORT algorithm from the TCGA **(A)**, CGGA-sequence **(B)**, and CGGA-array **(C)** databases. Immune infiltrates in two clusters based on the xCELL algorithm from the TCGA **(D)**, CGGA-sequence **(E)**, and CGGA-array **(F)** databases. *$p < 0.05$, **$p < 0.01$, ***$p < 0.001$, NS, no significant differences.

5A,C), CGGA-sequence ($p < 0.01$; **Figures 5E,G**) and CGGA-array ($p < 0.05$; **Figures 5I,K**) databases. Meanwhile, other immunological progress, including inhibitory cells Tregs, innate immunity, T cells, glycolysis, inhibitory molecules, priming activation, and IFNG response was also significantly enriched in cluster 2 from the TCGA ($p < 0.01$; **Figures 5B,D**), CGGA-sequence ($p < 0.05$; **Figures 5F,H**) and CGGA-array ($p < 0.05$; **Figures 5J,L**) databases.

Furthermore, we explored the expression profiles of immune escape-associated genes between cluster 1 and cluster 2 from the training and validation databases. Results indicated that antigen genes such as HLA-B, HLA-DPA1, HLA-DPB1, HLA-DQB2, HLA-DRA, HLA-DRB1, and MICB were upregulated in cluster 2 compared to cluster 1 from the three public databases ($p < 0.05$; **Figures 6A–C**). The expression of the co-inhibitory gene-SLAMF7 was higher in cluster 2 ($p < 0.05$; **Figures 6D–F**). The levels of ligand genes, including CD40LG, CD70, CXCL10, CXCL9, IL-10, TGFB1, and CEGFA, were higher in cluster 2, whereas the expression of CX3CL1 was lower in cluster 2 ($p < 0.05$; **Figures 6G–I**). The levels of receptor genes, including CD40, ICOS, IL2RA, LAG3, PDCD1, TNFRSF14, TNFRSF4, and TNFRSF9, were increased in cluster 2, whereas the expression of EDNRB and TLR-4 was lower in cluster 2 ($p < 0.05$; **Figures 6J–L**). In addition, the levels of cell adhesion genes, including ICAM-1 and ITGB2, were elevated in cluster 2 ($p < 0.05$; **Supplementary Figures S5A–C**). The expression of costimulatory genes, including CD28 and CD80, were higher in cluster 2 ($p < 0.05$; **Supplementary Figures S5D–F**). The expression of other genes, such as GZMA and PRF1, were overexpressed in cluster 2 ($p < 0.05$; **Supplementary Figures S5G–I**). These results demonstrated that the TNF genes played an essential role in the immune infiltration and were related to the immunosuppressive progress in the LGG TME.

Prediction of Sensitive Drugs

Next, we predicted the sensitive drugs between cluster 1 and cluster 2 from the public databases. The top 50 sensitive drugs between clusters 1 and 2 were exported from the CELLMINIER database (**Supplementary Table S3**). Data from the CTRP1

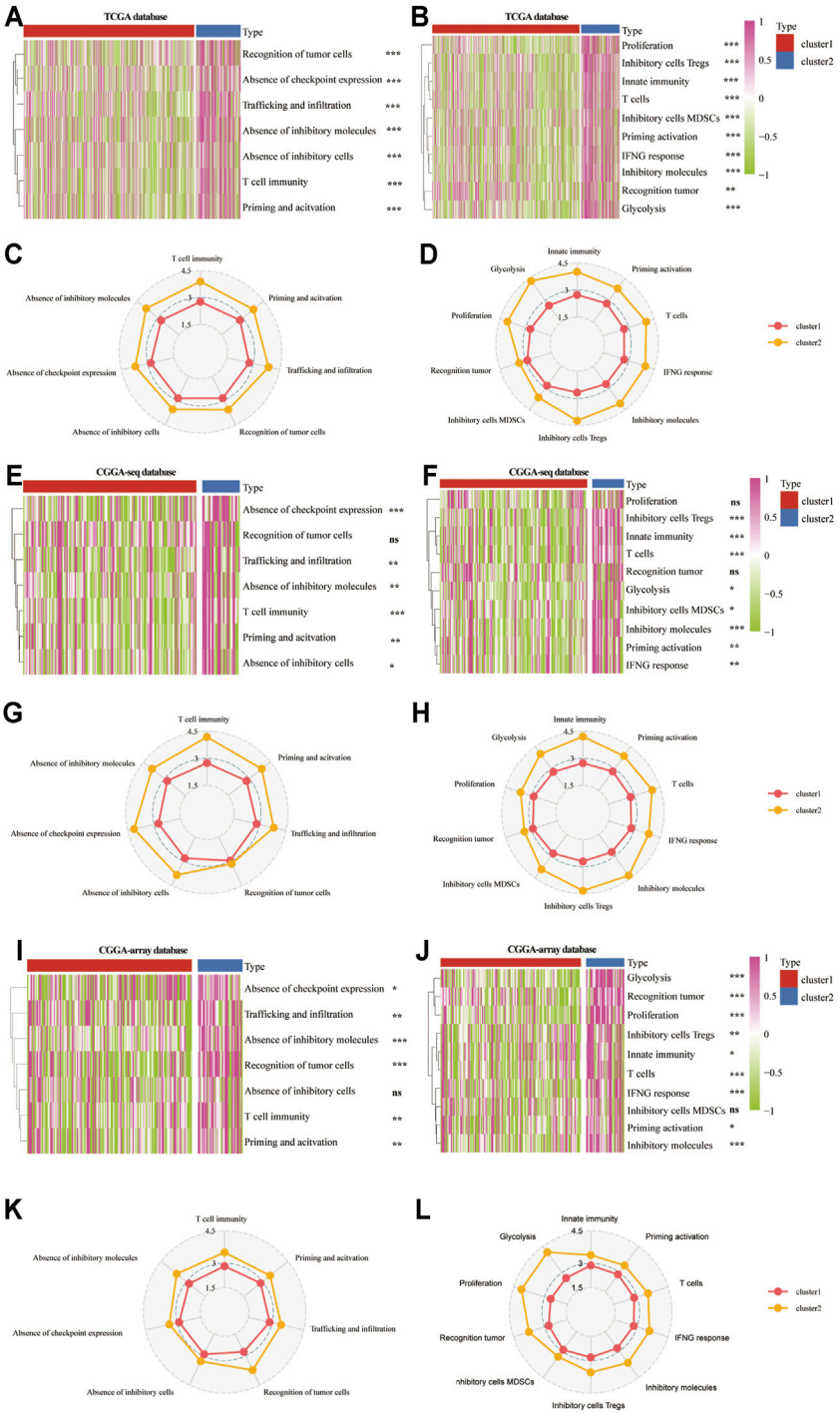

FIGURE 5 | The patient-specific landscape of the LGG tumor microenvironment in cluster 1 and cluster 2 from the training and validation cohorts. Heatmap shows the expression of immune landscapes in two clusters based on 2017 (left) and 2020 (right) immunogram algorithm from the TCGA **(A,B)**, CGGA-sequence **(E,F)**, and CGGA-array **(I,J)** databases. The radar chart shows the expression of the immune landscape in two clusters based on the 2017 (left) and 2020 (right) immunogram algorithm from the TCGA **(C,D)**, CGGA-sequence **(G,H)**, and CGGA-array **(K,L)** databases. *$p < 0.05$, **$p < 0.01$, ***$p < 0.001$, NS, no significant differences.

database showed that cluster 2 exhibited significantly more sensitivity to bortezomib, dasatinib, JW-7-52-1, phenformin, and THZ-2-49 than cluster 1 ($p < 0.001$; **Figures 7A,D**). In addition, the CTRP2 database showed that cluster 2 exhibited significant sensitivity to AZD5582 comparing with cluster 1 ($p < 0.001$; **Figures 7B,E**). In addition, the PRISM database showed that cluster 2 exhibited significant sensitivity to many drugs compared to cluster 1 ($p < 0.001$; **Figures 7C,F**).

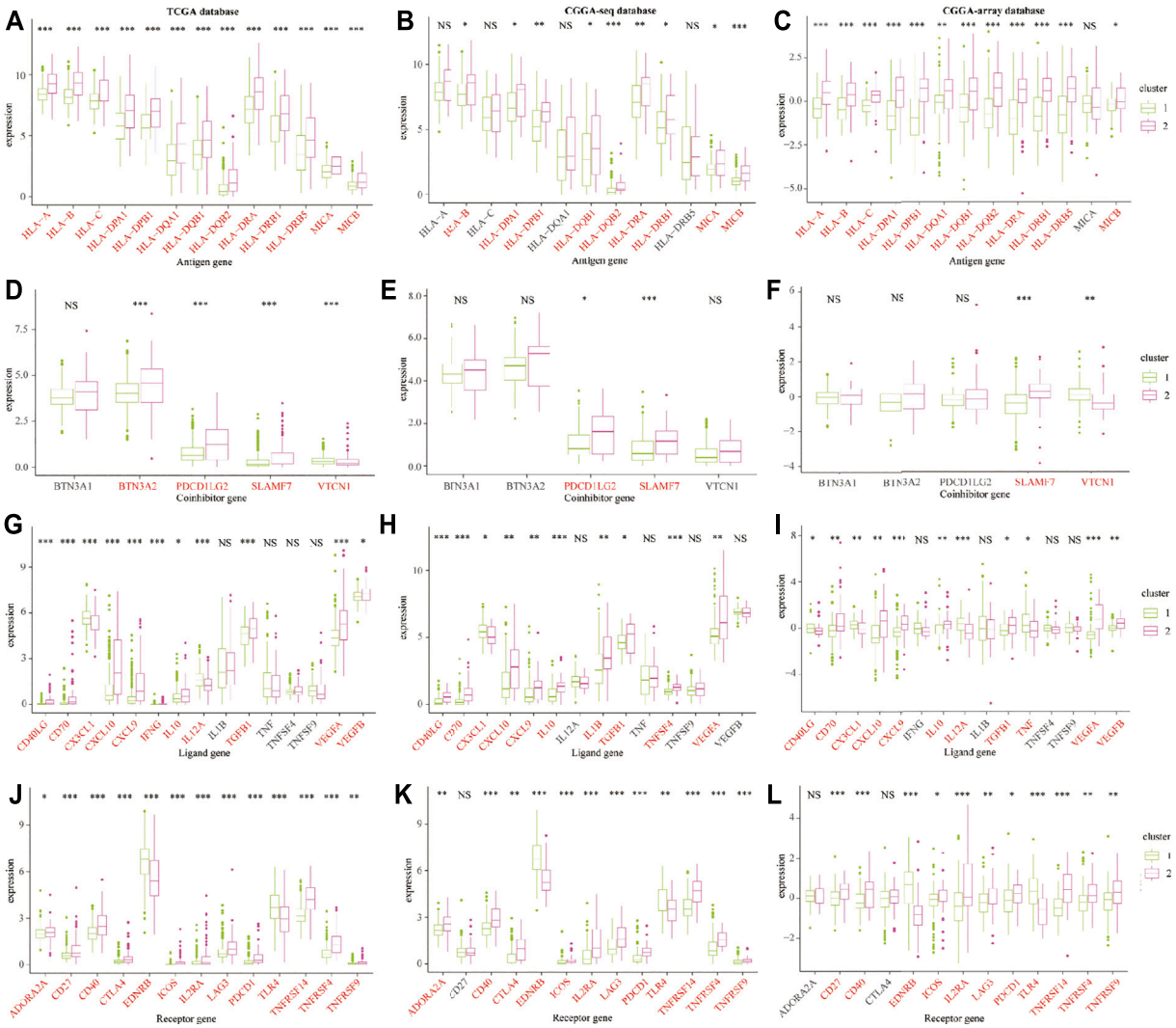

FIGURE 6 | The immune escape-associated gene expression in cluster 1 and cluster 2 from the training and validation cohorts. The expression of antigen genes in cluster 1 and cluster 2 from the TCGA **(A)**, CGGA-sequence **(B)**, and CGGA-array **(C)** databases. The expression of co-inhibitory genes in cluster 1 and cluster 2 from the TCGA **(D)**, CGGA-sequence **(E)**, and CGGA-array **(F)** databases. The expression of ligand genes in cluster 1 and cluster 2 from the TCGA **(G)**, CGGA-sequence **(H)**, and CGGA-array **(I)** databases. The expression of receptor genes in cluster 1 and cluster 2 from the TCGA **(J)**, CGGA-sequence **(K)**, and CGGA-array **(L)** databases. $^{*}p < 0.05$, $^{**}p < 0.01$, $^{***}p < 0.001$, NS, no significant differences.

Main Contributor Identification, Immune Infiltration, and Enrichment Pathway Analysis

Finally, we used three machine-learning methods-LASSO, XGBOOST, and BORUTA algorithms to identify the main contributors of the cluster model from RNF family members (**Figures 8A–E**). The result showed that TRIM8, TRAF5, and DTX2 are the top three contributors. Then, the association of those genes with clinical features was also mapped with heatmap (**Figure 8F**). The heatmap showed that cluster 2 has higher DTX2 and TRAF5 and a lower expression of TRIM8. Meanwhile, the results showed that the overexpressed DTX2 and TRAF5 were associated with IDH WT status, whereas the overexpressed TRIM8 were associated with IDH mutant status.

Patients in the high expression group of TRIM8 have a better outcome than the low expression group ($p < 0.001$; **Figure 9A**). On the contrary, patients in the high expression group of DTX2 ($p < 0.001$; **Figure 9C**) and TRAF5 ($p < 0.001$; **Figure 9E**) have a worse outcome than the low expression group. These data indicated that the high expression of TRIM8 in the LGGs TME might play a protective role, while the increased expression of DTX2 and TRAF5 in the LGG TME may act as a detrimental role. In addition, the CIBERSORT analysis showed that the most positively correlated cell with TRIM8 is monocyte, and the most negatively correlated cell is M1 macrophage (**Figure 9B**). The most positively correlated cell with DTX2 is the M2 macrophage, and the most negatively correlated cell is the memory B cell (**Figure 9D**). The most positively correlated cell with TRAF5 is the M1 macrophage, and the most negatively

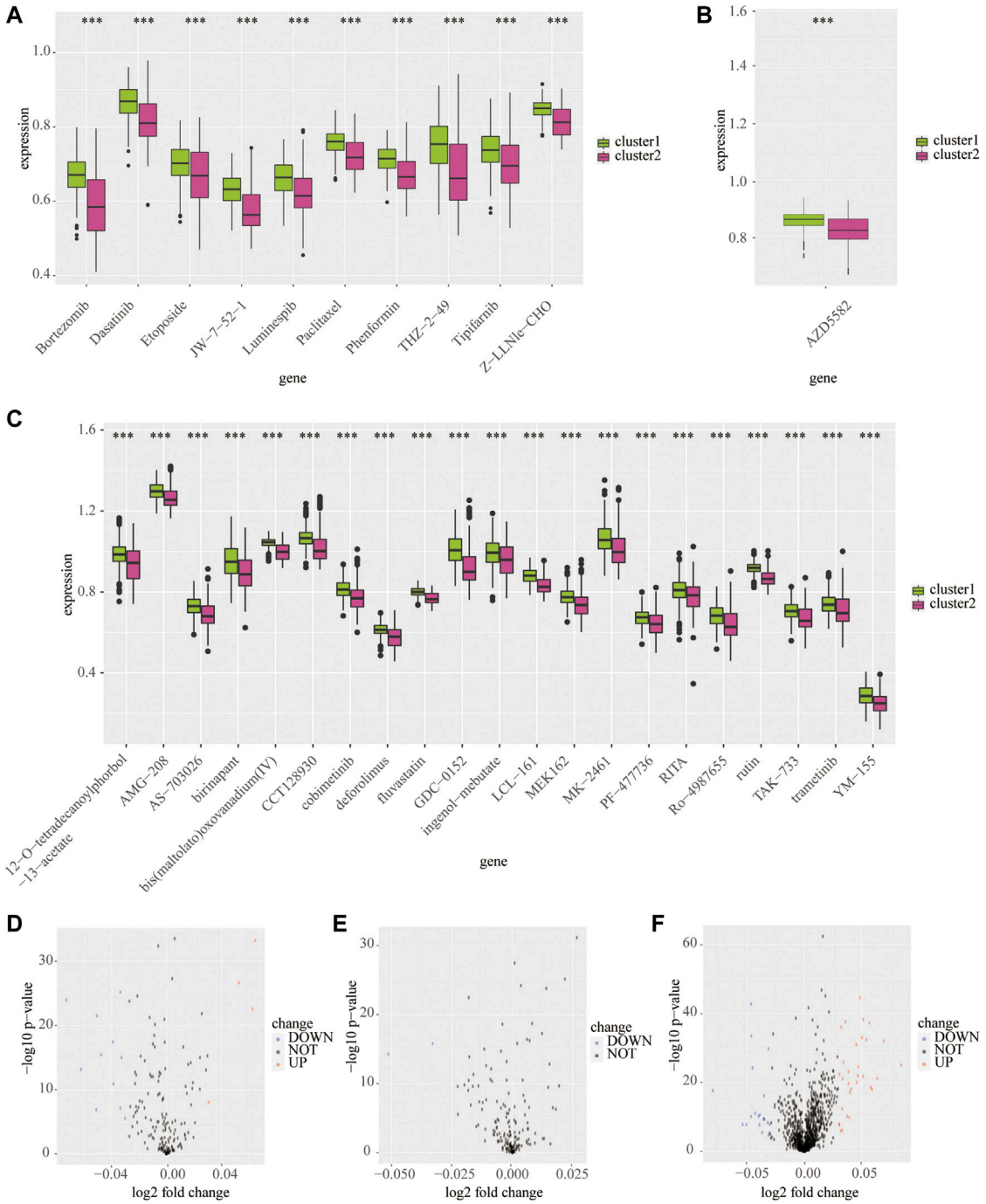

FIGURE 7 | Predicted potential sensitivity compounds based on the cluster model using public databases. The box plot shows sensitivity compounds between cluster 1 and cluster 2 based on the CTRP1 **(A)**, CTRP2 **(B)**, and PRISM **(C)** databases. The volcano plots shows sensitivity compounds between cluster 1 and cluster 2 based on the CTRP1 **(D)**, CTRP2 **(E)**, and PRISM **(F)** databases. ***$p < 0.001$.

correlated cell is the monocyte (**Figure 9F**). These results indicated that the monocyte and memory B cells in the TME might inhibit the LGG progress and contribute to a good outcome. At the same time, the macrophages in the TME may promote the LGG progress and lead to a worse outcome. In addition, we also used xCELL analysis to show the infiltrated immune cells related to the three genes in LGG TME (**Supplementary Figure S6**). Moreover, the enriched signaling pathways related to the three genes were also displayed by GO-based GSVA analysis (**Supplementary Figure S7**).

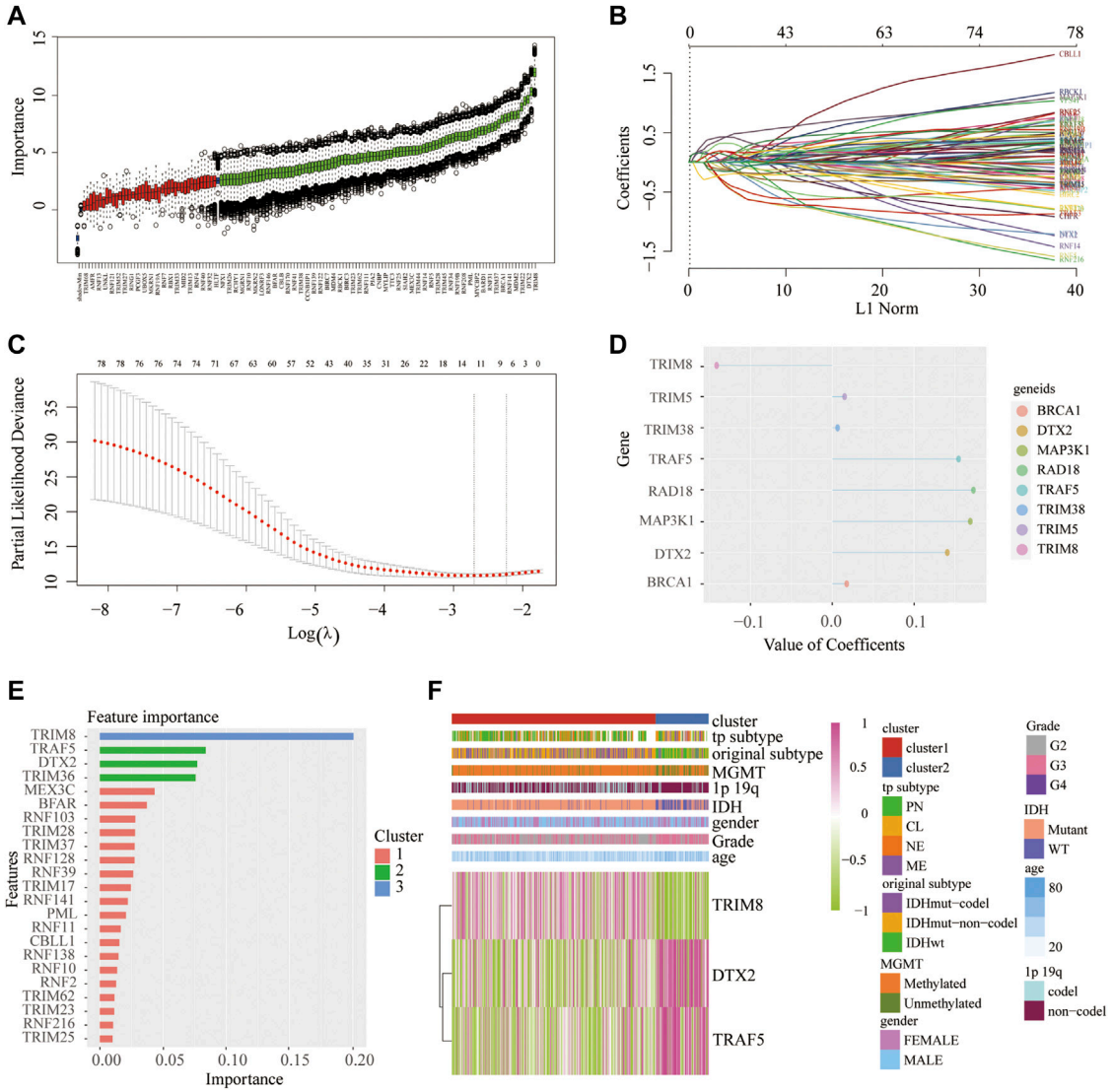

FIGURE 8 | Identification of main contributors of the cluster model from RNF family members. Identify main contributors of the cluster model from RNF family members by Boruta algorithm **(A)**, LASSO regression analysis **(B–D)**, and Xgboost algorithm **(E)**. Heatmap shows the expression of three main contributors in two clusters **(F)**.

DISCUSSION

Low-grade glioma is a group of heterogeneous neoplasms originating from the glial cells nearby neurons and accounts for more than 6% of all primary central nervous system (CNS) tumors in adults (Ostrom et al., 2019). With the rapid development of high-throughput sequencing technology, more and more novel biomarkers related to the prognosis of LGG have been discovered in recent years (Aquilanti et al., 2018; Hsu et al., 2019; Zhang et al., 2020; Zhang et al., 2021c). Recent research focuses on the predictive value, and pathogenic mechanism of RNF proteins have been conducted in several cancer types. For example, the expression level of RNF6 was upregulated in both tumor samples and cell lines of gastric cancer. Furthermore, knockdown of RNF6 significantly increased the cleavage of PARP and promoted cell apoptosis through the SHP-1/STAT3 signaling pathway, which eventually inhibits gastric cancer cell growth (Huang et al., 2018). In another study, RNF121 levels were found decreased in renal cell carcinoma samples than adjacent normal tissues (Zhao et al., 2014). Further research revealed that overexpressed RNF121 inhibited the growth and invasion of human renal cell carcinoma cells by activating NF-κB signaling pathways. However, the relevance between RNF proteins and LGG development remains poorly understood.

In this study, we explore the landscape of RNF proteins in the tumor microenvironment of LGG both from the TCGA and CGGA databases. We established a clustering model based on

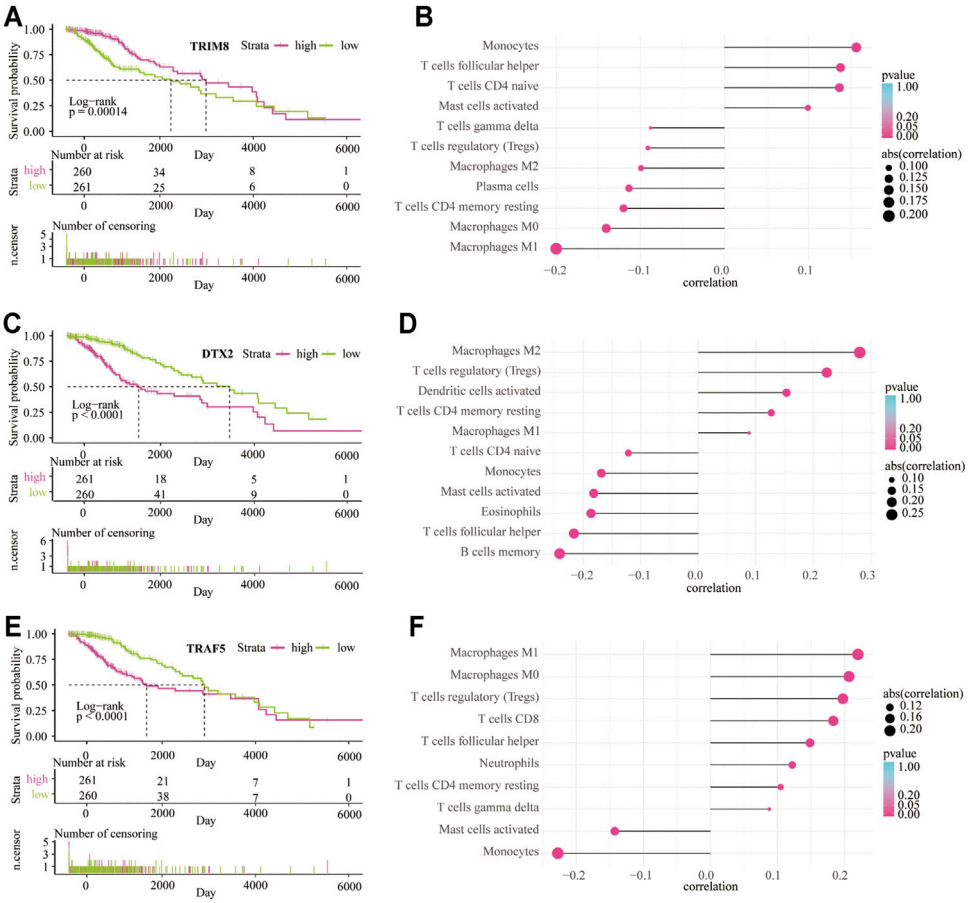

FIGURE 9 | The survival analysis and immune infiltrate are based on the expression of three main contributors. Kaplan–Meier overall survival curve between low-risk and high-risk groups based on the expression of TRIM8 **(A)**, DTX2 **(C)**, and TRAF5 **(E)**. CIBERSORT algorithm shows the relationship between the immune infiltrates and the expression of TRIM8 **(B)**, DTX2 **(D)**, and TRAF5 **(F)**.

the expression of RNF proteins and found a significant difference in prognosis between the two clusters. Molecular mutations, especially IDH enzyme mutation status, were associated with the outcome of LGG and GBM. Generally, IDH-mutant gliomas have a longer overall survival time than the IDH wide-type (WT) counterparts (Olar et al., 2015; Youssef and Miller, 2020). In the current study, we found that the status of IDH was different between the two clusters. This result means that RNF proteins might have a close relationship with the IDH mutant status of LGG. These data provide new insight into the mechanisms underlying the RNF proteins upon LGG progression.

Infiltrated immune cells and stromal cells in the TME influenced the tumor's response to the immune system. For example, upregulated tumor infiltrated $CD3^+$ and $CD8^+$ were associated with longer survival time with an integrated immunosuppressive system in the tumor microenvironment (Kmiecik et al., 2013). Tumor-associated M1-type macrophages are considered to exhibit pro-inflammatory and anti-tumoral effects, while tumor-associated M2-type macrophages are associated with anti-inflammatory and pro-tumoral functions (Madeddu et al., 2018; Macciò et al., 2020). It is well known that myeloid-derived suppressor cells (MDSCs) can act as the primary mediators of immune responses in many cancers and other pathological progress. Tregs can regulate immune suppression of anti-tumor immune response in the tumor microenvironment (Bronte et al., 2016; Li et al., 2020; Pokhrel et al., 2021). DCS identified and processed tumor-associated antigens in the tumor microenvironment and promoted anti-tumor immunity by modulating other immune cells' functions (Wculek et al., 2020). In this study, the GO and KEGG analysis indicated that the expression levels of RNF proteins were significantly accompanied by immune cells infiltration and checkpoint expression related signaling pathways in LGG, among which T cell and mast cell activation, DCs antigen processing and differentiation, Th17 cell differentiation, absence of checkpoint expression, inhibitory Tregs and MDSCs were most significant. In addition, the RNF proteins expression was significantly associated with tumor purity, immune score, and stromal score in the LGG TME based on the ESTIMATE algorithm.

Various immune cells in the LGG TME were related to the expression of RNF proteins, including macrophages, monocytes, plasma cells, CD4 memory T cells, Tregs, neutrophils, and mast cells. Meanwhile, large amounts of immune checkpoints were found to be different expressed between the two clusters. Taken together, we proposed that RNF proteins may be involved in the regulation of immune response in the LGG TME by recruiting immune cells and regulating the expression of immune checkpoints.

Furthermore, we identified three main contributors among RNF proteins: TRIM8, DTX2, and TRAF5. Results showed that the upregulated expression of DTX2 and TRAF5 were associated with IDH WT status and a poor outcome in LGG. In contrast, the elevated expression of TRIM8 was associated with IDH mutant status and a better prognosis in LGG. Furthermore, CIBERSORT and xCELL algorithms demonstrated that these three genes are essential in recruiting immune cells, such as monocytes, macrophages, T cells follicular helper, CD4 naïve T cells, Tregs, CD8 T cells.

Until right now, effective drugs for IDH WT LGG treatment are still limited. Finally, we discovered various small molecular drugs that exhibited sensitivity to cluster 2, such as bortezomib, dasatinib and phenformin, which have been proved to inhibit the growth of human glioma cells in previous studies (Jantas et al., 2018; Wang et al., 2018; Miklja et al., 2020). At the same time, we also discovered many new drugs sensitive to IDH WT glioma that has not been reported before, including AMG−208, JW−7−52−1, THZ−2−49, AZD5582, and so on. These small molecular drugs might help to improve the treatment effect of IDH WT LGG in the future.

To sum up, we established a clustering model based on the expression of RNF proteins, which can be applied to predict the outcome of LGG patients. In addition, we explored the relationship between the immune aspects in the LGG tumor microenvironment and RNF proteins. Moreover, we found three main contributors among RNF proteins that were closely associated with LGG progress. Importantly, we explored lots of sensitive drugs, which might help to improve the treatment effect of patients with LGG in the future. However, there are some limitations to this study. First of all, only public data was used for analysis in this study, which has not been verified with our data. Meanwhile, the fundamental function of RNF genes in regulating immune cells infiltration and checkpoints expression in the LGG TME was not explored through *in vivo* and *in vitro* studies. Secondly, we identified three key markers, but these three genes' role in LGG is still far from discovered in this paper. The specific mechanisms of RNF genes involved in LGG immunity need further exploration.

DATA AVAILABILITY STATEMENT

The original contributions presented in the study are included in the article/**Supplementary Material**, further inquiries can be directed to the corresponding authors.

AUTHOR CONTRIBUTIONS

Writing -Original Draft, Methodology, Validation, Visualization: JZ and ZW. Data Curation, Validation: HZ, ZD, and XL. Investigation: SL, FL, XZ, and ZL. Conceptualization, Methodology, Supervision, Project Administration and Funding Acquisition: KY and QC.

FUNDING

This study is supported by the National Nature Science Foundation of China (NO.82073893, NO. 81873635, NO. 81703622); the China Postdoctoral Science Foundation (NO. 2018M633002); the Natural Science Foundation of Hunan Province (NO. 2018JJ3838, NO. 2018SK2101, NO. 2019JJ50948); the Hunan Provincial Health and Health Committee Foundation of China (C2019186); Xiangya Hospital Central South University postdoctoral foundation; and the Fundamental Research Funds for the Central Universities of Central South University (No. 2021zzts1027).

ACKNOWLEDGMENTS

We acknowledge TCGA, CGGA and GEO database for providing their platforms and contributors for uploading their meaningful datasets.

SUPPLEMENTARY MATERIAL

The Supplementary Material for this article can be found online at: https://www.frontiersin.org/articles/10.3389/fcell.2021.754873/full#supplementary-material

Supplementary Figure S1 | Clustering analysis and predictive ability of the risk signature in the four datasets. Cluster analysis to obtain the best number of clusters in the TCGA **(A)**. Kaplan—Meier overall survival curve between two clusters from the Rembrandt dataset **(B)**. The AUC of the cluster model in the TCGA **(C)**, CGGA-sequence **(D)**, CGGA-array **(E)**, and Rembrandt **(F)** databases.

Supplementary Figure S2 | Enrichment of signaling pathways in cluster 2 from the training and validation cohorts. Gene set enrichment analysis in cluster 2 based on G.O. database from the TCGA **(A)**, CGGA-sequence **(B)**, and CGGA-array **(C)** databases. Gene set enrichment analysis in cluster 2 based on the KEGG database from the TCGA **(D)**, CGGA-sequence **(E)**, and CGGA-array **(F)** databases.

Supplementary Figure S3 | Immune infiltrates in cluster 1 and cluster 2 from the training and validation cohorts. Heatmap shows infiltrated immune cells in two clusters based on the CIBERSORT algorithm from the TCGA **(A)**, CGGA-sequence **(B)**, and CGG-aarray **(C)** databases. In addition, the heatmap shows infiltrated immune cells in two clusters based on the xCELL algorithm from the TCGA **(D)**, CGGA-sequence **(E)**, and CGGA-array **(F)** databases.

Supplementary Figure S4 | Immune landscapes in cluster 1 and cluster 2 from the training and validation cohorts. The tumor purity, estimate score, immune score, stromal score in cluster 1 and cluster 2 from the TCGA **(A)**, CGGA-sequence **(B)**, and CGGA-array **(C)** databases. $^{*}p < 0.05$, $^{**}p < 0.01$, $^{***}p < 0.001$.

Supplementary Figure S5 | Levels of immune escape associated genes in cluster 1 and cluster 2 from the training and validation cohorts. The expression of cell adhesion genes in cluster 1 and cluster 2 from the TCGA **(A)**, CGGA-sequence **(B)**,

and CGGA-array **(C)** databases. The expression of costimulatory genes in cluster 1 and cluster 2 from the TCGA **(D)**, CGGA-sequence **(E)**, and CGGA-array **(F)** databases. The expression of other genes in cluster 1 and cluster 2 from the TCGA **(G)**, CGGA-sequence **(H)**, and CGGA-array **(I)** databases. *$p < 0.05$, **$p < 0.01$, ***$p < 0.001$, NS: no significant differences.

Supplementary Figure S6 | Infiltrated immune cells are based on the expression of three main contributors. XCELL algorithm shows the relationship between the immune infiltrates and the expression of TRIM8 **(A)**, DTX2 **(B)**, and TRAF5 **(C)**.

Supplementary Figure S7 | Enrichment of signaling pathways based on the expression of three main contributors. GO enrichment analysis based on GSVA analysis of TRIM8 **(A)**, DTX2 **(B)**, and TRAF5 **(C)**.

Supplementary Table S1 | Total RNF family gene list from HGNC database.

Supplementary Table S2 | The clinicopathological characteristics of four public databases.

Supplementary Table S3 | Top 50 predicted drugs from the Cellminer database.

REFERENCES

Alexander, B. M., and Cloughesy, T. F. (2017). Adult Glioblastoma. *Jco* 35, 2402–2409. doi:10.1200/jco.2017.73.0119

Amal, H., Gong, G., Gjoneska, E., Lewis, S. M., Wishnok, J. S., Tsai, L.-H., et al. (2019). S-nitrosylation of E3 Ubiquitin-Protein Ligase RNF213 Alters Non-canonical Wnt/Ca+2 Signaling in the P301S Mouse Model of Tauopathy. *Transl Psychiatry* 9, 44. doi:10.1038/s41398-019-0388-7

An, Y., Wang, Q., Zhang, L., Sun, F., Zhang, G., Dong, H., et al. (2020). OSlgg: An Online Prognostic Biomarker Analysis Tool for Low-Grade Glioma. *Front. Oncol.* 10, 1097. doi:10.3389/fonc.2020.01097

Andrews, M. C., Duong, C. P. M., Gopalakrishnan, V., Iebba, V., Chen, W. S., Derosa, L., et al. (2021). Gut Microbiota Signatures Are Associated with Toxicity to Combined CTLA-4 and PD-1 Blockade. *Nat. Med.* 27, 1432. doi:10.1038/s41591-021-01406-6

Aquilanti, E., Miller, J., Santagata, S., Cahill, D. P., and Brastianos, P. K. (2018). Updates in Prognostic Markers for Gliomas. *Neuro Oncol.* 20, vii17–vii26. doi:10.1093/neuonc/noy158

Aran, D., Hu, Z., and Butte, A. J. (2017). xCell: Digitally Portraying the Tissue Cellular Heterogeneity Landscape. *Genome Biol.* 18, 220. doi:10.1186/s13059-017-1349-1

Aslan, K., Turco, V., Blobner, J., Sonner, J. K., Liuzzi, A. R., Núñez, N. G., et al. (2020). Heterogeneity of Response to Immune Checkpoint Blockade in Hypermutated Experimental Gliomas. *Nat. Commun.* 11, 931. doi:10.1038/s41467-020-14642-0

Baghban, R., Roshangar, L., Jahanban-Esfahlan, R., Seidi, K., Ebrahimi-Kalan, A., Jaymand, M., et al. (2020). Tumor Microenvironment Complexity and Therapeutic Implications at a Glance. *Cell Commun Signal* 18, 59. doi:10.1186/s12964-020-0530-4

Bowman, R. L., Wang, Q., Carro, A., Verhaak, R. G. W., and Squatrito, M. (2017). GlioVis Data portal for Visualization and Analysis of Brain Tumor Expression Datasets. *Neuonc* 19, 139–141. doi:10.1093/neuonc/now247

Bronte, V., Brandau, S., Chen, S.-H., Colombo, M. P., Frey, A. B., Greten, T. F., et al. (2016). Recommendations for Myeloid-Derived Suppressor Cell Nomenclature and Characterization Standards. *Nat. Commun.* 7, 12150. doi:10.1038/ncomms12150

Campbell, S. J., Edwards, R. A., Leung, C. C. Y., Neculai, D., Hodge, C. D., Dhe-Paganon, S., et al. (2012). Molecular Insights into the Function of RING Finger (RNF)-containing Proteins hRNF8 and hRNF168 in Ubc13/Mms2-dependent Ubiquitylation. *J. Biol. Chem.* 287, 23900–23910. doi:10.1074/jbc.m112.359653

Cham, K. L., Soga, T., and Parhar, I. S. (2018). Expression of RING Finger Protein 38 in Serotonergic Neurons in the Brain of Nile Tilapia, *Oreochromis niloticus*. *Front. Neuroanat.* 12, 109. doi:10.3389/fnana.2018.00109

Cham, K. L., Soga, T., and Parhar, I. S. (2017). RING Finger Protein 38 Is a Neuronal Protein in the Brain of Nile Tilapia, *Oreochromis niloticus*. *Front. Neuroanat.* 11, 72. doi:10.3389/fnana.2017.00072

De Vleeschouwer, S., and Bergers, G. (2017). *Glioblastoma: To Target the Tumor Cell or the Microenvironment*. Editor S. De Vleeschouwer (Brisbane: Glioblastoma).

Fang, S., Liang, J., Qian, T., Wang, Y., Liu, X., Fan, X., et al. (2017). Anatomic Location of Tumor Predicts the Accuracy of Motor Function Localization in Diffuse Lower-Grade Gliomas Involving the Hand Knob Area. *AJNR Am. J. Neuroradiol* 38, 1990–1997. doi:10.3174/ajnr.a5342

Funakoshi, Y., Hata, N., Kuga, D., Hatae, R., Sangatsuda, Y., Fujioka, Y., et al. (2021). Pediatric Glioma: An Update of Diagnosis, Biology, and Treatment. *Cancers (Basel)* 13, 758. doi:10.3390/cancers13040758

Galli, F., Aguilera, J. V., Palermo, B., Markovic, S. N., Nisticò, P., and Signore, A. (2020). Relevance of Immune Cell and Tumor Microenvironment Imaging in the New Era of Immunotherapy. *J. Exp. Clin. Cancer Res.* 39, 89. doi:10.1186/s13046-020-01586-y

Geng, R., Tan, X., Wu, J., Pan, Z., Yi, M., Shi, W., et al. (2017). RNF183 Promotes Proliferation and Metastasis of Colorectal Cancer Cells via Activation of NF-κB-IL-8 Axis. *Cell Death Dis* 8, e2994. doi:10.1038/cddis.2017.400

Giraldo, N. A., Sanchez-Salas, R., Peske, J. D., Vano, Y., Becht, E., Petitprez, F., et al. (2019). The Clinical Role of the TME in Solid Cancer. *Br. J. Cancer* 120, 45–53. doi:10.1038/s41416-018-0327-z

Gusev, Y., Bhuvaneshwar, K., Song, L., Zenklusen, J.-C., Fine, H., and Madhavan, S. (2018). The REMBRANDT Study, A Large Collection of Genomic Data from Brain Cancer Patients. *Sci. Data* 5, 180158. doi:10.1038/sdata.2018.158

Hodges, T. R., Ott, M., Xiu, J., Gatalica, Z., Swensen, J., Zhou, S., et al. (2017). Mutational Burden, Immune Checkpoint Expression, and Mismatch Repair in Glioma: Implications for Immune Checkpoint Immunotherapy. *Neuro Oncol.* 19, 1047–1057. doi:10.1093/neuonc/nox026

Hsu, J. B.-K., Chang, T.-H., Lee, G. A., Lee, T.-Y., and Chen, C.-Y. (2019). Identification of Potential Biomarkers Related to Glioma Survival by Gene Expression Profile Analysis. *BMC Med. Genomics* 11, 34. doi:10.1186/s12920-019-0479-6

Huang, Z., Cai, Y., Yang, C., Chen, Z., Sun, H., Xu, Y., et al. (2018). Knockdown of RNF6 Inhibits Gastric Cancer Cell Growth by Suppressing STAT3 Signaling. *Ott* 11, 6579–6587. doi:10.2147/ott.s174846

Jantas, D., Grygier, B., Gołda, S., Chwastek, J., Zatorska, J., and Tertil, M. (2018). An Endogenous and Ectopic Expression of Metabotropic Glutamate Receptor 8 (mGluR8) Inhibits Proliferation and Increases Chemosensitivity of Human Neuroblastoma and Glioma Cells. *Cancer Lett.* 432, 1–16. doi:10.1016/j.canlet.2018.06.004

Karasaki, T., Nagayama, K., Kuwano, H., Nitadori, J.-i., Sato, M., Anraku, M., et al. (2017). An Immunogram for the Cancer-Immunity Cycle: Towards Personalized Immunotherapy of Lung Cancer. *J. Thorac. Oncol.* 12, 791–803. doi:10.1016/j.jtho.2017.01.005

Kmiecik, J., Poli, A., Brons, N. H. C., Waha, A., Eide, G. E., Enger, P. Ø., et al. (2013). Elevated CD3+ and CD8+ Tumor-Infiltrating Immune Cells Correlate with Prolonged Survival in Glioblastoma Patients Despite Integrated Immunosuppressive Mechanisms in the Tumor Microenvironment and at the Systemic Level. *J. Neuroimmunology* 264, 71–83. doi:10.1016/j.jneuroim.2013.08.013

Kobayashi, Y., Kushihara, Y., Saito, N., Yamaguchi, S., and Kakimi, K. (2020). A Novel Scoring Method Based on RNA-Seq Immunograms Describing Individual Cancer-immunity Interactions. *Cancer Sci.* 111, 4031–4040. doi:10.1111/cas.14621

Kuhns, M., Trifunović, D., Huber, H., and Müller, V. (2020). The Rnf Complex Is a Na+ Coupled Respiratory Enzyme in a Fermenting Bacterium, Thermotoga Maritima. *Commun. Biol.* 3, 431. doi:10.1038/s42003-020-01158-y

Li, C., Jiang, P., Wei, S., Xu, X., and Wang, J. (2020). Regulatory T Cells in Tumor Microenvironment: New Mechanisms, Potential Therapeutic Strategies and Future Prospects. *Mol. Cancer* 19, 116. doi:10.1186/s12943-020-01234-1

Li, M. O., Wolf, N., Raulet, D. H., Akkari, L., Pittet, M. J., Rodriguez, P. C., et al. (2021). Innate Immune Cells in the Tumor Microenvironment. *Cancer Cell* 39, 725–729. doi:10.1016/j.ccell.2021.05.016

Liu, F., Huang, J., Liu, X., Cheng, Q., Luo, C., and Liu, Z. (2020). CTLA-4 Correlates with Immune and Clinical Characteristics of Glioma. *Cancer Cel Int* 20, 7. doi:10.1186/s12935-019-1085-6

Liu, L., Wong, C. C., Gong, B., and Yu, J. (2018). Functional Significance and Therapeutic Implication of Ring-type E3 Ligases in Colorectal Cancer. *Oncogene* 37, 148–159. doi:10.1038/onc.2017.313

Liu, Z.-y., Feng, S.-s., Zhang, Y.-h., Zhang, L.-y., Xu, S.-c., Li, J., et al. (2021). Competing Risk Model to Determine the Prognostic Factors and Treatment

Strategies for Elderly Patients with Glioblastoma. *Sci. Rep.* 11, 9321. doi:10.1038/s41598-021-88820-5

Macciò, A., Gramignano, G., Cherchi, M. C., Tanca, L., Melis, L., and Madeddu, C. (2020). Role of M1-Polarized Tumor-Associated Macrophages in the Prognosis of Advanced Ovarian Cancer Patients. *Sci. Rep.* 10, 6096. doi:10.1038/s41598-020-63276-1

Madeddu, C., Gramignano, G., Kotsonis, P., Coghe, F., Atzeni, V., Scartozzi, M., et al. (2018). Microenvironmental M1 Tumor-Associated Macrophage Polarization Influences Cancer-Related Anemia in Advanced Ovarian Cancer: Key Role of Interleukin-6. *Haematologica* 103, e388–e391. doi:10.3324/haematol.2018.191551

McKinnon, C., Nandhabalan, M., Murray, S. A., and Plaha, P. (2021). Glioblastoma: Clinical Presentation, Diagnosis, and Management. *BMJ* 374, n1560. doi:10.1136/bmj.n1560

Miklja, Z., Yadav, V. N., Cartaxo, R. T., Siada, R., Thomas, C. C., Cummings, J. R., et al. (2020). Everolimus Improves the Efficacy of Dasatinib in PDGFRα-Driven Glioma. *J. Clin. Invest.* 130, 5313–5325. doi:10.1172/jci133310

Miller, A. M., Shah, R. H., Pentsova, E. I., Pourmaleki, M., Briggs, S., Distefano, N., et al. (2019). Tracking Tumour Evolution in Glioma Through Liquid Biopsies of Cerebrospinal Fluid. *Nature* 565, 654–658. doi:10.1038/s41586-019-0882-3

Molinaro, A. M., Taylor, J. W., Wiencke, J. K., and Wrensch, M. R. (2019). Genetic and Molecular Epidemiology of Adult Diffuse Glioma. *Nat. Rev. Neurol.* 15, 405–417. doi:10.1038/s41582-019-0220-2

Newman, A. M., Steen, C. B., Liu, C. L., Gentles, A. J., Chaudhuri, A. A., Scherer, F., et al. (2019). Determining Cell Type Abundance and Expression from Bulk Tissues with Digital Cytometry. *Nat. Biotechnol.* 37, 773–782. doi:10.1038/s41587-019-0114-2

Olar, A., Wani, K. M., Alfaro-Munoz, K. D., Heathcock, L. E., van Thuijl, H. F., Gilbert, M. R., et al. (2015). IDH Mutation Status and Role of WHO Grade and Mitotic Index in Overall Survival in Grade II-III Diffuse Gliomas. *Acta Neuropathol.* 129, 585–596. doi:10.1007/s00401-015-1398-z

Ostrom, Q. T., Cioffi, G., Gittleman, H., Patil, N., Waite, K., Kruchko, C., et al. (2019). CBTRUS Statistical Report: Primary Brain and Other Central Nervous System Tumors Diagnosed in the United States in 2012-2016. *Neuro Oncol.* 21, v1–v100. doi:10.1093/neuonc/noz150

Peng, R., Zhang, P.-F., Yang, X., Wei, C.-Y., Huang, X.-Y., Cai, J.-B., et al. (2019). Overexpression of RNF38 Facilitates TGF-β Signaling by Ubiquitinating and Degrading AHNAK in Hepatocellular Carcinoma. *J. Exp. Clin. Cancer Res.* 38, 113. doi:10.1186/s13046-019-1113-3

Pokhrel, R. H., Acharya, S., Ahn, J.-H., Gu, Y., Pandit, M., Kim, J.-O., et al. (2021). AMPK Promotes Antitumor Immunity by Downregulating PD-1 in Regulatory T Cells via the HMGCR/p38 Signaling Pathway. *Mol. Cancer* 20, 133. doi:10.1186/s12943-021-01420-9

Reifenberger, G., Wirsching, H.-G., Knobbe-Thomsen, C. B., and Weller, M. (2017). Advances in the Molecular Genetics of Gliomas - Implications for Classification and Therapy. *Nat. Rev. Clin. Oncol.* 14, 434–452. doi:10.1038/nrclinonc.2016.204

Simon, T., Jackson, E., and Giamas, G. (2020). Breaking Through the Glioblastoma Micro-environment via Extracellular Vesicles. *Oncogene* 39, 4477–4490. doi:10.1038/s41388-020-1308-2

Tan, A. C., Ashley, D. M., López, G. Y., Malinzak, M., Friedman, H. S., and Khasraw, M. (2020). Management of Glioblastoma: State of the Art and Future Directions. *CA A. Cancer J. Clin.* 70, 299–312. doi:10.3322/caac.21613

Wang, L., Wang, X., Zhao, Y., Niu, W., Ma, G., Yin, W., et al. (2016). E3 Ubiquitin Ligase RNF126 Regulates the Progression of Tongue Cancer. *Cancer Med.* 5, 2043–2047. doi:10.1002/cam4.771

Wang, X., Guo, G., Guan, H., Yu, Y., Lu, J., and Yu, J. (2019). Challenges and Potential of PD-1/pd-L1 Checkpoint Blockade Immunotherapy for Glioblastoma. *J. Exp. Clin. Cancer Res.* 38, 87. doi:10.1186/s13046-019-1085-3

Wang, Y., Meng, Y., Zhang, S., Wu, H., Yang, D., Nie, C., et al. (2018). Phenformin and Metformin Inhibit Growth and Migration of LN229 Glioma Cells In Vitro and In Vivo. *Ott* 11, 6039–6048. doi:10.2147/ott.s168981

Wculek, S. K., Cueto, F. J., Mujal, A. M., Melero, I., Krummel, M. F., and Sancho, D. (2020). Dendritic Cells in Cancer Immunology and Immunotherapy. *Nat. Rev. Immunol.* 20, 7–24. doi:10.1038/s41577-019-0210-z

Wei, C.-Y., Zhu, M.-X., Yang, Y.-W., Zhang, P.-F., Yang, X., Peng, R., et al. (2019). Downregulation of RNF128 Activates Wnt/β-Catenin Signaling to Induce Cellular EMT and Stemness via CD44 and CTTN Ubiquitination in Melanoma. *J. Hematol. Oncol.* 12, 21. doi:10.1186/s13045-019-0711-z

Wilkerson, M. D., and Hayes, D. N. (2010). ConsensusClusterPlus: A Class Discovery Tool with Confidence Assessments and Item Tracking. *Bioinformatics* 26, 1572–1573. doi:10.1093/bioinformatics/btq170

Yoshihara, K., Shahmoradgoli, M., Martínez, E., Vegesna, R., Kim, H., Torres-Garcia, W., et al. (2013). Inferring Tumour Purity and Stromal and Immune Cell Admixture from Expression Data. *Nat. Commun.* 4, 2612. doi:10.1038/ncomms3612

Youssef, G., and Miller, J. J. (2020). Lower Grade Gliomas. *Curr. Neurol. Neurosci. Rep.* 20, 21. doi:10.1007/s11910-020-01040-8

Zhang, H., Chen, Z., Wang, Z., Dai, Z., Hu, Z., Zhang, X., et al. (2021). Correlation between APOBEC3B Expression and Clinical Characterization in Lower-Grade Gliomas. *Front. Oncol.* 11, 625838. doi:10.3389/fonc.2021.625838

Zhang, H., Dai, Z., Wu, W., Wang, Z., Zhang, N., Zhang, L., et al. (2021). Regulatory Mechanisms of Immune Checkpoints PD-L1 and CTLA-4 in Cancer. *J. Exp. Clin. Cancer Res.* 40, 184. doi:10.1186/s13046-021-01987-7

Zhang, H., He, J., Dai, Z., Wang, Z., Liang, X., He, F., et al. (2021). PDIA5 Is Correlated with Immune Infiltration and Predicts Poor Prognosis in Gliomas. *Front. Immunol.* 12, 628966. doi:10.3389/fimmu.2021.628966

Zhang, H., Wang, R., Yu, Y., Liu, J., Luo, T., and Fan, F. (2019). Glioblastoma Treatment Modalities Besides Surgery. *J. Cancer* 10, 4793–4806. doi:10.7150/jca.32475

Zhang, H., Zhou, Y., Cheng, Q., Dai, Z., Wang, Z., Liu, F., et al. (2020). PDIA3 Correlates with Clinical Malignant Features and Immune Signature in Human Gliomas. *Aging* 12, 15392–15413. doi:10.18632/aging.103601

Zhao, Y., Hongdu, B., Ma, D., and Chen, Y. (2014). Really Interesting New Gene finger Protein 121 Is a Novel Golgi-Localized Membrane Protein that Regulates Apoptosis. *Acta Biochim. Biophys. Sin (Shanghai)* 46, 668–674. doi:10.1093/abbs/gmu047

Zhao, Z., Meng, F., Wang, W., Wang, Z., Zhang, C., and Jiang, T. (2017). Comprehensive RNA-Seq Transcriptomic Profiling in the Malignant Progression of Gliomas. *Sci. Data* 4, 170024. doi:10.1038/sdata.2017.24

Conflict of Interest: The authors declare that the research was conducted in the absence of any commercial or financial relationships that could be construed as a potential conflict of interest.

Publisher's Note: All claims expressed in this article are solely those of the authors and do not necessarily represent those of their affiliated organizations, or those of the publisher, the editors and the reviewers. Any product that may be evaluated in this article, or claim that may be made by its manufacturer, is not guaranteed or endorsed by the publisher.

frontiers in Cell and Developmental Biology

ORIGINAL RESEARCH
published: 17 February 2022
doi: 10.3389/fcell.2022.740822

CMTM Family Genes Affect Prognosis and Modulate Immunocytes Infiltration in Grade II/III Glioma Patients by Influencing the Tumor Immune Landscape and Activating Associated Immunosuppressing Pathways

Zeyu Wang[1,2†], Jingwei Zhang[1,2†], Hao Zhang[1], Ziyu Dai[1], Xisong Liang[1], Shuwang Li[1], Renjun Peng[1], Xun Zhang[1], Fangkun Liu[1], Zhixiong Liu[1,2,3], Kui Yang[1] and Quan Cheng[1,2,3]**

[1]Department of Neurosurgery, Xiangya Hospital, Central South University, Changsha, China, [2]National Clinical Research Center for Geriatric Disorders, Changsha, China, [3]Clinical Diagnosis and Therapy Center for Glioma of Xiangya Hospital, Central South University, Changsha, China

Lower-grade glioma (LGG) is one of the most common primary tumor types in adults. The chemokine-like factor (CKLF)-like Marvel transmembrane domain-containing (CMTM) family is widely expressed in the immune system and can modulate tumor progression. However, the role of the CMTM family in LGG remains unknown. A total of 508 LGG patients from The Cancer Genome Atlas (TCGA) database were used as a training cohort, and 155 LGG patients from the Chinese Glioma Genome Atlas (CGGA) array database, 142 LGG patients from the CGGA RNA-sequencing database, and 168 LGG patients from the GSE108474 database were used as the validation cohorts. Patients were subdivided into two groups using consensus clustering. The ENET algorithm was applied to build a scoring model based on the cluster model. Finally, ESTIMATE, CIBERSORT, and xCell algorithms were performed to define the tumor immune landscape. The expression levels of the CMTM family genes were associated with glioma grades and isocitrate dehydrogenase (IDH) status. Patients in cluster 2 and the high-risk score group exhibited a poor prognosis and were enriched with higher grade, wild-type IDH (IDH-WT), 1p19q non-codeletion, MGMT promoter unmethylation, and IDH-WT subtype. Patients in cluster 1 and low-risk score group were associated with high tumor purity and reduced immune cell infiltration. Enrichment pathways analysis indicated that several essential pathways involved in tumor progression were associated with the expression of CMTM family genes. Importantly, PD-1, PD-L1, and PD-L2 expression levels were increased in cluster 2 and high-risk groups. Therefore, the CMTM family contributes to LGG progression through modulating tumor immune landscape.

Keywords: CMTM, lower-grade glioma, micro-environment, immune infiltration, prognosis

OPEN ACCESS

Edited by:
Mariane Tami Amano, Hospital Sirio Libanes, Brazil

Reviewed by:
Erico Tosoni Costa, Hospital Sirio Libanes, Brazil
Clarissa Ribeiro Reily Rocha, Federal University of São Paulo, Brazil

***Correspondence:**
Quan Cheng
chengquan@csu.edu.cn
Kui Yang
kui.yang@csu.edu.cn

†These authors have contributed equally to this work

Specialty section:
This article was submitted to Molecular and Cellular Pathology, a section of the journal Frontiers in Cell and Developmental Biology

Received: *13 July 2021*
Accepted: *03 January 2022*
Published: *17 February 2022*

Citation:
Wang Z, Zhang J, Zhang H, Dai Z, Liang X, Li S, Peng R, Zhang X, Liu F, Liu Z, Yang K and Cheng Q (2022) CMTM Family Genes Affect Prognosis and Modulate Immunocytes Infiltration in Grade II/III Glioma Patients by Influencing the Tumor Immune Landscape and Activating Associated Immunosuppressing Pathways. Front. Cell Dev. Biol. 10:740822. doi: 10.3389/fcell.2022.740822

INTRODUCTION

Gliomas originate from the neuroglial stem or progenitor cells and is the most common primary malignant brain tumor (Weller et al., 2015). Gliomas are classified into two categories according to the degree of malignancy, including glioblastoma (GBM) and lower-grade glioma (LGG). In addition, 2016 WHO classification of the central nervous system (CNS) tumors classified gliomas into astrocytic tumors, oligodendrogliomas, and not otherwise specified (NOS) not only based on histology but also molecular features, including isocitrate dehydrogenase (IDH) mutational and 1p/19q codeletion status (Wen and Huse, 2016; Wen and Huse, 2017). LGG has a relatively long growth period in adults. Therefore, surgical management, radiotherapy, and chemotherapy are the main treatments for LGG (Kleihues and Ohgaki, 1999; Taylor et al., 2019). Although people with LGG have a better prognosis than other aggressive tumor types in the CNS, the median overall survival (OS) of LGG is still far from satisfactory (Sidaway, 2020; Aiman and Rayi, 2021).

In recent years, numerous studies have focused on the immune infiltration of glioma. A close relationship has been shown between tumor-infiltrating immune cells and improved clinical outcomes in LGG (Bacolod et al., 2016; Wu et al., 2019a; Zhang et al., 2021a). The tumor microenvironment (TME) is the environment around a tumor that includes the surrounding blood vessels, infiltrated immune cells, tumor cells, cytokines, and the extracellular matrix (ECM) (Giraldo et al., 2019). TME is a dynamic and complex ecosystem that mediates tumor immunity, tumorigenesis, tumor growth, and migration. Microglia, macrophages, regulatory T cells (Tregs), and natural killer cells (NK) are the primary immune cells in the TME (Binnewies et al., 2018). These immune cells interact with tumor cells and play an essential role in modulating multiple immune processes in the TME. Importantly, they mediate the progress of tumor growth and metastasis. For example, $CD8^+$ T cells and $CD4^+$ T-helper 1 (Th1)-oriented T cells can directly kill tumor cells in an antigen-specific manner by secreting cytotoxic cytokines (Lim et al., 2020). Conversely, other immune cells, such as the M2 type of macrophages, express C-C motif chemokine receptor 2 (CCR2, receptor of CCL2), and which is an irreplaceable factor that promotes tumor metastasis. Inhibition of the CCL2-CCR2 pathway can effectively reduce tumor metastasis and eventually prolong the survival of mice (Qian et al., 2011). Therefore, TME-specific immunotherapy may provide promising targets in the treatment of LGG in the future.

The CKLF-like Marvel transmembrane domain-containing (CMTM) gene, which contains nine members (CMTM1-8 and CKLF), is a novel gene family reported in 2001 (Han et al., 2001). CMTM members are widely expressed in the immune system and are involved in several pathological processes (Delic et al., 2015). A recent study found that abnormal expression of CMTMs was implicated in the process of tumor growth and metastasis (Wu et al., 2019b; Wu et al., 2020). However, the specific role and mechanism remain elusive. Herein, we used clinical, mRNA sequencing, and microarray data of LGG patients from The Cancer Genome Atlas (TCGA), and Chinese Glioma Genome Atlas (CGGA) databases, and Gene Expression Omnibus (GEO) database (Bao et al., 2014; Fang et al., 2017; Zhao et al., 2017) to evaluate the predictive value of the CMTM family in LGG and elucidate the relationship between the CMTM family genes and immune infiltration in LGG TME.

MATERIALS AND METHODS

Datasets

The clinical and expression data of LGG patients were collected from TCGA database (http://cancergenome.nih.gov/) and CGGA database (http://www.cgga.org.cn). Data from TCGA (n = 508) were used as the training cohort and CGGA array data (CGGA301, mRNA microarray database, n = 155), CGGA RNA-sequencing (RNA-seq) data (CGGA325, mRNA sequencing database, n = 142), and GSE108474 data (n = 168) were used as validation cohorts. The LGG subtype was predicted by the Gliovis data portal (Bowman et al., 2017).

Consensus Clustering Analysis and Machine Learning

Consensus clustering analysis based on CMTMs was performed with the R package "ConsensusClusterPlus" (Wilkerson and Hayes, 2010). For the validation cohort, machine learning, support vector machine, was used to reproduce the clustering model with the R package "e1071". The heatmap and Sankey diagram were generated to illustrate the potential relationship between LGG clinical features and the clustering model.

Construction of the Risk Model

Differentially expressed genes (DEGs) between two clusters were identified with the R package 'limma'. Univariate Cox regression analysis and the ENET algorithm were further employed to filter out prognosis-associated genes. Finally, the risk was calculated based on principal component analysis (PCA) and hazard ratio (HR):

$$\text{Risk} = \text{Gene}(\text{HR} > 1)^*(\text{PC1} + \text{PC2}) - \text{Gene}(\text{HR} < 1)^*(\text{PC1} + \text{PC2}) \quad (2)$$

Biofunction Prediction

Gene ontology (GO) and Kyoto Encyclopedia of genes and genomes (KEGG) based on gene set variation analysis (GSVA) and gene set enrichment analysis (GSEA) were used to explore differential biofunction prediction activation between cluster 1 and cluster 2 samples, as well as samples in the high-risk and low-risk groups. Pathways with p value <0.05 are considered as statistically significant.

Tumor Immune Landscape

The landscape of immune cell infiltration was predicted with the R package 'ESTIMATE' (Yoshihara et al., 2013), CIBSERSORT algorithm (Newman et al., 2019), and xCell algorithm (Aran et al., 2017) as previously described.

Univariate and Multivariate Cox Regression Analysis

Univariate and multiple variate Cox regression analysis were performed with R package "survival", and results were presented with R package "forestplot".

Real-Time Quantitative PCR

Tumor tissue and normal tissue which was adherent to the tumor were collected during the surgery. One milliliter Trizol was added to 100 mg tissue, and tissue was grinded by a grinder (Servicebio, Wuhan, China). Then, RNA extraction was followed by the standard protocol. cDNA library was constructed following protocol of HiScript II Q RT SuperMix for qPCR (+g DNA wiper) (Vazyme, Nanjing, China). Steps of real-time quantitative PCR were set as previously reported (Wang et al., 2021), and primers are listed as below:

β-actin
Forward: ACCCTGAAGTACCCCATCGAG
Reverse: AGCACAGCCTGGATAGCAAC
CMTM3
Forward: AAGTACTCGGATGGGGCTTC
Reverse: TCTTCTGTCTTGTGGGCTGT
CMTM6
Forward: TTTCCACACATGACAGGACTTC
Reverse: GGCTTCAGCCCTAGTGGTAT
CMTM7
Forward: CCAAGAGTTACAACCAGAGCG
Reverse: CATCTGTGGACTGGGTTACAC
CMTM8
Forward: AACAATGACCTACACCAGGATTC
Reverse: AAGGCACTGCCGTTAAAGC
CKLF
Forward: CACAAGCCCCTGAACCATAT
Reverse: GCTTCCGGTAAATAAGGGCC

Statistical Analysis

The Wilcox test was used to compare the difference between two groups, and analysis of variance (ANOVA) was used to compare multiple groups. In addition, the Kaplan-Meier log-rank test was used for survival analyses. All analyses were performed with R (version 3.6.1), and GraphPad Prism (version 8.0.1).

RESULTS

Relationship Between CMTM Family Genes and Tumor Grade and IDH Status

To study the role of CMTM family genes in LGG, LGG data were selected from TCGA, CGGA array (CGGA301), and CGGA RNA-seq (CGGA325) databases (**Figure 1**). The description of samples from the TCGA, CGGA-seq, CGGA-array, and GSE108474 databases were shown in **Supplementary Table S1**. The relationship between the expression levels of each CMTM family gene and grade from the TCGA database (training cohort) was explored. Results showed that the expression level of CMTM1, CMTM3, CMTM6, CMTM7, CMTM8, and CKLF was elevated in high-grade gliomas (grade III; $p < 0.01$; **Figure 2A**). Conversely, the expression level of CMTM4 and CMTM5 was higher in LGG (grade II; $p < 0.01$; **Figure 2A**). Similarly, the expression levels of CMTM1, CMTM3, CMTM6, CMTM8, and CKLF were increased in grade III in the validation cohort (CGGA301; $p < 0.05$; **Figure 2B**). IDH mutational status is another critical marker that is related to patient prognosis. The result indicated that the levels of CMTM3, CMTM6, CMTM7, CMTM8, and CKLF were much higher in IDH-WT than in IDH-mutated gliomas in the TCGA database ($p < 0.001$; **Figure 2D**). Data from the CGGA301 database showed that only CMTM8 was upregulated in IDH-WT compared with the IDH mutational group ($p < 0.01$; **Figure 2E**), which could be due to fewer samples in CGGA301 than TCGA database. The expression level of CMTM5 was lower in IDH-WT gliomas in both TCGA and CGGA301 databases. Moreover, data from CGGA325 showed that whereas the mRNA levels of CMTM2, CMTM3, CMTM6, CMTM7, and CKLF were significantly elevated in both grade III and IDH-mutant groups, CMTM4 and CMTM5 expression levels were decreased in both grade III and IDH WT groups (all $p < 0.05$; **Figures 2C,F**). Overall, these results indicated that high levels of CMTM3, CMTM6, CMTM7, and CKLF might predicat a worse prognosis, while the high levels of CMTM4 and CMTM5 may be associated with favorable outcomes in LGG.

The expression of CMTM3, CMTM6, CMTM7, CMTM8, and CKLF were further verified on our own samples (**Supplementary Figure S1**). As illustrated, the expression of CMTM3, CMTM6, CMTM7, CMTM8, and CKLF in Grade II and III gliomas showed similar tendency as that in TCGA and CGGA databases.

Relationship Between Clusters of CMTM Family Genes and Glioma Prognosis

Unsupervised consensus clustering was used to classify patients into cluster 1 and cluster 2 in the training and validation cohorts. First, machine learning was used to reproduce the clustering model in the TCGA cohort (**Figure 3A**). Then, Kaplan-Meier analysis was used to reveal the outcome in the two clusters. Result in the TCGA database showed that patients in cluster 1 had a better prognosis compared with those in cluster 2 for OS, progression-free interval (PFI), and disease-specific survival (DSS) ($p < 0.0001$; **Figures 3B–D**). In the three validation cohorts, patients in cluster 1 also showed a better outcome for OS ($p < 0.01$; **Figures 3E,F**; **Supplementary Figure S5A**). The correlation between CMTM family expression, the cluster model, and corresponding clinical features were also mapped in TCGA (**Figure 3G**), CGGA-array database (**Figure 3H**), and CGGA RNA-sequence database (**Figure 3I**). Furthermore, the Sankey diagram from the TCGA database showed that numerous factors, including higher grade (grade III), IDH-WT, 1p/19q non-codeletion, and O6-methylguanine-DNA methyltransferase (MGMT) unmethylation, were associated with poor prognoses in cluster 2 (**Figure 3J**), which were verified in CGGA-array (**Figure 3K**) and CGGA RNA-seq (**Figure 3L**) databases. These results indicated that the expression of CMTM family genes was associated with patient prognosis in LGG.

Relationship Between CMTM Family Genes and Immune Cell Infiltration in LGG Microenvironment

To further verify the relationship between the expression of CMTM family genes and immune cell infiltrates in the LGG

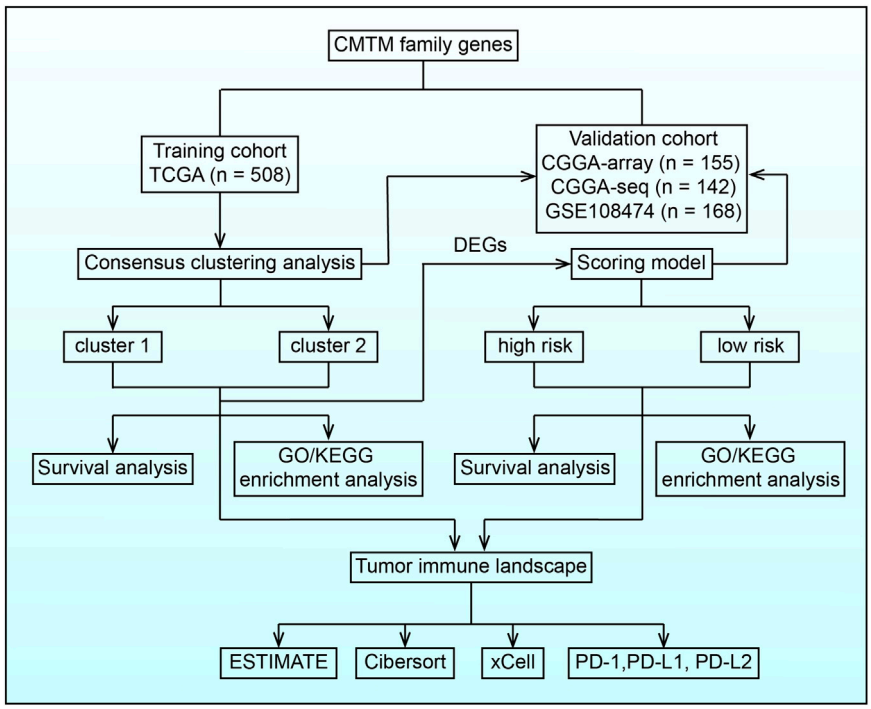

FIGURE 1 | Flow chart illustrating the proposed role of CMTM family genes in LGG.

microenvironment, the purity, ESTIMATE score, stromal score, and immune score were calculated in the two clusters in training and validation cohorts. ESTIMATE, stromal, and immune scores were higher in cluster 2 ($p < 0.001$), whereas tumor purity was lower ($p < 0.001$) in cluster 2 in training and validation cohorts (**Supplementary Figure S2**). Moreover, results from the xCell algorithm showed different immune cell infiltrates in cluster 1 and cluster 2 in training and validation cohorts (**Figures 4A–C**). The expression levels of dendritic cells (DCs), B cells, common lymphoid progenitor cells (CLPs), fibroblasts, macrophages (M1 and M2), mast cells, Th2 cells, and monocytes were significantly higher in cluster 2 in the three cohorts ($p < 0.05$). Contrarily, the expression levels of natural killer T (NKT) cells, and regulatory T cells (Tregs) were higher ($p < 0.05$) in cluster 1. Results from the CIBERSORT algorithm indicated that the levels of M1 and M2 macrophages were significantly higher in cluster 2 ($p < 0.01$; **Supplementary Figure S3**). However, the expression of CD4 naive T cells was higher in cluster 1 ($p < 0.001$). Collectively, these results revealed that many immune infiltrating cells were closely associated with the poor prognosis of patients in cluster 2.

Functional Enrichment Analysis in Clusters 1 and 2

GO/KEGG enrichment analysis based on GSEA and GSVA analyses were used to identify differential pathways activation between cluster 1 and cluster 2 samples. KEGG-based GSEA pathway analysis in TCGA and CGGA-array databases indicated that pathways associated with p53 signaling, programmed death-ligand 1 (PD-L1) expression, programmed cell death protein 1 (PD-1) checkpoint, and Th17 cell differentiation were highly enriched (**Figures 5A,B**) in cluster 2 samples. GO-based GSEA pathway analysis in TCGA and CGGA-array databases indicated that pathways associated with L-glutamate importation and glutamate secretion were highly enriched (**Figures 5C,D**) in cluster 1 samples while immune related pathways like negative regulation of mast cell activation were enriched in cluster 2 samples. Data from the CGGA RNA-seq cohort also supported those difference (**Supplementary Figures S4A,B**). Moreover, KEGG-based GSVA analysis, visualized by heatmap, showed different pathways in cluster 1 and cluster 2. In the TCGA database, pathways associated with negative regulation of mast cell activation, major histocompatibility complex (MHC) class II receptor activation, and protein complex were enriched in cluster 2. In addition, pathways associated with negative regulation of T cell migration, adverse effects of Toll-like receptor 4 (TLR4) signaling, positive regulation of glutamate secretion, glutamate biosynthetic process, and glutamate catabolic process were enriched in cluster 1 ($p < 0.05$; **Figure 5E**). In the CGGA-array dataset, the glutamate biosynthetic and catabolic process pathways were enriched in cluster 1 ($p < 0.05$). However, pathways associated with $CD8^+$ αβ T cell activation, antigen progress and presentation via MHC class I B cell, negative regulation of mast cells degranulation, and positive regulation of antigen progress and expression were enriched in cluster 2 ($p < 0.05$; **Figure 5F**). Similar results were also found in the CGGA RNA-seq dataset (**Supplementary Figure S4C**).

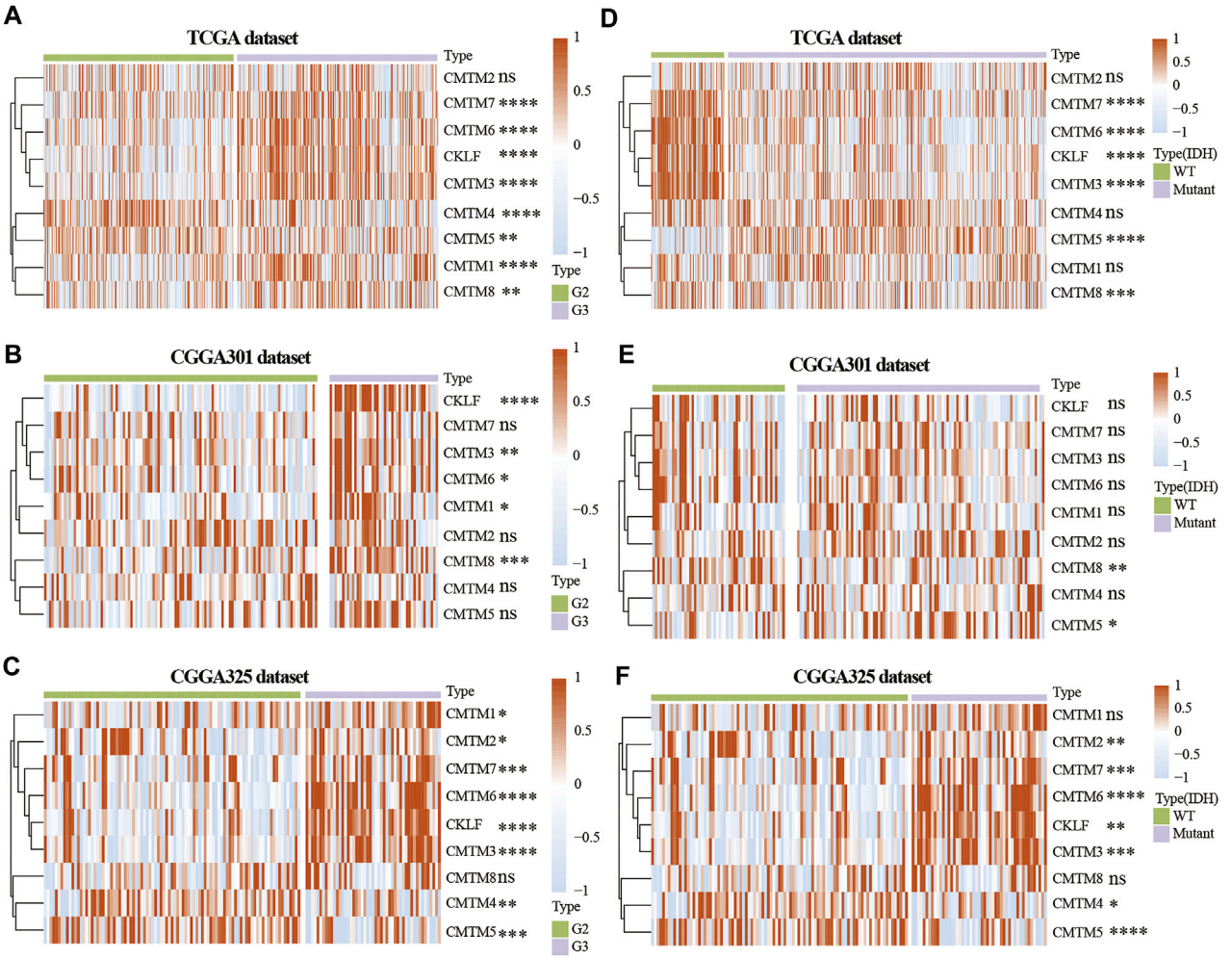

FIGURE 2 | Expression of CMTM family genes in LGG in training and validation cohorts. Expression of CMTM family genes in different grades in the TCGA **(A)**, CGGA301 **(B)**, and CGGA325 **(C)** datasets. Expression of CMTM family genes in different IDH subgroups in the TCGA **(D)**, CGGA301 **(E)**, and CGGA325 **(F)** datasets. The Wilcox test was used to compare the difference between two groups (ns: no significant difference, $*p < 0.05$, $**p < 0.01$, $***p < 0.001$, and $****p < 0.0001$).

Establishment of the Scoring Model Based on DEGs in the Training Cohort

Next, the scoring models (low-risk and high-risk groups) were constructed based on the DEGs from clusters 1 and 2 based on TCGA database (**Figure 6A**). Then, a total of 21 genes were identified as being independently associated with prognosis in the TCGA database by exploring the univariate Cox regression analysis and the ENET algorithm subsequently (**Figure 6B**). The risk score was calculated based on those genes. Univariate and multivariate Cox regression analysis in TCGA, CGGA RNA-seq, CGGA-array, and GSE108474 databases were shown in **Supplementary Table S2**. Kaplan-Meier analysis was used to evaluate survival differences between the two risk groups. It was found that patients in the low-risk group had a better prognosis compared with those in the high-risk group for OS, PFI, and DSS in the TCGA database ($p < 0.0001$; **Figures 6C–E**). In addition, patients in the low-risk group had a better outcome for OS in the three validation cohorts ($p < 0.0001$; **Figures 6F,G**; **Supplementary Figure S5B**).

From the heatmap of the scoring models, high levels of CMTM3, CMTM6, CMTM7, and CKLF were associated with increased risk scores in TCGA and the two CGGA databases (**Figures 6H–J**; **Supplementary Figure S5C**). However, high levels of CMTM4 and CMTM5 were associated with a low-risk score. Glioma subtype, 1p/19q co-deletion, grade II gliomas, IDH mutational status, and MGMT methylation were associated with lower-risk scores in TCGA and the two CGGA databases ($p < 0.001$; **Supplementary Figure S6**). Furthermore, most samples in cluster 2 belonged to the high-risk group. The Sankey diagram showed that samples from cluster 1, lower grade (grade II), IDH mutational status, 1p/19q co-deletion, and MGMT methylation were associated with favorable prognoses in the low-risk group (**Figures 6K–M**).

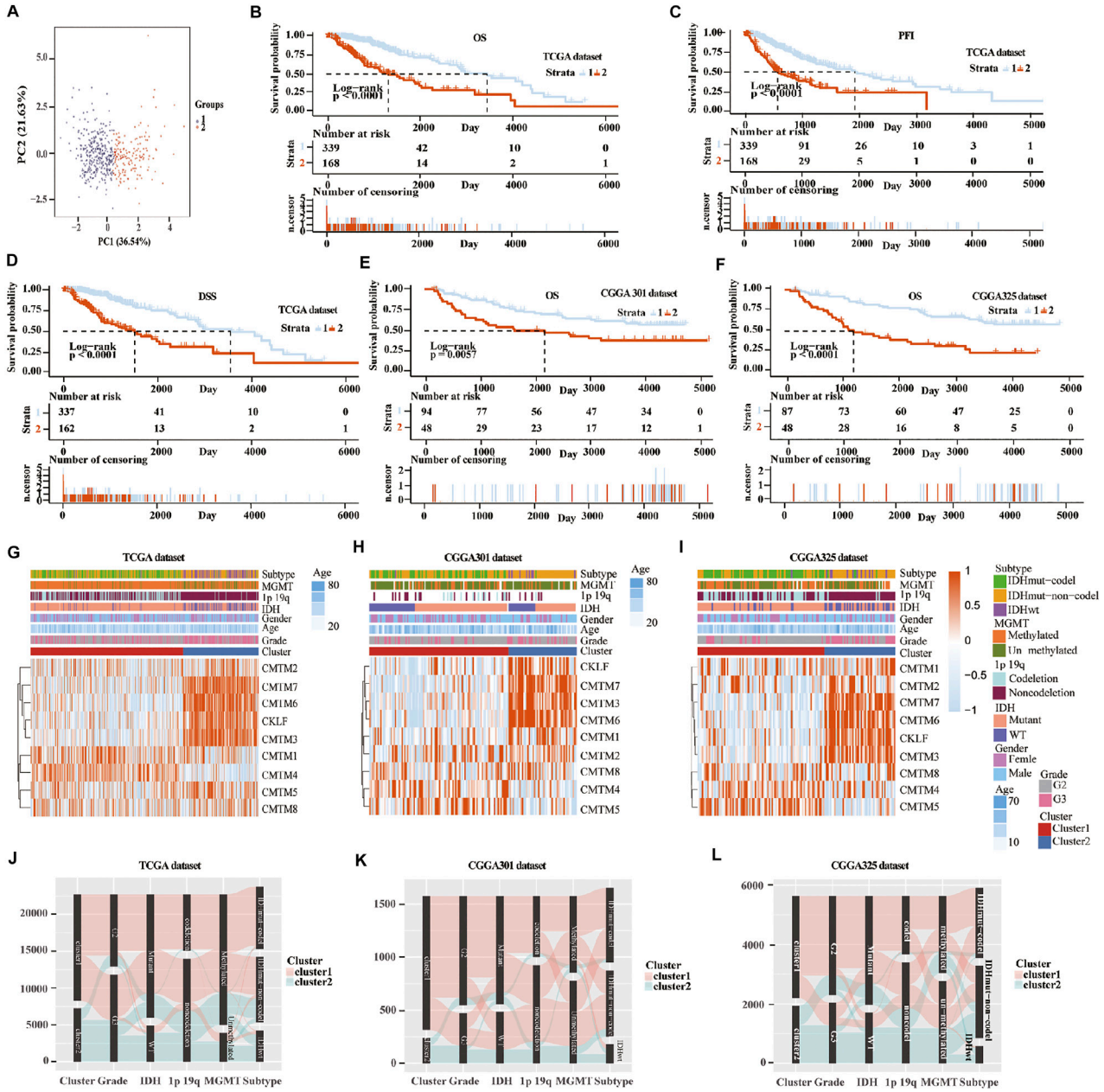

FIGURE 3 | Consensus clustering of samples into cluster 1 and cluster 2 in training and validation cohorts. **(A)** Principal component analysis (PCA) was applied to explore any clustering behavior of the samples in the TCGA database. Kaplan-Meier analysis of patients in cluster 1 and cluster 2 from the TCGA database for OS **(B)**, PFI **(C)**, and DSS **(D)**. (E) Kaplan-Meier analysis of patients in cluster 1 and cluster 2 from CGGA301 database for OS. **(F)** Kaplan-Meier analysis of patients in cluster 1 and cluster 2 from CGGA325 database for OS. Heatmap of different gliomas features and expression of CMTM in cluster 1 and cluster 2 from TCGA **(G)**, CGGA301 **(H)**, and CGGA325 **(I)** databases. Sankey diagram of different expression patterns of glioma features in cluster 1 and cluster 2 from TCGA **(J)**, CGGA301 **(K)**, and CGGA325 **(L)** databases, analyzed by the log-rank test.

Functional Enrichment Analysis in the Low- and High-Risk Group in the Training and Validation Cohorts

KEGG-based GSEA pathway analysis indicated p53 signaling, PD-L1 expression, PD-1 checkpoint, Th cell differentiation (Th1, Th2, and Th17), and TNF signaling were enriched in high-risk score group from the TCGA database (**Figure 7A**). GO-based GSEA pathway analysis indicated that cell-cell adhesion mediated by integrin, nature like cell proliferation, negative regulation of mast cell activation, restriction of antigen processing and presentation, and T cell activation pathways were also enriched in high-risk score group from the TCGA database (**Figure 7B**). Furthermore, KEGG-based GSVA analysis

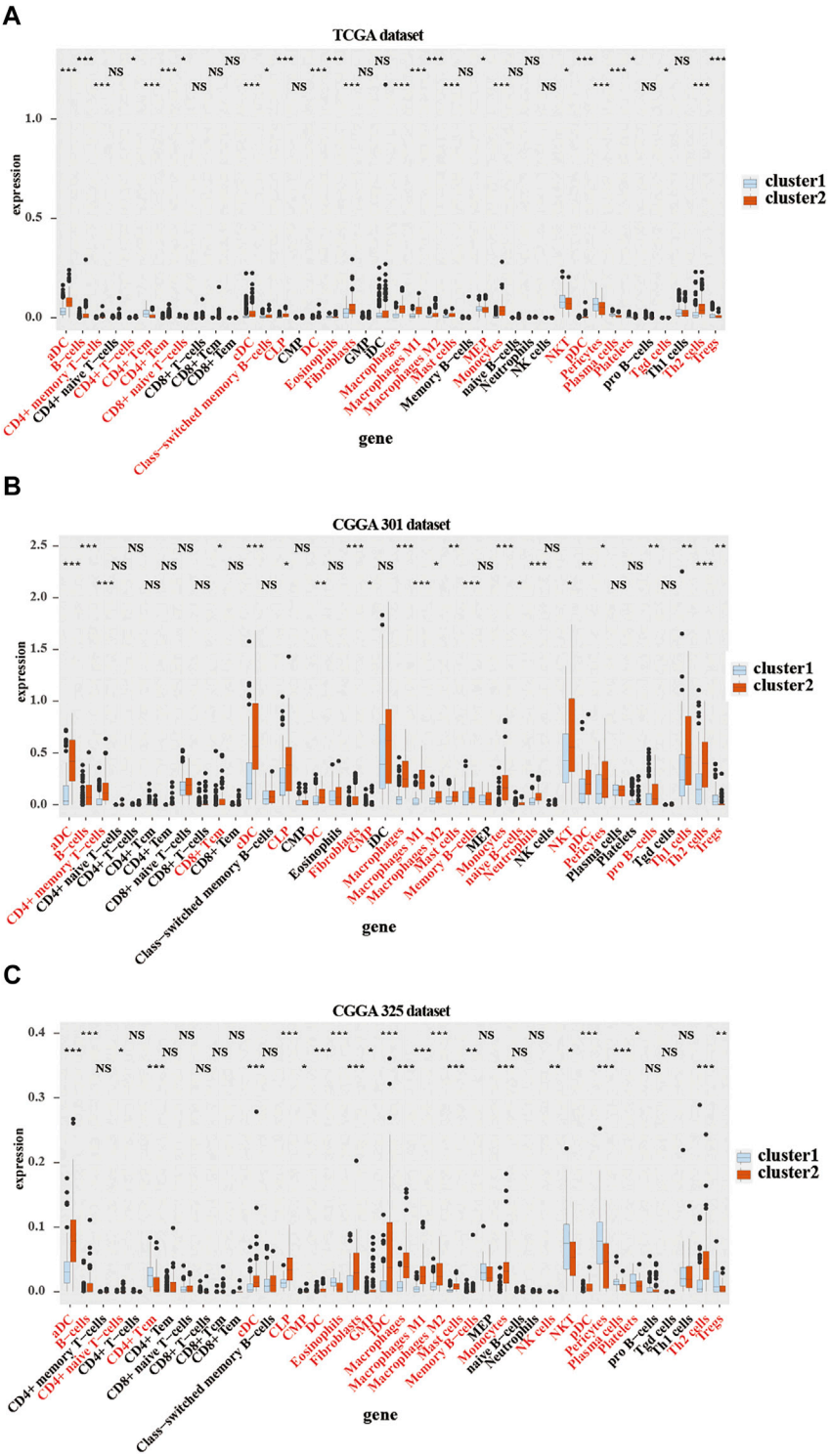

FIGURE 4 | Immune cells infiltration in cluster 1 and cluster 2 from TCGA and CGGA301 databases. xCELL algorithm of infiltrated immune cells in cluster 1 and cluster 2 from TCGA **(A)**, CGGA301 **(B)**, and CGGA301 **(C)** databases. The Wilcox test was used to compare the difference between the two groups (ns: no significant differences, $*p < 0.05$, $**p < 0.01$, and $***p < 0.001$).

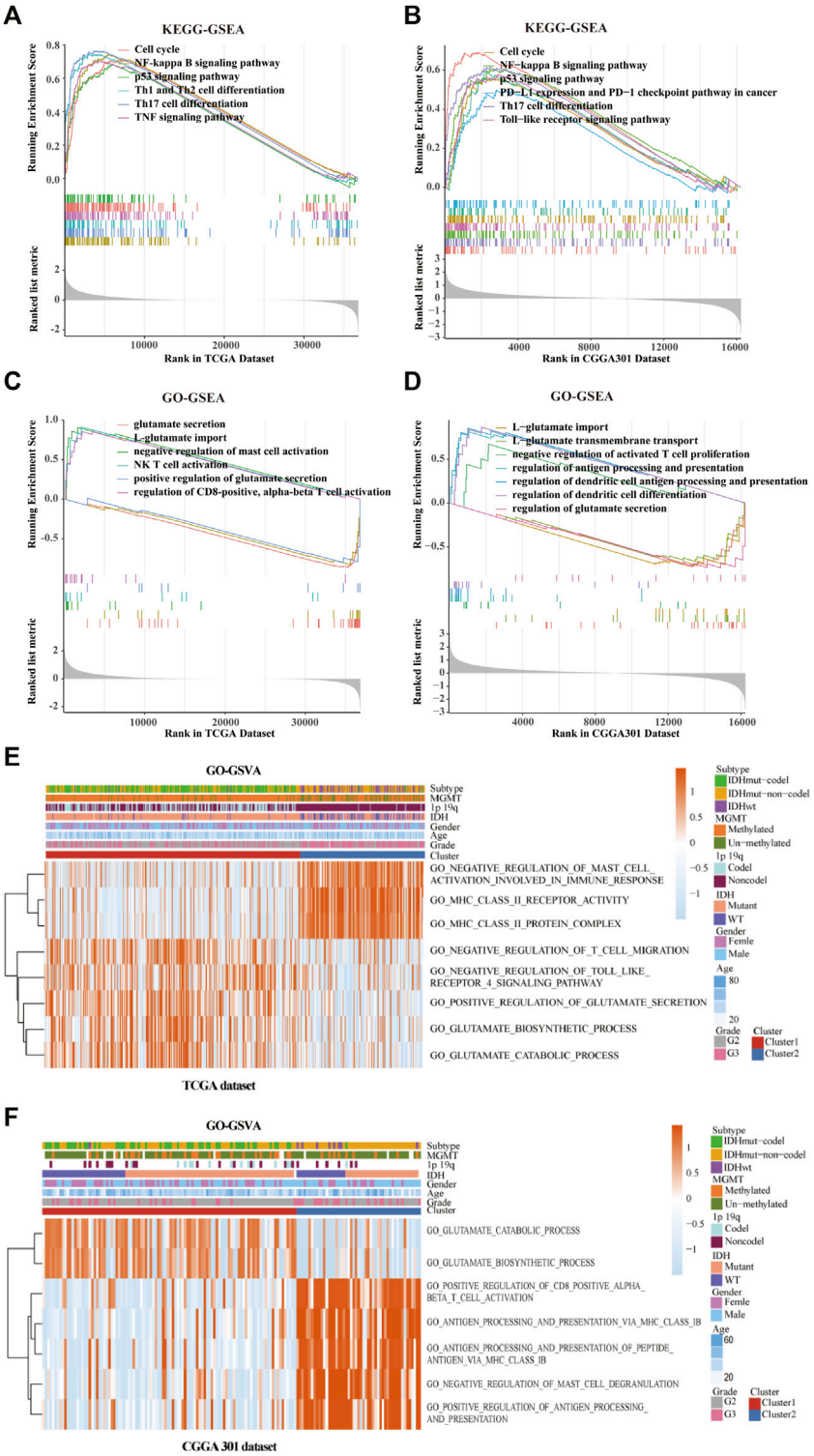

FIGURE 5 | Gene ontology (GO) and Kyoto Encyclopedia of Genes and Genomes (KEGG) enrichment analysis of the cluster model based on gene set enrichment analysis (GSEA) and gene set variation analysis (GSVA). Enriched pathways between cluster 1 and cluster 2 based on KEGG-based GSEA analysis in TCGA **(A)** and CGGA301 **(B)** databases. Enriched pathways between cluster 1 and cluster 2 based on GO-based GSEA analysis in TCGA **(C)** and CGGA301 **(D)** databases. Enriched pathways between cluster 1 and cluster 2 based on GO-based GSVA analysis in TCGA **(E)** and CGGA301 **(F)** databases.

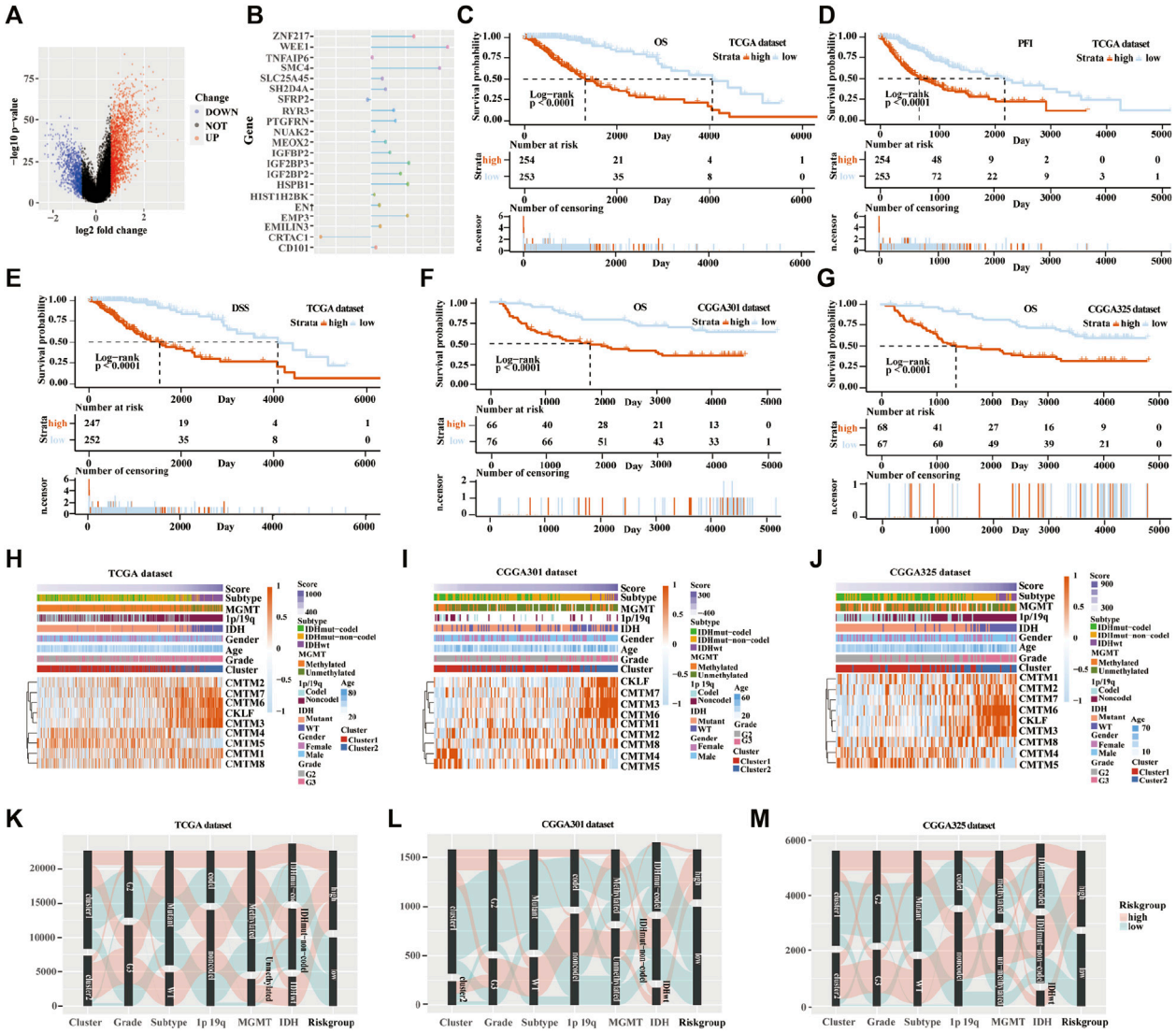

FIGURE 6 | Establishment and verification of the scoring model in the training and validation cohorts. **(A)** Volcano plot of differently expressed genes in the two clusters from TCGA database. **(B)** Elastic network map of 21 genes that were associated with prognosis in the two clusters from the TCGA database. Kaplan-Meier analysis of patients in low-risk and high-risk groups from the TCGA database for OS **(C)**, PFI **(D)**, and DSS **(E)**. **(F)** Kaplan-Meier analysis of patients in low-risk and high-risk groups from the CGGA301 database for OS. **(G)** Kaplan-Meier analysis of patients in low-risk and high-risk groups from the CGGA325 database for OS. Heatmap of different glioma features and expression of CMTM in the low-risk and high-risk groups from the TCGA **(H)**, CGGA301 **(I)**, and CGGA325 **(J)** databases. Sankey diagram of different expression patterns of glioma features in cluster 1 and cluster 2 from TCGA **(K)**, CGGA301 **(L)**, and CGGA325 **(M)** databases, analyzed by the log-rank test.

showed that the signaling pathways of p53, focal adhesion, cell adhesion molecules cams, antigen progress, and presentation were enriched in high-risk score group from the TCGA database (**Figure 7C**). In addition, GO-based GSVA analysis indicated that the signaling pathways of FAS, protein complex involved in cell adhesion, extracellular matrix binding, cellular response to radiation, cell apoptotic progress, lymphocyte activation involved in immune response, negative regulation of T cell, and lymphocyte differentiation were associated with the high-risk score in the TCGA database (**Figure 7D**).

Moreover, pathways associated with antigen process and presentation, NF-kappa B, p53 signaling, PD-L1 expression, PD-1 checkpoint, Th17 cell differentiation, and TLR signaling were enriched in high-risk score group from the CGGA-array database (**Figure 7E**). GO-based GSEA pathway analysis in the CGGA-array database indicated that cell-cell adhesion mediated by integrin, DC antigen processing and presentation, extracellular matrix disassembly, regulation of $CD8^{+}$, and alpha-beta T cell activation signaling were enriched high-risk score group (**Figure 7F**). KEGG-based GSVA analysis showed that

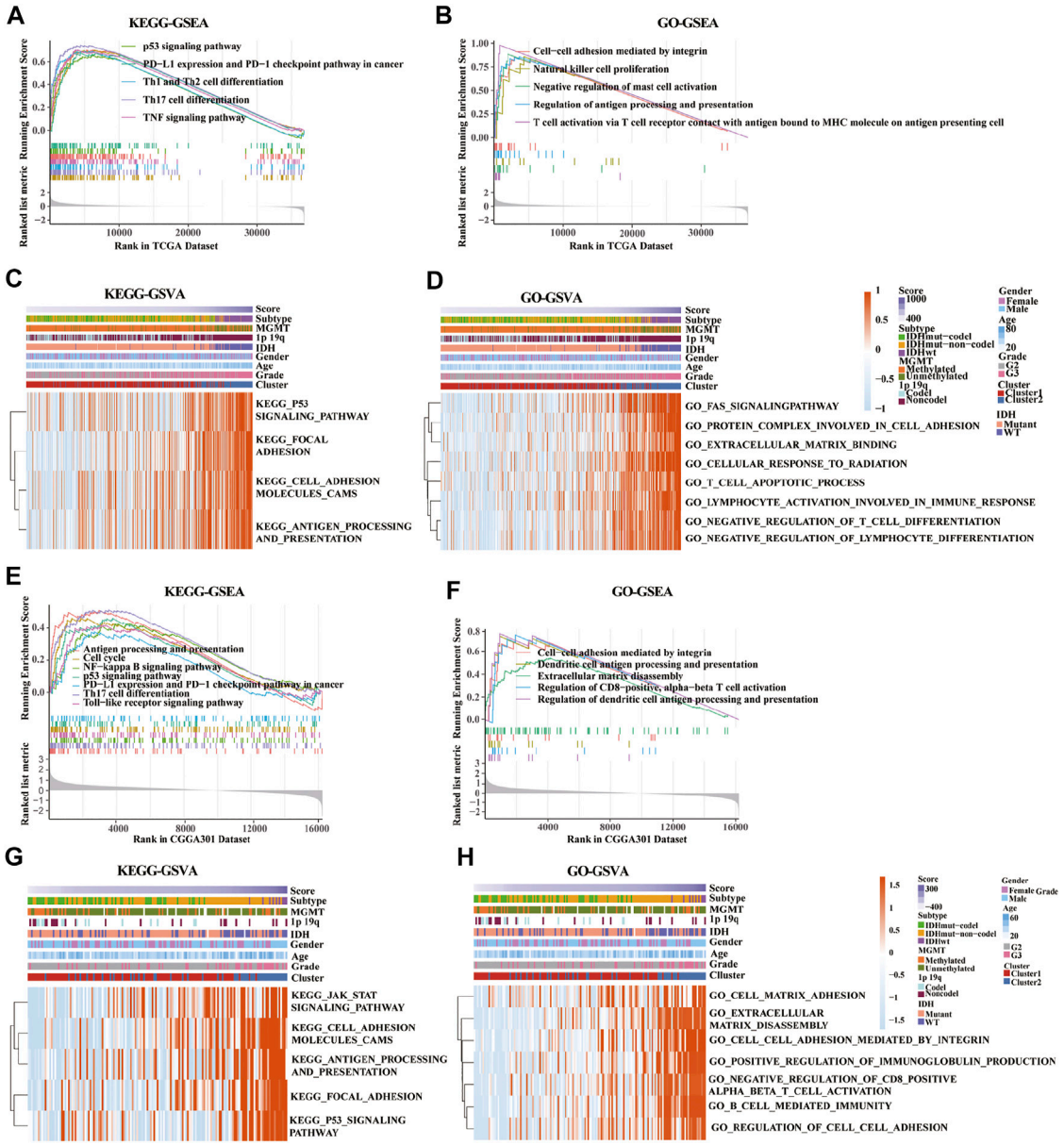

FIGURE 7 | Gene set enrichment analysis (GSEA) and gene set variation analysis (GSVA) of key pathways between low-risk and high-risk groups based on gene ontology (GO) and Kyoto Encyclopedia of Genes and Genomes (KEGG) databases. **(A,E)** Enriched pathways between low-risk and high-risk groups based on KEGG-based GSEA analysis in TCGA **(A)** and CGGA301 **(E)** databases. **(B,F)** Enriched pathways between low-risk and high-risk groups based on GO-based GSEA analysis in TCGA **(B)** and CGGA301 **(F)** databases. **(C,G)** Enriched pathways between low-risk and high-risk groups based on KEGG-based GSVA analysis in TCGA **(C)** and CGGA301 **(G)** databases. **(D,H)** Enriched pathways between low-risk and high-risk groups based on GO-based GSVA analysis in TCGA **(D)** and CGGA301 **(H)** databases.

JAK/STAT signaling, cell adhesion molecules cams, antigen processing and presentation, focal adhesion, and p53 signaling pathways were enriched, with a high-risk score in high-risk score group from the CGGA-array database (**Figure 7G**). Finally, GO-based GSVA analysis indicated that signaling pathways associated with cell-matrix adhesion, extracellular matrix disassembly, cell-cell adhesion mediated by integrin, regulation of immunoglobulin production, cell-cell adhesion, $CD8^+$, alpha-beta T cell activation, and cell-mediated immunity were enriched in high-risk score group from the CGGA-array database (**Figure 7H**). These results were also verified in the CGGA RNA-seq database (**Supplementary Figure S7**).

Expression of PD-1, PD-L1, and PD-L2 in Different Clusters and Score Groups

Pathways enrichment analysis indicated that immunocytes' function may be different between high and low score

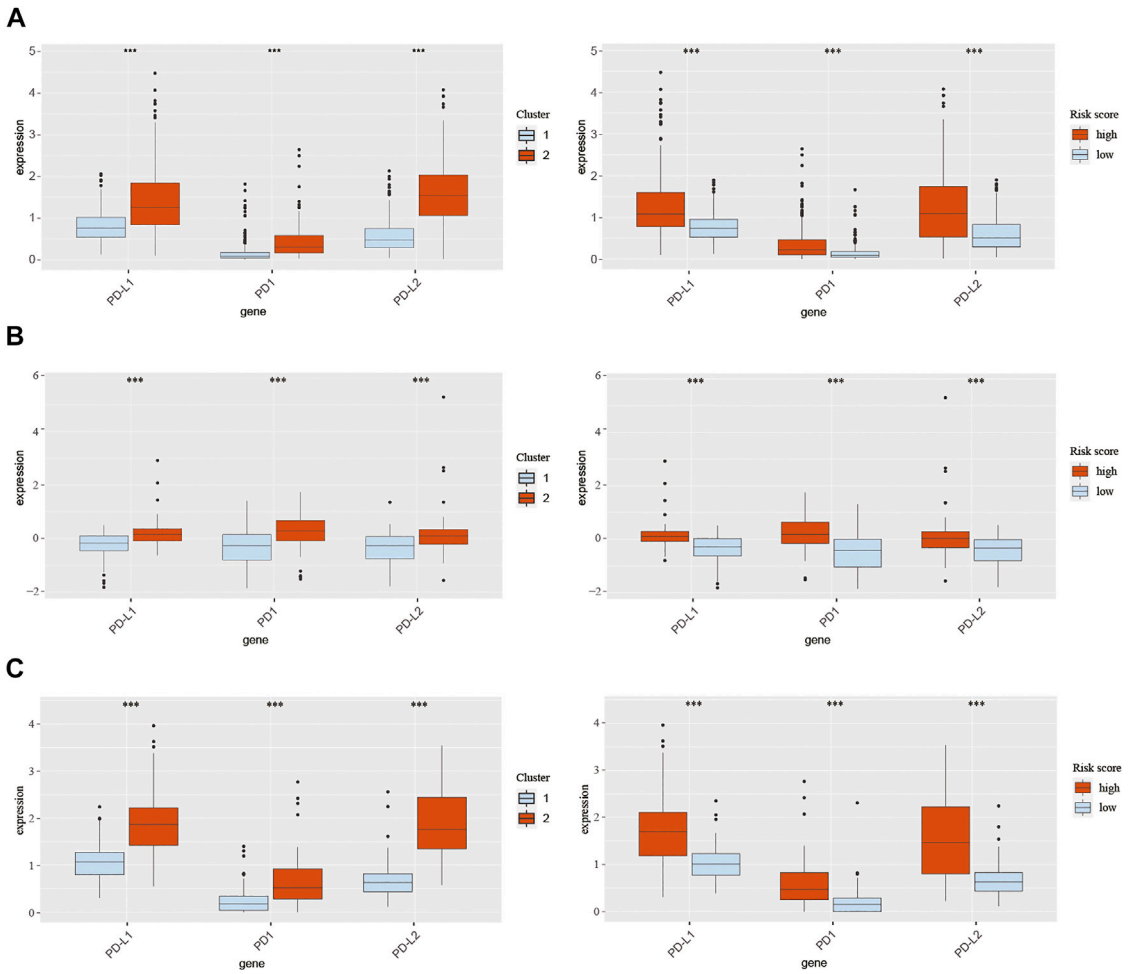

FIGURE 8 | Expression of PD-1, PD-L1, and PD-L2 in different clusters and risk groups in training and validation cohorts. **(A)** Expression of PD-1, PD-L1, and PD-L2 in cluster 1, cluster 2, the low-risk group, and the high-risk group from TCGA database. **(B)** Expression of PD-1, PD-L1, and PD-L2 in cluster 1, cluster 2, the low-risk group, and the high-risk group from the CGGA301 database. **(C)** Expression of PD-1, PD-L1, and PD-L2 in cluster 1, cluster 2, the low-risk group, and the high-risk group from the CGGA325 database. The Wilcox test was used to compare the difference between the two groups (***$p < 0.001$).

samples. Next, we explore the association between those two models and immune check point expression. The expression of CMTM family genes was previously found to be closely associated with immune checkpoints PD-1 and PD-L1. Therefore, PD-1, PD-L1, and PD-L2 expression levels were evaluated in different clusters and risk groups (**Figure 8**). Results indicated that the expression levels of PD-1, PD-L1, and PD-L2 were upregulated in cluster 2 and the high-risk group in all three cohorts ($p < 0.001$; **Figures 8A–C**). Together, those results implied an immunosuppressive microenvironment in high-risk samples.

DISCUSSION

LGG is a primary tumor that progresses slowly in the brain but eventually develops into high-grade secondary aggressive tumors, such as GBM (Bready and Placantonakis, 2019). The prognosis of LGG is affected by several factors, including age, grade, and molecular genetic mutations (IDH mutations, 1p/19q co-deletion, MGMT promoter methylation). IDH, a small molecular protein, is a key rate-limiting enzyme in the progress of energy metabolism. Numerous studies found that patients with IDH-mutated gliomas exhibited a better prognosis than those with IDH-WT (Hartmann et al., 2010; Turkalp et al., 2014). 1p/19q co-deletion is another valuable genetic marker for patients with gliomas. Zhao et al. evaluated 28 glioma studies with over 3400 cases and found that patients with co-deletion of chromosomal 1p/19q had a better PFS and OS than those with the entire chromosomal group (Zhao et al., 2014). MGMT promoter methylation is also a favorable molecular maker for a better clinical outcome in LGG (Mathur et al., 2020). In this paper, we found that patients with unmethylated MGMT promoter from the TCGA database tend to have a high-risk score, which suggests that MGMT promoter methylation may be related to the prognosis of LGG. However, the underlying mechanisms need to be explored in detail. In addition, since the

number of cases in the TCGA database is still a bit small, the difference is not particularly obvious.

Several studies have explored the relationship between the expression changes of various genes and the development of glioma to identify appropriate prognostic markers for patients with glioma (Zhang et al., 2021b; Zhang et al., 2021c; Wang et al., 2021). Besides, with the rapid development of high-throughput sequencing technology, numerous gene families have been identified. Therefore, a series of reliable databases have been produced, such as the Gene Expression Omnibus (GEO), TCGA, and CGGA datasets. In the present study, we used two public databases (TCGA and CGGA) to investigate the correlation between the expression levels of the CMTM gene family and the prognosis of LGG.

The CMTM gene family was first described in 2001. The nine members in this family are located on different chromosomes, which play an essential role in various physiological and pathological processes (Hara et al., 1988). Delic et al. systematically analyzed CMTM family genes in GBM and found that CMTM2, 3, and 6 were significantly upregulated, and CMTM4 and 8 were significantly downregulated (Delic et al., 2015). They found that elevated CMTM1 and CMTM3 expressions were significantly associated with shorter OS. In addition, they provided first insights into CMTM1 and CMTM 3 signals through human phosphokinase protein expression profiling assay, which may be regulated by growth factor receptor, Src family kinase, and WNT activation. This perfect work inspired us to explore the role of CMTM family genes in LGG. CMTM1 and CMTM2, located on chromosome 16q21, mainly participate in chemotaxis and regulation of signaling receptor activity under physiological conditions. Previous studies showed that the expression of CMTM1 increased significantly in various cancer samples, suggesting that CMTM1 may play a vital role in tumorigenesis (Song et al., 2021). An *In vitro* study in a breast cancer cell line found that CMTM1 eliminated TNF-α-induced apoptosis and eventually promoted breast cancer cell proliferation (Wang et al., 2014). In this study, we found that the expression of CMTM1 was higher in grade III glioma in the TCGA datasets. Previous studies indicated that CMTM2 is downregulated in liver cancer tissues, which is related to the outcome of liver cancer patients (Li et al., 2020). However, no significant differences were found in the expression of various grades and genetic characteristics in LGG in our study.

CMTM3, CMTM4, and CMTM5 are thought to bring about favorable prognostic factors in several cancer types (Zhang et al., 2014; Hu et al., 2015; Li et al., 2015). Previous studies found that overexpressed CMTM3 significantly inhibited cancer cell proliferation and migration by reducing the activity of Erk1/2 (Su et al., 2014). However, in the present study, we found that upregulated CMTM3 may predict a poor outcome in LGG. In a recent paper on tumor cell proliferation and migration, the author found that over-expression of CMTM3 was associated with low pathological grade, high recurrence/metastasis rate, and worse survival in pancreatic cancer (Zhou et al., 2021). CMTM3 was found to closely relate to cell proliferation and differentiation, Hedgehog signaling pathway, Wnt signaling pathway, ECM-receptor interaction, and pathways in cancer. These results showed that the current role of CMTM3 in tumor formation is complex and ambiguous. CMTM3 may participate in tumor immunity through a variety of mechanisms, including signaling pathways that inhibit tumor growth and promote tumorigenesis.

CMTM4 can prevent cell proliferation and migration through the AKT/STAT3 pathway (Xue et al., 2019). *In vivo* and *In vitro* studies proved that CMTM5 could suppress tumor growth by regulating P13K-AKT signaling (Xiao et al., 2015; Xu and Dang, 2017). Our study confirmed that CMTM4 and CMTM5 are highly expressed in glioma with lower grade and better prognostic subtypes; however, the specific molecular mechanism warrants further investigation.

Intervention targeting immune checkpoints is an effective strategy in tumor immunotherapy. Recent reports have shown that CMTM6 regulates PD-L1, a key immune checkpoint in numerous cancers. CMTM6 effectively reduced the expression of PD-L1 through the IFN-γ signaling pathway (Burr et al., 2017; Mezzadra et al., 2017). Other CMTM members, including CMTM7 (Huang et al., 2019), CMTM8 (Gao et al., 2015), and CKLF (Dunne et al., 2016) were identified as tumor suppressors. Liu et al. found that CMTM7 plays a vista role in regulating EGFR signaling in human non-small cell lung cancer, and the knockdown of CMTM7 induces the progression of cancer cells (Liu et al., 2015). Further studies revealed that CMTM8 could induce cell apoptosis through a mitochondria-mediated pathway in caspase-independent and caspase-dependent manners (Li et al., 2014). CKLF, the first member to be discovered in the CMTM family, is also identified as a promising therapeutic target in human tumors (Cai et al., 2020). In this study, it was found that CMTM6, CMTM7, CMTM8, and CKLF were highly expressed in grade III and IDH-WT gliomas. These results indicated that these CMTM family members might have a different role in glioma than classical tumors.

Moreover, two clusters were established according to the expression of CMTM family genes, and a scoring model was built based on DEGs in the two clusters. It was found that the expression of CMTM3, CMTM6, CMTM7, CMTM8, and CKLF were significantly increased in cluster 2 and high-risk groups, and the expression of CMTM4 and CMTM5 was increased dramatically in cluster 1 and the low-risk group. The reliability of this model for predicting the prognosis of glioma was proved and then verified using the two validation datasets (CGGA-array and CGGA RNA-seq databases). The immune landscapes in the TME were investigated and found that different immune infiltrating cells were upregulated in cluster 2, such as DCs, B cells, CLPs, fibroblasts, macrophages, mast cells, Th2 cells, and monocytes, which play a vital role in tumor immunity. These results demonstrated that CMTM family genes are critical in the immune infiltration process of LGG TME.

Furthermore, GO and KEGG enrichment analyses were used to identify several enriched pathways, including cell cycle, NF-kappa B signaling pathway, p53 signaling pathway, PD-L1 expression, PD-1 checkpoint pathway, Th1 and Th2 cell differentiation, and TNF signaling pathway. These key pathways play a critical role in the process of tumor formation, development, and metastasis. Mounting evidence

supports the role of the NF-kappa B pathway in the pathogenesis and resistance to treatment of glioma (Puliyappadamba et al., 2014). Especially, the common enriched pathways were p53 signaling pathway, PD-L1 expression, PD-1 checkpoint pathway, and Th17 cell differentiation based on the KEGG analysis. The p53 pathway is consisted of a network of genes and their products, which are designed to respond to various internal and external stress signals that affect the cell homeostasis mechanisms that monitor DNA replication, chromosome segregation, and cell division (Issaeva, 2019). Increasing studies have found that P53 signaling pathway can affect kinds of cellular processes, including maintenance of genome stability, metabolism, and longevity, and represents one of the most important and widely studied tumor suppressors (Stegh, 2012). Meanwhile, Th17 cells were identified as vital defenders against pathogens both in autoimmune disorders and cancer diseases (Knochelmann et al., 2018). In addition, PD-L1 and PD-1, which are negatively associated with immune checkpoint regulation, and have been proved to be predictive biomarkers of tumor immune therapy and are effective intervention targets in tumors (Chen et al., 2018). We found that PD-1, PD-L1, and PD-L2 expression levels were significantly upregulated in cluster 2 and high-risk groups in TCGA and CGGA databases. Importantly, the common enriched pathways were cell-cell adhesion mediated by integrin and regulation of antigen processing and presentation based on the GO analysis, which was found to take part in intercellular and cell-extracellular matrix interactions progress in multiple cancer types.

Generally, this study systematically described different expression patterns of CMTM family genes and their predictive value for patients with LGG. Furthermore, we explored the relationship between the expression of CMTM family genes and immune infiltrates in the TME. Overexpression of CMTM members is associated with crucial pathways implicated in tumor progression. The CMTM family can modulate LGG prognosis and tumor immunocytes infiltration even if the cluster model shows no statistical significance in multivariate Cox regression. But the scoring model is generated and constructed from the cluster model and shows better prognostic ability and more precise biofunction precision (Zhang et al., 2020). In sum, these findings underscore the importance of CMTM family genes as promising immunotherapeutic targets and could contribute to the discovery of novel immune checkpoints in LGG.

DATA AVAILABILITY STATEMENT

The datasets presented in this study can be found in online repositories. The names of the repository/repositories and accession number(s) can be found in the article/ **Supplementary Material**.

AUTHOR CONTRIBUTIONS

Writing—original draft, methodology, validation, and visualization: ZW and JZ. Data curation and validation: HZ, RP, ZD, and XL. Investigation: SL, FL, and XZ. Conceptualization, methodology, supervision, project administration, and funding acquisition: ZL, KY, and QC.

FUNDING

This study is supported by the National Nature Science Foundation of China (No. 82073893, 82172685, 81703622, and 81901268); the China Postdoctoral Science Foundation (No. 2018M633002); the Natural Science Foundation of Hunan Province (No. 2018JJ3838, 2019JJ50948); the Hunan Provincial Health and Health Committee Foundation of China (C2019186); Xiangya Hospital Central South University postdoctoral foundation; and the Fundamental Research Funds for the Central Universities of Central South University (No. 2021zzts1027).

ACKNOWLEDGMENTS

We acknowledge TCGA, CGGA and GEO database for providing their platforms and contributors for uploading their meaningful datasets.

SUPPLEMENTARY MATERIAL

The Supplementary Material for this article can be found online at: https://www.frontiersin.org/articles/10.3389/fcell.2022.740822/full#supplementary-material

REFERENCES

Aiman, W., and Rayi, A. (2021). *Low Grade Gliomas*. Treasure Island (FL): StatPearls.

Aran, D., Hu, Z., and Butte, A. J. (2017). xCell: Digitally Portraying the Tissue Cellular Heterogeneity Landscape. *Genome Biol.* 18, 220. doi:10.1186/s13059-017-1349-1

Bacolod, M. D., Talukdar, S., Emdad, L., Das, S. K., Sarkar, D., Wang, X.-Y., et al. (2016). Immune Infiltration, Glioma Stratification, and Therapeutic Implications. *Transl. Cancer Res.* 5, S652–S656. doi:10.21037/tcr.2016.10.69

Bao, Z.-S., Chen, H.-M., Yang, M.-Y., Zhang, C.-B., Yu, K., Ye, W.-L., et al. (2014). RNA-seq of 272 Gliomas Revealed a Novel, Recurrent PTPRZ1-MET Fusion Transcript in Secondary Glioblastomas. *Genome Res.* 24, 1765–1773. doi:10.1101/gr.165126.113

Binnewies, M., Roberts, E. W., Kersten, K., Chan, V., Fearon, D. F., Merad, M., et al. (2018). Understanding the Tumor Immune Microenvironment (TIME) for Effective Therapy. *Nat. Med.* 24, 541–550. doi:10.1038/s41591-018-0014-x

Bowman, R. L., Wang, Q., Carro, A., Verhaak, R. G. W., and Squatrito, M. (2017). GlioVis Data portal for Visualization and Analysis of Brain Tumor Expression Datasets. *Neuonc.* 19, 139–141. doi:10.1093/neuonc/now247

Bready, D., and Placantonakis, D. G. (2019). Molecular Pathogenesis of Low-Grade Glioma. *Neurosurg. Clin. North America* 30, 17–25. doi:10.1016/j.nec.2018.08.011

Burr, M. L., Sparbier, C. E., Chan, Y.-C., Williamson, J. C., Woods, K., Beavis, P. A., et al. (2017). CMTM6 Maintains the Expression of PD-L1 and Regulates Anti-tumour Immunity. *Nature* 549, 101–105. doi:10.1038/nature23643

Cai, X., Deng, J., Ming, Q., Cai, H., and Chen, Z. (2020). Chemokine-like Factor 1: A Promising Therapeutic Target in Human Diseases. *Exp. Biol. Med. (Maywood)* 245, 1518–1528. doi:10.1177/1535370220945225

Chen, R. Q., Liu, F., Qiu, X. Y., and Chen, X. Q. (2018). The Prognostic and Therapeutic Value of PD-L1 in Glioma. *Front. Pharmacol.* 9, 1503. doi:10.3389/fphar.2018.01503

Delic, S., Thuy, A., Schulze, M., Proescholdt, M. A., Dietrich, P., Bosserhoff, A.-K., et al. (2015). Systematic Investigation of CMTM Family Genes Suggests Relevance to Glioblastoma Pathogenesis and CMTM1 and CMTM3 as Priority Targets. *Genes Chromosomes Cancer* 54, 433–443. doi:10.1002/gcc.22255

Dunne, P. D., O'Reilly, P. G., Coleman, H. G., Gray, R. T., Longley, D. B., Johnston, P. G., et al. (2016). Stratified Analysis Reveals Chemokine-like Factor (CKLF) as a Potential Prognostic Marker in the MSI-Immune Consensus Molecular Subtype CMS1 of Colorectal Cancer. *Oncotarget* 7, 36632–36644. doi:10.18632/oncotarget.9126

Fang, S., Liang, J., Qian, T., Wang, Y., Liu, X., Fan, X., et al. (2017). Anatomic Location of Tumor Predicts the Accuracy of Motor Function Localization in Diffuse Lower-Grade Gliomas Involving the Hand Knob Area. *AJNR Am. J. Neuroradiol* 38, 1990–1997. doi:10.3174/ajnr.a5342

Gao, D., Hu, H., Wang, Y., Yu, W., Zhou, J., Wang, X., et al. (2015). CMTM8 Inhibits the Carcinogenesis and Progression of Bladder Cancer. *Oncol. Rep.* 34, 2853–2863. doi:10.3892/or.2015.4310

Giraldo, N. A., Sanchez-Salas, R., Peske, J. D., Vano, Y., Becht, E., Petitprez, F., et al. (2019). The Clinical Role of the TME in Solid Cancer. *Br. J. Cancer* 120, 45–53. doi:10.1038/s41416-018-0327-z

Han, W., Lou, Y., Tang, J., Zhang, Y., Chen, Y., Li, Y., et al. (2001). Molecular Cloning and Characterization of Chemokine-like Factor 1 (CKLF1), a Novel Human Cytokine with Unique Structure and Potential Chemotactic Activity. *Biochem. J.* 357, 127–135. doi:10.1042/bj3570127

Hara, N., Mineo, I., Kono, N., Yamada, Y., Kawachi, M., Kiyokawa, H., et al. (1988). Inosine and Adenosine Formation in Ischemic and Non-ischemic Contracting Muscles of Rats: Difference between Fast and Slow Muscles. *Res. Commun. Chem. Pathol. Pharmacol.* 60, 309–321.

Hartmann, C., Hentschel, B., Wick, W., Capper, D., Felsberg, J., Simon, M., et al. (2010). Patients with IDH1 Wild Type Anaplastic Astrocytomas Exhibit Worse Prognosis Than IDH1-Mutated Glioblastomas, and IDH1 Mutation Status Accounts for the Unfavorable Prognostic Effect of Higher Age: Implications for Classification of Gliomas. *Acta Neuropathol.* 120, 707–718. doi:10.1007/s00401-010-0781-z

Hu, F., Yuan, W., Wang, X., Sheng, Z., Yuan, Y., Qin, C., et al. (2015). CMTM3 Is Reduced in Prostate Cancer and Inhibits Migration, Invasion and Growth of LNCaP Cells. *Clin. Transl. Oncol.* 17, 632–639. doi:10.1007/s12094-015-1288-9

Huang, Z. M., Li, P. L., Yang, P., Hou, X. D., Yang, Y. L., Xu, X., et al. (2019). Overexpression of CMTM7 Inhibits Cell Growth and Migration in Liver Cancer. *Kaohsiung J. Med. Sci.* 35, 332–340. doi:10.1002/kjm2.12058

Issaeva, N. (2019). p53 Signaling in Cancers. *Cancers (Basel)* 11, 332. doi:10.3390/cancers11030332

Kleihues, P., and Ohgaki, H. (1999). Primary and Secondary Glioblastomas: from Concept to Clinical Diagnosis. *Neuro Oncol.* 1, 44–51. doi:10.1093/neuonc/1.1.44

Knochelmann, H. M., Dwyer, C. J., Bailey, S. R., Amaya, S. M., Elston, D. M., Mazza-McCrann, J. M., et al. (2018). When Worlds Collide: Th17 and Treg Cells in Cancer and Autoimmunity. *Cell Mol Immunol* 15, 458–469. doi:10.1038/s41423-018-0004-4

Li, H., Li, J., Su, Y., Fan, Y., Guo, X., Li, L., et al. (2014). A Novel 3p22.3 Gene CMTM7 Represses Oncogenic EGFR Signaling and Inhibits Cancer Cell Growth. *Oncogene* 33, 3109–3118. doi:10.1038/onc.2013.282

Li, M., Luo, F., Tian, X., Yin, S., Zhou, L., and Zheng, S. (2020). Chemokine-Like Factor-like MARVEL Transmembrane Domain-Containing Family in Hepatocellular Carcinoma: Latest Advances. *Front. Oncol.* 10, 595973. doi:10.3389/fonc.2020.595973

Li, T., Cheng, Y., Wang, P., Wang, W., Hu, F., Mo, X., et al. (2015). CMTM4 Is Frequently Downregulated and Functions as a Tumour Suppressor in clear Cell Renal Cell Carcinoma. *J. Exp. Clin. Cancer Res.* 34, 122. doi:10.1186/s13046-015-0236-4

Lim, A. R., Rathmell, W. K., and Rathmell, J. C. (2020). The Tumor Microenvironment as a Metabolic Barrier to Effector T Cells and Immunotherapy. *Elife* 9, e55185. doi:10.7554/eLife.55185

Liu, B., Su, Y., Li, T., Yuan, W., Mo, X., Li, H., et al. (2015). CMTM7 Knockdown Increases Tumorigenicity of Human Non-small Cell Lung Cancer Cells and EGFR-AKT Signaling by Reducing Rab5 Activation. *Oncotarget* 6, 41092–41107. doi:10.18632/oncotarget.5732

Mathur, R., Zhang, Y., Grimmer, M. R., Hong, C., Zhang, M., Bollam, S., et al. (2020). MGMT Promoter Methylation Level in Newly Diagnosed Low-Grade Glioma Is a Predictor of Hypermutation at Recurrence. *Neuro Oncol.* 22, 1580–1590. doi:10.1093/neuonc/noaa059

Mezzadra, R., Sun, C., Jae, L. T., Gomez-Eerland, R., de Vries, E., Wu, W., et al. (2017). Identification of CMTM6 and CMTM4 as PD-L1 Protein Regulators. *Nature* 549, 106–110. doi:10.1038/nature23669

Newman, A. M., Steen, C. B., Liu, C. L., Gentles, A. J., Chaudhuri, A. A., Scherer, F., et al. (2019). Determining Cell Type Abundance and Expression from Bulk Tissues with Digital Cytometry. *Nat. Biotechnol.* 37, 773–782. doi:10.1038/s41587-019-0114-2

Puliyappadamba, V. T., Hatanpaa, K. J., Chakraborty, S., and Habib, A. A. (2014). The Role of NF-Kb in the Pathogenesis of Glioma. *Mol. Cell Oncol.* 1, e963478. doi:10.4161/23723548.2014.963478

Qian, B.-Z., Li, J., Zhang, H., Kitamura, T., Zhang, J., Campion, L. R., et al. (2011). CCL2 Recruits Inflammatory Monocytes to Facilitate Breast-Tumour Metastasis. *Nature* 475, 222–225. doi:10.1038/nature10138

Sidaway, P. (2020). Low-grade Glioma Subtypes Revealed. *Nat. Rev. Clin. Oncol.* 17, 335. doi:10.1038/s41571-020-0380-4

Song, X., Zhang, S., Tian, R., Zheng, C., Xu, Y., Wang, T., et al. (2021). Expression and Clinical Significance of CMTM1 in Hepatocellular Carcinoma. *Open Med. (Wars)* 16, 217–223. doi:10.1515/med-2021-0221

Stegh, A. H. (2012). Targeting the P53 Signaling Pathway in Cancer Therapy - the Promises, Challenges and Perils. *Expert Opin. Ther. Targets* 16, 67–83. doi:10.1517/14728222.2011.643299

Su, Y., Lin, Y., Zhang, L., Liu, B., Yuan, W., Mo, X., et al. (2014). CMTM3inhibits Cell Migration and Invasion and Correlates with Favorable Prognosis in Gastric Cancer. *Cancer Sci.* 105, 26–34. doi:10.1111/cas.12304

Taylor, O. G., Brzozowski, J. S., and Skelding, K. A. (2019). Glioblastoma Multiforme: An Overview of Emerging Therapeutic Targets. *Front. Oncol.* 9, 963. doi:10.3389/fonc.2019.00963

Turkalp, Z., Karamchandani, J., and Das, S. (2014). IDHMutation in Glioma. *JAMA Neurol.* 71, 1319–1325. doi:10.1001/jamaneurol.2014.1205

Wang, J., Zhang, G., Zhang, Y., Luo, Y., Song, Q., Qiu, X., et al. (2014). CMTM1_v17 Is a Novel Potential Therapeutic Target in Breast Cancer. *Oncol. Rep.* 32, 1829–1836. doi:10.3892/or.2014.3429

Wang, Z., Su, G., Dai, Z., Meng, M., Zhang, H., Fan, F., et al. (2021). Circadian Clock Genes Promote Glioma Progression by Affecting Tumour Immune Infiltration and Tumour Cell Proliferation. *Cell Prolif.* 54, e12988. doi:10.1111/cpr.12988

Weller, M., Wick, W., Aldape, K., Brada, M., Berger, M., Pfister, S. M., et al. (2015). Glioma. *Nat. Rev. Dis. Primers* 1, 15017. doi:10.1038/nrdp.2015.17

Wen, P. Y., and Huse, J. T. (2017). World Health Organization Classification of Central Nervous System Tumors. *Continuum (Minneap Minn)* 23, 1531–1547. doi:10.1212/CON.0000000000000536

Wilkerson, M. D., and Hayes, D. N. (2010). ConsensusClusterPlus: a Class Discovery Tool with Confidence Assessments and Item Tracking. *Bioinformatics* 26, 1572–1573. doi:10.1093/bioinformatics/btq170

Wu, J., Li, L., Wu, S., and Xu, B. (2020). CMTM Family Proteins 1-8: Roles in Cancer Biological Processes and Potential Clinical Value. *Cancer Biol. Med.* 17, 528–542. doi:10.20892/j.issn.2095-3941.2020.0032

Wu, K., Li, X., Gu, H., Yang, Q., Liu, Y., and Wang, L. (2019). Research Advances in CKLF-like MARVEL Transmembrane Domain-Containing Family in Non-small Cell Lung Cancer. *Int. J. Biol. Sci.* 15, 2576–2583. doi:10.7150/ijbs.33733

Wu, S., Yang, W., Zhang, H., Ren, Y., Fang, Z., Yuan, C., et al. (2019). The Prognostic Landscape of Tumor-Infiltrating Immune Cells and Immune Checkpoints in Glioblastoma. *Technol. Cancer Res. Treat.* 18, 1533033819869949. doi:10.1177/1533033819869949

Xiao, Y., Yuan, Y., Zhang, Y., Li, J., Liu, Z., Zhang, X., et al. (2015). CMTM5 Is Reduced in Prostate Cancer and Inhibits Cancer Cell Growth *In Vitro* and *In Vivo*. *Clin. Transl. Oncol.* 17, 431–437. doi:10.1007/s12094-014-1253-z

Xu, G., and Dang, C. (2017). CMTM5 Is Downregulated and Suppresses Tumour Growth in Hepatocellular Carcinoma through Regulating PI3K-AKT Signalling. *Cancer Cel. Int*. 17, 113. doi:10.1186/s12935-017-0485-8

Xue, H., Li, T., Wang, P., Mo, X., Zhang, H., Ding, S., et al. (2019). CMTM4 Inhibits Cell Proliferation and Migration via AKT, ERK1/2, and STAT3 Pathway in Colorectal Cancer. *Acta Biochim. Biophys. Sin (Shanghai)* 51, 915–924. doi:10.1093/abbs/gmz084

Yoshihara, K., Shahmoradgoli, M., Martínez, E., Vegesna, R., Kim, H., Torres-Garcia, W., et al. (2013). Inferring Tumour Purity and Stromal and Immune Cell Admixture from Expression Data. *Nat. Commun.* 4, 2612. doi:10.1038/ncomms3612

Zhang, B., Wu, Q., Li, B., Wang, D., Wang, L., and Zhou, Y. L. (2020). m6A Regulator-Mediated Methylation Modification Patterns and Tumor Microenvironment Infiltration Characterization in Gastric Cancer. *Mol. Cancer* 19, 53. doi:10.1186/s12943-020-01170-0

Zhang, H., Chen, Z., Wang, Z., Dai, Z., Hu, Z., Zhang, X., et al. (2021). Correlation between APOBEC3B Expression and Clinical Characterization in Lower-Grade Gliomas. *Front. Oncol.* 11, 625838. doi:10.3389/fonc.2021.625838

Zhang, H., Cui, B., Zhou, Y., Wang, X., Wu, W., Wang, Z., et al. (2021). B2M Overexpression Correlates with Malignancy and Immune Signatures in Human Gliomas. *Sci. Rep.* 11, 5045. doi:10.1038/s41598-021-84465-6

Zhang, H., He, J., Dai, Z., Wang, Z., Liang, X., He, F., et al. (2021). PDIA5 Is Correlated with Immune Infiltration and Predicts Poor Prognosis in Gliomas. *Front. Immunol.* 12, 628966. doi:10.3389/fimmu.2021.628966

Zhang, H., Nan, X., Li, X., Chen, Y., Zhang, J., Sun, L., et al. (2014). CMTM5 Exhibits Tumor Suppressor Activity through Promoter Methylation in Oral Squamous Cell Carcinoma. *Biochem. Biophysical Res. Commun.* 447, 304–310. doi:10.1016/j.bbrc.2014.03.158

Zhao, J., Ma, W., and Zhao, H. (2014). Loss of Heterozygosity 1p/19q and Survival in Glioma: a Meta-Analysis. *Neuro Oncol.* 16, 103–112. doi:10.1093/neuonc/not145

Zhao, Z., Meng, F., Wang, W., Wang, Z., Zhang, C., and Jiang, T. (2017). Comprehensive RNA-Seq Transcriptomic Profiling in the Malignant Progression of Gliomas. *Sci. Data* 4, 170024. doi:10.1038/sdata.2017.24

Zhou, Z., Ma, Z., Li, Z., Zhuang, H., Liu, C., Gong, Y., et al. (2021). CMTM3 Overexpression Predicts Poor Survival and Promotes Proliferation and Migration in Pancreatic Cancer. *J. Cancer* 12, 5797–5806. doi:10.7150/jca.57082

Conflict of Interest: The authors declare that the research was conducted in the absence of any commercial or financial relationships that could be construed as a potential conflict of interest.

Publisher's Note: All claims expressed in this article are solely those of the authors and do not necessarily represent those of their affiliated organizations, or those of the publisher, the editors, and the reviewers. Any product that may be evaluated in this article, or claim that may be made by its manufacturer, is not guaranteed or endorsed by the publisher.

frontiers | Frontiers in Cell and Developmental Biology

ORIGINAL RESEARCH
published: 16 June 2022
doi: 10.3389/fcell.2022.742213

Heparanase 1 Upregulation Promotes Tumor Progression and Is a Predictor of Low Survival for Oral Cancer

André A. Nimtz Rodrigues[1,2†], *Lucilene Lopes-Santos*[1†], *Pammela A. Lacerda*[1], *Mariana F. Juste*[1], *Bruno Augusto Mariz*[3], *Débora C. Cajazeiro*[1], *Victoria Giacobbe*[1], *Rafael Borges*[1], *André Casarim*[2], *Giovanna De Sanctis Callegari*[4,5], *Fernando Antônio M. Claret Arcadipane*[2], *Ivan Aprahamian*[6], *Tuula Anneli Salo*[7], *Carine Ervolino De Oliveira*[8], *Ricardo D. Coletta*[3,9], *Taize M. Augusto*[1,6] and *Nilva K. Cervigne*[1,6,10]*

[1]Laboratory of Molecular Biology and Cell Culture (LBMCC), Faculty of Medicine of Jundiaí, Jundiaí, Brazil, [2]Department of Head and Neck Surgery, Faculty of Medicine of Jundiaí, Jundiaí, Brazil, [3]Department of Oral Diagnosis, School of Dentistry of Piracicaba, Campinas State University, Piracicaba, Brazil, [4]Independent Researcher, São Paulo, Brazil, [5]Institute of Pathology Cardoso de Almeida, Jundiaí, Brazil, [6]Department of Internal Medicine, Faculty of Medicine of Jundiaí, Jundai, Brazil, [7]Department of Oral and Maxillofacial Diseases, Faculty of Medicine, University of Helsinki, Helsinki, Finland, [8]Programa de Pós-graduação em Ciências Biológicas, Universidade Federal de Alfenas, Alfenas, Brazil, [9]School of Dentistry, University of Campinas, Piracicaba, Brazil, [10]Faculty of Medicine of Jundiaí, Jundiaí, Brazil

OPEN ACCESS

Edited by:
Rodrigo Nalio Ramos,
D'Or Institute for Research and Education (IDOR), Brazil

Reviewed by:
Xiang Chen,
Fudan University, China
Ana Karina Oliveira,
University of Virginia, United States

***Correspondence:**
Nilva K. Cervigne
nilva.cervigne@gmail.com
nilvafurlan@g.fmj.br

†These authors have contributed equally to this work and share first authorship

Specialty section:
This article was submitted to Molecular and Cellular Pathology, a section of the journal Frontiers in Cell and Developmental Biology

Received: 15 July 2021
Accepted: 07 April 2022
Published: 16 June 2022

Citation:
Rodrigues AAN, Lopes-Santos L, Lacerda PA, Juste MF, Mariz BA, Cajazeiro DC, Giacobbe V, Borges R, Casarim A, Callegari GDS, Claret Arcadipane FAM, Aprahamian I, Salo TA, De Oliveira CE, Coletta RD, Augusto TM and Cervigne NK (2022) Heparanase 1 Upregulation Promotes Tumor Progression and Is a Predictor of Low Survival for Oral Cancer. Front. Cell Dev. Biol. 10:742213. doi: 10.3389/fcell.2022.742213

Background: Oral cavity cancer is still an important public health problem throughout the world. Oral squamous cell carcinomas (OSCCs) can be quite aggressive and metastatic, with a low survival rate and poor prognosis. However, this is usually related to the clinical stage and histological grade, and molecular prognostic markers for clinical practice are yet to be defined. Heparanase (HPSE1) is an endoglycosidase associated with extracellular matrix remodeling, and although involved in several malignancies, the clinical implications of HPSE1 expression in OSCCs are still unknown.

Methods: We sought to investigate HPSE1 expression in a series of primary OSCCs and further explore whether its overexpression plays a relevant role in OSCC tumorigenesis. mRNA and protein expression analyses were performed in OSCC tissue samples and cell lines. A loss-of-function strategy using shRNA and a gain-of-function strategy using an ORF vector targeting HPSE1 were employed to investigate the endogenous modulation of HPSE1 and its effects on proliferation, apoptosis, adhesion, epithelial–mesenchymal transition (EMT), angiogenesis, migration, and invasion of oral cancer *in vitro*.

Results: We demonstrated that HPSE1 is frequently upregulated in OSCC samples and cell lines and is an unfavorable prognostic indicator of disease-specific survival when combined with advanced pT stages. Moreover, abrogation of HPSE1 in OSCC cells significantly promoted apoptosis and inhibited proliferation, migration, invasion, and epithelial–mesenchymal transition by significantly decreasing the expression of N-cadherin and vimentin. Furthermore, a conditioned medium of HPSE1-downregulated cells resulted in reduced vascular endothelial growth.

Conclusion: Our results confirm the overexpression of HPSE1 in OSCCs, suggest that HPSE1 expression correlates with disease progression as it is associated with several

important biological processes for oral tumorigenesis, and can be managed as a prognostic marker for patients with OSCC.

Keywords: oral squamous cell carcinoma, EMT, MEC, HPSE1, biomarker, prognosis

INTRODUCTION

Among the most common types of cancer in the world, oral squamous cell carcinoma (OSCC) is responsible for approximately 300,000 new cases per year (Chi et al., 2015), corresponding to more than 90% of malignant tumors of oral cavity (Moro et al., 2018). In Brazil, the incidence of OSCC is considered one of the highest in the world, corresponding to the fifth most common malignancy in men and the 12th most frequent in women among all cancers in the country (Instituto Nacional de Câncer José Alencar Gomes da Silva, 2019). OSCCs are characterized by having poor prognosis and low survival, with 5-year mortality rates below 60%. In addition, the metastatic dissemination to regional lymph nodes is frequent and strongly correlated with poor disease prognosis, and it is associated with an increased risk of distant metastasis and diminished survival (Alam et al., 2011). Heparanase 1 (HPSE1) is an endo-β-D-glucuronidase with endoglycosidase activity capable of cleaving heparan sulfate (HS), leading to extracellular matrix (ECM) remodeling in various physiological and pathological processes and regulating the release of various HS-linked molecules, such as cytokines and enzymes involved in inflammation, wound healing, and tumor invasion (Dempsey et al., 2000; Parish et al., 2001; Jin and Zhou, 2017). The metastatic potential of tumor cells also correlates with the ability to cleave heparan sulfate proteoglycans (Vlodavsky et al., 1992; Sanderson et al., 2017). HPSE1 activity was first linked to the metastatic potential of melanoma cells in 1983 (Nakajima et al., 1983). Since then, such an association has been observed in a growing number of solid and hematological tumors, including gastric (Zheng et al., 2010), head and neck (Mogler et al., 2011), cervix (Zeng et al., 2013), pancreas (Quiros et al., 2006; Hunter et al., 2014), prostate (Zhou et al., 2008), and breast cancers (Jiao et al., 2014) (Santos et al., 2014; Xia et al., 2014; Gross-Cohen et al., 2016). The role of HPSE1 in the metastatic process appears to be associated with its ability to confer invasive properties and angiogenic potential to tumor cells (Ilan et al., 2006; Nadir et al., 2006; Vreys and David, 2007). For this reason, the use of HPSE1 inhibitors has also been strongly speculated as a potential tool for anticancer drug development (Nadir et al., 2006; Zhu et al., 2006; Pisano et al., 2014; Masola et al., 2016).

Several *in vivo* studies based on HPSE1 inhibitors support the hypothesis of the major role of HPSE1 in cancer due to its HS cleaving activity of the ECM, which contributes to tumor invasion and metastasis (Masola et al., 2018). Vlodavsky et al. (2012) reported that heparanase activity is increased in the plasma of cancer patients, and decreased heparanase expression can inhibit tumor cell metastasis. Moreover, there is evidence that the expression of genes associated with aggressive tumor behavior can be positively regulated by HPSE1 (Nadir et al., 2006; Zetser et al., 2006; Purushothaman et al., 2008; Shah et al., 2018). Thus, increased expression of heparanase is strongly correlated with metastasis, tumor vascularity, and reduced postoperative survival in cancer patients (Ilan et al., 2006; Vreys and David, 2007; Zhang et al., 2012). Several studies have shown that heparanase inhibitors (Yang et al., 2007; Ostapoff et al., 2013; Nadanaka et al., 2014) and gene silencing (Edovitsky et al., 2004; Lerner et al., 2008) can inhibit tumor growth and metastasis, providing additional evidence for the role of heparanase in tumorigenesis.

Considering the dynamics of cancer growth and the role of HPSE1 as a key in several tumor processes, it is important to combine efforts to clarify the relevance of HPSE1 in OSCCs. Our data suggest a link between the expression of HPSE1 and its potential as a prognostic marker for OSCC and shed light on our understanding of the biology for oral cancer progression, such as evidence for the action of HPSE1 in inhibiting apoptosis, promoting proliferative signaling, regulating MMP expression and EMT to facilitate invasion and establishment of the pre-metastatic niche, and increasing the bioavailability of pro-angiogenic factors. Although further investigation to delineate the crucial mechanism of action of HPSE1 in oral cavity cancer is still needed, especially to determine HPSE1-targeted therapy, our study certainly has the potential to improve patient prognosis and make therapeutic approaches more suitable for patients with oral cavity cancer.

MATERIALS AND METHODS

Samples and Clinicopathological Data

Oral tumor tissues and non-cancerous contralateral oral mucosal tissue samples from 35 patients with OSCC were divided into two parts: one was fixed in formalin and embedded in paraffin for hematoxylin and eosin staining, as well as immunohistochemistry analysis, while the other samples were snap-frozen in liquid nitrogen and kept at −80°C until used for total RNA extraction. All these patients were diagnosed and treated at the Department of Head and Neck Surgery and Otorhinolaryngology, São Vicente de Paulo Hospital, Jundiaí, SP, Brazil. The initial diagnosis was based on clinical findings and confirmed by histopathological analysis of the specimens. A description of clinical–epidemiopathological data from all 35 OSCC patients is summarized in **Supplementary Table S1**. The *HPSE1* mRNA expression levels were analyzed in 31 fresh OSCC and 35 non-cancerous oral mucosal tissues by quantitative PCR (qRT-PCR). Clinicopathological features of the 31 OSCC patients, whose samples were analyzed for HPSE1 mRNA expression, are described in **Table 1**. Immunohistochemical analysis was also performed to confirm protein expression levels of HPSE1 in 32 of these OSCC tissue samples. After treatment, patients were regularly followed up, and the outcomes were categorized as disease-specific survival, time

TABLE 1 | Association of expression of heparanase 1 with clinicopathological parameters of tumors.

	Expression of heparanase 1		
	Low, *n* (%)	**High, *n* (%)**	***p* value**
Age (years)			
< 62	6 (40.0)	8 (50.0)	0.58
≥ 62	9 (60.0)	8 (50.0)	
Gender			
Male	11 (73.3)	12 (75.0)	0.92
Female	4 (26.7)	4 (25.0)	
Smoking habit			
No	12 (80.0)	13 (81.2)	0.93
Yes	3 (20.0)	3 (18.8)	
Drinking habit			
No	13 (86.7)	13 (81.2)	0.68
Yes	2 (13.3)	3 (18.8)	
pT stage			
pT1 + pT2	11 (73.3)	10 (62.5)	0.52
pT3 + pT4	4 (26.7)	6 (37.5)	
pN stage			
N0	10 (66.7)	4 (25.0)	***0.02**
N+	5 (33.3)	12 (75.0)	
pTNM			
Early stage (I and II)	8 (53.3)	3 (18.8)	***0.04**
Advanced stage (III and IV)	7 (46.7)	13 (81.2)	
Location			
Tongue and floor of mouth	12 (80.0)	9 (56.2)	0.16
Other	3 (20.0)	7 (43.8)	
Histological grade			
Well-differentiated	10 (66.7)	4 (25.0)	***0.02**
Moderately differentiated and poorly differentiated	5 (33.3)	12 (75.0)	
Treatment			
Surgery	12 (80.0)	16 (100)	0.06
Surgery + radiotherapy/chemotherapy	3 (20.0)	0	
Margin status (mm)			
≥ 5	14 (93.3)	15 (93.7)	0.96
< 5	1 (6.7)	1 (6.3)	
Perineural invasion			
No	8 (53.3)	6 (37.5)	0.38
Yes	7 (46,7)	10 (62.5)	
Lymphovascular invasion			
No	12 (80.0)	11 (68.7)	0.48
Yes	3 (20.0)	5 (31.3)	
Depth of invasion (mm)			
< 5	8 (53.3)	6 (37.5)	0.38
≥ 5	7 (46.7)	10 (62.5)	

**p < 0.05. In bold, significant association of Clinicopathological characteristics and HPSE1 overexpression in OSCC samples.*

from treatment initiation until death due to tumor or last known date alive, time from treatment initiation until the diagnosis of the first recurrence (local, regional, or distant), or last known date alive for those without recurrence. Also, normal oral tissues were obtained from five individuals without cancer subjected to standard third molar surgery procedures. Written informed consent was obtained from each individual, and this study was approved by the Institutional Ethics Committee of the Faculty of Medicine of Jundiaí, Jundiaí, SP, Brazil (protocol number 45091715.1.0000.5412).

Immunohistochemistry

Heparanase 1 (HPA, HPSE1) immunostaining was performed using the streptavidin–biotin–peroxidase complex method on 32 FFPE oral cancer specimens and five normal oral tissue specimens from non-cancerous individuals. Briefly, staining was performed using the standard method of deparaffinization and gradual rehydration, followed by heat-mediated antigen retrieval in 10 mM citric acid at pH 6.0 in a pressure cooker. The sections were further treated with 3% hydrogen peroxide to block endogenous peroxidase activity. Primary antibody incubation with polyclonal rabbit HPSE1 antibody (bs-1541R, Bioss Antibodies, United States), diluted 1:200, was carried out overnight, followed by the LSAB method (LSAB + System-HRP kit, Dako, United States). Detection was carried out using 3,3′-diaminobenzidine tetrahydrochloride (Sigma-Aldrich, United States) containing the 0.01% H_2O_2 detection system. Control reactions were performed by omission of the primary antibody. Immunoexpression of HPSE1 was analyzed semiquantitatively by the following criteria: the percentage of

cytoplasm positivity was graded from 0 to 4 (0: no staining; 1: 1–25% staining; 3: 51–75% staining; 4: 76–100% staining) and the intensity, from 0 to 3 (0: no staining; 1: weak staining; 2: moderate staining; 3: strong staining). Tumor final scores were calculated as the sum of both categories, and the samples were classified as presenting low (0–4) or high (5–7) expression of HPSE1.

Cell Culture

Human oral cancer cell lines SCC-4, SCC-9, SCC-15, SCC-25, and HSC-3, originally isolated from oral cancer (OSCC) of the human tongue, were obtained from the American Type Culture Collection (ATCC). The SCC-4, -9, -15, and -25 cells were grown in DMEM plus Ham's F12 medium (DMEM/F-12), supplemented with 10% fetal bovine serum (FBS, Life Technologies, Inc.), penicillin (100 U/ml), streptomycin (100 μg/ml), and 0.4 μg/ml hydrocortisone. HSC3 human oral cancer cell line was placed in DMEM supplemented with 10% FBS, 100 units/ml penicillin, 100 μg/ml streptomycin, and 2 mM glutamine. The HPSE1-silenced (HPSE1-) and -upregulated (HPSE+) clones derived from the SCC-9 line were cultured in the same maintenance medium with the addition of 0.25 μg/ml puromycin and 5 μg/ml geneticin, respectively, for these cell expansion. Non-transformed human gingival keratinocyte cell line (HGK), obtained from mucosal keratinocytes and found to be spontaneously immortalized, was cultured in a serum-free, low-calcium medium (Gibco's Keratinocyte-SFM; Invitrogen, United States) containing specific supplements and antibiotics, as previously described (Mäkelä et al., 1998; Rodrigues et al., 2017). Cells were maintained at 37°C in a humidified atmosphere of 5% CO_2.

Cell Cultures and Stable Cells Mediating Heparanase 1-Silencing and Heparanase 1 Upregulation

Considering that SCC-9 cell line had an intermediate expression level of HPSE1 within all four oral cell lines analyzed, we selected this cell line to carry out both gain- and loss-of-function *in vitro* experiments. Then, transduction of SCC-9 cells with control (scrRNA control cells) or shRNA HPSE1 sequences was performed using HuSH shRNA plasmid panel (short-hairpin RNA) following the manufacturer's instructions (OriGene Technologies, United States/HPSE1, human, cat. No. TR307138). Briefly, after transduction, the silenced cells were selected in the presence of 1 μg/ml of puromycin (Invitrogen, United States) for 2 weeks. For the gain-of-function strategy, the transduction of SCC-9 was performed using TrueORF cDNA clones and PrecisionShuttle vector system containing the human HPSE1 cDNA clone (ORF with C-terminal GFP tag) (cat. No. RG219659) along with control SSC-9 Mock transduced cells following the manufacturer's instructions (OriGene Technologies, United States). Then, after transduction, these cells were selected in the presence of 500 μg/ml of geneticin (ThermoFisher, United States) for 2 weeks. The insertion of the plasmids in the clones of transduced cells under- and overexpressing HPSE1 was confirmed by PCR with sequences 5′ primer and 3′ primer of the Origen Kit components before the expansion of the transduced clones.

Real-Time Quantitative PCR

Real-time quantitative PCR was carried out to determine the efficiency of HPSE 1 silencing and upregulation in oral cancer cell lines and to investigate HPSE1 expression in oral cancer and non-cancerous oral tissue samples. Total RNA was isolated and purified using the TRIzol reagent method in accordance with the manufacturer's protocol (Invitrogen, United States). Reverse transcription reactions were conducted with a single step with 1 ug of RNA (each sample) using the commercial kit Luna OneStep qPCR (Biolabs) in accordance with the manufacturer's protocol. All qRT-PCRs were prepared and run in triplicates using the quantitative thermal cycler 7500 Real-Time PCR-System (Applied Biosystem, United States). Gene expressions of *HPSE1* were determined by the relative quantification using the $2^{-\Delta\Delta Ct}$ method, and the housekeeping gene *PPIA* (cyclophilin A) was used as a reference gene for data normalization. For the *HPSE1* expression analysis in the clinical samples, a pool of five normal oral tissues from individuals without cancer was used as the reference for the relative quantification. The amplification conditions were standardized following the manufacturer's protocol as follows: 10 min at 55°C for enzyme activation, 1 min at 95°C for initial denaturation, followed by 45 cycles of denaturation at 95°C for 10 s, and 60 s at 60°C for pairing and extending the primers. At the end of amplification, an additional dissociation step was included (45 cycles with a decrease of 1°C every 15 s, starting at 95°C) to generate a dissociation curve (melting curve) necessary to confirm the specificity of the amplified product. Additionally, the expression analysis of markers relevant to invasion (i.e., EMT markers—E-cadherin, N-cadherin and vimentin; and ECM remodeling markers—MMP2 and MMP9) and angiogenesis (VEGFA) was carried out in cell lines and HPSE1-silenced and -upregulated clones, using qPCR as previously described (Rodrigues et al., 2017). The sequence of primers used is shown in **Supplementary Table S2**.

Western Blotting Analysis

Western blotting was performed to determine the HPSE1 protein expression levels of parental OSCC cell line (WT), and the silenced and upregulated clones. The cells were washed with cold PBS and lysed with a buffer containing 50 mM NaCl, 0.5% Triton X-100, 0.5 mg EDTA/mL, and 10 μL/ml cocktail protease inhibitor (cat. P-8340—Sigma Chemical Co., St. Louis, MO, United States). After centrifugation (10,000×g at 4°C, 10 min), protein concentrations were determined using the Bradford method following the manufacturer's instructions (Bio-Rad Protein Assay, Bio-Rad, United States). A total of 30 ug of protein was subjected to SDS-PAGE electrophoresis and transferred to nitrocellulose membranes (Bio-Rad, United States), which were blocked with non-fat dry milk (0.1% of PBS with Tween 20) and incubated overnight (4°C) with specific primary antibodies (HPSE1/1:1000, Bioss-Bs-1541R). The membranes were washed and incubated with horseradish peroxidase-conjugated secondary anti-rabbit

antibody (1:2000/Cell Signaling Technology), followed by detection with enhanced chemiluminescence (GE Healthcare, United States). Anti-β-actin was employed as the loading control (AC-74, Sigma Aldrich, St. Louis, MO). GAPDH (1: 1000/Santa Cruz Biotechnology- Sc-25778) was used as the loading control. Immunoreactive bands were detected using enhanced chemiluminescence (ECL) Western Blotting System (GE Healthcare, United States) by G-Box system (Syngene).

Immunofluorescence Assay

To determine the localization of HPSE1, we used the immunofluorescence assay. Briefly, the parental oral cancer cell line (W)T, stable inhibition clone shRNA HPSE1, and upregulated clone orfRNA HPSE1+ were plated/well at a density of 5×10^4 (24-well plate) containing sterile glass coverslips. The immunofluorescence (IF) samples were fixed in paraformaldehyde (4%), and the primary antibodies were diluted and applied to the cells (1: 250 −1 ml 3% BSA in TBS-T and 4 µL of HPA antibody −1). The secondary antibody solution (1: 1000 −1 ml of 3% BSA in TBS-T, 1 µL of Rabbit Alexa Fluor 488) was added to each cell/well, and then the cells were mounted onto glass slides with Vectashield mounting medium (Vector Labs, United States). The slides were visualized under a Leica fluorescence microscope (LEIKA, Germany) with a 40 × or ×60 × oil immersion objectives.

Cell Cycle Analysis

The distribution of cells in the cell cycle was evaluated by flow cytometry. Cells were incubated in DMEM/F-12 without serum for 24 h and then trypsinized, resuspended in 70% ethanol, treated with 10 µg/ml of RNAse (Sigma-Aldrich, United States), and stained with 50 µg/ml of propidium iodide (Sigma-Aldrich, United States). DNA contents were then analyzed using an FACSCalibur flow cytometer (BD Biosciences, United States).

Apoptosis Analysis

For the apoptosis assay, cells were resuspended in binding buffer (10 mM HEPES pH 7.4, 150 mM NaCl, 5 mM KCl, 1 mM $MgCl_2$, and 1.8 mM $CaCl_2$) containing Annexin V-Alexa Fluor 647 and 7-AAD (BD Biosciences, United States). Cell apoptosis, characterized by positivity for annexin V, was detected using an FACSCalibur flow cytometer (BD Biosciences, United States). A minimum of 10,000 events were analyzed for each sample.

Cell Viability and Proliferation Assay

Cell viability was determined using MTT assay (MTT, Sigma), as defined earlier by Alam et al., 2011. Briefly, 20 ml of MTT (5 mg/ml) was added to each well containing a density of 1×10^4 cells [parental OSCC cells, HPSE1-inhibited (shRNA HPSE1-) and -upregulated (orfRNA HPSE1+) clones]. After 3 h of incubation at 37°C, the cell supernatants were discarded, the MTT crystals were dissolved with DMSO, and the absorbance was measured at 570 nm at 12, 24, and 48 h. The percentage of viability was defined as the relative absorbance of transfected versus non-transfected control cells. The experiment was performed three independent times in quintuplicates.

Migration Assay

To analyze the movement of the cell toward the artificial space, a scratch was created in a monolayer confluent cell, the oral cancer cell lines, and their respective HPSE1-inhibited and -upregulated clones were plated at 5×10^4 in 12-well plates. When the cell monolayer reached 90–95% confluence, a scratch was made with a tip of 200 µL (time 0). Following 24 and 48 h, the images were recorded by a camera coupled to the inverted microscope (Nikon, Eclipse TS100) using Motic Image Plus 2.0 software.

Adhesion Assay

For the assay, 96-well plates were coated with 10 ug/cm^2 of type I collagen (Corning, Cat # 354236) in 100 ul of PBS for 24 h at 4°C. A quantity of 200 ul of PBS was used to wash the wells each three times, followed by covering with 200 ul of 3% BSA in PBS for 2 h at 37°C. Control wells were coated with only 3% BSA solution. Then, 3×10^3 cells were harvested and resuspended in 100 ul DMEM/F12 medium supplemented with 3% BSA, added to each well, and incubated at 37°C/5% CO_2 for 1 h. After washing the non-adherent cells, the remaining cells were fixed with 4% paraformaldehyde for 15 min and stained with 1% toluidine blue in 1% borax solution. The absorbance was measured at 650 nm by using an Epoch plate reader (Biotek).

Invasion Assay

Transwell (Corning, United States) assay was carried out to examine OSCC cell invasion. Briefly, the membranes were coated with 50 ul of gelatinous matrix Miogel (2.4 mg/ml) with type I collagen (0.8 mg/ml) (Corning, Cat # 354236) (Salo et al., 2015) and incubated for 12–16 h. Then, the cells were plated in 200 ul of DMEM/F12 medium without FBS (8×10^4 cells per well). As chemo-attractive, 500 ul of complete DMEM/F12 medium was added to the bottom layer of the inserts inside the wells, so the plates were incubated at 37°C/5% CO2 for 72 h. The invasion profile was assessed by carefully removing the formed membrane with cells from the inside of the insert.

The invading cells on the lower side of the insert were fixed in 4% paraformaldehyde for 15 min and stained with 1% toluidine blue in 1% borax solution. Then the cells were eluted in a 1% SDS solution for 5 min. Dye absorbance was measured at 650 nm in the Epoch plate reader (Biotek).

Tube Formation Assay

To verify the potential HPSE1 modulation in the capillary structure formation, the oral cancer cells, the lines, and their respective inhibited and upregulated clones were grown in a culture medium of 10% FBS. After 70% confluence, the cells were incubated with SFB 0% for more than 24 h, and the preconditioned medium from each cell was collected. A measure of 50 µl of gelatinous matrix Miogel (2.4 mg/ml) with type I collagen (0.8 mg/ml) (Corning, Cat # 354236) (Salo et al., 2015) was polymerized in 96-well plates. HUVECs were incubated without FBS in RPMI1640 medium for 24 h. The cells were suspended in RPMI-1640 and added to wells coated with Miogel at a density of 1×10^4 cell medium plus 80% the preconditioned medium and incubated at 37°C for 48 h. During the experimental period, cell morphology of capillary structures was observed and photo-documented at 12 and 24 h. The formation of the tube was

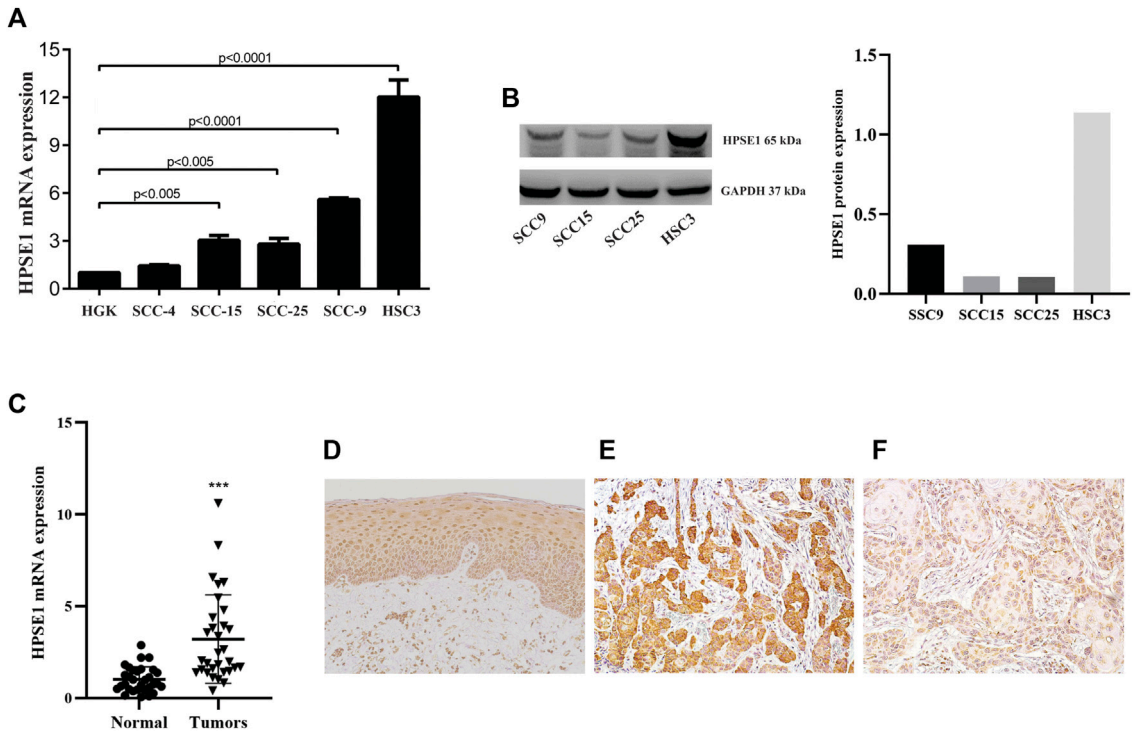

FIGURE 1 | HPSE1 is overexpressed in OSCCs patient samples and OSCC-derived cell lines. Total RNA from fresh samples and cell lines was converted to cDNA and subjected to qPCR. For gene expression analysis of tissue samples relative quantification was based on the comparison of a pool of five normal oral tissues, while the spontaneously immortalized but non-transformed epithelial cell line HGK was used as reference for comparison with OSCC-derived cell lines. The levels of HPSE1 mRNA were significantly higher in OSCC cell lines compared with HGK cells **(A)**. The high expression levels of protein HPSE1 were confirmed on OSCC-derived cell lines by Western Blot analysis **(B)**. The levels of HPSE1 mRNA were also significantly higher in OSCC tissue samples compared to normal oral mucosa **(C)**. Representative images in a high-power field (200×) of immunohistochemical analysis for HPSE1 in Normal oral tissue **(D)** and OSCC tissue preparations confirmed its higher expression at protein level; with a distinct cytoplasmic distribution and intensity in oral cancer samples expressing both higher **(E)** and lower **(F)** levels of HPSE1. Results were statistically determined by ANOVA followed by Tukey multiple comparison test, where $^{**}p < 0.005$, $^{***}p < 0.001$, and $^{****}p < 0.0001$.

examined and photographed under an inverted microscope. The quantification of antiangiogenic activity was done using Motic Image Plus 2.0 software and calculated by measuring the length of the tubule wall perimeter of endothelial cells.

Statistical Analysis

The expression of HPSE1 among different tissues was analyzed and compared using the Kruskal–Wallis test with Dunn's post hoc test, and the receiver operating characteristic (ROC) curve with area under the curve (AUC) was applied to compare the discriminatory ability of the HPSE1 between normal and tumor tissues. A chi-squared test was used to analyze the association of HPSE1 expression and clinicopathological features. The Kaplan–Meier method was used to construct survival curves that were compared using log-rank tests. The Cox proportional hazard model was used for univariate and multivariate survival analysis. For the multivariate analysis, the stepwise method, including the clinicopathological parameters verified in the univariate analysis as potential predictor variables, was performed to characterize the independent survival factors of OSCC patients. In this method, variables are sequentially included, and those that become non-significant are then removed. The final model is built only with variables displaying a p value ≤ 0.05. These statistical analyses were performed using MedCalc® statistical software, version 19.5.3 (MedCalc Software Ltd., Ostend, Belgium). All *in vitro* assays were performed at least three times, and data were analyzed using one- or two-way analysis of variance with repeated measures (RM-ANOVA) with post hoc comparisons based on Tukey's multiple comparisons test. These analyses were performed using GraphPad Prism software version 5.0. For all statistical analyses, the significance level was set at 5% ($p \leq 0.05$).

RESULTS

Heparanase 1 is Overexpressed in the Oral Squamous Cell Carcinoma Cell Lines and Tissues

The expression of HPSE1 was analyzed by qPCR, and the levels of HPSE1 mRNA were significantly higher in the OSCC cell lines SCC-15 ($p < 0.005$), SCC-25 ($p < 0.005$), SCC-9 ($p < 0.001$), and HSC-3 ($p < 0.0001$) compared with the immortalized, but not transformed, epithelial cell line HGK (**Figure 1A**). Western bloting analysis was carried to confirm HPSE1 expression in these OSCC cell lines (**Figure 1B**). The cell line SCC-9 was selected to carry out functional *in vitro* assays to investigate

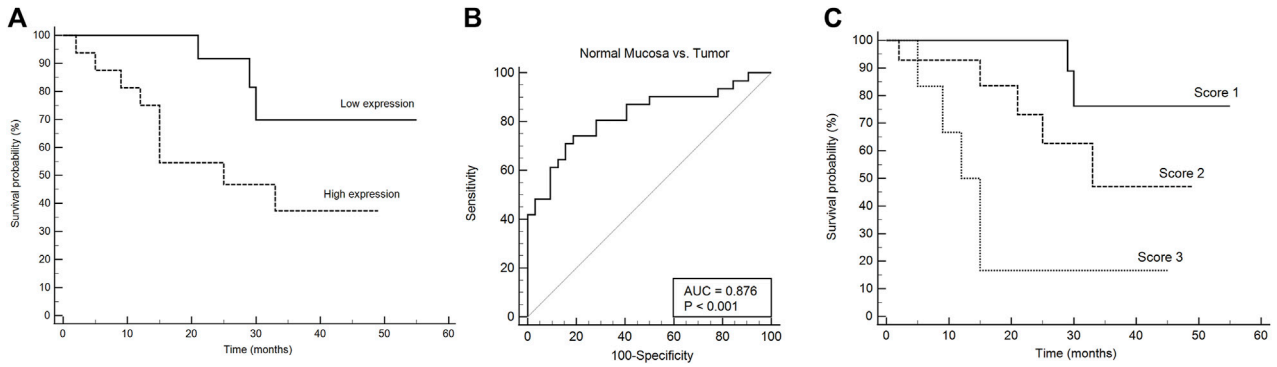

FIGURE 2 | HPSE1 overexpression discriminates OSCC and normal samples and predicts low patient survival. **(A)** Kaplan–Meier cumulative curves for disease-free survival of patients with OSCC as a function of HPSE1 expression, showing a 70% probability of death in patients with higher expression of HPSE1 compared with those with low expression. **(B)** Receiver operating characteristic (ROC) curves showing the ability of the HPSE1 overexpression distinguishes OSCC tumors from normal oral samples. **(C)** Kaplan–Meier of multivariate survival analysis combining HPSE1 expression levels with pT stages, where score 1: HPSE1 lower expressing samples associated with pT1/2, score 2: HPSE1 lower expressing samples associated with pT3/4 or higher HPSE1 with pT1/2, and score 3: HPSE1 higher expressing samples associated with pT3/4. These results confirmed that HPSE1 overexpression was significantly associated with higher grade tumors.

the HPSE1 role in oral cancer tumorigenesis. Of note, we checked the nuclear and cytoplasmic HPSE1 protein expression in the SCC-9 cell line; these OSCC cells showed higher HPSE1 expression in the cytoplasm compartment than in the non-malignant HGK cells, where the HPSE1 expression was more restricted to the nuclear fraction (**Supplementary Figure S1A**).

We also sought to determine HPSE1 mRNA expression levels in 35 fresh samples from OSCC and normal oral mucosa ($n = 40$). For that, equivalent concentrations of total RNA of these normal tissues were pooled and used as a reference for mRNA relative quantification. A significantly higher level of HPSE1 mRNA was observed in the group of tumors than the controls ($p < 0.001$, **Figure 1B**), and the variation on HPSE1 expression levels was very small among control samples. For instance, we also verified the HPSE1 expression pattern in a subset of 33 OSCCs, and in normal oral tissue (**Figure 1D**), by immunohistochemistry analysis. Interestingly, the immunostaining for tumor cells revealed that HPSE1 upregulation had marked staining intensity in the cytoplasm of OSCC tissues (**Figures 1E,F**). Immunoreactivity for HPSE1 was also detected in some inflammatory, endothelial, and stromal cells.

Expression of Heparanase 1 is Related to Reduced Survival of Oral Squamous Cell Carcinoma Patients

We then assessed the association between mRNA expression of *HPSE1* and the clinical prognosis of OSCC patients. Patients with *HPSE1* overexpression had a significantly poorer disease-specific survival rate than those with lower expression. The probability of death was approximately 70% among patients expressing higher levels of *HPSE1*, significantly "higher" than the ones expressing lower *HPSE1* (37%) ($p < 0.05$, **Figure 2A**). The receiver operating characteristic (ROC) curve showed the ability of the *HPSE1* higher expression in discriminate OSCC tumors and normal oral samples (AUC = 0.876, $p < 0.001$) (**Figure 2B**). Also, recurrence was diagnosed in 30% of patients with higher expression of *HPSE1* after up to a 55-month follow-up, compared with 6.25% for those with low HPSE1 expression.

To investigate the association between mRNA expression levels of *HPSE1* and clinicopathological features, 35 OSCC patients were divided into *HPSE1* lower and higher expressing subgroups, with the median value as the cutoff. Considering the clinicopathological characteristics of tumors (**Table 1**), the overexpression of *HPSE1* in OSCC tissues was significantly associated with moderately and poorly differentiated histological grades of tumors ($p = 0.02$). Our results also demonstrate a significant correlation between the expression of *HPSE1* in tumor cells and cervical lymph node metastasis (pN stage), in that patients with metastasis (N+) had significantly higher HPSE1 expression ($p = 0.02$). Approximately 81% of the advanced stage tumors (pTNM stages III and IV) demonstrated high levels of *HPSE1*, while only 18% of pTNM stages I and II tumors presented high *HPSE1* expression ($p = 0.04$). Univariate analysis for disease-specific survival of patients with the OSCC cohort is also provided in **Table 2**. This analysis revealed that tumor size (pT3+pT4) [7.81 (95% CI 1.78–34.12, $p = 0.006$)], pTNM advanced stages (III and IV) [3.48 (95% 1.09–11.14, $p = 0.035$)], and barely lymphovascular invasion and HPSE1 expression were prognostic factors of the presented OSCC cohort. For HPSE1, a hazard ratio (HR) of 3.21 (95% CI 1.00–10.25, $p = 0.047$) was found for higher *HPSE1* mRNA expression about low *HPSE1* levels. Similarly, the presence of invasion in lymph vasculature had an HR of 3.88 (95% CI 1.02–14.82, $p = 0.047$).

It was also observed that the size of the primary tumor (pT stage) was a risk factor for disease-specific survival [4.48 (95% CI 1.38–14.6, $p = 0.0126$)], but neither the local regional metastasis at diagnosis (pN stage) nor the expression of the HPSE1 mRNA itself (**Supplementary Figure S2**). To strengthen the prognostic data of the independent factors, we performed univariate and multivariate survival analyses by combining HPSE1 expression levels with the pT stage. For that, we categorized three different scores: score 1: HPSE1 lower expressing samples in association

TABLE 2 | Univariate analysis for disease-specific survival of patients with oral squamous cell carcinoma.

	Overall survival	
	HR (95% CI)	***p* value**
Age (years)		
< 61	1	0.54
≥ 61	1.42 (0.45–4.48)	
Gender		
Male	1	0.55
Female	0.64 (0.14–2.81)	
Smoking habit		
No	1	0.52
Yes	1.62 (0.36–7.24)	
Drinking habit		
No	1	0.24
Yes	2.73 (0.51–14.55)	
pT stage		
pT1 + pT2	1	***0.006**
pT3 + pT4	7.81 (1.78–34.12)	
pN stage		
N0	1	0.17
N+	2.23 (0.70–7.09)	
pTNM		
Early stage (I and II)	1	***0.035**
Advanced stage (III and IV)	3.48 (1.09–11.14)	
Location		
Tongue and floor of mouth	1	0.17
Other	2.34 (0.68–8.03)	
Tumor grading		
Well-differentiated	1	0.91
Moderately differentiated and poorly differentiated	0.93 (0.29–2.95)	
Treatment		
Surgery	1	***0.033**
Surgery + radiotherapy/chemotherapy	218.6 (1.50–31745.8)	
Margin status (mm)		
≥ 5	1	0.30
< 5	NA	
Perineural invasion		
No	1	0.17
Yes	2.24 (0.70–7.12)	
Lymphovascular invasion		
No	1	***0.047**
Yes	3.88 (1.02–14.82)	
Depth of invasion (mm)		
< 5	1	0.15
≥ 5	2.33 (0.72–7.49)	
Heparanase 1		
Low expression	1	***0.047**
High expression	3.21 (1.00–10.25)	

**p < 0.05. In bold, significant prognostic factors for OSCC cohort analyzed.*

with pT1/2, score 2: HPSE1 lower expressing samples in association with pT3/4 or higher HPSE1 with pT1/2, and score 3: HPSE1 higher expressing samples in association with pT3/4. The multivariate Cox regression analyses of the combination of HPSE1 expression and tumor size (pT) discriminated well and confirmed that overexpression of this enzyme is significantly associated with more aggressive tumors of high rank [HR: 3.22 (95% CI: 1.42–7.32, $p = 0.005$)] (**Figure 2C**). Together, these findings suggest that the expression levels of HPSE1 could be used in association with the clinicopathological parameters to better predict the poor prognosis of OSCCs. Considering the closer *p*-value for HPSE1 expression as an independent factor for OSCC prognosis, future studies should consider increasing the patient sample cohort.

Heparanase 1 Knockdown Increases Apoptosis and Suppresses the Proliferative Potentials of Oral Squamous Cell Carcinoma Cells

To gain insights into the role of HPSE1 in OSCC progression, HPSE1-silenced and -upregulated cells were achieved from the SCC-9 cell line by lentivirus-mediated shRNA and human GFP-tagged ORF plasmid, respectively. Conventionally, cells transduced with

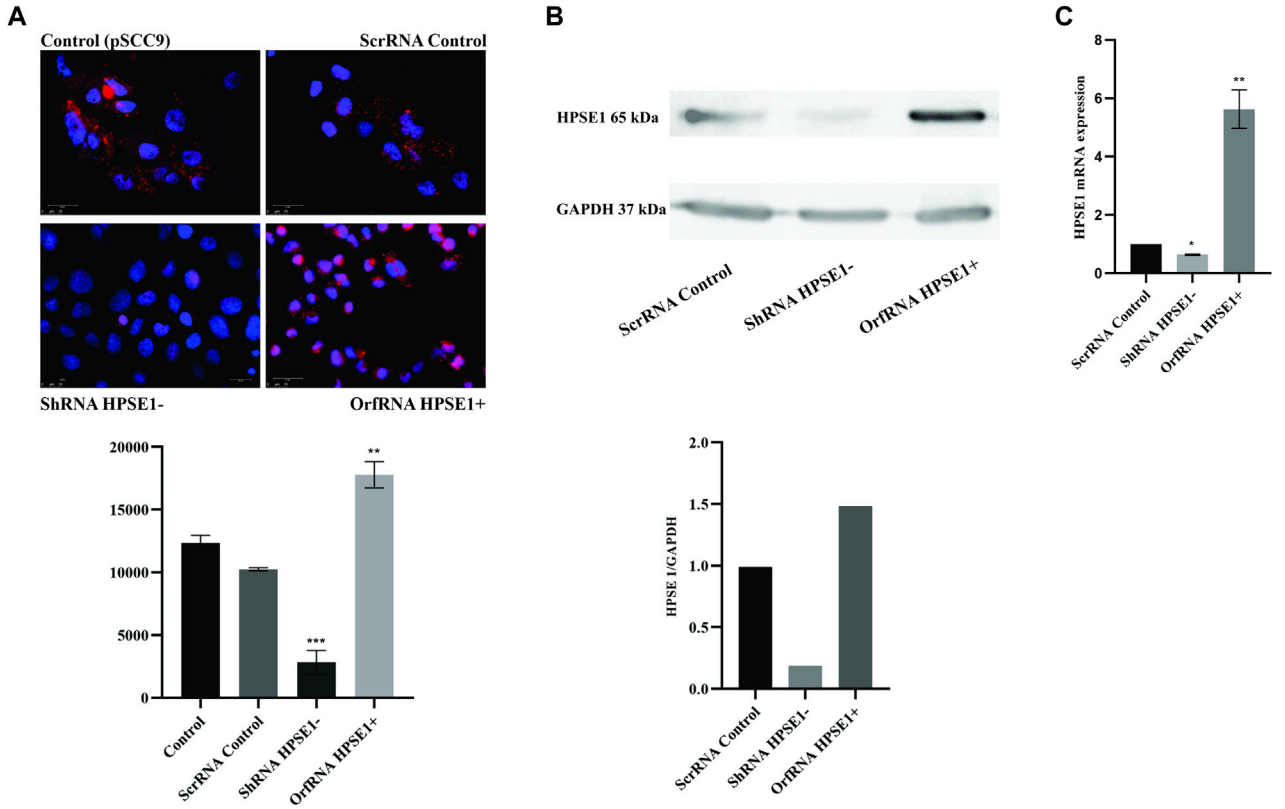

FIGURE 3 | HPSE1 knockdown and upregulation efficiency in OSCC cells. The efficiency of endogenous HPSE1 modulation was verified by Immunofluorescence **(A)**, Western Blot **(B)** and RT-qPCR **(C)** analyzes. For the loss-of-function strategy, SCC-9 cells were transduced with shRNA expressing a vector sequence against HPSE1 (shRNA HPSE1−) and empty vector (scrRNA control). For the gain-of-function strategy, SCC-9 cells were transduced with a ORF clone in a shuttle vector to enhance HPSE1 expression (orfRNA HPSE1+), along with mock-transduced cells as described in *Methods*. shRNA HPSE1− cells showed a significant reduction and orfRNA HPSE+ cells showed a significant upregulation of HPSE1 in both mRNA and protein levels compared to scrRNA control and parental mock-transduced SCC-9 control cells (pSCC9), without targeting sequences. Results were statistically determined by ANOVA, followed by Tukey's test, where $^{*}p < 0.05$, $^{**}p < 0.01$, $^{***}p < 0.001$, and $^{****}p < 0.0001$.

lentivirus carrying an shRNA-targeted sequence to HPSE1 exhibited a significant reduction in both HPSE1 protein ($p < 0.001$, **Figures 3A,B**) and mRNA ($p < 0.05$, **Figure 3C**) levels in comparison to parental SCC-9 cells (control) or cells transduced with the vector control (scrRNA), non-targeting sequence. Accordingly, cells transduced with the plasmid carrying a specific ORF sequence to enhance HPSE1 expression demonstrated a significant upregulation in both HPSE1 proteins ($p < 0.01$, **Figures 4A,B**) and mRNA ($p < 0.01$, **Figure 3C**) levels in comparison with parental and mock-transduced control cells. Of note, the cellular fraction analysis of the SCC-9 nuclear and cytoplasm compartments by WB analysis revealed that abrogation of HPSE1 protein expression was markedly reduced in the cytoplasmic fraction of shHPSE1-silenced cells and that ORF-mediated upregulation of HPSE1 enhanced cytoplasmatic expression of HPSE1 (**Supplementary Figures 1B,C**).

The specific shRNA against *HPSE1* drastically impaired the *in vitro* proliferation of SCC-9 cells ($p < 0.01$, **Figure 5A**). Accordingly, HPSE1 downregulation stimulates a significant increase in the cell amount at G0–G1 phases ($p < 0.001$) and an important reduction at the S phase ($p < 0.0001$) as compared to controls (**Figure 4C**). Conversely, orfHPSE1-upregulated cells showed enhancement in proliferation ($p < 0.0001$, **Figure 4A**), with marked reduction of cells at G0-G1 phases ($p < 0.001$) and an increase at the S phase ($p < 0.0001$, **Figure 4C**), compared to control cells. Also, HPSE1 upregulation was able to substantially decrease the number of cells in apoptosis ($p < 0.0001$, **Figure 4B**). Contrariwise, the number of apoptotic cells was significantly increased in SCC-9 shHPSE1-transfected cells ($p < 0.0001$, **Figure 4B**).

Heparanase 1 Overexpression Is Associated With Migration, Invasion, Extracellular Matrix Remodeling, and Acquisition of Epithelial–Mesenchymal Transition Properties of Oral Squamous Cell Carcinoma Cells

During the process of invasion and metastasis, the epithelial aspect of tumor cells is lost as the mesenchymal phenotype is evoked, which characterizes the process known as EMT. To acquire an understanding of the role of HPSE1 in the regulation of EMT

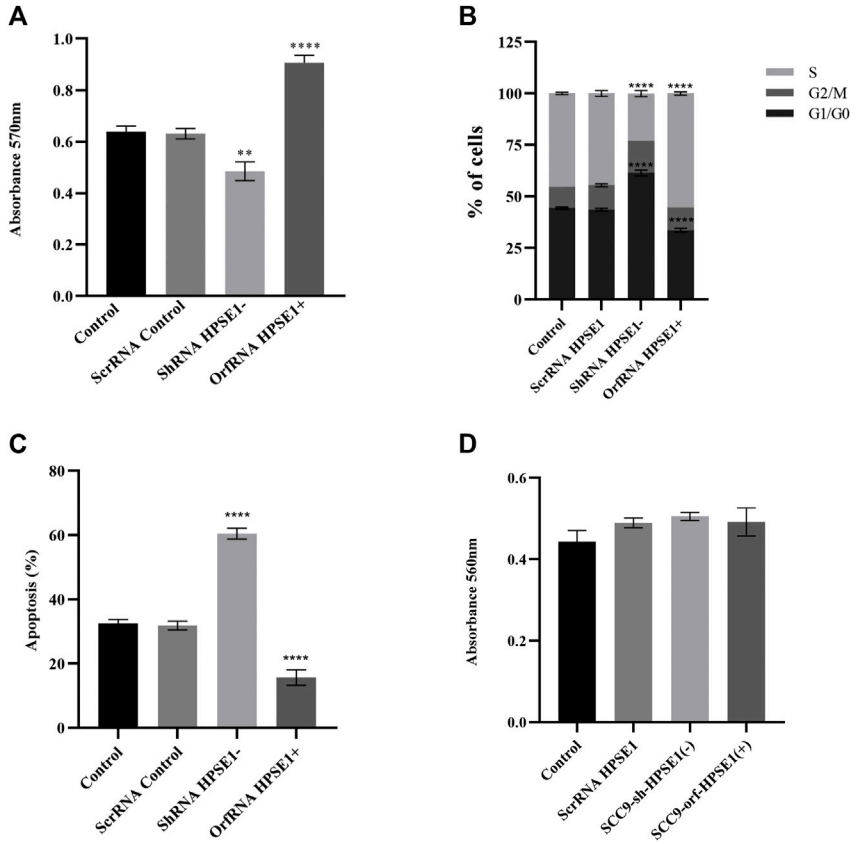

FIGURE 4 | Downregulation of HPSE1 inhibits proliferation and enhances apoptosis of OSCC cells. Cells were subjected to MTT cell proliferation **(A)**, DNA content cell cycle analysis **(B)**, and apoptosis **(C)** assays. **(A)** Cell Proliferation Assay of the OSCC SCC9 cell line (Control) compared to empty vector SCC9 control clone (ScrRNA control), HPSE1 inhibitory/silencing SCC9-ShRNA HPSE1– clone, and the HPSE1 overexpressing SCC9-OrfRNA HPSE1+ clone. **(B)** Quantification of cell cycle analysis was performed by flow cytometry after staining with propidium iodide for the SCC-9 control cells and the respectives HPSE1-modulated clones. Abrogation of HPSE1 induced arrest of the SCC-9 cells cycle in G1 phase, and its upregulation significantly induced cell proliferation. **(C)** Flow cytometric analysis of apoptosis showed a remarkable increase in the number of apoptotic cells in HPSE1-silenced cells (ShRNA HPSE1–), while SCC-9 overexpressing HPSE1 (Orf-RNA HPSE1+) exhibited a reduction in apoptosis. **(D)** No significant differences in cell adhesion properties were observed among any transduced clones modulating HPSE1 expression, compared to parental mock-transduced cells (control). Plots compose experimental triplicate analysis and were statistically calculated using ANOVA followed by Tukey's test, where $*p < 0.05$, $**p < 0.01$, $***p < 0.001$, and $****p < 0.0001$.

and invasion of oral cancer, we examined several features such as motility, invasiveness, adhesive capacity, expression of the epithelial marker E-cadherin, mesenchymal markers N-cadherin and vimentin, and ECM remodeling markers. The adhesive properties of HPSE1 in SCC9 cells were first investigated, and neither upregulation nor downregulation of HPSE1 affected SCC9 cell adhesion on surfaces coated with type 1 collagen (**Figure 4D**). Next, the scratch wound migration assay showed that upregulation of HPSE1 significantly enhanced the migration ($p < 0.001$, **Figure 5A**) and invasiveness ($p < 0.001$, **Figure 5B**) of SCC9-orfHPSE1 cells, whereas shHPSE1-silenced cells revealed significantly lower migration and invasion than the controls.

To further characterize the effects of HPSE1 on the expression of EMT and ECM remodeling makers, we examined the modulation of mRNA levels of *E-cadherin*, *vimentin*, *N-cadherin*, *Snail*, *Twist*, *MMP9*, and *MMP2* in HPS1-downregulated and -upregulated SCC9 cells by qRT-PCR. Significantly reduced levels of E-cadherin mRNA were observed in HPSE1-upregulated SCC9 cells ($p < 0.05$, **Figure 5C**). Concomitantly, HPSE1 increased the mRNA expression of the mesenchymal marker vimentin ($p < 0.05$), but not N-cadherin, and augmented the metalloproteinases MMP2 ($p < 0.01$) and MMP9 ($p < 0.0001$) (**Figure 5D**). Conversely, shHPSE1-silenced cells had upregulation of E-cadherin mRNA levels ($p < 0.01$), whereas diminishing expression of N-cadherin and vimentin was observed in these ShRNA SCC-9-transfected cells (**Figure 5C**) but not significatively compared to control cells. The mRNA expression of Snail, but not Twist, was higher in both down- and upregulated HPSE1-transfected SCC-9 cells, although it was much higher in the cells overexpressing HPSE1 (**Figure 5C**).

Downregulation of Heparanase 1 Abrogates Endothelium Tube Formation and Induces Vascular Endothelial Growth Factor A Expression

We next assembled an *in vitro* tube formation assay, using human umbilical vein endothelial cell (HUVEC), to directly assess the possible effects of HPSE1 on oral cancer angiogenesis. HUVECs composed

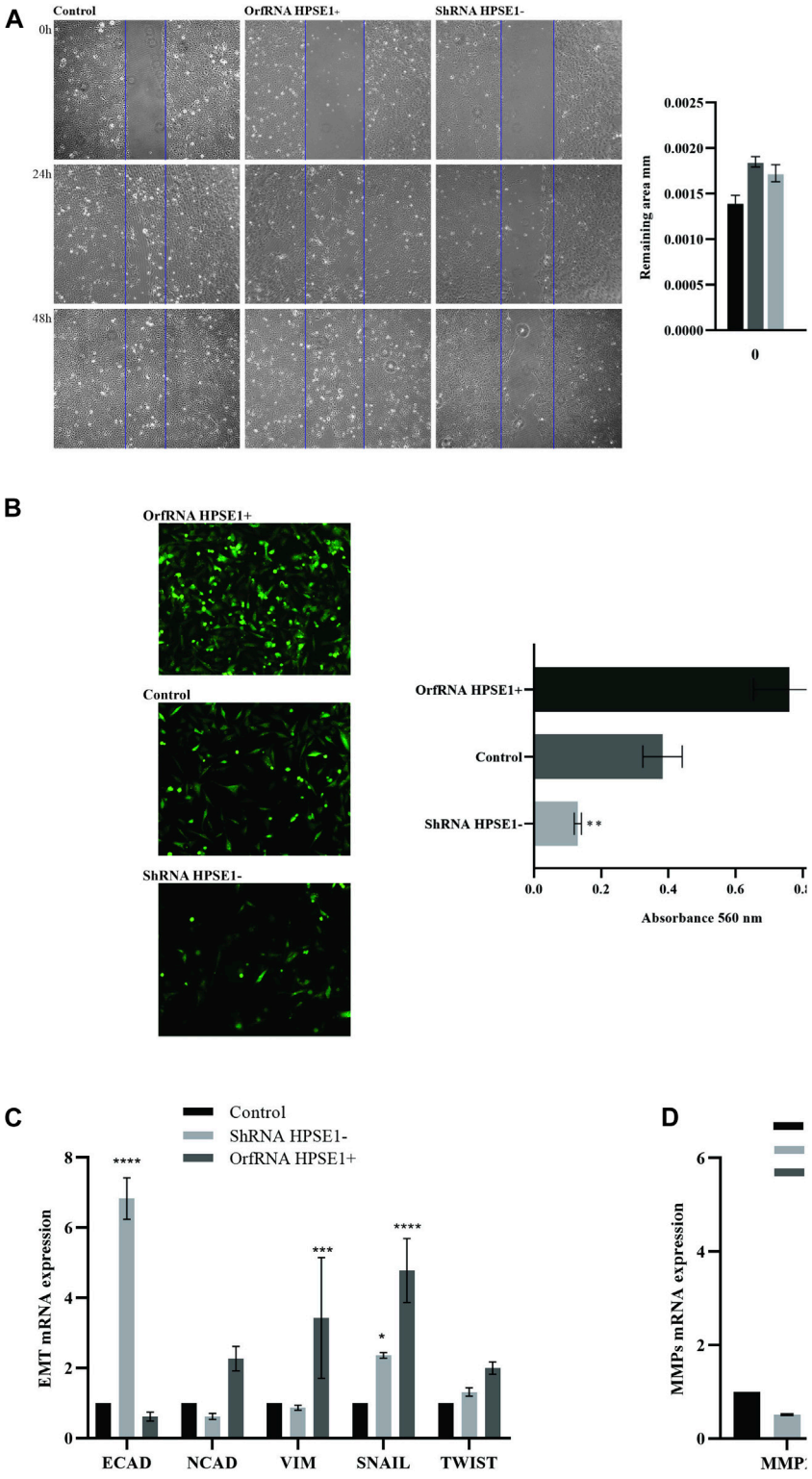

FIGURE 5 | Overexpression of HPSE1 is associated with migration, invasion, ECM remodeling, and acquisition of EMT properties. **(A)** Photomicrographs of cell lines were taken 0, 24, and 48 h after wounding (40X). The average width of the lacunae was measured. Migration of SCC-9 cells was significantly decreased in HPSE1-silenced cells (ShRNA HPSE1–) and increased in HPSE1-upregulated clones (OrfRNA HPSE1+). Migration analysis based on this assay showed that cells with lower expression of HPSE1 closed the scratch wound significantly slower than the SCC9 Control cells. **(B)** Invasion of SCC-9 cells was significantly inhibited by HPSE1 knockdown, and significantly enhanced after its upregulation. **(C)** Analysing EMT markers, the downregulation of HPSE1 significantly induced the expression of

(*Continued*)

FIGURE 5 | E-Cadherin (E-CAD), while OrfRNA HPSE1+ SCC9 clones overexpressing heparanase had a significant increasing of Vimentin (VIM) and SNAIL expressions. **(D)** The upregulation of HPSE1 significantly enhanced the expressions of MMP2 and MMP9. All the graphs compile experimental triplicate analyses, and the results were obtained by ANOVA followed by Tukey assay, where *$p < 0.05$, **$p < 0.01$, ***$p < 0.001$, and ****$p < 0.0001$.

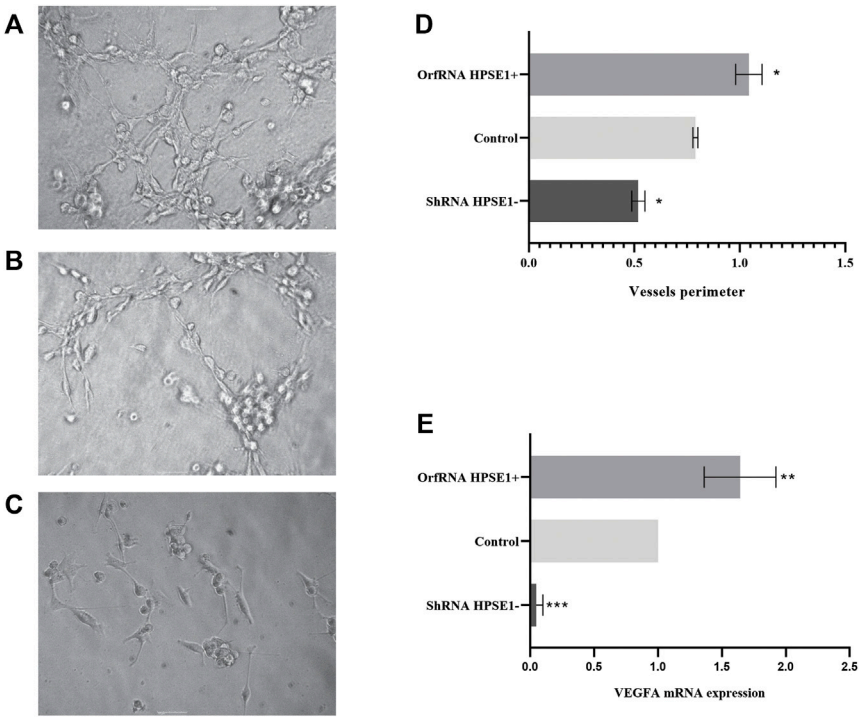

FIGURE 6 | Overexpression of HPSE1 enhances tumor neo-vascularization and induces VEGFA expression. HUVEC cells on a Miogel 2D layer co-culture. Photomicrograph of HUVEC endothelial cells added with preconditioned medium from OSCC cell lines and their respective clones after 12 h of experiment: **(A)** HUVEC cells incubated with preconditioned medium of SCC9-OrfRNA HPSE1+ clone overexpressing HPSE1 (100×); **(B)** HUVEC cells incubated with preconditioned medium of parental SCC9 (Control) (100×); **(C)** HUVEC cells incubated with preconditioned medium of SCC9-ShRNA HPSE1- clone with reduction of HPSE1 expression (100×). **(D)** Quantification of measures of the vessel circumference perimeter for each one of the conditions; the graph compiles two experimental triplicate analysis. **(E)** Gene expression analysis of endothelial growth factor VEGFA by qRT-PCR; the graph compiles folded expression values of relative quantification by ddCT obtained through comparison of clones OrfRNA HPSE1+ and ShRNA HPSE1– relative to the control SCC9 cells (normal reference = 1). Normalization of the analysis was performed using the endogenous control gene, PPIA. Statistical tests were performed using ANOVA followed by Tukey's test, where *$p < 0.05$, **$p < 0.01$, ***$p < 0.001$, and ****$p < 0.0001$.

interlaced tubes in Miogel (Salo et al., 2015) (**Figure 6**). HPSE1-depleted cells demonstrated a significantly lower number of tubes than control cells ($p < 0.05$, **Figures 6A–D**). Conversely, HPSE1 upregulation drastically promoted HUVEC tube formation ($p < 0.05$, **Figures 6A–D**). Afterward, we assessed whether endogenous HPSE1 modulation could interfere with the expression of the vascular endothelial growth factor A (VEGFA) gene, often associated with angiogenesis, vasculogenesis, and endothelial cell growth induction. As shown in **Figure 6E**, significantly reduced levels of VEGFA mRNA were observed in HPSE1-silenced SCC9 cells ($p < 0.001$), whereas markedly higher expression of VEGFA was detected in HPSE1-upregulated cells ($p < 0.01$) than the controls.

DISCUSSION

Although predictive factors such as age, clinical stage, and histological grade have been used to assess prognosis (Rodrigues et al., 2014; Almangush et al., 2015; Sawazaki-Calone et al., 2015), they still have poor predictive power. In addition to that, none of the currently molecular markers have yet been able to provide adequately knowledge to benefit these patients (Søland and Brusevold, 2013). Therefore, it is essential to identify biomarkers that can accurately identify and stratify low- and high-risk oral cancer patients, improving the capacity to predict those who would benefit from a more complex and intense treatment. The mammalian endoglycosidase HPSE1 is the predominant enzyme responsible for degrading heparan sulfate activity and is known to coordinate multiple biological activities to promote tumor growth, invasion, metastasis, angiogenesis, and inflammation (Vlodavsky et al., 2018). HPSE1 accomplishes this by cleaving heparan sulfate and thereby regulating the bioavailability of heparin-binding proteins, stimulating the tumor microenvironment (TME), resolving the tumor–host crosstalk, and inducing the activation of various genes, signaling pathways, and the

assembly of exosomes and autophagy (Vlodavsky et al., 2018). Taken together, these events ultimately influence tumor cell performance and their role in chemoresistance.

HPSE1 expression has also been previously shown to be elevated in several cancer types, including OSCC (Kurokawa et al., 2003; Väyrynen et al., 2018), and the overexpression was an indicator of worse prognosis (Rivara et al., 2016; Sanderson et al., 2017). So, in the present study, we sought to explore the potential roles of HPSE1 in OSCC biology. First, we confirmed that while heparanase mRNA and protein levels were expressed at very low levels in normal tissues, its expression was increased four times in primary tumors and was associated with poor prognosis, thus depicting the clinical relevance of HPSE1 in OSCC and positioning this enzyme as a valid drug target. Also, we verify that the probability of death was significantly higher among patients expressing higher levels of HPSE1 than the ones expressing lower levels. These results were in line with Vlodavsky et al. (2012) who also found that HPSE1 expression was associated with OSCC tumor invasion patterns in a xenograft model. Furthermore, high HPSE1 levels in primary tumor samples were significantly correlated with expanded malignity and the presence of metastatic disease (Hunter et al., 2014). These data corroborate with the suggestion that the upregulation of HPSE1 in primary tumors might increase its tendency to metastasize locally and remain remarkably upregulated in these tumor cells, which might as well successfully conquer distant organs (Vlodavsky et al., 2012).

Further analysis demonstrated that shortened disease-specific survival of OSCC patients was significantly associated with increased HPSE1 expression. In the univariate analyses, overexpression of HPSE1 proved to be a predictor of disease-specific survival along with consistent prognostic factors for OSCCs, such as tumors with high T classification, presence of cervical lymph node metastasis (N stage), and lymphovascular invasion. The multivariate Cox regression analyses of the combination of HPSE1 expression and tumor size (pT) confirmed that overexpression of this enzyme is significantly associated with higher grade more aggressive tumors. High levels of HPSE1 were also significantly associated with poorer prognosis, confirming HPSE1 as a prognosticator tool for OSCC. Indeed, recent studies reported the correlation of heparanase expression levels with a higher degree of the tumor, late stage, advanced tumor angiogenesis, and low patient survival (Jin and Zhou, 2017). Also, it is strongly suggested that dysregulated gene expression, a key feature of cancer, drives the overexpression of HPSE in the tumor microenvironment (TME), leading to pathological remodeling of the ECM and the release of cancer-promoting HSBPs (Hanahan and Weinberg, 2011; Hammond et al., 2014). HPSE also exhibits a variety of non-enzymatic functions, such as regulating gene expression, promoting cell adhesion, and tumor-promoting procoagulant activity (Nadir and Brenner, 2014; Sanderson et al., 2017). Thus, overexpression of HPSE in cancers promotes tumor growth and metastasis, leading to poor clinical prognosis (Rivara et al., 2016).

In the present study, we also showed that the localization of HPSE1 in oral cancer cells, from patients and cell lines, seemed to be correlated with the aggressiveness potential of those cells. Our results of immunohistochemical staining for heparanase showed marked positivity in oral cancer cells, particularly in the cytoplasmic compartment. Following these results, Leiser et al. (2011) reported that cytoplasmic localization of HPSE1 was associated with high-grade oral carcinomas.

Also, there have been pieces of evidence that the cytoplasmatic HPSE1 regulates the secretion, composition, and behavior of tumor cell-derived exosomes (Thompson et al., 2013). Other studies indicated that HPSE1 activates the syndecan–syntenin–ALIX pathway forming a linear axis that rules exosome formation (Roucourt et al., 2015; Rangarajan et al., 2020). Interestingly, ALIX-mediated syndecans and syntenin have been implicated in restraining exosome biogenesis, and HPSE1 was found to stimulate the secretion of exosomes and modify their composition and biological function (Vlodavsky et al., 2018). That scenario explains the relevant role of heparanase because once released, tumor-derived exosomes can travel through the body and impact resident cells at locations distal to the tumor, thereby aiding in the preparation of the pre-metastatic niche and influencing metastatic organotropism.

HPSE1 was also overexpressed in different OSCC-derived cell lines (up to 15-fold higher), and it seemed to be proportionally more highly expressed according to the malignant potential of these cell lines. We then modulated endogenous HPSE1 by generating stable OSCC cell lines expressing shRNA and ORF RNA-targeting HPSE1 to better understand the part of HPSE1 in the preclinical stage. We demonstrated that the abrogation of HPSE1 on oral cancer cells increases apoptosis, while suppressing proliferation, migration, invasion, epithelial–mesenchymal transition (EMT), and angiogenesis. In agreement with other studies, HPSE1 knockdown had expressive unfavorable effects on the viability and proliferative potential of OSCC cells (Ikuta et al., 2001; Tatsumi et al., 2020) as overexpression of HPSE1 increased the proliferation of OSCC cells. Per previous studies (Ikuta et al., 2001), we also demonstrated that HPSE1 regulates migration and invasion status of OSCC cells, which may explain why higher HPSE1 expression was significantly correlated with a worse prognosis.

In other cancers, HPSE1 activation has been linked to metastasis and tumor progression upholding. Chen et al. (2015) suggested an association between heparanase expression and cell adhesion, and metastasis in hepatocellular carcinoma cell lines. Previous studies (Tatsumi et al., 2020) also reported that HPSE1 played a role in the regulation of proliferation and autophagy in normal and malignant cells, conferring survival benefits and resistance to chemotherapy. We then explore the association of the proliferative process with HPSE1 expression in oral cancer biology. Our study confirmed that the increase in apoptosis resulted from HPSE1 suppression, as well as the inhibition of cell proliferation, while its overexpression reduced apoptosis and increased proliferation in these oral cancer cells. Furthermore, in the spontaneous bladder cancer mouse model, heparanase silencing significantly suppressed bladder cancer invasion. Our results showed that HPSE1

suppression significantly reduced the ability of cancer cells to migrate and invade, along with the modulation of the mRNA expression of EMT and ECM markers.

In this context, it is important to highlight that the TME is a cellular and a non-cellular environment that contains the tumor, and includes fibroblasts, surrounding blood vessels, bone marrow-derived immune cells, lymphocytes, signaling molecules, and an extracellular matrix. Also, the EMT involves a biological process by which cells transit between epithelial and mesenchymal states by decreasing cell–cell adhesion and increasing cell motility and metastasis. In cells with HPSE1 depletion, we observed an induction of E-cadherin and inhibition of vimentin, and the overexpression of HPSE1 promotes the EMT by upregulating these mesenchymal markers, an important phenotype for invasion and metastasis. The heparanase produced by cancer cells has also been suggested to cleave HS of the basement membrane (BM), which is necessary for them to infiltrate the BM of blood vessels during metastasis. In the ECM, HPSE1 can also discharge HS-bound growth factors and proteolytic enzymes, which promotes angiogenesis and proliferation of cancer cells, further assisting invasion and metastasis (Jayatilleke and Hulett, 2020). Traditionally, the ECM protein network, glycoproteins, and proteoglycans were noticed as an embedded scaffold furnishing a structural framework for cells to form tissue organs. Later, it was observed that the ECM played a role in the management of cell survival, proliferation, and differentiation. The enzymatic activity of HPSE leads to ECM remodeling by increasing bioavailability and function of heparan sulfate (HS)-binding proteins (HSBPs) (Cohen-Kaplan et al., 2008; Knelson et al., 2014), which are important components of the ECM due to their contribution to the maintenance of ECM structural integrity and regulatory functions (Sarrazin et al., 2011). In corroboration with our findings, high HPSE1 expression induced head and neck cancer progression (Cohen-Kaplan et al., 2008) and mammary adenocarcinoma cell invasion and metastasis correlated with loss of E-cadherin and gain of MMPs 2 and 9 levels (Welch et al., 1990).

Finally, as HPSE1 overexpression has been shown to strengthen tumor angiogenesis in other contexts, Vlodavsky et al. (2018) investigated the effects of HPSE1 silencing and overexpression on *in vitro* endothelial tube formation. As shown in the present study, the preconditioned medium overexpressing HPSE1 significantly enhanced and the HSPE1-inhibited preconditioned medium significantly decreased vascular tube formation compared to the preconditioned medium with HPSE1 wild-type (WT) expressing cells. Interestingly the formation of tubes structures of HUVEC cells treated with the preconditioned medium of HPSE1-overexpressing clones persisted, in contrast to those treated with preconditioned medium from the parental SCC9 control cells. When treated with the inhibition clone-preconditioned medium, there was a complete vessel breakdown after 24 h, suggesting a relevant role of HPSE1 in the maintenance of blood capillary vessels in the process of tumor angiogenesis. Thus, our data support the hypothesis that the level of HPSE1 produced by cancer cells can facilitate angiogenesis, which in turn supports tumor growth.

Angiogenesis, the formation of new blood vessels, has physiologic and pathological roles (Chung et al., 2010). To better understand the HPSE1 role in molecular pathways associated with angiogenesis, we evaluated the VEGFA gene expression profile in OSCC cell lines with modulated HPSE1 expression. Our results showed that VEGFA expression was increased in OSCC cell lines overexpressing HPSE1 and decreased in HPSE1-silenced OSCC cells when compared to OSCC cell line parental control. The VEGF-signaling pathway is a major regulator of tumor growth and metastasis (Vlodavsky et al., 2018). Heparanase aids tumor invasion by shattering the ECM, releasing angiogenic factors, and recruiting an angiogenic environment. Heparanase activity has been well implicated in cell dissemination associated with the processes of inflammation and angiogenesis (Parish et al., 2013), through the release of a combination of growth factors linked to bFGF, VEGF, and HB-EGF e KGF, which support neovascularization and wound healing. Zcharia et al. (2005) reported that high levels of heparanase in wound healing accelerated tissue repair and skin restoration, mediated mainly by an increased angiogenic response. These actions make heparanase a promising target for cancer therapy (Vlodavsky et al., 2018). Monoclonal antibodies against VEGFA were the first angiogenesis inhibitors authorized for the treatment of colon cancer patients with metastasis based on their survival benefit (Hurwitz et al., 2004) and could also be a tool to combat advanced oral cancer disease.

Of note, most local and distant metastatic cases had higher expression of HPSE1, while most non-metastatic cancers showed lower HPSE1 expression. That may be analogous to the HPSE1 role in various aspects of cancer metastasis (i.e., while in some cancer phases, heparanase assists ECM degradation; in others, it enhances neovascularization). Nevertheless, it is very reasonable that an outstanding correlation endures between heparanase expression and activity and the metastatic potential of oral cancer cells.

This report was the first to simultaneously investigate heparanase modulation (inhibition and induction) and its effects on the suppression of cancer migration, invasion, proliferation, apoptosis, and angiogenesis of oral cancer. However, our data have limitation on the correlation between HPSE1 and the EMT markers and VEGFA in clinical OSCC tissue specimens due to lack of any more samples available to perform such analyses. Thus, as a preclinical-based design, particularly in number of samples, this study has its limitation, and to gain more detailed insights into the molecular crisis involving the HPSE1-mediated OSCC progression, additional *in vivo* mechanistic studies are required.

CONCLUSION

Taken together, our results suggest that HPSE1 is overexpressed in patients with OSCC and OSCC-derived cell lines, upregulation of HPSE1 is significantly associated with poor outcome, and HPSE1 implicates an important role in OSCC migration, invasiveness, and the angiogenic process. On this basis, further

studies should be carried on to establish HPSE1 as a routine prognostic marker for patients with oral cavity cancer.

DATA AVAILABILITY STATEMENT

The original contributions presented in the study are included in the article/**Supplementary Material**, further inquiries can be directed to the corresponding author.

ETHICS STATEMENT

The studies involving human participants were reviewed and approved by Comitê de Ética e Pesquisa da Faculdade de Jundiaí (CEP/FMJ). The patients/participants provided their written informed consent to participate in this study.

AUTHOR CONTRIBUTIONS

NC, CO, and TA: conceived and designed the experiments; LL-S, MJ, PL, VG, DC, and NC: performed the experiments; AR, FC, PL, RB, GSC, and AC: contributed to clinical samples; BM: performed the immunohistochemical analysis; RC, LL-S, IA, and NC: analyzed the data; NC, LL-S, AR: wrote the manuscript; and all the authors revised and approved the final manuscript.

FUNDING

This work was supported by grants from Fundação de Amparo a Pesquisa do Estado de São Paulo-FAPESP, São Paulo, Brazil (NC, 2015/10029-1, 2018/16735-3) (TA, 2018/16735-3), and Coordenação de Aperfeiçoamento de Pessoal de Nível Superior-CAPES, Brasília, Brazil (PNPD) (88882.317191/2019-01).

SUPPLEMENTARY MATERIAL

The Supplementary Material for this article can be found online at: https://www.frontiersin.org/articles/10.3389/fcell.2022.742213/full#supplementary-material

Supplementary Figure S1 | Analysis of Immunofluorescence (IF) and Western Blot (WB) from OSCC cellular compartments. **(A)** In the SCC-9 cell line, nuclear and cytoplasmic HPSE1 protein expression was determined by IF and showed higher HPSE1 expression in the cytoplasmic compartment compared to the non-malignant HGK cells, in which HPSE1 expression was more restricted to the nuclear fraction. **(B)** Western blotting showing the distribution of HPSE1 protein expression pattern and its quantification **(C)** in SCC9 cells, and the respective suppressed (ShRNA) and upregulated (OrfRNA) derived clones within the subcellular compartments. The results showed a significant reduction in cytoplasmic protein levels of OSCC by HPSE1-shRNA silencing, while its induced upregulation significantly increased cytoplasmic HPSE1 expression in SCC-9 cells. N, Nucleus; C, Citoplasm.

Supplementary Figure S2 | Multivariate analyses showed a significant association of combinations of HPSE1 levels and pTNM **(A)**, pT **(B)**, and pN **(C)** stages for Disease Free-Survival. Survival curves indicated largely improved discriminatory ability.

REFERENCES

Alam, H., Sehgal, L., Kundu, S. T., Dalal, S. N., and Vaidya, M. M. (2011). Novel Function of Keratins 5 and 14 in Proliferation and Differentiation of Stratified Epithelial Cells. *MBoC* 22, 4068–4078. doi:10.1091/mbc.E10-08-0703

Almangush, A., Coletta, R. D., Bello, I. O., Bitu, C., Keski-Säntti, H., Mäkinen, L. K., et al. (2015). A Simple Novel Prognostic Model for Early Stage Oral Tongue Cancer. *Int. J. Oral Maxillofac. Surg.* 44, 143–150. doi:10.1016/j.ijom.2014.10.004

Chen, X.-P., Luo, J.-S., Tian, Y., Nie, C.-L., Cui, W., and Zhang, W.-D. (2015). Downregulation of Heparanase Expression Results in Suppression of Invasion, Migration, and Adhesion Abilities of Hepatocellular Carcinoma Cells. *Biomed. Res. Int.* 2015, 1–10. doi:10.1155/2015/241983

Chi, A. C., Day, T. A., and Neville, B. W. (2015). Oral Cavity and Oropharyngeal Squamous Cell Carcinoma-An Update. *CA: A Cancer J. Clinicians* 65, 401–421. doi:10.3322/caac.21293

Chung, A. S., Lee, J., and Ferrara, N. (2010). Targeting the Tumour Vasculature: Insights from Physiological Angiogenesis. *Nat. Rev. Cancer* 10, 505–514. doi:10.1038/nrc2868

Cohen-Kaplan, V., Doweck, I., Naroditsky, I., Vlodavsky, I., and Ilan, N. (2008). Heparanase Augments Epidermal Growth Factor Receptor Phosphorylation: Correlation with Head and Neck Tumor Progression. *Cancer Res.* 68, 10077–10085. doi:10.1158/0008-5472.CAN-08-2910

Dempsey, L. A., Brunn, G. J., and Platt, J. L. (2000). Heparanase, a Potential Regulator of Cell-Matrix Interactions. *Trends Biochemical Sciences* 25, 349–351. doi:10.1016/s0968-0004(00)01619-4

Edovitsky, E., Elkin, M., Zcharia, E., Peretz, T., and Vlodavsky, I. (2004). Heparanase Gene Silencing, Tumor Invasiveness, Angiogenesis, and Metastasis. *JNCI J. Natl. Cancer Inst.* 96, 1219–1230. doi:10.1093/jnci/djh230

Gross-Cohen, M., Feld, S., Doweck, I., Neufeld, G., Hasson, P., Arvatz, G., et al. (2016). Heparanase 2 Attenuates Head and Neck Tumor Vascularity and Growth. *Cancer Res.* 76, 2791–2801. doi:10.1158/0008-5472.CAN-15-1975

Hammond, E., Khurana, A., Shridhar, V., and Dredge, K. (2014). The Role of Heparanase and Sulfatases in the Modification of Heparan Sulfate Proteoglycans within the Tumor Microenvironment and Opportunities for Novel Cancer Therapeutics. *Front. Oncol.* 4, 195. doi:10.3389/fonc.2014.00195

Hanahan, D., and Weinberg, R. A. (2011). Hallmarks of Cancer: The Next Generation. *Cell* 144, 646–674. doi:10.1016/j.cell.2011.02.013

Hunter, K. E., Palermo, C., Kester, J. C., Simpson, K., Li, J.-P., Tang, L. H., et al. (2014). Heparanase Promotes Lymphangiogenesis and Tumor Invasion in Pancreatic Neuroendocrine Tumors. *Oncogene* 33, 1799–1808. doi:10.1038/onc.2013.142

Hurwitz, H., Fehrenbacher, L., Novotny, W., Cartwright, T., Hainsworth, J., Heim, W., et al. (2004). Bevacizumab Plus Irinotecan, Fluorouracil, and Leucovorin for Metastatic Colorectal Cancer. *N. Engl. J. Med.* 350, 2335–2342. doi:10.1056/NEJMoa032691

Ikuta, M., Podyma, K. A., Maruyama, K., Enomoto, S., and Yanagishita, M. (2001). Expression of Heparanase in Oral Cancer Cell Lines and Oral Cancer Tissues. *Oral Oncol.* 37, 177–184. doi:10.1016/S1368-8375(00)00077-4

Ilan, N., Elkin, M., and Vlodavsky, I. (2006). Regulation, Function and Clinical Significance of Heparanase in Cancer Metastasis and Angiogenesis. *Int. J. Biochem. Cel Biol.* 38, 2018–2039. doi:10.1016/j.biocel.2006.06.004

Instituto Nacional de Câncer José Alencar Gomes da Silva (2019). *Estimativa 2020 : incidência de câncer no Brasil*. Rio de Janeiro: Instituto Nacional de Câncer José Alencar Gomes da Silva.

Jayatilleke, K. M., and Hulett, M. D. (2020). Heparanase and the Hallmarks of Cancer. *J. Transl Med.* 18, 453. doi:10.1186/s12967-020-02624-1

Jiao, Q., Wu, A., Shao, G., Peng, H., Wang, M., Ji, S., et al. (2014). The Latest Progress in Research on Triple Negative Breast Cancer (TNBC): Risk Factors, Possible Therapeutic Targets and Prognostic Markers. *J. Thorac. Dis.* 6, 1329–1335. doi:10.3978/j.issn.2072-1439.2014.08.13

Jin, H., and Zhou, S. (2017). The Functions of Heparanase in Human Diseases. *Med. Chem.* 17, 541–548. doi:10.2174/1389557516666161101143 6

Knelson, E. H., Nee, J. C., and Blobe, G. C. (2014). Heparan Sulfate Signaling in Cancer. *Trends Biochem. Sci.* 39, 277–288. doi:10.1016/j.tibs.2014.03.001

Kurokawa, H., Katsube, K.-i., Podyma, K. A., Ikuta, M., Iseki, H., Nakajima, M., et al. (2003). Heparanase and Tumor Invasion Patterns in Human Oral Squamous Cell Carcinoma Xenografts. *Cancer Sci.* 94, 277–285. doi:10.1111/j.1349-7006.2003.tb01433.x

Leiser, Y., Abu-El-Naaj, I., Sabo, E., Akrish, S., Ilan, N., Ben-Izhak, O., et al. (2011). Prognostic Value of Heparanase Expression and Cellular Localization in Oral Cancer. *Head Neck* 33, 871–877. doi:10.1002/hed.21545

Lerner, I., Baraz, L., Pikarsky, E., Meirovitz, A., Edovitsky, E., Peretz, T., et al. (2008). Function of Heparanase in Prostate Tumorigenesis: Potential for Therapy. *Clin. Cancer Res.* 14, 668–676. doi:10.1158/1078-0432.CCR-07-1866

Mäkelä, M., Salo, T., and Larjava, H. (1998). MMP-9 from TNFα-Stimulated Keratinocytes Binds to Cell Membranes and Type I Collagen: A Cause for Extended Matrix Degradation in Inflammation? *Biochem. Biophysical Res. Commun.* 253, 325–335. doi:10.1006/bbrc.1998.9641

Masola, V., Bellin, G., Gambaro, G., and Onisto, M. (2018). Heparanase: A Multitasking Protein Involved in Extracellular Matrix (ECM) Remodeling and Intracellular Events. *Cells* 7, 236. doi:10.3390/cells7120236

Masola, V., Zaza, G., Gambaro, G., Onisto, M., Bellin, G., Vischini, G., et al. (2016). Heparanase: A Potential New Factor Involved in the Renal Epithelial Mesenchymal Transition (EMT) Induced by Ischemia/Reperfusion (I/R) Injury. *PLoS ONE* 11, e0160074. doi:10.1371/journal.pone.0160074

Mogler, C., Herold-Mende, C., Dyckhoff, G., Jenetzky, E., Beckhove, P., and Helmke, B. M. (2011). Heparanase Expression in Head and Neck Squamous Cell Carcinomas Is Associated with Reduced Proliferation and Improved Survival. *Histopathology* 58, 944–952. doi:10.1111/j.1365-2559.2011.03834.x

Moro, J. d. S., Maroneze, M. C., Ardenghi, T. M., Barin, L. M., and Danesi, C. C. (2018). Oral and Oropharyngeal Cancer: Epidemiology and Survival Analysis. *Einstein (São Paulo)* 16, eAO4248. doi:10.1590/S1679-45082018AO4248

Nadanaka, S., Purunomo, E., Takeda, N., Tamura, J.-i., and Kitagawa, H. (2014). Heparan Sulfate Containing Unsubstituted Glucosamine Residues. *J. Biol. Chem.* 289, 15231–15243. doi:10.1074/jbc.M113.545343

Nadir, Y., and Brenner, B. (2014). Heparanase Multiple Effects in Cancer. *Thromb. Res.* 133, S90–S94. doi:10.1016/S0049-3848(14)50015-1

Nadir, Y., Brenner, B., Zetser, A., Ilan, N., Shafat, I., Zcharia, E., et al. (2006). Heparanase Induces Tissue Factor Expression in Vascular Endothelial and Cancer Cells. *J. Thromb. Haemost.* 4, 2443–2451. doi:10.1111/j.1538-7836.2006.02212.x

Nakajima, M., Irimura, T., di Ferrante, D., di Ferrante, N., and Nicolson, G. L. (1983). Heparan Sulfate Degradation: Relation to Tumor Invasive and Metastatic Properties of Mouse B16 Melanoma Sublines. *Science* 220, 611–613. doi:10.1126/science.6220468

Ostapoff, K. T., Awasthi, N., Kutluk Cenik, B., Hinz, S., Dredge, K., Schwarz, R. E., et al. (2013). PG545, an Angiogenesis and Heparanase Inhibitor, Reduces Primary Tumor Growth and Metastasis in Experimental Pancreatic Cancer. *Mol. Cancer Ther.* 12, 1190–1201. doi:10.1158/1535-7163.MCT-12-1123

Parish, C. R., Freeman, C., and Hulett, M. D. (2001). Heparanase: a Key Enzyme Involved in Cell Invasion. *Biochim. Biophys. Acta (Bba) - Rev. Cancer* 1471, M99–M108. doi:10.1016/s0304-419x(01)00017-8

Parish, C. R., Freeman, C., Ziolkowski, A. F., He, Y. Q., Sutcliffe, E. L., Zafar, A., et al. (2013). Unexpected New Roles for Heparanase in Type 1 Diabetes and Immune Gene Regulation. *Matrix Biol.* 32, 228–233. doi:10.1016/j.matbio.2013.02.007

Pisano, C., Vlodavsky, I., Ilan, N., and Zunino, F. (2014). The Potential of Heparanase as a Therapeutic Target in Cancer. *Biochem. Pharmacol.* 89, 12–19. doi:10.1016/j.bcp.2014.02.010

Purushothaman, A., Chen, L., Yang, Y., and Sanderson, R. D. (2008). Heparanase Stimulation of Protease Expression Implicates it as a Master Regulator of the Aggressive Tumor Phenotype in Myeloma. *J. Biol. Chem.* 283, 32628–32636. doi:10.1074/jbc.M806266200

Quiros, R. M., Rao, G., Plate, J., Harris, J. E., Brunn, G. J., Platt, J. L., et al. (2006). Elevated Serum Heparanase-1 Levels in Patients with Pancreatic Carcinoma Are Associated with Poor Survival. *Cancer* 106, 532–540. doi:10.1002/cncr.21648

Rangarajan, S., Richter, J. R., Richter, R. P., Bandari, S. K., Tripathi, K., Vlodavsky, I., et al. (2020). Heparanase-enhanced Shedding of Syndecan-1 and its Role in Driving Disease Pathogenesis and Progression. *J. Histochem. Cytochem.* 68, 823–840. doi:10.1369/0022155420937087

Rivara, S., Milazzo, F. M., and Giannini, G. (2016). Heparanase: A Rainbow Pharmacological Target Associated to Multiple Pathologies Including Rare Diseases. *Future Med. Chem.* 8, 647–680. doi:10.4155/fmc-2016-0012

Rodrigues, P. C., Miguel, M. C. C., Bagordakis, E., Fonseca, F. P., de Aquino, S. N., Santos-Silva, A. R., et al. (2014). Clinicopathological Prognostic Factors of Oral Tongue Squamous Cell Carcinoma: a Retrospective Study of 202 Cases. *Int. J. Oral Maxillofac. Surg.* 43, 795–801. doi:10.1016/j.ijom.2014.01.014

Rodrigues, P. C., Sawazaki-Calone, I., Ervolino De Oliveira, C., Carneiro, C., Macedo, S., Dourado, M. R., et al. (2017). Fascin Promotes Migration and Invasion and Is a Prognostic Marker for Oral Squamous Cell Carcinoma. *Oncotarget* 8, 74736–74754. doi:10.18632/oncotarget.20360

Roucourt, B., Meeussen, S., Bao, J., Zimmermann, P., and David, G. (2015). Heparanase Activates the Syndecan-Syntenin-ALIX Exosome Pathway. *Cell Res* 25, 412–428. doi:10.1038/cr.2015.29

Salo, T., Sutinen, M., Hoque Apu, E., Sundquist, E., Cervigne, N. K., de Oliveira, C. E., et al. (2015). A Novel Human Leiomyoma Tissue Derived Matrix for Cell Culture Studies. *BMC Cancer* 15, 1. doi:10.1186/s12885-015-1944-z

Sanderson, R. D., Elkin, M., Rapraeger, A. C., Ilan, N., and Vlodavsky, I. (2017). Heparanase Regulation of Cancer, Autophagy and Inflammation: New Mechanisms and Targets for Therapy. *Febs J.* 284, 42–55. doi:10.1111/febs.13932

Santos, T. C. F. d., Gomes, A. M., Paschoal, M. E. M., Stelling, M. P., Rumjanek, V. M. B. D., Junior, A. d. R., et al. (2014). Heparanase Expression and Localization in Different Types of Human Lung Cancer. *Biochim. Biophys. Acta (Bba) - Gen. Subjects* 1840, 2599–2608. doi:10.1016/j.bbagen.2014.04.010

Sarrazin, S., Lamanna, W. C., and Esko, J. D. (2011). Heparan Sulfate Proteoglycans. *Cold Spring Harbor Perspect. Biol.* 3, a004952. doi:10.1101/cshperspect.a004952

Sawazaki-Calone, I., Rangel, A., Bueno, A., Morais, C., Nagai, H., Kunz, R., et al. (2015). The Prognostic Value of Histopathological Grading Systems in Oral Squamous Cell Carcinomas. *Oral Dis.* 21, 755–761. doi:10.1111/odi.12343

Shah, S., Fourgeaud, C., Derieux, S., Mirshahi, S., Contant, G., Pimpie, C., et al. (2018). The Close Relationship between Heparanase and Epithelial Mesenchymal Transition in Gastric Signet-Ring Cell Adenocarcinoma. *Oncotarget* 73, 33778–33787. doi:10.18632/oncotarget.26042

Søland, T. M., and Brusevold, I. J. (2013). Prognostic Molecular Markers in Cancer - Quo Vadis? *Histopathology* 63, 297–308. doi:10.1111/his.12184

Tatsumi, Y., Miyake, M., Shimada, K., Fujii, T., Hori, S., Morizawa, Y., et al. (2020). Inhibition of Heparanase Expression Results in Suppression of Invasion, Migration and Adhesion Abilities of Bladder Cancer Cells. *Ijms* 21, 3789. doi:10.3390/ijms21113789

Thompson, C. A., Purushothaman, A., Ramani, V. C., Vlodavsky, I., and Sanderson, R. D. (2013). Heparanase Regulates Secretion, Composition, and Function of Tumor Cell-Derived Exosomes. *J. Biol. Chem.* 288, 10093–10099. doi:10.1074/jbc.C112.444562

Väyrynen, O., Piippo, M., Jämsä, H., Väisänen, T., de Almeida, C. E. B., Salo, T., et al. (2018). Effects of Ionizing Radiation and HPSE1 Inhibition on the Invasion of Oral Tongue Carcinoma Cells on Human Extracellular Matrices *In Vitro*. *Exp. Cel Res.* 371, 151–161. doi:10.1016/j.yexcr.2018.08.005

Vlodavsky, I., Eldor, A., Haimovitz-Friedman, A., Matzner, Y., and Ishai-Michaeli, R. (1992). Expression of Heparanase by Platelets and Circulating Cells of the Immune System: Possible Involvement in Diapedesis and Extravasation. *Invasion Metastasis* 12, 112.

Vlodavsky, I., Beckhove, P., Lerner, I., Pisano, C., Meirovitz, A., Ilan, N., et al. (2012). Significance of Heparanase in Cancer and Inflammation. *Cancer Microenvironment* 5, 115–132. doi:10.1007/s12307-011-0082-7

Vlodavsky, I., Gross-Cohen, M., Weissmann, M., Ilan, N., and Sanderson, R. D. (2018). Opposing Functions of Heparanase-1 and Heparanase-2 in Cancer Progression. *Trends Biochem. Sci.* 43, 18–31. doi:10.1016/j.tibs.2017.10.007

Vreys, V., and David, G. (2007). Mammalian Heparanase: what Is the Message? *J. Cell. Mol. Med.* 11, 427–452. doi:10.1111/j.1582-4934.2007.00039.x

Welch, D. R., Fabra, A., and Nakajima, M. (1990). Transforming Growth Factor Beta Stimulates Mammary Adenocarcinoma Cell Invasion and Metastatic Potential. *Proc. Natl. Acad. Sci. U.S.A.* 87, 7678–7682. doi:10.1073/pnas.87.19.7678

Xia, F., Xu, J. C., Zhang, P., Zhang, Y. Y., Zhang, Q. W., Chao, Z. H., et al. (2014). Glucose-regulated Protein 78 and Heparanase Expression in Oral Squamous Cell Carcinoma: Correlations and Prognostic Significance. *World J. Surg. Onc* 12, 121. doi:10.1186/1477-7819-12-121

Yang, Y., MacLeod, V., Miao, H.-Q., Theus, A., Zhan, F., Shaughnessy, J. D., et al. (2007). Heparanase Enhances Syndecan-1 Shedding. *J. Biol. Chem.* 282, 13326–13333. doi:10.1074/jbc.M611259200

Zcharia, E., Zilka, R., Yaar, A., Yacoby-Zeevi, O., Zetser, A., Metzger, S., et al. (2005). Heparanase Accelerates Wound Angiogenesis and Wound Healing in Mouse and Rat Models. *FASEB j.* 19, 211–221. doi:10.1096/fj.04-1970com

Zeng, X., Tao, W., Mei, L., Huang, L., Tan, C., and Feng, S.-S. (2013). Cholic Acid-Functionalized Nanoparticles of star-shaped PLGA-Vitamin E TPGS Copolymer for Docetaxel Delivery to Cervical Cancer. *Biomaterials* 34, 6058–6067. doi:10.1016/j.biomaterials.2013.04.052

Zetser, A., Bashenko, Y., Edovitsky, E., Levy-Adam, F., Vlodavsky, I., and Ilan, N. (2006). Heparanase Induces Vascular Endothelial Growth Factor Expression: Correlation with P38 Phosphorylation Levels and Src Activation. *Cancer Res.* 66, 1455–1463. doi:10.1158/0008-5472.CAN-05-1811

Zhang, L., Riethdorf, S., Wu, G., Wang, T., Yang, K., Peng, G., et al. (2012). Meta-Analysis of the Prognostic Value of Circulating Tumor Cells in Breast Cancer. *Clin. Cancer Res.* 18, 5701–5710. doi:10.1158/1078-0432.CCR-12-1587

Zheng, L., Jiang, G., Mei, H., Pu, J., Dong, J., Hou, X., et al. (2010). Small RNA Interference-Mediated Gene Silencing of Heparanase Abolishes the Invasion, Metastasis, and Angiogenesis of Gastric Cancer Cells. *BMC Cancer* 10, 33–44. doi:10.1186/1471-2407-10-33

Zhou, Y., Song, B., Qin, W.-j., Zhang, G., Zhang, R., Luan, Q., et al. (2008). Heparanase Promotes Bone Destruction and Invasiveness in Prostate Cancer. *Cancer Lett.* 268, 252–259. doi:10.1016/j.canlet.2008.04.008

Zhu, Z., Navarro, E., Kussie, P., Liu, H., and Miao, H.-Q. (2006). Development of Heparanase Inhibitors for Anti-cancer Therapy. *Cmc* 13, 2101–2111. doi:10.2174/092986706777935230

Conflict of Interest: The authors declare that the research was conducted in the absence of any commercial or financial relationships that could be construed as a potential conflict of interest.

Publisher's Note: All claims expressed in this article are solely those of the authors and do not necessarily represent those of their affiliated organizations, or those of the publisher, the editors, and the reviewers. Any product that may be evaluated in this article, or claim that may be made by its manufacturer, is not guaranteed or endorsed by the publisher.

Advantages of publishing in Frontiers

OPEN ACCESS
Articles are free to read for greatest visibility and readership

FAST PUBLICATION
Around 90 days from submission to decision

HIGH QUALITY PEER-REVIEW
Rigorous, collaborative, and constructive peer-review

TRANSPARENT PEER-REVIEW
Editors and reviewers acknowledged by name on published articles

Frontiers
Avenue du Tribunal-Fédéral 34
1005 Lausanne | Switzerland

Visit us: www.frontiersin.org
Contact us: frontiersin.org/about/contact

REPRODUCIBILITY OF RESEARCH
Support open data and methods to enhance research reproducibility

DIGITAL PUBLISHING
Articles designed for optimal readership across devices

FOLLOW US
@frontiersin

IMPACT METRICS
Advanced article metrics track visibility across digital media

EXTENSIVE PROMOTION
Marketing and promotion of impactful research

LOOP RESEARCH NETWORK
Our network increases your article's readership